TICK AND TICK-BORNE PATHOGENS: MOLECULAR AND IMMUNE TARGETS FOR CONTROL STRATEGIES

EDITED BY: Abid Ali, Albert Mulenga and Itabajara Silva Vaz Jr
PUBLISHED IN: Frontiers in Physiology and Frontiers in Veterinary Science

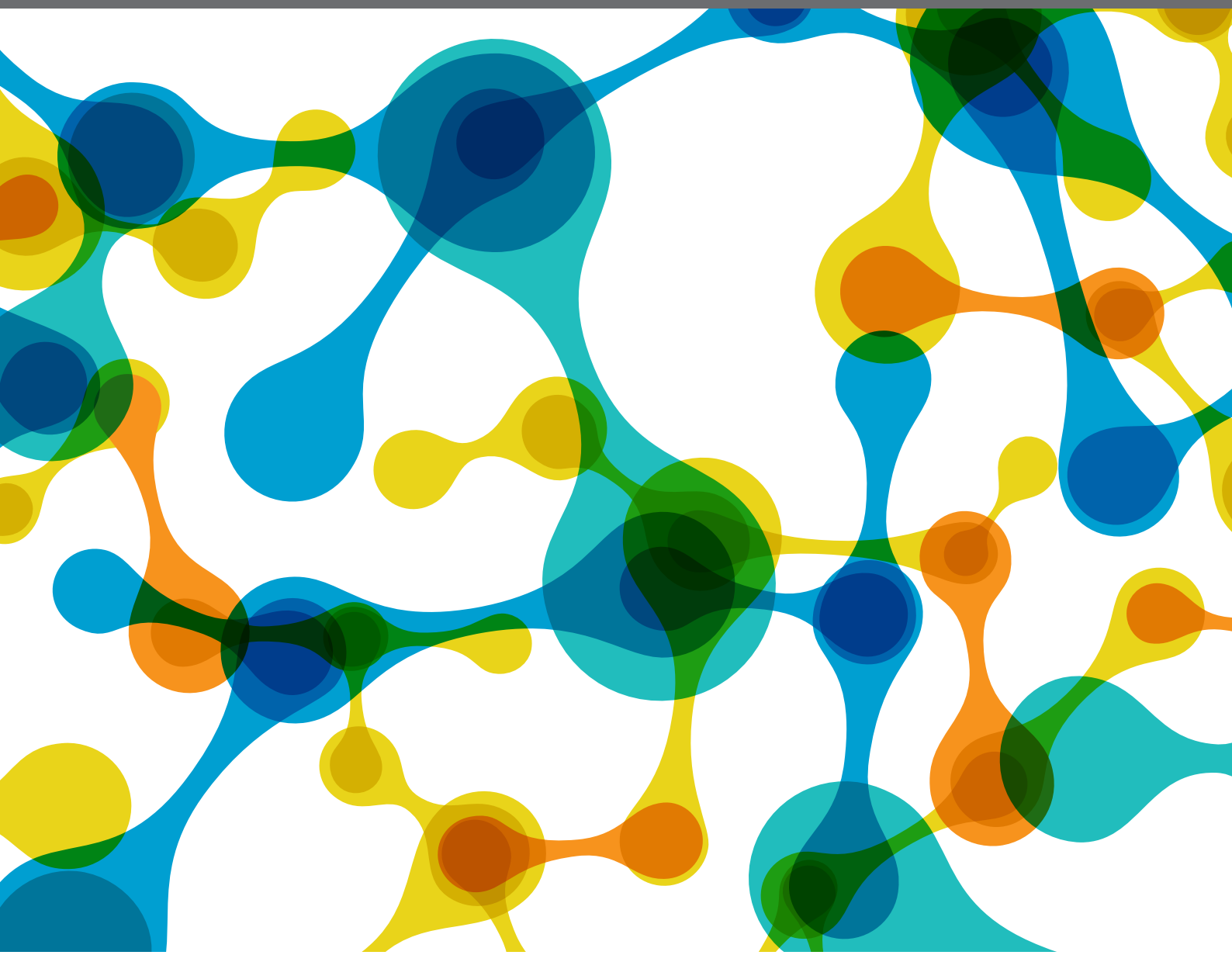

frontiers Research Topics

frontiers

ISSN 1664-8714
ISBN 978-2-88966-060-5
DOI 10.3389/978-2-88966-060-5

About Frontiers

Frontiers is more than just an open-access publisher of scholarly articles: it is a pioneering approach to the world of academia, radically improving the way scholarly research is managed. The grand vision of Frontiers is a world where all people have an equal opportunity to seek, share and generate knowledge. Frontiers provides immediate and permanent online open access to all its publications, but this alone is not enough to realize our grand goals.

Frontiers Journal Series

The Frontiers Journal Series is a multi-tier and interdisciplinary set of open-access, online journals, promising a paradigm shift from the current review, selection and dissemination processes in academic publishing. All Frontiers journals are driven by researchers for researchers; therefore, they constitute a service to the scholarly community. At the same time, the Frontiers Journal Series operates on a revolutionary invention, the tiered publishing system, initially addressing specific communities of scholars, and gradually climbing up to broader public understanding, thus serving the interests of the lay society, too.

Dedication to Quality

Each Frontiers article is a landmark of the highest quality, thanks to genuinely collaborative interactions between authors and review editors, who include some of the world's best academicians. Research must be certified by peers before entering a stream of knowledge that may eventually reach the public - and shape society; therefore, Frontiers only applies the most rigorous and unbiased reviews.
Frontiers revolutionizes research publishing by freely delivering the most outstanding research, evaluated with no bias from both the academic and social point of view. By applying the most advanced information technologies, Frontiers is catapulting scholarly publishing into a new generation.

What are Frontiers Research Topics?

Frontiers Research Topics are very popular trademarks of the Frontiers Journals Series: they are collections of at least ten articles, all centered on a particular subject. With their unique mix of varied contributions from Original Research to Review Articles, Frontiers Research Topics unify the most influential researchers, the latest key findings and historical advances in a hot research area! Find out more on how to host your own Frontiers Research Topic or contribute to one as an author by contacting the Frontiers Editorial Office: researchtopics@frontiersin.org

TICK AND TICK-BORNE PATHOGENS: MOLECULAR AND IMMUNE TARGETS FOR CONTROL STRATEGIES

Topic Editors:
Abid Ali, Abdul Wali Khan University Mardan, Pakistan
Albert Mulenga, Texas A&M University, United States
Itabajara Silva Vaz Jr, Federal University of Rio Grande do Sul, Brazil

Citation: Ali, A., Mulenga, A., Vaz, I. S. Jr, eds. (2020). Tick and Tick-Borne Pathogens: Molecular and Immune Targets for Control Strategies. Lausanne: Frontiers Media SA. doi: 10.3389/978-2-88966-060-5

Table of Contents

06 ***Editorial: Tick and Tick-Borne Pathogens: Molecular and Immune Targets for Control Strategies***
Abid Ali, Albert Mulenga and Itabajara Silva Vaz Jr.

10 ***Functional Evolution of Subolesin/Akirin***
Sara Artigas-Jerónimo, Margarita Villar, Alejandro Cabezas-Cruz, James J. Valdés, Agustín Estrada-Peña, Pilar Alberdi and José de la Fuente

27 ***A Continuing Exploration of Tick–Virus Interactions Using Various Experimental Viral Infections of Hard Ticks***
Melbourne Rio Talactac, Emmanuel P. Hernandez, Kozo Fujisaki and Tetsuya Tanaka

33 ***Preliminary Evaluation of Tick Protein Extracts and Recombinant Ferritin 2 as Anti-tick Vaccines Targeting* Ixodes ricinus *in Cattle***
Sarah Knorr, Juan Anguita, Julen T. Cortazar, Ondrej Hajdusek, Petr Kopáček, Jos J. Trentelman, Olivia Kershaw, Joppe W. Hovius and Ard M. Nijhof

44 ***Crucial Role for Basophils in Acquired Protective Immunity to Tick Infestation***
Hajime Karasuyama, Yuya Tabakawa, Takuya Ohta, Takeshi Wada and Soichiro Yoshikawa

52 ***Transcriptome and Proteome Response of* Rhipicephalus annulatus *Tick Vector to* Babesia bigemina *Infection***
Sandra Antunes, Joana Couto, Joana Ferrolho, Gustavo Seron Sanches, José Octavio Merino Charrez, Ned De la Cruz Hernández, Monica Mazuz, Margarita Villar, Varda Shkap, José de la Fuente and Ana Domingos

69 ***Modeling Modulation of the Tick Regulome in Response to* Anaplasma phagocytophilum *for the Identification of New Control Targets***
Sara Artigas-Jerónimo, Agustín Estrada-Peña, Alejandro Cabezas-Cruz, Pilar Alberdi, Margarita Villar and José de la Fuente

80 ***Chemical Equilibrium at the Tick–Host Feeding Interface:A Critical Examination of Biological Relevance in Hematophagous Behavior***
Ben J. Mans

107 ***The Transcriptome of the Salivary Glands of* Amblyomma aureolatum *Reveals the Antimicrobial Peptide Microplusin as an Important Factor for the Tick Protection Against* Rickettsia rickettsii *Infection***
Larissa A. Martins, Camila D. Malossi, Maria F. B. de M. Galletti, José M. Ribeiro, André Fujita, Eliane Esteves, Francisco B. Costa, Marcelo B. Labruna, Sirlei Daffre and Andréa C. Fogaça

120 ***Vitellogenin Receptor as a Target for Tick Control: A Mini-Review***
Robert D. Mitchell III, Daniel E. Sonenshine and Adalberto A. Pérez de León

129 ***Comparative Susceptibility of Different Populations of* Amblyomma sculptum *to* Rickettsia rickettsii**
Monize Gerardi, Alejandro Ramírez-Hernández, Lina C. Binder, Felipe S. Krawczak, Fábio Gregori and Marcelo B. Labruna

141 *Ultrastructural and Cytotoxic Effects of* **Metarhizium robertsii** *Infection on* **Rhipicephalus microplus** *Hemocytes*
Jéssica Fiorotti, Rubem Figueiredo Sadok Menna-Barreto, Patrícia Silva Gôlo, Caio Junior Balduino Coutinho-Rodrigues, Ricardo Oliveira Barbosa Bitencourt, Diva Denelle Spadacci-Morena, Isabele da Costa Angelo and Vânia Rita Elias Pinheiro Bittencourt

158 *Genetic Profiling Reveals High Allelic Diversity, Heterozygosity and Antigenic Diversity in the Clinical Isolates of the* **Theileria annulata** *From India*
Sonti Roy, Vasundhra Bhandari, Debabrata Dandasena, Shweta Murthy and Paresh Sharma

166 *Repurposing of Glycine-Rich Proteins in Abiotic and Biotic Stresses in the Lone-Star Tick (***Amblyomma americanum***)*
Rebekah Bullard, Surendra Raj Sharma, Pradipta Kumar Das, Sarah E. Morgan and Shahid Karim

179 *The Use of Tick Salivary Proteins as Novel Therapeutics*
Jindřich Chmelař, Jan Kotál, Anna Kovaříková and Michail Kotsyfakis

189 *Deciphering Biological Processes at the Tick-Host Interface Opens New Strategies for Treatment of Human Diseases*
Iveta Štibrániová, Pavlína Bartíková, Viera Holíková and Mária Kazimírová

210 *Seasonal Dynamics, Record of Ticks Infesting Humans, Wild and Domestic Animals and Molecular Phylogeny of* **Rhipicephalus microplus** *in Khyber Pakhtunkhwa Pakistan*
Abid Ali, Munsif Ali Khan, Hafsa Zahid, Pir Muhammad Yaseen, Muhammad Qayash Khan, Javed Nawab, Zia Ur Rehman, Muhammad Ateeq, Sardar Khan and Mohammad Ibrahim

225 *A Vaccinomics Approach for the Identification of Tick Protective Antigens for the Control of* **Ixodes ricinus** *and* **Dermacentor reticulatus** *Infestations in Companion Animals*
Marinela Contreras, Margarita Villar and José de la Fuente

244 *The Complete Mitochondrial Genome and Expression Profile of Mitochondrial Protein-Coding Genes in the Bisexual and Parthenogenetic* **Haemaphysalis longicornis**
Tianhong Wang, Shiqi Zhang, Tingwei Pei, Zhijun Yu and Jingze Liu

257 *TOR as a Regulatory Target in* **Rhipicephalus microplus** *Embryogenesis*
Camila Waltero, Leonardo Araujo de Abreu, Thayná Alonso, Rodrigo Nunes-da-Fonseca, Itabajara da Silva Vaz Jr. and Carlos Logullo

272 *The Cattle Fever Tick,* **Rhipicephalus microplus***, as a Model for Forward Pharmacology to Elucidate Kinin GPCR Function in the Acari*
Caixing Xiong, Dwight Baker and Patricia V. Pietrantonio

292 *Experimental* **Ixodes ricinus***-Sheep Cycle of* **Anaplasma phagocytophilum** *NV2Os Propagated in Tick Cell Cultures*
Consuelo Almazán, Lisa Fourniol, Clotilde Rouxel, Pilar Alberdi, Christelle Gandoin, Anne-Claire Lagrée, Henri-Jean Boulouis, José de la Fuente and Sarah I. Bonnet

304 *Tick Cell Lines in Research on Tick Control*
Ahmed Al-Rofaai and Lesley Bell-Sakyi

311 ***Global Transcription Profiles of* Anaplasma phagocytophilum *at Key Stages of Infection in Tick and Human Cell Lines and Granulocytes***
Curtis M. Nelson, Michael J. Herron, Xin-Ru Wang, Gerald D. Baldridge, Jonathan D. Oliver and Ulrike G. Munderloh

328 **Porin *Expression Profiles in* Haemaphysalis longicornis *Infected With* Babesia microti**
Weiqing Zheng, Rika Umemiya-Shirafuji, Qian Zhang, Kiyoshi Okado, Paul Franck Adjou Moumouni, Hiroshi Suzuki, Haiying Chen, Mingming Liu and Xuenan Xuan

frontiers in Physiology

EDITORIAL
published: 07 August 2020
doi: 10.3389/fphys.2020.00744

Editorial: Tick and Tick-Borne Pathogens: Molecular and Immune Targets for Control Strategies

Abid Ali[1]*, *Albert Mulenga*[2] and *Itabajara Silva Vaz Jr.*[3,4]

[1] Department of Zoology, Abdul Wali Khan University Mardan, Mardan, Pakistan, [2] Department of Veterinary Pathobiology, College of Veterinary Medicine, Texas A&M University, College Station, TX, United States, [3] Centro de Biotecnologia, Universidade Federal do Rio Grande do Sul, Porto Alegre, Brazil, [4] Faculdade de Veterinaria, Universidade Federal do Rio Grande do Sul, Porto Alegre, Brazil

Keywords: tick, tick-borne pathogens, control, molecular-targets, immune-targets

Editorial on the Research Topic

Tick and Tick-Borne Pathogens: Molecular and Immune Targets for Control Strategies

Ticks are obligate hematophagous ectoparasites of domestic animals, humans, and wildlife. Ticks can be found in areas around the world ranging from the Arctic to tropical regions, and are known for their negative impact. They are capable of transmitting a wide range of pathogens including protozoa, viruses, and bacteria including spirochetes and rickettsia. The resulting diseases can potentially cause major production losses in livestock, thereby reducing farming incomes, increasing cost to consumers, and threatening trade between regions and/or world markets. Climate change has an impact on the distribution of ticks and tick-borne pathogens because tick species select a set of ecological conditions and biotopes that determine their geographic distributions and outline risk areas for their associated pathogens' transmission. In particular, arthropod vectors such as ticks, are vulnerable to these climatic changes as their population, survival, and development depend on factor like vegetation, availability of a host, photoperiod, moister and climatic conditions. Tick density, distribution, and their capability of pathogen transmission are thus effected (Ali et al.; Gerardi et al.).

Novel approaches have emerged, and the limitations of present operational protocols have been reduced to improve and standardize the laboratory procedures to lower costs, and to obtain a better understanding of tick and tick-borne pathogen interactions. Convenient and low-cost techniques provide a great opportunity to identify new targets for the future control of TBVs (Talactac et al.). Almazán et al. showed that sheep inoculated with tick cells infected with the *Anaplasma phagocytophilum* developed an infection 4 days post-inoculation (dpi) and the infected nymphs of *Ixodes ricinus* were able to transmit the *A. phagocytophilum* to naive infested sheep. The sheep transmitted the bacteria to 2.7% nymphs engorged as larvae during persistent infection. Among several other tick-borne diseases, tropical theileriosis caused by *Theileria annulata* infection is a significant livestock disease—especially in crossbreed cattle. The current study highlights the genetic and allelic diversity present among the Indian *T. annulata* parasites and its vaccine using a microsatellite marker, *tams1* sequencing, and GBS. The findings indicate that a heterogeneous parasitic population is prevalent in India, causing theileriosis, which may render the vaccine ineffective due to their high diversity. Parasite diversity data will be helpful in revamping new vaccines to control the disease (Roy et al.).

The hemocytes of *Rhipicephalus microplus* females, after *Metarhizium robertsii* infection associated with the cytotoxicity, were evaluated. Cytoplasmic vacuoles were observed in hemocytes of infected female ticks with electron densities, and in lipid droplets in close contact to low electron

Edited and reviewed by:
Ioannis Eleftherianos, George Washington University, United States

***Correspondence:**
Abid Ali
uop_ali@yahoo.com

Specialty section:
This article was submitted to Invertebrate Physiology, a section of the journal Frontiers in Physiology

Received: *15 May 2020*
Accepted: *08 June 2020*
Published: *07 August 2020*

Citation:
Ali A, Mulenga A and Vaz IS Jr (2020) Editorial: Tick and Tick-Borne Pathogens: Molecular and Immune Targets for Control Strategies. Front. Physiol. 11:744. doi: 10.3389/fphys.2020.00744

density vacuoles, as well as the formation of autophagosomes and subcellular material in different stages of degradation. This study reported fungal cytotoxicity, analyzing ultrastructural effects on hemocytes of *R. microplus* infected with entomopathogenic fungi (Fiorotti et al.). The genes that are required by tick-borne pathogens, such as *A. phagocytophilum* for host invasion and proliferation, were studied. Among them, several genes were found to be upregulated within human and tick cell lines (HL-60 and ISE6). Genes with unknown functions were found to play a disproportionate role in the establishment of infection (Nelson et al.).

The effects of an experimental infection with *Rickettsia rickettsii* on the global gene expression profile of the *A. aureolatum* salivary gland (SG), was determined by next-generation RNA sequencing. A total of 260 coding sequences (CDSs) were modulated by infection, among which 161 were upregulated and 99 were downregulated. Regarding CDSs in the immunity category, one sequence encoding one microplusin-like antimicrobial peptide (AMP) was chosen because, when there is a *R. rickettsii* infection, microplusin is significantly upregulated in both the salivary glands and the midgut tissues of *A. aureolatum*. The expression of microplusin was significantly upregulated in the SG as well as in the midgut (MG) of infected *A. aureolatum*. The knockdown of microplusin expression by RNA interference caused a significant increase in the prevalence of infected ticks (Martins et al.).

The porin functions in *Haemaphysalis longicornis* blood feeding and *Babesia* infection, and the relationship between porin and porin-related apoptosis genes such as B-cell lymphoma (Bcl), cytochrome complex (Cytc), caspase 2 (Cas2), and caspase 8 (Cas8), was analyzed. Porin expression levels were higher in the infected vs. uninfected nymphs during blood feeding, except at 1-day-partially-fed and 0 to 1-day post-engorgement. The highest *B. microti* burden negatively affected porin mRNA levels in both nymphs and female adults. Porin knockdown affected body weight and *Babesia* infection levels and significantly downregulated the expression levels of Cytc and Bcl in *H. longicornis* female ticks. Finally, the obtained results suggest that *H. longicornis* porin might interfere with blood feeding and *B. microti* infection (Zheng et al.).

A large amount of genomic and proteomic data of different organisms are available in public data banks. The genomic and proteomic sequence information of pathogens can provide an aid in detection and characterization of the novel therapeutic targets and vaccine candidates. The regulome (transcription factors-target genes interactions) plays a critical role in the cell's response to pathogen infection. The application of regulomics to tick-pathogen interactions will advance the understanding of these molecular interactions and contribute to the identification of novel control targets, to control tick and tick-borne diseases. In this article, *in silico* approaches were applied to model how *A. phagocytophilum* infection modulates the tick vector regulome. This proof-of-concept study provided support for the use of a network analysis in the study of the regulome response to infection, resulting in new information on tick-pathogen interactions and potential targets for developing interventions, to control tick infestations and pathogen transmission (Artigas-Jerónimo, Villar et al.).

A first comprehensive report of tick fauna was published from a northern state of Pakistan, which revealed that tick species comprising of six genera, were infesting diverse hosts including humans. These tick species included *R. microplus*, *Hyalomma anatolicum, Argas persicus*, *H. impeltatum, R. turanicus*, *R. haemaphysaloides*, *R. annulatus*, *Haemaphysalis montgomeryi*, *H. indica*, and *H. punctate*. *H. marginatum*, *R. sanguineus*, and *H. longicornis*, *A. gervaisi*, *A. exornatum, A. latum, Dermacentor marginatus*. It is important to mention that *H. punctata*, *Amb. exornatum,* and *Amblyomma latum* correspond to imported tick populations (authors personal communication). The phylogenetic analysis of tick *R. microplus*, based on partial mitochondrial cytochrome oxidase subunit I (COX1), 16S ribosomal RNA (16S rRNA), and internal transcribed spacer 2 (ITS2) sequences, revealed that *R. microplus* prevalent in this region belong to clade C, which include ticks originating from Bangladesh, Malaysia, and India (Ali et al.).

Blood feeding by ticks requires prolonged contact with a host's tissue and blood, and it has been suggested that the co-evolution of ticks with their natural hosts has resulted in the selection of an appropriate set of salivary components that allow ticks to evade both specific and non-specific host immunity in order to successfully obtain blood (Bullard et al.). In their quest for a blood meal, ticks transmit pathogens and inject a cocktail of bioactive molecules into their vertebrate hosts. Tick-borne pathogens have developed mechanisms to survive in the arthropod vector by manipulating gene expression, based on the midgut or salivary environment (Gerardi et al.; Antunes et al.).

Although not a replacement for the whole organism, research on tick cell lines provides a foundation for studies at less expensive *in vitro,* an alternative to *in vivo* tick feeding experiments (Al-Rofaai and Bell-Sakyi). Acaricides are the main components of integrated tick control strategies—despite their limited success and the associated hazards. It is under this scenario that anti-tick vaccines have emerged as an alternative tool for tick control. The potential advantages of vaccine-based control strategies include: cost-effectiveness, avoidance of environmental contamination, prevention of drug-resistance, possible prevention of pathogen transmission, and its potential applicability in a wide variety of hosts. A comprehensive understanding of tick proteins and their physiological roles can help shed light on how these parasites overcome host defenses, revealing new molecules of potential use for tick control and therapeutic applications (Artigas-Jerónimo, Villar et al.). The identification of conserved proteins across various parasites or vectors may provide the opportunity to develop a viable universal vaccine for control of multiple arthropods infestations and a platform for further characterization of how their evolution can meet species-specific demands. For instance, the conserved functional evolution of subolesin/akirin correlates with the protective capacity shown by these proteins in vaccine formulations for the control of different

arthropod and pathogen species (Artigas-Jerónimo, Villar et al.).

Components of the tick salivary glands have attracted attention as candidate antigens for anti-tick vaccines. Knowledge about the role of tick salivary proteins in tick physiology is important for a better understanding of the host-parasite relationships, drug targets, and the search for a novel candidate antigen for vaccine development. Moreover, tick salivary molecules have been observed to potentially exert cytotoxic and cytolytic effects on various tumor cells that have anti-angiogenic properties. Therefore, research has been focused on the identification of major tick salivary protein families exploitable in medical applications such as immunomodulation, inhibition of hemostasis, and inflammation, and the potential, opportunities, and challenges in searching for novel tick-derived drugs have been discussed (Chmelar et al.; Štibrániová et al.). A review article described that the tick feeding site may be considered as a closed system and could be treated as an ideal equilibrium system. Several tick proteins may have functional relevant concentrations and affinities at the feeding site. The feeding site is not an ideal closed system, but leads to a possible overestimation of tick protein concentration at the feeding site, and consequently, an overestimation of functional relevance (Mans).

A kinin precursor sequence was predicted from several tick species, and all species showed an expansion of kinin paracopies. The "kinin core" (minimal active sequence) of tick kinins, FX1X2WGamide, is similar to insect sequences. A library of 14 small molecules, antagonists of mammalian neurokinin (NK) receptors, was screened using this endpoint assay and antagonists of NK receptors displayed selectivity (>10,000-fold) on the tick kinin receptor. Future approaches may accelerate kinin discoveries such as the identification of molecules for acaricide development (Xiong et al.).

Complete mitochondrial genomes of the bisexual and parthenogenetic populations were analyzed, and the expression of the mitochondrial protein-coding genes was evaluated. Single nucleotide polymorphism analysis showed that ∼200 bases were different, and the phylogenetic tree showed that the genetic distance between bisexual and parthenogenetic populations was lower than the subspecies. The expressions of the mitochondrial protein-coding genes, at different feeding stages of the bisexual and parthenogenetic population, revealed differences in expression patterns, which suggest that they might trigger specific energy utilization mechanisms due to their different reproductive strategies (Wang et al.).

Resistance to tick infestation by a vertebrate host reduces the chances of pathogen transmission (Lew-Tabor et al., 2017). Demonstrations of cellular and molecular mechanism underlying tick-resistance is also important for the development of an anti-tick vaccine. In a review article, the history on tick-resistance overviewed the recent findings, particularly the role of basophils in the tick-resistance manifestation. Basophil accumulation has been observed at the tick re-infestation site, even though the frequency of basophils among cellular infiltrates varies in different animal species. Skin-resident memory CD4+ T cells contribute to the recruitment of basophils to the tick re-infestation site through production of IL-3 in mice. Depletion of basophils before the tick re-infestation abolishes tick-resistance, demonstrating the crucial role of basophils in tick-resistance. The activation of basophils via IgE and its receptor FcεRI is essential, and histamine released from activated basophils functions as an important effector molecule in murine tick-resistance. First, tick infestation triggers the production of IgE against saliva antigens in the host, and blood-circulating basophils bind such IgE on the cell surface via FcεRI. In the second infestation, IgE-armed basophils are recruited to the tick-feeding sites and are activated by tick saliva antigens to release histamine that promotes epidermal hyperplasia, contributing to tick resistance (Karasuyama et al.).

Various approaches have been developed to obtain an effective vaccine against *R. microplus* and other ticks. The glycoprotein BM86, a tick gut epithelial cell protein, became the first commercial vaccine against tick infestation. However, this vaccine demonstrates quite variable efficacy and does not confer enough protection against several tick populations. Developing an anti-tick vaccine consisting of one or more common tick antigens, capable of triggering protective immune responses against heterologous tick challenges, would be economically and technically attractive. Additionally, elucidating the role of tick molecules may be a promising avenue for new approaches to developing therapeutic applications (Artigas-Jerónimo, Estrada-Peña et al.). A Vaccinomics based study, presented in an original research article, showed that recombinant ferritin 2 from *I. ricinus* (IrFER2) and tick protein extract (TPE) consisting of soluble proteins from the internal organs of partially fed *I. ricinus* females, conferred a strong immune response in calves and significantly reduced the feeding success of both nymphs and adults (Knorr et al.).

It has been suggested that a cocktail of candidate antigens might be more effective for the development of an effective tick vaccine (Parizi et al., 2012). Two *I. ricinus* proteins, heme lipoprotein and an uncharacterized secreted protein, and five *Dermacentor reticulatus* proteins, a glypican-like protein, secreted protein involved in homophilic cell adhesion, sulfate/anion exchanger, signal peptidase complex subunit 3, and uncharacterized secreted protein proteins, were identified as the most effective protective antigens resulting in vaccines that affect multiple tick developmental stages. The combination of some of these antigens might increase vaccine efficacy through antigen synergy for the control of tick infestations and may potentially affect pathogen infection and transmission (Contreras et al.).

Interfering in tick reproduction is an interesting target for the development of new methods for tick control, since ticks have fast reproduction rates and a large number of descendants. To maintain the tick embryo development during incubation, all supplements are derived from maternally derived nutrients. Therefore, the deposition of compounds in the egg occurs during egg formation and determine the success of embryo development and hatching. Since embryogenesis is a metabolically intensive process, the energy supplementation is vital for a perfect embryo development. The insulin signaling pathway regulates glucose homeostasis and protein kinase B (PKB, or AKT), glycogen synthase kinase 3 (GSK-3), and target of rapamycin (TOR) are key enzymes of this signaling pathway. Waltero et al. studied the

characterization of the TOR and two other downstream effectors, S6 kinase (S6K) and eukaryotic translation initiation factor 4E-binding protein 1 (4E-BP1), to determine the role of this enzyme in tick reproduction. Additionally, with the goal of identifying a useful target, Michael III et al. focused a detailed review on the knowledge of the molecular structure and functional role of the tick vitellogenin receptor. They related that inhibition of the expression of the receptor is possible to infer oocyte maturation, egg deposition, and pathogen transmission.

AUTHOR CONTRIBUTIONS

All authors listed have made a substantial, direct and intellectual contribution to the work, and approved it for publication.

FUNDING

This research was supported by NIH grant to AM (USA), CAPES and CNPq to IV (Brazil), and PSF and HEC to AA (Pakistan).

REFERENCES

Lew-Tabor, A. E., Ali, A., Rehman, G., Rocha-Garcia, G., Zangirolamo, A. F., Malardo, T., et al. (2017). Cattle tick *Rhipicephalus microplus*-host interface: a review of resistant and susceptible host responses. *Front. Cell Infect. Microbiol.* 7:506. doi: 10.3389/fcimb.2017.00506

Parizi, L. F., Reck, J., Oldiges, D. P., Guizzo, M. G., Seixas, A., Logullo, C., et al. (2012). Multi-antigenic vaccine against the cattle tick *Rhipicephalus (Boophilus) microplus*: a field evaluation. *Vaccine* 30, 6912–6917. doi: 10.1016/j.vaccine.2012.08.078

Conflict of Interest: The authors declare that the research was conducted in the absence of any commercial or financial relationships that could be construed as a potential conflict of interest.

frontiers in Physiology

REVIEW
published: 13 November 2018
doi: 10.3389/fphys.2018.01612

Functional Evolution of Subolesin/Akirin

*Sara Artigas-Jerónimo[1†], Margarita Villar[1†], Alejandro Cabezas-Cruz[2], James J. Valdés[3,4,5], Agustín Estrada-Peña[6], Pilar Alberdi[1] and José de la Fuente[1,7]**

[1] SaBio, Instituto de Investigación en Recursos Cinegéticos (IREC), CSIC, Universidad de Castilla-La Mancha (UCLM), Junta de Comunidades de Castilla – La Mancha (JCCM), Ciudad Real, Spain, [2] UMR BIPAR, INRA, ANSES, Ecole Nationale Vétérinaire d'Alfort, Université Paris-Est, Paris, France, [3] Faculty of Science, University of South Bohemia, České Budějovice, Czechia, [4] Institute of Parasitology, Biology Centre, Czech Academy of Sciences, České Budějovice, Czechia, [5] Department of Virology, Veterinary Research Institute, Brno, Czechia, [6] Facultad de Veterinaria, Universidad de Zaragoza, Zaragoza, Spain, [7] Department of Veterinary Pathobiology, Center for Veterinary Health Sciences, Oklahoma State University, Stillwater, OK, United States

The Subolesin/Akirin constitutes a good model for the study of functional evolution because these proteins have been conserved throughout the metazoan and play a role in the regulation of different biological processes. Here, we investigated the evolutionary history of Subolesin/Akirin with recent results on their structure, protein-protein interactions and function in different species to provide insights into the functional evolution of these regulatory proteins, and their potential as vaccine antigens for the control of ectoparasite infestations and pathogen infection. The results suggest that Subolesin/Akirin evolved conserving not only its sequence and structure, but also its function and role in cell interactome and regulome in response to pathogen infection and other biological processes. This functional conservation provides a platform for further characterization of the function of these regulatory proteins, and how their evolution can meet species-specific demands. Furthermore, the conserved functional evolution of Subolesin/Akirin correlates with the protective capacity shown by these proteins in vaccine formulations for the control of different arthropod and pathogen species. These results encourage further research to characterize the structure and function of these proteins, and to develop new vaccine formulations by combining Subolesin/Akirin with interacting proteins for the control of multiple ectoparasite infestations and pathogen infection.

Keywords: immune response, vaccine, interactome, regulome, phylogeny, tick, *Anaplasma phagocytophilum*

OPEN ACCESS

Edited by:
Itabajara Da Silva Vaz Jr., Universidade Federal do Rio Grande do Sul (UFRGS), Brazil

Reviewed by:
Sukanya Narasimhan, Yale University, United States
Carlos Alexandre Sanchez Ferreira, Pontifícia Universidade Católica do Rio Grande do Sul, Brazil

***Correspondence:**
José de la Fuente
jose_delafuente@yahoo.com

[†]These authors have contributed equally to this work

Specialty section:
This article was submitted to Invertebrate Physiology, a section of the journal Frontiers in Physiology

Received: *03 July 2018*
Accepted: *25 October 2018*
Published: *13 November 2018*

Citation:
Artigas-Jerónimo S, Villar M, Cabezas-Cruz A, Valdés JJ, Estrada-Peña A, Alberdi P and de la Fuente J (2018) Functional Evolution of Subolesin/Akirin. Front. Physiol. 9:1612. doi: 10.3389/fphys.2018.01612

INTRODUCTION

Akirin, from the Japanese "akiraka ni suru" meaning "making things clear," was first identified by Goto et al. (2008) as a key component of the immune deficiency (IMD) and Tumor necrosis factor (TNF)/Toll-like receptor (TLR)-nuclear factor-kappa B (NF-kB) (TNF/TLR) signaling pathways in *Drosophila melanogaster* and *Mus musculus*, respectively. However, previous reports identified *akirin* as a gene involved in developmental processes in flies (Peña-Rangel et al., 2002; DasGupta et al., 2005). Subolesin, from the Latin "suboles" meaning "progeny," was first reported in 2003 with its discovery as the candidate protective antigen 4D8 by expression library immunization in *Ixodes scapularis* (Almazán et al., 2003).

Gene orthology is a key concept in functional evolution (Koonin, 2005). Orthologs genes, defined as derived from a single ancestral gene that diverged during speciation, usually perform equivalent or identical functions, while paralogs that originated after gene duplication are considered to have more divergent functions (Koonin, 2005; Adipietro et al., 2012). Studies at genome level have identified many orthologs genes between divergent species, but the functional equivalency of the proteins encoded by these genes has not been fully characterized (Koonin, 2005).

Subolesin/Akirin are encoded by orthologs evolutionarily conserved throughout the metazoan that play a role in the regulation of different biological processes including immune response (de la Fuente et al., 2006a; Beutler and Moresco, 2008; Goto et al., 2008; Galindo et al., 2009; Macqueen, 2009; Macqueen and Johnston, 2009; Wan and Lenardo, 2010). Two *akirin* paralogs encoding Akirin1 and Akirin2 have been identified in vertebrates, but the functional homolog for invertebrate Subolesin/Akirin appears to be Akirin2 ortholog (Beutler and Moresco, 2008; Goto et al., 2008; Galindo et al., 2009; Macqueen and Johnston, 2009).

Understanding the function of the cell interactome (protein-protein physical and functional interactions) and regulome (transcription factors-target genes interactions) in response to infection is critical toward a better understanding of host-pathogen interactions and the identification of potential targets for new interventions for the prevention and control of tick infestations and tick-borne diseases (Rioualen et al., 2017; de la Fuente, 2018). Subolesin/Akirin are involved in both cell interactome and regulome, and constitute a good model for the study of the functional evolution of these processes in response to infection. In this review, we integrated the evolutionary history of Subolesin/Akirin with recent results on their structure and function in different species to provide insights into the functional evolution of these regulatory proteins, and their potential as vaccine antigens for the control of ectoparasite infestations and pathogen infection.

EVOLUTION OF SUBOLESIN/AKIRIN

The phylogenetic analysis of *subolesin*/*akirin* coding sequences using an updated sequence database (**Figure 1A** and **Supplementary Figure S1**) expanded the information on the evolution of these genes, and supported the results reported previously by Macqueen and Johnston (2009) that *akirin1* and *akirin2* are vertebrate-specific paralogs that form a separate clade from invertebrate *subolesin*/*akirin*. In some vertebrate species, Akirins constitute a family of paralog proteins that probably originated as a result of whole-genome duplications (Macqueen and Johnston, 2009; Macqueen et al., 2010a,b; Liu et al., 2015). After *akirin* duplication, *akirin1* evolved faster than *akirin2*, the ortholog of tick *subolesin* (**Figure 1A**; Macqueen and Johnston, 2009). Furthermore, the loss of some *akirin* paralogs may have also occurred after genome duplications (Macqueen et al., 2010b; Liu et al., 2015). For example, the *subolesin/akirin* gene family consists of a single member in invertebrates (*subolesin/akirin*), birds and reptiles (*subolesin/akirin2*), two members in amphibians and mammals (*akirin1* and *akirin2*), two to three members in teleosts, and more than three members in Salmonidae (Macqueen et al., 2010a,b; Liu et al., 2015).

The phylogenetic analysis of *subolesin* gene sequences was performed in 42 species belonging to 6 and 1 genera of hard (family Ixodidae) and soft (family Argasidae) ticks, respectively. The analysis corroborated previous results showing a reductive evolution in protein length (de la Fuente et al., 2006a; **Figure 1B**). The Subolesin amino acid (aa) sequence evolved from 173 to 184 aa in *Ornithodoros*, *Ixodes* and *Haemaphysalis* spp. to 161 aa in *Rhipicephalus* spp. (**Figure 1B**). It is generally accepted that evolution proceeds toward greater complexity at both the organismal and genomic levels. However, numerous examples of reductive evolution of parasites and symbionts have been described to challenge this notion (Wolf and Koonin, 2013). Wolf and Koonin (2013) proposed that quantitatively, the evolution of genomes appears to be dominated by reduction and simplification, punctuated by episodes of complexification. The reductive evolution process has been particularly documented in genomes that replicate within the domain of a host genome (Andersson and Kurland, 1998; Driscoll et al., 2017), but it has also been proposed to be involved in the origin of bacteria from eukaryotes (Staley, 2017). In arthropods, reductive evolution has been implicated in the evolutionary origin of other proteins such as type IV classical cadherins (Sasaki et al., 2017).

The protein length is subjected to systematic variation that relates to the cellular context in which it functions (Wang et al., 2011). For growth rate-optimized cells, the reduction in protein length constitutes an advantage by increasing their mass-normalized kinetic efficiencies (Ehrenberg and Kurland, 1984; Kurland et al., 2007; Wang et al., 2011). Consequently, shorter proteins that retain maximum functional rates are expected to support faster cell growth rates than longer proteins with similar kinetic characteristics. Wang et al. (2011) proposed the use of the terms "domain" and "linker" to refer to protein folded domains and nondomain regions, respectively. Proteins with nondomain sequences are proteins intrinsically unstructured or natively unfolded that lack a stable tertiary structure but have a dynamic range of conformations (Orengo and Thornton, 2005). These proteins appear to be more abundant in eukaryotes when compared to prokaryotes and are usually involved in binding and molecular recognition (Brown et al., 2011). Subolesin/Akirin were characterized as a linker with three predicted disordered nondomain regions that resulted in unstructured proteins (Prudencio et al., 2010; see also below). These results agreed with the findings of Wang et al. (2011) that the evolutionary reductive constraints on protein lengths are preferentially expressed in linker sequences.

It is difficult to establish a comprehensive record of ticks developmental rates because most of the experiments in previously published papers have been done at different regimes of temperature, relative humidity and photoperiod, all factors affecting the time in which ticks complete each developmental stage. However, data compiled by Hoogstraal (1956), Morel (2003) and Horak et al. (2018) under similar

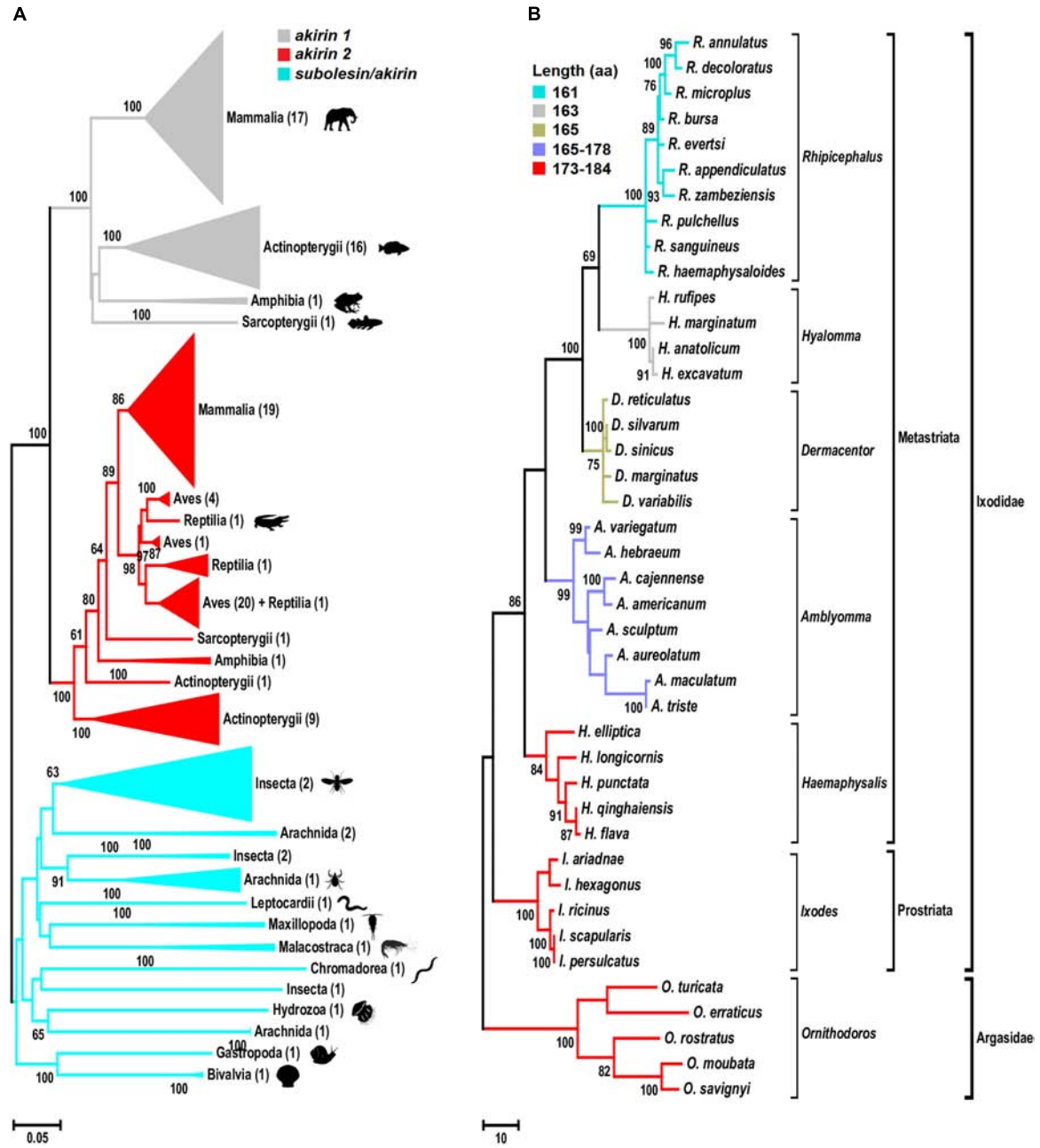

FIGURE 1 | Phylogenetic analysis of *akirin* and *subolesin* nucleotide sequences. **(A)** A Neighbor Joining (NJ) phylogenetic tree was constructed with 361 nucleotide sequences belonging to 152 families, 73 orders and 15 classes (Mammalia, Actinopterygii, Amphibia, Sarcopterygii, Aves, Reptilia, Arachnida, Malacostraca, Insecta, Leptocardii, Maxillopoda, Chromadorea, Hydrozoa, Gastropoda and Bivalvia) of animals. All branches were collapsed at the class level and the number of orders per cluster is shown inside brackets. GenBank accession numbers and species names are provided in **Supplementary Figure S1**. Sequences were aligned using MAFFT configured for the maximum accuracy (Katoh and Standley, 2013). The final alignment contained 303 gap-free sites. All ambiguous positions were removed for each sequence pair. The best-fit model of the sequence evolution was selected based on Corrected Akaike Information Criterion (cAIC) and Bayesian Information Criterion (BIC) implemented in Molecular Evolutionary Genetics Analysis (MEGA) version 7. The Kimura 2-parameter model, which showed the lowest values of cAIC and BIC, was chosen for tree reconstruction. The evolutionary history was inferred using the NJ method implemented in MEGA 7 (Kumar et al., 2016). The percentage of replicate trees in which the associated taxa clustered together in the bootstrap test (500 replicates) is shown next to the branches (Felsenstein, 1985). **(B)** Phylogenetic tree of tick *subolesin* sequences. A Maximum Parsimony (MP) phylogenetic tree was constructed with 42 nucleotide sequences belonging to 6 and 1 genera of hard (family Ixodidae) and soft (family Argasidae) ticks, respectively. Because the evolution of *subolesin* in ticks has been less studied when compared to akirins, MP was used to generate a robust hypothesis on the evolution of this molecule in ticks. Sequences were aligned using MAFFT configured for the maximum accuracy (Katoh and Standley, 2013). Then, using the MAFFT alignment as template, a condon aligment was build (HIV database; www.hiv.lanl.gov accessed on 29-12-2017). The final alignment contained 576 total sites of which 329 were gap-free. The evolutionary history was inferred using the MP method

(Continued)

FIGURE 1 | Continued
implemented in Molecular Evolutionary Genetics Analysis (MEGA) version 7 (Kumar et al., 2016). The percentage of replicate trees in which the associated taxa clustered together in the bootstrap test (500 replicates) is shown next to the branches (Felsenstein, 1985). The MP tree was obtained using the Subtree-Pruning-Regrafting (SPR) algorithm with search level 1 in which the initial trees were obtained by the random addition of sequences (10 replicates). Sequences were collected from Genbank and transcriptome projects and accession numbers are as follow: *Ixodes scapularis* (AY652654), *I. persulcatus* (KM888876), *I. ricinus* (JX193817), *I. ariadnae* (KM455971), *I. hexagonus* (JX193818), *Rhipicephalus evertsi* (JX193846), *R. appendiculatus* (DQ159967), *R. microplus* (EU301808), *R. sanguineus* (JX193845), *R. haemaphysaloides* (KP677498), *R. annulatus* (JX193844), *R. decoloratus* (JX193843), *R. zambeziensis* (GFPF01005851), *R. bursa* (GFZJ01017781), *R. pulchellus* (GACK01006228), *Dermacentor silvarum* (JX856138), *D. sinicus* (KM115649), *D. marginatus* (KU973622), *D. variabilis* (AY652657), *D. reticulatus* (JX193847), *Amblyomma variegatum* (JX193824), *A. hebraeum* (EU262598), *A. cajennense* (JX193823), *A. americanum* (JX193819), *A. maculatum* (JX193825), *A. aureolatum* (GFAC01005925), *A. triste* (GBBM01002796), *A. sculptum* (GFAA01000261), *Hyalomma anatolicum* (KT981976), *H. rufipes* (JX193849, *H. marginatum* (DQ159971), *H. excavatum* (GEFH01000904), *Haemaphysalis longicornis* (EU289292), *Hae. elliptica* (JX193850), *Hae. qinghaiensis* (EU326281, *Hae. flava* (KJ829652), *Hae. punctata* (DQ159972), *Ornithodoros moubata* (JX193852), *O. savignyi* (JX193851), *O. turicata* (GDIE01114362), *O. erraticus* (HM622148) and *O. rostratus* (GCJJ01005500).

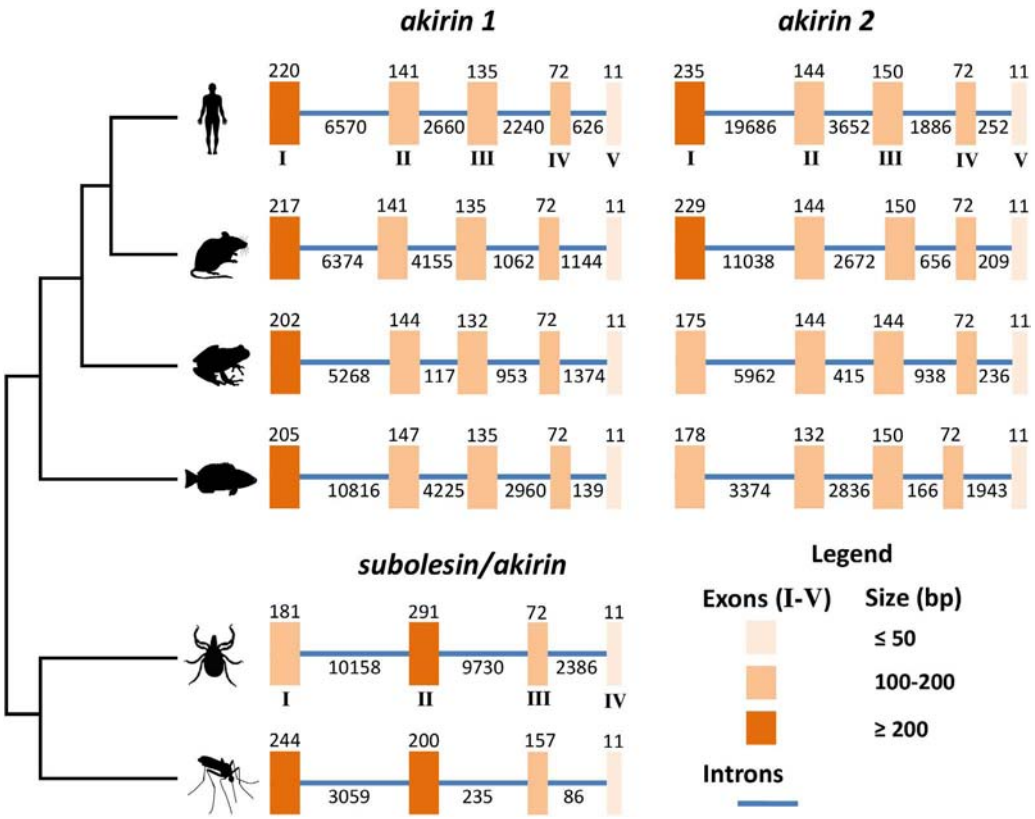

FIGURE 2 | Genomic organization of *subolesin/akirin* orthologs across selected eukaryotic species. The genomic organization of the coding regions of tick (*I. scapularis*), human (*Homo sapiens*), mouse (*M. musculus*), frog (*Xenopus laevis*), fish (*Danio rerio*) and mosquito (*Anopheles gambiae*) *subolesin/akirin* is shown. The genomic organization of human, mouse, frog and fish *akirins* was previously reported (Liu et al., 2015). The genomic organization of tick and mosquito *subolesin/akirin* was collected from VectorBase (https://www.vectorbase.org; Giraldo-Calderón et al., 2015). Latin numerals correspond to the size of exons/introns in base pairs.

conditions established that in the range of 24–28°C, ticks of the genera *Hyalomma* and *Rhipicephalus* complete their life cycle in about 33% less time than ticks of the genera *Ixodes* or *Amblyomma*. The *Hyalomma* and *Rhipicephalus* spp. are considered the two most recent genera of ticks, while *Ixodes* spp. and *Amblyomma* are among the most ancient splits of tick lineages (Mans et al., 2016; **Figure 1B**). Therefore, it is possible that the reductive evolution of Subolesin is associated with faster developmental rates in *Rhipicephalus* and *Hyalomma* spp. when compared to more ancient tick species even if they are sympatric. The faster developmental rate in recently evolved tick species may be associated with increasing cell growth rates that have been associated with reductive evolution (Wang et al., 2011). However, the complete association between existing data about developmental rates and evolutionary features of ticks requires further research.

At the genome level, *subolesin*/*akirin* exon-intron architecture shows a clear evolutionary pattern (**Figure 2**). As shown for *subolesin*/*akirin* coding sequences (**Figure 1A**), the vertebrate-specific paralogs form a separate clade from invertebrate genes

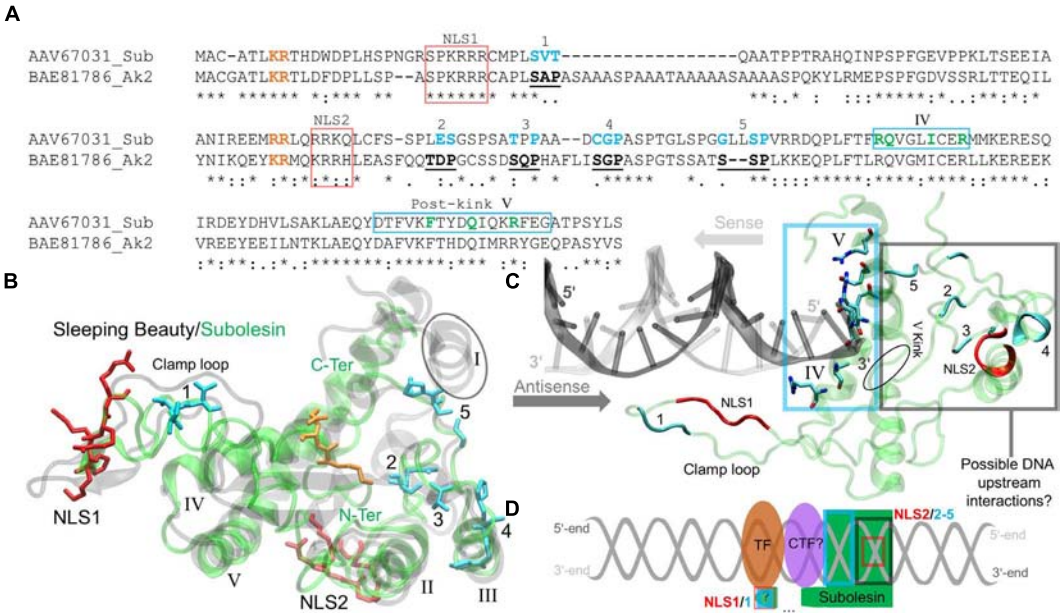

FIGURE 3 | The *I. scapularis* Subolesin structure and its interactions with DNA and transcription factors. **(A)** The pairwise sequence alignment of the *I. scapularis* Subolesin (Sub) and the rat Arkinin2 (Ak2), accession numbers indicated, was generated using the MAFFT alignment program at default settings (Katoh et al., 2017). The NLS 1 and 2 domains (red box), binding sites 1-5 (bold-underlined in Ak2 and cyan for Sub), and the novel DNA binding sites (green and enclosed in a cyan box) are shown. The residues color-coded orange are extensions of the NLS domains. **(B)** The superposed tertiary structures of Sleeping Beauty (transparent black) and Subolesin (transparent green) are represented with the clamp loop labeled and the five α-helices of Sleeping Beauty (PDB: 5CR4) annotated in roman numerals. The tertiary residue positions of the labeled Subolesin NLS domains and binding sites are, respectively, color-coded as in the pairwise alignment. The Subolesin termini positions are color-labeled (green). **(C)** The Subolesin-DNA complex, modeled from the Mos1-DNA (PDB: 3HOS) show the residues of the novel DNA-binding site on α-helices IV-V, enclosed by a cyan box that were predicted by I-TASSER (Zhang, 2008). The DNA prime ends are color-labeled for the respective directions (indicated by arrows) of the sense (gray) and antisense (dark gray) strands. The residue positions of the Subolesin clamp loop, NLS domains and binding sites are color-coded as in previous panels A and B. **(D)** The schematic representation of the upstream DNA (gray helix) interactions with Subolesin NLS2, binding sites 2-5, and the potential clamp loop interaction (via NLS1 and binding site 1) with an unknown co-transcription factor (CTF?) and unknown (?) transcription factor (TF).

(**Figure 2**). The *subolesin*/*akirin* genes evolved from 4 exons in invertebrates to 5 exons in vertebrates. The exon sizes showed a pattern of larger to shorter for vertebrate *akirin1* exons I to V and mosquito *akirin* exons I to IV (**Figure 2**). However, for tick *subolesin* and vertebrate *akirin2* genes, the size of exons II and III, respectively, were larger or similar than that of preceding exon (**Figure 2**). Furthermore, while the length of 11 nucleotides (nt) in the last exon was conserved across evolution, the length of the penultimate exon evolved from 157 nt in mosquitoes to 72 nt in ticks and vertebrates (**Figure 2**). However, the length of the exon-intron sequence increased from 3,992 nt in mosquitoes to 22,829 nt in ticks and then decreased to 8,862 nt in fish to increase back again to 26,088 nt in humans (**Figure 2**). These results do not correlate with genome sizes of these organisms (Gregory, 2005), and may originated from still unknown evolutionary events.

SUBOLESIN/AKIRIN STRUCTURE AND ITS INTERACTIONS WITH DNA AND TRANSCRIPTION FACTORS

Akirins are involved in cellular processes that are regulated by specific domains and binding sites. The rat Akirin2 (or 14-3-3β Interactant 1) described by Komiya et al. (2008) is 48% identical to the *I. scapularis* Subolesin and was previously used to identify the conserved Akirin nuclear localization signal (NLS) domains and its binding sites (Macqueen and Johnston, 2009). The pairwise sequence alignment shows that both NLS domains of the rat Akirin2 are conserved in Subolesin, but with variations in a few binding sites (**Figure 3A**). Subolesin binding sites 1 and 4 are similar to Akirin2 with Subolesin binding sites 2 and 3 each possessing a single substitution. The Subolesin binding site 5, however, has a double Leu insertion when compared to Akirin2 (**Figure 3A**). Currently there are no resolved Subolesin/Akirin structures and standard sequence-based bioinformatics methods lack parameters for locating structural homologs in the Protein Databank (PDB). Therefore, several logical steps were taken to correctly model the *I. scapularis* Subolesin. The Subolesin sequence (**Figure 3A**) was initially submitted to I-TASSER (Zhang, 2008), a protein multiple threading algorithm that is considered a top competitor in the Critical Assessment of Structure Prediction[1]. The I-TASSER algorithm resulted in five distinct Subolesin models that were then individually submitted to the DALI server (Holm and Laakso, 2016) for identifying PDB structural homologs of similar length with minimalα-carbon backbone deviations between the two global structures. Since

[1]http://predictioncenter.org

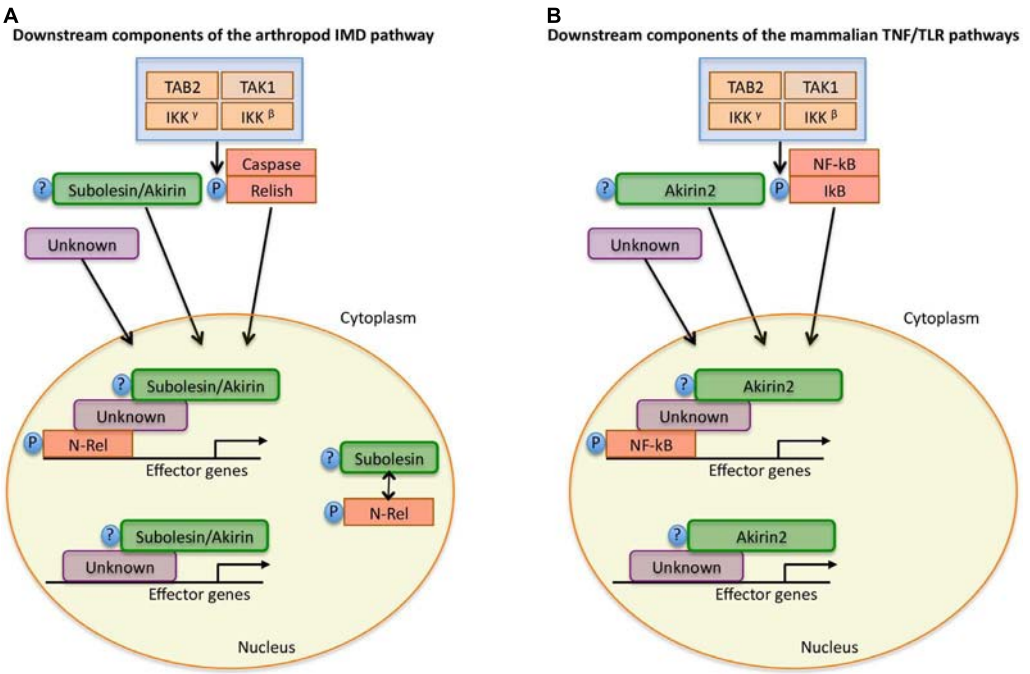

FIGURE 4 | Model for Subolesin/Akirin function in immune response pathways. A simplified annotation of the downstream components of the arthropod IMD and mammalian TNF/TLR pathways (Goto et al., 2008; Beutler and Moresco, 2008; de la Fuente et al., 2008; Naranjo et al., 2013; Shaw et al., 2017). **(A)** After activation of the arthropod IMD pathway, the TGF-β (TAK1), Tak1-binding protein 2 (TAB2) and the I-KB kinase (IKK) complex are recruited, which leads to phosphorylation of the NF-κB transcription factor, Relish. After phosphorylation, the N-terminal domain of Relish (N-Rel) is cleaved by Caspase-8 homolog Dredd or a similar Caspase and is translocated to the nucleus. Subolesin/Akirin may be post-translationally modified and translocated to the nucleus. In the nucleus, N-Rel interacts with Subolesin/Akirin through unknown proteins to drive the production of anti-microbial peptides and other effector genes. In ticks, N-Rel and Subolesin may be reciprocally regulated. **(B)** In mammals, the activation of the TNF/TLR signaling pathways also results in the recruitment of the TAB2-TAK1 and IKK complexes, which results in the phosphorylation of the inhibitory regulator of NF-kB, IkB, resulting in the NF-kB translocation to the nucleus. As in arthropods, Akirin2 may be post-translationally modified and translocated to the nucleus. Once in the nucleus, NF-kB interacts with Akirin2 through unknown proteins for the activation of gene expression. In both arthropods and mammals, Subolesin/Akirin are involved in the regulation of genes that are Relish/NF-kB independent.

Subolesin/Akirin are effectors of the IMD/TNF/TLR Relish/NF-kB signaling pathways (Goto et al., 2008; Naranjo et al., 2013), a match with homologous structures that potentially participate within these pathways was also a criterion in selecting an appropriate Subolesin model. This logical approach resulted in a Subolesin model homologous in structure, with only 7% residue conservation, to the genetically engineered catalytic domain of the transposase Sleeping Beauty (Ivics et al., 1997; Zanesi et al., 2013; **Figure 3B**).

As part of the *Tc1/mariner* transposon superfamily, the Sleeping Beauty transposase has been engineered for genetic screening studies, leading to the discovery of several genes activated by Sleeping Beauty transposon insertions that participate in the NF-kB signaling pathway (Zanesi et al., 2013). The Sleeping Beauty transposase sequence is composed of an N-terminus paired-like domain with a leucine zipper (∼90 residues long) and the C-terminus folds as the catalytic domain (Ivics et al., 1997). The catalytic domain of Sleeping Beauty was resolved with a DNA transposon end and modeled with a target DNA revealing the mechanism of hyperactive Sleeping Beauty mutation screening studies while discovering novel variants for future screenings (Voigt et al., 2016). The Sleeping Beauty crystal structure details that its catalytic domain has a global homology to Ribonuclease H (RNase H) (Voigt et al., 2016). The RNase H-like protein fold forms a catalytic triad (Asp-Asp-Glu) that coordinates metal ions involved in excision and insertions of DNA (Voigt et al., 2016). By resolving the Sleeping Beauty catalytic domain, Voigt et al. (2016) also discovered that the Gly-rich box (located on the clamp loop) is involved in protein-protein interactions, specifically with partnering monomers in the DNA complex. The conserved positions of the catalytic triad and the Gly-rich box, however, are not present in Subolesin/Akirin sequences.

Prior to acting in the *Tc1/mariner* transposon system, Sleeping Beauty must enter the nucleus. Passage to the nucleus is controlled by NLS domains that have a strong affinity to karyopherin/importin receptors, proteins responsible for transporting NLS-tagged "cargo" in and out of the nucleus via nuclear pores (Leung et al., 2003). The N-terminus of the Sleeping Beauty catalytic domain contains a NLS domain that is quite long (17 residues) and is actually a bipartite NLS (Ivics et al., 1997). A monopartite NLS domain has the formulation Lys-Lys/Arg-[X]-Lys-Lys/Arg, where [X] is any other (∼2) amino acids. A bipartite NLS domain has a linker sequence, where [X] is ∼10 residues long (Makkerh et al., 1996). Mutations of

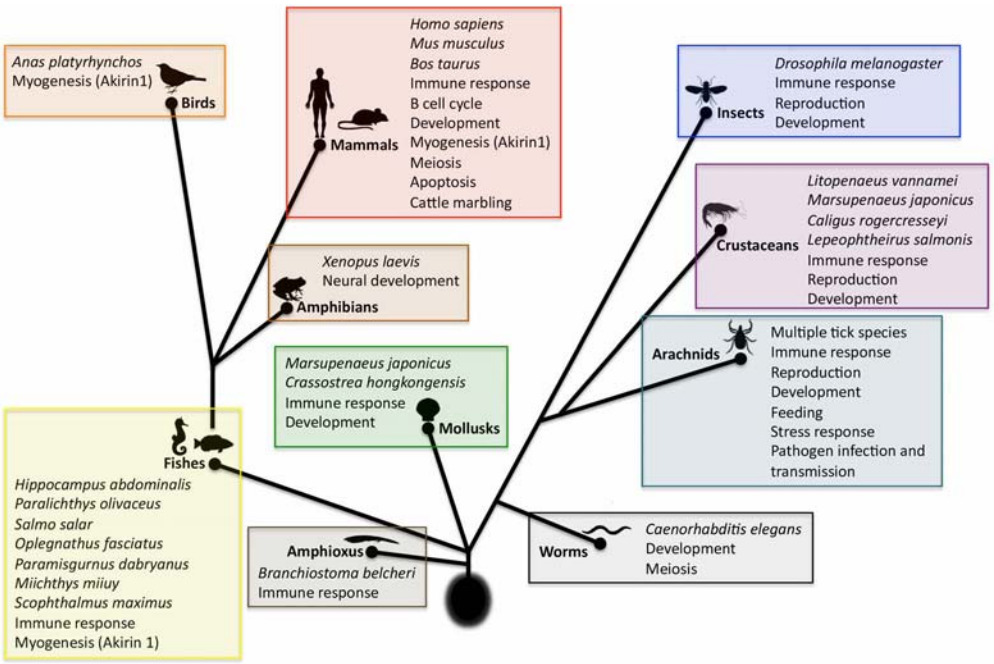

FIGURE 5 | Scheme of the evolution and function of Subolesin/Akirin | Functional annotations were done based on published results for Subolesin/Akirin2. References are in the text of the paper. Myogenesis, attributed exclusively to Akirin1, was included and labeled as such. For each taxa, species in which studies were conducted are shown.

these upstream NLS residues prior to the linker sequence [X] has shown to reduce protein entry into the nucleus (Dingwall et al., 1988), and inhibit NLS binding to karyopherin/importin receptors (Leung et al., 2003). These upstream, positively charged residue pairs are in the aligned sequences of **Figure 3A** (orange-labeled residues), indicating that Subolesin/Akirin2 NLS1 is bipartite. The two positively charged residues highlighted near NLS2 (**Figure 3A**) indicate that the NLS2 of Subolesin/Akirin is actually a longer monopartite domain. The modeled Subolesin structure has its NLS1 positioned on the clamp loop, which differs from Sleeping Beauty that is coordinated at the N-terminus α-helix (I) (**Figure 3B**). The Subolesin NLS2 domain, not present in the catalytic domain of Sleeping Beauty, is located on an α-helix (II) outside the central core of the protein. The absence of the catalytic triad of Sleeping Beauty (Voigt et al., 2016) and metal binding sites in Subolesin/Akirin support that these proteins do not act as a transposase. Additionally, the Subolesin/Akirin binding sites have long been recognized by mutation studies (Komiya et al., 2008), and Subolesin/Akirin RNA interference (RNAi) experiments have shown to disrupt the Relish signaling pathway (Goto et al., 2008; Naranjo et al., 2013). However, as discussed bellow, the Subolesin/Akirin interactome has not been fully characterized, and whether Subolesin/Akirin binding partners are only proteins or also include nucleic acids.

The superposed structures of Subolesin and Sleeping Beauty depict a global homology with a low α-carbon backbone deviation of 0.3 nm (**Figure 3B**). There are, however, missing and disordered secondary structures. The Sleeping Beauty catalytic domain has five β-sheets surrounded by five α-helices. As previously mentioned, the N-terminus α-helix I of Sleeping Beauty that contains its NLS domain is missing in the Subolesin model (encircled in **Figure 3B**), thereby shifting the Subolesin NLS1 domain to the clamp loop. Moreover, the β-sheets of Subolesin are highly disordered. Future experiments should resolve the stacking and conformations of the disordered Subolesin β-sheets by X-ray crystallography. Nevertheless, the remaining four α-helices (II-V) are structurally conserved, and the Subolesin/Akirin binding sites 2-5 are positioned on or approximating α-helix III (**Figure 3B**). As in the primary sequence (**Figure 3A**), the Subolesin/Akirin binding site 1 is structurally distant from the other sites, located on the N-terminus clamp loop near the position of NLS1 (**Figure 3B**). As a transposase, the clamp loop of the resolved Sleeping Beauty catalytic domain is not in its DNA-bound conformation. Therefore, Voigt et al. (2016) modeled the clamp loop after the DNA-bound transposase, Mos1, from *Drosophila mauritiana* (Richardson et al., 2009). The Mos1 also has poor sequence identity to Subolesin (<5%), but are structurally homologous with α-carbon backbone deviation of 0.34 nm. This led to a subsequent I-TASSER simulation using the template Mos1 as conducted by Voigt et al. (2016). The resulting model has Subolesin bound to a DNA duplex with an adequate clamp loop conformation that extends downstream the duplex (**Figure 3C**).

The Subolesin-DNA complex show several residues on α-helices IV and V that approximate the DNA 5′-end of the sense strand and the 3′-end of the antisense strand (**Figure 3C**).

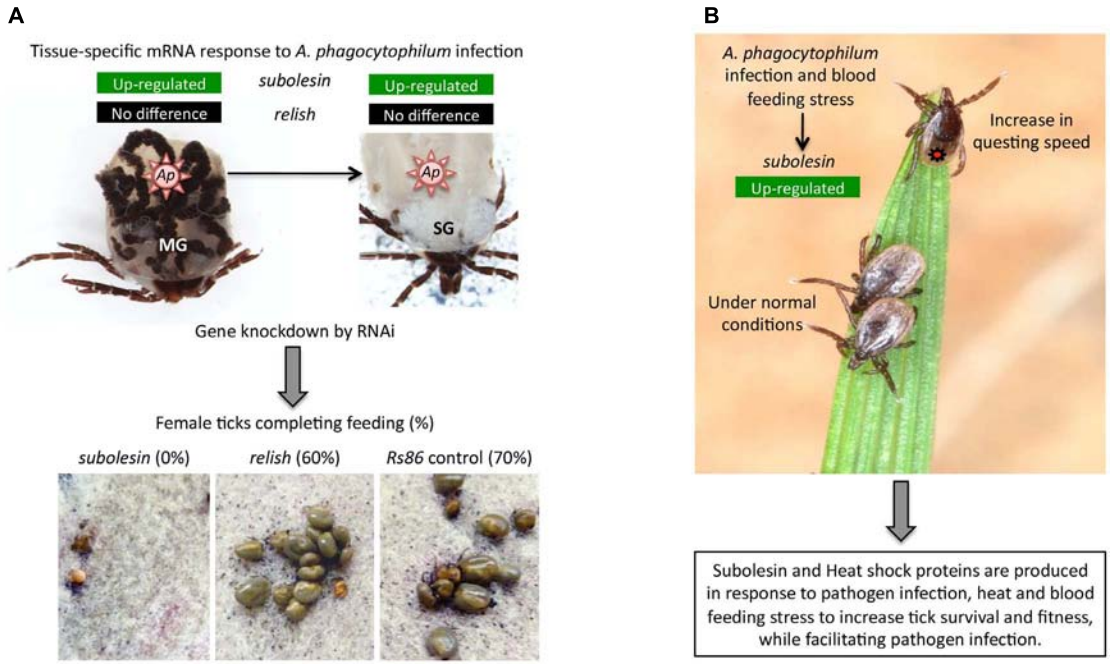

FIGURE 6 | Examples of the role of tick Subolesin in different biological processes | **(A)** Role of tick Subolesin in *A. phagocytophilum* infection and blood feeding. The transcriptomics analysis in different *I. scapularis* tick tissues showed that *subolesin* (ISCW023283) but not *relish* (ISCW018935) mRNA levels significantly increased in response to *A. phagocytophilum* (*Ap*) infection in both midgut (MG) and salivary glands (SG). In addition, the *subolesin* gene knockdown phenotype in ticks injected with dsRNA resulted in a significant reduction in the number of female ticks completing feeding, oviposition and fertility. Results were reported by Ayllón et al. (2015). Photo of dissected *I. scapularis* partially fed adult female ticks courtesy of K. M. Kocan (Oklahoma State University, United States). **(B)** Role of tick Subolesin in *A. phagocytophilum* infection, blood feeding and questing speed. The response to *A. phagocytophilum* and stress increases *subolesin* levels, which together with heat shock proteins improve tick questing speed and survival. Results were reported by Busby et al. (2012). Photo of questing *Ixodes ricinus* courtesy of L. Grubhoffer & J. Erhard (Biology Center of the AS CR, Institute of Parasitology, Czechia).

Four of the seven residues positioned on α-helix IV mainly interact with the phosphate backbone of the antisense strand. The remaining three residues that interact with both strands are after the pivotal kink of α-helix V (encircled in **Figure 3C**). The alignment in **Figure 3A** highlights these novel DNA-binding residues and indicates the α-helix on which they are positioned. The binding sites 2–5 and NLS2 are distal to the DNA interacting site, while the clamp loop containing NLS1 and binding site one is downstream the DNA duplex. Given the structural coordination of Subolesin bound to DNA (**Figure 3C**), binding sites 2–5 and NLS2 may interact with nucleotides upstream the DNA or with additional co-transcription factors (CTF) (**Figure 3D**). The transcription factors (TF) Relish/NF-kB form DNA-protein complexes with CTFs, and Subolesin is hypothesized to act as a CTF of Relish via an intermediate CTF (**Figure 3D** and described in the next section). Furthermore, the extended DNA downstream position of the Subolesin clamp loop with binding site one will hypothetically coordinate the CTF and possibly the TF (**Figure 3D**). If Subolesin is a CTF, how will it conform while the mRNA is being transcribed? Positively charged residues, specifically Lys, recognize RNA strands via electrostatic interactions (Law et al., 2006). Given conformational flexibility of the Subolesin clamp loop and the fact that it does not contain the Sleeping Beauty Gly-rich box, the proximity of positively charged Subolesin NLS1 domain residues downstream the DNA duplex may guide transcribing mRNAs for post-transcriptional processing.

FUNCTION OF SUBOLESIN/AKIRIN

The innate immune response acts as the first line of defense against pathogen infection in all metazoans, and constitutes the only immune response in invertebrates (Medzhitov et al., 1997; Shaw et al., 2017). It has been shown that invertebrate Subolesin/Akirin and vertebrate Akirin2 act in concert with Relish/NF-kB to induce the expression of a subset of downstream pathway elements in the IMD and TNF/TLR signaling pathways involved in the immune response to pathogen infection. This function of Subolesin/Akirin has been documented in ticks (de la Fuente et al., 2008, 2017a; Naranjo et al., 2013; Gulia-Nuss et al., 2016; Shaw et al., 2017), fruit fly (Beutler and Moresco, 2008; Goto et al., 2008; Wan and Lenardo, 2010; Bonnay et al., 2014), human (Goto et al., 2008), salmon (Macqueen et al., 2010b), shrimp (Hou et al., 2013), Japanese flounder (Yang et al., 2013), amphioxus (Yan et al., 2013), rock bream (Kasthuri et al., 2013), Chinese loach (Xue et al., 2014), Hong Kong oyster (Qu et al., 2014), turbot (Yang et al., 2011), sea louse (Valenzuela-Muñoz and Gallardo-Escárate, 2014), mouse

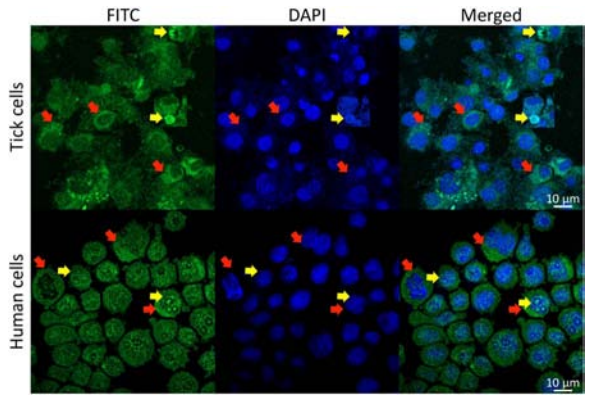

FIGURE 7 | Subcellular localization of Subolesin/Akirin2. Representative images of immunofluorescence analysis of *I. scapularis* ISE6 and human HL60 cells incubated with anti-Subolesin and anti-Akirin2 antibodies, respectively. The cells were fixed with 4% paraformaldehyde in PBS for 15 min, permeabilized with 0.5% Triton X-100 in PBS for 5 min and blocked with blocking buffer (3% BSA in PBS) for 1 h. Then, the cells were incubated overnight at 4°C with anti-Subolesin (Antunes et al., 2014) or anti-Akirin2 (Abcam, Cambridge, United Kingdom) antibodies (1/50 dilution in 3% BSA in PBS). After 3 washes with PBS, the slides were incubated with fluorescein isothiocyanate (FITC) conjugated anti-rabbit secondary antibodies (Sigma-Aldrich, St. Louis, MO, United States; green) at 1/160 dilution in 3% BSA in PBS for 1 h at room temperature. Cells were counterstained with ProLong Antifade containing 4′,6-diamidino-2-phenylindole (DAPI) (Molecular Probes, Eugene, OR, United States; blue), and imaged with a Zeiss LSM800 confocal microscope using a 63× oil immersion lens (Carl Zeiss, Oberkochen, Germany). Yellow arrows show examples of protein localization in the nucleus while red arrows illustrate protein localization in the cytoplasm.

(Beutler and Moresco, 2008; Goto et al., 2008; Wan and Lenardo, 2010; Tartey et al., 2015), croaker (Liu et al., 2015); shrimp (Liu Y. et al., 2016; Liu et al., 2016), and seahorse (Pavithiran et al., 2018; **Figures 4**, **5**).

Subolesin/Akirin are also involved in the Relish/NF-kB independent gene regulation (**Figure 4**), thus playing a role in various biological processes in addition to the immune response (**Figure 5**). These processes include animal reproduction and development, causing lethal embryonic or reduced growth phenotypes in knockout mice, fruit fly, ticks, and nematodes (Maeda et al., 2001; de la Fuente et al., 2006a; Goto et al., 2008; Carpio et al., 2013; Qu et al., 2014), metazoan myogenesis (Marshall et al., 2008; Salerno et al., 2009; Macqueen et al., 2010a; Mobley et al., 2014; Sun et al., 2016), *Xenopus* neural development (Liu et al., 2017), meiosis/carcinogenesis (Komiya et al., 2008; Macqueen et al., 2010b; Clemons et al., 2013), tick stress response, feeding, growth and reproduction (Almazán et al., 2003, 2005; de la Fuente et al., 2006a, 2008; Smith et al., 2009; Busby et al., 2012; Rahman et al., 2018), pathogen infection and transmission in ticks (de la Fuente et al., 2006b, 2016, 2017a; Zivkovic et al., 2010a,b; Busby et al., 2012; Hajdušek et al., 2013) and turbot (Yang et al., 2011), human glioblastoma cell apoptosis (Krossa et al., 2015), cattle marbling (Sasaki et al., 2009; Watanabe et al., 2011; Kim et al., 2013), and mouse mitogen-induced B cell cycle progression and humoral immune responses (Tartey et al., 2015). For example, as previously reported in *I. scapularis* and other tick species (de la Fuente and Kocan, 2006; de la Fuente et al., 2006a,b, 2011, 2013; Merino et al., 2013a; de la Fuente and Contreras, 2015), Subolesin appears to function in multiple biological processes such as tick response to infection, feeding, reproduction, development and stress response (**Figure 6**).

Akirin1 and Akirin2 have also different functions in vertebrates, which is illustrated by the role of Akirin1 in myogenesis while Akirin2 promotes meiosis/carcinogenesis (Macqueen and Johnston, 2009; Macqueen et al., 2010a,b; **Figure 4**). These different functions may be related to the Akirin subcellular localization. While Akirin1 is found in the nucleus, Subolesin/Akirin2 is located in both cytoplasm and nucleus (de la Fuente et al., 2011; Antunes et al., 2014; Krossa et al., 2015; Pavithiran et al., 2018; **Figure 7**). The subcellular localization of Subolesin/Akirin2 is probably related to its structure, which as discussed above contains NLS domains that are involved in protein transport in and out of the nucleus via nuclear pores (Leung et al., 2003).

In summary and based on current information, Subolesin/Akirin evolved with similar functions in both invertebrates and vertebrates (**Figure 5**). The annotation of some biological processes described in certain taxa only may be due to the presence of species-specific functions or more likely a consequence of the still incomplete characterization of Subolesin/Akirin function in the different species.

SUBOLESIN/AKIRIN ROLE IN CELL INTERACTOME AND REGULOME

Subolesin/Akirin are proteins without catalytic or DNA-binding capacity. How Subolesin/Akirin regulate gene expression is unknown but likely involve interactions with proteins with DNA-binding or chromatin-remodeling capacity (de la Fuente et al., 2008; Beutler and Moresco, 2008; Nowak and Baylies, 2012; Nowak et al., 2012; Naranjo et al., 2013). In this way, Subolesin/Akirin link the activities of transcription factors with those of chromatin remodeling complexes to influence gene expression in a context-dependent manner (Nowak and Baylies, 2012; Nowak et al., 2012). For example, Subolesin/Akirin and Akirin2 as key components of the innate immune response can directly or indirectly interact with other regulatory proteins such as "14-3-3" proteins, DNA methyltransferase-associated protein 1 (DMAP1) and the basic helix–loop–helix transcription factor (Twist) to up- or down-regulate transcription (Gonzalez and Baylies, 2005; Goto et al., 2008, 2014; Komiya et al., 2008; de la Fuente et al., 2008; Beutler and Moresco, 2008; Nowak et al., 2012; Naranjo et al., 2013; Tartey et al., 2014; Gulia-Nuss et al., 2016; Shaw et al., 2017).

The Subolesin/Akirin role in the cell interactome and regulome in response to different stimuli has not been characterized. Recently, we proposed a method based on the graph theory for the analysis of human and tick cell

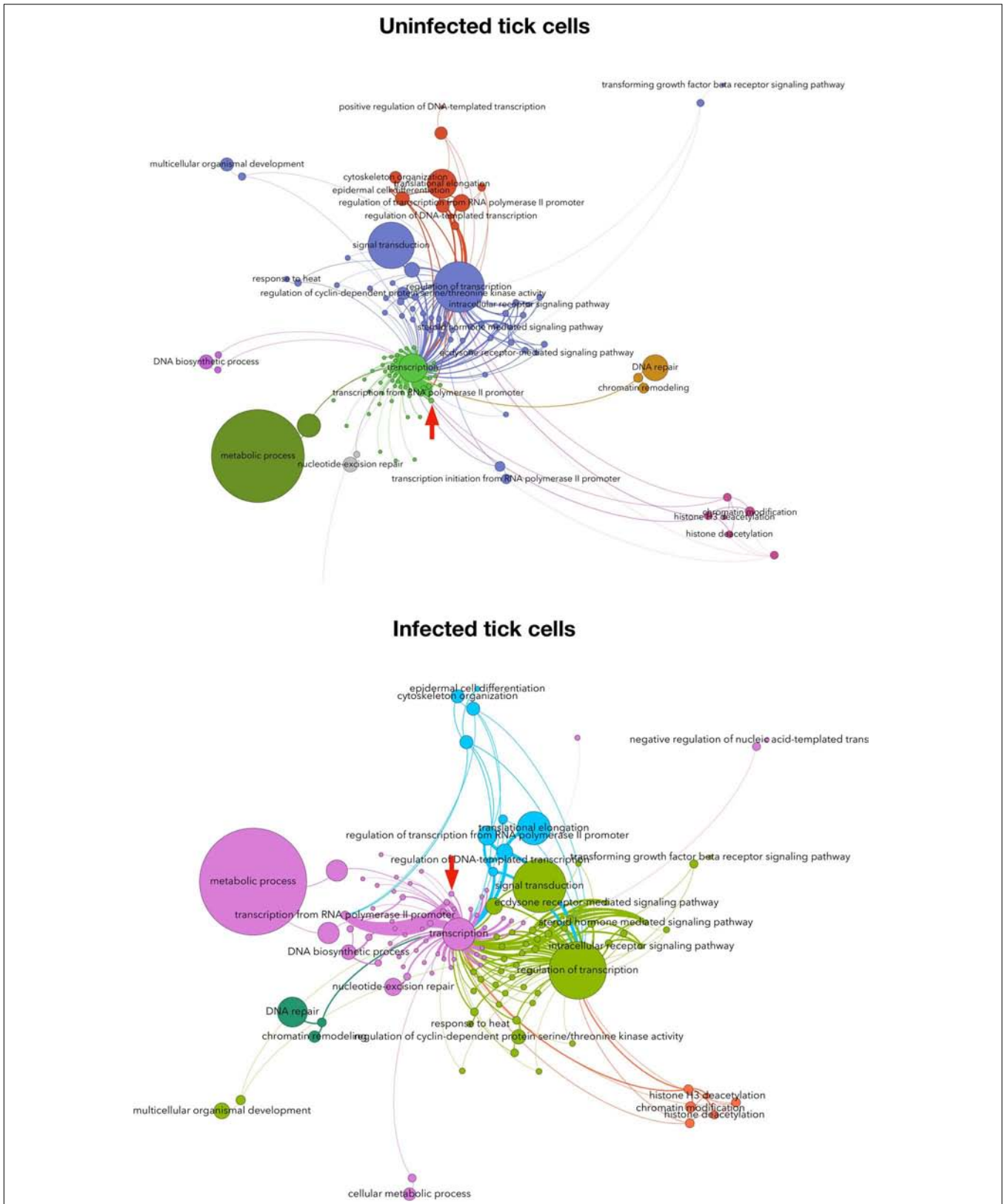

FIGURE 8 | Subolesin regulome in tick cells. The network of proteins and processes associated to transcription in tick cells uninfected and infected with *Anaplasma phagocytophilum*. The nodes (circles) are either proteins or processes (labeled). The size of each circle is proportional to its centrality index. The networks show

(Continued)

FIGURE 8 | Continued
clusters of interacting proteins and processes in colors. The width of each link is proportional to the strength of the interaction. The networks show the topology of the tick interactome and regulome. The networks were built with the annotated proteins represented in either uninfected or infected cells, and a directed network was built for each protein linked to the processes in which it is involved. The weight of each link is proportional to the number of reads of the protein. This weighted degree of each link was used to calculate the centrality indexes, mainly the Betweenness Centrality, which is represented in the panels. Only the proteins annotated as involved in processes associated with transcription (i.e., linked by one or more protein(s) simultaneously annotated as transcripiton or other cellular process). The topology of the networks was obtained with the Lovaine algorithm. In both networks, the topological position of Subolesin is marked with a red arrow. Methods were described in Estrada-Peña et al. (2018).

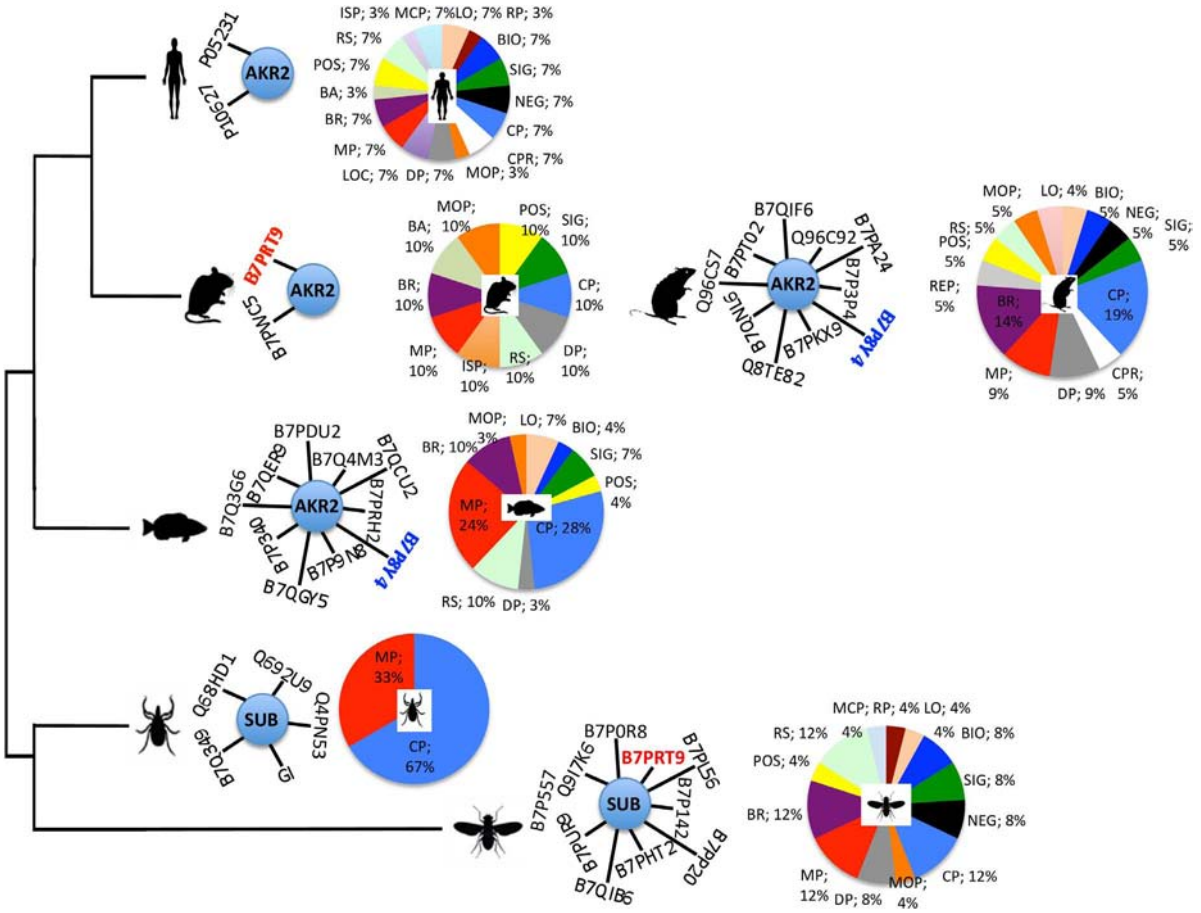

FIGURE 9 | Characterization of the Subolesin/Akirin2 interactome. The information on Subolesin/Akirin-protein physical and functional interactions was compiled from the String protein-protein interactions database v.10.5 (https://string-db.org). The central node of the networks represent Subolesin/Akirin2 while the edges correspond to the predicted functional associations. Only predictions with medium (or better) confidence (> 0.4) limited to the top 10 interactions with protein-protein interaction (PPI) enrichment p-value ≤ 0.5 were considered. To compare the different species, protein annotations were standardize by identity to *I. scapularis/I. ricinus-D. melanogaster-H. sapiens* order of priority (see **Supplementary Dataset S1** for complete annotations). For illustration purposes, the species included in the analysis correspond to *D. melanogaster*, *I. scapularis*, *Danio rerio*, *Mus musculus*, *Rattus norvegicus*, and *H. sapiens*. Identical proteins in two different species are highlighted in red and blue letters. The functional annotation of the Subolesin/Akirin2 interacting proteins according to the biological processes (level 2) in which they are involved was done using Blast2GO (www.blast2go.com), and represented in pies with different colors for each process and the percentage of proteins on each process. Abbreviations: LO, localization (sepia); RP, rhythmic process (sangria); BIO, biogenesis (blue); SIG, signaling (green); NEG, negative regulation of biological process (black); CP, cellular process (azure); CPR, cell proliferation (white); MCP, multi-organism process (sky); DP, developmental process (gray); LOC, locomotion (violet); MP, metabolic process (red); BR, biological regulation (byzantine); BA, biological adhesion (moss); POS, positive regulation of biological process (yellow); RS, response to stimulus (tea); ISP, immune system process (gold); MOP, multicellular organismal process (orange); REP, reproductive process (smoke). Color code was established according to color thesaurus (https://graf1x.com/list-of-colors-with-color-names/).

proteome in response to *A. phagocytophilum* infection (Estrada-Peña et al., 2018). This approach resulted in a network of interacting proteins and cell processes clustered in biological pathways, and ranked with indexes representing the topology of the proteome influenced by features of the interactome and regulome. The results evidenced differences in the response to *A. phagocytophilum* infection between human and tick cells, and supported that human neutrophils but not tick cells

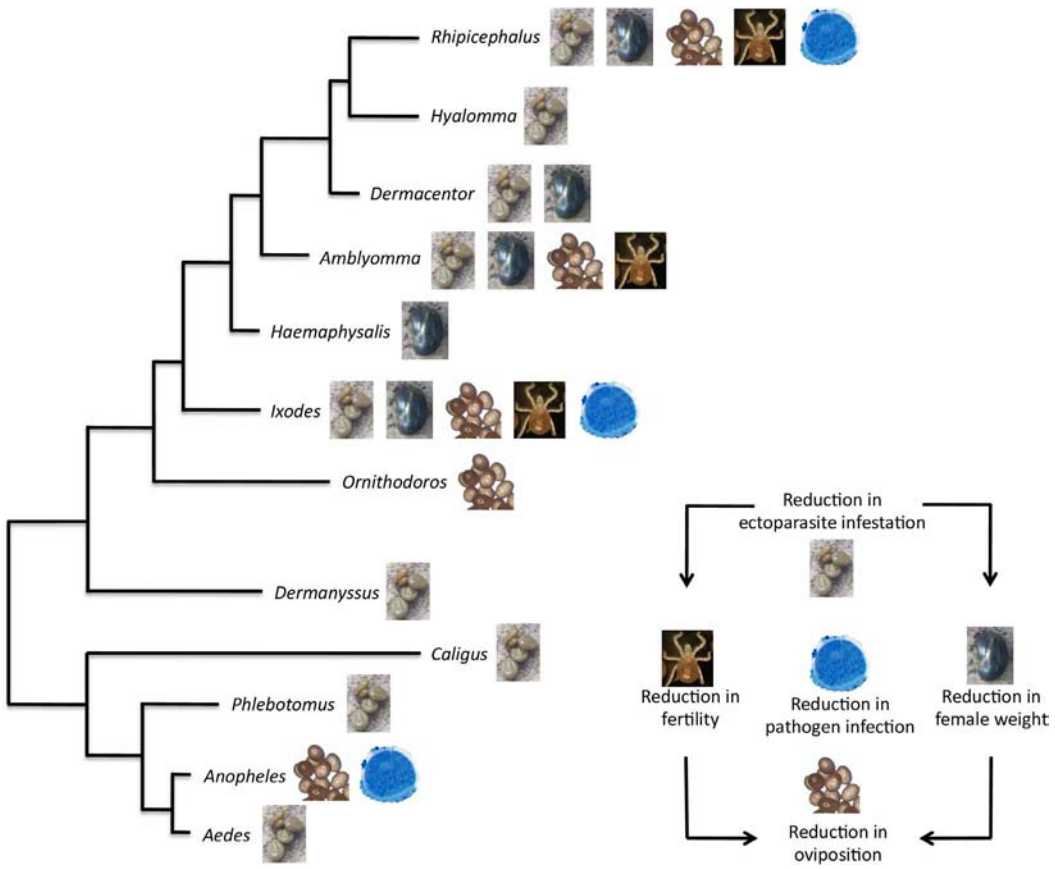

FIGURE 10 | Protective capacity of Subolesin/Akirin in vaccines for the control of arthropod ectoparasite infestations and pathogen infection. The effect of Subolesin/Akirin vaccination is shown on evolutionarily diverse arthropod genera. The effect of the vaccine was recorded on different phases of ectoparasite life cycle in the form of reduction in ectoparasite infestation (number of ectoparasites completing feeding), weight (weight of engorged female ectoparasites), oviposition (number of eggs per female), and fertility (number of larvae per female) in ectoparasites fed on vaccinated hosts when compared to controls. The reduction in pathogen infection was recorded as differences in pathogen levels between ectoparasites fed on vaccinated and control hosts.

limit pathogen infection through differential representation of ras-related proteins (Estrada-Peña et al., 2018). Herein, this method was applied to predict the position of Subolesin in the regulome of tick cells and in response to *A. phagocytophilum* infection (**Figure 8**). The results showed that Subolesin is deeply involved in the core of transcription processes but also in other secondary processes such as transcription from RNA polymerase II promoter, DNA repair, and chromatin remodeling (**Figure 8**). Furthermore, other processes that change in infected cells when compared to uninfected cells (i.e., signal transduction, regulation of transcription, and response to heat) are deeply linked to the central transcription process. The putative Subolesin role in these processes varied between infected and uninfected cells (the width of the lines is proportional to the importance of the link between proteins and processes; **Figure 8**). For example, it appears that particularly in infected cells other proteins but Subolesin have a more prominent role in the strong protein link with transcription and transcription from RNA polymerase II promoter processes (**Figure 8**). These results predict the role that Subolesin plays in the regulation of different biological processes, and its differential role in response to *A. phagocytophilum* infection in tick cells. However, the lack of a more prominent role for Subolesin may respond to the fact that this protein does not bind directly to DNA but interacts with other proteins to exert its regulatory function.

In an attempt to provide information on the Subolesin/Akirin interactome, the information on Subolesin/Akirin-protein physical and functional interactions was compiled from the String protein-protein interactions database[2] (**Figure 9** and **Supplementary Dataset S1**). Based on the analysis of protein-protein interactions, the results did not allow establishing an evolutionary signature of the Subolesin/Akirin2 interactome (**Figure 9**), probably due to the limited information available. Nevertheless, similar Subolesin/Akirin2 interacting proteins were described in fly and mouse (B7PRT9, Brahma/SWI2-related protein BRG-1) and in fish and rat (B7P8Y4, Arginyl-tRNA synthetase)

[2]https://string-db.org

suggesting possible evolutionarily conserved protein-protein interactions (**Figure 9**). To further gain insight into the evolution of the Subolesin/Akirin2 interactome, instead of looking only at protein-protein interactions, the interacting proteins were annotated according to the biological processes in which they are involved (**Figure 9**). The results of this analysis showed that the biological processes affected by the Subolesin/Akirin interactome are evolutionarily conserved, with metabolic process (MP), cellular process (CP) and biological regulation (BR) being among the most represented processes in all organisms (**Figure 9**).

PROTECTIVE CAPACITY OF SUBOLESIN/AKIRIN FOR THE CONTROL OF ECTOPARASITE VECTOR INFESTATIONS AND PATHOGEN INFECTION

Subolesin was discovered and characterized as a tick protective antigen for the control of *I. scapularis* infestations (Almazán et al., 2003, 2005; Sonenshine et al., 2006). Since then, Subolesin/Akirin showed a protective capacity in vaccines for the control of infestations by different arthropod species and pathogen infection and transmission (reviewed by de la Fuente et al., 2006a, 2011, 2013; de la Fuente and Kocan, 2006, 2014; Merino et al., 2013a,b; de la Fuente and Contreras, 2015). The putative mechanism for Subolesin vaccine protection was described by de la Fuente et al. (2011). They showed that by still unknown mechanisms anti-Subolesin antibodies could enter into tick cells where they can interact with cytosolic Subolesin to prevent its translocation to the nucleus and therefore the possibility to exert it regulatory functions.

The development of vaccines for the control of multiple arthropod ectoparasites constitutes a priority for targeting the various species infesting the same host (de la Fuente et al., 2011; Contreras and de la Fuente, 2016b). In this context, Subolesin/Akirin appears as a promising vaccine protective antigen due to its conservation in sequence and function through evolution (**Figures 1**, **5**, **9**). In fact, recent results support the potential of Subolesin/Akirin as a vaccine protective antigen for the control of multiple ectoparasite vector species and transmitted pathogens (**Figure 10**). The arthropod ectoparasite species in which Subolesin/Akirin have shown protective capacity by affecting different phases of their life cycles include the genera *Aedes, Anopheles, Phlebotomus, Caligus, Dermanyssus, Ornithodoros, Ixodes, Haemaphysalis, Amblyomma, Dermacentor, Hyalomma* and *Rhipicephalus* (Almazán et al., 2003, 2005, 2010, 2012; de la Fuente et al., 2006a, 2010, 2011, 2013; Canales et al., 2009; Harrington et al., 2009; Zivkovic et al., 2010a; Moreno-Cid et al., 2011, 2013; Carpio et al., 2011; Bensaci et al., 2012; Merino et al., 2011a,b, 2013b; Carreón et al., 2012; Manzano-Román et al., 2012, 2015; de la Fuente and Kocan, 2014; da Costa et al., 2014; Shakya et al., 2014; Torina et al., 2014; Contreras et al., 2015; de la Fuente and Contreras, 2015; Lu et al., 2016; Olds et al., 2016; Contreras and de la Fuente, 2016a; Kumar et al., 2017; Villar et al., 2017; **Figure 10**). The reduction in pathogen infection has been shown for tick-borne pathogens, *Anaplasma marginale*, *A. phagocytophilum*, *Borrelia burgdorferi* s.s. and *Babesia bovis*, and the mosquito-borne pathogen, *Plasmodium berghei* (de la Fuente et al., 2011; Merino et al., 2011b, 2013a; Bensaci et al., 2012; de la Fuente and Kocan, 2014; da Costa et al., 2014; **Figure 10**). Furthermore, protective epitopes were mapped in Subolesin/Akirin (Prudencio et al., 2010) and chimeric antigens were designed showing protective capacity in vaccinated hosts against tick infestations (Merino et al., 2013b; Contreras and de la Fuente, 2016a).

Considering the protective capacity shown by Subolesin/Akirin on different vector and pathogen species, future research directions will include the characterization of its protective capacity in other arthropod ectoparasite species, and the combination with other vector-derived and pathogen-derived antigens to increase vaccine efficacy for the control of both vector infestations and pathogen infection (Schetters et al., 2016; de la Fuente et al., 2017b; de la Fuente, 2018).

CONCLUSION AND FUTURE DIRECTIONS

Significant advances have been made recently toward understanding the evolution and function of Subolesin/Akirin. Our results suggest that Subolesin/Akirin evolved conserving not only its sequence and structure, but also its function and role in cell interactome and regulome in response to pathogen infection and other biological processes. However, major challenges remain in fully characterizing the interactome and function of these proteins, their role in the cell regulome in response to different stimuli, and how their evolution can meet species-specific demands. Furthermore, the structure of Subolesin/Akirin and interacting molecules should be resolved by X-ray crystallography to better understand their function. Finally, the conserved functional evolution of Subolesin/Akirin correlates with the protective capacity shown by these proteins in vaccine formulations for the control of different arthropod and pathogen species, and encourage further research to develop new vaccine formulations by combining Subolesin/Akirin with interacting proteins for the control of multiple ectoparasite infestations and pathogen infection.

AUTHOR CONTRIBUTIONS

JdlF conceived the paper. SA-J, MV, AC-C, JV, and AE-P performed the data analyses. PA and SA-J performed the microscopy studies. JF, SA-J, JV, and AC-C wrote the manuscript. All authors approved and contributed to the final version of the manuscript.

FUNDING

This work was financially supported by the Ministerio de Economía, Industria y Competitividad (Spain) grant BFU2016-79892-P. MV was funded by the Universidad de Castilla La Mancha, Spain. JV was supported by Project FIT (Pharmacology, Immunotherapy, nanoToxicology), funded by the European Regional Development Fund. The publication fee was partially supported by the CSIC Open Access Publication Support Initiative through its Unit of Information Resources for Research (URICI).

ACKNOWLEDGMENTS

We acknowledge a grant for the development of a research organization RVO: RO0516 from the Veterinary Research Institute, Brno, Czechia.

SUPPLEMENTARY MATERIAL

The Supplementary Material for this article can be found online at: https://www.frontiersin.org/articles/10.3389/fphys.2018.01612/full#supplementary-material

FIGURE S1 | Phylogenetic tree of akirin and subolesin nucleotide sequences. The figure displays a Neighbor Joining (NJ) phylogenetic tree of 361 nucleotide sequences belonging to 152 families, 73 orders and 15 classes. GenBank accession numbers and species names are shown. Tree reconstruction method was as described in **Figure 1**.

DATASET S1 | Annotation of the Subolesin/Akirin interactome. The information on Subolesin/Akirin-protein interactions was compiled from the literature and String protein-protein interactions database v.10.5 (https://string-db.org). Only predictions with medium (or better) confidence (0.4) limited to the top 10 interactions with protein-protein interaction (PPI) enrichment p-value ≤ 0.5 were considered. To compare the different species, protein annotations were standardize by identity to *I. scapularis/I. ricinus-D. melanogaster-H. sapiens* order of priority.

REFERENCES

Adipietro, K. A., Mainland, J. D., and Matsunami, H. (2012). Functional evolution of mammalian odorant receptors. *PLoS Genet.* 8:e1002821. doi: 10.1371/journal.pgen.1002821

Almazán, C., Blas-Machado, U., Kocan, K. M., Yoshioka, J. H., Blouin, E. F., Mangold, A. J., et al. (2005). Characterization of three *Ixodes scapularis* cDNAs protective against tick infestations. *Vaccine* 23, 4403–4416. doi: 10.1016/j.vaccine.2005.04.012

Almazán, C., Kocan, K. M., Bergman, D. K., Garcia-Garcia, J. C., Blouin, E. F., and de la Fuente, J. (2003). Identification of protective antigens for the control of *Ixodes scapularis* infestations using cDNA expression library immunization. *Vaccine* 21, 1492–1501. doi: 10.1016/S0264-410X(02)00683-7

Almazán, C., Lagunes, R., Villar, M., Canales, M., Rosario-Cruz, R., Jongejan, F., et al. (2010). Identification and characterization of *Rhipicephalus (Boophilus) microplus* candidate protective antigens for the control of cattle tick infestations. *Parasitol. Res.* 106, 471–479. doi: 10.1007/s00436-009-1689-1

Almazán, C., Moreno-Cantú, O., Moreno-Cid, J. A., Galindo, R. C., Canales, M., Villar, M., et al. (2012). Control of tick infestations in cattle vaccinated with bacterial membranes containing surface-exposed tick protective antigens. *Vaccine* 30, 265–272. doi: 10.1016/j.vaccine.2011.10.102

Andersson, S. G., and Kurland, C. G. (1998). Reductive evolution of resident genomes. *Trends Microbiol.* 6, 263–268. doi: 10.1016/S0966-842X(98)01312-2

Antunes, S., Merino, O., Mosqueda, J., Moreno-Cid, J. A., Bell-Sakyi, L., Fragkoudis, R., et al. (2014). Tick capillary feeding for the study of proteins involved in tick-pathogen interactions as potential antigens for the control of tick infestation and pathogen infection. *Parasit. Vectors* 7:42. doi: 10.1186/1756-3305-7-42

Ayllón, N., Villar, M., Galindo, R. C., Kocan, K. M., Šíma, R., López, J. A., et al. (2015). Systems biology of tissue-specific response to *Anaplasma phagocytophilum* reveals differentiated apoptosis in the tick vector *Ixodes scapularis*. *PLoS Genet.* 11:e1005120. doi: 10.1371/journal.pgen.1005120

Bensaci, M., Bhattacharya, D., Clark, R., and Hu, L. T. (2012). Oral vaccination with *Vaccinia virus* expressing the tick antigen subolesin inhibits tick feeding and transmission of *Borrelia burgdorferi*. *Vaccine* 30, 6040–6046. doi: 10.1016/j.vaccine.2012.07.053

Beutler, B., and Moresco, E. M. (2008). Akirins versus infection. *Nat. Immunol.* 9, 7–9. doi: 10.1038/ni0108-7

Bonnay, F., Nguyen, X. H., Cohen-Berros, E., Troxler, L., Batsche, E., Camonis, J., et al. (2014). Akirin specifies NF-κB selectivity of *Drosophila* innate immune response via chromatin remodeling. *EMBO J.* 33, 2349–2362. doi: 10.15252/embj.201488456

Brown, C. J., Johnson, A. K., Dunker, A. K., and Daughdrill, G. W. (2011). Evolution and disorder. *Curr. Opin. Struct. Biol.* 21, 441–446. doi: 10.1016/j.sbi.2011.02.005

Busby, A. T., Ayllón, N., Kocan, K. M., Blouin, E. F., de la Fuente, G., Galindo, R. C., et al. (2012). Expression of heat-shock proteins and subolesin affects stress responses, *Anaplasma phagocytophilum* infection and questing behavior in the tick, *Ixodes scapularis*. *Med. Vet. Entomol.* 26, 92–102. doi: 10.1111/j.1365-2915.2011.00973.x

Canales, M., Naranjo, V., Almazán, C., Molina, R., Tsuruta, S. A., Szabó, M. P. J., et al. (2009). Conservation and immunogenicity of the mosquito ortholog of the tick protective antigen, subolesin. *Parasitol. Res.* 105, 97–111. doi: 10.1007/s00436-009-1368-2

Carpio, Y., Basabe, L., Acosta, J., Rodríguez, A., Mendoza, A., Lisperger, A., et al. (2011). Novel gene isolated from *Caligus rogercresseyi*: a promising target for vaccine development against sea lice. *Vaccine* 29, 2810–2820. doi: 10.1016/j.vaccine.2011.01.109

Carpio, Y., García, C., Pons, T., Haussmann, D., Rodríguez-Ramos, T., Basabe, L., et al. (2013). Akirins in sea lice: first steps toward a deeper understanding. *Exp. Parasitol.* 135, 188–199. doi: 10.1016/j.exppara.2013.06.018

Carreón, D., Pérez de la Lastra, J. M., Almazán, C., Canales, M., Ruiz-Fons, F., Boadella, M., et al. (2012). Vaccination with BM86, subolesin and akirin protective antigens for the control of tick infestations in white tailed deer and red deer. *Vaccine* 30, 273–279. doi: 10.1016/j.vaccine.2011.10.099

Clemons, A. M., Brockway, H. M., Yin, Y., Kasinathan, B., Butterfield, Y. S., Jones, S. J., et al. (2013). Akirin is required for diakinesis bivalent structure and synaptonemal complex disassembly at meiotic prophase I. *Mol. Biol. Cell.* 24, 1053–1067. doi: 10.1091/mbc.E12-11-0841

Contreras, M., and de la Fuente, J. (2016a). Control of *Ixodes ricinus* and *Dermacentor reticulatus* tick infestations in rabbits vaccinated with the Q38 Subolesin/Akirin chimera. *Vaccine* 34, 3010–3013. doi: 10.1016/j.vaccine.2016.04.092

Contreras, M., and de la Fuente, J. (2016b). Vaccinomics approach to the development of vaccines for the control of multiple ectoparasite infestations. *Nova Acta Leopold.* 411, 185–200. doi: 10.1186/1471-2164-12-105

Contreras, M., Moreno-Cid, J. A., Domingos, A., Canales, M., Díez-Delgado, I., Pérez de la Lastra, J. M., et al. (2015). Bacterial membranes enhance the immunogenicity and protective capacity of the surface exposed tick Subolesin-*Anaplasma marginale* MSP1a chimeric antigen. *Ticks Tick Borne Dis.* 6, 820–828. doi: 10.1016/j.ttbdis.2015.07.010

da Costa, M., Pinheiro-Silva, R., Antunes, S., Moreno-Cid, J. A., Villar, M., de la Fuente, J., et al. (2014). Mosquito Akirin as a potential antigen for malaria control. *Malar. J.* 13:470. doi: 10.1186/1475-2875-13-470

DasGupta, R., Kaykas, A., Moon, R. T., and Perrimon, N. (2005). Functional genomic analysis of the Wnt-wingless signaling pathway. *Science* 308, 826–833. doi: 10.1126/science.1109374

de la Fuente, J. (2018). Controlling ticks and tick-borne diseases...looking forward. *Ticks Tick Borne Dis.* 9, 1354–1357. doi: 10.1016/j.ttbdis.2018.04.001

de la Fuente, J., Almazaìn, C., Blas-Machado, U., Naranjo, V., Mangold, A. J., Blouin, E. F., et al. (2006a). The tick protective antigen, 4D8, is a conserved protein involved in modulation of tick blood ingestion and reproduction. *Vaccine* 24, 4082–4095.

de la Fuente, J., Almazán, C., Blouin, E. F., Naranjo, V., and Kocan, K. M. (2006b). Reduction of tick infections with *Anaplasma marginale* and *A. phagocytophilum* by targeting the tick protective antigen subolesin. *Parasitol. Res.* 100, 85–91.

de la Fuente, J., Antunes, S., Bonnet, S., Cabezas-Cruz, A., Domingos, A., Estrada-Peña, A., et al. (2017a). Tick-pathogen interactions and vector competence: identification of molecular drivers for tick-borne diseases. *Front. Cell. Infect. Microbiol.* 7:114. doi: 10.3389/fcimb.2017.00114

de la Fuente, J., Contreras, M., Estrada-Peña, A., and Cabezas-Cruz, A. (2017b). Targeting a global health problem: vaccine design and challenges for the control of tick-borne diseases. *Vaccine* 35, 5089–5094. doi: 10.1016/j.vaccine.2017.07.097

de la Fuente, J., and Contreras, M. (2015). Tick vaccines: current status and future directions. *Expert Rev. Vaccines* 14, 1367–1376. doi: 10.1586/14760584.2015.1076339

de la Fuente, J., and Kocan, K. M. (2006). Strategies for development of vaccines for control of ixodid tick species. *Parasite Immunol.* 28, 275–283. doi: 10.1111/j.1365-3024.2006.00828.x

de la Fuente, J., and Kocan, K. M. (2014). "Development of vaccines for control of tick infestations and interruption of pathogen transmission," in *Biology of Ticks*, 2nd Edn, eds D. E. Sonenshine and R. M. Roe (New York, NY: Oxford University Press), 333–352.

de la Fuente, J., Manzano-Roman, R., Naranjo, V., Kocan, K. M., Zivkovic, Z., Blouin, E. F., et al. (2010). Identification of protective antigens by RNA interference for control of the lone star tick, *Amblyomma americanum*. *Vaccine* 28, 1786–1795. doi: 10.1016/j.vaccine.2009.12.007

de la Fuente, J., Maritz-Olivier, C., Naranjo, V., Ayoubi, P., Nijhof, A. M., Almazán, C., et al. (2008). Evidence of the role of tick subolesin in gene expression. *BMC Genomics* 9:372. doi: 10.1186/1471-2164-9-372

de la Fuente, J., Moreno-Cid, J. A., Canales, M., Villar, M., Pérez de la Lastra, J. M., Kocan, K. M., et al. (2011). Targeting arthropod subolesin/akirin for the development of a universal vaccine for control of vector infestations and pathogen transmission. *Vet. Parasitol.* 181, 17–22. doi: 10.1016/j.vetpar.2011.04.018

de la Fuente, J., Moreno-Cid, J. A., Galindo, R. C., Almazán, C., Kocan, K. M., Merino, O., et al. (2013). Subolesin/Akirin vaccines for the control of arthropod vectors and vector-borne pathogens. *Transbound. Emerg. Dis.* 60(Suppl. 2), 172–178. doi: 10.1111/tbed.12146

de la Fuente, J., Villar, M., Cabezas-Cruz, A., Estrada-Peña, A., Ayllón, N., and Alberdi, P. (2016). Tick-host-pathogen interactions: conflict and cooperation. *PLoS Pathog.* 12:e1005488. doi: 10.1371/journal.ppat.1005488

Dingwall, C., Robbins, J., Dilworth, S. M., Roberts, B., and Richardson, W. D. (1988). The nucleoplasmin nuclear location sequence is larger and more complex than that of SV-40 large T antigen. *J. Cell Biol.* 107, 841–849. doi: 10.1083/jcb.107.3.841

Driscoll, T. P., Verhoeve, V. I., Guillotte, M. L., Lehman, S. S., Rennoll, S. A., Beier-Sexton, M., et al. (2017). Wholly *Rickettsia*! Reconstructed metabolic profile of the quintessential bacterial parasite of eukaryotic cells. *mBio* 8:e859-17. doi: 10.1128/mBio.00859-17

Ehrenberg, M., and Kurland, C. G. (1984). Costs of accuracy determined by a maximal growth rate constraint. *Q. Rev. Biophys.* 17, 45–82. doi: 10.1017/S0033583500005254

Estrada-Peña, A., Villar, M., Artigas-Jerónimo, S., López, V., Alberdi, P., Cabezas-Cruz, A., et al. (2018). Use of graph theory to characterize human and arthropod vector cell protein response to infection. *Front. Cell. Infect. Microbiol.* 8:265. doi: 10.3389/fcimb.2018.00265

Felsenstein, J. (1985). Confidence limits on phylogenies: an approach using the bootstrap. *Evolution* 39, 783–791. doi: 10.1111/j.1558-5646.1985.tb00420.x

Galindo, R. C., Doncel-Pérez, E., Zivkovic, Z., Naranjo, V., Gortazar, C., Mangold, A. J., et al. (2009). Tick subolesin is an ortholog of the akirins described in insects and vertebrates. *Dev. Comp. Immunol.* 33, 612–617. doi: 10.1016/j.dci.2008.11.002

Giraldo-Calderón, G. I., Emrich, S. J., MacCallum, R. M., Maslen, G., Dialynas, E., Topalis, P., et al. (2015). VectorBase: an updated bioinformatics resource for invertebrate vectors and other organisms related with human diseases. *Nucleic Acids Res.* 43, D707–D713. doi: 10.1093/nar/gku1117

Gonzalez, K., and Baylies, M. (2005). "bhringi: A novel Twist co-regulator", in *Proceedings of the Program and Abstracts 46th Annual Drosophila Research Conference*, San Diego, CA, 46:320B.

Goto, A., Fukuyama, H., Imler, J. L., and Hoffmann, J. A. (2014). The chromatin regulator DMAP1 modulates activity of the nuclear factor B (NF-B) transcription factor Relish in the *Drosophila* innate immune response. *J. Biol. Chem.* 289, 20470–20476. doi: 10.1074/jbc.C114.553719

Goto, A., Matsushita, K., Gesellchen, V., El Chamy, L., Kuttenkeuler, D., Takeuchi, O., et al. (2008). Akirins are highly conserved nuclear proteins required for NF-kappaB-dependent gene expression in Drosophila and mice. *Nat. Immunol.* 9, 97–104. doi: 10.1038/ni1543

Gregory, T. R. (2005). *Animal Genome Size Database*. Avilable at: http://www.genomesize.com

Gulia-Nuss, M., Nuss, A. B., Meyer, J. M., Sonenshine, D. E., Roe, R. M., Waterhouse, R. M., et al. (2016). Genomic insights into the *Ixodes scapularis* tick vector of Lyme disease. *Nat. Commun.* 7:10507. doi: 10.1038/ncomms10507

Hajdušek, O., Šíma, R., Ayllón, N., Jalovecká, M., Perner, J., de la Fuente, J., et al. (2013). Interaction of the tick immune system with transmitted pathogens. *Front. Cell. Infect. Microbiol.* 3:26. doi: 10.3389/fcimb.2013.00026

Harrington, D., Canales, M., de la Fuente, J., de Luna, C., Robinson, K., Guy, J., et al. (2009). Immunisation with recombinant proteins subolesin and Bm86 for the control of *Dermanyssus gallinae* in poultry. *Vaccine* 27, 4056–4063. doi: 10.1016/j.vaccine.2009.04.014

Holm, L., and Laakso, L. M. (2016). Dali server update. *Nucleic Acids Res.* 44, W351–W355. doi: 10.1093/nar/gkw357

Hoogstraal, H. (1956). *African Ixodoidea. I. Ticks of the Sudan (with Special Reference to Equatoria Province and with Preliminary Reviews of the Genera Boophilus, Margaropus and Hyalomma)*. Washington, DC: Department of the Navy, 1101.

Horak, I. G., Heyne, H., Williams, R., Gallivan, G. J., Spickett, A. M., Bezuidenhout, J. D., et al. (2018). *The Ixodid Ticks (Acari: Ixodidae) of Southern Africa*. Hamburg: Springer, 675. doi: 10.1007/978-3-319-70642-9

Hou, F., Wang, X., Qian, Z., Liu, Q., Liu, Y., He, S., et al. (2013). Identification and functional studies of Akirin, a potential positive nuclear factor of NF-κB signaling pathways in the Pacific white shrimp, *Litopenaeus vannamei*. *Dev. Comp. Immunol.* 41, 703–714. doi: 10.1016/j.dci.2013.08.005

Ivics, Z., Hackett, P. B., Plasterk, R. H., and Izsvak, Z. (1997). Molecular reconstruction of Sleeping Beauty, a Tc1-like transposon from fish, and its transposition in human cells. *Cell* 91, 501–510. doi: 10.1016/S0092-8674(00)80436-5

Kasthuri, S. R., Umasuthan, N., Whang, I., Wan, Q., Lim, B. S., Jung, H. B., et al. (2013). Akirin2 homologues from rock bream, *Oplegnathus fasciatus*: genomic and molecular characterization and transcriptional expression analysis. *Fish Shellfish Immunol.* 35, 740–747. doi: 10.1016/j.fsi.2013.06.006

Katoh, K., Rozewicki, J., and Yamada, K. D. (2017). MAFFT online service: multiple sequence alignment, interactive sequence choice and visualization. *Brief. Bioinform.* doi: 10.1093/bib/bbx108 [Epub ahead of print].

Katoh, K., and Standley, D. M. (2013). MAFFT multiple sequence alignment software version 7: improvements in performance and usability. *Mol. Biol. Evol.* 30, 772–780. doi: 10.1093/molbev/mst010

Kim, H., Lee, S. K., Hong, M. W., Park, S. R., Lee, Y. S., Kim, J. W., et al. (2013). Association of a single nucleotide polymorphism in the akirin 2 gene with economically important traits in Korean native cattle. *Anim. Genet.* 44, 750–753. doi: 10.1111/age.12055

Komiya, Y., Kurabe, N., Katagiri, K., Ogawa, M., Sugiyama, A., Kawasaki, Y., et al. (2008). A novel binding factor of 14-3-3beta functions as a transcriptional repressor and promotes anchorage-independent growth, tumorigenicity, and metastasis. *J. Biol. Chem.* 283, 18753–18764. doi: 10.1074/jbc.M802530200

Koonin, E. V. (2005). Orthologs, paralogs, and evolutionary genomics. *Annu. Rev. Genet.* 39, 309–338. doi: 10.1371/journal.pgen.1002821

Krossa, S., Schmitt, A. D., Hattermann, K., Fritsch, J., Scheidig, A. J., Mehdorn, H. M., et al. (2015). Down regulation of Akirin-2 increases chemosensitivity in human glioblastomas more efficiently than Twist-1. *Oncotarget* 6, 21029–21045. doi: 10.18632/oncotarget.3763

Kumar, B., Manjunathachar, H. V., Nagar, G., Ravikumar, G., de la Fuente, J., Saravanan, B. C., et al. (2017). Functional characterization of candidate antigens of *Hyalomma anatolicum* and evaluation of its cross-protective efficacy against *Rhipicephalus microplus*. *Vaccine* 35, 5682–5692. doi: 10.1016/j.vaccine.2017.08.049

Kumar, S., Stecher, G., and Tamura, K. (2016). MEGA7: molecular evolutionary genetics analysis version 7.0 for bigger datasets. *Mol. Biol. Evol.* 33, 1870–1874. doi: 10.1093/molbev/msw054

Kurland, C. G., Canbäck, B., and Berg, O. G. (2007). The origins of modern proteomes. *Biochimie* 89, 1454–1463. doi: 10.1016/j.biochi.2007.09.004

Law, M. J., Linde, M. E., Chambers, E. J., Oubridge, C., Katsamba, P. S., Nilsson, L., et al. (2006). The role of positively charged amino acids and electrostatic interactions in the complex of U1A protein and U1 hairpin II RNA. *Nucleic Acids Res.* 34, 275–285. doi: 10.1093/nar/gkj436

Leung, S. W., Harreman, M. T., Hodel, M. R., Hodel, A. E., and Corbett, A. H. (2003). Dissection of the karyopherin alpha nuclear localization signal (NLS)-binding groove: functional requirements for NLS binding. *J. Biol. Chem.* 278, 41947–41953. doi: 10.1074/jbc.M307162200

Liu, N., Wang, X. W., Sun, J. J., Wang, L., Zhang, H. W., Zhao, X. F., et al. (2016). Akirin interacts with Bap60 and 14-3-3 proteins to regulate the expression of antimicrobial peptides in the kuruma shrimp (*Marsupenaeus japonicus*). *Dev. Comp. Immunol.* 55, 80–89. doi: 10.1016/j.dci.2015.10.015

Liu, T., Gao, Y., and Xu, T. (2015). Evolution of akirin family in gene and genome levels and coexpressed patterns among family members and rel gene in croaker. *Dev. Comp. Immunol.* 52, 17–25. doi: 10.1016/j.dci.2015.04.010

Liu, X., Xia, Y., Tang, J., Ma, L., Li, C., Ma, P., et al. (2017). Dual roles of Akirin2 protein during *Xenopus* neural development. *J. Biol. Chem.* 292, 5676–5684. doi: 10.1074/jbc.M117.777110

Liu, Y., Song, L., Sun, Y., Liu, T., Hou, F., and Liu, X. (2016). Comparison of immune response in Pacific white shrimp, *Litopenaeus vannamei*, after knock down of Toll and IMD gene *in vivo*. *Dev. Comp. Immunol.* 60, 41–52. doi: 10.1016/j.dci.2016.02.004

Lu, P., Zhou, Y., Yu, Y., Cao, J., Zhang, H., Gong, H., et al. (2016). RNA interference and the vaccine effect of a subolesin homolog from the tick *Rhipicephalus haemaphysaloides*. *Exp. Appl. Acarol.* 68, 113–126. doi: 10.1007/s10493-015-9987-z

Macqueen, D. (2009). Commentary on Galindo et Al. [Dev. Comp. Immunol. 33(4) (2009) 612-617]. *Dev. Comp. Immunol.* 33, 877; authorrely 878–879. doi: 10.1016/j.dci.2009.02.011

Macqueen, D. J., and Johnston, I. A. (2009). Evolution of the multifaceted eukaryotic akirin gene family. *BMC Evol. Biol.* 9:34. doi: 10.1186/1471-2148-9-34

Macqueen, D. J., Bower, N. I., and Johnston, I. A. (2010a). Positioning the expanded akirin gene family of Atlantic salmon within the transcriptional networks of myogenesis. *Biochem. Biophys. Res. Commun.* 200, 599–605. doi: 10.1016/j.bbrc.2010.08.110

Macqueen, D. J., Kristjánsson, B. K., and Johnston, I. A. (2010b). Salmonid genomes have a remarkably expanded akirin family, coexpressed with genes from conserved pathways governing skeletal muscle growth and catabolism. *Physiol. Genomics* 42, 134–148. doi: 10.1152/physiolgenomics.00045.2010

Maeda, I., Kohara, Y., Yamamoto, M., and Sugimoto, A. (2001). Large-scale analysis of gene function in *Caenorhabditis elegans* by high-throughput RNAi. *Curr. Biol.* 11, 171–176. doi: 10.1016/S0960-9822(01)00052-5

Makkerh, J. P., Dingwall, C., and Laskey, R. A. (1996). Comparative mutagenesis of nuclear localization signals reveals the importance of neutral and acidic amino acids. *Curr. Biol.* 6, 1025–1027. doi: 10.1016/S0960-9822(02)00648-6

Mans, B. J., De Castro, M. H., Pienaar, R., De Klerk, D., Gaven, P., Genu, S., et al. (2016). Ancestral reconstruction of tick lineages. *Ticks Tick Borne Dis.* 7, 509–535. doi: 10.1016/j.ttbdis.2016.02.002

Manzano-Román, R., Díaz-Martín, V., Oleaga, A., and Pérez-Sánchez, R. (2015). Identification of protective linear B-cell epitopes on the subolesin/akirin orthologues of *Ornithodoros* spp. soft ticks. *Vaccine* 33, 1046–1055. doi: 10.1016/j.vaccine.2015.01.015

Manzano-Román, R., Díaz-Martín, V., Oleaga, A., Siles-Lucas, M., and Pérez-Sánchez, R. (2012). Subolesin/akirin orthologs from *Ornithodoros* spp. soft ticks: cloning, RNAi gene silencing and protective effect of the recombinant proteins. *Vet. Parasitol.* 185, 248–259. doi: 10.1016/j.vetpar.2011.10.032

Marshall, A., Salerno, M. S., Thomas, M., Davies, T., Berry, C., Dyer, K., et al. (2008). Mighty is a novel promyogenic factor in skeletal myogenesis. *Exp. Cell Res.* 314, 1013–1029. doi: 10.1016/j.yexcr.2008.01.004

Medzhitov, R., and Janeway, C. A. Jr. (1997). Innate immunity: impact on the adaptive immune response. *Curr. Opin. Immunol.* 9, 4–9. doi: 10.1016/S0952-7915(97)80152-5

Merino, O., Alberdi, P., Pérez de la Lastra, J. M., and de la Fuente, J. (2013a). Tick vaccines and the control of tick-borne pathogens. *Front. Cell. Infect. Microbiol.* 3:30. doi: 10.3389/fcimb.2013.00030

Merino, O., Antunes, S., Mosqueda, J., Moreno-Cid, J. A., Pérez de la Lastra, J. M., Rosario-Cruz, R., et al. (2013b). Vaccination with proteins involved in tick-pathogen interactions reduces vector infestations and pathogen infection. *Vaccine* 31, 5889–5896. doi: 10.1016/j.vaccine.2013.09.037

Merino, O., Almazán, C., Canales, M., Villar, M., Moreno-Cid, J. A., Estrada-Peña, A., et al. (2011a). Control of *Rhipicephalus (Boophilus) microplus* infestations by the combination of subolesin vaccination and tick autocidal control after subolesin gene knockdown in ticks fed on cattle. *Vaccine* 29, 2248–2254. doi: 10.1016/j.vaccine.2011.01.050

Merino, O., Almazán, C., Canales, M., Villar, M., Moreno-Cid, J. A., Galindo, R. C., et al. (2011b). Targeting the tick protective antigen subolesin reduces vector infestations and pathogen infection by *Anaplasma marginale* and *Babesia bigemina*. *Vaccine* 29, 8575–8579. doi: 10.1016/j.vaccine.2011.09.023

Mobley, C. B., Fox, C. D., Ferguson, B. S., Amin, R. H., Dalbo, V. J., Baier, S., et al. (2014). L-leucine, beta-hydroxy-beta-methylbutyric acid (HMB) and creatine monohydrate prevent myostatin-induced Akirin-1/Mighty mRNA down-regulation and myotube atrophy. *J. Int. Soc. Sports Nutr.* 11:38. doi: 10.1186/1550-2783-11-38

Morel, P. C. (2003). *Les Tiques d'Afrique et du Bassin Meìditerraneìen (1965–1995)*. Can Tho: CI*RAD-EMVT*, 1342.

Moreno-Cid, J. A., Jiménez, M., Cornelie, S., Molina, R., Alarcón, P., Lacroix, M.-N., et al. (2011). Characterization of *Aedes albopictus* akirin for the control of mosquito and sand fly infestations. *Vaccine* 29, 77–82. doi: 10.1016/j.vaccine.2010.10.011

Moreno-Cid, J. A., Pérez de la Lastra, J. M., Villar, M., Jiménez, M., Pinal, R., Estrada-Peña, A., et al. (2013). Control of multiple arthropod vector infestations with subolesin/akirin vaccines. *Vaccine* 31, 1187–1196. doi: 10.1016/j.vaccine.2012.12.073

Naranjo, N., Ayllón, N., Pérez de la Lastra, J. M., Galindo, R. C., Kocan, K. M., Blouin, E. F., et al. (2013). Reciprocal regulation of NF-kB (Relish) and Subolesin in the tick vector, *Ixodes scapularis*. *PLoS One* 8:e65915. doi: 10.1371/journal.pone.0065915

Nowak, S. J., Aihara, H., Gonzalez, K., Nibu, Y., and Baylies, M. K. (2012). Akirin links twist-regulated transcription with the Brahma chromatin remodeling complex during embryogenesis. *PLoS Genet.* 8:e1002547. doi: 10.1371/journal.pgen.1002547

Nowak, S. J., and Baylies, M. K. (2012). Akirin: a context-dependent link between transcription and chromatin remodeling. *Bioarchitecture* 2, 209–213. doi: 10.4161/bioa.22907

Olds, C. L., Mwaura, S., Odongo, D. O., Scoles, G. A., Bishop, R., and Daubenberger, C. (2016). Induction of humoral immune response to multiple recombinant *Rhipicephalus appendiculatus* antigens and their effect on tick feeding success and pathogen transmission. *Parasit. Vectors* 9:484. doi: 10.1186/s13071-016-1774-0

Orengo, C. A., and Thornton, J. M. (2005). Protein families and their evolution-a structural perspective. *Annu. Rev. Biochem.* 74, 867–900. doi: 10.1146/annurev.biochem.74.082803.133029

Pavithiran, A., Bathige, S. D. N. K., Kugapreethan, R., Priyathilaka, T. T., Yang, H., Kim, M. J., et al. (2018). A comparative study of three akirin genes from big belly seahorse *Hippocampus abdominalis*: molecular, transcriptional and functional characterization. *Fish Shellfish Immunol.* 74, 584–592. doi: 10.1016/j.fsi.2018.01.025

Peña-Rangel, M. T., Rodriguez, I., and Riesgo-Escovar, J. R. (2002). A misexpression study examining dorsal thorax formation in *Drosophila melanogaster*. *Genetics* 160, 1035–1050.

Prudencio, C. R., Pérez de la Lastra, J. M., Canales, M., Villar, M., and de la Fuente, J. (2010). Mapping protective epitopes in the tick and mosquito subolesin ortholog proteins. *Vaccine* 28, 5398–5406. doi: 10.1016/j.vaccine.2010.06.021

Qu, F., Xiang, Z., Zhang, Y., Li, J., Zhang, Y., and Yu, Z. (2014). The identification of the first molluscan Akirin2 with immune defense function in the Hong Kong oyster *Crassostrea hongkongensis*. *Fish Shellfish Immunol.* 41, 455–465. doi: 10.1016/j.fsi.2014.09.029

Rahman, M. K., Saiful Islam, M., and You, M. (2018). Impact of subolesin and cystatin knockdown by RNA interference in adult female *Haemaphysalis longicornis* (Acari: Ixodidae) on blood engorgement and reproduction. *Insects* 9:E39. doi: 10.3390/insects9020039

Richardson, J. M., Colloms, S. D., Finnegan, D. J., and Walkinshaw, M. D. (2009). Molecular architecture of the Mos1 paired-end complex: the structural basis of DNA transposition in a eukaryote. *Cell* 138, 1096–1108. doi: 10.1016/j.cell.2009.07.012

Rioualen, C., Da Costa, Q., Chetrit, B., Charafe-Jauffret, E., Ginestier, C., and Bidaut, G. (2017). HTS-Net: an integrated regulome-interactome approach for establishing network regulation models in high-throughput screenings. *PLoS One* 12:e0185400. doi: 10.1371/journal.pone.0185400

Salerno, M. S., Dyer, K., Bracegirdle, J., Platt, L., Thomas, M., Siriett, V., et al. (2009). Akirin1 (Mighty), a novel promyogenic factor regulates muscle regeneration and cell chemotaxis. *Exp. Cell Res.* 315, 2012–2021. doi: 10.1016/j.yexcr.2009.04.014

Sasaki, M., Akiyama-Oda, Y., and Oda, H. (2017). Evolutionary origin of type IV classical cadherins in arthropods. *BMC Evol. Biol.* 17:142. doi: 10.1186/s12862-017-0991-2

Sasaki, S., Yamada, T., Sukegawa, S., Miyake, T., Fujita, T., Morita, M., et al. (2009). Association of a single nucleotide polymorphism in akirin 2 gene with marbling in Japanese Black beef cattle. *BMC Res. Notes* 2:131. doi: 10.1186/1756-0500-2-131

Schetters, T., Bishop, R., Crampton, M., Kopáček, P., Lew-Tabor, A., Maritz-Olivier, C., et al. (2016). Cattle tick vaccine researchers join forces in CATVAC. *Parasit. Vectors* 9:105. doi: 10.1186/s13071-016-1386-8

Shakya, M., Kumar, B., Nagar, G., de la Fuente, J., and Ghosh, S. (2014). Subolesin: a candidate vaccine antigen for the control of cattle tick infestations in Indian situation. *Vaccine* 32, 3488–3494. doi: 10.1016/j.vaccine.2014.04.053

Shaw, D. K., Wang, X., Brown, L. J., Oliva Chávez, A. S., Reif, K. E., Smith, A. A., et al. (2017). Infection-derived lipids elicit an immune deficiency circuit in arthropods. *Nat. Commun.* 8:14401. doi: 10.1038/ncomms14401

Smith, A., Guo, X., de la Fuente, J., Naranjo, N., Kocan, K. M., and Kaufman, W. R. (2009). The impact of RNA interference of the subolesin and voraxin genes in male *Amblyomma hebraeum* (Acari: Ixodidae) on female engorgement and oviposition. *Exp. Appl. Acarol.* 47, 71–86. doi: 10.1007/s10493-008-9195-1

Sonenshine, D. E., Kocan, K. M., and de la Fuente, J. (2006). Tick control: further thoughts on a research agenda. *Trends Parasitol.* 22, 550–551. doi: 10.1016/j.pt.2006.09.003

Staley, J. T. (2017). Domain Cell Theory supports the independent evolution of the Eukarya, Bacteria and Archaea and the Nuclear Compartment Commonality hypothesis. *Open Biol.* 7:170041. doi: 10.1098/rsob.170041

Sun, W., Huang, H., Ma, S., Gan, X., Zhu, M., Liu, H., et al. (2016). Akirin2 could promote the proliferation but not the differentiation of duck myoblasts via the activation of the mTOR/p70S6K signaling pathway. *Int. J. Biochem. Cell. Biol.* 79, 298–307. doi: 10.1016/j.biocel.2016.08.032

Tartey, S., Matsushita, K., Imamura, T., Wakabayashi, A., Ori, D., Mino, T., et al. (2015). Essential function for the nuclear protein Akirin2 in B cell activation and humoral immune responses. *J. Immunol.* 195, 519–527. doi: 10.4049/jimmunol.1500373

Tartey, S., Matsushita, K., Vandenbon, A., Ori, D., Imamura, T., Mino, T., et al. (2014). Akirin2 is critical for inducing inflammatory genes by bridging IκB-ζ and the SWI/SNF complex. *EMBO J.* 33, 2332–2348. doi: 10.15252/embj.201488447

Torina, A., Moreno-Cid, J. A., Blanda, V., Fernández de Mera, I. G., Pérez de la Lastra, J. M., Scimeca, S., et al. (2014). Control of tick infestations and pathogen prevalence in cattle and sheep farms vaccinated with the recombinant Subolesin-Major Surface Protein 1a chimeric antigen. *Parasit. Vectors* 7:10. doi: 10.1186/1756-3305-7-10

Valenzuela-Muñoz, V., and Gallardo-Escárate, C. (2014). TLR and IMD signaling pathways from *Caligus rogercresseyi* (Crustacea: Copepoda): *in silico* gene expression and SNPs discovery. *Fish Shellfish Immunol.* 36, 428–434. doi: 10.1016/j.fsi.2013.12.019

Villar, M., Marina, A., and de la Fuente, J. (2017). Applying proteomics to tick vaccine development: where are we? *Expert Rev. Proteomics* 14, 211–221. doi: 10.1080/14789450.2017.1284590

Voigt, F., Wiedemann, L., Zuliani, C., Querques, I., Sebe, A., Mates, L., et al. (2016). Sleeping Beauty transposase structure allows rational design of hyperactive variants for genetic engineering. *Nat. Commun.* 7:11126. doi: 10.1038/ncomms11126

Wan, F., and Lenardo, M. J. (2010). The nuclear signaling of NF-kappaB: current knowledge, new insights, and future perspectives. *Cell Res.* 20, 24–33. doi: 10.1038/cr.2009.137

Wang, M., Kurland, C. G., and Caetano-Anollés, G. (2011). Reductive evolution of proteomes and protein structures. *Proc. Natl. Acad. Sci U.S.A.* 108, 11954–11958. doi: 10.1073/pnas.1017361108

Watanabe, N., Satoh, Y., Fujita, T., Ohta, T., Kose, H., Muramatsu, Y., et al. (2011). Distribution of allele frequencies at TTN g.231054C > T, RPL27A g.3109537C > T and AKIRIN2 c.*188G > A between Japanese Black and four other cattle breeds with differing historical selection for marbling. *BMC Res. Notes* 4:10. doi: 10.1186/1756-0500-4-10

Wolf, Y. I., and Koonin, E. V. (2013). Genome reduction as the dominant mode of evolution. *Bioessays* 35, 829–837. doi: 10.1002/bies.201300037

Xue, X., Wang, L., Chen, Y., Zhang, X., Luo, H., Li, Z., et al. (2014). Identification and molecular characterization of an Akirin2 homolog in Chinese loach (*Paramisgurnus dabryanus*). *Fish Shellfish Immunol.* 36, 435–443. doi: 10.1016/j.fsi.2013.12.021

Yan, J., Dong, X., Kong, Y., Zhang, Y., Jing, R., and Feng, L. (2013). Identification and primary immune characteristics of an amphioxus akirin homolog. *Fish Shellfish Immunol.* 35, 564–571. doi: 10.1016/j.fsi.2013.05.020

Yang, C. G., Wang, X. L., Wang, L., Zhang, B., and Chen, S. L. (2011). A new Akirin1 gene in turbot (*Scophthalmus maximus*): molecular cloning, characterization and expression analysis in response to bacterial and viral immunological challenge. *Fish Shellfish Immunol* 30, 1031–1041. doi: 10.1016/j.fsi.2011.01.028

Yang, C. G., Wang, X. L., Zhang, B., Sun, B., Liu, S. S., and Chen, S. L. (2013). Screening and analysis of PoAkirin1 and two related genes in response to immunological stimulants in the Japanese flounder (*Paralichthys olivaceus*). *BMC Mol. Biol.* 14:10. doi: 10.1186/1471-2199-14-10

Zanesi, N., Balatti, V., Riordan, J., Burch, A., Rizzotto, L., Palamarchuk, A., et al. (2013). A Sleeping Beauty screen reveals NF-kB activation in CLL mouse model. *Blood* 121, 4355–4358. doi: 10.1182/blood-2013-02-486035

Zhang, Y. (2008). I-TASSER server for protein 3D structure prediction. *BMC Bioinformatics* 9:40. doi: 10.1186/1471-2105-9-40

Zivkovic, Z., Esteves, E., Almazán, C., Daffre, S., Nijhof, A. M., Kocan, K. M., et al. (2010a). Differential expression of genes in salivary glands of male *Rhipicephalus (Boophilus) microplus* in response to infection with *Anaplasma marginale*. *BMC Genomics* 11:186. doi: 10.1186/1471-2164-11-186

Zivkovic, Z., Torina, A., Mitra, R., Alongi, A., Scimeca, S., Kocan, K. M., et al. (2010b). Subolesin expression in response to pathogen infection in ticks. *BMC Immunol.* 11:7. doi: 10.1186/1471-2172-11-7

Conflict of Interest Statement: The authors declare that the research was conducted in the absence of any commercial or financial relationships that could be construed as a potential conflict of interest.

frontiers in Physiology

MINI REVIEW
published: 04 December 2018
doi: 10.3389/fphys.2018.01728

A Continuing Exploration of Tick–Virus Interactions Using Various Experimental Viral Infections of Hard Ticks

*Melbourne Rio Talactac[1,2], Emmanuel P. Hernandez[2], Kozo Fujisaki[3] and Tetsuya Tanaka[2]**

[1] Department of Clinical and Population Health, College of Veterinary Medicine and Biomedical Sciences, Cavite State University, Cavite, Philippines, [2] Laboratory of Infectious Diseases, Joint Faculty of Veterinary Medicine, Kagoshima University, Kagoshima, Japan, [3] National Agriculture and Food Research Organization, Tsukuba, Japan

To fully unravel the ixodid ticks' role as vectors of viral pathogens, their susceptibility to new control measures, and their ability to develop acaricide resistance, acclimatization of ticks under laboratory conditions is greatly needed. However, the unique and complicated feeding behavior of these ticks compared to that of other hematophagous arthropods requires efficient and effective techniques to infect them with tick-borne viruses (TBVs). In addition, relatively expensive maintenance of animals for blood feeding and associated concerns about animal welfare critically limit our understanding of TBVs. This mini review aims to summarize the current knowledge about the artificial infection of hard ticks with viral pathogens, which is currently used to elucidate virus transmission and vector competence and to discover immune modulators related to tick–virus interactions. This review will also present the advantages and limitations of the current techniques for tick infection. Fortunately, new artificial techniques arise, and the limitations of current protocols are greatly reduced as researchers continuously improve, streamline, and standardize the laboratory procedures to lower cost and produce better adoptability. In summary, convenient and low-cost techniques to study the interactions between ticks and TBVs provide a great opportunity to identify new targets for the future control of TBVs.

Keywords: tick-borne viruses, ixodid ticks, virus infection, blood feeding, tick–virus interactions

OPEN ACCESS

Edited by:
Itabajara Da Silva Vaz Jr., Universidade Federal do Rio Grande do Sul (UFRGS), Brazil

Reviewed by:
Mark Stenglein, Colorado State University, United States
Marcos Henrique Ferreira Sorgine, Universidade Federal do Rio de Janeiro, Brazil

****Correspondence:***
Tetsuya Tanaka
k6199431@kadai.jp

Specialty section:
This article was submitted to Invertebrate Physiology, a section of the journal Frontiers in Physiology

Received: *24 September 2018*
Accepted: *16 November 2018*
Published: *04 December 2018*

Citation:
Talactac MR, Hernandez EP, Fujisaki K and Tanaka T (2018) A Continuing Exploration of Tick–Virus Interactions Using Various Experimental Viral Infections of Hard Ticks. Front. Physiol. 9:1728. doi: 10.3389/fphys.2018.01728

INTRODUCTION

Ticks are the most economically important vectors of livestock diseases (Arthur, 1962) and are considered second to mosquitoes in transmitting human diseases (de la Fuente et al., 2008; Socolovschi et al., 2009). Among the pathogens transmitted by these bloodsucking ectoparasites, tick-borne viruses (TBVs) present a severe health risk to both humans and domestic animals (Hoogstraal, 1973). TBVs comprise a wide range of viruses classified into eight virus families: *Asfarviridae*, *Nairoviridae, Peribunyaviridae, Phenuiviridae*, *Flaviviridae*, *Orthomyxoviridae*, *Rhabdoviridae*, and *Reoviridae* (Brackney and Armstrong, 2016; Kazimírová et al., 2017). Among these viral families, *Nairoviridae* and *Flaviviridae* are considered to have the TBVs of most importance to public health, including the tick-borne encephalitis virus (TBEV) and the Crimean–Congo hemorrhagic fever virus (CCHFV), which are known to cause severe clinical symptoms in humans (Nuttall et al., 1994; Labuda and Nuttall, 2004; Brackney and Armstrong, 2016; Kazimírová et al., 2017).

Of the 900 currently known tick species, less than 10% are implicated as virus vectors, and these include the *Ornithodoros* and *Argas* genera for the argasid ticks and *Ixodes*, *Haemaphysalis*, *Hyalomma*, *Amblyomma*, *Dermacentor*, and *Rhipicephalus* genera in ixodid ticks (Labuda and Nuttall, 2004; de la Fuente et al., 2017).

Although the role of ticks in the transmission of viruses has been known for over a century (Mansfield et al., 2017), the understanding of tick–virus interactions important for tick antiviral immunity, pathogen replication, and transmission of the virus to an animal host remains limited and at an early stage (Mitzel et al., 2007; Kopacek et al., 2010; Liu et al., 2012). Moreover, the diversity of tick-borne viruses has been less thoroughly studied than that of mosquito-borne viruses (Yoshii et al., 2015).

In addition, ixodid ticks differ essentially from other blood-feeding insects in terms of their digestive physiology, feeding behavior (Obenchain and Galun, 1982), and the long duration of the blood meal, which can take up to several weeks (Waladde and Rice, 1982). Moreover, tick attachment at feeding sites on the host requires correct physical and chemical stimuli for a successful engorgement (Guerin et al., 2000).

Since it is estimated that TBVs spend more than 95% of their life cycle within the tick vector (de la Fuente et al., 2017), a very intimate and highly specific association between tick vector species and the transmitted TBVs is normally maintained (Brites-Neto et al., 2015). With this in mind, artificial viral infection of ticks using experimental laboratory techniques can greatly improve our understanding of tick–virus interaction, particularly transmission pathways and vector competence. A comprehensive review of artificial tick infections using pathogens other than TBVs and the ixodid (hard) tick life cycle has already been made by Bonnet and Liu (2012). In this mini review, different techniques for the viral infection of hard ticks were presented, indicating their advantages and limitations with respect to their application to viral transmission and vector competency studies (summarized in **Table 1**).

METHODS FOR INFECTING TICKS

Direct Feeding on Infected Host

Infesting ticks on infected natural hosts remains the method most closely resembling the normal acquisition of a virus in the wild. Direct feeding on infected host can be facilitated by using feeding bags (**Figures 1a,b**) or feeding chambers (**Figures 1c,d**). However, the maintenance and handling of animal hosts can be expensive and difficult, particularly for wild animals (Bonnet and Liu, 2012). The direct feeding technique also lacks the capacity to quantify the pathogen dose acquired by the tick during or post feeding. The technique may also not be appropriate for virus strains not suited for replication in the vertebrate hosts (Mitzel et al., 2007). In addition, it remains a challenge to synchronize viremia with tick feeding, and for ethical reasons, the use of alternative artificial methods in infecting ticks without the use of laboratory animals is still preferred (Bonnet and Liu, 2012).

Various hosts, mostly small laboratory animals, have already been infected for direct tick acquisition of the virus. *Dermacentor andersoni* ticks were previously infected by infesting rabbits injected intravenously with large doses of the Powassan virus (Chernesky, 1969). Laboratory mice were also previously used to study severe fever with thrombocytopenia syndrome virus (SFTSV) transmission by *Haemaphysalis longicornis* (Luo et al., 2015), while *Rhipicephalus appendiculatus* specimens were infected with the Thogoto virus (THOV) by allowing them to feed on THOV-infected Syrian hamsters (Booth et al., 1989). Transmission of West Nile virus from infected mice to naïve *I. ricinus* nymphs through direct blood feeding was also previously observed (Lawrie et al., 2004).

Co-feeding Infection

Non-viremic transmission, or co-feeding transmission (**Figure 2c**), is an important transmission mechanism for TBVs established by Jones et al. (1987). It occurs between infected and uninfected ticks when they co-feed in close proximity on susceptible hosts, even when these hosts do not develop viremia (Alekseev and Chunikhin, 1990; Labuda et al., 1993; Jones et al., 1997; Labuda et al., 1997a,b). Though co-feeding is an established natural tick infection method, it requires an animal host for feeding and may not produce high infection rates, as transmission of the virus from infected and uninfected ticks greatly depends on the proximity or distance among feeding ticks.

Co-feeding experiments were mostly conducted in small laboratory or wild animals. Virus transmission experiments using yellow-necked mice (*Apodemus flavicollis*) and bank voles (*Clethrionomys glareolus*) (Labuda et al., 1996, 1997b), BALB/c mice (Khasnatinov et al., 2009; Slovák et al., 2014), European hedgehog (*Erinaceus europaeus*), striped field mouse (*A. agrarius*) European pine vole (*Pitymys subterraneus*), and common pheasant (*Phaseanus colchicus*) (Labuda et al., 1993) were used to study TBEV transmission by *I. ricinus.*

Co-feeding transmission of the Louping ill virus on *I. ricinus* was also evaluated in mountain hares (*Lepus timidus*), New Zealand white rabbits (*Oryctolagus cuniculus*) and red deer (*Cervus elaphus*) (Jones et al., 1997). Non-viremic transmission was also established for Thogoto virus (THOV) on *R. appendiculatus* (Jones et al., 1987, 1997) and CCHFV on *Hyalomma truncatum*, *H. impeltatum* (Gordon et al., 1993) and *Amblyomma variegatum* (Gonzalez et al., 1991) using guinea pigs (*Cavia porcellus*). Co-feeding transmission was also observed for Bhanja virus and Palma virus in *D. marginatus, D. reticulatus*, and *I. ricinus* ticks infested on mice (Labuda et al., 1997a) and Heartland virus in *Amblyomma americanum* infested on rabbits (Godsey et al., 2016). Lastly, co-feeding transmission of THOV was recently demonstrated in *H. longicornis* ticks infested on BALB/c mice (Talactac et al., 2018).

Membrane-Feeding Methods

Another alternative to tick infestation is through membrane feeding. Membranes from animal and non-animal origin (e.g., silicone membranes) are usually utilized, with variable success, to feed ticks. This method could also be used for studies on

TABLE 1 | Summary of the techniques used to artificially infect ticks with representative ticks and viruses, their major advantages/disadvantages and associated references.

Tick-infection methods	Tick species	Virus studied	Main advantages	Main disadvantages
Direct feeding on infected host	*D. andersoni* *H. longicornis* *R. appendiculatus*	Powassan virus[1] SFTS virus[2] Thogoto virus[3]	Can infect a greater number of ticks; resembles the normal acquisition	Requires animal host; lacks quantification of acquired viral load
Co-feeding infection	*I. ricinus*	TBEV[4–8] Louping ill virus[9] Bhanja virus[5]	An established natural viral infection of ticks	Requires animal host; greatly depends on the distance among feeding ticks
	D. marginatus	Palma virus[5]		
	R. appendiculatus	Thogoto virus[9,10]		
	H. truncatum	CCHFV[11]		
	A. americanum	Heartland virus[12]		
	H. longicornis	Thogoto virus[13]		
Membrane-feeding method	*I. ricinus* *I. ricinus* *D. reticulatus*	Bluetongue virus[14] African swine fever virus[15]	Reduces variation within a given treatment group	Requires chemical and physical stimuli to enhance tick attachment; depends on the length of the hypostome; long attachment time
Capillary feeding	*A. variegatum* *R. appendiculatus*	Dugbe virus[16]	Mimics the natural route of infection; can estimate the amount of introduced pathogen	Complicated maintenance of the integrity of the mouthparts of the ticks after removal
	I. ricinus *D. reticulatus*	Bluetongue virus[14]		
Percoxal injection	*H. longicornis*	Langat virus[17,18]	Can estimate the amount of pathogen to be introduced	Requires a microinjector; may produce higher tick mortality due to injury
	A. variegatum	Thogoto virus[19]		
	I. ricinus	TBEV[4–6,8,20]		
		Louping ill virus[9]		
Anal pore injection	*H. truncatum*	CCHFV[21]		
	I. ricinus	TBEV[19]		
	H. longicornis	Langat virus[17]		
Infection by immersion	*I. scapularis*	LGTV[22,23]	Low cost; relatively simple artificial method; can synchronously infect ticks with a defined virus stock	May not generate cohorts of infected ticks with equal pathogen burden
	A. americanum	Heartland virus[12]		

[1]*Chernesky (1969)*, [2]*Luo et al. (2015)*, [3]*Booth et al. (1989)*, [4]*Labuda et al. (1996)*, [5]*Labuda et al. (1997a)*, [6]*Khasnatinov et al. (2009)*, [7]*Slovák et al. (2014)*, [8]*Labuda et al. (1993)*, [9]*Jones et al. (1997)*, [10]*Jones et al. (1987)*, [11]*Gordon et al. (1993)*, [12]*Godsey et al. (2016)*, [13]*Talactac et al. (2018)*, [14]*Bouwknegt et al. (2010)*, [15] *De carvalho Ferreira et al. (2014)*, [16]*Steele and Nuttall (1989)*, [17]*Talactac et al. (2016)*, [18]*Talactac et al. (2017b)*, [19]*Kaufman and Nuttall (1996)*, [20]*Belova et al. (2012)*, [21]*Gonzalez et al. (1989)*, [22]*McNally et al. (2012)*, *and* [23]*Tumban et al. (2011)*.

the dynamics of pathogen transmission, since it can reduce the variation within a given treatment group because the blood meal from the same donor reduces the variation that may arise from individual tick–host relationships (Krober and Guerin, 2007).

However, this method requires chemical and physical stimuli to enhance attachment by hard ticks to membranes (Kuhnert, 1996). Its use may also depend on the length of the hypostome in all life stages of the hard ticks to be studied (Krober and Guerin, 2007). In addition, this type of artificial feeding is more challenging for ixodid ticks, since they require longer time for attachment (de Moura et al., 1997. This method was previously used in infecting *I. ricinus*, *I. hexagonus*, *D. reticulatus*, and *R. bursa* with the Bluetongue virus (Bouwknegt et al., 2010). The unlikely involvement of *I. ricinus* and *D. reticulatus* as biological vectors of African swine fever virus was also shown using membrane feeding (De carvalho Ferreira et al., 2014).

Infection Through Capillary Feeding

The introduction of pathogens to ixodid ticks via capillary feeding was first attempted by Chabaud (1950). In this technique, the ticks are normally pre-fed on animals, followed by a careful mechanical removal of ticks from the host. Eventually, a capillary tube containing the pathogen is placed over the tick's mouthparts, and the tick is immobilized on a slide (Burgdorfer, 1957; Bouwknegt et al., 2010). Capillary feeding provides a number of advantages, especially that it mimics the natural route of infection of ticks, and it can estimate the amount of pathogen to be introduced. However, maintaining the integrity of the mouthparts of the ticks after removal is crucial for a successful capillary feeding (Bonnet and Liu, 2012). This technique was previously used in infecting *A. variegatum* and *R. appendiculatus* with the Dugbe virus (Steele and Nuttall, 1989) and *I. ricinus*, *I. hexagonus*, *D. reticulatus*, and *R. bursa* with the Bluetongue virus (Bouwknegt et al., 2010).

Infection Through Injection

Direct injection of the virus inoculum through the cuticle (between the coxa and trochanter) has the advantage of estimating the viral dose received by the ticks (**Figure 2a**). However, this method bypasses the midgut barrier of ticks

FIGURE 1 | Feedings bags are glued or taped to clean-shaven ears of long-eared rabbit to allow tick engorgement **(a)**. *Haemaphysalis longicornis* nymphs infested on a rabbit's ear **(b)**. A mouse with a feeding chamber attached on its back **(c)**. Ixodes persulcatus adult ticks infested on a mouse via chamber feeding **(d)**. Tick infestation using feeding bags or chamber feeders can be readily utilized to infect ticks with viruses via direct feeding on infected hosts.

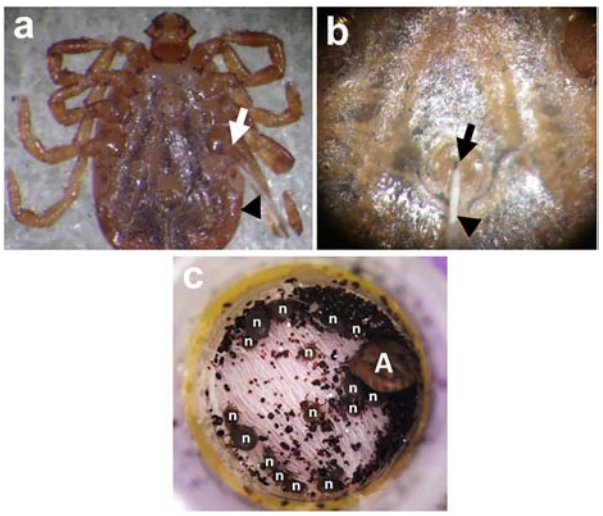

FIGURE 2 | Percoxal **(a)** and anal pore/rectal **(b)** injections to *H. longicornis* adult ticks. Infection is accomplished by injecting the virus inoculum containing an estimated virus titer using glass microneedles (black arrowheads) at the joint of the tick coxa and trochanter of the 4th pair of legs (white arrow) or into the tick's anal aperture (black arrow). After injection, ticks will be kept for 24 h in a 25°C incubator to observe for any mortality arising from possible injury due to the injection. Co-feeding **(c)** between a THOV-infected *H. longicornis* adult (A) and smaller uninfected/naïve nymphs (n). The ticks were infested on mice using feeding chamber/capsule method. All engorged nymphs post infestation will be collected and allowed to molt. Twenty-one days after molting, newly emerged adult ticks will be examined for either the presence of infectious virions or viral RNA using a focus formation assay or real-time PCR, respectively.

during feeding, making it unrepresentative of the natural route of infection for ticks (Mitzel et al., 2007). This technique also requires a microinjector to efficiently introduce the inoculum into the tick and may produce higher tick mortality due to injection injury (Rechav et al., 1999). Previous studies using this technique include the infection of *H. longicornis* with the Langat virus (Talactac et al., 2016, 2017a), *A. variegatum* with the Thogoto virus (Kaufman and Nuttall, 1996), *I. ricinus* with TBEV (Labuda et al., 1993, 1996, 1997b; Khasnatinov et al., 2009; Belova et al., 2012), and the Louping ill virus (Jones et al., 1997). *D. marginatus*, *D. reticulatus*, and *I. ricinus* ticks also previously received percoxal injections with the Bhanja and Palma viruses (Labuda et al., 1997a). Alternatively, anal pore or rectal injection of the virus directly into the gut of the tick can be used (**Figure 2b**), though it also requires skill to avoid puncturing the gut upon injection. This method has been used to infect *H. truncatum* with CCHFV (Gonzalez et al., 1989), *I. ricinus* with TBEV (Belova et al., 2012), and *H. longicornis* with Langat virus (Talactac et al., 2017b) and THOV (Talactac et al., 2018).

Infection Through Immersion

Infection of ticks through immersion provides a low cost and relatively simple artificial method, since it can synchronously infect a large number of ticks with a defined virus stock. The ticks are believed to be infected when they successfully swallowed the immersion medium containing the virus; with the ingested virus ultimately reaching the midgut (Mitzel et al., 2007). The virus can also possibly penetrate the tick's exoskeletons, especially the immature ones. Larvae and nymphs have less sturdy exoskeleton, since arthropods must be able to hydrolyze the chitin for cuticle degradation and development during the immature stages (You et al., 2003). However, its major limitation is the generation of cohorts of infected ticks with an equal pathogen burden (Kariu et al., 2011). Infection of ticks using this method was previously reported for *I. scapularis* infected with Langat virus (Tumban et al., 2011; McNally et al., 2012), the dengue virus (Tumban et al., 2011), and TBEV (Mitzel et al., 2007) and for *A. americanum* infected with the Heartland virus (Godsey et al., 2016).

CONCLUSION

To fully understand the interaction of ticks with TBVs, efficient techniques for the artificial infection and maintenance of tick colonies under laboratory conditions are crucial. As emphasized in this mini review, it is the unique but complicated feeding behavior of ixodid ticks that makes studies related to virus transmission, vector competence, and other aspects of tick–virus

interaction a challenging endeavor. However, with the availability of these alternative feeding methods and techniques to infect ticks with different viruses of public health importance, the potential for studies on TBVs to catch up with the advances in mosquito-borne viral disease research is no longer a far-fetched scenario. In addition, the limitations of current techniques do not outweigh importance of studying TBVs. Understanding the interactions between ticks and the TBVs they transmit offers a great opportunity to identify new targets for the future control of TBVs.

AUTHOR CONTRIBUTIONS

All authors listed have made a substantial, direct and intellectual contribution to the work, and approved it for publication.

FUNDING

This study was supported by the Japan Society for the Promotion of Science (JSPS) KAKENHI grant No. 15H05264, 16H05028, and 17K19328, the Takeda Science Foundation, and the Japanese Government Ministry of Education, Culture, Sports, Science and Technology Scholarship (Monbukagakusho: MEXT) for doctoral fellowship.

ACKNOWLEDGMENTS

We are grateful to K. Kusakisako of the Laboratory of Infectious Diseases, Joint Faculty of Veterinary Medicine, Kagoshima University, for his helpful comments and suggestions regarding this manuscript.

REFERENCES

Alekseev, A. N., and Chunikhin, S. P. (1990). Exchange of tick-borne encephalitis virusbetween Ixodidae simultaneously feeding on animals with subthreshold levels of viraemia. *Med. Parazitol.* 2, 48–50.

Arthur, D. G. (1962). *Ticks and Disease*. Oxford: Pergamon Press.

Belova, O. A., Burenkova, L. A., and Karganova, G. G. (2012). Different tick-borne encephalitis virus (TBEV) prevalences in unfed versus partially engorged ixodid ticks evidence of virus replication and changes in tick behavior. *Ticks Tick Borne Dis.* 3, 240–246. doi: 10.1016/j.ttbdis.2012.05.005

Bonnet, S., and Liu, X. Y. (2012). Laboratory artificial infection of hard ticks: a tool for the analysis of tick-borne pathogen transmission. *Acarologia.* 52, 453–464. doi: 10.1051/acarologia/20122068

Booth, T. F., Davies, C. R., Jones, L. D., Staunton, D., and Nuttall, P. A. (1989). Anatomical basis of thogoto virus infection in BHK cell culture and in the ixodid tick vector, *Rhipicephalus appendiculatus*. *J. Gen. Virol.* 70, 1093–1104. doi: 10.1099/0022-1317-70-5-1093

Bouwknegt, C., van Rijn, P. A., Schipper, J. J. M., Hölzel, D., Boonstra, J., Nijhof, A. M., et al. (2010). Potential role of ticks as vectors of bluetongue virus. *Exp. Appl. Acarol.* 52, 183–192. doi: 10.1007/s10493-010-9359-7

Brackney, D. E., and Armstrong, P. M. (2016). Transmission and evolution of tick-borne viruses. *Curr. Opin. Virol.* 21, 67–74. doi: 10.1016/j.coviro.2016.08.005

Brites-Neto, J., Duarte, K. M. R., and Martins, T. F. (2015). Tick-borne infections in human and animal population worldwide. *Vet. World* 8, 301–315. doi: 10.14202/vetworld.2015.301-315

Burgdorfer, W. (1957). Artificial feeding of ixodid ticks for studies on the transmission of disease agents. *J. Infect. Dis.* 100, 212–214. doi: 10.1093/infdis/100.3.212

Chabaud, A. G. (1950). Sur la nutrition artificielle destiques. *Ann. Parasitol. Hum. Comp.* 25, 142–147. doi: 10.1051/parasite/1950251042

Chernesky, M. A. (1969). Powassan virus transmission by ixodid ticks infected after feeding on viremic rabbits injected intravenously. *Can. J. Microbiol.* 6, 521–526. doi: 10.1139/m69-090

De carvalho Ferreira, H. C., Tudela Zúquete, S., Wijnveld, M., Weesendorp, E., Jongejan, F., Stegeman, A., et al. (2014). No evidence of African swine fever virus replication in hard ticks. *Ticks Tick Borne Dis.* 5, 582–589. doi: 10.1016/j.ttbdis.2013.12.012

de la Fuente, J., Antunes, S., Bonnet, S., Cabezas-Cruz, A., Domingos, A. G., and Estrada-Peña, A. (2017). Tick-pathogen interactions and vector competence: identification of molecular drivers for tick-borne diseases. *Front. Cell. Infect. Microbiol.* 7:114. doi: 10.3389/fcimb.2017.00114

de la Fuente, J., Estrada-Pena, A., Venzal, J. M., Kocan, K. M., and Sonenshine, D. E. (2008). Overview: ticks as vectors of pathogens that cause disease in humans and animals. *Front. Biosci.* 13:6938–6946. doi: 10.2741/3200

de Moura, S. T., da Fonseca, A. H., Fernandes, C. G., and Butler, J. F. (1997). Artificial feeding of *Amblyomma cajennense* (Fabricius, 1787) (Acari:Ixodidae) through silicone membrane. *Mem. Inst. Oswaldo Cruz.* 92, 545–548. doi: 10.1590/S0074-02761997000400019

Godsey, M. S., Savage, H. M., Burkhalter, K. L., Bosco-Lauth, A. M., and Delorey, M. J. (2016). Transmission of heartland virus (Bunyaviridae: Phlebovirus) by experimentally infected *Amblyomma americanum* (Acari: Ixodidae). *J. Med. Entomol.* 53, 1226–1233. doi: 10.1093/jme/tjw080

Gonzalez, J. P., Cornet, J. P., Wilson, M. L., and Camicas, J. L. (1991). Crimean-Congo haemorrhagic fever virus replication in adult *Hyalomma truncatum* and *Amblyomma variegatum* ticks. *Res. Virol.* 142, 483–488. doi: 10.1016/0923-2516(91)90071-A

Gonzalez, J. P., NDiaye, M., Diop, A., and Wilson, M. L. (1989). "Laboratoire d'Ecologie Virale," in *Rapport Annuel De l'Institut Pasteur De Dakar*, ed. J. P. Digoutte (Dakar: Institut Pasteur), 100–110.

Gordon, S. W., Linthicum, K. J., and Moulton, J. R. (1993). Transmission of crimean-congo hemorrhagic fever virus in two species of hyalomma ticks from infected adults to cofeeding immature forms. *Am. J. Trop. Med. Hyg.* 48, 576–580. doi: 10.4269/ajtmh.1993.48.576

Guerin, P. M., Kröber, T., McMahon, C., Guerenstein, P., Grenacher, S., Vlimant, M., et al. (2000). Chemosensory and behavioural adaptations of ectoparasitic arthropods. *Nova Acta Leopold.* 83, 213–229.

Hoogstraal, H. (1973). "Viruses and ticks," in *Viruses and Invertebrates*, ed. A. J. Gibbs (The Hague: North-Holland Publishings), 351–390.

Jones, L. D., Davies, C. R., Steele, G. M., and Nuttall, P. A. (1987). A novel mode of arbovirus transmission involving a nonviremic host. *Science* 237, 775–777. doi: 10.1126/science.3616608

Jones, L. D., Gaunt, M., Hails, R. S., Laurenson, K., Hudson, P. J., Reid, H., et al. (1997). Transmission of louping ill virus between infected and uninfected ticks co-feeding on mountain hares. *Med. Vet. Entomol.* 11, 172–176. doi: 10.1111/j.1365-2915.1997.tb00309.x

Kariu, T., Coleman, A. S., Anderson, J. F., and Pal, U. (2011). Methods for rapid transfer and localization of lyme disease pathogens within the tick gut. *J. Vis. Exp.* 48:2544. doi: 10.3791/2544

Kaufman, W. R., and Nuttall, P. A. (1996). *Amblyomma variegatum* (Acari: Ixodidae): mechanism and control of arbovirus secretion in tick saliva. *Exp. Parasitol.* 82, 316–323. doi: 10.1006/expr.1996.0039

Kazimírová, M., Thangamani, S., Bartíková, P., Hermance, M., Holíková, V., Štibrániová, I., et al. (2017). Tick-Borne Viruses and Biological Processes at the Tick-Host-Virus Interface. *Front. Cell. Infect. Microbiol.* 7:339. doi: 10.3389/fcimb.2017.00339

Khasnatinov, M. A., Ustanikova, K., Frolova, T. V., Pogodina, V. V., Bochkova, N. G., and Levina, L. S. (2009). Non-hemagglutinating flaviviruses: molecular mechanisms for the emergence of new strains via adaptation to European ticks. *PLoS One* 4:e7295. doi: 10.1371/journal.pone.0007295

Kopacek, P., Hajdusek, O., Buresova, V., and Daffre, S. (2010). Tick innate immunity. *Adv. Exp. Med. Biol.* 708, 137–162. doi: 10.1007/978-1-4419-80595_8

Krober, T., and Guerin, P. M. (2007). In vitro feeding assays for hard ticks. *Trends Parasitol.* 23, 445–449. doi: 10.1016/j.pt.2007.07.010

Kuhnert, F. (1996). Feeding of hard ticks in vitro: new perspectives for rearing and for the identification of systemic acaricides. *ALTEX*. 13, 76–87.

Labuda, M., Alves, M. J., Elečková, E., Kožuch, O., and Filipe, A. R. (1997a). Transmission of tick-borne bunyaviruses by cofeeding ixodid ticks. *Acta Virol.* 41, 325–328.

Labuda, M., Kozuch, O., Zuffová, E., Elecková, E., Hails, R. S., and Nuttall, P. A. (1997b). Tick-borne encephalitis virus transmission between ticks cofeeding on specific immune natural rodent hosts. *Virology* 235, 138–143.

Labuda, M., Austyn, J. M., Zuffova, E., Kozuch, O., Fuchsberger, N., Lysy, J., et al. (1996). Importance of localized skin infection in tick-borne encephalitis virus transmission. *Virology* 219, 357–366. doi: 10.1006/viro.1996.0261

Labuda, M., and Nuttall, P. A. (2004). Tick-borne viruses. *Parasitology* 129, S221–S245. doi: 10.1017/S0031182004005220

Labuda, M., Nuttall, P. A., Kozuch, O., Elecková, E., Williams, T., and Zuffová, E. (1993). Nonviremic transmission of tick-borne encephalitis virus: a mechanism for arbovirus survival in nature. *Experientia* 49, 802–805. doi: 10.1007/BF01923553

Lawrie, C. H., Uzcátegui, N. Y., Gould, E. A., and Nuttall, P. A. (2004). Ixodid and argasid tick species and west nile virus. *Emerg. Infect. Dis.* 10, 653–657. doi: 10.3201/eid1004.030517

Liu, L., Dai, J., Zhao, Y. O., Narasimhan, S., Yang, Y., Zhang, L., et al. (2012). Ixodes scapularis JAK-STAT pathway regulates tick antimicrobial peptides, thereby controlling the agent of human granulocytic anaplasmosis. *J. Infect. Dis.* 206, 1233–1241. doi: 10.1093/infdis/jis484

Luo, L., Zhao, L., Wen, H., Zhang, Z., Liu, J., Fang, L., et al. (2015). *Haemaphysalis longicornis* ticks as reservoir and vector of severe fever with thrombocytopenia syndrome virus in China. *Emerg. Infect. Dis.* 21, 1770–1776. doi: 10.3201/eid2110

Mansfield, K. L., Jizhou, L., Phipps, L. P., and Johnson, N. (2017). Emerging tick-borne viruses in the twenty-first century. *Front. Cell. Infect. Microbiol.* 7:298. doi: 10.3389/fcimb.2017.00298

McNally, K. L., Mitzel, D. N., Anderson, J. M., Ribeiro, J. M. C., Valenzuela, J. G., Myers, T. G., et al. (2012). Differential salivary gland transcript expression profile in ixodes scapularis nymphs upon feeding or flavivirus infection. *Ticks Tick Borne Dis.* 3, 18–26. doi: 10.1016/j.ttbdis.2011.09.003

Mitzel, D. N., Wolfinbarger, J. B., Long, R. D., Masnick, M., Best, S. M., and Bloom, M. E. (2007). Tick-borne flavivirus infection in ixodes scapularis larvae: development of a novel method for synchronous viral infection of ticks. *Virology* 365, 410–418. doi: 10.1016/j.virol.2007.03.057

Nuttall, P. A., Jones, L. D., Labuda, M., and Kaufman, W. R. (1994). Adaptations of arboviruses to ticks. *J. Med. Entomol.* 31, 1–9. doi: 10.1093/jmedent/31.1.1

Obenchain, F. D., and Galun, R. (1982). *The Physiology of Ticks*. Oxford: Pergamon Press.

Rechav, Y., Zyzak, M., Fielden, L. J., and Childs, J. E. (1999). Comparison of methods for introducing and producing artificial infection of ixodid ticks (Acari: Ixodidae) with *Ehrlichia chaffeensis*. *J. Med. Entomol.* 36, 414–419. doi: 10.1093/jmedent/36.4.414

Slovák, M., Kazimírová, M., Siebenstichová, M., Ustaníková, K., Klempa, B., Gritsun, T., et al. (2014). Survival dynamics of tick-borne encephalitis virus in ixodes ricinus ticks. *Ticks Tick Borne Dis.* 5, 962–969. doi: 10.1016/j.ttbdis.2014.07.019

Socolovschi, C., Mediannikov, O., Raoult, D., and Parola, P. (2009). The relationship between spotted fever group rickettsiae and ixodid ticks. *Vet. Res.* 40:34. doi: 10.1051/vetres/2009017

Steele, G. M., and Nuttall, P. A. (1989). Difference in vector competence of two species of sympatric ticks, *Amblyomma variegatum* and *Rhipicephalus appendiculatus*, for Dugbe virus (Nairovirus, Bunyaviridae). *Virus Res.* 14, 73–84. doi: 10.1016/0168-1702(89)90071-3

Talactac, M. R., Yada, Y., Yoshii, K., Hernandez, E. P., Kusakisako, K., Maeda, H., et al. (2017a). Characterization and antiviral activity of a newly identified defensin-like peptide, HEdefensin, in the hard tick *Haemaphysalis longicornis*. *Dev. Comp. Immunol.* 68, 98–107. doi: 10.1016/j.dci.2016.11.013

Talactac, M. R., Yoshii, K., Hernandez, E. P., Kusakisako, K., Galay, R. L., Fujisaki, K., et al. (2017b). Synchronous langat virus infection of *Haemaphysalis longicornis* using anal pore picroinjection. *Viruses.* 9:189. doi: 10.3390/v9070189

Talactac, M. R., Yoshii, K., Hernandez, E. P., Kusakisako, K., Galay, R. L., Fujisaki, K., et al. (2018). Vector competence of *Haemaphysalis longicornis* ticks for a Japanese isolate of the thogoto virus. *Sci. Rep.* 8:9300. doi: 10.1038/s41598-018-27483-1

Talactac, M. R., Yoshii, K., Maeda, H., Kusakisako, K., Hernandez, E. P., Tsuji, N., et al. (2016). Virucidal activity of *Haemaphysalis longicornis* longicin P4 peptide against tick-borne encephalitis virus surrogate langat virus. *Parasit. Vectors.* 9:59. doi: 10.1186/s13071-016-1344-5

Tumban, E., Mitzel, D. N., Maes, N. E., Hanson, C. T., Whitehead, S. S., and Hanley, K. A. (2011). Replacement of the 3' untranslated variable region of mosquito-borne dengue virus with that of tick-borne langat virus does not alter vector specificity. *J. Gen. Virol.* 92, 841–848. doi: 10.1099/vir.0.026997-0

Waladde, S. M., and Rice, M. J. (1982). "The sensory basis of tick feeding behaviour," in *Physiology of Ticks*, eds F. D. Obenchain and R. Galun (Oxford: Pergamon Press), 71–118.

Yoshii, K., Okamoto, N., Nakao, R., Klaus-Hofstetter, R., Yabu, T., Masumoto, H., et al. (2015). Isolation of the thogoto virus from a *Haemaphysalis longicornis* in Kyoto City, Japan. *J. Gen. Virol.* 96, 2099–2103. doi: 10.1099/vir.0.000177

You, M., Xuan, X., Tsuji, N., Kamio, T., Taylor, D., Suzuki, N., et al. (2003). Identification and molecular characterization of a chitinase from the hard tick *Haemaphysalis longicornis*. *J. Biol. Chem.* 278, 8556–8563. doi: 10.1074/jbc.M206831200

Conflict of Interest Statement: The authors declare that the research was conducted in the absence of any commercial or financial relationships that could be construed as a potential conflict of interest.

frontiers in Physiology

ORIGINAL RESEARCH
published: 05 December 2018
doi: 10.3389/fphys.2018.01696

Preliminary Evaluation of Tick Protein Extracts and Recombinant Ferritin 2 as Anti-tick Vaccines Targeting *Ixodes ricinus* in Cattle

*Sarah Knorr[1], Juan Anguita[2,3], Julen T. Cortazar[2], Ondrej Hajdusek[4], Petr Kopáček[4], Jos J. Trentelman[5], Olivia Kershaw[6], Joppe W. Hovius[5] and Ard M. Nijhof[1]**

[1] Institute for Parasitology and Tropical Veterinary Medicine, Freie Universität Berlin, Berlin, Germany, [2] Center for Cooperative Research in Biosciences (CIC bioGUNE), Derio, Spain, [3] Ikerbasque, Basque Foundation for Science, Bilbao, Spain, [4] Institute of Parasitology, Biology Centre, Czech Academy of Sciences, České Budějovice, Czechia, [5] Center for Experimental and Molecular Medicine, Academic Medical Center, University of Amsterdam, Amsterdam, Netherlands, [6] Institute of Veterinary Pathology, Freie Universität Berlin, Berlin, Germany

OPEN ACCESS

Edited by:
Itabajara Da Silva Vaz Jr., Universidade Federal do Rio Grande do Sul (UFRGS), Brazil

Reviewed by:
Lucas Tirloni, National Institute of Allergy and Infectious Diseases (NIAID), United States
Adriana Seixas, Federal University of Health Sciences of Porto Alegre, Brazil

***Correspondence:**
Ard M. Nijhof
ard.nijhof@fu-berlin.de

Specialty section:
This article was submitted to Invertebrate Physiology, a section of the journal Frontiers in Physiology

Received: *23 August 2018*
Accepted: *12 November 2018*
Published: *05 December 2018*

Citation:
Knorr S, Anguita J, Cortazar JT, Hajdusek O, Kopáček P, Trentelman JJ, Kershaw O, Hovius JW and Nijhof AM (2018) Preliminary Evaluation of Tick Protein Extracts and Recombinant Ferritin 2 as Anti-tick Vaccines Targeting Ixodes ricinus in Cattle. Front. Physiol. 9:1696. doi: 10.3389/fphys.2018.01696

Anti-tick vaccines have the potential to be an environmentally friendly and cost-effective option for tick control. In vaccine development, the identification of efficacious antigens forms the major bottleneck. In this study, the efficacy of immunization with recombinant ferritin 2 and native tick protein extracts (TPEs) against *Ixodes ricinus* infestations in calves was assessed in two immunization experiments. In the first experiment, each calf (n = 3) was immunized twice with recombinant ferritin 2 from *I. ricinus* (IrFER2), TPE consisting of soluble proteins from the internal organs of partially fed *I. ricinus* females, or adjuvant, respectively. In the second experiment, each calf (n = 4) was immunized with protein extracts from the midgut (ME) of partially fed females, the salivary glands (SGE) of partially fed females, a combination of ME and SGE, or adjuvant, respectively. Two weeks after the booster immunization, calves were challenged with 100 females and 200 nymphs. Blood was collected from the calves before the first and after the second immunization and fed to *I. ricinus* females and nymphs using an *in vitro* artificial tick feeding system. The two calves vaccinated with whole TPE and midgut extract (ME) showed hyperemia on tick bite sites 2 days post tick infestation and exudative blisters were observed in the ME-vaccinated animal, signs that were suggestive of a delayed type hypersensitivity (DTH) reaction. Significantly fewer ticks successfully fed on the three animals vaccinated with TPE, SGE, or ME. Adults fed on the TPE and ME vaccinated animals weighed significantly less. Tick feeding on the IrFER2 vaccinated calf was not impaired. The *in vitro* feeding of serum or fresh whole blood collected from the vaccinated animals did not significantly affect tick feeding success. Immunization with native *I. ricinus* TPEs thus conferred a strong immune response in calves and significantly reduced the feeding success of both nymphs and adults. *In vitro* feeding of serum or blood collected from vaccinated animals to ticks did not affect tick feeding, indicating that antibodies alone were not responsible for the observed vaccine immunity.

Keywords: *Ixodes ricinus*, anti-tick vaccine, salivary glands extract, midgut extract, ferritin, artificial tick feeding

INTRODUCTION

Ixodes ricinus is a tick species which is widespread in Europe and can transmit various bacterial, protozoal and viral pathogens of medical and veterinary importance, including the causal agents of Lyme borreliosis, tick-borne encephalitis (TBE) virus and babesiosis. Multiple studies have shown that the incidence of both Lyme borreliosis and TBE in several European countries have increased over the last decades (Smith and Takkinen, 2006; Fulop and Poggensee, 2008; Sykes and Makiello, 2017; Radzisauskiene et al., 2018). Lyme borreliosis is also the most common zoonotic vector-borne pathogen in the United States where *I. scapularis*, a sister species of *I. ricinus*, is the main arthropod vector (Schwartz et al., 2017).

The abundance and activity of *I. ricinus* ticks depends on abiotic factors, including relative humidity and temperature, as well as biotic factors such as adequate vegetation cover and vertebrate host availability (Randolph et al., 2002). *I. ricinus* is a three-host tick species with a broad host range; larvae and nymphs feed predominantly on rodents and birds, whereas the key reproduction hosts for adults are larger mammals (Gray et al., 1998). Control of *I. ricinus* and associated tick-borne diseases include personal preventive measures, such as the avoidance of tick habitats and a prompt removal of attached ticks, as well as environmental-based approaches, including habitat modification, a reduction of host densities or treatment of wildlife hosts with acaricides (Pound et al., 2012; Sprong et al., 2018). Another alternative targeted at controlling the tick vector is the use of anti-tick vaccines that would interfere with tick feeding and survival or pathogen transmission (Parizi et al., 2012; Sprong et al., 2014).

The first observations that animals repeatedly infested with ticks can develop an immune response that results in the rejection of ticks and that injection of tick extracts may also result in a partial immunity were made by William Trager in the 1930s (Trager, 1939a,b). This and similar studies formed the foundation for work by Australian scientists which led to the identification of the Bm86 antigen. This antigen is the principal component of the only commercialized anti-tick vaccine targeting an ectoparasite, the one-host tick *Rhipicephalus microplus*, to date (reviewed in Willadsen, 2004). The Bm86 protein was identified following multiple cycles of biochemical fractionation of immunogenic tick midgut extracts (MEs) followed by immunization trials with parasite challenges, with increasingly simpler protein mixtures being used for immunization in each successive cycle (Willadsen et al., 1989). Immunization with recombinant Bm86 was subsequently shown to be effective against *R. microplus* and a number of other tick species and homologs of Bm86 were identified in all main ixodid tick genera (de Vos et al., 2001; Nijhof et al., 2007). Immunization with two Bm86 orthologs isolated from *I. ricinus* was, however, not effective against conspecific tick infestations in rabbits (Coumou et al., 2015). More promising results for *I. ricinus* were obtained by immunization of rabbits with recombinant ferritin 2 (FER2). This protein is secreted by the tick midgut into the hemocoel and acts as an iron transporter, thus playing a pivotal role in the iron metabolism of ticks (Hajdusek et al., 2009). Immunization with recombinant FER2 in rabbits resulted in a reduction in tick numbers, engorgement weight and fertility rate of *I. ricinus* females feeding on immunized animals. Similar effects were observed for *R. annulatus* and *R. microplus* ticks feeding on cattle immunized with recombinant *R. microplus* FER2 (RmFER2) (Hajdusek et al., 2010). Other recombinant proteins that were evaluated for their efficacy in controlling *Ixodes* infestations in rabbits, mice and guinea pigs include subolesin (Almazan et al., 2005), tick cement protein 64TRP (Trimnell et al., 2005), the elastase inhibitor Iris (Prevot et al., 2007), sialostatin L2 (Kotsyfakis et al., 2008), a putative metalloprotease (Metis 1) (Decrem et al., 2008), anti-complement proteins IRAC I and IRAC II (Gillet et al., 2009), a cyclin-dependent kinase (Gomes et al., 2015), and aquaporin (Contreras and de la Fuente, 2017).

In this pilot study, we aimed to investigate if immunization of cattle to reduce *I. ricinus* tick feeding and reproduction is possible. To this purpose, we evaluated the use of recombinant FER2 as well as native tissue extracts. The cow was chosen as an animal model since it is a suitable host for infestations with high numbers of *I. ricinus* and also because large blood volumes can be safely drawn without affecting the animal's health (Wolfensohn and Lloyd, 2013). This facilitated the subsequent evaluation of collected antisera within an artificial tick feeding system (ATFS) to study individual components of the immunological response on tick feeding (Contreras et al., 2017).

MATERIALS AND METHODS

Calves and Ticks

Six-month-old Holstein-Friesian calves were purchased from a local dairy farm. Calves were housed on pastures of the Institute for Parasitology and Tropical Veterinary Medicine in Berlin during the first 7 weeks of the study (d0–d49). The pastures were considered to be free of ticks; natural tick infestations were not observed during this period. One week prior to tick challenge, they were moved to an enclosed cattle pen for the duration of the tick infestation. *I. ricinus* ticks for the *in vivo* challenge originated from the tick breeding unit of the Institute for Parasitology and Tropical Veterinary Medicine of the Freie Universität Berlin. For the *in vitro* feeding experiments, half of the adult *I. ricinus* ticks originated from the tick breeding unit. Prior to use, these were mixed with an equal number of adult *I. ricinus* ticks collected from the vegetation in and around Berlin, as previous (unpublished) work suggested that this might improve the attachment rate of ticks in the ATFS. All animal experiments were conducted with approval of the commission for animal experiments (LAGeSo, Berlin, registration number G0210/15).

Vaccine Preparation

Native Tick Protein Extracts

For the preparation of native tick protein extracts (TPEs), female *I. ricinus* ticks were prefer for 3–5 days on rabbits. Partially fed females weighing ∼30 to 70 mg were manually detached and washed for 30 s in 70% ethanol. They were subsequently dissected on a glass slide under ice-cold phosphate buffered saline (PBS, pH

7.2). The internal organs (midguts, salivary glands, Malpighian tubules, trachea, synganglia, and ovaries), were dissected and stored in PBS on ice. For preparation of the TPE used in the first immunization study, all internal organs except the midguts were pooled together. For the second immunization study, only the salivary glands and midguts were used for preparation of the salivary gland extract (SGE) and ME, respectively. Tissues were homogenized in an ultrasound homogenizer (Hielscher, UP100H) followed by centrifugation at 15,000 *g* for 30 min at 4°C. The supernatant of each extract was sterile filtered (0.2 μm non-pyrogenic filters, Sarstedt Germany) and stored at −20°C until use. Protein concentrations were measured by the CB-X™ Protein Assay (G Biosciences, United States) according to the manufacturer's instructions.

Ferritin 2 (FER 2)

Recombinant protein ferritin 2 from *I. ricinus* (IrFER2) was expressed in *E. coli* strain BL21 as previously described (Hajdusek et al., 2010).

Prior to immunization, TPE, SGE, and ME or recombinant IrFER2 were emulsified in a homogenizer (IKA Turrax T25 Mixer) with 1.5 mg saponin in 1 mL of Montanide ISA V50 adjuvant (SEPPIC, France) as specified by the adjuvant's manufacturer.

Study Outline

All calves were vaccinated intramuscularly (i.m.) twice at an interval of 6 weeks. Two weeks after the second immunization, each calf was challenged with ticks. The first study was performed with three calves: one calf received 100 μg IrFER2, the second calf ∼12 mg TPE (4 ME: 1 other internal organs), and the third calf was vaccinated with Montanide ISA 50 adjuvant and saponin only. The second study was performed with four calves: one calf was vaccinated with ∼6 mg SGE, one with ∼9 mg ME, one with a ∼8 mg combination of ME and SGE (4 ME : 1 SGE) and a control calf with Montanide ISA 50 adjuvant and saponin only.

Tick Challenge

Two weeks after the second immunization, each animal was infested with 200 nymphs, 100 adult males, and 100 *I. ricinus* females. The ticks were equally divided over two linen bags, which were attached to the basis of the unshaved ears using adhesive tape (Leukoplast, BSN medical, Hamburg, Germany).

Following a resting period of 2 days to allow ticks to attach undisturbed, bags were checked twice per day and engorged nymphs or females were removed and weighed. Adult females were subsequently stored individually and nymphs were stored in small batches in glass tubes. The tubes containing the ticks were stored in a desiccator with 80% relative humidity (RH), which was placed in a climate chamber at 20°C and a light-dark-cycle of 14–10 h.

In vitro Tick Feeding

The ATFS used for the feeding of plasma or whole blood from the vaccinated calves to *I. ricinus* ticks *in vitro* was based on a previously published protocol (Krober and Guerin, 2007) which was further optimized in house (Krull et al., 2017). In short, tick feeding units were made of borosilicate glass tubes with a 28 mm inner diameter, 2 mm wall thickness, and height of 65 mm. The feeding units were closed on one end with a silicone membrane with a thickness of 80–120 μm for adults and 70–90 μm for nymphs. The silicone membranes were attached to the tick feeding unit using silicone glue. A square piece of glass fiber mosquito netting, approximately 20 mm × 20 mm in size, was glued to the silicone membrane inside the feeding units used for adult ticks to provide tactile stimuli. Silicone glue was applied to two sides of the square mosquito netting only, leaving sufficient space for ticks to crawl underneath the netting. Bovine hair extract (Krull et al., 2017) and bovine hair were dispersed over the silicone membrane to stimulate tick attachment. Ten females with 5–7 males, or 50 nymphs were placed in each feeding unit, which was subsequently placed in a climate chamber set at 20°C, 80% RH, 5% CO_2 and 14 h light–10 h dark cycle.

Before the first (d0) and 2 weeks after the second immunization (d56), 1.5 L blood was collected from each calf. Blood was centrifuged at 3,500 *g* for 30 min at 4°C to separate blood cells and plasma. Plasma was collected and stored at −20°C until use.

For the first study and nymphal tick feeding of the second study, collected plasma was mixed with the erythrocyte and buffy coat layer of bovine blood collected at a local slaughterhouse. Blood cells were washed twice and subsequently stored at 4°C in modified Vega y Martinez phosphate-buffered saline solution containing 20% glucose (Zweygarth et al., 1995). Blood cells were overlaid with two-thirds of buffer. Blood cells and stored plasma were mixed in a 2:1 ratio, resulting in whole blood with a packed cell volume (PCV) of 33%. Ticks were subsequently fed using the ATFS. Before each feeding, gentamycin (10 mg/mL) and 0.1 M adenosine triphosphate (ATP) were added to the blood meal.

During the second study, blood for the *in vitro* feeding of *I. ricinus* adults was collected from each calf on day 55, day 62, and day 68 in the presence of heparin (20 I.U./mL) and glucose (2 g/L). Prior to *in vitro* feeding, it was supplemented with gentamycin (10 mg/mL) and 0.1 M ATP and preheated to 37°C on a hot plate (Hot Plate 062, Labotect, Göttingen, Germany). Blood was changed twice per day. Detached and replete adults and nymphs were weighed and stored individually in a desiccator with 80% RH at RT.

Enzyme-Linked Immunosorbent Assay (ELISA)

Blood was collected weekly from each calf in a serum tube (Microvette®, Sarstedt, Germany). After coagulation, blood samples were centrifuged at 2,800 *g* for 5 min. The serum was subsequently withdrawn and stored until use at −20°C. A 96-well plate (F-bottom, Medium binding; Greiner Bio-one) was coated with 2.5 μg/mL TPE, ME or SGE or 0.5 μg/mL IrFER2 in coating buffer (0.05 M carbonate-bicarbonate; pH 9.6) at 20°C for 1 h and at 4°C overnight. Serum samples diluted 1:200 in 0.05% PBS-Tween were added to each well and the plate was incubated at 37°C for 30 min. Mouse anti-bovine IgG antibody, horseradish peroxidase-conjugated (Acris Antibodies GmbH) was diluted

1:5000 in 0.05% PBS-T and incubated at 37°C for 30 min. O-phenylenediamine (OPD-P9187, Sigma Aldrich) was used as substrate and resulting color was measured with Epoch Microplate Spectrophotometer (BioTek) at 492 nm. The plate was washed three times with 0.05% PBS-Tween after each incubation step.

IgM, IgG1, and IgG2 antibody titration experiments were performed using eight serial dilutions, from 1:100 to 1:12,800, of sera from the first and second immunization experiment. Here, the amount of total protein used for coating was 0.5 μg/mL in carbonate buffer. The plates were then washed, blocked with 1% fetal bovine serum in PBS, incubated with the sera dilutions followed by specific secondary antibodies against bovine IgG1, IgG2, and IgM conjugated with horseradish peroxidase (Bio-Rad). The ELISAs were developed using HRP substrate (Kirkegaard and Perry Laboratories, Gaithersburg, MD, United States) and read at 450 nm.

Western Blot

Five micrograms of purified Ferritin 2 or tissue extracts were resolved in 4–20% precast polyacrylamide gels (Bio-Rad) and transferred to nitrocellulose membranes (Bio-Rad). The membranes were blocked for 2 h in PBS + 5% skim milk, followed by incubation with calf sera in PBS containing 0.1% Tween 20 (PBST) at 1:1000 dilution for 2 h. The membranes were washed three times with PBST, and incubated with a 1:10,000 dilution of anti-bovine IgG (Life Technologies) conjugated with horseradish peroxidase for a period of 1 h. After extensive washing the membranes were briefly incubated with HRP substrate (SuperSignal West Femto Maximum Sensitivity Substrate, Life Technologies) and developed in a ChemiDoc Gel Imaging System (Bio-Rad).

Skin Sample Collection and Histological Processing

Biopsies were taken from euthanized animals of the second study at d68 from areas where ticks had fed and processed using routine histological techniques.

Statistical Analyses

Engorgement weight of adult ticks and nymphs were analyzed using GraphPad Prism version 5.03 for Windows, GraphPad Software, La Jolla, CA, United States[1]. For normally distributed data one-way ANOVA followed by Bonferroni's multiple comparison test was performed. Kruskal-Wallis test and Dunn's post-test was conducted for data with non-Gaussian distribution. $P \leq 0.05$ was considered significant for all tests. *P*-values for number of ticks and molting rate of nymphs were calculated with mid-p-exact test using OpenEpi version 3.01[2]. *P*-values were adjusted according to Holm correction in RStudio version 3.4.3.

[1]http://www.graphpad.com

[2]http://openepi.com

RESULTS

Immune Response

Indirect ELISA-results demonstrated that the IrFER2 and TPE vaccinated calf each developed antibody titers against recombinant IrFER2 and native TPE, respectively. Serum from the TPE vaccinated animal did not clearly recognize IrFER2 (**Figure 1**). These results were confirmed by Western blot, which also showed that immune sera from the TPE-immunized animal recognized ME, SGE and ovary proteins. Recombinant IrFER2 and native tick proteins were not recognized by pre-immune sera of the IrFER2 and TPE-immunized animals, respectively (**Figure 2**).

Calves from the second study, immunized with ME, SGE or a combination thereof developed higher antibody titers compared to the TPE-vaccinated calf from the first study. The calf immunized with ME showed a strong immune response against both ME and SGE and developed the highest antibody titer of all vaccinated calves (**Figure 3**). Antibody titration experiments predominantly showed a IgG1 and, to a lesser extent, IgG2 response in sera from the ME and SGE-immunized calves and the calf immunized with a combination of ME and SGE. A clear IgM response was not detected (**Figure 4**).

Tick Challenge

Two days post tick infestation, hyperemia and oedema on the tick bite sites on the ears of TPE vaccinated calf were observed (**Figure 5**). These reactions were not observed on the ears of the IrFER2 vaccinated or control calf. On the negative control, 70 female ticks engorged, with a mean weight of 245.8 ± 85.3 mg. This was not statistically different from the IrFER2-vaccinated animal, on which 87 ticks engorged with a mean weight of with 268.6 ± 82.0 mg. Only 22 ticks fed to repletion on the TPE-immunized calf, with a significantly reduced engorgement weight of 126.6 ± 86.9 mg ($p \leq 0.001$). The results for the nymphs fed on the TPE-vaccinated calf showed a similar trend: 14 from 200 nymphs were able to engorge compared to 128/200 and 145/200 nymphs from the control and IrFER2-vaccinated animal, respectively, but there was no significant difference between the engorgement weights (**Table 1**).

Control and SGE vaccinated calves of the second study did not show a clear skin response at 2 days post tick infestation. The calf immunized with a combination of SGE and ME showed similar inflammatory signs on the tick bite sites with hyperemia as observed in the first study. The ME vaccinated animal showed a severe cutaneous reaction with a papular reaction at the tick attachment site with serous exudation 2 days post infestation (**Figure 6**). Histological examination of the ears could only be performed at d68 post immunization after the tick infestation in the second immunization experiment. It showed an extensive infiltration of the dermis with eosinophils and macrophages in the ears of animals immunized with SGE, ME and a combination of both extracts that was absent in the skin of the control animal (**Figure 7**).

Adults fed on SGE (187.8 ± 102.4 mg, $n = 63$) or SGE and ME (140.6 ± 89.5 mg, $n = 25$) immunized calves had a significantly

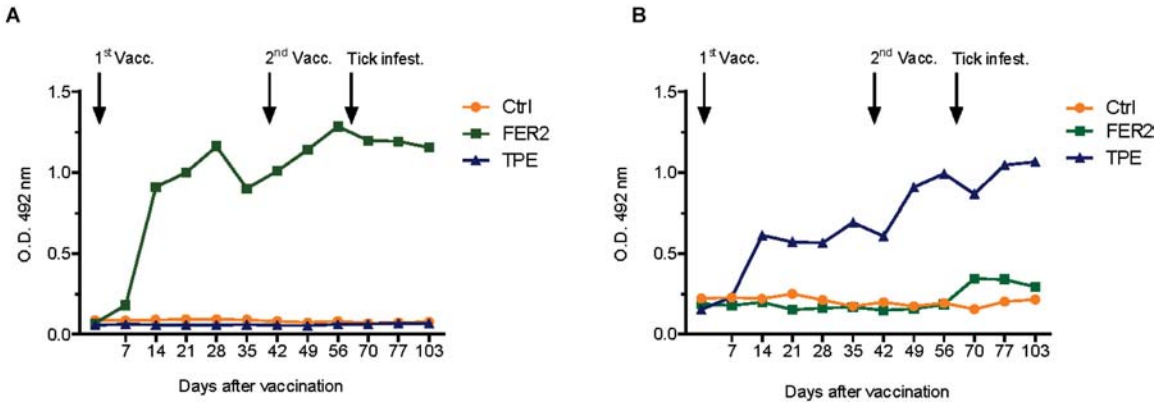

FIGURE 1 | Antibody response in vaccinated animals of the first cattle immunization study. Bovine serum (diluted 1:200) antibody titers to **(A)** recombinant ferritin 2 (FER2) and **(B)** tick protein extract (TPE) were determined by indirect ELISA in cattle vaccinated with FER2, TPE, and adjuvant control.

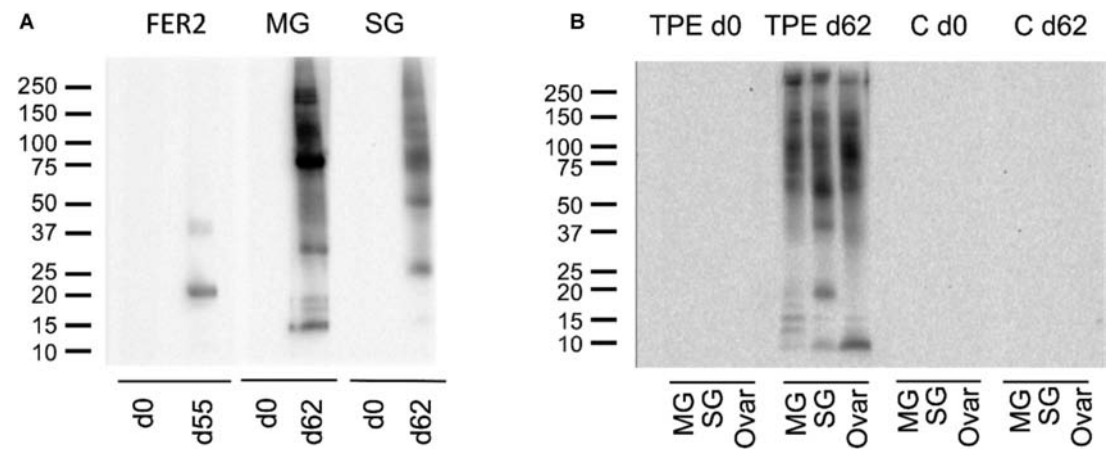

FIGURE 2 | (A) Western blot of recombinant ferritin 2 (FER2), native midgut (MG), and salivary gland (SG) extracts, probed with pre-immune and immune sera of calves vaccinated with recombinant ferritin 2 (lanes 1 and 2) and tick protein extract (lanes 3 to 6); **(B)** western blot of native MG, SG, and Ovaries (Ovar) extracts, probed with pre-immune and immune sera of the calf vaccinated with tick protein extracts (TPE) and the control calf (C).

($p \leq 0.001$) lower engorgement weight compared to adults fed on control (262.2 ± 70.8 mg, $n = 69$). Only two adult ticks were able to engorge on the ME vaccinated calf, with a significantly lower engorgement weight (79.0 ± 19.7 mg) in comparison to the control ($p \leq 0.05$). For all vaccinated calves, a reduced number (SGE $n = 23$; ME $n = 11$; SGE and ME $n = 20$) of nymphs could engorge compared to the Ctrl ($n = 92$), but no significant differences between engorgement weights were observed. Mean engorgement weights and statistical results for adult ticks and nymphs of the second study are shown in **Table 2**.

In vitro Tick Feeding

For the first study, the percentage of ticks that attached and successfully fed in the ATFS ranged from 33 to 44% per group for females and from 35 to 42% for nymphs. No significant differences in number of ticks that completed feeding and their engorgement weights were found. The attachment and engorgement rates of the second study were comparable to that of the first and ranged from 24 to 44% for both females and nymphs. Slightly higher female engorgement weights compared to that of the first *in vitro* study were recorded. Again, an effect of *in vitro* feeding of either stored plasma or fresh whole blood on tick engorgement was not observed. Mean engorgement weights and statistical results for adult ticks and nymphs of 1st and 2nd immunization study are shown in **Tables 1**, **2**, respectively.

DISCUSSION

Immunization with recombinant IrFER2 or native tick proteins elicited a clear antibody response in the immunized animals. Interestingly, sera of the animal vaccinated with ME also recognized salivary gland antigens in the indirect ELISA and vice versa (**Figure 3**), suggesting the presence of common epitopes in both ME and SGE. Similar findings were previously reported in cattle vaccinated with *R. microplus* gut membrane antigens (Opdebeeck and Daly, 1990) and recent data for *I. ricinus* also

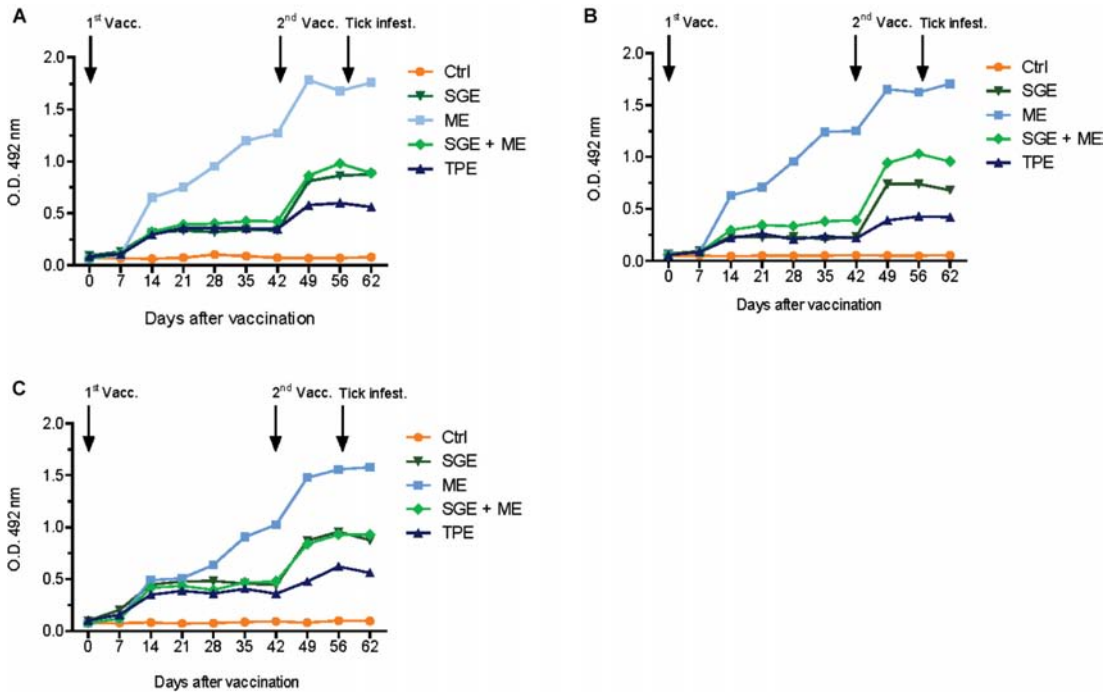

FIGURE 3 | Antibody response in vaccinated animals of the second cattle immunization study. Bovine serum (diluted 1:200) antibody titers to **(A)** midgut extract (ME), **(B)** salivary gland extract (SGE), and **(C)** SGE and ME were determined by indirect ELISA in cattle vaccinated with ME, SGE and a combination of ME and SGE and the adjuvant control. For comparison purposes, serum from the TPE-vaccinated animal from the first immunization study was also included in the ELISA.

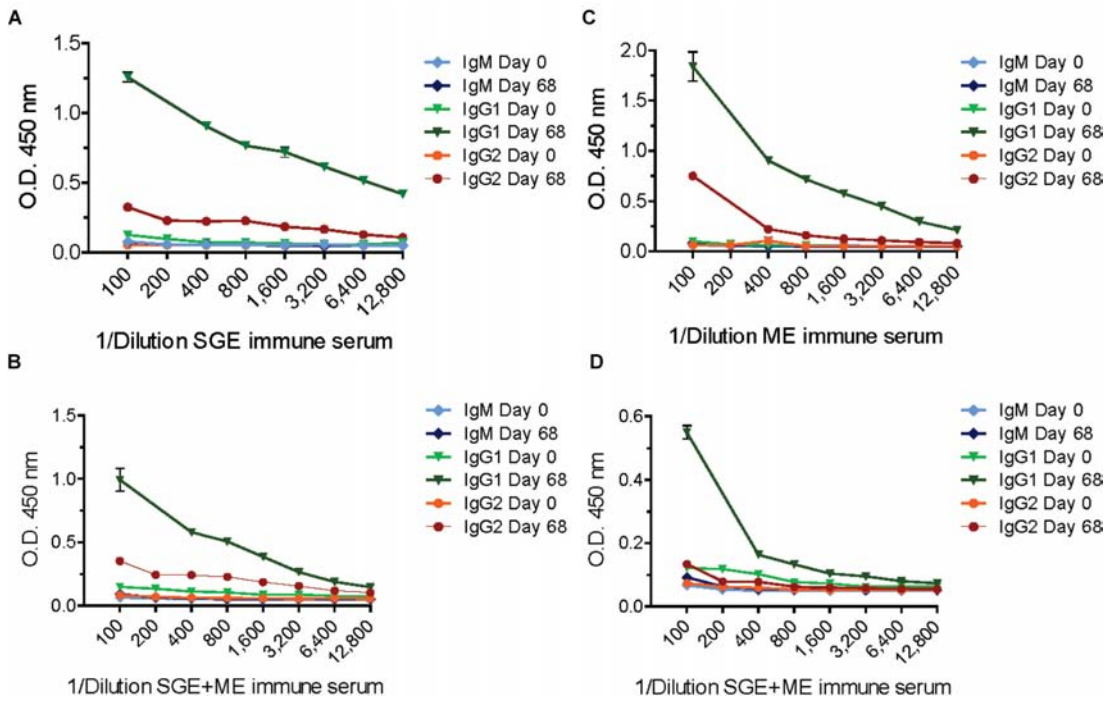

FIGURE 4 | Titrated IgM, IgG1, and IgG2 antibody response in animals vaccinated with salivary gland extract (SGE), midgut extract (ME) or a combination of both SGE and ME (SGE+ME). Plates were coated with 0.5 μg/mL SGE **(A,B)** or ME **(C,D)**, respectively.

FIGURE 5 | Photograph of the ear from the TPE vaccinated cow, 2 days after tick infestation, showing hyperaemia and oedema around the tick feeding sites.

indicates the presence of shared transcripts and proteins between salivary glands and midguts (Schwarz et al., 2014; Perner et al., 2016). It is not known if these common epitopes are peptides or carbohydrates; efforts to deglycosylate the tissue extracts by enzymatic deglycosylation or sodium hydroxide to investigate this in more detail were not successful (data not shown). It is also striking that the strongest cutaneous response was observed in the ME-vaccinated animals, with a marked papular swelling at the tick attachment site and extensive serous exudate, a finding that supports the presence of shared epitopes between ME and saliva proteins. The regurgitation of midgut proteins during the feeding process might form an alternative explanation for the observed cutaneous response. There is some evidence that ticks may regurgitate gut contents during feeding (Brown, 1988) and it has also been suggested that pathogens might be transmitted by this route (Burgdorfer et al., 1989). However, the presence of a pharyngeal valve in ticks, which is considered to be an effective barrier preventing regurgitation, argues against this, making regurgitation of gut contents a little understood and controversial phenomenon (Sonenshine and Anderson, 2014). The skin reaction became apparent at 48 h after the ticks were placed on the ear, which together with the observed response is indicative of a type IV delayed hypersensitivity (DTH) reaction. Nymphs in particular might have become trapped in the exudate and died as a result, which may have contributed to the low number of ticks recovered from this animal. DTH reactions have also been observed in immunization studies targeting other hematophagous arthropods; immunization with a 15 kD salivary gland protein of the sandfly vector of leishmaniosis, *Phlebotomus papatasi* (Valenzuela et al., 2001) resulted in a humoral and strong DTH responses upon subsequent exposure to *P. papatasi* and immunization with the 64 TRP antigen derived from the cement cone of *R. appendiculatus* ticks was also shown to induce strong humoral and DTH responses (Trimnell et al., 2005).

Although the FER2 immunized calf developed a high antibody titer, tick feeding on this calf was not impaired. This is in contrast to previous findings of a immunization experiment in which the tick number, engorgement weight, oviposition and fertility of *I. ricinus* feeding on immunized rabbits ($n = 2$) were reduced after threefold immunization with 100 μg IrFER2 (Hajdusek et al., 2010). The small group size or use of individual animals in both studies, animal species-specific differences and differences in the immunization schedule might explain these contrasting findings. Recombinant IrFER2 produced in *E. coli* was not recognized by serum from the TPE vaccinated animal. This can be explained by the assumption that the amount of ferritin 2 in the TPE was minute, as it is mainly expressed in the midgut but secreted into the tick plasma, which was the only tissue where the protein could previously be detected by Western Blot (Hajdusek et al., 2009).

Immunization of calves with native TPEs from adult ticks was more successful in inhibiting tick feeding. Immunization with extracts containing midgut proteins (TPE, ME and a combination of both ME and SGE) in particular resulted in a significant reduction in the number of females and nymphs that fed successfully and also in a significant reduction in the engorgement weights of females. As the native proteins were extracted from adult females, the observed effect on nymphs could be explained by the presence of conserved proteins in both nymph and adult ticks. A recent proteomic study indeed showed a considerable overlap between proteins identified in nymphal and adult salivary glands and midguts (Schwarz et al., 2014).

The effect of immunization with soluble midgut proteins prepared from adult ticks on tick feeding has been previously evaluated for a number of metastriate tick species, including *Amblyomma variegatum*, *Dermacentor andersoni*, *Hyalomma anatolicum*, *H. dromedarii*, *R. annulatus, R. microplus*, *R. appendiculatus*, *R. sanguineus* and the soft tick *Ornithodoros erraticus* (Allen and Humphreys, 1979; Jongejan et al., 1989; Wong and Opdebeeck, 1989; Rechav et al., 1992; Kimaro and Opdebeeck, 1994; Szabo and Bechara, 1997; Banerjee et al., 2003; Manzano-Roman et al., 2006; Nikpay and Nabian, 2016). The reported efficacy of immunization of these trials was, however, rarely as high as reported in this study, with reductions in tick numbers ranging from 63% for ticks feeding on the animal immunized with a combination of SGE and ME, to 97% in the ME-immunized animal. This could again be due to the small number of animals used in this study and/or the mechanical disturbance of ticks caused by the serous exudate at the tick feeding site in the ME-vaccinated animal, but it does indicate that the immunization procedure followed was successful and that the development of tick immunity against *I. ricinus* through immunization in cattle is possible. The optimal amount of native TPEs that confers tick immunity in animals is not known; amounts used in previous studies with cattle ranged from three immunizations with 100 μg salivary gland proteins (Nikpay and Nabian, 2016) to one immunization with 200 mg midgut protein followed by three booster immunizations with 150 mg midgut protein (Essuman et al., 1991). Differences in the tick and host species used, as well as differences in the preparation of antigen extracts and the presentation of vaccine efficacy, make it difficult to draw any conclusions on this matter from previous studies. We therefore followed a pragmatic approach by using the maximum amount of proteins that could be extracted from the partially fed females, which turned out to be in the range of ∼6 to ∼12 mg protein.

TABLE 1 | Tick challenge and *in vitro* tick feeding results of 1st study.

Study	Life stage		Ctrl	TPE	IrFER2	TPE d0
Tick challenge	Adults	No	70^{ab}	22^{ac}	87^{bc}	
		EW (mg)	245.8 ± 85.3^{d}	126.6 ± 86.9^{de}	268.6 ± 82.0^{e}	
	Nymphs	No	128^{f}	14^{fg}	145^{g}	
		EW (mg)	3.6 ± 0.9	3.1 ± 1.0	3.5 ± 0.9	
		Molting rate (%)	70^{h}	36^{hi}	71^{i}	
		Sex of nymphs	54♀ 35♂	2♀ 3♂	59♀ 44♂	
In vitro	Adults	No	39	33	44	40
		EW (mg)	193.8 ± 74.8	177.8 ± 71.9	190.9 ± 79.3	201.4 ± 74.8
	Nymphs	No	84	79	70	
		EW (mg)	2.6 ± 0.9	2.7 ± 0.9	2.6 ± 0.8	
		Molting rate (%)	45^{j}	49^{k}	9^{jk}	
		Sex of nymphs	16♀ 20♂	27♀ 17♂	2♀ 4♂	

No, number of engorged ticks; EW, engorgement weight. Mean values ± SD tested in a one-way analysis of variance (ANOVA) followed by Kruskal-Wallis test for multi-group comparisons. P-values for number of ticks and molting rate (in percent) were tested by mid-p-exact test. P-values were adjusted according to Holm correction. Significantly differences are indicated by letters and p-values. The sex of nymphs was determined after molting.

[a]Mid-P-exact test, p-value adjustment by Holm correction; $p < 0.0001$. [b]Mid-P-exact test, p-value adjustment by Holm correction; $P = 0.0036$. [c]Mid-P-exact test, p-value adjustment by Holm correction; $p < 0.0001$. [d]Kruskal-Wallis test, Dunn's post hoc-test; $p < 0.0001$. [e]Kruskal-Wallis test, Dunn's post hoc-test; $p < 0.0001$. [f]Mid-P-exact test, p-value adjustment by Holm correction; $p < 0.0001$. [g]Mid-P-exact test, p-value adjustment by Holm correction; $p < 0.0001$. [h]Mid-P-exact test, p-value adjustment by Holm correction; $P = 0.0355$. [i]Mid-P-exact test, p-value adjustment by Holm correction; $P = 0.0355$. [j]Mid-P-exact test, p-value adjustment by Holm correction; $p < 0.0001$. [k]Mid-P-exact test, p-value adjustment by Holm correction; $p < 0.0001$.

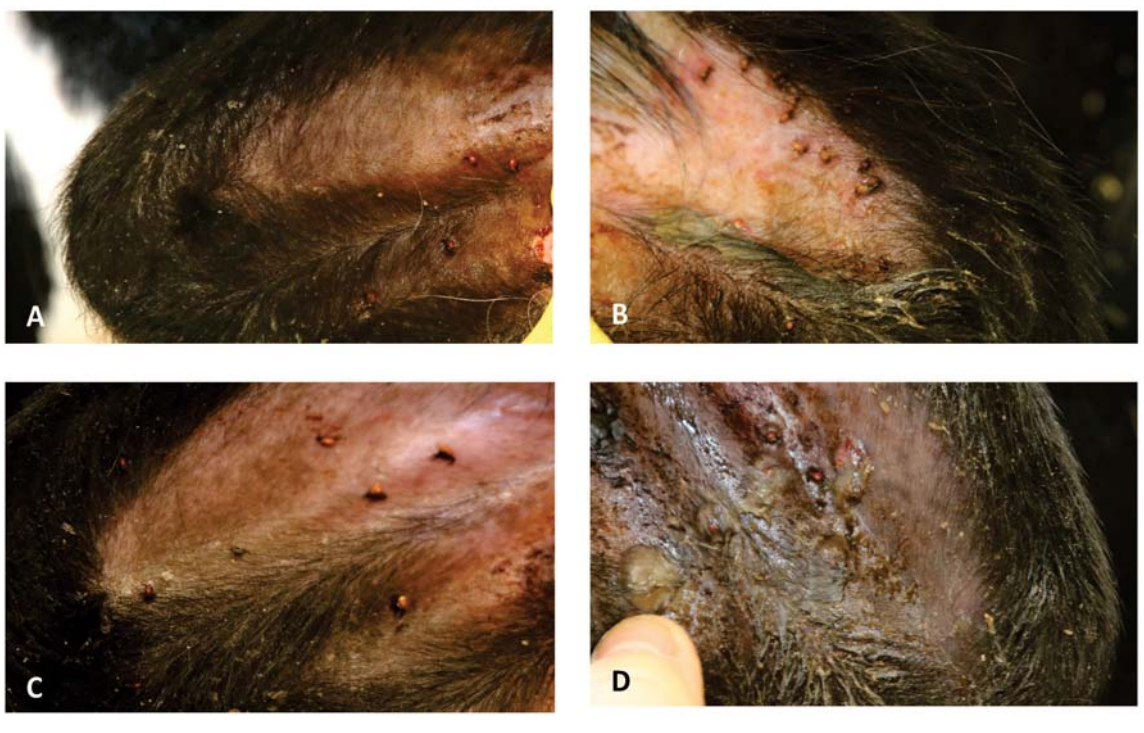

FIGURE 6 | Photographs of the ears from the vaccinated calves of the second immunization experiment, 2 days post-infestation. **(A)** Control animal; **(B)** SGE+ME-immunized calf; **(C)** SGE-immunized calf; **(D)** ME-immunized calf.

Feeding of blood from the vaccinated animals *in vitro* using the ATFS showed that the humoral response of the immunized animals alone did not affect tick feeding. It differs in this regard to the mode of action of the Bm86 vaccine, where the *in vitro* feeding of IgG1 antibodies in particular was shown to cause tick gut damage in *R. microplus* (Kemp et al., 1989). Further identification of the tissue extract antigens that were primarily responsible for the observed protective immune responses would be of great interest in the future development of vaccines targeting *I. ricinus* ticks.

Control of *Ixodes* tick infestations in important reproduction hosts such as deer by using the "4-Poster" acaricide dispensing

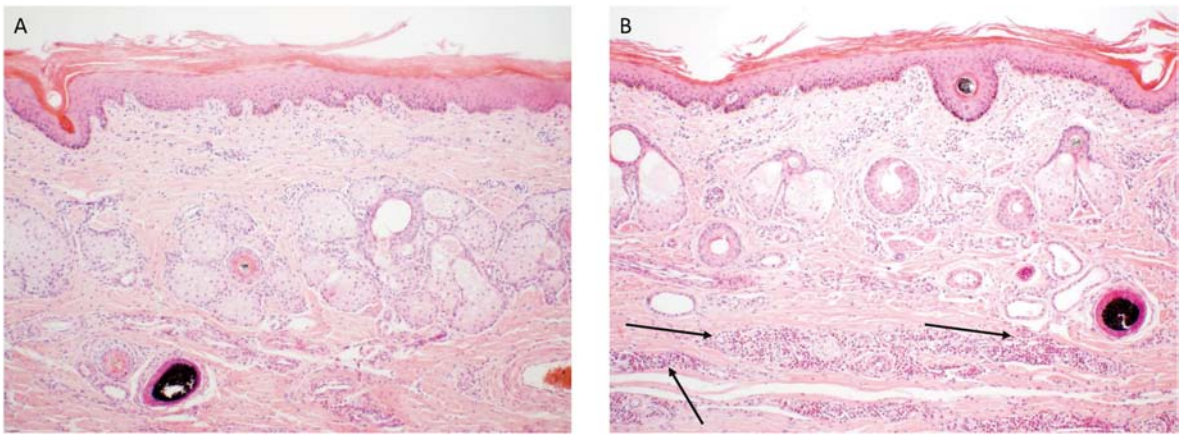

FIGURE 7 | Histopathology of the ear skin from the control **(A)** and ME-immunized animal **(B)**. The arrows indicate the mixed inflammatory infiltrate mainly composed of eosinophils and macrophages in the dermis of the ME-immunized animal. The biopsies were taken at d68 post immunization and stained with hematoxylin and eosin (100× magnification).

TABLE 2 | Tick challenge and *in vitro* tick feeding results of 2nd study.

Study	Life stage		Ctrl	SGE+ME	ME	SGE
Tick challenge	Adults	No	67^{ab}	25^{acd}	2^{bce}	63^{de}
		EW (mg)	262.1 ± 70.8^{fg}	140.6 ± 89.5^{f}	79.0 ± 19.7	187.8 ± 102.4^{g}
	Nymphs	No	92^{hij}	20^{h}	11^{i}	23^{j}
		EW (mg)	3.5 ± 1.0	3.2 ± 1.0	3.6 ± 0.7	3.8 ± 1.1
		Molting rate (%)	86^{k}	15^{kl}	55^{m}	100^{lm}
		Sex of nymphs	42♀ 37♂	0♀ 3♂	6♀ 0♂	15♀ 8♂
In vitro	Adults	No	23	23	18	32
		EW (mg)	256.4 ± 102.5	205.3 ± 68.9	195.7 ± 72.0	239.3 ± 92.4
	Nymphs	No	48^{no}	87^{n}	65	76^{o}
		EW (mg)	2.8 ± 0.9	2.8 ± 0.9	2.7 ± 0.9	2.7 ± 0.8
		Molting rate (%)	54^{pq}	34	26^{p}	29^{q}
		Sex of nymphs	10♀ 16♂	8♀ 22♂	5♀ 12♂	7♀ 15♂

No, number of engorged ticks; EW, engorgement weight. Mean values ± SD tested in a one-way analysis of variance (ANOVA) followed by Kruskal-Wallis test for multi-group comparisons. P-values for number of ticks and molting rate (in percent) were tested by mid-p-exact test. P-values were adjusted according to Holm correction. Significantly differences are indicated by letters and p-values. The sex of nymphs was determined after molting.

[a]Mid-P-exact test, p-value adjustment by Holm correction; $p < 0.0001$. [b]Mid-P-exact test, p-value adjustment by Holm correction; $p < 0.0001$. [c]Mid-P-exact test, p-value adjustment by Holm correction; $p < 0.0001$. [d]Mid-P-exact test, p-value adjustment by Holm correction; $p < 0.0001$. [e]Mid-P-exact test, p-value adjustment by Holm correction; $p < 0.0001$. [f]Kruskal-Wallis test, Dunn's post hoc-test; $p < 0.0001$. [g]Kruskal-Wallis test, Dunn's post hoc-test; $p < 0.0001$. [h]Mid-P-exact test, p-value adjustment by Holm correction; $p < 0.0001$. [i]Mid-P-exact test, p-value adjustment by Holm correction; $p < 0.0001$. [j]Mid-P-exact test, p-value adjustment by Holm correction; $p < 0.0001$. [k]Mid-P-exact test, p-value adjustment by Holm correction; $p < 0.0001$. [l]Mid-P-exact test, p-value adjustment by Holm correction; $p < 0.0001$. [m]Mid-P-exact test, p-value adjustment by Holm correction; $p = 0.0133$. [n]Mid-P-exact test, p-value adjustment by Holm correction; $P = 0.0002$. [o]Mid-P-exact test, p-value adjustment by Holm correction; $P = 0.0127$. [p]Mid-P-exact test, p-value adjustment by Holm correction; $P = 0.0173$. [q]Mid-P-exact test, p-value adjustment by Holm correction; $P = 0.0292$.

device was shown to significantly reduce nymphal tick densities in the northeastern United States over time (Brei et al., 2009). Immunization of wildlife hosts against ticks could form an alternative means of reducing tick abundance and the risk for acquiring tick-borne diseases, but will depend on the identification of effective antigens and the availability of suitable vaccine delivery systems such as oral immunization or ballistic delivery of vaccines (Sharma and Hinds, 2012).

Although this work was limited by the small number of animals used due to cost constraints, the results nevertheless indicate that tick immunity against *I. ricinus* can be elicited in cattle upon immunization with native TPEs. Future work will focus on the analysis of immunogenic antigens to identify potential tick-protective vaccine candidates.

ETHICS STATEMENT

This study was carried out in accordance with the recommendations of the Landesamt for Gesundheit and Soziales, Berlin, Germany. The protocol was approved by the Landesamt für Gesundheit und Soziales, under registration number G0210/15.

AUTHOR CONTRIBUTIONS

SK, JA, JT, JH, and AN conceived and designed the study. OH and PK contributed materials. SK, JC, JA, and AN performed the experiments. OK performed the histopathological analyses. SK and AN analyzed the data and drafted the manuscript. All authors read and approved the final manuscript submitted for publication.

FUNDING

This study was financed through the 'Anti-tick vaccines to prevent tick-borne diseases in Europe' (ANTIDotE) project, funded by the European Community's Seventh Framework Program under grant agreement 602272. OH was partially supported by the Czech Science Foundation grant no. 17-27386S. AN received financial support by the Federal Ministry of Education and Research (BMBF) under project number 01KI1720 as part of the 'Research Network Zoonotic Infectious Diseases.' CIC bioGUNE is accredited as a Severo Ochoa Center of Excellence by the Spanish Ministry of Economy and Competitiveness (MINECO) (SEV-2016-0644).

ACKNOWLEDGMENTS

We thank Peggy Hoffmann-Köhler, Gabriela Loosová, and Estíbaliz Atondo for their technical assistance.

REFERENCES

Allen, J. R., and Humphreys, S. J. (1979). Immunisation of guinea pigs and cattle against ticks. *Nature* 280, 491–493. doi: 10.1038/280491a0

Almazan, C., Blas-Machado, U., Kocan, K. M., Yoshioka, J. H., Blouin, E. F., Mangold, A. J., et al. (2005). Characterization of three *Ixodes scapularis* cDNAs protective against tick infestations. *Vaccine* 23, 4403–4416. doi: 10.1016/j.vaccine.2005.04.012

Banerjee, D. P., Kumar, R., Kumar, S., and Sengupta, P. P. (2003). Immunization of crossbred cattle (*Bos indicus* x *Bos taurus*) with fractionated midgut antigens against *Hyalomma anatolicum* anatolicum. *Trop. Anim. Health Prod.* 35, 509–519. doi: 10.1023/A:1027325717124

Brei, B., Brownstein, J. S., George, J. E., Pound, J. M., Miller, J. A., Daniels, T. J., et al. (2009). Evaluation of the United States department of agriculture northeast area-wide tick control project by meta-analysis. *Vector Borne Zoonotic Dis.*9, 423–430. doi: 10.1089/vbz.2008.0150

Brown, S. J. (1988). Evidence for regurgitation by *Amblyomma americanum*. *Vet. Parasitol.* 28, 335–342. doi: 10.1016/0304-4017(88)90081-7

Burgdorfer, W., Hayes, S. F., and Corwin, D. (1989). Pathophysiology of the Lyme disease spirochete, *Borrelia burgdorferi*, in ixodid ticks. *Rev. Infect. Dis.* 11(Suppl. 6), S1442–S1450. doi: 10.1093/clinids/11.Supplement_6.S1442

Contreras, M., Alberdi, P., Fernandez, De Mera, I. G., Krull, C., Nijhof, A., et al. (2017). Vaccinomics approach to the identification of candidate protective antigens for the control of tick vector infestations and *Anaplasma phagocytophilum* infection. *Front. Cell. Infect. Microbiol.* 7:360. doi: 10.3389/fcimb.2017.00360

Contreras, M., and de la Fuente, J. (2017). Control of infestations by *Ixodes ricinus* tick larvae in rabbits vaccinated with aquaporin recombinant antigens. *Vaccine* 35, 1323–1328. doi: 10.1016/j.vaccine.2017.01.052

Coumou, J., Wagemakers, A., Trentelman, J. J., Nijhof, A. M., and Hovius, J. W. (2015). Vaccination against Bm86 Homologues in rabbits does not impair *Ixodes ricinus* feeding or oviposition. *PLoS One* 10:e0123495. doi: 10.1371/journal.pone.0123495

de Vos, S., Zeinstra, L., Taoufik, O., Willadsen, P., and Jongejan, F. (2001). Evidence for the utility of the Bm86 antigen from *Boophilus microplus* in vaccination against other tick species. *Exp. Appl. Acarol.* 25, 245–261. doi: 10.1023/A:1010609007009

Decrem, Y., Mariller, M., Lahaye, K., Blasioli, V., Beaufays, J., Zouaoui Boudjeltia, K., et al. (2008). The impact of gene knock-down and vaccination against salivary metalloproteases on blood feeding and egg laying by *Ixodes ricinus*. *Int. J. Parasitol.* 38, 549–560. doi: 10.1016/j.ijpara.2007.09.003

Essuman, S., Dipeolu, O. O., and Odhiambo, T. R. (1991). Immunization of cattle with a semi-purified fraction of solubilized membrane-bound antigens extracted from the midgut of the tick *Rhipicephalus appendiculatus*. *Exp. Appl. Acarol.* 13, 65–73. doi: 10.1007/Bf01268941

Fulop, B., and Poggensee, G. (2008). Epidemiological situation of Lyme borreliosis in Germany: surveillance data from six Eastern German States, 2002 to 2006. *Parasitol. Res.* 103(Suppl. 1), S117–S120. doi: 10.1007/s00436-008-1060-y

Gillet, L., Schroeder, H., Mast, J., Thirion, M., Renauld, J. C., Dewals, B., et al. (2009). Anchoring tick salivary anti-complement proteins IRAC I and IRAC II to membrane increases their immunogenicity. *Vet. Res.* 40:51. doi: 10.1051/vetres/2009034

Gomes, H., Moraes, J., Githaka, N., Martins, R., Isezaki, M., Vaz Ida, S., et al. (2015). Vaccination with cyclin-dependent kinase tick antigen confers protection against Ixodes infestation. *Vet. Parasitol.* 211, 266–273. doi: 10.1016/j.vetpar.2015.05.022

Gray, J. S., Kahl, O., Robertson, J. N., Daniel, M., Estrada-Pena, A., Gettinby, G., et al. (1998). Lyme borreliosis habitat assessment. *Zentralbl. Bakteriol.* 287, 211–228. doi: 10.1016/S0934-8840(98)80123-0

Hajdusek, O., Almazan, C., Loosova, G., Villar, M., Canales, M., Grubhoffer, L., et al. (2010). Characterization of ferritin 2 for the control of tick infestations. *Vaccine* 28, 2993–2998. doi: 10.1016/j.vaccine.2010.02.008

Hajdusek, O., Sojka, D., Kopacek, P., Buresova, V., Franta, Z., Sauman, I., et al. (2009). Knockdown of proteins involved in iron metabolism limits tick reproduction and development. *Proc. Natl. Acad. Sci. U.S.A.* 106, 1033–1038. doi: 10.1073/pnas.0807961106

Jongejan, F., Pegram, R. G., Zivkovic, D., Hensen, E. J., Mwase, E. T., Thielemans, M. J., et al. (1989). Monitoring of naturally acquired and artificially induced immunity to *Amblyomma variegatum* and *Rhipicephalus appendiculatus* ticks under field and laboratory conditions. *Exp. Appl. Acarol.* 7, 181–199. doi: 10.1007/BF01194059

Kemp, D. H., Pearson, R. D., Gough, J. M., and Willadsen, P. (1989). Vaccination against *Boophilus microplus*: localization of antigens on tick gut cells and their interaction with the host immune system. *Exp. Appl. Acarol.* 7, 43–58. doi: 10.1007/BF01200452

Kimaro, E. E., and Opdebeeck, J. P. (1994). Tick infestations on cattle vaccinated with extracts from the eggs and the gut of *Boophilus microplus*. *Vet. Parasitol.* 52, 61–70. doi: 10.1016/0304-4017(94)90036-1

Kotsyfakis, M., Anderson, J. M., Andersen, J. F., Calvo, E., Francischetti, I. M., Mather, T. N., et al. (2008). Cutting edge: immunity against a "silent" salivary antigen of the Lyme vector *Ixodes scapularis* impairs its ability to feed. *J. Immunol.* 181, 5209–5212. doi: 10.4049/jimmunol.181.8.5209

Krober, T., and Guerin, P. M. (2007). In vitro feeding assays for hard ticks. *Trends Parasitol.* 23, 445–449. doi: 10.1016/j.pt.2007.07.010

Krull, C., Bohme, B., Clausen, P. H., and Nijhof, A. M. (2017). Optimization of an artificial tick feeding assay for *Dermacentor reticulatus*. *Parasit. Vectors* 10:60. doi: 10.1186/s13071-017-2000-4

Manzano-Roman, R., Encinas-Grandes, A., and Perez-Sanchez, R. (2006). Antigens from the midgut membranes of *Ornithodoros erraticus* induce lethal anti-tick immune responses in pigs and mice. *Vet. Parasitol.* 135, 65–79. doi: 10.1016/j.vetpar.2005.08.004

Nijhof, A. M., Taoufik, A., De La Fuente, J., Kocan, K. M., De Vries, E., and Jongejan, F. (2007). Gene silencing of the tick protective antigens, Bm86, Bm91 and subolesin, in the one-host tick *Boophilus microplus* by RNA interference. *Int. J. Parasitol.* 37, 653–662. doi: 10.1016/j.ijpara.2006.11.005

Nikpay, A., and Nabian, S. (2016). Immunization of cattle with tick salivary gland extracts. *J. Arthropod Borne Dis.* 10, 281–290.

Opdebeeck, J. P., and Daly, K. E. (1990). Immune responses of infected and vaccinated Hereford cattle to antigens of the cattle tick, *Boophilus microplus*. *Vet. Immunol. Immunopathol.* 25, 99–108. doi: 10.1016/0165-2427(90)90113-7

Parizi, L. F., Githaka, N. W., Logullo, C., Konnai, S., Masuda, A., Ohashi, K., et al. (2012). The quest for a universal vaccine against ticks: cross-immunity insights. *Vet. J.* 194, 158–165. doi: 10.1016/j.tvjl.2012.05.023

Perner, J., Provaznik, J., Schrenkova, J., Urbanova, V., Ribeiro, J. M., and Kopacek, P. (2016). RNA-seq analyses of the midgut from blood- and serum-fed *Ixodes ricinus* ticks. *Sci. Rep.* 6:36695. doi: 10.1038/srep36695

Pound, J. M., Lohmeyer, K. H., Davey, R. B., Miller, J. A., and George, J. E. (2012). Efficacy of amitraz-impregnated collars on white-tailed deer (Artiodactyla: Cervidae) in reducing free-living populations of lone star ticks (Acari: Ixodidae). *J. Econ. Entomol.* 105, 2207–2212. doi: 10.1603/EC12219

Prevot, P. P., Couvreur, B., Denis, V., Brossard, M., Vanhamme, L., and Godfroid, E. (2007). Protective immunity against *Ixodes ricinus* induced by a salivary serpin. *Vaccine* 25, 3284–3292. doi: 10.1016/j.vaccine.2007.01.008

Radzisauskiene, D., Zagminas, K., Asokliene, L., Jasionis, A., Mameniskiene, R., Ambrozaitis, A., et al. (2018). Epidemiological patterns of tick-borne encephalitis in Lithuania and clinical features in adults in the light of the high incidence in recent years: a retrospective study. *Eur. J. Neurol.* 25, 268–274. doi: 10.1111/ene.13486

Randolph, S. E., Green, R. M., Hoodless, A. N., and Peacey, M. F. (2002). An empirical quantitative framework for the seasonal population dynamics of the tick *Ixodes ricinus*. *Int. J. Parasitol.* 32, 979–989. doi: 10.1016/S0020-7519(02)00030-9

Rechav, Y., Spickett, A. M., Dauth, J., Tembo, S. D., Clarke, F. C., Heller-Haupt, A., et al. (1992). Immunization of guinea-pigs and cattle against adult *Rhipicephalus appendiculatus* ticks using semipurified nymphal homogenates and adult gut homogenate. *Immunology* 75, 700–706.

Schwartz, A. M., Hinckley, A. F., Mead, P. S., Hook, S. A., and Kugeler, K. J. (2017). Surveillance for Lyme disease – United States, 2008-2015. *MMWR Surveill. Summ.* 66, 1–12. doi: 10.15585/mmwr.ss6622a1

Schwarz, A., Tenzer, S., Hackenberg, M., Erhart, J., Gerhold-Ay, A., Mazur, J., et al. (2014). A systems level analysis reveals transcriptomic and proteomic complexity in *Ixodes ricinus* midgut and salivary glands during early attachment and feeding. *Mol. Cell. Proteomics* 13, 2725–2735. doi: 10.1074/mcp.M114.039289

Sharma, S., and Hinds, L. A. (2012). Formulation and delivery of vaccines: ongoing challenges for animal management. *J. Pharm. Bioallied Sci.* 4, 258–266. doi: 10.4103/0975-7406.103231

Smith, R., and Takkinen, J. (2006). Lyme borreliosis: Europe-wide coordinated surveillance and action needed? *Euro Surveill.* 11, E060622060621.

Sonenshine, D. E., and Anderson, J. M. (2014). "Mouthparts and digestive system: anatomy and molecular biology of feeding and digestion," in *Biology of Ticks*, eds D. E. Sonenshine and M. D. Roe (New York, NY: Oxford University Press), 122–162.

Sprong, H., Azagi, T., Hoornstra, D., Nijhof, A. M., Knorr, S., Baarsma, M. E., et al. (2018). Control of Lyme borreliosis and other *Ixodes ricinus*-borne diseases. *Parasit. Vectors* 11:145. doi: 10.1186/s13071-018-2744-5

Sprong, H., Trentelman, J., Seemann, I., Grubhoffer, L., Rego, R. O., Hajdusek, O., et al. (2014). ANTIDotE: anti-tick vaccines to prevent tick-borne diseases in Europe. *Parasit. Vectors* 7:77. doi: 10.1186/1756-3305-7-77

Sykes, R. A., and Makiello, P. (2017). An estimate of Lyme borreliosis incidence in Western Europe. *J Public Health* 39, 74–81. doi: 10.1093/pubmed/fdw017

Szabo, M. P., and Bechara, G. H. (1997). Immunisation of dogs and guinea pigs against *Rhipicephalus sanguineus* ticks using gut extract. *Vet. Parasitol.* 68, 283–294. doi: 10.1016/S0304-4017(96)01079-5

Trager, W. (1939a). Acquired immunity to ticks. *J. Parasitol.* 25, 57–81. doi: 10.2307/3272160

Trager, W. (1939b). Further observations on acquired immunity to the tick *Dermacentor variabilis* Say. *J. Parasitol.* 25, 137–139. doi: 10.2307/3272354

Trimnell, A. R., Davies, G. M., Lissina, O., Hails, R. S., and Nuttall, P. A. (2005). A cross-reactive tick cement antigen is a candidate broad-spectrum tick vaccine. *Vaccine* 23, 4329–4341. doi: 10.1016/j.vaccine.2005.03.041

Valenzuela, J. G., Belkaid, Y., Garfield, M. K., Mendez, S., Kamhawi, S., Rowton, E. D., et al. (2001). Toward a defined anti-*Leishmania* vaccine targeting vector antigens: characterization of a protective salivary protein. *J. Exp. Med.* 194, 331–342. doi: 10.1084/jem.194.3.331

Willadsen, P. (2004). Anti-tick vaccines. *Parasitology* 129(Suppl.), S367–S387. doi: 10.1017/S0031182003004657

Willadsen, P., Riding, G. A., Mckenna, R. V., Kemp, D. H., Tellam, R. L., Nielsen, J. N., et al. (1989). Immunologic control of a parasitic arthropod. Identification of a protective antigen from *Boophilus microplus*. *J. Immunol.* 143, 1346–1351.

Wolfensohn, S., and Lloyd, M. (2013). *Handbook of Laboratory Animal Management and Welfare*. Oxford: Wiley-Blackwell.

Wong, J. Y., and Opdebeeck, J. P. (1989). Protective efficacy of antigens solubilized from gut membranes of the cattle tick, *Boophilus microplus*. *Immunology* 66, 149–155.

Zweygarth, E., Just, M. C., and De Waal, D. T. (1995). Continuous in vitro cultivation of erythrocytic stages of *Babesia equi*. *Parasitol. Res.* 81, 355–358. doi: 10.1007/BF00931544

Conflict of Interest Statement: The authors declare that the research was conducted in the absence of any commercial or financial relationships that could be construed as a potential conflict of interest.

frontiers in Physiology

REVIEW
published: 07 December 2018
doi: 10.3389/fphys.2018.01769

Crucial Role for Basophils in Acquired Protective Immunity to Tick Infestation

Hajime Karasuyama[1], Yuya Tabakawa[1], Takuya Ohta[1], Takeshi Wada[1,2] and Soichiro Yoshikawa[1]**

[1] Department of Immune Regulation, Graduate School of Medical and Dental Sciences, Tokyo Medical and Dental University, Tokyo, Japan, [2] Division of Molecular Medicine, Institute of Advanced Medical Sciences, Tokushima University, Tokushima, Japan

OPEN ACCESS

Edited by:
Abid Ali,
Abdul Wali Khan University Mardan, Pakistan

Reviewed by:
Ben J. Mans,
Agricultural Research Council, South Africa
Shahid Karim,
University of Southern Mississippi, United States

***Correspondence:**
Hajime Karasuyama
karasuyama.mbch@tmd.ac.jp
Soichiro Yoshikawa
yoshisou.mbch@tmd.ac.jp

Specialty section:
This article was submitted to Invertebrate Physiology, a section of the journal Frontiers in Physiology

Received: *13 August 2018*
Accepted: *23 November 2018*
Published: *07 December 2018*

Citation:
Karasuyama H, Tabakawa Y, Ohta T, Wada T and Yoshikawa S (2018) Crucial Role for Basophils in Acquired Protective Immunity to Tick Infestation. Front. Physiol. 9:1769. doi: 10.3389/fphys.2018.01769

Ticks are blood-sucking arthropods that can transmit various pathogenic organisms to host animals and humans, causing serious infectious diseases including Lyme disease. Tick feeding induces innate and acquired immune responses in host animals, depending on the combination of different species of animals and ticks. Acquired tick resistance (ATR) can diminish the chance of pathogen transmission from infected ticks to the host. Hence, the elucidation of cellular and molecular mechanism underlying ATR is important for the development of efficient anti-tick vaccines. In this review article, we briefly overview the history of studies on ATR and summarize recent findings, particularly focusing on the role for basophils in the manifestation of ATR. In several animal species, including cattle, guinea pigs, rabbits and mice, basophil accumulation is observed at the tick re-infestation site, even though the frequency of basophils among cellular infiltrates varies in different animal species, ranging from approximately 3% in mice to 70% in guinea pigs. Skin-resident, memory $CD4^+$ T cells contribute to the recruitment of basophils to the tick re-infestation site through production of IL-3 in mice. Depletion of basophils before the tick re-infestation abolishes ATR in guinea pigs infested with *Amblyomma americanum* and mice infested with *Haemaphysalis longicornis*, demonstrating the crucial role of basophils in the manifestation of ATR. The activation of basophils via IgE and its receptor FcεRI is essential for ATR in mice. Histamine released from activated basophils functions as an important effector molecule in murine ATR, probably through promotion of epidermal hyperplasia which interferes with tick attachment or blood feeding in the skin. Accumulating evidence suggests the following scenario. The 1^{st} tick infestation triggers the production of IgE against tick saliva antigens in the host, and blood-circulating basophils bind such IgE on the cell surface via FcεRI. In the 2^{nd} infestation, IgE-armed basophils are recruited to tick-feeding sites and stimulated by tick saliva antigens to release histamine that promotes epidermal hyperplasia, contributing to ATR. Further studies are needed to clarify whether this scenario in mice can be applied to ATR in other animal species and humans.

Keywords: basophil, mast cell, tick resistance, IgE, histamine

INTRODUCTION

Ticks, particularly ixodid family members, are blood-sucking ectoparasites of vertebrates and can transmit various pathogens to animals and humans during blood feeding for days, causing serious infectious diseases, including Lyme disease, babesiosis, Rocky Mountain spotted fever, human monocytic ehrlichiosis and severe fever with thrombocytopenia syndrome (Gratz, 1999; Parola and Raoult, 2001; de la Fuente et al., 2008; Embers and Narasimhan, 2013; Wikel, 2013; Yamaji et al., 2018). Besides tick-borne infectious diseases, some people with the experience of tick bites show recurrent episodes of anaphylaxis, a life-threatening systemic allergic reaction, after eating red meat or treating with anticancer monoclonal antibodies (Platts-Mills and Commins, 2013; Steinke et al., 2015). Thus, tick infestation is of medical and veterinary public health importance.

Host defense mechanism is a threat to successful blood feeding by ticks and hence must be counteracted. To this end, ticks inject saliva containing various bioactive substances into the host during tick infestation, including vasodilator and antihemostatic, antiinflammatory and immunosuppressive reagents (Wikel, 2013). On the other hand, some animals, such as mice, guinea pigs, rabbits and cattle, have been shown to develop the resistance to tick feeding after single or multiple tick infestations, depending on the combination of animal species/strains and tick species (Trager, 1939; Wikel, 1996). This acquired tick resistance (ATR) is commonly assessed by several parameters, including the reduction in the number and/or body weight of engorged ticks or tick death when sensitized animals are re-infested with ticks. ATR was first described in 1938 by Trager who found that after infestation with *Dermacentor variabilis*, guinea pigs develop resistance to subsequent tick infestations (Trager, 1939). Since then, ATR has been further characterized by using cattle and laboratory animals including guinea pigs (Wikel, 1996). ATR is not restricted to the skin lesion of previous tick bites and can be observed in un-infested skin of sensitized animals, indicating the contribution of systemic responses rather than a localized response at the previously infested skin lesion. Moreover, ATR can be transferred to naive animals with sera or cells isolated from previously infested animals (Wikel and Allen, 1976; Brown and Askenase, 1981; Askenase et al., 1982), suggesting that ATR is a type of immune reaction. Importantly, ATR can diminish the chance of pathogen transmission from infected ticks to host animals and humans (Bell et al., 1979; Wikel et al., 1997; Nazario et al., 1998; Burke et al., 2005; Dai et al., 2009). Therefore, the elucidation of cellular and molecular mechanisms underlying ATR is important for developing efficient anti-tick vaccines that can minimize the transmission of pathogens causing serious infectious diseases.

Basophils are the least abundant granulocytes and account for less than 1% of peripheral blood leukocytes (Galli, 2000). They are named after basophilic granules in the cytoplasm that stain with basic dye, as first documented by Paul Ehrlich in 1879. In addition to basophilic granules, blood-circulating basophils share some phenotypic properties with tissue-resident mast cells, such as the surface expression of the high-affinity IgE receptor FcεRI and the release of allergy-inducing chemical mediators, including histamine, in response to various stimuli (Galli, 2000; Stone et al., 2010). Therefore, basophils have often been erroneously considered as minor and redundant relatives or blood-circulating precursors of tissue-resident mast cells (Falcone et al., 2000). It is now accepted well that basophils and mast cells are distinct cell lineages, and that basophils play crucial and non-redundant roles distinct from those played by mast cells (Voehringer, 2017; Karasuyama et al., 2018; Varricchi et al., 2018). Basophils contribute to protective immunity, particularly to parasitic infections while they are involved in the pathogenesis of various disorders, including allergic and autoimmune disorders.

In this review article, we summarize recent advances in our understanding of the cellular and molecular mechanisms underlying ATR, particularly focusing on the role of basophils identified mainly in mouse models of tick infestation.

BASOPHILS ARE KEY EFFECTOR CELLS IN THE MANIFESTATION OF ATR

In Guinea Pigs

An early study described that cutaneous reactions at tick-feeding sites in tick-resistant guinea pigs were characterized by granulocytic inflammatory infiltrates, edema, and epidermal hyperplasia whereas the 1st tick-feeding site in previously uninfested guinea pigs showed minimal skin reactivity (Trager, 1939). Accumulation of numerous basophils and eosinophils, with basophils comprising up to 70% of cellular infiltrates, was detected at tick-feeding sites of guinea pigs that manifested ATR (Allen, 1973). Such basophil-rich cutaneous reaction was referred as cutaneous basophil hypersensitivity (CBH) and extensively studied in 1970s and early 1980s (Katz, 1978). Basophil depletion in *A. americanum*-infested guinea pigs by using antiserum raised against basophils abolished ATR (Brown et al., 1982), demonstrating the important role for basophils in ATR. Basophil infiltration at the site of tick re-infestation was also observed in cattle and rabbits (Allen et al., 1977; Brossard and Fivaz, 1982), even though the frequency of basophils among cellular infiltrates varied, and the functional role of basophils in these animals has not yet been determined to our knowledge. Thus, it remained elusive whether the important finding on basophils in guinea pig ATR can be generalized to other animal species and humans.

In Mice

A previous study reported that basophil infiltration was hardly detected at the tick-feeding site of WBB6F1-+/+ mice during re-infestation with *H. longicornis*, in spite of the fact that the mice showed ATR (Matsuda et al., 1990). Mast cell-deficient WBB6F1-W/W^v mice failed to manifest ATR, and adoptive transfer of mast cells conferred ATR on these mice (Matsuda et al., 1985, 1987, 1990), suggesting that mast cells in place of basophils contributed to ATR in mice, unlike in guinea pigs. On the contrary, other studies reported that the same mast cell-deficient strain of mice showed ATR to another tick species *Dermacentor variabilis* (denHollander and Allen, 1985; Steeves and Allen, 1991). Murine basophils had been notoriously difficult to identify owing to their fewer basophilic granules compared

to those in other animals and humans, and therefore, electron microscopic examination was needed to identify them in tissue sections (Urbina et al., 1981; Dvorak et al., 1982; Dvorak, 2000). Notably, the infiltration of basophils, along with eosinophils and neutrophils, was detected by electron microscopy at the tick-feeding site in the 3rd infestation with *D. variabilis* in both mast cell-sufficient and -deficient mice (Steeves and Allen, 1991). Thus, the mechanism underlying ATR in mice, including the distinct roles played by basophils and mast cells, and the influence of different genetic background of both mice and ticks remained to be clarified.

Recent characterization of cell surface markers on murine basophils (Min et al., 2004; Voehringer et al., 2004) and the identification of murine basophil-specific serine protease, mouse mast cell protease-8 (mMCP-8) (Poorafshar et al., 2000; Ugajin et al., 2009) have enabled us to identify and isolate murine basophils much more easily. Taking the advantage of a mMCP-8-specific mAb TUG8 (Ugajin et al., 2009), we demonstrated that mMCP-8-expressing basophils are recruited to the tick-feeding site and make a cluster around the tick mouthpart during the 2nd but rarely the 1st infestation with *H. longicornis* in C57BL/6 mice (Wada et al., 2010). Intravital fluorescence microscopic analysis, using *Mcpt8*^{GFP} (green basophil) mice in that only basophils express green fluorescent protein (GFP), confirmed the basophil accumulation at the 2nd but not 1st tick-feeding site (Ohta et al., 2017; **Figure 1**). Basophils represented less than 5% of leukocytes at the 2nd tick-feeding site in mice, much fewer than in guinea pigs, while monocytes/macrophages, neutrophils and eosinophils were abundant. Importantly, we found that basophil depletion by treating mice with basophil-depleting mAbs, either anti-FcεRIα (MAR-1) or anti-CD200R3 (Ba103), just before the 2nd tick infestation completely abolished ATR with no apparent effect on the number of other types of cells, including monocytes/macrophages, neutrophils and eosinophils (Wada et al., 2010). The essential role of basophils in ATR was further demonstrated by diphtheria toxin-mediated ablation of basophils in genetically engineered *Mcpt8*^{DTR} mice in that only basophils expressed diphtheria toxin receptors (Wada et al., 2010). Of note, we also demonstrated that mast cell-deficient *Kit*$^{W-sh/W-sh}$ C57BL/6 mice failed to manifest ATR, confirming the importance of mast cells in ATR reported previously (Matsuda et al., 1985, 1987, 1990). Thus, mast cells, in addition to basophils, appear to contribute to ATR in C57BL/6 mice infested with *H. longicornis*, in contrast to ATR in *D. variabilis*-infested WBB6F1-+/+ mice in that mast cells are dispensable (denHollander and Allen, 1985; Steeves and Allen, 1991).

In Humans

Basophil infiltration was detected in humans at the tick-feeding sites and in the skin lesions of scabies (Ito et al., 2011; Nakahigashi et al., 2013; Kimura et al., 2017). Of note, a patient lacking basophils and eosinophils reportedly suffered from widespread scabies (Juhlin and Michaelsson, 1977). These observations suggest the possible involvement of basophils in protective immunity to ectoparasites, including ticks.

BASOPHIL ACTIVATION THROUGH IgE AND ITS RECEPTOR FcεRI IS ESSENTIAL FOR ATR

It was shown in guinea pigs that transfer of serum from previously infested animals conferred ATR on naive animals (Wikel and Allen, 1976; Brown and Askenase, 1981; Askenase et al., 1982). Similarly, in mice, transfer of serum from tick-infested but not un-infested mice conferred ATR on naive mice (Matsuda et al., 1990), suggesting the involvement of tick-specific antibodies in ATR. Of note, the heat treatment of the serum at 56°C for 2 h abolished the ATR transfer activity (Matsuda et al., 1990), indicating that antibodies of IgE isotype contribute to the manifestation of ATR. Consistent with this observation, we demonstrated that both antibody-deficient μMT mice and *Fcer1g*$^{-/-}$ mice, that lack the expression of high affinity IgE receptor FcεRI, failed to show ATR (Wada et al., 2010). This

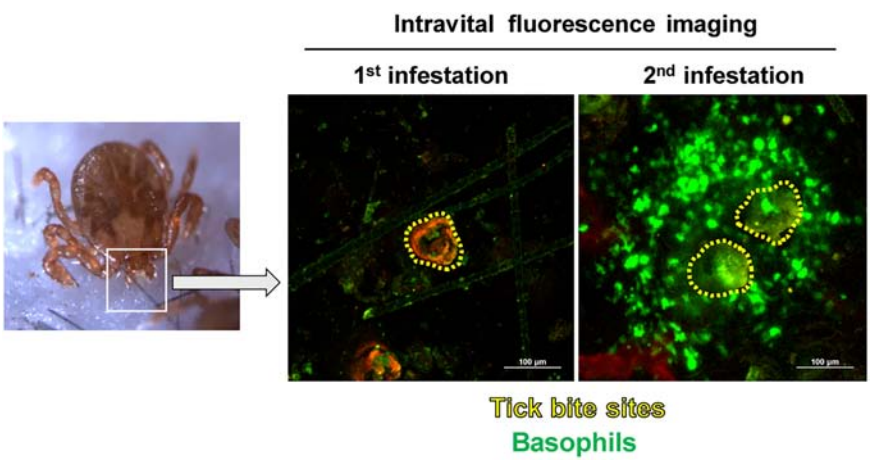

FIGURE 1 | Basophils accumulate at the tick-feeding site during the 2nd but not 1st tick infestation. *Mcpt8*^{GFP} (green basophil) mice were infested with ticks one or twice and subjected to intravital fluorescence imaging analysis of green basophils at tick-feeding sites on day 2 of the 1st or 2nd infestation.

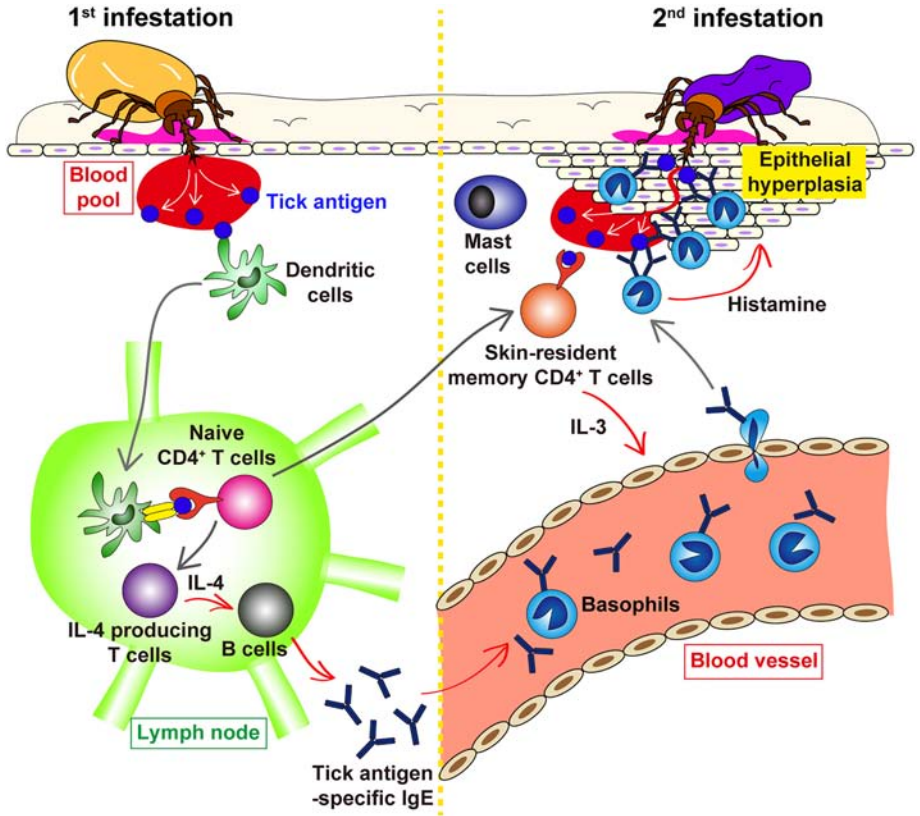

FIGURE 2 | Schematic view of the proposed mechanism underlying ATR. In the 1st tick infestation (left panel), dendritic cells in the skin take up tick saliva antigens and move to the draining lymph node where they present tick antigens to naive CD4+ T cells, leading to the generation of IL-4-producing T cells. T cell-derived IL-4 stimulates B cells to produce tick antigen-specific IgE that in turn circulates in the peripheral blood and bind to the surface of blood-circulating basophils via FcεRI. Some of tick antigen-specific CD4+ T cells generated in the lymph node migrate into the skin throughout the body and are retained as skin-resident, memory CD4+ T cells. In the 2nd tick infestation (right panel), such skin-resident, memory CD4+ T cells are stimulated with tick antigens to produce IL-3 that in turn promotes the recruitment of IgE-armed basophils from the peripheral blood to the tick-feeding site. IgE-armed basophils are activated with tick antigens to release histamine that acts on keratinocyte, resulting in epidermal hyperplasia that may interfere with tick attachment or blood feeding in the skin, and hence contribute to ATR. The role of skin mast cells in ATR remains elusive.

suggested the following scenario (**Figure 2**). The 1st infestation triggers the production of IgE against tick saliva antigens, and basophils and mast cells bind IgE on the cell surface via FcεRI. In the 2nd infestation, tick saliva antigens delivered into the tick-feeding site bind to IgE on these cells, leading to the cross-linking of FcεRI and hence activation of these cells that may contribute to ATR.

Intriguingly, mast cell-deficient $Kit^{W-sh/W-sh}$ C57BL/6 mice reconstituted with mast cells derived from $Fcer1g^{-/-}$ mice could manifest ATR as did mice reconstituted with wild-type mast cells (Wada et al., 2010), indicating that FcεRI on mast cells is dispensable for IgE-mediated ATR. In contrast, adoptive transfer of basophils isolated from previously infested wild-type, but not $Fcer1g^{-/-}$, mice conferred ATR on naive mice (Wada et al., 2010). These results suggested that basophils rather than mast cells play a critical role in IgE-dependent ATR through FcεRI-mediated activation, even though both types of cells contribute to ATR.

Ticks inject a plethora of substances, including proteins, into the host during feeding (Wikel, 2013). However, it remains ill-defined which components among tick saliva injected are the major targets of IgE that is involved in ATR, even though a series of tick saliva antigens recognized by sera from tick-infested animals and humans have been identified (Brown et al., 1984; Brown, 1988; Mayoral et al., 2004). It was demonstrated that infestation with *A. americanum* can induce a strong IgE response to tick saliva antigens including the carbohydrate α-gal, which is also present in red meats such as beef and pork. The production of such anti-α-gal IgE in tick-infested people can lead to anaphylaxis after ingestion of red meats (Platts-Mills and Commins, 2013; Steinke et al., 2015). It remains to be investigated whether anti-α-gal IgE is involved in ATR.

Molecular characterization of tick salivary components has demonstrated that different members among the same multi-gene family are expressed at distinct time points during tick feeding (Karim and Ribeiro, 2015). For example, two cystatin genes from *Ixodes scapularis* change their expression reciprocally during feeding (Kotsyfakis et al., 2007; Karim and Ribeiro, 2015). Such antigenic variation or sialome switch during tick feeding is considered as a possible mechanism by which ticks avoid host

immune responses. It remains to be determined whether such variation can affect the production of anti-tick IgE and hence IgE-mediated ATR, and whether IgE raised against one family member is cross-reactive to other members of the same family.

Host-derived IgG molecules containing blood meal pass through the midgut barrier of *Rhipicephalus appendiculatus* into the hemolymph and are excreted via the saliva back into the host during feeding. IgG binding proteins detected in the tick hemolymph and salivary glands are thought to contribute to this excretion of IgG, as a strategy by which ticks evade the damage caused by host antibodies (Wang and Nuttall, 1999). IGBP-MA, a member of IgG binding proteins has been shown to bind to IgE (Wang and Nuttall, 2013). Further studies are needed to examine whether such IgG binding proteins can interfere with IgE-mediated ATR in the host and whether the host raises antibodies against them to neutralize their activity.

BASOPHIL-DERIVED HISTAMINE IS AN IMPORTANT EFFECTOR MOLECULE IN ATR

Biologically active molecules, such as histamine and proteases, stored in the secretary granules in basophils and mast cells have been implicated as effectors of ATR. It was reported in cattle that the tick resistance is correlated with hypersensitivity to tick antigens and the amount of histamine at the tick-feeding site (Willadsen et al., 1979). Moreover, administration of antihistamine in cattle resulted in higher tick numbers (Tatchell and Bennett, 1969) whereas the injection of histamine into the cattle skin promoted tick detachment (Kemp and Bourne, 1980). Similar observations were reported in guinea pigs (Wikel, 1982), suggesting the possible involvement of histamine to ATR. However, the cellular source of histamine responsible for ATR and the mechanism underlying histamine-mediated ATR remained ill-defined.

We have recently addressed these questions by analyzing C57BL/6 mice infested with *H. longicornis*, in that both basophils and mast cells contribute to ATR (Wada et al., 2010). Treatment of mice with histamine H1 antagonist during the 2nd infestation abolished ATR (Tabakawa et al., 2018). Consistent with this, mice deficient for histamine production due to the lack of histidine decarboxylase (HDC) failed to show ATR (Tabakawa et al., 2018). Moreover, repeated injection of histamine or histamine H1 receptor agonist beneath the tick-infested site during the 1st infestation inhibited the tick feeding in wild-type mice (Tabakawa et al., 2018). These observations illustrated the important role of the histamine-histamine H1 receptor axis in the manifestation of ATR in mice, consistent with previous studies in guinea pigs and cattle (Tatchell and Bennett, 1969; Willadsen et al., 1979; Wikel, 1982).

Both basophils and mast cells are well-known producers of histamine, and therefore supposed to contribute to ATR through histamine release. Unexpectedly, however, adoptive transfer of histamine-deficient mast cells reconstituted ATR in mast cell-deficient $Kit^{W-sh/W-sh}$ C57BL/6 mice as did that of wild-type mast cells (Tabakawa et al., 2018), indicating that mast cell-derived histamine is dispensable for ATR. In contrast, adoptive transfer of wild-type but not histamine-deficient basophils conferred ATR on basophil-depleted *Mcpt8*^{DTR} mice (Tabakawa et al., 2018), demonstrating the crucial role of basophil-derived histamine in the manifestation of ATR.

Intravital imaging analysis of cells at the 2nd tick feeding site demonstrated that basophils make a cluster within the epidermis and surround a tick mouthpart. In contrast, mast cells are mostly scattered in the dermis rather than epidermis and localized more distantly from the tick mouthpart (Tabakawa et al., 2018). It is well known that histamine has a short half-life. Therefore, basophil-derived histamine may be much more effective than mast cell-derived in the manifestation of ATR, considering the fact that higher numbers of basophils are localized closer to a tick mouthpart, compared to mast cells.

Previous studies reported that histamine promotes itching and grooming response in the skin, resulting in removal of ticks in host animals (Koudstaal et al., 1978). In the mouse mode of tick infestation, ticks are placed inside of a small tube attached to the skin. Therefore, the effect of host grooming on tick feeding is minimized, implying other mechanisms underlying histamine-mediated ATR. Mice deficient for histamine H1 receptor failed to manifest ATR (Tabakawa et al., 2018), indicating that histamine acts on host cells rather than ticks. We detected the thickening of the epidermis and the formation of basophil cluster within the thickened epidermis at the 2nd but not 1st tick-feeding site in mice (Tabakawa et al., 2018) as reported previously in guinea pigs (Trager, 1939; Allen, 1973). This epidermal hyperplasia was absent in histamine-deficient or basophil-deficient mice (Tabakawa et al., 2018), suggesting that basophil-derived histamine is involved in epidermal hyperplasia. Considering that keratinocytes express functional H1 receptor (Ohsawa and Hirasawa, 2014) and that histamine promotes the proliferation of keratinocytes (Maurer et al., 1997; Albrecht and Dittrich, 2015), histamine released from basophil localized in the epidermis perhaps induces the thickening of the epidermis that may interfere with tick attachment or blood-sucking in the skin during the 2nd infestation (**Figure 2**).

Histamine-binding proteins (HBPs) have been identified in tick saliva (Paesen et al., 1999; Sangamnatdej et al., 2002; Mans et al., 2008). They show high-affinity binding to histamine and can efficiently compete for histamine with its native receptor. Thus, they may interfere with histamine-induced host responses at tick feeding sits, including itching and grooming. However, it remains to be determined whether tick HBPs can give any impact on histamine-mediated ATR in the host and whether the host raises antibodies against them to neutralize their activity. Mast cells and basophils are the major source of histamine at tick feeding sites. Basophils accumulate at tick feeding sites during the 1st but not 2nd infestation while mast cells always reside there. Given that higher numbers of basophils are localized closer to a tick mouthpart, compared to mast cells, during the 2nd infestation (Tabakawa et al., 2018), the concentration of histamine near tick mouthparts should be much higher during the 2nd infestation compared to the 1st infestation. Therefore, one may assume that HBPs might be less effective in sequestering histamine at the 2nd tick-feeding site in which ATR is executed. The influence of HBPs

on histamine-mediated ATR could be explored by generating HBP-deficient ticks in future studies.

It has been reported that *H. longicornis*, *Dermacentor andersoni*, and *Boophilus microplus* larval ticks are highly reactive to histamine in the induction of tick resistance while *A. americanum* and *Ixodes holocyclus* ticks are less responsive to histamine (Bagnall, 1975; Kemp and Bourne, 1980; Wikel, 1982; Brown and Askenase, 1985). The former tick species have shorter mouthparts than the latter (Suppan et al., 2017), suggesting the possibility that histamine-induced thickening of the epidermis prevents the former's but not the latter's mouthparts from penetrating into the dermis in order to form blood pools. This may explain the differential responsiveness to histamine among tick species in terms of ATR induction. Alternatively, but not mutually exclusively, it is possible that the presence or absence (or differential amounts) of HBPs in different tick species is correlated in part with differential reactivity to histamine in the induction of tick resistance.

SKIN-RESIDENT MEMORY CD4$^+$ T CELLS ARE RESPONSIBLE FOR BASOPHIL RECRUITMENT TO THE 2nd TICK-FEEDING SITE

Basophils circulate in the peripheral blood under homeostatic conditions, and they infiltrate the skin at the tick-feeding site during the 2nd but not 1st infestation. Importantly, the recruitment of basophils can be observed in previously uninfested skin, far from the 1st infestation site, of sensitized animals, implicating that the 1st tick infestation may induce systemic alteration in the skin throughout the body, so that basophils can readily infiltrate the tick re-infestation site anywhere in the body. We have recently demonstrated in mice that skin CD4$^+$ memory T cells play an important role in basophil recruitment to the 2nd tick-feeding site, leading to ATR (Ohta et al., 2017). Tick antigen-specific CD4$^+$ effector T cells are generated during the 1st tick infestation and distributed to the skin all over the body, and some of them are retained as skin-resident memory T cells (**Figure 2**). In the 2nd tick infestation, tick saliva antigens delivered into the skin stimulate these memory T cells present in the skin to produce IL-3 that is required for basophil recruitment to the 2nd tick-feeding site (Ohta et al., 2017). Even though the exact mechanism underlying IL-3-mediated basophil recruitment remains to be clarified, IL-3 might promote basophil adhesion to endothelium (Bochner et al., 1990; Korpelainen et al., 1996; Lim et al., 2006), leading to transendothelial migration of basophils and their accumulation in the skin.

AN UNSOLVED ISSUE: THE ROLE OF MAST CELLS IN ATR

As described above, mast cells contribute to ATR in mice infested with *H. longicornis* (Matsuda et al., 1985, 1987, 1990) whereas they are dispensable for ATR in *D. variabilis*-infested mice (denHollander and Allen, 1985; Steeves and Allen, 1991). As far as we are aware, the involvement of mast cells to ATR has not yet been documented in other animal species. In the case of mice infested with *H. longicornis*, histamine derived from basophils but not mast cells is essential for the manifestation of ATR (Tabakawa et al., 2018), even though both basophils and mast cells are involved in ATR (Wada et al., 2010). The deficiency of either basophils or mast cells almost completely abolishes ATR (Wada et al., 2010), suggesting that the role of these cells may not be additive. Of note, the number of basophils accumulating at the 2nd tick-feeding site is comparable between mast cell-sufficient and -deficient mice (Wada et al., 2010), indicating that mast cells are not prerequisite for basophil recruitment. Nevertheless, closer examination with intravital imaging revealed that basophils accumulating at the 2nd tick-feeding site are more motile and less-clustered around a tick mouthpart in mast cell-deficient mice than in mast cell-sufficient mice (Tabakawa et al., 2018). Therefore, one may assume that mast cells may contribute to ATR by directly or indirectly regulating basophil behavior. Further studies are needed for elucidating how mast cells contribute to the manifestation of ATR.

CONCLUSION

Recent development of a series of analytical tools in laboratory animals has advanced our understanding of the cellular and molecular mechanism underlying ATR. In several animal species, basophil accumulation is observed at the tick re-infestation site (**Figure 1**), and basophil depletion abolishes ATR in guinea pigs and mice, demonstrating the crucial role of basophils in the manifestation of ATR. The 1st tick infestation triggers the production of IgE against tick saliva antigens. In the 2nd infestation, IgE-armed basophils are recruited to the tick-feeding site and stimulated by tick saliva antigens to release histamine that functions as a key effector in ATR, probably through promotion of the epidermal hyperplasia that in turn interferes with tick attachment or blood feeding in the skin (**Figure 2**). Further studies on the detailed mechanism underlying ATR, including the role of mast cells, may help develop the strategy to prevent tick infestation and tick-borne diseases.

AUTHOR CONTRIBUTIONS

HK has substantially contributed to the literature review and drafted the manuscript. SY contributed to the discussion and drafting, and editing of the manuscript. YT, TO, and TW reviewed and edited the manuscript.

FUNDING

This work was supported by research grants from Japanese Ministry of Education, Culture, Sports, Science and Technology [15H05786 (HK) and 17K15719 (SY)] and TMDU President's Young Researchers Award (SY).

REFERENCES

Albrecht, M., and Dittrich, A. M. (2015). Expression and function of histamine and its receptors in atopic dermatitis. *Mol. Cell Pediatr.* 2, 16–23. doi: 10.1186/s40348-015-0027-1

Allen, J. R. (1973). Tick resistance: basophils in skin reactions of resistant guinea pigs. *Int. J. Parasitol.* 3, 195–200. doi: 10.1016/0020-7519(73)90024-6

Allen, J. R., Doube, B. M., and Kemp, D. H. (1977). Histology of bovine skin reactions to *Ixodes holocyclus* neumann. *Can. J. Comp. Med.* 41, 26–35.

Askenase, P. W., Bagnall, B. G., and Worms, M. J. (1982). Cutaneous basophil-associated resistance to ectoparasites (ticks). I. Transfer with immune serum or immune cells. *Immunology* 45, 501–511.

Bagnall, B. G. (1975). *Cutaneous Immunity to the Tick Ixodes Holocyclus*. Ph.D. thesis, University of Sydney, Sydney.

Bell, J. F., Stewart, S. J., and Wikel, S. K. (1979). Resistance to tick-borne *Francisella tularensis* by tick-sensitized rabbits: allergic klendusity. *Am. J. Trop. Med. Hyg.* 28, 876–880. doi: 10.4269/ajtmh.1979.28.876

Bochner, B. S., Mckelvey, A. A., Sterbinsky, S. A., Hildreth, J. E., Derse, C. P., Klunk, D. A., et al. (1990). IL-3 augments adhesiveness for endothelium and CD11b expression in human basophils but not neutrophils. *J. Immunol.* 145, 1832–1837.

Brossard, M., and Fivaz, V. (1982). *Ixodes ricinus* L.: mast cells, basophils and eosinophils in the sequence of cellular events in the skin of infested or re-infested rabbits. *Parasitology* 85(Pt 3), 583–592.

Brown, S. J. (1988). Characterization of tick antigens inducing host immune resistance. II. Description of rabbit-acquired immunity to *Amblyomma americanum* ticks and identification of potential tick antigens by Western blot analysis. *Vet. Parasitol.* 28, 245–259. doi: 10.1016/0304-4017(88)90112-4

Brown, S. J., and Askenase, P. W. (1981). Cutaneous basophil responses and immune resistance of guinea pigs to ticks: passive transfer with peritoneal exudate cells or serum. *J. Immunol.* 127, 2163–2167.

Brown, S. J., and Askenase, P. W. (1985). Rejection of ticks from guinea pigs by anti-hapten-antibody-mediated degranulation of basophils at cutaneous basophil hypersensitivity sites: role of mediators other than histamine. *J. Immunol.* 134, 1160–1165.

Brown, S. J., Galli, S. J., Gleich, G. J., and Askenase, P. W. (1982). Ablation of immunity to *Amblyomma americanum* by anti-basophil serum: cooperation between basophils and eosinophils in expression of immunity to ectoparasites (ticks) in guinea pigs. *J. Immunol.* 129, 790–796.

Brown, S. J., Shapiro, S. Z., and Askenase, P. W. (1984). Characterization of tick antigens inducing host immune resistance. I. Immunization of guinea pigs with *Amblyomma americanum*-derived salivary gland extracts and identification of an important salivary gland protein antigen with guinea pig anti-tick antibodies. *J. Immunol.* 133, 3319–3325.

Burke, G., Wikel, S. K., Spielman, A., Telford, S. R., Mckay, K., and Krause, P. J. (2005). Hypersensitivity to ticks and Lyme disease risk. *Emerg. Infect. Dis.* 11, 36–41.

Dai, J., Wang, P., Adusumilli, S., Booth, C. J., Narasimhan, S., Anguita, J., et al. (2009). Antibodies against a tick protein, Salp15, protect mice from the Lyme disease agent. *Cell Host Microbe* 6, 482–492. doi: 10.1016/j.chom.2009.10.006

de la Fuente, J., Estrada-Pena, A., Venzal, J. M., Kocan, K. M., and Sonenshine, D. E. (2008). Overview: ticks as vectors of pathogens that cause disease in humans and animals. *Front. Biosci.* 13:6938–6946. doi: 10.2741/3200

denHollander, N., and Allen, J. R. (1985). *Dermacentor variabilis*: resistance to ticks acquired by mast cell-deficient and other strains of mice. *Exp. Parasitol.* 59, 169–179. doi: 10.1016/0014-4894(85)90069-4

Dvorak, A. M. (2000). The mouse basophil, a rare and rarely recognized granulocyte. *Blood* 96, 1616–1617.

Dvorak, A. M., Nabel, G., Pyne, K., Cantor, H., Dvorak, H. F., and Galli, S. J. (1982). Ultrastructural identification of the mouse basophil. *Blood* 59, 1279–1285.

Embers, M. E., and Narasimhan, S. (2013). Vaccination against Lyme disease: past, present, and future. *Front. Cell Infect. Microbiol.* 3:6. doi: 10.3389/fcimb.2013.00006

Falcone, F. H., Haas, H., and Gibbs, B. F. (2000). The human basophil: a new appreciation of its role in immune responses. *Blood* 96, 4028–4038.

Galli, S. J. (2000). Mast cells and basophils. *Curr. Opin. Hematol.* 7, 32–39. doi: 10.1097/00062752-200001000-00007

Gratz, N. G. (1999). Emerging and resurging vector-borne diseases. *Annu. Rev. Entomol.* 44, 51–75. doi: 10.1146/annurev.ento.44.1.51

Ito, Y., Satoh, T., Takayama, K., Miyagishi, C., Walls, A. F., and Yokozeki, H. (2011). Basophil recruitment and activation in inflammatory skin diseases. *Allergy* 66, 1107–1113. doi: 10.1111/j.1398-9995.2011.02570.x

Juhlin, L., and Michaelsson, G. (1977). A new syndrome characterised by absence of eosinophils and basophils. *Lancet* 1, 1233–1235. doi: 10.1016/S0140-6736(77)92440-0

Karasuyama, H., Miyake, K., Yoshikawa, S., and Yamanishi, Y. (2018). Multifaceted roles of basophils in health and disease. *J. Allergy Clin. Immunol.* 142, 370–380. doi: 10.1016/j.jaci.2017.10.042

Karim, S., and Ribeiro, J. M. C. (2015). An insight into the sialome of the lone star tick, amblyomma americanum, with a glimpse on its time dependent gene expression. *PLoS One* 10:e0131292. doi: 10.1371/journal.pone.0131292

Katz, S. I. (1978). Recruitment of basophils in delayed htpersensitivity reactions. *J. Invest. Dermatol.* 71, 70–75. doi: 10.1111/1523-1747.ep12544415

Kemp, D. H., and Bourne, A. (1980). Boophilus microplus: the effect of histamine on the attachment of cattle-tick larvae–studies *in vivo* and *in vitro*. *Parasitology* 80, 487–496. doi: 10.1017/S0031182000000950

Kimura, R., Sugita, K., Ito, A., Goto, H., and Yamamoto, O. (2017). Basophils are recruited and localized at the site of tick bites in humans. *J. Cutan. Pathol.* 44, 1091–1093. doi: 10.1111/cup.13045

Korpelainen, E. I., Gamble, J. R., Vadas, M. A., and Lopez, A. F. (1996). IL-3 receptor expression, regulation and function in cells of the Vasculature. *Immunol. Cell Biol.* 74, 1–7. doi: 10.1038/icb.1996.1

Kotsyfakis, M., Karim, S., Andersen, J. F., Mather, T. N., and Ribeiro, J. M. (2007). Selective cysteine protease inhibition contributes to blood-feeding success of the tick *Ixodes scapularis*. *J. Biol. Chem.* 282, 29256–29263. doi: 10.1074/jbc.M703143200

Koudstaal, D., Kemp, D. H., and Kerr, J. D. (1978). Boophilus microplus: rejection of larvae from British breed cattle. *Parasitology* 76, 379–386. doi: 10.1017/S0031182000048241

Lim, L. H. K., Burdick, M. M., Hudson, S. A., Mustafa, F. B., Konstantopoulos, K., and Bochner, B. S. (2006). Stimulation of human endothelium with IL-3 induces selective basophil accumulation *in vitro*. *J. Immunol.* 176, 5346–5353. doi: 10.4049/jimmunol.176.9.5346

Mans, B. J., Ribeiro, J. M. C., and Andersen, J. F. (2008). Structure, function, and evolution of biogenic amine-binding proteins in soft ticks. *J. Biol. Chem.* 283, 18721–18733. doi: 10.1074/jbc.M800188200

Matsuda, H., Fukui, K., Kiso, Y., and Kitamura, Y. (1985). Inability of genetically mast cell-deficient W/W^v mice to acquire resistance against larval *Haemaphysalis longicornis* ticks. *J. Parasitol.* 71, 443–448. doi: 10.2307/3281535

Matsuda, H., Nakano, T., Kiso, Y., and Kitamura, Y. (1987). Normalization of anti-tick response of mast cell-deficient W/W^v mice by intracutaneous injection of cultured mast cells. *J. Parasitol.* 73, 155–160. doi: 10.2307/3282361

Matsuda, H., Watanabe, N., Kiso, Y., Hirota, S., Ushio, H., Kannan, Y., et al. (1990). Necessity of IgE antibodies and mast cells for manifestation of resistance against larval *Haemaphysalis longicornis* ticks in mice. *J. Immunol.* 144, 259–262.

Maurer, M., Opitz, M., Henz, B. M., and Paus, R. (1997). The mast cell products histamine and serotonin stimulate and TNF-(inhibits the proliferation of murine epidermal keratinocytes in situ. *J. Dermatol. Sci.* 16, 79–84. doi: 10.1016/S0923-1811(97)00043-1

Mayoral, T. N., Merino, F. J., Serrano, J. L., Fernánndez-Soto, P., Encinas, A., Xe Rez, S., et al. (2004). Detection of antibodies to tick salivary antigens among patients from a region of spain. *Eur. J. Epidemiol.* 19, 79–83. doi: 10.1023/B:EJEP.0000013252.97826.10

Min, B., Prout, M., Hu-Li, J., Zhu, J., Jankovic, D., Morgan, E. S., et al. (2004). Basophils produce IL-4 and accumulate in tissues after infection with a Th2-inducing parasite. *J. Exp. Med.* 200, 507–517. doi: 10.1084/jem.20040590

Nakahigashi, K., Otsuka, A., Tomari, K., Miyachi, Y., and Kabashima, K. (2013). Evaluation of basophil infiltration into the skin lesions of tick bites. *Case Rep. Dermatol.* 5, 48–51. doi: 10.1159/000348650

Nazario, S., Das, S., De Silva, A. M., Deponte, K., Marcantonio, N., Anderson, J. F., et al. (1998). Prevention of *Borrelia burgdorferi* transmission in guinea pigs by tick immunity. *Am. J. Trop. Med. Hyg.* 58, 780–785. doi: 10.4269/ajtmh.1998.58.780

Ohsawa, Y., and Hirasawa, N. (2014). The role of histamine H1 and H4 receptors in atopic dermatitis: from basic research to clinical study. *Allergol. Int.* 63, 533–542. doi: 10.2332/allergolint.13-RA-0675

Ohta, T., Yoshikawa, S., Tabakawa, Y., Yamaji, K., Ishiwata, K., Shitara, H., et al. (2017). Skin $CD4^+$ memory T cells play an essential role in acquired anti-tick immunity through interleukin-3-mediated basophil recruitment to tick-feeding sites. *Front. Immunol.* 8:1348. doi: 10.3389/fimmu.2017.01348

Paesen, G. C., Adams, P. L., Harlos, K., Nuttall, P. A., and Stuart, D. I. (1999). Tick histamine-binding proteins: isolation, cloning, and three-dimensional structure. *Mol. Cell.* 3, 661–671. doi: 10.1016/S1097-2765(00)80359-7

Parola, P., and Raoult, D. (2001). Ticks and tick-borne bacterial diseases in humans: an emerging infectious threat. *Clin. Infect. Dis.* 32, 897–928. doi: 10.1086/319347

Platts-Mills, T. A., and Commins, S. P. (2013). Emerging antigens involved in allergic responses. *Curr. Opin. Immunol.* 6, 769–774. doi: 10.1016/j.coi.2013.09.002

Poorafshar, M., Helmby, H., Troye-Blomberg, M., and Hellman, L. (2000). MMCP-8, the first lineage-specific differentiation marker for mouse basophils. Elevated numbers of potent IL-4-producing and MMCP-8-positive cells in spleens of malaria-infected mice. *Eur. J. Immunol.* 30, 2660–2668. doi: 10.1002/1521-4141(200009)30:9<2660::AID-IMMU2660>3.0.CO;2-I

Sangamnatdej, S., Paesen, G. C., Slovak, M., and Nuttall, P. A. (2002). A high affinity serotonin- and histamine-binding lipocalin from tick saliva. *Insect Mol. Biol.* 11, 79–86. doi: 10.1046/j.0962-1075.2001.00311.x

Steeves, E. B., and Allen, J. R. (1991). Tick resistance in mast cell-deficient mice: histological studies. *Int. J. Parasitol.* 21, 265–268. doi: 10.1016/0020-7519(91)90020-8

Steinke, J. W., Platts-Mills, T. A., and Commins, S. P. (2015). The alpha-gal story: lessons learned from connecting the dots. *J. Allergy Clin. Immunol.* 135, 589–596. doi: 10.1016/j.jaci.2014.12.1947

Stone, K. D., Prussin, C., and Metcalfe, D. D. (2010). IgE, mast cells, Basophils, and Eosinophils. *J. Allergy Clin. Immunol.* 125, S73–S80. doi: 10.1016/j.jaci.2009.11.017

Suppan, J., Engel, B., Marchetti-Deschmann, M., and Nurnberger, S. (2017). Tick attachment cement - reviewing the mysteries of a biological skin plug system. *Biol. Rev. Camb. Philos. Soc.* 2, 1056–1076. doi: 10.1111/brv.12384

Tabakawa, Y., Ohta, T., Yoshikawa, S., Elisabeth, J. R., Yamaji, K., Ishiwata, K., et al. (2018). Histamine released from skin-infiltrating basophils but not mast cells is crucial for acquired tick resistance in mice. *Front. Immunol.* 9:1540. doi: 10.3389/fimmu.2018.01540

Tatchell, R. J., and Bennett, G. F. (1969). Boophilus microplus: antihistaminic and tranquillizing drugs and cattle resistance. *Exp. Parasitol.* 26, 369–377. doi: 10.1016/0014-4894(69)90130-1

Trager, W. (1939). Acquired Immunity to Ticks. *J. Parasitol.* 25, 57–81. doi: 10.2307/3272160

Ugajin, T., Kojima, T., Mukai, K., Obata, K., Kawano, Y., Minegishi, Y., et al. (2009). Basophils preferentially express mouse mast cell protease 11 among the mast cell tryptase family in contrast to mast cells. *J. Leukoc. Biol.* 86, 1417–1425. doi: 10.1189/jlb.0609400

Urbina, C., Ortiz, C., and Hurtado, I. (1981). A new look at basophils in mice. *Int. Arch. Allergy Appl. Immunol.* 66, 158–160. doi: 10.1159/000232814

Varricchi, G., Raap, U., Rivellese, F., Marone, G., and Gibbs, B. F. (2018). Human mast cells and basophils-How are they similar how are they different? *Immunol. Rev.* 282, 8–34. doi: 10.1111/imr.12627

Voehringer, D. (2017). Recent advances in understanding basophil functions *in vivo*. *F1000Res* 6:1464. doi: 10.12688/f1000research.11697.1

Voehringer, D., Shinkai, K., and Locksley, R. M. (2004). Type 2 immunity reflects orchestrated recruitment of cells committed to IL-4 production. *Immunity* 20, 267–277. doi: 10.1016/S1074-7613(04)00026-3

Wada, T., Ishiwata, K., Koseki, H., Ishikura, T., Ugajin, T., Ohnuma, N., et al. (2010). Selective ablation of basophils in mice reveals their nonredundant role in acquired immunity against ticks. *J. Clin. Invest.* 120, 2867–2875. doi: 10.1172/JCI42680

Wang, H., and Nuttall, P. A. (1999). Immunoglobulin-binding proteins in ticks: new target for vaccine development against a blood-feeding parasite. *Cell Mol. Life Sci.* 56, 286–295. doi: 10.1007/s000180050430

Wang, H., and Nuttall, P. A. (2013). Methods of Administrating IGBPMA to Treat type I Hypersensitivity. U.S. Patent No 8,343,504. Wiltshire, GB: Natural Environment Research Council.

Wikel, S. (2013). Ticks and tick-borne pathogens at the cutaneous interface: host defenses, tick countermeasures, and a suitable environment for pathogen establishment. *Front. Microbiol.* 4:337. doi: 10.3389/fmicb.2013.00337

Wikel, S. K. (1982). Histamine content of tick attachment sites and the effects of H1 and H2 histamine antagonists on the expression of resistance. *Ann. Trop. Med. Parasitol.* 76, 179–185. doi: 10.1080/00034983.1982.11687525

Wikel, S. K. (1996). Host immunity to ticks. *Annu. Rev. Entomol.* 41, 1–22. doi: 10.1146/annurev.en.41.010196.000245

Wikel, S. K., and Allen, J. R. (1976). Acquired resistance to ticks. I. Passive transfer of resistance. *Immunology* 30, 311–316.

Wikel, S. K., Ramachandra, R. N., Bergman, D. K., Burkot, T. R., and Piesman, J. (1997). Infestation with pathogen-free nymphs of the tick *Ixodes scapularis* induces host resistance to transmission of Borrelia burgdorferi by ticks. *Infect. Immun.* 65, 335–338.

Willadsen, P., Wood, G. M., and Riding, G. A. (1979). The relation between skin histamine concentration, histamine sensitivity, and the resistance of cattle to the tick, *Boophilus microplus*. *Z. Parasitenkd* 59, 87–93. doi: 10.1007/BF00927849

Yamaji, K., Aonuma, H., and Kanuka, H. (2018). Distribution of tick-borne diseases in Japan: past patterns and implications for the future. *J. Infect. Chemother.* 24, 499–504. doi: 10.1016/j.jiac.2018.03.012

Conflict of Interest Statement: The authors declare that the research was conducted in the absence of any commercial or financial relationships that could be construed as a potential conflict of interest.

frontiers in Physiology

ORIGINAL RESEARCH
published: 02 April 2019
doi: 10.3389/fphys.2019.00318

Transcriptome and Proteome Response of *Rhipicephalus annulatus* Tick Vector to *Babesia bigemina* Infection

Sandra Antunes[1], Joana Couto[1], Joana Ferrolho[1], Gustavo Seron Sanches[1], José Octavio Merino Charrez[2], Ned De la Cruz Hernández[2], Monica Mazuz[3], Margarita Villar[4], Varda Shkap[3], José de la Fuente[4,5] and Ana Domingos[1]*

[1] Global Health and Tropical Medicine, Instituto de Higiene e Medicina Tropical, Universidade Nova de Lisboa, Lisbon, Portugal, [2] Facultad de Medicina Veterinaria y Zootecnia, Universidad Autónoma de Tamaulipas, Ciudad Victoria, Mexico, [3] Kimron Veterinary Institute, Bet Dagan, Israel, [4] SaBio, Instituto de Investigación en Recursos Cinegéticos, IREC, CSIC-UCLM-JCCM, Ciudad Real, Spain, [5] Department of Veterinary Pathobiology, Center for Veterinary Health Sciences, Oklahoma State University, Stillwater, OK, United States

OPEN ACCESS

Edited by:
Itabajara Da Silva Vaz Jr., Federal University of Rio Grande do Sul, Brazil

Reviewed by:
Mauro Mandrioli, University of Modena and Reggio Emilia, Italy
Claudio Mafra, Universidade Federal de Viçosa, Brazil
Tae Kim, Texas A&M University, United States

***Correspondence:**
Sandra Antunes
santunes@ihmt.unl.pt

Specialty section:
This article was submitted to Invertebrate Physiology, a section of the journal Frontiers in Physiology

Received: *10 January 2019*
Accepted: *11 March 2019*
Published: *02 April 2019*

Citation:
Antunes S, Couto J, Ferrolho J, Sanches GS, Merino Charrez JO, De la Cruz Hernández N, Mazuz M, Villar M, Shkap V, de la Fuente J and Domingos A (2019) Transcriptome and Proteome Response of Rhipicephalus annulatus Tick Vector to Babesia bigemina Infection. Front. Physiol. 10:318. doi: 10.3389/fphys.2019.00318

A system biology approach was used to gain insight into tick biology and interactions between vector and pathogen. *Rhipicephalus annulatus* is one of the main vectors of *Babesia bigemina* which has a massive impact on animal health. It is vital to obtain more information about this relationship, to better understand tick and pathogen biology, pathogen transmission dynamics, and new potential control approaches. In ticks, salivary glands (SGs) play a key role during pathogen infection and transmission. RNA sequencing obtained from uninfected and *B. bigemina* infected SGs obtained from fed female ticks resulted in 6823 and 6475 unigenes, respectively. From these, 360 unigenes were found to be differentially expressed ($p < 0.05$). Reversed phase liquid chromatography–mass spectrometry identified a total of 3679 tick proteins. Among them 406 were differently represented in response to *Babesia* infection. The omics data obtained suggested that *Babesia* infection lead to a reduction in the levels of mRNA and proteins ($n = 237$ transcripts, $n = 212$ proteins) when compared to uninfected controls. Integrated transcriptomics and proteomics datasets suggested a key role for stress response and apoptosis pathways in response to infection. Thus, six genes coding for GP80, death-associated protein kinase (DAPK-1), bax inhibitor-1 related (BI-1), heat shock protein (HSP), heat shock transcription factor (PHSTF), and queuine trna-ribosyltransferase (QtRibosyl) were selected and RNA interference (RNAi) performed. Gene silencing was obtained for all genes except *phstf.* Knockdown of *gp80*, *dapk-1*, and *bi-1* led to a significant increase in *Babesia* infection levels while *hsp* and *QtRibosyl* knockdown resulted in a non-significant decrease of infection levels when compared to the respective controls. Gene knockdown did not affect tick survival, but engorged female weight and egg production were affected in the *gp80*, *dapk-1*, and *QtRibosyl*-silenced groups in comparison to controls. These results advanced our understanding of tick–*Babesia* molecular interactions, and suggested new tick antigens as putative targets for vaccination to control tick infestations and pathogen infection/transmission.

Keywords: proteomics, transcriptomics, *Rhipicephalus annulatus*, *Babesia bigemina*, vector–pathogen interactions, apoptosis, stress response

INTRODUCTION

Babesiosis is a worldwide tick-borne hemoprotozoa disease caused by intra-erythrocytic parasites of the genus *Babesia* (Beugnet and Moreau, 2015; Lempereur et al., 2017). The disease may range from asymptomatic carrier to more severe states, characterized by hemolytic anemia, fever, hemoglobinuria, and occasionally death, affecting a large variety of mammals, including pets, farm, and wild animals and also humans (Schnittger et al., 2012). Human infection is mainly due to *Babesia microti* or *Babesia divergens*, and although it rarely occurs, it has been considered an emerging zoonosis due to the growing number of fatal cases (Leiby, 2006; Schnittger et al., 2012). In contrast, cattle babesiosis, caused by either *Babesia bovis* or *B. bigemina*, is an important disease causing high morbidity and mortality, thus leading to severe economic losses to the cattle industry (Chauvin et al., 2009). The tick species *R. annulatus* and *Rhipicephalus microplus*, the most important ticks of cattle in tropical and subtropical regions, conduce a negative impact on meat, milk, and leather productions and are considered as the main vectors and reservoirs of *B. bovis* and *B. bigemina* (Bock et al., 2004).

The application of chemical acaricides is the method of choice for tick control. However, it results in environmental contamination, selection of resistant ticks, and presence of residues in meat and milk, potentially harmful for animals and humans (Corson et al., 2001; Ghosh et al., 2007). To reduce these negative impacts, much attention has been directed to the development of new approaches that are efficient and at the same time environmentally friendly. Vaccination, as a prophylactic measure, stands out representing a promising and sustainable alternative for the control of ticks and tick-borne pathogens (Almazan et al., 2018). A vaccine targeting both tick fitness and pathogen competence is an attractive choice requiring the identification of tick molecules with a dual effect.

Several studies, based on omics approaches, have been conducted to understand the tick–pathogen interactions, identifying possible new vaccine candidates (Villar et al., 2017). System biology approaches have been efficiently used to characterize vector and pathogen interactions: in *Drosophila melanogaster*, one of the most well studied genetic model organisms (McTaggart et al., 2015), and *Anopheles* spp. mosquitoes (Domingos et al., 2017). The characterization of tick organs response to infection using technologies such as transcriptomics, proteomics, and functional genomics improved current knowledge on tick–pathogen interactions and allowed the development of new strategies and/or the identification of targets for tick and disease control. Also, research has shown that during the long-lasting tick–pathogen co-evolution, microorganisms have developed important strategies to manipulate or modulate tick response to infection, without impairing tick survival, enhancing their capacity of infection, replication, and transmission guaranteeing the survival of both (de la Fuente et al., 2016; Šimo et al., 2017). In *Ixodes scapularis*, the effect of *Anaplasma phagocytophilum* infection on tissue-specific responses and on cellular pathways, such as apoptosis or stress response, which can be activated in a certain tissue in response to infection in order to contain parasite evasion and or improve immune response, have been extensively studied (Alberdi et al., 2015; Ayllon et al., 2015; Villar et al., 2015; Cabezas-Cruz et al., 2017). However, there is limited knowledge on tick vector responses to *Babesia* spp. infection. *Babesia* parasites invade several tick tissues including the midgut, salivary glands (SGs), and ovaries, affecting tick fitness. Some tick molecules such as calreticulin, a calcium binding protein, kunitz-type serine protease inhibitors, lachesin, vitellogenins, among others, have been identified as having a role on tick–*Babesia* interface (Zhou et al., 2006; Rachinsky et al., 2008; Antunes et al., 2017, 2018). Scarce information is available regarding the mechanisms used by *B. bigemina* to infect, develop, multiply, and survive inside the tick vector. Additionally, the impact of parasite infection at tick transcriptome and proteome levels, particularly on the molecular pathways affected by *B. bigemina*, is still to be investigated.

The overall objective of this study was to deepen the understanding on the complex *R. annulatus* response to *B. bigemina* infection. To conclude on mRNA and protein levels of *R. annulatus* in response to *B. bigemina* infection, the present research combined transcriptomics and proteomics analysis to obtain a sialotranscriptome and proteome by RNA sequencing (RNA-seq) and reversed phase liquid chromatography–mass spectrometry (RP-LC–MS/MS). Research focused on genes and proteins that were found differentially expressed or represented after infection. Six genes were further studied by RNAi-mediated gene silencing including genes related to apoptosis and stress response. This work represents the first report concerning the effect of *B. bigemina* infection on the sialotranscriptome and proteome of *R. annulatus*, and in the influence of the presence of the parasite on specific and crucial cellular pathways, constituting an important step further on the development of new measures for ticks and parasite control.

MATERIALS AND METHODS

Ethics Statement

Animal experiments were conducted according with the "Guide for Care and Use of Laboratory Animals" of the institutions involved in the study, following protocols approved by the Committee on the Ethics of Animal Experiments and the principle of the three Rs, to replace, reduce, and refine the use of animals for scientific purposes.

Rhipicephalus annulatus and *Babesia bigemina*

R. annulatus adult ticks were obtained from a laboratory colony free of tick-transmissible infections maintained at the Kimron Veterinary Institute, Israel. Six-month-old Friesian calves were tested for the presence of antibodies against *Babesia* spp. using an immunofluorescence assay, as described previously (Shkap et al., 2005), and were kept under strict tick-free conditions. To obtain *B. bigemina*-infected ticks, one calf was splenectomized and inoculated intravenously with 1×10^6 *B. bigemina* (Moledet strain) cryopreserved parasites a fortnight later. Once the peak of

parasitemia was reached, ticks were fed for 1 week inside cotton bags attached with non-toxic silicone glue GE Advantage Silicone Sealant (General Electric, New York, NY, United States) to a shaved area on the dorsal region of the animal. Similarly, a naïve calf was used to obtain uninfected ticks. Detached adult female ticks from the infected and naïve calf were maintained at 28°C and 80% humidity.

Sialome

Sample Preparation and Probe-Based qPCR Detection of *Babesia bigemina*

A total of 30 uninfected and 30 *B. bigemina*-infected female ticks were used for tissue isolation. Ticks were washed twice in distilled water, once in 75% (v/v) ethanol, and one last wash in water. Ticks were dissected and the SGs extracted under a Motic SMZ-171B stereomicroscope (Motic Instruments Inc., Xiamen, China), using ice-cold phosphate buffer saline (PBS). Total RNA from 10 SGs obtained from each group was extracted using TriReagent (Sigma–Aldrich, St. Louis, MO, United States), according to the manufacturer's instructions. RNA concentration and integrity were evaluated by analysis of rRNA band integrity using Agilent 2100 Bioanalyzer (Agilent Technologies Inc., Santa Clara, CA, United States). cDNA was synthesized from 100 ng of total RNA using the iScript cDNA Synthesis Kit (Bio-Rad, Hercules, CA, United States), following the manufacturer's protocol. To determine the presence of *B. bigemina* in the SGs, probe-based qPCR reactions were carried out as described before for the detection of 18S rRNA of *B. bigemina* (Kim et al., 2007). Briefly, triplicate 20 μl reactions were prepared with 10 μl of Probe Xpert Fast Probe 2× Mastermix (GRISP Research Solutions, Porto, Portugal), 400 nM of each primer, 100 nM of probe, 1 μl of cDNA template, and nuclease-free water up to the final volume. The qPCR was carried out in a CFX Connect™ Real-Time PCR Detection System thermal cycler (Bio-Rad, Hercules, CA, United States) with a thermal cycling profile of 10 min at 95°C, followed by 45 cycles of 20 s at 95°C and 1 min at 55°C. Negative controls were prepared with no template. Positive controls were prepared with *B. bigemina* Moledet strain purified DNA. A standard curve was constructed with fivefold serial dilutions of the positive control DNA to determine reaction efficiency. Data were analyzed using the Bio-Rad CFX Manager Software version 3.1 (Bio-Rad, Hercules, CA, United States). Samples with quantification cycle (Cq) values above 39 were considered negative for the presence of the pathogen. After *B. bigemina* infection confirmation, the remaining 20 SGs from infected or uninfected ticks were grouped in two pools, and the total RNA, for RNA-seq was extracted as described above.

RNA Sequencing and Analysis

Library preparation was performed using TruSeq RNA kit (Illumina, San Diego, CA, United States), following the manufacturer's instructions. Shortly, prior to cDNA library construction magnetic beads with Oligo (dT) were used to enrich poly (A) mRNA from 1 μg of total-RNA. Purified mRNA was disrupted into short fragments. Two different fragmentation conditions were applied so that a "shorter" and a "longer" preparation were made for both the control (uninfected) and the *B. bigemina* infected RNA samples. Next, the purified mRNA was disrupted into short fragments, and double-stranded cDNA was immediately synthesized. cDNA was subjected to end-repair and adenylation, then connected with sequencing adapters. Suitable fragments, purified by size selection protocol with AMPure XP beads (Beckman Coulter, Pasadena, CA, United States), were selected as templates for PCR amplification. The final library sizes and qualities were evaluated by electrophoresis using an Agilent High Sensitivity DNA Kit (Agilent Technologies Inc.); fragment size range was between 287 and 296 bp for the short insert and 397 and 436 bp for the longer insert preparations. Subsequently, libraries were pooled and titrated using qPCR to obtain an accurate estimation of concentration. Cluster generation was performed in a Cluster Station (Illumina, San Diego, CA, United States) and the libraries sequenced using a GAIIx equipment (Illumina, San Diego, CA, United States), with a 2 × 100 cycle sequencing reads separated by a paired-end turnaround. Image analysis was performed using the HiSeq control Software version 1.8.4. (Illumina, San Diego, CA, United States) at Parque Científico de Madrid, Spain.

Assembly and Analysis of Transcripts

Reads were trimmed where the error probability was higher than 0.05. To get an optimal assembly, the sequence reads included were only those that the two members of the pair remained after filtering and trimming. Oases Software (Velvet, version 1.2.10) suitable for short paired-end reads assemblies (Schulz et al., 2012) was used selecting the mode of single assembly, i.e., not merged. For the two conditions, a kmer of 83 was selected for being close to the total length of the read (115 bp), avoiding misassembles. The Transcriptome Shotgun Assembly (TSA) project was submitted to the DDBJ/EMBL/GenBank under accession numbers GBJT00000000 and GBJS00000000 for uninfected and infected ticks, respectively. Functional annotation of each transcript was conducted based on the Basic Local Alignment Search Tool (BLAST[1]) and the results inferred by similarity to UniProt database[2] reference proteins. The minimum similarity threshold required for annotating a transcript was a BLAST *E*-value $< 10^{-10}$. A total of 34,095 reference proteins, considered to be representative on the UniRef90 clusters belonging to the taxonomic node Chelicerata, were downloaded from the UniProt database (January 2015). Chelicerata is eight levels above the *Rhipicentor reticulatus* taxon (Madder et al., 2014). Each selected protein belonged only to one cluster, showing 90% similarity with all members of that cluster. A protein-centred analysis of the differential expression was performed for the *de novo* transcriptome comparison. For the UniGene cluster formation, in each sample, for a set of transcripts annotated with the same UniProt, the longer nucleotide sequence was chosen to be the representative of each UniGene. Functional data were curated using Blast2GO platform version 4.0.7 available at https://www.blast2go.com (Conesa et al., 2005; Götz et al., 2008). Manual annotation was done with sequences retrieving no hits needed by compiling information from UniProt, RefSeq, GO,

[1]https://blast.ncbi.nlm.nih.gov/Blast.cgi

[2]https://www.uniprot.org/

Panther, KEGG, Pfam, and NCBI databases. For the uninfected and infected condition comparison, transcripts were clustered by proteins. When two transcripts were annotated under the same UniProt they were included in the same cluster; and when the same protein cluster was present in both conditions, the protein cluster expression levels were compared. The software edgeR, for Empirical Analysis of Digital Gene Expression Data in R [Bioconductor version: Release (3.7)] (Robinson et al., 2010), was used to compare the mRNA expression levels detected in samples.

Transcriptomics Data Normalization and Validation

For transcriptomics data normalization, four reference genes were selected including *tubulin-beta-2B chain*, *elongation factor 1*, *cyclophilin*, and *transcription factor TFIID* (Robinson et al., 2010). Since no biological replicates were used, a biological coefficient of variation (BCV) was firstly selected to 0.4. Considering that if the BCV was perfectly approximated, the *p*-value for the four genes would have to be 1, the lowest *p*-value obtained for any of these four genes was selected. This corresponded to the *transcription factor TFIID* that had a $p = 0.465$ (for BCV = 0.4). All the genes with a *p*-value higher than 0.465 were selected as genes without differential expression to approximate the dispersion. The dispersion and the BCV were analyzed for this set of 2719 theoretically housekeeping genes. A BCV = 0.6 was obtained after approximating the dispersion of the housekeeping genes and this BCV value was used to select the differentially expressed genes in response to infection. For RNA-seq data validation, 10 paired SGs obtained individually from each uninfected and *B. bigemina*-infected *R. annulatus* female ticks (previously screened for infection), respectively, were used in triplicate. **Supplementary Table S1** shows the primer sets used for qPCR and their respective final concentrations and annealing temperatures. Briefly, 10 μl triplicate reactions were prepared with 5 μl iTaq™ Universal SYBR® Green Supermix (Bio-Rad, Hercules, CA, United States), specific primer concentration, 1 μl of cDNA template, and nuclease-free water up to the final volume. The qPCR was carried out in a CFX Connect™ Real-Time PCR Detection System thermal cycler (Bio-Rad, Hercules, CA, United States), with a thermal cycling profile of 10 min at 95°C, followed by 45 cycles of 15 s at 95°C and 45 s at specific-annealing temperature. Negative controls were prepared with no template. A standard curve was constructed with fivefold serial dilutions of *R. annulatus* cDNA to determine reaction efficiency. To ensure that only one amplicon was formed, a melting curve was performed at the end of every reaction (55–95°C; 0.5°C/s melt rates). To confirm correct fragment amplification, gel electrophoresis was performed, the fragments were sequenced by the chain termination method at StabVida (Lisbon, Portugal) and the resulting sequence was analyzed against the sequences available at the NCBI nucleotide database[3]. The CFX Manager™ Software (Bio-Rad, Hercules, CA, United States) was used to analyze the gene expression data between conditions and reference gene validation was based on the geNorm algorithm (Vandesompele et al., 2002) and on the expression stability value M of each reference gene ($M < 1$).

[3]https://blast.ncbi.nlm.nih.gov/Blast.cgi

Proteome

Sample Preparation

A total of 16 uninfected and 16 *B. bigemina*-infected engorged female ticks obtained as described in the section "*Rhipicephalus annulatus* and *Babesia bigemina*" were equally divided into two different biological samples for each group. Ticks were dissected, cuticle removed, and washed in 10 mM PBS to eliminate the maximum host blood possible. Internal tick tissues were homogenized with a glass homogenizer (20 strokes) in lysis buffer [0.25 M de sucrose, 10 mM Tris–HCl pH 7.5, 1 mM $MgCl_2$, 0.7% DDM, 0.5% ASB detergent, supplemented with Complete protease inhibitor cocktail (Roche, Basel, Switzerland)] in a ratio of 1 ml of buffer *per* gram of sample. Samples were sonicated for 1 min in an ultrasonic cooled bath (JP Selecta, Barcelona, Spain) followed by 10 s of vortex. After three cycles of sonication-vortex, the homogenates were centrifuged at 200 × *g* for 5 min at 4°C, to remove cellular debris. The supernatants were then collected and protein concentration was determined using the Bicinchoninic Acid (BCA) Assay (Thermo Scientific, San Jose, CA, United States), according to the manufacturer's instructions.

Proteomics

One-hundred and fifty grams of protein extracts *per* group were on-gel concentrated by SDS–PAGE and trypsin digested as described previously (Villar et al., 2014). The desalted protein digest was re-suspended in 0.1% formic acid and analyzed by RP-LC–MS/MS technique using an Easy-nLC II system coupled to an ion trap LTQ mass spectrometer (Thermo Scientific, San Jose, CA, United States). Peptides were concentrated (on-line) by RP chromatography using a 0.1 × 20 mm C18 RP precolumn (Thermo Scientific, San Jose, CA, United States), and then separated using a 0.075 × 100 mm C18 RP column (Thermo Scientific, San Jose, CA, United States) operating at 0.3 ml/min. Peptides were eluted using a 180 min gradient from 5 to 40% solvent B (Solvent A: 0.1% formic acid in water, solvent B: 0.1% formic acid in acetonitrile). Electrospray (ESI) ionization was performed using a Fused-silica PicoTip Emitter ID 10 mm (New Objective, Woburn, MA, United States) interface. Peptides were detected in survey scans from 400 to 1600 amu (1 mscan), followed by 15 data dependent MS/MS scans (Top 15), using an isolation width of two mass-to-charge ratio units, normalized collision energy of 35%, and dynamic exclusion applied during 30 s periods.

Data Analysis

The MS/MS raw files were searched against a compiled database containing all sequences from Ixodidae, *Bos taurus*, and *Babesia* (135,071, 32,156, and 23,215 Uniprot entries in September 2017, respectively)[4] and with a database created from transcriptomics data (Holt et al., 2002; Evans et al., 2012), according to the Proteomics Informed by Transcriptomics (PIT) technique using the SEQUEST algorithm (Proteome Discoverer 1.4, Thermo Scientific, San Jose, CA, United States). The following constraints were used for the searches: tryptic cleavage after

[4]http://www.uniprot.org

Arg and Lys, up to two missed cleavage sites, and tolerances of 1 Da for-precursor ions and 0.8 Da for MS/MS fragment ions, and the searches were performed allowing optional Met oxidation and Cys carbamidomethylation. A false discovery rate (FDR) < 0.05 was considered as a condition for successful peptide assignments and at least two peptides *per* protein in at least one sample analyzed were the necessary condition for protein identification (**Supplementary Table S2**). Two biological replicates were used for each of uninfected and *B. bigemina*-infected ticks. For the quantitative analysis of tick proteins, after discarding *Babesia* and host proteins, the total number of peptide-spectrum matches (PSMs) for each tick protein was normalized against the total number of PSMs in ticks and compared between uninfected and infected ticks by χ^2-test statistics with Bonferroni correction in the IDEG6 Software[5] ($p = 0.05$). Only proteins that showed no significant differences between replicates and significant differences between the two conditions in at least three of the uninfected *versus* infected pair comparisons were considered as differentially represented (**Supplementary Table S3**). The mass spectrometry proteomics data have been deposited at the PeptideAtlas repository[6] with the dataset identifier PASS01339[7].

Gene and Protein Ontology Analysis

Gene ontology (GO) terms were assigned to differentially expressed genes and represented proteins with the Software Tool for Rapid Annotation of Proteins (STRAP) version 1.5 (Cardiovascular Proteomics Centre of Boston University School of Medicine at http://www.bumc.bu.edu/cardiovascularproteomics/cpctools/strap/). For the analysis, two categories of GO terms were evaluated that included the Biological Process (BP) and Molecular Function (MF). Chord diagrams were generated to display GO and the expression/representation of apoptotic and stress response-related UniProt IDs by using the GOplot R package in RStudio (Version 1.1.453) (Walter et al., 2015).

Proteomics Data Validation

Proteomics data validation was conducted by Western blot using two commercial mouse monoclonal antibodies targeting homologous amino acids sequences between tick and mouse and an in-house rabbit anti-subolesin polyclonal antibody (**Supplementary Table S4**). Ten engorged female ticks of each condition (uninfected and infected) were dissected, internal organs were rinsed in PBS and used to extract proteinaceous content using TriReagent (Sigma–Aldrich, St. Louis, MO, United States), according to the manufacturer's instructions. Elution was performed in 1× PBS, supplemented with 1% sodium dodecyl sulfate (SDS) and 1% protease inhibitor cocktail (Amresco, Solon, OH, United States). Protein concentration was assessed by spectrophotometry using a NanoDrop ND-1000 (Thermo Fisher Scientific). Fifty micrograms of protein extracts from each condition were re-suspended in Laemmli buffer (Bio-Rad, Hercules, CA, United States) containing 5% (v/v) of 2-β-mercaptoethanol, separated on a 12.5% discontinuous SDS–PAGE gel and transferred overnight at a constant 25 V to a nitrocellulose membrane, with a pore size of 0.2 μm (Bio-Rad, Hercules, CA, United States), using the Mini Trans-Blot® Electrophoretic Transfer Cell (Bio-Rad, Hercules, CA, United States). Membranes were stained with Ponceau S and blocked with 5% (w/v) nonfat dry milk (Bio-Rad, Hercules, CA, United States) in PBS containing 0.05% (v/v) Tween 20 (PBS-T) at room temperature (RT), for 1 h. In parallel, polyacrylamide gels were stained with BlueSafe (NZYTech, Lisbon, Portugal) for 1 h at RT. Membranes were washed with Tris-buffered saline complemented with 0.05% (v/v) Tween 20 (TBS-T) and incubated with the primary antibody diluted according to the manufacturer or literature (**Supplementary Table S4**), for 90 min at RT. After washing, membranes were incubated with a goat anti-mouse Polyvalent Immunoglobulins (G, A, M) – Alkaline Phosphate secondary antibody (1:3000; Sigma–Aldrich, St. Louis, MO, United States) for 1 h at RT, and afterward washed with TBS-T. The antigen–antibody complexes were detected using the alkaline phosphatase (AP) conjugate substrate kit (Bio-Rad, Hercules, CA, United States) and the protein band intensities were estimated using ImageJ Software (version 1.51K) (Schneider et al., 2012).

RNA Interference Assay

Ticks and dsRNA Synthesis

For the RNAi assay, *R. annulatus* pathogen-free adult ticks were obtained from the laboratory colony established at Knipling-Bushland U.S. Livestock Insects Research Laboratory and Veterinary Pest Genomics Center, Texas, United States, and maintained on cattle at the tick rearing facilities at the University of Tamaulipas, Mexico, as described in the section "*Rhipicephalus annulatus* and *Babesia bigemina*." For the RNAi-mediated gene-silencing assays, gene-specific double stranded (ds) RNA was synthesized using as template the sequences assembled in this study and sequences publicly available in GenBank. In particular, *Rhipicephalus pulchellus* TSA GACK01000273, GACK01006332, GACK01002259, and GACK01006752, *Amblyomma maculatum* transcript JO843858 and *R. microplus* transcript U49934. Fragments of interest were amplified using the iProof™ High-Fidelity PCR Kit (Bio-Rad, Hercules, CA, United States), with specific primers containing T7 promoter (**Supplementary Table S5**) and previously synthesized cDNA. Briefly, PCR reactions of 50 μL were prepared with 1× iProof HF Buffer, 10 mM of dNTP mix, 0.5 μM of each primer, 1 mM of $MgCl_2$, 0.02 U/μl proof DNA polymerase, and 1 μl of template cDNA. The cycling conditions were as follows: initial denaturation at 98°C for 3 min, 35 cycles of denaturation at 98°C for 10 s, annealing at specific temperature (**Supplementary Table S5**) for 30 s and extension at 72°C for 15 s; and a final extension at 72°C for 10 min. To confirm correct fragment amplification, gel electrophoresis was performed on a 0.5× TBE 1.2% (w/v) agarose gel, purified using the Zigmoclean™ Gel DNA Recovery Kit (Zymo Research, Irvine, CA, United States), and the fragments sequenced at StabVida (Caparica, Portugal).

[5]http://compgen.bio.unipd.it/bioinfo/software/

[6]http://www.peptideatlas.org/

[7]http://www.peptideatlas.org/PASS/PASS01339

The resulting sequence was compared against the sequences available at the NCBI nucleotide database[8]. After correct confirmation of the amplified sequences, dsRNA was synthesized using the MEGAscript RNAi Kit (Ambion, Austin, TX, United States) accordingly with instructions provided by the manufacturer, purified, and analyzed by spectrophotometry and agarose gel.

Tick Inoculation and Cattle Infestation

Thirty pathogen-free *R. annulatus* unfed female ticks *per* group were injected with 1×10^{11} to 1×10^{12} molecules of specific dsRNA in the right spiracular plate, using a Hamilton syringe (Sigma) with a 1 in. × 33-gauge needle. The control group was injected with the same volume of elution buffer, similar to what has been described in other studies (Hussein et al., 2015; Ferrolho et al., 2017). While the use of unrelated dsRNA is now a well-established control in species with full genome annotation, the *R. annulatus* genome is not annotated thus increasing the possibility of off targets in silencing assays. After injection, ticks were kept in an acclimatized room at 22–25°C and 95% relative humidity, for 6 h before infestation. Two 6-month-old calves were inoculated intravenously with 2 ml of cryopreserved *B. bigemina*-infected blood (1×10^6 infected erythrocytes) (field strain from Chiapas, Mexico). Cattle infection was confirmed by visual examination of blood smears. The cattle infestation was conducted as described in **Figure 1**. Ticks were monitored daily, at the second day unattached ticks were removed and the remaining were allowed to feed on the infected calves for 7 days. After this period, attached ticks were manually removed and stored in a humidity chamber until further use. SGs from 10 detached ticks *per* silenced-group were dissected and stored in RNA*later* (Ambion, Austin, TX, United States). The remaining 20 female ticks of each group were kept in individual pierced 1.5 ml microfuge tubes, under the laboratory conditions described above, for oviposition.

Efficiency of Gene Silencing, *B. bigemina* Infection Levels, and Tick Fitness

Gene silencing efficiency in SG was determined by comparing mRNA levels between specific dsRNA-injected and control groups by qPCR as described in the Section "Transcriptomics Data Normalization and Validation." Quantitative PCR was carried out in both SG and ovaries for the 18S rRNA of *B. bigemina*, following a previously described protocol (Antunes et al., 2012), and the effect of gene silencing in infection was evaluated by a Student's *t*-test ($p = 0.05$). Engorged female weight (EFW), egg mass weight (EMW), and egg production efficiency (EPE) were determined for each collected tick and analyzed between silenced and control groups by Student's *t*-test with unequal variance ($p > 0.05$). The EPE was calculated according to the formula EPE = (EMW/EFW) × 100. Tick ability to feed was determined by the ratio of engorged female ticks collected

[8]https://blast.ncbi.nlm.nih.gov/Blast.cgi

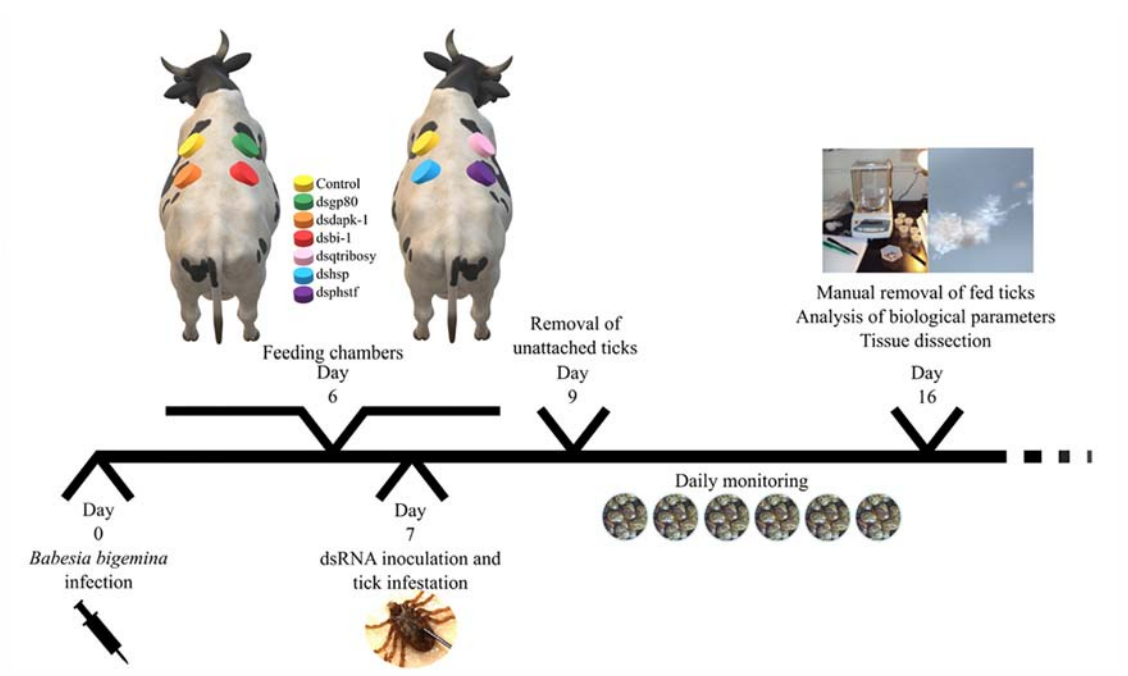

FIGURE 1 | Experimental design of silencing assay. Two 6 months-old calves were inoculated intravenously with *B. bigemina*-infected blood. After 6 days, cotton cloth chambers were glued to the calf skin (one day before infestation). In day 7, thirty specific-dsRNA inoculated female ticks were added to its respective feeding chambers together with thirty males. Two days after infestation (day 9) unattached ticks were removed from the patches. Ticks were monitored daily and allowed to feed on the infected calves for 7 days. After this period, attached ticks were manually removed and stored in a humidity chamber until further use (analysis of biological parameters and tissue dissection).

from the feeding chambers to the total number of female ticks added initially, and statistically compared with the Chi-square test ($p > 0.05$) with the null hypothesis that tick mortality was independent of gene silencing.

RESULTS

R. annulatus Female Sialotranscriptome: Assembly and Annotation

All the SG tested from *R. annulatus* female ticks fed on a *B. bigemina* infected calve were found to be positive for infection, while no infection was found on the SG of female ticks fed on the naïve calve. This enabled the production of a pool of infected SG and an uninfected SG pool to proceed with RNA-seq. With 40,573 988 high-quality paired-end reads, two transcriptomes were assembled, from the control and the infected samples. The assembly resulted in 33,379 putative transcripts in the control sample (33,118 with length < 200 bp) and 30,435 for the infected one (30,301 with length < 200 bp). After the first step of annotation, only the alignments (BLAST) with *e*-value minor than 10^{-10} were selected to infer functional annotation, resulting in 16,564 transcripts for the control and 15,037 for the infected sample. From these, 6823 unigenes with 1,374,576 ± 1,787,133 (Ave ± *SE*) estimated counts per protein were identified in the control population and 6475 unigenes with 1,182,677 ± 1,494,052 (Ave ± *SE*) in the infected group. Moreover, 884 unigenes were found to be exclusive to the infected samples while 1232 to the control samples (**Supplementary Table S2**). GO analysis of the obtained sialotranscriptome resulted in 69 sequences without BLAST hits, 877 sequences with BLAST hits without annotation, 473 with mapping without annotation, and 6286 sequences were functionally annotated. **Supplementary Figures S1, S2** summarizes the functional annotation of the sialotranscriptome of *R. annulatus* female ticks. These multi-level charts show relevant functions from the general levels to the specific ones. The GO annotation highlights BPs such as single-organism cellular process, regulation of cellular process, gene expression or transport, and MF related to protein binding, hydrolase activity, or transferase activity. Using a BCV of 0.6, 360 unigenes were found to be differentially expressed ($p < 0.05$), whereas 123 were up regulated and 237 down regulated (**Figure 2**). Automated functional annotation was performed using Blast2GO and unigenes that did not retrieve GO terms were manually annotated. GO level 2 charts are shown in **Figures 3**, **4**. The most represented BP were cellular and metabolic processes with 125 and 133 sequences, respectively. These categories include all processes carried out at the cellular level (e.g., apoptosis or homeostasis) and chemical reactions and pathways, including anabolism and catabolism, by which living organisms transform chemical substances. Biological regulation and regulation of BPs were represented by 48 and 44 sequences. Response to stimulus, including processes such as stress, immune, or redox state responses, was represented by 30 sequences. BP, such as growth or detoxification with a single representative, were included in the "other" BP category. Regarding the assignments of MF, the classes with higher representation, binding and catalytic activity, with 148 and 129 sequences, respectively, followed by transporter activity, with 26 sequences were found. With the exception of structural molecule activity, all the other classes contained more down regulated than up regulated transcripts.

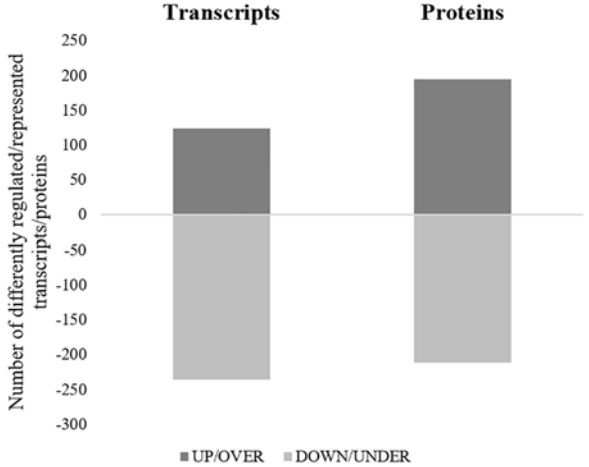

FIGURE 2 | Representation of differentially regulated/represented transcripts/proteins of *R. annulatus* females in response to *B. bigemina* infection. For each approach, the number of transcripts (left column) or proteins (right column) differently regulated or represented are shown. Dark gray = up-regulated transcripts/over-represented proteins, Light gray = down-regulated transcripts/under-represented proteins.

Validation of RNA-Seq Results

To confirm differential gene expression, qPCR was performed on individual SGs. The levels of mRNA genes related to stress response encoding for the following proteins were analyzed: (1) small heat shock protein (HSP) II (UniProt ID:E0YPC0), (2) putative 60 kDa HSP (UniProt ID:L7M6W4), (3) putative heat shock hsp20 protein (UniProt ID:L7M7M1), (4) HSP 90 (UniProt ID:F1CGQ9), (5) Hsp70, putative (UniProt ID:L7M6A7), (6) putative selenoprotein k (UniProt ID:L7M5G4), (7) glutathione peroxidase (UniProt ID:Q2XW15), (8) thioredoxin peroxidase (UniProt ID:L7M1W2), (9) adenylate kinase isoenzyme 6 (UniProt ID:L7M323), (10) tumor rejection antigen-Gp96 (UniProt ID:B7QC85), (11) putative HSP (UniProt ID:L7MFS4), (12) serum amyloid A protein-like (UniProt ID:A6N9S3), (13) dual oxidase 1 (UniProt ID:B7PVC0), (14) putative HSP (UniProt ID:L7M4B9), and (15) putative heat shock transcription factor (PHSTF) (UniProt ID:L7MFL0). In addition, genes encoding for proteins related to apoptosis metabolic pathway were selected for validation of RNAseq by qPCR: (16) cytochrome c oxidase Subunit 1 (UniProt ID:A0A059VIA9), (17) putative death-associated protein kinase dapk-1 (DAPK-1) (UniProt ID:L7MKM3), (18) putative apoptosis inhibitor 5 (UniProt ID:L7LVN8), (19) bax inhibitor-1 related (BI-1) (UniProt ID:G3MPQ7), (20) putative apoptosis antagonizing transcription factor (UniProt ID:L7MAJ6), (21) mitochondrial ribosome small subunit component mediator of apoptosis dap3 (UniProt ID:L7M383) and (22) queuine trna-ribosyltransferase (QtRibosyl) (UniProt ID:L7M340), and

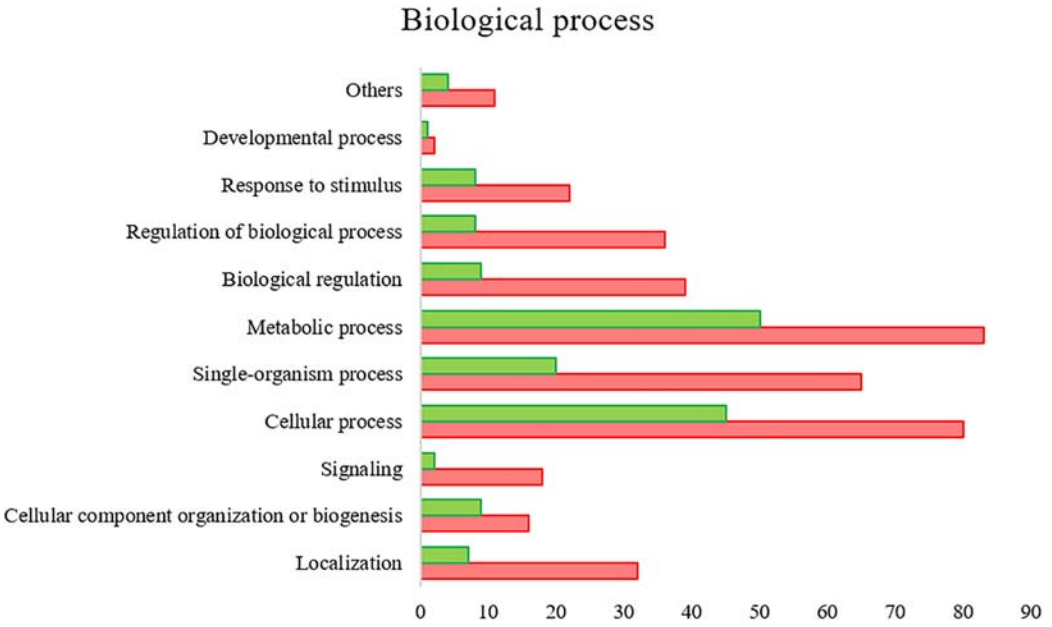

FIGURE 3 | *R. annulatus* SGs transcriptional response to *B. bigemina* infection based on GO BP (level 2) of encoded proteins. Red bars represent down regulated genes, green bars represent up regulated genes with statistical significance ($p < 0.05$).

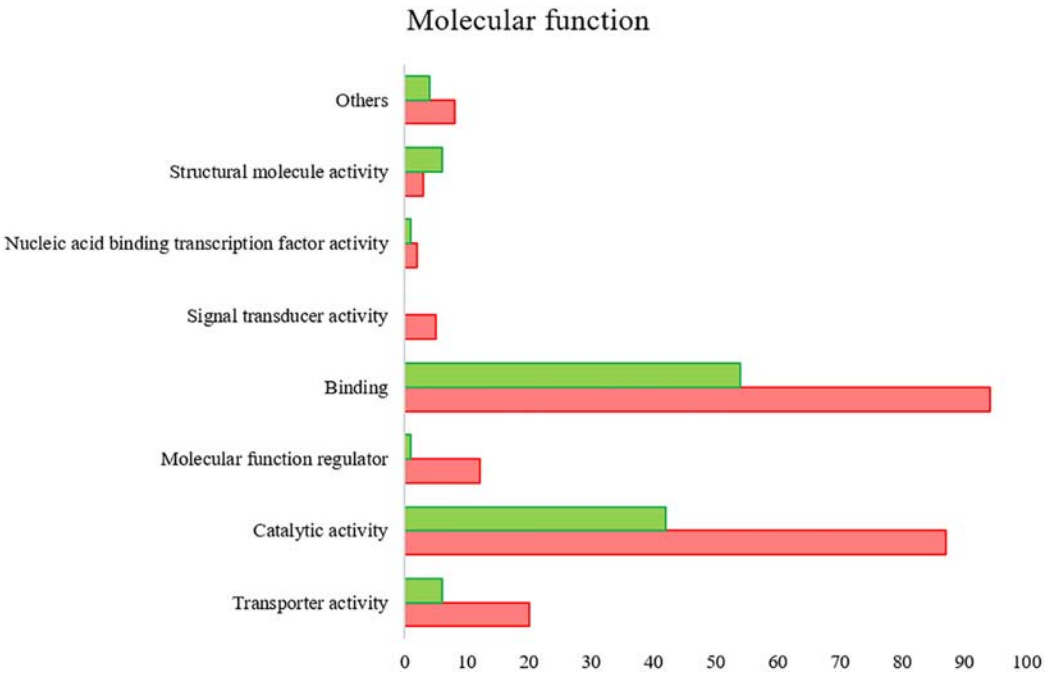

FIGURE 4 | *R. annulatus* SGs transcriptional response to *B. bigemina* infection based on GO MF (level 2) of encoded proteins. Red bars represent down regulated genes, green bars represent up regulated genes with statistical significance ($p < 0.05$).

(23) GP80 (UniProt ID:Q17174) related to proteolysis and lipid transport, respectively (**Supplementary Figure S3**). A moderate positive correlation between the mRNA levels by RNA-Seq and qPCR was obtained (Pearson's correlation coefficient 0.6387, $p = 0.001$).

Proteomics of the *R. annulatus* Female Ticks in Response to *B. bigemina* Infection

Proteomics analysis identified a total of 4,594 proteins in *R. annulatus* female ticks (**Supplementary Table S2**), where

80.08% (n = 3,679) were peptide sequences related to ticks while the remaining were mainly associated with the bovine host. **Supplementary Figure S2** summarizes the functional annotation of the proteome of *R. annulatus* in multi-level charts. When comparing uninfected and *B. bigemina*-infected samples, 406 proteins were found differently represented ($p < 0.05$) and those were annotated using Blast2GO and UniProt-related databases (**Supplementary Table S3**). The proteomics data showed that *Babesia* infection leads to a higher number of under-represented proteins (n = 212), in comparison to over-represented (n = 194) (**Figure 2**). GO analysis contributed for the annotation of 89.41% differentially represented proteins (n = 363), while only 43 proteins were classified as "Unknown" due to the absence of annotation. The level 2 GO terms for BP and MF are shown in **Figures 5**, **6**. The most represented GO terms were cellular, metabolic, and single-organism processes (BP, **Figure 5**), binding, catalytic, and nucleic acid-binding transcription factor activity (MF, **Figure 6**). Focusing on BPs identified herein, only cellular component organization or biogenesis, and cellular and metabolic processes, showed a higher number of over-represented proteins than under-represented. Regarding the MFs, with the exception of structural molecule activity, all were found to be under-represented.

Validation of Proteomics by Western Blot

For the validation of proteomics results, three antibodies against apoptotic and stress-related proteins, Ran, clathrin, and subolesin (4D8), were used for western blot analysis using proteinaceous extracts of fed-uninfected and fed-*Babesia*-infected ticks (**Supplementary Table S4**). The results corroborated proteomics data, showing that in response to *B. bigemina* infection Ran protein (UniProt ID: B7QIB6) is over-represented (Proteomics fold change = $+\infty$; band intensity: NI = non-determinated, I = 5,849,430) while Clathrin (UniProt ID: B7PUK8) was down-regulated (Proteomics fold change = -3.7; band intensity: NI = 11,493.492, I = 5,064.865). The 4D8 protein was found to be over-represented in *Babesia*-infected ticks in comparison to the uninfected ticks (Proteomics fold change = $+\infty$; band intensity: NI = 5,8119.247, I = 11,2021.586) (**Supplementary Figure S4**).

Stress Response and Apoptosis: A System Biology Approach

All apoptotic and stress response-related molecules from transcriptomics and proteomics results were selected to further generate a chord diagram that displays the modulation of gene expression or protein production and its function (**Figure 7**). Eighteen and seven UniProt ID's were found to be related to stress response and apoptosis, respectively. GO clusters such as regulation of BPs, response to stimulus, biological regulation, detoxification, and antioxidant activity were intertwined with these two pathways. Consistent and significant results between transcriptomics and qPCR approaches allowed the identification of three molecules, of which two were up-regulated HSP and putative heat shock-related protein (UniProt IDs: L7MFS4 and L7M4B9, respectively) and DAPK-1 was found down-regulated (UniProt ID: L7MKM3). From this dataset, only two targets were

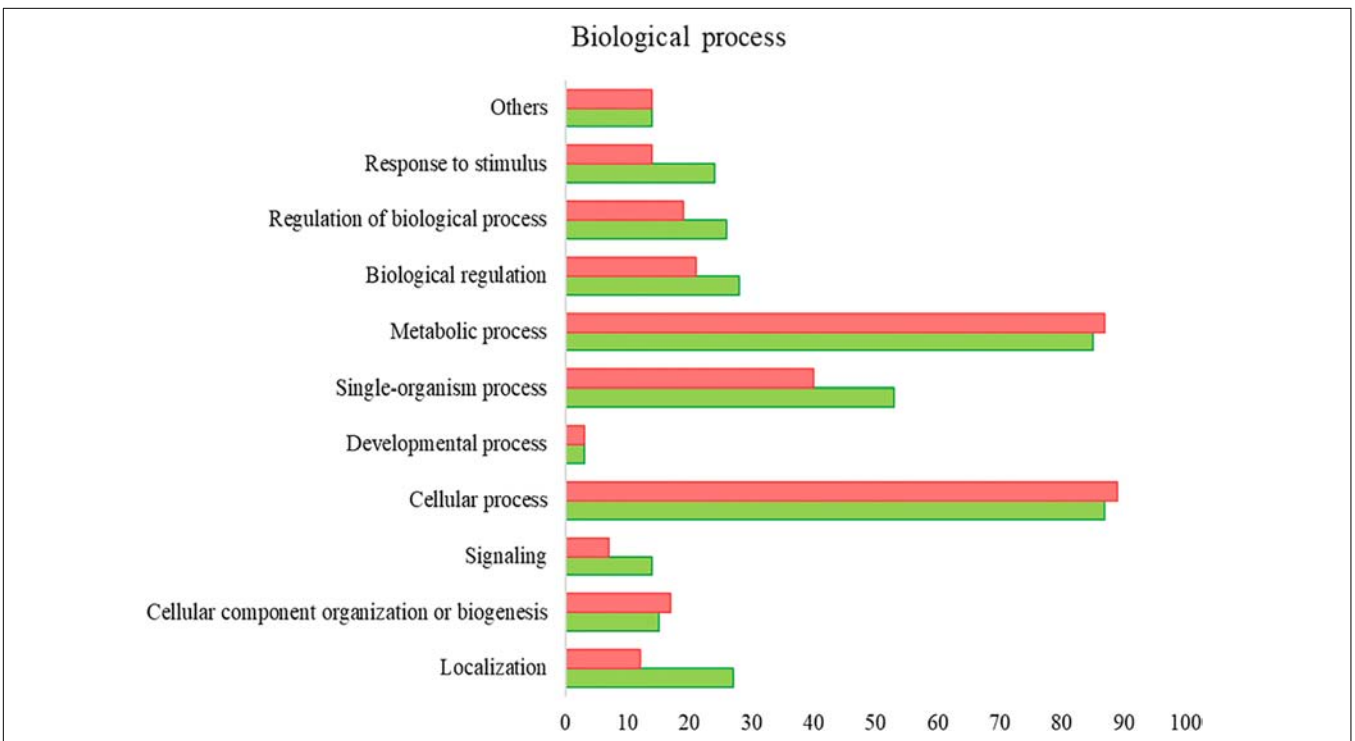

FIGURE 5 | Gene ontology of the proteins from *R. annulatus* in response to *B. bigemina* infection. GO terms and its representation of BP (level 2). Green bars show over-represented proteins and red bars under-represented proteins with statistical significance ($p < 0.05$).

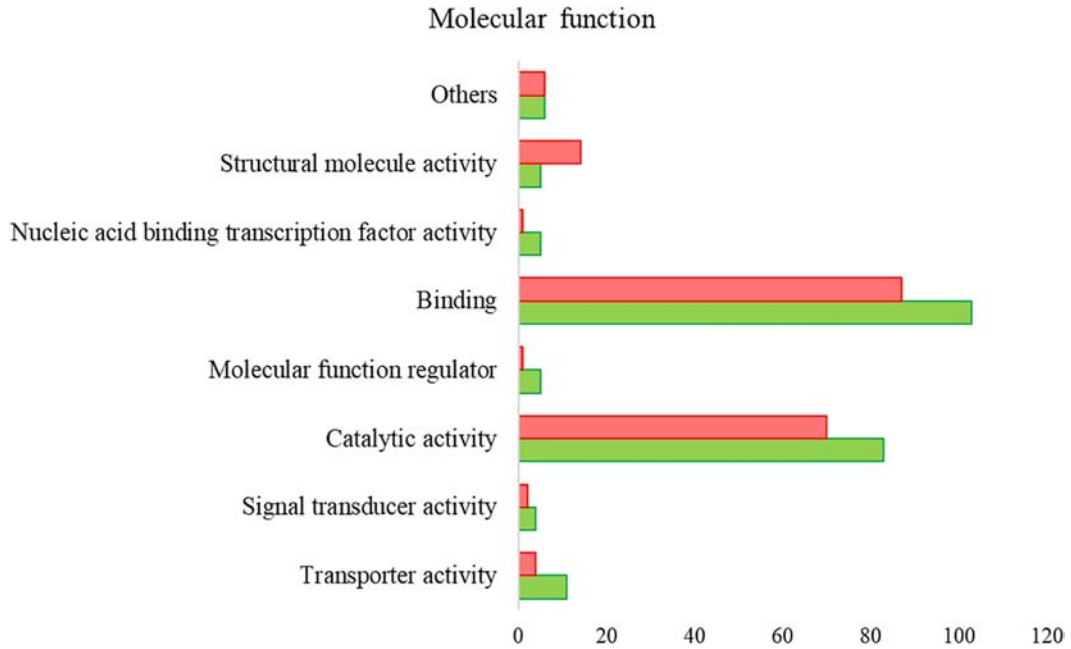

FIGURE 6 | Gene ontology of the proteins from *R. annulatus* in response to *B. bigemina* infection. GO terms and its representation of MF (level 2). Green bars show over-represented proteins and red bars under-represented proteins with statistical significance ($p < 0.05$).

identified in both transcriptomics and proteomics databases, a putative heat shock-related protein (UniProt ID: L7M4B9) and serum amyloid A protein-like (UniProt ID: A6N9S3), with specific modulation of their expression and representation. Four UniProt IDs demonstrated an opposite correlation between cellular protein levels and mRNA abundance, glutathione peroxidase putative heat shock-related protein, PHSTF, and putative apoptosis inhibitor 5 (UniProt IDs: Q2XW15, L7M4B9, L7MFL0, and L7LVN8, respectively).

Selection of Genes for RNA Interference

To gain insight into the functional role of identified tick vector genes/proteins in response to *Babesia* infection, targets for RNAi were selected based on their role in highly represented BPs such as apoptosis and stress response, and differential mRNA/protein levels in response to infection (**Table 1**). Two genes encoding for stress response-related proteins were selected (UniProt ID: L7MFS4 and L7MFL0), identified as being more expressed/represented in infected ticks. The first is a member of the HSP90 family, which is described as being able to regulate a specific subset of cellular signaling proteins that have been implicated in disease processes, particularly in ticks where they have been shown to have a role in virus replication (Weisheit et al., 2015). Transcriptional activation of heat shock genes relies on specific regulators such as the HSTF. Subsequently, a reduction of expression of such regulators may have a higher impact on activation of cellular stress response. Evidence of apoptosis manipulation in tick host cells by infecting pathogens has been demonstrated previously (Ayllon et al., 2015; Alberdi et al., 2016), which lead to the parallel selection of DAPK-1 and BI-1 genes (UniProt ID: L7MKM3 and G3MPQ7). The first, a pro-apoptotic kinase initially identified in vertebrate models, is involved in autophagy and tumor suppression (Inbal et al., 2002) and correspondent mRNA levels were found to be down regulated. The second, with an anti-apoptotic role (Lisak et al., 2015), appears to be under-represented in the current study. In the invertebrates *Drosophila* and *C. elegans* the role of DAPK-1 and related kinases has been briefly addressed revealing additional functions (Chuang and Chisholm, 2014). In ticks no functional studies have been performed so far with these two targets. The protein GP80 (UniProt ID: Q17174) is acknowledged to have a role in lipid transport and vitellogenesis (Tellam et al., 2002) thus correspondent reduction in mRNA levels is expected to deeply affect tick physiological parameters. QtRibosyl (UniProt ID: L7M340) is implicated in transfer RNAs (tRNAs) hypermodification, which in its turn are central players in nuclei acid translation (Lorenz et al., 2017). Particularly, queuine or Q-tRNA participate in many cellular functions, such as cell proliferation inhibition and stress (Vinayak and Pathak, 2009). In ticks, information of the impact of *QtRibosyl* depletion in tick physiological parameters, as well as in pathogen invasion, is still missing.

Functional Studies

Assessment of Gene Silencing and *B. bigemina* Infection

The results of gene knockdown efficiency in SG and its effect on *B. bigemina* infection in both SG and ovaries are shown in **Table 2**. Silencing was achieved for target genes *gp80* (98.6%), *bi-1* (92%), *hsp* (88.5%), and *QtRibosyl* (71.4%), as opposed to

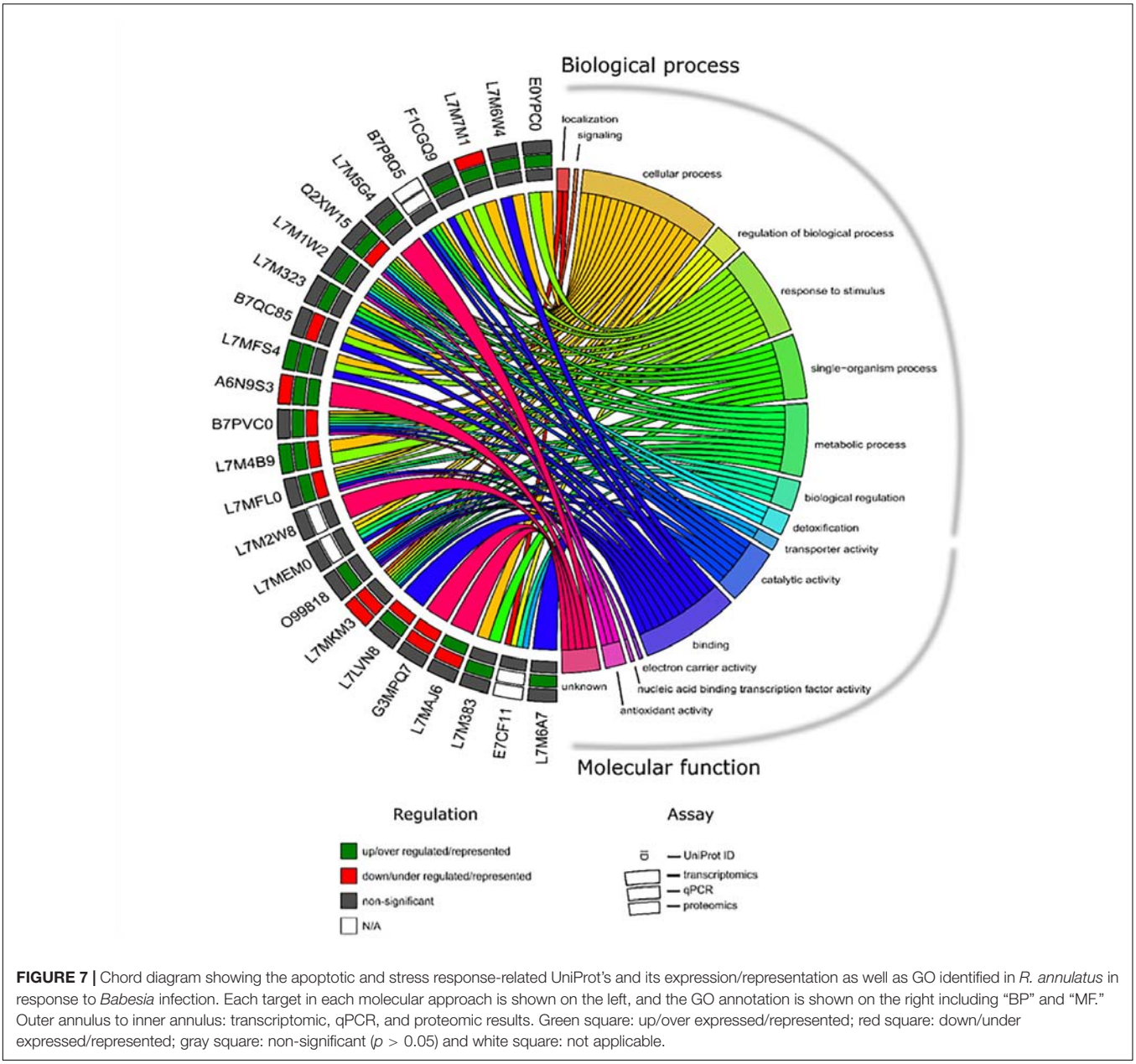

FIGURE 7 | Chord diagram showing the apoptotic and stress response-related UniProt's and its expression/representation as well as GO identified in *R. annulatus* in response to *Babesia* infection. Each target in each molecular approach is shown on the left, and the GO annotation is shown on the right including "BP" and "MF." Outer annulus to inner annulus: transcriptomic, qPCR, and proteomic results. Green square: up/over expressed/represented; red square: down/under expressed/represented; gray square: non-significant ($p > 0.05$) and white square: not applicable.

TABLE 1 | Targets selected for RNAi assays, BPs in which are involved, and their representation on transcriptomics and proteomics analysis.

Gene	Encoding protein (Uniprot ID)	Biological process	mRNA (fold-change) infected/uninfected		Protein infected/uninfected
			RNA seq	qPCR	
gp80	Q17174	Lipid transport	−7.0*	−7.67*	
Death-associated protein kinase-1	L7MKM3	Apoptotic process	−3.31*	−3.35*	
Bax inhibitor 1	G3MPQ7	Apoptotic process	0.231	−1.724	−∞
Heat shock protein	L7MFS4	Stress response	3.25*	3.027*	
Heat shock transcription factor	L7MFLO	Stress response	0.07	1.293	+∞
Queuine trna-ribosyltransferase	L7M340	tRNA modification	0.15	4.18*	−∞

*Red color indicates a significant down regulation or representation of the genes/proteins, the green color indicates a significant up regulation or representation of the genes/proteins while the gray color corresponds to non-significant regulation of the genes/proteins. *$p < 0.05$.*

phstf. Despite testing different conditions, levels of *dapk-1* mRNA were not detected on the ds*dapk-1* inoculated ticks, suggesting an efficient knockdown. Silencing of *gp80*, *dapk-1*, and *bi-1* lead to a significant increase of infection levels in tick SG ($p < 0.05$) with a ratio of 2.29, 19.75, and 4.39, respectively. Knockdown of the remaining targets resulted in a non-significant decrease of infection levels of SG in comparison to the control group. Regarding the ovaries, a significant reduction of *B. bigemina* levels ($p < 0.05$) (ratio 0.16) was observed in response to *gp80* knockdown and in the remaining groups a non-significant increase was detected.

Biological and Reproductive Parameters of Tick After RNAi

Biological and reproductive parameters of *R. annulatus* female ticks injected with specific dsRNA before feeding are shown in **Table 3**. In all cases, the results obtained demonstrate that dsRNA inoculation did not affect the tick feeding ability (Chi-square, $p > 0.05$). Knockdown of *gp80*, *dapk-1*, *bi-1*, and *QtRibosyl* resulted in significantly lower female weights after feeding, in comparison to their respective controls ($p < 0.05$), and also in lower weight of laid eggs ($p < 0.05$). Females belonging to the *gp80*, *dapk*-1, and *QtRibosyl* silenced groups showed a significant ($p < 0.05$) reduction in EPE in comparison with their respective controls, which was not observed in the bi-1 silenced group. Four fed females belonging to the *QtRibosyl* silenced group were not able to lay eggs. *phstf* dsRNA inoculation resulted in lower female weight, egg mass, and EPE, but no statistical analysis was performed since silencing was not demonstrated.

DISCUSSION

Phylogenetic studies on certain pathogens and their tick vectors revealed a deep-rooted co-evolutionary relationship (de la Fuente et al., 2010; Antunes et al., 2017). The origin of piroplasmids could be traced back over millions of years to the time when tick species emerged, suggesting that *Babesia* parasites co-evolved with early tick lineages and their vertebrate hosts (Silva et al., 2011). Some pathogens may have a modest impact

TABLE 2 | Efficiency of gene knockdown by RNAi and its influence on *B. bigemina* infection levels in *R. annulatus* female ticks.

	Group	Gene silencing (%)	*B. bigemina* levels SG (Ave ± *SD*)	Test/Ct (Ave)	*B. bigemina* levels Ovaries (Ave ± *SD*)	Test/Ct (Ave)
Calf 1	*gp80*	∼98.6	$4.74e^{-04} \pm 1.53e^{-04}$	2.29*	$8.34e^{-06} \pm 7.39e^{-06}$	0.16*
	Death-associated protein kinase-1	[a]	$4.09e^{-03} \pm 4.23e^{-03}$	19.75*	$2.26e^{-04} \pm 2.29e^{-04}$	4.18
	Bax inhibitor 1 related	∼92	$9.07e^{-03} \pm 9.91e^{-04}$	4.39	$1.06e^{-04} \pm 7.02e^{-05}$	1.96
	Control	–	$2.07e^{-04} \pm 1.23e^{-03}$	–	$5.40e^{-05} \pm 3.83e^{-05}$	–
Calf 2	*Heat shock protein*	∼88.5	$1.80e^{-03} \pm 2.16e^{-03}$	0.67	$7.27e^{-05} \pm 4.53e^{-05}$	2.46
	Heat shock transcription factor	ND	–	–	–	–
	Queuine trna-ribosyltransferase	∼71.4	$1.86e^{-03} \pm 2.35e^{-03}$	0.69	$4.91e^{-05} \pm 2.89e^{-05}$	1.67
	Control	–	$2.70e^{-03} \pm 3.88e^{-03}$	–	$2.96e^{-05} \pm 1.79e^{-05}$	–

*Thirty female R. annulatus ticks per group were injected with specific dsRNA or elution buffer as control. Ticks were allowed to feed in separated patches on calves experimentally infected with B. bigemina. Gene knockdown was analyzed by qPCR in 10 individual SGs per group by comparing mRNA levels between specific dsRNA-injected and control ticks using the CFX Manager™ Software by means of the Pfaff method, *$p < 0.05$. The B. bigemina infection levels were determined in tick SG and ovaries by qPCR of the pathogen 18S rRNA gene and normalized against tick 16S rRNA using the ddCq method ($2^{-Cq_{target}-Cq_{control}}$). Infection rate was calculated by the ratio of silenced per control groups. The mRNA levels and B. bigemina infection in ticks were compared between specific dsRNA injected and control ticks by a Student's t-test (*$p < 0.05$). ds, double-stranded; ND, not demonstrated; a, mRNA levels not detected in the silenced group.*

TABLE 3 | Evaluation of biological and reproductive parameters of *R. annulatus* female ticks injected with specific-dsRNA.

	Group	*n*	Attach (%)	EFW (mg Ave ± SD)	*n*	EMW (mg Ave ± SD)	EPE (Ave ± SD)
Calf 1	*gp80*	20	66.7	186 ± 56*	10	64 ± 21*	40.967 ± 7.280*
	death-associated protein kinase	17	56.7	144 ± 61*	7	52 ± 24*	37.330 ± 3.882*
	Bax inhibitor 1 related	18	60.0	200 ± 74*	8	71 ± 30*	47.622 ± 9.297
	Control	22	73.3	233 ± 35	12	113 ± 20	48.588 ± 3.735
Calf 2	*Heat shock protein*	19	63.3	226 ± 41	9	115 ± 29	50.763 ± 6.237
	Heat shock transcription factor	17	56.7	216 ± 41[a]	7	76 ± 10[a]	39.719 ± 3.335[a]
	Queuine trna-ribosyltransferase	20	66.7	149 ± 56*	10	59 ± 25*[b]	21.705 ± 19.982*
	Control	20	66.7	242 ± 45	10	124 ± 28	50.015 ± 2.881

Thirty R. annulatus female ticks per group were injected with dsRNA or elution buffer as control. Ticks were allowed to feed in separated patches on calves experimentally infected with B. bigemina. All attached ticks were collected after 7 days of feeding, weighed, and held in an acclimatized room. Ten ticks per group were randomly selected and SG dissected. The remaining were allowed to lay eggs. Tick ability to feed was evaluated as the ratio of removed ticks to the total number of ticks placed on the lamb using Chi-square test ($p < 0.05$). Female tick weight after feeding, EMW, and EPE were compared between dsRNA and unrelated dsRNA ticks by Student's t-test. The EPE was calculated according to the formula EPE = (EMW/EFW) × 100. N, number of samples used in the statistical analysis of the subsequent parameters; EFW, engorged female weight; EMW, egg mass weight; EPE, egg production efficiency; *, statistical difference when compared to the control group. [a]No statistical analysis was performed due to no gene knockdown. [b]Four females didn't laid eggs.*

upon their vector and/or host, while others greatly influence host fitness and may manipulate host gene expression to favor infection, dissemination, and transmission (Cen-Aguilar et al., 1998; Mercado-Curiel et al., 2011; Antunes et al., 2017, 2018; Cornejo et al., 2017). We have found in our previous studies that the presence of *Babesia* in ticks induces a transcriptional shift (Antunes et al., 2012), particularly in the SGs (Antunes et al., 2018). Herein, a systems biology approach was applied to gain a more refined understanding on the complex interplay between *B. bigemina* and its tick vector *R. annulatus*. Our results identified *dapk-1*, *bi-1*, *gp80*, and *QtRibosyl* genes, that have important roles in apoptosis and vitellogenesis, and demonstrated that *Babesia* infection fundamentally affects key processes in SG tick cells.

It has been well documented that apoptosis is a highly regulated form of cell death. This process ensures a cell or organ to respond adequately to stress, thus limiting the risk of a disease or an infection that may compromise the ability of an organism to survive. Since its discovery, apoptosis has been extensively studied and its molecular regulation is now well understood. One of the critical components of this cell death pathway is *dapk-1*, a pro-apoptotic kinase, which can also regulate autophagy. Typically, *dapk-1* has been studied in the context of its suppression in tumor growth and metastasis but additional roles emerged in last years (Farag and Roh, 2019). In this study, we have shown that exposure of ticks to *B. bigemina* significantly down regulated the transcription of *dapk-1* in tick SG cells. This might have a significant impact upon the survival and propagation of *Babesia* parasites in its vector host. Inhibition of apoptosis in ticks and tick cells toward infection and survival is a strategy previously described in *Anaplasma* infection (Ayllon et al., 2015; Alberdi et al., 2016). Furthermore, silencing *dapk-1* led to a substantial increase in *B. bigemina* infection in the SG cells of ticks that fed on an infected calf. After a tick takes a blood meal, the SGs enlarge, then degenerate, and become atrophied. Recent evidence has demonstrated that SG transformation into a vestigial state is due to caspase-1-mediated apoptosis, limiting the potential for pathogen transmission (Yu et al., 2017). It is therefore interesting to observe the ability of *B. bigemina* infection to selectively restrict a vital gene within the apoptotic pathway. By blocking the apoptosis process, the parasite might very likely survive and persist in the tissue and further facilitate dissemination of the infection throughout the tick, and subsequent transmission to another host. In the event of apoptosis occurring in SGs, the parasite might be eliminated, likely *via* its destruction following the engulfment of the apoptotic bodies it is occupying. The *dapk-1* silenced ticks had significant lower weight than the control ticks, after a blood meal which might be attributed to the increased virulence observed, as this knockdown was not a spurious consequence of elevated biting rates. Such impact in female ticks has been previously described after silencing apoptosis-related genes in *A. phagocytophilum* infection in the tick vector *I. scapularis* (Ayllon et al., 2013, 2015). To the best of our knowledge, our study is the first ever reported to identify *dapk-1* from a high-resolution multi-omic screen of any *Rhipicephalus* tick species infected with *Babesia* parasites. Further research will seek to elucidate the molecular mechanism underlying *dapk-1* suppression in these cells and its functional significance.

The BI-1-related protein (UniProt ID: G3MPQ7) belongs to the Bax inhibitory protein-like family, exhibiting a highly conserved BI-1 domain throughout eukaryotes and prokaryotes (Lisak et al., 2015). Sequence analyses showed a high homology to an *Amblyomma triste* putative growth hormone-induced protein (UniProt ID: A0A023GIS5) and a growth hormone-inducible transmembrane protein-like from *Rhipicephalus zambeziensis* (UniProt ID: A0A224YYC2), also known as transmembrane BAX inhibitor motif (TMBIM) containing protein 5 supporting its anti-apoptotic role (Reimers et al., 2007; Rojas-Rivera and Hetz, 2015). TMBIM5 is recognized to be the only member from the TMBIM family of proteins localized mainly in the inner mitochondrial membrane and directly involved in the outer mitochondrial membrane permeability. Down regulation of such a protein leads to the release of pro-apoptotic proteins from the mitochondria, whereas overexpression results in the stabilization of cytochrome c at the inner membrane (Oka et al., 2008). Herein, the *R. annulatus* putative ortholog protein was found to be down regulated in response to infection, suggesting that under invasion there is an induction of cell apoptosis. However, reinforcement of gene down regulation resulted in the increase of *B. bigemina* levels in the SGs. Interestingly, the expression of this gene was also found to be down regulated in many types of cancer suggesting that the functional impact of its regulation is not fully understood yet (Rojas-Rivera and Hetz, 2015). Our results point to interactions between *Babesia* parasites and the tick apoptosis-related molecules, which requires further investigation with a special reference to this particular metabolic pathway.

In ticks, vitellogenesis is the process of yolk formation with the material accumulating in the developing oocyte and characterized by the synthesis of vitellogenins (Vg) during the reproductive period (Coons et al., 1989). GP80 is a processed product from vitellogenin, encoded by one *Vg* gene (Thompson et al., 2007; Taheri et al., 2014), and for simplicity we will maintain, herein, the GP80 nomenclature. Multiple *Vgs* have been described in ticks (Boldbaatar et al., 2010; Rodriguez et al., 2016; Xavier et al., 2018). Sequence analysis demonstrate a high similarity of *gp80* to *Vg-1* (UniProt ID: A0A034WTV5). In this study, *B. bigemina* infection led to a significant down regulation of *gp80* transcription, which is in contrast to our previous study results (Antunes et al., 2012). A possible explanation for this discrepancy relies on the different tissues analyzed in the two studies. In the present one, only SGs were targeted, whereas Vgs are considered to be absent and are thought to be functionally replaced by the hemelipoglyco-carrier protein (CP) (Donohue et al., 2009). Encountering transcription of the *gp80* in this organ suggests that *Rhipicephalus* SGs possess genes highly similar to Vgs, sharing many molecular features to since similar results were attained in SGs of *Rhipicephalus bursa* (Antunes et al., 2018). Our data revealed a significant decline in engorged female *R. annulatus* weight, EMW, and EPE, when *gp80* was silenced, upon feeding on an infected calf in accordance to previous studies (Boldbaatar et al., 2010; Antunes et al., 2018). Keeping

in mind that the silencing methodology is not tissue specific, our results suggest that a decreased expression of *Vgs* leads to a reduction in lipid transport and normal production of energy (ATP) provided by lipid disruption, leading to an abnormal or delayed development of ovaries and eggs. A consequent increase in *B. bigemina* infectivity in SG was observed by silencing *gp80* and a parallel decrease was detected in the ovaries. This parasite sustains transmission via both horizontal and vertical routes, through feeding and eggs production, respectively, which imply that a parasite-driven strategy to restrict vitellogenin synthesis is less likely. This data suggest that the host may redirect resources away from cell defense against pathogens toward processes with a more urgent demand such as egg production. Therefore, once facing lack of *Vgs* transcription, which will ultimately affect progeny, cells efforts will go to compensate this process, leaving SG cells more prone to infection and pathogen dissemination. However, the opposite scenario was observed in the ovaries, whereas a decrease of the levels of *B. bigemina* was detected suggesting that parasite transmission is hampered by the GP80 deficiency. A similar effect has been observed in *Laodelphax striatellus* whereas the transmission of a virus is facilitated by the expression of an insect-specific *Vg* (Huo et al., 2018). In fact, it seems that the process of vitellogenesis is critical for efficient pathogen transovarial transmission and is has been suggested that *Babesia* may directly interact with a Vg receptor (Boldbaatar et al., 2008; Hussein et al., 2019). Targeting vitellogenesis to control tick infestation is a very attractive approach, since the inhibition or disruption of such process may result in tick female mortality, decreased egg production, and viability and, ultimately, have an effect on pathogens with transovarial transmission such as *Babesia* spp.

Transfer RNAs are primarily involved in translation, functioning as adaptors from DNA to proteins (Pathak et al., 2007; Lorenz et al., 2017). One of the most important tRNA hypermodification is the replacement of guanosine by an analog, the nucleoside queuosine (Vinayak and Pathak, 2009), resulting in queuine-tRNA (Q-tRNA) and implicating a cascade of enzymatic reactions (Betat et al., 2010). This Q-tRNA have been shown to correlate with diverse cell processes including stress tolerance, cell proliferation, tumor growth, and protein translation (Fergus et al., 2015; Tuorto et al., 2018). QtRibosyl, herein designated as QtRibosyl, is an enzyme involved in the chemical reaction that results in queuosine base modification (Deshpande and Katze, 2001; Fergus et al., 2015). In the present study, the expression of *QtRibosyl* was found to be up regulated while protein levels were found to be down regulated in response to infection. This may be due to several biological factors such as the occurrence of post-transcriptional and post-translational modifications but also due to methodological constraints (Maier et al., 2009; Ayllon et al., 2015; Villar et al., 2015). Interestingly, the human ortholog enzyme gene (*Queuine tRNA-ribosyltransferase catalytic subunit 1-QTRT1*) has been found differentially regulated in some cancer tissues. It has been shown that, as a consequence, the Q-tRNA deficiency is associated with different neoplastic tissues and may even correlate with tumor grade (Vinayak and Pathak, 2009; Fergus et al., 2015). A high expression of such enzyme suggests that the cell needs to produce Q-tRNA either to promote the activity of antioxidant enzymes, secure protein folding, or to maintain high glycolytic rate (Pathak et al., 2008; Fergus et al., 2015; Tuorto et al., 2018), processes which have been demonstrated to occur in infected ticks (Villar et al., 2015; Cabezas-Cruz et al., 2017). Moreover, the present study demonstrated that efficient knockdown of *QtRibosyl* affected tick parameters and led to a marked reduction of female weight, egg mass, and EPE. These findings are clearly supporting the role of Q-tRNA in cell proliferation and glycolytic metabolism. A non-significant reduction of *Babesia* infection in tick SG was also observed, which can be related to a deficit on cellular ATP pools, which in its turn results in a shortage of nutrients essential for parasite multiplication (Trager, 1974).

Stimulation of a cell stress response by pathogens in ticks has been previously reported (Mulenga et al., 2003; Villar et al., 2010; Busby et al., 2012; Weisheit et al., 2015). Herein, two heat shock-related genes were targeted: the *hsp* which was found to be up regulated upon infection and the *phstf* that showed a similar expression in SG on both conditions. Knockdown of *hsp* did not significantly affected the studied parameters, although further studies centered in this biologically relevant pathway in ticks should be performed to deepen our understanding on tick–*Babesia* interface.

Our study has pinpointed interesting tick proteins interacting with *Babesia*. Still, due to its transovarial and transstadial transmission capacity, future studies focusing on early feeding time points, other tick stages, or other tissues, such as ovaries, are needed to fully understand the molecular dynamics at the tick–pathogen interface.

CONCLUSION

For many intracellular parasites, the host cell is no longer an opponent but rather an assistant, evolving to efficiently and precisely manipulate their host. Accordingly, in ticks, *Anaplasma* bacteria are able to subordinate cell BPs such as apoptosis and glycogenesis. The present study shed some light regarding the *Rhipicephalus–Babesia* interface by making use of transcriptomics and proteomics allied to gene functional analysis. The results obtained point out a strong parasitic pressure over cellular functions, of which processes like apoptosis and stress response stand out. The genes *dapk-1*, *QtRibosyl*, and *gp80* were characterized with regard to their role on tick reproductive parameters and interaction with *Babesia* infection, and showed to be highly influential functional molecules. The importance of understanding the tick biology and tick–pathogen molecular interactions is of the outmost importance in the discovery of suitable vaccine candidates to control tick populations and tick-borne diseases.

DATA AVAILABILITY

The datasets generated for this study can be found in DDBJ/EMBL/GenBank and PeptideAtlas repository, Accession numbers GBJT00000000, GBJS00000000, and identifier PASS01339, respectively.

AUTHOR CONTRIBUTIONS

SA, JdlF, and AD designed the study. VS, MM, and JMC were responsible for tick rearing. SA, JC, JF, MV, and JdlF performed transcriptomics and proteomics analyses. SA and JC performed qPCR assays and western blots. JMC, ND, SA, JC, and JF performed the RNA interference studies. SA, JC, JdlF, GS, and AD performed data analysis and wrote the manuscript. All authors edited and approved the final manuscript.

FUNDING

RHIBAB - PTDC/CVT/112050/2009 "Differential expression and functional characterization of tick (*Rhipicephalus annulatus*) genes in response to pathogen infection (*B. bigemina*)." SA is the recipient of a post-doctoral grant supported by FCT (SFRH/BPD/108957/2015), JC and JF are the recipients of Ph.D. grants supported by the FCT (SFRH/BD/121946/2016 and SFRH/BD/122894/2016, respectively).

ACKNOWLEDGMENTS

The authors would like to acknowledge Fundação para a Ciência e Tecnologia (FCT) for funds to GHTM – UID/Multi/04413/2013.

SUPPLEMENTARY MATERIAL

The Supplementary Material for this article can be found online at: https://www.frontiersin.org/articles/10.3389/fphys.2019.00318/full#supplementary-material

REFERENCES

Alberdi, P., Ayllón, N., Cabezas-Cruz, A., Bell-Sakyi, L., Zweygarth, E., Stuen, S., et al. (2015). Infection of *Ixodes* spp. tick cells with different *Anaplasma phagocytophilum* isolates induces the inhibition of apoptotic cell death. *Ticks Tick Borne Dis.* 6, 758–767. doi: 10.1016/j.ttbdis.2015.07.001

Alberdi, P., Espinosa, P. J., Cabezas-Cruz, A., and de la Fuente, J. (2016). *Anaplasma phagocytophilum* manipulates host cell apoptosis by different mechanisms to establish infection. *Vet. Sci.* 3:E15. doi: 10.3390/vetsci3030015

Almazan, C., Tipacamu, G. A., Rodriguez, S., Mosqueda, J., and Perez de Leon, A. (2018). Immunological control of ticks and tick-borne diseases that impact cattle health and production. *Front. Biosci.* 23, 1535–1551. doi: 10.2741/4659

Antunes, S., Couto, J., Ferrolho, J., Rodrigues, F., Nobre, J., Santos, A. S., et al. (2018). *Rhipicephalus bursa* sialotranscriptomic response to blood feeding and *Babesia ovis* infection: identification of candidate protective antigens. *Front. Cell. Infect. Microbiol.* 8:116. doi: 10.3389/fcimb.2018.00116

Antunes, S., Galindo, R. C., Almazan, C., Rudenko, N., Golovchenko, M., Grubhoffer, L., et al. (2012). Functional genomics studies of *Rhipicephalus* (*Boophilus) annulatus* ticks in response to infection with the cattle protozoan parasite, *Babesia bigemina*. *Int. J. Parasitol.* 42, 187–195. doi: 10.1016/j.ijpara.2011.12.003

Antunes, S., Rosa, C., Couto, J., Ferrolho, J., and Domingos, A. (2017). Deciphering *Babesia*-vector interactions. *Front. Cell. Infect. Microbiol.* 7:429. doi: 10.3389/fcimb.2017.00429

Ayllon, N., Villar, M., Busby, A. T., Kocan, K. M., Blouin, E. F., Bonzon-Kulichenko, E., et al. (2013). *Anaplasma phagocytophilum* inhibits apoptosis and promotes cytoskeleton rearrangement for infection of tick cells. *Infect. Immun.* 81, 2415–2425. doi: 10.1128/iai.00194-13

Ayllon, N., Villar, M., Galindo, R. C., Kocan, K. M., Sima, R., Lopez, J. A., et al. (2015). Systems biology of tissue-specific response to *Anaplasma phagocytophilum* reveals differentiated apoptosis in the tick vector *Ixodes scapularis*. *PLoS Genet.* 11:e1005120. doi: 10.1371/journal.pgen.1005120

Betat, H., Rammelt, C., and Mörl, M. (2010). tRNA nucleotidyltransferases: ancient catalysts with an unusual mechanism of polymerization. *Cell. Mol. Life Sci.* 67, 1447–1463. doi: 10.1007/s00018-010-0271-4

Beugnet, F., and Moreau, Y. (2015). Babesiosis. *Rev. Sci. Tech.* 34, 627–639. doi: 10.20506/rst.34.2.2385

Bock, R., Jackson, L., De Vos, A., and Jorgensen, W. (2004). Babesiosis of cattle. *Parasitology* 129, S247–S269. doi: 10.1017/s0031182004005190

Boldbaatar, D., Battsetseg, B., Matsuo, T., Hatta, T., Umemiya-Shirafuji, R., Xuan, X., et al. (2008). Tick vitellogenin receptor reveals critical role in oocyte development and transovarial transmission of *Babesia* parasite. *Int. J. Biochem. Cell Biol.* 86, 331–344. doi: 10.1139/o08-071

Boldbaatar, D., Umemiya-Shirafuji, R., Liao, M., Tanaka, T., Xuan, X. N., and Fujisaki, K. (2010). Multiple vitellogenins from the *Haemaphysalis longicornis* tick are crucial for ovarian development. *J. Insect. Physiol.* 56, 1587–1598. doi: 10.1016/j.jinsphys.2010.05.019

Busby, A. T., Ayllón, N., Kocan, K. M., Blouin, E. F., de la Fuente, G., Galindo, R. C., et al. (2012). Expression of heat shock proteins and subolesin affects stress responses, *Anaplasma phagocytophilum* infection and questing behaviour in the tick, *Ixodes scapularis*. *Med. Vet. Entomol* 26, 92–102. doi: 10.1111/j.1365-2915.2011.00973.x

Cabezas-Cruz, A., Alberdi, P., Valdés, J. J., Villar, M., and de la Fuente, J. (2017). *Anaplasma phagocytophilum* infection subverts carbohydrate metabolic pathways in the tick vector, *Ixodes scapularis*. *Front. Cell. Infect. Microbiol.* 7:23. doi: 10.3389/fcimb.2017.00023

Cen-Aguilar, J. F., Rodriguez-Vivas, R. I., Dominguez-Alpizar, J. L., and Wagner, G. G. (1998). Studies on the effect of infection by *Babesia* sp. on oviposition of *Boophilus microplus* engorged females naturally infected in the Mexican tropics. *Vet. Parasitol.* 78, 253–257. doi: 10.1016/s0304-4017(98)00148-4

Chauvin, A., Moreau, E., Bonnet, S., Plantard, O., and Malandrin, L. (2009). *Babesia* and its hosts: adaptation to long-lasting interactions as a way to achieve efficient transmission. *Vet. Res.* 40:37. doi: 10.1051/vetres/2009020

Chuang, M., and Chisholm, A. D. (2014). Insights into the functions of the death associated protein kinases from *C. elegans* and other invertebrates. *Apoptosis* 19, 392–397. doi: 10.1007/s10495-013-0943-2

Conesa, A., Gotz, S., Garcia-Gomez, J. M., Terol, J., Talon, M., and Robles, M. (2005). Blast2GO: a universal tool for annotation, visualization and analysis in functional genomics research. *Bioinformatics* 21, 3674–3676. doi: 10.1093/bioinformatics/bti610

Coons, L. B., Lamoreaux, W. J., Rosell-Davis, R., and Tarnowski, B. I. (1989). Onset of vitellogenin production and vitellogenesis, and their relationship to changes in the midgut epithelium and oocytes in the tick *Dermacentor variabilis*. *Exp. Appl. Acarol.* 6, 291–305. doi: 10.1007/BF01193301

Cornejo, E., Schlaermann, P., and Mukherjee, S. (2017). How to rewire the host cell: a home improvement guide for intracellular bacteria. *J. Cell Biol.* 216, 3931–3948. doi: 10.1083/jcb.201701095

Corson, M. S., Teel, P. D., and Grant, W. E. (2001). Influence of acaricide resistance on cattle-fever tick (Boophilus spp.) infestations in semi-arid thornshrublands: a simulation approach. *Exp. Appl. Acarol.* 25, 171–184. doi: 10.1023/A:1010674303962

de la Fuente, J., Estrada-Peña, A., Cabezas-Cruz, A., and Kocan, K. M. (2016). *Anaplasma phagocytophilum* uses common strategies for infection of ticks and vertebrate hosts. *Trends Microbiol.* 24, 173–180. doi: 10.1016/j.tim.2015.12.001

de la Fuente, J., Kocan, K. M., Blouin, E. F., Zivkovic, Z., Naranjo, V., Almazán, C., et al. (2010). Functional genomics and evolution of tick-*Anaplasma* interactions and vaccine development. *Vet. Parasitol.* 167, 175–186. doi: 10.1016/j.vetpar.2009.09.019

Deshpande, K. L., and Katze, J. R. (2001). Characterization of cDNA encoding the human tRNA-guanine transglycosylase (TGT) catalytic subunit. *Gene* 265, 205–212. doi: 10.1016/S0378-1119(01)00368-7

Domingos, A., Pinheiro-Silva, R., Couto, J., do Rosário, V., and de la Fuente, J. (2017). The *Anopheles gambiae* transcriptome - a turning point for malaria control. *Insect. Mol. Biol* 26, 140–151. doi: 10.1111/imb.12289

Donohue, K. V., Khalil, S. M. S., Sonenshine, D. E., and Roe, R. M. (2009). Heme-binding storage proteins in the Chelicerata. *J. Insect. Physiol.* 55, 287–296. doi: 10.1016/j.jinphys.2009.01.002

Evans, V. C., Barker, G., Heesom, K. J., Fan, J., Bessant, C., and Matthews, D. A. (2012). De novo derivation of proteomes from transcriptomes for transcript and protein identification. *Nat. Methods* 9, 1207–1211. doi: 10.1038/nmeth.2227

Farag, A. K., and Roh, E. J. (2019). Death-associated protein kinase (DAPK) family modulators: current and future therapeutic outcomes. *Med. Res. Rev.* 39, 349–385. doi: 10.1002/med.21518

Fergus, C., Barnes, D., Alqasem, M. A., and Kelly, V. P. (2015). The queuine micronutrient: charting a course from microbe to man. *Nutrients* 7, 2897–2929. doi: 10.3390/nu7042897

Ferrolho, J., Antunes, S., Sanches, G. S., Couto, J., Evora, P. M., Rosa, C., et al. (2017). Ferritin 1 silencing effect in *Rhipicephalus sanguineus* sensu lato (Acari: Ixodidae) during experimental infection with *Ehrlichia canis*. *Ticks Tick Borne Dis.* 8, 174–184. doi: 10.1016/j.ttbdis.2016.10.015

Ghosh, S., Azhahianambi, P., and Yadav, M. P. (2007). Upcoming and future strategies of tick control: a review. *J. Vector Borne Dis.* 44, 79–89.

Götz, S., García-Gómez, J. M., Terol, J., Williams, T. D., Nagaraj, S. H., Nueda, M. J., et al. (2008). High-throughput functional annotation and data mining with the Blast2GO suite. *Nucleic Acids Res.* 36, 3420–3435. doi: 10.1093/nar/gkn176

Holt, R. A., Subramanian, G. M., Halpern, A., Sutton, G. G., Charlab, R., Nusskern, D. R., et al. (2002). The genome sequence of the malaria mosquito *Anopheles gambiae*. *Science* 298, 129–149. doi: 10.1126/science.1076181

Huo, Y., Yu, Y., Chen, L., Li, Q., Zhang, M., Zhiyu, S., et al. (2018). Insect tissue-specific vitellogenin facilitates transmission of plant virus. *PLoS Pathog.* 14:e1006909. doi: 10.1371/journal.ppat.1006909

Hussein, H. E., Johnson, W. C., Taus, N. S., Suarez, C. E., Scoles, G. A., and Ueti, M. W. (2019). Silencing expression of the *Rhipicephalus microplus* vitellogenin receptor gene blocks *Babesia bovis* transmission and interferes with oocyte maturation. *Parasit. Vectors* 12:7. doi: 10.1186/s13071-018-3270-1

Hussein, H. E., Scoles, G. A., Ueti, M. W., Suarez, C. E., Adham, F. K., Guerrero, F. D., et al. (2015). Targeted silencing of the Aquaporin 2 gene of *Rhipicephalus (Boophilus) microplus* reduces tick fitness. *Parasit. Vectors* 8:618. doi: 10.1186/s13071-015-1226-2

Inbal, B., Bialik, S., Sabanay, I., Shani, G., and Kimchi, A. (2002). DAP kinase and DRP-1 mediate membrane blebbing and the formation of autophagic vesicles during programmed cell death. *J. Cell Biol.* 157, 455–468. doi: 10.1083/jcb.200109094

Kim, C., Iseki, H., Herbas, M. S., Yokoyama, N., Suzuki, H., Xuan, X., et al. (2007). Development of TaqMan-based real-time PCR assays for diagnostic detection of *Babesia bovis* and *Babesia bigemina*. *Am. J. Trop. Med. Hyg.* 77, 837–841. doi: 10.4269/ajtmh.2007.77.837

Leiby, D. A. (2006). Babesiosis and blood transfusion: flying under the radar. *Vox Sang* 90, 157–165. doi: 10.1111/j.1423-0410.2006.00740.x

Lempereur, L., Beck, R., Fonseca, I., Marques, C., Duarte, A., Santos, M., et al. (2017). Guidelines for the detection of *Babesia* and *Theileria* parasites. *Vector Borne Zoonotic Dis.* 17, 51–65. doi: 10.1089/vbz.2016.1955

Lisak, D. A., Schacht, T., Enders, V., Habicht, J., Kiviluoto, S., Schneider, J., et al. (2015). The transmembrane Bax inhibitor motif (TMBIM) containing protein family: tissue expression, intracellular localization and effects on the ER CA^{2+}-filling state. *Biochim. Biophys. Acta* 1853, 2104–2114. doi: 10.1016/j.bbamcr.2015.03.002

Lorenz, C., Lünse, C. E., and Mörl, M. (2017). tRNA modifications: impact on structure and thermal adaptation. *Biomolecules* 7:E35. doi: 10.3390/biom7020035

Madder, M., Horak, I., and Stoltsz, H. (2014). *Tick Identification, Faculty of Veterinary Science*. Hatfield: University of Pretoria, 58.

Maier, T., Güell, M., and Serrano, L. (2009). Correlation of mRNA and protein in complex biological samples. *FEBS Lett.* 583, 3966–3973. doi: 10.1016/j.febslet.2009.10.036

McTaggart, S. J., Cézard, T., Garbutt, J. S., Wilson, P. J., and Little, T. J. (2015). Transcriptome profiling during a natural host-parasite interaction. *BMC Genomics* 16:643. doi: 10.1186/s12864-015-1838-0

Mercado-Curiel, R. F., Palmer, G. H., Guerrero, F. D., and Brayton, K. A. (2011). Temporal characterisation of the organ-specific *Rhipicephalus microplus* transcriptional response to *Anaplasma marginale* infection. *Int. J. Parasitol.* 41, 851–860. doi: 10.1016/j.ijpara.2011.03.003

Mulenga, A., Macaluso, K. R., Simser, J. A., and Azad, A. F. (2003). Dynamics of Rickettsia-tick interactions: identification and characterization of differentially expressed mRNAs in uninfected and infected *Dermacentor variabilis*. *Insect. Mol. Biol.* 12, 185–193. doi: 10.1046/j.1365-2583.2003.00400.x

Nijhof, A. M., Balk, J. A., Postigo, M., and Jongejan, F. (2009). Selection of reference genes for quantitative RT-PCR studies in *Rhipicephalus (Boophilus) microplus* and *Rhipicephalus appendiculatus* ticks and determination of the expression profile of Bm86. *BMC Mol. Biol.* 10:112. doi: 10.1186/1471-2199-10-112

Oka, T., Sayano, T., Tamai, S., Yokota, S., Kato, H., Fujii, G., et al. (2008). Identification of a novel protein MICS1 that is involved in maintenance of mitochondrial morphology and apoptotic release of cytochrome c. *Mol. Biol. Cell* 19, 2597–2608. doi: 10.1091/mbc.e07-12-1205

Pathak, C., Jaiswal, Y. K., and Vinayak, M. (2007). Possible involvement of queuine in regulation of cell proliferation. *Biofactors* 29, 159–173. doi: 10.1002/biof.5520290401

Pathak, C., Jaiswal, Y. K., and Vinayak, M. (2008). Queuine promotes antioxidant defence system by activating cellular antioxidant enzyme activities in cancer. *Biosci. Rep.* 28, 73–81. doi: 10.1042/BSR20070011

Prudencio, C. R., Pérez de la Lastra, J. M., Canales, M., Villar, M., and de la Fuente, J. (2010). Mapping protective epitopes in the tick and mosquito subolesin ortholog proteins. *Vaccine* 28, 5398–5406. doi: 10.1016/j.vaccine.2010.06.021

Rachinsky, A., Guerrero, F. D., and Scoles, G. A. (2008). Proteomic profiling of *Rhipicephalus (Boophilus) microplus* midgut responses to infection with *Babesia bovis*. *Vet. Parasitol.* 152, 294–313. doi: 10.1016/j.vetpar.2007.12.027

Reimers, K., Choi, C. Y., Bucan, V., and Vogt, P. M. (2007). The growth-hormone inducible transmembrane protein (Ghitm) belongs to the Bax inhibitory protein-like family. *Int. J. Biol. Sci.* 3, 471–476. doi: 10.7150/ijbs.3.471

Robinson, M. D., McCarthy, D. J., and Smyth, G. K. (2010). edgeR: a Bioconductor package for differential expression analysis of digital gene expression data. *Bioinformatics* 26, 139–140. doi: 10.1093/bioinformatics/btp616

Rodriguez, P. B. R., Cruz, R. R., Garcia, D. I. D., Gutierrez, R. H., Quintanilla, R. E. L., Sahagun, D. O., et al. (2016). Identification of immunogenic proteins from ovarian tissue and recognized in larval extracts of Rhipicephalus (Boophilus) microplus, through an immunoproteomic approach. *Exp. Parasitol.* 170, 227–235. doi: 10.1016/j.exppara.2016.10.005

Rojas-Rivera, D., and Hetz, C. (2015). TMBIM protein family: ancestral regulators of cell death. *Oncogene* 34, 269–280. doi: 10.1038/onc.2014.6

Schneider, C. A., Rasband, W. S., and Eliceiri, K. W. (2012). NIH Image to ImageJ: 25 years of image analysis. *Nat. Methods* 9, 671–675. doi: 10.1038/nmeth.2089

Schnittger, L., Rodriguez, A. E., Florin-Christensen, M., and Morrison, D. A. (2012). *Babesia*: a world emerging. *Infect. Genet. Evol.* 12, 1788–1809. doi: 10.1016/j.meegid.2012.07.004

Schulz, M. H., Zerbino, D. R., Vingron, M., and Birney, E. (2012). Oases: robust de novo RNA-seq assembly across the dynamic range of expression levels. *Bioinformatics* 28, 1086–1092. doi: 10.1093/bioinformatics/bts094

Shkap, V., Leibovitz, B., Krigel, Y., Hammerschlag, J., Marcovics, A., Fish, L., et al. (2005). Vaccination of older *Bos taurus* bulls against bovine babesiosis. *Vet. Parasitol.* 129, 235–242. doi: 10.1016/j.vetpar.2005.01.013

Silva, J. C., Egan, A., Friedman, R., Munro, J. B., Carlton, J. M., and Hughes, A. L. (2011). Genome sequences reveal divergence times of malaria parasite lineages. *Parasitology* 138, 1737–1749. doi: 10.1017/S0031182010001575

Šimo, L., Kazimirova, M., Richardson, J., and Bonnet, S. I. (2017). The essential role of tick salivary glands and saliva in tick feeding and pathogen transmission. *Front. Cell. Infect. Microbiol.* 7:281. doi: 10.3389/fcimb.2017.00281

Taheri, M., Nabian, S., Ranjbar, M., Fard, R. M. N., Sadeghian, A. G., and Sazmand, A. (2014). Study of vitellogenin in *Boophilus annulatus* tick larvae and its immunological aspects. *Trop. Biomed.* 31, 398–405.

Tellam, R. L., Kemp, D., Riding, G., Briscoe, S., Smith, D., Sharp, P., et al. (2002). Reduced oviposition of *Boophilus microplus* feeding on sheep vaccinated with vitellin. *Vet. Parasitol.* 103, 141–156. doi: 10.1016/S0304-4017(01)00573-8

Thompson, D. M., Khalil, S. M. S., Jeffers, L. A., Sonenshine, D. E., Mitchell, R. D., Osgood, C. J., et al. (2007). Sequence and the developmental and tissue-specific regulation of the first complete vitellogenin messenger RNA from ticks

responsible for heme sequestration. *Insect. Biochem. Mol. Biol.* 37, 363–374. doi: 10.1016/j.ibmb.2007.01.004

Trager, W. (1974). Some aspects of intracellular parasitism. *Science* 183, 269–273. doi: 10.1126/science.183.4122.269

Tuorto, F., Legrand, C., Cirzi, C., Federico, G., Liebers, R., Müller, M., et al. (2018). Queuosine-modified tRNAs confer nutritional control of protein translation. *EMBO J.* 37:e99777. doi: 10.15252/embj.201899777

Vandesompele, J., De Preter, K., Pattyn, F., Poppe, B., Van Roy, N., De Paepe, A., et al. (2002). Accurate normalization of real-time quantitative RT-PCR data by geometric averaging of multiple internal control genes. *Genome Biol.* 3:research0034.1. doi: 10.1186/gb-2002-3-7-research0034

Villar, M., Ayllon, N., Alberdi, P., Moreno, A., Moreno, M., Tobes, R., et al. (2015). Integrated metabolomics, transcriptomics and proteomics identifies metabolic pathways affected by *Anaplasma phagocytophilum* Infection in Tick Cells. *Mol. Cell Proteomics* 14, 3154–3172. doi: 10.1074/mcp.M115.051938

Villar, M., Ayllon, N., Busby, A. T., Galindo, R. C., Blouin, E. F., Kocan, K. M., et al. (2010). Expression of Heat Shock and other stress response proteins in ticks and cultured tick cells in response to Anaplasma spp. infection and heat shock. *Int. J. Genomics Proteomics* 2010:657261. doi: 10.1155/2010/657261

Villar, M., Marina, A., and de la Fuente, J. (2017). Applying proteomics to tick vaccine development: where are we? *Expert Rev. Proteomics* 14, 211–221. doi: 10.1080/14789450.2017.1284590

Villar, M., Popara, M., Ayllon, N., Fernandez de Mera, I. G., Mateos-Hernandez, L., Galindo, R. C., et al. (2014). A systems biology approach to the characterization of stress response in *Dermacentor reticulatus* tick unfed larvae. *PLoS One* 9:e89564. doi: 10.1371/journal.pone.0089564

Vinayak, M., and Pathak, C. (2009). Queuosine modification of tRNA: its divergent role in cellular machinery. *Biosci. Rep.* 30, 135–148. doi: 10.1042/BSR20090057

Walter, W., Sánchez-Cabo, F., and Ricote, M. (2015). GOplot: an R package for visually combining expression data with functional analysis. *Bioinformatics* 31, 2912–2914. doi: 10.1093/bioinformatics/btv300

Weisheit, S., Villar, M., Tykalová, H., Popara, M., Loecherbach, J., Watson, M., et al. (2015). *Ixodes scapularis* and *Ixodes ricinus* tick cell lines respond to infection with tick-borne encephalitis virus: transcriptomic and proteomic analysis. *Parasit. Vectors* 8:599. doi: 10.1186/s13071-015-1210-x

Xavier, M. A., Tirloni, L., Pinto, A. F. M., Diedrich, J. K., Yates, J. R., Mulenga, A., et al. (2018). A proteomic insight into vitellogenesis during tick ovary maturation. *Sci. Rep.* 8:4698. doi: 10.1038/s41598-018-23090-2

Yu, X., Zhou, Y., Cao, J., Zhang, H., Gong, H., and Zhou, J. (2017). Caspase-1 participates in apoptosis of salivary glands in *Rhipicephalus haemaphysaloides*. *Parasit. Vectors* 10:225. doi: 10.1186/s13071-017-2161-1

Zhou, J., Ueda, M., Umemiya, R., Battsetseg, B., Boldbaatar, D., Xuan, X., et al. (2006). A secreted cystatin from the tick *Haemaphysalis longicornis* and its distinct expression patterns in relation to innate immunity. *Insect Biochem. Mol. Biol.* 36, 527–535. doi: 10.1016/j.ibmb.2006.03.003

Conflict of Interest Statement: The authors declare that the research was conducted in the absence of any commercial or financial relationships that could be construed as a potential conflict of interest.

frontiers in Physiology

BRIEF RESEARCH REPORT
published: 18 April 2019
doi: 10.3389/fphys.2019.00462

Modeling Modulation of the Tick Regulome in Response to *Anaplasma phagocytophilum* for the Identification of New Control Targets

Sara Artigas-Jerónimo[1†], Agustín Estrada-Peña[2†], Alejandro Cabezas-Cruz[3], Pilar Alberdi[1], Margarita Villar[1] and José de la Fuente[1,4]*

[1] SaBio, Instituto de Investigación en Recursos Cinegéticos IREC-CSIC-UCLM-JCCM, Ciudad Real, Spain, [2] Facultad de Veterinaria, Universidad de Zaragoza, Zaragoza, Spain, [3] UMR BIPAR, INRA, ANSES, Ecole Nationale Vétérinaire d'Alfort, Université Paris-Est, Maisons-Alfort, France, [4] Department of Veterinary Pathobiology, Center for Veterinary Health Sciences, Oklahoma State University, Stillwater, OK, United States

OPEN ACCESS

Edited by:
Abid Ali,
Abdul Wali Khan University Mardan, Pakistan

Reviewed by:
Shahid Karim,
University of Southern Mississippi, United States
Snorre Stuen,
Norwegian School of Veterinary Science, Norway

***Correspondence:**
José de la Fuente
jose_delafuente@yahoo.com

[†] *These authors have contributed equally to this work*

Specialty section:
This article was submitted to Invertebrate Physiology, a section of the journal Frontiers in Physiology

Received: *21 February 2019*
Accepted: *04 April 2019*
Published: *18 April 2019*

Citation:
Artigas-Jerónimo S, Estrada-Peña A, Cabezas-Cruz A, Alberdi P, Villar M and de la Fuente J (2019) Modeling Modulation of the Tick Regulome in Response to Anaplasma phagocytophilum for the Identification of New Control Targets. Front. Physiol. 10:462. doi: 10.3389/fphys.2019.00462

Ticks act as vectors of pathogens affecting human and animal health worldwide, and recent research has focused on the characterization of tick-pathogen interactions using omics technologies to identify new targets for developing novel control interventions. The regulome (transcription factors-target genes interactions) plays a critical role in cell response to pathogen infection. Therefore, the application of regulomics to tick-pathogen interactions would advance our understanding of these molecular interactions and contribute to the identification of novel control targets for the prevention and control of tick infestations and tick-borne diseases. However, limited information is available on the role of tick regulome in response to pathogen infection. In this study, we applied complementary *in silico* approaches to modeling how *Anaplasma phagocytophilum* infection modulates tick vector regulome. This proof-of-concept research provided support for the use of network analysis in the study of regulome response to infection, resulting in new information on tick-pathogen interactions and potential targets for developing interventions for the control of tick infestations and pathogen transmission. Deciphering the precise nature of circuits that shape the tick regulome in response to pathogen infection is an area of research that in the future will advance our knowledge of tick-pathogen interactions, and the identification of new antigens for the control of tick infestations and pathogen infection/transmission.

Keywords: regulome, transcription, tick, *Ixodes scapularis*, *Anaplasma phagocytophilum*, ISE6 cells, vaccine

INTRODUCTION

Ticks (Acari: Ixodida) are major vectors of pathogens affecting human and animal health worldwide, and consequently the focus of research for developing novel control interventions (de la Fuente, 2018). Among tick-transmitted pathogens, *Anaplasma phagocytophilum* (Alphaproteobacteria: Rickettsiales) is mainly transmitted by *Ixodes* spp. and the causative agent of human and animal anaplasmosis and tick-borne fever in small ruminants (Severo et al., 2015).

Recent developments in tick genomics have advanced research using latest omics technologies for the characterization of tick-host-pathogen interactions and the identification of candidate protective antigens (de la Fuente et al., 2016c,a, 2017; Gulia-Nuss et al., 2016; Shaw et al., 2017; de la Fuente, 2018). Vaccinomics, a holistic perspective based on the use of omics technologies and bioinformatics in a systems biology approach for the characterization of tick-host-pathogen molecular interactions is our platform for the identification of candidate vaccine antigens (de la Fuente and Merino, 2013; de la Fuente et al., 2016a, 2018; Contreras et al., 2017). In this context, tick cell lines constitute a valuable resource because it is a proven model for the study of tick-pathogen and particularly tick-*A. phagocytophilum* interactions, easy manipulation without animal experimentation, and the fact that *A. phagocytophilum* infects mainly one cell type in vertebrates (neutrophils) but multiple cell types in ticks better resembled by these cell lines (Munderloh et al., 1994; Severo et al., 2015; Villar et al., 2015; Bell-Sakyi et al., 2018).

The regulome (transcription factors-target genes interactions) and interactome (protein-protein physical and functional interactions) play a critical role in cell response to different stimuli including pathogen infection. Both regulome and interactome are implicated in transcriptional regulation, which is one of the most fundamental mechanisms for controlling the amount of protein produced by cells under different environmental and physiological conditions and developmental stages (Gronostajski et al., 2011; Vaquerizas et al., 2012; Shih et al., 2016; Rioualen et al., 2017). Therefore, the application of regulomics and interactomics to host/tick-pathogen interactions would advance our understanding of these molecular interactions and contribute to the identification of new control targets for the prevention and control of tick infestations and tick-borne diseases (de la Fuente et al., 2018; Artigas-Jerónimo et al., 2018a,b; Estrada-Peña et al., 2018).

Few studies have addressed the role of the regulome or regulon (part of the regulome including a set of genes that share a common regulatory element binding site) in the interaction between tick-borne pathogens and vertebrate hosts (i.e., Bugrysheva et al., 2015; Boyle et al., 2019). However, limited information is available on the role of tick regulome in response to pathogen infection (Artigas-Jerónimo et al., 2018b).

In this study, we applied complementary *in silico* approaches to modeling how *A. phagoctophilum* infection modulates tick vector regulome, and the possibilities for the identification of new control target antigens. This proof-of-concept research provided new information on tick-pathogen interactions and potential targets for developing interventions for the control of tick infestations and pathogen infection.

MATERIALS AND METHODS

Datasets

The RNA sequencing (RNAseq) datasets of differential expression of *I. scapularis* transcription factors (TF) and target genes (TG) in response to *A. phagocytophilum* infection was obtained from previously published transcriptomics analyses in ISE6 cells, and fed adult female midguts and salivary glands (Ayllón et al., 2015; Villar et al., 2015). Gene ontology (GO) level-3 annotations for biological processes (BP) were conducted using Blast2GO software (version 3.0)[1] (Villar et al., 2014; **Supplementary Dataset 1**). The RNAseq data is available at http://dx.doi.org/10.5061/dryad.50kt0 and http://www.ncbi.nlm.nih.gov/geo/query/acc.cgi?acc=GSE68881.

Network Analysis of the Tick Regulome in Response to Infection

A network of interactions followed by a co-correspondence analysis (CoCA) was used for the integration of TF and TG interactions (regulome) of *I. scapularis* tick response to *A. phagocytophilum* infection. The methodology to build the network of interactions between proteins and functional metabolic processes has been previously described and validated (Estrada-Peña et al., 2018). This network consists of a set of nodes that are connected by edges where nodes are the interacting items, and links between nodes represent the strength with which they interact. In this development, a TF or TG is the source node and the cell metabolic process(es) in which it is involved are the target(s). The edge linking both nodes has a weight, which is the expression of either TF or TG. Networks were built separately for infected and uninfected *I. scapularis* ISE6 cells, salivary glands and midguts. Only TF and TG with GO functional annotations were included in the networks (**Supplementary Dataset 1**). Centrality is a fundamental property of a network because it refers to nodes that connect high score nodes (Opsahl et al., 2010; Estrada-Peña et al., 2018). In this context, "high score" applies to other nodes with high importance in the network. We calculated the importance of a node in the "traffic" between different nodes of the network using Betweenness Centrality (BNC), giving a higher score to a node that sits on many shortest paths of other node pairs (Barthelemy, 2004; Estrada-Peña et al., 2018). In our context, it is an indicator of the relative importance of a TF/TG in the links between two or more processes. Other calculated indexes included the PageRank (PR), a measure of the importance of the nodes linking with a given node, and the Weighted Degree (WD), which was calculated from the expression profile of each TF/TG linking to a cell process (Estrada-Peña et al., 2018).

The interactions between TF and TG were demonstrated using CoCA. Only TF/TG with values of BNC or PR higher than zero were included. We did the CoCA using the indexes of centrality obtained from the network explained above. The function "coca" of the package "cocorresp" was used for the R programming environment (Simpson, 2016). Data on BNC, PR and WD of each infected and uninfected datasets from ISE6 cells, salivary glands and midguts were entered into separate CoCAs. The analysis aimed to relate two different datasets from uninfected and infected samples to find patterns that are common to both and associating the TF and TG that are close in the reduced multivariate space and establishing correspondences. The plotting of the scores in the two first axes of the reduced space gives the interaction between TF and TG, i.e., the closer

[1] www.blast2go.com

they are in the space, the higher is the expected interaction. The method produces a cloud of interacting TF and TG. To improve the resolution of the charts, we plotted only TF/TG that were at a maximum of two score units of distance. We assumed that other TG separated by more than 2 score units from the values of TF were not interacting with these TF.

In silico Prediction of TF-TG Interactions

Putative DNA binding sites in TG for TF present only in infected tick ISE6 cells were predicted based on published information for TF-interacting sequences in other species, and the *I. scapularis* genomic scaffold whole genome shotgun sequence using cisTargetX[2] and direct search for TF binding sequences in the predicted 5′ gene regulatory regions of the *I. scapularis* genome (**Supplementary Dataset 2**; Potier et al., 2012; Rougemont and Naef, 2012; Vaquerizas et al., 2012). The BP with higher representation in the upregulated than in downregulated regulome (peptidase inhibitor and stress response) in response to infection were selected for further characterization of TF-TG interactions.

RNA Interference (RNAi) for Gene Knockdown in Tick ISE6 Cells

The *I. scapularis* ISE6 cells (provided by U.G. Munderloh, University of Minnesota, United States) was maintained in L-15B300 medium as described previously (Munderloh et al., 1994). Four different TF (HSF, Ap-2, Arx and Hox; **Supplementary Dataset 2**) were silenced using two siRNAs for each TF (HSF: 5′ GCA CUC AGG GCC AGG AUU A 3′ and 5′ CCU CGG AAG CAG ACA GGA A 3′; Ap-2: 5′ AGA AAG AGG ACA CGA AGA A 3′ and 5′ CCA AGA AAG AGG ACA CGA A 3′; Arx: 5′ CCA AGA AAG AGG ACA CGA A 3′ and 5′ GAC CGA AGC CAG AGU GCA A 3′; Hox: 5′ CCU CCA GCU UCA ACA CAU A 3′ and 5′ ACG CCA CGG CCG AGC UUA A 3′) provided by Dharmacon (GE Healthcare Dharmacon Inc., Lafayette, CO, United States). As control, two *Rs86* siRNAs (5′ CGG UAA AUG UCG AAG CAA A 3′ and 5′ GCG AAU AUG AAG UCG GUA A 3′) were used. The siRNA experiments were conducted by incubating ISE6 tick cells with 100 nM of each siRNA diluted in 100 μl of serum-free medium in 24-well plates using four wells per treatment. To facilitate siRNA transfection, DharmaFECT (GE Healthcare Dharmacon Inc.) was used following manufacturer's recommendations. After 24 h, 0.5 ml/well of fresh medium was added. After 48 h of siRNA exposure, medium containing siRNA was removed and replaced with 1 ml fresh medium alone or containing cell free *A. phagocytophilum* NY18 obtained as previously reported (de la Fuente et al., 2005). Cells were incubated for a total of 72 h, and then collected for DNA and RNA extraction.

Determination of Gene Knockdown and TG mRNA Levels by RT-qPCR

Total RNA was extracted from ISE6 cells using All Prep DNA/RNA/PROTEIN Mini Kit (Qiagen, Hilden, Germany) following manufacturer's recommendations. Gene knockdown levels after TF RNAi were assessed for TF and TG by RT-qPCR on RNA samples using gene-specific oligonucleotide primers (**Supplementary Table 1**), the Kapa SYBR Fast One-Step RT-qPCR Kit (Kapa Biosystems, Roche Holding AG, Basel, Switzerland), and the QIAGEN Rotor-Gene Real-Time PCR Detection System (Qiagen). A dissociation curve was run at the end of the reaction to ensure that only one amplicon was formed and that the amplicons denatured consistently in the same temperature range for every sample. The mRNA levels were normalized against tick *rps4* using the genNorm method [Delta-Delta-Ct (ddCt) method] as described previously (Ayllón et al., 2013). Normalized Ct values were compared between test siRNAs-treated tick cells and controls treated with *Rs86* siRNA by Chi^2-test ($p = 0.05$; $n = 4$ biological replicates).

Determination of *A. phagocytophilum* DNA Levels by qPCR

Total DNA was extracted from infected cells using an All Prep DNA/RNA/Protein Mini Kit (Qiagen, Hilden, Germany). DNA samples were analyzed by qPCR using gene-specific primers for *A. phagocytophilum msp4* as previously described (Ayllón et al., 2013). Normalized against tick *rps4* Ct values were compared between test siRNAs-treated tick cells and controls treated with *Rs86* siRNA by Chi^2-test ($p = 0.001$; $n = 2$–4 biological replicates).

RESULTS AND DISCUSSION

Rationale and Experimental Design

The tick regulome in response to *A. phagocytophilum* infection was characterized in the *I. scapularis* tick vector to provide insights into tissue-specific regulome profiles, and the identification of potential targets for the control of tick infestations and pathogen infection/transmission. The experimental design included two independent methods for the *in silico* characterization of the tick regulome in response to *A. phagocytophilum* using transcriptomics data previously obtained from infected *I. scapularis* ISE6 cells, and fed female midguts and salivary glands (**Supplementary Figure 1A**). The first approach was based on a network analysis in which the nodes were either TF or TG together with their corresponding GO BP annotations, and the link between two nodes represented the expression of the gene (**Supplementary Figure 1B**). The indexes of centrality were calculated separately for each network of uninfected and infected samples, and only nodes of TF and TG with indexes of centrality higher than zero were used for co-correspondence CoCA analysis (**Supplementary Figure 1B**). The second approach was used in parallel with network analysis, and consisted in the *in silico* prediction of TF-TG interactions based on described TF recognition sequences by searching in the *I. scapularis* genomic scaffold whole genome shotgun sequence (**Supplementary Figure 1C**). This analysis was focused on TF present only in infected ISE6 cells, and TG in BP overrepresented in the upregulated than in the downregulated regulome in response to infection as a proof-of-concept to facilitate the

[2]https://omictools.com/cistargetx-tool

identification of candidate target antigens for development of vaccines and other control measures. The results of the network analysis were then plotted with TF and TG together in the reduced space to demonstrate that the position of the TF correlates with the TG that are near to these TF after the CoCA (**Supplementary Figure 1D**). Finally, the results of both approaches were compared, and the TF-TG interactions predicted by both methods were functionally characterized by RNAi in *A. phagocytophilum*-infected and uninfected tick ISE6 cells (**Supplementary Figure 1E**).

The *I. scapularis* Regulome Shows Tissue-Specific Signatures in Response to *A. phagocytophilum* Infection

For the construction of networks, a total of 144, 86, and 93 TF (**Supplementary Dataset 3**), and 5225, 3919, and 4341 TG (**Supplementary Dataset 4**) were used derived from tick ISE6 cells, salivary glands and midguts, respectively. Tick midgut did not show detectable differences in the network indexes of TF BP between uninfected and infected samples (close to 100% BNC; **Figure 1A**). However, the TF multicell development and anatomical structure development processes increased to near 200% in infected versus uninfected ISE6 cells (**Figure 1A**). The network centrality of all the TF processes showed a clear increase in infected salivary glands when compared to unifected controls (**Figure 1A**). The multicell development process was represented in TF from ISE6 cells only (**Figure 1A**).

Other than minor variations in the network indexes of the TF, each test showed different TF that were present or absent in either uninfected or infected samples. Four TF were detected only in uninfected ISE6 cells, and other 4 were recorded only in infected ISE6 cells (**Figure 1B**). The most prominent TF in ISE6 cells (ISCW01819) was completely inhibited in infected ISE6 cells (**Figure 1B**). The pattern was more complex in the salivary glands showing up to 17 TF recorded only in infected, and 4 in uninfected samples (**Figure 1C**). Nine TF were recorded only in uninfected and 8 only in infected midgut (**Figure 1D**). As in ISE6 cells, the three most highly represented TF in uninfected midgut were not recorded in infected samples (**Figure 1D**). The number of TG detected only in uninfected or infected samples varied from 197 (uninfected) to 206 (infected) ISE6 cells, 159 (uninfected) to 585 (infected) salivary glands, and 360 (uninfected) to 129 (infected) midgut.

Every detected TF that was unique for uninfected or infected samples was included in CoCA. Based on the values of network indexes of TG, 70 TG in uninfected and 88 TG in infected ISE6 cells, 5 TG in uninfected and 58 TG in infected salivary glands, and 43 TG in uninfected and 25 TG in infected midgut were included in the analysis. The results from multivariate analyses showed a clear correspondence between TF and TG recorded only in uninfected or infected samples while the origin of the first correspondence axis (value = 0) separated completely TF and TG occurring only in either uninfected or infected samples (**Figures 2A–C** and **Supplementary Figures 2A–C**). These analyses suggested that the TF closer to individual TG are likely to regulate the expression of these genes (**Figures 2A–C** and **Supplementary Figures 2A–C**).

These results evidenced tissue-specific differences between infected and uninfected cells, thus supporting previous findings at the mRNA, protein and metabolic levels in *I. scapularis* ISE6 cells, a model for hemocytes, midgut and salivary glands, which are involved in *A. phagocytophilum* life cycle in the tick vector (Ayllón et al., 2015; Villar et al., 2015; reviewed by de la Fuente et al., 2017). These results evidenced that the regulome regulates various BP involved in tick-*A. phagocytophilum* interactions (**Figures 1A, 3A** and **Supplementary Dataset 2**), a finding previously reported in other organisms (Shih et al., 2016; Casella et al., 2017).

A. phagocytophilum Modulates the Tick Regulome to Upregulate Biological Processes That Facilitate Pathogen Infection

To complement the network analysis approach to tick regulome study, the putative DNA binding sites were characterized *in silico* for TF and TG in the upregulated regulome in response to infection in tick vector ISE6 cells (**Figures 3A,B** and **Supplementary Dataset 2**). In particular, the peptidase inhibitor and stress response BP with higher representation in the upregulated than in downregulated regulome (**Figure 3A**) were selected for further characterization of TF-TG interactions (**Figure 3B**).

The results showed a correlation between complementary *in silico* approaches (**Figure 4A**), therefore providing support for the network analysis of the regulome to predict at the transcriptomics level the most significant TF-TG interactions in response to stimuli such as pathogen infection.

To characterize the functional implications of selected TF-TG interactions predicted by both methodological approaches (**Figures 3B**, **4A**), RNAi was used in ISE6 cells to knockdown the expression of TF and characterize the effect on TG mRNA and *A. phagocytophilum* DNA levels (**Figures 4B–D**). The results showed that after 77–87% (average ± S.D., 81 ± 4%) TF silencing (**Figure 4B**), the levels of all predicted TG except for ISCW011771 and ISCW012363 decreased when compared to *Rs86* siRNA-treated controls (**Figure 4C**). The two TG that were not downregulated after TF knockdown had the lowest mRNA levels (**Figure 4C**), which could affect the possibility of detecting differences between test and control cells. Alternatively, other TF or interacting proteins could be involved in the regulation of these genes. Nevertheless, except for ISCW011771 and ISCW012363 the results supported the prediction that these TF are implicated in the regulation of TG. Nevertheless, these TF-TG interactions should be corroborated in future experiments using different *in vitro* protein-DNA binding assays (Yang, 1998; Forde and McCutchen-Maloney, 2002; Deplancke and Gheldof, 2012; Ogawa and Biggin, 2012).

Regarding *A. phagocytophilum* infection, the results showed a 96–97% decrease in pathogen DNA levels after TF knockdown (**Figure 4D**). These results suggested that the TF

A

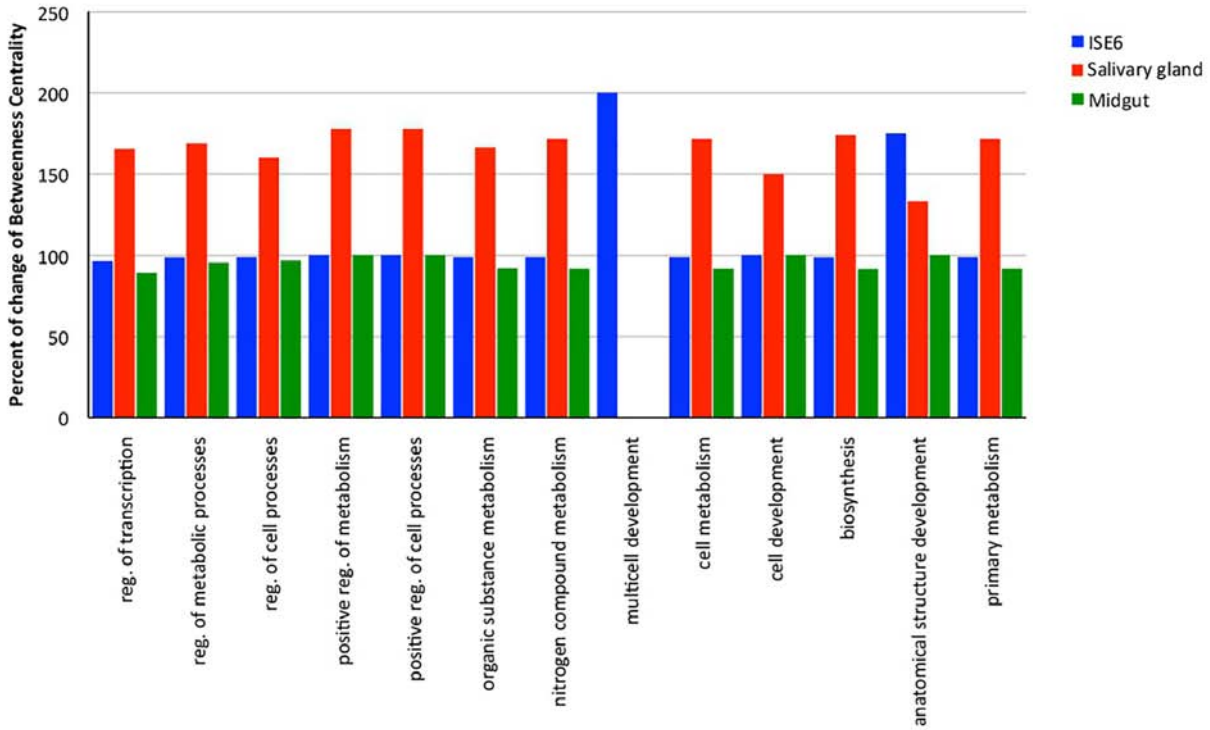

B

TF	BNC (u)	BNC (i)
ISCW006446	0.0	39.1
ISCW007820	0.0	19.7
ISCW021026	0.0	38.7
ISCW021207	0.0	39.1
ISCW008705	17.2	0.0
ISCW010324	17.2	0.0
ISCW012614	17.2	0.0
ISCW015819	93.5	0.0

C

TF	BNC (u)	BNC (i)
ISCW017832	0.0	99.0
ISCW011969	0.0	57.2
ISCW021026	0.0	56.9
ISCW023660	0.0	55.3
ISCW011796	0.0	55.3
ISCW000140	0.0	55.3
ISCW010324	0.0	15.8
ISCW018799	0.0	15.8
ISCW002484	0.0	15.8
ISCW017749	0.0	15.8
ISCW019692	0.0	15.8
ISCW019283	0.0	15.8
ISCW019280	0.0	15.8
ISCW021939	0.0	15.8
ISCW017821	0.0	15.8
ISCW020382	0.0	15.8
ISCW012211	0.0	10.8
ISCW020450	16.5	0.0
ISCW020450	16.5	0.0
ISCW024501	93.9	0.0
ISCW024501	93.9	0.0

D

TF	BNC (u)	BNC (i)
ISCW019692	0.0	15.1
ISCW024501	0.0	92.0
ISCW019280	0.0	15.1
ISCW004287	0.0	89.4
ISCW009030	0.0	15.1
ISCW015741	0.0	15.1
ISCW019283	0.0	15.1
ISCW013477	0.0	15.1
ISCW012211	15.1	0.0
ISCW012211	15.1	0.0
ISCW018799	21.8	0.0
ISCW019287	21.8	0.0
ISCW003117	21.8	0.0
ISCW008179	99.6	0.0
ISCW017832	102.3	0.0
ISCW017832	102.3	0.0
ISCW020382	279.1	0.0

FIGURE 1 | Changes in the expression of TF in tick ISE6 cells, salivary gland and midgut in response to *A. phagocytophilum* infection. **(A)** The percentage change of the index Betweenness Centrality (BNC) infection among uninfected and infected target organs in the 13 BP GO annotations. **(B)** Values of BNC of the 8 TF that showed the highest changes between uninfected BNC (u) and infected BNC (i) ISE6 cells. **(C)** Values of BNC of the 21 TF that showed the highest changes between uninfected BNC (u) and infected BNC (i) salivary glands. **(D)** Values of BNC of the 17 TF that showed the highest changes between uninfected BNC (u) and infected BNC (i) midgut. Abbreviations: reg., regulation; (u), uninfected; (i), infected.

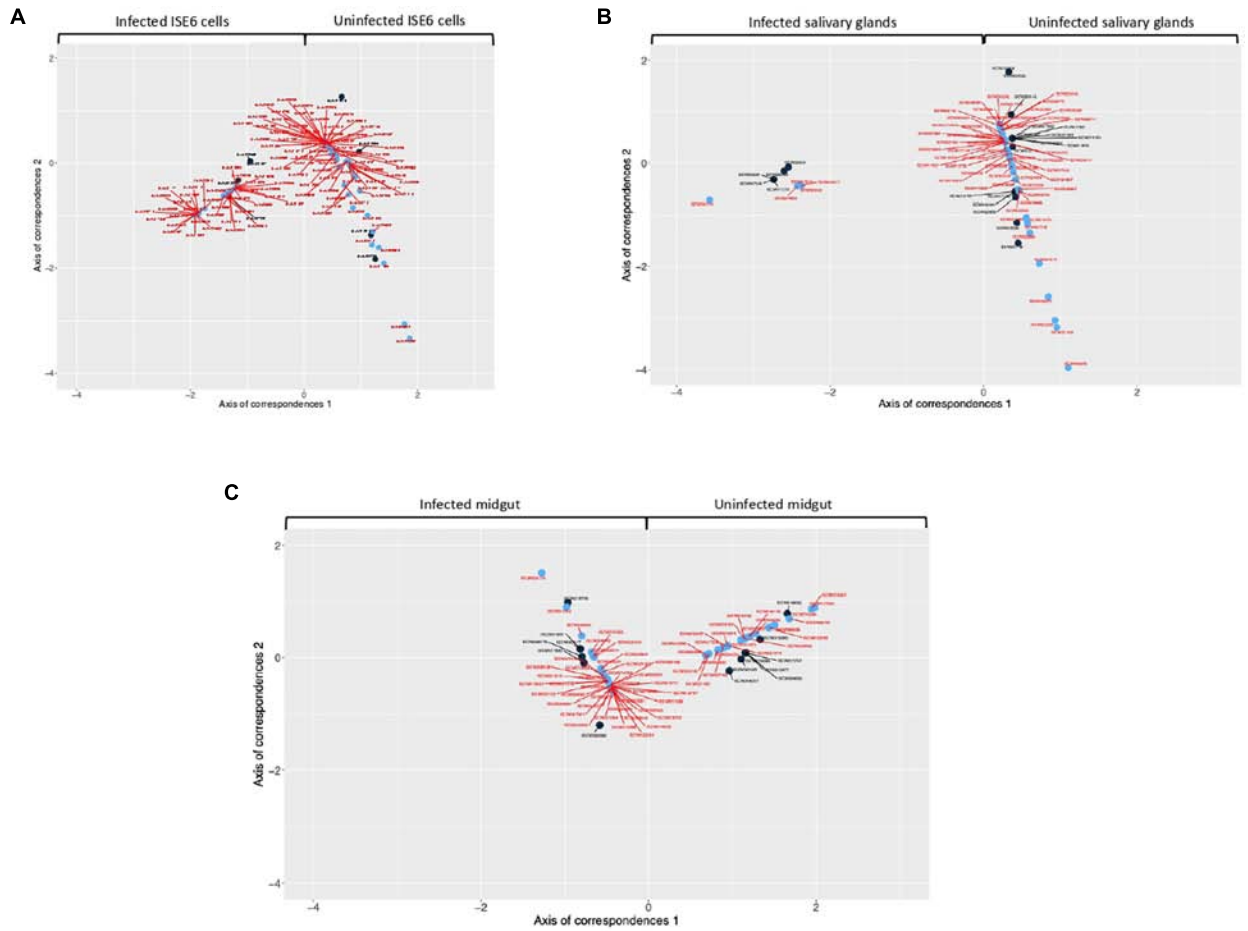

FIGURE 2 | Co-correspondence analysis (CoCA) of TF and TG in uninfected and *A. phagocytophilum*-infected samples. CoCA was conducted in *I. scapularis* **(A)** ISE6 cells, **(B)** salivary glands and **(C)** midgut. The charts show the position of TF (black symbol and label) and TG (blue symbol and red label) after the CoCA of the indexes of centrality. The TF and associated TG with highest values of centrality in the network of infected cells appear together at negative values of the Axis 1 (n = 4, 4, and 9 in ISE6 cells, salivary glands and midgut, respectively). The TF and the associated TG with highest values of centrality in the network of uninfected cells appear together at positive values of the Axis 1 (n = 4, 17, and 8 in ISE6 cells, salivary glands and midgut, respectively). High-resolution images are shown in **Supplementary Figures 2A–C**.

and corresponding TG are upregulated by *A. phagocytophilum* to facilitate pathogen infection.

Characterization of TF and Upregulated TG in Response to Infection as Putative Control Targets

The TF implicated in the regulation of selected TG included heat shock transcription factor (HSF), Ap-2, Aristaless-related homeobox gene (Arx) and Hox (**Figure 3B**). These TF has been described before to function in different transcriptionally regulated processes in other species. The mammalian Ap-2 TF has been shown to be involved in transcriptional activation and DNA binding/dimerization (Williams and Tjian, 1991). The HSF family has been implicated in the regulation of different physiological processes including cell response to stress and infection (Gomez-Pastor et al., 2018). Hox and Arx are members of a family of essential developmental regulators that bind to homeodomains target DNA sequences to regulate embryogenesis and neuronal processes in different organisms (Pellerin et al., 1994; Cho et al., 2012).

Few studies in other host-pathogen models have shown that some of these TF facilitate pathogen infection and therefore has been proposed as potential targets for control interventions. In primary peripheral blood monocytes, HSF1 is upregulated by human cytomegalovirus (HCMV) for pathogen survival, and has been suggested as a potential control target (Peppenelli et al., 2018). The tick-borne pathogen, *Ehrlichia chaffeensis*, upregulates the expression of certain Hox genes to facilitate infection through epigenetic mechanisms in human monocytic leukemia cells (THP-1) (Mitra et al., 2018). However, the role of these TF during pathogen infection in ticks has not been investigated before.

The BP modulated by the regulome of selected TF-TG interactions with a putative role in facilitating *A. phagocytophilum* infection included peptidase inhibitor

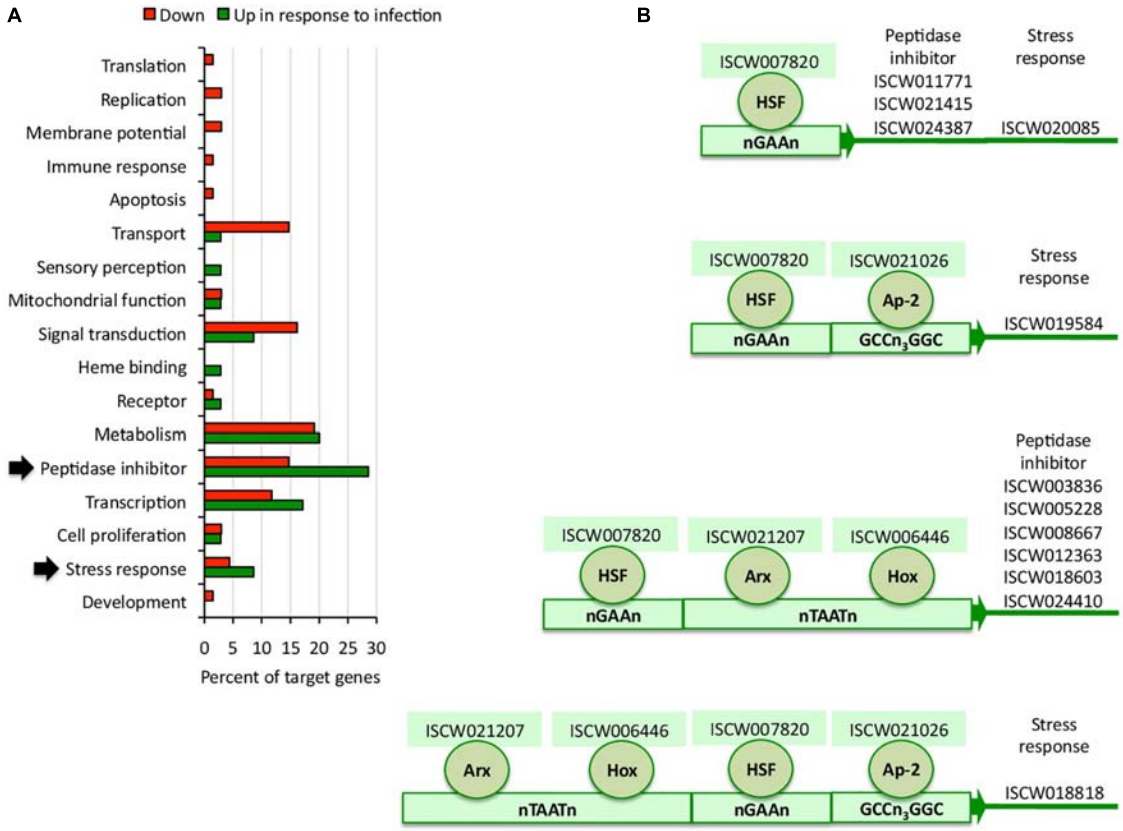

FIGURE 3 | Biological processes affected by the tick ISE6 cells regulome in response to *A. phagocytophilum* infection. **(A)** Upregulated and downregulated target genes in the *in silico* predicted tick ISE6 cells regulome in response to *A. phagocytophilum* infection were grouped according to their BP. The BP with higher representation in the upregulated than in downregulated regulome in response to infection (arrows) were selected for characterization of TF-TG interactions. **(B)** Predicted regulatory DNA motifs according to regulatory factors identified by RNAseq in infected cells only and involved in the control of upregulated target genes annotated in the peptidase inhibitor and stress response BP with higher representation in the upregulated than in downregulated regulome.

and stress response (**Figure 3A** and **Supplementary Dataset 2**). The stress response upregulated TG included genes coding for peroxinectin and uncharacterized protein with heme binding and peroxidase activity (n = 2), and glutathione peroxidase with glutathione peroxidase activity. The peptidase inhibitor TG encoded for a carboxypeptidase inhibitor precursor with carboxipeptidase and metalloendopeptidase inhibitor activity, uncharacterized protein, Kunitz-type proteinase inhibitor 5 II, serpin-2 precursors and secreted salivary gland peptides with serine-type endopeptidase inhibitor activity (n = 6), and cystatin and salivary cystatin-L with cysteine-type endopeptidase inhibitor activity (n = 2).

These proteins are involved in key physiological processes during tick life cycle such as heme/iron metabolism and detoxification and tick-host interactions (Chmelar et al., 2016; de la Fuente et al., 2016a). Glutathione peroxidase belongs to the glutathione antioxidant defense system and protects eukaryotic cells from oxidative damage (Espinosa-Diez et al., 2015). Glutathione peroxidase levels and activity are affected in different ways by *Anaplasma marginale* infection in both vertebrate and tick cells (Reddy et al., 1988; More et al., 1989; Kalil et al., 2017; Esmaeilnejad et al., 2018). While the activity and expression of glutathione peroxidase and other components of the antioxidant system was lower in *A. marginale*-infected cattle and water buffaloes (Reddy et al., 1988; More et al., 1989; Esmaeilnejad et al., 2018), glutathione peroxidase coding gene was upregulated in embryonic *Rhipicephalus microplus* BME26 cells in response to *A. marginale* infection (Kalil et al., 2017). These results showed that *A. marginale* infection induces a differential response of the glutathione antioxidant defense system in the vertebrate and tick hosts. RNAi-mediated gene silencing of glutathione peroxidase and other antioxidant defense system genes increased *A. marginale* infection in BME26 cells, suggesting that the antioxidant response mediated by this molecule might play a role in the control of infection in ticks (Kalil et al., 2017). Another of the identified tick TG, peroxinectin, is a cell adhesion protein involved in melanization of pathogens in invertebrates (Sritunyalucksana et al., 2001; Cerenius and Söderhäll, 2004), was upregulated in crayfish resistant to white spot syndrome virus, and susceptible crayfish failed to upregulate this gene in response to viral infection (Yi et al., 2017). Strong cellular adhesion in response to the invading agent during crustacean encapsulation defense reaction was proposed as a

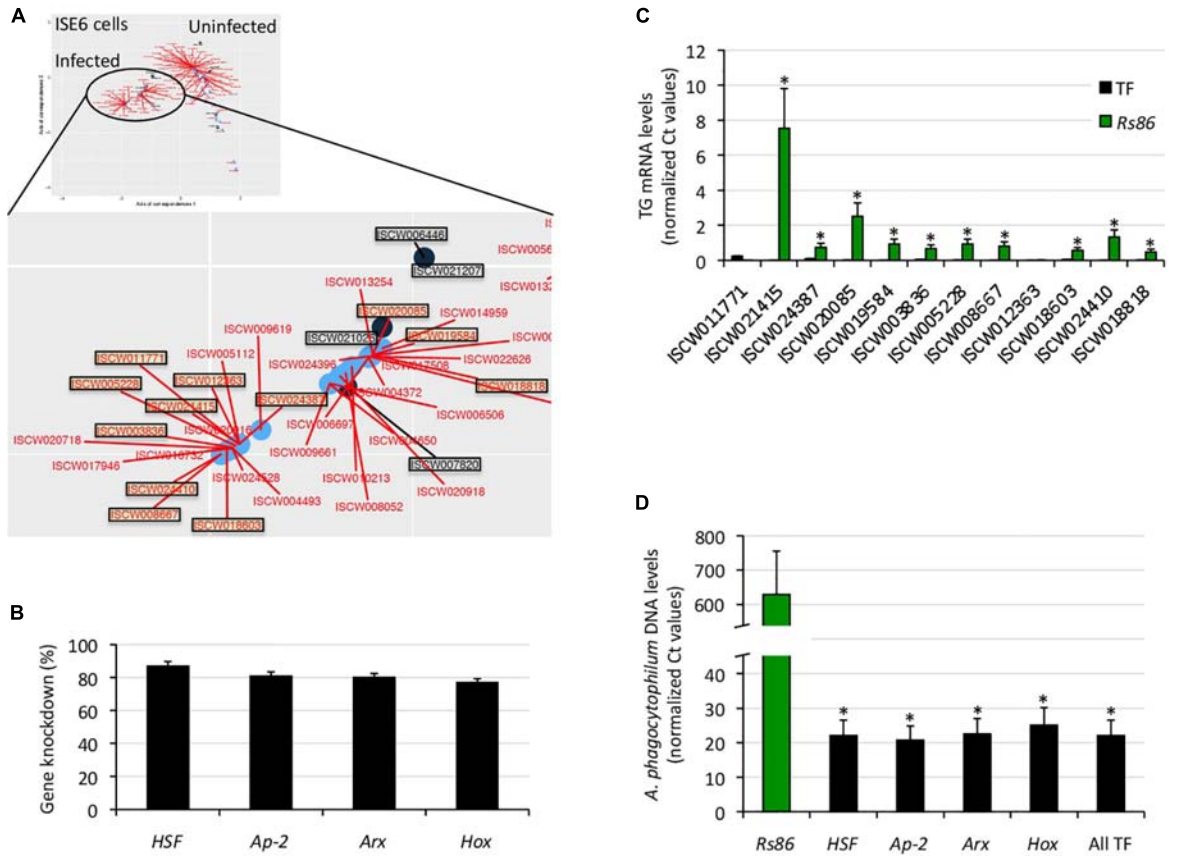

FIGURE 4 | Functional characterization of selected TF-TG components of the tick ISE6 cells regulome. **(A)** The predictive results of network analysis and *in silico* prediction of TF-TG interactions were compared in infected ISE6 cells. The TF-TG interactions predicted by both methods (squared in black letter for TF and red letter for TG) were then functionally characterized by RNAi in tick ISE6 cells. **(B)** Percentage of TF gene knockdown with respect to Rs86 siRNA control in ISE6 cells. Normalized against tick *rps4* Ct values were compared between test siRNAs-treated tick cells and controls treated with *Rs86* siRNA by Chi^2-test ($p < 0.05$; $n = 4$ biological replicates). **(C)** The TG mRNA levels were determined by qRT-PCR in ISE6 cells after TF gene knockdown or treatment with control *Rs86* siRNA. Normalized against tick *rps4* Ct values (average + S.E.) were compared between test siRNAs-treated tick cells and controls treated with *Rs86* siRNA by Chi^2-test (*$p < 0.001$; $n = 4$ biological replicates). **(D)** The *A. phagocytophilum* DNA levels were determined by qPCR in ISE6 cells after TF gene knockdown or treatment with control *Rs86* siRNA. Normalized against tick *rps4* Ct values (average + S.D.) were compared between test siRNAs-treated tick cells and controls treated with *Rs86* siRNA by Chi^2-test (*$p < 0.001$; $n = 2$–4 biological replicates).

protective mechanism mediated by peroxinectin in infected crayfish. The heme-binding lipoprotein (HELP), a transporter of heme in ticks, was previously found to be upregulated and downregulated in midguts and salivary glands, respectively, of *A. phagocytophilum*-infected ticks (Villar et al., 2016). HELP, together with Vitellogenin 1 and 2, was proposed to transport heme to other tick tissues such as salivary glands (Hajdusek et al., 2009). The uncharacterized protein with heme binding activity identified in this study may have a function similar to HELP, suggesting that *A. phagocytophilum* affects hemoglobin primary cleavage and heme transport in tick midguts and salivary glands, possibly to regulate the levels of heme in a tissue-specific manner with potential effects for pathogen and vector survival. The expression of Kunitz-type proteinase inhibitors have been found to be modified in several tick species in response to infection by tick-borne pathogens such as *Bartonella henselae* (Liu et al., 2014), flavivirus (McNally et al., 2012), *Babesia bigemina* (Antunes et al., 2012), and *A. marginale* (Zivkovic et al., 2010). Kunitz peptides are moonlighting proteins that perform multiple functions within the feeding lesion (Schwarz et al., 2014). Upregulation of Kunitz proteins in salivary glands of ticks infected with *B. henselae* (Liu et al., 2014) and flavivirus (McNally et al., 2012) may be associated with host immunity modulation at the feeding site. In contrast to upregulation, it is less clear why Kunitz peptides, including a Kunitz-type proteinase inhibitor 5, would be dowregulated in salivary glands following *A. marginale* infection (Zivkovic et al., 2010). Additional studies show that the expression of Kunitz peptides is complex and may be related to the tick and pathogen species (Rachinsky et al., 2007; Antunes et al., 2012).

These preliminary evidences based on selected TF-TG interactions support that the analysis of tick regulome in response to different stimuli such as pathogen infection could provide potential targets for the control of tick infestations and pathogen infection/transmission. Furthermore, some of these

protein families have been proposed as protective antigens using a rational approach for the identification of tick vaccine protective antigens (de la Fuente et al., 2016a). As recently proposed (de la Fuente et al., 2018), the combination of regulomics with intelligent Big Data analytic techniques may contribute to the high throughput identification of candidate vaccine antigens.

CONCLUSION

Our modeling of the modulation of the tick regulome in response to *A. phagocytophilum* infection provided new insights into the mechanisms that target specific functions in different tick tissues. These results supported the use of network analysis for the study of regulome response to infection. Although general mechanisms affected by *A. phagocytophilum* infection may be conserved even between tick and human cells (de la Fuente et al., 2016b), the effect of vector-pathogen co-evolution on pathogen isolates adaptation to grow in tick cells (Alberdi et al., 2015) may result in differences between isolates in the modulation of the tick cell regulome. Future research should be directed at validating the results of the network analysis for regulomics studies and the characterization of TF-TG interactions. Deciphering the precise nature of circuits that shape the tick regulome in response to pathogen infection is an area of research that in the future will advance our knowledge of tick-pathogen interactions, and the identification of new targets for the control of tick infestations and pathogen infection/transmission.

DATA AVAILABILITY

All datasets generated for this study are included in the manuscript and/or the **Supplementary Files**.

AUTHOR CONTRIBUTIONS

MV, AE-P, AC-C, and JdlF conceived the study and designed the experiments. SA-J, PA, and MV performed the experiments. AE-P, MV, AC-C, and JdlF performed the data analysis. JdlF, SA-J, AE-P, and AC-C wrote the manuscript. All authors approved and contributed to the final version of the manuscript.

FUNDING

This research was financially supported by the Ministerio de Economía, Industria y Competitividad, Spain grant BFU2016-79892-P. MV was funded by the Universidad de Castilla La Mancha, Spain.

SUPPLEMENTARY MATERIAL

The Supplementary Material for this article can be found online at: https://www.frontiersin.org/articles/10.3389/fphys.2019.00462/full#supplementary-material

REFERENCES

Alberdi, P., Ayllón, N., Cabezas-Cruz, A., Bell-Sakyi, L., Zweygarth, E., Stuen, S., et al. (2015). Infection of *Ixodes* spp. tick cells with different *Anaplasma phagocytophilum* isolates induces the inhibition of apoptotic cell death. *Ticks Tick Borne Dis.* 6, 758–767. doi: 10.1016/j.ttbdis.2015.07.001

Antunes, S., Galindo, R. C., Almazán, C., Rudenko, N., Golovchenko, M., Grubhoffer, L., et al. (2012). Functional genomics studies of *Rhipicephalus (Boophilus) annulatus* ticks in response to infection with the cattle protozoan parasite, *Babesia bigemina*. *Int. J. Parasitol.* 42, 187–195. doi: 10.1016/j.ijpara.2011.12.003

Artigas-Jerónimo, S., de la Fuente, J., and Villar, M. (2018a). Interactomics and tick vaccine development: new directions for the control of tick-borne diseases. *Expert Rev. Proteomics* 15, 627–635. doi: 10.1080/14789450.2018.1506701

Artigas-Jerónimo, S., Villar, M., Cabezas-Cruz, A., Valdés, J. J., Estrada-Peña, A., Alberdi, P., et al. (2018b). Functional evolution of Subolesin/Akirin. *Front. Physiol.* 9:1612. doi: 10.3389/fphys.2018.01612

Ayllón, N., Villar, M., Busby, A. T., Kocan, K. M., Blouin, E. F., Bonzón-Kulichenko, E., et al. (2013). *Anaplasma phagocytophilum* inhibits apoptosis and promotes cytoskeleton rearrangement for infection of tick cells. *Infect. Immun.* 81, 2415–2425. doi: 10.1128/IAI.00194-13

Ayllón, N., Villar, M., Galindo, R. C., Kocan, K. M., Šíma R., López, J. A., et al. (2015). Systems biology of tissue-specific response to *Anaplasma phagocytophilum* reveals differentiated apoptosis in the tick vector *Ixodes scapularis*. *PLoS Genet.* 11:e1005120. doi: 10.1371/journal.pgen.1005120

Barthelemy, M. (2004). Betweenness centrality in large complex networks. *Eur. Phys. J. B* 38, 163–168. doi: 10.1140/epjb/e2004-00111-4

Bell-Sakyi, L., Darby, A., Baylis, M., and Makepeace, B. L. (2018). The Tick Cell Biobank: a global resource for in vitro research on ticks, other arthropods and the pathogens they transmit. *Ticks Tick Borne Dis.* 9, 1364–1371. doi: 10.1016/j.ttbdis.2018.05.015

Boyle, W. K., Groshong, A. M., Drecktrah, D., Boylan, J. A., Gherardini, F. C., Blevins, J. S., et al. (2019). DksA controls the response of the Lyme disease spirochete *Borrelia burgdorferi* to starvation. *J. Bacteriol.* 201:e00582-18. doi: 10.1128/JB.00582-18

Bugrysheva, J. V., Pappas, C. J., Terekhova, D. A., Iyer, R., Godfrey, H. P., Schwartz, I., et al. (2015). Characterization of the RelBbu regulon in *Borrelia burgdorferi* reveals modulation of glycerol metabolism by (p)ppGpp. *PLoS One* 10:e0118063. doi: 10.1371/journal.pone.0118063

Casella, L. G., Weiss, A., Pérez-Rueda, E., Ibarra, J. A., and Shaw, L. N. (2017). Towards the complete proteinaceous regulome of *Acinetobacter baumannii*. *Microb. Genom.* 3:mgen000107. doi: 10.1099/mgen.0.000107

Cerenius, L., and Söderhäll, K. (2004). The prophenoloxidase-activating system in invertebrates. *Immunol. Rev.* 198, 116–126. doi: 10.1111/j.0105-2896.2004.00116.x

Chmelar, J., Kotal, J., Karim, S., Kopacek, P., Francischetti, I. M. B., Pedra, J. H. F., et al. (2016). Sialomes and mialomes: a systems-biology view of tick tissues and tick-host interactions. *Trends Parasitol.* 32, 242–254. doi: 10.1016/j.pt.2015.10.002

Cho, S. J., Valles, Y., Kim, K. M., Ji, S. C., Han, S. J., and Park, S. C. (2012). Additional duplicated Hox genes in the earthworm: *Perionyx excavatus* Hox genes consist of eleven paralog groups. *Gene* 493, 260–266. doi: 10.1016/j.gene.2011.11.006

Contreras, M., Alberdi, P., Fernández de Mera, I. G., Krull, C., Nijhof, A., Villar, M., et al. (2017). Vaccinomics approach to the identification of candidate protective antigens for the control of tick vector infestations and *Anaplasma phagocytophilum* infection. *Front. Cell. Infect. Microbiol.* 7:360. doi: 10.3389/fcimb.2017.00360

de la Fuente, J. (2018). Controlling ticks and tick-borne diseases...looking forward. *Ticks Tick Borne Dis.* 9, 1354–1357. doi: 10.1016/j.ttbdis.2018.04.001

de la Fuente, J., Antunes, S., Bonnet, S., Cabezas-Cruz, A., Domingos, A., Estrada-Peña, A., et al. (2017). Tick-pathogen interactions and vector competence:

identification of molecular drivers for tick-borne diseases. *Front. Cell. Infect. Microbiol.* 7:114. doi: 10.3389/fcimb.2017.00114

de la Fuente, J., Ayoubi, P., Blouin, E. F., Almazán, C., Naranjo, V., and Kocan, K. M. (2005). Gene expression profiling of human promyelocytic cells in response to infection with *Anaplasma phagocytophilum*. *Cell. Microbiol.* 7, 549–559. doi: 10.1111/j.1462-5822.2004.00485.x

de la Fuente, J., and Merino, O. (2013). Vaccinomics, the new road to tick vaccines. *Vaccine* 31, 5923–5929. doi: 10.1016/j.ttbdis.2018.04.001

de la Fuente, J., Villar, M., Estrada-Peña, A., and Olivas, J. A. (2018). High throughput discovery and characterization of tick and pathogen vaccine protective antigens using vaccinomics with intelligent Big Data analytic techniques. *Expert Rev. Vaccines* 17, 569–576. doi: 10.1080/14760584.2018

de la Fuente, J., Kopáček, P., Lew-Tabor, A., and Maritz-Olivier, C. (2016a). Strategies for new and improved vaccines against ticks and tick-borne diseases. *Parasite Immunol.* 38, 754–769. doi: 10.1111/pim.12339

de la Fuente, J., Villar, M., Cabezas-Cruz, A., Estrada-Peña, A., Ayllón, N., and Alberdi, P. (2016b). Tick-host-pathogen interactions: conflict and cooperation. *PLoS Pathog.* 12:e1005488. doi: 10.1371/journal.ppat.1005488

de la Fuente, J., Waterhouse, R. M., Sonenshine, D. E., Roe, M. R., Ribeiro, J. M., Sattelle, D. B., et al. (2016c). Tick genome assembled: new opportunities for research on tick-host-pathogen interactions. *Front. Cell. Infect. Microbiol.* 6:103. doi: 10.3389/fcimb.2016.00103

Deplancke, B., and Gheldof, N. (2012). *Gene Regulatory Networks Methods and Protocols*. New York, NY: Human Press.

Esmaeilnejad, B., Tavassoli, M., Samiei, A., Hajipour, N., Imani-Baran, A., and Farhang-Pajuh, F. (2018). Evaluation of oxidative stress and antioxidant status, serum trace mineral levels and cholinesterases activity in cattle infected with *Anaplasma marginale*. *Microb. Pathog.* 123, 402–409. doi: 10.1016/j.micpath.2018.07.039

Espinosa-Diez, C., Miguel, V., Mennerich, D., Kietzmann, T., Sánchez-Pérez, P., Cadenas, S., et al. (2015). Antioxidant responses and cellular adjustments to oxidative stress. *Redox Biol.* 6, 183–197. doi: 10.1016/j.redox.2015.07.008

Estrada-Peña, A., Villar, M., Artigas-Jerónimo, S., López, V., Alberdi, P., Cabezas-Cruz, A., et al. (2018). Use of graph theory to characterize human and arthropod vector cell protein response to infection. *Front. Cell. Infect. Microbiol.* 8:265. doi: 10.3389/fcimb.2018.00265

Forde, C. E., and McCutchen-Maloney, S. L. (2002). Characterization of transcription factors by mass spectrometry and the role of SELDI-MS. *Mass Spectrom. Rev.* 21, 419–439. doi: 10.1002/mas.10040

Gomez-Pastor, R., Burchfiel, E. T., and Thiele, D. J. (2018). Regulation of heat shock transcription factors and their roles in physiology and disease. *Nat. Rev. Mol. Cell Biol.* 19, 4–19. doi: 10.1038/nrm.2017.73

Gronostajski, R. M., Guaneri, J., Lee, D. H., and Gallo, S. M. (2011). The NFI-Regulome Database: a tool for annotation and analysis of control regions of genes regulated by Nuclear Factor I transcription factors. *J. Clin. Bioinforma.* 1:4. doi: 10.1186/2043-9113-1-4

Gulia-Nuss, M., Nuss, A. B., Meyer, J. M., Sonenshine, D. E., Roe, R. M., Waterhouse, R. M., et al. (2016). Genomic insights into the Ixodes scapularis tick vector of Lyme disease. *Nat. Commun.* 7:10507. doi: 10.1038/ncomms10507

Hajdusek, O., Sojka, D., Kopacek, P., Buresova, V., Franta, Z., Sauman, I., et al. (2009). Knockdown of proteins involved in iron metabolism limits tick reproduction and development. *Proc. Natl. Acad. Sci. U.S.A.* 106, 1033–1038. doi: 10.1073/pnas.0807961106

Kalil, S. P., Rosa, R. D. D., Capelli-Peixoto, J., Pohl, P. C., Oliveira, P. L., Fogaça, A. C., et al. (2017). Immune-related redox metabolism of embryonic cells of the tick *Rhipicephalus microplus* (BME26) in response to infection with *Anaplasma marginale*. *Parasit. Vectors.* 10:613. doi: 10.1186/s13071-017-2575-9

Liu, X. Y., de la Fuente, J., Cote, M., Galindo, R. C., Moutailler, S., Vayssier-Taussat, M., et al. (2014). IrSPI, a tick serine protease inhibitor involved in tick feeding and *Bartonella henselae* infection. *PLoS Negl. Trop. Dis.* 8:e2993. doi: 10.1371/journal.pntd.0002993

McNally, K. L., Mitzel, D. N., Anderson, J. M., Ribeiro, J. M., Valenzuela, J. G., Myers, T. G., et al. (2012). Differential salivary gland transcript expression profile in Ixodes scapularis nymphs upon feeding or flavivirus infection. *Ticks Tick Borne Dis.* 3, 18–26. doi: 10.1016/j.ttbdis.2011.09.003

Mitra, S., Dunphy, P. S., Das, S., Zhu, B., Luo, T., and McBride, J. W. (2018). *Ehrlichia chaffeensis* TRP120 effector targets and recruits host polycomb group proteins for degradation to promote intracellular infection. *Infect. Immun.* 86:e00845-17. doi: 10.1128/IAI.00845-17

More, T., Reddy, G. R., Sharma, S. P., and Singh, L. N. (1989). Enzymes of oxidant defence system of leucocytes and erythrocytes in bovine anaplasmosis. *Vet. Parasitol.* 31, 333–337. doi: 10.1016/0304-4017(89)90082-4

Munderloh, U., Liu, Y., Wang, M., Chen, C., and Kurtti, T. (1994). Establishment, maintenance and description of cell lines from the tick *Ixodes scapularis*. *J. Parasitol.* 80, 533–543.

Ogawa, N., and Biggin, M. D. (2012). High-throughput SELEX determination of DNA sequences bound by transcription factors *in vitro*. *Methods Mol. Biol.* 786, 51–63. doi: 10.1007/978-1-61779-292-2_3

Opsahl, T., Agneessens, F., and Skvoretz, J. (2010). Node centrality in weighted networks: generalizing degree and shortest paths. *Soc. Networks* 32, 245–251. doi: 10.1016/j.socnet.2010.03.006

Pellerin, I., Schnabel, C., Catron, K. M., and Abate, C. (1994). Hox proteins have different affinities for a consensus DNA site that correlate with the positions of their genes on the Hox cluster. *Mol. Cell Biol.* 14, 4532–4545. doi: 10.1128/mcb.14.7.4532

Peppenelli, M. A., Miller, M. J., Altman, A. M., Cojohari, O., and Chan, G. C. (2018). Aberrant regulation of the Akt signaling network by human cytomegalovirus allows for targeting of infected monocytes. *Antiviral Res.* 158, 13–24. doi: 10.1016/j.antiviral.2018.07.015

Potier, D., Atak, Z. K., Sanchez, M. N., Herrmann, C., and Aerts, S. (2012). Using cisTargetX to predict transcriptional targets and networks in *Drosophila*. *Methods Mol. Biol.* 786, 291–314. doi: 10.1007/978-1-61779-292-2_18

Rachinsky, A., Guerrero, F. D., and Scoles, G. A. (2007). Differential protein expression in ovaries of uninfected and *Babesia*-infected southern cattle ticks, *Rhipicephalus (Boophilus) microplus*. *Insect Biochem. Mol. Biol.* 37, 1291–1308. doi: 10.1016/j.ibmb.2007.08.001

Reddy, G. R., More, T., Sharma, S. P., and Singh, L. N. (1988). The oxidant defence system in water-buffaloes (*Bubalus bubalis*) experimentally infected with *Anaplasma marginale*. *Vet. Parasitol.* 27, 245–249. doi: 10.1016/0304-4017(88)90039-8

Rioualen, C., Da Costa, Q., Chetrit, B., Charafe-Jauffret, E., Ginestier, C., and Bidaut, G. (2017). HTS-Net: an integrated regulome-interactome approach for establishing network regulation models in high-throughput screenings. *PLoS One* 12:e0185400. doi: 10.1371/journal.pone.0185400

Rougemont, J., and Naef, F. (2012). Computational analysis of protein-DNA interactions from ChIP-seq data. *Methods Mol. Biol.* 786, 263–273. doi: 10.1007/978-1-61779-292-2_16

Schwarz, A., Cabezas-Cruz, A., Kopecký, J., and Valdés, J. J. (2014). Understanding the evolutionary structural variability and target specificity of tick salivary Kunitz peptides using next generation transcriptome data. *BMC Evol. Biol.* 14:4. doi: 10.1186/1471-2148-14-4

Severo, M. S., Pedra, J. H. F., Ayllón, N., Kocan, K. M., and de la Fuente, J. (2015). "*Anaplasma*," in *Molecular Medical Microbiology*, 2nd Edn, Vol. 3, eds Y. W. Tang, M. Sussman, D. Liu, I. Poxton, and J. Schwartzman (London: Academic Press), 2033–2042.

Shaw, D. K., Wang, X., Brown, L. J., Oliva Chávez, A. S., Reif, K. E., Smith, A. A., et al. (2017). Infection-derived lipids elicit an immune deficiency circuit in arthropods. *Nat. Commun.* 8:14401. doi: 10.1038/ncomms14401

Shih, H. Y., Sciumè, G., Mikami, Y., Guo, L., Sun, H. W., Brooks, S. R., et al. (2016). Developmental acquisition of regulomes underlies innate lymphoid cell functionality. *Cell* 165, 1120–1133. doi: 10.1016/j.cell.2016.04.029

Simpson, G. L. (2016). *cocorresp: Co-Correspondence Analysis Ordination Methods. R package version 0.3-0*. Available at: http://cran.r-project.org/package=cocorresp (accessed June, 2018).

Sritunyalucksana, K., Wongsuebsantati, K., Johansson, M. W., and Söderhäll, K. (2001). Peroxinectin, a cell adhesive protein associated with the proPO system from the black tiger shrimp, *Penaeus monodon*. *Dev. Comp. Immunol.* 25, 353–363. doi: 10.1016/s0145-305x(01)00009-x

Vaquerizas, J. M., Teichmann, S. A., and Luscombe, N. M. (2012). How do you find transcription factors? computational approaches to compile and annotate repertoires of regulators for any genome. *Methods Mol. Biol.* 786, 3–19. doi: 10.1007/978-1-61779-292-2_1

Villar, M., Ayllón, N., Alberdi, P., Moreno, A., Moreno, M., Tobes, R., et al. (2015). Integrated metabolomics, transcriptomics and proteomics identifies metabolic pathways affected by *Anaplasma phagocytophilum* infection in tick cells. *Mol. Cell. Proteomics* 14, 3154–3172. doi: 10.1074/mcp.M115.051938

Villar, M., López, V., Ayllón, N., Cabezas-Cruz, A., López, J. A., Vázquez, J., et al. (2016). The intracellular bacterium *Anaplasma phagocytophilum* selectively manipulates the levels of vertebrate host proteins in the tick vector Ixodes scapularis. *Parasit. Vectors* 9:467. doi: 10.1186/s13071-016-1747-3

Villar, M., Popara, M., Ayllón, N., Fernández de Mera, I. G., Mateos-Hernández, L., Galindo, R. C., et al. (2014). A systems biology approach to the characterization of stress response in *Dermacentor reticulatus* tick unfed larvae. *PLoS One* 9:e89564. doi: 10.1371/journal.pone.0089564

Williams, T., and Tjian, R. (1991). Analysis of the DNA-binding and activation properties of the human transcription factor AP-2. *Genes Dev.* 5, 670–682. doi: 10.1101/gad.5.4.670

Yang, V. W. (1998). Eukaryotic transcription factors: identification, characterization and functions. *J. Nutr.* 128, 2045–2051. doi: 10.1093/jn/128.11.2045

Yi, S., Li, Y., Shi, L., and Zhang, L. (2017). Novel Insights into Antiviral gene regulation of red swamp crayfish, *Procambarus clarkii*, infected with white spot syndrome virus. *Genes* 8:E320. doi: 10.3390/genes8110320

Zivkovic, Z., Esteves, E., Almazán, C., Daffre, S., Nijhof, A. M., Kocan, K. M., et al. (2010). Differential expression of genes in salivary glands of male *Rhipicephalus (Boophilus) microplus* in response to infection with *Anaplasma marginale*. *BMC Genomics* 11:186. doi: 10.1186/1471-2164-11-186

Conflict of Interest Statement: The authors declare that the research was conducted in the absence of any commercial or financial relationships that could be construed as a potential conflict of interest.

frontiers in Physiology

REVIEW
published: 01 May 2019
doi: 10.3389/fphys.2019.00530

Chemical Equilibrium at the Tick–Host Feeding Interface: A Critical Examination of Biological Relevance in Hematophagous Behavior

Ben J. Mans[1,2,3]*

[1] Epidemiology, Parasites and Vectors, Agricultural Research Council-Onderstepoort Veterinary Research, Pretoria, South Africa, [2] Department of Veterinary Tropical Diseases, University of Pretoria, Pretoria, South Africa, [3] Department of Life and Consumer Sciences, University of South Africa, Pretoria, South Africa

OPEN ACCESS

Edited by:
Abid Ali,
Abdul Wali Khan University Mardan, Pakistan

Reviewed by:
Jose Ribeiro,
National Institute of Allergy and Infectious Diseases (NIAID), United States
Tae Kim,
Texas A&M University, United States
Jan Perner,
Institute of Parasitology (ASCR), Czechia

***Correspondence:**
Ben J. Mans
mansb@arc.agric.za

Specialty section:
This article was submitted to Invertebrate Physiology, a section of the journal Frontiers in Physiology

Received: *12 March 2019*
Accepted: *15 April 2019*
Published: *01 May 2019*

Citation:
Mans BJ (2019) Chemical Equilibrium at the Tick–Host Feeding Interface: A Critical Examination of Biological Relevance in Hematophagous Behavior. Front. Physiol. 10:530. doi: 10.3389/fphys.2019.00530

Ticks secrete hundreds to thousands of proteins into the feeding site, that presumably all play important functions in the modulation of host defense mechanisms. The current review considers the assumption that tick proteins have functional relevance during feeding. The feeding site may be described as a closed system and could be treated as an ideal equilibrium system, thereby allowing modeling of tick–host interactions in an equilibrium state. In this equilibrium state, the concentration of host and tick proteins and their affinities will determine functional relevance at the tick–host interface. Using this approach, many characterized tick proteins may have functional relevant concentrations and affinities at the feeding site. Conversely, the feeding site is not an ideal closed system, but is dynamic and changing, leading to possible overestimation of tick protein concentration at the feeding site and consequently an overestimation of functional relevance. Ticks have evolved different possible strategies to deal with this dynamic environment and overcome the barrier that equilibrium kinetics poses to tick feeding. Even so, cognisance of the limitations that equilibrium binding place on deductions of functional relevance should serve as an important incentive to determine both the concentration and affinity of tick proteins proposed to be functional at the feeding site.

Keywords: tick, host, feeding, affinity, equilibrium, function, relevance

BIOLOGICAL ACTIVITY AT THE TICK FEEDING INTERFACE

Biological function is central to the understanding of life and organismal biology. The context that function confers is exemplified in the frustration felt when a gene or protein of interest can only be annotated as a hypothetical protein with unknown function. Conversely, the ease of annotation by homology has made genome sequencing and assignment of function to orthologs an almost mundane task (Giles and Emes, 2017). Even so, biochemical characterization remains central to the elucidation and confirmation of new function and the understanding of functional mechanism. From a biochemical reductionist perspective, biological function may be explained within a structural mechanistic context as the action of a gene, surface, motif or residue that result

in a chemical reaction, activation or inhibition of an enzyme or receptor, or even a physiological process such as blood clotting or platelet aggregation. The current review considers biological function at the tick–host interface from this reductionist perspective (Elgin, 2010). Even so, it was recently suggested that before or during evolution of new function by gene duplicates, and before negative selection maintain the adaptive advantage conferred by such new functions, new duplicates may exist in a state of undefined or non-optimized function, where protein expression is maintained while functional space is explored by random mutation: the playground hypothesis of neutral evolution (Mans et al., 2017). There is also an increasing recognition that most proteins may exhibit "promiscuous activity," i.e., irrelevant secondary activities (Copley, 2015, 2017). In addition, given the possibility that a biochemical assay may yield results for a broad class of proteins with diverse functions, or even results without biological meaning, it raise the question whether any particular measured function is relevant within a biological or physiological context. The current review therefore also considers functional relevance at the tick–host interface from this perspective.

Sabbatani (1899), after reading Haycraft's work on the anti-clotting effects of the oral secretions from leeches (Haycraft, 1884), made the first prescient deduction that all hematophagous organisms must secrete components that interfere or regulate host defenses, such as the hemostatic system. He tested this by showing that crude whole body tick extracts led to *in vitro* inhibition of blood clotting and that injecting this extract into various animals led to prolongation of blood coagulation *in vivo*. He also injected what may very well be the first fractionation of tick proteins to show that this purified preparation retained its inhibitory properties. Sabbatani's deduction has been confirmed by extensive research into tick–host interactions that established a veritable pharmacopeia of bioactive components secreted by ticks during feeding (reviewed in Mans and Neitz, 2004a; Francischetti et al., 2009; Mans et al., 2016). However, a question that must have plagued him and remains relevant today, is whether *in vitro* and even *in vivo* observations can be causally linked with biological relevant activity at the feeding site, i.e., do what we measure in a test tube really function as a modulator of host defenses during feeding? The observation that ticks can cause paralysis in a host (Hovell, 1824 cited in Scott, 1921) and the presence of salivary glands in ticks (von Siebold and Stannius, 1854; Leydig, 1855; Heller, 1858), must have suggested that ticks can secrete substances into the host. Phenotypic changes in the host such as itching or ecchymosis after tick bite also suggested that ticks secrete substances into the host (Nuttall et al., 1908). Secretion and therefore presence would imply activity at the feeding site. However, the presence of toxic and anti-hemostatic molecules in tick eggs, but not salivary glands or saliva, showed that measurement of biological activity in crude extracts does not necessarily imply function at the tick–host interface (Hoeppli and Feng, 1933; de Meillon, 1942; Riek, 1957, 1959; Gregson, 1973; Neitz et al., 1981; Viljoen et al., 1985; Mans et al., 2004a). This implication was recognized soon after Sabbatani's seminal study, when researchers extended his observations by proving that anti-hemostatic and toxic activities were present in salivary glands of ticks (Nuttall and Strickland, 1908; Cornwall and Patton, 1914; Ross, 1926; Hoeppli and Feng, 1933). It would take a number of years before anti-hemostatic and toxic activity could be showed to be secreted in tick saliva itself. This had to await chemical means, such as pilocarpine, or mechanical means, such as infra-red light, to stimulate salivation in order to obtain adequate quantities of salivary secretion for demonstration of biological activity (Howell, 1966; Tatchell, 1967; Neitz et al., 1969, 1978; Dickinson et al., 1976; Ribeiro et al., 1985, 1987; Ribeiro and Spielman, 1986; Ribeiro et al., 1991). However, as Tatchell (1967) indicated: salivary secretions obtained with exogenous stimulants should be treated with caution, since it is unclear whether such secretions represent the total saliva complement or even represent saliva, since cement is not found in such secretions. This may be a pertinent observation since cement may readily form during feeding on artificial membranes (Kröber and Geurin, 2007), arguing that induced salivation is not entirely the same as salivation during actual feeding.

Confirmation of secretion during feeding remains a crucial component of validation of biological relevance (Law et al., 1992). This may be achieved to various extents, by direct determination of the presence of a specific activity or molecule in saliva, or detection of host-derived antibodies generated against components secreted during feeding (Ribeiro et al., 1991; Oleaga-Pérez et al., 1994; Mulenga et al., 2003). Detection in the salivary glands or salivary gland extract (SGE) may be used as an indication of secretion, especially if a secretory peptide signal is present in the immature protein sequence (Nielsen, 2017). The latter have been extensively used to identify potential secretory components during transcriptome analysis (reviewed in Mans et al., 2016). However, secretion of some proteins without canonical signal peptides and non-salivary gland derived proteins via apocrine or alternative secretion has complicated the distinction of true and false positive secretory components (Mulenga et al., 2003; Díaz-Martín et al., 2013b; Oliveira et al., 2013; Tirloni et al., 2014, 2015), thereby also obscuring deduction of biological relevance (Mans et al., 2016). Not all salivary gland proteins with signal peptides are necessarily secreted during feeding (Nielsen, 2017), nor are all secretory proteins secreted at the same time, such as the case for hard ticks, that show differential expression over the course of several days of feeding (McSwain et al., 1982; Paesen et al., 1999; Wang et al., 2001b; de Castro et al., 2016, 2017; Kim et al., 2017; Perner et al., 2018). Transcriptome and proteome data also shows a weak correlation (Schwarz et al., 2014). While this may be ascribed to technical limitations in the proteomic and transcriptomic analysis of complex samples from non-model organisms, it further complicates the assessment of the final relevant concentration of protein present during feeding.

The Equilibrium State and Functional Correlates

Le Chatelier's principle states that an equilibrium system will tend to counteract changes to the system to maintain its equilibrium. In biological systems this is overcome by enzymes that create intermediate states to catalyze non-reversible chemical reactions.

In the case of receptor-ligand or protein-inhibitor binding, the affinity of the receptor for the ligand and the relative receptor and ligand concentrations determines the bound state at equilibrium (**Figure 1**). The affinity between molecules is expressed as the equilibrium dissociation constant (K_D) that range for most biological systems from the fM to mM range (Smith et al., 2012). The K_D is the ligand concentration at which 50% of the receptor is occupied at equilibrium (**Figure 1**). At a ligand concentration 10-fold the K_D, a receptor would be 91% saturated and above this concentration almost all of the receptor will be occupied. However, at a ligand concentration 10-fold less than the K_D, only 9% of the receptor would be occupied by the ligand and below this concentration essentially no binding occurs. At concentrations of the ligand that is equal to its K_D, only 50% of the receptor will be occupied if the stoichiometry of binding is 1:1. The K_D is therefore also considered to reflect a physiological relevant concentration (Sears et al., 2007). Concentrations of salivary proteins at the feeding site would therefore be physiologically relevant only at concentrations equal or exceeding their affinities for their targets by 10-fold or more if 50–100% receptor occupancy is necessary for effective inhibition. The K_i (inhibitor constant) is determined for inhibitors of enzyme active sites and reflect the concentration necessary to reduce enzyme activity by half. It is generally used in the characterization of inhibitors using enzyme kinetics and depends on both enzyme affinity for substrate and inhibitor affinity for enzyme. Even so, it is similar to the K_D and should produce similar values when enzyme activity is measured at physiological concentrations. Another measurement analogous to the K_D is the IC_{50} value of an inhibitor. The IC_{50} value (half-maximal inhibitory concentration) is the concentration at which 50% inhibition of function is observed. This is generally determined for complex processes such as inhibition of platelet aggregation, blood clotting, or cell migration. This value would ultimately depend on the concentration of receptor or number of cells used in an assay, but would be close to the K_D if physiologically relevant receptor or cell concentrations were used. Another measure that may indicate physiological relevance is the stoichiometric inhibition ratio (SI). This ratio indicate physiological relevance when an inhibitor interact with an enzyme or receptor close to equimolar ratios, since this imply high affinity, so that for example an SI = 2 imply saturation of receptor at $2K_D$. This may be seen for suicide inhibitors that bind irreversible to the enzyme active site. In enzyme kinetics the K_m (Michaelis constant) is the substrate concentration that allows an enzyme to attain half V_{max}. V_{max} is the maximum reaction rate of the enzyme when saturated with substrate. While the K_m is dependent on rate constants rather than ligand concentration it is also an indication of affinity and provide an estimate of relevant concentrations of substrates where an enzyme will function. For example, if a given agonist functions at concentrations 10-fold lower than the K_m, the enzyme will not be able to effectively remove this agonist from the system and neutralize its effect. The K_D, K_i, IC_{50}, SI, and K_m are therefore all useful to assess the physiological relevance of any biological activity. The reader is referred to Kuriyan et al. (2013) for a general treatment of protein-ligand affinity.

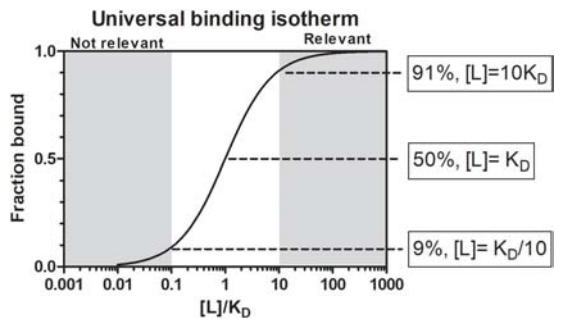

FIGURE 1 | The universal binding isotherm express the relationship between receptor occupation by a ligand (fraction bound) and the equilibrium dissociation constant (K_D) with regard to the concentration of ligand present for a 1:1 interaction at equilibrium. At a ligand concentration that equals the K_D (1K_D), 50% of the receptor will be occupied. At a ligand concentration 10-fold more than the K_D (10K_D), 91% of the receptor will be occupied. Above this concentration a given ligand should be physiologically significant. At a ligand concentration 10-fold less than the K_D (K_D/10) only 9% of the receptor will be occupied. Below this concentration physiological significance should be suspect. Between 10K_D and K_D/10 a gray area exist where physiological significance will depend on environmental factors.

Another measure of potential functional activity is the amount of salivary gland equivalents that may have a measurable impact or functionality. For example, ∼0.125 salivary gland equivalents from the tick *Ornithodoros kalahariensis* (previously *Ornithodoros savignyi*, Bakkes et al., 2018), was able to increase clotting time for the APTT test by 400%, 0.4% of a salivary gland could inhibit fXa ∼100 and 0.07% could inhibit thrombin by ∼100% (Gaspar et al., 1995). As such, any function that may be measured from the equivalent of 2 salivary glands (∼1 tick) or less that has an appreciable effect on some function may indicate the presence of relevant functionality. Even so, if characterizing crude extracts, it should be considered that the sum of multiple functions may be measured and that individual activities may be much less.

Whether a molecule will have relevant biological activity at the feeding site depends on their affinities for their respective ligands or receptors and whether they are secreted at relevant biological concentrations. In terms of chemical equilibrium, this implies that inhibitors or kratagonists (dealt with below) needs to be present at the feeding site at higher concentrations than the K_D for their respective receptors or ligands. At concentrations below the K_D little or no binding will occur and inhibitors may not be effective or physiologically relevant. In addition to satisfying concentration requirements, competition between host-derived substrates, ligands or receptors and tick-derived inhibitors, enzymes or scavengers for activating biomolecules will determine whether potential host-modulatory molecules may be biologically significant. This is essentially determined by the comparative affinities of host vs. tick-derived receptor-ligand interaction. Again, the biological relevance of host-derived agonists will be determined by their active concentrations at the feeding site. Effective concentration may also be determined by protein turnover or half-life at the feeding site. This will

depend on secretion into the feeding site, concentration and sequestration at the feeding site and protein stability. In the case of secretory proteins, most have disulphide bonds that increase their stability (Mans et al., 2016), contributing toward their effective concentrations. Modulation of host defenses at the tick–host interface therefore depends on interplay between these factors, with the implication that tick-derived antagonists need to be present at higher concentrations than host-derived agonists and have higher affinities for their shared targets (**Figure 2**).

The Feeding Site: Effective Volume Determines Functionality

The equilibrium state is an ideal closed state and the feeding site may be considered as such. However, while the feeding site may have a defined volume approximating a closed state, the feeding site itself may be dynamic with constant changes in concentration of both host and tick proteins. Ticks ingests blood meal and salivary components, since ticks alternately salivate and ingest blood meal (Arthur, 1970; Kemp et al., 1982), thereby removing both volume and active components from the feeding site. These repetitive doses of saliva, alternating by sucking events may be considered to be independent equilibrium events and in such a case may suggest that estimates of concentration at the feeding site may be lower than described below. Tick-derived molecules may also be removed into the general systemic system of the host or the general area around the feeding site, as evidenced by the systemic effects seen during paralysis and tick toxicoses (Mans et al., 2004a). Influx of blood or lymph into the feeding site may also dilute tick-derived proteins as seen in the case of edema (Kemp et al., 1982). As such, while the feeding site itself has been described as a hematoma or cavity that seems self-contained, the site itself may be much more dynamic than a defined cavity of blood.

A critical question remains as to what extent the feeding site may be reduced to a biochemical reaction in a test tube, i.e., can we measure the feeding site, calculate the feeding site volume and determine the amount of saliva secreted by the tick to derive estimations of biological concentrations at the feeding site? However, the feeding site is a complex and dynamic environment that changes constantly as determined by both the tick and the host (Nuttall, 2019). For example, ticks secrete enzymes that degrade the extracellular matrix over time, increasing the feeding site volume, while host wound healing responses will tend to counteract an increase in feeding site volume (Wikel, 2017). On the other hand, host inflammatory responses such as edema and cellular infiltration will tend to increase the feeding site volume, while hard ticks actively secrete excess blood-meal derived water back into the host, which will further contribute to feeding site volume, dilution and drainage of salivary proteins. As such, feeding site volumes have been conservatively estimated at 10–50 μl (Mans et al., 2008a,b). However, feeding site volume differs between larvae, nymphs and adults, whether natural or secondary hosts are parasitized and whether hosts are naïve or immune (Tatchell and Moorhouse, 1968; Brown and Knapp, 1980a,b; Brown et al., 1983). Natural hosts tend to present smaller feeding lesions, while secondary hosts can produce large lesions due to inflammatory responses (Brown and Knapp, 1980a,b; Brown et al., 1983).

Protein Concentration at the Feeding Site and Functionally Suspect Proteins

It may be estimated what concentrations can be expected for the average secreted protein at the feeding site, by asking what

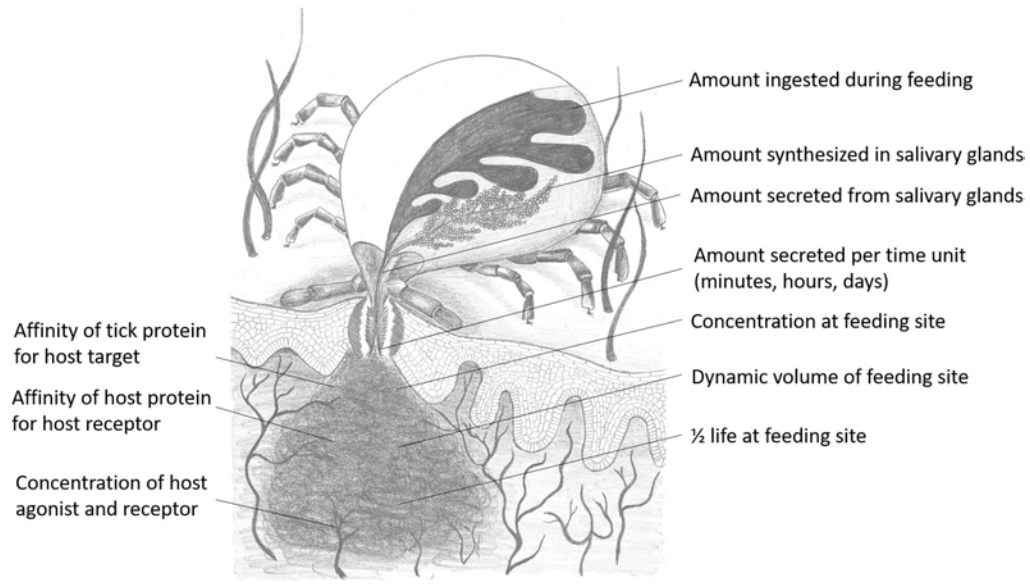

FIGURE 2 | Parameters that influence functional relevance at the feeding site for any salivary gland protein secreted during feeding. Drawing courtesy of Ronel Pienaar.

the highest protein concentration may be. In this regard, the lipocalins are known to be some of the most abundant proteins synthesized in tick salivary glands (Mans, 2011; Mans et al., 2017). The TSGP1-4 lipocalins from the soft tick *O. kalahariensis* has been characterized in detail. They each make up ∼5% of the total soluble salivary gland protein, comprising ∼20% of the total soluble protein content (Mans et al., 2001; Mans and Neitz, 2004b). In this case the total protein that may be secreted by a tick during a feeding event comprise ∼6 μg protein with molecular masses of ∼15 kDa each. Similarly, the savignygrins (Mr ∼ 7 kDa) also make up ∼3% of the total salivary gland protein with ∼4 μg of protein secreted during a feeding event (Mans et al., 2002b). In the case of the lipocalins from the soft ticks *Argas monolakensis*, the histamine binding protein AM-10 (Mr ∼ 16 kDa) comprise ∼23% of the total soluble protein (Mans et al., 2008b,c), and in this case equates with 4.6 μg of protein secreted during feeding. These concentrations are likely to be the highest estimates, since it is known that hard ticks secrete ∼30–300 times less protein than soft ticks in their saliva at any given feeding stage (Ribeiro, 1987; Dharampaul et al., 1993). The upper limit for any given protein in the adult tick salivary gland may thus be assumed to be ∼10 μg with a dynamic protein concentration range of 10,000-fold (1 ng–10 μg). If it is also assumed that nymphs have 10-fold and larvae 100-fold lower salivary concentrations than adults some interesting observations may be made regarding feeding site concentrations. For the purpose of the current study, the feeding site volumes were estimated from the studies of Brown and Knapp (1980a,b) with feeding cavities for larvae from 0.1 to 50 nl, nymphs from 5 to 150 nl, and adults from 10 nl to 10 μl. Using these assumptions concentration fluctuation at the feeding site can be estimated at various salivary gland protein concentrations and molecular masses of proteins. Under these assumptions the concentrations at the feeding site do not differ extensively between larvae, nymphs or adults, even though feeding site volume and effective salivary gland concentrations may differ (**Figure 3**). Allowing for the concentration ranges estimated, maximum concentrations at the feeding site may range from nM to mM, and may even range from nM to μM for salivary gland concentrations such as 0.1, 0.01, or 0.001 μg for adults, nymphs, or larvae, respectively, that may be considered to be more representative of the average protein concentration. These concentrations may be an over estimation since the dynamic nature of the feeding site and the rate at which protein is secreted may never approximate these total estimated concentrations.

In ticks the IC_{50}, K_D, and K_i values range from pM–mM and falls within the concentration expected at the feeding site (**Figures 3**, **4**). IC_{50} values generally tend to range from 10 nM to 10 μM (**Figure 2**). Conversely, K_D values range from 1 nM to 1 μM, while K_i values range from 10 pM to 10 nM. The higher IC_{50} values is probably due to the use of *in vitro* assays that measure complex reactions such as platelet aggregation, blood clotting, complement or cell migration. These systems do not necessarily represent true *in vivo* conditions and may be artificial to some extent, i.e., much higher concentrations of agonists or cell numbers are needed for observation than what is found under physiological conditions. The K_D values may represent true affinities, while the K_i values are dependent on the enzyme and substrate concentrations used, and the lower pM values may be due to the availability of chromogenic and fluorogenic substrates that enable sensitive measurement of enzyme activity. In this case, some of the affinities may be overestimated.

A number of tick proteins characterized have affinities, inhibition constants or IC_{50} values in the nM or pM range, which would probably be functional at the feeding site (**Figure 4** and **Table 1**). For some, concentrations at the feeding site may be estimated based on yields of purified inhibitor and these are generally in the same range as the affinities or higher, suggesting biological relevant concentrations at the feeding site (**Table 1**). For a number of proteins, estimates of concentrations at the feeding site is not available and the low nM to pM range of their K_D, K_i, or IC_{50} values is the only indication of functional relevance. A number of proteins also present extraordinary high concentration estimates at the feeding sites (>1 M), which may indicate that these proteins may not have been completely purified at the time of their characterization, or may reflect that they derived from whole body extracts and not tick salivary glands, which may suggest that these inhibitors originate from multiple organs (Ibrahim et al., 2001a,b). In many cases, the concentration of inhibitors that may occur at the feeding site has not been determined (**Table 1**). This will remain a major impediment in the assessment of functional relevance at the feeding site, since we are probably over rather than underestimating feeding site concentrations. To further consider functional relevance it is necessary to unpack the salivary gland repertoire into its functional modalities.

TICK FEEDING AND MODULATION OF HOST DEFENSES

Ticks need to modulate their vertebrate host's defense mechanisms to obtain a successful blood-meal (Francischetti et al., 2009). In this regard, ticks secrete numerous proteins during feeding that function as inhibitors, enzymes, or kratagonists that use a variety of mechanisms to overcome host defenses (Mans, 2011; Mans et al., 2016) (**Figure 5**).

Inhibitors That Target Enzyme Active Sites and/or Substrate-Binding Exosites

Various enzymes are involved in host hemostasis and many are part of enzyme cascades such as the blood clotting or complement cascade that enable efficient control as well as rapid response to injury or infection (Francischetti et al., 2009). Inhibitors for these cascades are found in all ticks. Inhibitors of blood-clotting enzymes generally target the active and exosites and inhibit primary enzymatic activity of thrombin, fXa, kallikrein, kallikrein-fXIIa–fXIa, fXa-TF-VIIa, plasmin, fV or carboxypeptidase B, thereby inhibiting formation or dissolution of the fibrin clot (**Table 1** including references). Inhibitors may also target enzymes that may induce platelet aggregation such as cathepsin G, or enzymes involved in inflammation such as cathepsin B, C, H, L, S, and V, chymase,

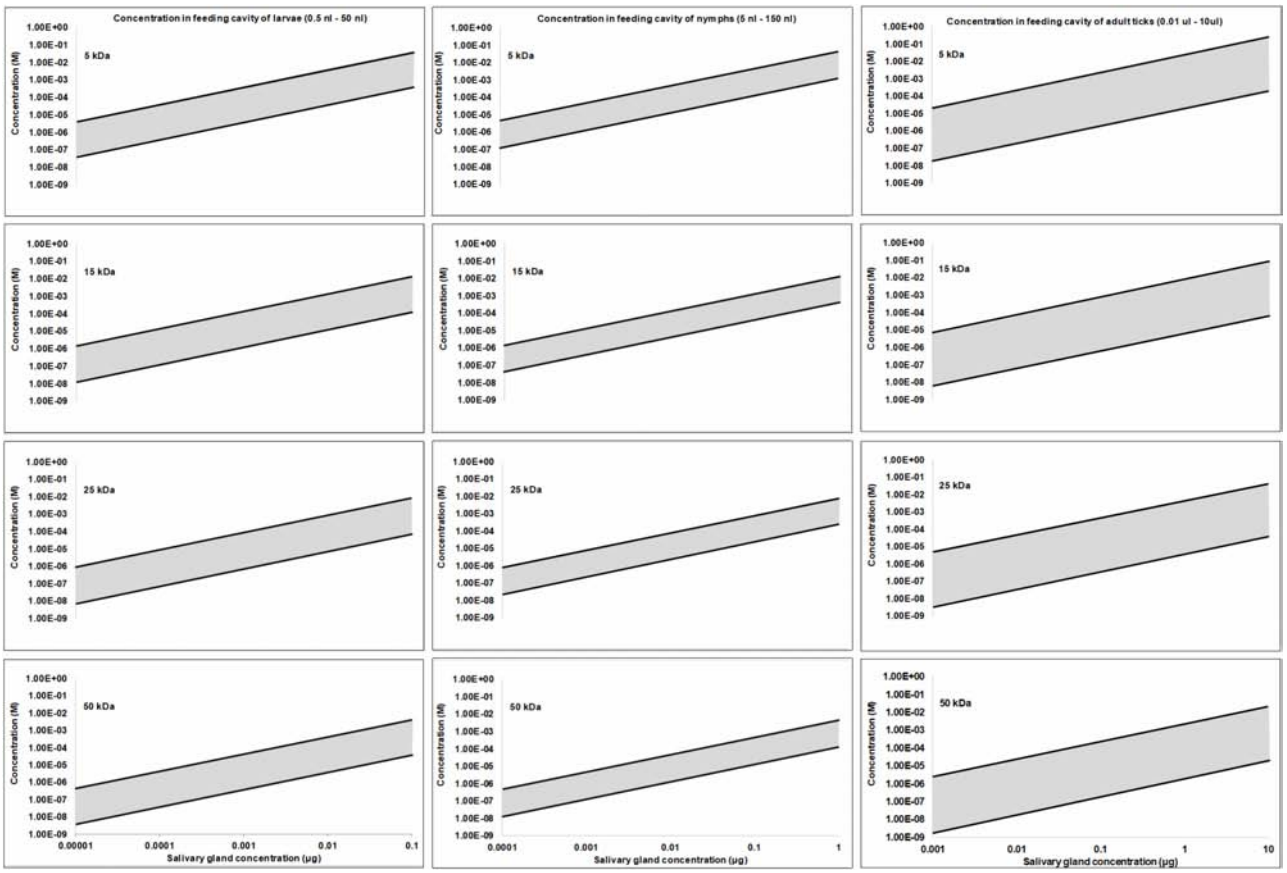

FIGURE 3 | Protein concentration estimates at the feeding site for larvae, nymphs and adults. Feeding sites volumes were estimated from Brown and Knapp (1980a; 1980b) and salivary concentrations were simulated over a 10,000-fold range assuming a maximum concentration of 10 µg in adults, 1 µg in nymphs and 0.1 µg in larvae.

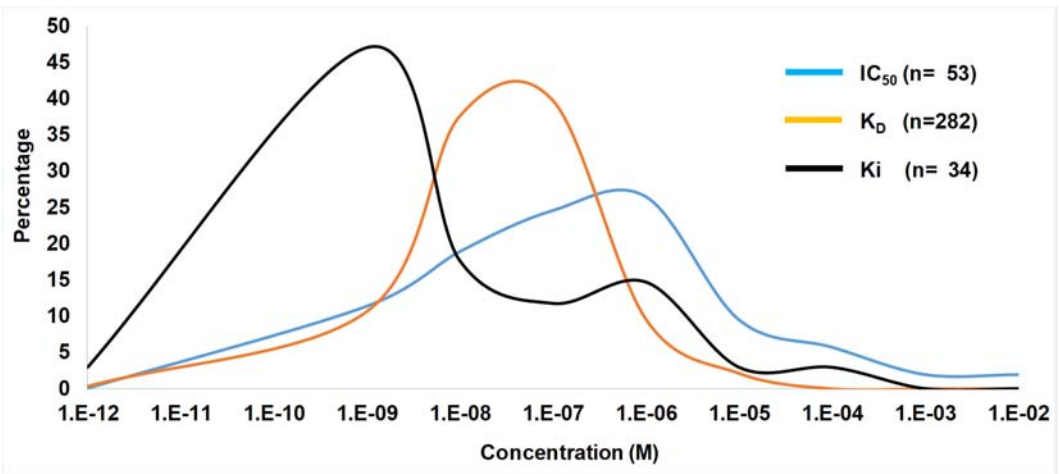

FIGURE 4 | Ranges of IC_{50}, K_D, and K_i values from the tick literature. Indicated are frequency distribution curves of values obtained from **Table 1** and references therein.

TABLE 1 | Tick inhibitors of host defenses considered to have relevant physiological function.

Protein	Tick	Target	Affinity (K_D, K_i, K_m, IC_{50})	Concentration (Minimum–Maximum)	References
Apyrase	*Ixodes scapularis*	ATP/ADP	N/A	Activity in saliva	Ribeiro et al., 1985
Apyrase	*Ornithodoros moubata*	ATP/ADP	N/A	Activity in saliva	Ribeiro et al., 1991
Apyrase	*Ornithodoros kalahariensis*	ATP/ADP	$K_m \sim 1$ mM	Activity in saliva 1 μM–1 mM	Mans, 1997; Mans et al., 1998b
Ir-CPI	*Ixodes ricinus*	fXIIa, fXIa, Plasmin	$K_D \sim 16$–38 nM	Unknown	Decrem et al., 2009
PAI	*Ixodes sinensis*	Platelets	$IC_{50} \sim 250$ nM	Unknown	Liu et al., 2005
Savignygrin	*Ornithodoros kalahariensis*	$\alpha_{IIb}\beta_3$	$IC_{50} \sim 130$ nM; $K_D \sim 60$ nM	55 μM–57 mM	Mans et al., 2002b; Mans and Neitz, 2004c
Monogrin	*Argas monolakensis*	$\alpha_{IIb}\beta_3$	$IC_{50} \sim 150$ nM	10 μM–10 mM	Mans et al., 2008a
Variabilin	*Dermacentor variabilis*	$\alpha_{IIb}\beta_3$	$IC_{50} \sim 150$ nM	2.7 μM–2.7 mM	Wang et al., 1996
Disagregin	*Ornithodoros moubata*	$\alpha_{IIb}\beta_3$	$IC_{50} \sim 104$ nM; $K_D \sim 40$ nM	20 μM–20 μM	Karczewski et al., 1994
YY-39	*Ixodes scapularis*	$\alpha_{IIb}\beta_3$	$IC_{50} \sim 4$–20 μM	Unknown	Tang et al., 2015
TAI	*Ornithodoros moubata*	$\alpha_2\beta_1$	$IC_{50} \sim 5$–8 nM; $K_D \sim 40$ nM	50 nM–50 μM	Karczewski et al., 1995
Moubatin	*Ornithodoros moubata*	TXA_2	$IC_{50} \sim 50$ nM $K_D \sim 24$ nM	1.5 μM–1.5 mM	Waxman and Connolly, 1993; Mans and Ribeiro, 2008b
TSGP2	*Ornithodoros kalahariensis*	LTB_4	$K_D \sim 18$ nM	38 μM–38 mM	Mans et al., 2001; Mans and Ribeiro, 2008b
TSGP3	*Ornithodoros kalahariensis*	TXA_2; LTB_4	$K_D \sim 5$–21 nM	38 μM–38 mM	Mans et al., 2001; Mans and Ribeiro, 2008b
Ir-LBP	*Ixodes ricinus*	LTB_4	$K_D \sim 0.5$ nM	Detected in saliva	Beaufays et al., 2008
TSGP4	*Ornithodoros kalahariensis*	LTC_4	$K_D < 2$ nM	35 μM–35 mM	Mans et al., 2001; Mans and Ribeiro, 2008a
AM-33	*Argas monolakensis*	LTC_4	$K_D \sim 2$ nM	3.5 μM–3.5 mM	Mans et al., 2008c; Mans and Ribeiro, 2008a
TSGP1	*Ornithodoros kalahariensis*	Histamine Serotonin	$K_D < 3$ nM; $K_D \sim 6$ nM	32 μM–32 mM	Mans et al., 2001, 2008b
OP-3	*Ornithodoros parkeri*	Histamine Serotonin	$K_D \sim 106$ nM; $K_D \sim 116$ nM	Detected in SGE	Francischetti et al., 2008 Mans and Ribeiro, 2008b
OtLip	*Ornithodoros turicata*	Histamine	Unknown	Unknown	Neelakanta et al., 2018
Monomine	*Argas monolakensis*	Histamine	$K_D \sim 7$ nM	29 μM–28 mM	Mans et al., 2008b,c
Monotonin	*Argas monolakensis*	Serotonin	$K_D < 2$ nM	10 μM–10 mM	Mans et al., 2008b,c
Is-14	*Ixodes scapularis*	Histamine Serotonin	$K_D \sim 427$ nM; $K_D < 2$	Unknown	Mans et al., 2008c
Is-15	*Ixodes scapularis*	Histamine Serotonin	$K_D \sim 746$ nM; $K_D < 2$	Unknown	Mans et al., 2008c
HBP1-3	*Rhipicephalus appendiculatus*	Histamine	$K_D \sim 1$–18 nM	Detected in SGE	Paesen et al., 1999
SHBP	*Dermacentor reticulatus*	Histamine Serotonin	$K_D \sim 1$–2 nM $K_D \sim 0.6$ nM	Unknown	Sangamnatdej et al., 2002
Savignin	*Ornithodoros kalahariensis*	Thrombin	$K_i \sim 5$ pM	850 nM–1 mM	Nienaber et al., 1999
P5	*Hyalomma dromedarii*	Thrombin	$K_i \sim 500$ nM	30 μM–30 mM	Ibrahim and Masoud, 2018
Sculptin	*Amblyomma sculptum*	Thrombin	$IC_{50} \sim 2$ pM $K_i \sim 18$ pM;	Unknown	Iqbal et al., 2017
Avathrin	*Amblyomma variegatum*	Thrombin	$IC_{50} \sim 7$ nM $K_i \sim 545$ pM	Unknown	Iyer et al., 2017
Boophilin	*Rhipicephalus microplus*	Thrombin	$IC_{50} \sim 1$ μM $K_i \sim 101$, 0.5–2 nM $K_D \sim 116$ nM	Unknown	Macedo-Ribeiro et al., 2008; Soares et al., 2012; Assumpção et al., 2016
RmS-15	*Rhipicephalus microplus*	Thrombin	SI ∼ 2	Unknown	Rodriguez-Valle et al., 2015; Xu T. et al., 2016
Hyalomin-1	*Hyalomma rufipes*	Thrombin	$K_i \sim 12$ nM $K_D \sim 19$ nM	Unknown	Jablonka et al., 2015

(Continued)

TABLE 1 | Continued

Protein	Tick	Target	Affinity (K_D, K_i, K_m, IC_{50})	Concentration (Minimum–Maximum)	References
rIxscS-1E1	*Ixodes scapularis*	Thrombin	SI ∼ 4	Unknown	Ibelli et al., 2014
Monobin	*Argas monolakensis*	Thrombin	K_i ∼ 6 pM	400 nM–400 μM	Mans et al., 2008a
Chimadanin	*Haemaphysalis longicornis*	Thrombin	IC_{50} ∼ 300 nM	Unknown	Nakajima et al., 2006
Madanins	*Haemaphysalis longicornis*	Thrombin	K_D ∼ 3–4 μM; K_i ∼ 31–55 nM	Unknown	Iwanaga et al., 2003; Figueiredo et al., 2013
Variegin	*Amblyomma variegatum*	Thrombin	IC_{50} ∼ 1 nM; K_i ∼ 10 pM	Unknown	Kazimírová et al., 2002; Koh et al., 2007
NTI-2	*Hyalomma dromedarii*	Thrombin	K_i ∼ 211 nM	3.8 mM–3.8 M	Ibrahim et al., 2001b
Americanin	*Amblyomma americanum*	Thrombin	K_i ∼ 0.073 nM	100 nM–100 μM	Zhu et al., 1997a
Saliva	*Amblyomma americanum*	fXa; Thrombin	100% I ∼ 0.3 SU	Unknown	Zhu et al., 1997b
Ornithodorin	*Ornithodoros moubata*	Thrombin	K_i ∼ 1 pM	Unknown	van de Locht et al., 1996
Anticoagulant	*Ixodes holocyclus*	Clotting	IC_{50} ∼ 0.25 SGU	Unknown	Anastopoulos et al., 1991
Ixin	*Ixodes ricinus*	Thrombin	IC_{50} ∼ 0.6 SGU	Unknown	Hoffmann et al., 1991
Calcaratin	*Rhipicephalus calcaratus*	Thrombin	Unknown	Unknown	Motoyashiki et al., 2003
Haemathrin	*Haemaphysalis bispinosa*	Thrombin	IC_{50} ∼ 40 μM	Unknown	Brahma et al., 2017
Microphilin	*Rhipicephalus microplus*	Thrombin	IC_{50} ∼ 6–42 μM	17 μM–17 mM	Ciprandi et al., 2006
BmAP	*Rhipicephalus microplus*	Thrombin	IC_{50} ∼ 100 nM–1 μM	333 nM–33 μM	Horn et al., 2000
NTI-1	*Hyalomma dromedarii*	Thrombin	K_i ∼ 11.7 μM	650 μM–6.5 M	Ibrahim et al., 2001b
HLS2	*Haemaphysalis longicornis*	Thrombin	IC_{50} ∼ μM	Unknown	Imamura et al., 2005
IRS-2	*Ixodes ricinus*	Cathepsin G; Chymase	IC_{50} ∼ 4–11 nM	Unknown	Chmelař et al., 2011
AamS6	*Amblyomma americanum*	Undefined	All tests μM range; no parameters	Immunogenic	Chalaire et al., 2011; Mulenga et al., 2013
Penthalaris	*Ixodes scapularis*	Tissue factor pathway	IC_{50} ∼ 100 pM	Unknown	Francischetti et al., 2004
Ixolaris	*Ixodes scapularis*	Tissue factor pathway fXa	IC_{50} ∼ pM range	Unknown	Francischetti et al., 2002; Monteiro et al., 2005
Hd_fXaI	*Hyalomma dromedarii*	fXa	K_i ∼ 134 nM	0.3 mM–300 mM	Ibrahim et al., 2001a
Anticoagulant	*Rhipicephalus appendiculatus*	fXa	450% clotting time increase for 2 SGU	100 nM–125 μM	Limo et al., 1991
TAP	*Ornithodoros moubata*	fXa	K_i ∼ 0.6 nM	8 μM–8 mM	Waxman et al., 1990
fXaI	*Ornithodoros kalahariensis*	fXa	K_i ∼ 0.8 nM	250 nM–250 μM	Gaspar et al., 1996
Salp14	*Ixodes scapularis*	fXa	IC_{50} ∼ 150 nM	Immunogenic	Narasimhan et al., 2002
Amblyomin-X	*Amblyomma sculptum*	fXa	IC_{50} ∼ 10 μM; K_i ∼ 4 μM	Unknown	Batista et al., 2010; Branco et al., 2016
TIX-5	*Ixodes scapularis*	fV	IC_{50} ∼ 3.2 μM; all tests μM range	Immunogenic	Schuijt et al., 2011, 2013
Rhipilin-1	*Rhipicephalus haemaphysaloides*	Elastase	SI ∼ 6	Unknown	Cao et al., 2013
BmTI-A	*Rhipicephalus microplus*	Elastase; Kallikrein	K_i ∼ 1.4 nM; K_i ∼ 120 nM	Unknown	Tanaka et al., 1999
Iris	*Ixodes ricinus*	Elastase TNF-α	IC_{50} ∼ μM IC_{50} ∼ 50 nM	Unknown	Leboulle et al., 2002; Prevot et al., 2006, 2009
RsTIQ 2, 5, 7	*Rhipicephalus sanguineus*	Elastase; plasmin	K_i ∼ 1–38 nM	Unknown	Sant'Anna Azzolini et al., 2003
Haemaphysalin	*Haemaphysalis longicornis*	fXIIa	IC_{50} ∼ 50–100 nM; K_D ∼ 3 nM	Unknown	Kato et al., 2005
AAS19	*Amblyomma americanum*	Plasmin; Thrombin	SI ∼ 3–9	Unknown	Kim et al., 2015; Radulović and Mulenga, 2017

(Continued)

TABLE 1 | Continued

Protein	Tick	Target	Affinity (K_D, K_i, K_m, IC_{50})	Concentration (Minimum–Maximum)	References
TdPI	*Rhipicephalus appendiculatus*	Tryptase	K_i < 1.5 nM	Unknown	Paesen et al., 2007
Tryptogalinin	*Ixodes scapularis*	Plasmin Tryptase	K_i ∼ 5.83 nM K_i ∼ 10 pM	Unknown	Valdés et al., 2013
Sialostatin L	*Ixodes scapularis*	Cathepsin L	IC_{50} ∼ 5 nM; K_i ∼ 95 pM	Detected in saliva	Kotsyfakis et al., 2006
Sialostatin L2	*Ixodes scapularis*	Cathepsin L	IC_{50} ∼ 70 pM; K_i ∼ 65 pM	Unknown	Kotsyfakis et al., 2007
Iristatin	*Ixodes ricinus*	Cathepsin L and C	IC_{50} ∼ 500 nM–3 μM	Unknown	Kotál et al., 2019
OmC2	*Ornithodoros moubata*	Cathepsin L and S	IC_{50} ∼ 150 pM; K_i ∼ 65 pM	Detected in saliva	Grunclová et al., 2006; Salát et al., 2010
BrBmcys2b	*Rhipicephalus microplus*	Cathepsin B and L	K_i ∼ 1–3 nM	Detected in saliva	Parizi et al., 2013
RHcyst-2	*Rhipicephalus haemaphysaloides*	Cathepsin S	IC_{50} ∼ 100 pM	Detected in saliva	Wang et al., 2015
TCI	*Rhipicephalus bursa*	Carboxy-peptidase	K_i ∼ 1–4 nM	150 nM–150 μM	Arolas et al., 2005
HITCI	*Haemaphysalis longicornis*	Carboxy-peptidase	IC_{50} ∼ 10 μM	Unknown	Gong et al., 2007
Evasin-1	*Rhipicephalus sanguineus*	CCL3; CCL8; CCL18	K_D ∼ 160 pM; K_D ∼ 810 pM; K_D ∼ 3 nM	Detected in saliva	Frauenschuh et al., 2007
Evasin-3	*Rhipicephalus sanguineus*	CXCL1; CXCL8	K_D ∼ 340 pM; K_D ∼ 700 pM;	Detected in saliva	Déruaz et al., 2008
Evasin-4	*Rhipicephalus sanguineus*	CCL1-CCL27	K_D ∼ 10–700 pM;	Detected in saliva	Déruaz et al., 2013
P1243 (AAM-02)	*Amblyomma americanum*	CCL1-CCL27	K_D ∼ 1–100 nM	Unknown	Alenazi et al., 2018
P1156	*Ixodes ricinus*	CXCL1-8	K_D ∼ 3–70 nM	Unknown	Alenazi et al., 2018
RPU-01, RPU-02, AAM-01, AAM-02, ACA-01, ACA-02, AMA-01, ATR-02, IRI-01	*Rhipicephalus pulchellus Amblyomma americanum Amblyomma cajennense Ixodes ricinus Ixodes holocyclus*	Eotaxin-1; Eotaxin-2; Eotaxin-3; MCP-1; MCP-2; MCP-3	K_D ∼ 5–1,000 nM	Unknown	Hayward et al., 2018
P991, P985, P546, P974, P983, P1181, P1182, P1183, P1180, P467	*Amblyomma maculatum Amblyomma triste Amblyomma parvum Rhipicephalus pulchellus*	CCL2, CCL3, CCL4, CCL7, CCL8, CCL11, CCL13,CCL14, CCL16, CL17, CCL18,CCL19 CCL20,CCL21, CCL22, CL23 CCL24,CCL27, CCL28, CCL25	K_D ∼ 1 pM–3 μM	Unknown	Singh et al., 2017
P672	*R. pulchellus*	CCL3, CCL8, CCL11, CCL13, CCL14, CCL16, CCL18, CCl23	K_D ∼ 1–10 nM; IC50 ∼ 2–6 nM	Unknown	Eaton et al., 2018
OMCI	*Ornithodoros moubata*	C5 complement	IC_{50} ∼ 12–27 nM K_D ∼ 18 nM K_D < 100 pM	29 μM–29 mM	Nunn et al., 2005; Hepburn et al., 2007; Macpherson et al., 2018
TSGP2	*Ornithodoros kalahariensis*	C5 complement	K_D ∼ 26 nM	38 μM–38 mM	Mans et al., 2001; Mans and Ribeiro, 2008b
TSGP3	*Ornithodoros kalahariensis*	C5 complement	K_D ∼ 14 nM	38 μM–38 μM	Mans et al., 2001; Mans and Ribeiro, 2008b
RaCI	*Rhipicephalus appendiculatus*	C5 complement	IC_{50}-6–21 nM	Unknown	Jore et al., 2016

(Continued)

TABLE 1 | Continued

Protein	Tick	Target	Affinity (K_D, K_i, K_m, IC_{50})	Concentration (Minimum–Maximum)	References
Isac; Salp9; Salp20	*Ixodes scapularis*	C3 complement	IC_{50} ∼ 200 nM	Detected in saliva	Valenzuela et al., 2000; Soares et al., 2005; Tyson et al., 2007, 2008
IRAC; IxAC	*Ixodes ricinus*	C3 complement	IC_{50} ∼ 10–50 nM	Unknown	Daix et al., 2007; Schroeder et al., 2007; Couvreur et al., 2008
HT1-12	*Ixodes holocyclus*	Presynapse	IC_{50} ∼ 1–10 mM	Detected in saliva	Chand et al., 2016
Salp15	*Ixodes scapularis*	T cell proliferation IL2 production CD4	K_D ∼ 47 nM	Detected in saliva	Anguita et al., 2002; Garg et al., 2006
Longistatin	*Haemaphysalis longicornis*	RAGE	K_D ∼ 72 nM	Detected in saliva	Anisuzzaman et al., 2014
Adrenomedullin	*Ornithodoros moubata*	Vasodilation	IC_{50} ∼ 7 nM	Unknown	Iwanaga et al., 2014
Ra-KLP	*Rhipicephalus appendiculatus*	maxiK channels	AC_{50} ∼ 1 μM	Unknown	Paesen et al., 2009
Ixonnexin	*Ixodes scapularis*	Plasminogen-tPA	K_m ∼ 70–200 nM K_D ∼ 4–19 nM	Detected in saliva	Assumpção et al., 2018

Indicated are relative affinity reported as the dissociation equilibrium constant (K_D), inhibitory constant (K_i), Michaelis constant (K_m), stoichiometric inhibition ration (SI), or inhibitory concentration (IC_{50}). Salivary gland unit (SGU) refers to a fraction of a salivary gland. Minimum and maximum concentrations were calculated based on yields per tick reported and a feeding site volume of 10 nl–10 μl. Were indicated that proteins were detected in saliva or salivary gland extract (SGE), this was done with either western blot, affinity pull-down or proteomics.

elastase, and tryptase (**Table 1** and references therein). Targeting of enzyme active sites or substrate-binding exosites prevent binding of the substrate to the enzyme, thereby blocking its downstream effects. Most of these inhibitors have affinity measurements ranging from low pM to nM and for those whose concentrations could be estimated, would be present at relevant concentrations (**Table 1**).

With regard to host protein concentrations and affinities, prothrombin occurs at ∼1.4 μM in plasma, although only sub μM quantities are generally converted to thrombin (Butenas and Mann, 2002). Fibrinogen and fibrin has a low affinity site for thrombin with K_D ∼ 2–5 μM and a high affinity site with K_D ∼ 100 nM, while occurring at a plasma concentration of ∼7.6 μM. In addition, the K_D for the thrombin platelet receptor GP1bα is ∼50–200 nM (Adams and Huntington, 2006). It is therefore not unexpected that inhibitors would have K_D values in the low nM or pM range, while also occurring at low nM to μM concentration ranges to allow efficient competition with fibrinogen. fX occur at a plasma concentration of ∼170 nM, while fXa concentrations found in the clot range from 2 to 16 nM (Butenas and Mann, 2002). These concentrations also correlate with K_i values of tick inhibitors that are in the low nM range or below (**Table 1**). Other blood clotting factors have even lower concentrations ranging from low nM to pM concentrations in plasma (Butenas and Mann, 2002). Neutrophil derived proteases such as elastase or cathepsin G can reach concentrations of 100 nM at the site of release and is sufficient to induce platelet aggregation (Ferrer-Lopez et al., 1990). Again, the low nM IC_{50} or K_D values for the tick inhibitors correspond with the host target concentrations, supporting functional relevance at the tick feeding site (**Table 1**). Some clotting enzyme inhibitors have K_i or IC_{50} values in the μM ranges (**Table 1**). While estimates indicate that tick proteins may achieve such high concentrations at the feeding site, it remains crucial to confirm that they actually do.

Inhibitors That Target Sites Distant From Enzyme Active Sites

Inhibitors may target enzymes at sites distant from the active site, thereby disrupting complex assembly and downstream activation and include inhibitors of C5 complement such as *Ornithodoros moubata* complement inhibitor (OMCI) and *Rhipicephalus appendiculatus* complement inhibitor (RaCI) (Nunn et al., 2005; Jore et al., 2016). OMCI binds to the C5d, CUB, and C345c domains of C5, while RaCI binds to the MG1, MG2, and C5d domains (Jore et al., 2016). In both cases, these domains and the inhibitor binding sites are distant from C5a or the C5 convertase binding sites suggesting that these inhibitors do not directly inhibit interaction of convertases with C5, but probably inhibit rearrangement of domains within C5 that is necessary for activation to occur (Jore et al., 2016). Other complement inhibitors from soft ticks include the OMCI homologs TSGP2 and TSGP3 from *O. kalahariensis* (Mans and Ribeiro, 2008b). These inhibitors have K_D values in the low nM range (**Table 1**). A recent study that used site-specific immobilization of OMCI and multicycle kinetics indicated that the K_D may even be in the low pM ranges indicating that assay design can affect estimations of affinity (Macpherson et al., 2018). These inhibitors also show quite high expected concentrations at the feeding site, which is mostly due to their functioning as kratagonists (section below). Complement C5 occur at a concentration of ∼370 nM in plasma and its activator (C3/C5 convertase) show K_m values of 5–16 nM for the classical and alternative complement pathways (Rawal and Pangburn, 2001, 2003). Therefore, even at low nM concentrations and the high concentrations of

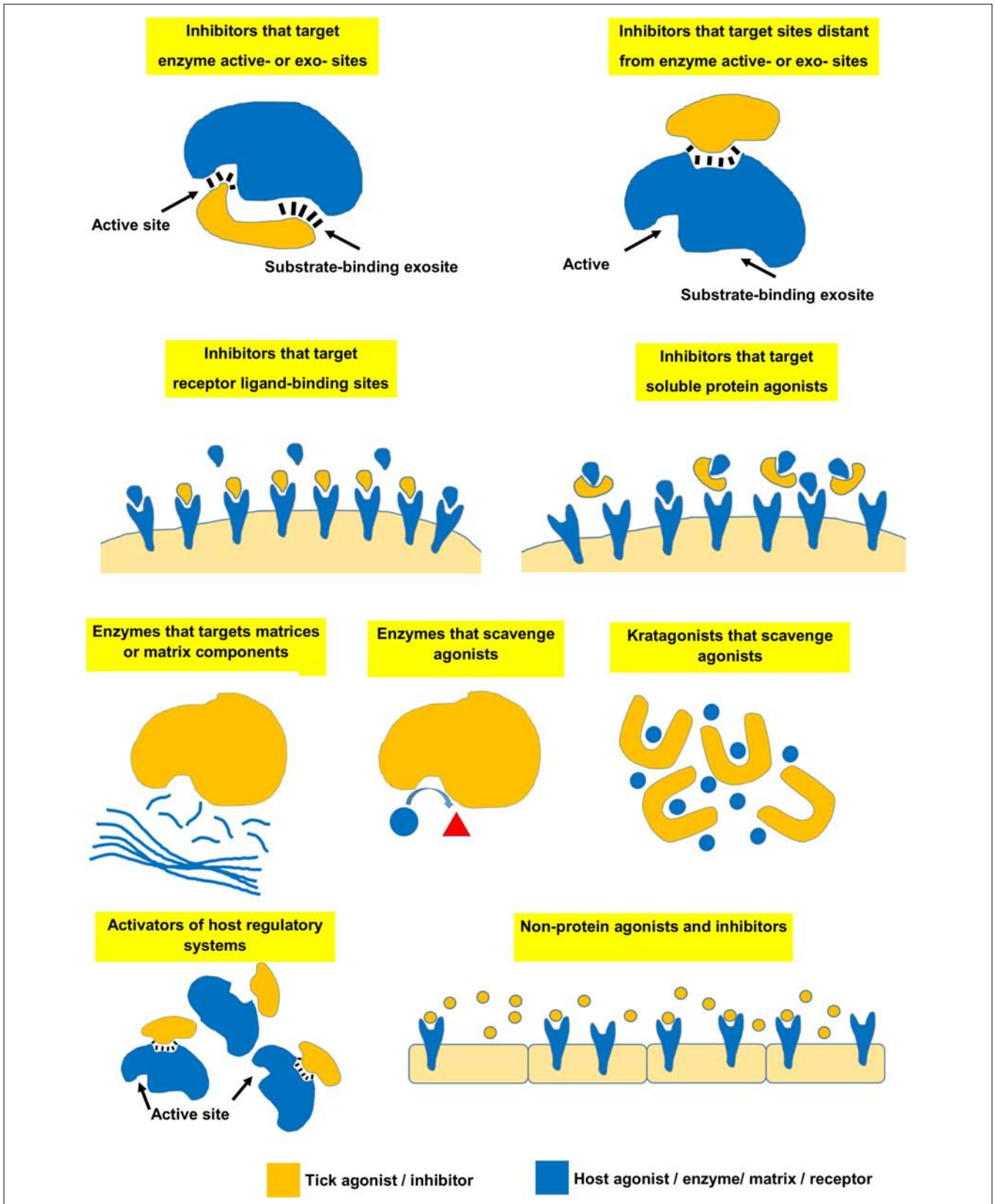

FIGURE 5 | Various mechanisms used by ticks to modulate vertebrate host defenses.

inhibitor expected at the feeding site, the tick proteins should be functionally relevant. Hard ticks also possess complement inhibitors that belong to the Isac/IRAC family (Valenzuela et al., 2000). These inhibitors target the C3 convertase complex (C3bBbP) of the alternative pathway and dissociate this complex, preventing binding of the convertase to C3. IC_{50} values that range from 10 to 200 nM has been reported (**Table 1**). Of these inhibitors, Salp20 specifically target properdin of the C3 convertase complex and bind with a K_D∼0.6 nM, which is much lower than the K_D of properdin (>85 nM) for C3b (Tyson et al., 2008). As such, these inhibitors should be functionally relevant at the feeding site although affinities for all homologs have not yet been determined. The blood-clotting inhibitor ixolaris targets the heparin-binding exosite of fXa, thereby disrupting formation of the prothrombinase complex with an IC_{50} in the pM range (Francischetti et al., 2002; Monteiro et al., 2005). It would therefore be expected to be functionally relevant.

Inhibitors That Target Receptor Ligand-Binding Sites

Inhibitors that target cell receptors thereby blocking binding of natural ligands and receptor activation includes fibrinogen receptor (GPIIbIIIa; $\alpha_{IIb}\beta_3$) antagonists that inhibit platelet aggregation induced by any agonist (Karczewski et al., 1994; Wang et al., 1996; Mans et al., 2002b, 2008a; Tang et al., 2015). It has been shown that these inhibitors can also compete with bound fibrinogen to disaggregate aggregated platelets (Mans et al., 2002a). Binding to the fibrinogen receptor do not seem to result in outside-in signaling by these agonists. Inhibitors that target fibrinogen receptors need to be present at high concentrations, since platelets possess high numbers of the $\alpha_{IIb}\beta_3$ integrin on their surface (∼80,000 receptors/platelet) (Wagner et al., 1996). This could result in concentrations of active receptor of ∼39 nM at the feeding site. The affinity constant (K_D) for fibrinogen is ∼1.4 μM, while fibrinogen occur in 10-fold excess (Frojmovic et al., 1994). It is therefore not unexpected that inhibitors would have K_D values in the nM range to bind to the receptor, while also occurring at μM concentrations to effectively compete with fibrinogen. Conversely, inhibitors with K_D or IC_{50} values above 1 μM may not be effective inhibitors.

Tick adhesion inhibitor (TAI) inhibits adhesion of platelets to collagen with an IC_{50} ∼ 8 nM (Karczewski et al., 1995). Competitive inhibition (IC_{50} ∼ 5 nM) of binding of the monoclonal antibody Gi9 to the platelet collagen receptor GPIa-IIa ($\alpha_2\beta_1$) confirmed targeting of this receptor by TAI (Karczewski et al., 1995). The collagen receptor (GP1a/IIa) occur at low receptor numbers on platelets (800 receptors/platelet) resulting in a concentration of ∼400 pM at the feeding site (Coller et al., 1989). The affinity of collagen for platelets is also ∼35–90 nM (Jung and Moroi, 1998). It is therefore not surprising that the affinity for collagen receptor antagonists may be in the low nM range, with similar low nM concentrations at the feeding site.

Longistatin binds to the V domain of the receptor for advanced glycation end products (RAGE) with a K_D ∼ 72 nM, thereby inhibiting ligand-induced inflammation in tissues (Anisuzzaman et al., 2014). It has been detected at the feeding site using host antibodies and would therefore presumably be present at nM concentrations (Anisuzzaman et al., 2010). The concentration for RAGE is in the low pM ranges (Bopp et al., 2008) and longistatin should therefore be able to saturate the receptor at nM concentrations.

Inhibitors that target receptors and upon binding induce antagonistic responses do exist. Salp15 binds to the CD4 coreceptor on T cells with a K_D ∼ 47 nM and inhibits T-cell receptor ligation induced activation resulting in immunosuppression (Anguita et al., 2002; Garg et al., 2006). Salp15 also interact with DC-SIGN on dendritic cells (DC) to activate the serine\threonine kinase Raf-1. This leads to modulation of Toll-like receptor induced DC activation (Hovius et al., 2008). However, in the latter case no affinity assessment was done, so it remains difficult to assess the biological relevance of this at the tick-feeding site. The CD4 coreceptor occurs at ∼16–664 pM (Platt et al., 1998), and if Salp15 occur at concentrations equal or above its K_D for the CD4 coreceptor should saturate the receptor and will be biologically relevant. The neurotoxins from *Ixodes holocyclus* are presumed to target and inhibit presynaptic P/Q-type voltage gated calcium channels (Chand et al., 2016). Recombinant holocyclotoxins have IC_{50} values ranging from 5 to 12 μM, which seem to be orders of magnitude higher than the concentrations present in saliva (Chand et al., 2016), suggesting that a discrepancy still exist between the identified toxins and crude salivary composition (Pienaar et al., 2018).

Inhibitors That Target Soluble Protein Agonists

A number of soluble host protein agonists exist that play a role in inflammation and immunity. These generally bind to receptors on leukocytes to activate cellular responses and cellular migration and are collectively known as cytokines or chemokines (Sokol and Luster, 2015). Leukocytes include eosinophils, mast cells, monocytes, neutrophils and natural killer cells that migrate along chemokine concentration gradients caused by release of chemokines from sites of infection or inflammation (Moore et al., 2018). A large number of chemokines exist that have specificities for different cell types. Chemokines are classified based on their conserved disulphide bond patterns. C chemokines possess a single disulphide bond and consist of two chemokines (XCL1 and XCL2). CC chemokines (β-chemokines) possess two disulphide bonds, with adjacent cysteines near the N-terminal and consist of 28 chemokines (CCL1–CCL28), described thus far. CXC chemokines (α-chemokines) possess two disulphide bonds with the adjacent cysteines near the N-terminal separated by a single amino acid and consist of 17 chemokines (CXCL1–CXCL17), described to date. A number of inhibitors from ticks that interact directly with these soluble agonists and prevent binding to their receptors have been described and are known as the evasins (Frauenschuh et al., 2007; Déruaz et al., 2008). It has been shown that evasins can bind to a wide array of cytokines or chemokines (**Table 1**). Their K_D values range from low pM to nM.

In the case of chemokines where leukocytes respond to concentration gradients for directional chemotaxis, the measured gradients suggest that these may range across low pM to several hundred nM (Moore et al., 2018). Naturally formed gradients depend on various factors that will influence the concentration gradient, notably, the type of cell secreting the chemokine, the amount secreted that depend on environmental cues, the presence of flow-induced shear stress and interaction of the chemokines with the extracellular matrix (Moore et al., 2018). Depending on the K_D of the evasins (low nM), chemotaxis may only be efficiently inhibited somewhere along the concentration gradient and not across the whole range, especially since competition of evasins for different chemokines might occur.

Enzymes That Target Matrices or Matrix Components

Ticks feed from a feeding cavity where blood pools (Tatchell and Moorhouse, 1968). The feeding site needs to be remodeled to form this cavity (Wikel, 2017). Ticks may secrete a variety of enzymes that will enable such remodeling. This includes hyaluronidase that targets hyaluronic acid, a major component of the extracellular matrix (Neitz et al., 1978). Salivary transcriptomes also indicate that an abundant class of enzymes are the metalloproteases (Mans et al., 2016). While their role in feeding site remodeling has not been established beyond doubt, the general assumption is that these enzymes would play a role in remodeling (Mans, 2016; Wikel, 2017). Other metalloproteases that has been identified with a defined function include fibrin(ogen)ase activity that remove fibrinogen, both substrate for thrombin or platelet aggregation, or fibrin that forms the blood clot (Francischetti et al., 2003). Longistatin, a small EF-hand protein can hydrolyze α, β, and γ chains of fibrinogen, activates plasminogen to plasmin, degrade fibrin and dissolve fibrin clots (Anisuzzaman et al., 2011, 2012). Other enzymes that may target the fibrin clot without a direct interaction include plasminogen activators such as enolase that promote degradation of the fibrin clot via activation of the host enzyme plasminogen to plasmin (Díaz-Martín et al., 2013a; Xu X.L. et al., 2016). A serine protease that potentially activates protein C, a potent anticoagulant has also been identified in saliva of *Ixodes scapularis* (Pichu et al., 2014). For these "activating" enzymes the physiological effective concentrations in saliva may be low (pM–nM ranges) and detection of function in saliva (not salivary gland extract) may be enough to infer functional significance given their amplification/catalyzing nature.

Enzymes That Perform Scavenging Functions

Some enzymes may perform scavenging functions by targeting bioactive molecules and catalyzing chemical reactions that inactivate or remove these molecules. This may prevent activation of receptors, or induce antagonistic responses in receptors by removal of activating ligand. In ticks, the enzyme apyrase (ATP-diphosphohydrolase; EC 3.6.2.5) hydrolyse ATP that function in inflammation (Faas et al., 2017), as well as ADP that induce platelet aggregation (Ribeiro et al., 1985, 1991; Mans et al., 1998a, 2008a). Apyrase was able to disaggregate platelets aggregated by ADP and caused platelet shape change from an activated spherical back to discoid form (Mans et al., 1998b, 2000), suggesting that bound ADP could be scavenged from its platelet receptor. Apyrase activity has been found in saliva or salivary glands of most ticks studied and have been assigned to the 5′-nucleotidase family (Stutzer et al., 2009). Family members have been found in all tick transcriptomes studied to date (Mans et al., 2016). Kinetic parameters from purified apyrase indicated a $K_m \sim 1$ mM for ATP and ADP and high turnover number (10^6 s^{-1}) and K_{cat}/K_m ratio (10^9 $M^{-1}s^{-1}$) (Mans et al., 1998b). These numbers indicate a highly efficient enzyme that would rapidly hydrolyze high local concentrations of ADP or ATP. Given the relatively high concentration of apyrase found in tick salivary glands (Mans et al., 1998b), it would probably also be functionally relevant. Another enzyme found in ticks that perform scavenging functions is a metallo dipeptidyl carboxypeptidase responsible for salivary kininase activity and breakdown of anaphylatoxin and bradykinin, involved in inflammation, pain and vasoconstriction (Ribeiro and Spielman, 1986; Ribeiro and Mather, 1998; Bastiani et al., 2002). In all cases of "scavenging" enzymes, the enzymes need to be able to rapidly remove host-derived agonist to levels below their functional ranges.

Kratagonists That Perform Scavenging Functions

Kratagonists are related to "scavenging" enzymatic functions, by scavenging or mopping up of bioactive molecules, but without chemically changing their structures. Kratagonists may have similar functional activity as "scavenging" enzymes, such as preventing activation of receptors by ligands, or competitive removal of ligand from receptors causing an antagonistic response (Ribeiro and Arcà, 2009; Andersen and Ribeiro, 2017). The term kratagonist was recently coined to describe the abundant proteins found in saliva of most hematophagous organisms that function in a scavenging capacity (Ribeiro and Arcà, 2009). The name derives from the Greek "to arrest or to seize" and was appropriately proposed independently by the Greek compatriots Babis Savakis and Michalis Kotsyfakis (Ribeiro and Arcà, 2009). Recently the etymology of the name was redefined to indicate "hold" or "grab/capture" and "agonist" (Andersen and Ribeiro, 2017; Arcà and Ribeiro, 2018). In ticks a large number of kratagonists have been described, that all belong to the lipocalin family. Lipocalin structure is composed of an eight stranded anti-parallel β-barrel closed off at one end by an N-terminal 3_{10}-helix, with a C-terminal α-helix anchored to the side of the barrel by disulphide bonds. This gives lipocalins the distinct appearance of a cup with an open end, where ligands can access the cup and bind in the cavity inside the barrel. Specificity is conferred by residues inside the barrel, as well as four loops that allow access to the barrel (Flower, 1996). The original name of lipocalin was assigned to "extracellular proteins capable of enclosing lipophiles within their structure to minimize solvent contact"

(Pervaiz and Brew, 1987). Subsequently, lipocalins were defined based on conserved sequence or structural motifs (Flower, 1996). Scavenging functions performed by tick lipocalins include scavenging of histamine and serotonin (Paesen et al., 1999; Sangamnatdej et al., 2002; Mans et al., 2008b; Neelakanta et al., 2018), leukotriene B4 (Beaufays et al., 2008; Mans and Ribeiro, 2008b; Roversi et al., 2013), leukotriene C4 (Mans and Ribeiro, 2008a), thromboxane A2 (Mans and Ribeiro, 2008b), and cholesterol (Preston et al., 2013; Roversi et al., 2017).

In the case of small chemical agonists that are scavenged by either enzymes or kratagonists, the concentrations at which they activate their respective receptors are important. Platelets secrete ADP and ATP at 3–7 μM concentrations, which are also the concentration necessary for primary and secondary aggregation (Packham and Rand, 2011). Apyrase from ticks has been shown to effectively inhibit platelet aggregation at these activator concentrations, at enzyme concentrations well below the expected secretory levels (Mans et al., 1998b). Basophils and mast cells may secrete histamine to attain local concentrations of 20 μM in the skin that can lead to inflammatory responses when histamine binds to its receptors with K_D ∼ 10 nM–30 μM (Petersen, 1997; MacGlashan, 2003). Serotonin is secreted by platelets at local concentrations of ∼5 μM where it can cause vasoconstriction and platelet aggregation by binding to various serotonin receptors with K_i ∼ 10 nM–1 μM (Watts et al., 2012). The very high concentrations of biogenic amine binding kratagonists at the feeding site (μM–mM) and their low affinities (low nM) indicate that they will be biologically relevant at the feeding site (**Table 1**).

Leukotriene B_4 secreted by neutrophils may reach high concentrations at the site of neutrophil release (∼950 nM) (Lewis et al., 1982). The affinity of LTB_4 for its neutrophil receptor BLT1 ranges from 0.1 to 2 nM (Yokomizo, 2015). Again, the low affinities observed for the LTB_4 scavengers and their high concentrations (μM) at the feeding sites would make them relevant competitors at the feeding site.

Cysteinyl leukotrienes can only be detected in plasma during inflammatory reactions such as asthma attacks and then occur at concentrations of ∼100–765 pM (Sasagawa et al., 1994). It has been shown to cause vasoconstriction and vasopermeability at a concentration of ∼100 nM, and bind with affinities from 5 to 35 nM to its receptors (Drazen et al., 1980; Krilis et al., 1983; Ghiglieri-Bertez et al., 1986; Prié et al., 1995). Scavengers of LTC_4 and LTD_4 have K_D values below 2 nM and also occur at μM concentrations (**Table 1**). It is therefore also expected that they would be physiologically relevant during feeding.

Thromboxane A_2 is released from platelets at concentrations of 11–35 nM, which is capable of inducing platelet aggregation and bind to platelet receptors with K_D ∼ 4 nM (Hamberg et al., 1975; Dorn and DeJesus, 1991). The high concentrations of the TXA_2 kratagonists at the feeding site (μM–mM) and their low affinities (low nM) suggest that they would be able to neutralize TXA_2 binding to its receptor during feeding (**Table 1**).

Activators of Host Regulatory Systems

The majority of tick host modulatory mechanisms described so far comprise inhibitors. However, activators may also play important roles since these may target the natural regulatory feedback systems of host hemostasis. Plasminogen activators that result in degradation of the fibrin clot have already been discussed. Recently, a small peptide named ixonnexin that belongs to the basic tail family was described that act by promoting interaction of plasminogen and tissue plasminogen activator (tPA) by forming a enzymatically productive ternary complex that forms plasmin to promote fibrinolysis (Assumpção et al., 2018). Ixonnexin interacts with both plasminogen and tPA with similar K_D values (4–20 nM). Such an activator would need to be present at similar or higher concentrations than the target enzymes to be functionally relevant. In the case of ixonnexin, plasminogen and tPA occur at plasma concentrations of ∼2 μM and 100 pM, respectively (MacGregor and Prowse, 1983; Assumpção et al., 2018). While no exact concentration has been established for ixonnexin, it has been estimated to occur at high concentrations in saliva (Assumpção et al., 2018). It has also been suggested that all basic tail proteins may perform this function, including the fXa inhibitor Salp14, since this family in which the C-terminal is rich in basic amino acids such as lysine and arginine mimics the C-terminal lysine present in fibrin that serves as recognition site for plasminogen and tPA lysine binding sites (Assumpção et al., 2018).

The adrenomedullins are a special case of tick-derived inhibitors that bind to host calcitonin-receptor-like receptor and receptor activity-modifying protein receptor complexes to cause vasodilation (Iwanaga et al., 2014). These inhibitors have not converged to mimic host adrenomedullin, but have been acquired via horizontal gene transfer from a mammalian host (Iwanaga et al., 2014). At systemic concentrations of ∼7 nM it reduced blood pressure by almost 50% (**Table 1**). It may therefore be assumed that secretion of such low quantities during feeding may result in local vasodilatory effects. However, it's presence in saliva at functional concentrations still needs to be confirmed.

An activator of MaxiK channels have been described in *R. appendiculatus*, where it presumably play a role in regulation of blood vessel tonus and blood flow (Paesen et al., 2009). It invoked a half maximal response in MaxiK channels at 1 μM. Its functionality at the feeding site remains to be resolved.

Non-protein Agonists and Inhibitors

Ticks may also secrete non-protein agonists that could affect the host's defense mechanisms. As such, ixodid ticks secrete prostaglandin E2 (PGE2), a potent vasodilator, at ∼40–500 ng/ml saliva (Ribeiro et al., 1985, 1992; Inokuma et al., 1994). Concentrations of PGE2 may range from 79 nM to 994 μM in adults at the feeding site, which would be pharmacologically active, since the K_D of the PGE2 receptor is ∼0.7 nM (Davis and Sharif, 2000). Another non-protein mechanism for modulating host inflammatory and pain

sensing responses was recently reported that involved secretion of saliva-specific microRNAs that was detected in salivary exosomes using next-generation sequencing (Hackenberg et al., 2017; Hackenberg and Kotsyfakis, 2018). The efficiency of exosomal miRNA will depend on the concentrations of exosomes in saliva, the specificity of the exosomes for specific cell types and the concentration of miRNA inside the exosomes (Hu et al., 2012). As yet, the functional relevance of saliva-derived exosomal miRNA still needs to be confirmed, with their kinetics of inhibition resolved, since the question remains whether a single exosome would only target a single lymphocyte or epithelial cell, in which case the effectiveness of inhibition would be determined by the number of cells that can be neutralized at the feeding site. It would, however, add another complex repertoire to the ticks expanding modulatory mechanisms.

STRATEGIES TO CIRCUMVENT THE AFFINITY/EQUILIBRIUM BARRIER

It is evident that the majority of tick proteins thus far characterized would have physiological functionality at the feeding site (**Figure 3** and **Table 1**). However, expression and secretion of high concentrations of secretory proteins via the salivary secretory granules may be restricted to very few proteins given physical constraints of granule packaging (Mans and Neitz, 2004b). The dynamic nature of the feeding site may also make the actual concentrations of tick proteins present at any given moment much more haphazard than expected. The concentrations at the feeding site may very well be 100–10,000-fold lower than estimated, in which case concentrations may drop to pM–nM for most proteins, which may be below the K_D values for many proteins. To address this, ticks may employ various alternative strategies that allow adequate expression and optimal use of secreted proteins at the feeding site that allow ticks to circumvent or eliminate the problems posed by an equilibrium system (**Figure 6**). The next section discusses such strategies in more detail.

Redundancy as Means to Control Complexity and Chaos

The host's defense systems such as the clotting, platelet aggregation, complement and inflammatory cascades are part of one big redundant integrated feedback system that allows rapid response as well as control of the system (Delvaeye and Conway, 2009; Deppermann and Kubes, 2016; Wiegner et al., 2016). It has been argued that this redundancy is mimicked in the complexity of functions observed in the salivary glands of blood-feeding arthropods (Ribeiro, 1995). Conversely, it has been argued that the complexity observed in the functional salivary repertoire of ticks is due to a highly optimized system of defense shaped by evolution (Nuttall, 2019). However, redundancy may serve the purpose of dealing with a highly dynamic and chaotic system, as may be seen at the feeding site, which is in constant flux with ever changing concentrations of target and inhibitor molecules. Targeting of many different host proteins at once, even if not at optimal concentrations, may disrupt a redundant system enough to allow successful feeding. In this environment no protein needs to be 100% effective, but only good enough to get the job done. This may allow non-optimal proteins to function at the feeding site, or be maintained while evolving more optimized functions as postulated in the playground hypothesis of neutral evolution (Mans et al., 2017). The question then becomes a matter of how much inhibition of the host's defense systems would be necessary to ensure successful feeding. In this regard, three observations could be made: firstly, that inefficient inhibition was surely a given during the early stages of adaptation to a blood-feeding lifestyle since protein functions were still optimized by natural selection. Secondly, since ticks had to switch hosts throughout their evolution, we have no evidence that ticks are not still adapting to new hosts, and functions that seem to be only partially effective may indeed still be optimized in future through natural selection. Thirdly, given the relatively high concentrations that may be obtained at the feeding site, even if proteins may only be partially effective, may allow for selection of these non-optimal functions to improve efficiency, again supporting a neutral evolution of function hypothesis (Mans et al., 2017). These arguments should, however, not serve as a *carte blanche* to support every claim of functional significance in blood-feeding, since the contribution of salivary derived proteins to species fitness has not been elucidated yet or even proven beyond doubt.

Fast Feeding, Storage and Secretion of a Large Bolus of Salivary Proteins

Soft ticks feed within minutes to hours to repletion, drop off, digest the blood meal slowly over the course of weeks to months, lay a small egg batch and can then feed several times more using the same pattern (Mans and Neitz, 2004a). During fast feeding most salivary proteins may be secreted in the course of 10–30 min and will be replenished within several days after feeding. Secretory proteins are stored in large granules up to 10 μM in diameter that effectively fill the salivary gland cells to their maximum extent (Mans and Neitz, 2004b; Mans et al., 2004b). The protein profiles of soft tick SGE attest to this, since protein spectra rarely show the presence of genomic DNA, in contrast to SGE from hard ticks that predominantly show genomic DNA/RNA, while the protein peak and concentration is obscured (**Figure 7**). This strategy from soft ticks allows concentrations of proteins that can overcome relatively high equilibrium dissociation constants by sheer concentration effects alone. Hard ticks utilize this strategy to some extent, since different salivary gland cells are filled with secretory granules over the course of the feeding period that can last several days to weeks (Binnington and Kemp, 1980). However, the amount of protein found in crude salivary gland extract rarely exceeds the concentrations of genomic DNA and is generally less than what would be observed for soft ticks (**Figure 7**), and may range from 5 to 60 μg total soluble protein over the course of feeding for a small tick such as *R. appendiculatus* (Wang and Nuttall, 1994). Similarly,

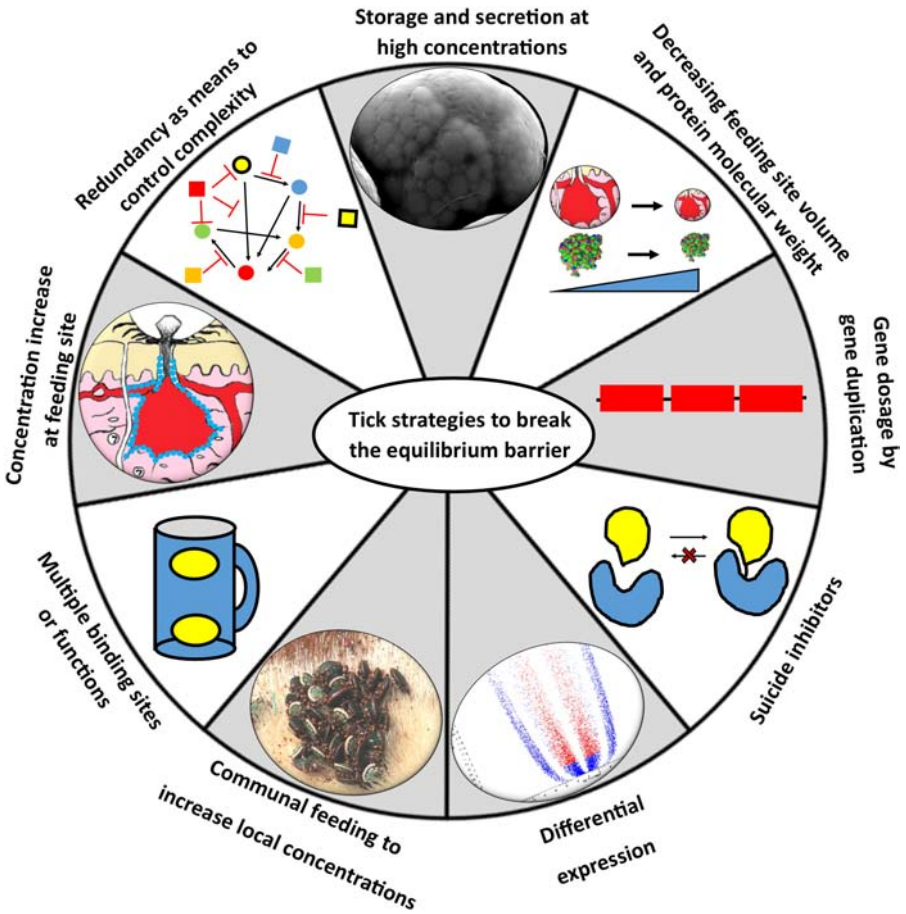

FIGURE 6 | Strategies to circumvent the equilibrium barrier. Ticks can use various strategies to increase local concentrations at the feeding site to satisfy equilibrium binding conditions.

concentrations in pilocarpine-induced salivary secretions in hard ticks are generally lower than soft ticks, with soft ticks attaining ∼20–40 mg/ml and hard ticks ranging from 700 to 60 μg/ml over the course of feeding (Howell et al., 1975; Ribeiro, 1987; Ribeiro et al., 1991; Dharampaul et al., 1993; Chand et al., 2016).

Communal Feeding to Increase Local Concentrations at the Feeding Site

Hard ticks feed for several days to weeks and mating on the host (or off the host for some *Ixodes* species) during the slow pre-feeding phase is required before the rapid engorgement phase can occur (Kiszewski et al., 2001). To allow mate finding, males secrete attraction-aggregation-attachment pheromones that result in ticks clustering and co-feeding at the same feeding site (Sonenshine, 2004). In a similar manner, specific tick species generally have preference sites of attachment on the host, presumably due to host environmental cues. While males do not engorge or take a significant blood meal, they do attach and secrete salivary components into the communal feeding site that apparently assist females in blood meal acquisition (Wang et al., 1998, 2001a). Creation of a communal locality where all ticks contribute to the localized but systemic feeding site may result in combined concentrations that overcome affinity restricted barriers.

Gene Dosage and Cumulative Contributions From Multigene Families

Proteins may be maintained as gene duplicates to allow high level expression from each family member (Mans et al., 2017). While each member may by itself completely inhibit host functions, even partial inhibition by each gene duplicate can result in complete inhibition. This is a relatively simple example of the gene dosage effect that has been observed for fibrinogen receptor antagonists (Mans et al., 2003a, 2008a) and LTB_4 scavengers (Mans et al., 2003b; Mans and Ribeiro, 2008b). It has been proposed that multigene families express different antigenic variable family members at low concentration levels to escape the immune system, the varying epitope hypothesis (Couvreur et al., 2008; Chmelař et al., 2016b). In this scenario, the low-level expressed proteins cumulatively target

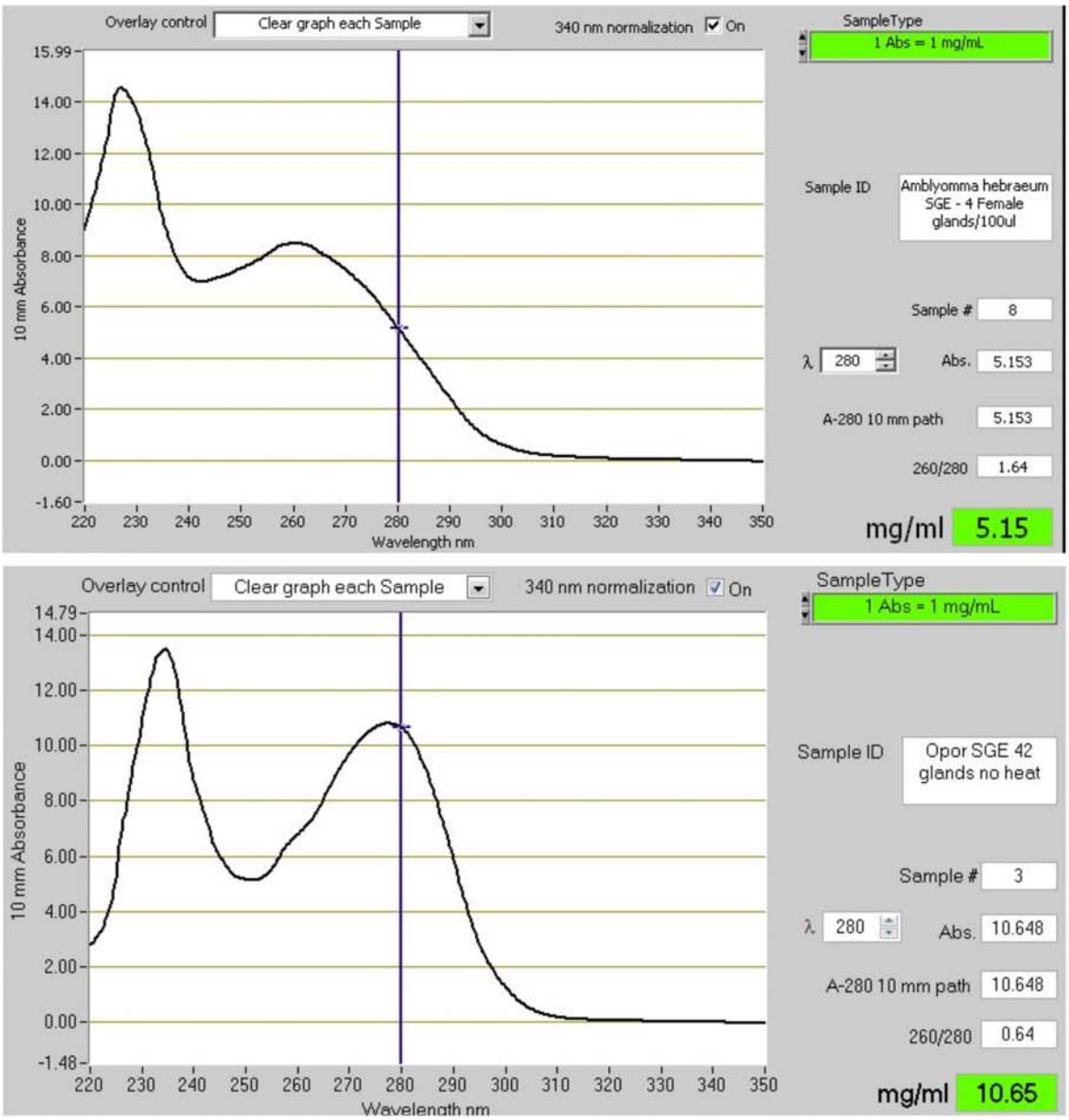

FIGURE 7 | The absorbance spectra of salivary gland extracts (SGE) from hard and soft ticks. The top graph shows the spectrum of SGE of 4 glands from *Amblyomma hebraeum* suspended in 100 μl water. Based on the 280 nm absorbance a single gland would have a soluble protein concentration of ∼128 μg. Bradford determination indicated a concentration closer to ∼60 μg/gland. The bottom graph shows the spectrum of SGE of 42 glands from *Ornithodoros phacochoerus* suspended in 500 μl water. Based on the 280 nm absorbance a single gland would have a soluble protein concentration of ∼127 μg. Bradford determination indicated a concentration of ∼125 μg/gland. These absorbance spectra are representative of hard and soft tick SGE in general.

the same receptor to attain a combined concentration that would allow receptor saturation and inhibition. This may be possible, even if expressed at concentrations well below the equilibrium dissociation constant, since the inhibitory effects may be summed if the inhibitors act in a mutually exclusive manner (1:1 receptor-ligand binding with no synergistic effects) (Chou and Talalay, 1977). A cumulative effect was recently shown for the holocyclotoxins from the paralysis tick, *Ixodes holocyclus*, where at least 19 holocyclotoxin genes were expressed at low levels that showed a cumulative paralysis effect when combined (Rodriguez-Valle et al., 2017). It should be noted that while immune evasion was proposed as reason for the multiplicity of gene family members, low level expression of multiple genes to attain a cumulative threshold concentration that allows effective inhibition may also be possible and may fit with the overall neutral evolution of tick salivary gland proteins previously proposed (Mans et al., 2017). Low-level expression may in this scenario also be a function of the

constitutive differential expression observed in hard ticks, where the extreme high expression levels observed in soft ticks due to accumulation in granules may not be attainable. Even so, it remains to be quantitatively proven that cumulative contributions to attain a threshold concentration occur at the feeding site.

Increasing Concentration at the Feeding Site

The vertebrate host uses localized cues and responses to maintain and regulate haemostasis. As such, wounds or breakdown in system integrity are detected by exposure of localized collagen or other extracellular matrix components, activation of platelets and exposure of procoagulant platelet surfaces, initiation of blood-clotting and the complement cascade on activated platelet surfaces (Delvaeye and Conway, 2009; Deppermann and Kubes, 2016; Wiegner et al., 2016). In a similar manner, targeting of tick-derived bioactive molecules to activated surfaces, whether tick or host surfaces can increase local concentrations and prevent loss or dilution of components via blood meal ingestion or systemic diffusion. Salivary proteins have been found in tick cement where they presumably function as inhibitors of host defenses, or to prevent recognition of cement as a foreign or activation surface for host defenses (Bullard et al., 2016). Proteins such as apyrase have asymmetric charged surfaces (Stutzer et al., 2009), suggesting that these would be attracted to activated negatively charged platelet membranes. Other tick proteins has been shown to interact with membranes or have higher inhibitory activity in the presence of membranes, suggesting that these proteins may be concentrated on activated membrane surfaces at the feeding site (Ehebauer et al., 2002; Schuijt et al., 2013). Some Kunitz-domain inhibitors such as ixolaris have long carboxy-termini rich in serine and threonine residues that can be the site of glycosylation (Francischetti et al., 2002). These would create mucin tails that would be sticky and allow concentration on the walls of the feeding cavity preventing removal and increasing concentration (Francischetti et al., 2009). This may be a general strategy for glycosylated tick proteins (Uhlír et al., 1994).

Increasing Effective Concentration Using Multiple Binding Sites or Multiple Functions

In the case of some tick lipocalins their effective concentration is increased by possessing two independent binding sites for histamine or one for histamine and one for serotonin (Paesen et al., 2000; Sangamnatdej et al., 2002; Mans et al., 2008b). This increase their capacity for scavenging twofold. Another variation on this may be proteins that can potentially target many independent ligands or targets and may therefore have multiple functions. While this certainly expands the potential of proteins to work within a complex redundant environment, the most effective of these would be proteins that have independent function and mechanisms. For example, targeting of complement C5 and LTB_4 allows OMCI and its homologs to inhibit both complement and LTB_4 mediated inflammation at the same time (Nunn et al., 2005; Mans and Ribeiro, 2008b; Roversi et al., 2013). In this case, both functions target the two key non-redundant mediators of neutrophil recruitment during inflammation that seems to be intricately linked (Sadik et al., 2018). This is a remarkable convergence of function in a single protein (Mans et al., 2017). On the other hand, if the functional mechanisms are not independent, i.e., use the same site for ligand binding or the same protein surface to target different proteins, competition between targets will effectively lower the concentration of available inhibitor, thereby impacting its functionality. This may be seen for moubatin and its homologs that bind both LTB_4 and TXA_2 within the same lipocalin cavity at similar affinities (Mans and Ribeiro, 2008b). If both LTB_4 and TXA_2 are present at similar concentrations, the effective scavenging capability may be halved. One way to compensate for this may be multiple proteins or very high concentrations at the feeding site as observed for moubatin, TSGP2 and TSGP3. The same problem would face many of the enzyme inhibitors that can inhibit two or more enzymes from a specific class such as the cystatins, where the presence of many different host enzymes at the feeding site would lead to competition with the tick inhibitors. Similarly, the evasins can bind to many chemokines with similar affinities that may lead to competition of evasins for different chemokines, thereby reducing their effectivity.

Suicide Inhibitors

Inhibitors that bind in a 1:1 manner to their target enzymes, and then serve as substrate, resulting in the formation of a covalent enzyme-inhibitor complex, circumvent the equilibrium dissociation problem completely. Their initial affinities need only to be high enough for the enzyme to catalyze its reaction and form the covalent complex to result in permanent inhibition. In ticks, such inhibitors are found in the serpins that target various enzymes of the clotting cascade (Chmelař et al., 2017). Serpins form covalent complexes with their respective serine proteases after cleavage (Whisstock et al., 2010).

Differential Expression

Ixodid ticks express different proteins at different periods during feeding (McSwain et al., 1982; Paesen et al., 1999; Wang et al., 2001b; Kim et al., 2017; Perner et al., 2018). Possible reasons proposed for this include antigenic variation to escape the immune system (Chmelař et al., 2016b), or responses to changes at the feeding site such as wound healing (Francischetti et al., 2005). Differential expression may also occur as salivary gland morphology changes during the course of feeding and different cell types play different roles in the feeding process (Binnington and Kemp, 1980). As such, differential expression may allow increased concentration spikes of proteins in specific feeding windows.

Minimizing Feeding Site Volume

Comparison of adult, nymphal, and larval concentrations at the feeding site indicates that the relative concentrations remain constant between the various life stages even though salivary gland concentrations may differ several fold (**Figure 3**). This is mostly due to the differences observed in feeding cavity

size that scale relative to the life stage and tick size. If this observation holds for all tick species it would imply that smaller ticks compensate by creating smaller feeding cavities. Feeding cavity size may then be related to protein concentration secreted during feeding.

Smaller Proteins Allow Higher Molar Concentrations

The majority of secretory salivary proteins in ticks have low molecular masses below 25 kDa. This include the majority of highly abundant protein families such as the basic tail secretory, Kunitz-BPTI and lipocalin families (Mans et al., 2008c, 2016; Mans, 2011). Lower molecular masses allow higher relative molar concentrations at the feeding site, which could result in an up to a 10-fold difference between a 5 and 50 kDa protein (**Figure 3**).

FUNCTIONAL RELEVANCE AND MECHANISM

Understanding the mechanism of action (how a given protein works) is important in accessing functional relevance. As example, the case of moubatin may be considered. Originally moubatin was identified as a specific inhibitor of collagen-induced platelet aggregation with an $IC_{50} \sim 50$ nM, that did not affect ADP, arachidonic acid, thrombin, ristocetin, or calcium ionophore A23187 induced platelet aggregation (Waxman and Connolly, 1993). Subsequently, recombinant moubatin was shown to inhibit collagen-induced platelet aggregation with $IC_{50} \sim 100$ nM but did not inhibit adhesion to collagen (Keller et al., 1993). At high concentrations (5.8 μM) of moubatin and low concentrations of ADP (2 μM) 40% inhibition of ADP-induced platelet aggregation was observed, suggesting that the cyclooxygenase pathway may be targeted. It was also shown that moubatin at these high concentrations could inhibit the TXA_2 mimetic U46619 and competed with the TXA_2 receptor antagonist SQ29548 for binding to platelet membranes with $IC_{50} \sim 10$ μM (Keller et al., 1993). The leech inhibitor LAPP did not compete with SQ29548 binding to platelets, indicating that different receptors were targeted. Moubatin also did not inhibit binding of the monoclonal antibody Gi9 that inhibited adhesion to collagen and interacts with integrin $\alpha_2\beta_1$, the proposed receptor for adhesion to collagen. At the time, moubatin did not share sequence homology with any inhibitor of collagen-induced platelet aggregation or with collagen, and did not contain the RGD motif important in integrin recognition. From the complex data above it was suggested that moubatin might be a TXA_2 receptor antagonist (Keller et al., 1993). Subsequently, it was shown that moubatin's mechanism of collagen-induced platelet aggregation is exclusively via scavenging of TXA_2 with $K_D \sim 20$ nM, by gain and loss of function mutations in TSGP2 and TSGP3, respectively, two closely related homologs (Mans and Ribeiro, 2008b). In retrospect, it may be considered that the only inhibitory paradigms at the time were interaction with either collagen or specific platelet receptors and that the kratagonist paradigm as formulated recently did not exist. Interpreting the moubatin results from the previous paradigms may have been logical, even if the high IC_{50} observed for SQ29548 should have raised flags. It may now be suggested that moubatin was scavenging SQ29548 (a TXA_2 mimetic), albeit with low affinity and did not compete for the receptor. Several lines of evidence converged on moubatin as scavenger of TXA_2: the evidence that moubatin belonged to the lipocalin family (Paesen et al., 1999; Mans et al., 2003b); the fact that lipocalins are highly abundant in salivary glands and that abundant proteins generally act as scavengers, i.e., the kratagonist paradigm (Mans et al., 2001, 2003b; Mans and Neitz, 2004a,b; Calvo et al., 2006); the inhibitory effect of moubatin on the TXA_2 mimetic U46619 (Keller et al., 1993), and the observation that a closely related protein, OMCI bound ricinoleic acid, suggesting that moubatin may bind prostaglandins and thromboxanes (Roversi et al., 2007). The gain of function mutation in TSGP2 of R85G and a similar complete loss of function for TSGP3 with the mutation G85R, allowed unambiguous confirmation of functional relevance as TXA_2 scavengers (Mans and Ribeiro, 2008b). It not only highlighted the reductionist paradigm in elucidation of function, but also showed how elucidation of mechanism may inform on which function is considered relevant. As such, moubatin is an inhibitor of collagen-induced platelet aggregation, but perform this function by scavenging the secondary agonist TXA_2. Its mechanism is primarily as kratagonist and not as receptor or ligand neutralizing inhibitor. Once mechanism is clarified the parameters necessary to assess functional significance can be better defined. In this case, that any homolog has to bind TXA_2 in the low nM range, be present at high concentrations and possess the R85G substitution to be functionally relevant.

SYSTEMS BIOLOGY, BIOINFORMATICS AND FUNCTIONAL RELEVANCE

While the majority of functions found in ticks may be assigned functional significance (**Table 1**), enough reports in the literature indicate that caution should be exercised when evaluating functional relevance. This is compounded by advances in technology that allow systems approaches to the analysis of salivary gland protein dynamics and bioinformatics that allows functional analysis *in silico*. As such, recent advances in technology, both in next-generation transcriptome sequencing and proteomics, has allowed an unprecedented view of salivary gland dynamics from a systems perspective (Schwarz et al., 2014; Chmelař et al., 2016a; Mans et al., 2016; Kim et al., 2017). This has indicated how ticks differentially up- or down-regulate proteins during various time intervals in feeding, which suggest that ticks actively respond to the feeding environment, reflecting a fine tuned adaptation to the hosts defense mechanisms. While the systems paradigm clearly show how dynamic expression may be in ticks, inferences regarding function rests on inference by homology or annotation. For example, a recent excellent proteomic study followed the expression profile of *I. scapularis* sampled every 24 h until detachment and indicated differential expression for a large number of lipocalins annotated as histamine-binding proteins (Kim et al., 2017). The discussion

focused on the functionality of lipocalins as histamine scavengers and how the data would support tick responses to host immunity and feeding. Interestingly, a functional study into biogenic amine binding lipocalins that specifically targeted *I. scapularis* lipocalins with biogenic amine binding motifs, failed to find any histamine-binding lipocalins, but only identified serotonin-binding lipocalins with a single binding site (Mans et al., 2008b). While this does not exclude the possibility that histamine-binding lipocalins exist in *Ixodes* ticks, the results thus far do not support it. Similarly, bioinformatic analysis predicted high affinity binding of histamine and serotonin in lipocalins from *Ixodes ricinus*, for which none of the critical residues involved in biogenic amine binding was conserved (Valdés et al., 2016). Molecular docking also recently predicted nM affinities for cystatins from *Ixodes persulcatus* without experimental verification of affinities or target enzymes (Rangel et al., 2017). While such bioinformatic and systems approaches can certainly direct research to proteins of interest, the data should be used with caution to infer functional relevance, especially if the possibility exists that some of these proteins may be only transiently expressed or at concentrations too low for functionality. For systems biology to come of age, we need accurate dissection of the feeding site in real-time to quantify fluxes in protein concentration while performing quality control with validated functions.

IS FUNCTIONAL RELEVANCE RELEVANT?

It may be considered whether it really matters whether a measured function is relevant during feeding, given the emerging recognition that all proteins may be moonlighting to some extent. From this perspective, any function present in tick saliva should be relevant at some level and our goal for the next few decades would be to assign functions to salivary proteins, whether relevant or not. A more comprehensive understanding would later emerge once we have gathered enough data to truly assess relevance. This position is appealing since it buys some time for dubious functions. It is, however, also a philosophical "everything goes" viewpoint (Feyerabend, 1975), that makes distinguishing important from trivial function very difficult. The same issue has been raised with regard to whether all ticks are venomous, or whether only some ticks secrete toxins that may cause the various well recognized forms of tick paralysis and toxicoses (Pienaar et al., 2018). By treating all ticks as venomous, the meaning of toxicity is obscured. Similarly, by treating all functions in saliva as relevant at the feeding site, even if their functional parameters suggest that they would not be relevant, may obscure those central in the feeding process from peripheral functions.

FUNCTIONAL RELEVANCE FROM A PRACTICAL PERSPECTIVE

The use of tick salivary proteins as therapeutic agents within a clinical or pharmaceutical setting remains an important and promising goal (Mans, 2005). From this perspective any function determined for a protein need not be functionally relevant at the tick feeding site, as long as the specific parameters for use has been determined that would allow it to function under clinical or therapeutic controlled conditions. For example, the half-life of OMCI could be improved >50-fold by PASylation, making it more relevant for clinical use (Kuhn et al., 2016). In a similar vein, anti-tick vaccines may be developed against proteins with unknown functions or even irrelevant function, as long as the vaccine shows efficacy, as for example for hidden antigens (Nuttall et al., 2006). On the other hand, development of vaccines against exposed antigens may work better if antigens with real functional significance at the feeding site can be defined, their mechanism of action elucidated and this information used to rationally design target strategies that would neutralize function at the feeding site effectively.

CONCLUSION

Functional relevance is determined by the concentration of tick proteins at the feeding site as well as their affinity for their respective host targets. The current review showed that the majority of proteins found in tick saliva or salivary glands thus far characterized will be functional at the tick feeding site. It was also shown how ticks may circumvent the problems presented by an equilibrium system. Even so, inferring functional relevance without estimating concentration or affinity at the feeding site remains a risky endeavor. Future aims in salivary gland biology should focus on quantification of protein concentration secreted during feeding as well as in the actual feeding site. This should provide more accurate estimates of functional relevance.

AUTHOR CONTRIBUTIONS

BM conceptualized the study and wrote the manuscript.

FUNDING

This work was supported by the Economic Competitive Support Programme (30/01/V010), the National Research Foundation (NRF) Incentive Funding (IFR2011032400016) for Rated Researchers (NRF-Mans), and the National Research Foundation (NRF) Competitive Funding for Rated Researchers (CPRR180101296400). The funding bodies had no role in study design, data collection, analysis and interpretation, decision to publish, or preparation of the manuscript.

ACKNOWLEDGMENTS

Ronel Pienaar is thanked for assistance with the graphic figures in the study. The reviewers are thanked for constructive criticism and additional ideas that improved the study.

REFERENCES

Adams, T. E., and Huntington, J. A. (2006). Thrombin–Cofactor interactions. Structural insights into regulatory mechanisms. *Arterioscler. Thromb. Vasc. Biol.* 26, 1738–1745. doi: 10.1161/01.atv.0000228844.65168.d1

Alenazi, Y., Singh, K., Davies, G., Eaton, J. R. O., Elders, P., Kawamura, A., et al. (2018). Genetically engineered two-warhead evasins provide a method to achieve precision targeting of disease-relevant chemokine subsets. *Sci. Rep.* 8:6333. doi: 10.1038/s41598-018-24568-9

Anastopoulos, P., Thurn, M. J., and Broady, K. W. (1991). Anticoagulant in the tick *Ixodes holocyclus*. *Aust. Vet. J.* 68, 366–367. doi: 10.1111/j.1751-0813.1991.tb00740.x

Andersen, J. F., and Ribeiro, J. M. C. (2017). "Salivary kratagonists: scavengers of host physiological effectors during blood feeding," in *Arthropod Vector: Controller of Disease Transmission*, Vol. 2, eds S. K. Wikel, S. Aksoy, and G. Dimopoulos (Amsterdam: Elsevier), 51–63. doi: 10.1016/b978-0-12-805360-7.00004-6

Anguita, J., Ramamoorthi, N., Hovius, J. W., Das, S., Thomas, V., Persinski, R., et al. (2002). Salp15, an *Ixodes scapularis* salivary protein, inhibits CD4(+) T cell activation. *Immunity* 16, 849–859. doi: 10.1016/s1074-7613(02)00325-4

Anisuzzaman, M., Hatta, T., Miyoshi, T., Matsubayashi, M., Islam, M. K., Alim, M. A., et al. (2014). Longistatin in tick saliva blocks advanced glycation end-product receptor activation. *J. Clin. Invest.* 124, 4429–4444. doi: 10.1172/jci74917

Anisuzzaman, M., Islam, K., Alim, M. A., Miyoshi, T., Hatta, T., Yamaji, K., et al. (2011). Longistatin, a plasminogen activator, is key to the availability of blood-meals for ixodid ticks. *PLoS Pathog.* 7:e1001312. doi: 10.1371/journal.ppat.1001312

Anisuzzaman, M., Islam, K., Alim, M. A., Miyoshi, T., Hatta, T., Yamaji, K., et al. (2012). Longistatin is an unconventional serine protease and induces protective immunity against tick infestation. *Mol. Biochem. Parasitol.* 182, 45–53. doi: 10.1016/j.molbiopara.2011.12.002

Anisuzzaman, M., Islam, K., Miyoshi, T., Alim, M. A., Hatta, T., Yamaji, K., et al. (2010). Longistatin, a novel EF-hand protein from the ixodid tick *Haemaphysalis longicornis*, is required for acquisition of host blood-meals. *Int. J. Parasitol.* 40, 721–729. doi: 10.1016/j.ijpara.2009.11.004

Arcà, B., and Ribeiro, J. M. (2018). Saliva of hematophagous insects: a multifaceted toolkit. *Curr. Opin. Insect Sci.* 29, 102–109. doi: 10.1016/j.cois.2018.07.012

Arolas, J. L., Lorenzo, J., Rovira, A., Castellà, J., Aviles, F. X., and Sommerhoff, C. P. (2005). A carboxypeptidase inhibitor from the tick *Rhipicephalus bursa*: isolation, cDNA cloning, recombinant expression, and characterization. *J. Biol. Chem.* 280, 3441–3448. doi: 10.1074/jbc.m411086200

Arthur, D. R. (1970). Tick feeding and its implications. *Adv. Parasitol.* 8, 275–292. doi: 10.1016/s0065-308x(08)60258-4

Assumpção, T. C., Ma, D., Mizurini, D. M., Kini, R. M., Ribeiro, J. M., Kotsyfakis, M., et al. (2016). In vitro mode of action and anti-thrombotic activity of boophilin, a multifunctional Kunitz protease inhibitor from the midgut of a tick vector of babesiosis, *Rhipicephalus microplus*. *PLoS Negl. Trop. Dis.* 10:e0004298. doi: 10.1371/journal.pntd.0004298

Assumpção, T. C., Mizurini, D. M., Ma, D., Monteiro, R. Q., Ahlstedt, S., Reyes, M., et al. (2018). Ixonnexin from tick saliva promotes fibrinolysis by interacting with plasminogen and tissue-type plasminogen activator, and prevents arterial thrombosis. *Sci. Rep.* 8:4806. doi: 10.1038/s41598-018-22780-1

Bakkes, D. K., De Klerk, D., Latif, A. A., and Mans, B. J. (2018). Integrative taxonomy of Afrotropical *Ornithodoros* (*Ornithodoros*) (Acari: Ixodida: Argasidae). *Ticks Tick Borne Dis.* 9, 1006–1037. doi: 10.1016/j.ttbdis.2018.03.024

Bastiani, M., Hillebrand, S., Horn, F., Kist, T. B., Guimarães, J. A., and Termignoni, C. (2002). Cattle tick *Boophilus microplus* salivary gland contains a thiol-activated metalloendopeptidase displaying kininase activity. *Insect Biochem. Mol. Biol.* 32, 1439–1446. doi: 10.1016/s0965-1748(02)00064-4

Batista, I. F., Ramos, O. H., Ventura, J. S., Junqueira-de-Azevedo, I. L., Ho, P. L., and Chudzinski-Tavassi, A. M. (2010). A new factor Xa inhibitor from *Amblyomma cajennense* with a unique domain composition. *Arch. Biochem. Biophys.* 493, 151–156. doi: 10.1016/j.abb.2009.10.009

Beaufays, J., Adam, B., Menten-Dedoyart, C., Fievez, L., Grosjean, A., Decrem, Y., et al. (2008). Ir-LBP, an *Ixodes ricinus* tick salivary LTB4-binding lipocalin, interferes with host neutrophil function. *PLoS One* 3:e3987. doi: 10.1371/journal.pone.0003987

Binnington, K. C., and Kemp, D. H. (1980). Role of tick salivary glands in feeding and disease transmission. *Adv. Parasitol.* 18, 315–339. doi: 10.1016/s0065-308x(08)60403-0

Bopp, C., Hofer, S., Weitz, J., Bierhaus, A., Nawroth, P. P., Martin, E., et al. (2008). sRAGE is elevated in septic patients and associated with patients outcome. *J. Surg. Res.* 147, 79–83. doi: 10.1016/j.jss.2007.07.014

Brahma, R. K., Blanchet, G., Kaur, S., Kini, R. M., and Doley, R. (2017). Expression and characterization of haemathrins, madanin-like thrombin inhibitors, isolated from the salivary gland of tick *Haemaphysalis bispinosa* (Acari: Ixodidae). *Thromb. Res.* 152, 20–29. doi: 10.1016/j.thromres.2017.01.012

Branco, V. G., Iqbal, A., Alvarez-Flores, M. P., Sciani, J. M., de Andrade, S. A., Iwai, L. K., et al. (2016). Amblyomin-X having a Kunitz-type homologous domain, is a noncompetitive inhibitor of FXa and induces anticoagulation in vitro and in vivo. *Biochim. Biophys. Acta* 1864, 1428–1435. doi: 10.1016/j.bbapap.2016.07.011

Brown, S. J., and Knapp, F. W. (1980a). *Amblyomma americanum*: sequential histological analysis of larval and nymphal feeding sites on guinea pigs. *Exp. Parasitol.* 49, 188–205. doi: 10.1016/0014-4894(80)90116-2

Brown, S. J., and Knapp, F. W. (1980b). *Amblyomma americanum*: sequential histological analysis of adult feeding sites on guinea pigs. *Exp. Parasitol.* 49, 303–318. doi: 10.1016/0014-4894(80)90067-3

Brown, S. J., Worms, M. J., and Askenase, P. W. (1983). *Rhipicephalus appendiculatus*: larval feeding sites in guinea pigs actively sensitized and receiving immune serum. *Exp. Parasitol.* 55, 111–120. doi: 10.1016/0014-4894(83)90004-8

Bullard, R., Allen, P., Chao, C. C., Douglas, J., Das, P., Morgan, S. E., et al. (2016). Structural characterization of tick cement cones collected from in vivo and artificial membrane blood-fed lone star ticks (*Amblyomma americanum*). *Ticks Tick Borne Dis.* 7, 880–892. doi: 10.1016/j.ttbdis.2016.04.006

Butenas, S., and Mann, K. G. (2002). Blood coagulation. *Biochemistry* 67, 3–12.

Calvo, E., Mans, B. J., Andersen, J. F., and Ribeiro, J. M. (2006). Function and evolution of a mosquito salivary protein family. *J. Biol. Chem.* 281, 1935–1942. doi: 10.1074/jbc.m510359200

Cao, J., Shi, L., Zhou, Y., Gao, X., Zhang, H., Gong, H., et al. (2013). Characterization of a new Kunitz-type serine protease inhibitor from the hard tick *Rhipicephalus hemaphysaloides*. *Arch. Insect Biochem. Physiol.* 84, 104–113. doi: 10.1002/arch.21118

Chalaire, K. C., Kim, T. K., Garcia-Rodriguez, H., and Mulenga, A. (2011). *Amblyomma americanum* (L.) (Acari: Ixodidae) tick salivary gland serine protease inhibitor (serpin) 6 is secreted into tick saliva during tick feeding. *J. Exp. Biol.* 214, 665–673. doi: 10.1242/jeb.052076

Chand, K. K., Lee, K. M., Lavidis, N. A., Rodriguez-Valle, M., Ijaz, H., Koehbach, J., et al. (2016). Tick holocyclotoxins trigger host paralysis by presynaptic inhibition. *Sci. Rep.* 6:29446. doi: 10.1038/srep29446

Chmelař, J., Kotál, J., Karim, S., Kopacek, P., Francischetti, I. M. B., Pedra, J. H. F., et al. (2016a). Sialomes and mialomes: a systems-biology view of tick tissues and tick-host interactions. *Trends Parasitol.* 32, 242–254. doi: 10.1016/j.pt.2015.10.002

Chmelař, J., Kotál, J., Kopecký, J., Pedra, J. H., and Kotsyfakis, M. (2016b). All for one and one for all on the tick-host battlefield. *Trends Parasitol.* 32, 368–377. doi: 10.1016/j.pt.2016.01.004

Chmelař, J., Kotál, J., Langhansová, H., and Kotsyfakis, M. (2017). Protease inhibitors in tick saliva: the role of serpins and cystatins in tick-host-pathogen interaction. *Front. Cell. Infect. Microbiol.* 7:216. doi: 10.3389/fcimb.2017.00216

Chmelař, J., Oliveira, C. J., Rezacova, P., Francischetti, I. M., Kovarova, Z., Pejler, G., et al. (2011). A tick salivary protein targets cathepsin G and chymase and inhibits host inflammation and platelet aggregation. *Blood* 117, 736–744. doi: 10.1182/blood-2010-06-293241

Chou, T.-C., and Talalay, P. (1977). A simple generalized equation for the analysis of multiple inhibition of Michaelis-Mentin kinetics systems. *J. Biol. Chem.* 252, 6438–6442.

Ciprandi, A., de Oliveira, S. K., Masuda, A., Horn, F., and Termignoni, C. (2006). *Boophilus microplus*: its saliva contains microphilin, a small thrombin inhibitor. *Exp. Parasitol.* 114, 40–46. doi: 10.1016/j.exppara.2006.02.010

Coller, B. S., Beer, J. H., Scudder, L. E., and Steinberg, M. H. (1989). Collagen-platelet interactions: evidence for a direct interaction of collagen with platelet GPIa/IIa and an indirect interaction with platelet GPIIb/IIIa mediated by adhesive proteins. *Blood* 74, 182–192.

Copley, S. D. (2015). An evolutionary biochemist's perspective on promiscuity. *Trends Biochem. Sci.* 40, 72–78. doi: 10.1016/j.tibs.2014.12.004

Copley, S. D. (2017). Shining a light on enzyme promiscuity. *Curr. Opin. Struct. Biol.* 47, 167–175. doi: 10.1016/j.sbi.2017.11.001

Cornwall, J. W., and Patton, W. S. (1914). Some observations on the salivary secretion of the commoner blood-sucking insects and ticks. *Indian J. Med. Res.* 2, 569–593.

Couvreur, B., Beaufays, J., Charon, C., Lahaye, K., Gensale, F., Denis, V., et al. (2008). Variability and action mechanism of a family of anticomplement proteins in *Ixodes ricinus*. *PLoS One* 3:e1400. doi: 10.1371/journal.pone.0001400

Daix, V., Schroeder, H., Praet, N., Georgin, J. P., Chiappino, I., Gillet, L., et al. (2007). *Ixodes* ticks belonging to the *Ixodes ricinus* complex encode a family of anticomplement proteins. *Insect Mol. Biol.* 16, 155–166. doi: 10.1111/j.1365-2583.2006.00710.x

Davis, T. L., and Sharif, N. A. (2000). Pharmacological characterization of [3H]-prostaglandin E2 binding to the cloned human EP4 prostanoid receptor. *Br. J. Pharmacol.* 130, 1919–1926. doi: 10.1038/sj.bjp.0703525

de Castro, M. H., de Klerk, D., Pienaar, R., Latif, A. A., Rees, D. J., and Mans, B. J. (2016). De novo assembly and annotation of the salivary gland transcriptome of *Rhipicephalus appendiculatus* male and female ticks during blood feeding. *Ticks and Tick-borne Dis.* 7, 536–548. doi: 10.1016/j.ttbdis.2016.01.014

de Castro, M. H., de Klerk, D., Pienaar, R., Rees, D. J. G. R., and Mans, B. J. (2017). Sialotranscriptomics of *Rhipicephalus zambeziensis* reveal intricate expression profiles of secretory proteins and suggest tight temporal transcriptional regulation during blood feeding. *Parasit. Vectors* 10:384.

de Meillon, B. (1942). A toxin from the eggs of South African ticks. *S. Afr. J. Med. Sci.* 7, 226–235.

Decrem, Y., Rath, G., Blasioli, V., Cauchie, P., Robert, S., Beaufays, J., et al. (2009). Ir-CPI, a coagulation contact phase inhibitor from the tick *Ixodes ricinus*, inhibits thrombus formation without impairing hemostasis. *J. Exp. Med.* 206, 2381–2395. doi: 10.1084/jem.20091007

Delvaeye, M., and Conway, E. M. (2009). Coagulation and innate immune responses: can we view them separately? *Blood* 114, 2367–2374. doi: 10.1182/blood-2009-05-199208

Deppermann, C., and Kubes, P. (2016). Platelets and infection. *Semin. Immunol.* 28, 536–545. doi: 10.1016/j.smim.2016.10.005

Déruaz, M., Bonvin, P., Severin, I. C., Johnson, Z., Krohn, S., Power, C. A., et al. (2013). Evasin-4, a tick-derived chemokine-binding protein with broad selectivity can be modified for use in preclinical disease models. *FEBS J.* 280, 4876–4887. doi: 10.1111/febs.12463

Déruaz, M., Frauenschuh, A., Alessandri, A. L., Dias, J. M., Coelho, F. M., Russo, R. C., et al. (2008). Ticks produce highly selective chemokine binding proteins with antiinflammatory activity. *J. Exp. Med.* 205, 2019–2031. doi: 10.1084/jem.20072689

Dharampaul, S., Kaufman, W. R., and Belosevic, M. (1993). Differential recognition of saliva antigens from the ixodid tick *Amblyomma hebraeum* (Acari: Ixodidae) by sera from infested and immunized rabbits. *J. Med. Entomol.* 30, 262–266. doi: 10.1093/jmedent/30.1.262

Díaz-Martín, V., Manzano-Román, R., Oleaga, A., Encinas-Grandes, A., and Pérez-Sánchez, R. (2013a). Cloning and characterization of a plasminogen-binding enolase from the saliva of the argasid tick *Ornithodoros moubata*. *Vet. Parasitol.* 191, 301–314. doi: 10.1016/j.vetpar.2012.09.019

Díaz-Martín, V., Manzano-Román, R., Valero, L., Oleaga, A., Encinas-Grandes, A., and Pérez-Sánchez, R. (2013b). An insight into the proteome of the saliva of the argasid tick *Ornithodoros moubata* reveals important differences in saliva protein composition between the sexes. *J. Proteomics* 80, 216–235. doi: 10.1016/j.jprot.2013.01.015

Dickinson, R. G., O'Hagan, J. E., Schotz, M., Binnington, K. C., and Hegarty, M. P. (1976). Prostaglandin in the saliva of the cattle tick *Boophilus microplus*. *Aust. J. Exp. Biol. Med. Sci.* 54, 475–486.

Dorn, G. W. II, and DeJesus, A. (1991). Human platelet aggregation and shape change are coupled to separate thromboxane A2-prostaglandin H2 receptors. *Am. J. Physiol.* 260, H327–H334.

Drazen, J. M., Austen, K. F., Lewis, R. A., Clark, D. A., Goto, G., Marfat, A., et al. (1980). Comparative airway and vascular activities of leukotrienes C-1 and D *in vivo* and *in vitro*. *Proc. Natl. Acad. Sci. U.S.A.* 77, 4354–4358.

Eaton, J. R. O., Alenazi, Y., Singh, K., Davies, G., Geis-Asteggiante, L., Kessler, B., et al. (2018). The N-terminal domain of a tick evasin is critical for chemokine binding and neutralization and confers specific binding activity to other evasins. *J. Biol. Chem.* 293, 6134–6146. doi: 10.1074/jbc.RA117.000487

Ehebauer, M. T., Mans, B. J., Gaspar, A. R., and Neitz, A. W. (2002). Identification of extrinsic blood coagulation pathway inhibitors from the tick *Ornithodoros savignyi* (Acari: Argasidae). *Exp. Parasitol.* 101, 138–148. doi: 10.1016/s0014-4894(02)00102-9

Elgin, M. (2010). "Reductionism in biology: an example of biochemistry," in *The Present Situation in the Philosophy of Science. The Philosophy of Science in a European Perspective*, Vol. 1, ed. F. Stadler (Dortrecht: Spinger).

Faas, M. M., Sáez, T., and de Vos, P. (2017). Extracellular ATP and adenosine: the Yin and Yang in immune responses? *Mol. Aspects. Med.* 55, 9–19. doi: 10.1016/j.mam.2017.01.002

Ferrer-Lopez, P., Renesto, P., Schattner, M., Bassot, S., Laurent, P., and Chignard, M. (1990). Activation of human platelets by C5a-stimulated neutrophils: a role for cathepsin G. *Am. J. Physiol.* 258, C1100–C1107.

Feyerabend, P. (1975). *Against Method: Outline of an Anarchistic Theory of Knowledge*. Brooklyn, NY: Verso Books, 339.

Figueiredo, A. C., de Sanctis, D., and Pereira, P. J. (2013). The tick-derived anticoagulant madanin is processed by thrombin and factor Xa. *PLoS One* 8:e71866. doi: 10.1371/journal.pone.0071866

Flower, D. R. (1996). The lipocalin protein family: structure and function. *Biochem. J.* 318, 1–14. doi: 10.1042/bj3180001

Francischetti, I. M., Mans, B. J., Meng, Z., Gudderra, N., Veenstra, T. D., Pham, V. M., et al. (2008). An insight into the sialome of the soft tick, *Ornithodorus parkeri*. *Insect Biochem. Mol. Biol.* 38, 1–21. doi: 10.1016/j.ibmb.2007.09.009

Francischetti, I. M., Mather, T. N., and Ribeiro, J. M. (2003). Cloning of a salivary gland metalloprotease and characterization of gelatinase and fibrin(ogen)lytic activities in the saliva of the Lyme disease tick vector *Ixodes scapularis*. *Biochem. Biophys. Res. Commun.* 305, 869–875. doi: 10.1016/s0006-291x(03)00857-x

Francischetti, I. M., Mather, T. N., and Ribeiro, J. M. (2004). Penthalaris, a novel recombinant five-Kunitz tissue factor pathway inhibitor (TFPI) from the salivary gland of the tick vector of Lyme disease, *Ixodes scapularis*. *Thromb. Haemost.* 91, 886–898. doi: 10.1160/th03-11-0715

Francischetti, I. M., Mather, T. N., and Ribeiro, J. M. (2005). Tick saliva is a potent inhibitor of endothelial cell proliferation and angiogenesis. *Thromb. Haemost.* 94, 167–174. doi: 10.1160/th04-09-0566

Francischetti, I. M., Sa-Nunes, A., Mans, B. J., Santos, I. M., and Ribeiro, J. M. (2009). The role of saliva in tick feeding. *Front. Biosci.* 14:2051–2088.

Francischetti, I. M., Valenzuela, J. G., Andersen, J. F., Mather, T. N., and Ribeiro, J. M. (2002). Ixolaris, a novel recombinant tissue factor pathway inhibitor (TFPI) from the salivary gland of the tick, *Ixodes scapularis*: identification of factor X and factor Xa as scaffolds for the inhibition of factor VIIa/tissue factor complex. *Blood* 99, 3602–3612. doi: 10.1182/blood-2001-12-0237

Frauenschuh, A., Power, C. A., Déruaz, M., Ferreira, B. R., Silva, J. S., Teixeira, M. M., et al. (2007). Molecular cloning and characterization of a highly selective chemokine-binding protein from the tick *Rhipicephalus sanguineus*. *J. Biol. Chem.* 282, 27250–27258. doi: 10.1074/jbc.m704706200

Frojmovic, M. M., Mooney, R. F., and Wong, T. (1994). Dynamics of platelet glycoprotein IIb-IIIa receptor expression and fibrinogen binding. I. Quantal activation of platelet subpopulations varies with adenosine diphosphate concentration. *Biophys. J.* 67, 2060–2068. doi: 10.1016/s0006-3495(94)80689-7

Garg, R., Juncadella, I. J., Ramamoorthi, N., Ashish Ananthanarayanan, S. K., Thomas, V., Rincón, M., et al. (2006). Cutting edge: CD4 is the receptor for the tick saliva immunosuppressor, Salp15. *J. Immunol.* 177, 6579–6583. doi: 10.4049/jimmunol.177.10.6579

Gaspar, A. R., Crause, J. C., and Neitz, A. W. (1995). Identification of anticoagulant activities in the salivary glands of the soft tick, *Ornithodoros savignyi*. *Exp. Appl. Acarol.* 19, 117–127. doi: 10.1007/bf00052551

Gaspar, A. R., Joubert, A. M., Crause, J. C., and Neitz, A. W. (1996). Isolation and characterization of an anticoagulant from the salivary glands of the tick, *Ornithodoros savignyi* (Acari: Argasidae). *Exp. Appl. Acarol.* 20, 583–598. doi: 10.1007/bf00052809

Ghiglieri-Bertez, C., Cristol, J. P., and Bonne, C. (1986). High-affinity binding site for leukotriene C4 in human erythrocytes. *Biochim. Biophys. Acta* 879, 97–102. doi: 10.1016/0005-2760(86)90271-7

Giles, T. C., and Emes, R. D. (2017). Inferring function from homology. *Meth. Mol. Biol.* 1526, 23–40. doi: 10.1007/978-1-4939-6613-4_2

Gong, H., Zhou, J., Liao, M., Hatta, T., Harnnoi, T., Umemiya, R., et al. (2007). Characterization of a carboxypeptidase inhibitor from the tick *Haemaphysalis longicornis*. *J. Insect Physiol.* 53, 1079–1087. doi: 10.1016/j.jinsphys.2007.06.008

Gregson, J. D. (1973). *Tick Paralysis: An Appraisal of Natural and Experimental Data*. Ottawa, ON: Information Division, Canada Department of Agriculture. doi: 10.1016/j.jinsphys.2007.06.008

Grunclová, L., Horn, M., Vancová, M., Sojka, D., Franta, Z., Mares, M., et al. (2006). Two secreted cystatins of the soft tick *Ornithodoros moubata*: differential expression pattern and inhibitory specificity. *Biol Chem.* 387, 1635–1644.

Hackenberg, M., and Kotsyfakis, M. (2018). Exosome-mediated pathogen transmission by arthropod vectors. *Trends Parasitol.* 34, 549–552. doi: 10.1016/j.pt.2018.04.001

Hackenberg, M., Langenberger, D., Schwarz, A., Erhart, J., and Kotsyfakis, M. (2017). *In silico* target network analysis of *de novo*-discovered, tick saliva-specific microRNAs reveals important combinatorial effects in their interference with vertebrate host physiology. *RNA* 23, 1259–1269. doi: 10.1261/rna.061168.117

Hamberg, M., Svensson, J., and Samuelsson, B. (1975). Thromboxanes: a new group of biologically active compounds derived from prostaglandin endoperoxides. *Proc. Natl. Acad. Sci. U.S.A.* 72, 2994–2998. doi: 10.1073/pnas.72.8.2994

Haycraft, J. B. (1884). Ueber die Einwirkung eines Sekretes des officinellen Blutegels auf die Gerinnbarkeit des Blutes. *Arch. für exp. Pathol. u. Pharmakol.* 18:209. doi: 10.1007/bf01833843

Hayward, J., Sanchez, J., Perry, A., Huang, C., Rodriguez Valle, M., Canals, M., et al. (2018). Ticks from diverse genera encode chemokine-inhibitory evasin proteins. *J. Biol. Chem.* 292, 15670–15680. doi: 10.1074/jbc.m117.807255

Heller, C. (1858). Zur anatomie von *Argas persicus*. *Sitzungberichte d. Kaiserl. Akad. Wien* 30, 297–326.

Hepburn, N. J., Williams, A. S., Nunn, M. A., Chamberlain-Banoub, J. C., Hamer, J., Morgan, B. P., et al. (2007). In vivo characterization and therapeutic efficacy of a C5-specific inhibitor from the soft tick *Ornithodoros moubata*. *J. Biol. Chem.* 282, 8292–8299. doi: 10.1074/jbc.m609858200

Hoeppli, R., and Feng, L. C. (1933). Experimental studies on ticks. *Chin. Med. J.* 47, 29–43.

Hoffmann, A., Walsmann, P., Riesener, G., Paintz, M., and Markwardt, F. (1991). Isolation and characterization of a thrombin inhibitor from the tick *Ixodes ricinus*. *Pharmazie* 46, 209–212.

Horn, F., dos Santos, P. C., and Termignoni, C. (2000). *Boophilus microplus* anticoagulant protein: an antithrombin inhibitor isolated from the cattle tick saliva. *Arch. Biochem. Biophys.* 384, 68–73. doi: 10.1006/abbi.2000.2076

Hovius, J. W., de Jong, M. A., den Dunnen, J., Litjens, M., Fikrig, E., van der Poll, T., et al. (2008). Salp15 binding to DC-SIGN inhibits cytokine expression by impairing both nucleosome remodeling and mRNA stabilization. *PLoS Pathog.* 4:e31. doi: 10.1371/journal.ppat.0040031

Howell, C. J. (1966). Collection of salivary gland secretion from the argasid *Ornithodoros savignyi* (Audouin) (1827) by the use of a pharmacological stimulant. *J. S. Afr. Vet. Med. Assoc.* 37, 236–239.

Howell, C. J., Neitz, A. W. H., and Potgieter, D. J. J. (1975). Some toxic and chemical properties of the oral secretion of the sand tampan, *Ornithodoros savignyi* (Audouin) (1827). *Onderstepoort J. Vet. Res.* 43, 99–102.

Hu, G., Drescher, K. M., and Chen, X. M. (2012). Exosomal miRNAs: biological properties and therapeutic potential. *Front. Genet.* 3:56. doi: 10.3389/fgene.2012.00056

Ibelli, A. M., Kim, T. K., Hill, C. C., Lewis, L. A., Bakshi, M., Miller, S., et al. (2014). A blood meal-induced *Ixodes scapularis* tick saliva serpin inhibits trypsin and thrombin, and interferes with platelet aggregation and blood clotting. *Int. J. Parasitol.* 44, 369–379. doi: 10.1016/j.ijpara.2014.01.010

Ibrahim, M. A., Ghazy, A. H., Maharem, T. M., and Khalil, M. I. (2001a). Factor Xa (FXa) inhibitor from the nymphs of the camel tick *Hyalomma dromedarii*. *Comp. Biochem. Physiol. B Biochem. Mol. Biol.* 130, 501–512. doi: 10.1016/s1096-4959(01)00459-6

Ibrahim, M. A., Ghazy, A. H., Maharem, T., and Khalil, M. (2001b). Isolation and properties of two forms of thrombin inhibitor from the nymphs of the camel tick *Hyalomma dromedarii* (Acari: Ixodidae). *Exp. Appl. Acarol.* 25, 675–698.

Ibrahim, M. A., and Masoud, H. M. M. (2018). Thrombin inhibitor from the salivary gland of the camel tick *Hyalomma dromedarii*. *Exp. Appl. Acarol.* 74, 85–97. doi: 10.1007/s10493-017-0196-9

Imamura, S., da Silva Vaz Junior, I., Sugino, M., Ohashi, K., and Onuma, M. (2005). A serine protease inhibitor (serpin) from *Haemaphysalis longicornis* as an anti-tick vaccine. *Vaccine* 23, 1301–1311. doi: 10.1016/j.vaccine.2004.08.041

Inokuma, H., Kemp, D. H., and Willadsen, P. (1994). Comparison of prostaglandin E2 (PGE2) in salivary gland of *Boophilus microplus*, *Haemaphysalis longicornis* and *Ixodes holocyclus*, and quantification of PGE2 in saliva, hemolymph, ovary and gut of *B. microplus*. *J. Vet. Med. Sci.* 56, 1217–1218. doi: 10.1292/jvms.56.1217

Iqbal, A., Goldfeder, M. B., Marques-Porto, R., Asif, H., Souza, J. G., Faria, F., et al. (2017). Revisiting antithrombotic therapeutics; sculptin, a novel specific, competitive, reversible, scissile and tight binding inhibitor of thrombin. *Sci. Rep.* 7:1431. doi: 10.1038/s41598-017-01486-w

Iwanaga, S., Isawa, H., and Yuda, M. (2014). Horizontal gene transfer of a vertebrate vasodilatory hormone into ticks. *Nature Comm.* 5:3373. doi: 10.1038/ncomms4373

Iwanaga, S., Okada, M., Isawa, H., Morita, A., Yuda, M., and Chinzei, Y. (2003). Identification and characterization of novel salivary thrombin inhibitors from the ixodidae tick, *Haemaphysalis longicornis*. *Eur. J. Biochem.* 270, 1926–1934. doi: 10.1046/j.1432-1033.2003.03560.x

Iyer, J. K., Koh, C. Y., Kazimirova, M., Roller, L., Jobichen, C., Swaminathan, K., et al. (2017). Avathrin: a novel thrombin inhibitor derived from a multicopy precursor in the salivary glands of the ixodid tick, *Amblyomma variegatum*. *FASEB J.* 31, 2981–2995. doi: 10.1096/fj.201601216R

Jablonka, W., Kotsyfakis, M., Mizurini, D. M., Monteiro, R. Q., Lukszo, J., Drake, S. K., et al. (2015). Identification and mechanistic analysis of a novel tick-derived inhibitor of Thrombin. *PLoS One* 10:e0133991. doi: 10.1371/journal.pone.0133991

Jore, M. M., Johnson, S., Sheppard, D., Barber, N. M., Li, Y. I., Nunn, M. A., et al. (2016). Structural basis for therapeutic inhibition of complement C5. *Nat. Struct. Mol. Biol.* 23, 378–386. doi: 10.1038/nsmb.3196

Jung, S. M., and Moroi, M. (1998). Platelets interact with soluble and insoluble collagens through characteristically different reactions. *J. Biol. Chem.* 273, 14827–14837. doi: 10.1074/jbc.273.24.14827

Karczewski, J., Endris, R., and Connolly, T. M. (1994). Disagregin is a fibrinogen receptor antagonist lacking the Arg-Gly-Asp sequence from the tick, *Ornithodoros moubata*. *J. Biol. Chem.* 269, 6702–6708.

Karczewski, J., Waxman, L., Endris, R. G., and Connolly, T. M. (1995). An inhibitor from the argasid tick *Ornithodoros moubata* of cell adhesion to collagen. *Biochem. Biophys. Res. Commun.* 208, 532–541. doi: 10.1006/bbrc.1995.1371

Kato, N., Iwanaga, S., Okayama, T., Isawa, H., Yuda, M., and Chinzei, Y. (2005). Identification and characterization of the plasma kallikrein-kinin system inhibitor, haemaphysalin, from hard tick, *Haemaphysalis longicornis*. *Thromb. Haemost.* 93, 359–367. doi: 10.1160/th04-05-0319

Kazimírová, M., Jancinová, V., Petríková, M., Takác, P., Labuda, M., and Nosál, R. (2002). An inhibitor of thrombin-stimulated blood platelet aggregation from the salivary glands of the hard tick *Amblyomma variegatum* (Acari: Ixodidae). *Exp. Appl. Acarol.* 28, 97–105. doi: 10.1007/978-94-017-3526-1_7

Keller, P. M., Waxman, L., Arnold, B. A., Schultz, L. D., Condra, C., and Connolly, T. M. (1993). Cloning of the cDNA and expression of moubatin, an inhibitor of platelet aggregation. *J. Biol. Chem.* 268, 5450–5456.

Kemp, D. H., Stone, B. F., and Binnington, K. C. (1982). "Tick attachment and feeding: role of the mouthparts, feeding apparatus, salivary gland secretions and the host response," in *Physiology of Ticks*, eds F. D. Obenchain and R. Galun (Oxford: Pergamon Press).

Kim, T. K., Tirloni, L., Pinto, A. F., Moresco, J., Yates, J. R. III, da Silva Vaz, I. Jr., et al. (2017). *Ixodes scapularis* tick saliva proteins sequentially secreted every 24 h during blood feeding. *PLoS Negl. Trop. Dis.* 10:e0004323. doi: 10.1371/journal.pntd.0004323

Kim, T. K., Tirloni, L., Radulovic, Z., Lewis, L., Bakshi, M., Hill, C., et al. (2015). Conserved *Amblyomma americanum* tick serpin19, an inhibitor of blood clotting factors Xa and XIa, trypsin and plasmin, has anti-haemostatic functions. *Int. J. Parasitol.* 45, 613–627. doi: 10.1016/j.ijpara.2015.03.009

Kiszewski, A. E., Matuschka, F. R., and Spielman, A. (2001). Mating strategies and spermiogenesis in ixodid ticks. *Annu. Rev. Entomol.* 46, 167–182.

Koh, C. Y., Kazimirova, M., Trimnell, A., Takac, P., Labuda, M., Nuttall, P. A., et al. (2007). Variegin, a novel fast and tight binding thrombin inhibitor from the tropical bont tick. *J. Biol. Chem.* 282, 29101–29113. doi: 10.1074/jbc.m705600200

Kotál, J., Stergiou, N., Buša, M., Chlastáková, A., Beránková, Z., Řezáčová, P., et al. (2019). The structure and function of Iristatin, a novel immunosuppressive tick salivary cystatin. *Cell Mol. Life Sci.*

Kotsyfakis, M., Karim, S., Andersen, J. F., Mather, T. N., and Ribeiro, J. M. (2007). Selective cysteine protease inhibition contributes to blood-feeding success of the tick *Ixodes scapularis*. *J. Biol. Chem.* 282, 29256–29263. doi: 10.1074/jbc.m703143200

Kotsyfakis, M., Sá-Nunes, A., Francischetti, I. M., Mather, T. N., Andersen, J. F., and Ribeiro, J. M. (2006). Antiinflammatory and immunosuppressive activity of sialostatin L, a salivary cystatin from the tick *Ixodes scapularis*. *J. Biol. Chem.* 281, 26298–26307. doi: 10.1074/jbc.m513010200

Krilis, S., Lewis, R. A., Corey, E. J., and Austen, K. F. (1983). Specific receptors for leukotriene C4 on a smooth muscle cell line. *J. Clin. Invest.* 72, 1516–1519. doi: 10.1172/jci111109

Kröber, T., and Geurin, P. M. (2007). In vitro feeding assays for hard ticks. *Trends Parasitol.* 23, 445–449. doi: 10.1016/j.pt.2007.07.010

Kuhn, N., Schmidt, C. Q., Schlapschy, M., and Skerra, A. (2016). PASylated Coversin, a C5-specific complement inhibitor with extended pharmacokinetics, shows enhanced anti-hemolytic activity *in vitro*. *Bioconjug. Chem.* 27, 2359–2371. doi: 10.1021/acs.bioconjchem.6b00369

Kuriyan, J., Konforti, B., and Wemmer, D. (2013). *The Molecules of Life: Physical and Chemical Principles*. Routledge: Garland Science, Taylor & Francis Group, 1008.

Law, J. H., Ribeiro, J. M. C., and Wells, M. A. (1992). Biochemical insights derived from insect diversity. *Ann. Rev. Biochem.* 64, 87–111. doi: 10.1146/annurev.biochem.61.1.87

Leboulle, G., Crippa, M., Decrem, Y., Mejri, N., Brossard, M., Bollen, A., et al. (2002). Characterization of a novel salivary immunosuppressive protein from *Ixodes ricinus* ticks. *J. Biol. Chem.* 277, 10083–10089.

Lewis, R. A., Mencia-Huerta, J. M., Soberman, R. J., Hoover, D., Marfat, A., Corey, E. J., et al. (1982). Radioimmunoassay for leukotriene B4. *Proc. Natl. Acad. Sci. U.S.A.* 79, 7904–7908.

Leydig, F. (1855). Zum feineren Bau der Arthropoden. *Müller's Archiv. f. Anat. Physiol. u. wiss. Med.* 1855, 376–480.

Limo, M. K., Voigt, W. P., Tumbo-Oeri, A. G., Njogu, R. M., and ole-MoiYoi, O. K. (1991). Purification and characterization of an anticoagulant from the salivary glands of the ixodid tick *Rhipicephalus appendiculatus*. *Exp. Parasitol.* 72, 418–429. doi: 10.1016/0014-4894(91)90088-e

Liu, Y. H., Xu, C. H., Liu, Z. G., Liang, J. G., and Lai, R. (2005). Isolation and purification of an inhibitor on platelet aggregation from *Ixodes sinensis*. *Zhongguo Ji Sheng Chong Xue Yu Ji Sheng Chong Bing Za Zhi* 23, 424–427.

Macedo-Ribeiro, S., Almeida, C., Calisto, B. M., Friedrich, T., Mentele, R., Stürzebecher, J., et al. (2008). Isolation, cloning and structural characterisation of boophilin, a multifunctional Kunitz-type proteinase inhibitor from the cattle tick. *PLoS One* 3:e1624. doi: 10.1371/journal.pone.0001624

MacGlashan, D. Jr. (2003). Histamine: a mediator of inflammation. *J. Allergy Clin. Immunol.* 112, S53–S59.

MacGregor, I. R., and Prowse, C. V. (1983). Tissue plasminogen activator in human plasma measured by radioimmunoassay. *Thromb. Res.* 31, 461–474. doi: 10.1016/0049-3848(83)90410-3

Macpherson, A., Liu, X., Dedi, N., Kennedy, J., Carrington, B., Durrant, O., et al. (2018). The rational design of affinity-attenuated OmCI for the purification of complement C5. *J. Biol. Chem.* 293, 14112–14121. doi: 10.1074/jbc.RA118.004043

Mans, B. J. (1997). *Biochemical Properties of a Platelet Aggregation Inhibitor of the tick, Ornithodoros savignyi*. . doi: 10.1074/jbc.ra118.004043

Mans, B. J. (2005). Tick histamine-binding proteins and related lipocalins: potential as therapeutic agents. *Curr. Opin. Investig. Drugs* 6, 1131–1135.

Mans, B. J. (2011). Evolution of vertebrate hemostatic and inflammatory control mechanisms in blood-feeding arthropods. *J. Innate Immun.* 3, 41–51. doi: 10.1159/000321599

Mans, B. J. (2016). "Glandular matrices and secretions: blood- feeding arthropods," in *Extracellular Composite Matrices in Arthropods*, eds E. Cohen and B. Moussian (Switzerland: Springer), 625–688. doi: 10.1007/978-3-319-40740-1_17

Mans, B. J., Andersen, J. F., Schwan, T. G., and Ribeiro, J. M. (2008a). Characterization of anti-hemostatic factors in the argasid, *Argas monolakensis*: implications for the evolution of blood-feeding in the soft tick family. *Insect Biochem. Mol. Biol.* 38, 22–41. doi: 10.1016/j.ibmb.2007.09.002

Mans, B. J., Ribeiro, J. M., and Andersen, J. F. (2008b). Structure, function, and evolution of biogenic amine-binding proteins in soft ticks. *J. Biol. Chem.* 283, 18721–18733. doi: 10.1074/jbc.M800188200

Mans, B. J., Andersen, J. F., Francischetti, I. M., Valenzuela, J. G., Schwan, T. G., Pham, V. M., et al. (2008c). Comparative sialomics between hard and soft ticks: implications for the evolution of blood-feeding behavior. *Insect Biochem. Mol. Biol.* 38, 42–58. doi: 10.1016/j.ibmb.2007.09.003

Mans, B. J., Coetzee, J., Louw, A. I., Gaspar, A. R., and Neitz, A. W. (2000). Disaggregation of aggregated platelets by apyrase from the tick, *Ornithodoros savignyi* (Acari: Argasidae). *Exp. Appl. Acarol.* 24, 271–282.

Mans, B. J., de Castro, M. H., Pienaar, R., de Klerk, D., Gaven, P., Genu, S., et al. (2016). Ancestral reconstruction of tick lineages. *Ticks Tick Borne Dis.* 7, 509–535. doi: 10.1016/j.ttbdis.2016.02.002

Mans, B. J., Featherston, J., de Castro, M. H., and Pienaar, R. (2017). Gene duplication and protein evolution in tick-host interactions. *Front. Cell Infect. Microbiol.* 7:413. doi: 10.3389/fcimb.2017.00413

Mans, B. J., Gaspar, A. R., Louw, A. I., and Neitz, A. W. (1998a). Apyrase activity and platelet aggregation inhibitors in the tick *Ornithodoros savignyi* (Acari: Argasidae). *Exp. Appl. Acarol.* 22, 353–366.

Mans, B. J., Gasper, A. R., Louw, A. I., and Neitz, A. W. (1998b). Purification and characterization of apyrase from the tick, *Ornithodoros savignyi*. *Comp. Biochem. Physiol. B Biochem. Mol. Biol.* 120, 617–624. doi: 10.1016/s0305-0491(98)10061-5

Mans, B. J., Venter, J. D., Vrey, P. J., Louw, A. I., and Neitz, A. W. (2001). Identification of putative proteins involved in granule biogenesis of tick salivary glands. *Electrophoresis* 22, 1739–1746. doi: 10.1002/1522-2683(200105)22%3A9%3C1739%3A%3Aaid-elps1739%3E3.0.co%3B2-7

Mans, B. J., Louw, A. I., and Neitz, A. W. (2002a). Disaggregation of aggregated platelets by savignygrin, a αIIbβ3 antagonist from *Ornithodoros savignyi*. *Exp. Appl. Acarol.* 27, 231–239.

Mans, B. J., Louw, A. I., and Neitz, A. W. (2002b). Savignygrin, a platelet aggregation inhibitor from the soft tick *Ornithodoros savignyi*, presents the RGD integrin recognition motif on the Kunitz-BPTI fold. *J. Biol. Chem.* 277, 21371–22378.

Mans, B. J., Louw, A. I., and Neitz, A. W. (2003a). The influence of tick behavior, biotope and host specificity on concerted evolution of the platelet aggregation inhibitor savignygrin, from the soft tick *Ornithodoros savignyi*. *Insect Biochem. Mol. Biol.* 33, 623–629. doi: 10.1016/s0965-1748(03)00047-x

Mans, B. J., Louw, A. I., and Neitz, A. W. (2003b). The major tick salivary gland proteins and toxins from the soft tick, *Ornithodoros savignyi*, are part of the tick Lipocalin family: implications for the origins of tick toxicoses. *Mol. Biol. Evol.* 20, 1158–1167. doi: 10.1093/molbev/msg126

Mans, B. J., and Neitz, A. W. (2004a). Adaptation of ticks to a blood-feeding environment: evolution from a functional perspective. *Insect Biochem. Mol. Biol.* 34, 1–17. doi: 10.1016/j.ibmb.2003.09.002

Mans, B. J., and Neitz, A. W. (2004b). Molecular crowding as a mechanism for tick secretory granule biogenesis. *Insect Biochem. Mol. Biol.* 34, 1187–1193. doi: 10.1016/j.ibmb.2004.07.007

Mans, B. J., and Neitz, A. W. (2004c). The mechanism of αIIbβ3 antagonism by savignygrin and its implications for the evolution of anti-hemostatic strategies in soft ticks. *Insect Biochem. Mol. Biol.* 34, 573–584. doi: 10.1016/s0965-1748(04)00038-4

Mans, B. J., Gothe, R., and Neitz, A. W. (2004a). Biochemical perspectives on paralysis and other forms of toxicoses caused by ticks. *Parasitology* 129, S95–S111.

Mans, B. J., Venter, J. D., Coons, L. B., Louw, A. I., and Neitz, A. W. H. (2004b). A reassessment of argasid tick salivary gland ultrastructure from an immunocytochemical perspective. *Exp. Appl. Acarol.* 33, 119–129. doi: 10.1023/b%3Aappa.0000030012.47964.b3

Mans, B. J., and Ribeiro, J. M. (2008a). A novel clade of cysteinyl leukotriene scavengers in soft ticks. *Insect Biochem. Mol. Biol.* 38, 862–870. doi: 10.1016/j.ibmb.2008.06.002

Mans, B. J., and Ribeiro, J. M. (2008b). Function, mechanism and evolution of the moubatin-clade of soft tick lipocalins. *Insect Biochem. Mol. Biol.* 38, 841–852. doi: 10.1016/j.ibmb.2008.06.007

McSwain, J. L., Essenberg, R. C., and Sauer, J. R. (1982). Protein changes in the salivary glands of the female lone star tick, *Amblyomma americanum*, during feeding. *J. Parasitol.* 68, 100–106.

Monteiro, R. Q., Rezaie, A. R., Ribeiro, J. M., and Francischetti, I. M. (2005). Ixolaris: a factor Xa heparin-binding exosite inhibitor. *Biochem. J.* 387, 871–877. doi: 10.1042/bj20041738

Moore, J. E. Jr., Brook, B. S., and Nibbs, R. J. B. (2018). Chemokine transport dynamics and emerging recognition of their role in immune function. *Curr. Opin. Biomed. Eng.* 5, 90–95. doi: 10.1016/j.cobme.2018.03.001

Motoyashiki, T., Tu, A. T., Azimov, D. A., and Ibragim, K. (2003). Isolation of anticoagulant from the venom of tick, *Boophilus calcaratus*, from Uzbekistan. *Thromb. Res.* 110, 235–241. doi: 10.1016/s0049-3848(03)00409-2

Mulenga, A., Kim, T., and Ibelli, A. M. (2013). *Amblyomma americanum* tick saliva serine protease inhibitor 6 is a cross-class inhibitor of serine proteases and papain-like cysteine proteases that delays plasma clotting and inhibits platelet aggregation. *Insect Mol. Biol.* 22, 306–319. doi: 10.1111/imb.12024

Mulenga, A., Macaluso, K. R., Simser, J. A., and Azad, A. F. (2003). The American dog tick, *Dermacentor variabilis*, encodes a functional histamine release factor homolog. *Insect Biochem. Mol. Biol.* 33, 911–919. doi: 10.1016/s0965-1748(03)00097-3

Nakajima, C., Imamura, S., Konnai, S., Yamada, S., Nishikado, H., Ohashi, K., et al. (2006). A novel gene encoding a thrombin inhibitory protein in a cDNA library from *Haemaphysalis longicornis* salivary gland. *J. Vet. Med Sci.* 68, 447–452. doi: 10.1292/jvms.68.447

Narasimhan, S., Koski, R. A., Beaulieu, B., Anderson, J. F., Ramamoorthi, N., Kantor, F., et al. (2002). A novel family of anticoagulants from the saliva of *Ixodes scapularis*. *Insect Mol. Biol.* 11, 641–650. doi: 10.1046/j.1365-2583.2002.00375.x

Neelakanta, G., Sultana, H., Sonenshine, D. E., and Andersen, J. F. (2018). Identification and characterization of a histamine-binding lipocalin-like molecule from the relapsing fever tick *Ornithodoros turicata*. *Insect Mol. Biol.* 27, 177–187. doi: 10.1111/imb.12362

Neitz, A. W., Howell, C. J., Potgieter, D. J., and Bezuidenhout, J. D. (1978). Proteins and free amino acids in the salivary secretion and haemolymph of the tick *Amblyomma hebraeum*. *Onderstepoort J. Vet. Res.* 45, 235–240.

Neitz, A. W., Prozesky, L., Bezuidenhout, J. D., Putterill, J. F., and Potgieter, D. J. (1981). An investigation into the toxic principle in eggs of the tick *Amblyomma hebraeum*. *Onderstepoort J. Vet. Res.* 48, 109–117.

Neitz, A. W. H., Howell, C. J., and Potgieter, D. J. J. (1969). Purification of the toxic component in the oral secretion of the sand tampan *Ornithodoros savignyi* (Audouin) (1827). *J. S. Afr. Chem. Ind.* 22, 142–149.

Nielsen, H. (2017). Predicting secretory proteins with SignalP. *Methods Mol. Biol.* 1611, 59–73. doi: 10.1007/978-1-4939-7015-5_6

Nienaber, J., Gaspar, A. R., and Neitz, A. W. (1999). Savignin, a potent thrombin inhibitor isolated from the salivary glands of the tick *Ornithodoros savignyi* (Acari: Argasidae). *Exp. Parasitol.* 93, 82–91. doi: 10.1006/expr.1999.4448

Nunn, M. A., Sharma, A., Paesen, G. C., Adamson, S., Lissina, O., Willis, A. C., et al. (2005). Complement inhibitor of C5 activation from the soft tick *Ornithodoros moubata*. *J. Immunol.* 174, 2084–2091. doi: 10.4049/jimmunol.174.4.2084

Nuttall, G. H. F., and Strickland, C. (1908). On the presence of an anticoagulin in the salivary glands and intestines of *Argas persicus*. *Parasitology* 1, 302–310. doi: 10.1017/s0031182000003590

Nuttall, G. H. F., Warburton, C., Cooper, W. F., and Robinson, L. E. (1908). *Ticks. A Monograph of the Ixodoidae. Part I: The Argasidae*. Cambridge: Cambridge University Press. doi: 10.1017/s0031182000003590

Nuttall, P. A. (2019). Wonders of tick saliva. *Ticks Tick Borne Dis.* 10, 470–481. doi: 10.1016/j.ttbdis.2018.11.005

Nuttall, P. A., Trimnell, A. R., Kazimirova, M., and Labuda, M. (2006). Exposed and concealed antigens as vaccine targets for controlling ticks and tick-borne diseases. *Parasite Immunol.* 28, 155–163. doi: 10.1111/j.1365-3024.2006.00806.x

Oleaga-Pérez, A., Pérez-Sánchez, R., Astigarraga, A., and Encinas-Grandes, A. (1994). Detection of pig farms with *Ornithodoros erraticus* by pig serology. Elimination of non-specific reactions by carbohydrate epitopes of salivary antigens. *Vet. Parasitol.* 52, 97–111. doi: 10.1016/0304-4017(94)90040-x

Oliveira, C. J., Anatriello, E., de Miranda-Santos, I. K., Francischetti, I. M., Sá-Nunes, A., Ferreira, B. R., et al. (2013). Proteome of *Rhipicephalus sanguineus* tick saliva induced by the secretagogues pilocarpine and dopamine. *Ticks Tick Borne Dis.* 4, 469–477. doi: 10.1016/j.ttbdis.2013.05.001

Packham, M. A., and Rand, M. L. (2011). Historical perspective on ADP-induced platelet activation. *Purinergic. Signal.* 7, 283–292. doi: 10.1007/s11302-011-9227-x

Paesen, G. C., Adams, P. L., Harlos, K., Nuttall, P. A., and Stuart, D. I. (1999). Tick histamine-binding proteins: isolation, cloning, and three-dimensional structure. *Mol. Cell* 3, 661–671. doi: 10.1016/s1097-2765(00)80359-7

Paesen, G. C., Adams, P. L., Nuttall, P. A., and Stuart, D. L. (2000). Tick histamine-binding proteins: lipocalins with a second binding cavity. *Biochim. Biophys. Acta* 1482, 92–101. doi: 10.1016/s0167-4838(00)00168-0

Paesen, G. C., Siebold, C., Dallas, M. L., Peers, C., Harlos, C., Nuttall, P. A., et al. (2009). An ion-channel modulator from the saliva of the brown ear tick has a highly modified Kunitz/BPTI structure. *J. Mol. Biol.* 389, 734–747. doi: 10.1016/j.jmb.2009.04.045

Paesen, G. C., Siebold, C., Harlos, K., Peacey, M. F., Nuttall, P. A., and Stuart, D. I. (2007). A tick protein with a modified Kunitz fold inhibits human tryptase. *J. Mol. Biol.* 368, 1172–1186. doi: 10.1016/j.jmb.2007.03.011

Parizi, L. F., Githaka, N. W., Acevedo, C., Benavides, U., Seixas, A., Logullo, C., et al. (2013). Sequence characterization and immunogenicity of cystatins from the cattle tick Rhipicephalus (Boophilus) microplus. *Ticks Tick Borne Dis.* 4, 492–499. doi: 10.1016/j.ttbdis.2013.06.005

Perner, J., Kropáčková, S., Kopáček, P., and Ribeiro, J. M. C. (2018). Sialome diversity of ticks revealed by RNAseq of single tick salivary glands. *PLoS Negl. Trop. Dis.* 12:e0006410. doi: 10.1371/journal.pntd.0006410

Pervaiz, S., and Brew, K. (1987). Homology and structure-function correlations between alpha 1-acid glycoprotein and serum retinol-binding protein and its relatives. *FASEB J.* 1, 209–214. doi: 10.1096/fasebj.1.3.3622999

Petersen, L. J. (1997). Quantitative measurement of extracellular histamine concentrations in intact human skin in vivo by the microdialysis technique: methodological aspects. *Allergy* 52, 547–555. doi: 10.1111/j.1398-9995.1997.tb02598.x

Pichu, S., Ribeiro, J. M., Mather, T. N., and Francischetti, I. M. (2014). Purification of a serine protease and evidence for a protein C activator from the saliva of the tick, *Ixodes scapularis*. *Toxicon* 77, 32–39. doi: 10.1016/j.toxicon.2013.10.025

Pienaar, R., Neitz, A. W. H., and Mans, B. J. (2018). Tick paralysis: solving an Enigma. *Vet. Sci.* 5:53. doi: 10.3390/vetsci5020053

Platt, E. J., Wehrly, K., Kuhmann, S. E., Chesebro, B., and Kabat, D. (1998). Effects of CCR5 and CD4 cell surface concentrations on infections by macrophagetropic isolates of human immunodeficiency virus type 1. *J. Virol.* 72, 2855–2864.

Preston, S. G., Majtán, J., Kouremenou, C., Rysnik, O., Burger, L. F., Cabezas Cruz, A., et al. (2013). Novel immunomodulators from hard ticks selectively reprogramme human dendritic cell responses. *PLoS Pathog.* 9:e1003450. doi: 10.1371/journal.ppat.1003450

Prevot, P. P., Adam, B., Boudjeltia, K. Z., Brossard, M., Lins, L., Cauchie, P., et al. (2006). Anti-hemostatic effects of a serpin from the saliva of the tick *Ixodes ricinus*. *J. Biol. Chem.* 281, 26361–26369. doi: 10.1074/jbc.m604197200

Prevot, P. P., Beschin, A., Lins, L., Beaufays, J., Grosjean, A., Bruys, L., et al. (2009). Exosites mediate the anti-inflammatory effects of a multifunctional serpin from the saliva of the tick *Ixodes ricinus*. *FEBS J.* 276, 3235–3246. doi: 10.1111/j.1742-4658.2009.07038.x

Prié, S., Guillemette, G., Boulay, G., Borgeat, P., and Sirois, P. (1995). Leukotriene C4 receptors on guinea pig tracheocytes. *J. Pharmacol. Exp. Ther.* 275, 312–318.

Radulović, ŽM., and Mulenga, A. (2017). Heparan sulfate/heparin glycosaminoglycan binding alters inhibitory profile and enhances anticoagulant function of conserved *Amblyomma americanum* tick saliva serpin 19. *Insect Biochem. Mol. Biol.* 80, 1–10. doi: 10.1016/j.ibmb.2016.11.002

Rangel, C. K., Parizi, L. F., Sabadin, G. A., Costa, E. P., Romeiro, N. C., Isezaki, M., et al. (2017). Molecular and structural characterization of novel cystatins

from the taiga tick *Ixodes persulcatus*. *Ticks Tick Borne Dis.* 8, 432–441. doi: 10.1016/j.ttbdis.2017.01.007

Rawal, N., and Pangburn, M. (2001). Formation of high-affinity C5 convertases of the alternative pathway of complement. *J. Immunol.* 166, 2635–2642. doi: 10.4049/jimmunol.166.4.2635

Rawal, N., and Pangburn, M. K. (2003). Formation of high affinity C5 convertase of the classical pathway of complement. *J. Biol. Chem.* 278, 38476–38483. doi: 10.1074/jbc.m307017200

Ribeiro, J. M. (1987). *Ixodes dammini*: salivary anti-complement activity. *Exp. Parasitol.* 64, 347–353. doi: 10.1016/0014-4894(87)90046-4

Ribeiro, J. M., and Arcà, B. (2009). From sialomes to the sialoverse: an insight into salivary potion of blood-feeding insects. *Adv. In. Insect Physiol.* 37, 59–118. doi: 10.1371/journal.pone.0044612

Ribeiro, J. M., Evans, P. M., MacSwain, J. L., and Sauer, J. (1992). *Amblyomma americanum*: characterization of salivary prostaglandins E2 and F2 alpha by RP-HPLC/bioassay and gas chromatography-mass spectrometry. *Exp. Parasitol.* 74, 112–116. doi: 10.1016/0014-4894(92)90145-z

Ribeiro, J. M., and Mather, T. N. (1998). *Ixodes scapularis*: salivary kininase activity is a metallo dipeptidyl carboxypeptidase. *Exp. Parasitol.* 89, 213–221. doi: 10.1006/expr.1998.4296

Ribeiro, J. M. C. (1995). How ticks make a living. *Parasitol. Today* 11, 91–93. doi: 10.1016/0169-4758(95)80162-6

Ribeiro, J. M. C., Endris, T. M., and Endris, R. (1991). Saliva of the soft tick *Ornithodoros moubata*, contains anti-platelet and apyrase activity. *Comp. Biochem. Physiol.* 100, 109–112. doi: 10.1016/0300-9629(91)90190-n

Ribeiro, J. M. C., Makoul, G., Levine, J., Robinson, D., and Spielman, A. (1985). Antihemostatic, antiinflammatory, and immunosuppressive properties of the saliva of a tick *Ixodes dammini*. *J. Exp. Med.* 161, 332–344. doi: 10.1084/jem.161.2.332

Ribeiro, J. M. C., and Spielman, A. (1986). *Ixodes dammini*: salivary anaphylatoxin inactivating activity. *Exp. Parasitol.* 62, 292–297. doi: 10.1016/0014-4894(86)90034-2

Riek, R. F. (1957). Studies on the reactions of animals to infestation with ticks. *Aust. J. Agric. Res.* 8, 215–223.

Riek, R. F. (1959). Studies on the reactions of animals to infestation with ticks. *Aust. J. Agric. Res.* 10, 604–613.

Rodriguez-Valle, M., Moolhuijzen, P., Barrero, R. A., Ong, C. T., Busch, G., Karbanowicz, T., et al. (2017). Transcriptome and toxin family analysis of the paralysis tick, *Ixodes holocyclus*. *Int. J. Parasitol.* 48, 71–82. doi: 10.1016/j.ijpara.2017.07.007

Rodriguez-Valle, M., Xu, T., Kurscheid, S., and Lew-Tabor, A. E. (2015). *Rhipicephalus microplus* serine protease inhibitor family: annotation, expression and functional characterisation assessment. *Parasit. Vectors* 8:7. doi: 10.1186/s13071-014-0605-4

Ross, I. C. (1926). An experimental study of tick paralysis in Australia. *Parasitology* 18, 410–429. doi: 10.1186/s13071-018-3061-8

Roversi, P., Johnson, S., Preston, S. G., Nunn, M. A., Paesen, G. C., Austyn, J. M., et al. (2017). Structural basis of cholesterol binding by a novel clade of dendritic cell modulators from ticks. *Sci. Rep.* 7:16057. doi: 10.1038/s41598-017-16413-2

Roversi, P., Lissina, O., Johnson, S., Ahmat, N., Paesen, G. C., Ploss, K., et al. (2007). The structure of OMCI, a novel lipocalin inhibitor of the complement system. *J. Mol. Biol.* 369, 784–793. doi: 10.1016/j.jmb.2007.03.064

Roversi, P., Ryffel, B., Togbe, D., Maillet, I., Teixeira, M., Ahmat, N., et al. (2013). Bifunctional lipocalin ameliorates murine immune complex-induced acute lung injury. *J. Biol. Chem.* 288, 18789–18802. doi: 10.1074/jbc.M112.420331

Sabbatani, L. (1899). Fermento anticoagulante del' *Ixodes ricinus*. *Arch. Ital. Biol.* 31, 37–53.

Sadik, C. D., Miyabe, Y., Sezin, T., and Luster, A. D. (2018). The critical role of C5a as an initiator of neutrophil-mediated autoimmune inflammation of the joint and skin. *Semin. Immunol.* 37, 21–29. doi: 10.1016/j.smim.2018.03.002

Salát, J., Paesen, G. C., Rezácová, P., Kotsyfakis, M., Kovárová, Z., Sanda, M., et al. (2010). Crystal structure and functional characterization of an immunomodulatory salivary cystatin from the soft tick *Ornithodoros moubata*. *Biochem. J.* 429, 103–112. doi: 10.1042/BJ20100280

Sangamnatdej, S., Paesen, G. C., Slovak, M., and Nuttall, P. A. (2002). A high affinity serotonin- and histamine-binding lipocalin from tick saliva. *Insect Mol. Biol.* 11, 79–86. doi: 10.1046/j.0962-1075.2001.00311.x

Sant'Anna Azzolini, S., Sasaki, S. D., Torquato, R. J., Andreotti, R., Andreotti, E., and Tanaka, A. S. (2003). *Rhipicephalus sanguineus* trypsin inhibitors present in the tick larvae: isolation, characterization, and partial primary structure determination. *Arch. Biochem. Biophys.* 417, 176–182. doi: 10.1016/s0003-9861(03)00344-8

Sasagawa, M., Satoh, T., Takemoto, A., Hasegawa, T., Suzuki, E., and Arakawa, M. (1994). Blood levels of leukotrienes (LTC4, D4, E4, B4) in asthmatic patients during attack and remission. *Arerugi* 43, 28–36.

Schroeder, H., Daix, V., Gillet, L., Renauld, J. C., and Vanderplasschen, A. (2007). The paralogous salivary anti-complement proteins IRAC I and IRAC II encoded by *Ixodes ricinus* ticks have broad and complementary inhibitory activities against the complement of different host species. *Microbes Infect.* 9, 247–250. doi: 10.1016/j.micinf.2006.10.020

Schuijt, T. J., Bakhtiari, K., Daffre, S., Deponte, K., Wielders, S. J., Marquart, J. A., et al. (2013). Factor Xa activation of factor V is of paramount importance in initiating the coagulation system: lessons from a tick salivary protein. *Circulation* 128, 254–266. doi: 10.1161/CIRCULATIONAHA.113.003191

Schuijt, T. J., Narasimhan, S., Daffre, S., DePonte, K., Hovius, J. W., Van't Veer, C., et al. (2011). Identification and characterization of *Ixodes scapularis* antigens that elicit tick immunity using yeast surface display. *PLoS One* 6:e15926. doi: 10.1371/journal.pone.0015926

Schwarz, A., Tenzer, S., Hackenberg, M., Erhart, J., Gerhold-Ay, A., Mazur, J., et al. (2014). A systems level analysis reveals transcriptomic and proteomic complexity in *Ixodes ricinus* midgut and salivary glands during early attachment and feeding. *Mol. Cell. Proteomics* 13, 2725–2735. doi: 10.1074/mcp.M114.039289

Scott, E. (1921). Hume and Hovell's journey to Port Phillip. *Roy. Aust. Hist. Soc.* 7, 289–380.

Sears, D. W., Thompson, S. E., and Saxon, S. R. (2007). Reversible ligand binding reactions: why do biochemistry students have trouble connecting the dots? *Biochem. Mol. Biol. Educ.* 35, 105–118. doi: 10.1002/bmb.29

Singh, K., Davies, G., Alenazi, Y., Eaton, J. R. O., Kawamura, A., and Bhattacharya, S. (2017). Yeast surface display identifies a family of evasins from ticks with novel polyvalent CC chemokine-binding activities. *Sci. Rep.* 7:4267. doi: 10.1038/s41598-017-04378-1

Smith, R. D., Engdahl, A. L., Dunbar, J. B. Jr., and Carlson, H. A. (2012). Biophysical limits of protein-ligand binding. *J. Chem. Inf. Model.* 52, 2098–2106. doi: 10.1021/ci200612f

Soares, C. A., Lima, C. M., Dolan, M. C., Piesman, J., Beard, C. B., and Zeidner, N. S. (2005). Capillary feeding of specific dsRNA induces silencing of the Isac gene in nymphal *Ixodes scapularis* ticks. *Insect Mol. Biol.* 14, 443–452. doi: 10.1111/j.1365-2583.2005.00575.x

Soares, T. S., Watanabe, R. M., Tanaka-Azevedo, A. M., Torquato, R. J., Lu, S., Figueiredo, A. C., et al. (2012). Expression and functional characterization of Boophilin, a thrombin inhibitor from *Rhipicephalus* (Boophilus) microplus midgut. *Vet. Parasitol.* 187, 521–528. doi: 10.1016/j.vetpar.2012.01.027

Sokol, C. L., and Luster, A. D. (2015). The chemokine system in innate immunity. *Cold Spring Harb. Perspect. Biol.* 7:a016303. doi: 10.1101/cshperspect.a016303

Sonenshine, D. E. (2004). Pheromones and other semiochemicals of ticks and their use in tick control. *Parasitology* 129, S405–S425.

Stutzer, C., Mans, B. J., Gaspar, A. R., Neitz, A. W., and Maritz-Olivier, C. (2009). *Ornithodoros savignyi*: soft tick apyrase belongs to the 5'-nucleotidase family. *Exp. Parasitol.* 122, 318–327. doi: 10.1016/j.exppara.2009.04.007

Tanaka, A. S., Andreotti, R., Gomes, A., Torquato, R. J., Sampaio, M. U., and Sampaio, C. A. (1999). A double headed serine proteinase inhibitor–human plasma kallikrein and elastase inhibitor–from *Boophilus microplus* larvae. *Immunopharmacology* 45, 171–177. doi: 10.1016/s0162-3109(99)00074-0

Tang, J., Fang, Y., Han, Y., Bai, X., Yan, X., Zhang, Y., et al. (2015). YY-39, a tick anti-thrombosis peptide containing RGD domain. *Peptides* 68, 99–104. doi: 10.1016/j.peptides.2014.08.008

Tatchell, R. J. (1967). A modified method for obtaining tick oral secretion. *J. Parasitol.* 53, 1106–1107.

Tatchell, R. J., and Moorhouse, D. E. (1968). The feeding processes of the cattle tick *Boophilus microplus* (Canestrini). II. The sequence of host-tissue changes. *Parasitology* 58, 441–459.

Tirloni, L., Islam, M. S., Kim, T. K., Diedrich, J. K., Yates, J. R. III, Pinto, A. F., et al. (2015). Saliva from nymph and adult females of *Haemaphysalis longicornis*: a proteomic study. *Parasit. Vectors* 8:338. doi: 10.1186/s13071-015-0918-y

Tirloni, L., Reck, J., Terra, R. M., Martins, J. R., Mulenga, A., Sherman, N. E., et al. (2014). Proteomic analysis of cattle tick *Rhipicephalus* (Boophilus) microplus saliva: a comparison between partially and fully engorged females. *PLoS One* 9:e94831. doi: 10.1371/journal.pone.0094831

Tyson, K., Elkins, C., Patterson, H., Fikrig, E., and de Silva, A. (2007). Biochemical and functional characterization of Salp20, an *Ixodes scapularis* tick salivary protein that inhibits the complement pathway. *Insect Mol. Biol.* 16, 469–479. doi: 10.1111/j.1365-2583.2007.00742.x

Tyson, K. R., Elkins, C., and de Silva, A. M. (2008). A novel mechanism of complement inhibition unmasked by a tick salivary protein that binds to properdin. *J. Immunol.* 180, 3964–3968. doi: 10.4049/jimmunol.180.6.3964

Uhlír, J., Grubhoffer, L., Borskı, I., and Dusbábek, F. (1994). Antigens and glycoproteins of larvae, nymphs and adults of the tick *Ixodes ricinus*. *Med. Vet. Entomol.* 8, 141–150. doi: 10.1111/j.1365-2915.1994.tb00154.x

Valdés, J. J., Cabezas-Cruz, A., Sima, R., Butterill, P. T., Růžek, D., and Nuttall, P. A. (2016). Substrate prediction of *Ixodes ricinus* salivary lipocalins differentially expressed during *Borrelia afzelii* infection. *Sci. Rep.* 6:32372. doi: 10.1038/srep32372

Valdés, J. J., Schwarz, A., Cabeza de Vaca, I., Calvo, E., Pedra, J. H., Guallar, V., et al. (2013). Tryptogalinin is a tick Kunitz serine protease inhibitor with a unique intrinsic disorder. *PLoS One* 8:e62562. doi: 10.1371/journal.pone.0062562

Valenzuela, J. G., Charlab, R., Mather, T. N., and Ribeiro, J. M. (2000). Purification, cloning, and expression of a novel salivary anticomplement protein from the tick, *Ixodes scapularis*. *J. Biol. Chem.* 275, 18717–18723. doi: 10.1074/jbc.m001486200

van de Locht, A., Stubbs, M. T., Bode, W., Friedrich, T., Bollschweiler, C., Höffken, W., et al. (1996). The ornithodorin-thrombin crystal structure, a key to the TAP enigma? *EMBO J.* 15, 6011–6017. doi: 10.1002/j.1460-2075.1996.tb00989.x

Viljoen, G. J., Neitz, A. W. H., Prozesky, L., Bezuidenhout, J. D., and Vermeulen, N. M. J. (1985). Purification and properties of tick egg toxic proteins. *Insect Biochem.* 15, 475–482. doi: 10.1016/0020-1790(85)90060-5

von Siebold, C. T. H., and Stannius, H. (1854). *Comparative Anatomy*. London: Trubner and Company.

Wagner, C. L., Mascelli, M. A., Neblock, D. S., Weisman, H. F., Coller, B. S., and Jordan, R. E. (1996). Analysis of GPIIb/IIIa receptor number by quantification of 7E3 binding to human platelets. *Blood* 88, 907–914.

Wang, H., Kaufman, W. R., Cui, W. W., and Nuttall, P. A. (2001b). Molecular individuality and adaptation of the tick *Rhipicephalus appendiculatus* in changed feeding environments. *Med. Vet. Entomol.* 15, 403–412. doi: 10.1046/j.0269-283x.2001.00328.x

Wang, H., Hails, R. S., Cui, W. W., and Nuttall, P. A. (2001a). Feeding aggregation of the tick *Rhipicephalus appendiculatus* (Ixodidae): benefits and costs in the contest with host responses. *Parasitology* 123, 447–453.

Wang, H., and Nuttall, P. A. (1994). Comparison of the proteins in salivary glands, saliva and haemolymph of *Rhipicephalus appendiculatus* female ticks during feeding. *Parasitology* 109, 517–523.

Wang, H., Paesen, G. C., Nuttall, P. A., and Barbour, A. G. (1998). Male ticks help their mates to feed. *Nature* 391, 753–754. doi: 10.1038/35773

Wang, X., Coons, L. B., Taylor, D. B., Stevens, S. E. Jr., and Gartner, T. K. (1996). Variabilin, a novel RGD-containing antagonist of glycoprotein IIb-IIIa and platelet aggregation inhibitor from the hard tick *Dermacentor variabilis*. *J. Biol. Chem.* 271, 17785–17790. doi: 10.1074/jbc.271.30.17785

Wang, Y., Yu, X., Cao, J., Zhou, Y., Gong, H., Zhang, H., et al. (2015). Characterization of a secreted cystatin from the tick *Rhipicephalus haemaphysaloides*. *Exp. Appl. Acarol.* 67, 289–298. doi: 10.1007/s10493-015-9946-8

Watts, S. W., Morrison, S. F., Davis, R. P., and Barman, S. M. (2012). Serotonin and blood pressure regulation. *Pharmacol. Rev.* 64, 359–388. doi: 10.1124/pr.111.004697

Waxman, L., and Connolly, T. M. (1993). Isolation of an inhibitor selective for collagen-stimulated platelet aggregation from the soft tick *Ornithodoros moubata*. *J. Biol. Chem.* 268, 5445–5449.

Waxman, L., Smith, D. E., Arcuri, K. E., and Vlasuk, G. P. (1990). Tick anticoagulant peptide (TAP) is a novel inhibitor of blood coagulation factor Xa. *Science* 248, 593–596. doi: 10.1126/science.2333510

Whisstock, J. C., Silverman, G. A., Bird, P. I., Bottomley, S. P., Kaiserman, D., Luke, C. J., et al. (2010). Serpins flex their muscle: II. Structural insights into target peptidase recognition, polymerization, and transport functions. *J. Biol. Chem.* 285, 24307–24312. doi: 10.1074/jbc.R110.141408

Wiegner, R., Chakraborty, S., and Huber-Lang, M. (2016). Complement-coagulation crosstalk on cellular and artificial surfaces. *Immunobiology* 221, 1073–1079. doi: 10.1016/j.imbio.2016.06.005

Wikel, S. (2017). "Arthropod modulation of wound healing. in arthropod vector," in *Controller of Disease Transmission*, Vol. 2, eds S. K. Wikel, S. Aksoy, and G. Dimopoulos (Amsterdam: Elsevier), 31–50. doi: 10.1016/b978-0-12-805360-7.00003-4

Xu, T., Lew-Tabor, A., and Rodriguez-Valle, M. (2016). Effective inhibition of thrombin by *Rhipicephalus microplus* serpin-15 (RmS-15) obtained in the yeast *Pichia pastoris*. *Ticks Tick Borne Dis.* 7, 180–187. doi: 10.1016/j.ttbdis.2015.09.007

Xu, X. L., Cheng, T. Y., and Yang, H. (2016). Enolase, a plasminogen receptor isolated from salivary gland transcriptome of the ixodid tick *Haemaphysalis flava*. *Parasitol. Res.* 115, 1955–1964. doi: 10.1007/s00436-016-4938-0

Yokomizo, T. (2015). Two distinct leukotriene B4 receptors, BLT1 and BLT2. *J. Biochem.* 157, 65–71. doi: 10.1093/jb/mvu078

Zhu, K., Bowman, A. S., Brigham, D. L., Essenberg, R. C., Dillwith, J. W., and Sauer, J. R. (1997a). Isolation and characterization of Americanin, a specific inhibitor of thrombin, from the salivary glands of the lone star tick *Amblyomma americanum* (L.). *Exp. Parasitol.* 87, 30–38. doi: 10.1006/expr.1997.4175

Zhu, K., Sauer, J. R., Bowman, A. S., and Dillwith, J. W. (1997b). Identification and characterization of anticoagulant activities in the saliva of the lone star tick, *Amblyomma americanum* (L.). *J. Parasitol.* 83, 38–43.

Conflict of Interest Statement: The author declares that the research was conducted in the absence of any commercial or financial relationships that could be construed as a potential conflict of interest.

frontiers in Physiology

ORIGINAL RESEARCH
published: 03 May 2019
doi: 10.3389/fphys.2019.00529

The Transcriptome of the Salivary Glands of *Amblyomma aureolatum* Reveals the Antimicrobial Peptide Microplusin as an Important Factor for the Tick Protection Against *Rickettsia rickettsii* Infection

Larissa A. Martins[1], Camila D. Malossi[1†], Maria F. B. de M. Galletti[1†], José M. Ribeiro[2], André Fujita[3], Eliane Esteves[4], Francisco B. Costa[5], Marcelo B. Labruna[5], Sirlei Daffre[1] and Andréa C. Fogaça[1]*

[1] Departamento de Parasitologia, Instituto de Ciências Biomédicas, Universidade de São Paulo, São Paulo, Brazil, [2] Laboratory of Malaria and Vector Research, National Institute of Allergy and Infectious Diseases, Bethesda, MD, United States, [3] Departamento de Ciência da Computação, Instituto de Matemática e Estatística, Universidade de São Paulo, São Paulo, Brazil, [4] Departamento de Imunologia, Instituto de Ciências Biomédicas, Universidade de São Paulo, São Paulo, Brazil, [5] Departamento de Medicina Veterinária Preventiva e Saúde Animal, Faculdade de Medicina Veterinária e Zootecnia, Universidade de São Paulo, São Paulo, Brazil

The salivary glands (SG) of ixodid ticks play a pivotal role in blood feeding, producing both the cement and the saliva. The cement is an adhesive substance that helps the attachment of the tick to the host skin, while the saliva contains a rich mixture of antihemostatic, anti-inflammatory, and immunomodulatory substances that allow ticks to properly acquire the blood meal. The tick saliva is also a vehicle used by several pathogens to be transmitted to the vertebrate host, including various bacterial species from the genus *Rickettsia*. *Rickettsia rickettsii* is a tick-borne obligate intracellular bacterium that causes the severe Rocky Mountain spotted fever. In Brazil, the dog yellow tick *Amblyomma aureolatum* is a vector of *R. rickettsii*. In the current study, the effects of an experimental infection with *R. rickettsii* on the global gene expression profile of *A. aureolatum* SG was determined by next-generation RNA sequencing. A total of 260 coding sequences (CDSs) were modulated by infection, among which 161 were upregulated and 99 were downregulated. Regarding CDSs in the immunity category, we highlight one sequence encoding one microplusin-like antimicrobial peptide (AMP) (Ambaur-69859). AMPs are important effectors of the arthropod immune system, which lack the adaptive response of the immune system of vertebrates. The expression of microplusin was confirmed to be significantly upregulated in the SG as well as in the midgut (MG) of infected *A. aureolatum* by a quantitative polymerase chain reaction preceded by reverse transcription. The knockdown of the microplusin expression by RNA interference caused a significant increase in the prevalence of infected ticks in relation to the control. In addition, a higher rickettsial load of one order of magnitude was recorded in both the MG and SG of ticks that received microplusin-specific

OPEN ACCESS

Edited by:
Albert Mulenga,
Texas A&M University, United States

Reviewed by:
Abid Ali,
Abdul Wali Khan University Mardan, Pakistan
Daniele Pereira Castro,
Fundação Oswaldo Cruz (Fiocruz), Brazil
Shahid Karim,
The University of Southern Mississippi, United States

****Correspondence:***
Andréa C. Fogaça
deafog@usp.br

†Present address:
Camila D. Malossi,
Instituto de Biotecnologia, Universidade Estadual Paulista, Botucatu, Brazil
Maria F. B. de M. Galletti,
Rickettsial Zoonoses Branch, Division of Vector-Borne Diseases, National Center for Emerging and Zoonotic Infectious Diseases, Centers for Disease Control and Prevention, Atlanta, GA, United States

Specialty section:
This article was submitted to Invertebrate Physiology, a section of the journal Frontiers in Physiology

Received: *23 November 2018*
Accepted: *12 April 2019*
Published: *03 May 2019*

Citation:
Martins LA, Malossi CD, Galletti MFBM, Ribeiro JM, Fujita A, Esteves E, Costa FB, Labruna MB, Daffre S and Fogaça AC (2019) The Transcriptome of the Salivary Glands of Amblyomma aureolatum Reveals the Antimicrobial Peptide Microplusin as an Important Factor for the Tick Protection Against Rickettsia rickettsii Infection. Front. Physiol. 10:529. doi: 10.3389/fphys.2019.00529

dsRNA. No effect of microplusin knockdown was observed on the *R. rickettsii* transmission to rabbits. Moreover, no significant differences in tick engorgement and oviposition were recorded in ticks that received dsMicroplusin, demonstrating that microplusin knockdown has no effect on tick fitness. Further studies must be performed to determine the mechanism of action of this AMP against *R. rickettsii*.

Keywords: spotted fever, tick-rickettsiae interaction, immune, microplusin, antimicrobial peptide, salivary glands, transcriptome, RNAi

INTRODUCTION

Ticks are obligate blood feeding arthropods and their success in acquiring the host's blood depends essentially on the physiological functions performed by the salivary glands (SG) (Bowman and Sauer, 2004; Sonenshine and Roe, 2013). Primarily, SG are osmoregulation organs that revert the excess of fluids and ions from the blood meal back into the host's circulation via saliva. In this manner, the nutrients are concentrated and both the volume and the ionic composition of the hemolymph are regulated (Kaufman, 2010). The tick saliva also contains a myriad of biomolecules with diverse pharmacological activities, including anticoagulation, antiplatelet, vasodilatory, anti-inflammatory, and immunomodulatory, enabling blood uptake (Francischetti et al., 2009; Kazimirova and Stibraniova, 2013; Kotal et al., 2015; Simo et al., 2017). Infectious agents, including viruses, bacteria, and protozoa, use tick saliva as a vehicle to be transmitted to a vertebrate host (Dantas-Torres et al., 2012; Simo et al., 2017). In addition, the biological properties of the tick saliva were previously reported to benefit the transmission of viruses and bacteria to the host (Kaufman, 2010; Kazimirova and Stibraniova, 2013; Simo et al., 2017). Besides saliva, SG also produce the cement, an adhesive substance that covers the tick mouthparts and helps the attachment to the host skin, seals the feeding lesion, and prevents the contact of tick mouthparts with the host's immune factors (Suppan et al., 2018).

Rickettsia rickettsii is a tick-borne obligate intracellular bacterium that causes the life-threatening Rocky Mountain spotted fever (RMSF). *R. rickettsii* colonizes the endothelial cells of the vertebrate host, causing an intense vasculitis that can lead to the failure of important organs, including the brain, lungs, and kidneys. Antibiotic treatment is available, but it is effective only if performed within a few days of illness onset (Chapman et al., 2006; Dantas-Torres, 2007; Chen and Sexton, 2008). Nonetheless, the non-specificity of clinical manifestations, such as fever, headache, and myalgia, associated with the late detection of antibodies to *R. rickettsii* in serological tests, make early diagnosis difficult (Dantas-Torres, 2007). As a consequence, fatality rates of the disease are still high, reaching approximately 40% in Brazil (Labruna, 2009). Specifically in the State of São Paulo, lethality rates can overpass 70% [official data from São Paulo State Health Secretary (2007–2018)].

In Brazil, *Amblyomma sculptum* [formerly named *Amblyomma cajennense* (Nava et al., 2014)] and *Amblyomma aureolatum* are implicated as vectors of *R. rickettsii* (Labruna, 2009). The tick midgut (MG) is the first tick organ that interacts with rickettsiae acquired within the blood meal. The rickettsiae then need to reach the SG to be transmitted to the vertebrate host via saliva. Importantly, rickettsiae are not only collected from the hemolymph by the tick SG, but actively proliferate in this organ (Socolovschi et al., 2009). We previously showed that the infection with *R. rickettsii* modulates the global gene expression profile of the MG of both *A. sculptum* and *A. aureolatum* (Martins et al., 2017). The majority of modulated coding sequences (CDSs) of *A. aureolatum*, which is more susceptible to the *R. rickettsii* infection than *A. sculptum* (Labruna et al., 2008), were downregulated in response to infection (Martins et al., 2017). On the other hand, most *A. sculptum* CDSs, including immune factors, were upregulated in the MG of infected ticks. In the current study, we determined the global transcriptional profile of *A. aureolatum* SG in response to an infection with *R. rickettsii* by next-generation RNA sequencing (RNA-seq). Ticks were infected by feeding on infected hosts, mimicking a natural infection. RNA-seq data were validated by a quantitative polymerase chain reaction preceded by reverse transcription (RT-qPCR). The coding sequence (CDS) of one antimicrobial peptide with similarity to the microplusin of *Rhipicephalus microplus* (Fogaca et al., 2004), which was significantly induced by infection, was targeted for functional characterization using RNA interference (RNAi). Besides generating a transcript databank of *A. aureolatum* SG, our data showed that microplusin is one important factor of tick-rickettsiae interactions.

MATERIALS AND METHODS

Ethics Statement

The procedures adopted for the experiments involving vertebrate animals were approved by the Institutional Animal Care and Use Committees from the Faculty of Veterinary Medicine (protocol number 1423/2008) and the Institute of Biomedical Sciences (protocol number 128/2011), University of São Paulo, São Paulo, Brazil.

R. rickettsii-Infected and Uninfected Ticks

Adult ticks, infected or not with the highly virulent Taiaçu strain of *R. rickettsii*, were obtained using the procedure previously detailed in Pinter and Labruna (2006) and Galletti et al. (2013). Off-host phases were held in an incubator at 25°C and 95% relative humidity. The SG and MG of each tick were dissected and separately transferred to 100 μL of RNA*later*® Solution (Thermo Fisher Scientific, United States).

Nucleic Acid Extraction

The SG and MG of each adult tick were homogenized and submitted to a simultaneous isolation of genomic DNA (gDNA) and total RNA using the InviTrap® Spin Cell RNA Mini Kit (Stratatec, Germany) according to the manufacturer's specifications.

Real-Time Quantitative PCR (qPCR) to *R. rickettsii* Quantification

Genomic DNA was utilized as a template to quantify the total number of rickettsiae in tick organs by real-time quantitative PCR (qPCR) using a hydrolysis probe for the citrate synthase gene (*glt*A) of *R. rickettsii*, as previously described (Galletti et al., 2013). gDNA samples extracted from non-infected ticks were also analyzed to confirm the absence of infection. All samples were analyzed in three technical replicates.

RNA-Seq, Assembly, and Annotation

The RNA extracted from the SG of ten *A. aureolatum* harboring between 7.00×10^4 and 1.00×10^5 rickettsiae was pooled to generate the infected sample. The RNA extracted from the SG of ten non-infected *A. aureolatum* was also combined to generate the control sample. Each tick contributed equally for the composition of the two pool samples, which were submitted to a high throughput mRNA sequencing (RNA-seq), together with RNA samples from the MG of non-infected and infected *A. aureolatum* (Martins et al., 2017) and from the SG of fed and unfed *A. sculptum* (Esteves et al., 2017). To that end, all samples were tagged and multiplex sequenced in four lanes using a HiSeq™ sequencing system (Illumina, United States) at the North Carolina State University facility (NC, United States). A total of around 242 million reads of 101 base pairs were obtained for *A. aureolatum* samples using the single read and submitted to a bioinformatics analysis as detailed before (Karim et al., 2011; Esteves et al., 2017; Martins et al., 2017).

Paired comparisons of the number of reads hitting each CDS were calculated by chi-squared test to detect significant differences between the gene expression in SG of *A. aureolatum* infected (AaI) and non-infected (AaC). Normalized fold-ratios of the sample reads were computed by adjusting the numerator by a factor based on the ratio of the total number of reads in each sample and adding one to the denominator to avoid division by zero. The minimum considered fold-change in infected ticks in relation to control ticks was larger than five and $p < 0.05$.

The complete dataset was organized in a hyperlinked spreadsheet as previously reported (Ribeiro et al., 2004) and a table with links (**Supplementary Table 1**) may be downloaded from https://s3.amazonaws.com/proj-bip-prod-publicread/transcriptome/Amb_aureolatum/SupplementaryTable1.zip.

The raw data were deposited to the Sequence Read Archives (SRA) of the NCBI under the BioProject PRJNA344771 [raw reads runs SRR4301100 (SG of control *A. aureolatum*) and SRR4301110 (SG of infected *A. aureolatum*)]. The Transcriptome Shotgun Assembly (TSA) project has been deposited at DDBJ/EMBL/GenBank under the accession code GFAC00000000. Only CDSs representing 90% of the sequences of known proteins or larger than 250 amino acids were deposited.

The amino acid sequence of the protein encoded by the CDS Ambaur-69859 (GenBank protein ID: JAT93257.1), whose code one AMP was similar to the microplusin of *R. microplus* (Fogaca et al., 2004), was used as query in blastp searches against both Transcriptome Shotgun Assembly (tsa_nr; NCBI) and UniProtKB/Swiss-Prot (swissprot) databases with the phylum Arthropoda (taxid: 6656) as filter. The protein sequence of a given tick species with the best match with *A. aureolatum* was selected as representative for that species and used to perform multiple sequence alignment (MSA) using the multiple sequence comparison by log-expectation (MUSCLE) tool (Edgar, 2004a,b) with default parameters at the European Bioinformatics Institute (EMBL-EBI) website (McWilliam et al., 2013; Li et al., 2015). A phylogenetics analysis of microplusins (**Supplementary Table 2**) was performed with the Maximum Likelihood (ML) method with the Jones-Taylor-Thornton (JTT) matrix-based substitution model (Jones et al., 1992) using MEGA X (Kumar et al., 2018) software.

Validation of RNA-Seq Data Using Real-Time Quantitative PCR Proceeded by Reverse Transcription (RT-qPCR)

Five hundred nanogram of the total RNA extracted from the SG of non-infected (AaC) or infected (AaI) ticks were treated with RQ1 RNase-free DNase (Promega, United States) and reverse transcribed (RT) into cDNA using M-MLV Reverse Transcriptase (Thermo Fisher Scientific, United States), as detailed by the manufacturer. The resulting cDNA was used as a template in qPCR with the Maxima SYBR Green/ROX qPCR MasterMix (Thermo Fisher Scientific, United States) and specific primers for selected CDSs (**Supplementary Table 3**). Primers were designed using Primer3 (Rozen and Skaletsky, 2000) and synthesized by Thermo Fisher Scientific (United States). qPCR was performed on a StepOne Plus thermocycler (Thermo Fisher Scientific, United States) using the following program: 95°C for 10 min followed by 40 cycles at 95°C for 15 s, 60°C for 60 s, and 72°C for 20 s. The $2^{-\Delta\Delta Ct}$ equation was utilized to calculate the relative expression of select genes in infected versus non-infected ticks or exposed versus infected ticks (Livak and Schmittgen, 2001). The encoding gene of the ribosomal protein S3A was used as reference (Martins et al., 2017). At least three biological replicates of each group were analyzed. Student's *t*-test was used to statistically validate the differentially expressed CDSs.

RNA Interference in Ticks

The knockdown of microplusin (CDS Ambaur-69859) was induced by injection of double-stranded RNA (dsRNA) into adult tick hemocoel as described by Kocan et al. (2011). Briefly, specific primers containing T7 promoter sequence (**Supplementary Table 3**) were used to amplify the target sequence (Ambaur-69859) by PCR. The non-related dsRNA of the merozoite surface protein 1 (MSP1) of *Plasmodium falciparum* was used as control (**Supplementary Table 3**; Kalil et al., 2017). The resulting products were purified using PCR Purification GeneJet™ kit

TABLE 1 | Selected CDSs of *A. aureolatum* salivary glands differentially expressed by infection with *R. rickettsii*.

CDS	Annotation	Functional class	Fold-change	
			RNA-seq	RT-qPCR
Ambaur-1956	Cytochrome P450	Detoxification/oxidation	9.16	NA
Ambaur-60624	Cytochrome P450		5.02	NA
Ambaur-67466	Cytochrome P450		5.32	NA
Ambaur-45304	Cytochrome P450		5.48	NA
Ambaur-36571	Cytochrome P450		9.12	NA
AmbarSigP-56564	Cytochrome P450		8.01	NA
Ambaur-60175	Cytochrome P450		11.74	2.27*
Ambaur-61062	Cytochrome P450		0.17	NA
Ambaur-47534	Glutathione *S*-transferase		5.16	NA
Ambaur-23052	Glutathione *S*-transferase		7.49	NA
Ambaur-18924	Peptidoglycan recognition protein	Immunity	5.81	NA
AmbarSigP-61895	α-Macroglobulin		22.12	NA
AmbarSigP-5190	α-Macroglobulin		17.87	0.65
Ambaur-69859	Microplusin		8.52	4.71*
Ambaur-25218	Microplusin		5.93	NA
AmbarSigP-22173	Microplusin	Secreted	0.10	0.44*
Ambaur-50152	5.3 kDa antibacterial peptide		0.00	NA
Ambaur-19862	5.3 kDa antibacterial peptide		0.16	0.005
AmbarSigP-47654	Lipocalin		37.90	3.12
Ambaur-47378	Basic tail protein		6.42	133,707.32**
AmbarSigP-70152	Basic tail protein		0.02	0.05**
Ambaur-6577	8.9 kDa protein		0.05	0.18
Ambaur-54200	Secreted protein		0.13	141.58*
Ambaur-4333	Salivary secreted protein of 21.3 kDa	Unknown conserved	11.46	0.79
Ambaur-22275	Polyubiquitin	Proteasome machinery	5.84	NA
Ambaur-53071	Histone 2B	Nuclear regulation	6.44	NA

Only CDSs with statistically significant differences in expression in the salivary glands of infected vs. control (non-infected) ticks, identified by RNA-seq analysis, are presented. Some CDSs were additionally analyzed by RT-qPCR ($p < 0.05$ and **$p < 0.01$; Student's t-test). NA, relative expression not analyzed by RT-qPCR.*

(Thermo Fisher Scientific, United States). One microgram of the purified cDNA was utilized to synthesize dsRNAs using the T7 Ribomax Express RNAi System kit (Promega, United States).

To evaluate the effects of gene silencing on the acquisition of *R. rickettsii*, non-infected adult ticks were injected with 10^{11} molecules of either dsMicroplusin (333 base pairs) or dsMSP1 (666 base pairs) in 69 nL of PBS (12 ticks in each group). An injection was administered in the coxal membrane located at the base of the fourth leg using Nanoject II equipment (Drummond). After injection, ticks were kept in an incubator at 25°C and 95% RH for 24 h. Ticks were fed on infected rabbits during the bacteremia peak. After 3 days, ticks were manually removed, and SG and MG were dissected as described above.

To evaluate the effects of silencing on the transmission of *R. rickettsii*, adult ticks infected during feeding of the larval stage were injected with specific dsRNA using the same equipment and procedure described above (60 ticks in each group). Twenty-four hours after dsRNA administration, ticks were allowed to feed on non-infected rabbits (30 ticks per rabbit). After 5 days, six ticks from each group were manually removed and SG were dissected. The rectal temperature of rabbits was monitored daily and fever was considered when the temperature was higher than 40°C. Skin biopsies of the rabbits were performed on days 3, 10, and 21 after the beginning of tick feeding using 3 mm punches under local anesthesia. In addition, blood samples of all rabbits were collected on days 0 and 21 postinfestation for immunofluorescence assays (IFA), as detailed by Horta et al. (2008).

To determine the effects of gene silencing on *A. aureolatum* fitness, non-infected adults were injected with either dsMicroplusin or dsMSP1. Ticks fed on one non-infected dog until they were completely engorged. Females were individually weighted and transferred to an incubator at 25°C and 95% RH. After the end of oviposition, the egg mass of each female was weighted. The fertility rate was obtained by calculating the ratio between the weight of the egg mass and the weight of each female.

To evaluate gene silencing, total RNA extracted from tick organs was used as a template in RT-qPCR following the same procedure described above. To calculate the percentage of gene silencing in ticks injected with dsMicroplusin, we considered the levels of their respective transcripts in the control group as 100%. The gDNA extracted from tick organs and from skin biopsies of rabbits was used as a template in qPCR for *R. rickettsii* quantification, as described above. Differences in the microplusin gene expression, rickettsial load, and tick fitness parameters were analyzed between dsMicroplusin and dsMSP1

groups by Mann–Whitney test using GraphPad Prism version 7.0 for Windows (GraphPad Software, United States) and considered significant when $p < 0.05$.

RESULTS

Identification of Differentially Expressed CDSs in SG of *A. aureolatum* Ticks in Response to the *R. rickettsii* Infection

Approximately 242 million reads were obtained from the analysis of RNA samples extracted from *A. aureolatum* organs by RNA-seq, among which nearly 110 million reads corresponded to SG samples [number of reads in SG infected (AaI): 50,475,296; number of reads in SG control (AaC): 59,846,982]. The total of 242 million reads was assembled into 11,906 CDSs from which 11,903 are expressed in SG and 11,888 in MG (**Supplementary Table 1**).

From the 11,903 CDSs expressed in SG, 161 were upregulated by infection while 99 were downregulated (**Supplementary Table 1** and **Table 1**). The majority of modulated CDSs encode putative secreted proteins (72 upregulated and 68 downregulated) (**Figure 1**), including lipocalins and Kunitz-type inhibitors. Twelve CDSs of putative secreted lipocalins were downregulated by infection, while only six were upregulated. Regarding CDSs encoding putative secreted Kunitz-type inhibitors, seven were downregulated and only one was upregulated by infection (**Supplementary Table 1**). The functional classes detoxification/oxidation, transposon elements, signal transduction, protein modification, transporter and channels, metabolism, and extracellular matrix comprise CDSs mostly upregulated by infection (**Figure 1**). In the detoxification/oxidation category, seven CDSs encoding cytochrome P450 (CYP) were upregulated in the SG of infected ticks, while only one was downregulated (**Supplementary Table 1**, **Table 1**, and **Figure 1**). In addition, two glutathione *S*-transferase (GST) CDSs were upregulated in response to infection and none was downregulated (**Supplementary Table 1** and **Table 1**).

The functional categories of nuclear regulation, proteasome machinery, storage, and transcription factors are represented exclusively by upregulated CDSs and each of them is composed of only one CDS (**Figure 1**). Among them, we highlight one polyubiquitin (Ambaur-22275) and one histone 2B (Ambaur-53071) encoding sequences, included in proteasome machinery and nuclear regulation categories, respectively. In the immunity category, five CDSs were upregulated by infection: one peptidoglycan receptor protein (PGRP; Ambaur-18924), two α-macroglobulins (AmbarSigP-61895 and AmbarSigP-5190), and two antimicrobial peptides (AMPs) similar to the microplusin of *R. microplus* (Fogaca et al., 2004) (Ambaur-69859 and Ambaur-25218) (**Table 1**). Moreover, one CDS of a trypsin-inhibitor like (TIL) (Ambaur-46428), a type of protease inhibitor previously reported to exhibit antimicrobial activity (Fogaca et al., 2006; Wang et al., 2015), was also upregulated by *R. rickettsii*. Conversely, one microplusin (AmbarSigP-22173) and two 5.3 kDa antimicrobial peptides (Ambaur-50152 and Ambaur-19862), were downregulated in infected ticks in relation to the control (**Supplementary Table 1** and **Table 1**).

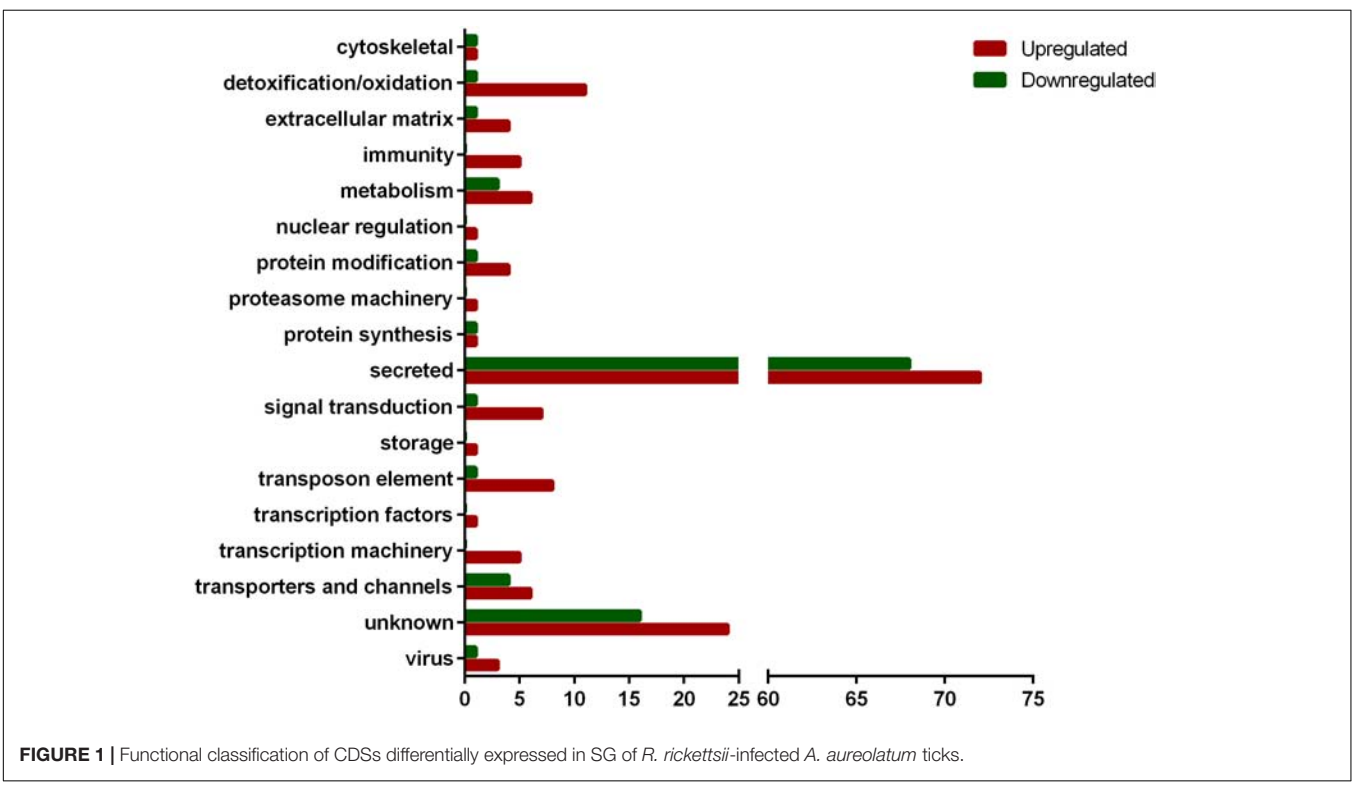

FIGURE 1 | Functional classification of CDSs differentially expressed in SG of *R. rickettsii*-infected *A. aureolatum* ticks.

The expression of 11 CDSs was further analyzed by RT-qPCR (**Table 1**). Five of them [two microplusins (Ambaur-69859 and AmbarSigP-22173), one cytochrome P450 (Ambaur-60175), and two basic tail proteins (Ambaur-47378 and AmbarSigP-70152)] were significantly modulated in infected versus control ticks, exhibiting the same transcriptional profile observed in RNA-seq. Three additional CDSs [one 5.3 kDa antimicrobial peptide (Ambaur-19862), one lipocalin (AmbarSigP-47654) and one 8.9 kDa protein (Ambaur-6577)] presented the same expression pattern previously obtained by RNA-seq, but their expression levels in infected ticks were not significantly different in relation to control ticks. Likewise, the transcription of the CDSs Ambaur-4333 and AmbarSigP-5190, which encode a salivary secreted protein of 21.3 kDa and an α-macroglobulin, respectively, was not significantly different in infected versus control ticks. One CDS of a putative secreted protein (Ambaur-54200) presented the opposite pattern obtained by RNA-seq, detected as significantly upregulated in infected ticks by RT-qPCR.

Microplusin Functional Study on *R. rickettsii* Acquisition and Transmission

Besides being significantly upregulated by infection in SG of infected ticks, the CDS Ambaur-69859, which encodes the antimicrobial peptide microplusin, was also upregulated in MG (**Figure 2**). The MSA analysis of the amino acid sequence of *A. aureolatum* microplusin with microplusins of different species of soft and hard ticks showed that all sequences present a conserved signal peptide as well as six conserved cysteine residues (**Figure 3A**). The mature peptide of all sequences starts with two histidine residues, except for *Amblyomma triste*, which sequence starts with an aspartate residue followed by two histidine residues. All of them also exhibit a histidine-rich C-terminal with a variable number of histidine residues after the last cysteine residue, ranging from two (*A. triste* and *Hyalomma excavatum*) to 12 (*Ixodes ricinus*). The phylogenetic tree showed that all species in the genus *Amblyomma* cluster together, with the exception of *A. triste* (**Figure 3B**). In fact, this last species is the most distant sequence in relation to the *Amblyomma* cluster and lays with soft ticks (genera *Argas* and *Ornithodoros*). The hard ticks *R. microplus* and *H. excavatum* cluster together and with other species in the genus *Rhipicephalus*. Microplusins of the two analyzed species of the genus *Ixodes* (*Ixodes ricinus* and *Ixodes scapularis*) also cluster together and are close to soft ticks.

The CDS Ambaur-69859 was selected for the functional studies assessed by RNAi experiments. Specific dsRNA for either microplusin or MSP1 (control) were injected into the hemocoel of *A. aureolatum*. A survival rate of 100% was obtained 24 h post-injection and ticks were then fed on infected rabbits. A high efficiency of microplusin silencing of around 97.9% in the MG (**Figure 4A**) and 99.8% in the SG (**Figure 4B**) was obtained. A higher prevalence of ticks with infected MG was obtained in the group of ticks that received dsMicroplusin (58.3%) in comparison with the control group (16.7%). The prevalence of ticks with infected SG was also higher in the dsMicroplusin group (33.3%) than in the dsMSP1 group (8.3%). In addition, the rickettsial load of one order of magnitude was higher in the MG of ticks that received dsMicroplusin, with significant differences in comparison to the control (**Figure 4C**). The rickettsial load was also higher in SG of ticks from dsMicroplusin group, although not significant (**Figure 4D**).

The effects of microplusin knockdown on the transmission of *R. rickettsii* to rabbits were also evaluated. To that end, *R. rickettsii*-infected ticks were injected with either dsMicroplusin or dsMSP1. Despite the fact that the microplusin expression had been significantly silenced in the group that received dsMicroplusin in relation to the control group (**Figure 5A**), no difference was identified between both groups. All rabbits exhibited fever, were *R. rickettsii*-positive in skin biopsies and/or died during the course of infestation, independently on the tick group that they were exposed to (**Table 2**). The rickettsial load in the SG of ticks removed from the rabbits 5 days after the beginning of feeding was similar in both groups (**Figure 5B**).

To evaluate the effect of microplusin knockdown on the fitness of *A. aureolatum* adult females (**Figure 6**), engorged females were weighted (**Figure 6A**) as well as their laid eggs (**Figure 6B**) and used to calculate their fertility rate (**Figure 6C**). No significant difference was detected among all fitness parameters in microplusin silenced ticks when compared to the control group.

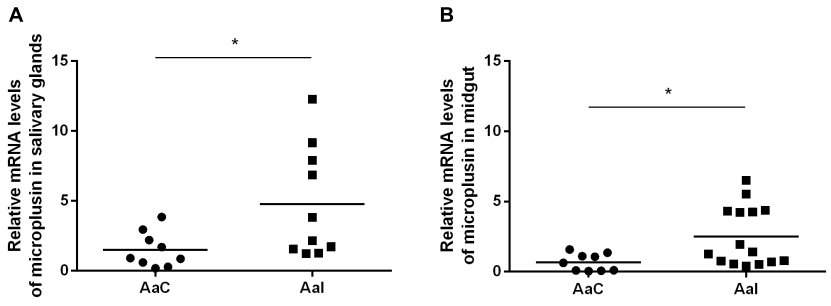

FIGURE 2 | Relative expression of microplusin in salivary glands **(A)** and midgut **(B)** of ticks infected (AaI) or not (control; AaC) with *R. rickettsii* by RT-qPCR (*$p < 0.05$; Mann–Whitney test).

A

```
Amblyomma triste                MHSKMLVSLMLVGLLGLASADHHRPQSVCALEGDAQRALVECIRGNLDEPTTTKLQAVKERLQCEELHCVFVKICERNNGTLEH
Rhipicephalus zambeziensis      MKA-FLVCALLATVATVSFAHH---LELCKKQDEQLKTELQCIGLHISAEANQSFDKALKTLGCQDRSCVIRKLCAGND--LEG
Rhipicephalus appendiculatus    MKA-FLVCALLATVATVSFAHH---LELCKKQDEQLKTELQCIGLHISAEANQSFDKAMKTLGCQDRSCVIRKLCAGND--LEG
Rhipicephalus pulchellus        MKA-FMVCALLATFAAVCFAHH---LELCKKQDDQLRTELQCIGLHISAEANQSFNKAVKTLGCQDWSCVIRKLCVGND--LEA
Amblyomma maculatum             MNAVFASCMFVAAFVAATSAHH---LELCKKSDEVLATELECIKQHIPASTGAAFGDAMQKLQCSNPSCAVRKMCEGND--LEG
Amblyomma hebraeum              MNAVFASCLIVAALVAFASAHH---LELCKKNDQVLATELECIKQHIPAETNAAFDEAVTKLQCSDRSCAIRKLCEGND--LEG
Amblyomma aureolatum            MNAVFASCLFVATLVAAASAHH---LELCKKTDQVLATELECIKQHIPATTNAAFDDAVQKLKCSDRSCAIRKMCEGND--LEG
Amblyomma americanum            MKAVLASSLFVAALVAATSAHH---LELCKKNDQVLATELECIKQHIPESTNAAFDDTVQKLECSDRSCAIRKMCEGND--LEA
Amblyomma sculptum              MKAVFASCLFVVALVAAASAHH---LELCKKNDQVLATELECIKQHIPESTNAAFDDAVKKLECSDRSCAIRKMCEGND--LEG
Hyalomma excavatum              MKAVFLSALLVVALVASSSAHH---LELCKKTDDVLVTELECIKHHITPPVNVAFDDAVQQLGCPDRACAIRKMCATND--LEA
Rhipicephalus microplus         MKAIFVSALLVVALVASTSAHH---QELCTKGDDALVTELECIRLRISPETNAAFDNAVQQLNCLNRACAYRKMCATNN--LEQ
Ixodes ricinus                  MKS-LLVCLVLAVVVLVASGHH---VELCKKNDAELKEALTCITSKLPEALNTKFNEVEKQVGCNDKSCVFEKLCKEGD--LDE
Ixodes scapularis               MKS-LLVCLVLAVLVLVASGHH---VELCKNNDAELKEALTCITSKLPAALNTKFSHVEKQLGCNDKSCVFGKLCKAGD--LDE
Argas monolakensis              MKS-LLVLALLAFGAVLVSAHH---LEMCEKSTDELREQLVCHRQHATGAFNAKLDQVNRQLRCNNDICTFKKLCDAPD--FLT
Ornithodoros parkeri            MKG-FFSVAALAAVLLLASSHH---LDLCDKDDQELRDQLQCQRNQATAEFKRKFDRVNRQLQCDSDLCSIRKMCAEPD--FLT
Ornithodoros turicata           MKG-LFGVAVLAAVVLLASAHH---LELCKKADKPLKDQLKCQRDHATPAFNSKFDSVNKQLQCDSDFCTIRKLCAEPD--FET
Ornithodoros coriaceus          MKG-LLGVAVLAVVVFVASAHH---LDLCQKDDQELREQLKCQXDHAAAEFNRKFDRVNRQLQCDSDFCSVRKMCAEPD--FET
                                *:. :    :.       . *    .:*          : *   .        :  .   : * .  *   *:*   :  :

Amblyomma triste                SGNAFFEDNEKLALRNAVVTC-------------------RDGA--HH-----------
Rhipicephalus zambeziensis      AMADHFTKAQITEIHNAATTCDPEAG--------------HGHH--HPH----------
Rhipicephalus appendiculatus    AMADHFTKAQITEIHNAATTCDPEAG--------------HGHH--HPH----------
Rhipicephalus pulchellus        AMANHFTKSQISEIHSASTICDPEAG--------------HSHH--HH-----------
Amblyomma maculatum             AMAKYFTTEQIKHVHDAATTCDPDAS--------------HDHG--HDHGH--------D
Amblyomma hebraeum              AMAKYFTPEQIKHVHDAALTCDPDAR--------------HDHD--HDHGHGHGHDHDPH
Amblyomma aureolatum            AMAKFFTTEQIKHIHDASTTCAPDAH--------------HGHD--HSHDH----GH--H
Amblyomma americanum            AMAKFFTAEQIKHVHDAATTCDPDAH--------------HDHG--HDHGHDHGDGH--H
Amblyomma sculptum              AMAKFFTAEQIKHVHDAATTCDPDSH--------------HDHG--HDHGH--------H
Hyalomma excavatum              AMSIYFSKEQISEIHDAATACDPDVQ--------------HGEG--H------------
Rhipicephalus microplus         AMSVYFTNEQIKEIHDAATACDPEAH--------------HEHD--H------------
Ixodes ricinus                  ALKKHFTAAEVQTLHTTATDCDHSHGHEHSHGHEHGHGQEHGHG--HH-----------
Ixodes scapularis               ALKKHFTAAEIKTFHTTATDCDHSHGHEHS----------HGHG--HH-----------
Argas monolakensis              ELRKYFTESEINELHELANQCDPDAH--------------HDHPHCHPH----------
Ornithodoros parkeri            ALKRFFTEGEIEELHELANQCDAAAMDS------------HGQD--PH-----------
Ornithodoros turicata           ALKKFFTESEIQVLHELANHCDPDSPTGHDM---------HAHD--HHH----------
Ornithodoros coriaceus          ALKKYFTESEVEVLHHLANHCDRDSH--------------HDHD--HHH----------
                                    .*   :   ..     *                    .
```

B

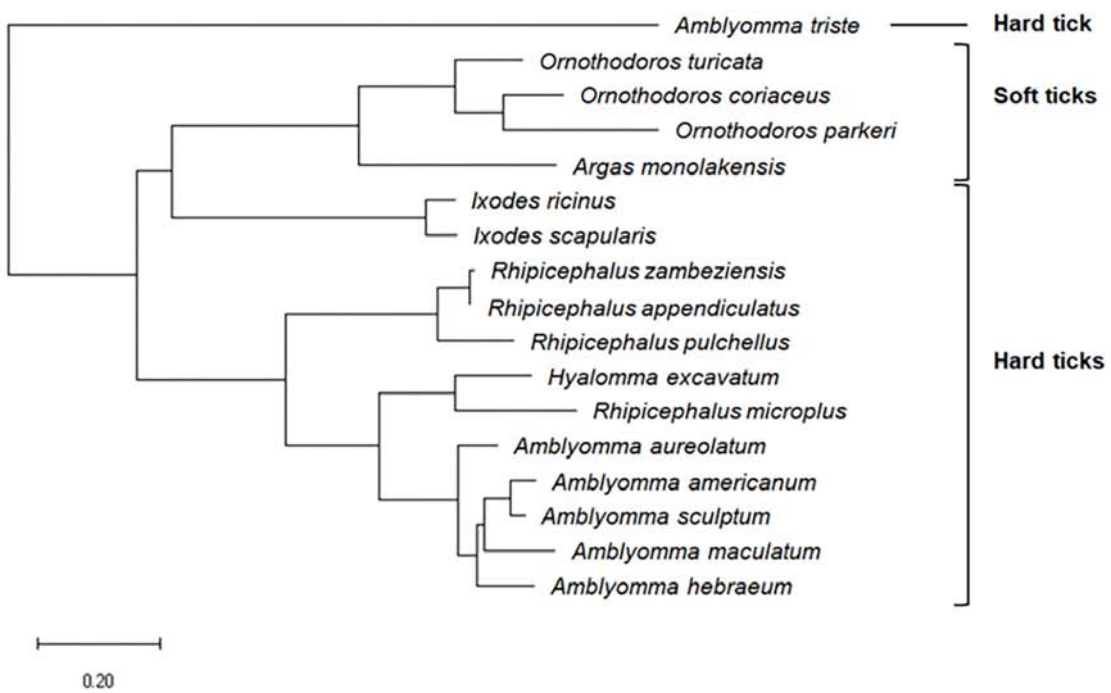

FIGURE 3 | MSA and phylogenetic analysis of microplusins. **(A)** Multiple sequence alignment of protein sequences was performed using MUSCLE method. Asterisks highlight the conserved cysteine residues; italic letters show the signal peptide; bold letters indicate histidine residues in the C-terminal. **(B)** A phylogenetic tree was constructed with protein sequences using Maximum Likelihood (ML) method. The analysis involved 17 amino acid sequences (accession numbers available in **Supplementary Table 2**). Bar scale at the bottom indicates 20% amino acid divergence.

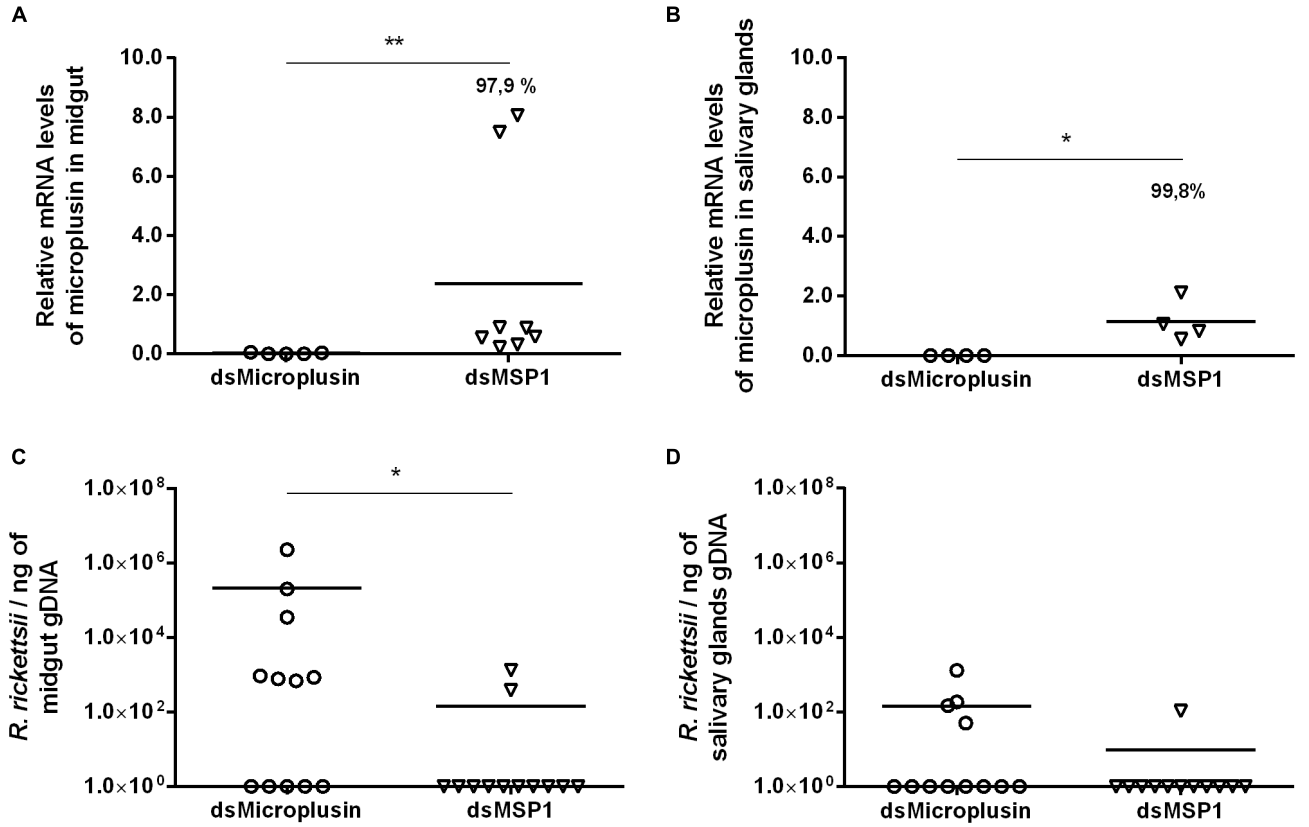

FIGURE 4 | Effect of RNAi-mediated silencing of microplusin in *R. rickettsii* acquisition by *A. aureolatum*. Specific dsRNA for either microplusin (dsMicroplusin) or MSP1 (dsMSP1; control) were injected into the hemocoel of non-infected ticks. After 24 h, ticks were fed on *R. rickettsii*-infected rabbits for 3 days. The relative expression of microplusin in midgut **(A)** and salivary glands **(B)** of ticks injected with dsMicroplusin in relation to the control was assessed by RT-qPCR and the rickettsial load in MG **(C)** and SG **(D)** by qPCR (*$p < 0.05$ and **$p < 0.005$; Mann–Whitney test).

DISCUSSION

Pathogens acquired by ticks within the blood meal have to overcome several barriers within ticks, including the MG, hemolymph, and SG, to be efficiently transmitted to another host. Each of these organs plays a decisive role in the tick vector competence for a particular pathogen (Ueti et al., 2007; Hajdušek et al., 2013). We have previously reported the effects of *R. rickettsii* on the global gene expression profile of the MG of *A. aureolatum* and *A. sculptum* (Martins et al., 2017). In the current study, we report the transcriptional profile of the SG of *A. aureolatum* in response to infection with this same pathogen. To date, the availability of, albeit partial, genomes of ticks is restricted to *I. scapularis* (Gulia-Nuss et al., 2016). Therefore, this transcriptomic study provides a rich source for tick sequences in the genus *Amblyomma*.

Around 242 million reads obtained by RNA-seq of RNA samples extracted from organs of *A. aureolatum* were assembled into 11,906 CDSs. Transcripts of the majority of assembled CDSs were detected with at least one read in tick SG, among which 21.2% encode proteins with a signal peptide for secretion. This result is in accordance with the secretory role played by tick SG (Bowman and Sauer, 2004; Kaufman, 2010). CDSs of putative secreted proteins count for 53.8% of the total of sequences modulated by *R. rickettsii* infection. From those, we highlight CDSs of lipocalins and Kunitz inhibitors, which were mostly downregulated by infection. Lipocalins are proteins of tick saliva that possess the property of binding the inflammatory mediators histamine and serotonin and, therefore, they play an anti-inflammatory role (Paesen et al., 1999; Sangamnatdej et al., 2002). A tendency of higher *Babesia bovis* infection, despite not significant, was observed in the larval progeny of lipocalin-silenced *R. microplus* females (Bastos et al., 2009). Besides downregulation in SG, our previous study showed that most CDSs of lipocalins were also downregulated in the MG of *A. aureolatum* in response to *R. rickettsii* infection. In contrast to the *A. aureolatum* pattern, all modulated CDSs of lipocalins were upregulated in the MG of infected *A. sculptum* (Martins et al., 2017). Therefore, it is possible that inflammatory components acquired within the blood meal exert a detrimental effect on the MG epithelium, enabling *A. aureolatum* to be more susceptible to infection than *A. sculptum*.

Most of the CDSs of Kunitz inhibitors modulated by infection were downregulated in the SG of *A. aureolatum*, as previously described for the tick MG (Martins et al., 2017). Conversely, all modulated CDSs of Kunitz inhibitors were upregulated in the

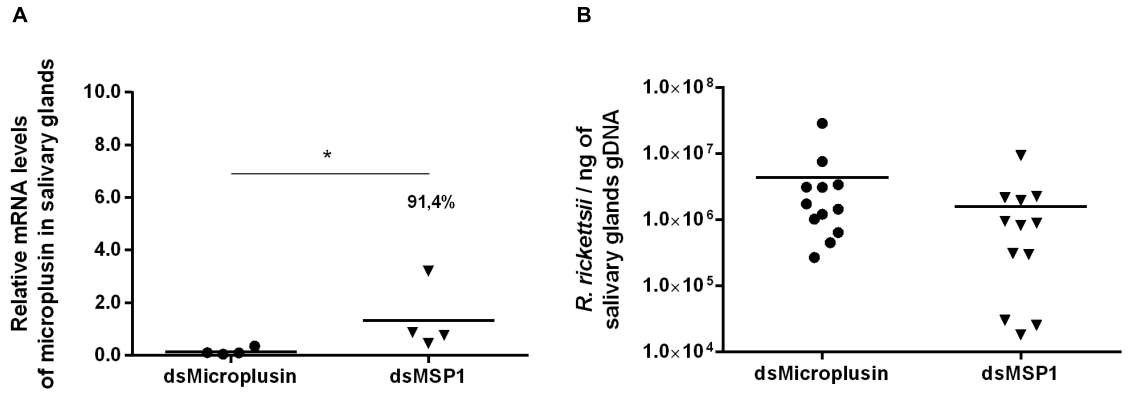

FIGURE 5 | Relative expression of microplusin and rickettsial load in ticks used to evaluate the effects of gene-knockdown on *R. rickettsii* transmission to rabbits. Specific dsRNA for either microplusin (dsMicroplusin) or MSP1 (dsMSP1; control) were injected into the hemocoel of *R. rickettsii*-infected ticks. After 24 h, ticks were fed on non-infected rabbits for 5 days. The relative expression of microplusin **(A)** and the rickettsial load **(B)** in SG of ticks injected with dsMicroplusin in relation to the control were assessed by RT-qPCR and by qPCR, respectively (*$p < 0.05$; Mann–Whitney test).

TABLE 2 | Effect of RNAi-mediated silencing of microplusin in *R. rickettsii* transmission to rabbits.

Tick group	Rabbit	Fever (>40°C)	Skin biopsy positive in qPCR	Death	IFA
dsMicroplusin	1	On days 7–8th	1.33×10^2	On day 11th	NA
	2	On days 7–10th	–	–	+
dsMSP1	3	On days 7–12th	–	–	+
	4	On days 8–9th	3.18×10^2	On day 13th	NA

Specific dsRNA for either microplusin (dsMicroplusin) or MSP1 (dsMSP1; control) were injected into the hemocoel of infected ticks. After 24 h, ticks were fed on non-infected rabbits. The temperature of all animals was daily evaluated, and it was considered fever when >40°C. gDNA extracted from skin biopsies of rabbits was used as template in qPCR for R. rickettsii detection. Blood samples of survive rabbits were collected on day 21 postinfestation and tested for anti-R. rickettsii reactive antibodies by IFA. NA, not analyzed.

MG of infected *A. sculptum* (Martins et al., 2017). It is known that Kunitz inhibitors of tick saliva exert an inhibitory activity on blood coagulation, assuring the acquisition of a fluid blood meal (Corral-Rodriguez et al., 2009; Francischetti et al., 2009). Moreover, it was previously reported that a Kunitz inhibitor of *Dermacentor variabilis* possesses a bacteriostatic effect against the non-virulent *Rickettsia montanensis* (Ceraul et al., 2008) and that its knockdown increases tick infection (Ceraul et al., 2011). Therefore, it is plausible to suppose that Kunitz inhibitors may also exhibit an antimicrobial activity against *R. rickettsii*, controlling infection in the MG of *A. sculptum* and culminating in a low susceptibility to infection.

Considering upregulated CDSs identified in the current study, some are included in the detoxification/oxidation category and code CYPs and GSTs. CYPs constitute an ancient protein family ubiquitous in nature and have been described to play different roles, being involved in pesticide detoxification as well as in the synthesis of different important endogenous molecules, such as hormones (Werck-Reichhart and Feyereisen, 2000). Sixty-eight CDSs of CYPs were detected in the *A. aureolatum* transcriptome, among which seven were upregulated and only one was downregulated in the SG of infected ticks. The upregulation of CYP genes in response to infection was previously reported, for instance in the mosquito *Aedes aegypti* (Behura et al., 2011) and in the honeybee *Apis mellifera* (Cornman et al., 2013). Intriguingly, the knockdown of CYP by RNAi reduced the infection of the mosquito *Anopheles gambiae* by *Plasmodium berghei* (Felix and Silveira, 2011). GSTs, which are involved in the detoxification of xenobiotics and oxidative stress (Pavlidi et al., 2018), were also previously reported to be upregulated by infection in arthropods, such as ticks (Mulenga et al., 2003; Mercado-Curiel et al., 2011; Bifano et al., 2014). For instance, one CDS of glutathione *S*-transferase was upregulated in the cell line BME26 of *R. microplus* and also in both MG and SG adult males by infection with *Anaplasma marginale*, the causative agent of bovine anaplasmosis. However, GST knockdown induced by RNAi presented no effect in either the acquisition of *A. marginale* by ticks or transmission to calves (Bifano et al., 2014). On the other hand, GST-knockdown reduced the acquisition of *A. marginale* by the tick *D. variabilis*, suggesting that the susceptibility response obtained by GST-silencing depends on the tick species and/or the pathogen strain (Kocan et al., 2009).

One polyubiquitin (Ambaur-22275), included in proteasome machinery category, was also upregulated in the SG of infected *A. aureolatum*. The upregulation of a polyubiquitin was previously reported to occur in the cell line IDE8 of *I. scapularis* in response to the infection of *A. marginale* (de la Fuente et al., 2007). The ubiquitination of proteins is a well-known signal for the degradation of protein in the proteasome, but it is also involved in the signaling of many other cellular processes

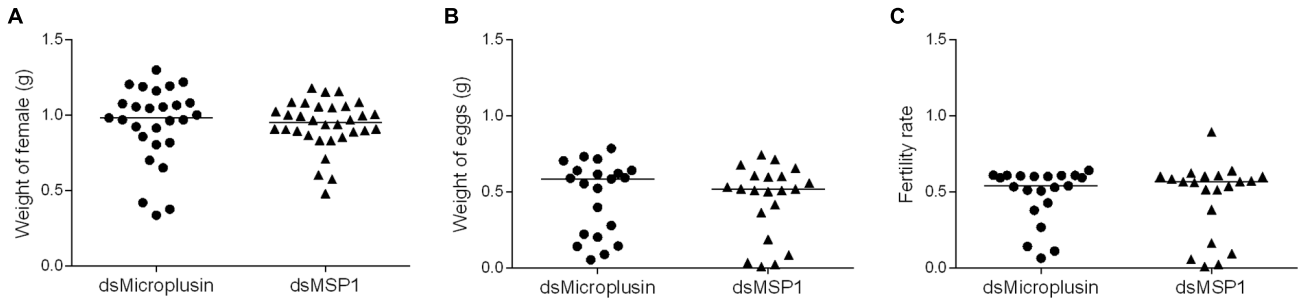

FIGURE 6 | Effects of RNAi-mediated silencing of microplusin on tick fitness. Specific dsRNA for either microplusin (dsMicroplusin) or MSP1 (dsMSP1; control) were injected into the hemocoel of non-infected ticks. After 24 h, ticks were fed on one non-infected dog. The weight of engorged ticks **(A)**, weight of the egg mass **(B)**, and fertility rate **(C)** were recorded.

(Welchman et al., 2005). Interestingly, the knockdown of the E3 [named x-linked inhibitor of apoptosis protein (XIAP)] of *I. scapularis* by RNAi restricted the proliferation of *Anaplasma phagocytophilum*, the causative agent of human granulocytic anaplasmosis (Severo et al., 2013).

The transcriptional level of one sequence coding for a histone 2B (Ambaur-53071), included in nuclear regulation, was also higher in the SG of infected *A. aureolatum*. The upregulation of histone 2B expression was already observed in the SG and MG of the tick *I. scapularis* infected with *A. phagocytophilum* (Cabezas-Cruz et al., 2016). The knockdown of the histone 2B of *I. scapularis* by RNAi was reported to impair the invasion of the cell line ISE6 by *Rickettsia felis*, an agent of flea-borne spotted fever. Moreover, it was shown that histone 2B interacts with the outer membrane protein B of *R. felis*, suggesting that it might play a role in cell invasion (Thepparit et al., 2010).

Some immunity components were also differentially expressed in the SG of infected *A. aureolatum*. Among them, one sequence encoding PGRP (Ambaur-18924) was upregulated. PGRPs are classified into non-catalytic or catalytic depending on the presence of an amidase catalytic site. The non-catalytic PGRPs act as pathogen pattern recognition receptors and activate the Toll and Imd pathways, as demonstrated in *Drosophila*. On the other hand, catalytic PGRPs cleave peptidoglycan, acting as either effectors, by exerting an antibacterial activity, or negative regulators of the immune response, by performing the clearance of peptidoglycan (Palmer and Jiggins, 2015). As the PGRP putatively coded by CDS Ambaur-18924 exhibits the amidase catalytic site (data not shown), it may play a role as an effector or negative regulator of tick immune signaling pathways. Two α-macroglobulins (AmbarSigP-61895 and AmbarSigP-5190) were also upregulated by infection. Alpha-macroglobulins are members of the family of thioester-containing proteins (TEPs) (Buresova et al., 2011; Urbanova et al., 2015). Interestingly, the knockdown of α2-macroglobulins mediated by RNAi diminished the phagocytosis of *Chryseobacterium indologenes* by the hemocytes of *I. ricinus* (Buresova et al., 2011). Additionally, the transcriptional levels of one trypsin-inhibitor like (TIL) encoding sequence (Ambaur-46428), a type of protease inhibitors that exhibit antimicrobial activity (Fogaca et al., 2006; Wang et al., 2015), was also higher in infected *A. aureolatum* ticks.

The immune system of invertebrates, including arthropods, is simpler than the immune system of vertebrates, lacking the adaptive response (Baxter et al., 2017). In this context, effector molecules, such as the aforementioned factors and AMPs, play a central role, acting directly against pathogens (Bulet et al., 2004). Interestingly, it was previously reported that the AMP defensin-2 reduces the *R. montanensis* load in the MG of the tick *D. variabilis* (Pelc et al., 2014). In addition, it was shown that this AMP causes the death of *R. montanensis* through lysis and leakage of cytoplasmic proteins (Pelc et al., 2014). Two microplusin CDSs (Ambaur-69859 and Ambaur-25218) were upregulated in the SG of *A. aureolatum* ticks by *R. rickettsii*. Besides being significantly upregulated by infection in the SG of infected ticks, the CDS Ambaur-69859 was also detected to be upregulated in MG. Microplusin is a 10,204 kDa AMP that was originally identified in the hemolymph (Fogaca et al., 2004) and lately in the ovary and eggs (Esteves et al., 2009) of *R. microplus*. Interestingly, this AMP is also upregulated in the SG and MG of *A. marginale*-infected *R. microplus* (Capelli-Peixoto et al., 2017). We therefore targeted the microplusin encoded by the CDS Ambaur-69859 to analyze the effects of its knockdown in the acquisition of the bacterium *R. rickettsii* by *A. aureolatum*. A higher prevalence of infected ticks was obtained in the dsMicroplusin injected group than in the control group, showing that microplusin silencing benefited *R. rickettsii* establishment within the tick. Moreover, the rickettsial load was also higher in both SG and MG of ticks that received dsMicroplusin, demonstrating that this AMP is important for the control of infection in both organs. On the other hand, microplusin knockdown showed no detectable effect on the transmission of *R. rickettsii* to rabbits. All together, these results show that microplusin plays a protective role against tick infection by *R. rickettsii* but does not exert any detectable effect on the bacterial transmission to rabbits after SG had already been infected by this bacterium. In addition, ticks that received either dsMicroplusin or dsMSP1 showed no significant differences in engorgement and oviposition, showing that the silencing of this AMP presents no effect on tick fitness.

The MSA analysis of the amino acid sequence of *A. aureolatum* microplusin with the amino acid sequences of microplusins of different species of ticks showed all of them exhibit six conserved cysteine residues and a histidine-rich

C-terminal. Interestingly, the histidine-rich C-terminal of the microplusins of *R. microplus* (Silva et al., 2009, 2011) and *A. hebraeum* (Lai et al., 2004), which is named hebraein, was enrolled with their antimicrobial activity. Indeed, the histidine residues of the microplusin of *R. microplus* have the property of chelating metallic ions, such as copper, affecting the respiration of the Gram-positive bacterium *Micrococcus luteus* (Silva et al., 2009) and the fungus *Cryptococcus neoformans* (Silva et al., 2011). In addition, the copper-binding property of microplusin also alters the melanization and formation of the polysaccharide capsule of *C. neoformans* (Silva et al., 2011). Therefore, it would be interesting to determine the mechanism of action of microplusin against *R. rickettsii*.

CONCLUSION

In conclusion, our data show that *R. rickettsii* exerts a modulatory effect on the transcriptional profile the SG of *A. aureolatum*. Moreover, RNAi experiments demonstrated that the knockdown of one microplusin increases the susceptibility of ticks to infection, suggesting that this is one important factor for the control of *R. rickettsii*. The functional characterization of the additional CDSs modulated by infection is warranted and might reveal other factors that interfere with the acquisition and/or transmission of this tick-borne pathogen.

ETHICS STATEMENT

All procedures involving vertebrate animals were carried out according to the Brazilian National Law number 11794 and approved by the Institutional Animal Care and Use Committees from the Faculty of Veterinary Medicine and Zootechnics (protocol number 1423/2008) and the Institute of Biomedical Sciences (protocol number 128/2011), University of São Paulo, São Paulo, Brazil. This study does not involve experimentation with human beings.

AUTHOR CONTRIBUTIONS

ACF designed the experiments. LM, CM, MG, and FC generated the biological samples. LM, CM, and MG performed the experiments. JR performed the bioinformatics data analysis. LM, ACF, JR, and AF analyzed the RNA-seq, RNAi, and RT-qPCR data. JR, AF, and LM performed the statistical data analysis. ACF, JR, AF, ML, EE, and SD contributed to reagents, materials, and analysis tools. ACF and LM wrote the manuscript. SD, MG, ML, AF, and JR critically revised the manuscript. All authors read and approved the final manuscript.

FUNDING

This work was supported by funds from the São Paulo Research Foundation (FAPESP; Grants 2008/053570-0 and 2013/26450-2), the National Council for Scientific and Technological Development [CNPq; Grants CNPq 573959/2008-0; The National Institutes of Science and Technology Program in Molecular Entomology (INCT-EM)], the Coordination for the Improvement of Higher Education Personnel (CAPES), and the Provost for Research of the University of São Paulo [Research Support Center on Bioactive Molecules from Arthropod Vectors (NAP-MOBIARVE 12.1.17661.1.7)]. MG and LM were, respectively, supported by doctoral and master's fellowships from FAPESP. SD received a CNPq research productivity scholarship (304382/2017-5). JR was supported by the Intramural Research Program of the National Institute of Allergy and Infectious Diseases.

ACKNOWLEDGMENTS

We would like to thank Pedro Cesar Ferreira de Souza for technical assistance in tick colony maintenance. This work utilized the computational resources of the NIH HPC Biowulf cluster (http://hpc.nih.gov).

SUPPLEMENTARY MATERIAL

The Supplementary Material for this article can be found online at: https://www.frontiersin.org/articles/10.3389/fphys.2019.00529/full#supplementary-material

REFERENCES

Bastos, R. G., Ueti, M. W., Guerrero, F. D., Knowles, D. P., and Scoles, G. A. (2009). Silencing of a putative immunophilin gene in the cattle tick *Rhipicephalus* (*Boophilus*) *microplus* increases the infection rate of *Babesia bovis* in larval progeny. *Parasit. Vectors* 2:57. doi: 10.1186/1756-3305-2-57

Baxter, R. H., Contet, A., and Krueger, K. (2017). Arthropod innate immune systems and vector-borne diseases. *Biochemistry* 56, 907–918. doi: 10.1021/acs.biochem.6b00870

Behura, S. K., Gomez-Machorro, C., Harker, B. W., deBruyn, B., Lovin, D. D., Hemme, R. R., et al. (2011). Global cross-talk of genes of the mosquito Aedes aegypti in response to dengue virus infection. *PLoS Negl. Trop. Dis.* 5:e1385. doi: 10.1371/journal.pntd.0001385

Bifano, T. D., Ueti, M. W., Esteves, E., Reif, K. E., Braz, G. R., Scoles, G. A., et al. (2014). Knockdown of the *Rhipicephalus microplus* cytochrome c oxidase subunit III gene is associated with a failure of anaplasma marginale transmission. *PLoS One* 9:e98614. doi: 10.1371/journal.pone.0098614

Bowman, A. S., and Sauer, J. R. (2004). Tick salivary glands: function, physiology and future. *Parasitology* 129(Suppl.), S67–S81.

Bulet, P., Stocklin, R., and Menin, L. (2004). Anti-microbial peptides: from invertebrates to vertebrates. *Immunol. Rev.* 198, 169–184. doi: 10.1111/j.0105-2896.2004.0124.x

Buresova, V., Hajdusek, O., Franta, Z., Loosova, G., Grunclova, L., Levashina, E. A., et al. (2011). Functional genomics of tick thioester-containing proteins reveal the ancient origin of the complement system. *J. Innate Immun.* 3, 623–630. doi: 10.1159/000328851

Cabezas-Cruz, A., Alberdi, P., Ayllon, N., Valdes, J. J., Pierce, R., Villar, M., et al. (2016). *Anaplasma phagocytophilum increases the levels of histone modifying enzymes to inhibit cell apoptosis and facilitate pathogen infection in the tick vector Ixodes scapularis*. *Epigenetics* 11, 303–319. doi: 10.1080/15592294.2016.1163460

Capelli-Peixoto, J., Carvalho, D. D., Johnson, W. C., Scoles, G. A., Fogaca, A. C., Daffre, S., et al. (2017). The transcription factor relish controls *Anaplasma marginale* infection in the bovine tick *Rhipicephalus microplus*. *Dev. Comp. Immunol.* 74, 32–39. doi: 10.1016/j.dci.2017.04.005

Ceraul, S. M., Chung, A., Sears, K. T., Popov, V. L., Beier-Sexton, M., Rahman, M. S., et al. (2011). A Kunitz protease inhibitor from Dermacentor variabilis, a vector for spotted fever group rickettsiae, limits *Rickettsia montanensis* invasion. *Infect. Immun.* 79, 321–329. doi: 10.1128/IAI.00362-10

Ceraul, S. M., Dreher-Lesnick, S. M., Mulenga, A., Rahman, M. S., and Azad, A. F. (2008). Functional characterization and novel rickettsiostatic effects of a Kunitz-type serine protease inhibitor from the tick *Dermacentor variabilis*. *Infect. Immun.* 76, 5429–5435. doi: 10.1128/IAI.00866-08

Chapman, A. S., Murphy, S. M., Demma, L. J., Holman, R. C., Curns, A. T., McQuiston, J. H., et al. (2006). Rocky mountain spotted fever in the United States, 1997-2002. *Vector Borne Zoonot. Dis.* 6, 170–178.

Chen, L. F., and Sexton, D. J. (2008). What's new in Rocky Mountain spotted fever? *Infect. Dis. Clin. N. Am.* 22, 415–432, 7–8. doi: 10.1016/j.idc.2008.03.008

Cornman, R. S., Lopez, D., and Evans, J. D. (2013). Transcriptional response of honey bee larvae infected with the bacterial pathogen *Paenibacillus larvae*. *PLoS One* 8:e65424. doi: 10.1371/journal.pone.0065424

Corral-Rodriguez, M. A., Macedo-Ribeiro, S., Barbosa Pereira, P. J., and Fuentes-Prior, P. (2009). Tick-derived Kunitz-type inhibitors as antihemostatic factors. *Insect Biochem. Mol. Biol.* 39, 579–595. doi: 10.1016/j.ibmb.2009.07.003

Dantas-Torres, F. (2007). Rocky mountain spotted fever. *Lancet Infect. Dis.* 7, 724–732.

Dantas-Torres, F., Chomel, B. B., and Otranto, D. (2012). Ticks and tick-borne diseases: a one health perspective. *Trends Parasitol.* 28, 437–446. doi: 10.1016/j.pt.2012.07.003

de la Fuente, J., Blouin, E. F., Manzano-Roman, R., Naranjo, V., Almazan, C., Perez de la Lastra, J. M., et al. (2007). Functional genomic studies of tick cells in response to infection with the cattle pathogen, *Anaplasma marginale*. *Genomics* 90, 712–722. doi: 10.1016/j.ygeno.2007.08.009

Edgar, R. C. (2004a). MUSCLE: a multiple sequence alignment method with reduced time and space complexity. *BMC Bioinformatics* 5:113. doi: 10.1186/1471-2105-5-113

Edgar, R. C. (2004b). MUSCLE: multiple sequence alignment with high accuracy and high throughput. *Nucleic Acids Res.* 32, 1792–1797. doi: 10.1093/nar/gkh340

Esteves, E., Fogaca, A. C., Maldonado, R., Silva, F. D., Manso, P. P., Pelajo-Machado, M., et al. (2009). Antimicrobial activity in the tick *Rhipicephalus* (*Boophilus*) microplus eggs: cellular localization and temporal expression of microplusin during oogenesis and embryogenesis. *Dev. Comp. Immunol.* 33, 913–919. doi: 10.1016/j.dci.2009.02.009

Esteves, E., Maruyama, S. R., Kawahara, R., Fujita, A., Martins, L. A., Righi, A. A., et al. (2017). Analysis of the salivary gland transcriptome of unfed and partially fed *Amblyomma sculptum* ticks and descriptive proteome of the saliva. *Front. Cell Infect. Microbiol.* 7:476. doi: 10.3389/fcimb.2017.00476

Felix, R. C., and Silveira, H. (2011). The interplay between tubulins and P450 cytochromes during Plasmodium berghei invasion of *Anopheles gambiae* midgut. *PLoS One* 6:e24181. doi: 10.1371/journal.pone.0024181

Fogaca, A. C., Almeida, I. C., Eberlin, M. N., Tanaka, A. S., Bulet, P., and Daffre, S. (2006). Ixodidin, a novel antimicrobial peptide from the hemocytes of the cattle tick *Boophilus microplus* with inhibitory activity against serine proteinases. *Peptides* 27, 667–674. doi: 10.1016/j.peptides.2005.07.013

Fogaca, A. C., Lorenzini, D. M., Kaku, L. M., Esteves, E., Bulet, P., and Daffre, S. (2004). Cysteine-rich antimicrobial peptides of the cattle tick *Boophilus microplus*: isolation, structural characterization and tissue expression profile. *Dev. Comp. Immunol.* 28, 191–200. doi: 10.1016/j.dci.2003.08.001

Francischetti, I. M., Sa-Nunes, A., Mans, B. J., Santos, I. M., and Ribeiro, J. M. (2009). The role of saliva in tick feeding. *Front. Biosci.* 14, 2051–2088.

Galletti, M. F., Fujita, A., Nishiyama, M. Y. Jr., Malossi, C. D., Pinter, A., Soares, J. F., et al. (2013). Natural blood feeding and temperature shift modulate the global transcriptional profile of *Rickettsia rickettsii* infecting its tick vector. *PLoS One* 8:e77388. doi: 10.1371/journal.pone.0077388

Gulia-Nuss, M., Nuss, A. B., Meyer, J. M., Sonenshine, D. E., Roe, R. M., Waterhouse, R. M., et al. (2016). Genomic insights into the *Ixodes scapularis* tick vector of lyme disease. *Nat. Commun.* 7:10507. doi: 10.1038/ncomms10507

Hajdušek, O., Šíma, R., Ayllon, N., Jalovecká, M., Perner, J., de la Fuente, J., et al. (2013). Interaction of the tick immune system with transmitted pathogens. *Front. Cell. Infect. Microbiol.* 3:26. doi: 10.3389/fcimb.2013.00026

Horta, M. C., Moraes-Filho, J., Casagrande, R. A., Saito, T. B., Rosa, S. C., Ogrzewalska, M., et al. (2008). Experimental Infection of opossums *Didelphis aurita* by *Rickettsia rickettsii* and evaluation of the transmission of the infection to ticks *Amblyomma cajennense*. *Vector Borne Zoonotic Dis.* 9, 109–118. doi: 10.1089/vbz.2008.0114

Jones, D. T., Taylor, W. R., and Thornton, J. M. (1992). The rapid generation of mutation data matrices from protein sequences. *Comput. Appl. Biosci.* 8, 275–282. doi: 10.1093/bioinformatics/8.3.275

Kalil, S. P., Rosa, R. D. D., Capelli-Peixoto, J., Pohl, P. C., Oliveira, P. L., Fogaca, A. C., et al. (2017). Immune-related redox metabolism of embryonic cells of the tick Rhipicephalus microplus (BME26) in response to infection with *Anaplasma marginale*. *Parasit. Vectors* 10:613. doi: 10.1186/s13071-017-2575-9

Karim, S., Singh, P., and Ribeiro, J. M. (2011). A deep insight into the sialotranscriptome of the gulf coast tick, *Amblyomma maculatum*. *PLoS One* 6:e28525. doi: 10.1371/journal.pone.0028525

Kaufman, W. R. (2010). Ticks physiological aspects with implications for pathogen transmission. *Ticks Tick Borne Dis.* 1, 11–22. doi: 10.1016/j.ttbdis.2009.12.001

Kazimirova, M., and Stibraniova, I. (2013). Tick salivary compounds: their role in modulation of host defences and pathogen transmission. *Front. Cell Infect. Microbiol.* 3:43. doi: 10.3389/fcimb.2013.00043

Kocan, K. M., Blouin, E., and de la Fuente, J. (2011). RNA interference in ticks. *J. Vis. Exp.* 2011:2474.

Kocan, K. M., Zivkovic, Z., Blouin, E. F., Naranjo, V., Almazan, C., Mitra, R., et al. (2009). Silencing of genes involved in *Anaplasma marginale*-tick interactions affects the pathogen developmental cycle in *Dermacentor variabilis*. *BMC Dev. Biol.* 9:42. doi: 10.1186/1471-213X-9-42

Kotal, J., Langhansova, H., Lieskovska, J., Andersen, J. F., Francischetti, I. M. B., Chavakis, T., et al. (2015). Modulation of host immunity by tick saliva. *J. Proteo.* 128, 58–68. doi: 10.1016/j.jprot.2015.07.005

Kumar, S., Stecher, G., Li, M., Knyaz, C., and Tamura, K. (2018). MEGA X: molecular evolutionary genetics analysis across computing platforms. *Mol. Biol. Evol.* 35, 1547–1549. doi: 10.1093/molbev/msy096

Labruna, M. B. (2009). Ecology of rickettsia in South America. *Ann. N.Y. Acad. Sci.* 1166, 156–166. doi: 10.1111/j.1749-6632.2009.04516.x

Labruna, M. B., Ogrzewalska, M., Martins, T. F., Pinter, A., and Horta, M. C. (2008). Comparative susceptibility of larval stages of *Amblyomma aureolatum*, *Amblyomma cajennense*, and *Rhipicephalus sanguineus* to infection by *Rickettsia rickettsii*. *J. Med. Entomol.* 45, 1156–1159. doi: 10.1603/0022-2585(2008)45%5B1156:csolso%5D2.0.co;2

Lai, R., Takeuchi, H., Lomas, L. O., Jonczy, J., Rigden, D. J., Rees, H. H., et al. (2004). A new type of antimicrobial protein with multiple histidines from the hard tick, *Amblyomma hebraeum*. *FASEB J.* 18, 1447–1449. doi: 10.1096/fj.03-1154fje

Li, W., Cowley, A., Uludag, M., Gur, T., McWilliam, H., Squizzato, S., et al. (2015). The EMBL-EBI bioinformatics web and programmatic tools framework. *Nucleic Acids Res.* 43, W580–W584. doi: 10.1093/nar/gkv279

Livak, K. J., and Schmittgen, T. D. (2001). Analysis of relative gene expression data using real-time quantitative PCR and the 2(-delta delta C(T) method. *Methods* 25, 402–408. doi: 10.1006/meth.2001.1262

Martins, L. A., Galletti, M., Ribeiro, J. M., Fujita, A., Costa, F. B., Labruna, M. B., et al. (2017). The distinct transcriptional response of the midgut of *Amblyomma sculptum* and *Amblyomma aureolatum* ticks to *Rickettsia rickettsii* correlates to their differences in susceptibility to infection. *Front. Cell Infect. Microbiol.* 7:129. doi: 10.3389/fcimb.2017.00129

McWilliam, H., Li, W., Uludag, M., Squizzato, S., Park, Y. M., Buso, N., et al. (2013). Analysis tool web services from the EMBL-EBI. *Nucleic Acids Res.* 41, W597–W600. doi: 10.1093/nar/gkt376

Mercado-Curiel, R. F., Palmer, G. H., Guerrero, F. D., and Brayton, K. A. (2011). Temporal characterisation of the organ-specific *Rhipicephalus microplus* transcriptional response to *Anaplasma marginale* infection. *Int. J. Parasitol.* 41, 851–860. doi: 10.1016/j.ijpara.2011.03.003

Mulenga, A., Macaluso, K. R., Simser, J. A., and Azad, A. F. (2003). Dynamics of *Rickettsia*-tick interactions: identification and characterization of differentially expressed mRNAs in uninfected and infected *Dermacentor variabilis*. *Insect Mol. Biol.* 12, 185–193. doi: 10.1046/j.1365-2583.2003.00400.x

Nava, S., Beati, L., Labruna, M. B., Caceres, A. G., Mangold, A. J., and Guglielmone, A. A. (2014). Reassessment of the taxonomic status of *Amblyomma cajennense* () with the description of three new species, *Amblyomma tonelliae* n. sp., *Amblyomma interandinum* n. sp. and *Amblyomma patinoi* n. sp., and reinstatement of *Amblyomma mixtum*, and *Amblyomma sculptum* (*Ixodida*: *Ixodidae*). *Ticks Tick Borne Dis.* 5, 252–276. doi: 10.1016/j.ttbdis.2013.11.004

Paesen, G. C., Adams, P. L., Harlos, K., Nuttall, P. A., and Stuart, D. I. (1999). Tick histamine-binding proteins: isolation, cloning, and three-dimensional structure. *Mol. Cell.* 3, 661–671. doi: 10.1016/s1097-2765(00)80359-7

Palmer, W. J., and Jiggins, F. M. (2015). Comparative genomics reveals the origins and diversity of arthropod immune systems. *Mol. Biol. Evol.* 32, 2111–2129. doi: 10.1093/molbev/msv093

Pavlidi, N., Vontas, J., and Van Leeuwen, T. (2018). The role of glutathione S-transferases (GSTs) in insecticide resistance in crop pests and disease vectors. *Curr. Opin. Insect Sci.* 27, 97–102. doi: 10.1016/j.cois.2018.04.007

Pelc, R. S., McClure, J. C., Sears, K. T., Chung, A., Rahman, M. S., and Ceraul, S. M. (2014). Defending the fort: a role for defensin-2 in limiting *Rickettsia montanensis* infection of *Dermacentor variabilis*. *Insect Mol. Biol.* 23, 457–465. doi: 10.1111/imb.12094

Pinter, A., and Labruna, M. B. (2006). Isolation of *Rickettsia rickettsii* and *Rickettsia bellii* in cell culture from the tick *Amblyomma aureolatum* in Brazil. *Ann. N.Y. Acad. Sci.* 1078, 523–529. doi: 10.1196/annals.1374.103

Ribeiro, J. M., Topalis, P., and Louis, C. (2004). AnoXcel: an Anopheles gambiae protein database. *Insect Mol. Biol.* 13, 449–457. doi: 10.1111/j.0962-1075.2004.00503.x

Rozen, S., and Skaletsky, H. (2000). Primer3 on the WWW for general users and for biologist programmers. *Methods Mol. Biol.* 132, 365–386. doi: 10.1385/1-59259-192-2:365

Sangamnatdej, S., Paesen, G. C., Slovak, M., and Nuttall, P. A. (2002). A high affinity serotonin- and histamine-binding lipocalin from tick saliva. *Insect Mol. Biol.* 11, 79–86. doi: 10.1046/j.0962-1075.2001.00311.x

Severo, M. S., Choy, A., Stephens, K. D., Sakhon, O. S., Chen, G., Chung, D. W., et al. (2013). The E3 ubiquitin ligase XIAP restricts *Anaplasma phagocytophilum* colonization of *Ixodes scapularis* ticks. *J. Infect. Dis.* 208, 1830–1840. doi: 10.1093/infdis/jit380

Silva, F. D., Rezende, C. A., Rossi, D. C., Esteves, E., Dyszy, F. H., Schreier, S., et al. (2009). Structure and mode of action of microplusin, a copper II-chelating antimicrobial peptide from the cattle tick *Rhipicephalus* (*Boophilus*) *microplus*. *J. Biol. Chem.* 284, 34735–34746. doi: 10.1074/jbc.M109.016410

Silva, F. D., Rossi, D. C., Martinez, L. R., Frases, S., Fonseca, F. L., Campos, C. B., et al. (2011). Effects of microplusin, a copper-chelating antimicrobial peptide, against *Cryptococcus neoformans*. *FEMS Microbiol. Lett.* 324, 64–72. doi: 10.1111/j.1574-6968.2011.02386.x

Simo, L., Kazimirova, M., Richardson, J., and Bonnet, S. I. (2017). The essential role of tick salivary glands and saliva in tick feeding and pathogen transmission. *Front. Cell Infect. Microbiol.* 7:281. doi: 10.3389/fcimb.2017.00281

Socolovschi, C., Mediannikov, O., Raoult, D., and Parola, P. (2009). The relationship between spotted fever group *Rickettsiae* and *ixodid* ticks. *Vet. Res.* 40:34. doi: 10.1051/vetres/2009017

Sonenshine, D. E., and Roe, R. M. (2013). *Biology of Ticks*, Vol. 1. New York, NY: Oxford University Press, 560.

Suppan, J., Engel, B., Marchetti-Deschmann, M., and Nurnberger, S. (2018). Tick attachment cement - reviewing the mysteries of a biological skin plug system. *Biol. Rev. Camb. Philos. Soc.* 93, 1056–1076. doi: 10.1111/brv.12384

Thepparit, C., Bourchookarn, A., Petchampai, N., Barker, S. A., and Macaluso, K. R. (2010). Interaction of *Rickettsia felis* with histone H2B facilitates the infection of a tick cell line. *Microbiology* 156, 2855–2863. doi: 10.1099/mic.0.041400-0

Ueti, M. W., Reagan, J. O., Jr., Knowles, D. P., Jr., Scoles, G. A., Shkap, V., Palmer, G. H., et al. (2007). Identification of midgut and salivary glands as specific and distinct barriers to efficient tick-borne transmission of *Anaplasma marginale*. *Infect. Immun.* 75, 2959–2964. doi: 10.1128/IAI.00284-07

Urbanova, V., Sima, R., Sauman, I., Hajdusek, O., and Kopacek, P. (2015). Thioester-containing proteins of the tick *Ixodes ricinus*: gene expression, response to microbial challenge and their role in phagocytosis of the yeast *Candida albicans*. *Dev. Comp. Immunol.* 48, 55–64. doi: 10.1016/j.dci.2014.09.004

Wang, Y. W., Tan, J. M., Du, C. W., Luan, N., Yan, X. W., Lai, R., et al. (2015). A novel trypsin inhibitor-like cysteine-rich peptide from the frog *Lepidobatrachus laevis* containing proteinase-inhibiting activity. *Nat. Prod. Bioprospect.* 5, 209–214. doi: 10.1007/s13659-015-0069-z

Welchman, R. L., Gordon, C., and Mayer, R. J. (2005). Ubiquitin and ubiquitin-like proteins as multifunctional signals. *Nat. Rev. Mol. Cell Biol.* 6, 599–609. doi: 10.1038/nrm1700

Werck-Reichhart, D., and Feyereisen, R. (2000). Cytochromes P450: a success story. *Genome Biol.* 1:REVIEWS3003.

Conflict of Interest Statement: The authors declare that the research was conducted in the absence of any commercial or financial relationships that could be construed as a potential conflict of interest.

frontiers in Physiology

MINI REVIEW
published: 21 May 2019
doi: 10.3389/fphys.2019.00618

Vitellogenin Receptor as a Target for Tick Control: A Mini-Review

Robert D. Mitchell III[1], Daniel E. Sonenshine[2,3] and Adalberto A. Pérez de León[1]**

[1] USDA-ARS, Knipling-Bushland U.S. Livestock Insects Research Laboratory, Veterinary Pest Genomics Center, Kerrville, TX, United States, [2] Laboratory for Malaria and Vector Research, National Institute of Allergy and Infectious Diseases, National Institutes of Health, Rockville, MD, United States, [3] Department of Biological Sciences, Old Dominion University, Norfolk, VA, United States

While much effort has been put into understanding vitellogenesis in insects and other organisms, much less is known of this process in ticks. There are several steps that facilitate yolk formation in developing oocytes of which the vitellogenin receptor (VgR) is a key component. The tick VgR binds vitellogenin (Vg) circulating in the hemolymph to initiate receptor-mediated endocytosis and its transformation into vitellin (Vn). The conversion of Vg into Vn, the final form of the yolk protein, occurs inside oocytes of the female tick ovary. Vn is critical to tick embryos since it serves as the nutritional source for their development, survival, and reproduction. Recent studies also suggest that pathogenic microbes, i.e., *Babesia* spp., that rely on ticks for propagation and dissemination likely "hitchhike" onto Vg molecules as they enter developing oocytes through the VgR. Suppressing VgR messenger RNA synthesis via RNA interference (RNAi) completely blocked *Babesia* spp. transmission into developing tick oocytes, thereby inhibiting vertical transmission of these pathogenic microbes from female to eggs. To date, VgRs from only four tick species, *Dermacentor variabilis*, *Rhipicephalus microplus*, *Amblyomma hebraeum*, and *Haemaphysalis longicornis*, have been fully sequenced and characterized. In contrast, many more VgRs have been described in various insect species. VgR is a critical component in egg formation and maturation that can serve as a precise target for tick control. However, additional research will help identify unique residues within the receptor that are specific to ticks or other arthropod disease vectors while avoiding cross-reactivity with non-target species. Detailed knowledge of the molecular structure and functional role of tick VgRs will enable development of novel vaccines to control ticks and tick-borne diseases.

Keywords: tick, vitellogenin receptor, vitellogenesis, RNAi, reproduction, tick-borne pathogens, vector control, vaccine

OPEN ACCESS

Edited by:
Abid Ali,
Abdul Wali Khan University Mardan, Pakistan

Reviewed by:
Carlos Termignoni,
Federal University of Rio Grande do Sul, Brazil
Rika Umemiya-Shirafuji,
Obihiro University of Agriculture and Veterinary Medicine, Japan
Adriana Seixas,
Federal University of Health Sciences of Porto Alegre, Brazil

****Correspondence:***
Robert D. Mitchell III
Robert.Mitchell@ars.usda.gov
Adalberto A. Pérez de León
Beto.PerezdeLeon@ars.usda.gov

Specialty section:
This article was submitted to Invertebrate Physiology, a section of the journal Frontiers in Physiology

Received: *04 March 2019*
Accepted: *02 May 2019*
Published: *21 May 2019*

Citation:
Mitchell RD III, Sonenshine DE and Pérez de León AA (2019) Vitellogenin Receptor as a Target for Tick Control: A Mini-Review. Front. Physiol. 10:618. doi: 10.3389/fphys.2019.00618

INTRODUCTION

Ticks are ectoparasites that blood feed on hosts found across diverse habitats ranging from the darkest caverns to the hottest deserts. They harbor a greater variety of pathogenic microbes, including bacteria, viruses, and protozoans, than any other arthropod group (Anderson and Magnarelli, 2008; Sonenshine and Roe, 2013a). Tick-borne pathogens are transmitted via the bite of an infected tick to a susceptible host. Successful transmission can result in debilitating or even lethal diseases like Lyme disease (causative agent *Borrelia burgdorferi*), Rocky Mountain spotted

fever (causative agent *Rickettsia rickettsia*) and babesiosis (causative agent *Babesia* spp.) in humans, domesticated animals, and wildlife. Tick bites can also elicit a severe immune response as tick saliva carries a broad assortment of pharmacologically active molecules directed to inhibit host defenses (Alarcon-Chaidez et al., 2006; Nicholson et al., 2019; Nuttall, 2019). Ticks are masters of stealthy blood feeding and often remain undetected on an unsuspecting host for several hours or days as they feed. Hard ticks in the family Ixodidae typically feed for several days while soft ticks in the family Argasidae feed much more rapidly usually within minutes or only 1–2 h (Sonenshine and Roe, 2013b; Eisen, 2018). The injurious effects of tick bites and tick-transmitted diseases result in billions of dollars in damage annually to humans, livestock, and wildlife. Additional losses are incurred by the need to purchase and administer acaricides, medical and veterinary costs for treating affected humans and livestock, and other costs such as permanent damage to animal hides and reduction in meat quality and milk production from infested livestock (Giraldo-Ríos and Hurtado, 2018; Mac et al., 2019). Global climate change exacerbates these difficulties by increasing the habitable range of ticks, including Canada and Nordic countries. Current control measures continue to fail resulting in widespread resistance to multiple classes of acaricides (Bowman and Nuttall, 2008; Sonenshine, 2018; Boulanger et al., 2019). Discovering new or alternative targets to enhance or replace existing methods is required to maintain effective tick control efforts and vector-borne disease prevention.

Vitellogenesis is a critical mechanism in tick reproduction and a process that can be targeted for tick control. Vitellogenin (Vg) is synthesized in the fat body and midgut of a female tick after mating and transported through the hemolymph, captured by surface receptors called vitellogenin receptors (VgRs), and endocytosed into developing oocytes within the ovaries. Endocytosed Vg is transformed to vitellin (Vn), the functional form of the yolk protein found in oocytes, which provides nutrients essential for the developing embryos (Khalil et al., 2011; Xavier et al., 2018). VgRs, which are large transmembrane proteins of approximately 200 kilodaltons, serve as "gatekeepers" regulating the entry of Vg and pathogenic microbes discussed herein. Captured Vg is transported into developing oocytes via receptor-mediated endocytosis across clathrin-coated pits that are normally distributed evenly across a developing oocyte's outer surface. Besides ticks, VgRs are found in vertebrates and other invertebrate organisms including crustaceans, and a wide variety of other arthropods. However, while they share key motifs critical to proper functionality, tick VgRs are different enough from VgRs of other organisms to be candidate vaccine targets (Roe et al., 2008; Kopáček et al., 2019).

Of the approximately 702 hard tick and 193 soft tick species (Guglielmone et al., 2010), only four tick VgRs have been successfully cloned and sequenced, namely, *Dermacentor variabilis*, *Rhipicephalus microplus*, *Amblyomma hebraeum*, and *Haemaphysalis longicornis* (**Table 1**). This is in stark contrast to the many more VgRs described in insect species. This marked disparity highlights the need for research on VgRs as targets to innovate tick control technologies. Advanced molecular techniques and next-generation sequencing can be applied to realize that potential. While the genomes of *Ixodes scapularis*, *Ixodes ricinus*, and *R. microplus* are now available, the genomes of other ticks of medical and veterinary importance must also be sequenced to further understand the role of VgRs in reproduction and tick-borne disease transmission to craft highly specific "designer molecules" for safer tick control (Cramaro et al., 2015; Gulia-Nuss et al., 2016; Barrero et al., 2017; Murgia et al., 2019).

This mini-review addresses current knowledge of the structure and function of VgRs from the American dog tick, *D. variabilis*, the southern cattle fever or Asian blue tick, *R. microplus*, the tropical bont tick, *A. hebraeum*, and the Asian longhorned tick, *H. longicornis*. Suppression of tick VgRs is explored as a method to eliminate ticks as well as prevent transmission of tick-borne pathogenic microbes transovarially to the next generation. Further avenues of tick VgR research are also discussed.

TICK VITELLOGENIN RECEPTOR STRUCTURE AND FUNCTION

Tick VgRs, derived from a single gene, are members of the low-density lipoprotein receptor (LDLR) gene superfamily and share the common multi-domain architecture of other LDLRs (with a few exceptions discussed later) including: (1) ligand-binding domains (LBDs) consisting of clusters of cysteine-rich repeats, (2) cysteine-rich epidermal growth factor (EGF)-precursor homology domains, (3) an O-linked sugar domain, (4) a transmembrane domain, and (5) a cytoplasmic domain as shown in **Figure 1A** (Sappington and Raikhel, 1998; Tufail and Takeda, 2009). The two LBDs in ticks, where circulating Vg binds, consist of multiple modularly clustered cysteine-rich repeats, called LDLR class A (LDLRA) repeats, which are approximately 40 amino acids long and are disulfide-bonded in the pattern C_I–C_{III}, C_{II}–C_V, and C_{IV}–C_{VI} (Goldstein et al., 1985). There is also a cluster of acidic residues in each repeat that generally follows the pattern (CDxxxDCxDGSDE), which is conserved between the fourth and sixth cysteines of all insect VgRs. This cluster of acidic residues within each LBD is critical for proper disulfide bond folding and ligand-binding to the domain (Blacklow and Kim, 1996; Fass et al., 1997). The LBD closest to the N-terminus, ligand-binding domain 1 (LBD1), in all tick VgRs described so far contains four LDLRA repeats while the LBD closest to the C-terminus, ligand-binding domain 2 (LBD2), contains eight, in contrast to the two LBDs found in insect VgRs where LBD1 contains five repeats while there are eight in LBD2. This difference contributes to insect LBD1 and LBD2 only having an approximately 35% identity with tick VgR LBDs (Boldbaatar et al., 2008; Smith and Kaufman, 2013).

In organisms less closely related evolutionarily to ticks, the number of repeats can vary substantially including vertebrate VgRs that have only a single 7- or 8-repeat LBD (Yamamoto et al., 1986; Okabayashi et al., 1996). As shown in **Figure 1**, LBD1 in *R. microplus*, *H. longicornis*, and *A. hebraeum* is 83, 89, and 78% identical (i.e., amino acids match exactly) to the *D. variabilis* LBD1, respectively. LBD2 in *R. microplus*, *H. longicornis*, and *A. hebraeum* is 84, 73, and 77% identical to the *D. variabilis* LBD2, respectively. This suggests that treatments targeting LBDs

of tick VgRs may cross-react with multiple tick species while not targeting insects or other unrelated organisms. Additionally, there are essentially twice as many targets to interrogate in some of the more ancestral species since a second LBD seems to disappear in higher organisms. It is possible that genetic duplication occurred early in the molecular evolution of tick VgRs to generate new genetic material and was subsequently lost in higher organisms as VgR function became more specialized.

Tick EGF-precursor homology domains, which follow immediately after LBD1 and LBD2, contain four cysteine-rich LDLR class B (LDLRB) repeats in each domain. This contrasts insect VgRs that have four LDLRB repeats in the first domain but only three repeats in the second. However, unlike LDLRA repeats, LDLRB repeats follow the disulfide-binding pattern C_I–C_{III}, C_{II}–C_{IV}, and C_V–C_{VI} (Sappington and Raikhel, 2005). There are also EGF-like repeats of approximately 40 amino acids that exist singly or in pairs within these domains. Some of these EGF-like repeats bind calcium to maintain stability of the domain and prevent proteolytic degradation (**Figure 1A**; Rao et al., 1995). Each tick EGF-precursor homology domain, as in other organisms, contains six YWXD motifs that form a β-propeller. The β-propeller is thought to function as an acid-dependent ligand release mechanism in endosomes but may also play an active role in ligand binding, although this has only been proposed in larger members of the lipoprotein receptor family (Andersen et al., 2013). However, not all algorithms pinpoint six YWXD motifs in this region in ticks and other organisms; research on this domain confirmed that the motif is not always absolutely conserved but there are always six repeats that must be present for functionality. Therefore, all β-propeller domains shown in **Figure 1A** are represented by six YWXD motifs even though they may have initially been reported as having less. The EGF-precursor homology domains may also serve as spacer regions to maintain adequate distance between LBDs and ensure that only ligands of certain sizes are retained by VgRs (Springer, 1998; Innerarity, 2002; Jeon and Blacklow, 2003; Andersen et al., 2013).

Smith and Kaufman (2013) reported only three EGF-like repeats in the EGF-precursor homology domain present following LBD1 in *H. longicornis*, but alternative algorithms, like the SMART algorithm, identify four EGF-like repeats in that domain (Smith and Kaufman, 2013; Letunic and Bork, 2018). The presence of three or four EGF-like repeats in that domain in *H. longicornis* is likely inconsequential as the basic elements are present for that domain to be fully functional in either

TABLE 1 | Tick vitellogenin receptor (VgR) sequence information available to date.

Species	Common name	Protein name	Source	Acc.#	UniProt ID	Size[B]
Ixodes scapularis	Black-legged tick; Deer tick	Vitellogenin receptor, putative	Genomic	EEC16350.1	B7QBX8	810
Ixodes scapularis	Black-legged tick; Deer tick	Vitellogenin receptor, putative	Genomic	EEC20133.1	B7QMR1	1200
Rhipicephalus microplus[A]	Southern cattle tick	Vitellogenin receptor	cDNA	AUQ44344.1	A0A2I7G3Y1	1799
Rhipicephalus microplus	Southern cattle tick	Vitellogenin receptor, partial	cDNA	AMZ04157.1	A0A1W5KSB7	788
Amblyomma hebraeum[A]	Tropical bont tick	Vitellogenin receptor	cDNA	AGQ57038.1	U5KCA6	1801
Dermacentor variabilis[A]	American dog tick	Vitellogenin receptor	cDNA	AAZ31260.3	Q45VP9	1798
Haemaphysalis longicornis[A]	Bush tick	Vitellogenin receptor, partial	cDNA	BAG14342.1	B1Q2W6	1781
Ornithodoros erraticus	European soft tick	Vitellogenin receptor	cDNA	–	A0A293LRH2	874
Ornithodoros erraticus	European soft tick	Vitellogenin receptor	cDNA	–	A0A293M1D3	1278
Ornithodoros erraticus	European soft tick	Vitellogenin receptor	cDNA	–	A0A293N0S6	459
Ornithodoros erraticus	European soft tick	Vitellogenin receptor	cDNA	–	A0A293LLZ8	640
Ornithodoros erraticus	European soft tick	Vitellogenin receptor	cDNA	–	A0A293LUB6	505
Ornithodoros brasiliensis	Mouro tick	Vitellogenin receptor	cDNA	–	A0A1D2AJA7	219
Ornithodoros brasiliensis	Mouro tick	Vitellogenin receptor	cDNA	–	A0A1D2AIF9	166
Ixodes ricinus	Castor bean tick	Putative vitellogenin receptor	cDNA	JAA65139.1	A0A0K8R3T2	140
Ixodes ricinus	Castor bean tick	Putative vitellogenin receptor	cDNA	JAC91887.1	A0A090X7C9	221
Ixodes ricinus	Castor bean tick	Putative vitellogenin receptor	cDNA	JAB68489.1	V5GWI7	133
Ixodes ricinus	Castor bean tick	Putative vitellogenin receptor	cDNA	JAA73497.1	A0A0K8RQX7	100
Amblyomma cajennense	Cayenne tick	Putative vitellogenin receptor	cDNA	JAC21573.1	A0A023FLL9	336
Amblyomma cajennense	Cayenne tick	Putative vitellogenin receptor	cDNA	JAC24396.1	A0A023FRH2	389
Rhipicephalus appendiculatus	Brown ear tick	Vitellogenin receptor	cDNA	–	A0A2D1UEP7	187
Rhipicephalus appendiculatus	Brown ear tick	Vitellogenin receptor	cDNA	–	A0A131Z1S4	286
Ornithodoros turicata	Relapsing fever tick	Putative vitellogenin receptor	cDNA	–	A0A2R5LQ71	265
Rhipicephalus pulchellus	Zebra tick	Vitellogenin receptor	cDNA	JAA55785.1	L7LVF0	286
Ornithodoros moubata	African relapsing fever tick	Vitellogenin receptor	cDNA	–	A0A1Z5L4E0	226
Ornithodoros moubata	African relapsing fever tick	Vitellogenin receptor	cDNA	–	A0A1Z5L2N2	79

There are 26 sequences available between the National Center for Biotechnology Information (NCBI) and the Universal Protein Database (UniProt) that identify as whole or partial tick VgRs of which 4 have been functionally characterized (Accession numbers: AUQ44344.1; AGQ57038.1; AAZ31260.3; BAG14342.1).
[A] *Functionally characterized.*
[B] *Length in amino acids.*

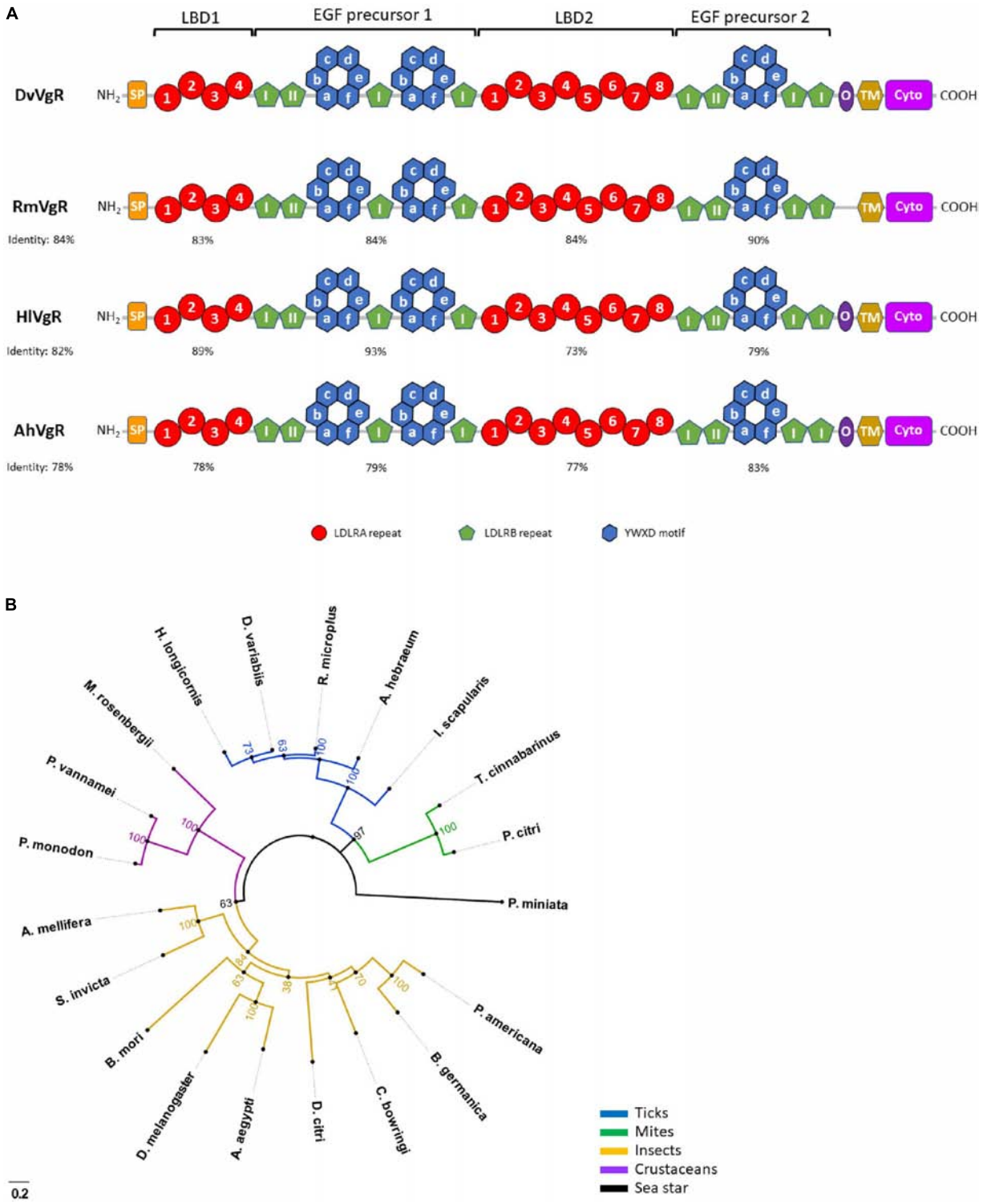

FIGURE 1 | Tick vitellogenin receptor (VgR) structure and phylogeny in relation to VgRs from other organisms. **(A)** Tick VgRs from *D. variabilis* (DvVgR), *R. microplus* (RmVgR), *H. longicornis* (HlVgR), and *A. hebraeum* (AhVgR). Percentages under the species identifier represent the percent identity of that species with the full-length VgR amino acid sequence of *D. variabilis*. Percentages under the four highlighted domains represent the percent identity of that region in relation to the *D. variabilis* VgR amino acid sequence. LBD1, ligand-binding domain 1; EGF precursor 1, epidermal growth factor (EGF)-precursor homology domain 1; LBD2, ligand-binding domain 2; EGF precursor 2, epidermal growth factor (EGF)-precursor homology domain 2; "I" inside green pentagon, EGF-like repeat within LDLRB repeat of LBD (non-calcium binding); "II" inside green pentagon, EGF-like repeat within LDLRB repeat of LBD (calcium binding); SP, signal peptide; TM,

(Continued)

FIGURE 1 | Continued
transmembrane domain; O, O-linked sugar domain; Cyto, cytoplasmic domain. **(B)** Unrooted maximum likelihood tree showing the phylogenetic relationship between VgRs from 5 tick species (AAZ31260.3, *Dermacentor variabilis*; AGQ57038.1, *Amblyomma hebraeum*; AUQ44344.1, *Rhipicephalus microplus*; BAG14342.1, *Haemaphysalis longicornis*; EEC20133.1, *Ixodes scapularis*), 2 mite species (ANS13820.1, *Tetranychus cinnabarinus*; AHN48901.1, *Panonychus citri*), 9 insect species (AAK15810.1, *Aedes aegypti*; AAB60217.1, *Drosophila melanogaster*; BAC02725.2, *Periplaneta americana*; CAJ19121.1, *Blattella germanica*; AAP92450.1, *Solenopsis invicta*; XP_026295652.1, *Apis mellifera*; ADK94452.1, *Bombyx mori*; AZN28756.1, *Colaphellus bowringi*; XP_026689064.1, *Diaphorina citri*), 3 crustacean species (ADK55596.1, *Macrobrachium rosenbergii*; ROT71709.1, *Penaeus vannamei*; ABW79798.1, *Penaeus monodon*), and a sea star (AMR68937.1, *Patiria miniata*). Bootstrap values from 1000 simulations are displayed at the nodes. Number and letter combinations in parenthesis are Accession Numbers. Figure design modeled after figure from Smith and Kaufman (2013).

scenario. The EGF-precursor homology domain closest to the N-terminus in *R. microplus*, *H. longicornis*, and *A. hebraeum* is 84, 93, and 79% identical to the same domain in *D. variabilis*, respectively (**Figure 1A**), while the EGF-precursor homology domain closest to the C-terminus in *R. microplus*, *H. longicornis*, and *A. hebraeum* is 84, 73, and 77% identical to the same domain in *D. variabilis*, respectively.

The O-linked sugar domain, a region rich in serine and threonine residues, is found in most, but not all, vertebrae and invertebrate VgRs. Research findings suggest that it may provide rigidity to the receptor as it extends into the extracellular space, afford protection from denaturation, or modulate proteolytic cleavage of the ectodomain (Gent and Braakman, 2004; Tufail and Takeda, 2009). The O-linked sugar domain is present in the VgR of *D. variabilis*, *H. longicornis*, and *A. hebraeum*, but is absent from the *R. microplus* VgR (Seixas et al., 2018). A hydrophobic transmembrane domain is present in all VgRs that tethers the receptor to the plasma membrane. Experiments disabling this region resulted in inactive, truncated receptors (Schneider and Nimpf, 2003). A cytoplasmic domain of all four tick species also contains typical leucine-leucine/leucine-isoleucine (LL/LI) and conserved FXNPXF sequences indicative of internalization signals in VgRs from other organism. These conserved residues play a critical role in receptor internalization as they are responsible for delivering ligand-bound receptors to internal endosomes where ligands are removed, and the receptors are recycled back to the cell surface (Trowbridge, 1991). Phylogenic analysis shows that ticks form a distinct clade when their VgRs are compared to those of mites, insects, crustaceans, and a sea star (**Figure 1B**). However, the functional significance of structural variations between tick VgRs and those of other invertebrates and vertebrates remains to be determined.

SILENCING VITELLOGENIN RECEPTOR HALTS EGG FORMATION AND DEPOSITION

RNA interference (RNAi) was utilized to ascertain the functionality of tick VgRs from *D. variabilis*, *H. longicornis*, *A. hebraeum*, and *R. microplus*. Mitchell et al. (2007) reported for the first time successful knockdown of a VgR in any acarine species. By disabling VgR messenger RNAs (mRNAs) the receptor was rendered ineffective and substantial amounts of Vg accumulated in the hemolymph of treated ticks rather than in the oocytes. Northern blot analysis revealed that VgR mRNAs from *D. variabilis* were abundant in the ovaries of vitellogenic females, but other female tissues and male whole-body extracts showed no VgR mRNAs. This observation revealed VgR expression to be tissue- and sex-specific. In these experiments, newly emerged unfed females were injected with 0.5 μg of double-stranded RNA (dsRNA) and placed on a rabbit host. These females were allowed to mate with introduced males and feed to repletion (∼8 days), then collected, and held 0–4 days post drop-off (when they were presumably fully vitellogenic, i.e., flooding nutrients into developing oocytes) before being dissected for assessment. In the PBS-injected control group the oocytes were almost completely brown from Vg uptake 2 days post drop-off (oocyte growth stage 4 as described in Balashov, 1972). In stark contrast, most of the RNAi-treated oocytes had not progressed past stage 2 in their development, which is typical of previtellogenic oocytes, the ovary was largely white in color, and mated females did not lay eggs.

Subsequently, *H. longicornis* (Boldbaatar et al., 2008), *A. hebraeum* (Smith and Kaufman, 2013), and *R. microplus* (Seixas et al., 2018) VgRs were sequenced, characterized, and shown to share structural features with the *D. variabilis* receptor. **Table 1** shows all tick VgR sequences that are currently available in the NCBI and UniProt databases (UniProt Consortium, 2007; Lipman et al., 2015). Molecular studies were conducted to determine functionality and similar results were obtained to the *D. variabilis* work. *H. longicornis* females injected with 1.0 μg VgR-dsRNA did not lay eggs and their ovaries were predominantly white upon inspection 7 days post drop-off. In *A. hebraeum*, 1.0 μg VgR-dsRNA was injected into females and transcript suppression was observed, but blockage of Vg entering oocytes at the level of the previous studies was not achieved. It was suggested that this tick species may require an additional unknown vitellogenin uptake factor (VUF) for yolk uptake (Smith and Kaufman, 2013), but such a factor remains to be identified. The most recent tick VgR described was that of *R. microplus* where 8.0 μg VgR-dsRNA was injected into partially engorged females that were then artificially bloodfed for 28 h before dissection. RNAi treatment halted Vg uptake as in previous experiments and hatching rates were significantly reduced compared to controls. An interesting additional observation was made where part-fed ticks that reached a certain weight (>35 mg) were not significantly affected by VgR-dsRNA introduction, which suggested a developmental threshold for efficacy. Further studies need to determine the amount of dsRNA necessary to fully inhibit vitellogenesis and pathogen migration across the VgR in all tick species, the

optimal time and methods of delivery, and whether or not a VUF is involved.

VITELLOGENIN RECEPTOR PHYSIOLOGY AND TICK-BORNE PATHOGENS

Transovarial transmission is an important process for the maintenance of tick-borne pathogens (Randolph, 1994). Silencing VgR in *H. longicornis* not only halted oocyte development, but it also blocked *Babesia gibsoni* transmission from the midgut into oocytes (Boldbaatar et al., 2008). *B. gibsoni* is a protozoan that causes canine babesiosis, a disease whose clinical manifestations in dogs can range from mild fever and lethargy to multi-organ failure and death (Solano-Gallego et al., 2016). This observation had not been previously described in ticks even though researchers knew the tick ovary played an important role in pathogen transovarial transmission. Hussein et al. (2019) demonstrated a similar finding in *R. microplus* where silencing the VgR blocked *B. bovis* transmission and inhibited ovary maturation. This study also reported that while >90% of the females in all test groups laid eggs, the egg masses from the VgR-dsRNA-treated group were misshapen, and weighed less than half (43 ± 3.36 mg) of the buffer-injected (121 ± 4.94 mg) and untreated groups (109 ± 4.32 mg).

MICROBIAL HIJACKING OF VITELLOGENESIS THROUGH VITELLOGENIN RECEPTOR

As noted in the preceding section, inhibiting the VgR of *R. microplus*, an arthropod of great economic importance to the livestock industry globally, blocked transmission of *B. bovis* to maturing oocytes just as *B. gibsoni* transmission was blocked by silencing the *H. longicornis* VgR. *B. bovis*, the causative agent of bovine babesiosis, causes millions of dollars of damage annually by destroying cow hides, disrupting meat production, and disturbing milk production (Bock et al., 2004). Pathogen transmission from adult to young at the VgR interface should be examined further for potential intervention to control tick-borne diseases. Recently, it was demonstrated that vertical transmission of the rice stripe virus (RSV) in *Laodelphax striatellus*, the small brown planthopper, occurs when RSV hitchhikes by binding to Vg entering developing oocytes through VgR-mediated endocytosis (He et al., 2018). A similar mechanism may have evolved among tick-borne pathogens for transovarial transmission to the progeny of infected gravid females. Additionally, it is hypothesized that ticks have more than one site of Vg synthesis, as was observed in *L. striatellus* (Rosell-Davis and Coons, 1989). Compelling evidence exists supporting tick Vg synthesis in the fat body, midgut, and some ovary tissue of various species (Thompson et al., 2007; Boldbaatar et al., 2010; Khalil et al., 2011; Smith and Kaufman, 2014; Ramírez Rodríguez et al., 2016). Only Vg from planthopper hemocytes bound RSV, which suggests a conformational difference whereby specific viral surface peptides could allow this interaction to occur (Huo et al., 2019).

TICK CONTROL STRATEGIES EXPLOITING VITELLOGENIN RECEPTOR

In addition to injection, RNAi can be delivered effectively orally or topically to ticks and other arthropods for control purposes (Killiny et al., 2014; Marr et al., 2014). Therefore, VgR-dsRNA could potentially be applied directly to ticks or potential hosts or, alternatively, delivered parenterally for systemic host protection. To improve transport and control release, organic nanocarriers like liposomes or inorganic nanoparticles could be employed to improve dsRNA survivability or target specific tissues or cellular compartments (Lombardo et al., 2019). The rapid development of genome editing technologies, like those based on CRISPR/Cas9 (Sun et al., 2017), present the opportunity for biotechnology approaches targeting tick VgRs.

Vaccine development utilizing recombinant tick VgRs should be thoroughly appraised to inhibit oocyte maturation, egg deposition, and pathogen transmission (Xavier et al., 2018). VgRs are desirable targets because tick species have a single gene copy and as far as we know they are expressed only in the ovary. Although tick VgRs appear inaccessible to specific host antibodies, it is known that ticks have a "leaky gut" whereby antibodies could reach, and bind concealed VgRs (Kemp et al., 1989; da Silva Vaz et al., 1996; Jeffers and Roe, 2008; Hope et al., 2010). "Concealed" antigens may not be part of the typical tick-host interaction but can still be exploited to elicit an anti-tick immunological response. However, bioengineering of the recombinant protein may be required to enhance immunogenicity and overcome the need for frequent booster vaccinations to continually stimulate the specific anti-tick immune response (Opdebeeck, 1994; Willadsen, 2008). Reverse vaccinology could be applied to develop VgR-based anti-tick vaccines whereby epitopes would be identified to produce subunit vaccines or by using such sequences to produce chimeras containing other relevant peptide sequences (Guerrero et al., 2012; Miller et al., 2012; Valle and Guerrero, 2018).

FUTURE DIRECTIONS

Tick VgRs are candidates for innovative tick control technologies as they play a critical role in tick reproduction and the transovarial transmission of tick-borne pathogens. Conserved structural characteristics suggests that designer molecules targeting VgRs could be tick-specific. However, tick VgRs

also share structural characteristics with other arthropod pests. Biotechnological advances offer the opportunity to exploit this feature to innovate control technologies that are safer for non-target species and other, more simplistic vaccines.

CONTRIBUTION TO THE FIELD STATEMENT

While much effort has been put into understanding vitellogenesis in insects and other organisms, much less is known of this process in ticks. There are several steps that facilitate yolk formation in developing oocytes of which the VgR is a key component. The tick VgR binds Vg circulating in the hemolymph to initiate receptor-mediated endocytosis and its transformation into vitellin (Vn). The conversion of Vg into Vn, the final form of the yolk protein, occurs inside oocytes of the female tick ovary. Vn is critical to tick embryos since it serves as the nutritional source for their development, survivability, and ultimately for the continuation of the species. Recent studies also suggest that pathogenic microbes, i.e., *Babesia* spp., that rely on ticks for propagation and dissemination likely "hitchhike" onto Vg molecules as they enter developing oocytes through VgRs. Suppressing VgR messenger RNA synthesis via RNA interference (RNAi) completely blocked *Babesia* spp. transmission into developing tick oocytes, thereby inhibiting vertical transmission of these pathogenic microbes from female to eggs. Detailed knowledge of the molecular structure and functional role of tick VgRs enables biotechnological applications to innovate control technologies for integrated management of ticks and tick-borne diseases.

DATA AVAILABILITY

No datasets were generated or analyzed for this study.

AUTHOR CONTRIBUTIONS

RM and APL conceived the idea. RM wrote the manuscript. APL and DS reviewed and revised the manuscript.

FUNDING

This study was funded by the United States Department of Agriculture's Agricultural Research Service (USDA-ARS) under project number 3094-32000-039-00-D. RM was funded by the USDA-ARS through the Oak Ridge Institute for Science and Education (ORISE). The USDA is an equal opportunity provider and employer.

ACKNOWLEDGMENTS

We gratefully acknowledge Dr. Pia U. Olafson from the USDA-ARS, Knipling-Bushland, U.S. Livestock Insects Research Laboratory, Veterinary Pest Genomics Center, Kerrville, TX, United States, for her assistance in refining the phylogenetic tree.

REFERENCES

Alarcon-Chaidez, F., Ryan, R., Wikel, S., Dardick, K., Lawler, C., Foppa, I. M., et al. (2006). Confirmation of tick bite by detection of antibody to *Ixodes calreticulin* salivary protein. *Clin. Vacc. Immunol.* 13, 1217–1222. doi: 10.1128/cvi.00201-06

Andersen, O. M., Dagil, R., and Kragelund, B. B. (2013). New horizons for lipoprotein receptors: communication by β-propellers. *J. Lipid Res.* 54, 2763–2774. doi: 10.1194/jlr.M039545

Anderson, J. F., and Magnarelli, L. A. (2008). Biology of ticks. *Infect. Dis. Clin. North Am.* 22, 195–215. doi: 10.1016/j.idc.2007.12.006

Balashov, Y. S. (1972). Bloodsucking ticks (Ixodoidea)-vectors of disease in man and animals. *Entomol Soc Am.* 8, 161–376.

Barrero, R. A., Guerrero, F. D., Black, M., McCooke, J., Chapman, B., Schilkey, F., et al. (2017). Gene-enriched draft genome of the cattle tick *Rhipicephalus microplus*: assembly by the hybrid Pacific biosciences/Illumina approach enabled analysis of the highly repetitive genome. *Int. J. Parasitol.* 47, 569–583. doi: 10.1016/j.ijpara.2017.03.007

Blacklow, S. C., and Kim, P. S. (1996). Protein folding and calcium binding defects arising from familial hypercholesterolemia mutations of the LDL receptor. *Nat. Struct. Biol.* 3, 758–762. doi: 10.1038/nsb0996-758

Bock, R., Jackson, L., De Vos, A., and Jorgensen, W. (2004). Babesiosis of cattle. *Parasitology* 129, S247–S269.

Boldbaatar, D., Battsetseg, B., Matsuo, T., Hatta, T., Umemiya-Shirafuji, R., Xuan, X., et al. (2008). Tick vitellogenin receptor reveals critical role in oocyte development and transovarial transmission of *Babesia* parasite. *Biochem. Cell. Biol.* 864, 331–344. doi: 10.1139/o08-071

Boldbaatar, D., Umemiya-Shirafuji, R., Liao, M., Tanaka, T., Xuan, X., and Fujisaki, K. (2010). Multiple vitellogenins from the *Haemaphysalis longicornis* tick are crucial for ovarian development. *J. Insect Physiol.* 56, 1587–1598. doi: 10.1016/j.jinsphys.2010.05.019

Boulanger, N., Boyer, P., Talagrand-Reboul, E., and Hansmann, Y. (2019). Ticks and tick-borne diseases. *Med. Mal. Infect.* 49, 87–97. doi: 10.1016/j.medmal.2019.01.007

Bowman, A. S., and Nuttall, P. A. (2008). *Ticks: Biology, Disease and Control*. Cambridge: Cambridge University Press.

UniProt Consortium (2007). The universal protein resource (UniProt). *Nucleic Acids Res.* 36, D190–D195.

Cramaro, W. J., Revets, D., Hunewald, O. E., Sinner, R., Reye, A. L., and Muller, C. P. (2015). Integration of *Ixodes ricinus* genome sequencing with transcriptome and proteome annotation of the naïve midgut. *BMC Genomics* 16, 871. doi: 10.1186/s12864-015-1981-7

da Silva Vaz, I. Jr., Martinez, R. H. M., Oliveira, A., Heck, A., Logullo, C., Gonzales, J. C., et al. (1996). Functional bovine immunoglobulins in *Boophilus microplus* hemolymph. *Vet. Parasitol.* 62, 155–160. doi: 10.1016/0304-4017(95)00851-9

Eisen, L. (2018). Pathogen transmission in relation to duration of attachment by *Ixodes scapularis* ticks. *Ticks Tick Borne Dis.* 9, 535–542. doi: 10.1016/j.ttbdis.2018.01.002

Fass, D., Blacklow, S., Kim, P. S., and Berger, J. M. (1997). Molecular basis of familial hypercholesterolaemia from structure of LDL receptor module. *Nature* 388, 691–693. doi: 10.1038/41798

Gent, J., and Braakman, I. (2004). Low-density lipoprotein receptor structure and folding. *Cell. Mol. Life Sci.* 61, 2461–2470. doi: 10.1007/s00018-004-4090-3

Giraldo-Ríos, C., and Hurtado, O. J. B. (2018). "Economic and health impact of the ticks in production animals," in *Ticks and Tick-Borne Pathogens*, eds M. Abubakar and P. K. Perera (London: IntechOpen), doi: 10.5772/intechopen.81167

Goldstein, J. L., Brown, M. S., Anderson, R. G., Russell, D. W., and Schneider, W. J. (1985). Receptor-mediated endocytosis: concepts emerging from the LDL receptor system. *Ann. Rev. Cell Biol.* 1, 1–39. doi: 10.1146/annurev.cellbio.1.1.1

Guerrero, F. D., Miller, R. J., and de León, A. A. P. (2012). Cattle tick vaccines: many candidate antigens, but will a commercially viable product emerge? *Int. J. Parasitol.* 42, 421–427. doi: 10.1016/j.ijpara.2012.04.003

Guglielmone, A. A., Robbins, R. G., Apanaskevich, D. A., Petney, T. N., Estrada-Peña, A., Horak, I. G., et al. (2010). The *Argasidae*, *Ixodidae* and *Nuttalliellidae* (*Acari: Ixodida*) of the world: a list of valid species names. *Zootaxa* 2528, 1–28.

Gulia-Nuss, M., Nuss, A. B., Meyer, J. M., Sonenshine, D. E., Roe, R. M., Waterhouse, R. M., et al. (2016). Genomic insights into the *Ixodes scapularis* tick vector of Lyme disease. *Nat. Commun.* 7, 10507. doi: 10.1038/ncomms10507

He, K., Lin, K., Ding, S., Wang, G., and Li, F. (2018). The vitellogenin receptor has an essential role in vertical transmission of rice stripe virus during oogenesis in the small brown plant hopper. *Pest Manag. Sci.* 75, 1370–1382. doi: 10.1002/ps.5256

Hope, M., Jiang, X., Gough, J., Cadogan, L., Josh, P., Jonsson, N., et al. (2010). Experimental vaccination of sheep and cattle against tick infestation using recombinant 5'-nucleotidase. *Parasit. Immunol.* 32, 135–142. doi: 10.1111/j.1365-3024.2009.01168.x

Huo, Y., Yu, Y., Liu, Q., Liu, D., Zhang, M., Liang, J., et al. (2019). Rice stripe virus hitchhikes the vector insect vitellogenin ligand-receptor pathway for ovary entry. *Philos. Trans. R. Soc. B* 374, 20180312. doi: 10.1098/rstb.2018.0312

Hussein, H. E., Johnson, W. C., Taus, N. S., Suarez, C. E., Scoles, G. A., and Ueti, M. W. (2019). Silencing expression of the *Rhipicephalus microplus* vitellogenin receptor gene blocks *Babesia bovis* transmission and interferes with oocyte maturation. *Parasit. Vectors* 12, 7. doi: 10.1186/s13071-018-3270-1

Innerarity, T. L. (2002). LDL receptor's β-propeller displaces LDL. *Science* 298, 2337–2339. doi: 10.1126/science.1080669

Jeffers, L. A., and Roe, R. M. (2008). The movement of proteins across the insect and tick digestive system. *J. Insect Physiol.* 54, 319–332. doi: 10.1016/j.jinsphys.2007.10.009

Jeon, H., and Blacklow, S. C. (2003). An intramolecular spin of the LDL receptor β propeller. *Structure* 11, 133–136. doi: 10.1016/s0969-2126(03)00010-8

Kemp, D., Pearson, R., Gough, J., and Willadsen, P. (1989). Vaccination against *Boophilus microplus*: localization of antigens on tick gut cells and their interaction with the host immune system. *Exp. Appl. Acarol.* 7, 43–58. doi: 10.1007/bf01200452

Khalil, S. M., Donohue, K. V., Thompson, D. M., Jeffers, L. A., Ananthapadmanaban, U., Sonenshine, D. E., et al. (2011). Full-length sequence, regulation and developmental studies of a second vitellogenin gene from the American dog tick. *Dermacentor variabilis. J. Insect Physiol.* 57, 400–408. doi: 10.1016/j.jinsphys.2010.12.008

Killiny, N., Hajeri, S., Tiwari, S., Gowda, S., and Stelinski, L. L. (2014). Double-stranded RNA uptake through topical application, mediates silencing of five CYP4 genes and suppresses insecticide resistance in *Diaphorina citri*. *PLoS One* 9, e110536. doi: 10.1371/journal.pone.0110536

Kopáček, P., Perner, J., Sojka, D., Šíma, R., and Hajdušek, O. (2019). "Molecular targets to impair blood meal processing in ticks," in *Ectoparasites: Drug Discovery Against Moving Targets*, eds C. Meng and A. Sluder (Weinheim: Wiley-VCH Verlag GmbH & Co. KGaA), 141–165.

Letunic, I., and Bork, P. (2018). 20 years of the SMART protein domain annotation resource. *Nucleic Acids Res.* 46, D493–D496. doi: 10.1093/nar/gkx922

Lipman, D. J., Karsch-Mizrachi, I., Ostell, J., Clark, K., and Sayers, E. W. (2015). GenBank. *Nucleic Acids Res.* 44, D67–D72. doi: 10.1093/nar/gkv1276

Lombardo, D., Kiselev, M. A., and Caccamo, M. T. (2019). Smart nanoparticles for drug delivery application: development of versatile nanocarrier platforms in biotechnology and nanomedicine. *J. Nanomater.* 2019, 1–26. doi: 10.1155/2019/3702518

Mac, S., da Silva, S. R., and Sander, B. (2019). The economic burden of Lyme disease and the cost-effectiveness of Lyme disease interventions: a scoping review. *PLoS One* 14, e0210280. doi: 10.1371/journal.pone.0210280

Marr, E. J., Sargison, N. D., Nisbet, A. J., and Burgess, S. T. (2014). RNA interference for the identification of ectoparasite vaccine candidates. *Parasit. Immunol.* 36, 616–626. doi: 10.1111/pim.12132

Miller, R., Estrada-Peña, A., Almazán, C., Allen, A., Jory, L., Yeater, K., et al. (2012). Exploring the use of an anti-tick vaccine as a tool for the integrated eradication of the cattle fever tick *Rhipicephalus* (*Boophilus*) annulatus. *Vaccine* 30, 5682–5687. doi: 10.1016/j.vaccine.2012.05.061

Mitchell, R. D. III, Ross, E., Osgood, C., Sonenshine, D. E., Donohue, K. V., Khalil, S. M., et al. (2007). Molecular characterization, tissue-specific expression and RNAi knockdown of the first vitellogenin receptor from a tick. *Insect Biochem. Mol. Biol.* 37, 375–388. doi: 10.1016/j.ibmb.2007.01.005

Murgia, M. V., Bell-Sakyi, L., de la Fuente, J., Kurtti, T. J., Makepeace, B. L., Mans, B., et al. (2019). Meeting the challenge of tick-borne disease control: a proposal for 1000 Ixodes genomes. *Ticks Tick Borne Dis.* 10, 213–218. doi: 10.1016/j.ttbdis.2018.08.009

Nicholson, W. L., Sonenshine, D. E., Noden, B. H., and Brown, R. N. (2019). "Ticks (Ixodida)," in *Medical and Veterinary Entomology*, eds G. R. Mullen and L. A. Durden (San Diego, CA: Academic Press, an imprint of Elsevier), 603–672.

Nuttall, P. A. (2019). Wonders of tick saliva. *Ticks Tick Borne Dis.* 10, 470–481. doi: 10.1016/j.ttbdis.2018.11.005

Okabayashi, K., Shoji, H., Nakamura, T., Hashimoto, O., Asashima, M., and Sugino, H. (1996). cDNA cloning and expression of the *Xenopus laevis* vitellogenin receptor. *Biochem. Biophys. Res. Commun.* 224, 406–413.

Opdebeeck, J. (1994). Vaccines against blood-sucking arthropods. *Vet. Parasitol.* 54, 205–222. doi: 10.1016/0304-4017(94)90091-4

Ramírez Rodríguez, P. B., Cruz, R. R., García, D. I. D., Gutiérrez, R. H., Quintanilla, R. E. L., Sahagún, D. O., et al. (2016). Identification of immunogenic proteins from ovarian tissue and recognized in larval extracts of *Rhipicephalus (Boophilus) microplus*, through an immunoproteomic approach. *Exp. Parasitol.* 170, 227–235. doi: 10.1016/j.exppara.2016.10.005

Randolph, S. E. (1994). "The relative contributions of transovarial and transstadial transmission to the maintenance of tick-borne diseases," in *Lyme Borreliosis*, eds J. S. Axford and D. H. E. Rees (Boston MA: Springer), 131–134. doi: 10.1007/978-1-4615-2415-1_21

Rao, Z., Handford, P., Mayhew, M., Knott, V., Brownlee, G. G., and Stuart, D. (1995). The structure of a Ca^{2+}-binding epidermal growth factor-like domain: its role in protein-protein interactions. *Cell* 82, 131–141. doi: 10.1016/0092-8674(95)90059-4

Roe, R. M., Donohue, K. V., Khalil, S. M., and Sonenshine, D. E. (2008). Hormonal regulation of metamorphosis and reproduction in ticks. *Front. Biosci.* 13, 7250–7268.

Rosell-Davis, R., and Coons, L. B. (1989). Relationship between feeding, mating, vitellogenin production and vitellogenesis in the tick *Dermacentor variabilis*. *Exp. Appl. Acarol.* 7, 95–105. doi: 10.1007/bf01200456

Sappington, T. W., and Raikhel, A. S. (1998). Molecular characteristics of insect vitellogenins and vitellogenin receptors. *Insect Biochem. Mol. Biol.* 28, 277–300. doi: 10.1016/s0965-1748(97)00110-0

Sappington, T. W., and Raikhel, A. S. (2005). "Insect vitellogenin/yolk protein receptors," in *Progress in Vitellogenesis. Reproductive Biology of Invertebrates*, eds T. W. Sappington and A. S. Raikhel (Enfield, USA: Science Publishers, Inc), 229–264.

Schneider, W., and Nimpf, J. (2003). LDL receptor relatives at the crossroad of endocytosis and signaling. *Cell. Mol. Life Sci.* 60, 892–903. doi: 10.1007/s00018-003-2183-z

Seixas, A., Alzugaray, M. F., Tirloni, L., Parizi, L. F., Pinto, A. F. M., Githaka, N. W., et al. (2018). Expression profile of *Rhipicephalus microplus* vitellogenin receptor during oogenesis. *Ticks Tick Borne Dis.* 9, 72–81. doi: 10.1016/j.ttbdis.2017.10.006

Smith, A. D., and Kaufman, R. W. (2013). Molecular characterization of the vitellogenin receptor from the tick, *Amblyomma hebraeum* (*Acari: Ixodidae*). *Insect Biochem. Mol. Biol.* 43, 1133–1141. doi: 10.1016/j.ibmb.2013.10.002

Smith, A. D., and Kaufman, W. R. (2014). Molecular characterization of two vitellogenin genes from the tick, *Amblyomma hebraeum* (Acari: Ixodidae). *Ticks Tick Borne Dis.* 5, 821–833. doi: 10.1016/j.ttbdis.2014.06.001

Solano-Gallego, L., Sainz, Á, Roura, X., Estrada-Peña, A., and Miró, G. (2016). A review of canine babesiosis: the European perspective. *Parasit. Vectors* 9, 336. doi: 10.1186/s13071-016-1596-0

Sonenshine, D. E. (2018). Range expansion of tick disease vectors in North America: implications for spread of tick-borne disease. *Int. J. Environ. Res. Public Health* 15, 478. doi: 10.3390/ijerph15030478

Sonenshine, D. E., and Roe, R. M. (2013a). *Biology of Ticks, Vol. 1*. Oxford: Oxford University Press.

Sonenshine, D. E., and Roe, R. M. (2013b). *Biology of Ticks, Vol. 2*. Oxford: Oxford University Press.

Springer, T. A. (1998). An extracellular β-propeller module predicted in lipoprotein and scavenger receptors, tyrosine kinases, epidermal growth factor precursor, and extracellular matrix components. *J. Mol. Biol.* 283, 837–862. doi: 10.1006/jmbi.1998.2115

Sun, D., Guo, Z., Liu, Y., and Zhang, Y. (2017). Progress and prospects of CRISPR/Cas systems in insects and other arthropods. *Front. Physiol.* 8, 608. doi: 10.3389/fphys.2017.00608

Thompson, D. M., Khalil, S. M., Jeffers, L. A., Sonenshine, D. E., Mitchell, R. D., Osgood, C. J., et al. (2007). Sequence and the developmental and tissue-specific regulation of the first complete vitellogenin messenger RNA from ticks responsible for heme sequestration. *Insect Biochem. Mol. Biol.* 37, 363–374. doi: 10.1016/j.ibmb.2007.01.004

Trowbridge, I. S. (1991). Endocytosis and signals for internalization. *Curr. Opin. Cell. Biol* 3, 634–641. doi: 10.1016/0955-0674(91)90034-v

Tufail, M., and Takeda, M. (2009). Insect vitellogenin/lipophorin receptors: molecular structures, role in oogenesis, and regulatory mechanisms. *J. Insect Physiol.* 55, 87–103. doi: 10.1016/j.jinsphys.2008.11.007

Valle, M. R., and Guerrero, F. D. (2018). Anti-tick vaccines in the omics era. *Front. Biosci.* 10, 122–136. doi: 10.2741/e812

Willadsen, P. (2008). "Anti-tick vaccines," in *Ticks: Biology, Disease and Control*, eds A. S. Bowman and P. A. Nuttall (Cambridge: Cambridge University Press), 424–446. doi: 10.1017/cbo9780511551802.020

Xavier, M. A., Tirloni, L., Pinto, A. F. M., Diedrich, J. K., Yates, J. R. III, Mulenga, A., et al. (2018). A proteomic insight into vitellogenesis during tick ovary maturation. *Sci. Rep.* 8, 4698. doi: 10.1038/s41598-018-23090-2

Yamamoto, T., Bishop, R. W., Brown, M. S., Goldstein, J. L., and Russell, D. W. (1986). Deletion in cysteine-rich region of LDL receptor impedes transport to cell surface in WHHL rabbit. *Science* 232, 1230–1237. doi: 10.1126/science.3010466

Conflict of Interest Statement: The authors declare that the research was conducted in the absence of any commercial or financial relationships that could be construed as a potential conflict of interest.

frontiers in Physiology

ORIGINAL RESEARCH
published: 28 May 2019
doi: 10.3389/fphys.2019.00653

Comparative Susceptibility of Different Populations of *Amblyomma sculptum* to *Rickettsia rickettsii*

*Monize Gerardi, Alejandro Ramírez-Hernández, Lina C. Binder, Felipe S. Krawczak†, Fábio Gregori and Marcelo B. Labruna**

Department of Preventive Veterinary Medicine and Animal Health, Faculty of Veterinary Medicine, University of São Paulo, São Paulo, Brazil

OPEN ACCESS

Edited by:
Itabajara Da Silva Vaz Jr., Federal University of Rio Grande do Sul, Brazil

Reviewed by:
Ben J. Mans, Agricultural Research Council, South Africa
José M. Venzal, Universidad de la República, Uruguay

***Correspondence:**
Marcelo B. Labruna
labruna@usp.br

†Present address:
Felipe S. Krawczak, Setor de Medicina Veterinária Preventiva, Escola de Veterinária e Zootecnia, Universidade Federal de Goiás, Goiânia, Brazil

Specialty section:
This article was submitted to Invertebrate Physiology, a section of the journal Frontiers in Physiology

Received: *02 April 2019*
Accepted: *09 May 2019*
Published: *28 May 2019*

Citation:
Gerardi M, Ramírez-Hernández A, Binder LC, Krawczak FS, Gregori F and Labruna MB (2019) Comparative Susceptibility of Different Populations of Amblyomma sculptum to Rickettsia rickettsii. Front. Physiol. 10:653. doi: 10.3389/fphys.2019.00653

The bacterium *Rickettsia rickettsii* is the etiological agent of Brazilian spotted fever (BSF), which is transmitted in Brazil mainly by the tick *Amblyomma sculptum.* Herein, larvae and nymphs of six populations of *A. sculptum* were exposed to *R. rickettsii* by feeding on needle-inoculated guinea pigs, and thereafter reared on uninfected guinea pigs or rabbits. Two tick populations were exposed to autochthone *R. rickettsii* strains, whereas four tick populations were exposed to non-autochthone strains. The six geographically different populations of *A. sculptum* showed different susceptibilities to *R. rickettsii*, higher among the two tick populations that were exposed to their autochthone *R. rickettsii* strain. In addition, higher rates of transovarial transmission of *R. rickettsii* and vector competence success also included the two tick populations that were exposed to autochthone *R. rickettsii* strains. These results indicate that the susceptibility of *A. sculptum* to *R. rickettsii* varies among different tick populations, with a clear bias for higher susceptibility to an autochthone *R. rickettsii* strain that has already coevolved with a tick population for some time. Our results demonstrated that the *R. rickettsii* infection induces higher mortality of engorged larvae and nymphs, and tend to reduce the reproductive fitness of engorged females. All together, these results might explain the low *R. rickettsii*-infection rates of *A. sculptum* under natural conditions (usually <1%), and indicate that an *A. sculptum* population should not be able to sustain a *R. rickettsii* infection for successive tick generations without the creation of new cohorts of infected ticks via horizontal transmission on vertebrate rickettsemic hosts (amplifying hosts). Finally, despite of the ubiquitous distribution of *A. sculptum* in southeastern and central-western Brazil, most of the populations of this tick species are devoid of *R. rickettsii* infection. This scenario might be related to two major factors: (i) insufficient numbers of susceptible amplifying hosts; and (ii) lower susceptibilities of many tick populations. While the first factor has been demonstrated by mathematical models in previous studies, the second is highlighted by the results observed in the present study.

Keywords: spotted fever group *Rickettsia*, experimental infection, vector competence, transovarial transmission, transstadial maintenance

INTRODUCTION

The bacterium *Rickettsia rickettsii* is the etiological agent of Brazilian spotted fever (BSF), the deadliest tick-borne disease of the New World. In southeastern Brazil, 776 cases of BSF were laboratory-confirmed in humans from 2007 to 2015, with an overall case-fatality rate of 55% (Oliveira et al., 2016). While several tick species of the genus *Amblyomma* have been implicated in the transmission of *R. rickettsii* to humans in South America (Labruna et al., 2014), *Amblyomma sculptum* (formerly called as *Amblyomma cajennense* in southeastern Brazil) is the most important vector, since most of the BSF-confirmed cases have been associated to this tick species (Pinter et al., 2011; Krawczak et al., 2014; Labruna et al., 2017).

Amblyomma sculptum, a member of the *A. cajennense* species complex, is by far the most frequent human-biting tick species in Brazil (Guglielmone et al., 2006; Ramos et al., 2014; Martins et al., 2016). While this may suggest a high exposure of humans to *R. rickettsii* infection, the incidence of BSF has been as low as 0.14/100,000 inhabitants (Oliveira et al., 2016), thanks to the very low *R. rickettsii*-infection rates among *A. sculptum* populations, reported to be between 0.05 and 1.28% (Guedes et al., 2005, 2011; Krawczak et al., 2014; Labruna et al., 2017). The very low *R. rickettsii*-infection rates of *A. sculptum* under natural conditions has been attributed to the lower susceptibility of this tick species to the bacterium when compared to other tick species that are found with much higher infection rates under natural conditions, such as *Amblyomma aureolatum* and *Rhipicephalus sanguineus* sensu lato (s.l.) (Labruna et al., 2008, 2011; Pacheco et al., 2011; Ogrzewalska et al., 2012; Soares et al., 2012).

Amblyomma sculptum has a ubiquitous distribution in southeastern and central-western Brazil (Martins et al., 2016); however, only a few populations of this tick species have been found infected by *R. rickettsii* (Sangioni et al., 2005; Pacheco et al., 2007, 2009; Soares et al., 2012). This scenario could be linked to different susceptibilities to *R. rickettsii* infection among different populations of *A. sculptum*. Previous studies that quantified the susceptibility of *A. sculptum* to *R. rickettsii* employed a rickettsial strain that was originally isolated from *A. aureolatum* ticks in an area without *A. sculptum* (Labruna et al., 2008; Soares et al., 2012). Therefore, more reliable data could be obtained with additional studies employing *A. sculptum*-derived *R. rickettsii* strains. Based on the above statements, the present study evaluated the comparative susceptibility of different populations of *A. sculptum* to the infection by *R. rickettsii*, using two rickettsial strains that were originally isolated from *A. sculptum* in Brazil.

MATERIALS AND METHODS

Ethics Statements

This study has been approved by the Institutional Animal Care and Use Committee (IACUC) of the Faculty of Veterinary Medicine of the University of São Paulo (protocols 3104/2013 and 5948070314). Field capture of ticks was authorized by the Brazilian Ministry of the Environment (permit SISBIO Nos. 43259-1 and 11459-1).

Ticks

A total of six geographically distinct populations of *A. sculptum* were used in this study, as detailed in **Table 1**. From five populations, unfed adults were collected on the vegetation by dragging or dry ice traps following Terassini et al. (2010) or Szabó et al. (2009), and brought alive to the laboratory, where adult ticks were allowed to feed on tick-naïve rabbits, in order to establish five independent tick colonies. From a sixth tick population (E-ITU), engorged females were collected from capybaras (*Hydrochoerus hydrochaeris*) and brought to the laboratory to start a tick colony.

For all six tick colonies, off-host conditions were provided by an incubator set for a temperature of 27°C, 85% relative humidity and photoperiod 0:24 (light:dark). Our experimental infestations were started with the F_1 larvae (first lab generation) of each of the six tick colonies. Before starting the experiments, we had the following evidence that these ticks were free of rickettsial infection: all engorged females that yielded the F_1 larvae, as well as a small sample of their egg batches were negative by real-time PCR for the genus *Rickettsia* (protocol described below) at the end of oviposition; and all rabbits remained seronegative to *R. rickettsii* (protocol described below) 21 days after being infested with field-collected adult ticks.

Among the six colonies of *A. sculptum*, three were from BSF-endemic areas in which fatal cases of BSF have been reported recently, in association with the transmission by *A. sculptum*. Three other colonies were from areas where BSF was never reported (non-endemic areas), which include a highly anthropic area in the state of São Paulo, and two natural areas with a rich biodiversity (**Table 1**).

Rickettsia rickettsii Strains

Two strains of *R. rickettsii* were used in this study, strain Itu and strain Pampulha. The former was isolated from *A. sculptum* collected in a BSF-endemic area in Itu municipality (Krawczak et al., 2014), the same area where we collected *A. sculptum* adult ticks to form our E-ITU tick colony. The later was collected in the Pampulha Lake area, a BSF-endemic area in Belo Horizonte City (Labruna et al., 2017), where we collected *A. sculptum* adult ticks to form our E-PAM tick colony. Both *R. rickettsii* strains were originally isolated through the inoculation of guinea pigs with field-collected *A. sculptum* tick homogenate and subsequently adaptation of the strain to Vero cell culture (Krawczak et al., 2014; Labruna et al., 2017). However, only the guinea pig lineage of each strain (never *in vitro* cultured) was used for experimental infections in the present study. For this purpose, each rickettsial strain has been maintained through guinea pig passages in our laboratory, and in each passage we have cryopreserved fragments of infected spleen, lung, liver, and brain. In the present study, we used fragments of these four organs of the third guinea pig passage of each isolate to inoculate guinea pigs, as described below.

TABLE 1 | General characteristics of the local origin of the *Amblyomma sculptum* populations that originated the six tick colonies used in the present study.

Tick colony code	Origin (municipality, state)	Conservation status of the origin	Main hosts sustaining the *A. sculptum* population	Status for Brazilian spotted fever (*R. rickettsii*)	References
E-ITU	Itu, São Paulo	Highly anthropic, low biodiversity	Capybaras	Endemic	Krawczak et al., 2014
E-PIC	Piracicaba, São Paulo	Highly anthropic, low biodiversity	Capybaras	Endemic	Perez et al., 2008
E-PAM	Belo Horizonte, Minas Gerais	Highly anthropic, low biodiversity	Capybaras	Endemic	Labruna et al., 2017
NE-PIS	Pirassununga, São Paulo	Highly anthropic, low biodiversity	Capybaras	Non-endemic	Horta et al., 2007
NE-POC	Poconé, Mato Grosso	Natural area, high biodiversity	Tapirs, peccaries	Non-endemic	Melo et al., 2016
NE-GSV	Chapada Gaúcha, Minas Gerais	Natural area, high biodiversity	Tapirs, peccaries	Non-endemic	Barbieri et al., 2019

Tick Infestation Protocols

Throughout this study, larvae and nymphs were allowed to feed on tick-naïve adult male (or female in a few cases) guinea pigs, whereas adult ticks were allowed to feed on tick-naïve adult male domestic rabbits. In either case, tick infestations were performed inside cotton sleeves (10–20 cm diameter) that were glued to the shaved back of each animal, as previously described (Pinter et al., 2002; Horta et al., 2009). Ticks (larvae, nymphs or adults, 20–30 days old) were released into the sleeve. Larval infestations consisted of approximately 500–1500 larvae per guinea pig; nymphal infestations consisted of 80–100 nymphs per guinea pig; and adult infestations consisted of 7–20 couples per rabbit. The sleeves were opened daily, and the detached engorged ticks were removed, counted and immediately taken to the incubator where molting (for engorged larvae and nymphs) or oviposition (for engorged females) was observed daily. Engorged females were individually weighed in an electronic balance (precision of 0.0001 g) at the detachment day. Molting success (survivorship) was determined for engorged larvae and nymphs whereas the following biological parameters were determined for engorged females: feeding period (number of days from placement of the ticks on the host to the detachment), oviposition success (proportion of engorged females that successfully oviposited), preoviposition period (number of days from detachment to the beginning of oviposition) and egg mass incubation period (number of days from the beginning of oviposition to the hatching of the first larva). Additionally, the total egg mass laid by each female was weighed at the end of oviposition and a conversion efficiency index (CEI = mg egg mass/mg engorged female $\times$ 100), which measures the efficiency with which a tick species converts body weight into eggs (Drummond and Whetstone, 1970), was determined for each female that oviposited. Percentage of hatching for each female egg mass was visually estimated according to Labruna et al. (2000). During the experiment, animals were fed with commercial pellets and water *ad libitum*.

Experimental Procedures

Most of the experimental procedures used in this study were exactly the same that were used in a previous study at our laboratory, in which an *A. sculptum* population from Pedreira, state of São Paulo, was experimentally infected with *R. rickettsii* strain Taiaçu, previously isolated from the tick *A. aureolatum* (Soares et al., 2012). These procedures were adopted, so most of our results can be compared to the results reported by Soares et al. (2012), as presented below in the Discussion section.

In the present study, the strain Itu of *R. rickettsii* was used for experimental infection of five tick colonies: E-ITU, E-PIC, NE-PIS, NE-POC, and NE-GSV. The strain Pampulha of *R. rickettsii* was used for experimental infection of only the E-PAM tick colony. With these procedures, we had two tick colonies exposed to autochthone strains of *R. rickettsii* (E-ITU to strain Itu; E-PAM to strain Pampulha), and four tick colonies exposed to a non-autochthone strain of *R. rickettsii* (E-PIC, NE-PIS, NE-POC, and NE-GSV to strain Itu); in the latter case, one tick colony (E-PIC) was from a BSF-endemic area, while the remaining three tick colonies were from BSF non-endemic areas. In addition, NE-POC and NE-GSV were from highly preserved areas with rich biodiversity, whereas NE-PIS was from a highly anthropic area (**Table 1**).

Procedures of experimental infection of ticks with *R. rickettsii* and the follow up infestations, from F_1 larvae to F_3 larvae (or F_3 nymphs for a single tick colony) were the same for each tick colony, and are summarized in **Figure 1**. In all cases, the initial exposition of ticks to *R. rickettsii* infection consisted of ticks (larvae or nymphs) feeding on *R. rickettsii*-infected guinea pigs. For this purpose, samples from our stock of cryopreserved guinea pig-infected organs were thawed at room temperature, crushed in a mortar with brain–heart infusion (BHI) and the resultant homogenate was used to inoculate guinea pigs intraperitoneally, as previously described (Soares et al., 2012). At the same day of guinea pig inoculation, these animals were infested with ticks. During the F_1 generation, three experimental groups of ticks (GL, GN, and CG) were formed in each colony. GL and GN consisted

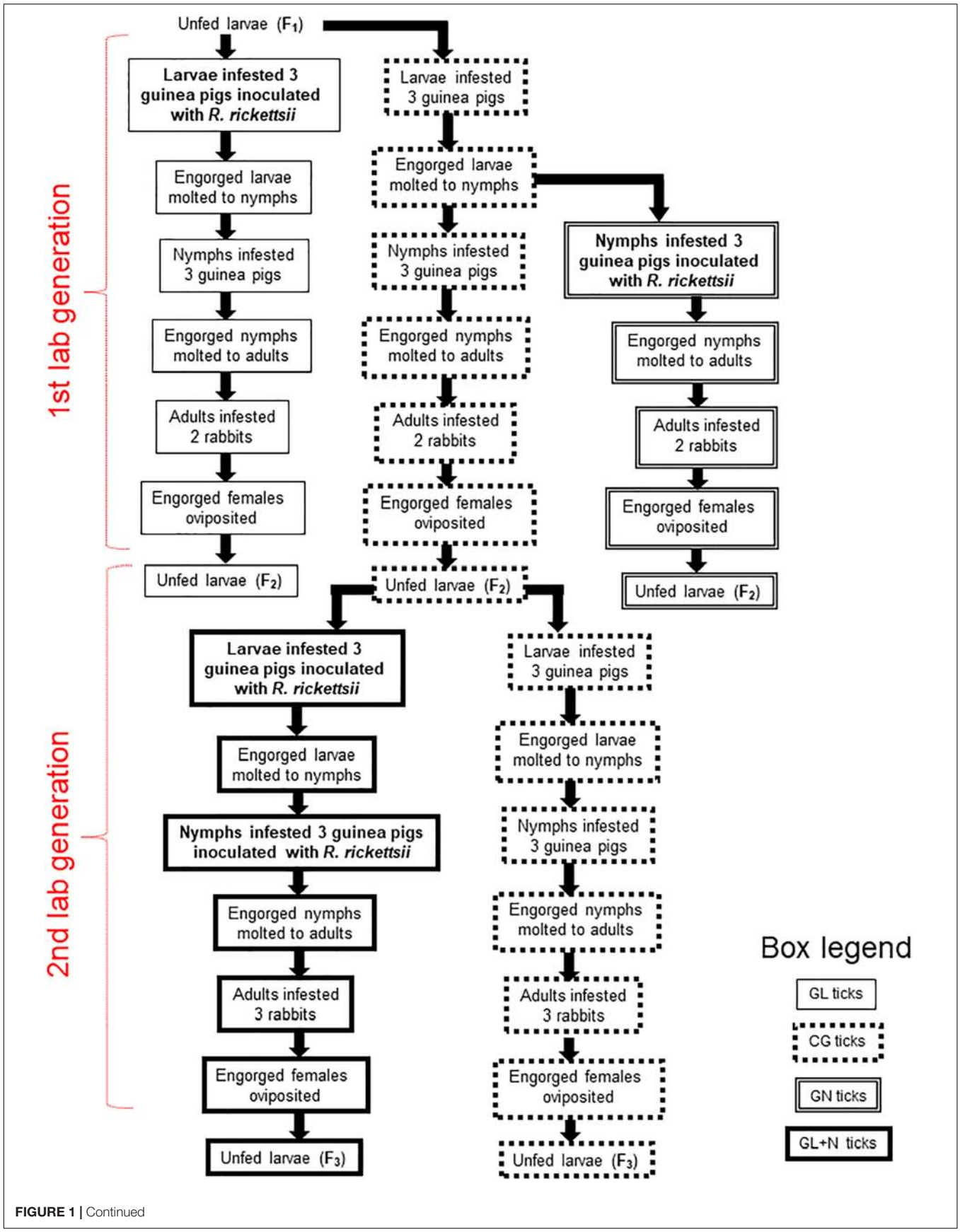

FIGURE 1 | Continued

FIGURE 1 | Diagram illustrating experimental procedures with each of the six colonies of *Amblyomma sculptum* ticks from F_1 larvae to F_3 larvae. GL and GN ticks were exposed to *Rickettsia rickettsii*-inoculated guinea pigs during the F_1 larval and nymphal stages, respectively, and thereafter, they were reared through the F_2 larval stage on susceptible animals (guinea pigs for larvae and nymphs; rabbits for adult ticks). GL + N ticks were dually exposed to *R. rickettsii*-inoculated guinea pigs, firstly during the F_2 larval stage, secondly during the F_2 nymphal stage, and then reared through the F_3 larval stage on susceptible rabbits. CG ticks were the uninfected control group, always exposed to susceptible guinea pigs or rabbits in parallel to the infected groups.

of ticks that were exposed to *R. rickettsii*-inoculated guinea pigs during the F_1 larval or nymphal stages, respectively, and thereafter they were reared through the F_2 larval stage on susceptible hosts (guinea pigs or rabbits). CG was the uninfected control group, always exposed to susceptible, uninfected hosts (**Figure 1**).

In the second lab generation of the study, F_2 larvae of the uninfected control group (CG) of each tick colony were exposed to *R. rickettsii*-inoculated guinea pigs, and the resultant nymphs were also exposed to *R. rickettsii*-inoculated guinea pigs, forming the GL + N group (ticks with dual exposure to *R. rickettsii*-inoculated guinea pigs). These ticks were reared through the F_3 larval or nymphal stage, with ticks feeding on susceptible, uninfected hosts. In parallel, CG ticks were reared through the F_3 larval stage, always exposed to susceptible, uninfected hosts (**Figure 1**).

Guinea Pig and Rabbit Evaluation

All infested animals had their rectal temperature measured from 0 to 21 days post-inoculation or infestation (dpi). Guinea pigs were considered febrile when rectal temperature was >39.5°C (Monteiro, 1931); rabbits were considered febrile when rectal temperature was >40.0°C (Monteiro, 1933). The occurrence of scrotal reactions (edema, congestion, necrosis), typical of *R. rickettsii* acute infection in guinea pigs and rabbits (Monteiro, 1933), were annotated. In all infestations, approximately 0.5–1.0 mL of blood was obtained from each guinea pig or rabbit at days 0 and 21 dpi. Guinea pig blood samples were collected intra-cardiacally under anesthesia (20 mg/Kg xylazine + 20 mg/kg cetamin + 1 mg/kg acepromazin), while rabbit samples were collected through the central ear vein. Samples were centrifuged to obtain sera, which were tested for seroconversion to *R. rickettsii*, as described below. If any guinea pig or rabbit died before 21 dpi, it was subjected to necropsy, when we tried to obtain a blood sample through cardiac puncture. In addition, a lung sample was collected and evaluated by PCR for rickettsial infection, using the protocol described below.

Molecular Analysis

Throughout the study, samples of unfed larvae, nymphs and adults, eggs, and engorged females at the end of oviposition, were tested by PCR for detection of rickettsial DNA. For this purpose, DNA was extracted from eggs (in pools of ≈50 eggs or individually), unfed larvae (in pools of ≈50 larvae or individually), and unfed nymphs by the boiling method, as previously described (Horta et al., 2005), and from unfed adult ticks or engorged females at the end of oviposition by the guanidine isothiocyanate-phenol technique (Sangioni et al., 2005). Guinea pig or rabbit lung fragments were submitted to DNA extraction using the DNeasy tissue Kit (Qiagen, Chatsworth, CA, United States). Blank tubes were always included in the DNA extraction procedures, as negative controls of this step.

Extracted DNA samples were tested by a Taqman real-time PCR assay targeting the rickettsial *gltA* gene, as described (Soares et al., 2012). The sensitivity of this PCR assay was determined to be one DNA copy of *R. rickettsii* (Labruna et al., 2004). Tick DNA samples that were shown to contain no rickettsial DNA by the real-time PCR described above were tested by a conventional PCR protocol targeting the tick mitochondrial 16S rRNA gene, as previously described (Mangold et al., 1998). If the tick sample yielded no product by this PCR, it was considered that DNA extraction was not successful, and the sample was discarded from the study. Random samples of F_1 adult ticks, positive by the real-time PCR assay, were further tested using a conventional PCR assay targeting a 532-bp fragment of the rickettsial *ompA* gene, as described (Regnery et al., 1991); PCR products were DNA-sequenced and the resultant sequences were submitted to BLAST analysis[1] in order to confirm the identity of the *Rickettsia* species.

Serological Analysis

Guinea pig and rabbit blood serum samples were individually tested by the indirect immunofluorescence assay (IFA) using crude antigens derived from *R. rickettsii* strain Taiaçu, as previously described (Labruna et al., 2007). Each serum was diluted in two-fold increments with PBS from 1:64 to the endpoint titer (Labruna et al., 2007). A commercial fluorescein isothiocyanate-labeled goat anti-rabbit IgG (Sigma Diagnostics, St. Louis, MO, United States) or rabbit anti-guinea pig IgG (Sigma Diagnostics) was used. In each slide, a serum previously shown to be non-reactive (negative control) and a known reactive serum (positive control) were tested at the 1:64 dilution. These serum samples were from the study of Soares et al. (2012).

Statistical Analyses

The proportions of ticks that successfully molted or oviposited fertile eggs from different groups, the proportion of *R. rickettsii*-infected ticks from different colonies, and fatality rates of inoculated guinea pigs were compared by using the chi-square test. Reproductive parameters of engorged females were compared between colonies/groups by using the *t*-test, after the Kolmogorov–Smirnov normality test. Analyses were performed using the program Epi Info™ version 7 (chi-square) and Minitab® 18.1 (*t*-Student). Significant differences were considered for $P < 0.05$.

[1] www.ncbi.nlm.nih.gov/blast

Phylogenetic Analyses of Ticks

In order to perform a comparative genetic analysis of *R. rickettsii*-infected and uninfected ticks of each colony, we generated partial sequences of the tick mitochondrial 16S rRNA gene and the tick second internal transcribed spacer (ITS2). Noteworthy, the uninfected tick samples were composed by adult ticks that were exposed to *R. rickettsii* infection (through feeding as larvae and/or nymphs on rickettsemic guinea pigs), but were shown to contain no rickettsial DNA when tested as unfed adults by the real-time PCR protocol described above.

From each tick colony, DNA of *R. rickettsii*-infected and uninfected ticks were submitted to two PCR protocols, one targeting a ≈460-bp fragment of the tick mitochondrial 16S rRNA gene (Mangold et al., 1998) and one targeting a ≈1,100-bp of the tick nuclear ribosomal region, which includes the entire ITS2, as previously described (Marrelli et al., 2007). All PCR products were treated with ExoSap (USB, Cleveland, OH, United States) and sequenced in an ABI automated sequencer (Applied Biosystems/Thermo Fisher Scientific, model ABI 3500 Genetic Analyzer, Foster City, CA, United States) with the same primers used for PCR. The consensus 16S rRNA sequences were aligned by using Clustal/W v.1.8.1 (Thompson et al., 1994), including the 16S rRNA sequence of *Amblyomma tonelliae* from Paraguay retrieved from GenBank (KF179349), which was used as the outgroup. A nucleotide identity matrix was calculated by using the Bioedit software v.7.0.5.3 (Hall, 1999). A phylogenetic tree was generated with the Maximum Likelihood criteria (Tamura 3-parameter model) for the 16S rRNA mitochondrial gene partial nucleotide sequences (410 sites on the dataset) and 1,000 bootstrap replicates using Mega X software (Kumar et al., 2018).

RESULTS

Inoculated Guinea Pigs

In order to form the *R. rickettsii*-infected tick cohorts, larvae and nymphs of the six colonies were exposed to *R. rickettsii* by feeding on guinea pigs that had been inoculated with homogenates of *R. rickettsii*-infected guinea pig organs. A total of 72 guinea pigs were inoculated, which all but one developed fever that started 3–8 dpi (median: 4; mean: 3.9 ± 0.9), and lasted for 3–11 days (median: 5; mean: 5.4 ± 2.0) (**Supplementary Tables S1–S12**). Ticks that had fed on the only non-febrile-inoculated guinea pig (guinea pig G.P.78) were discarded from the study (**Supplementary Table S6**). Rickettsial infection was confirmed in all febrile guinea pigs by seroconversion to *R. rickettsii* at 21 dpi (endpoint titers ranging from 16,384 to 65,536; median: 32,768) or by detection of rickettsial DNA in a lung sample collected from those guinea pigs that died during the febrile period. For instance, 53 out of 71 guinea pigs died during the febrile period (**Supplementary Tables S1–S12**), resulting in an overall fatality rate of 74%. Considering the two *R. rickettsii* strains separately, fatality rates were 75% (45/60) for strain Itu, and 72% (8/11) for strain Pampulha ($P > 0.05$). Larval or nymphal feeding periods lasted from 3 to 10 days, with most of the engorged ticks detaching between 4 and 7 dpi. Since larval and nymphal infestations were performed at the same day of guinea pig inoculation, tick feeding period overlapped with the febrile period, a condition that certifies that these ticks fed during the rickettsemic period; hence, they were exposed to *R. rickettsii*.

Rickettsial Infection in GL Ticks

The GL ticks consisted of F_1 larvae initially exposed to *R. rickettsii* by feeding on rickettsemic guinea pigs, and thereafter, reared until F_2 unfed larvae by feeding on susceptible hosts. After F_1 acquisition larval feeding, rickettsial infection rates of F_1 nymphs (transstadial perpetuation of *R. rickettsii* from larvae to nymphs) varied from 0 to 16% among the six tick colonies, with higher rates for the two tick colonies that were exposed to autochthone *R. rickettsii* strains, namely E-ITU and E-PAM (**Table 2**). Infestation of these F_1 nymphs on susceptible guinea pigs resulted in successful rickettsial transmission (fever followed by death or seroconversion with high endpoint titers) in all three guinea pigs exposed to E-ITU and E-PAM nymphs, only one guinea pig exposed to NE-PIS or NE-GSV, and none of the guinea pigs exposed to E-PIC and NE-POC (**Table 3**). Transstadial perpetuation of *R. rickettsii* from F_1 nymphs to adults were observed by DNA detection only in E-ITU and E-PAM ticks (33 and 47%, respectively), which were infected with autochthone *R. rickettsii* strains (**Table 2**).

TABLE 2 | Tick-*Rickettsia rickettsii* acquisition (feeding on rickettsemic guinea pig) and maintenance (transstadial perpetuation and transovarial transmission).

Tick colony	Transstadial perpetuation: larvae to nymphs[a]			Transstadial perpetuation: nymphs to adults[b]			Transovarial transmission rate[c]		
	GL[d]	GN	GL + N[d]	GL	GN	GL + N	GL	GN	GL + N
E-ITU	4/25 (16)[a]	–	3/36 (8)[a]	5/15 (33)	0/15 (0)	9/15 (60)	2/16 (12)	3/11 (27)	4/20 (20)
E-PIC	1/40 (3)[a,b]	–	3/30 (10)[a]	0/10 (0)	0/30 (0)	0/30 (0)	0 (0/0)	0 (0/0)	0/2 (0)
E-PAM	3/36 (8)[a,b]	–	9/22 (41)[b,c]	7/15 (47)	10/15 (67)	5/15 (33)	1/7 (14)	1/6 (17)	0/4 (0)
NE-PIS	1/55 (2)[b]	–	0/10 (0)[a]	0/25 (0)	3/28 (11)	20/30 (67)	2/11 (18)	1/15 (7)	3/19 (16)
NE-POC	1/80 (1)[b]	–	0/15 (0)[a]	0/20 (0)	0/15 (0)	3/15 (20)	0 (0/0)	0 (0/0)	1/8 (13)
NE-GSV	0/48 (0)[b]	–	5/31 (16)[a,c]	0/16 (0)	4/22 (18)	7/30 (23)	0/5 (0)	1/6 (17)	3/11 (27)

GL, R. rickettsii-acquisition feeding as larvae; GN, R. rickettsii-acquisition feeding as nymphs; and GL + N, dual R. rickettsii acquisition-feeding, as larvae and as nymphs. [a]No. PCR-positive unfed nymphs/no. unfed nymphs tested (% infection). [b]No. PCR-positive unfed adults/no. unfed adults tested (% infection). [c]No. females with PCR-positive eggs or larvae/no. PCR-positive females at the end of oviposition (% transovarial transmission). [d]Different letters in the same column mean significantly different infection rates ($P < 0.05$).

TABLE 3 | Results of rickettsial transmission by ticks (vector competence) of six colonies of *Amblyomma sculptum* that were allowed to feed on susceptible hosts (guinea pigs for larvae and nymphs; rabbits for adults).

Tick colony	No. hosts that became infected by *R. rickettsii*/no. infested hosts[a]									Total (%)
	GL ticks			GN ticks			GL + N ticks			
	F_1 nymphs	F_1 adults	F_2 larvae	F_1 adults	F_2 larvae	F_2 nymphs	F_2 adults	F_3 larvae	F_3 nymphs	
E-ITU	3/3	2/2	–	2/2	–	–	3/3	2/2	1/1	13/13 (100)
E-PIC	0/3	0/2	–	0/2	–	–	1/3	–	–	1/10 (10)
E-PAM	3/3	1/2	1/1	1/2	1/1	–	0/1	–	–	7/10 (70)
NE-PIS	1/3	1/2	–	2/2	1/1	1/1	2/3	–	–	8/12 (67)
NE-POC	0/3	0/2	–	0/2	–	–	3/3	–	–	3/10 (30)
NE-GSV	1/3	1/2	–	1/2	–	–	2/3	2/3	–	7/13 (54)

Previous to these infestations, Rickettsia rickettsii-acquisition feedings were performed on rickettsemic guinea pigs that were infested with F_1 larvae (GL ticks), F_1 nymphs (GN ticks) and F_2 larvae and nymphs (GL + N ticks). GL, R. rickettsii-acquisition feeding as larvae; GN, R. rickettsii-acquisition feeding as nymphs; and GL + N, dual R. rickettsii acquisition-feeding, as larvae and as nymphs. [a]Hosts were considered infected by R. rickettsii when they became febrile after tick infestation, and the infection was confirmed by seroconversion with high endpoint titers to R. rickettsii or by detection of rickettsial DNA in their lungs if they died during the febrile period. –, not done.

Infestation of F_1 adults on susceptible rabbits resulted in successful rickettsial transmission (fever followed by death or seroconversion with high endpoint titers) in all two rabbits exposed to E-ITU ticks, and one out of two rabbits exposed to E-PAM, NE-PIS, and NE-GSV adults, and none of the two rabbits exposed to either E-PIC or NE-POC (**Table 3**). Transovarial transmission of *R. rickettsii* was observed by DNA detection in engorged females of only the E-ITU, E-PAM, and NE-PIS tick colonies. In these cases, the transovarial transmission rate (no. females with PCR-positive eggs or larvae/no. PCR-positive females at the end of oviposition × 100) varied from 12 to 18% (**Table 2**). For these infected females with rickettsial transovarial transmission, we calculated the filial infection rate (No. infected eggs or larvae/No. tested eggs or larvae × 100), which was 100% for either E-ITU or E-PAM ticks (infected with autochthone *R. rickettsii* strains), and 0–10% for NE-PIS ticks (infected with non-autochthone *R. rickettsii* strain) (**Supplementary Table S13**). The transovarial acquisition infection of E-PAM F_2-infected larvae was confirmed by allowing part of these larvae to feed on a guinea pig, which became ill and seroconverted to *R. rickettsii* (guinea pig G.P. 73 in **Supplementary Table S5**).

Rickettsial Infection in GN Ticks

The GN ticks consisted of F_1 nymphs initially exposed to *R. rickettsii* by feeding on rickettsemic guinea pigs, and thereafter, reared until F_2 unfed larvae or nymphs by feeding on susceptible hosts. After F_1 acquisition nymphal feeding, rickettsial infection rates of F_1 adults (transstadial perpetuation of *R. rickettsii* from nymphs to adults) were observed by DNA detection in ticks of only three tick colonies, 67% for E-PAM, 11% for NE-PIS, and 18% for NE-GSV (**Table 2**). Infestation of these F_1 adults on susceptible rabbits resulted in successful rickettsial transmission (fever followed by death or seroconversion with high endpoint titers) in all two rabbits exposed to either E-ITU, E-PAM or NE-PIS ticks, and one out of two rabbits exposed to NE-GSV adults, and none of the two rabbits exposed to either E-PIC or NE-POC (**Table 3**). Transovarial transmission of *R. rickettsii* was observed by DNA detection in engorged females of the E-ITU, E-PAM, NE-PIS, and NE-GSV tick colonies. In these cases, the transovarial transmission rate varied from 7 to 27% (**Table 2**). For these infected females with rickettsial transovarial transmission, the filial infection rates were 90–100% for E-ITU, 60% for E-PAM, 10–50% for NE-PIS, and 70% for NE-GSV (**Supplementary Table S13**). The transovarial acquisition infection of either E-PAM or NE-PIS F_2-infected larvae was confirmed by allowing part of these larvae to feed on guinea pigs, which became ill and seroconverted to *R. rickettsii* (guinea pigs G.P.74 in **Supplementary Table S5**, and G.P.102 in **Supplementary Table S7**). Moreover, NE-PIS F_2 nymphs (molted from the engorged larvae that had fed on G.P.102) were also able to transmit *R. rickettsii* to guinea pig G.P.103 (**Tables 3** and **Supplementary Table S7**).

Rickettsial Infection in GL + N Ticks

The GL + N ticks consisted of F_2 uninfected ticks that were dually exposed to *R. rickettsii* by feeding on rickettsemic guinea pigs during both larval and nymphal feeding, and thereafter, reared until F_3 larvae or nymphs by feeding on susceptible hosts. After F_2 acquisition nymphal feeding, rickettsial infection rates of F_2 nymphs (transstadial perpetuation of *R. rickettsii* from larvae to nymphs) were observed by DNA detection in ticks of four tick colonies, 41% for E-PAM, 16% for NE-GSV, 10% for E-PIC, and 8% for E-ITU ticks (**Table 2**). After the second acquisition feeding (F_2 nymphs on rickettsemic guinea pigs), rickettsial infection rates of F_2 adults (transstadial perpetuation of *R. rickettsii* from nymphs to adults) were observed in ticks of five out of the six tick colonies, 67% for NE-PIS, 60% for E-ITU, 33% for E-PAM, 23% for NE-GSV, and 20% for NE-POC ticks; rickettsial infection was not detected in any of the E-PIC adult ticks (**Table 2**). Infestation of these F_2 adults on susceptible rabbits resulted in successful rickettsial transmission (fever followed by death or seroconversion with high endpoint titers) in all three rabbits exposed to either E-ITU or NE-POC ticks, two out of three rabbits exposed to either NE-PIS or NE-GSV ticks, and one out of three rabbits exposed to E-PIC adults. Rickettsial transmission was not observed in any

TABLE 4 | Molting success according to *Amblyomma sculptum* tick generations (F_1 or F_2), tick stages (larvae or nymph) and experimental groups (CG, GL, GN, and GL + N).

Tick colonies	No. ticks that molted/no. engorged ticks (% molting success)[a]									
	F_1 larvae[b]		F_1 nymphs			F_2 larvae[b]			F_2 nymphs	
	CG	GL	CG	GL	GN	CG	GL + N		CG	GL + N
E-ITU	273/300 (91)[a]	126/300 (42)[b]	242/242 (100)[a]	190/276 (69)[b]	175/234 (75)[b]	243/300 (81)[a]	166/300 (55)[b]		246/257 (96)[a]	254/289 (88)[b]
E-PIC	267/300 (89)[a]	264/300 (88)[a]	255/256 (99)[a]	258/270 (96)[b]	272/272 (100)[a]	274/300 (91)[a]	159/300 (53)[b]		278/280 (99)[a]	253/269 (94)[b]
E-PAM	208/300 (69)[a]	199/300 (66)[a]	237/242 (98)[a]	240/283 (86)[b]	271/280 (97)[a]	283/300 (94)[a]	171/300 (57)[b]		129/145 (89)[a]	106/159 (67)[b]
NE-PIS	260/300 (87)[a]	247/300 (82)[a]	204/204 (100)[a]	232/248 (94)[b]	209/210 (99)[a]	283/300 (94)[a]	176/300 (59)[b]		192/192 (100)[a]	212/212 (100)[a]
NE-POC	217/300 (72)[a]	191/300 (64)[b]	202/207 (98)[a]	186/204 (91)[b]	160/171 (94)[a,b]	263/300 (88)[a]	186/300 (62)[b]		247/260 (95)[a]	236/245 (96)[a]
NE-GSV	294/300 (98)[a]	272/300 (91)[b]	173/183 (95)[a]	272/278 (98)[a]	173/222 (78)[b]	285/300 (95)[a]	193/300 (64)[b]		214/216 (99)[a]	180/225 (80)[b]

CG, uninfected control group, never exposed to R. rickettsii infection; GL, R. rickettsii-acquisition feeding as larvae; GN, R. rickettsii-acquisition feeding as nymphs; and GL + N, dual R. rickettsii acquisition-feeding, as larvae and as nymphs. [a]Different letters in the same line for the same tick generation and stage mean significantly different molting success values ($P < 0.05$). [b]Due to the high number of engorged larvae recovered from guinea pigs, molting success was observed in a sample of 300 viable engorged larvae from each generation of each tick colony.

of the two rabbits exposed to either E-PIC or NE-POC, and in the one exposed to E-PAM ticks (**Table 3**). Transovarial transmission of *R. rickettsii* was observed in engorged females of four colonies, with transovarial transmission rates of 27% for NE-GSV, 20% for E-ITU, 16% for NE-PIS, and 13% for NE-POC. There was no transovarial transmission in E-PIC and E-PAM ticks (**Table 2**). For the infected females with rickettsial transovarial transmission, the filial infection rates were 30–100% for NE-GSV, 0–100% for E-ITU, 50–100% for NE-PIS, and 100% for NE-POC (**Supplementary Table S13**). The transovarial acquisition infection of either E-ITU or NE-GSV F_2-infected larvae was confirmed by allowing part of these larvae to feed on guinea pigs, which became ill and seroconverted to *R. rickettsii* (guinea pigs G.P.28 and G.P.29 in **Table S2**, and G.P.171 and G.P.172 in **Table S12**). Moreover, E-ITU F_2 nymphs (molted from the engorged larvae that had fed on G.P.29) were also able to transmit *R. rickettsii* to guinea pig G.P.30 (**Tables 3** and **Supplementary Table S2**).

CG Ticks and Additional Molecular Tests

Each of the six tick colonies had its own CG group, which consisted of uninfected ticks that were reared in parallel to each of the infected groups, always exposed to susceptible guinea pigs or rabbits. During all infestations from F_1 larvae to F_2 adults, all animals remained afebrile and did not seroconvert to *R. rickettsii*. Moreover, larvae, nymphs and adult ticks were always negative by PCR, indicating absence of rickettsiae in this tick control group (**Supplementary Tables S1**–**S12**).

All *Rickettsia*-negative samples from the six experimental groups yielded amplicons by the PCR assay targeting the tick 16S rRNA gene, indicating that DNA extraction was successful. The only few exceptions, five tick samples that failed to amplify the tick 16S rRNA gene, were discarded from the study. Random samples of two *R. rickettsii*-infected F_1 adult ticks per colony yielded *ompA* amplicons that generated DNA sequences 100% identical to the sequence of *R. rickettsii* strain Taiaçu from GenBank (KU321853).

Tick Molting Success and Reproductive Performance

Molting success rates of engorged larvae to nymphs were higher for CG (uninfected ticks) than for GL or GL + N (exposed to *R. rickettsii*) ticks in all six tick colonies, with statistically significant differences ($P < 0.05$) in most of the cases (**Table 4**). A similar trend was observed for engorged nymphs, which displayed significantly higher ($P < 0.05$) molting success for CG ticks in most of the times when compared to GL, GN or GL + N ticks (**Table 4**). Hence, exposure to *R. rickettsii* infection caused higher mortality rates of engorged larvae and nymphs of all six tick colonies.

Overall, the reproductive performance of engorged females of the uninfected ticks tended to be higher than those of the *R. rickettsii*-infected ticks, as demonstrated by higher engorged female weight, egg mass weight, CEI, and % egg hatching values of the uninfected females (**Supplementary Tables S14**–**S19**). However, only in a few cases these values were significantly

different ($P < 0.05$) between uninfected and infected females of the same tick group, as for example, the engorged female weight and % egg hatching values in the GL group of E-ITU ticks (**Supplementary Table S14**), engorged female weight and CEI values in the GL + N group of E-PIC ticks (**Supplementary Table S15**), the CEI values in the GL group of E-PAM ticks (**Supplementary Table S16**), and the % egg hatching values in the GL group of NE-PIS ticks (**Supplementary Table S17**) and the GL + N group of NE-POC ticks (**Supplementary Table S18**).

Tick Molecular and Phylogenetic Analyses

Regarding the mitochondrial 16S rRNA gene, we generated partial sequences from a total of 98 *R. rickettsii*-infected ticks (4–43 sequences from each of the six colonies) and from 138 uninfected ticks (15–43 ticks from each of the six colonies) (**Supplementary Table S20**). Ticks of each colony yielded a single haplotype, except for the E-PAM ticks, which yielded two distinct haplotypes (A and B). E-PIC and NE-PIS ticks shared the same haplotype, as also did NE-GSV and NE-POC ticks, and also E-ITU and part of the E-PAM ticks; the other part of E-PAM yielded a unique haplotype (**Supplementary Table S21**). Despite these inter-colony differences, *R. rickettsii*-infected and uninfected ticks of the same colony shared a single haplotype. Even among E-PAM ticks (the only colony that generated more than one haplotype), each of the two haplotypes were shared by both infected and uninfected ticks. Differences among the seven haplotypes of *A. sculptum* ranged from 0% (between the above identical haplotypes) to 3.3% [between E-PAM (haplotype B) and either NE-PIS or E-PIC]. E-PAM haplotypes A and B differed by 3% (**Supplementary Table S21**). The phylogenetic tree containing these seven 16S rRNA haplotypes shows two major clusters, one containing E-ITU, E-PAM (haplotype A), E-PIC and NE-PIS ticks, which segregated under high bootstrap support (96%) from the other clade that contains NE-GSV, NE-POC, and E-PAM (haplotype B) (**Figure 2**).

Regarding the nuclear ITS2 nuclear gene, we generated partial sequences of 557-bp from a total of 77 *R. rickettsii*-infected ticks (3–40 sequences from each of the six colonies) and from 112 uninfected ticks (8–40 ticks from each of the six colonies). All these sequences were identical to each other, and when submitted to BLAST analysis, they were 100% identical to several *A. sculptum* sequences from Brazil (KU169885-KU169888).

DISCUSSION

Exposure of ticks of six geographically different populations of *A. sculptum* to *R. rickettsii* acquisition feeding and transmission revealed different susceptibilities among the six tick populations. After larval acquisition feeding (GL ticks), these differences were clearly in favor of higher infection rates for the two tick colonies that were exposed to their autochthone *R. rickettsii* strain, namely strain Itu for E-ITU ticks, and strain Pampulha for E-PAM ticks. Rickettsial infection rates in F_1 unfed nymphs of these two colonies were significantly higher than those observed in the other four tick colonies, which were exposed to *R. rickettsii* strain Itu. These differences among GL ticks were even more remarkable for the F_1 adult stage, as shown by 33 and 47% rickettsial detection in unfed adults of E-ITU and E-PAM ticks, in contrast to 0% for the remaining tick colonies (**Table 2**). The same trend was somewhat observed when *R. rickettsii* acquisition feeding occurred during the nymphal stage (GN ticks) or during both larval and nymphal feeding (GL + GN ticks), as shown by generally higher rickettsial infection rates among E-PAM and E-ITU ticks. While comparable infection rates were sometimes observed in ticks of the other colonies, it is noteworthy that 0% infection rates were observed several times for E-PIC, NE-PIS, NE-POC and NE-GSV ticks. In addition, highest rates of transovarial transmission of *R. rickettsii* also included E-PAM and E-ITU ticks, while 0% rates were more frequent on the other tick colonies (**Table 2**). These results were corroborated by the vector competence infestations, which resulted in more events of successful transmission of *R. rickettsii* when susceptible hosts were infested by E-PAM and E-ITU ticks; i.e., 70–100% successful transmission versus 10–67% (**Table 3**). All together, these results indicate that the susceptibility of *A. sculptum* to *R. rickettsii* varies among different tick populations, with a clear bias for higher susceptibility to an autochthone *R. rickettsii* strain that has already coevolved with a tick population for some time.

Soares et al. (2012) evaluated the susceptibility of an *A. sculptum* population by an *A. aureolatum*-derived strain of *R. rickettsii*, using the same type of protocols of the present study. Their results for the GL group (acquisition feeding during the larva stage) were comparable with our results for the tick colonies that were exposed to a non-autochthone *R. rickettsii* strain, although their GN group (acquisition feeding during the nymphal stage) displayed infection rates similar or superior to all GN groups of the present study. On the other hand, most of the transovarial acquisition infection-larvae of the study of Soares et al. (2012) failed to transmit *R. rickettsii* to guinea pigs, contrasting to the high vector competence of the transovarial acquisition infection-larvae of the present study. These results reinforce our above statement that suggests the existence of some adaptive interaction of *R. rickettsii* strains with its natural tick populations. Interestingly, our molecular analyses of two tick genes (16S rRNA and ITS2) showed that ticks of the two most *R. rickettsii*-susceptible populations of the present study (E-PAM and E-ITU) shared the same 16S rRNA haplotype (**Figure 2**), suggesting a genetic role in the tick-*R. rickettsii* interaction. However, further studies are needed to investigate this interaction more deeply, which could also be affected by tick endosymbionts, as for example, bacteria of the genera *Coxiella*, which have been reported to infect some *A. sculptum* (reported as *A. cajennense*) populations (Machado-Ferreira et al., 2011; Duron et al., 2015).

Regardless of the different susceptibilities of *A. sculptum* populations to *R. rickettsii*, Soares et al. (2012) and the present study clearly demonstrated that this tick species is partially refractory to *R. rickettsii* infection, in conjunction with relatively low transovarial transmission rates, always <50%. In addition, our results demonstrated that the *R. rickettsii* infection induces

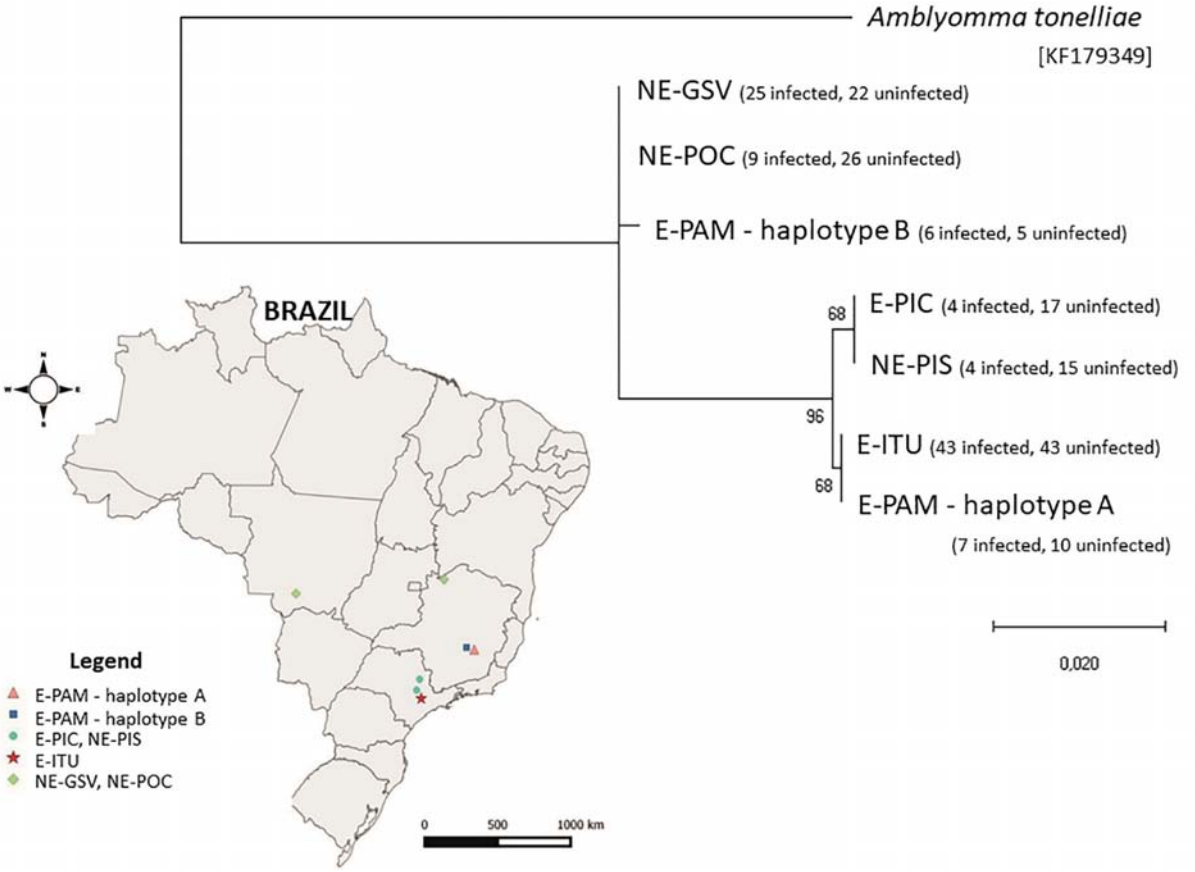

FIGURE 2 | Maximum likelihood tree based on the Tamura 3-parameter model for the 16S rRNA mitochondrial gene partial nucleotide sequences of six tick colonies (E-ITU, E-PIC, E-PAM, NE-PIS, NE-POC, and NE-GSV) of *Amblyomma sculptum* (410 sites on the dataset). The sequence of *Amblyomma tonelliae* from Paraguay (KF179349) was used as outgroup. The numbers at each node are bootstrap values greater than 60% from 1,000 replicates. The tree is drawn to scale, with branch lengths measured in the number of substitutions per site. The map of Brazil indicates the geographical location of each of the seven *A. sculptum* haplotypes from the tree. The numbers of sequences obtained for infected and uninfected ticks for each haplotype are shown within parentheses.

higher mortality of engorged larvae and nymphs, and tend to reduce the reproductive fitness of engorged females; this later impairment was also demonstrated by Soares et al. (2012). While these findings have been used to explain the low *R. rickettsii*-infection rates of *A. sculptum* under natural conditions, usually <1% (Krawczak et al., 2014; Labruna et al., 2017), they indicate that an *A. sculptum* population should not be able to sustain a *R. rickettsii* infection for successive tick generations without the creation of new cohorts of infected ticks via horizontal transmission on vertebrate rickettsemic hosts (amplifying hosts). In this case, capybaras have been incriminated as the main amplifying host of *R. rickettsii* for *A. sculptum* ticks in most of the BSF-endemic areas of Brazil (Souza et al., 2009; Polo et al., 2017). Finally, despite the ubiquitous distribution of *A. sculptum* in southeastern and central-western Brazil (Martins et al., 2016), most of the populations of this tick species are devoid of *R. rickettsii* infection (Sangioni et al., 2005; Pacheco et al., 2007, 2009). This scenario might be related to two major factors: (i) insufficient numbers of susceptible amplifying hosts; and (ii) lower susceptibilities of many tick populations. While the first factor has been demonstrated by mathematical models (Polo et al., 2017), the second is highlighted by the results observed in the present study.

DATA AVAILABILITY

The raw data supporting the conclusions of this manuscript will be made available by the authors, without undue reservation, to any qualified researcher.

ETHICS STATEMENT

This study has been approved by the Institutional Animal Care and Use Committee (IACUC) of the Faculty of Veterinary Medicine of the University of São Paulo (protocols 3104/2013 and 5948070314). Field capture of ticks was authorized by the Brazilian Ministry of the Environment (permit SISBIO Nos. 43259-1 and 11459-1).

AUTHOR CONTRIBUTIONS

MG and ML designed the experiments. MG, AR-H, LB, and FK performed the experiments. MG, FG, and ML analyzed the data and wrote the manuscript. All authors read and approved the final manuscript.

FUNDING

This research was supported by the Fundação de Amparo a Pesquisa do Estado de São Paulo (FAPESP Grants 2013/14222-5 and 2013/18046-7).

ACKNOWLEDGMENTS

We thank João Fábio Soares, Francisco Borges Costa, and Jonas Moraes-Filho for their valuable help during experiments. Special acknowledgment to all animals that involuntarily gave their lives for this study to be concluded.

SUPPLEMENTARY MATERIAL

The Supplementary Material for this article can be found online at: https://www.frontiersin.org/articles/10.3389/fphys.2019.00653/full#supplementary-material

REFERENCES

Barbieri, A. R. M., Szabó, M. P. J., Costa, F. B., Martins, T. F., Soares, H. S., Pascoli, G., et al. (2019). Species richness and seasonal dynamics of ticks with notes on rickettsial infection in a natural park of the cerrado biome in Brazil. *Ticks Tick Borne Dis.* 10, 442–453. doi: 10.1016/j.ttbdis.2018.12.010

Drummond, R. O., and Whetstone, T. M. (1970). Oviposition of the gulf coast tick. *J. Econ. Entomol.* 66, 130–133.

Duron, O., Noël, V., McCoy, K. D., Bonazzi, M., Sidi-Boumedine, K., Morel, O., et al. (2015). The recent evolution of a maternally-inherited endosymbiont of ticks led to the emergence of the Q fever pathogen, *Coxiella burnetii*. *PLoS Pathog.* 11:e1004892. doi: 10.1371/journal.ppat.1004892

Guedes, E., Leite, R. C., Prata, M. C. A., Pacheco, R. C., Walker, D. H., and Labruna, M. B. (2005). Detection of Rickettsia rickettsii in the tick *Amblyomma cajennense* in a new Brazilian spotted fever-endemic area in the state of minas gerais. *Mem. Inst. Oswaldo Cruz* 100, 841–845. doi: 10.1590/s0074-02762005000800004

Guedes, E., Leite, R. C., Pacheco, R. C., Silveira, I., and Labruna, M. B. (2011). *Rickettsia* species infecting *Amblyomma* ticks from an area endemic for Brazilian spotted fever in Brazil. *Rev. Bras. Parasitol. Vet.* 20, 308–311. doi: 10.1590/s1984-29612011000400009

Guglielmone, A. A., Beati, L., Barros-Battesti, D. M., Labruna, M. B., Nava, S., Venzal, J. M., et al. (2006). Ticks (Ixodidae) on humans in South America. *Exp. Appl. Acarol.* 40, 83–100. doi: 10.1007/s10493-006-9027-0

Hall, T. A. (1999). BioEdit: a user-friendly biological sequence alignment editor and analysis program for Windows 95/98/NT. *Nucleic Acids Symp. Ser.* 41, 95–98.

Horta, M. C., Pinter, A., Cortez, A., Soares, R. M., Gennari, S. M., Schumaker, T. T. S., et al. (2005). *Rickettsia felis* (Rickettsiales: Rickettsiaceae) in *Ctenocephalides felis felis* (Siphonaptera: Pulicidae) in the state of São Paulo, Brazil. *Arq. Bras. Med. Vet. Zootec.* 57, 321–325. doi: 10.1590/s0102-09352005000300008

Horta, M. C., Labruna, M. B., Pinter, A., Linardi, P. M., and Schumaker, T. T. (2007). Rickettsia infection in five areas of the state of São Paulo, Brazil. *Mem. Inst. Oswaldo Cruz* 102, 793–801. doi: 10.1590/s0074-02762007000700003

Horta, M. C., Moraes-Filho, J., Casagrande, R. A., Saito, T. B., Rosal, S. C., Martins, T. F., et al. (2009). Experimental infection of opossums *Didelphis aurita* by *Rickettsia rickettsii* and evaluation of the transmission of the infection to ticks *Amblyomma cajennense*. *Vector Borne Zoonotic Dis.* 9, 109–118. doi: 10.1089/vbz.2008.0114

Krawczak, F. S., Nieri-Bastos, F. A., Nunes, F. P., Soares, J. F., Moraes-Filho, J., and Labruna, M. B. (2014). Rickettsial infection in *Amblyomma cajennense* ticks and capybaras (*Hydrochoerus hydrochaeris*) in a Brazilian spotted fever-endemic area. *Parasit. Vectors* 7:7. doi: 10.1186/1756-3305-7-7

Kumar, S., Stecher, G., Li, M., Knyaz, C., and Tamura, K. (2018). MEGA X. Molecular evolutionary genetics analysis across computing platforms. *Mol. Biol. Evol.* 35, 1547–1549. doi: 10.1093/molbev/msy096

Labruna, M. B., Leite, R. C., Faccini, J. L. H., and Ferreira, F. (2000). Life-cycle of the tick *Haemaphysalis leporis-palustris* (Acari: Ixodidae) under laboratory conditions. *Exp. Appl. Acarol.* 24, 683–694.

Labruna, M. B., Whitworth, T., Horta, M. C., Bouyer, D. H., McBride, J. W., Pinter, A., et al. (2004). *Rickettsia* species infecting *Amblyomma cooperi* ticks from an area in the state of São Paulo, Brazil, where Brazilian spotted fever is endemic. *J. Clin. Microbiol.* 42, 90–98. doi: 10.1128/jcm.42.1.90-98.2004

Labruna, M. B., Horta, M. C., Aguiar, D. M., Cavalcante, G. T., Pinter, A., Gennari, S. M., et al. (2007). Prevalence of *Rickettsia* infection in dogs from the urban and rural areas of monte negro municipality, western Amazon, Brazil. *Vector Borne Zoonotic Dis.* 7, 249–255. doi: 10.1089/vbz.2006.0621

Labruna, M. B., Ogrzewalska, M., Martins, T. F., Pinter, A., and Horta, M. C. (2008). Comparative susceptibility of larval stages of *Amblyomma aureolatum, Amblyomma cajennense*, and *Rhipicephalus sanguineus* to infection by *Rickettsia rickettsii*. *J. Med. Entomol.* 45, 1156–1159. doi: 10.1093/jmedent/45.6.1156

Labruna, M. B., Ogrzewalska, M., Soares, J. F., Martins, T. F., Soares, H. S., Moraes-Filho, J., et al. (2011). Experimental infection of *Amblyomma aureolatum* ticks with *Rickettsia rickettsii*. *Emerg. Infect. Dis.* 17, 829–834. doi: 10.3201/eid1705.101524

Labruna, M. B., Santos, F. C., Ogrzewalska, M., Nascimento, E. M., Colombo, S., Marcili, A., et al. (2014). Genetic identification of rickettsial isolates from fatal cases of Brazilian spotted fever and comparison with *Rickettsia rickettsii* isolates from the American continents. *J. Clin. Microbiol.* 52, 3788–3791. doi: 10.1128/JCM.01914-14

Labruna, M. B., Krawczak, F. S., Gerardi, M., Binder, L. C., Barbieri, A. R. M., Paz, G. F., et al. (2017). Isolation of *Rickettsia rickettsii* from the tick *Amblyomma sculptum* from a Brazilian spotted fever–endemic area in the Pampulha Lake region, southeastern Brazil. *Vet. Parasitol. Reg. Stud. Rep.* 8, 82–85. doi: 10.1016/j.vprsr.2017.02.007

Machado-Ferreira, E., Dietrich, G., Hojgaard, A., Levin, M., Piesman, J., Zeidner, N. S., et al. (2011). Coxiella symbionts in the Cayenne tick *Amblyomma cajennense*. *Microb. Ecol.* 62, 134–142. doi: 10.1007/s00248-011-9868-x

Mangold, A. J., Bargues, M. D., and Mas-Coma, S. (1998). Mitochondrial 16SrDNA sequences and phylogenetic relationships of species of *Rhipicephalus* and other tick genera among Metastriata (Acari: Ixodidae). *Parasitol. Res.* 84, 478–484. doi: 10.1007/s004360050433

Marrelli, M. T., Souza, L. F., Marques, R. C., Labruna, M. B., Matioli, S. R., Tonon, A. P., et al. (2007). Taxonomic and phylogenetic relationships between neotropical species of ticks from genus *Amblyomma* (Acari: Ixodidae) inferred from second internal transcribed spacer sequences of rDNA. *J. Med. Entomol.* 44, 222–228. doi: 10.1603/0022-2585(2007)44%5B222:taprbn%5D2.0.co;2

Martins, T. F., Barbieri, A. R., Costa, F. B., Terassini, F. A., Camargo, L. M., Peterka, C. R., et al. (2016). Geographical distribution of *Amblyomma cajennense* (sensu lato) ticks (Parasitiformes: Ixodidae) in Brazil, with description of the nymph of *A. cajennense (sensu stricto)*. *Parasit. Vectors* 9:186. doi: 10.1186/s13071-016-1460-2

Melo, A. L., Witter, R., Martins, T. F., Pacheco, T. A., Alves, A. S., Chitarra, C. S., et al. (2016). A survey of tick-borne pathogens in dogs and their ticks in the Pantanal biome, Brazil. *Med. Vet. Entomol.* 30, 112–116. doi: 10.1111/mve.12139

Monteiro, J. L. (1931). Estudos sobre o typho exanthematico de S. Paulo. *Mem. Inst. Butantan* 6, 5–135.

Monteiro, J. L. (1933). Comportamento experimental do Coelho aos virus do typho Exanthemático de São Paulo e da febre maculosa das Montanhas Rochosas. *Mem. Inst. Butantan* 8, 3–80.

Ogrzewalska, M., Saraiva, D. G., Moraes-Filho, J., Martins, T. F., Costa, F. B., Pinter, A., et al. (2012). Epidemiology of brazilian spotted fever in the atlantic forest, state of São Paulo, Brazil. *Parasitology* 139, 1283–1300. doi: 10.1017/s0031182012000546

Oliveira, S., Guimarães, J., Reckziegel, G., Costa, B., Araújo-Vilges, K., Fonseca, L., et al. (2016). An update on the epidemiological situation of spotted fever in Brazil. *J. Venom. Anim. Toxins Incl. Trop. Dis.* 22:22. doi: 10.1186/s40409-016-0077-4

Pacheco, R. C., Horta, M. C., Moraes-Filho, J., Ataliba, A. C., Pinter, A., and Labruna, M. B. (2007). Rickettsial infection in capybaras (*Hydrochoerus hydrochaeris*) from São Paulo, Brazil: serological evidence for infection by *Rickettsia bellii* and *Rickettsia parkeri*. *Biomedica* 27, 364–371.

Pacheco, R. C., Horta, M. C., Pinter, A., Moraes-Filho, J., Martins, T. F., Nardi, M. S., et al. (2009). Pesquisa de *Rickettsia* spp. em carrapatos *Amblyomma cajennense* e *Amblyomma dubitatum* no Estado de São Paulo. *Rev. Soc. Bras. Med. Trop.* 42, 351–353. doi: 10.1590/s0037-86822009000300023

Pacheco, R. C., Moraes-Filho, J., Guedes, E., Silveira, I., Richtzenhain, L. J., Leite, R. C., et al. (2011). Rickettsial infections of dogs, horses and ticks in Juiz de Fora, southeastern Brazil, and isolation of *Rickettsia rickettsii* from *Rhipicephalus sanguineus* ticks. *Med. Vet. Entomol.* 25, 148–155. doi: 10.1111/j.1365-2915.2010.00915.x

Perez, C. A., Almeida, A. F., Almeida, A., Carvalho, V. H., Balestrin, D. C., Guimarães, M. S., et al. (2008). Ticks of genus *Amblyomma* (Acari: Ixodidae) and their relationship with hosts in endemic area for spotted fever in the State of São Paulo. *Rev. Bras. Parasitol. Vet.* 17, 210–217.

Pinter, A., Franca, A., Souza, C., Sabbo, C., Mendes, E., Pereira, F., et al. (2011). Febre maculosa brasileira. *BEPA Suplemento* 8, 19–24.

Pinter, A., Labruna, M. B., and Faccini, J. L. (2002). The sex ratio of *Amblyomma cajennense* (Acari: Ixodidae) with notes on the male feeding period in the laboratory. *Vet. Parasitol.* 105, 79–88. doi: 10.1016/S0304-4017(01)00650-1

Polo, G., Mera Acosta, C., Labruna, M. B., and Ferreira, F. (2017). Transmission dynamics and control of *Rickettsia rickettsii* in populations of *Hydrochoerus hydrochaeris* and *Amblyomma sculptum*. *PLoS Negl. Trop. Dis.* 11:e0005613. doi: 10.1371/journal.pntd.0005613

Ramos, V. N., Osava, C. F., Piovezan, U., and Szabó, M. P. (2014). Ticks on humans in the pantanal wetlands, Brazil. *Ticks Tick Borne Dis.* 5, 497–499. doi: 10.1016/j.ttbdis.2014.03.004

Regnery, R. L., Spruill, C. L., and Plikaytis, B. D. (1991). Genotypic identification of rickettsiae and estimation of intraspecies sequence divergence for portions of two rickettsial genes. *J. Bacteriol.* 173, 1576–1589. doi: 10.1128/jb.173.5.1576-1589.1991

Sangioni, L. A., Horta, M. C., Vianna, M. C. B., Gennari, S. M., Soares, R. S., Galvão, M. A. M., et al. (2005). Rickettsial infection in animals and Brazilian spotted fever endemicity. *Emerg. Infect. Dis.* 11, 265–270. doi: 10.3201/eid1102.040656

Soares, J. F., Soares, H. S., Barbieri, A. M., and Labruna, M. B. (2012). Experimental infection of the tick *Amblyomma cajennense*, Cayenne tick, with *Rickettsia rickettsii*, the agent of Rocky Mountain spotted fever. *Med. Vet. Entomol.* 26, 139–151. doi: 10.1111/j.1365-2915.2011.00982.x

Souza, C. E., Moraes-Filho, J., Ogrzewalska, M., Uchoa, F. C., Horta, M. C., Souza, S. S., et al. (2009). Experimental infection of capybaras *Hydrochoerus hydrochaeris* by *Rickettsia rickettsii* and evaluation of the transmission of the infection to ticks *Amblyomma cajennense*. *Vet. Parasitol.* 161, 116–121. doi: 10.1016/j.vetpar.2008.12.010

Szabó, M. P., Labruna, M. B., Garcia, M. V., Pinter, A., Castagnolli, K. C., Pacheco, R. C., et al. (2009). Ecological aspects of the free-living ticks (Acari: Ixodidae) on animal trails within Atlantic rainforest in south-eastern Brazil. *Ann. Trop. Med. Parasitol.* 103, 57–72. doi: 10.1179/136485909X384956

Terassini, F. A., Barbieri, F. S., Albuquerque, S., Szabó, M. P., Camargo, L. M., and Labruna, M. B. (2010). Comparison of two methods for collecting free-living ticks in the Amazonian forest. *Ticks Tick Borne Dis.* 1, 194–196. doi: 10.1016/j.ttbdis.2010.08.002

Thompson, J. D., Higgins, D. G., and Gibson, T. J. (1994). CLUSTALW: improving the sensitivity of progressive multiple sequence alignment through sequence weighting, position specific gap penalties and weight matrix choice. *Nucleic Acids Res.* 22, 4673–4680. doi: 10.1093/nar/22.22.4673

Conflict of Interest Statement: The authors declare that the research was conducted in the absence of any commercial or financial relationships that could be construed as a potential conflict of interest.

frontiers in Physiology

ORIGINAL RESEARCH
published: 29 May 2019
doi: 10.3389/fphys.2019.00654

Ultrastructural and Cytotoxic Effects of *Metarhizium robertsii* Infection on *Rhipicephalus microplus* Hemocytes

*Jéssica Fiorotti[1], Rubem Figueiredo Sadok Menna-Barreto[2], Patrícia Silva Gôlo[3], Caio Junior Balduino Coutinho-Rodrigues[1], Ricardo Oliveira Barbosa Bitencourt[1], Diva Denelle Spadacci-Morena[4], Isabele da Costa Angelo[5] and Vânia Rita Elias Pinheiro Bittencourt[3]**

[1] Programa de Pós-Graduação em Ciências Veterinárias, Instituto de Veterinária, Universidade Federal Rural do Rio de Janeiro, Seropédica, Brazil, [2] Laboratório de Biologia Celular, IOC, Fundação Oswaldo Cruz, Rio de Janeiro, Brazil, [3] Departamento de Parasitologia Animal, Instituto de Veterinária, Universidade Federal Rural do Rio de Janeiro, Seropédica, Brazil, [4] Laboratório de Fisiopatologia, Instituto Butantan, São Paulo, Brazil, [5] Departamento de Epidemiologia e Saúde Pública, Instituto de Veterinária, Universidade Federal Rural do Rio de Janeiro, Seropédica, Brazil

OPEN ACCESS

Edited by:
Itabajara Da Silva Vaz Jr., Federal University of Rio Grande do Sul, Brazil

Reviewed by:
Renata Silva Matos, Universidade Federal de Juiz de Fora, Brazil
Karim Christina Furquim Isler, Universidade Estadual Paulista Júlio de Mesquita Filho, Brazil

***Correspondence:**
Vânia Rita Elias Pinheiro Bittencourt
vaniabit@ufrrj.br

Specialty section:
This article was submitted to Invertebrate Physiology, a section of the journal Frontiers in Physiology

Received: *04 March 2019*
Accepted: *09 May 2019*
Published: *29 May 2019*

Citation:
Fiorotti J, Menna-Barreto RFS, Gôlo PS, Coutinho-Rodrigues CJB, Bitencourt ROB, Spadacci-Morena DD, Angelo IC and Bittencourt VREP (2019) Ultrastructural and Cytotoxic Effects of Metarhizium robertsii Infection on Rhipicephalus microplus Hemocytes. Front. Physiol. 10:654. doi: 10.3389/fphys.2019.00654

Metarhizium is an entomopathogenic fungus widely employed in the biological control of arthropods. Hemocytes present in the hemolymph of invertebrates are the cells involved in the immune response of arthropods. Despite this, knowledge about *Rhipicephalus microplus* hemocytes morphological aspects as well as their role in response to the fungal infection is scarce. The present study aimed to analyze the hemocytes of *R. microplus* females after *Metarhizium robertsii* infection, using light and electron microscopy approaches associated with the cytotoxicity evaluation. Five types of hemocytes (prohemocytes, spherulocytes, plasmatocytes, granulocytes, and oenocytoids) were described in the hemolymph of uninfected ticks, while only prohemocytes, granulocytes, and plasmatocytes were observed in fungus-infected tick females. Twenty-four hours after the fungal infection, only granulocytes and plasmatocytes were detected in the transmission electron microscopy analysis. Hemocytes from fungus-infected tick females showed several cytoplasmic vacuoles with different electron densities, and lipid droplets in close contact to low electron density vacuoles, as well as the formation of autophagosomes and subcellular material in different stages of degradation could also be observed. *M. robertsii* propagules were more toxic to tick hemocytes in the highest concentration tested (1.0×10^8 conidia mL^{-1}). Interestingly, the lowest fungus concentration did not affect significantly the cell viability. Microanalysis showed that cells granules from fungus-infected and uninfected ticks had similar composition. This study addressed the first report of fungal cytotoxicity analyzing ultrastructural effects on hemocytes of *R. microplus* infected with entomopathogenic fungi. These results open new perspectives for the comprehension of ticks physiology and pathology, allowing the identification of new targets for the biological control.

Keywords: entomopathogenic fungi, cell death, fungal infection, tick, immunity

INTRODUCTION

Ticks are obligate hematophagous ectoparasites relevant to public and veterinary health (De la Fuente et al., 2008; Kernif et al., 2016). The cattle tick, *Rhipicephalus microplus*, has an enormous negative impact on livestock. The economic impact has increased, particularly in tropical countries and financial losses of USD 3.24 billion per year only in Brazil have been reported (Grisi et al., 2014). The improper use of chemical acaricides is frequently reported and causes the raising of resistant tick populations in addition to the environmental, meat, and milk contamination. Accordingly, alternative control methods using entomopathogenic fungi have been studied to decrease the use of these chemicals (Schank and Vainstein, 2010; Camargo et al., 2012; Perinotto et al., 2017).

Metarhizium anisopliae sensu lato (s.l.) is a complex of species of cosmopolitan entomopathogenic fungi which includes species that can infect specific hosts, as *Metarhizium acridum* with Orthoptera insects, or a wider range of insect groups, such as *Metarhizium robertsii* and *M. anisopliae* sensu stricto (s.s.). These fungi are also considered endophytes and rhizosphere competent (Hu et al., 2014; Vega, 2018). All *R. microplus* life stages have been shown to be sensitive to entomopathogenic fungal infection (Alonso-Díaz et al., 2007; Leemon and Jonsson, 2008), either *in vitro* assays (Perinotto et al., 2017), associated with chemical acaricides (Bahiense et al., 2008; Webster et al., 2015), or *in vivo* tests using available commercial products (Camargo et al., 2016).

Metarhizium infection starts with the fungal propagule attachment on the hosts' surface and active penetration (Madelin et al., 1967). After penetration, the hyphae present in the hemolymph differentiate into blastospores and the host dies due to a set of occurrences such as: physical damage, pathological changes occurring in the hemolymph, histolytic action, blocking of the digestive system, and even production of micotoxins (Bidochka et al., 1997; Alves, 1998; Roberts and St Leger, 2004). Nevertheless, the host can fight against the fungal infection triggering its immune system by starting processes such as phagocytosis, nodule formation, melanization, encapsulation, and secretion of antimicrobial peptides (Kopácek et al., 2010; Hajdušek et al., 2013).

Tick immune system is composed of humoral and cellular defense responses (Schmidt et al., 2001; Lavine and Strand, 2002). In general, the humoral immune response involves several antimicrobial peptides, reactive oxygen species and enzymatic cascades that regulate coagulation and hemolytic melanization processes (Gillespie et al., 1997; Smith and Pal, 2014). The cellular reactions are triggered immediately after the microorganism invasion and directly involve the attack of these microorganisms by hemocytes (Tan et al., 2013). Hemocytes are circulating cells present in the hemolymph that also be found connected to the fatty body, nephrocytes, and salivary glands (Sterba et al., 2011). Innate immune mechanisms have already been reported for several invertebrates (Brayner et al., 2007; Nation, 2016; Iacovone et al., 2018), including ticks (Gillespie et al., 1997; Johns et al., 2001; Feitosa et al., 2015), considering phagocytosis as the most important innate response (Bayne, 1990; Ehlers et al., 1992), that in ticks is mediated mainly by granulocytes and plasmatocytes (Dolp, 1970; Fujisaki et al., 1975; Kuhn and Haug, 1995; Zhioua et al., 1996; Inoue et al., 2001; Borovicková and Hypsa, 2005; Feitosa et al., 2018). Despite this, little has been reported about cellular immune response in *R. microplus* ticks, since most studies are based on the tick humoral responses (Nakajima et al., 2003; Fogaça et al., 2004; Angelo et al., 2014; Chávez et al., 2017).

Hemocytes are extremely relevant for studies about interactions between the host and its pathogens (Jones, 1962; Crossley, 1975; Lackie, 1980; Gupta, 1986; Paskewitz and Christensen, 1996; Chen and Lu, 2018; Iacovone et al., 2018). Arthropods' hemocytes classification and terminology were framed mostly based on insect studies, while this literature is still scarce for ticks (Nevermann et al., 1991; Borovicková and Hypsa, 2005; Araújo et al., 2008; Cunha et al., 2009; Laughton et al., 2011). Additionally, compared to insects, literature about the cell response of ticks challenged with pathogens is poorly explored.

Studies reported that circulating hemocytes of adult mosquitoes infected with pathogens may decrease (Hillyer et al., 2005; Castillo et al., 2006, 2011; Brayner et al., 2007; Bryant and Michael, 2014) and have their morphology altered (Au et al., 2003; Kwon et al., 2014). It is known that the number of circulating hemocytes of *R. microplus* ticks infected with entomopathogenic fungi dropped off in comparison to uninfected females (De Paulo et al., 2018), despite this, to the present date, alterations in the morphology of hemocytes from *R. microplus* ticks infected with pathogens have not been reported yet, as studies were conducted mainly with *R. sanguineus* and *Dermacentor variabilis* ticks (Eggenberger et al., 1990; Ceraul et al., 2002; Feitosa et al., 2015, 2018). Undoubtedly, further approaches to understand the immune system of ticks have to overcome the discussion of hemocyte types, especially when its identification is based just on morphological analyzes, while histochemical differentiation and functional aspects are largely neglected. Accordingly, the aim of this study was to analyze the hemocytes of *R. microplus* females infected or not by *M. robertsii*, using light microscopy, cytotoxicity test, transmission electron microscopy (TEM), and transmission electron microscopy with energy-dispersive X-ray spectrometer (TEM-EDS).

MATERIALS AND METHODS

Fungal Isolate and Tick Obtainment

One fungal isolate, *M. robertsii* ARSEF 2575, was used in the present study. The fungal isolate was obtained from the Agriculture Research Service Collection of Entomopathogenic Fungal Cultures (ARSEF) (USDA-US Plant, Soil and Nutrition Laboratory, Ithaca, NY, United States). Cultures were grown on PDA (potato dextrose agar) at 25°C ± 1°C and ≥80 relative humidity (RH) for 14 days. A conidial suspension was used to infect the ticks.

Rhipicephalus microplus fully engorged ticks were obtained from artificially infested animals [the present experiment was part of a project approved by the Veterinary Institute Ethics Committee of the Federal Rural University of Rio de Janeiro (CEUA UFRRJ no. 037/2014)]. After collection on the stalls

floor, fully engorged tick females were immersed in running water followed by 0.05% sodium hypochlorite solution for three min, then dried, identified and weighed for homogeneous division of the groups.

Entomopathogenic Fungi Inoculation Into *R. microplus* Ticks

Fungal suspensions were prepared by suspending *M. robertsii* ARSEF 2575 conidia in 0.1% polyoxyethylene sorbitan monooleate (Tween®80) sterile aqueous solution (v/v). For fungal inoculation, engorged females were divided into seven homogeneously weighed groups with 20 females each (for the bioassay) and three homogeneously weighed groups with 20 females each (for the microscopy analysis). The negative control group did not receive any treatment (tick females under physiological conditions), and treated females were inoculated with 5 μL of ARSEF 2575 fungal suspension or 5 μL 0.1% Tween®80 aqueous solution (v/v) into the foramen located between the dorsal scutum and the capitulum, using an insulin syringe (Johns et al., 1998). All the experiments were performed in triplicate (except the bioassay) and repeated three times.

Bioassay With Engorged Females

Tick females were homogeneously weighed based on the Yule's formula (Sampaio, 2002). Groups were inoculated as mentioned before and divided as follows: A group was treated with 5 μL 0.1% Tween®80 aqueous solution (v/v) and the fungus-infected groups were infected with six different fungal concentrations (1.0×10^3, 10^4, 10^5, 10^6, 10^7 or 10^8 conidia mL^{-1}). Fungal suspensions were adjusted to each concentration using Neubauer's chamber. Fungal concentrations that were used in the present bioassay were the same used in the forward described cell viability test. The highest concentration (1.0×10^8 conidia mL^{-1}) was defined based on the concentration commonly used for topical treatments in ticks. Tick females were maintained at $27 \pm 1°C$ and ≥80% RH in the dark. Tick mortality was recorded 24 and 48 h after the treatments.

Hemolymph Collection

Ticks infected with fungi (each tick infected with 5 μL of 1.0×10^7 conidia mL^{-1}, a sublethal concentration), ticks inoculated with Tween®80 aqueous solution (v/v) and the negative control group (ticks under physiological conditions, a untreated group) had their hemolymph collected according to Angelo et al. (2010) through the ruptured cuticle at the dorsal surface of the tick female using a needle, 24 h after infection. The hemolymph drops were collected with a capillary glass coupled to a flexible rubber. Samples were placed in microtubes containing 30 μL protease inhibitor cocktail (Inhibit®Sigma-Aldrich) and 82 μL saline buffer (1.5 M NaCl, 50 mM EDTA, pH 7.2). Microtubes were kept on ice throughout the collection.

Cell Viability Test

Three hundred engorged tick females were used for the cell viability test. Hemolymph of uninfected females was collected and the hemocytes harvested according to De Paulo et al. (2018). Hemocytes were resuspended in 50 mL sterilized Leibovitz's L-15 culture medium (Gibco®) at double strength, supplemented with 20% fetal bovine serum (FBS), 2 g. L^{-1} glucose, and 100 UI mL^{-1} penicillin, adjusted to pH 7.0–7.2. Cells were then seeded into 96 well plates at 5×10^4 cells mL^{-1} in a final volume of 170 μL culture medium. Cells were allowed to attach to the well surface for 1 h. Hemocytes were then exposed to 10 μL conidial suspensions using six different concentrations (1.0×10^3, 10^4, 10^5, 10^6, 10^7, or 10^8 conidia mL^{-1}) chosen to make it possible to assemble a kinetic curve. 24 h after fungal exposure, 20 μL of resazurin (Sigma-Aldrich) at 0.13 mg mL^{-1} were added in each well, and the plate incubated for 1, 2, 3, and 4 h. Fluorescence was read using a microplate reader Chameleon (Hidex®) at 530 nm excitation and 590 nm emission. Relative hemocyte viability was calculated considered unexposed cells as controls (≈100% viability). Experiments were carried out in triplicate and repeated three times with new engorged females and a new batch of fungus.

Light Microscopy Analysis

Hemolymph Smear

Drops from total hemolymph (plasma and hemocytes) of untreated ticks (negative control group), ticks inoculated with 0.1% Tween®80 and ticks infected with 10^7 conidia mL^{-1} were collected 24 h after infection and placed directly onto glass slides, dried at room temperature for 20–30 min, and fixed in methanol PA (Sigma-Aldrich) for 3 min. Slides were then stained with Giemsa (Sigma-Aldrich) [diluted 1:9 in buffered distilled water Brayner et al. (2005)] for 30 min, rapidly washed with buffered distilled water, and observed by light microscope. Five stained slides were performed per group. One hundred cells per slide were count for differential hemocytes counts. Differential hemocytes counts were expressed based on the amount of each hemocyte type in the total cells counted.

Hemocytes in Historesin

For light microscopy, hemocytes from ticks infected with 10^7 conidia mL^{-1} (collected 24 h after infection) and hemocytes from Tween-inoculated ticks were removed from plasma (De Paulo et al., 2018) and immediately immersed in 4% paraformaldehyde in 0.2 M Millonig buffer (pH 7. 2) for 6 h at room temperature. Samples were then centrifuged at $500 \times g$ for 3 min, supernatant was discarded, the hemocytes pellet dehydrated in ascending ethanol series (70–100%), embedded in pure historesin overnight, and finally embedded in historesin plus hardener (Leica) at 4°C for 24 h. Three micrometers thick histological sections were stained with methylene blue for morphological studies. The sections were observed and photographed under a DM LS (Leica) light microscope coupled to a DFC420 camera (Leica) and Leica Application Suite version 3.1.0 imaging software.

Transmission Electron Microscopy

Hemocytes from infected ticks (10^7 conidia mL^{-1}), ticks inoculated with Tween®80 and untreated ticks were collected 24 h after infection, removed from plasma (De Paulo et al., 2018), and fixed in 2% glutaraldehyde for 3 h at 4°C. The samples were then centrifuged at $500 \times g$ for 3 min, the supernatant was

discarded, the cells' pellet was washed in 0.2 M Millonig buffer for 15 min, centrifuged at 500 × *g* for 3 min, and then post-fixed in 1% OsO_4 at room temperature for 3 h. After that, pellets were washed in Millonig buffer, dehydrated in ascending acetone series (30, 50, 70, 90, and 100%), pre-embedded in Polybed 812 resin-acetone (1:1) overnight at room temperature, and embedded in pure resin at room temperature for 8 h. After resin polymerization (72 h) at 60°C, ultrathin sections were obtained, stained with uranyl acetate and lead citrate. The examination was performed in Jeol 100 CX II and LEO EM 906E transmission electron microscope.

X-Ray Microanalysis of Cells Granules

The chemical composition of *R. microplus* granulocytes' granules was determined by energy-dispersive X-ray spectrometer (TEM-EDS, H7650/Hitachi H-700 FA). Hemocytes from Tween-inoculated ticks and fungus-infected ticks (10^7 conidia mL^{-1}) were prepared as described for transmission electron microscopy and a quantitative characteristic of ions and maps of their distribution were obtained with a Hitachi H-8100 TEM microscope (Hitachi, Tokyo, Japan) equipped with energy-dispersive X-ray spectrometer (EDS, OXFORD INCA x-sight, Abingdon, Oxfordshire, United Kingdom).

Statistical Analysis

Bioassay data were analyzed by one-way ANOVA followed by Newman-Keuls Multiple Comparison Test ($P \leq 0.05$). Cell viability data were analyzed by one-way ANOVA followed by Tukey's test for pair-wise comparisons ($P \leq 0.05$). For analysis of hemocytes populations, multiple *t*-tests were used for pair-wise comparisons ($P \leq 0.05$). All data were analyzed through GraphPad Prism version 5.00 for Windows (GraphPad Software, San Diego, CA, United States).

RESULTS

Bioassay With Engorged Females

Conidia of *M. robertsii* isolate ARSEF 2575 used to infect adult females had 98% germination after incubation for 24 h at 27 ± 1°C and ≥80% RH. Females' mortality percent is shown in **Figure 1**. In general, tick mortality was proportional to conidial concentration, (i.e., the higher the conidial concentration, the higher the tick mortality) (**Figures 1A,B**). Ticks infected with 10^7 conidia mL^{-1} showed 21% ± 2.35 mortality 24 h after infection and 48% ± 2.35 mortality 48 h after infection, while ticks infected with 10^8 conidia mL^{-1} had 31,66% ± 2.0 and 83,3% ± 4.71 mortality 24 and 48 h after infection, respectively.

Cell Viability Test

The kinetic curve shows hemocytes viability 24 h after fungal exposure in different times of incubation with resazurin (**Figure 2**). It was possible to observe that hemocytes viability was similar 3 and 4 h after incubation (**Figure 2**). *M. robertsii* ARSEF 2575 conidia were more toxic to *R. microplus* hemocytes at 10^7 conidia mL^{-1} and 10^8 conidia mL^{-1}, reducing cell viability in 15, 53% ± 1.58 and 36.1% ± 1.48 24 h after the fungal addition, respectively (**Figure 3**). Despite lower fungal concentrations (10^3, 10^4, 10^5, and 10^6 conidia mL^{-1}) can also influence cell viability, drastic reductions started at the higher concentrations (i.e., 10^7 and 10^8).

Light Microscopy Analysis

Prohemocytes, spherulocytes, granulocytes, plasmatocytes, and oenocytoids were observed in both engorged *R. microplus* females under physiological conditions and tween-inoculated ticks after Giemsa staining. The concentration of these hemocytes was the same for both groups (**Figure 4**). On the other hand, when engorged females were infected with *M. robertsii*, spherulocytes and oenocytoids were not observed. In addition, prohemocytes and granulocytes were present in the same amounts in controls and fungus-infected groups, only plasmatocytes amounts were statistically different between uninfected (negative control and tween-inoculated) and infected groups. All cells had the basophilic nucleus and the following characteristics: Prohemocytes (ranging from 8 to 10 μm) as relatively small cells, with large nucleus (**Figures 5A**, **6A**). Granulocytes (measuring approximately 12 to 15 μm) as circular cells that were observed in two different forms: with a more central

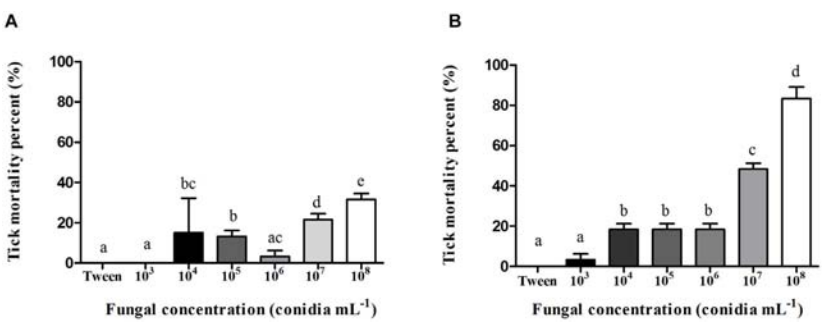

FIGURE 1 | Mean percent (%) mortality and standard deviation of *Rhipicephalus microplus* adult females infected with *Metarhizium robertsii* ARSEF 2575 conidia in different concentrations (1.0×10^3, 10^4, 10^5, 10^6, 10^7 and 10^8 conidia mL^{-1}). Each group had 20 tick females. Mortality percent was recorded **(A)** 24 h and **(B)** 48 h after fungal inoculation. Mean values (±) standard deviation followed for the same letter do not differ statistically by ANOVA test ($P \geq 0.05$). The bioassay was conducted three times, on three different days, using new ticks and conidial preparations each day.

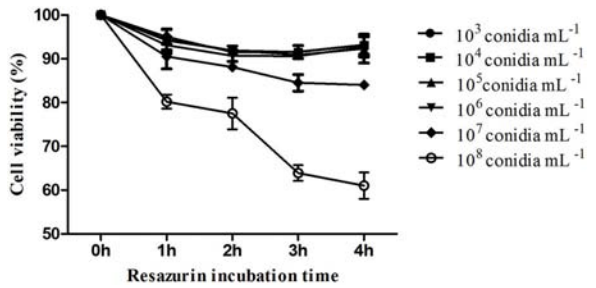

FIGURE 2 | *In vitro* cytotoxic assay of *Metarhizium robertsii* ARSEF 2575 against *Rhipicephalus microplus* hemocytes using a resazurin-based assay (to evaluate cell viability). *R. microplus* hemocytes were exposed to different concentrations (1.0×10^3, 10^4, 10^5, 10^6, 10^7, and 10^8 conidia mL^{-1}) of fungal suspensions. Twenty-four hours after exposure, resazurin was used for four different incubation times (1, 2, 3, and 4 h). ANOVA followed by Tukey's test was used. Experiments were repeated with at least three independent biological samples.

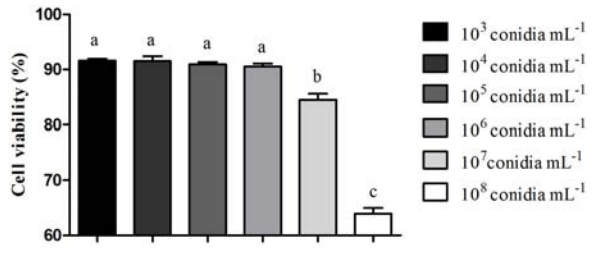

FIGURE 3 | Effect of *Metarhizium robertsii* on the cellular proliferation of *Rhipicephalus microplus* hemocytes at 3 h incubation with resazurin. Mean values (±) standard deviation followed for the same letter do not differ statistically by ANOVA test ($P \geq 0.05$). Experiments were repeated with at least three independent biological samples.

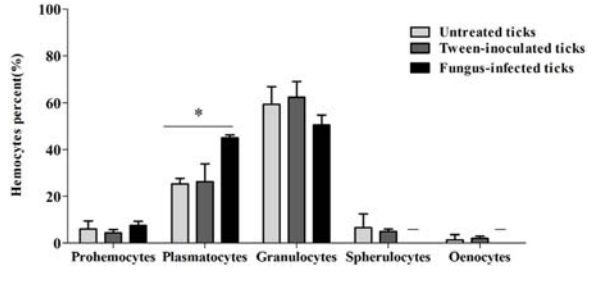

FIGURE 4 | Mean percent and standard deviation of *Rhipicephalus microplus* hemocytes population (prohemocytes, granulocytes, plasmatocytes, spherulocytes and oenocytoids) of untreated tick females (ticks under physiological conditions), tween-inoculated ticks and fungus-infected ticks. *R. microplus* females were infected with *Metarhizium robertsii* ARSEF 2575. Mean values (±) standard deviation followed by * differ statistically by multiple *t*-tests ($P \leq 0.05$). A total of 100 cells were counted in each slide (five slides were analyzed for each group). Experiments were repeated with at least three independent biological samples.

nucleus or eccentric nucleus (**Figures 5B,C**, **6B,C**). Spherulocytes (measuring approximately 12 to 15 μm) had oval shape, with spherules in the cytoplasm (**Figures 5D**, **6D**). Plasmatocytes (measuring approximately 20 μm) presented a varied shape, with the nucleus displaced of the central region of the cell; some plasmatocytes had pseudopodia (**Figures 5E**, **6E**). Oenocytoids were larger-sized (approximately 20 μm) exhibiting the nucleus displaced of the central region of the cells (**Figures 5F**, **6F**). Additionally, spherulocytes, plasmatocytes, and oenocytoids exhibited poorly Giemsa-stained areas (**Figures 5D–F**, **6D–F**). Granulocytes from fungus-infected ticks showed fewer granules than hemocytes from untreated or tween-inoculated ticks. Prohemocytes were similar in uninfected or fungus-infected females (**Figure 5A**, **6A**, **7A**). The cells' cytoplasm from infected ticks showed heterogeneity (**Figure 7B**) and also intense vacuolization (**Figure 7C**).

Historesin analysis was used to compare the hemocytes types [i.e., prohemocytes, granulocytes, and plasmatocytes (**Figure 8**)] observed in both fungus-infected and tween-inoculated ticks. After fungal infection, prohemocytes had the same morphology than the prohemocytes from tween-inoculated tick females (**Figures 8A,D**). Despite this, granulocytes apparently lost granules, since cells from infected females had fewer granules than the granulocytes from uninfected ticks (**Figures 8B,E**). Plasmatocytes of fungus-infected females also showed morphological changes, exhibiting vacuoles in their cytoplasm (**Figures 8C,F**).

Transmission Electron Microscopy Analysis

Based on presence or absence of granules, cell shape, presence or absence of pseudopodia, nucleus location, endocytic activity, endoplasmic reticulum and homogeneity of the cytoplasm, *R. microplus* hemocytes were classified as follows: Prohemocytes: small cells with a large and central nucleus, none or few granules, and mitochondria (**Figures 9A**, **10A**). Granulocytes: exhibited central or eccentric nuclei, cytoplasmic projections and lots of granules with different electron densities (**Figures 9B,C**, **10B,C**). Spherulocytes: large cells with homogeneous electron densities spherules occupying virtually the entire cytoplasm (**Figures 9D**, **10D**). Plasmatocytes: variable sized cells with no or few granular inclusions in the cytoplasm and pseudopodia (**Figures 9E,F**, **10E,F**). Oenocytoids were not observed in TEM analysis. No differences were observed between untreated and tween-inoculated tick females, except granulocytes from ticks under physiological conditions apparently exhibited more plasma membrane projections (**Figures 9C**, **10C**).

Some morphological differences were observed in hemocytes of *R. microplus* ticks after fungal infection. Twenty-four hours after infection, prohemocytes, spherulocytes and oenocytoids could not be observed, only granulocytes and plasmatocytes. Plasmatocytes had intense cytoplasmic vacuolization and double wall fungal conidia in the cytoplasm (**Figures 11A–D**), suggesting phagocytosis of conidia. In addition, these cells displayed autophagosome with material at different stages of degradation, plasma membrane rupture, suggesting a necrosis process, healthy mitochondria, nucleus with normal appearance and an increased endoplasmic reticulum. Granulocytes from fungus-infected ticks had fewer granules than granulocytes of uninfected

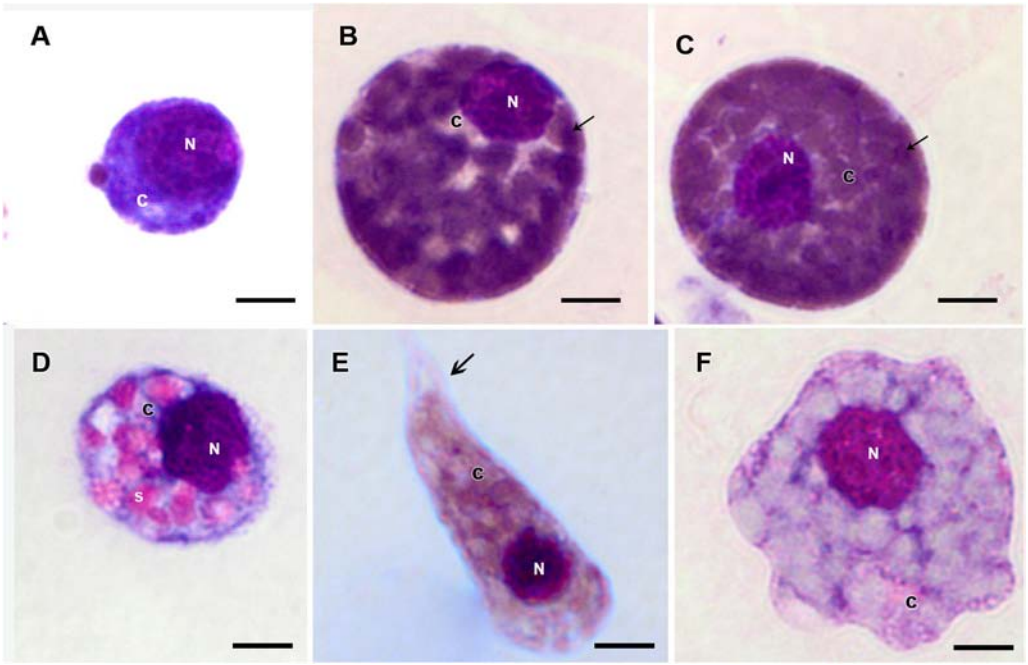

FIGURE 5 | Hemocytes representation found in the hemolymph of *R. microplus* engorged females under physiological conditions (untreated ticks) after Giemsa staining. **(A)** Prohemocyte, **(B,C)** Granulocyte, **(D)** Spherulocyte, **(E)** Plasmatocyte and **(F)** Oenocyte. Nucleus (N), cytoplasm (c), granules (thin black arrow), spherules (s) and pseudopodia (thick black arrow). Bars = 5 μm.

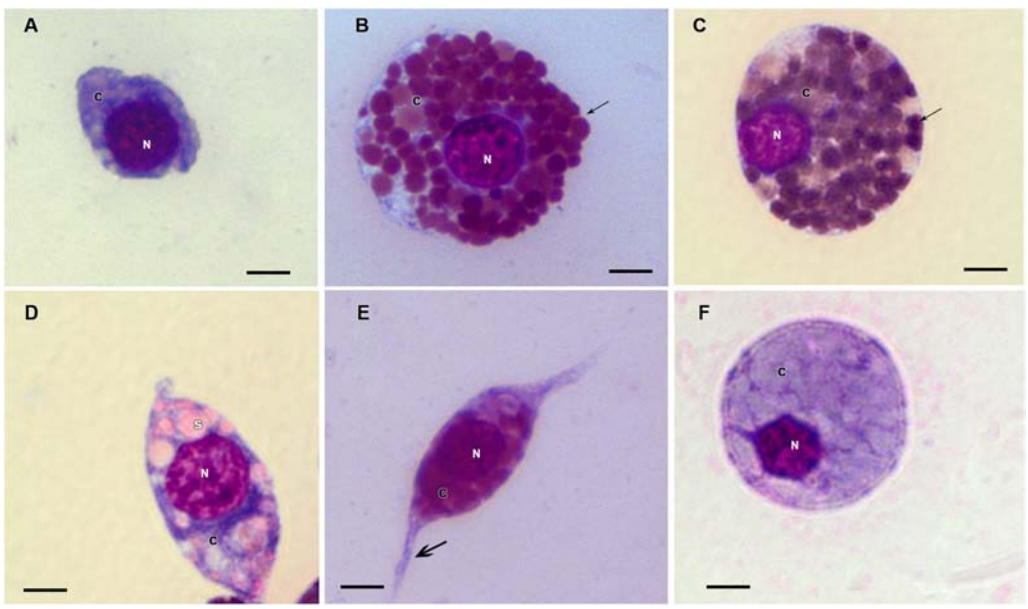

FIGURE 6 | Hemocytes representation found in the hemolymph of *R. microplus* engorged females from tween-inoculated ticks after Giemsa staining. **(A)** Prohemocyte, **(B,C)** Granulocyte, **(D)** Spherulocyte, **(E)** Plasmatocyte and **(F)** Oenocyte. Nucleus (N), cytoplasm (c), granules (thin black arrow), spherules (s) and pseudopodia (thick black arrow). Bars = 5 μm.

ticks, also exhibited autophagosomes with material at different stages of degradation and the presence of multivesicular bodies (**Figures 11E,F**). Hemocytes from fungus-infected tick females had nuclei showing extensive regions of euchromatin, several cytoplasmic vacuoles with different electron densities, subcellular material in degradation stage or already degraded, and the presence of autophagosome or multivesicular bodies, suggesting an autophagy process (**Figure 11**).

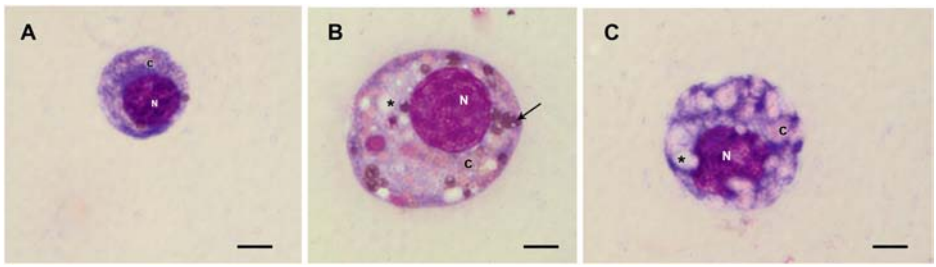

FIGURE 7 | Hemocytes representation found in the hemolymph of *R. microplus* engorged females from fungus-infected ticks after Giemsa staining. **(A)** Prohemocyte, **(B)** Granulocyte and **(C)** Plasmatocyte. Nucleus (N), cytoplasm (c), vacuoles (*) and granules (thin black arrow). Bars = 5 μm.

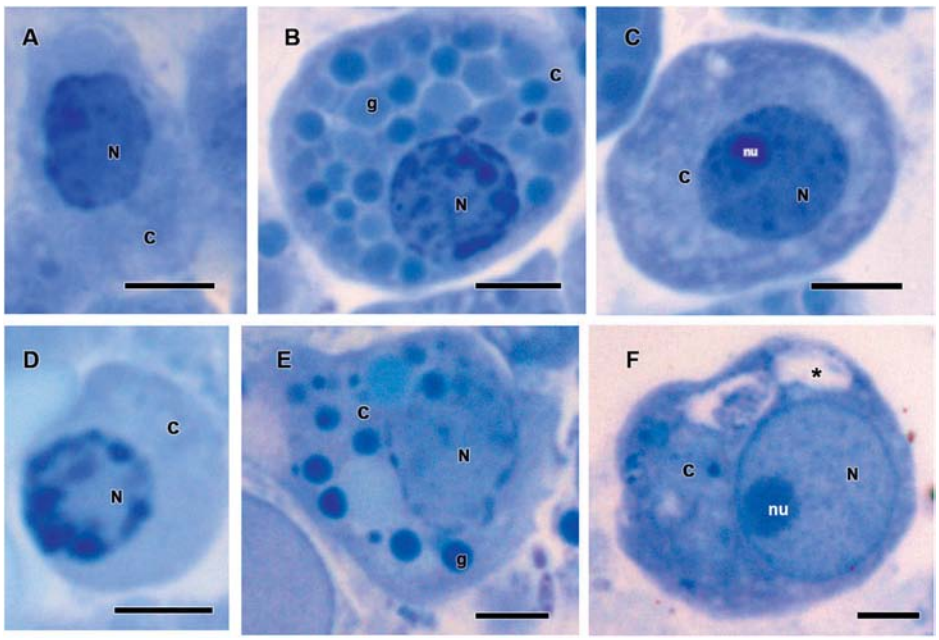

FIGURE 8 | Hemocytes representation found in the hemolymph of *Rhipicephalus microplus* engorged females **(A–C)** inoculated with 0.1% Tween®80 aqueous solution (v/v) or **(D–F)** infected with *Metarhizium robertsii* after methylene blue staining. Prohemocytes **(A)** from tween-inoculated ticks and **(D)** from fungus-infected ticks; granulocytes **(B)** from tween-inoculated ticks and **(E)** from fungus-infected ticks; plasmatocytes from **(C)** tween-inoculated group and **(F)** from fungus-infected ticks. Nucleus (N), cytoplasm (c), nucleolus (nu), granule (g) and vacuoles (*). Bars = 5 μm.

Characterization of Cells Granules by Microanalysis

Microanalysis demonstrated that *M. robertsii* ARSEF 2575 infection did not affect the composition of *R. microplus* granulocytes' electron dense granules (**Figure 12**). Granules of granulocytes from tween-inoculated ticks and fungus-infected ticks were composed only by oxygen and carbon.

DISCUSSION

Some entomopathogenic fungi are known to be highly virulent to ticks, as well as to different species of insects (Roberts and St Leger, 2004; Wang and St Leger, 2006; Leemon and Jonsson, 2008; Samish et al., 2014; Perinotto et al., 2017). Interestingly, entomopathogenic fungi have a variety of mechanisms that can neutralize the host defenses, such as the production of secondary metabolites able to suppress the insect immune system (Dubovskiy et al., 2013). This suppression of immune reactions is one of the main mechanisms governing the outcome of relations between a host and an invader. Furthermore, *Metarhizium* spreads in nutrient-rich hemocoel through immunological evasion and adaptation to osmotic stress (Wang and St Leger, 2006; Huang et al., 2015). Here, *M. robertsii* ARSEF 2575 was virulent to *R. microplus* engorged females after fungal inoculation. Several factors are involved in the virulence of a fungal isolate to arthropods, especially ticks that are much less susceptible than insects (Rot et al., 2013; Erler and Ates, 2015; Mohammadyani et al., 2016; Alves et al., 2017; Fischhoff et al., 2017). Distinct fungal virulence to different populations of the same host (Perinotto et al., 2012), host species, life stage of the host (i.e., some species and stages are more susceptible than

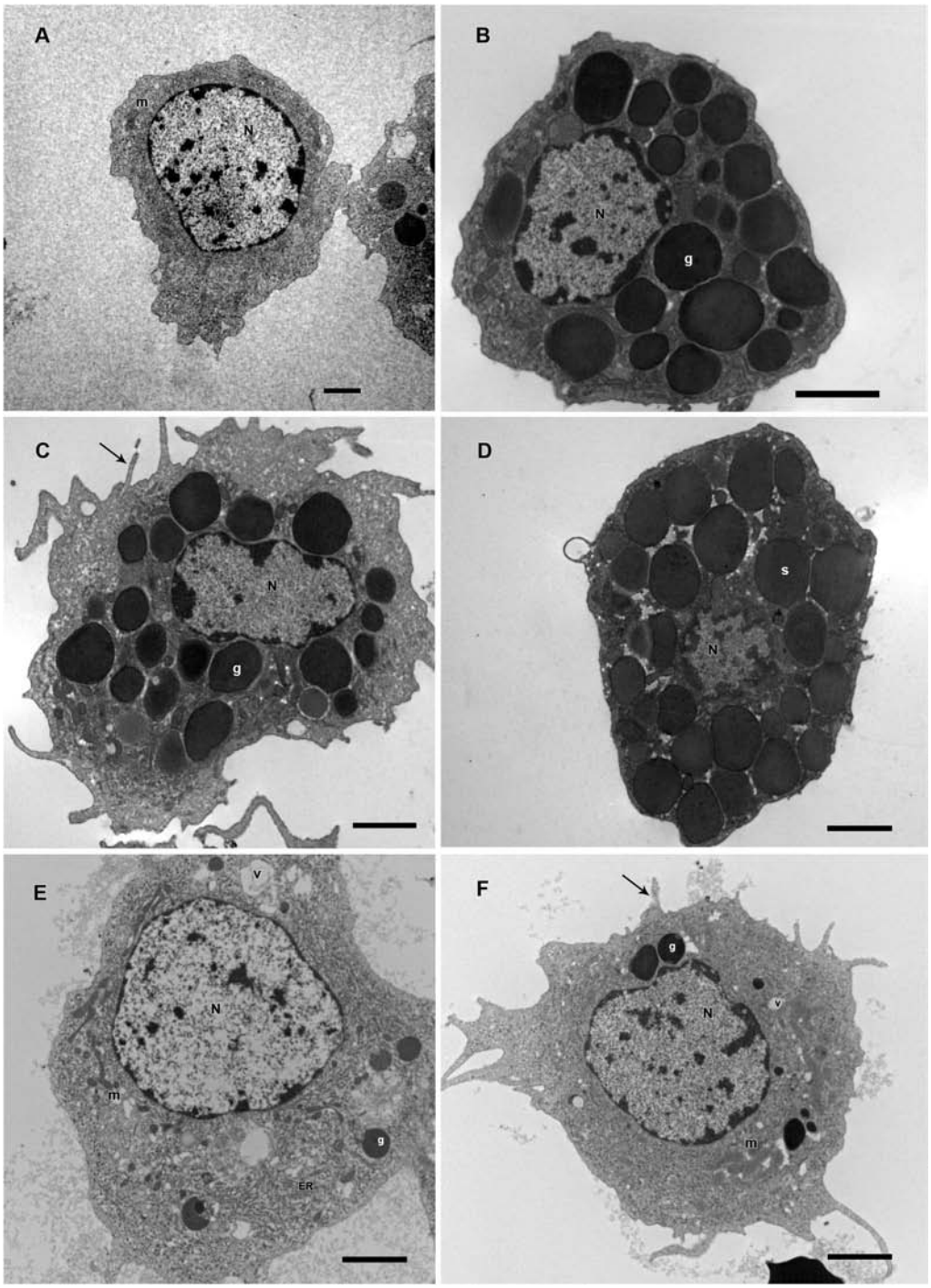

FIGURE 9 | Electromicrographs of *R. microplus* hemocytes in normal physiological conditions (untreated-ticks). **(A)** Prohemocyte with nucleus (N) and mitochondria (m) in its cytoplasm. **(B,C)** Granulocytes with nucleus (N), electron dense granules (g), and plasma membrane projection (black arrow). **(D)** Spherulocyte with nucleus (N) and spherules (s) in the cytoplasm. **(E,F)** Plasmatocytes with nucleus (N), mitochondria (m), endoplasmic reticulum (ER), electron dense granules (g), vacuole (v), and plasma membrane projections (black arrow). Bars = 2 μm.

others), and the quantity of fungal propagules applied to the arthropod pest (Alden et al., 2001; Ment et al., 2012) are some of these factors. Analyzing the results of the present study, the highest fungal concentration (i.e., 1.0×10^8 conidia mL^{-1}, the one more frequently used for tick control) in the longest time of infection (i.e., 48 h) yielded the best tick mortality rate; while the lowest fungal concentrations (i.e., 1.0×10^4, 10^5, and 10^6 conidia mL^{-1}) resulted in similar mortality rates. Despite the longer

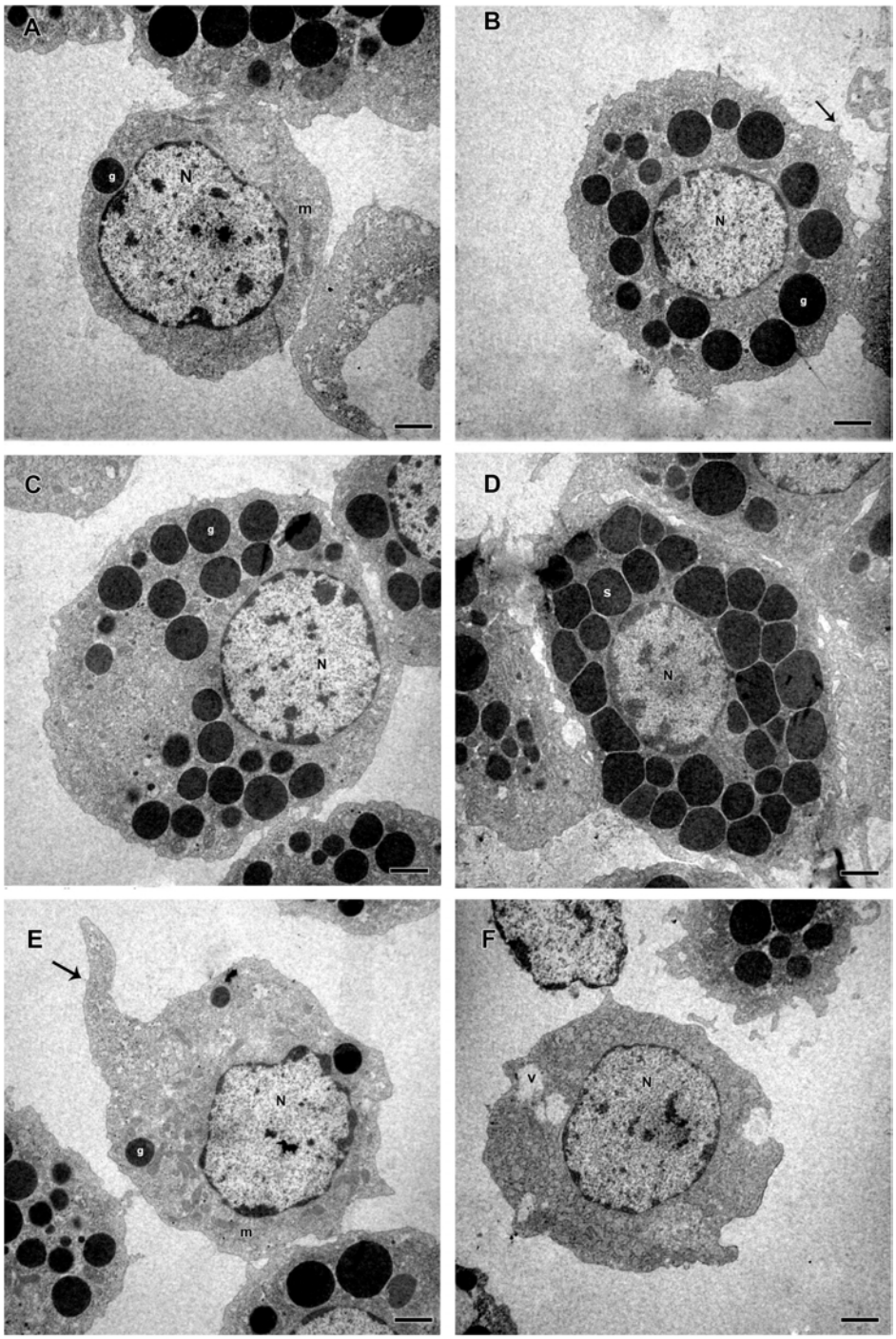

FIGURE 10 | Electromicrographs of hemocytes from *R. microplus* engorged females inoculated with 0.1% Tween®80 aqueous solution (v/v). **(A)** Prohemocyte with nucleus (N), electron dense granule (g) and mitochondria (m) in its cytoplasm. **(B,C)** Granulocytes with nucleus (N), electron dense granules (g), and plasma membrane projection (black arrow). **(D)** Spherulocyte with nucleus (N) and spherules (s) in the cytoplasm. **(E,F)** Plasmatocytes with nucleus (N), mitochondria (m), electron dense granules (g), vacuole (v), and pseudopodia (black arrow). Bars = 2 μm.

time of infection, greater the negative effects for the host. The mortality rates of ticks 48 h after fungal inoculation in the higher doses, prevented the hemolymph collection since hemolymph collected from near-to-death or dead females is not colorless but red, suggesting midgut disruption and fungal colonization of organs such as ovaries (Liu et al., 2009; Ment et al., 2012; Sanchez-Roblero et al., 2012; De Paulo et al., 2018). The same happens with the hemolymph collected 24 h after inoculation with the highest

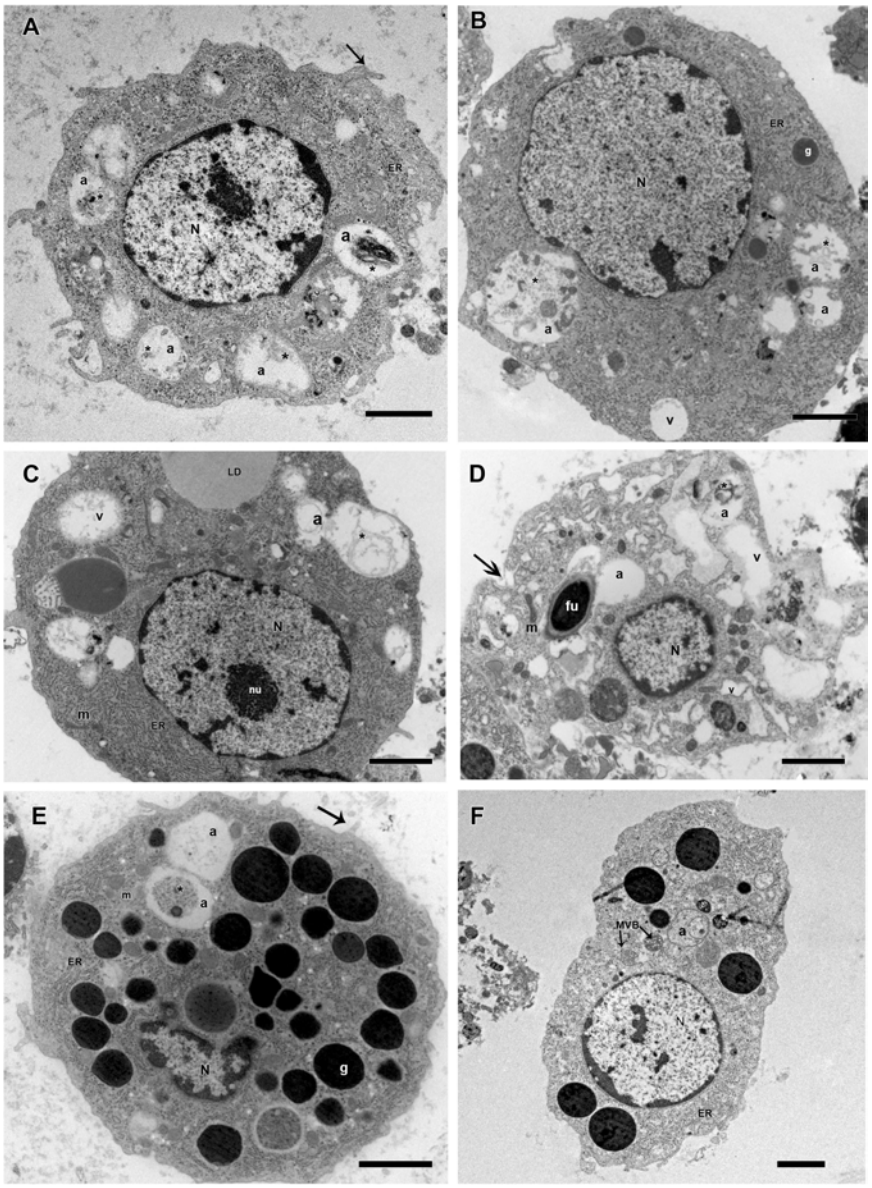

FIGURE 11 | Electromicrographs of *R. microplus* hemocytes from fungus-infected ticks. **(A)** Plasmatocyte with nucleus (N), endoplasmic reticulum (ER), autophagosome (a) with material at different stages of degradation (*) and plasma membrane projection (black arrow). **(B)** Plasmatocyte with nucleus (N), electron dense granules (g), vacuolization (v), endoplasmic reticulum (ER), autophagosome (a) with material at different stages of degradation (*). **(C)** Plasmatocyte with nucleus (N), nucleolus (nu), mitochondria (m), endoplasmic reticulum (ER), presence of lipid droplets (LD) adjacent to low electron density vacuoles (v) and autophagosome (a) with material at different stages of degradation (*). **(D)** Plasmatocyte with nucleus (N), double wall fungal conidia in the cytoplasm (fu), intense vacuolization (v), mitochondria (m), plasma membrane rupture (black arrow) and autophagosome (a) with material at different stages of degradation (*). **(E)** Granulocyte with nucleus (N), electron dense granules (g), mitochondria (m), endoplasmic reticulum (ER), plasma membrane projection (black arrow) and autophagosome (a) with material at different stages of degradation (*). **(F)** Granulocyte with nucleus (N), endoplasmic reticulum (ER), autophagosome (a) and multivesicular bodies (MVB). Bars = 2 μm.

fungal concentration (1.0×10^8 conidia mL^{-1}). Accordingly, the ultrastructural and cytotoxic analyses of hemocytes from fungus-infected ticks were performed with hemolymph collected 24 h after fungal inoculation after inoculation with 1.0×10^7 conidia mL^{-1}.

During the fungal infectious process, the arthropod can fight the pathogen through humoral and cellular immunity; the last one is mediated by hemocytes (Sterba et al., 2011). The present study demonstrated that the entomopathogen *M. robertsii* negatively affected *R. microplus* tick hemocytes, possibly causing cell death. The kinetic curve of the hemocytes viability test 24 h after exposure to *M. robertsii* showed that the highest resazurin activation (i.e., the lowest hemocytes viability) occurred with 3 h of incubation, after this time, activity remained stable. There

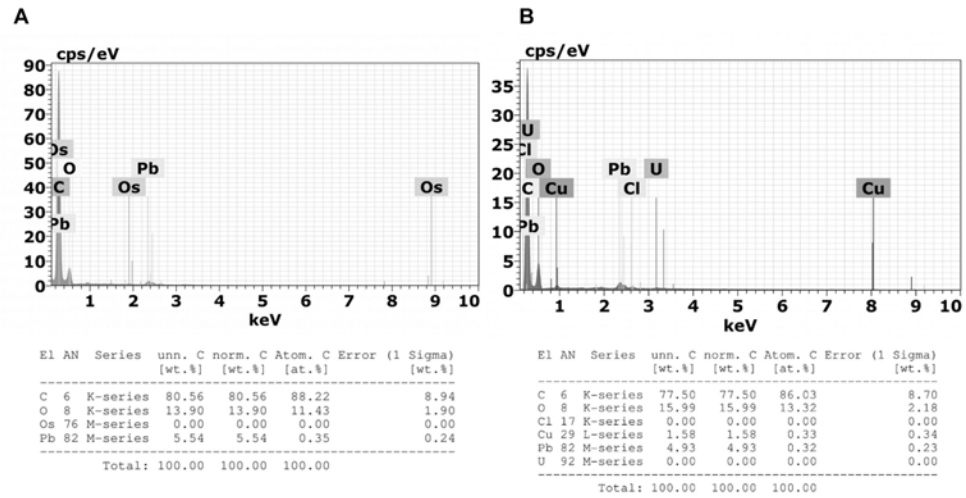

FIGURE 12 | Emission spectra obtained by Energy Dispersive X-Ray Spectroscopy (X-EDS) in TEM performed on 3 μm sections of **(A)** granulocytes from tween-inoculated ticks and **(B)** granulocytes from fungus-infected ticks. Spectra obtained focusing the incident electron beam on the granulocyte electron-dense granules of which characteristic energies of non-X-ray emission are evident. Multiple X-EDS analyses have been performed in each group; the ones that exhibited a pattern in common with the rest of the acquired spectra are shown. It is also possible to observe the presence of copper (Cu), a component of the TEM supporting grid; osmium (Os), used as fixative; lead (Pb), and uranium (U) that are used as staining.

are no studies involving resazurin and tick hemocytes, or even evaluating entomopathogenic fungal toxicity to these cells. Most studies with arthropod hemocytes are focused on MTT [3-(4,5-dimethylthiazol-2-yl)-2,5-diphenyl tetrazolium bromide] (Jose et al., 2011) and assays performed over heavy metal toxicity (Katsumiti et al., 2014, 2015; Minguez et al., 2014). Analyze the cells' viability is crucial for toxicity tests and MTT is widely used, however, it has lower sensibility and needs a higher incubation time in comparison to resazurin, once MTT measures the mitochondrial dehydrogenate (Mosmann, 1983). In addition, resazurin test is easy to be performed because it does not need culture media removal or organic solvents (Mosmann, 1983; Xu et al., 2015).

Studies about *R. microplus* cellular morphology and ultrastructure are scarce; for this reason, hemocytes identification through light and transmission microscopy was based on other tick species and other arthropods (Carneiro and Daemon, 1997; Borovicková and Hypsa, 2005; Habeeb and El-Hag, 2008; Feitosa et al., 2015, 2018). Silva et al. (2006) studies with light microscopy reported six hemocytes types in *R. microplus* hemolymph described as prohemocytes, granulocytes, plasmatocytes, spherulocytes, adipohemocytes, and oenocytoids. The last two were found to be less abundant. In the present study, only five cell types were observed: prohemocytes, granulocytes with different morphologies, plasmatocytes, spherulocytes, and oenocytoids, also diverging from studies with *R. sanguineus*, where adipohemocytes were also reported (Feitosa et al., 2015). After fungal infection, it was possible to observe that prohemocytes morphology was similar to prohemocytes from uninfected *R. microplus* ticks, unlike granulocytes and plasmatocytes. Granulocytes from fungus-infected ticks apparently lost granules and plasmatocytes of infected females showed cytoplasm vacuolization. The morphological alterations of plasmatocytes suggested the phagocytic activity and also may indicate a process to cell death, already reported by Sharma et al. (2008) and Shaurub et al. (2014). Some cells from untreated or treated ticks exhibited poorly stained areas (**Figures 5–7**), what is suggested to be a result of the differences between intracellular components. Accordingly, further studies are needed to characterize those areas for a better understanding of the organelles present in these cells.

Electron microscopy is very important for hemocytes characterization. Despite this, until the present date, the ultrastructural description of *R. microplus* hemocytes was not available in the literature. Accordingly, the morphological descriptions in the present study were compared with other tick species (Borovicková and Hypsa, 2005; Habeeb and El-Hag, 2008; Feitosa et al., 2015, 2018). Here, prohemocytes had similar morphology to those described by Habeeb and El-Hag (2008) and Feitosa et al. (2015) for other tick species. In the ultrastructure analysis, these cells showed ribosomes and mitochondria, but little endoplasmic reticulum and Golgi. The similar morphological characteristics of this hemocyte reported by this and other studies may be related to its function, since the prohemocyte is considered the precursor of other hemocytes (Lavine and Strand, 2002; Kavanagh and Reeves, 2004). Nevertheless, the origin of the other hemocytes is still unclear (Nation, 2016).

Plasmatocytes were abundant, polymorphic, had either central or eccentric nuclei, vesicles with different sizes, small vacuoles and mitochondria (Sonenshine and Roe, 2014). However, in the present study, cytoplasmic and pseudopodia projections, and an agranular or slightly granular cytoplasm were observed, in contrast to the findings of Feitosa et al. (2015) that described plasmatocytes with only small granulations. This and other

studies suggested that this cell type is strongly involved in the immune response, through the removal of apoptotic cells, but mainly due to phagocytosis and encapsulation of pathogens, analogous to the actions of monocytes in vertebrates (Tojo et al., 2000; Lavine and Strand, 2002; Jiang et al., 2009; Honti et al., 2014).

Insect granulocytes are generally elliptic cells showing protease activity with acid phosphatase in the lysosomal compartments (Nation, 2016). For other tick species such as *Ornithodoros moubata* and *Ixodes ricinus*, granulocytes were distinguished in two types, based on the electron density and maturation of their granules (Borovicková and Hypsa, 2005; Sonenshine and Roe, 2014), while for *R. sanguineus* differentiation of granulocytes types was described based on cell maturation (Feitosa et al., 2015). In the present study, these cells had granules with different sizes, different electron densities and also diverse nucleus position in the cytoplasm. Despite this, we did not distinguish these cells in different types, since it was necessary to investigate the granules' composition before staggering additional classifications.

Spherulocytes are less abundant cells in the hemolymph, however, in *R. sanguineus* they appear to be more abundant (Carneiro and Daemon, 1997; Feitosa et al., 2015). In the present study, these cells present spherules in the cytoplasm and less organelles corroborating with other studies with insects (Brayner et al., 2005) and tick (Sonenshine and Hynes, 2008). In insects, this cell type is suggested to be involved with tissue renewal, transport of substances such as hormones and even production of some hemolymph proteins (Negreiro et al., 2004).

Adipohemocytes are cells found in insects and some tick species with varying sized and shape lipid droplets, throughout the entire cytoplasm, some mitochondria, and eccentric nucleus (Cunha et al., 2009). In *Aedes aegypti*, this cell type is considered the second most abundant and may have some granules (Hillyer et al., 2003). In ticks, a study with *R. sanguineus* reported this cellular type was rarely found in the hemolymph (Feitosa et al., 2015). In the present study, this cell type was not observed, endorsing other studies with ticks (Borovicková and Hypsa, 2005; Habeeb and El-Hag, 2008). The absence of these cells in the present study is suggested to reflect its low abundance or absence in *R. microplus* hemolymph, or a misclassification since these cells are microscopically identical fat body cells or can even be mistaken by plasmatocytes with lipid droplets (Gupta, 1985; Hillyer et al., 2003; Nation, 2016).

Oenocytoids are cells the exhibit varied size and shape, without pseudopodia, and usually with an eccentric nucleus (Gupta, 1985). They are non-phagocytic cells but may be involved in the encapsulation process (Eggenberger et al., 1990). At light microscopy these cells show homogeneous cytoplasm or small refractory granulations (Carneiro and Daemon, 1997). Transmission microscopy revels few organelles, but some mitochondria and electron luscent vesicles may be present (Giulianini et al., 2003). In ticks, this hemocyte type is not abundant (Silva et al., 2006; Feitosa et al., 2015). In the present study few oenocytoids were detected and only at light microscopy. It is suggested that the low abundance of these cells is due to its easy disruption associated with calcium mobilization that activates protein kinase C and open calcium channels, inducing increased intracellular osmotic pressure, causing cell disruption (Shrestha et al., 2015).

Hemocytes have several functions, featuring protection against pathogens, production and secretion of peroxidases, encapsulation and phagocytosis (Nation, 2016). The interactions between entomopathogenic fungi and tick hemocytes are not well elucidated, so the morphological characterization of these cells and the changes caused by the infectious process can help to investigate the lower susceptibility that these arthropods have toward entomopathogenic agents.

Granulocytes from fungus-infected ticks showed apparently fewer granules and some cells also exhibited vacuolization. These cells are guided to initiate, mediate and terminate the encapsulation process, forming a monolayer on the foreign agent (Sonenshine and Hynes, 2008). Despite this, in the present study, encapsulation processes of *M. robertsii* conidia by granulocytes were not observed, possibly due to the infection stage here analyzed (24 h after infection), considered advanced.

Plasmatocytes from fungus-infected ticks exhibited cytoplasmic vacuolization and double wall fungal conidia in the cytoplasm, suggesting a process of conidia phagocytosis. Vacuolization in plasmatocytes was also observed in other arthropod species after pathogens challenging (Sharma et al., 2008; Shaurub et al., 2014). In addition, in the present study, cells from tick-infected ticks lost its filopodia, endorsing Ghasemi et al. (2013) reports, and exhibited an increased endoplasmic reticulum. The endoplasmic reticulum is a membranous network which is responsible for protein biosynthesis, for example, and also acts as calcium storage (Berridge et al., 2003). For this reason, endoplasmic reticulum has significant importance in cellular stimuli, nutrient availability or redox status. When one cell has abundance of this organelle, it means this cell is trying to produce and secrete more protein seeking to control adversities in the intracellular media (Zhang and Kaufman, 2008). Nevertheless, further studies are needed to investigate the complete process of phagocytosis or fungal internalization and the resulting autophagy hemocytes.

Non-visualization of other cell types such as prohemocytes, spherulocytes and oenocytoids in the tick hemolymph after fungal infection is suggested to reflect the reduction in the concentration of these cell types considering that these cells do not have specific functions in the cellular immune response, and, for that reason, they are supposed to be more vulnerable to the pathogenic infection (Lavine and Strand, 2002; Cunha et al., 2009). Prohemocytes may also be in a lower concentration because these cells may have differentiated into granulocytes and plasmatocytes (Feitosa et al., 2015). Additionally, secondary metabolites produced by *Metarhizium* can cause hemocytes apoptosis reducing the number of circulating hemocytes in the hemolymph (Wiegand et al., 2000).

The encapsulation of pathogens or foreign bodies is one of the most common defense processes in arthropods succeeding to encompass larger targets such as nematodes (Bronskill, 1962;

Peters and Ehlers, 1997; Mastore et al., 2015). In insects, granulocytes are responsible for this process, in which several layers of the cells surround the pathogen, forming a capsule and inactivating it by the production of free radicals (Nappi and Ottaviani, 2000). In ticks, the process remains evident in plasmatocytes (Kopácek et al., 2000). In the present study, neither encapsulation nor nodulation processes were observed.

The fungal parasitism in arthropod cells has been reported for the fungus *Microsporidium*, which are eukaryotes, obligate parasites of several animal species and was also considered an entomopathogenic fungus (Polar et al., 2008). A large number of pathogens are able to survive in host cells, such as *Histoplasma capsulatum* fungus that can be phagocytosed by human alveolar macrophages and still is capable of multiplying itself within the cell (Newman et al., 2006). Supposedly, intracellular colonization of the fungus support itself, allowing some type of latency with a negative impact for the arthropod host health, although some factors as the nutritional stress can cause a rapid fungal growth, leading to host desiccation and arthropod death (Kurtti and Keyhani, 2008).

Exposure of insect hemocytes to pathogens such as viruses, bacteria, protozoa, and other microorganisms can trigger a cell response to the infection (Nation, 2016). Cells populations increase in hemolymph as a feedback to the infection process until the pathogens are eliminated. Nevertheless, when microorganisms are highly pathogenic, cells will be leaning to start autophagy processes. Additionally, the autophagic pathway seems to play an important role during the pathogen-host cell interaction, favoring or hindering the infection. Autophagy refers to the mechanism of degradation of cytoplasmic components through the lysosomal route, selectively or non-selectively. This process occurs physiologically throughout the cell cycle, but it is exacerbated under stress conditions such as nutritional deprivation. Autophagy promotes cell cycle modulation, growth, antigenic presentation, cytokine production, and degradation of intracellular pathogens in certain cell types (Munz, 2009). The imbalance of the autophagic pathway (increase or decrease) can lead to cell death (Kroemer and Levine, 2008). In the present study, an autophagosome was observed in hemocytes from fungus-infected ticks, suggesting an autophagic processes.

Previous studies involving autophagy were limited to its role in non-selective recycling of intracellular material to the lysosome, in response to starvation (Mizushima et al., 2004; Kroemer et al., 2010). Nevertheless, autophagy is now recognized as a process with several specialized functions, including elimination of large endogenous material in a selective way, such as mitophagy and xenophagy. Autophagosomes are identified by multiple assays, including fluorescent dyes and TEM ultrastructural analysis (Klionsky et al., 2012). Studies with *Drosophila melanogaster* and *Caenorhabditis elegans* demonstrated the contribution of autophagy to innate immune response, mainly when adaptive immunity is absent (Benjamin et al., 2013; Yin et al., 2016; Zimmermann et al., 2016; Kmiec et al., 2017). In *D. melanogaster*, autophagy is promoted by host pattern recognition receptors (PRRs), whereas in *C. elegans*, xenophagy is used to target *Microsporidia* (Bakowski et al., 2014). Recent studies started to unveil the involvement of autophagy with host tolerance rather than resistance to infection caused by extracellular pathogens (Kuo et al., 2018). Nevertheless, more investigation is required to elucidate why ticks are more tolerant to entomopathogenic fungi than insects, focusing especially in autophagy studies, since ticks have short life cycle.

The present study demonstrated the first evaluation of *R. microplus* hemocytes using transmission electron microscopy and elucidated some aspects associated to this tick's cellular immune response to entomopathogenic fungi through cytotoxicity, TEM, and bioassay analysis, seeking to understand this host's higher tolerance to entomopathogenic fungi in comparison to insects. Our study unveiled important observations necessary for the comprehension of tick physiology and tick pathology, supporting the progress of new strategies for the biological control of ticks.

DATA AVAILABILITY

The raw data supporting the conclusions of this manuscript will be made available by the authors, without undue reservation, to any qualified researcher.

ETHICS STATEMENT

This study was carried out in accordance with the project approved by the Ethics Committee for the Use of Animals of the Veterinary Institute, Federal Rural University of Rio de Janeiro (CEUA UFRRJ n°. 037/2014).

AUTHOR CONTRIBUTIONS

JF, CC-R, PG, IA, RM-B, and VB conceived and designed the study. JF, CC-R, and RB performed the experiments. DS-M helped with histological analyses. DS-M and RM-B helped with transmission electron microscopy analyses. JF and PG analyzed the data and drafted the manuscript. All authors read and approved the final manuscript.

FUNDING

This study was financed in part by the Coordenacão de Aperfeiçoamento de Pessoal de Nível Superior (CAPES) from Brazil, finance code 001, Fundação Carlos Chagas Filho de Amparo à Pesquisa do Estado do Rio de Janeiro (FAPERJ), and Conselho Nacional de Desenvolvimento Científico e Tecnológico (CNPq) from Brazil. VB is a CNPq researcher.

ACKNOWLEDGMENTS

We would like to thank Dr. Flávio J. H. Tommasini Vieira Ramos (Instituto Militar de Engenharia - IME) for helping in EDS analysis.

REFERENCES

Alden, L., Demoling, F., and Baath, E. (2001). Rapid method of determining factors limiting bacterial growth in soil. *Appl. Environ. Microbiol.* 67, 1830–1838. doi: 10.1128/AEM.67.4.1830-1838.2001

Alonso-Díaz, M. A., García, L., Galindo-Velasco, E., Lezama-Gutierrez, R., Angel-Sahagún, C. A., Rodríguez-Vivas, R. I., et al. (2007). Evaluation of *Metarhizium anisopliae* (Hyphomycetes) for the control of *Boophilus microplus* (Acari: Ixodidae) on naturally infested cattle in the Mexican tropics. *Vet. Parasitol.* 147, 336–340. doi: 10.1016/j.vetpar.2007.03.030

Alves, F. M., Bernardo, C. C., Paixão, F. R. S., Barreto, L. P., Luz, C., Humber, R. A., et al. (2017). Heat-stressed *Metarhizium anisopliae*: viability (*in vitro*) and virulence (*in vivo*) assessments against the tick *Rhipicephalus sanguineus*. *Parasitol. Res.* 116, 111–121. doi: 10.1007/s00436-016-5267-z

Alves, S. B. (1998). *Controle Microbiano de Insetos*. Piracicaba: FEALQ.

Angelo, I. C., Fernandes, E. K. K., Bahiense, T. C., Perinotto, W. M. S., Moraes, A. P. R., Terra, A. L. M., et al. (2010). Efficiency of *Lecanicillium lecanii* to control the tick *Rhipicephalus microplus*. *Vet. Parasitol.* 172, 317–322. doi: 10.1016/j.vetpar.2010.04.038

Angelo, I. C., Gôlo, P. S., Perinotto, W. M. S., Camargo, M. G., Coutinho-Rodrigues, C. J. B., Campanhon, I. B., et al. (2014). Detection of serpins involved in cellular immune response of *Rhipicephalus microplus* challenged with fungi. *Biocontrol Sci. Technol.* 24, 351–360. doi: 10.1080/09583157.2013.863269

Araújo, H. C., Cavalcanti, M. G., Santos, S. S., Alves, L. C., and Brayner, F. A. (2008). Hemocytes ultrastructure of *Aedes aegypti* (Diptera: Culicidae). *Micron* 39, 184–189. doi: 10.1016/j.micron.2007.01.003

Au, C., Dean, P., Reynolds, S. E., and Ffrench-Constant, R. H. (2003). Effect of the insect pathogenic bacterium *Photorhabdus* on insect phagocytes. *Cell. Microbiol.* 6, 89–95. doi: 10.1046/j.1462-5822.2003.00345.x

Bahiense, T. C., Fernandes, É. K. K., Angelo, I. C., Perinotto, W. M. S., and Bittencourt, V. R. E. P. (2008). Performance of *Metarhizium anisopliae* and its combination with deltamethrin against a pyrethroid-resistant strain of *Boophilus microplus* in a stall test. *Ann. N. Y. Acad. Sci.* 1149, 242–245. doi: 10.1196/annals.1428.031

Bakowski, M. A., Desjardins, C. A., Smelkinson, M. G., Dunbar, T. L., Lopez-Moyado, I. F., Rifkin, S. A., et al. (2014). Ubiquitin-mediated response to *microsporidia* and virus infection in *C. elegans*. *PLoS Pathog.* 10:e1004200. doi: 10.1371/journal.ppat.1004200

Bayne, C. J. (1990). Phagocytosis and non-self recognition in invertebrates. Phagocytosis appears to be an ancient line of defense. *Bioscience* 40, 723–731. doi: 10.2307/1311504

Benjamin, J. L., Sumpter, R. Jr., Levine, B., and Hooper, L. V. (2013). Intestinal epithelial autophagy is essential for host defense against invasive bacteria. *Cell Host Microbe* 13, 723–734. doi: 10.1016/j.chom.2013.05.004

Berridge, M. J., Bootman, M. D., and Roderick, H. L. (2003). Calcium signalling: dynamics, homeostasis and remodelling. *Nat. Rev. Mol. Cell Biol.* 4, 517–529. doi: 10.1038/nrm1155

Bidochka, M. J., Walsh, S. R. A., Ramos, M. E., St Leger, R. J., Carruthers, R. I., Silver, J. C., et al. (1997). Cloned DNA probes distinguish endemic and exotic *Entomophaga grylli* fungal pathotype infections in grasshopper life stages. *Mol. Ecol.* 6, 303–308. doi: 10.1046/j.1365-294X.1997.00187.x

Borovicková, B., and Hypsa, V. (2005). Ontogeny of tick hemocytes: a comparative analysis of *Ixodes ricinus* and *Ornithodoros moubata*. *Exp. Appl. Acarol.* 35, 317–333. doi: 10.1007/s10493-004-2209-8

Brayner, F. A., Araujo, H. R., Cavalcanti, M. G., Alves, L. C., and Peixoto, C. A. (2005). Ultrastructural characterization of the hemocytes of *Culex quinquefasciatus* (Diptera: Culicidae). *Micron* 36, 359–367. doi: 10.1016/j.micron.2004.11.007

Brayner, F. A., Araujo, H. R., Santos, S. S., Cavalcanti, M. G., Alves, L. C., Souza, J. R., et al. (2007). Haemocyte population and ultrastructural changes during the immune response of the mosquito *Culex quinquefasciatus* to microfilariae of *Wuchereria bancrofti*. *Med. Vet. Entomol.* 21, 112–120. doi: 10.1111/j.1365-2915.2007.00673.x

Bronskill, J. F. (1962). Encapsulation of rhabditoid nematodes in mosquitoes. *Can. J. Zool.* 40, 1269–1275. doi: 10.1139/z62-103

Bryant, W. B., and Michael, K. (2014). Blood feeding induces hemocyte proliferation and activation in the African malaria mosquito, *Anopheles gambiae* Giles. *J. Exp. Biol.* 217, 1238–1245. doi: 10.1242/jeb.094573

Camargo, M. G., Gôlo, P. S., Angelo, I. C., Perinotto, W. M. S., Sa, F. A., Quinelato, S., et al. (2012). Effect of oil-based formulations of acaripathogenic fungi to control *Rhipicephalus microplus* ticks under laboratory conditions. *Vet. Parasitol.* 188, 140–147. doi: 10.1016/j.vetpar.2012.03.012

Camargo, M. G., Nogueira, M. R. S., Marciano, A. F., Perinotto, W. M. S., Coutinho-Rodrigues, C. J. B., Scott, F. B., et al. (2016). *Metarhizium anisopliae* for controlling *Rhipicephalus microplus* ticks under field conditions. *Vet. Parasitol.* 223, 38–42. doi: 10.1016/j.vetpar.2016.04.014

Carneiro, M. E., and Daemon, E. (1997). Caracterização dos tipos celulares presentes na hemolinfa de adultos de *Rhipicephalus sanguineus* (Latreille, 1806) (IXODOIDEA: Ixodidae) em diferentes estados nutricionais. *Rev. Bras. Parasitol. Vet.* 6, 1–9.

Castillo, J., Brown, M. R., and Strand, M. R. (2011). Blood feeding and insulin-like peptide 3 stimulate proliferation of hemocytes in the mosquito *Aedes aegypti*. *PLoS Pathog.* 7:e1002274. doi: 10.1371/journal.ppat.1002274

Castillo, J. C., Robertson, A. E., and Strand, M. R. (2006). Characterization of hemocytes from the mosquitoes *Anopheles gambiae* and *Aedes aegypti*. *Insect. Biochem. Mol. Biol.* 36, 891–903. doi: 10.1016/j.ibmb.2006.08.010

Ceraul, S. M., Sonenshine, D. E., and Hynes, W. L. (2002). Resistance of the tick *Dermacentor variabilis* (Acari: Ixodidae) following challenge with the bacterium *Escherichia coli* (Enterobacteriales: Enterobacteriaceae). *J. Med. Entomol.* 39, 376–383. doi: 10.1603/0022-2585-39.2.376

Chávez, A. S. O., Shaw, D. K., Munderloh, U. G., and Pedra, J. H. (2017). Tick humoral responses: marching to the beat of a different drummer. *Front. Microbiol.* 8:223. doi: 10.3389/fmicb.2017.00223

Chen, K., and Lu, Z. (2018). Immune responses to bacterial and fungal infections in the silkworm, *Bombyx mori*. *Dev. Comp. Immunol.* 83, 3–11. doi: 10.1016/j.dci.2017.12.024

Crossley, A. C. (1975). The cytophysiology of insect blood. *Adv. Insect Physiol.* 11, 117–221. doi: 10.1016/s0065-2806(08)60163-0

Cunha, F. M., Wanderley-Teixeira, V., Teixeira, A. A. C., Albuquerque, A. C., Alves, L. C., and Lima, L. A. (2009). Caracterização dos hemócitos de operários de *Nasutitermes coxipoensis* (Holmgren) (Isoptera: Termitidae) e avaliação hemocitária após parasitismo por *Metarhizium anisopliae*. *Neotrop. Entomol.* 38, 293–297. doi: 10.1590/S1519-566X2009000200021

De la Fuente, J., Estrada-Pena, A., Venzal, J. M., Kocan, K. M., and Sonenshine, D. E. (2008). Overview: ticks as vectors of pathogens that cause disease in humans and animals. *Front. Biosci.* 13, 6938–6946.

De Paulo, J. F., Camargo, M. G., Coutinho-Rodrigues, C. J. B., Marciano, A. F., Freitas, M. C., Da Silva, E. M., et al. (2018). *Rhipicephalus microplus* infected by *Metarhizium*: unveiling hemocyte quantification, GFP-fungi virulence, and ovary infection. *Parasitol. Res.* 117, 1847–1856. doi: 10.1007/s00436-018-5874-y

Dolp, R. M. (1970). Biochemical and physiological studies of certain ticks (Ixodoidea). Qualitative and quantitative studies of hemocytes. *J. Med. Entomol.* 7, 277–288. doi: 10.1093/jmedent/7.3.277

Dubovskiy, I. M., Whitten, M. M. A., Yaroslavtseva, O. N., Greig, C., Kryukov, V. Y., Grizanova, K. V., et al. (2013). Can insects develop resistance to insect pathogenic fungi? *PLoS One* 8:e60248. doi: 10.1371/journal.pone.0060248

Eggenberger, L. R., Lamoreaux, W. J., and Coons, L. B. (1990). Hemocytic encapsulation of implants in the tick *Dermacentor variabilis*. *Exp. Appl. Acarol.* 9, 279–287. doi: 10.1007/BF01193434

Ehlers, S., Mielke, M. E., Blankenstein, T., and Hahn, H. (1992). Kinetic analysis of cytokine gene expression in the livers of naive and immune mice infected with *Listeria monocytogenes*. The immediate early phase in innate resistance and acquired immunity. *J. Immunol.* 149, 3016–3022.

Erler, F., and Ates, A. O. (2015). Potential of two entomopathogenic fungi, *Beauveria bassiana* and *Metarhizium anisopliae* (Coleoptera: Scarabaeidae), as biological control agents against the June beetle. *J. Insect Sci.* 15:44. doi: 10.1093/jisesa/iev029

Feitosa, A. P. S., Alves, L. C., Chaves, M. M., Veras, D. L., Silva, E. M., Alianca, A. S. S., et al. (2015). Hemocytes of *Rhipicephalus sanguineus* (Acari: Ixodidae): characterization, population abundance, and ultrastructural changes following challenge with *Leishmania infantum*. *J. Med. Entomol.* 52, 1193–1202. doi: 10.1093/jme/tjv125

Feitosa, A. P. S., Alves, L. C., Chaves, M. M., Veras, D. L., Vasconcelos de Deus, D. M., Portela Juniora, N. C., et al. (2018). Assessing the cellular and humoral immune response in *Rhipicephalus sanguineus* sensu lato (Acari: Ixodidae)

infected with *Leishmania infantum* (Nicolle, 1908). *Ticks Tick Borne Dis.* 9, 1421–1430. doi: 10.1016/j.ttbdis.2018.06.007

Fischhoff, I. R., Keesing, F., and Ostfeld, R. S. (2017). The tick biocontrol agent *Metarhizium brunneum* (=*M. anisopliae*) (strain F52) does not reduce non-target arthropods. *PLoS One* 12:e0187675. doi: 10.1371/journal.pone.0187675

Fogaça, A. C., Lorenzini, D. M., Kaku, L. M., Esteves, E., Bulet, P., and Daffre, S. (2004). Cysteine-rich antimicrobial peptides of the cattle tick *Boophilus microplus*: isolation, structural characterization and tissue expression profile. *Dev. Comp. Immunol.* 28, 191–200. doi: 10.1016/j.dci.2003.08.001

Fujisaki, K., Kitaoka, S., and Morii, T. (1975). Hemocyte types and their primary cultures in the argasid tick, *Ornithodoros moubata* Murray (Ixodoidea). *Appl. Entomol. Zool.* 10, 30–39. doi: 10.1303/aez.10.30

Ghasemi, V., Moharramipour, S., and Jalali Sendi, J. (2013). Circulating hemocytes of Mediterranean flour moth, *Ephestia kuehniella* Zell. (Lep.:Pyralidae) and their response to thermal stress. *Invertebrate Surviv. J.* 10, 128–140.

Gillespie, J. P., Kanost, M. R., and Trenczek, T. (1997). Biological mediators of insect immunity. *Annl. Rev. Entomol.* 42, 611–643. doi: 10.1146/annurev.ento.42.1.611

Giulianini, P. G., Bertolo, F., Battistella, S., and Amirante, S. A. (2003). Ultrastructure of the hemocytes of *Cetonischema aeruginosa* larvae (Coleoptera, Scarabaeidae): involvement of both granulocytes and oenocytoids in in vivo phagocytosis. *Tissue Cell* 35, 243–251. doi: 10.1016/S0040-8166(03)00037-5

Grisi, L., Leite, R. C., Martins, J. R. S., Barros, A. T. M., Andreotti, R., Cançado, P. D., et al. (2014). Reassessment of the potencial economic impact of cattle parasites in Brazil. *Rev. Bras. Parasitol. Vet.* 23, 150–156. doi: 10.1590/S1984-29612014042

Gupta, A. P. (1985). *Cellular Elements in the Hemolymph: Comprehensive Insect Physiology, Biochemistry and Pharmacology*. Oxford: Pergamon Press, 402–444.

Gupta, A. P. (1986). "Arthropod immunocytes: identification, structure, and analogies to the functions of vertebrate B- and T-lymphocytes," in *Hemocytic and Humoral Immunity in Arthropod*, ed. A. P. Gupta (Hoboken, NJ: John Wiley & Sons), 3–57.

Habeeb, S. M., and El-Hag, H. A. A. (2008). Ultrastructural changes in hemocyte cells of hard tick (*Hyalomma dromedarii*: Ixodidae): a model of *Bacillus thuringiensis* var. *thuringiensis* H14;-endotoxin mode of action. *Am. Eurasian J. Agric. Environ. Sci.* 3, 829–836.

Hajdušek, O., Sima, R., Ayllon, N., Jalovecka, M., Perner, J., de la Fuente, J., et al. (2013). Interaction of the tick immune system with transmitted pathogens. *Front. Cell. Infect. Microbiol.* 3:26. doi: 10.3389/fcimb.2013.00026

Hillyer, J. F., Schmidt, S. L., and Christensen, B. M. (2003). Hemocyte-mediated phagocytosis and melanization in the mosquito *Armigeres subalbatus* following immune challenge by bacteria. *Cell Tissue Res.* 313, 117–127. doi: 10.1007/s00441-003-0744-y

Hillyer, J. F., Schmidt, S. L., Fuchs, J. F., Boyle, J. P., and Christensen, B. M. (2005). Age-associated mortality in immune challenged mosquitoes (*Aedes aegypti*) correlates with a decrease in haemocyte numbers. *Cell. Microbiol.* 7, 39–51. doi: 10.1111/j.1462-5822.2004.00430.x

Honti, V., Csordas, G., Kurucz, E., Markus, R., and Ando, I. (2014). The cell-mediated immunity of *Drosophila melanogaster*: hemocyte lineages, immune compartments, microanatomy and regulation. *Dev. Comp. Immunol.* 42, 47–56. doi: 10.1016/j.dci.2013.06.005

Hu, X., Xiao, G., Zheng, P., Shang, Y., Su, Y., Zhang, X., et al. (2014). Trajectory and genomic determinants of fungal-pathogen speciation and host adaptation. *Proc. Natl. Acad. Sci. U.S.A.* 111, 16796–16801. doi: 10.1073/pnas.1412662111

Huang, W., Shang, Y., Chen, P., Gao, Q., and Wang, C. (2015). MrpacC regulates sporulation, insect cuticle penetration and immune evasion in *Metarhizium robertsii*. *Environ. Microbiol.* 17, 994–1008. doi: 10.1111/1462-2920.12451

Iacovone, A., Ris, N., Poirié, M., and Gatti, J. L. (2018). Time-course analysis of *Drosophila suzukii* interaction with endoparasitoid wasps evidences a delayed encapsulation response compared to *D. melanogaster*. *PLoS One* 13:e0201573. doi: 10.1371/journal.pone.0201573

Inoue, N., Hanada, K., Tsuji, N., Igarashi, I., Nagasawa, H., Mikami, T., et al. (2001). Characterization of phagocytic hemocytes in *Ornithodorosmoubata* (Acari: Ixodidae). *J. Med. Entomol.* 38, 514–519. doi: 10.1603/0022-2585-38.4.514

Jiang, R., Kim, E. H., Gong, J. H., Kwon, H. M., Kim, C. H., Ryu, K. H., et al. (2009). Three pairs of protease-serpin complexes cooperatively regulate the insect innate immune responses. *J. Biol. Chem.* 284, 35652–35658. doi: 10.1074/jbc.M109.071001

Johns, R., Sonenshine, D. E., and Hynes, W. L. (1998). Control of bacterial infections in the hard tick *Dermacentor variabilis* (Acari: Ixodidae): evidence for the existence of antimicrobial proteins in tick hemolymph. *J. Med. Entomol.* 35, 458–464. doi: 10.1093/jmedent/35.4.458

Johns, R., Sonenshine, D. E., and Hynes, W. L. (2001). Identification of a defensin from the hemolymph of the American dog tick, *Dermacentorvariabilis*. *Insect Biochem. Mol. Biol.* 31, 857–865. doi: 10.1016/S0965-1748(01)00031-5

Jones, J. C. (1962). Current concepts concerning insect hemocytes. *Am. Zoo1.* 2, 209–246. doi: 10.1093/icb/2.2.209

Jose, S., Mohandas, A., Philip, R., and Bright Singh, I. S. (2011). Primary haemocyte culture of *Penaeus monodon* as an in vitro model for white spot syndrome virus titration, viral and immune related gene expression and cytotoxicity assays. *J. Invertebr. Pathol.* 105, 312–321. doi: 10.1016/j.jip.2010.08.006

Katsumiti, A., Gilliland, D., Arostegui, I., and Cajaraville, M. P. (2014). Cytotoxicity and cellular mechanisms involved in the toxicity of CdS quantum dots in hemocytes and gill cells of the mussel *Mytilus galloprovincialis*. *Aquat. Toxicol.* 153, 39–52. doi: 10.1016/j.aquatox.2014.02.003

Katsumiti, A., Gilliland, D., Arostegui, I., and Cajaraville, M. P. (2015). Mechanisms of toxicity of Ag nanoparticles in comparison to bulk and ionic Ag on mussel hemocytes and gill cells. *PLoS One* 10:e0129039. doi: 10.1371/journal.pone.0129039

Kavanagh, K., and Reeves, E. P. (2004). Exploiting the potential of insects for in vivo pathogenicity testing of microbial pathogens. *FEMS Microbiol. Rev.* 28, 101–112. doi: 10.1016/j.femsre.2003.09.002

Kernif, T., Leulmi, H., Raoult, D., and Parola, P. (2016). Emerging tick-borne bacterial pathogens. *Microbiol. Spectr.* 4:EI10-0012-2016. doi: 10.1128/microbiolspec.ei10-0012-2016

Klionsky, D. J., Abdalla, F. C., Abeliovich, H., Abraham, R. T., Acevedo-Arozena, A., Adeli, K., et al. (2012). Guidelines for the use and interpretation of assays for monitoring autophagy. *Autophagy* 8, 445–544. doi: 10.4161/auto.19496

Kmiec, Z., Cyman, M., and Slebioda, T. J. (2017). Cells of the innate and adaptive immunity and their interactions in inflammatory bowel disease. *Adv. Med. Sci.* 62, 1–16. doi: 10.1016/j.advms.2016.09.001

Kopácek, P., Hajdusek, O., Buresova, V., and Daffre, S. (2010). "Tick innate immunity," in *Invertebrate Immunity. Advances in Experimental Medicine and Biology*, Vol. 708, ed. K. Söderhäll (Boston, MA: Springer).

Kopácek, P., Weise, C., Saravanan, T., Vitova, K., and Grubhoffer, L. (2000). Characterization of an alpha-macroglobulin-like glycoprotein isolated from the plasma of the soft tick *Ornithodoros moubata*. *Eur. J. Biochem.* 267, 465–475. doi: 10.1046/j.1432-1327.2000.01020.x

Kroemer, G., and Levine, B. (2008). Autophagic cell death: the story of a misnomer. *Nat. Rev. Mol. Cell Biol.* 9, 1004–1010. doi: 10.1038/nrm2529

Kroemer, G., Mariño, G., and Levine, B. (2010). Autophagy and the integrated stress response. *Mol. Cell* 40, 280–293. doi: 10.1016/j.molcel.2010.09.023

Kuhn, K. H., and Haug, T. (1995). Ultrastructural, cytochemical, and immunocytochemical characterization of haemocytes of the hard tick *Ixodes ricinus* (Acari: Chelicerata). *Cell Tissue Res.* 277, 493–504. doi: 10.1007/BF00300222

Kuo, C. J., Hansen, M., and Troemel, E. (2018). Autophagy and innate immunity: insights from invertebrate model organisms. *Autophagy* 14, 233–242. doi: 10.1080/15548627.2017.1389824

Kurtti, T. J., and Keyhani, N. O. (2008). Intracellular infection of tick cell lines by the entomopathogenic fungus *Metarhizium anisopliae*. *Microbiology* 154, 1700–1709. doi: 10.1099/mic.0.2008/016667-0

Kwon, H., Bang, K., and Cho, S. (2014). Characterization of the hemocytes in larvae of *Protaetia brevitarsis seulensis*: involvement of granulocyte-mediated phagocytosis. *PLoS One* 9:e103620. doi: 10.1371/journal.pone.0103620

Lackie, A. M. (1980). Invertebrate immunity. *Parazitology* 80, 393–412.

Laughton, A. M., Boots, M., and Siva-Jothy, M. T. (2011). The ontogeny of immunity in the honey bee, *Apis mellifera* L. following an immune challenge. *J. Insect Physiol.* 57, 1023–1032. doi: 10.1016/j.jinsphys.2011.04.020

Lavine, M. D., and Strand, M. R. (2002). Insect hemocytes and their role in immunity. *Insect Biochem. Mol. Biol.* 32, 1295–1309. doi: 10.1016/S0965-1748(02)00092-9

Leemon, D. M., and Jonsson, N. N. (2008). Laboratory studies on Australian isolates of *Metarhizium anisopliae* as a biopesticide for the cattle tick *Boophilus microplus*. *J. Invertebr. Pathol.* 97, 40–49. doi: 10.1016/j.jip.2007.07.006

Liu, W., Xie, Y., Xue, J., Gao, Y., Zhang, Y., Zhang, X., et al. (2009). Histopathological changes of *Ceroplastes japonicus* infected by *Lecanicillium lecanii*. *J. Invertebr. Pathol.* 101, 96–105. doi: 10.1016/j.jip.2009.03.002

Madelin, M. F., Robinson, R. E., and Williams, R. S. (1967). Appressorium like structures in insect parasitizing deuteromycetes. *J. Invertebr. Pathol.* 9, 404–412. doi: 10.1016/0022-2011(67)90078-X

Mastore, M., Arizza, V., Manachini, B., and Brivio, M. F. (2015). Modulation of immune responses of *Rhynchophorus ferrugineus* (Insecta: Coleoptera) induced by the entomopathogenic nematode *Steinernema carpocapsae* (Nematoda: Rhabditida). *Insect Sci.* 22, 748–760. doi: 10.1111/1744-7917.12141

Ment, D., Churchill, A. C. L., Glazer, I., Rehner, S. A., Rot, A., Donzelli, B. G. G., et al. (2012). Resistant ticks inhibit *Metarhizium* infection prior to haemocoel invasion by reducing fungal viability on the cuticle surface. *Environ. Microbiol.* 14, 1570–1583. doi: 10.1111/j.1462-2920.2012.02747.x

Minguez, L., Halm-Lemeille, M. P., Costil, K., Bureau, R., Lebel, J. M., and Serpentini, A. (2014). Assessment of cytotoxic and immunomodulatory properties of four antidepressants on primary cultures of abalone hemocytes (*Haliotis tuberculata*). *Aquat. Toxicol.* 153, 3–11. doi: 10.1016/j.aquatox.2013.10.020

Mizushima, N., Yamamoto, A., Matsui, M., Yoshimori, T., and Ohsumi, Y. (2004). In vivo analysis of autophagy in response to nutrient starvation using transgenic mice expressing a fluorescent autophagosome marker. *Mol. Biol. Cell* 15, 1101–1111. doi: 10.1091/mbc.e03-09-0704

Mohammadyani, M., Karimi, J., Taheri, P., Sadeghi, H., and Zare, R. (2016). Entomopathogenic fungi as promising biocontrol agents for the rosaceous longhorn beetle, *Osphranteria coerulescens*. *Biocontrol* 6, 579–590. doi: 10.1007/s10526-016-9745-0

Mosmann, T. (1983). Rapid colorimetric assay for cellular growth and survival: application to proliferation and cytotoxicity assays. *J. Immunol. Methods* 65, 55–63. doi: 10.1016/0022-1759(83)90303-4

Munz, C. (2009). Enhancing immunity through autophagy. *Annu. Rev. Immunol.* 27, 423–449. doi: 10.1146/annurev.immunol.021908.132537

Nakajima, Y., Ogihara, K., Taylor, D., and Yamakawa, M. (2003). Antibacterial hemoglobin fragments from the midgut of the soft tick, *Ornithodoros moubata* (Acari: Argasidae). *J. Med. Entomol.* 40, 78–81. doi: 10.1603/0022-2585-40.1.78

Nappi, A. J., and Ottaviani, E. (2000). Cytotoxicity and cytotoxic molecules in invertebrates. *Bioessays* 22, 469–480. doi: 10.1002/(sici)1521-1878(200005)22:5<469::aid-bies9>3.0.co;2-4

Nation, J. L. (2016). *Insect Physiology and Biochemistry*. Gainesville, FL: University of Florida.

Negreiro, M. C. C., Andrade, F. G., and Falleiros, A. M. F. (2004). Sistema imunológico de defesa em insetos: uma abordagem em lagartas da soja, *Anticarsia gemmatalis* Hübner (Lepidoptera: Noctuidae), resistentes ao AgMNPV. *Semin. Ciênc. Agrár.* 25, 293–308. doi: 10.5433/1679-0359

Nevermann, L., Xylander, W. E. R., and Seifert, G. (1991). The hemocytes of the centipede *Lithobius forficatus* (Chilo-poda, Lithobiomorpha). *Zoomorphology* 110, 317–327. doi: 10.1111/j.1744-7410.2012.00264.x

Newman, S. L., Gootee, L., Hilty, J., and Morris, R. E. (2006). Human macrophages do not require phagosome acidification to mediate fungistatic/fungicidal activity against *Histoplasma capsulatum*. *J. Immunol.* 176, 1806–1813. doi: 10.4049/jimmunol.176.3.1806

Paskewitz, S. M., and Christensen, B. M. (1996). "Immune responses of vectors," in *The Biology of Disease vectors*, eds B. J. Beaty and W. C. Marquardt (Niwot, CO: University Press of Colorado), 371–392.

Perinotto, W. M. S., Angelo, I. C., Golo, P. S., Camargo, M. G., Quinelato, S., Sa, F. A., et al. (2017). In vitro pathogenicity of different *Metarhizium anisopliae* s.l. isolates in oil formulations against *Rhipicephalus microplus*. *Biocontrol Sci. Technol.* 27, 338–347. doi: 10.1080/09583157.2017.1289151

Perinotto, W. M. S., Angelo, I. C., Golo, P. S., Quinelato, S. B., Camargo, M. G., Sa, F. A., et al. (2012). Susceptibility of different populations of ticks to entomopathogenic fungi. *Exp. Parasitol.* 130, 257–260. doi: 10.1016/j.exppara.2011.12.003

Peters, A., and Ehlers, R. U. (1997). Encapsulation of the entomopathogenic nematodes *Steinernema feltiae* in *Tipula oleracea*. *J. Invertebr. Pathol.* 69, 218–222. doi: 10.1006/jipa.1996.4648

Polar, P., Moore, D., Kairo, M. T. K., and Ramsubhag, A. (2008). Topically applied myco-acaricides for the control of cattle ticks: overcoming the challenges. *Exp. Appl. Acarol.* 46, 119–148. doi: 10.1007/s10493-008-9170-x

Roberts, D. W., and St Leger, R. J. (2004). *Metarhizium* spp., cosmopolitan insect pathogenic fungi: mycological aspects. Adv. Appl. Microbiol. 54, 1–70. doi: 10.1016/S0065-2164(04)54001-7

Rot, A., Gindin, G., Ment, D., Mishoutchenko, A., Glazer, I., and Samish, M. (2013). On-host control of the brown dog tick *Rhipicephalus sanguineus* Latreille (Acari: Ixodidae) *by Metarhizium brunneum* (Hypocreales: Clavicipitaceae). *Vet. Parasitol.* 193, 229–237. doi: 10.1016/j.vetpar.2012.11.020

Samish, M., Rot, A., Ment, D., Barel, S., Glazer, I., and Gindin, G. (2014). Efficacy of the entomopathogenic fungus *Metarhizium brunneum* in controlling the tick *Rhipicephalus annulatus* under field conditions. *Vet. Parasitol.* 206, 258–266. doi: 10.1016/j.vetpar.2014.10.019

Sampaio, I. B. M. (2002). *Estatística Aplicada à Experimentação Animal*. Belo Horizonte: FEPMVZ.

Sanchez-Roblero, R., Huerta, G., Valle, J., Gomez, J., and Toledo, J. (2012). Effect of *Beauveria bassiana* on the ovarian development and reproductive potential of *Anastrepha ludens* (Diptera: Tephritidae). *Biocontrol Sci. Technol.* 22, 1045–1091. doi: 10.1080/09583157.2012.713090

Schank, A., and Vainstein, M. H. (2010). *Metarhizium anisopliae* s.l. enzymes and toxins. *Toxicon* 56, 1267–1274. doi: 10.1016/j.toxicon.2010.03.008

Schmidt, O., Theopold, U., and Strand, M. R. (2001). Innate immunity and its evasion and suppression by hymenopteran endoparasitoids. *Bioessays* 23, 344–351. doi: 10.1002/bies.1049

Sharma, P. R., Sharma, O. P., and Saxena, B. P. (2008). Effect of sweet flag rhizome oil (*Acorus calamus*) on hemogram and ultrastructure of hemocytes of the tobacco armyworm, *Spodoptera litura* (Lepidoptera: Noctuidae). *Micron* 39, 544–551. doi: 10.1016/j.micron.2007.07.005

Shaurub, E. H., Abdel-Meguide, A., and Abd El-Aziz, N. (2014). Quantificative and ultrastructural changes in the heamocytes of *Spodoptera littoralis* (Boisd.) treated individually or in combination with *Spodoptera littoralis* multicapside nucleopolyhedrovirus (SpliMNPV) and Azadirachtin. *Micron* 65, 62–68. doi: 10.1016/j.micron.2014.04.010

Shrestha, S., Park, J., Ahn, S. J., and Kim, Y. (2015). Pge2 mediates oenocytoid cell lysis via a sodium-potassium-chloride cotransporter. *Arch. Insect Biochem. Physiol.* 89, 218–229. doi: 10.1002/arch.21238

Silva, S. B., Savastano, G., and Bittencourt, V. R. E. P. (2006). Tipos celulares envolvidos na resposta imune de fêmeas de *Boophilus microplus* inoculados com *Metarhizium anisopliae* e *Penicillium* sp. *Rev. Bras. Med. Vet.* 15, 128–131.

Smith, A. A., and Pal, U. (2014). Immunity-related genes in *Ixodes scapularis* – perspectives from genome information. *Microbiology* 4:116. doi: 10.3389/fcimb.2014.00116

Sonenshine, D. E., and Hynes, W. L. (2008). Molecular characterization and related aspects of the innate immune response in ticks. *Front. Biosci.* 13, 7046–7063.

Sonenshine, D. E., and Roe, R. M. (2014). *Biology of Ticks*, 2nd Edn. Oxford: Oxford University Press, 560.

Sterba, J., Dupejova, J., Fiser, M., Vancova, M., and Grubhoffer, L. (2011). Fibrinogen-related proteins in ixodid ticks. *Parasit. Vectors* 4:127. doi: 10.1186/1756-3305-4-127

Tan, J., Xu, M., Zhang, K., Wang, X., Chen, S., Li, T., et al. (2013). Characterization of hemocytes proliferation in larval silkworm *Bombyx mori*. *J. Insect Physiol.* 59, 595–603. doi: 10.1016/j.jinsphys.2013.03.008

Tojo, S., Naganuma, F., Arakawa, K., and Yokoo, S. (2000). Involvement of both granular cells and plasmatocytes in phagocytic reactions in the greater wax moth, *Galleria mellonella*. *J. Insect Physiol.* 46, 1129–1135. doi: 10.1016/s0022-1910(99)00223-1

Vega, F. E. (2018). The use of fungal entomopathogens as endophytes in biological control: a review. *Mycologia* 110, 4–30. doi: 10.1080/00275514.2017.1418578

Wang, C., and St Leger, R. J. (2006). A collagenous protective coat enables *Metarhizium anisopliae* to evade insect immune responses. *Proc. Natl. Acad. Sci. U.S.A.* 103, 6647–6652. doi: 10.1073/pnas.0601951103

Webster, A., Reck, J., Santi, L., Souza, U. A., Dall'Agnol, B., Klafke, G. M., et al. (2015). Integrated control of an acaricide-resistant strain of the cattle tick *Rhipicephalus microplus* by applying *Metarhizium anisopliae* associated with cypermethrin and chlorpyriphos under field conditions. *Vet. Parasitol.* 207, 302–308. doi: 10.1016/j.vetpar.2014.11.021

Wiegand, C., Levin, D., Gillespie, J. P., Willott, E., Kanost, M. R., and Trenczek, T. (2000). Monoclonal antibody M13 identifies a plasmatocyte membrane protein and inhibits encapsulation and spreading reactions of *Manduca sexta* hemocytes. *Arch. Insect Biochem. Physiol.* 45, 95–108. doi: 10.1002/1520-6327(200011)45:3<95::aid-arch1>3.0.co;2-0

Xu, M., McCanna, D. J., and Sivak, J. G. (2015). Use of the viability reagent PrestoBlue in comparison with alamarBlue and MTT to assess the viability of human corneal epithelial cells. *J. Pharmacol. Toxicol. Methods* 71, 1–7. doi: 10.1016/j.vascn.2014.11.003

Yin, Z., Pascual, C., and Klionsky, D. J. (2016). Autophagy: machinery and regulation. *Microb. Cell* 3, 588–596. doi: 10.15698/mic2016.12.546

Zhang, K., and Kaufman, R. J. (2008). From endoplasmic-reticulum stress to the inflammatory response. *Nature* 454, 455–462. doi: 10.1038/nature07203

Zhioua, E., Lebrun, R. A., Johnson, P. W., and Ginsberg, H. S. (1996). Ultrastructure of the haemocytes of *Ixodes scapularis* (Acari: Ixodidae). *Acarologia* 3, 173–179.

Zimmermann, A., Kainz, K., Andryushkova, A., Hofer, S., Madeo, F., and Carmona-Gutierrez, D. (2016). Autophagy: one more Nobel Prize for yeast. *Microb. Cell* 3, 579–581. doi: 10.15698/mic2016.12.544

Conflict of Interest Statement: The authors declare that the research was conducted in the absence of any commercial or financial relationships that could be construed as a potential conflict of interest.

frontiers in Physiology

ORIGINAL RESEARCH
published: 07 June 2019
doi: 10.3389/fphys.2019.00673

Genetic Profiling Reveals High Allelic Diversity, Heterozygosity and Antigenic Diversity in the Clinical Isolates of the *Theileria annulata* From India

*Sonti Roy[1,2†], Vasundhra Bhandari[1†], Debabrata Dandasena[1], Shweta Murthy[1] and Paresh Sharma[1]**

[1] National Institute of Animal Biotechnology, Hyderabad, India, [2] Manipal Academy of Higher Education, Manipal, India

OPEN ACCESS

Edited by:
Abid Ali,
Abdul Wali Khan University Mardan, Pakistan

Reviewed by:
Muhammad Imran Rashid,
University of Veterinary and Animal Sciences, Pakistan
Mohamed Gharbi,
National Veterinary School of Sidi Thabet, Tunisia

***Correspondence:**
Paresh Sharma
paresh@niab.org.in;
pareshsharma21@gmail.com

[†]Share first authorship

Specialty section:
This article was submitted to Invertebrate Physiology, a section of the journal Frontiers in Physiology

Received: 21 January 2019
Accepted: 13 May 2019
Published: 07 June 2019

Citation:
Roy S, Bhandari V, Dandasena D, Murthy S and Sharma P (2019) Genetic Profiling Reveals High Allelic Diversity, Heterozygosity and Antigenic Diversity in the Clinical Isolates of the Theileria annulata From India. Front. Physiol. 10:673. doi: 10.3389/fphys.2019.00673

Tropical theileriosis caused by *Theileria annulata* infection is a significant livestock disease affecting cattle health and productivity resulting in substantial monetary losses in several countries. Despite the use of an effective vaccine for disease control still, a high incidence of infection is reported from India. One of the many reasons behind the ineffective disease control can be the existence of genetically diverse *T. annulata* parasite population in India. Therefore, studies focusing on understanding the genotypes are warranted. In this study, we have performed a genetic analysis of the Indian *T. annulata* field cell lines and the vaccine line using microsatellite markers, Genotyping based sequencing (GBS) and *tams1* gene polymorphism. The degree of allelic diversity and multiplicity of the infection was determined to be high in the Indian population. No geographical sub-structuring and linkage disequilibrium were observed in the population. High population diversity was found which were similar with countries like Oman, Tunisia, and Turkey in contrast to Portugal and China. The presence of multiple genotypes as determined by microsatellite marker genotyping, GBS analysis and *tams1* gene polymorphism point toward a panmictic parasite population in India. These findings are the first report from India which would help in understanding the evolution and diversity of the *T. annulata* population in the country and can help in designing more effective strategies for controlling the disease.

Keywords: *Theileria annulata*, genetic profiling, microsatellite markers, genotyping based sequencing, antigenic diversity

INTRODUCTION

In India, tropical theileriosis accounts for high mortality and economic loss to the livestock industry (George et al., 2015). The disease is caused by *Theileria annulata* belonging to the phylum apicomplexan, its life cycles requires a vector (ixodid tick) and host (cattle or buffalo). Currently, a live attenuated schizont lymphocyte cell line is used as a vaccine for controlling the *T. annulata* infection in India (Chakraborty et al., 2017). Despite the availability of a licensed vaccine and a theileriocidal drug, buparvaquone (BPQ), the disease still represents a severe threat to animal

health and productivity especially to the crossbreed cattle. The major disadvantages with the current vaccine are the requirement of re-vaccination after every 3 years, maintenance of cold chain and transportation in liquid nitrogen. Additionally, cases of drug resistance were also reported from the field (Mhadhbi et al., 2010, 2015; Sharifiyazdi et al., 2012). Another important aspect which may reduce the vaccine effectiveness will be the presence of heterogeneous parasite population in the field. Hence, it is essential to investigate the genetic diversity of the *T. annulata* parasites currently prevalent in India.

The life cycle of the *Theileria* parasites involved both asexual and sexual reproduction, with later responsible for genetic recombination but restricted to the tick (Mans et al., 2015). As parasite diversity is mainly driven by recombination events, it is having a crucial role in deciding the fate of the parasite control measures. Previous reports have shown genetic diversity among the *T. annulata* parasites using a panel of 10 micro and minisatellite markers, *tams1* gene PCR, and indirect fluorescence assay (IFA) (Shiels et al., 1986; Dickson and Shiels, 1993; Katzer et al., 1998; Gubbels et al., 2000a,b; Wang et al., 2014). The genetic diversity of *T. annulata* parasites using microsatellite marker have been reported previously from various countries like Oman (Al-Hamidhi et al., 2015), Sudan, Tunisia, Turkey, (Weir et al., 2007, 2011) Portugal (Gomes et al., 2016), and China (Yin et al., 2018). However, the parasite diversity studies from India are very scarce; the few available reports are based on IFA and PCR using 18S *rRNA* and *tams1* genes (Manuja et al., 2006; Wang et al., 2014; George et al., 2015). With significant advancement in the field of genomics and genotyping and with the availability of the *T. annulata* whole genome sequence, the likelihoods of genotype-based population genetic studies are open. The genetic resolution of the parasite diversity can be improved by studying more number of markers, like in closely related parasite *Theileria parva and Plasmodium falciparum* (Campino et al., 2011; Henson et al., 2012; Hayashida et al., 2013; Hemmink et al., 2016; Chen et al., 2017). Genotyping based sequencing (GBS) is one such next-generation sequencing based strategy which can identify variants/SNPs for high diversity species with accuracy and cost-effectiveness (Elshire et al., 2011; Gurgul et al., 2018).

It is significant to study the genetic diversity of the *T. annulata* parasite for developing new vaccines, new therapies, and designing more effective disease controlling strategies. In this study, we have used the *T. annulata* live attenuated vaccine line and parasite cell lines isolated from animals infected by *T. annulata* for understanding the antigenic, allelic, and genotypic diversity of the Indian parasite population. Our study will not only help in understanding the genetic diversity in the Indian *T. annulata* parasites but also provide a comparative account with parasites from different countries and vaccine line currently in use.

MATERIALS AND METHODS

In vitro Culture of *Theileria* Cell Lines

Theileria annulata infected lymphocyte cell lines were established by culturing the peripheral blood mononuclear cells (PBMCs) isolated from the whole blood of the infected cattle from the states of Telangana and Andhra Pradesh in India. The infected animals were cross breed (Jersey breed) and had never been vaccinated against tropical theileriosis. The cell lines were grown in the RPMI 1640 medium at 37°C as per standard protocol (George et al., 2015). The vaccine cell line (V) was purchased from the Indian Immunologicals Ltd., Hyderabad. The DNA was extracted from the parasite lines using standard phenol/chloroform method and was confirmed by PCR using *T. annulata* surface protein (*Tasp*) primers as mentioned in **Table 1**.

Micro and Mini Satellite Marker Analysis

The known micro (TS 5, 9, 12, and 16) and minisatellite (TS 6, 8, 15, 20, 25, and 31) markers were used for genotyping *T. annulata* parasites (Weir et al., 2007). The 5′ end of the forward primers of all ten loci were fluorescently labeled with FAM dye. The PCR was done using locus-specific primers to amplify all the markers as mentioned before (Weir et al., 2007, 2011). The purified PCR product was then run on the ABI 3730Xl genetic analyzer with ROX labeled GS500 standard size marker for genotyping analyses. Further analyses was carried out by GeneMarker V2.7. The allele count was analyzed for each locus in the range of 100–500 bp. The peaks higher than 32% of the predominant peak was used for scoring allele to avoid minor amplification or PCR artifacts and a predominant allele at each locus is used to prepare the multilocus genotype (MLG) for each sample (**Table 2**; Weir et al., 2007, 2011). The MLG data was used to calculate the genetic distance matrix and heterozygosity at each locus using GenAlEx 6.5 software (Peakall and Smouse, 2012). The genetic distance matrix was used for performing PCoA analysis using GenAlEx 6.5 software. $^{A}I_{S}$ (index of Association), V_{D} (Variance of the pairwise differences), L_{MC} (Upper 95% confidence limits of Monte Carlo simulation), and L_{PARA} (parametric tests) were calculated using Lian 3.7 (Haubold and Hudson, 2000).

Genotyping Based Sequencing

The DNA isolated from the 6 parasite strains (C1, C2, V, C4, C5, and C6) was checked for its quality and quantity using Nanodrop and Qubit. Genomic DNA (300 ng) was digested by double digestion using PstI-HF and MluCl restriction enzyme at 37°C for 4 h. The resulting digested fragments were directly ligated to a pair of restriction site-specific adapters at 20°C for 1 h using T4 DNA ligase. The adapter-ligated fragments were subjected to PCR amplification (10 cycles) to amplify the adapter-ligated fragments and to add sample specific dual index barcodes (Nextera XT v2 Index Kit, Illumina,

TABLE 1 | Primers used in the study.

Primer name	Sequence (5′–3′)	Product size	TM
Tasp For	ATGAAATTCTTCTACCTTTTTG	1065 bp	60
Tasp Rev	ACAACAATCTTCGTTAATGCGA		
Tams For	ATGTTGTCCAGGACCACCCTC	858 bp	55
Tams Rev	TTAAAGGAAGTAAAGGACTGA		

TABLE 2 | Allele diversity among the different parasite strains for the 10 micro and Mini satellite markers.

Sample ID	Chr 1		Chr 2		Chr 3			Chr 4		
	TS15	TS16	TS20	TS31	TS8	TS9	TS12	TS5	TS6	TS25
C1	3	4	3	4	3	2	4	3	6	1
C2	2	1	5	12	6	3	3	2	7	6
C3	5	4	4	15	12	3	9	4	20	2
C4	7	7	3	7	4	2	1	2	20	2
C5	7	2	6	6	4	7	11	5	6	5
C6	5	1	4	7	12	2	2	1	4	2
V	3	2	3	16	3	4	5	2	20	2
Tunisia	8	12	13	18	24	22	18	8	16	7
Turkey	7	7	10	10	8	9	10	6	10	7

Chr, Chromosome.

United States). The amplified Illumina-compatible sequencing library was quantified by Qubit fluorometer (Thermo Fisher Scientific, MA, United States) and its fragment size distribution was analyzed on Agilent 2200 Tape Station. The library was used to run the Illumina single-end sequencing (75X1, NextSeq) for all the samples. The raw reads quality from the Illumina run were checked using FastQC. *T. annulata* genome specific reads were separated through alignment using Bowtie2, and aligned reads from each of the samples were used for variant identification. A merged FASTQ file was generated for all the six samples using the good reads for the organism. This merged FASTQ file was aligned to the reference genome of *T. annulata* (GCF_000003225.3) using Bowtie2. The alignment quality was checked using Qualimap software. To filter out low-quality SNPs/variants, the TASSEL-GBS pipeline was used for filtering minor allele frequency (MAF) and inbreeding coefficient. The consensus sequence generated from the run for each cell line was used for performing a multiple sequence alignment using ClustalW algorithm. The Ankara genome sequence was also included in the analysis as a control. Gblocks program was used to identify the conserved stretches in the genomes. Finally, MEGA7 program was used to calculate the phylogenetic distance between the parasite strains and for drawing a phylogenetic tree using the consensus sequence (Wang et al., 2014). The evolutionary history and phylogenetic tree were generated using the neighbor-joining method.

Tams1 Based Antigenic Diversity Analysis

The DNA isolated from the seven parasite strains was used for amplifying the *tams1* gene using for and rev primers (**Table 1**). The purified PCR products of 858 bp were then cloned into the pBSK vector using the TA cloning method followed by Sanger's sequencing to confirm the *tams1* gene. The sequencing results were further confirmed by checking the specificity of the sequence using blast analysis. The previously published *tams1* gene sequences from the three continents Asia, Africa and Europe were used for calculating the phylogenetic relationship between the strains using MEGA7 software (Wang et al., 2014). Accession number of the sequences that were used U222888.1 (Ankara), Z48739.1 (Ankara), GU130193.1 (Iraq: Kurdistan), AF214819.1 (Mauritania), JX683683.1 (Gansu: China), AF214911.1 (Turkey: Ankara), AF214872.1 (Tunisia: Northern), AY672541.1 (Iran), EU563912.1 (China: Xinjiang), AF214828.1 (Portugal), AF214860.1 (Italy: Northern Sicily), AF214812.1 (Spain: Cáceres), EF618726.1 (India: Chennai), EF618728.1 (India: Chennai), JX648210.1 (South India: Tamil Nadu), AF214840.1 (India: Hissar), AF214891.1 (Tunisia: Northern), AF214861.1 (Italy: Northern Sicily), AF214908.1 (Turkey: Ankara), AF214806.1 (Spain: Cáceres), AF214797.1 (Bahrain), GU130190.1 (Iraq:Kurdistan region), AB690863.1 (Srilanka: Polonnaruwa), GU130192.1 (Iraq: Kurdistan region), EF092918.1 (Iran: Qazvin Boein Zahra). These sequences were collected from the NCBI site and imported in MEGA7 software and aligned using the ClustalW method. The evolutionary history and phylogenetic tree were generated using the neighbor-joining method.

Ethics Statement

Collection of less than 5 ml of blood, in accordance with national legislation, is exempt from ethical approval requirements.

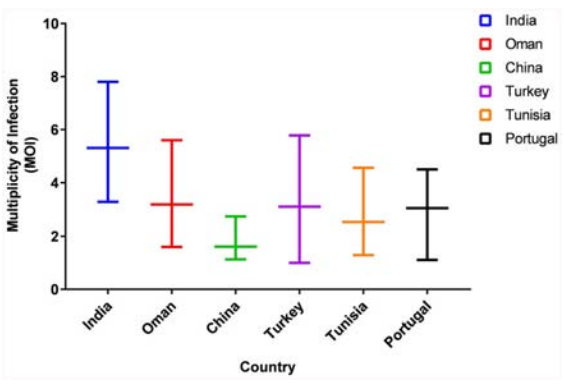

FIGURE 1 | Comparison of Multiplicity of Infection (MOI) in Six countries. The graph represents the range of MOI in six countries.

TABLE 3 | Comparison of heterozygosity and linkage equilibrium analysis.

Country	He	I_A^S	V_D	L_{MC}	L_{PARA}	Linkage
India	0.82041	0.0191	0.4571	0.6571	0.5732	LE
Oman	0.8307	0.019	1.4595	1.29	1.29	LD
China	0.5	0.1224	2.6253	1.5727	1.5635	LD
Turkey	0.8817	0.0207	1.0671	0.9495	0.944	LD
Tunisia	0.8841	0.0117	0.9534	0.9128	0.9088	LD
Portugal	0.625	0.0272	2.0247	1.8679	1.8521	LD

He, Estimated heterozygosity; I_A^S, Standard index of association; V_D, Mismatch variance (linkage analysis); L_{MC}, Upper 95% confidence limits of Monte Carlo simulation; L_{PARA}, Parametric tests; LD, Linkage disequilibrium; LE, Linkage equilibrium.

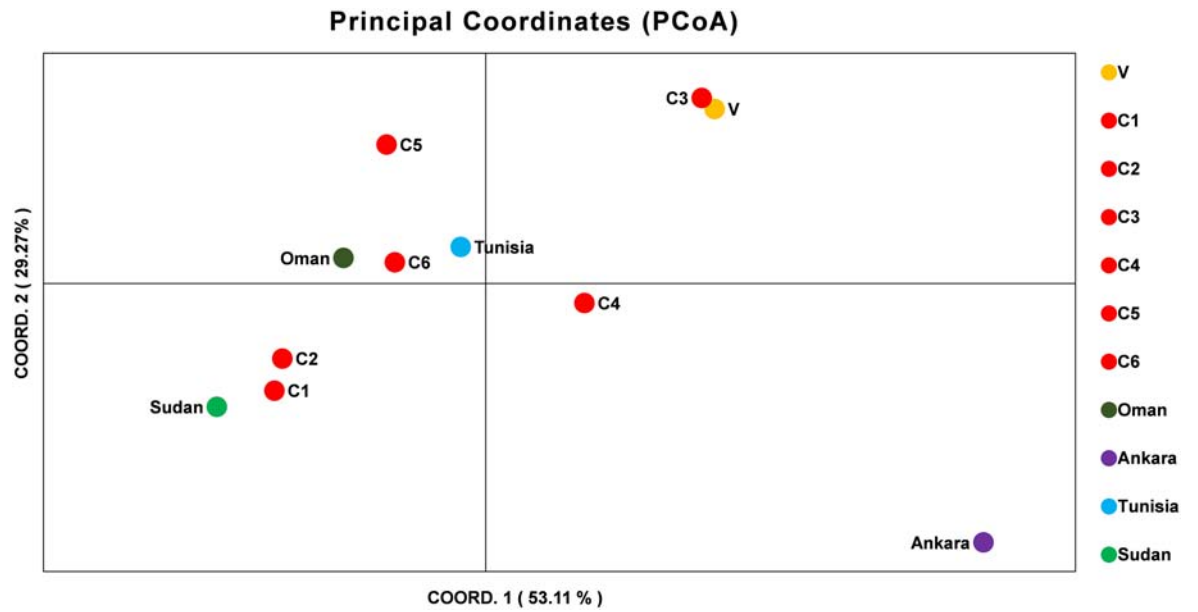

FIGURE 2 | Principal Component Analysis (PCoA) of *T. annulata* parasite population from India, Oman, Ankara, Sudan, and Tunisia. PCoA analysis based on the MLG profiles of the *T. annulata* parasites was done to understand the geographical distribution of the parasites in different countries. The two coordinates along with the proportional of variance (%) used for doing the analysis are shown in *X* and *Y* axis.

Further, professional veterinarians collected blood samples after obtaining oral consent from farm owner.

RESULTS

High Allelic Diversity Observed in the Indian Parasite Populations

Microsatellite analysis was done for the seven parasite cell lines (C1, C2, C3, C4, C5, C6, V) using the 10 markers. All the markers showed high polymorphisms in the Indian parasites although in few cell lines a single allele was observed for TS16, TS12, TS5, and TS25. The diversity of alleles ranged from one to twenty among the Indian parasite cell lines. In C3, C4, and V, highest polymorphism (n = 20) was observed for TS6 marker. Whereas low polymorphism (n = 1) was observed against markers TS16, TS12, TS5, and TS25 in C2, C6, C4, and C1 cell lines (**Table 2**).

The MOI for the Indian parasitic cell lines ranged from 3.3 to 7.8, with an average MOI of 5.31 (**Figure 1**). The MOI range of the Indian population was higher when compared to the parasite from Sudan, Oman, China, Portugal, and Turkey which ranged from 1.0 to 5.78.

High Population Diversity, Linkage Equilibrium and No Geographical Sub Structuring Seen in the Indian Population

The allelic profiles were used to create MLG data set for each marker using the predominant allele for the Indian population. The MLG data was further used for calculating heterozygosity, linkage disequilibrium and the genetic distance between the parasite strains. The estimated heterozygosity (H_e) for the Indian population was found to be 0.82041 which was determined by using the predominant allele dataset for each marker and averaged across all ten loci (**Table 3**). For understanding the Indian population differentiation, linkage analysis was performed by calculating values of I^S_A = 0.0191 and V_D = 0.4571 which was found to be less than L_{MC} = 0.6571 and L_{PARA} = 0.5732

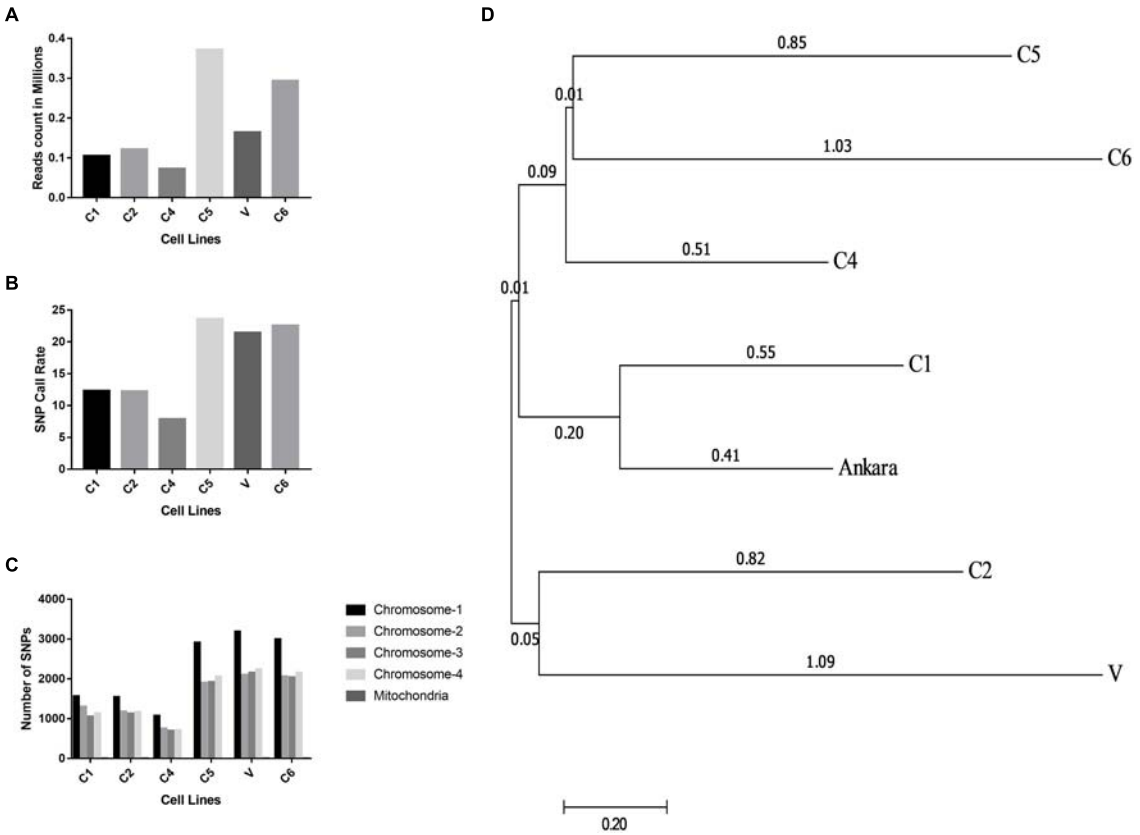

FIGURE 3 | Distribution of reads, SNP call rates and Phylogenetic relationship determined from the GBS analysis. **(A)** The figure shows the read count in millions generated using the GBS experiments done for the six different *T. annulata* cell lines. **(B)** The figure shows the SNP call rate between the six cells lines used for the GBS when compared to the Ankara reference strain. **(C)** The figure shows SNP distribution within the four chromosomes and mitochondria for the six cell lines used for the GBS study. **(D)** The evolutionary distances were computed using the maximum composite likelihood method and are in the units of the number of base substitutions per site. The analysis involved seven nucleotide sequences. Bootstrap values are shown next to the nodes. Evolutionary analysis was performed with MEGA7.

indicating linkage equilibrium (LE). The PCoA analysis showed no specific geographical distribution between the Indian parasites when compared to the parasites from other countries like Oman, Sudan, Tunisia, and Turkey. The analysis showed C1 and C2 parasites cluster with Sudan while C5 and C6 with Tunisia and Oman suggesting allelic similarities. The C3 and V clustered together in a separate cluster while C4 and parasite from Turkey didn't cluster with anyone. The variation among the samples was found to be 53.11 and 29.27% for the first and second coordinates of the graph, respectively (**Figure 2**).

GBS Identified Genetic Polymorphisms Among the Different *Theileria* Parasites

The Illumina reads generated after sequencing were aligned with the *T. annulata* Ankara strain for identifying *T. annulata* specific sequences and SNPs in the Indian parasite cell lines. The alignment helped in constructing a consensus DNA sequence for the six parasites. The GBS sequencing results showed that all the six parasites were well represented and had an average read count of 0.18 million/sample (**Figure 3A**). The distribution of SNP call rate for the samples ranged from 7.87 to 23.61% and was represented for the individual samples (**Figure 3B**). The SNPs were well distributed among the four *T. annulata* chromosomes (Chr) with Chr 1 having the highest number 3210 SNPs followed by Chr 2, 3, 4, and mitochondrial DNA in all the samples (**Figure 3C**). The phylogenetic relationship between the Indian parasites (n = 6) were calculated based on the SNPs detected in the GBS sequences including the Ankara parasite sequence. The analysis identified C1 and C6 close to the Ankara sequence based on the genetic polymorphisms in the respective sequences. C4 and C5 were clustered together while C2 showed similarity with V (**Figure 3D**).

Antigenic Diversity Was Observed for the *tams1* Gene Among the Parasites

The phylogenetic analysis was performed based on the neighbor-joining method using the *tams1* gene sequences of seven Indian parasites (GenBank accession IDs MK034698-MK034704) and 25 previously reported parasites. The clusters were divided into two groups on the basis of previously published data (Wang et al., 2014). C1, C2, and

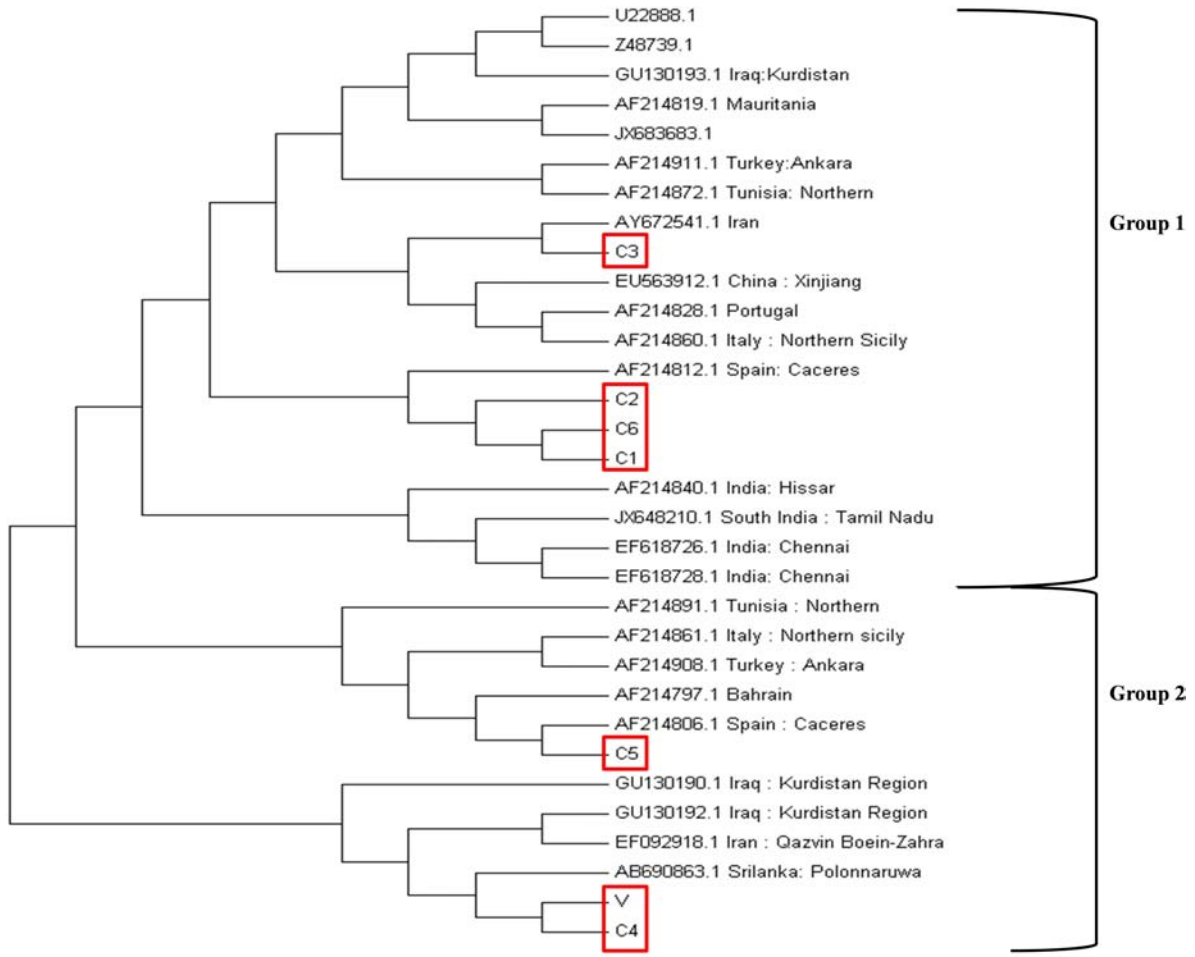

FIGURE 4 | Phylogenetic tree based on the *tams1* gene sequences from different countries. The evolutionary history was inferred using the neighbor-joining method. The percentage of replicate trees in which the associated taxa clustered together in the bootstrap test (1000 replicates) are shown next to the branches. The evolutionary distances were computed using the maximum composite likelihood method and are in the units of the number of base substitutions per site. The analysis involved 32 nucleotide sequences. All positions containing gaps and missing data were eliminated. There were a total of 363 positions in the final dataset. Evolutionary analysis was concluded in MEGA7.

C6 were clustered in group 1 while C4, C5, and V were in group 2 (**Figure 4**). The Indian isolates were distributed in both groups along with other countries like Spain, Italy, Tunisia, Iran, Bahrain, Turkey, and Iraq.

DISCUSSION

Despite the availability of a vaccine against *T. annulata*, theileriosis is frequently reported in India (George et al., 2015). The genetic diversity among the parasite strains can be one of the reasons for the failure to constraint the disease. This is the first report from India, where the genetic and allelic structure of the Indian parasites cell lines was investigated which revealed antigenic and allelic diversity among the parasite population. The parasite diversity data will be helpful in revamping or designing new vaccines for controlling the disease. *Theileria* infected bovine lymphocyte cell lines were utilized for understanding the parasite diversity in India using microsatellite markers, *tams1* gene-based antigenic diversity and GBS analysis. The vaccine strain from India and the already published data for other worldwide *T. annulata* strains were used for understanding and comparing the diversity among the parasite cell lines.

The microsatellite data analysis showed high population diversity among Indian parasites, which is in line with previous findings from Oman, Tunisia, and Turkey though less diversity was reported from Portugal and China (Weir et al., 2007, 2011; Al-Hamidhi et al., 2015; Gomes et al., 2016; Yin et al., 2018). The presence of multiple genotypes in each sample represented by high MOI values has been previously shown to be linked to high transmission intensity in related parasites like *P. falciparum* (Pinkevych et al., 2015). The MOI values were found to be higher when compared with values reported from other countries (Weir et al., 2007, 2011; Al-Hamidhi et al., 2015; Gomes et al., 2016; Yin et al., 2018). The allelic analysis showed the presence of

unique alleles when compared with previously reported alleles. The Indian parasite population was found to be in LE in contrast to LD that is reported for the majority of countries. In China, LE was observed region wise, however, LD was reported when the same analysis was done by taking samples from different regions as a population (Yin et al., 2018). The small sample size can be one of the reasons for the detection of LE in the Indian population and further studies with more samples are needed to verify the same. Despite the high genetic diversity, the population structure was found to be panmictic as represented using the PCoA analysis. The PCoA analysis clustered Indian parasites with Oman, Sudan, and Tunisia while least similarity was found with Turkey isolate. The Indian parasite population didn't show any geographical sub-structuring based on the PCoA analysis when analyzed with other country strains like Oman, Tunisia, Sudan, and Turkey.

The *tams1* gene has been shown to be a promising candidate for carrying antigenic diversity studies in *T. annulata* parasites (Gubbels et al., 2000b; Wang et al., 2014). There are contradictory reports with respect to *tams1* gene sequence with some suggesting no geographic specificity and other showing region specificity based on the gene polymorphism (Gubbels et al., 2000b; Wang et al., 2014). Our results showed Indian parasite strains to be clustered in both group 1 and 2 which is different from the previous report which showed them to be present in only group 1 (Wang et al., 2014).

The GBS analysis also confirmed the genetic diversity among the Indian parasites. The analysis showed few strains from India to be similar to Ankara strain from Turkey based on the diversity in the parasite genome. The phylogenetic tree showed a panmictic parasite population in India based on the genetic diversity. The major limitation associated with next-generation sequencing methods like GBS is the purity of the DNA sample, which in case of *T. annulata* parasites is tricky as it is difficult to separate the pure parasite from the host lymphocyte cell. The presence of host DNA in the sample has led to low SNP call rate for the parasite in our GBS study. In future, we plan to use more powerful techniques like WGS with high coverage to better understand the genetic diversity and the genome of the Indian parasite strains.

The current study not only highlights the genetic and allelic diversity present among the Indian *T. annulata* but also compares it with the isolates reported from other countries. It also sheds light on the genetic and allelic diversity among the Indian parasite and the vaccine by the use of microsatellite marker, *tams1* sequencing and GBS. These findings indicate that a heterogeneous parasitic population is prevailing in India causing theileriosis and may render the vaccine ineffective due to high diversity. It is essential to perform genetic diversity studies including the parasite population from different parts of India to map the diversity among the overall natural parasite population. It will help in identifying new vaccine targets and policy to control the disease.

AUTHOR CONTRIBUTIONS

PS designed the study. SR, VB, DD, and SM performed the experiments. SR, VB, and PS compiled and analyzed the data. VB and PS wrote the manuscript.

FUNDING

This work was funded by DBT extramural funded project (BT/PR10526/ADV/90/161/2014) and National Institute of Animal Biotechnology-DBT, Hyderabad.

ACKNOWLEDGMENTS

We would like to acknowledge the farm owners and veterinarians from Telangana and Andhra Pradesh for their providing samples.

REFERENCES

Al-Hamidhi, S. H., Tageldin, M., Weir, W., Al-Fahdi, A., Johnson, E. H., Bobade, P., et al. (2015). Genetic diversity and population structure of *Theileria annulata* in Oman. *PLoS One* 10:e0139581. doi: 10.1371/journal.pone.0139581

Campino, S., Auburn, S., Kivinen, K., Zongo, I., Ouedraogo, J.-B., Mangano, V., et al. (2011). Population genetic analysis of *Plasmodium falciparum* parasites using a customized illumina goldengate genotyping assay. *PLoS One* 6:e20251. doi: 10.1371/journal.pone.0020251

Chakraborty, S., Roy, S., Mistry, H. U., Murthy, S., George, N., Bhandari, V., et al. (2017). Potential sabotage of host cell physiology by apicomplexan parasites for their survival benefits. *Front. Immunol.* 8:1261. doi: 10.3389/fimmu.2017.01261

Chen, S.-B., Wang, Y., Kassegne, K., Xu, B., Shen, H.-M., and Chen, J.-H. (2017). Whole-genome sequencing of a *Plasmodium vivax* clinical isolate exhibits geographical characteristics and high genetic variation in China-Myanmar border area. *BMC Genomics* 18:131. doi: 10.1186/s12864-017-3523-y

Dickson, J., and Shiels, B. R. (1993). Antigenic diversity of a major merozoite surface molecule in *Theileria annulata*. *Mol. Biochem. Parasitol.* 57, 55–64. doi: 10.1016/0166-6851(93)90243-Q

Elshire, R. J., Glaubitz, J. C., Sun, Q., Poland, J. A., Kawamoto, K., Buckler, E. S., et al. (2011). A robust, simple genotyping-by-sequencing (GBS) approach for high diversity species. *PLoS One* 6:e19379. doi: 10.1371/journal.pone.0019379

George, N., Bhandari, V., Reddy, D. P., and Sharma, P. (2015). Molecular and phylogenetic analysis revealed new genotypes of *Theileria annulata* parasites from India. *Parasit. Vectors* 8:468. doi: 10.1186/s13071-015-1075-z

Gomes, J., Salgueiro, P., Inácio, J., Amaro, A., Pinto, J., Tait, A., et al. (2016). Population diversity of *Theileria annulata* in Portugal. *Infect. Genet. Evol.* 42, 14–19. doi: 10.1016/j.meegid.2016.04.023

Gubbels, M. J., d'Oliveira, C., and Jongejan, F. (2000a). Development of an indirect tams1 enzyme-linked immunosorbent assay for diagnosis of *Theileria annulata* infection in cattle. *Clin. Vaccine Immunol.* 7, 404–411. doi: 10.1128/CDLI.7.3.404-411.2000

Gubbels, M. J., Katzer, F., Hide, G., Jongejan, F., and Shiels, B. R. (2000b). Generation of a mosaic pattern of diversity in the major merozoite-piroplasm surface antigen of *Theileria annulata*. *Mol. Biochem. Parasitol.* 110, 23–32. doi: 10.1016/S0166-6851(00)00253-X

Gurgul, A., Miksza-Cybulska, A., Szmatoła, T., Jasielczuk, I., Piestrzyńska-Kajtoch, A., Fornal, A., et al. (2018). Genotyping-by-sequencing performance in selected livestock species. *Genomics* 111, 186–195. doi: 10.1016/j.ygeno.2018.02.002

Haubold, B., and Hudson, R. R. (2000). LIAN 3.0: detecting linkage disequilibrium in multilocus data. *Bioinformatics* 16, 847–849. doi: 10.1093/bioinformatics/16.9.847

Hayashida, K., Abe, T., Weir, W., Nakao, R., Ito, K., Kajino, K., et al. (2013). Whole-genome sequencing of *Theileria parva* strains provides insight into parasite migration and diversification in the african continent. *DNA Res.* 20, 209–220. doi: 10.1093/dnares/dst003

Hemmink, J. D., Weir, W., MacHugh, N. D., Graham, S. P., Patel, E., Paxton, E., et al. (2016). Limited genetic and antigenic diversity within parasite isolates used in a live vaccine against *Theileria parva*. *Int. J. Parasitol.* 46, 495–506. doi: 10.1016/j.ijpara.2016.02.007

Henson, S., Bishop, R. P., Morzaria, S., Spooner, P. R., Pelle, R., Poveda, L., et al. (2012). High-resolution genotyping and mapping of recombination and gene conversion in the protozoan *Theileria parva* using whole genome sequencing. *BMC Genomics* 13:503. doi: 10.1186/1471-2164-13-503

Katzer, F., Mckellar, S., Miled, L., D'Oliveira, C., and Shiels, B. (1998). Selection for antigenic diversity of Tams1, the major merozoite antigen of *Theileria annulata*. *Ann. N. Y. Acad. Sci.* 849, 96–108. doi: 10.1111/j.1749-6632.1998.tb11039.x

Mans, B. J., Pienaar, R., and Latif, A. A. (2015). A review of *Theileria* diagnostics and epidemiology. *Int. J. Parasitol.* 4, 104–118. doi: 10.1016/j.ijppaw.2014.12.006

Manuja, A., Malhotra, D. V., Sikka, V. K., Sangwan, A. K., Sharma, R., Kumar, B., et al. (2006). Isolates of *Theileria annulata* collected from different parts of India show phenotypic and genetic diversity. *Vet. Parasitol.* 137, 242–252. doi: 10.1016/j.vetpar.2006.01.021

Mhadhbi, M., Chaouch, M., Ajroud, K., Darghouth, M. A., and BenAbderrazak, S. (2015). Sequence polymorphism of cytochrome b gene in *Theileria annulata* tunisian isolates and its association with buparvaquone treatment failure. *PLoS One* 10:e0129678. doi: 10.1371/journal.pone.0129678

Mhadhbi, M., Naouach, A., Boumiza, A., Chaabani, M. F., BenAbderazzak, S., and Darghouth, M. A. (2010). In vivo evidence for the resistance of *Theileria annulata* to buparvaquone. *Vet. Parasitol.* 169, 241–247. doi: 10.1016/j.vetpar.2010.01.013

Peakall, R., and Smouse, P. E. (2012). GenAlEx 6.5: genetic analysis in Excel. Population genetic software for teaching and research-an update. *Bioinformatics* 28, 2537–2539. doi: 10.1093/bioinformatics/bts460

Pinkevych, M., Petravic, J., Bereczky, S., Rooth, I., Färnert, A., and Davenport, M. P. (2015). Understanding the relationship between *Plasmodium falciparum* growth rate and multiplicity of infection. *J. Infect. Dis.* 211, 1121–1127. doi: 10.1093/infdis/jiu561

Sharifiyazdi, H., Namazi, F., Oryan, A., Shahriari, R., and Razavi, M. (2012). Point mutations in the *Theileria annulata* cytochrome b gene is associated with buparvaquone treatment failure. *Vet. Parasitol.* 187, 431–435. doi: 10.1016/j.vetpar.2012.01.016

Shiels, B., McDougall, C., Tait, A., and Brown, C. G. D. (1986). Antigenic diversity of *Theileria annulata* macroschizonts. *Vet. Parasitol.* 21, 1–10. doi: 10.1016/0304-4017(86)90137-8

Wang, J., Yang, X., Wang, Y., Jing, Z., Meng, K., Liu, J., et al. (2014). Experimental immunology genetic diversity and phylogenetic analysis of Tams1 of *Theileria annulata* isolates from three continents between 2000 and 2012. *Cent. Eur. J. Immunol.* 4, 476–484. doi: 10.5114/ceji.2014.47732

Weir, W., Ben-Miled, L., Karagenç, T., Katzer, F., Darghouth, M., Shiels, B., et al. (2007). Genetic exchange and sub-structuring in *Theileria annulata* populations. *Mol. Biochem. Parasitol.* 154, 170–180. doi: 10.1016/j.molbiopara.2007.04.015

Weir, W., Karagenç, T., Gharbi, M., Simuunza, M., Aypak, S., Aysul, N., et al. (2011). Population diversity and multiplicity of infection in *Theileria annulata*. *Int. J. Parasitol.* 41, 193–203. doi: 10.1016/j.ijpara.2010.08.004

Yin, F., Liu, Z., Liu, J., Liu, A., Salih, D. A., Li, Y., et al. (2018). Population genetic analysis of *Theileria annulata* from six geographical regions in china, determined on the basis of micro- and mini-satellite markers. *Front. Genet.* 9:50. doi: 10.3389/fgene.2018.00050

Conflict of Interest Statement: The authors declare that the research was conducted in the absence of any commercial or financial relationships that could be construed as a potential conflict of interest.

frontiers in Physiology

ORIGINAL RESEARCH
published: 18 June 2019
doi: 10.3389/fphys.2019.00744

Repurposing of Glycine-Rich Proteins in Abiotic and Biotic Stresses in the Lone-Star Tick (*Amblyomma americanum*)

Rebekah Bullard[1,2†], Surendra Raj Sharma[1†], Pradipta Kumar Das[3], Sarah E. Morgan[3] and Shahid Karim[1]*

[1] Department of Cell and Molecular Biology, School of Biological, Environmental and Earth Sciences, The University of Southern Mississippi, Hattiesburg, MS, United States, [2] Department of Pathobiological Sciences, Louisiana State University, Baton Rouge, LA, United States, [3] School of Polymer Science and Engineering, The University of Southern Mississippi, Hattiesburg, MS, United States

OPEN ACCESS

Edited by:
Abid Ali,
Abdul Wali Khan University Mardan, Pakistan

Reviewed by:
Lucas Tirloni,
National Institute of Allergy and Infectious Diseases (NIAID), United States
Sandra Maruyama,
Federal University of São Carlos, Brazil

***Correspondence:**
Shahid Karim
Shahid.karim@usm.edu

[†] *These authors have contributed equally to this work*

Specialty section:
This article was submitted to Invertebrate Physiology, a section of the journal Frontiers in Physiology

Received: *11 March 2019*
Accepted: *31 May 2019*
Published: *18 June 2019*

Citation:
Bullard R, Sharma SR, Das PK, Morgan SE and Karim S (2019) Repurposing of Glycine-Rich Proteins in Abiotic and Biotic Stresses in the Lone-Star Tick (Amblyomma americanum). Front. Physiol. 10:744. doi: 10.3389/fphys.2019.00744

Tick feeding requires the secretion of a huge number of pharmacologically dynamic proteins and other molecules which are vital for the formation of the cement cone, the establishment of the blood pool and to counter against the host immune response. Glycine-rich proteins (GRP) are found in many organisms and can function in a variety of cellular processes and structures. The functional characterization of the GRPs in the tick salivary glands has not been elucidated. GRPs have been found to play a role in the formation of the cement cone; however, new evidence suggests repurposing of GRPs in the tick physiology. In this study, an RNA interference approach was utilized to silence two glycine-rich protein genes expressed in early phase of tick feeding to determine their functional role in tick hematophagy, cement cone structure, and microbial homeostasis within the tick host. Additionally, the transcriptional regulation of GRPs was determined after exposure to biotic and abiotic stresses including cold and hot temperature, injury, and oxidative stress. This caused a significant up-regulation of AamerSigP-34358, Aam-40766, AamerSigP-39259, and Aam-36909. Our results suggest ticks repurpose these proteins and further functional characterization of GRPs may help to design novel molecular strategies to disrupt the homeostasis and the pathogen transmission.

Keywords: ticks, cement proteins, glycine-rich proteins, salivary glands, *Amblyomma americanum*

INTRODUCTION

The Lone-Star tick *Amblyomma americanum* is of significant health concern in the United States, given its expanding geographic range and vector-competence for diseases such as by *Ehrlichia chaffeensis*, *Borrelia lonestari*, *Ehrlichia ewingii*, *Francisella tularensis*, *Theileria cervi* and heartland virus (Childs and Paddock, 2003; Goddard and Varela-Stokes, 2009). *A. americanum* has recently been associated with delayed anaphylaxis to red meat and is the first recorded example of an ectoparasite causing food allergy in the United States (Commins et al., 2011; Crispell et al., 2019). The bites from *A. americanum* are causing this unusual allergic reaction to meat (Platts-Mills and Commins, 2013).

Ticks are the most successful group of organisms and have developed the hematophagous trait to feed on vertebrate blood. During the attachment phase, the tick must establish a firm attachment by secreting multiple pharmacologically active proteins and other compounds in its saliva. Some of these compounds solidify once inside the host skin to form a proteinaceous matrix called the cement cone (Bishop et al., 2002; Bullard R. et al., 2016). This cement cone protects the hypostome (mouth part) while also anchoring the tick into the host dermis. Ticks of both long (Longirostrata) and short (Brevirostrata) mouthpart species secrete this proteinaceous matrix. Analysis of multiple adhesives from various species of glue-producing insects showed a prevalence of glycine in many of the proteins identified. Of all the adhesives tested, each species contained at least one protein which was classified as glycine rich, with 11–36% glycine content (27/33 proteins). Other amino acids also overrepresented include serine (12–33% in 17 proteins) and alanine (12–17% in 2 proteins) (Zhang et al., 2013).

Saliva molecules interact with the host immune system to assist the tick in establishing a liquid blood pool. Previous data have confirmed the proteins secreted through the saliva are not constituently expressed throughout the entirety of the blood meal, but are rather differentially expressed (Karim et al., 2011; Karim and Ribeiro, 2015). These proteins are responsible for mediating the host response by preventing clot formation, wound healing, immune system activation, and inflammatory cascades (Childs and Paddock, 2003). In addition to the modulation of the host immune system, some of the secreted proteins accumulate around the tick mouthparts and harden to form a cement cone which has previously been described in detail from our lab (Bullard R. et al., 2016). Proteomic analysis of these cones have identified multiple protein families such as GRPs, protease inhibitors, mucins and various uncharacterized cement cone proteins among these GRPs are predominant (Bullard R. et al., 2016; Bullard R.L. et al., 2016). One class of proteins found in the cement cone, GRP, has documented roles of physiological functions and structural characteristics in a variety of organisms (Zottich et al., 2013; Xu et al., 2014; Bullard R. et al., 2016).

GRPs are known to be a major structural component of spider silk (Winkler and Kaplan, 2000; Xia et al., 2010; Tokareva et al., 2013), insect cuticles (Zhang et al., 2008), and plant cell walls (Mousavi and Hotta, 2005). GRPs have also been implicated in anti-microbial activity (Wang et al., 2008), anti-freeze functions (Graham and Davies, 2005; Mok et al., 2010), RNA-binding (Kim et al., 2007), and anti-platelet aggregation (Schemmer et al., 2013). Starvation responsive, injury induced response, and defense against microbes and predators have been lined with the GRPs expression in insect hemolymph (Baba et al., 1987; Taniai et al., 2014; Yi et al., 2014; Pentzold et al., 2016).

It is currently unknown if the GRPs which are upregulated during the stress response play a role in mediating the stress directly or indirectly by interfering with the gene expression. Our work on the transcriptome analysis of *A. americanum* salivary glands identified various differentially and constitutively expressed GRPs, among which 14 glycine-rich proteins contained signal peptides, and 24 lacked signal peptides (Karim and Ribeiro, 2015). In this study, a sample of tick GRPs are analyzed to identify the types of glycine repeats found within the sequence. The transcripts of two GRPs up-regulated during early tick feeding are depleted using RNA interference to examine their functional role in tick hematophagy. The transcriptional expression of these GRPs was also determined in ticks with abiotic and biotic stresses. After evaluation of the feeding phenotypes of the knockdown ticks, further analysis of GRP expression is performed to identify functions in microbial maintenance and the tick's response to stressful stimuli.

MATERIALS AND METHODS

Ethics Statement

All animal experiments were carried out in strict accordance with recommendations in the Guide for the Care and Use of Laboratory Animals of the National Institutes of Health, United States. The protocol of tick feeding on sheep (#15101501.1) was approved by the Institutional Animal Care and Use Committee of University of Southern Mississippi.

Materials

All common laboratory supplies, and chemicals were purchased from Sigma-Aldrich (St. Louis, MO, United States), Fisher Scientific (Grand Island, NY, United States), or Bio-Rad (Hercules, CA, United States) unless otherwise specified.

Bioinformatics Analysis

Coding sequences of GRPs were obtained from *A. americanum* transcriptome study (Karim and Ribeiro, 2015) and various biological databases. Sequences were aligned using muscle alignment tool[1] and graphically presented via Snapegene viewer.

Ticks and Tissue Dissection

Ticks were purchased from the Oklahoma State University Tick Rearing Facility. Adult unfed male and female *A. americanum* were kept according to standard practices (Patrick and Hair, 1975) at room temperature (25°C) with approximately 90% relative humidity for a photoperiod of 14 h light/10 h dark. Ticks were infested on a sheep and partially blood-fed females were pulled after 5 days of post-infestation to obtain tissues. The blood-fed female *A. americanum* were dissected within 4 h of removal and collection from the sheep. Tick salivary glands were dissected as described previously (Karim and Ribeiro, 2015). Salivary gland tissues were pooled and stored in RNAlater (Life Technologies, Carlsbad, CA, United States) at −80°C until further use.

Transcriptional Gene Expression Analysis

RNA Isolation and cDNA Synthesis

The methods to extract total RNA and cDNA synthesis were conducted as described previously (Bullard R.L. et al., 2016). RNA was extracted from the pooled-dissected tick salivary glands

[1] http://www.ebi.ac.uk

and cDNA was synthesized from these samples to determine the transcriptional expression of GRPs. Briefly, frozen tick tissues were placed on ice to thaw and RNAlater was carefully removed with precision pipetting. RNA was isolated from the time point pooled salivary glands using illustra RNAspin Mini kit (GE Healthcare Life sciences) protocols. RNA concentration was measured using a NanoDrop spectrophotometer and stored at −80°C or used immediately. To synthesize cDNA, 2 μg of RNA were reverse transcribed using the iScript cDNA synthesis kit (Bio-Rad). The reverse transcription reaction was then set-up in a Bio-Rad thermocycler under the following conditions: 5 min at 25°C, 30 min at 42°C, 5 min at 85°C, and hold at 10°C. The resultant cDNA was diluted to a working concentration of 25 ng/μL with nuclease-free water and stored at −20°C until used (Bullard R.L. et al., 2016).

Reverse Transcription Quantitative PCR (RT-qPCR) Assay

A list of all genes tested in this study is provided in **Supplementary Table S1**. The transcript level of GRPs was quantified by a RT-qPCR assay as described earlier (Bullard R.L. et al., 2016). Briefly, 50 ng of cDNA was used in a total of 20 μL reaction using SYBR Green supermix with 300 nM of each gene specific primer. The samples were subjected to the following thermocycling conditions: 95°C for 30 s; 35 cycles of 95°C for 5 s and 60°C for 30 s with a fluorescence reading after each cycle; followed by a melt curve from 65 to 95°C in 0.5°C increments. Each reaction was performed in triplicate along with no template controls. Gene expression was normalized using ubiquitin as the reference gene and compared against treatment control.

DsRNA Synthesis and Tick Injections

The gene of interest was amplified using gene specific primers and purified using the QIAquick PCR Purification Kit (QIAGEN, Germany). Gene specific T7 promoter sequences were added to the 5′ and 3′ end of the purified product using PCR and were purified. The purified T7 PCR products was confirmed by sequencing and transcribed into dsRNA using the T7 Quick High Yield RNA Synthesis Kit (New England Biolabs, Ipswich, MA, United States). The dsRNA produced was purified via ethanol precipitation and the concentration was measured using a NanoDrop spectrophotometer and was analyzed on a 2% Agarose gel. Individual unfed female ticks were injected with irrelevant (GFP dsRNA) and target gene dsRNAs (AamersigP-41539, and Aam-40766) using a 31-gauge needle to a final concentration of 500 ng as described previously (Bullard R.L. et al., 2016). Ticks were kept overnight at 37°C to determine trauma/death related to microinjections. Next day ticks are infested on sheep. The ticks were infested on a sheep the next day. Attachment was monitored daily and photographed. Ticks attached within 24 h of infestation were considered attached and monitored until repletion. Partially blood-fed ticks (5 days post-infestation) were pulled and dissected for gene expression analysis.

Quantification of Total Bacterial Load

The total bacterial load in tick tissues was determined using the method described previously (Narasimhan et al., 2014; Budachetri and Karim, 2015). Briefly, a 25 μl volume reaction mixture contained 25 ng of tissue cDNA, 200 (μM 16S RNA gene primer and iTaq Universal SYBR Green Supermix (Bio-Rad) followed by qPCR assay using following conditions: 94°C for 5 min followed by 35 cycles at 94°C for 30 s, 60°C for 30 s, and 72°C for 30 s. A standard curve was used to determine the copy number of each gene. The bacterial copy number was normalized against *A. americanum* ubiquitin copy number in control tissues and gene silenced tick. All samples were run in triplicate.

Stress Exposure

Cold Stress

Supplementary Figure S1 illustrates the approaches utilized to determine the stress induced expression of glycine-rich proteins at organismal and tissue level. A total of 15 unfed female ticks were incubated at 4°C in an incubator with 90% relative humidity and a photoperiod of 14 h light/10 h dark cycle for a month to mimic winter like conditions. GRP gene expression was determined in the whole tick and dissected tissues. A total of 3 individual ticks were crushed to extract total RNA, while five pairs of salivary glands were pooled for the expression studies.

Heat Stress

A total of 15 unfed female adult ticks were kept at 40°C in an incubator with 42% relative humidity and a photoperiod of 14 h light/10 h dark cycle for 1 week. The expression of selected GRP genes was measured at both tissue and organismal levels as described above.

Injury Stress

Fifteen female ticks were injured by piercing the cuticle or pulling a hind leg from the tick. The ticks were placed in a 25°C incubator with 90% relative humidity maintaining photoperiod of 14 h light/10 h dark cycle to recover from the injury for 1 week. GRP expression was measured in both pooled salivary gland tissues (from five ticks) and in individually crushed whole ticks.

Oxidative Stress

Fifteen female ticks were injected with 10 mM Paraquat to induce a high oxidative stress environment in the tick tissues and allowed to recover over a 48-h period in 25 (°C incubator with 90% relative humidity maintaining photoperiod of 14 h light/10 h dark cycle. GRP expression was measured in both dissected salivary glands (pooled salivary glands from five ticks) and in crushed whole ticks (three individual ticks). In order to control for any transcriptional changes due to the injection, data from the injury stress exposed ticks were used for normalization.

Atomic Force Microscopy, Quantitative Nanoscale Mechanical Characterization (AFM-QNM) of the Tick Cement Cone

The cones from the *in vivo* fed ticks and from the artificially membrane fed ticks were sectioned along their lengths via cryo-microtoming. The thickness of each section was 20 (μm. The sections were then analyzed via AFM-QNM. AFM-QNM was performed with a Dimension Icon (Bruker) instrument in tapping mode. Silicon nitride probes (RTESP from Bruker)

with a typical resonance frequency of 324–358 kHz, spring constant of 20–80 N/m, length of 115–135 μm, and tip radius of 8 nm were utilized for the imaging. A relative calibration method using a standard polystyrene film of 2.7 GPa (from Bruker) was utilized. The AFM images were captured at a scan rate of 1 Hz and 256 × 256 pixels of data points were collected. Images were taken at different locations (at least three) across the surface. NanoScope 5.30r2 software was used to capture the images. The height images were analyzed via NanoScope Analysis 1.5 (Bruker) image processing software.

Data Analysis

All data are expressed as mean (SEM unless otherwise stated. Statistical significance between the two experimental groups or their respective controls was determined by the *t*-test using Graph Pad prism 7 (La Jolla, CA, United States). P-values of <0.05 were considered significant. Transcriptional expression levels were determined using Bio-Rad software (Bio-Rad CFX MANAGER v.3.1), and the expression values were considered significant if the P-value was 0.05 when compared with the control.

RESULTS

Bioinformatic Analysis of GRP Sequences

GRPs are characterized purely by the overabundance of glycine in the protein's sequence. This complicates typical bioinformatic analyses which would predict structure and function by comparing the unknown protein's sequence to other well described proteins. GRP sequences provide little information since they are not classified based on structural and functional aspects. Sequence identity is insignificant as the sheer number of glycine residues account for most of the homologous residues. To determine if the GRPs selected from the *A. americanum* sialotranscriptome (Karim and Ribeiro, 2015) could be grouped, the tripeptide and penta-peptide repeats commonly found in GRPs were used as a way to group the proteins (**Table 1**). When compared in this way, a possible pattern begins to emerge. GRPs with fewer amino acids typically have the GGX repeat whereas proteins with more than 200 amino acids have a near equal mixture of GGX and GXG repeats. While GXXXG repeats are found in these proteins, they are not more abundant than the tripeptide repeats listed. Interestingly, a scanning for motif identification of all nine GRPs in Prosite, only showed the presence of a motif in AamerSigP-34358 (PISGGSGGVRLPGQSGSKPG: T RNA ligase signature motif) (**Table 1**). Multiple sequence alignment of all selected nine GRP amino acid sequences only showed GGX and GXG repeats (**Supplementary Figure S2**). This pattern does not hold true when looking at GRPs from other organisms or even other ticks of the same species, so this information may not be a usable criterion for identifying GRP classes.

Expression of GRPs After the Depletion of a GRP Transcript and Cement Cone Analysis

The injection of dsRNA-AamerSigP-41539 (GXG/GGX) effectively depleted AamerSigP-41539 transcripts by >95% (data not shown). Each of the remaining GRPs were also analyzed to determine any off-target or compensatory effects (**Figure 1A**). Although the GRP transcript was significantly reduced, there was no measurable change in the ability of the tick to attach to the host, maintain a firm attachment, or ability to feed successfully (**Figure 1B**). Two GRPs, AamerSigP-39259 (GGX/GXG) and Aam-36909 (GGX/GXG), are over expressed when AamerSigP-41539 is depleted (**Figure 1A**). Interestingly, the depletion of AamerSigP-41539 also results in the depletion of Aam-41540 (GGX) and Aam-3099 but there is no significant change in AamerSig-34358 or Aam-40766 (**Figure 1A**).

Similar methods were used to elucidate the impact of gene silencing of an additional GRP, Aam-40766 (GGX/GXG). The depletion of Aam-40766 transcripts were verified using qRT-PCR and impact of gene silencing was monitored as feeding progressed. As seen with AamerSigP-41539, the depletion of Aam-40766 yielded no significant changes in attachment or engorgement weight (**Figure 2B**). The expression of the other GRPs was measured to identify compensatory mechanisms (**Figure 2A**). The depletion of Aam-40766 resulted in the reduction of five other GRPs (Aam-41235, AamerSigP-41913, AamerSigP-41539, Aam-41540, and Aam-3099). The other GRPs tested showed no change in expression levels.

Only a few cones from Aa-41539 depleted ticks and irrelevant double stranded RNA injected ticks were collected with cement cones attached at the tick mouthparts. However, it is important to note that of all the ticks fed, less than 10 cones were collected which made it difficult to determine whether the lack of cement cones from knocked-down ticks is due to a change in phenotype or just a complication of cement cone retrieval. AFM-QNM analysis of cone (**Figure 3**) recovered from control (irrelevant double stranded RNA injected) ticks showed that the modulus of the cone varies in different regions of cone. More specifically, the modulus of the cone decreases (2.9; 4.6; 7.1 GPa) as the cement penetrates deep into the host skin. Similarly, AFM-QNM analysis of the cement cone obtained from an AamSigP-41539 (**Figure 4**) depleted tick showed smaller than average modulus (2.5 and 6.2 GPa) in comparison to related section of cones (2.9 and 7.1 GPa) from control ticks.

Impact of GRP Silencing on Total Microbial Load

GRPs have been implicated in a variety of functional roles throughout the animal and plant world. Given that no measurable difference was observed in attachment or feeding in the GRP depleted ticks, it is possible that GRPs AamerSigP-41539 and Aam-40766 may play a role in pharmacological characteristics of tick saliva. To determine if tick GRPs may play a role in maintaining bacterial communities, the total bacterial load was calculated by measuring 16S rRNA in the

TABLE 1 | Protein characteristics and tripeptide repeats of nine AaGRPS.

Gene ID	Number of amino acids	Molecularweight (kDa)	Noteworthyamino acidprevalence	Noteworthy amino acid repeats/motif	GRPs class based on amino acid repeats
Aam-41235 (GBZX01001012.1)	107	10.0	22.4%Gly 22.4% Ser 15.0% Ala	GGX	Class I
AamerSigP-34358 (GBZX01000232.1)	205	18.7	30.7% Gly 17.1% Ser 13.2% Pro	GGX/GXG/ PISGGSGGVRLP GQSGSKPG	Class I /III
Aam-40766 (GBZX01000067.1)	310	29.4	27.7% Gly 19% Ser 11% Ala	GGX/GXG	Class I/III
AamerSigP-39259	54	51.7	22.2% Gly 16.7% Ser 13.0% Ala	GGX/GXG	Class I/III
AamerSigP-41913 (GBZX01000836.1)	116	11.8	19.8% Gly	GGX	Class I
AamerSigP-41539 (GBZX01000853.1)	116	11.6	24.1% Gly 13.8% Ala 10.3% Ser	GXG/GGX	Class I/III
Aam-41540 (GBZX01001942.1)	222	22.6	20.3% Gly 13.1% Ala	GGX	Class I
Aam-36909 (GBZX01000052.1)	325	UD	29.2% Gly 20.6% Ser	GGX/GXG	Class I/III
Aam-3099 (GBZX01000254.1)	202	20.0	23.3% Gly 15.3% Ala	N/A	N/A

GRP classes are categorized based on presence of amino acid sequence repeats.

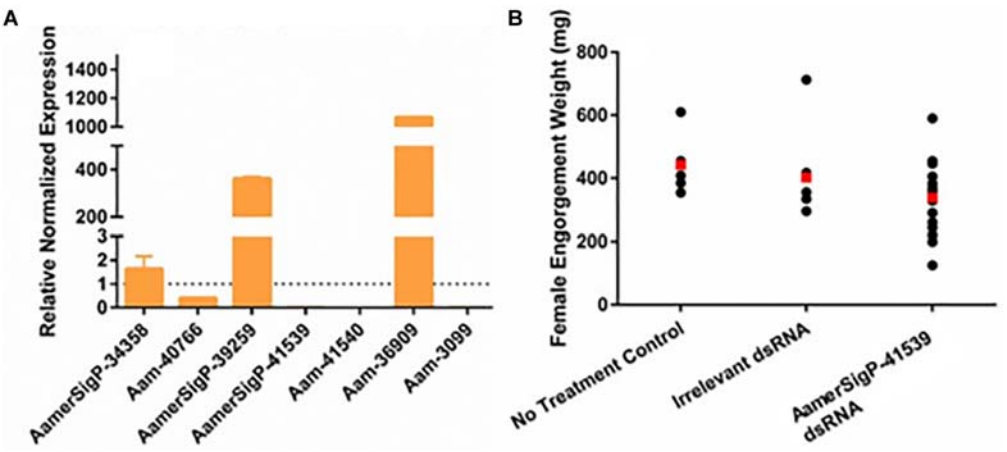

FIGURE 1 | RNA interference-based silencing of AamerSigP-41539 (glycine-rich protein gene) in the lone-star tick (*Amblyomma americanum*). **(A)** Compensatory transcriptional expression of selected grp genes was determined in AamerSigP-41539 silenced partially blood-fed tick salivary glands. **(B)** Mass of replete or forcibly removed 12 days fed female ticks. Ubiquitin was used as a housekeeping gene to normalize the transcriptional expression.

tissue. In the irrelevant dsRNA injected ticks, after 5 days of feeding, there were approximately 20 16S rRNA molecules for every 10,000 tick Ubiquitin (**Figure 5A**). However, in the case of AamerSigP-41539 deficient ticks, this increases to 400 16S rRNA molecules for every 10,000 ubiquitin. This 20-fold increase signifies that AamerSigP-41539 is at least partially responsible for the maintaining of microbial homeostasis within the tick salivary glands (**Figure 5A**). The exact mechanism of this role is yet to be determined. Additional studies on this protein, it's mechanism and how it affects microbial growth requires further investigation. In contrast to the significant bacterial growth in AamerSigP-41539 depleted ticks, when Aam-40766 is knocked down, the change in 16S rRNA is only 2-fold (**Figure 3B**). It should be noted that the AamerSigP-41539 ticks were partially fed for 5 days while the Aam-40766 ticks were partially fed for 8 days. This could have an effect on the magnitude difference between the two studies. It was noticed during data analysis of all datasets (including those not shown here) that GRPs were upregulated even in non-relevant dsRNA injections such as GFP. During RNAi, the ticks are subjected to injections and high humidity heat conditions to recover from injury trauma. Previous research in plants has shown the increased presence of GRPs during wound healing. A tick GRP responsible for wound healing would explain these results. A look into the expression of GRPs

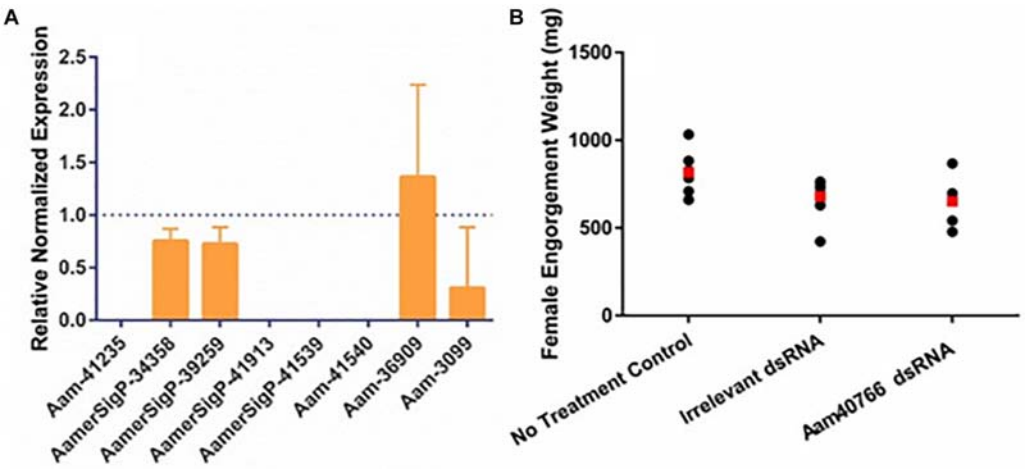

FIGURE 2 | RNA-interference based gene silencing of Aam-40766 (glycine-rich protein gene) in the lone-star tick (*A. americanum*). **(A)** Transcriptional expression of Aam-40766 and other glycine-rich proteins in the gene silenced partially blood-fed tick tissues. **(B)** Mass of replete or forcibly removed 12 days fed female ticks. Ubiquitin was used as a housekeeping gene to normalize the transcriptional expression.

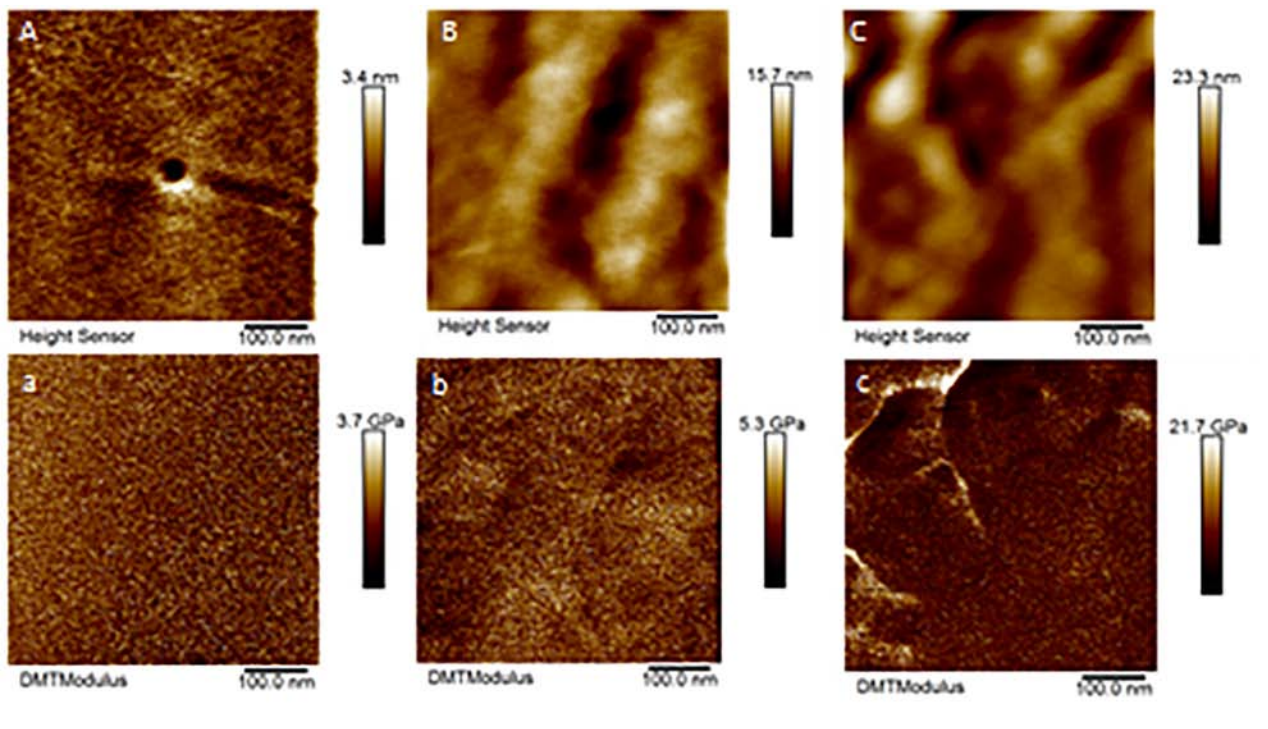

FIGURE 3 | AFM-QNM images of the cement cone obtained from a naturally fed tick. **(A,a)**, **(B,b)**, **(C,c)** are the height and modulus images of the section 1, 2, and 3 of the cement cones, respectively. An average modulus of 2.9, 4.6, 7.1 GPa was obtained for the section 1, 2, and 3, respectively.

during stress conditions and other known GRP functions were then performed.

Effect of Abiotic Stress on GRP Transcript Levels

To further identify potential GRP functions within the salivary glands, ticks were exposed to low temperatures, high temperatures, injury, and oxidative stress to identify stress related GRPs (**Figure 6**). The GRP expression profile of tick tissues after cold exposure shows the differential expression of many GRPs. The cold temperature presumably decreases the metabolic rate of the tick which down regulates many proteins (**Figure 6A**). The decreased expression of Aam-41235 (4-fold), Aam-36909 (2-fold), Aam-3099 (9-fold), and the complete depletion of Aam-41540 transcripts are conceivably due to this

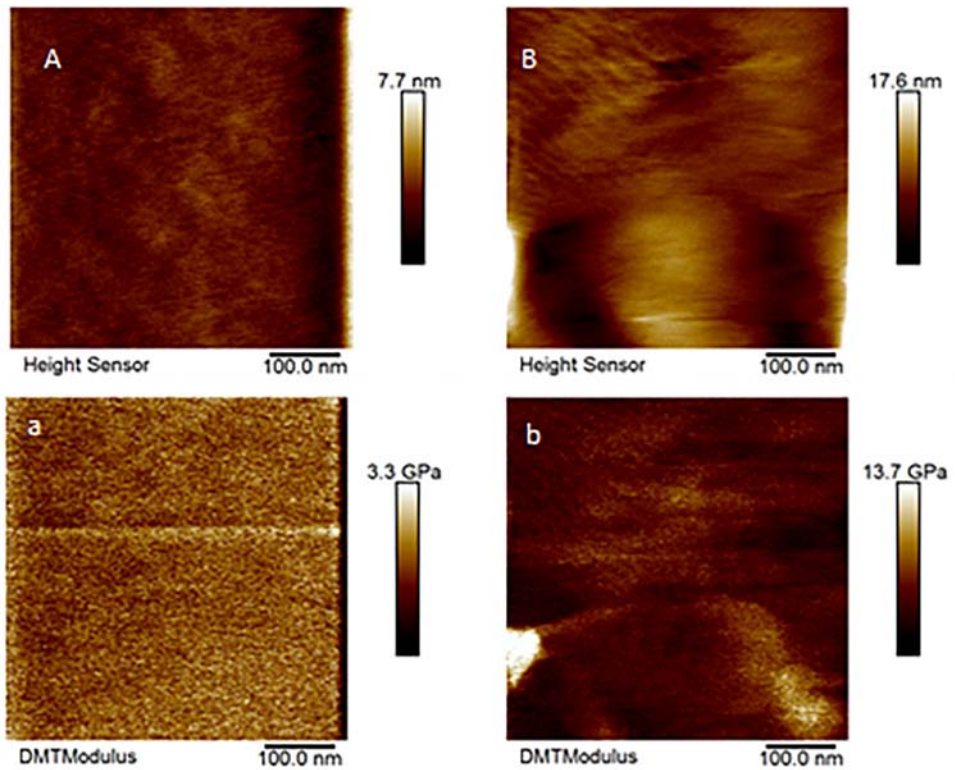

FIGURE 4 | AFM-QNM images of the cement cone obtained from an Aam-41539 silenced tick. **(A,a)**, and **(B,b)** are the height and modulus images of the section 1, and 2 of the cement cones, respectively. An average modulus of 2.5, and 6.2 GPa was obtained for the section 1, and 2, respectively.

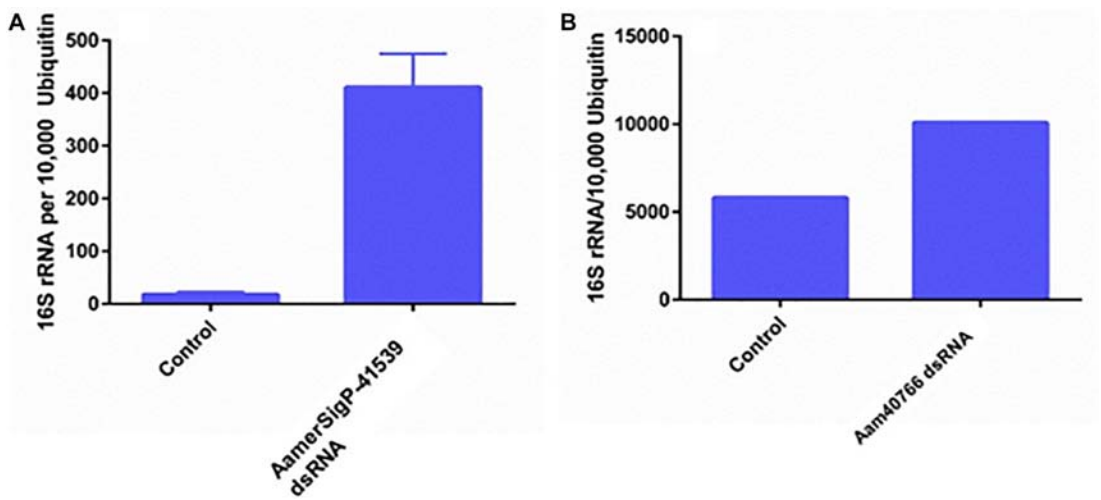

FIGURE 5 | Total bacterial load in GRP silenced tick tissues. The ticks from both irrelevant dsRNA (GFP) and target genes were blood feed and partially fed ticks were removed from the host past 5 days infestation. Within 2 h of tick removal from the hosts, the ticks were dissected to isolate salivary glands and stored in RNAlater before RNA extraction and cDNA synthesis. Total bacterial loads were estimated by qPCR and reference to ubiquitin in the tick salivary glands. **(A)** Changes in 16S rRNA abundance after depletion of AamerSigP-41539. **(B)** Changes in 16S rRNA abundance after depletion of Aam-40766.

decrease in metabolic rate or the GRP is not expressed in the unfed time stages. The low temperature, however, does cause an increase in AamerSigP-34358 (29-fold), Aam-40766 (2-fold), and AamerSigP-39259 (7-fold). An increase in the temperature also affects the GRP expression profile in the whole tick samples. When the ticks are exposed to high temperatures (**Figure 6B**), there is a decrease in Aam-41235 (20-fold), AamerSigP-41539 (2-fold), and Aam-3099 (31-fold). But there is an increase

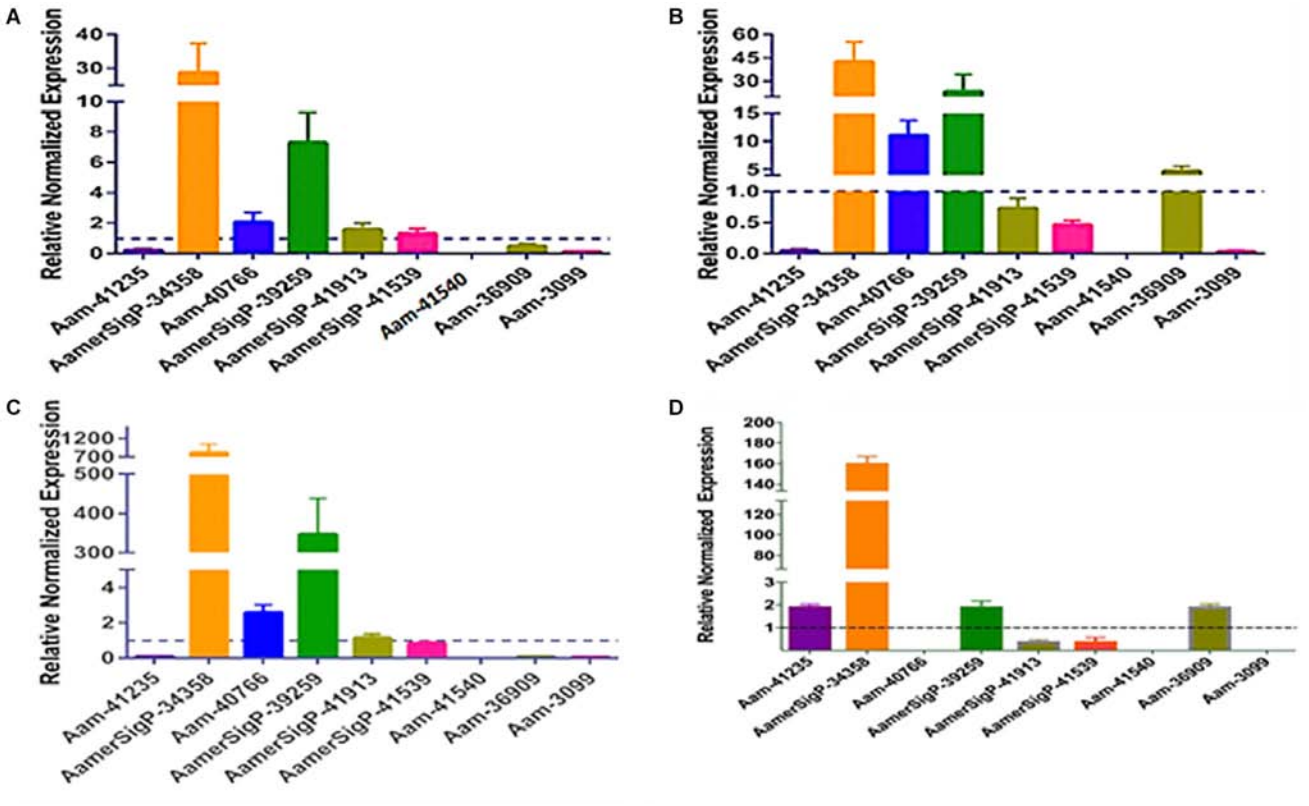

FIGURE 6 | Transcriptional expression of tick GRP genes in unfed ticks after stress exposure. Quantitative reverse transcriptase PCR (qRt-PCR) was used to determine the transcriptional expression levels of tick GRPs. **(A)** cold temperature, **(B)** hot/humid temperature, **(C)** injury, and **(D)** oxidative stress. The expression levels in tick control samples were set to 1, as represented by dashed lines. Ubiquitin was used as a housekeeping gene to normalize the transcriptional expression.

in many of the other GRPs including AamerSigP-34358 (43-fold), Aam-40766 (11-fold), AamerSigP-39259 (23-fold), and Aam-36909 (5-fold). The GRP expression of injured ticks was also measured. These tick samples had a decrease in GRPs such as Aam-41235 (10-fold), Aam-36909 (11-fold), and Aam-3099 (13-fold). The expression of AamerSigP-34358 and AamerSigP-39259 were again upregulated like the other stress conditions; however, the fold change is much higher (83-, and 347-fold, respectively). Similarly, oxidative stress in the whole tick showed upregulation of signal peptides namely AmerSigP-34358 (160 fold); AamerSigP-39259 (2 fold). Two GRPs such as Aam-41235 and Aam-36909 were found to be upregulated by two-fold while hypothetical secreted peptides AamerSigp-41539 and AamerSigp-41913 were found to be down-regulated; however, there was no expression of Aam-41540, Aam-40766, and Aam-3099 under oxidative stress in the whole tick.

The gene expression in the salivary glands show a similar change when exposed to stress (**Figure 7**). The salivary glands of ticks exposed to the low temperature (**Figure 5A**) have an increase of AamerSigP-34358 (6.6-fold), AamerSigP-39259 (3-fold), and Aam-36909 (8-fold). There is a significant decrease in Aam-40766 (6-fold), however, no change is seen in Aam-3099. Aam-41235 did not amplify in the salivary glands, and AamerSigP-41913, AamerSigP-41539, and Aam-41540 were not tested due to limited sample availability. Under heat stress there was upregulation of two signal peptides, AamerSigP-34358 and AamerSigP-39259 by three-fold and seven-fold, respectively. However, protein Aam-40766 was slightly upregulated while other proteins such as Aam-36909 and Aam-3099 was downregulated by eight-fold and seven-fold, respectively while there was no expression of Aam-41539.

Similar results are seen in salivary glands after an injury has occurred to the tick (**Figure 7C**). A decrease in Aam-40766 (8-fold) and the non-amplification of Aam-41235 and Aam-3099 show a change in the salivary glands from preparing for attachment and blood feeding to dealing with the trauma of the injury. Although the salivary glands are not directly injured by the removal of one of the hind legs, there is an increase in AamerSigP-34358 (88-fold), AamerSigP-39259 (34-fold), and a slight increase of Aam-36909 (2.4-fold). As the tick is feeding, it encounters a wide range of reactive oxygen species, which can cause oxidative stress in the tick. The GRP expression after injection with paraquat is similar to that of cold and injured ticks (**Figure 7D**). There is no amplification in Aam-41235 or Aam-3099, a decrease in Aam-40766 (17-fold) and an increase in AamerSigP-34358 (24-fold), AamerSigP-39259 (8-fold), and Aam-3099 (3-fold).

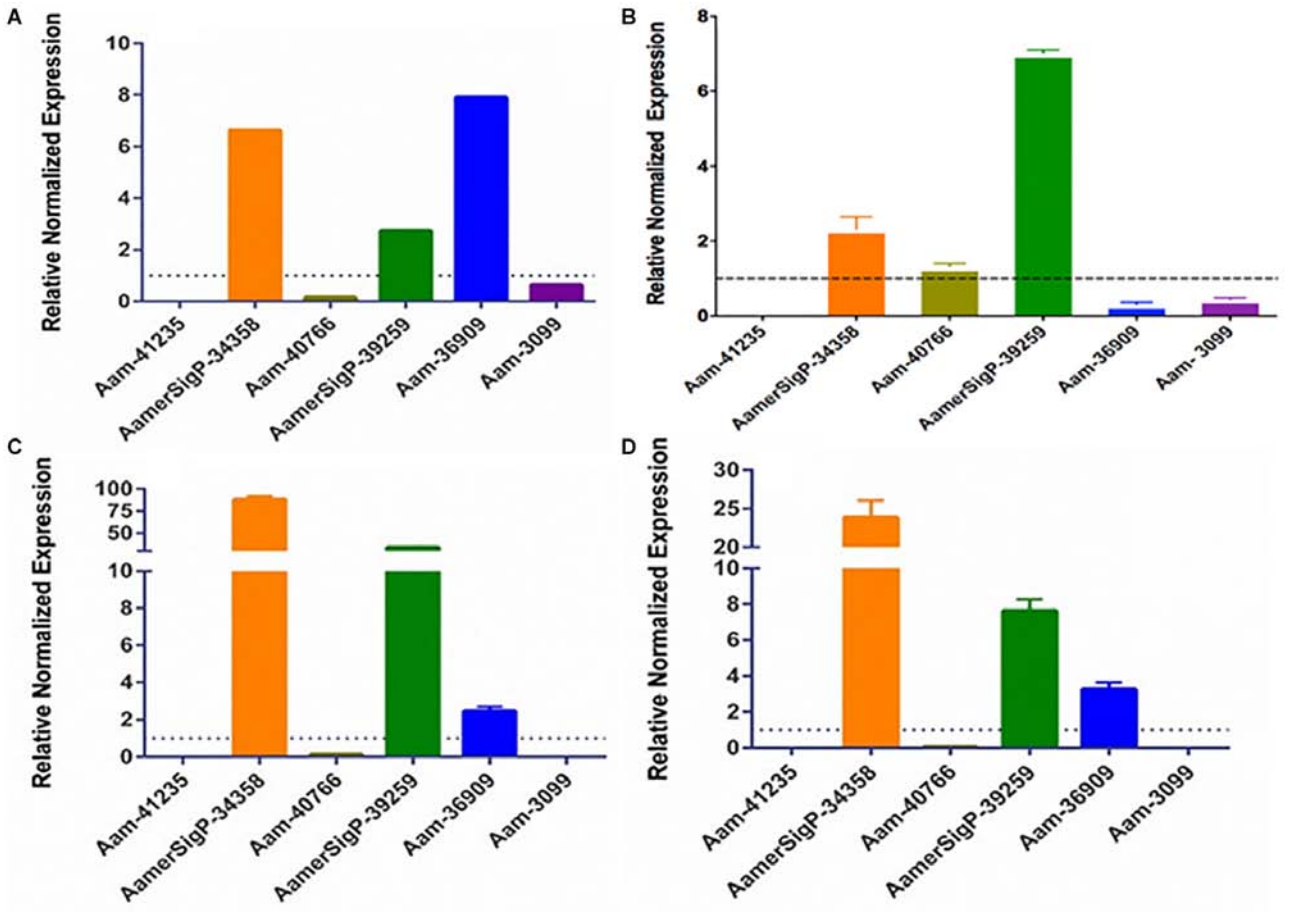

FIGURE 7 | Transcriptional expression of tick GRP genes in unfed tick salivary glands after stress exposure. Quantitative reverse transcriptase PCR (qRt-PCR) was used to determine the transcriptional expression levels of tick GRPs. **(A)** cold temperature, **(B)** hot/humid temperature, **(C)** injury, and **(D)** oxidative stress. The expression levels in tick control samples were set to 1, as represented by dashed lines. Ubiquitin was used as a housekeeping gene to normalize the transcriptional expression.

DISCUSSION

The functional characterization of novel molecules regulating diverse physiological responses in ticks, is very important for targeted control of ticks. To catalog the salivary transcripts, we have carried out a comprehensive RNA-Seq analysis of the *A. americanum* salivary glands (Karim and Ribeiro, 2015). From the sialotranscriptome data, identification of several GRPs prompted us to characterize their functional role in tick hematophagy. Existing literature indicated that GRPs are responsible for mediating the host response by preventing clot formation, wound healing, immune system activation, and inflammatory cascades (Francischetti et al., 2009). However, in many insects and arthropods, GRPs play a significant structural role. From spider silk to barnacle glue, GRPs are necessary for adhesion and strength. The selection of both Aam-40766 and AamerSigP-41539 was based on their up-regulation during early phase of tick feeding on the host as reported in our published work (Bullard R.L. et al., 2016). It was hypothesized that the reduction of GRP transcripts up-regulated during early phase of tick feeding would interfere with cement cone formation thereby, making attachment difficult both at the initial attachment and throughout the prolonged blood meal. This was not the case as well as no change in blood meal uptake was observed (**Figures 1B**, **2B**). This lack of lethal phenotypic change could be due to prepackaged GRPs synthesized before the injection of dsRNA. The existence of these proteins prior to the initiation of feeding would allow the tick to immediately utilize these proteins to establish the bite site and begin cement cone formation. Previously in this research group, we have shown that transcript depletion alone was not sufficient to change the feeding phenotype but when combined with protein inhibitors, a lethal phenotype was observed (Kumar et al., 2016). Hence, this indicates that RNAi alone might not be the perfect tool to study genes involved in attachment on the host, which are expressed early tick feeding stages.

Ticks must use their barbed mouthparts (hypostome) to pierce deeply into the host's dermis (skin), then incase the hypostome in a narrow secreted cement cone. In addition to maintaining a stealthy but secure attachment, the cement cone

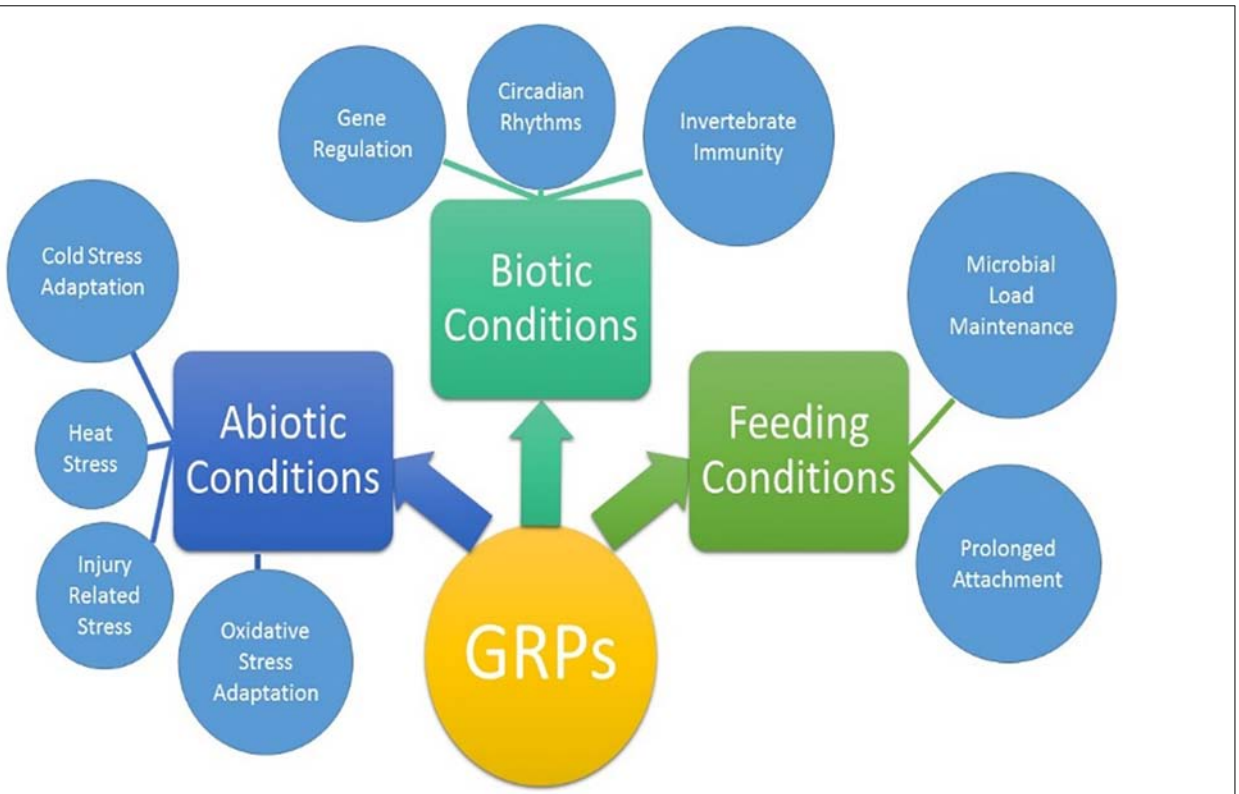

FIGURE 8 | Proposed biological activities of GRPs in tick biology. The extent of which each GRP participates in all listed physiological processes are not yet clear.

provides a conducive environment for the injection of pathogenic microbes into the host. Cement cones have been shown to contain a number of GRPs, which display significant structural and functional heterogeneity across the animal and plant kingdoms, suggesting their involvement in multiple physiological processes (**Figure 8**). The AFM-QNM result of related microtome section of cement cone indicated significant variation of their modulus. Cement which is close to the epidermis of the host skin exhibited higher modulus and the cement formed deep inside the host skin had lower modulus among control and Aam-41539 silenced ticks which indicates that of Aam-41539 might have vital role in proper cone development. Since Aam-41539 is highly expressed in early feeding stage along with the slight changes seen in cone development and homologous peptide sequence have been identified in previous cone proteome analysis it can be expected that this GRP might have direct or indirect roles in the development of cone (Karim and Ribeiro, 2015; Bullard R. et al., 2016; Hollmann et al., 2018). While removing the ticks from the host, care was taken to ensure maximum cone retrieval; however, it was not possible to collect cones from each test condition at the same point of feeding. This is a complication of this area of research and therefore cannot be considered indicative of changes in the cement cone formation without significant investigation.

The tick genome is incredibly large and contains multiple copies of structurally and functionally similar proteins. Previous data from this lab has shown these proteins are not expressed all at once or all throughout the blood meal but rather during small time frames of the blood meal (Bullard R.L. et al., 2016). This could be evolutionarily designed so that the tick is able to switch through all of the available genes to prevent detection from the host immune system. This becomes more complicated when applying this concept to GRPs. Because of the way GRPs are identified, it is possible that the nine selected nine GRPs may posses variety of functions. This would not fit into the switching hypothesis as the expression of one GRP would not compensate for another. The GRP expression in AamerSigP41539 depleted ticks, shows the upregulation of three Aa-GRPs (AamerSigP-34358, AamerSigP-39259, and Aam-36909, **Figure 1A**). However, when these results are compared to the gene expression in ticks suffering from injury stress, the same genes are upregulated. It is unlikely that the changes in the gene expression are a response from the tick to compensate for the loss of function from AamerSigP-41539 but rather a response to the injection injury during the delivery of the double stranded RNA.

There is a class of GRPs with antimicrobial activities in insects. Glycine rich antimicrobial peptides (GR-AMPs) are typically small peptides and can act on the microbes in a bacteriostatic fashion. Gloverins, an anti-microbial peptide isolated from *Hyalophora gloveri*, contains 18% glycine and has no significant similarities to known antimicrobial peptides. Antimicrobial peptides can range from only a few dozen residues to a few hundred as gloverins and attacins (Yi et al., 2013). Based on this criterion, the AaGRPs could serve as antimicrobial peptides. Another family of glycine rich antimicrobial peptides

are plasticins from South American hylid frogs (Scorciapino et al., 2013). Plasticins are able to disrupt the membrane mimetic environments (Carlier et al., 2015)such as a cell membrane of evading pathogens.

The increase in 16S rRNA is used as a measure of bacterial growth in the salivary glands. However, each bacterial cell contains more than 1 copy of 16S rRNA and so the increase cannot be taken as a true increase of bacteria. In the case of Aam-40766 depleted ticks, there is a 2-fold increase of 16S rRNA molecules (**Figure 5B**). This increase could be due to an increase in bacteria or to an increase of protein production in the bacteria or a mixture of both. The 20-fold increase of 16S rRNA in AamerSigP-41539 depleted ticks (**Figure 5A**), however, cannot be attributed solely to an increase in protein production. This increase must be due, at least in part, to an increase in bacteria cells.

In plants, GRPs are well documented to exhibit differential expression during multiple stress conditions. In Arabidopsis, a glycine rich domain protein (*AtGRDP2*) which is expressed throughout plant development and when AtGRDP2 is functionally not present there is a decrease in plant growth (Ortega-Amaro et al., 2015). The over expression of this protein results in increased growth and increased tolerance to stress conditions such as increase salinity (Ortega-Amaro et al., 2015). GRPs have also been differentially expressed in *Bombyx mori* after periods of starvation, although the exact mechanism involved has not yet been identified (Taniai et al., 2014). The lone-star ticks have expanded their geographic range into new areas of the northern and mid-western United States (Munzon et al., 2016; Sonenshine, 2018). Range expansion of *A. americanum* presents a significant public health threat in northeastern and southern Canada (Springer et al., 2015). The northward expansion of this tick's geographic range is consistent with climate change. This also suggests the possibility of adaptive evolution in distinct tick populations from New York, Oklahoma, and historic populations in the Carolinas (Munzon et al., 2016). To explore the role of AaGRPs in the stress response, ticks were exposed to various stress conditions such as cold temperature, hot temperature, oxidative stress, and injury (**Figures 6**, **7**). When the gene expression of stressed salivary glands is compared to stressed whole ticks, it becomes apparent that some of the genes are differentially expressed in different tissues. This is most evident in the expression of Aam-40766 and Aam-36909. In stressed salivary glands (**Figure 7**), Aam-40766 is down regulated in each of the conditions. However, when the whole tick is used, Aam-40766 is upregulated which indicates there might be tissue specific regulation of Aa-40766 expression. It is also possible that this protein is utilized by other tick tissues and is not necessary for blood feeding. Contrary to this, Aam-36909 is down regulated in cold stress and injury stress of whole ticks (**Figure 6**) but is upregulated in both of those stress conditions in the salivary glands. Aam-36909 may play a role in a cellular process in the salivary glands which is necessary for proper function but is not present to any large extent in the other tissues. More work is required to determine the mechanism of stress mediation.

CONCLUSION

Gene depletion of two GRPs by RNAi revealed that identifying the GRPs responsible for cement cone formation will be much more difficult than depleting a few proteins. The redundant nature of the tick genome allows for many levels of compensatory mechanisms. While the gene expression of GRPs after AamerSigP-41539 depletion seems to reveal one such compensatory mechanism, further investigation of the GRP functions revealed that this is a response to the injection injury not to the depletion of AamerSigP-41539. The identification of the effect of stress on GRP expression renders routine studies impossible. An attempt was made at knocking down AamerSigP-34358 which is upregulated during the early feeding as well as during stress. The injection of the double stranded RNA increased the transcripts to such a level that the "depleted" ticks contained more transcripts than the no treatment controls. Therefore, to determine the functions of GRPs, other methods must be developed which do not induce a stress on the tick.

The finding that GRPs are involved in the stress response of the ticks leads to the question of why these genes are over expressed during the feeding stages. Typically feeding is not considered a stress on the tick as it is a necessary process. A new hypothesis has emerged from the data presented here that individual GRPs may play multiple roles during different stages of the tick life cycle. The GRPs may function as antimicrobial or serve any of the other necessary functions for blood feeding when a tick is attached to the host but during times of molting, fasting, or overwintering the same GRPs may be repurposed for stress mediation. A growing body of evidence suggest that GRPs are involved in the physiological and evolutionary adaptation of organisms to abiotic and biotic stresses (**Figure 8**). The role of GRPs remain mostly elusive in the context of cement cone assembly, covert attachment, and cone disassembly. The diversity of functions and structural domains, together with different but specific expression patterns, indicate that this complex protein group can be implicated in numerous physiological functions (**Figure 8**). Ticks are uniquely adapted to variety of stress including prolonged feeding, abiotic, and biotic stresses during its life cycle. More work is required to fully elucidate the functions of the proteins, and recombinant protein expression will be key to that process. A functional characterization of GRPs may help to design novel molecular strategy to disrupt the homeostasis and hence the pathogen transmission.

DATA AVAILABILITY

All datasets generated for this study are included in the manuscript and/or the **Supplementary Files**.

AUTHOR CONTRIBUTIONS

RB and SK conceived and designed the experiments. RB, SRS, PKD, and SK performed the experiments. RB, SEM, and SK analyzed the data. SEM and SK contributed reagents, materials, and analysis tools. RB, SRS, and

SK wrote the manuscript. All authors have read and approved the final version of the manuscript.

FUNDING

This work was supported by grants from the National Institutes of General Medical Sciences awards (Grant Nos. R15 GM123431 and P20 GM103476). The funders had no role in study design, data collection, analysis, decision to publish, or manuscript preparation.

SUPPLEMENTARY MATERIAL

The Supplementary Material for this article can be found online at: https://www.frontiersin.org/articles/10.3389/fphys.2019.00744/full#supplementary-material

FIGURE S1 | Experimental design to examine the transcriptional expression of glycine-rich proteins at organismal and tissue level after stress exposure.

FIGURE S2 | Multiple sequence alignment of selected glycine-rich proteins. Sequences are highlighted based on amino acid property and conservation.

TABLE S1 | List of primers used in this study.

REFERENCES

Baba, K., Okada, M., Kawano, T., Komano, H., and Natori, S. (1987). Purification of Sarcotoxin III, a new antibacterial protein of Sarcophaga peregrina. *J. Biochem.* 102, 69–74. doi: 10.1093/oxfordjournals.jbchem.a122042

Bishop, R., Lambson, B., Wells, C., Pandit, P., Osaso, J., Nkonge, C., et al. (2002). A cement protein of the tick *Rhipicephalus appendiculatus*, located in the secretory e cell granules of the type III salivary gland acini, induces strong antibody responses in cattle. *Int. J. Parasitol.* 32, 833–842. doi: 10.1016/s0020-7519(02)00027-9

Budachetri, K., and Karim, S. (2015). An insight into the functional role of thioredoxin reductase, a selenoprotein, in maintaining normal native microbiota in the Gulf Coast tick (*Amblyomma maculatum*). *Insect Mol. Biol.* 24, 570–581. doi: 10.1111/imb.12184

Bullard, R., Allen, P., Chao, C. C., Douglas, J., Das, P., Morgan, S. E., et al. (2016). Structural characterization of tick cement cones collected from in vivo and artificial membrane blood-fed Lone Star ticks (*Amblyomma americanum*). *Tick Tick Borne Dis.* 7, 880–892. doi: 10.1016/j.ttbdis.2016.04.006

Bullard, R. L., Williams, J., and Karim, S. (2016). Temporal gene expression analysis and RNA silencing of single and multiple members of gene family in the Lone Star Tick *Amblyomma americanum*. *PLoS One* 11:e0147966. doi: 10.1371/journal.pone.0147966

Carlier, L., Joanne, P., Khemtémourian, L., Lacombe, C., Nicolas, P., El Amri, C., et al. (2015). Investigating the role of GXXXG motifs in helical folding and self-association of plasticins, Gly/Leu-rich antimicrobial peptides. *Biophys. Chem.* 196, 40–52. doi: 10.1016/j.bpc.2014.09.004

Childs, J. E., and Paddock, C. D. (2003). The ascendancy of *Amblyomma americanum* as a vector of pathogens affecting humans in the United States. *Annu. Rev. Entomol.* 48, 307–337.

Commins, S. P., James, H. R., Kelly, L. A., Pochan, S. L., Workman, L. J., Perzanowski, M. S., et al. (2011). The relevance of tick bites to the production of IgE antibodies to the mammalian oligosaccharide galactose-α-1,3-galactose. *J. Allergy Clin. Immunol.* 127, 1286–1293. doi: 10.1016/j.jaci.2011.02.019

Crispell, G., Commins, S. P., Archer-Hartmann, S. A., Choudhary, S., Dharmarajan, G., Azadi, P., et al. (2019). Discovery of alpha-gal-containing antigens in North American tick species believed to induce red meat allergy. *Front. Immunol.* 10:1056. doi: 10.3389/fimmu.2019.01056

Francischetti, I. M. B., Sa'-Nunes, A., Mans, B. J., Santos, I. M., and Ribeiro, J. M. C. (2009). The role of saliva in tick feeding. *Front. Biosci.* 14:2051–2088. doi: 10.2741/3363

Goddard, J., and Varela-Stokes, A. S. (2009). Role of the lone star tick, *Amblyomma americanum* (L.), in human and animal diseases. *Vet. Parasitol.* 160, 1–12. doi: 10.1016/j.vetpar.2008.10.089

Graham, L., and Davies, P. (2005). Glycine-rich antifreeze proteins from snow fleas. *Science* 310:461. doi: 10.1126/science.1115145

Hollmann, T., Kim, T. K., Tirloni, L., Radulović, ŽM., Pinto, A. F. M., Diedrich, J. K., et al. (2018). Identification and characterization of proteins in the *Amblyomma americanum* tick cement cone. *Int. J. Parasitol.* 48, 211–224. doi: 10.1016/j.ijpara.2017.08.018

Karim, S., and Ribeiro, J. M. (2015). An insight into the sialome of the lone star tick, *Amblyomma americanum*, with a glimpse on its time dependent gene expression. *PLoS One* 10:e0131292. doi: 10.1371/journal.pone.0131292

Karim, S., Singh, P., and Ribeiro, J. M. C. (2011). A deep insight into the sialotranscriptome of the Gulf Coast tick, *Amblyomma maculatum*. *PLoS One* 6:e28525. doi: 10.1371/journal.pone.0028525

Kim, J. S., Park, S. J., Kwak, K. J., Kim, Y. O., Kim, J. Y., Song, J., et al. (2007). Cold shock domain proteins and glycine-rich RNA-binding proteins from Arabidopsis thaliana can promote the cold adaptation processes in *Escherichia coli*. *Nucleic Acid Res.* 35, 506–516. doi: 10.1093/nar/gkl1076

Kumar, D., Budachetri, K., Meyers, V. C., and Karim, S. (2016). Assessment of the tick antioxidant response to exogenous oxidative stressors and insight into the role of catalase in the reproductive fitness of the Gulf Coast tick (*Amblyomma maculatum*). *Insect Mol. Biol.* 25, 283–294. doi: 10.1111/imb.12218

Mok, Y. F., Lin, F. H., Graham, L. A., Celik, Y., Braslavsky, I., and Davies, P. L. (2010). Structural basis for the superior activity of the large isoform of snow flea antifreeze protein. *Biocehmistry* 49, 2593–2603. doi: 10.1021/bi901929n

Mousavi, A., and Hotta, Y. (2005). Glycine-rich proteins. *Appl. Biochem. Biotechnol.* 120, 169–174. doi: 10.1385/abab:120:3:169

Munzon, J. D., Atkinson, J. K., Henn, B. M., and Benach, J. L. (2016). Population and evolutionary genomics of *Amblyomma americanum*, an expanding arthropod disease vector. *Genome Biol. Evol.* 8, 1351–1360. doi: 10.1093/gbe/evw080

Narasimhan, S., Rajeevan, N., Liu, L., Zhao, Y. O., Heisig, J., Pan, J., et al. (2014). Gut microbiota of the tick vector *Ixodes scapularis* modulate colonization of the Lyme disease spirochete. *Cell Host Microbe* 15, 58–71. doi: 10.1016/j.chom.2013.12.001

Ortega-Amaro, M. A., Rodríguez-Hernández, A. A., Rodríguez-Kessler, M., Hernández-Lucero, E., Rosales-Mendoza, S., Ibáñez-Salazar, A., et al. (2015). Overexpression of AtGRDP2, a novel glycine-rich domain protein, accelerates plant growth and improves stress tolerance. *Front. Plant Sci.* 5:782. doi: 10.3389/fpls.2014.00782

Patrick, C. D., and Hair, J. A. (1975). Laboratory rearing procedures, and equipment for. (multi)-host ticks (Acarina: Ixodidae). *J. Med. Entomol.* 12, 389–390. doi: 10.1093/jmedent/12.3.389

Pentzold, S., Zagrobelny, M., Khakimov, B., Engelsen, S. B., Clausen, H., Petersen, B. L., et al. (2016). Lepidopteran defense droplets- a comppsite physical and chemical weapon against potential predators. *Sci. Rep.* 6:22407. doi: 10.1038/srep22407

Platts-Mills, T. A., and Commins, S. P. (2013). Emerging antigens involved in allergic responses. *Curr. Opin. Immunol.* 25, 769–774. doi: 10.1016/j.coi.2013.09.002

Schemmer, P., Zhong, Z., Galli, U., Wheeler, M. D., Xiangli, L., Bradford, B., et al. (2013). Glycine reduces platelet aggregation. *Amino Acids* 44, 925–931. doi: 10.1007/s00726-012-1422-8

Scorciapino, M. A., Manzo, G., Rinaldi, A. C., Sanna, R., Casu, M., Pantic, J. M., et al. (2013). Conformational analysis of the frog skin peptide, plasticin-l1, and its effects on production of proinflammatory cytokines by macrophages. *Biochemistry* 52, 7231–7241. doi: 10.1021/bi4008287

Sonenshine, D. E. (2018). Range expansion of tick disease vectors in North America: implications for spread of tick-borne disease. *Int. J. Environ. Res. Public Health* 15:E478. doi: 10.3390/ijerph15030478

Springer, Y. P., Jarnevich, C. S., Barnett, D. T., Monaghan, A. J., and Eisen, R. J. (2015). Modeling the present and future geographic distribution of the Lone

star tick, *Amblyomma americanum* (Ixodida: Ixodidae), in the continental United States. *Am. J. Trop. Med. Hyg.* 93, 875–890. doi: 10.4269/ajtmh.15-0330

Taniai, K., Hirayama, C., Mita, K., and Asaoka, K. (2014). Starvation-responsive glycine-rich proteins gene in the silkwork *Bombyx mori*. *J. Comp. Physiol. B* 184, 827–834. doi: 10.1007/s00360-014-0846-8

Tokareva, O., Jacobsen, M., Buehler, M., Wong, J., and Kaplan, D. L. (2013). Structure-function-property-design interplay in biopolymers: Spider silk. *Acta Biomater.* 10, 1612–1626. doi: 10.1016/j.actbio.2013.08.020

Wang, J., Hu, C., Wu, Y., Stuart, A., Amemiya, C., Berriman, M., et al. (2008). Characterization of the antimicrobial peptide attacin loci from *Glossina morsitans*. *Insect Mol. Biol.* 17, 293–302. doi: 10.1111/j.1365-2583.2008.00805.x

Winkler, S., and Kaplan, D. L. (2000). Molecular biology of spider silk. *J. Biotechnol.* 74, 85–93. doi: 10.1016/s1389-0352(00)00005-2

Xia, X. X., Qian, Z. G., Ki, C. S., Park, Y. H., Kaplan, D. L., and Lee, S. Y. (2010). Native-sized recombinant spider silk protein produced in metabolically engineered *Escherichia coli* results in a strong fiber. *PNAS* 107, 14059–14063. doi: 10.1073/pnas.1003366107

Xu, T., Gu, L., Choi, M. J., Kim, R. J., Suh, M. C., and Kang, H. (2014). Comparative functional analysis of wheat (*Triticum aestivum*) zinc finger-containing glycine-rich RNA-binding proteins in response to abiotic stresses. *PLoS One* 9:e96877. doi: 10.1371/journal.pone.0096877

Yi, H. Y., Chowdhury, M., Huang, Y. D., and Yu, X. Q. (2014). Insect antimicrobial peptides and their applications. *Appl. Microbiol. Biotechnol.* 98, 5807–5822. doi: 10.1007/s00253-014-5792-6

Yi, H.-Y., Deng, X.-J., Yang, W.-Y., Zhou, C.-Z., Cao, Y., and Yu, X.-Q. (2013). Gloverins of the silkworm Bombyx mori: structural and binding properties and activities. *Insect Biochem. Mol. Biol.* 43, 612–625. doi: 10.1016/j.ibmb.2013.03.013

Zhang, J., Goyer, C., and Pelletier, Y. (2008). Environmenal stresses induce the expression of putative glycine-rich insect culticular protein genes in adult *Leptinotarsa decemlineata* (Say). *Insect Mol. Biol.* 17, 209–216. doi: 10.1111/j.1365-2583.2008.00796.x

Zhang, M., Zhou, F., Chu, Y., Zhao, Z., and An, C. (2013). Identification and expression profile analysis of antimicrobial peptide/protein in Asian Corn Borer, *Ostrinia furnacalis* (Guenee). *Int. J. Biol. Sci.* 9, 1004–1012. doi: 10.7150/ijbs.6813

Zottich, U., Da Cunha, M., Carvalho, A. O., Dias, G. B., Casarin, N., Vasconcelos, I. M., et al. (2013). An antifungal peptide from *Coffea canephora* seeds with sequence homology to glycine-rich proteins exerts membrane permeabilization and nuclear localization in fungi. *Biochim. Biophys. Acta Gen. Subj.* 1830, 3509–3516. doi: 10.1016/j.bbagen.2013.03.007

Conflict of Interest Statement: The authors declare that the research was conducted in the absence of any commercial or financial relationships that could be construed as a potential conflict of interest.

The handling Editor declared a past co-authorship with one of the authors SK.

frontiers in Physiology

MINI REVIEW
published: 26 June 2019
doi: 10.3389/fphys.2019.00812

The Use of Tick Salivary Proteins as Novel Therapeutics

*Jindřich Chmelař[1], Jan Kotál[1,2], Anna Kovaříková[1] and Michail Kotsyfakis[1,2]**

[1] Department of Medical Biology, Faculty of Science, University of South Bohemia in České Budějovice, České Budějovice, Czechia, [2] Laboratory of Genomics and Proteomics of Disease Vectors, Biology Centre CAS, Institute of Parasitology, České Budějovice, Czechia

The last three decades of research into tick salivary components have revealed several proteins with important pharmacological and immunological activities. Two primary interests have driven research into tick salivary secretions: the search for suitable pathogen transmission blocking or "anti-tick" vaccine candidates and the search for novel therapeutics derived from tick salivary components. Intensive basic research in the field of tick salivary gland transcriptomics and proteomics has identified several major protein families that play important roles in tick feeding and overcoming vertebrate anti-tick responses. Moreover, these families contain members with unrealized therapeutic potential. Here we review the major tick salivary protein families exploitable in medical applications such as immunomodulation, inhibition of hemostasis and inflammation. Moreover, we discuss the potential, opportunities, and challenges in searching for novel tick-derived drugs.

Keywords: ticks, therapeutics, immunomodulation, salivary proteins, anti-inflammatory proteins, hemostasis

OPEN ACCESS

Edited by:
Itabajara Da Silva Vaz Jr., Federal University of Rio Grande do Sul, Brazil

Reviewed by:
Nathalie Boulanger, Université de Strasbourg, France
Tae Kim, Texas A&M University, United States

***Correspondence:**
Michail Kotsyfakis
mich_kotsyfakis@yahoo.com

Specialty section:
This article was submitted to Invertebrate Physiology, a section of the journal Frontiers in Physiology

Received: *25 April 2019*
Accepted: *11 June 2019*
Published: *26 June 2019*

Citation:
Chmelař J, Kotál J, Kovaříková A and Kotsyfakis M (2019) The Use of Tick Salivary Proteins as Novel Therapeutics. Front. Physiol. 10:812. doi: 10.3389/fphys.2019.00812

INTRODUCTION

The data being generated in the high-throughput era are rapidly shifting research and development efforts toward novel and precise therapeutics that target specific pathological mechanisms and populations and diminish harmful side-effects (Paul et al., 2010; Jorgensen, 2011). Drug discovery pipelines can take a number of different forms including high-throughput screening of compound libraries or compounds similar to existing drugs, drug repurposing (Shim and Liu, 2014; Grammer and Lipsky, 2017), target-oriented molecular design, target searching using systems pharmacology approaches (Huang et al., 2014; Zhou et al., 2016), and searching for novel bioactive substances in various organisms. The latter approach is becoming increasingly attractive, as massive screening has proven to be less cost-effective than anticipated and, with rapid development in mass spectrometry, narrowing of active fractions to individual compounds is becoming easier (Wang et al., 2019). Apart from medicinal plants and/or herbal mixtures (Li and Weng, 2017), other sources – such as arthropods and parasites – have also proven to be useful (Cherniack, 2011; Ratcliffe et al., 2014; El-Tantawy, 2015). Unlike plant products that usually kill or repel herbivores and pests and have diverse effects on vital vertebrate physiology, parasitic proteins evolved to target specific vertebrate defense mechanisms. For example, the leech *Hirudo officinalis* produces the strongest known natural anti-coagulant hirudin, and hirudin and its artificial derivatives like bivalrudin are now used in clinical practice to treat coagulation disorders. Similarly, tick salivary proteins hold promise for the treatment of those processes they subvert, particularly immune-related diseases and hemostatic disorders.

TICK SALIVARY SECRETIONS AND TICK-HOST-PATHOGEN INTERACTIONS

Ticks are obligate blood-feeding ectoparasites of vertebrates including lizards, birds, and mammals (Jongejan and Uilenberg, 2004). As such, they must cope with diverse host defense mechanisms (Ribeiro and Francischetti, 2003; Francischetti et al., 2009) triggered by the bite/injury itself and the concomitant infection. The infections transmitted by ticks can be passive, such as from pathogens like poxviruses or apicomplexa present in blood on the tick hypostome or regurgitated during feeding (Tuppurainen et al., 2011; Hammer et al., 2016), and/or active when ticks are vectors for pathogens. Ticks can transmit bacteria of the genera *Borrelia*, *Anaplasma, Rickettsia, Francisella*, and others; protozoan parasites of the genus *Babesia*; and several viruses, with tick-borne encephalitis virus a major tick-transmitted viral pathogen in humans (Swanson et al., 2006; Coipan et al., 2013; Berggoetz et al., 2014; Jahfari et al., 2016; Kazimirova et al., 2017; Dehhaghi et al., 2019). Early works on tick saliva (Wikel, 1982; Ribeiro et al., 1985) showed that ticks actively modulate and/or inhibit host defense mechanisms, thus enabling the tick to complete its blood meal and facilitate pathogen transmission, as reviewed elsewhere (Francischetti et al., 2009; Wikel, 2013; Kotal et al., 2015). The latter effect has been described as saliva-assisted (originally saliva-activated) transmission (SAT) (Nuttall and Labuda, 2004, 2008), and several molecules have been described as SAT factors (Kazimirova and Stibraniova, 2013). It has been hypothesized that targeting salivary factors using a vaccine could block pathogen transmission (Neelakanta and Sultana, 2015), but despite successful vaccination and RNA interference experiments, such vaccines have yet to be clinically effective for most tick species (Neelakanta and Sultana, 2015). This is at least in part due to high functional redundancy among salivary components (Chmelar et al., 2016) or because salivary proteins are often beneficial but not indispensable for pathogen transmission (Pospisilova et al., 2019). However, from another perspective, these proteins represent a diverse and abundant library of pharmacoactive molecules with potential for medical exploitation. The functions and activities of numerous salivary components have been described and reviewed elsewhere (Chmelar et al., 2012, 2017; Kazimirova and Stibraniova, 2013; Simo et al., 2017). Here we review tick salivary protein families with potential for medical use, and in doing so we highlight that tick salivary secretions represent a unique source of novel drugs that are only just starting to be exploited and translated for clinical benefit.

TICK SALIVARY PROTEIN FAMILIES WITH THERAPEUTIC POTENTIAL

Thanks to comprehensive transcriptomic and proteomic studies of tick salivary glands and saliva, 10s of protein families have been identified in ticks (Oleaga et al., 2007; Oliveira et al., 2013; Schwarz et al., 2013; Mudenda et al., 2014; Tirloni et al., 2014, 2015, 2017; Karim and Ribeiro, 2015; Xu et al., 2015; Yu et al., 2015; de Castro et al., 2016; Kim et al., 2016; Esteves et al., 2017; Ribeiro et al., 2017). Some have been experimentally proven to possess anti-inflammatory, anti-hemostatic, anti-complement, and/or immunomodulatory activities, as reviewed elsewhere (Chmelar et al., 2012; Kazimirova and Stibraniova, 2013). Several diverse but abundant secreted protein groups have been repeatedly identified in transcriptomes from tick salivary glands. Their experimentally evidenced activities are summarized in **Figures 1, 2**, and their potential medical uses are discussed in detail below.

Lipocalins

Lipocalins form a large family of barrel-shaped proteins with specific folds creating pockets that usually bind hydrophobic molecules such as steroids or lipids. Lipocalins form the largest and most diverse protein family in ticks. They were originally described as histamine-binding proteins (Paesen et al., 1999) but were later found to bind other biogenic amines such as serotonin (Sangamnatdej et al., 2002; Mans et al., 2008b) and bioactive lipids (leukotrienes, thromboxanes, or cholesterol) (Keller et al., 1993; Beaufays et al., 2008; Mans and Ribeiro, 2008; Roversi et al., 2017). Apart from binding small hydrophobic molecules, tick lipocalins can also bind larger proteins such as the C5 component of the complement cascade (Nunn et al., 2005; Fredslund et al., 2008). The lipocalin from the tick *Ornithodoros moubata* (Coversin) displayed a therapeutic effect in disease models (Soltys et al., 2009; Romay-Penabad et al., 2014; Pischke et al., 2017) and is already being tested in clinical trials for the treatment of thrombotic microangiopathy (Brocklebank and Kavanagh, 2017; Goodship et al., 2017). The lipocalin Japanin from *Rhipicephalus appendiculatus* was found to modulate dendritic cell differentiation, thus altering subsequent T cell-dependent cellular responses (Preston et al., 2013). Several other tick lipocalins have been successfully tested in other disease models; for example, histamine binding lipocalin Ha24 from *Hyalomma asiaticum* inhibited cell recruitment and histamine secretion in a mouse experimental asthma model (Wang et al., 2016), and rEV131 and rEV504 from *R. appendiculatus* inhibited allergic asthma and acute respiratory distress syndrome by scavenging histamine (Couillin et al., 2004; Ryffel et al., 2005; Weston-Davies et al., 2005). Therefore, tick lipocalins are proven drug candidates that target hemostasis, complement, inflammation, and acquired immunity.

Protease Inhibitors

Endogenous protease inhibitors regulate many physiological processes in mammals, and their dysregulation leads to some serious diseases and even cancer development. Several protease inhibitor families have been identified in tick saliva. Serine protease inhibitors form four groups – Kunitz-domain inhibitors, serpins, trypsin inhibitor-like cysteine-rich domain inhibitors (TIL-domain inhibitors), and Kazal-domain inhibitors – while the cysteine protease inhibitors usually belong to the cystatin family. Tick protease inhibitors and their functions are reviewed elsewhere (Schwarz et al., 2012; Blisnick et al., 2017; Porter et al., 2017; Parizi et al., 2018), and the therapeutic potential of serpins and cystatins was outlined in

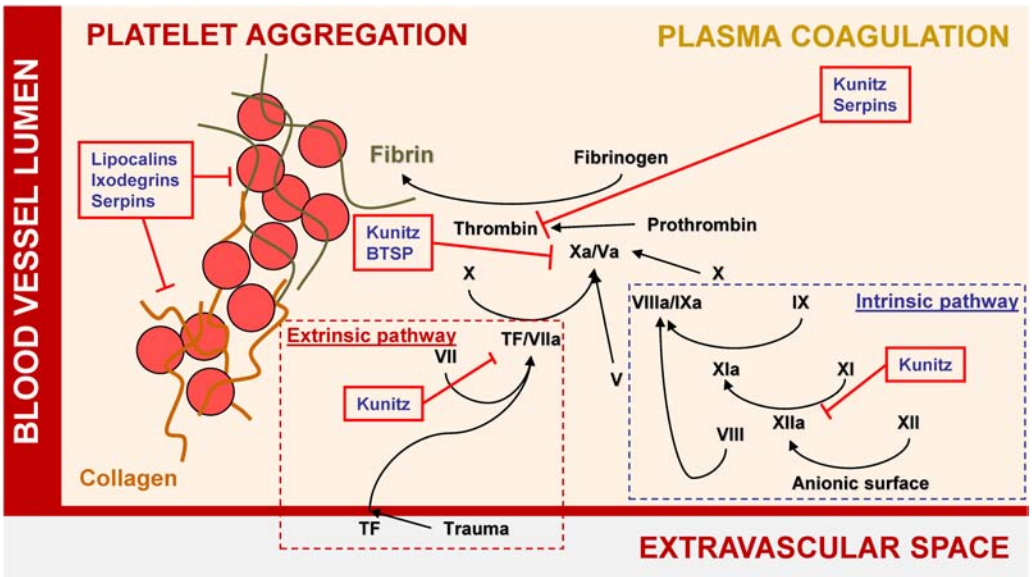

FIGURE 1 | Major tick salivary protein families and their roles in hemostasis.

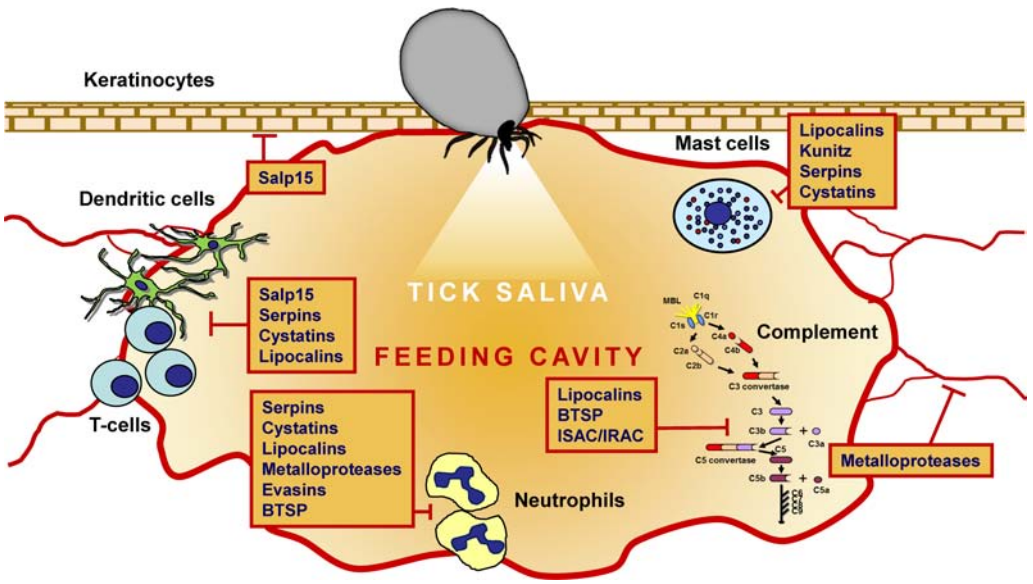

FIGURE 2 | The immunomodulatory and anti-complement activities of the major tick-secreted protein families.

our previous review (Chmelar et al., 2017). Here we discuss the therapeutic potential of the other two groups, Kunitz- and TIL-domain inhibitors.

Kunitz-Domain Protease Inhibitors

The Kunitz-domain protease inhibitors are the second largest family of secreted salivary proteins. Ticks possess Kunitz inhibitors with one to seven Kunitz domains, and most have been characterized as anti-coagulants that inhibit various proteases in the coagulation cascade (Corral-Rodriguez et al., 2009; Chmelar et al., 2012). Other family members possess anti-platelet activity due to integrin binding (see section "Disintegrins"). Their anti-platelet and anti-coagulatory properties make Kunitz inhibitors interesting as novel and target-specific drugs. Indeed, a Kunitz-domain protein Ir-CPI (*Ixodes ricinus* contact phase inhibitor) was shown to be a very efficient inhibitor of the contact phase of the coagulation cascade (Decrem et al., 2009), which is now being exploited in pre-clinical testing[1]. As well as hemostasis regulation, the Kunitz inhibitors Ixolaris and Amblyommin-X have displayed anti-cancer therapeutic potential

[1]www.bioxodes.com

(Carneiro-Lobo et al., 2009; Chudzinski-Tavassi et al., 2010; Barboza et al., 2015; de Souza et al., 2016).

Similar to lipocalins, Kunitz-domain tick inhibitors are a large and diverse group of proteins that could be used in drug development for human disease. Their highest potential lies in their anti-hemostatic properties, for which several Kunitz inhibitors have already been patented.

TIL-Domain Inhibitors

TIL-domain inhibitors represent another abundant group of tick salivary protease inhibitors. TIL-domain inhibitors are small (6–9 kDa), structurally conserved proteins with five disulfide bridges. Their inhibitory activity against trypsin was originally described in the parasitic nematode *Ascaris lumbricoides*. Proteins with the same cysteine scaffold were subsequently described as anti-coagulants in the helminth *Ancylostoma caninum* (Stassens et al., 1996) or in the skin secretions in the frog *Bombina bombina* (Mignogna et al., 1996). Moreover, they have also been identified in bee hemolymph (Bania et al., 1999) and as toxins in *Scorpiops jendeki* scorpion venom (Chen et al., 2013). The TIL-domain structure has been resolved, and the loop with the active P1 site is also recognized in non-tick proteins (Huang et al., 1994; Mignogna et al., 1996; Bania et al., 1999; Cierpicki et al., 2000). In addition to its anti-protease activity, scorpion TIL-domain inhibitor Sj7170 stimulated tumor growth and metastasis formation (Song et al., 2014). TIL-domain inhibitors play a regulatory role in *Drosophila* seminal fluid (Lung et al., 2002), and TIL domains are present in the large complex molecule of von Willebrand factor (Zhou et al., 2012), albeit with unknown function.

In tick salivary glands, TIL-domain inhibitors were the most abundant and diverse protein family with 108 members in *R. appendiculatus* and 64 in *I. ricinus* (Lieskovska et al., 2015; de Castro et al., 2016), suggesting that they are important in host defenses. Moreover, due to their conserved structure and known active site, TIL-domain inhibitors seem to be good candidates for protein engineering.

Disintegrins

Disintegrins form a large group of proteins that were originally described in snake venom as 60–80 kDa cysteine-rich proteins containing an integrin-binding motif Arg-Gly-Asp (RGD). This domain is also typical in extracellular matrix proteins and enables platelet binding via integrins and subsequent thrombus formation. RGD domains in soluble proteins such as disintegrins prevent platelet aggregation, which is crucial for the success of hematophagous parasites (Assumpcao et al., 2012). Three Kunitz domain-containing disintegrins have been functionally characterized: disagregin from *O. moubata*, which shows low similarity to Kunitz inhibitors and does not actually contain an RGD domain (Karczewski et al., 1994; Karczewski and Connolly, 1997); savignygrin from *Ornithodoros savignyi* (Mans et al., 2002a,b); and monogrins from *Argas monolakensis* (Mans et al., 2008a). Another group of tick disintegrins includes variabilin (Wang et al., 1996), which was the only group member characterized and later named ixodegrins (Ixodida + disintegrins) after their discovery in the *Ixodes pacificus* transcriptome (Francischetti et al., 2005). Variabilin was shown to block the binding of fibrinogen to integrin αIIbβ3 (Wang et al., 1996). The second tick protein characterized in the ixodegrin family was YY-39 from *Ixodes scapularis*, which was shown to bind integrin αIIbβ3 and thus compete with fibrinogen binding to platelets (Tang et al., 2015). Ixodegrins are structurally similar to snake venom disintegrins and usually contain RGD or KGD domains. Given their properties, they may be candidate therapeutics as novel anti-thrombotic agents.

Basic Tail Secreted Proteins (BTSPs)

The first BTSP family member was identified and described as one of 14 immunodominant antigens in *I. scapularis* and named Salp14 (Das et al., 2001). More homologs were subsequently found in the transcriptomes of *I. scapularis* (Valenzuela et al., 2002) and other tick species, where BTSP usually forms one of the most abundant and diverse putatively secreted groups (Francischetti et al., 2005; Schwarz et al., 2013; Karim and Ribeiro, 2015; de Castro et al., 2016). Salp14 and its smaller homolog Salp9Pac are anti-coagulants important for tick feeding, as evidenced by RNA interference studies in ticks (Narasimhan et al., 2002, 2004). Another BTSP family member, Ixonnexin, promoted fibrinolysis by accelerating plasminogen activation and inhibiting factor Xa (Assumpcao et al., 2018). An immunogen originally named P8 (Schuijt et al., 2011b) displayed lectin binding properties and acted as a complement inhibitor (Schuijt et al., 2011a), thus protecting *Borrelia* spirochetes from complement attack (Wagemakers et al., 2016).

The BTSP family contains 100s of members, some with modifications such as acidic tails or no tail instead of basic tails, which are usually composed of lysine and arginine residues (Francischetti et al., 2008). They work as anti-coagulants and specific complement inhibitors, both of which are very attractive drug targets.

Salp15

Wikel (1982) observed that tick infestation inhibited mitogen-induced guinea-pig T cell proliferation. Since, then, many effects of tick saliva on T cell function have been described (Kotal et al., 2015). The best characterized tick salivary protein with a direct effect on T cells is Salp15 from *I. scapularis* (Anguita et al., 2002), a member of a large family of heavily glycosylated proteins that seem to be unique to prostriate ticks such as *Ixodes* spp. (Wang et al., 2014). Salp15 binds specifically to the CD4 co-receptor on T cells, thus inhibiting cell signaling, reducing IL-2 production, and promoting $CD4^+$ T cell activation (Anguita et al., 2002; Garg et al., 2006; Juncadella et al., 2007). The immunomodulatory potential of Salp15 has been tested in several *in vivo* models with promising therapeutic results, e.g., in inhibiting HIV infection (Juncadella et al., 2008), experimental autoimmune encephalomyelitis (Juncadella et al., 2010), transplantation rejection (Tomas-Cortazar et al., 2017), and asthma (Paveglio et al., 2007). In addition to its anti-$CD4^+$ T cell effect, Salp15 is also a suppressor of dendritic cell function (Hovius et al., 2008; den Dunnen et al., 2009), suggesting another

use in targeted therapy. In addition, Salp15 inhibited TLR2-dependent inflammation and production of antimicrobial peptides by keratinocytes (Marchal et al., 2011). Apart from its immunomodulatory activities (Juncadella and Anguita, 2009), it has also been associated with protection of *Borrelia* spirochetes from the immune system (Ramamoorthi et al., 2005; Dai et al., 2009).

Metalloproteases

Metalloproteases form large group of physiologically important enzymes that play a role in extracellular matrix degradation, protein shedding from the cell surface, and enzyme activation. Tick salivary metalloproteases accelerate fibrinolysis (Francischetti et al., 2003; Beaufays et al., 2008), thus their function is anti-hemostatic. Two proteins from *I. scapularis* from the ADAMTS family (a disintegrin and metalloprotease with thrombospondin motifs) significantly inhibited neutrophil function, broadening the range of possible metalloprotease activities (Guo et al., 2009). The abundancy and diversity of metalloproteases in tick saliva is high; however, using them as therapeutics can be problematic due to their stability and the long-term maintenance of their activity.

Evasins

Chemokines play a role in cell recruitment to inflammation sites and therefore play crucial roles in promoting inflammatory responses (Charo and Ransohoff, 2006). Evasins form a family of chemokine-binding proteins first identified in *Rhipicephalus sanguineus* (Frauenschuh et al., 2007; Deruaz et al., 2008). Homologs were also found in *Amblyomma* and *Ixodes* species; however, in *Ixodes*, the homology is very weak (Hayward et al., 2017). Evasin-1 and evasin-4 bind CC chemokine members, while evasin-3 is specific for CXC chemokines (Frauenschuh et al., 2007; Deruaz et al., 2008). Evasin-1 can inhibit neutrophil, T cell, and macrophage migration and the production of inflammatory cytokines, from which originates its therapeutic potential. Evasin-1 has shown benefit in the treatment of pulmonary fibrosis (Russo et al., 2011) and graft versus host disease (Castor et al., 2010). Evasin-4 can interact with at least 18 CC chemokines, inhibit eosinophil recruitment (Vieira et al., 2009; Deruaz et al., 2013), and was effective against post-infarction myocardial injury and remodeling (Braunersreuther et al., 2013). Evasin-3 effectively inhibited myocardial reperfusion (Montecucco et al., 2010) and neutrophil recruitment (Deruaz et al., 2008), thereby reducing atherosclerotic vulnerability for ischemic stroke (Copin et al., 2013). Evasin-3 was also shown to inhibit neutrophil-mediated inflammation in a mouse acute pancreatitis model (Montecucco et al., 2014). The therapeutic potential of evasins is reviewed in Bonvin et al. (2016).

TICK PROTEINS AND BIOENGINEERING

The preceding discussion highlights that tick salivary proteins can target every possible immune mechanism and therefore have the potential to be used as drugs, especially against disorders of hemostasis, immune-mediated inflammatory diseases, and also against tumor growth. Indeed, many tick molecules have been patented for these reasons (Nuttall and Paesen, 2000; Nunn, 2004; Chudzinski-Tavassi et al., 2005); moreover, Coversin has already been, and continues to be, tested in clinical trials (ClinicalTrials.gov: NCT03829449, NCT03427060, NCT02591862, NCT03588026) for paroxysmal nocturnal hemoglobinuria and microscopic and thrombotic microangiopathy (Brocklebank and Kavanagh, 2017; Goodship et al., 2017). However, the pharmacokinetics and pharmacodynamics of tick proteins can limit their therapeutic potential. Similar to any large molecule of exogenous origin, tick salivary proteins display strong immunogenicity. This can be overcome using several modifications such as PEGylation [attachment of polyethylene glycol (PEG) polymers], which should, in addition to decreasing immunogenicity, improve solubility (Veronese and Mero, 2008; Jokerst et al., 2011). Another possibility is humanization of the proteins, in which potential T cell epitopes are eliminated or changed. This approach has been used with great success for monoclonal antibodies designed predominantly for cancer treatment by the fusion of the hypervariable parts of mouse-derived monoclonal antibodies to human heavy chains (De Groot and Scott, 2007). A similar approach could be used for tick serpins, where the reactive center loop (RCL), which is responsible for serpin specificity, would be of tick origin, and the conserved serpin scaffold would be of human origin (Silverman et al., 2010; Whisstock et al., 2010). The concept of creating novel serpins by combining the RCL and scaffold from different serpins has been proven with the fusion of the furin inhibitor B8 and the mutant variant of α1-antitrypsin (Izaguirre et al., 2013, 2019). Furthermore, a novel extracellular inhibitor of human granzyme B was produced by combining mouse RCL and a human scaffold into a single chimera (Marcet-Palacios et al., 2015). Despite these promising results, there is no experimental evidence that the same approach would be successful for tick salivary molecules as well. Our understanding of the interaction between tick salivary secretion and host immune system is still incomplete, and immune tolerance is not the only obstacle in turning tick proteins into drugs.

In addition to immunogenicity, small proteins and peptides, which many tick salivary proteins are, usually have a short circulatory half-life. This problem can be solved by fusing the studied protein with the Fc fragment of human IgG. Such a fusion was performed with evasin-4 but without success (Bonvin et al., 2016). PASylation – protein conjugation with the polymeric sequence of Pro, Ala, and Ser – is a relatively new method similar to PEGylation that can prolong protein half-life in the circulation by several days (Schlapschy et al., 2013). There are ways to modify tick salivary proteins to improve their pharmacodynamics and pharmacokinetics, some of which have already been successfully used, such as PASylation of Coversin (see section "Lipocalins"), which inhibited its degradation in plasma (Kuhn et al., 2016).

CONCLUDING REMARKS

Based on experimental evidence and/or the membership of proteins to well-described families, the function of some tick proteins has been proven or at least inferred. For some families, functional knowledge is still lacking. Therefore, tick salivary proteins remain rather poorly explored with respect to their therapeutic applications. Most efforts aiming to develop new drugs from ticks focus on the two largest families, Kunitz-domain inhibitors and lipocalins, as these groups contain new members with novel functions via several genetic mechanisms (Mans et al., 2008b; Schwarz et al., 2014). However, other groups deserve attention as well, such as TIL-domain protease inhibitors, Salp15, evasins, and many others. This minireview summarizes the main protein groups to emphasize the therapeutic potential of tick salivary proteins and some of the problems faced with clinical translation.

AUTHOR CONTRIBUTIONS

JC, JK, and AK wrote the manuscript. JC prepared the figures. MK reviewed and edited the manuscript.

FUNDING

This work was supported by the Grant Agency of the Czech Republic (19-14704Y to JC and 19-07247S to MK) and by the ERD Funds, projectCePaVip OPVVV (No. 384 CZ.02.1.01/0.0/0.0/16_019/0000759 to MK).

ACKNOWLEDGMENTS

We thank the Nextgenediting for editorial support.

REFERENCES

Anguita, J., Ramamoorthi, N., Hovius, J. W., Das, S., Thomas, V., Persinski, R., et al. (2002). Salp15, an ixodes scapularis salivary protein, inhibits CD4(+) T cell activation. *Immunity* 16, 849–859. doi: 10.1016/s1074-7613(02)00325-4

Assumpcao, T. C., Mizurini, D. M., Ma, D., Monteiro, R. Q., Ahlstedt, S., Reyes, M., et al. (2018). Ixonnexin from tick saliva promotes fibrinolysis by interacting with plasminogen and tissue-type plasminogen activator, and prevents arterial thrombosis. *Sci. Rep.* 8:4806. doi: 10.1038/s41598-018-22780-1

Assumpcao, T. C., Ribeiro, J. M., and Francischetti, I. M. (2012). Disintegrins from hematophagous sources. *Toxins* 4, 296–322. doi: 10.3390/toxins4050296

Bania, J., Stachowiak, D., and Polanowski, A. (1999). Primary structure and properties of the cathepsin G/chymotrypsin inhibitor from the larval hemolymph of *Apis mellifera*. *Eur J. Biochem.* 262, 680–687. doi: 10.1046/j.1432-1327.1999.00406.x

Barboza, T., Gomes, T., Mizurini, D. M., Monteiro, R. Q., Konig, S., Francischetti, I. M., et al. (2015). (99m)Tc-ixolaris targets glioblastoma-associated tissue factor: in vitro and pre-clinical applications. *Thromb. Res.* 136, 432–439. doi: 10.1016/j.thromres.2015.05.032

Beaufays, J., Adam, B., Menten-Dedoyart, C., Fievez, L., Grosjean, A., Decrem, Y., et al. (2008). Ir-LBP, an ixodes ricinus tick salivary LTB4-binding lipocalin, interferes with host neutrophil function. *PLoS One* 3:e3987. doi: 10.1371/journal.pone.0003987

Berggoetz, M., Schmid, M., Ston, D., Wyss, V., Chevillon, C., Pretorius, A. M., et al. (2014). Protozoan and bacterial pathogens in tick salivary glands in wild and domestic animal environments in South Africa. *Ticks Tick Borne Dis.* 5, 176–185. doi: 10.1016/j.ttbdis.2013.10.003

Blisnick, A. A., Foulon, T., and Bonnet, S. I. (2017). Serine protease inhibitors in ticks: an overview of their role in tick biology and tick-borne pathogen transmission. *Front. Cell Infect. Microbiol.* 7:199. doi: 10.3389/fcimb.2017.00199

Bonvin, P., Power, C. A., and Proudfoot, A. E. (2016). Evasins: therapeutic potential of a new family of chemokine-binding proteins from ticks. *Front. Immunol.* 7:208. doi: 10.3389/fimmu.2016.00208

Braunersreuther, V., Montecucco, F., Pelli, G., Galan, K., Proudfoot, A. E., Belin, A., et al. (2013). Treatment with the CC chemokine-binding protein Evasin-4 improves post-infarction myocardial injury and survival in mice. *Thromb. Haemost.* 110, 807–825. doi: 10.1160/TH13-04-0297

Brocklebank, V., and Kavanagh, D. (2017). Complement C5-inhibiting therapy for the thrombotic microangiopathies: accumulating evidence, but not a panacea. *Clin. Kidney J.* 10, 600–624. doi: 10.1093/ckj/sfx081

Carneiro-Lobo, T. C., Konig, S., Machado, D. E., Nasciutti, L. E., Forni, M. F., Francischetti, I. M., et al. (2009). Ixolaris, a tissue factor inhibitor, blocks primary tumor growth and angiogenesis in a glioblastoma model. *J. Thromb. Haemost.* 7, 1855–1864. doi: 10.1111/j.1538-7836.2009.03553.x

Castor, M. G., Rezende, B., Resende, C. B., Alessandri, A. L., Fagundes, C. T., Sousa, L. P., et al. (2010). The CCL3/macrophage inflammatory protein-1alpha-binding protein evasin-1 protects from graft-versus-host disease but does not modify graft-versus-leukemia in mice. *J. Immunol.* 184, 2646–2654. doi: 10.4049/jimmunol.0902614

Charo, I. F., and Ransohoff, R. M. (2006). The many roles of chemokines and chemokine receptors in inflammation. *N. Engl. J. Med.* 354, 610–621. doi: 10.1056/nejmra052723

Chen, Z., Wang, B., Hu, J., Yang, W., Cao, Z., Zhuo, R., et al. (2013). SjAPI, the first functionally characterized Ascaris-type protease inhibitor from animal venoms. *PLoS One* 8:e57529. doi: 10.1371/journal.pone.0057529

Cherniack, E. P. (2011). Bugs as drugs, part two: worms, leeches, scorpions, snails, ticks, centipedes, and spiders. *Altern. Med. Rev.* 16, 50–58.

Chmelar, J., Calvo, E., Pedra, J. H., Francischetti, I. M., and Kotsyfakis, M. (2012). Tick salivary secretion as a source of antihemostatics. *J. Proteomics* 75, 3842–3854. doi: 10.1016/j.jprot.2012.04.026

Chmelar, J., Kotal, J., Kopecky, J., Pedra, J. H. F., and Kotsyfakis, M. (2016). All for one and one for all on the tick-host battlefield. *Trends Parasitol.* 32, 368–377. doi: 10.1016/j.pt.2016.01.004

Chmelar, J., Kotal, J., Langhansova, H., and Kotsyfakis, M. (2017). Protease inhibitors in tick saliva: the role of serpins and cystatins in tick-host-pathogen interaction. *Front. Cell Infect. Microbiol.* 7:216. doi: 10.3389/fcimb.2017.00216

Chudzinski-Tavassi, A. M., De-Sa-Junior, P. L., Simons, S. M., Maria, D. A., De Souza Ventura, J., Batista, I. F., et al. (2010). A new tick Kunitz type inhibitor, Amblyomin-X, induces tumor cell death by modulating genes related to the cell cycle and targeting the ubiquitin-proteasome system. *Toxicon* 56, 1145–1154. doi: 10.1016/j.toxicon.2010.04.019

Chudzinski-Tavassi, A. M., Maria, D. A., Batista, I. F., and Ho, P. L. (2005). *Kunitz-Type Recombinant Inhibitor*. U.S. Patent No. WO2006029492A1.

Cierpicki, T., Bania, J., and Otlewski, J. (2000). NMR solution structure of Apis mellifera chymotrypsin/cathepsin G inhibitor-1 (AMCI-1): structural similarity with *Ascaris* protease inhibitors. *Protein Sci.* 9, 976–984. doi: 10.1110/ps.9.5.976

Coipan, E. C., Jahfari, S., Fonville, M., Maassen, C. B., Van Der Giessen, J., Takken, W., et al. (2013). Spatiotemporal dynamics of emerging pathogens in questing *Ixodes ricinus*. *Front. Cell Infect. Microbiol.* 3:36. doi: 10.3389/fcimb.2013.00036

Copin, J. C., Da Silva, R. F., Fraga-Silva, R. A., Capettini, L., Quintao, S., Lenglet, S., et al. (2013). Treatment with Evasin-3 reduces atherosclerotic vulnerability for ischemic stroke, but not brain injury in mice. *J. Cereb. Blood Flow Metab.* 33, 490–498. doi: 10.1038/jcbfm.2012.198

Corral-Rodriguez, M. A., Macedo-Ribeiro, S., Barbosa Pereira, P. J., and Fuentes-Prior, P. (2009). Tick-derived Kunitz-type inhibitors as antihemostatic factors. *Insect. Biochem. Mol. Biol.* 39, 579–595. doi: 10.1016/j.ibmb.2009.07.003

Couillin, I., Maillet, I., Vargaftig, B. B., Jacobs, M., Paesen, G. C., Nuttall, P. A., et al. (2004). Arthropod-derived histamine-binding protein prevents murine allergic asthma. *J. Immunol.* 173, 3281–3286. doi: 10.4049/jimmunol.173.5.3281

Dai, J., Wang, P., Adusumilli, S., Booth, C. J., Narasimhan, S., Anguita, J., et al. (2009). Antibodies against a tick protein, Salp15, protect mice from the Lyme disease agent. *Cell Host Microbe.* 6, 482–492. doi: 10.1016/j.chom.2009.10.006

Das, S., Banerjee, G., Deponte, K., Marcantonio, N., Kantor, F. S., and Fikrig, E. (2001). Salp25D, an *Ixodes scapularis* antioxidant, is 1 of 14 immunodominant antigens in engorged tick salivary glands. *J. Infect. Dis.* 184, 1056–1064. doi: 10.1086/323351

de Castro, M. H., De Klerk, D., Pienaar, R., Latif, A. A., Rees, D. J., and Mans, B. J. (2016). De novo assembly and annotation of the salivary gland transcriptome of *Rhipicephalus appendiculatus* male and female ticks during blood feeding. *Ticks Tick Borne Dis.* 7, 536–548. doi: 10.1016/j.ttbdis.2016.01.014

De Groot, A. S., and Scott, D. W. (2007). Immunogenicity of protein therapeutics. *Trends Immunol.* 28, 482–490. doi: 10.1016/j.it.2007.07.011

de Souza, J. G., Morais, K. L., Angles-Cano, E., Boufleur, P., De Mello, E. S., Maria, D. A., et al. (2016). Promising pharmacological profile of a Kunitz-type inhibitor in murine renal cell carcinoma model. *Oncotarget* 7, 62255–62266. doi: 10.18632/oncotarget.11555

Decrem, Y., Rath, G., Blasioli, V., Cauchie, P., Robert, S., Beaufays, J., et al. (2009). Ir-CPI, a coagulation contact phase inhibitor from the tick *Ixodes ricinus*, inhibits thrombus formation without impairing hemostasis. *J. Exp. Med.* 206, 2381–2395. doi: 10.1084/jem.20091007

Dehhaghi, M., Kazemi Shariat Panahi, H., Holmes, E. C., Hudson, B. J., Schloeffel, R., and Guillemin, G. J. (2019). Human tick-borne diseases in Australia. *Front. Cell Infect. Microbiol.* 9:3. doi: 10.3389/fcimb.2019.00003

den Dunnen, J., Gringhuis, S. I., and Geijtenbeek, T. B. (2009). Innate signaling by the C-type lectin DC-SIGN dictates immune responses. *Cancer Immunol. Immunother.* 58, 1149–1157. doi: 10.1007/s00262-008-0615-1

Deruaz, M., Bonvin, P., Severin, I. C., Johnson, Z., Krohn, S., Power, C. A., et al. (2013). Evasin-4, a tick-derived chemokine-binding protein with broad selectivity can be modified for use in preclinical disease models. *FEBS J.* 280, 4876–4887. doi: 10.1111/febs.12463

Deruaz, M., Frauenschuh, A., Alessandri, A. L., Dias, J. M., Coelho, F. M., Russo, R. C., et al. (2008). Ticks produce highly selective chemokine binding proteins with antiinflammatory activity. *J. Exp. Med.* 205, 2019–2031. doi: 10.1084/jem.20072689

El-Tantawy, N. L. (2015). Helminthes and insects: maladies or therapies. *Parasitol. Res.* 114, 359–377. doi: 10.1007/s00436-014-4260-7

Esteves, E., Maruyama, S. R., Kawahara, R., Fujita, A., Martins, L. A., Righi, A. A., et al. (2017). Analysis of the salivary gland transcriptome of unfed and partially fed amblyomma sculptum ticks and descriptive proteome of the saliva. *Front. Cell Infect. Microbiol.* 7:476. doi: 10.3389/fcimb.2017.00476

Francischetti, I. M., Mather, T. N., and Ribeiro, J. M. (2003). Cloning of a salivary gland metalloprotease and characterization of gelatinase and fibrin(ogen)lytic activities in the saliva of the Lyme disease tick vector *Ixodes scapularis*. *Biochem. Biophys. Res. Commun.* 305, 869–875. doi: 10.1016/s0006-291x(03)00857-x

Francischetti, I. M., Meng, Z., Mans, B. J., Gudderra, N., Hall, M., Veenstra, T. D., et al. (2008). An insight into the salivary transcriptome and proteome of the soft tick and vector of epizootic bovine abortion, *Ornithodoros coriaceus*. *J. Proteomics* 71, 493–512. doi: 10.1016/j.jprot.2008.07.006

Francischetti, I. M., My Pham, V., Mans, B. J., Andersen, J. F., Mather, T. N., Lane, R. S., et al. (2005). The transcriptome of the salivary glands of the female western black-legged tick *Ixodes pacificus* (Acari: Ixodidae). *Insect. Biochem. Mol. Biol.* 35, 1142–1161. doi: 10.1016/j.ibmb.2005.05.007

Francischetti, I. M., Sa-Nunes, A., Mans, B. J., Santos, I. M., and Ribeiro, J. M. (2009). The role of saliva in tick feeding. *Front. Biosci.* 14, 2051–2088. doi: 10.2741/3363

Frauenschuh, A., Power, C. A., Deruaz, M., Ferreira, B. R., Silva, J. S., Teixeira, M. M., et al. (2007). Molecular cloning and characterization of a highly selective chemokine-binding protein from the tick *Rhipicephalus sanguineus*. *J. Biol. Chem.* 282, 27250–27258. doi: 10.1074/jbc.m704706200

Fredslund, F., Laursen, N. S., Roversi, P., Jenner, L., Oliveira, C. L., Pedersen, J. S., et al. (2008). Structure of and influence of a tick complement inhibitor on human complement component 5. *Nat. Immunol.* 9, 753–760. doi: 10.1038/ni.1625

Garg, R., Juncadella, I. J., Ramamoorthi, N., Ashish Ananthanarayanan, S. K., Thomas, V., Rincón, M., et al. (2006). Cutting edge: CD4 is the receptor for the tick saliva immunosuppressor, Salp15. *J. Immunol.* 177, 6579–6583. doi: 10.4049/jimmunol.177.10.6579

Goodship, T. H. J., Pinto, F., Weston-Davies, W. H., Silva, J., Nishimura, J. I., Nunn, M. A., et al. (2017). Use of the complement inhibitor coversin to treat HSCT-associated TMA. *Blood Adv.* 1, 1254–1258. doi: 10.1182/bloodadvances.2016002832

Grammer, A. C., and Lipsky, P. E. (2017). Drug repositioning strategies for the identification of novel therapies for rheumatic autoimmune inflammatory diseases. *Rheum. Dis. Clin. North Am.* 43, 467–480. doi: 10.1016/j.rdc.2017.04.010

Guo, X., Booth, C. J., Paley, M. A., Wang, X., Deponte, K., Fikrig, E., et al. (2009). Inhibition of neutrophil function by two tick salivary proteins. *Infect. Immun.* 77, 2320–2329. doi: 10.1128/IAI.01507-08

Hammer, J. F., Jenkins, C., Bogema, D., and Emery, D. (2016). Mechanical transfer of Theileria orientalis: possible roles of biting arthropods, colostrum and husbandry practices in disease transmission. *Parasit. Vectors* 9:34. doi: 10.1186/s13071-016-1323-x

Hayward, J., Sanchez, J., Perry, A., Huang, C., Rodriguez Valle, M., Canals, M., et al. (2017). Ticks from diverse genera encode chemokine-inhibitory evasin proteins. *J. Biol. Chem.* 292, 15670–15680. doi: 10.1074/jbc.M117.807255

Hovius, J. W., De Jong, M. A., Den Dunnen, J., Litjens, M., Fikrig, E., Van Der Poll, T., et al. (2008). Salp15 binding to DC-SIGN inhibits cytokine expression by impairing both nucleosome remodeling and mRNA stabilization. *PLoS Pathog.* 4:e31. doi: 10.1371/journal.ppat.0040031

Huang, C., Zheng, C., Li, Y., Wang, Y., Lu, A., and Yang, L. (2014). Systems pharmacology in drug discovery and therapeutic insight for herbal medicines. *Brief. Bioinform.* 15, 710–733. doi: 10.1093/bib/bbt035

Huang, K., Strynadka, N. C., Bernard, V. D., Peanasky, R. J., and James, M. N. (1994). The molecular structure of the complex of *Ascaris* chymotrypsin/elastase inhibitor with porcine elastase. *Structure* 2, 679–689. doi: 10.1016/s0969-2126(00)00068-x

Izaguirre, G., Arciniega, M., and Quezada, A. G. (2019). Specific and selective inhibitors of proprotein convertases engineered by transferring serpin b8 reactive-site and exosite determinants of reactivity to the serpin alpha1PDX. *Biochemistry* 58, 1679–1688. doi: 10.1021/acs.biochem.8b01295

Izaguirre, G., Qi, L., Lima, M., and Olson, S. T. (2013). Identification of serpin determinants of specificity and selectivity for furin inhibition through studies of alpha1PDX (alpha1-protease inhibitor Portland)-serpin B8 and furin active-site loop chimeras. *J. Biol. Chem.* 288, 21802–21814. doi: 10.1074/jbc.M113.462804

Jahfari, S., Hofhuis, A., Fonville, M., Van Der Giessen, J., Van Pelt, W., and Sprong, H. (2016). Molecular detection of tick-borne pathogens in humans with tick bites and erythema migrans, in the Netherlands. *PLoS Negl. Trop Dis.* 10:e0005042. doi: 10.1371/journal.pntd.0005042

Jokerst, J. V., Lobovkina, T., Zare, R. N., and Gambhir, S. S. (2011). Nanoparticle PEGylation for imaging and therapy. *Nanomedicine* 6, 715–728. doi: 10.2217/nnm.11.19

Jongejan, F., and Uilenberg, G. (2004). The global importance of ticks. *Parasitology* 129, S3–S14.

Jorgensen, J. T. (2011). A challenging drug development process in the era of personalized medicine. *Drug Discov. Today* 16, 891–897. doi: 10.1016/j.drudis.2011.09.010

Juncadella, I. J., and Anguita, J. (2009). The immunosuppresive tick salivary protein, Salp15. *Adv. Exp. Med. Biol.* 666, 121–131. doi: 10.1007/978-1-4419-1601-3_10

Juncadella, I. J., Bates, T. C., Suleiman, R., Monteagudo-Mera, A., Olson, CM., Jr., Navasa, N., et al. (2010). The tick saliva immunosuppressor, Salp15, contributes to Th17-induced pathology during experimental autoimmune encephalomyelitis. *Biochem. Biophys. Res. Commun.* 402, 105–109. doi: 10.1016/j.bbrc.2010.09.125

Juncadella, I. J., Garg, R., Ananthnarayanan, S. K., Yengo, C. M., and Anguita, J. (2007). T-cell signaling pathways inhibited by the tick saliva immunosuppressor, Salp15. *FEMS Immunol. Med. Microbiol.* 49, 433–438. doi: 10.1111/j.1574-695x.2007.00223.x

Juncadella, I. J., Garg, R., Bates, T. C., Olivera, E. R., and Anguita, J. (2008). The Ixodes scapularis salivary protein, salp15, prevents the association of HIV-1

gp120 and CD4. *Biochem. Biophys. Res. Commun.* 367, 41–46. doi: 10.1016/j.bbrc.2007.12.104

Karczewski, J., and Connolly, T. M. (1997). The interaction of disagregin with the platelet fibrinogen receptor, glycoprotein IIb-IIIa. *Biochem. Biophys. Res. Commun.* 241, 744–748. doi: 10.1006/bbrc.1997.7881

Karczewski, J., Endris, R., and Connolly, T. M. (1994). Disagregin is a fibrinogen receptor antagonist lacking the Arg-Gly-Asp sequence from the tick, *Ornithodoros moubata*. *J. Biol. Chem.* 269, 6702–6708.

Karim, S., and Ribeiro, J. M. (2015). An insight into the sialome of the lone star tick, amblyomma americanum, with a glimpse on its time dependent gene expression. *PLoS One* 10:e0131292. doi: 10.1371/journal.pone.0131292

Kazimirova, M., and Stibraniova, I. (2013). Tick salivary compounds: their role in modulation of host defences and pathogen transmission. *Front. Cell Infect. Microbiol.* 3:43. doi: 10.3389/fcimb.2013.00043

Kazimirova, M., Thangamani, S., Bartikova, P., Hermance, M., Holikova, V., Stibraniova, I., et al. (2017). Tick-borne viruses and biological processes at the tick-host-virus interface. *Front. Cell Infect. Microbiol.* 7:339. doi: 10.3389/fcimb.2017.00339

Keller, P. M., Waxman, L., Arnold, B. A., Schultz, L. D., Condra, C., and Connolly, T. M. (1993). Cloning of the cDNA and expression of moubatin, an inhibitor of platelet aggregation. *J. Biol. Chem.* 268, 5450–5456.

Kim, T. K., Tirloni, L., Pinto, A. F., Moresco, J., Yates, J. R. III, Da Silva Vaz, I., et al. (2016). Ixodes scapularis tick saliva proteins sequentially secreted every 24 h during blood feeding. *PLoS Negl. Trop Dis.* 10:e0004323. doi: 10.1371/journal.pntd.0004323

Kotal, J., Langhansova, H., Lieskovska, J., Andersen, J. F., Francischetti, I. M., Chavakis, T., et al. (2015). Modulation of host immunity by tick saliva. *J. Proteomics* 128, 58–68. doi: 10.1016/j.jprot.2015.07.005

Kuhn, N., Schmidt, C. Q., Schlapschy, M., and Skerra, A. (2016). PASylated coversin, a C5-Specific complement inhibitor with extended pharmacokinetics, shows enhanced anti-hemolytic activity in vitro. *Bioconjug. Chem.* 27, 2359–2371. doi: 10.1021/acs.bioconjchem.6b00369

Li, F. S., and Weng, J. K. (2017). Demystifying traditional herbal medicine with modern approach. *Nat. Plants* 3:17109. doi: 10.1038/nplants.2017.109

Lieskovska, J., Palenikova, J., Sirmarova, J., Elsterova, J., Kotsyfakis, M., Campos Chagas, A., et al. (2015). Tick salivary cystatin sialostatin L2 suppresses IFN responses in mouse dendritic cells. *Parasite Immunol.* 37, 70–78. doi: 10.1111/pim.12162

Lung, O., Tram, U., Finnerty, C. M., Eipper-Mains, M. A., Kalb, J. M., and Wolfner, M. F. (2002). The Drosophila melanogaster seminal fluid protein Acp62F is a protease inhibitor that is toxic upon ectopic expression. *Genetics* 160, 211–224.

Mans, B. J., Andersen, J. F., Schwan, T. G., and Ribeiro, J. M. (2008a). Characterization of anti-hemostatic factors in the argasid, Argas monolakensis: implications for the evolution of blood-feeding in the soft tick family. *Insect. Biochem. Mol. Biol.* 38, 22–41. doi: 10.1016/j.ibmb.2007.09.002

Mans, B. J., Ribeiro, J. M., and Andersen, J. F. (2008b). Structure, function, and evolution of biogenic amine-binding proteins in soft ticks. *J. Biol. Chem.* 283, 18721–18733. doi: 10.1074/jbc.M800188200

Mans, B. J., Louw, A. I., and Neitz, A. W. (2002a). Disaggregation of aggregated platelets by savignygrin, a alphaIIbeta3 antagonist from *Ornithodoros savignyi*. *Exp. Appl. Acarol.* 27, 231–239.

Mans, B. J., Louw, A. I., and Neitz, A. W. (2002b). Savignygrin, a platelet aggregation inhibitor from the soft tick *Ornithodoros savignyi*, presents the RGD integrin recognition motif on the Kunitz-BPTI fold. *J. Biol. Chem.* 277, 21371–21378. doi: 10.1074/jbc.m112060200

Mans, B. J., and Ribeiro, J. M. (2008). Function, mechanism and evolution of the moubatin-clade of soft tick lipocalins. *Insect. Biochem. Mol. Biol.* 38, 841–852. doi: 10.1016/j.ibmb.2008.06.007

Marcet-Palacios, M., Ewen, C., Pittman, E., Duggan, B., Carmine-Simmen, K., Fahlman, R. P., et al. (2015). Design and characterization of a novel human Granzyme B inhibitor. *Protein Eng. Des. Sel.* 28, 9–17. doi: 10.1093/protein/gzu052

Marchal, C., Schramm, F., Kern, A., Luft, B. J., Yang, X., Schuijt, T. J., et al. (2011). Antialarmin effect of tick saliva during the transmission of Lyme disease. *Infect. Immun.* 79, 774–785. doi: 10.1128/IAI.00482-10

Mignogna, G., Pascarella, S., Wechselberger, C., Hinterleitner, C., Mollay, C., Amiconi, G., et al. (1996). BSTI, a trypsin inhibitor from skin secretions of Bombina bombina related to protease inhibitors of nematodes. *Protein Sci.* 5, 357–362. doi: 10.1002/pro.5560050220

Montecucco, F., Lenglet, S., Braunersreuther, V., Pelli, G., Pellieux, C., Montessuit, C., et al. (2010). Single administration of the CXC chemokine-binding protein Evasin-3 during ischemia prevents myocardial reperfusion injury in mice. *Arterioscler. Thromb. Vasc. Biol.* 30, 1371–1377. doi: 10.1161/ATVBAHA.110.206011

Montecucco, F., Mach, F., Lenglet, S., Vonlaufen, A., Gomes Quindere, A. L., Pelli, G., et al. (2014). Treatment with Evasin-3 abrogates neutrophil-mediated inflammation in mouse acute pancreatitis. *Eur. J. Clin. Invest.* 44, 940–950. doi: 10.1111/eci.12327

Mudenda, L., Pierle, S. A., Turse, J. E., Scoles, G. A., Purvine, S. O., Nicora, C. D., et al. (2014). Proteomics informed by transcriptomics identifies novel secreted proteins in *Dermacentor andersoni* saliva. *Int. J. Parasitol.* 44, 1029–1037. doi: 10.1016/j.ijpara.2014.07.003

Narasimhan, S., Koski, R. A., Beaulieu, B., Anderson, J. F., Ramamoorthi, N., Kantor, F., et al. (2002). A novel family of anticoagulants from the saliva of Ixodes scapularis. *Insect. Mol. Biol.* 11, 641–650. doi: 10.1046/j.1365-2583.2002.00375.x

Narasimhan, S., Montgomery, R. R., Deponte, K., Tschudi, C., Marcantonio, N., Anderson, J. F., et al. (2004). Disruption of Ixodes scapularis anticoagulation by using RNA interference. *Proc. Natl. Acad. Sci. U.S.A.* 101, 1141–1146. doi: 10.1073/pnas.0307669100

Neelakanta, G., and Sultana, H. (2015). Transmission-blocking vaccines: focus on anti-vector vaccines against tick-borne diseases. *Arch. Immunol. Ther. Exp.* 63, 169–179. doi: 10.1007/s00005-014-0324-8

Nunn, M. A. (2004). *Complement Inhibitors From Ticks*. U.S. Patent No. WO2004106369A2.

Nunn, M. A., Sharma, A., Paesen, G. C., Adamson, S., Lissina, O., Willis, A. C., et al. (2005). Complement inhibitor of C5 activation from the soft tick *Ornithodoros moubata*. *J. Immunol.* 174, 2084–2091. doi: 10.4049/jimmunol.174.4.2084

Nuttall, P. A., and Labuda, M. (2004). Tick-host interactions: saliva-activated transmission. *Parasitology* 129, S177–S189.

Nuttall, P. A., and Labuda, M. (2008). "Saliva-assisted transmission of tick-borne pathogens," in *Ticks: Biology, Disease and Control*, eds A. S. Bowman and P. A. Nuttall (Cambridge: Cambridge University Press), 205–219. doi: 10.1017/cbo9780511551802.011

Nuttall, P. A., and Paesen, G. C. (2000). *Tryptase Inhibitor*. U.S. Patent No. WO2001005823A2.

Oleaga, A., Escudero-Poblacion, A., Camafeita, E., and Perez-Sanchez, R. (2007). A proteomic approach to the identification of salivary proteins from the argasid ticks *Ornithodoros moubata* and *Ornithodoros erraticus*. *Insect. Biochem. Mol. Biol.* 37, 1149–1159. doi: 10.1016/j.ibmb.2007.07.003

Oliveira, C. J., Anatriello, E., De Miranda-Santos, I. K., Francischetti, I. M., Sa-Nunes, A., Ferreira, B. R., et al. (2013). Proteome of *Rhipicephalus sanguineus* tick saliva induced by the secretagogues pilocarpine and dopamine. *Ticks Tick Borne Dis.* 4, 469–477. doi: 10.1016/j.ttbdis.2013.05.001

Paesen, G. C., Adams, P. L., Harlos, K., Nuttall, P. A., and Stuart, D. I. (1999). Tick histamine-binding proteins: isolation, cloning, and three-dimensional structure. *Mol. Cell* 3, 661–671. doi: 10.1016/s1097-2765(00)80359-7

Parizi, L. F., Ali, A., Tirloni, L., Oldiges, D. P., Sabadin, G. A., Coutinho, M. L., et al. (2018). Peptidase inhibitors in tick physiology. *Med. Vet. Entomol.* 32, 129–144. doi: 10.1111/mve.12276

Paul, S. M., Mytelka, D. S., Dunwiddie, C. T., Persinger, C. C., Munos, B. H., Lindborg, S. R., et al. (2010). How to improve R&D productivity: the pharmaceutical industry's grand challenge. *Nat. Rev. Drug Discov.* 9, 203–214.

Paveglio, S. A., Allard, J., Mayette, J., Whittaker, L. A., Juncadella, I., Anguita, J., et al. (2007). The tick salivary protein, Salp15, inhibits the development of experimental asthma. *J. Immunol.* 178, 7064–7071. doi: 10.4049/jimmunol.178.11.7064

Pischke, S. E., Gustavsen, A., Orrem, H. L., Egge, K. H., Courivaud, F., Fontenelle, H., et al. (2017). Complement factor 5 blockade reduces porcine myocardial infarction size and improves immediate cardiac function. *Basic Res. Cardiol.* 112:20. doi: 10.1007/s00395-017-0610-9

Porter, L. M., Radulovic, Z. M., and Mulenga, A. (2017). A repertoire of protease inhibitor families in *Amblyomma americanum* and other tick species: inter-species comparative analyses. *Parasit. Vectors* 10:152. doi: 10.1186/s13071-017-2080-1

Pospisilova, T., Urbanova, V., Hes, O., Kopacek, P., Hajdusek, O., and Sima, R. (2019). Tracking of Borrelia afzelii transmission from infected Ixodes ricinus nymphs to mice. *Infect. Immun.* 87:e00896-18. doi: 10.1128/IAI.00896-18

Preston, S. G., Majtan, J., Kouremenou, C., Rysnik, O., Burger, L. F., Cabezas Cruz, A., et al. (2013). Novel immunomodulators from hard ticks selectively reprogramme human dendritic cell responses. *PLoS Pathog.* 9:e1003450. doi: 10.1371/journal.ppat.1003450

Ramamoorthi, N., Narasimhan, S., Pal, U., Bao, F., Yang, X. F., Fish, D., et al. (2005). The Lyme disease agent exploits a tick protein to infect the mammalian host. *Nature* 436, 573–577. doi: 10.1038/nature03812

Ratcliffe, N., Azambuja, P., and Mello, C. B. (2014). Recent advances in developing insect natural products as potential modern day medicines. *Evid. Based Complement. Alternat. Med.* 2014:904958. doi: 10.1155/2014/904958

Ribeiro, J. M., and Francischetti, I. M. (2003). Role of arthropod saliva in blood feeding: sialome and post-sialome perspectives. *Annu. Rev. Entomol.* 48, 73–88. doi: 10.1146/annurev.ento.48.060402.102812

Ribeiro, J. M., Makoul, G. T., Levine, J., Robinson, D. R., and Spielman, A. (1985). Antihemostatic, antiinflammatory, and immunosuppressive properties of the saliva of a tick, *Ixodes dammini*. *J. Exp. Med.* 161, 332–344. doi: 10.1084/jem.161.2.332

Ribeiro, J. M., Slovak, M., and Francischetti, I. M. (2017). An insight into the sialome of *Hyalomma* excavatum. *Ticks Tick Borne Dis.* 8, 201–207. doi: 10.1016/j.ttbdis.2016.08.011

Romay-Penabad, Z., Carrera Marin, A. L., Willis, R., Weston-Davies, W., Machin, S., Cohen, H., et al. (2014). Complement C5-inhibitor rEV576 (coversin) ameliorates in-vivo effects of antiphospholipid antibodies. *Lupus* 23, 1324–1326. doi: 10.1177/0961203314546022

Roversi, P., Johnson, S., Preston, S. G., Nunn, M. A., Paesen, G. C., Austyn, J. M., et al. (2017). Structural basis of cholesterol binding by a novel clade of dendritic cell modulators from ticks. *Sci. Rep.* 7:16057. doi: 10.1038/s41598-017-16413-2

Russo, R. C., Alessandri, A. L., Garcia, C. C., Cordeiro, B. F., Pinho, V., Cassali, G. D., et al. (2011). Therapeutic effects of evasin-1, a chemokine binding protein, in bleomycin-induced pulmonary fibrosis. *Am. J. Respir. Cell Mol. Biol.* 45, 72–80. doi: 10.1165/rcmb.2009-0406OC

Ryffel, B., Couillin, I., Maillet, I., Schnyder, B., Paesen, G. C., Nuttall, P., et al. (2005). Histamine scavenging attenuates endotoxin-induced acute lung injury. *Ann. N. Y. Acad. Sci.* 1056, 197–205. doi: 10.1196/annals.1352.034

Sangamnatdej, S., Paesen, G. C., Slovak, M., and Nuttall, P. A. (2002). A high affinity serotonin- and histamine-binding lipocalin from tick saliva. *Insect. Mol. Biol.* 11, 79–86. doi: 10.1046/j.0962-1075.2001.00311.x

Schlapschy, M., Binder, U., Borger, C., Theobald, I., Wachinger, K., Kisling, S., et al. (2013). PASylation: a biological alternative to PEGylation for extending the plasma half-life of pharmaceutically active proteins. *Protein Eng. Des. Sel.* 26, 489–501. doi: 10.1093/protein/gzt023

Schuijt, T. J., Coumou, J., Narasimhan, S., Dai, J., Deponte, K., Wouters, D., et al. (2011a). A tick mannose-binding lectin inhibitor interferes with the vertebrate complement cascade to enhance transmission of the lyme disease agent. *Cell Host Microbe.* 10, 136–146. doi: 10.1016/j.chom.2011.06.010

Schuijt, T. J., Narasimhan, S., Daffre, S., Deponte, K., Hovius, J. W., Van't Veer, C., et al. (2011b). Identification and characterization of *Ixodes scapularis* antigens that elicit tick immunity using yeast surface display. *PLoS One* 6:e15926. doi: 10.1371/journal.pone.0015926

Schwarz, A., Cabezas-Cruz, A., Kopecky, J., and Valdes, J. J. (2014). Understanding the evolutionary structural variability and target specificity of tick salivary Kunitz peptides using next generation transcriptome data. *BMC Evol. Biol.* 14:4. doi: 10.1186/1471-2148-14-4

Schwarz, A., Valdes, J. J., and Kotsyfakis, M. (2012). The role of cystatins in tick physiology and blood feeding. *Ticks Tick Borne Dis.* 3, 117–127. doi: 10.1016/j.ttbdis.2012.03.004

Schwarz, A., Von Reumont, B. M., Erhart, J., Chagas, A. C., Ribeiro, J. M., and Kotsyfakis, M. (2013). De novo Ixodes ricinus salivary gland transcriptome analysis using two next-generation sequencing methodologies. *FASEB J.* 27, 4745–4756. doi: 10.1096/fj.13-232140

Shim, J. S., and Liu, J. O. (2014). Recent advances in drug repositioning for the discovery of new anticancer drugs. *Int. J. Biol. Sci.* 10, 654–663. doi: 10.7150/ijbs.9224

Silverman, G. A., Whisstock, J. C., Bottomley, S. P., Huntington, J. A., Kaiserman, D., Luke, C. J., et al. (2010). Serpins flex their muscle: I. Putting the clamps on proteolysis in diverse biological systems. *J. Biol. Chem.* 285, 24299–24305. doi: 10.1074/jbc.R110.112771

Simo, L., Kazimirova, M., Richardson, J., and Bonnet, S. I. (2017). The essential role of tick salivary glands and saliva in tick feeding and pathogen transmission. *Front. Cell Infect. Microbiol.* 7:281. doi: 10.3389/fcimb.2017.00281

Soltys, J., Kusner, L. L., Young, A., Richmonds, C., Hatala, D., Gong, B., et al. (2009). Novel complement inhibitor limits severity of experimentally myasthenia gravis. *Ann. Neurol.* 65, 67–75. doi: 10.1002/ana.21536

Song, Y., Gong, K., Yan, H., Hong, W., Wang, L., Wu, Y., et al. (2014). Sj7170, a unique dual-function peptide with a specific alpha-chymotrypsin inhibitory activity and a potent tumor-activating effect from scorpion venom. *J. Biol. Chem.* 289, 11667–11680. doi: 10.1074/jbc.M113.540419

Stassens, P., Bergum, P. W., Gansemans, Y., Jespers, L., Laroche, Y., Huang, S., et al. (1996). Anticoagulant repertoire of the hookworm *Ancylostoma caninum*. *Proc. Natl. Acad. Sci. U.S.A.* 93, 2149–2154. doi: 10.1073/pnas.93.5.2149

Swanson, S. J., Neitzel, D., Reed, K. D., and Belongia, E. A. (2006). Coinfections acquired from ixodes ticks. *Clin. Microbiol. Rev.* 19, 708–727. doi: 10.1128/cmr.00011-06

Tang, J., Fang, Y., Han, Y., Bai, X., Yan, X., Zhang, Y., et al. (2015). YY-39, a tick anti-thrombosis peptide containing RGD domain. *Peptides* 68, 99–104. doi: 10.1016/j.peptides.2014.08.008

Tirloni, L., Islam, M. S., Kim, T. K., Diedrich, J. K., Yates, J. R. III, Pinto, A. F., et al. (2015). Saliva from nymph and adult females of *Haemaphysalis longicornis*: a proteomic study. *Parasit. Vectors* 8:338. doi: 10.1186/s13071-015-0918-y

Tirloni, L., Kim, T. K., Pinto, A. F. M., Yates, J. R. III, Da Silva Vaz, I. Jr., et al. (2017). Tick-host range adaptation: changes in protein profiles in unfed adult *Ixodes scapularis* and *Amblyomma americanum* saliva stimulated to feed on different hosts. *Front. Cell Infect. Microbiol.* 7:517. doi: 10.3389/fcimb.2017.00517

Tirloni, L., Reck, J., Terra, R. M., Martins, J. R., Mulenga, A., Sherman, N. E., et al. (2014). Proteomic analysis of cattle tick *Rhipicephalus* (Boophilus) microplus saliva: a comparison between partially and fully engorged females. *PLoS One* 9:e94831. doi: 10.1371/journal.pone.0094831

Tomas-Cortazar, J., Martin-Ruiz, I., Barriales, D., Pascual-Itoiz, M. A., De Juan, V. G., Caro-Maldonado, A., et al. (2017). The immunosuppressive effect of the tick protein, Salp15, is long-lasting and persists in a murine model of hematopoietic transplant. *Sci. Rep.* 7:10740. doi: 10.1038/s41598-017-11354-2

Tuppurainen, E. S., Stoltsz, W. H., Troskie, M., Wallace, D. B., Oura, C. A., Mellor, P. S., et al. (2011). A potential role for ixodid (hard) tick vectors in the transmission of lumpy skin disease virus in cattle. *Transbound. Emerg. Dis.* 58, 93–104. doi: 10.1111/j.1865-1682.2010.01184.x

Valenzuela, J. G., Francischetti, I. M., Pham, V. M., Garfield, M. K., Mather, T. N., and Ribeiro, J. M. (2002). Exploring the sialome of the tick *Ixodes scapularis*. *J. Exp. Biol.* 205, 2843–2864.

Veronese, F. M., and Mero, A. (2008). The impact of PEGylation on biological therapies. *BioDrugs* 22, 315–329. doi: 10.2165/00063030-200822050-00004

Vieira, A. T., Fagundes, C. T., Alessandri, A. L., Castor, M. G., Guabiraba, R., Borges, V. O., et al. (2009). Treatment with a novel chemokine-binding protein or eosinophil lineage-ablation protects mice from experimental colitis. *Am. J. Pathol.* 175, 2382–2391. doi: 10.2353/ajpath.2009.090093

Wagemakers, A., Coumou, J., Schuijt, T. J., Oei, A., Nijhof, A. M., Van 't Veer, C., et al. (2016). An *Ixodes ricinus* tick salivary lectin pathway inhibitor protects borrelia burgdorferi sensu lato from human complement. *Vector Borne Zoonotic Dis.* 16, 223–228. doi: 10.1089/vbz.2015.1901

Wang, X., Coons, L. B., Taylor, D. B., Stevens, S. E. Jr., and Gartner, T. K. (1996). Variabilin, a novel RGD-containing antagonist of glycoprotein IIb-IIIa and platelet aggregation inhibitor from the hard tick *Dermacentor variabilis*. *J. Biol. Chem.* 271, 17785–17790. doi: 10.1074/jbc.271.30.17785

Wang, X., Huang, Y., Niu, S. B., Jiang, B. G., Jia, N., Van Der Geest, L., et al. (2014). Genetic diversity of Salp15 in the Ixodes ricinus complex (Acari: Ixodidae). *PLoS One* 9:e94131. doi: 10.1371/journal.pone.0094131

Wang, X. J., Ren, J. L., Zhang, A. H., Sun, H., Yan, G. L., Han, Y., et al. (2019). Novel applications of mass spectrometry-based metabolomics in herbal medicines and its active ingredients: current evidence. *Mass Spectrom Rev.* [Epub ahead of print]

Wang, Y., Li, Z., Zhou, Y., Cao, J., Zhang, H., Gong, H., et al. (2016). Specific histamine binding activity of a new lipocalin from *Hyalomma* asiaticum (Ixodidae) and therapeutic effects on allergic asthma in mice. *Parasit. Vectors* 9:506. doi: 10.1186/s13071-016-1790-0

Weston-Davies, W., Couillin, I., Schnyder, S., Schnyder, B., Moser, R., Lissina, O., et al. (2005). Arthropod-derived protein EV131 inhibits histamine action and allergic asthma. *Ann. N. Y. Acad. Sci.* 1056, 189–196. doi: 10.1196/annals.1352.009

Whisstock, J. C., Silverman, G. A., Bird, P. I., Bottomley, S. P., Kaiserman, D., Luke, C. J., et al. (2010). Serpins flex their muscle: II. Structural insights into target peptidase recognition, polymerization, and transport functions. *J. Biol. Chem.* 285, 24307–24312. doi: 10.1074/jbc.R110.141408

Wikel, S. (2013). Ticks and tick-borne pathogens at the cutaneous interface: host defenses, tick countermeasures, and a suitable environment for pathogen establishment. *Front. Microbiol.* 4:337. doi: 10.3389/fmicb.2013.00337

Wikel, S. K. (1982). Influence of Dermacentor andersoni infestation on lymphocyte responsiveness to mitogens. *Ann. Trop Med. Parasitol.* 76, 627–632. doi: 10.1080/00034983.1982.11687593

Xu, X. L., Cheng, T. Y., Yang, H., Yan, F., and Yang, Y. (2015). De novo sequencing, assembly and analysis of salivary gland transcriptome of *Haemaphysalis* flava and identification of sialoprotein genes. *Infect. Genet. Evol.* 32, 135–142. doi: 10.1016/j.meegid.2015.03.010

Yu, X., Gong, H., Zhou, Y., Zhang, H., Cao, J., and Zhou, J. (2015). Differential sialotranscriptomes of unfed and fed *Rhipicephalus haemaphysaloides*, with particular regard to differentially expressed genes of cysteine proteases. *Parasit. Vectors* 8:597. doi: 10.1186/s13071-015-1213-7

Zhou, W., Wang, Y., Lu, A., and Zhang, G. (2016). Systems pharmacology in small molecular drug discovery. *Int. J. Mol. Sci.* 17:246. doi: 10.3390/ijms17020246

Zhou, Y. F., Eng, E. T., Zhu, J., Lu, C., Walz, T., and Springer, T. A. (2012). Sequence and structure relationships within von Willebrand factor. *Blood* 120, 449–458. doi: 10.1182/blood-2012-01-405134

Conflict of Interest Statement: The authors declare that the research was conducted in the absence of any commercial or financial relationships that could be construed as a potential conflict of interest.

frontiers in Physiology

REVIEW
published: 03 July 2019
doi: 10.3389/fphys.2019.00830

Deciphering Biological Processes at the Tick-Host Interface Opens New Strategies for Treatment of Human Diseases

Iveta Štibrániová[1], Pavlína Bartíková[1], Viera Holíková[1] and Mária Kazimírová[2]*

[1] Biomedical Research Center, Institute of Virology, Slovak Academy of Sciences, Bratislava, Slovakia, [2] Institute of Zoology, Slovak Academy of Sciences, Bratislava, Slovakia

Ticks are obligatory blood-feeding ectoparasites, causing blood loss and skin damage in their hosts. In addition, ticks also transmit a number of various pathogenic microorganisms that cause serious diseases in humans and animals. Ticks evolved a wide array of salivary bioactive compounds that, upon injection into the host skin, inhibit or modulate host reactions such as hemostasis, inflammation and wound healing. Modulation of the tick attachment site in the host skin involves mainly molecules which affect physiological processes orchestrated by cytokines, chemokines and growth factors. Suppressing host defense reactions is crucial for tick survival and reproduction. Furthermore, pharmacologically active compounds in tick saliva have a promising therapeutic potential for treatment of some human diseases connected with disorders in hemostasis and immune system. These disorders are often associated to alterations in signaling pathways and dysregulation or overexpression of specific cytokines which, in turn, affect mechanisms of angiogenesis, cell motility and cytoskeletal regulation. Moreover, tick salivary molecules were found to exert cytotoxic and cytolytic effects on various tumor cells and have anti-angiogenic properties. Elucidation of the mode of action of tick bioactive molecules on the regulation of cell processes in their mammalian hosts could provide new tools for understanding the complex changes leading to immune disorders and cancer. Tick bioactive molecules may also be exploited as new pharmacological inhibitors of the signaling pathways of cytokines and thus help alleviate patient discomfort and increase patient survival. We review the current knowledge about tick salivary peptides and proteins that have been identified and functionally characterized in *in vitro* and/or *in vivo* models and their therapeutic perspective.

Keywords: tick saliva, immunomodulation, host defense, pharmacological molecules, immunological disorders

OPEN ACCESS

Edited by:
Itabajara Da Silva Vaz Jr., Federal University of Rio Grande do Sul, Brazil

Reviewed by:
Anderson Sa-Nunes, University of São Paulo, Brazil
Melina Garcia Guizzo, Biology Centre (ASCR), Czechia

***Correspondence:**
Pavlína Bartíková
virupaca@savba.sk

Specialty section:
This article was submitted to Invertebrate Physiology, a section of the journal Frontiers in Physiology

Received: *19 April 2019*
Accepted: *17 June 2019*
Published: *03 July 2019*

Citation:
Štibrániová I, Bartíková P, Holíková V and Kazimírová M (2019) Deciphering Biological Processes at the Tick-Host Interface Opens New Strategies for Treatment of Human Diseases. Front. Physiol. 10:830. doi: 10.3389/fphys.2019.00830

INTRODUCTION

For centuries, humans have exploited arthropods (insects, scorpions, spiders, centipedes, ticks) and other invertebrates (leeches, hookworms, snails, etc.) and their products (honey, royal jelly, venom, propolis, etc.) or biologically active substances derived from them as valuable resources to treat various diseases (Cherniack, 2010, 2011; Chen et al., 2018; Koh et al., 2018). Their properties range from immunomodulatory, analgesic, anti-bacterial, anti-coagulant, anticancer, diuretic and anesthetic to anti-rheumatic. Many human cultures, especially in Asia, Africa and South America,

have used arthropods in traditional medicine and highly appreciated their therapeutic potential. In some cases, whole organisms, in others individual ingredients have been used. The capabilities of maggots (larvae of blowflies) feeding on necrotic tissues to heal wounds are among well-studied medical application of insects (maggot therapy) (Wolf and Hansson, 2003). Of other invertebrates, medicinal leeches have been applied, e.g., in reconstructive microsurgery, and in treatment of phlebitis (Eldor et al., 1996) or osteoarthritis (Michalsen et al., 2002). Anticoagulants designed based on their product, hirudin and its derivatives, have been used as antithrombotics (Markwardt, 2002; Chudzinski-Tavassi et al., 2018; Koh et al., 2018). Endoparasitic helminths have been used to cure inflammatory bowel diseases (Buning et al., 2008), and cantharidin, a derivate from blister beetles, has been applied for warts, molluscum contagiosum (Moed et al., 2001) and in anticancer therapy (Efferth et al., 2005; Liu and Chen, 2009). The enormous richness and diversity of arthropods, the wide range of biological activities exerted by their products, the use of some species and their products or derivatives as drugs against common and important diseases suggest that arthropods are a rich, and yet unexplored and unexploited source of potentially useful compounds for development of new therapeutic agents for modern medicine (Pemberton, 1999).

Among blood-feeding arthropods, ticks occupy a unique position. Their parasitic lifestyle resulted in development of a wide spectrum of evasive and disarming mechanisms of host defense reactions. Tick salivary glands produce and secrete into the feeding site in the host skin an impressive amount and variety of bioactive molecules modulating hemostatic, inflammatory and immune responses as well as wound healing. The composition of tick saliva is highly complex and changes through the feeding process. There are a few comprehensive and recent reviews on the composition and role of saliva in tick feeding and tick-host-pathogen interactions (Francischetti et al., 2009; Kotal et al., 2015; Blisnick et al., 2017; Šimo et al., 2017; Nuttall, 2018; Wikel, 2018). They all highlight the fact that only an integrated understanding of the physiological roles of tick bioactive molecules and their mode of action can elucidate complex changes in the mammalian hosts, leading to immune disorders and cancer, and disclose therapeutically valuable molecules. This review is focused on identified tick salivary peptides and proteins with known structure and function(s) which are promising candidates for development of drugs and their recombinant forms have been tested in disease models *in vitro* and/or *in vivo*. Non-peptide molecules (e.g., nucleosides, lipids) contained in tick saliva are beyond the scope of this paper.

TICKS AND PHARMACOLOGICAL PROPERTIES OF THEIR SALIVA

Ticks are blood feeders and bioactive compounds in their saliva have a promising therapeutic potential for treatment of some human diseases associated with hemostatic and immunological disorders (Mans, 2005; Hovius et al., 2008; Francischetti, 2010; Štibrániová et al., 2013; Sousa et al., 2015; Bonvin et al., 2016; Chudzinski-Tavassi et al., 2016, 2018; Chmelar et al., 2017; Murfin and Fikrig, 2017; Parizi et al., 2018). Tick salivary glands, a paired organ consisting of acini in grape-like clusters, produce saliva secreted by the feeding tick into the host primarily to enable blood feeding by suppressing local hemostatic and host immune responses (Francischetti et al., 2009; Kazimírová and Štibrániová, 2013; Wikel, 2013; Kotal et al., 2015; Šimo et al., 2017; Nuttall, 2018). Tick feeding, in addition, enables host infection with pathogenic microorganisms carried by ticks. Cutting-edge high-throughput technologies used during the last decade for studying composition and function of tick saliva have revealed its complexity (Ribeiro et al., 2006; Francischetti et al., 2011; Radulovič et al., 2014; Kotsyfakis et al., 2015; Tan et al., 2015; Xu et al., 2015; de Castro et al., 2016; Mans, 2016; Bonnet et al., 2018); not surprisingly, considering the tick's biology and their parasitic lifestyle, i.e., strict hematophagy, short-term (soft ticks) to long-lasting feeding (hard ticks) on the vertebrate host, and broad spectrum of hosts. The composition of tick saliva is complex and changes with biological factors such as gender, developmental stage, feeding stage and/or the presence/absence of microorganisms, pathogenic as well non-pathogenic (Liu et al., 2014; Ayllón et al., 2015; Kotsyfakis et al., 2015; Yu et al., 2015; Bonnet et al., 2017, 2018).

Tick saliva is a mixture of proteins, peptides and non-peptide molecules that interfere with various components of hemostasis, wound healing, and both arms of the immune system of the vertebrate hosts, including enzymes, cytokines, complement, antibodies, cell signaling components, immune cells (Francischetti et al., 2009; Mans, 2016; Nuttall, 2018; Wikel, 2018). In addition, cytotoxic and cytolitic activities acting against different cell types, impairment of cancer cells migration and signaling pathways, as well as anti-angiogenic properties have been demonstrated for saliva of different hard tick species (Kazimirova et al., 2006; Poole et al., 2013; Holíková et al., 2018; Sousa et al., 2018; de Sá Jr. et al., 2019; Gradowski do Nascimento et al., 2019), showing that tick saliva is an important source for designing new anticancer drugs (Kazimírová, 2011; Sousa et al., 2015; Chudzinski-Tavassi et al., 2016). Proteinaceous components of the tick saliva are grouped into families like lipocalins, proteins with Kunitz type domain, metalloproteases, serpins, cystatins, basic-tail secreted proteins, small peptide inhibitors, some protein families unique to ticks, and proteins and peptides of unknown structure and function (Ribeiro et al., 2006; Francischetti et al., 2009; Chmelar et al., 2012). Interestingly, a high redundancy and multifunctionality of the tick salivary compounds has been revealed, whereby many of them can target multiple components of hemostasis and, in addition, also components of the immune system (Francischetti et al., 2009; Chmelar et al., 2016; Šimo et al., 2017).

PROTEASE INHIBITORS

Transcriptome and proteome studies of tick salivary glands (SGs) discovered an enormous protein diversity and unique proteins belonging to novel protein families with unknown functions (Francischetti et al., 2011; Radulovič et al., 2014;

Kotsyfakis et al., 2015; Mans, 2016; Esteves et al., 2017). Many of these proteins are differentially expressed during the feeding process (Mans et al., 2008; Kotsyfakis et al., 2015).

Enzyme activity inhibitors represent a very abundant group and include, among others, protease inhibitors containing the Kunitz domain, serine protease inhibitors (serpins), cysteine proteinase inhibitors (cystatins), peptides of the hirudin-like/madanin/variegin superfamily, and basic tail proteins (de Miranda Santos et al., 2004; Francischetti et al., 2005, 2009; Ribeiro et al., 2006; Garcia et al., 2014; Liu and Bonnet, 2014; Parizi et al., 2018).

Kunitz Domain Containing Proteins

Members of the Kunitz domain family, the one of the larger protein families expressed in tick salivary glands, have been functionally characterized primarily as anti-hemostatic agents that block or inhibit host blood coagulation and/or platelet aggregation (Corral-Rodriguez et al., 2009; Chmelar et al., 2012; Parizi et al., 2018), but some of them have been found to display multiple functions, e.g., ixolaris (de Oliveira et al., 2012) or Amblyomin X (Chudzinski-Tavassi et al., 2010).

Hemostasis is the first line of defense against the tick bite and the first stage of wound healing. It comprises a series of physiological processes that stop bleeding at the site of vascular injury by formation of a hemostatic plug. Three major mechanisms are involved in hemostasis: (i) vasoconstriction – termination of bleeding from damaged blood vessels, (ii) coagulation – production of a fibrin clot, (iii) formation of a platelet plug. The enzymes in the coagulation cascade are activated through different pathways, depending on various endogenous and exogenous factors (Hoffman et al., 2009). Ticks have evolved various and effective countermeasures against the different mechanisms of the vertebrate hemostatic system and can target single or multiple host coagulation factors (Maritz-Olivier et al., 2007; Francischetti et al., 2009; Kazimírová et al., 2010; Chmelar et al., 2012; Šimo et al., 2017). Thrombin is the main target for majority of the identified tick anticoagulants (**Table 1**) and inhibition of thrombin generation is one of the main strategies to prevent thrombosis (Kazimírová et al., 2010; Chmelar et al., 2012). However, drugs that target other coagulation factors, e.g., factor Xa (FXa) would be an alternative treatment when thrombin generation has already occurred (Yeh et al., 2012). In spite of the wide range of different identified inhibitors derived from tick salivary glands, due to strict criteria for clinical use, only a limited number passed pre-clinical and clinical tests. For example, only preliminary validations of the tick anticoagulant peptide (TAP) has been performed *in vivo* using animal models, but TAP has never been tested in humans due to a slow onset of action and because its antigenicity, and a single study performed for ixolaris in a rat model awaits future validation (Maritz-Olivier et al., 2007). However, as tick anticoagulants bind specifically to their target molecules, they are important molecular tools to study and increase our understanding of the mechanisms of host blood coagulation. Examples include the mapping of thrombin exosites by ornithodorin derived from *Ornithodoros moubata* (van der Locht et al., 1996), understanding the prothrombinase complex formation by using ixolaris from *I. scapularis* (Monteiro et al., 2005), or characterization of the molecular mechanisms that maintain the procofactor state of circulating FV and the conversion of FV to active cofactor FVa by means of recombinant TIXC-5 from *I. scapularis* (Aleman and Wolberg, 2013; Schuijt et al., 2013). In addition, information on the structure and function of tick-derived anticoagulants can be used in designing synthetic peptides as a basis for development of novel drugs (Maritz-Olivier et al., 2007; Koh et al., 2018).

The **tick anticoagulant peptide TAP** is the first Kunitz-domain protease inhibitor identified in tick saliva that was functionally characterized and prepared in recombinant form. It was originally isolated from the soft tick *O. moubata* (Waxman et al., 1990). TAP is a single Kunitz domain direct slow, tight-binding competitive inhibitor of FXa, with a unique binding mode and high affinity to FXa (Wei et al., 1998). Recombinant forms of TAP (rTAP) have been tested in a variety of animal models of venous and arterial thrombosis showing that the molecule was more effective than heparin and was at least as effective as hirudin, but produced less bleeding (Yeh et al., 2012). For example, in an *in vivo* study, following an infusion into rhesus monkeys rTAP inhibited generation of fibrinopeptide A induced by thromboplastin (Neeper et al., 1990). In another study, the antithrombotic effect of rTAP was tested and compared with heparin in a baboon model of arterial thrombosis. The results also demonstrated the antithrombotic effect of rTAP without alterations of primary hemostasis (Schaffer et al., 1991). In a mouse carotid artery thrombosis model, TAP-antibody targeting activated platelets fusion protein was more effective than enoxaparin without prolonged bleeding time in comparison to conventional anticoagulants (Stoll et al., 2007). These results initiated speculations that drugs targeting FXa could be safer than thrombin inhibitors, although TAP has not been tested in humans (Yeh et al., 2012). In addition, direct FXa inhibitors, including TAP, could potentially be used in prevention of other diseases, such as atherosclerosis or atrial fibrillation, because FXa as well as thrombin are involved in mediation of protease-activated receptor signaling and modulation of cellular mechanisms in the abovementioned pathophysiological processes (Spronk et al., 2014).

Ornithodorin from *O. moubata* was the first thrombin inhibitor identified in a soft tick. It has two domains of the Kunitz basic pancreatic trypsin inhibitor (BPTI) family. The N-terminal domain binds to the active site of thrombin, the C-terminal domain binds at the fibrinogen recognition exosite. Ornithodorin is a slow, tight-binding, competitive inhibitor of thrombin (van der Locht et al., 1996).

Another tick Kunitz domain protease inhibitor with promising antithrombotic and anti-tumor therapeutic usage, **Ixolaris,** a two-Kunitz domain inhibitor that displays homology to the tissue factor (TF) pathway inhibitor (TFPI), was obtained by screening the cDNA library derived from salivary glands of *Ixodes scapularis* (Francischetti et al., 2002, 2004). Ixolaris inhibits factor VIIa (FVIIa)/TF–induced factor (FX) activation by binding to the FXa exosite (Francischetti et al., 2002) and also binds plasmatic FX, decreases heparin-catalyzed inhibition by antithrombin III, and impairs binding of FXa to plasmatic

TABLE 1 | Examples of tick salivary molecules of therapeutic interest in human diseases.

Molecule	Main function: Target(s) Proposed drug	Tick species	References
Protease inhibitors			
Serine protease inhibitors - Kunitz domain containing proteins			
TAP	Anticoagulant: FXa Antithrombotic	*Ornithodoros moubata*	Waxman et al., 1990; Corral-Rodriguez et al., 2009
Ornithodorin	Anticoagulant: thrombin Antithrombotic	*O. moubata*	van der Locht et al., 1996
Ixolaris	Anticoagulant: inhibitor of contact system proteins (VIIa/tissue factor-induced FX, FXa) Antithrombotic, antitumor (glioblastoma, melanoma)	*Ixodes scapularis*	Francischetti et al., 2002; Nazareth et al., 2006; Carneiro-Lobo et al., 2009; de Oliveira et al., 2012
Amblyomin-X	Anticoagulant: FXa, FVIIa/TF complex activity, prothombin conversion Antitumor, anti-angiogenetic	Amblyomma sculptum (formerly *A. cajennense*)	Batista et al., 2010; Drewes et al., 2012, 2015; Maria et al., 2013; Pacheco et al., 2014; Branco et al., 2016; Chudzinski-Tavassi et al., 2016
BmTI-A	Anticoagulant: inhibitor of contact system proteins, inhibits plasmin, elastase, and plasma kallikrein Inhibitor of wound healing and vessel formation Anti-angiogenetic	*Rhipicephalus. (Boophilus) microplus*	Tanaka et al., 1999; Soares et al., 2016
Ir-CPI	Anticoagulant: inhibitor of contact system proteins, blocks FXII, FXI, and kallikrein activation Antithrombotic	*Ixodes ricinus*	Decrem et al., 2009
TdPI	Immunomodulation: innate immune responses, inflammation, inhibitor of human skin β-tryptase Anti-inflammatory	*Rhipicephalus appendiculatus*	Paesen et al., 2007
Tryptogalinin	Immunomodulation: innate immune responses, inhibitor of human skin β-tryptase Anti-inflammatory	*I. scapularis*	Valdés et al., 2013
Haemangin	Wound healing, angiogenesis: inhibits angiogenesis and neovascularization Anti-angiogenetic	*Haemaphysalis longicornis*	Islam et al., 2009
Disagregin	Antiplatelet agent: inhibitor of glycoprotein IIb/IIIa (integrin αIIbβ3) Antithrombotic	*O. moubata*	Karczewski et al., 1994
Serine protease inhibitors – Serpin domain family			
Iris	Anticoagulant: thrombin, FXa Immunosuppression: pro-inflammatory cytokines Drug acting in regulation of TNF-alpha overexpression	*I. ricinus*	Leboulle et al., 2002; Prevot et al., 2009
IRS-2	Immunomodulation: innate immune responses – T cells, T17 cells, cathepsin G, chymase Treatment of autoimmune diseases	*I. ricinus*	Chmelar et al., 2011; Palenikova et al., 2015
Cystatins (cysteine protease inhibitors)			
Sialostatin L	Immunomodulation: acquired immune responses – cathepsin L and V, papain, dendritic cells maturation Immunosuppressive drug for asthma attack	*I. scapularis*	Kotsyfakis et al., 2006; Sa-Nunes et al., 2009; Horka et al., 2012; Klein et al., 2015; Lieskovská et al., 2015b
Sialostatin L2	Immunomodulation: acquired immune responses - cathepsin L, V and S, papain, interferon Anti-inflammatory	*I. scapularis*	Kotsyfakis et al., 2007; Chen et al., 2014; Lieskovská et al., 2015a,b
Iristatin	Immunomodulation: innate immune responses Immunotherapeutic	*I. ricinus*	Kotál et al., 2019
DsCystatin	Immunomodulation: cathepsin L and B, pro-inflammatory cytokines, TLR signaling pathway Anti-inflammatory	*Dermacentor silvarum*	Sun et al., 2018

(Continued)

TABLE 1 | Continued

Molecule	Main function: Target(s) Proposed drug	Tick species	References
Hirudin-like/Madanin/Variegin superfamily			
Variegin	Anticoagulant: thrombin Antithrombotic	*Amblyomma variegatum*	Koh et al., 2007, 2011; Kazimírová et al., 2015
Avathrin	Anticoagulant: thrombin Antithrombotic, coating of medical devices	*A. variegatum*	Iyer et al., 2017, 2019
Sculptin	Anticoagulant: thrombin Antithrombotic	*A. sculptum*	Iqbal et al., 2017
Madanin-1, 2, chimadanin	Anticoagulant: thrombin Antithrombotic	*H. longicornis*	Iwanaga et al., 2003; Thompson et al., 2017
Hyalomin 1	Anticoagulant: thrombin Antithrombotic	*Hyalomma marginatum*	Jablonka et al., 2015
Basic tail-secreted proteins			
Salp14	Anticoagulant: FXa Antithrombotic	*I. scapularis*	Narasimhan et al., 2002
Ixonnexin	Modulator of haemostasis: promotes fibrinolysis Antithrombotic	*I. scapularis*	Assumpção et al., 2018
Lipocalins			
OmCI	Complement: inhibitor of C5 activation Coversin: second-generation complement inhibitor; acute and chronic inflammation	*O. moubata*	Nunn et al., 2005; Roversi et al., 2007; Barratt-Due et al., 2011
Moubatin and other lipocalins of the moubatin clade from soft ticks	Antiplatelet agent: inhibition of platelet aggregation, binds to thromboxane A2 Antithrombotic	*O. moubata*	Waxman and Connolly, 1993; Mans and Ribeiro, 2008; Francischetti, 2010
Ra-HBPs	Innate immune responses: histamine-binding Anti-inflammatory	*R. appendiculatus*	Paesen et al., 1999; Mans, 2005
SHBP	Innate immune responses: histamine and serotonine-binding Anti-inflammatory	*D. reticulatus*	Sangamnatdej et al., 2002
Japanin	Immunomodulation: monocyte-derived dendritic cells, reprogrammes dendritic cell responses Immunotherapeutic (autoimmune disorders, allergies, transplant rejection, acute and chronic inflammatory diseases)	*R. appendiculatus*	Preston et al., 2013; Roversi et al., 2017
HA24	Innate immune responses: histamine-binding Anti-inflammatory	*Hyalomma asiaticum*	Wang et al., 2016
Ixodegrin superfamily			
Variabilin	Antiplatelet agent: inhibitor of glycoprotein IIb/IIIa (integrin αIIbβ3) Antithrombotic	*Dermacentor variabilis*	Wang et al., 1996
YY-39	Antiplatelet agent: blocks platelet adhesion to soluble collagen and bind to glycoprotein IIb/IIIa Antithrombotic	*Ixodes pacificus*	Tang et al., 2015
Metastriate-specific families			
Evasins	Innate immune responses: chemokine binding Anti-inflammatory (myocarditis, arthritis), anti-fibrotic	*Rhipicephalus sanguineus* and other hard ticks	Hajnicka et al., 2005; Frauenschuh et al., 2007; Deruaz et al., 2008; Hayward et al., 2017; Singh et al., 2017; Eaton et al., 2018
Small immunoregulatory peptides			
Hyalomin-A and -B	Innate immune responses: pro-inflammatory cytokine inhibitor Anti-inflammatory	*H. asiaticum asiaticum*	Wu et al., 2010
Amregulin	Innate immune responses: pro-inflammatory cytokine inhibitor Anti-inflammatory	*A. variegatum*	Tian et al., 2016
~8 kDa tick-derived C5 inhibitors			
RaCI	Complement: inhibitor of C5 activation Anti-inflammatory	*R. appendiculatus*	Matthijs et al., 2016

(Continued)

TABLE 1 | Continued

Molecule	Main function: Target(s) Proposed drug	Tick species	References
Prostriate-specific families			
Isac protein family			
Isac	Complement: inhibition of the alternative complement pathway (AP) by destabilizing the C3 convertase Anti-inflammatory	*I. scapularis*	Valenzuela et al., 2000
Salp 20	Complement: inhibits the AP by binding properdin and dissociating active C3 convertase Anti-inflammatory	*I. scapularis*	Tyson et al., 2007; Hourcade et al., 2016
Irac I, II	Complement: inhibition of AP by destabilizing the C3 convertase Anti-inflammatory	*I. ricinus*	Daix et al., 2007
IxACs	Complement: inhibits the AP by binding properdin Anti-inflammatory	*I. ricinus*	Couvreur et al., 2008
Family of 15 kDa salivary proteins			
Salp15	Immunosuppression: multifunctional, $CD4^+$ T cells, dendritic cells Immunosuppressive therapy in transplantation	*I. scapularis*	Anguita et al., 2002; Hovius et al., 2008; Tomás-Cortázar et al., 2017
Putative secreted salivary gland proteins			
TIX-5 (formerly P23)	Anticoagulatio: inhibitor of FXa-mediated FV activation	*I. scapularis*	Schuijt et al., 2011, 2013
EF-hand calcium-binding proteins			
Longistatin	Anticoagulant: plasminogen activator, degrades fibrin clots, antagonist to RAGE and suppresses inflammation during severe tissue injury Antithrombotic RAGE-regulated diseases, e.g.; Alzheimer's disease, psoriasis, diabetic complications and tumorigenesis	*H. longicornis*	Anisuzzaman et al. (2010, 2011, 2014, 2015)
Glycine-rich, or proline-rich, collagen-like superfamily	Glycine-rich cement proteins – cement cone, prevent loss of fluids and secures tick mouthparts in the skin New medical adhesives	Various species of hard ticks	Suppan et al., 2018

TAP, tick anticoagulant peptide; BmTI-A, Boophilus microplus trypsin inhibitor A; Ir-CPI, coagulation contact phase inhibitor from Ixodes ricinus; TdPI, tick-derived peptidase inhibitor; Iris, I. ricinus immunosuppressor; IRS-2, I. ricinus serpin 2; DsCystatin, Dermacentor silvarum cystatin; Ra-HBPs, Rhipicephalus appendiculatus histamine-binding proteins; SHBP, Dermacentor reticulatus serotonin-histamine binding protein; OmCI, Ornithodoros moubata complement inhibitor; HA, Hyalomma asiaticum; RaCI, R. appendiculatus complement inhibitor; Isac, Ixodes scapularis anticomplement; Irac, I. ricinus anticomplement; Salp, salivary protein; IxACs, Ixodes anticomplement proteins; YY-39, ixodegrin from I. pacificus; TIX-5, tick inhibitor of factor Xa toward factor V.

or immobilized heparin (Monteiro et al., 2005). By using a rat model, application of ixolaris resulted in effective antithrombotic activity, without hemorrhage and bleeding (Nazareth et al., 2006). Several evidences showed close correlation between thrombosis and cancer (Timp et al., 2013). Ixolaris was shown to block TF-dependent procoagulant activity in human melanoma cell lines and inhibit their metastatic potential as well as tumor angiogenesis in mice, without evidence of bleeding (de Oliveira et al., 2012). Ixolaris was also associated with reduced tumor vascularization and expression of vascular endothelial growth factor (VEGF) in a human glioblastoma model (Carneiro-Lobo et al., 2009, 2012). All this makes ixolaris a promising agent for anticancer therapy. In a recent study, the therapeutic potential of Ixolaris in chronic infections with immunodeficiency virus (HIV) has been demonstrated (Schechter et al., 2017). Despite effective anti-HIV infection therapy, persistent inflammation involving activated monocytes and their product (e.g., soluble TF) can result in cardiovascular and thromboembolic diseases (Funderburg and Lederman, 2014). In a non-human primate model, pigtail macaques chronically infected with Simian immunodeficiency virus (SIV) exhibited high numbers of monocytes expressing TF and producing proinflammatory cytokines such as tumor necrosis factor (TNF)-α, interleukin (IL)-1β and IL-6, simultaneously leading to coagulopathy and inflammation. *In vitro,* low doses of Ixolaris inhibited TF activity (formation of FXa) in peripheral blood mononuclear cells (PBMCs) derived from chronically SIV-infected macaques and in unstimulated and LPS-stimulated PBMCs originating from anti-HIV therapy naïve and treated HIV^+ suppressed humans, but without effect on TF expression or cytokine production (Schechter et al., 2017). *In vivo,* administration of Ixolaris to pigtails macaques showed reduced levels of IL-17 and decreased expression of Glut-1, CD80 and CD86 (i.e., markers associated with activation of lymphocytes), and resulted in lower concentration of $CD4^+$ and $CD8^+$ T cells ($HLA\text{-}DR^+$, $CD38^+$) and reduced expression of TF by $CD14^+$ monocytes. In addition, Ixolaris-treated animals showed reduced plasma D-dimer levels, indicating cardiovascular comorbidities, lower

SIV viremia and no developing disease up to 100 days after infection. This study has suggested a great potential of Ixolaris in anticoagulant therapy of HIV+ humans and in treatment of other inflammatory diseases (Schechter et al., 2017).

Amblyomin-X is a non-competitive inhibitor of FXa identified in salivary glands of *Amblyomma cajennense* (currently *A. sculptum*) ticks (Batista et al., 2010). It contains a single Kunitz domain and is able to inhibit FXa, prothrombinase and tenase activities (Morais et al., 2014; Branco et al., 2016). In an *in vitro* murine melanoma model, Amblyomin-X decreased tumor mass and reduced metastasis as well as induced apoptosis (Chudzinski-Tavassi et al., 2010; Ventura et al., 2013). It also displays cytotoxic activity on several human tumor cells, among them SK-Mel-28 (human melanoma) or Mia-PaCa-2 (human pancreatic adeno-carcinoma) cell lines, but not on non-tumor cells (Simons et al., 2011), and promotes apoptosis probably by targeting the ubiquitin-proteasome system (Chudzinski-Tavassi et al., 2010). In addition, Amblyomin-X induces apoptosis in murine renal adenocarcinoma (RENCA) cells, mitochondrial damage and the production of reactive oxygen species (ROS) (Akagi et al., 2012; Maria et al., 2013). Amblyomin-X impairs cell migration and causes actin cytoskeleton disruption in human tumor cells (Schmidt et al., 2018). In addition, tumor regression and the reduction of lung metastasis after administration of recombinant Amblyomin-X have been observed in animal models (de Souza et al., 2016). Apart its effects on tumor growth, Amblyomin-X displays antiangiogenic properties and inhibits vascular endothelial growth factor A (VEGF-A)-induced angiogenesis in both the dorsal subcutaneous tissue of mice and the chicken chorioallantoic membrane by modulation of endothelial cell proliferation and adhesion, especially of membrane expression of platelet-endothelial cell adhesion molecule-1 (PECAM-1) (Drewes et al., 2012, 2015), suggesting the possible application of Amblyomin-X as a local inhibitor to undesired neovascularization. Recently, the protein is being developed as anti-tumor drug and is under preclinical evaluations, undergoing pharmacokinetic and toxicity investigations in animals (Boufleur et al., 2019; Maria et al., 2019). These studies revealed that Amblyomin-X did not cause any mortality in mice, toxicity signs were observed only at higher doses, and there was no accumulation of Amblyomin-X in any organ.

Rhipicephalus (Boophilus) microplus possess a trypsin inhibitor A, **BmTI-A**, a two Kunitz domain inhibitor involved in counteracting host hemostasis. BmTI-A blocks neutrophil elastase, plasma kallikrein (Tanaka et al., 1999), trypsin and plasmin and, according to the latest information, it inhibits angiogenesis in a vessel formation assay *in vitro* (Soares et al., 2016). Neutrophil elastase is a serine proteinase secreted by neutrophils and macrophages during inflammation and destroys bacteria. It belongs to the same family as chymotrypsin and is closely related to other cytotoxic immune serine proteases, such as granzymes and cathepsin G. Abnormal expression of neutrophil elastase can cause emphysema, a chronic obstructive pulmonary disease. In elastase-induced experimental emphysema, BmTI-A minimizes parenchymal lesions in mice, suggesting the potential application of this inhibitor in emphysema treatment (Lourenço et al., 2014).

Ixodes ricinus- derived inhibitor of contact phase, **Ir-CPI,** with one Kunitz domain inhibits the intrinsic coagulation pathway by interference with FXIIa, FXIa and kallikrein. In addition, it protects Ir-CPI treated mice against collagen- and epinephrine-induced thromboembolism without increasing bleeding (Decrem et al., 2009).

Tick-derived protease inhibitor, **TdPI,** was identified in salivary glands of *Rhipicephalus appendiculatus* females (Paesen et al., 2007). TdPI is only expressed during the first 4 h after tick attachment and manipulates host immune defenses during the tick feeding process. It is a glycosylated Kunitz-related potent inhibitor of human β-tryptase and trypsin and moderately affects human plasmin (Paesen et al., 2007; Bronsoms et al., 2011). Human β-tryptases, specific serine proteases of mast cells, together with leukocyte elastase and chymase, are involved in inflammation and different aspects of tissue remodeling (Caughey, 2007). Beta-tryptase is a clinically useful marker of mast cells and their activation and in addition, it contributes to the pathogenesis of allergic inflammatory disorders, e.g., asthma. Thus, β-tryptase is a potential therapeutic target of tryptase inhibitors which have therapeutic potential in asthma (Sommerhoff and Schaschke, 2007). TdPI is able to penetrate mouse mast cells and may block the autocatalytic activation of tryptase required for its biological action (Paesen et al., 2007). Thus, TdPI-derived drugs could be used as inhibitors of mast cell tryptase in the control of injury caused by parasites, and in the treatment of allergies.

Tryptogalinin, an *I. scapularis* salivary Kunitz-type protein, was found to inhibit a number of serine proteases involved in inflammation and vertebrate immunity: β-tryptase, β-trypsin, α-chymotrypsin, plasmin, matriptase and elastase, showing a potential broad effect against mast cell proteins and other host enzymes (Valdés et al., 2013). Tryptogalinin is phylogenetically related to TdPI and provides another example when understanding of the structure and function of a tick protein could help in engineering highly specific pharmacological agents.

Haemangin was identified as a salivary Kunitz inhibitor in *Haemaphysalis lonigicornis* which is up-regulated during blood feeding (Islam et al., 2009). It strongly inhibits trypsin, chymotrypsin and plasmin and thereby supporting plasmin-dependent fibrinolysis inhibition and indicating its antiproteolytic potential on angiogenic cascades (Islam et al., 2009). Haemangin also blocks chick aortic explant angiogenesis and neovascularization of chick chorioalantoic membrane, demonstrating that it can inhibit both pre-existing vessel angiogenesis and neovascularization. Haemangin also impedes differentiation, proliferation, and tube formation and significantly induces expression of a variety of genes involved in apoptosis, angiogenesis and wound healing in human umbilical vein endothelial (HUVEC) cells (Islam et al., 2009).

Disagregin is a Kunitz-type protein derived from *O. moubata* that inhibits activation of platelet aggregation through integrin aIIbb3 (Karczewski et al., 1994). It does not contain the RGD motif that binds to the fibrinogen-binding site and thus, it is

unique in its sequence as well as function and could serve to design therapeutically useful antithrombotics.

Serine Protease Inhibitors – Serpin Domain Family

Serpins form one of the largest families of serine protease inhibitors ubiquitously distributed in nature, yet abundant in ticks (Francischetti et al., 2009). Several next-generation sequencing transcriptome studies revealed a high number of transcripts, e.g., over 150 in genus *Amblyomma*, around 20 in *Rhipicephalus* and at least 36 in *I. ricinus*, but only 20 tick serpins from different tick species have been functionally characterized. One of their functions is manipulation of host innate immune responses by impacting enzymes released from neutrophils, mast and dendritic cells (DCs).

The first tick serpin affecting host immune defenses was identified in salivary glands of *I. ricinus* and was named **Iris** (Leboulle et al., 2002). It inhibits T cells and splenocytes proliferation and alters cytokines levels of PBMC (Leboulle et al., 2002). It also suppresses coagulation and fibrinolysis by inhibition of thrombin, FXa and tissue plasminogen activator (Prevot et al., 2006). In addition, Iris inhibits secretion of TNF-α after binding on monocyte/macrophage cells (Prevot et al., 2009). Thus, Iris modulates multiple host processes simultaneously via independent mechanisms and potentially can serve for design of therapeutic for TNF-α overexpression induced pathological situations.

Ixodes ricinus serpin 2 **(IRS-2)** is a serine protease inhibitor that specifically inhibits two proteases, cathepsin G and chymase (**Figure 1**) that are secreted in mammals by stimulated neutrophils and mast cells, respectively. Cathepsin G is involved in tissue remodeling during inflammation, thus IRS-2 postpones this process, as well as platelet aggregation resulting in facilitating feeding (Chmelar et al., 2011). IRS-2 also modulates production of IL-6 by DCs, and subsequently differentiation and maturation of T helper 17 cells (Th17) via the IL-6/STAT-3 (Signal Transducer and Activator of Transcription 3) signaling pathway (Palenikova et al., 2015). In addition, IRS-2 impedes the paw edema development and the influx of neutrophils in an animal model of acute inflammation (Chmelar et al., 2011).

Cystatins (Cysteine Protease Inhibitors)

Cystatins represent a large superfamily of reversible and tight-binding inhibitors of papain-like cysteine proteases and legumains (Abrahamson et al., 2003). They regulate diverse vertebrate biological processes such as development of immune system, epidermal homeostasis, antigen presentation, neutrophil chemotaxis during inflammation, or apoptosis. Tick cystatins can interfere with both, innate and adaptive immune responses of the vertebrate host (Lieskovská et al., 2015a,b). Over the last decade, around 20 cystatins from various hard and soft ticks have been identified and biochemically analyzed for their role in the tick's physiology and blood feeding (Schwarz et al., 2012). All these cystatins are effective inhibitors of papain-like cysteine proteases, but not of legumain and belong to two of four existing cystatin subgroups, namely type 1 cystatins/stefins) and type 2 cystatins. While stefins are known to be primarily intracellular cytoplasmic proteins, type 2 are expressed and secreted in salivary glands and midgut and therefore have been more intensively studied in ticks. **Sialostatin L** was found first in the salivary glands of *I. scapularis* ticks by a sialotranscriptome study (Valenzuela, 2002) and later **Sialostatin L2** was described (Kotsyfakis et al., 2007).

Sialostatin L exerts miscellaneous immunosuppressive effects on mammalians. It is a potent inhibitor of lysosomal cysteine cathepsins L, C, V, S, X (**Figure 1**) and papain, proliferation of CD4+ cells and cytotoxic T cells (Kotsyfakis et al., 2006, 2007, 2010; Sa-Nunes et al., 2009), migration of neutrophils during acute inflammation, secretion of cytokines by mast cells, DCs and lymphocytes, and shows preventive potential against autoimmune diseases (Kotsyfakis et al., 2006; Sa-Nunes et al., 2009). On one side, mammalian cathepsins S, L, and V represent key players in the vertebrate immunity through their participation in the antigen presentation processes of DCs and macrophages, on the other hand, they are involved in many pathological processes, such as psoriasis, muscular dystrophy, neurodegenerative disorders, cancer, etc. Sialostatin L strongly decreases the production of IL-9 by Th9 cells, essentially involved in the induction of asthma symptoms. Application of sialostatin L almost completely abrogates airway hyperresponsiveness and eosinophilia in a model of experimental asthma and experimental data suggest its preventing effect in this disease model (Horka et al., 2012), probably by suppressing mast cell-derived IL-9 production by inhibiting IRF4 (Klein et al., 2015). In a mouse model of multiple sclerosis, *in vivo* administration of Sialostatin L during the immunization phase of experimental autoimmune encephalomyelitis pointedly prevents disease symptoms associated with decreased production of IFN-γ and IL-17 and proliferation of specific T cell (Sa-Nunes et al., 2009).

Sialostatin L2 impairs cathepsins C, L, S and V, diminishes secretion of IL-1b and IL-18 by macrophages and inhibits maturation of caspase-1. Upon infection with bacterial agents (e.g., *Anaplasma phagocytophilum*), Sialostatin L2 can significantly attenuate the severity of the disease due to its anti-inflammatory effects (Chen et al., 2014). Sialostatin L2 was found to suppress the interferon mediated immune response and enhance TBEV replication in murine DCs (Lieskovská et al., 2015a) and impair the production of proinflammatory chemokines in murine DCs upon infection with *Borrelia burgdorferi* (Lieskovská et al., 2015a).

Iristatin, a novel type 2 cystatin was identified in *I. ricinus* (Kotál et al., 2019). It suppresses vertebrate cathepsins C and L with similar affinity as sialostatins, production of T-cell derived cytokines, such as pro-inflammatory IFN-γ and IL-2 by stimulated Th1 cells, anti-inflammatory cytokine IL-4 by Th2 cells and IL-2 and IL-9 by Th9 cells, without effect on IL-17 production by Th17 cells. In mast cells, it blocks IL-9 and IL-6 production, but not IL-4. Furthermore, Iristatin inhibits OVA antigen-induced murine CD4+ T-cell proliferation *in vitro* and *in vivo* leukocyte (neutrophils and myeloid cells) recruitment in a mouse model of thioglycollate induced peritonitis. Iristatin with such a broad-spectrum of immunosuppressive activities may be useful in the therapy of immune-mediated diseases.

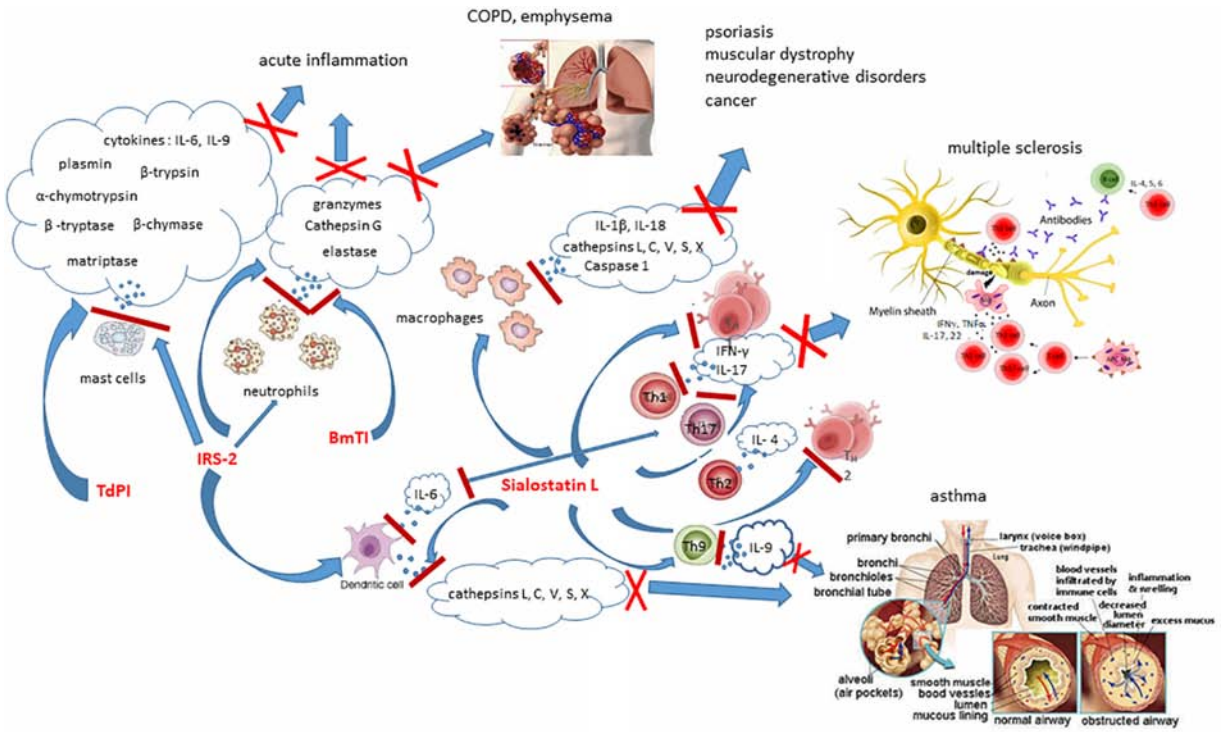

FIGURE 1 | Effects of selected tick salivary proteins on host immune cells and their potential therapeutic usage to treat immunological disorders. IRS-2, BmTI, and Sialostatin L modulate functions of enzymes released by immune cells, resulting in inhibition of their biological and pathological functions.

DsCystatin was identified by screening of the cDNA of *Dermacentor silvarum* salivary glands (Sun et al., 2018). DsCystatin impairs the activities of human cathepsins L and B and the expression of pro-inflammatory cytokines IFNγ, TNFα, and IL6 in mouse bone marrow-derived macrophages. It inhibits activation of mouse bone marrow-derived DCs and activation of NFκB in TLR2 and TLR4 signaling pathways. In a mouse arthritis model, DsCystatin suppresses joint inflammation induced by CFA and *B. burgdorferi*. DsCystatin could potentially be used in the cure of inflammatory diseases.

Small Peptide Inhibitors of the Hirudin-Like/Madanin/Variegin Superfamily

This superfamily comprises mainly small antithrombins and is probably specific to metastriate ticks (Francischetti et al., 2009).

Variegin is a 32-residue peptide derived from the salivary glands of partially fed female *Amblyomma variegatum* ticks. Its C-terminal tail displays homology to hirudin and is one of the smallest thrombin inhibitors in nature (Koh et al., 2007). It is a direct thrombin inhibitor and binds to thrombin from the active site to exosite-I (Koh et al., 2011). Upon binding, variegin is cleaved by thrombin, and its cleavage product continues to inhibit the thrombin active site in a non-competitive manner (Koh et al., 2009). Variegin is structurally and functionally similar to, but is more potent than bivalirudin (hirulog), a drug used for the treatment of patients with acute coronary syndromes (Lincoff et al., 2004; Stone et al., 2006). Pharmacokinetic studies involving rats confirmed that variegin, similar to other small peptide antithrombins, e.g., bivalirudin, was rapidly excreted by the renal route, which makes it suitable for short-lasting intravenous anticoagulation during surgical procedures[1].

Variegin-like thrombin inhibitors are probably synthesized in ticks as larger precursors that can be processed into multiple variants. Iyer et al. (2017) described **avathrin,** a new variegin-like thrombin inhibitor in *A. variegatum*. Similar to variegin, avathrin is a fast, tight-binding competitive inhibitor interacting with the thrombin active site and exosite-I after binding to thrombin. Avathrin is cleaved by thrombin, but the C-terminal cleavage product continues to exert prolonged inhibition. Avathrin prevented thrombosis better than hirulog-1 in a $FeCl_3$-induced murine carotid artery thrombosis model (Iyer et al., 2017, 2019). Variegin-like peptides represent perspective candidates for designing anticoagulants to prevent arterial and venous thrombosis during invasive procedures and for coating of medical devices.

Sculptin, a new thrombin inhibitor was identified in the transcriptome of salivary glands of *Amblyomma sculptum* (formerly *A. cajennense*) (Iqbal et al., 2017). Scupltin consists of 168 amino acid residues, has four similar repeats, shares few similarities with hirudin, but is more similar with serine protease inhibitors of the antistasin family. Sculptin is a novel class of competitive, specific and reversible thrombin

[1]https://patents.google.com/patent/US9217027

inhibitors and its mechanism of inhibition slightly differs from hirudin. Sculptin is cleaved by thrombin, but its fragments have no thrombin inhibitory activity. In contrast, fragments produced after hydrolysis by FXa are able to inhibit thrombin independently. Sculptin and its independent domain(s) have a potential to become novel antithrombotic drugs.

Madanin-1, 2 and **chimadanin** are small, cystein-free (∼6 kDa) specific antithrombins isolated from the salivary glands of *H. longicornis* (Iwanaga et al., 2003). These peptides behave as cleavable competitive inhibitors of thrombin, bind to the active site and exosite II of the enzyme, and lose their affinity to thrombin upon proteolysis (Figueiredo et al., 2013; Thompson et al., 2017). Tyrosine sulfation of madanin-1 and chimadanin are crucial for their thrombin inhibitory activity. A dramatic increase in their potency was observed following tyrosine sulfation, with the sulfated tyrosine residues binding to exosite II of thrombin. The importance of tyrosine sulfation and the unique binding mode of these peptides make them promising candidates for the development of next generation thrombin inhibitors (Thompson et al., 2017).

Hyalomin 1, a 59-residue cystein-free peptide was identified in the salivary gland transcriptome of *Hyalomma marginatum rufipes*. The peptide is a selective and competitive inhibitor of thrombin, interacting with both the active site and exosite I of the enzyme (Jablonka et al., 2015). Hyalomin-1 also inhibits the thrombin-mediated activation of FXI, thrombin-mediated platelet aggregation, and the activation of FV by thrombin. It is cleaved by thrombin and cleavage region and the C-terminal fragment inhibited the enzyme similar to the full-length peptide. Testing of hyalomin-1 in a mouse model of thrombosis increased arterial occlusion time, making the peptide as another candidate for development of antithrombotic drugs.

Basic Tail-Secreted Proteins (BTSP)

This family comprises over hundred proteins that were found primarily in *Ixodes* species (Francischetti et al., 2009; Chmelar et al., 2012). In spite some homologs from metastriate ticks were identified, BTSP seem to be typical for prostriate ticks. Most members of this protein family contain a basic carboxy terminus (tail) (Francischetti et al., 2009). Only two BTSP have been functionally characterized. They include anticoagulants with novel mode of action, derived from salivary glands of *I. scapularis*: salivary protein 14 (Salp14), and Ixonnexin.

Salp14, a 9.8 kDa protein, was found to impair the intrinsic pathway of coagulation and specifically inhibit FXa, but it does not inhibit other proteases (Narasimhan et al., 2002).

Ixonnexin is a 11.8 kDa salivary protein, displaying homology to Salp14 (Assumpção et al., 2018). It also interacts with FXa, but in addition, promotes fibrinolysis *in vitro* by enzymatically productive ternary complex through binding to tissue type plasminogen activator (t-PA) and plasminogen. In *in vivo* experiments, ixonnexin was found to inhibit $FeCl_3$-induced thrombosis in mice and appears as a novel modulator of fibrinolysis that can be involved in studies on participation of plasmin in ischemic events, tumor growth and metastasis.

LIPOCALINS

Lipocalins, a family of ubiquitous barrel-shaped proteins with low molecular weight, perform multiple biological functions, including the regulation of cell homeostasis and immune responses via sequestering small hydrophobic molecules such as vitamins, steroids, histamine, serotonin, prostaglandin, involved in modulation of platelet aggregation, vasoconstriction and inflammation (Schlehuber and Skerra, 2005). Lipocalins are a protein family with a large expansion in ticks; in soft ticks they act as anti-complement factors (Nunn et al., 2005; Tambourgi and van den Berg, 2014), inhibitors of platelet aggregation (Keller et al., 1993; Waxman and Connolly, 1993) and toxins (Mans et al., 2003), while in hard ticks they scavenge biogenic amines such as histamine and serotonin (Paesen et al., 1999; Sangamnatdej et al., 2002) or leukotriene B4 (LTB4) (Beaufays et al., 2008). Tick lipocalins are considered outliers since they lack the three structural conserved motifs typical of the general lipocalin family, which are apparently designed to accommodate charged, hydrophilic ligands. Unlike other lipocalins, tick lipocalins harbor two internal binding sites, the H for histamine with high affinity and the L also for histamine but weakly (Paesen et al., 2000).

OmCI (*O. moubata* Complement Inhibitor), a 16.8-kDa protein from *O. moubata,* is the first described natural complement inhibitor from ticks, targeting specifically the C5 activation step in the complement cascade (Nunn et al., 2005; Roversi et al., 2007; Mans and Ribeiro, 2008; Barratt-Due et al., 2011).

The vertebrate complement system is a key member of innate defenses against infection, maintaining tissue homeostasis and orchestrating the crosstalk between adaptive and innate immunity (Harris, 2018). However, it is also involved in common and serious diseases, among them in many autoimmune diseases such as rheumatoid arthritis, diabetes mellitus type 1, systemic lupus erythematosus, multiple sclerosis, and myasthenia gravis (Mollnes et al., 2002). Complement can be activated by four pathways (classical, alternative, lectin, and thrombin) (Duncan et al., 2007; Thiel, 2007; Zipfel et al., 2007a,b). Although, complement association with disease has driven a boom in complement drug discovery based on natural sources, very few drugs have progressed to late-stage clinical studies due to high target concentration and turnover, unwanted side effects and lack of clarity around disease mechanism (Tambourgi and van den Berg, 2014).

OmCI binds directly to C5 and thus inhibits cleavage into anaphylatoxin C5a and C5b, a subunit of the membrane attack complex (MAC; C5b-9) and prevents MAC-mediated lysis and destruction of red blood cells in paroxysmal nocturnal hemoglobinuria (PNH) and tissue destruction in various other complement-mediated inflammatory and autoimmune diseases (Hepburn et al., 2007; Fredslund et al., 2008). In addition, OmCI captures the inflammatory mediator leukotriene B4, a potent chemotactic agent and activator of neutrophils (Yoshikai, 2001). A recombinant form of OmCI (known as Coversin and rEV576) has shown efficacy in numerous animal models of complement-mediated diseases and successfully accomplished a

phase Ia clinical trial. The protein is protective in rat experimental models of passive and active autoimmune myasthenia gravis. OmCI-treated animals exhibited fewer symptoms and a markedly attenuated inflammatory response (Hepburn et al., 2007; Soltys et al., 2009). Coversin, if not bound to C5, has a very short plasma half-life and requires frequent dosing. N-terminal conjugation with a 600 amino acid polypeptide composed of Pro, Ala, and Ser has improved the pharmacokinetics of Coversin by extending the half-time, slowing kidney clearance, and considerably reducing background hemolysis of erythrocytes. Moreover, Coversin reduced lysis of erythrocyte as effectively as its non-conjugated form in a clinically relevant *in vitro* model of the complement-mediated disease, PNH (Kuhn et al., 2016).

Moubatin is a lipocalin derived from salivary glands of *O. moubata*. It inhibits platelet aggregation induced by collagen (Keller et al., 1993; Waxman and Connolly, 1993) and binds to thromboxane A_2, a potent platelet aggregation agonist and vasoconstrictor (Mans and Ribeiro, 2008). Moubatin was found to relax rat aorta pre-constricted by U46619 (a thromboxane A_2 mimetic) and inhibit its contraction induced by U46619 (Mans and Ribeiro, 2008).

The hard tick *R. appendiculatus* has two types of salivary lipocalins that are structurally resolved, bind different ligands and have separate functions, namely, *R. appendiculatus*-histamine binding proteins, **Ra-HBPs** (Paesen et al., 1999) and **Japanin** (Preston et al., 2013). The high-affinity Ra-HBPs were identified in both genders of the tick: RaHBP1 and 2 are specific for females, Ra-HBP3 is associated with males. Ra-HBP1 and 2 are around 20 kDa unglycosylated monomeric proteins secreted by the tick females during the early feeding stage, while Ra-HBP3 is a glycosylated dimeric protein produced throughout feeding. Ra-HBP2 and 3 show strong affinity to histamine whereas affinity of Ra-HBP1 is weak. Ra-HBP2 has been proposed for therapeutic use since it sequesters two histamine molecules, with different affinities, thereby reducing inflammatory responses (Paesen et al., 1999, 2000).

Serotonin-histamine binding protein, **SHBP,** identified in *Dermacentor reticulatus* ticks (Sangamnatdej et al., 2002) is a lipocalin simultaneously binding serotonin and histamine. Serotonin represents a key neurotransmitter of the central nervous system and is also involved in a number of neurological disorders (Dinan, 1996). Similarly to histamine, serotonin is a key mediator of inflammation (Askenase et al., 1980) produced by mast cells and platelets.

The described histamine binding proteins and related protein family members were under investigation as potential therapeutic agents for the treatment of various diseases: Ra-HBP2 (as rEV-131) for conjunctivitis (Nuttall and Paesen, 2001b), allergic rhinitis and asthma (Nuttall and Paesen, 2001a), carcinoid syndrome and rheumatoid arthritis (Weston-Davies, 2004), Dr-SHBP for treatment of carcinoid syndrome with high production of serotonin (Schnirer et al., 2003) and post-chemotherapy emesis with nausea and vomiting due to various neurotransmitters involving serotonin. The latter treatment focused on serotonin receptor antagonists (Hesketh, 2004). In both cases, SHBP primarily targets serotonin, with secondary anti-inflammatory effects due to its histamine-binding capabilities.

In a murine allergic asthma model, the intranasal administration of Ra-HBP2 to immunized mice before antigen challenge prevented airway hyper-reactivity by 70%, and also abrogated peribronchial inflammation, pulmonary eosinophilia, mucus hypersecretion, and IL-4 and IL-5 secretion and effectively reduced airway resistance, comparable with budesonide, the conventionally prescribed corticosteroid (Couillin et al., 2004). In a corticosteroid-resistant LPS-induced murine model of acute respiratory distress syndrome, rEV-131 decreased bronchoconstriction, activation and influx of neutrophils. In phase I and II clinical trial this lipocalin showed safety and pharmacological activity in treatment of allergy in humans (Schlehuber and Skerra, 2005).

Japanin is a 17.7 kDa *N*-glycosylated lipocalin which exists in complex with cholesterol (Preston et al., 2013; Roversi et al., 2017). It reprograms DCs, antigen-presenting cells, so they no longer respond to a wide spectrum of stimuli *in vitro* specific for immune recognition. DCs, resident cells within most peripheral tissues (including skin), represent a bridge between innate and adaptive immunity as the important initiators and modulators of T cell responses. Japanin blocks differentiation of DCs from monocytes and on one side impedes upregulation of co-stimulatory molecules and pro-inflammatory cytokines in response to stimuli and on other side it promotes upregulation of co-inhibitory molecules and the anti-inflammatory cytokine IL-10 (Preston et al., 2013). Although the exact mechanism by which Japanin modulates DCs has not been fully described, the molecule may represent a novel tool to modulate DCs with possible therapeutic applications, such as prevention or treatment of transplant rejection or autoimmune diseases.

HA24, identified in the salivary glands of the tick *Hyalomma asiaticum,* represents a new lipocalin protein with particular histamine binding capacity (Wang et al., 2016). Its recombinant form binds specifically to histamine in a dose-dependent manner, and can provide palliation from allergic asthma in mice (Yanan et al., 2016).

IXODEGRIN SUPERFAMILY

Ixodegrins include cysteine-rich proteins containing the RGD (Arg-Gly-Asp) or KGD (Lys-Gly-Asp) motif that interfere with fibrinogen binding to platelets and exert antiplatelet activities (Francischetti et al., 2009). As GPIIb/IIIa inhibitors are widely used clinically during coronary interventions (Hashemzadeh et al., 2008), tick-derived disintegrins could also serve as candidates for drug design.

Variabilin, derived from salivary glands of *Dermacentor variabilis,* is 5-kDa RGD-containing disintegrin and was the first RGD-containing antagonist isolated from ticks (Wang et al., 1996). It blocks ADP-induced platelet aggregation and prevents integrin aIIbb3 binding to immobilized fibrinogen. It also an antagonist of the vitronectin receptor αvβ3 and attenuates osteosarcoma cell adhesion to vitronectin. Its sequence differs from other known naturally occurring antagonists of GPIIb-IIIa.

Ixodegrins identified in *Ixodes pacificus* and *I. scapularis* salivary gland transcriptomes display sequence homology

to variabilin, including the RGD domain (Francischetti et al., 2005, 2009). Using the sequence of ixodegrin in the *I. pacificus* transcriptome (Francischetti et al., 2005), the molecule **YY-39** was synthesized and refolded for studies on its effects on platelets and thrombosis *in vivo* (Tang et al., 2015). YY-39 decreased adenosine diphosphate (ADP)-, thrombin- and thromboxane A_2-induced platelet aggregation. In addition, it inhibited platelet adhesion to soluble collagen and bound to purified GPIIb/IIIa. YY-39 also reduced thrombus weight in an *in vivo* experimental rat arteriovenous shunt model and as well as blocked thrombosis in a carrageenan-induced mouse tail thrombosis model. However, in the tested animal models, YY-39 showed little bleeding complication, which makes the molecule a promising antithrombotic agent.

METASTRIATE-SPECIFIC FAMILIES

Over thirty families of proteins have been found exclusively in metastriate ticks (Francischetti et al., 2009), but only a few have been functionally characterized. These include small immunoregulatory proteins that modulate vertebrate immune responses, mainly acting on cytokines and chemokines.

Cytokines, a diverse group of small secreted proteins (interleukins, growth factors, chemokines), represent key humoral controllers of cells in their interactions and communications and regulators of processes under normal, developmental and pathological conditions (inflammation, wound healing). Cytokine through binding to their specific receptors orchestrate immune responses, including the recruitment of immune cells into the site of inflammation. Uncontrolled expressions of cytokines are associated with inflammatory, autoimmunity even with cancer, thus members of cytokine networks are targets for development of new effective therapeutics. Ticks either suppress production of cytokines by various immune cells or directly inhibit cytokines by binding ligands. However, from all anticytokine activities described in different tick species (Hajnická et al., 2001; Hajnicka et al., 2005, 2011; Vančová et al., 2007, 2010; Peterková et al., 2008; Slovák et al., 2014), only hyalomins (Wu et al., 2010), Amregulin (Tian et al., 2016) and chemokine binding factors named Evasins derived from *Rhipicephalus sanguineus* (Frauenschuh et al., 2007; Deruaz et al., 2008) have been functionally and structurally characterized.

Small Immunoregulatory Peptides

Hyalomin-A and -B were identified in salivary glands of the hard tick *Hyalomma asiaticum asiaticum* (Wu et al., 2010). Both immunosuppressant peptides exert significant anti-inflammatory activities, either directly by inhibiting LPS-induced production of inflammatory cytokines – TNF-α, monocyte chemotactic protein-1and IFN-γ in mouse splenocytes or indirectly by stimulating secretion of immunosuppressant cytokine IL-10. Moreover, both hyalomins scavenge free radical 2,2′-azinobis 3-ethylbenzothiazoline-6-sulfonic acid ($ABTS^{+)}$ radicals *in vitro* and inhibit adjuvant-induced arthritis in mice *in vivo*.

Tian et al. (2016) structurally and functionally characterized a small immunosuppressant peptide **Amregulin** from *A. variegatum*. Amregulin inhibits *in vitro* secretion of inflammatory cytokines – TNF-α, IL-8, IL-1 and IFN-γ by LPS stimulated rat splenocytes in a dose-dependent manner. Like hyalomins, this peptide shows concentration dependent antioxidant activity by scavenging free radical $ABTS^{+}$, but not 2,2-diphenyl-1-picrylhydrazyl (DPPH) and by reducing ferric ions (Fe^{3+}) to Fe^{2+}. Amregulin also significantly inhibits Freuds adjuvant-induced paw inflammation in mouse models *in vivo*.

Evasins

Three salivary glycoproteins, found in the brown dog tick *R. sanguineus,* are secreted during a feeding and bind to host chemokines, thus inhibiting the host inflammatory response (Frauenschuh et al., 2007; Deruaz et al., 2008). **Evasin-1** and **-3** are high specific binders of only three CC chemokines (CCL3, CCL4, and CCL18) and a subset of CXC chemokines (CXCL1, -2, -3, -5, -8), respectively, whereas **Evasin-4** demonstrated more promiscuity effect by interaction with at least 18 chemokines of the CC subfamily. Evasin-1 in a dose-dependent manner reduced CCL3-induced influx of neutrophils in a peritoneal cell recruitment assay and showed high efficiency in reducing fibrosis resulted from neutrophil infiltration into the lung after bleomycin treatment, and also decreased the mortality observed in this model (Russo et al., 2011). Evasin-3 is effective in several neutrophil-dependent disease models with regards to its *in vitro* effect mentioned above. Montecucco et al. (2014) demonstrated beneficial effects of Evasin-3 and partially of Evasin-4 on inflammatory processes in pancreas and lungs in a mouse model of acute pancreatitis (AP). Evasin-3 treatment of mice with cerulein-induced AP decreased recruitment of neutrophils, production of ROS and apoptosis in the lungs and inhibited necrosis and apoptosis of neutrophils and macrophages in the pancreas. Evasin-4 only decreased the abundance of macrophages in lungs, without any effects in the pancreas. A dose-dependent Evasin-3 inhibition of CXCL8 induced leukocyte infiltration into the peritoneal cavity is determined. In an antigen-induced arthritis by BSA, intradermal injection of Evasin-3 significantly suppresses disease symptoms. In case of ischemic reperfusion injury, Evasin-3 showed higher efficiency than Evasin-1, even though only Evasin-1 effectively inhibited first DCs recruitment to the site of infection with *Leishmania major*, mediated by CCL3 released from neutrophils (Charmoy et al., 2010). Moreover, Evasin-1 is able to reduce skin inflammation observed in D6−/− mice in response to 12-*O*-tetradecanoylphorbol-13-acetate (Deruaz et al., 2008). Castor et al. (2010) studied effects of Evasin-1 on pathogenesis of acute graft-versus-host disease (GVHD) in mice, induced by transplantation of C57BL/6J murine splenocytes to B6D2F1 mice. GVHD is a complication occurring in allogeneic bone marrow transplantation with significant morbidity and mortality in humans (Ferrara and Deeg, 1991), and is characteristic by CCL3 expression and CCL3-induced recruitment and proliferation of T cells. Although application of Evasin-1 did not interfere with GVH-leukemia in mice, Evasin-1 treatment reduced levels of IFN-γ and

CCL5, but not TNF-α, reduced the number of $CD4^+$ and $CD8^+$ T cells infiltrating the small intestine and the damage of intestine and liver. In addition, Evasin-1 also ameliorated GVHD and provided partial relief from symptoms, whereby the effect was comparable to glucocorticosteroid dexamethasone and was similar to protection observed in $CCL3^{-/-}$ mice. Furthermore, both Evasin-3 and -4 effectively reduce post-infarction myocardial injury and remodeling (Braunersreuther et al., 2013) and Evasin-4 is effective in DSS-induced colitis (Vieira et al., 2009). Because of its broad CC chemokine-binding spectrum, Evasin-4 is considered the most suitable candidate for design of a therapeutic agent. By sequence similarity searches in transcriptomes of hard ticks, mainly of the *Rhipicephalus*, *Amblyomma*, and *Ixodes* genera, over 250 putative evasin sequences were detected (Hayward et al., 2017). Eight of them were expressed in *Escherichia coli* and exhibited high-affinity binding to human chemokines. They were classified into C8 and C6 evasins. By using the yeast surface display method, Singh et al. (2017) detected ten novel polyvalent CC-chemokine binding evasin-like molecules from eight hard tick species of the *Rhipicephalus* and *Amblyomma* genera. One of them, P672 from *Rhipicephalus pulchellus*, was found to bind to CCL8 and its properties could be altered by homology modeling, demonstrating that the function of tick evasins can be manipulated to design novel drugs (Eaton et al., 2018).

∼8 kDa Tick-Derived C5 Inhibitors

RaCI (Rhipicephalus appendiculatus C5 Inhibitor) belongs to a novel protein family of ∼8 kDa tick-derived C5 inhibitors. It was identified in the transcriptome of *R. appendiculatus* salivary glands (Matthijs et al., 2016) and its sequence shares no similarity to previously characterized tick complement inhibitors. RaCI binds human C5 and blocks the generation of C5a and membrane attack complex formation. RaCI exhibits cross-species reactivity which can be used in disease models on animal to test therapeutic efficacy of drug candidates. The small size of RaCI in comparison with the previously described OmCI and retaining its potency after its further reducing may potentially aid drug administration. As OmCI and RaCI target different sites on C5 (C5d-CUB and C5d-MG1-MG2, respectively), RaCI may be used to tune therapeutic effects of complement 5 inhibitors.

PROSTRIATE-SPECIFIC FAMILIES

Out of the six protein families included in this group, only members of one group, i.e., the Isac protein family, have been characterized functionally. This group comprises salivary anti-complement proteins derived from *I. scapularis* and *I. ricinus* (Francischetti et al., 2009).

Isac Protein Family

Several tick saliva molecules with promising anti-complement activities have been identified and characterized in ticks of the *Ixodes* genus: **Isac** and **Salp20** in *I. scapularis* (Valenzuela et al., 2000; Tyson et al., 2007), **Irac I, Irac II** (Daix et al., 2007), and **IxACs** (Couvreur et al., 2008) in *I. ricinus*. Isac and Irac proteins specifically inhibit the alternative pathway (AP) of complement via blocking C3 convertase, whereby this inhibition can lead to immunosuppression or diminishing of opsonization. On the other hand, depletion of serum C3 detected in neuromuscular junction, an important factor determining severity of myasthenia gravis, is appreciated in some patients with this autoimmune neuromuscular transmission diseases. Salp20, displaying homology to Isac, inhibits the AP by binding properdin, which is a positive regulator of this pathway (Tyson et al., 2008; Hourcade et al., 2016). Couvreur et al. (2008) cloned and expressed proteins from *I. ricinus*, named IxACs, showing 40% identity to Isac and Irac. IxACs also inhibit the AP by binding to properdin.

Family of 15 kDa Salivary Proteins

Salp15, a 15 kDa immunosuppressive cystein-rich glycoprotein, was identified in salivary glands of *I. scapularis* (Anguita et al., 2002). It inhibits directly the activation of CD4+ T cells through binding on the coreceptor CD4, which results in signaling pathway inhibition, reduced IL-2 production and CD25 (IL-2Rα) expression (Juncadella et al., 2007; Garg et al., 2014), and also indirectly via inhibition of DCs functions by binding on lectin type. Salp15 binding to CD4 is persistent and induces a long-lasting immunomodulatory effect, probably due to induction of an increased expression of the ectoenzyme, CD73, in regulatory T cells and increased production of adenosine (Tomás-Cortázar et al., 2017). This immunomodulatory protein is a promising candidate for treatment of T-cell-mediated autoimmune diseases involving asthma or allogeneic transplant tolerance. Paveglio et al. (2007) tested Salp15 in a mouse model of human allergic asthma with typical imbalance of CD4+ T cells toward Th2 cells and overproduction of cytokines IL-4, IL-5, and IL-13, leading to production of IgE, eosinophilpoiesis, production and secretion of mucus. Mice were intra-peritoneally sensitized with OVA in aluminum hydroxide in combination with or without Salp15, followed by OVA-aerosol treatment. Salp15 significantly reduced all features of allergic asthma mentioned above thus effectively prevented the development of experimental asthma. An opposite effect of Salp15 was detected in a mouse model of multiple sclerosis, experimental autoimmune encephalomyelitis (EAE), the progression of which is directly associated with Th17 and Th1 cells secreting IL-17 and IFN-γ, respectively (El-behi et al., 2010). Surprisingly, application of Salp15 led to enhanced activation of Th17 cells and consequently to increased production of IL-17 and development of severe EAE in mice *in vivo* and to induced differentiation of Th17 cells with IL-6 and without TGF-β *in vitro*. Salp15 did neither affect infiltration of T cells to the central nervous system, nor the development of antibody responses against the eliciting peptide $PLP_{139-151}$ or the presence of IFN-γ in the sera. The reported effect can be associated with repression of IL-2 during T cell differentiation, which could be achieved also by TGF-β and/or other immunosuppressants (Juncadella et al., 2010).

Putative Secreted Salivary Gland Proteins

TIX-5 ('Tick Inhibitor of factor Xa toward factor V,' formerly P23) was originally identified as a salivary antigen by screening *I. scapularis* nymphal salivary gland yeast surface display library with nymph-immune rabbit sera (Schuijt et al., 2011). Recombinant P23 demonstrated anti-coagulant activity. The anticoalgulant properties of P23 renamed to TIX-5 were further characterized (Schuijt et al., 2013). The studies show that TIX-5 specifically inhibits FXa-mediated factor V (FV) activation involving the B-domain of FV and reveal that activation of FV by FXa is a crucial event in the initiation of thrombin generation. The data not only elucidate a unique molecular mechanism by which ticks inhibit host blood coagulation, but propose a revised blood coagulation scheme in which direct FXa-mediated FV activation occurs in the initiation phase of coagulation. These findings could potentially results in novel therapeutic approaches for anticoagulation (Aleman and Wolberg, 2013).

EF-Hand Calcium-Binding Proteins

Longistatin was the first EF-hand calcium-binding protein identified and characterized from salivary glands of an ixodid tick, *H. longicornis* (Anisuzzaman et al., 2010). The protein was found to function as an anticoagulant and plasminogen activator, hydrolyze fibrinogen and delay fibrin clot formation (Anisuzzaman et al., 2011). Moreover, longistatin modulates host immune responses and inflammation associated with tick bites by binding to the receptor for advanced glycation end products (RAGE) that mediates immune cell activation and is highly expressed in the host skin at inflammatory sites (Anisuzzaman et al., 2014). Due to its ability to block RAGE, longistatin may be a therapeutic tool against RAGE-regulated diseases such as Alzheimer's disease, psoriasis, diabetic complications and tumorigenesis (Anisuzzaman et al., 2015).

GLYCINE-RICH, OR PROLINE-RICH, COLLAGEN-LIKE SUPERFAMILY

This superfamily of proteins produced in tick salivary glands is subdivided to a number of subgroups and includes, e.g., cuticle proteins, collagens, small and large GGY peptides, metastriate spider-like cement protein, Ixodes-specific collagen-like small peptides, metastriate and argasidae proteins distantly related to Ixodes collagen-like proteins, etc. (for details see Francischetti et al., 2009). Of interest to medical applications are proteins associated with tick cement. The main function of the cement is to anchor mouthparts of the feeding tick to the host skin and seal the feeding lesion during attachment. There are important differences in the strategy of attachment of metastriate and prostriate ticks as well as in the ultrastructure, mechanical properties and chemical composition of their cement (for review see Suppan et al., 2018). Metastriate ticks having shorter mouthparts produce an abundant cement protein cone, whereas prostriate ticks have longer mouthparts that allow mechanical attach into the host dermis, and thus produce less cement.

Considering the adhesive and sealing properties of tick cement, its potential applications as a template for biomimetic tissue adhesives is proposed (Suppan et al., 2018). Currently available tissue glues contain toxic substances, have weak bonding forces, and/or do not cover all possible fields of application in surgery and microsurgery (for review see Suppan et al., 2018). However, to be able replace currently used tissue glues by adhesives developed based on the structure and function of tick cement, the adhesive molecules produced in tick salivary glands need to be further explored.

CONCLUSION

The mammalian hemostatic and immune systems represent robust complex networks, comprising diverse humoral and cellular biological structures and processes that are essential for protection against disease, injuries or any other potentially damaging disturbers. Hemostasis belongs to the first line of defense and prevents from blood loss after damage of blood vessels. Functioning properly, both the hemostatic and the immune system identify a variety of threats and the immune system distinguishes them from the own healthy tissue. Hemostatic and immune pathways are closely interconnected. Any disorders of the immune system can result in immunodeficiency, autoimmune diseases, inflammatory diseases, even cancer, in which events of innate and adaptive immune responses, but also coagulation factors participate. Current treatment options of such diseases have often limited effectiveness, are accompanied by many side effects or are insufficient. Therefore researchers are looking for alternative medicaments derived from nature, for example, from plants, animals, or microorganisms. Ticks are astounding "pharmacologists." Their saliva contains hundreds of proteins and low molecular weight effectors with immunomodulatory, anti-inflammatory, anti-clotting and anti-platelet as well as antitumor and antiangiogenic properties with high affinity, avidity and selectivity for their targets in the host defense mechanisms. Moreover, many of the tick-derived molecules show specific, yet unknown functions and modes of action. Thus, ticks are promising sources for discovering and designing new medical treats targeting various pathways of the mammalian physiology. In addition to their high target specificity, tick-derived products have a low risk of microbial resistance, toxicity and immunogenicity (Simons et al., 2011). However, the exploration and exploitation of the pharmacological potential of ticks is still in its infancy. The candidates for designing novel drugs mentioned in this study have been tested in various animal models of human diseases and have shown promising continues. Unfortunately, only a few of them advanced to pre-clinical investigations, e.g., TAP, Ra-HBP, Dr-SBP, OmCI, or Amblyomin-X. The tick lipocalin RaHBP exhibited high ligand specificity and affinity and data from clinical trial exhibited beneficial effects in human allergy. Lipocalins are promising new therapy candidates based on their natural ligand-binding functions to store and transport small compounds, which together with their structure (small polypeptide chain) led to

design of artificial binding proteins "anticalins" with novel specificities, for example as transporters for pharmaceuticals. In general, it is a very long way from basic research to translation to the clinical praxis and, according to Murfin and Fikrig (2017), with many gaps and lacks. It is known that arthropod molecules are unstable, have a short half-life (for example OmCI mentioned in this review) or are cytotoxic, thus they require improved pharmacokinetics, optimization of dosage, delivery way, etc. (Ratcliffe et al., 2014). Another complication in drug development based on tick molecules is the identification of the mode of action of individual molecules within the complex mixture of saliva, where synergistic effect of molecules is presumed in the context of tick feeding. Thus, for therapeutic benefit identification of the interacting partners would be necessary. Last but not least, the high costs of development of new drugs designed on the basis of tick molecules is very relevant, thus the approval processes are not very attractive. However, only profound basic studies of the biological functions of tick molecules can lead to discovery and approval of new therapeutic agents.

AUTHOR CONTRIBUTIONS

PB, IŠ, VH, and MK conducted the literature search and wrote the manuscript. MK prepared the table. IŠ prepared the figure. All authors critically read and revised the manuscript.

FUNDING

This work was supported by the Grant agency of Slovak Republic (VEGA 2/0047/18 and VEGA 2/0172/19) and Slovak Research and Development Agency (APVV-0737-12).

REFERENCES

Abrahamson, M., Alvarez-Fernandez, M., and Nathanson, C. M. (2003). Cystatins. *Biochem. Soc. Symp*. 70, 179–199.

Akagi, E. M., de Sá Júnior, P. L., Simons, S. M., Bellini, M. H., Barreto, S. A., and Chudzinski-Tavassi, A. M. (2012). Pro-apoptotic effects of amblyomin-X in murine renal cell carcinoma "in vitro". *Biomed. Pharmacother.* 66, 64–69. doi: 10.1016/j.biopha.2011.11.015

Aleman, M. M., and Wolberg, A. S. (2013). Tick spit shines a light on the initiation of coagulation. *Circulation* 128, 203–205. doi: 10.1161/circulationaha.113.003800

Anguita, J., Ramamoorthi, N., Hovius, J. W. R., Das, S., Thomas, V., Persinski, R., et al. (2002). Salp15, an *Ixodes scapularis* salivary protein, inhibits CD4+ T cell activation. *Immunity* 16, 849–859. doi: 10.1016/S1074-7613(02)00325-324

Anisuzzaman, Alim, M. A., and Tsuji, N. (2015). Longistatin in tick-saliva targets RAGE. *Oncotarget* 6, 35133–35134. doi: 10.18632/oncotarget.6032

Anisuzzaman, Hatta, T., Miyoshi, T., Matsubayashi, M., Islam, M. K., Alim, M. A., et al. (2014). Longistatin in tick saliva blocks advanced glycation end-product receptor activation. *J. Clin. Invest.* 124, 4429–4444. doi: 10.1172/jci74917

Anisuzzaman, Islam, M. K., Alim, M. A., Miyoshi, T., Hata, T., Yamaji, K., et al. (2011). Longistatin, a plasminogen activator, is key to the availability of blood-meals for ixodid ticks. *PLoS Pathog.* 7:e1001312. doi: 10.1371/journal.ppat.1001312

Anisuzzaman, Islam, M. K., Miyoshim, T., Alim, M. A., Hatta, T., Yamaji, K., et al. (2010). Longistatin, a novel EF-hand protein from the ixodid tick *Haemaphysalis longicornis*, is required for acquisition of host blood-meals. *Int. J. Parasitol.* 40, 721–729. doi: 10.1016/j.ijpara.2009.11.004

Askenase, P. W., Bursztajn, S., Gershon, M. D., and Gershon, R. K. (1980). T cell-dependent mast cell degranulation and release of serotonin in murine delayed-type hypersensitivity. *J. Exp. Med.* 152, 1358–1374. doi: 10.1084/jem.152.5.1358

Assumpção, T. C., Mizurini, D. M., Ma, D., Monteiro, R. Q., Ahlstedt, S., Reyes, M., et al. (2018). Ixonnexin from tick saliva promotes fibrinolysis by interacting with plasminogen and tissue-type plasminogen activator, and prevents arterial thrombosis. *Sci. Rep.* 8:4806. doi: 10.1038/s41598-018-22780-22781

Ayllón, N., Villar, M., Galindo, R. C., Kocan, K. M., Šíma, R., López, J. A., et al. (2015). Systems biology of tissue-specific response to *Anaplasma phagocytophilum* reveals differentiated apoptosis in the tick vector ixodes scapularis. *PLoS Genet.* 11:e1005120. doi: 10.1371/journal.pgen.1005120

Barratt-Due, A., Thorgersen, E. B., Lindstad, J. K., Pharo, A., Lisina, O., Lambris, J. D., et al. (2011). *Ornithodoros moubata* complement inhibitor is an equally effective C5 inhibitor in pigs and humans. *J. Immunol.* 187, 4913–4919. doi: 10.4049/jimmunol.1101000

Batista, I. F. C., Ramos, O. H. P., Ventura, J. S., Junqueira-de-Azevedo, I. L. M., Ho, P. L., and Chudzinski-Tavassi, A. M. (2010). A new factor xa inhibitor from *Amblyomma cajennense* with a unique domain composition. *Arch. Biochem. Biophys.* 493, 151–156. doi: 10.1016/j.abb.2009.10.009

Beaufays, J., Adam, B., Decrem, Y., Prévôt, P. P., Santini, S., Brasseur, R., et al. (2008). Ixodes ricinus tick lipocalins: identifications, cloning, phylogenetic analysis and biochemical characterization. *PLoS One* 3:e3941. doi: 10.1371/journal.pone.0003941

Blisnick, A. A., Foulon, T., and Bonnet, S. I. (2017). Serine protease inhibitors in ticks: an overview of their role in tick biology and tick-borne pathogen transmission. *Front. Cell Infect. Microbiol.* 7:199. doi: 10.3389/fcimb.2017.00199

Bonnet, S., Kazimírová, M., Richardson, J., and Šimo, L. (2018). "„Tick saliva and its role in pathogen transmission"," in *Skin and Arthropod Vectors*, ed. N. Boulanger (Amsterdam: Elsevier), 121–192.

Bonnet, S. I., Binetruy, F., Hernández-Jarguín, A. M., and Duron, O. (2017). The tick microbiome: why non-pathogenic microorganisms matter in tick biology and pathogen transmission. *Front. Cell Infect. Microbiol.* 7:236. doi: 10.3389/fcimb.2017.00236

Bonvin, P., Power, C. A., and Proudfoot, A. E. (2016). Evasins: therapeutic potential of new family of chemokine-binding proteins from ticks. *Front. Immunol.* 7:208. doi: 10.3389/fimmu.2016.00208

Boufleur, P., Sciani, J. M., Goldfeder, M., Faria, F., Branco, V., and Chudzinski-Tavassi, A. M. (2019). Biodistribution and pharmacokinetics of amblyomin-X, a novel antitumour protein drug in healthy mice. *Eur. J. Drug. Metab. Pharmacokinet.* 44, 111–120. doi: 10.1007/s13318-018-0500-z

Branco, V. G., Iqbal, A., Alvarez-Flores, M. P., Sciani, J. M., de Andrade, S. A., Iwai, L. K., et al. (2016). Amblyomin-X having a Kunitz-type homologous domain is a noncompetitive inhibitor of FXa and induces anticoagulation *in vitro* and *in vivo*. *Biochim. Biophys. Acta* 1864, 1428–1435. doi: 10.1016/j.bbapap.2016.07.011

Braunersreuther, V., Montecucco, F., Pelli, G., Galan, K., Proudfoot, A. E., Belin, A., et al. (2013). Treatment with the CC chemokine-binding protein Evasin-4 improves post-infarction myocardial injury and survival in mice. *Thromb. Haemost.* 110, 807–825. doi: 10.1160/TH13-04-0297

Bronsoms, S., Pantoja-Uceda, D., Gabrijelcic-Geiger, D., Sanglas, L., Aviles, F. X., Santoro, J., et al. (2011). Oxidative folding and structural analyses of a Kunitz-Related Inhibitor and its disulfide intermediates: functional implications. *J. Mol. Biol.* 414, 427–441. doi: 10.1016/j.jmb.2011.10.018

Buning, J., Homann, N., von Smolinski, D., Borcherding, F., Noack, F., Stolte, M., et al. (2008). Helminths as governors of inflammatory bowel disease. *Gut* 57, 1182–1183. doi: 10.1136/gut.2008.152355

Carneiro-Lobo, T. C., Konig, S., Machado, D. E., Nasciutti, L. E., Forni, M. F., Francischetti, I. M. B., et al. (2009). Ixolaris, a tissue factor inhibitor, blocks primary tumor growth and angiogenesis in a glioblastoma model. *J. Thromb. Haemost.* 7, 1855–1864. doi: 10.1111/j.1538-7836.2009.03553.x

Carneiro-Lobo, T. C., Schaffner, F., Disse, J., Ostergaard, H., Francischetti, I. M. B., Monteiro, R. Q., et al. (2012). The tick-derived inhibitor ixolaris prevents tissue factor signaling on tumor cells. *J. Thromb. Haemost.* 10, 1849–1858. doi: 10.1111/j.1538-7836.2012.04864.x

Castor, M. G. M., Rezende, B., Resende, C. B., Alessandri, A. L., Fagundes, C. T., Sousa, L. P., et al. (2010). The CCL3/macrophage inflammatory protein-1α–binding protein evasin-1 protects from graft-versus-host disease but does not modify graft-versus-leukemia in mice. *J. Immunol.* 184, 2646–2654. doi: 10.4049/jimmunol.0902614

Caughey, G. H. (2007). Mast cell tryptases and chymases in inflammation and host defense. *Immunol. Rev.* 217, 141–154. doi: 10.1111/j.1600-065X.2007.00509.x

Charmoy, M., Brunner-Agten, S., Aebischer, D., Auderset, F., Launois, P., Milon, G., et al. (2010). Neutrophil-derived CCL3 is essential for the rapid recruitment of dendritic cells to the site of Leishmania major inoculation in resistant mice. *PLoS Pathog.* 6:e1000755. doi: 10.1371/journal.ppat.1000755

Chen, G., Wang, X., Severo, M. S., Sakhon, O. S., Sohail, M., Brown, L. J., et al. (2014). The tick salivary protein sialostatin L2 inhibits caspase-1-mediated inflammation during *Anaplasma phagocytophilum* infection. *Infect. Immun.* 82, 2553–2564. doi: 10.1128/IAI.01679-14

Chen, N., Xu, S., Zhang, Y., and Wang, F. (2018). Animal protein toxins: origins and therapeutic applications. *Biophys. Rep.* 4, 233–242. doi: 10.1007/s41048-018-0067-x

Cherniack, P. E. (2010). Bugs as drugs, Part 1: insects. the "New" alternative medicine for the 21st century? *Altern. Med. Rev.* 15, 124–135. doi: 10.1128/9781555819705

Cherniack, P. E. (2011). Bugs as drugs, part two_ worms, leeches, scorpions, snails, ticks, centipedes, and spiders. *Altern. Med. Rev.* 16, 50–58.

Chmelar, J., Calvo, E., Pedra, J. H. F., Francischetti, I. M. B., and Kotsyfakis, M. (2012). Tick salivary secretion as a source of antihemostatics. *J. Proteomics* 75, 3842–3854. doi: 10.1016/j.jprot.2012.04.026

Chmelar, J., Kotál, J., Kopecký, J., Pedra, J. H. F., and Kotsyfakis, M. (2016). All for one and one for all on the tick-host battlefield. *Trends Parasitol.* 32, 368–377. doi: 10.1016/j.pt.2016.01.004

Chmelar, J., Kotál, J., Langhansová, H., and Kotsyfakis, M. (2017). Protease inhibitors in tick saliva: the role of serpins and cystatins in tick-host-pathogen interaction. *Front. Cell Infect. Microbiol.* 7:216. doi: 10.3389/fcimb.2017.00216

Chmelar, J., Oliveira, C. J., Rezacova, P., Francischetti, I. M. B., Kovarova, Z., Pejler, G., et al. (2011). A tick salivary protein targets cathepsin G and chymase and inhibits host inflammation and platelet aggregation. *Blood* 117, 736–744. doi: 10.1182/blood-2010-06-293241

Chudzinski-Tavassi, A. M., de-Sá-Júnior, P. L., Simons, S. M., Maria, D. A., de Souza Ventura, J., de Fatima Correia Batista, I., et al. (2010). A new tick Kunitz type inhibitor, Amblyomin-X, induces tumor cell death by modulating genes related to the cell cycle and targeting the ubiquitin-proteasome system. *Toxicon* 56, 1145–1154. doi: 10.1016/j.toxicon.2010.04.019

Chudzinski-Tavassi, A. M., Faria, F., and Alvarez Flores, M. P. (2018). "Anticoagulants from hematophagous," in *Anticoagulant Drugs*, ed. M. Božič-Mijovski (Rijeka: IntechOpen), doi: 10.5772/intechopen.78025

Chudzinski-Tavassi, A. M., Morais, K. L. P., Pacheco, M. T. F., Pasqualoto, K. F. M., and de Souza, J. G. (2016). Tick salivary gland as potential natural source for the discovery of promising antitumor drug candidates. *Biomed. Pharmacother.* 77, 14–19. doi: 10.1016/j.biopha.2015.11.003

Corral-Rodriguez, M. A., Macedo-Ribeiro, S., Pereira, P. J. B., and Fuentes-Prior, P. (2009). Tick-derived Kunitz-type inhibitors as antihemostatic factors. *Insect Biochem. Mol. Biol.* 39, 579–595. doi: 10.1016/j.ibmb.2009.07.003

Couillin, I., Maillet, I., Vargaftig, B. B., Jacobs, M., Paesen, G. C., Nuttall, P. A., et al. (2004). Arthropod-derived histamine-binding protein prevents murine allergic asthma. *J. Immunol.* 173, 3281–3286. doi: 10.4049/jimmunol.173.5.3281

Couvreur, B., Beaufays, J., Charon, C., Lahaye, K., Gensale, F., Denis, V., et al. (2008). Variability and action mechanism of a family of anticomplement proteins in *Ixodes ricinus*. *PLoS One* 3:e1400. doi: 10.1371/journal.pone.0001400

Daix, V., Schroeder, H., Praet, N., Georgin, J. P., Chiappino, I., Gillet, L., et al. (2007). Ixodes ticks belonging to the *Ixodes ricinus* complex encode a family of anticomplement proteins. *Insect Mol. Biol.* 16, 155–166. doi: 10.1111/j.1365-2583.2006.00710.x

de Castro, M. H., de Klerk, D., Pienaar, R., Latif, A. A., Rees, D. J. G., and Mans, B. J. (2016). De novo assembly and annotation of the salivary gland transcriptome of *Rhipicephalus appendiculatus* male and female ticks during blood feeding. *Ticks Tick Borne Dis.* 7, 536–548. doi: 10.1016/j.ttbdis.2016.01.014

de Miranda Santos, I. K. F., Valenzuela, J. G., Ribeiro, J. M. C., de Castro, M. H., Costa, J. N., Costa, A. M., et al. (2004). Gene discovery in *Boophilus microplus*, the cattle tick: the transcriptomes of ovaries, salivary glands, and hemocytes. *Ann. N. Y. Acad. Sci.* 1026, 242–246. doi: 10.1196/annals.1307.037

de Oliveira, A. S., Lima, L. G., Mariano-Oliveira, A., Machado, D. E., Nasciutti, L. E., Andersen, J. F., et al. (2012). Inhibition of tissue factor by ixolaris reduces primary tumor growth and experimental metastasis in a murine model of melanoma. *Thromb. Res.* 130, 163–170. doi: 10.1016/j.thromres.2012.05.021

de Souza, J. G., Morais, K. L. P., Anglés-Cano, E., Boufleur, P., de Mello, E. S., Maria, D. A., et al. (2016). Promising pharmacological profile of a Kunitz-type inhibitor in murine renal cell carcinoma model. *Oncotarget* 7, 62255–62266. doi: 10.18632/oncotarget.11555

de Sá Jr, P. L., Camara, D. A. D., Sciani, J. M., Porcacchia, A. S., Fonseca, P. M. M., Mendonca, R. Z., et al. (2019). Antiproliferative and antiangiogenic effect of *Amblyomma sculptum* (Acari: Ixodidae) crude saliva in endothelial cells in vitro. *Biomed. Pharmacother.* 110, 353–361. doi: 10.1016/j.biopha.2018.11.107

Decrem, Y., Rath, G., Blasioli, V., Cauchie, P., Robert, S., Beaufays, J., et al. (2009). Ir-CPI, a coagulation contact phase inhibitor from the tick *Ixodes ricinus*, inhibits thrombus formation without impairing hemostasis. *J. Exp. Med.* 206, 2381–2395. doi: 10.1084/jem.20091007

Deruaz, M., Frauenschuh, A., Alessandri, A. L., Dias, J. M., Coelho, F. M., Russo, R. C., et al. (2008). Ticks produce highly selective chemokine binding proteins with antiinflammatory activity. *J. Exp. Med.* 205, 2019–2031. doi: 10.1084/jem.20072689

Dinan, T. G. (1996). Serotonin: current understanding and the way forward. *Int. Clin. Psychopharmacol.* 11(Suppl. 1), 19–21.

Drewes, C. C., Dias, R. Y., Branco, V. G., Cavalcante, M. F., Souza, J. G., Abdalla, D. S. P., et al. (2015). Post-transcriptional control of Amblyomin-X on secretion of vascular endothelial growth factor and expression of adhesion molecules in endothelial cells. *Toxicon* 101, 1–10. doi: 10.1016/j.toxicon.2015.04.002

Drewes, C. C., Dias, R. Y., Hebeda, C. B., Simons, S. M., Barreto, S. A., Ferreira Junior, J. M., et al. (2012). Actions of the Kunitz-type serine protease inhibitor amblyomin-X on VEGF-A-induced angiogenesis. *Toxicon* 60, 333–340. doi: 10.1016/j.toxicon.2012.04.349

Duncan, R. C., Wijeyewickrema, L. C., and Pike, R. N. (2007). The initiating proteases of the complement system: controlling the cleavage. *Biochimie* 90, 387–395. doi: 10.1016/j.biochi.2007.07.023

Eaton, J. R. O., Alenazi, Y., Singh, K., Davies, G., Geis-Asteggiante, L., Kessler, B., et al. (2018). The N-terminal domain of a tick evasin is critical for chemokine binding and neutralization and confers specific binding activity to other evasins. *J. Biol. Chem.* 293, 6134–6146. doi: 10.1074/jbc.RA117.000487

Efferth, T., Rauh, R., Kahl, S., Tomicic, M., Bochzelt, H., Tome, M. E., et al. (2005). Molecular modes of action of cantharidin in tumor cells. *Biochem. Pharmacol.* 69, 811–818. doi: 10.1016/j.bcp.2004.12.003

El-behi, M., Rostami, A., and Ciric, B. (2010). Current views on the roles ofTh1 and Th17 cells in experimental autoimmune encephalomyelitis. *J. Neuroimmune Pharmacol.* 5, 189–197. doi: 10.1007/s11481-009-9188-9189

Eldor, A., Orevi, M., and Rigbi, M. (1996). The role of the leech in medical therapeutics. *Blood Rev.* 10, 201–209. doi: 10.1016/s0268-960x(96)90000-4

Esteves, E., Maruyama, S. R., Kawahara, R., Fujita, A., Martins, L. A., Righi, A. A., et al. (2017). Analysis of the salivary gland transcriptome of unfed, and partially fed *Amblyomma sculptum* ticks, and descriptive proteome of the saliva. *Front. Cell Infect. Microbiol.* 7:476. doi: 10.3389/fcimb.2017.00476

Ferrara, J. L., and Deeg, H. J. (1991). Graft-versus-host disease. *N. Engl. J. Med.* 324, 667–674.

Figueiredo, A. C., de Sanctis, D., and Pereira, P. J. B. (2013). The tick-derived anticoagulant madanin is processed by thrombin and factor Xa. *PLoS One* 8:e71866. doi: 10.1371/journal.pone.0071866

Francischetti, I. M. B. (2010). Platelet aggregation inhibitors from hematophagous animals. *Toxicon* 56, 1130–1144. doi: 10.1016/j.toxicon.2009.12.003

Francischetti, I. M. B., Anderson, J. M., Manoukis, N., Pham, V. M., and Ribeiro, J. M. C. (2011). An insight into the sialotranscriptome and proteome of the coarse bontlegged tick, *Hyalomma marginatum rufipes*. *J. Proteomics* 74, 2892–2908. doi: 10.1016/j.jprot.2011.07.015

Francischetti, I. M. B., Mather, T. N., and Ribeiro, J. M. C. (2004). Penthalaris, a novel recombinant five-Kunitz tissue factor pathway inhibitor (TFPI) from

the salivary gland of the tick vector of Lyme disease, *Ixodes scapularis*. *Thromb. Haemost.* 91, 886–898. doi: 10.1160/TH03-11-0715

Francischetti, I. M. B., Pham, V. M., Mans, B. J., Andersen, J. F., Mather, T. N., Lane, R. S., et al. (2005). The transcriptome of the salivary glands of the female western black-legged tick *Ixodes pacificus* (Acari: Ixodidae). *Insect Biochem. Mol. Biol.* 35, 1142–1161. doi: 10.1016/j.ibmb.2005.05.007

Francischetti, I. M. B., Sa-Nunes, A., Mans, B. J., Santos, I. M., and Ribeiro, J. M. C. (2009). The role of saliva in tick feeding. *Front. Biosci.* 14, 2051–2088.

Francischetti, I. M. B., Valenzuela, J. G., Andersen, J. F., Mather, T. N., and Ribeiro, J. M. C. (2002). Ixolaris, a novel recombinant tissue factor pathway inhibitor (TFPI) from the salivary gland of the tick, *Ixodes scapularis*: identification of factor X and factor Xa as scaffolds for the inhibition of factor VIIa/tissue factor complex. *Blood* 99, 3602–3612. doi: 10.1182/blood-2001-12-0237

Frauenschuh, A., Power, C. A., Deruaz, M., Ferreira, B. R., Silva, J. S., Teixeira, M. M., et al. (2007). Molecular cloning and characterization of a highly selective chemokine-binding protein from the tick *Rhipicephalus sanguineus*. *J. Biol. Chem.* 282, 27250–27258. doi: 10.1074/jbc.m704706200

Fredslund, F., Laursen, N. S., Roversi, P., Jenner, L., Oliveira, C. L., Pedersen, J. S., et al. (2008). Structure of and influence of a tick complement inhibitor on human complement component 5. *Nat. Immunol.* 9, 753–760. doi: 10.1038/ni.1625

Funderburg, N. T., and Lederman, M. M. (2014). Coagulation and morbidity in treated HIV infection. *Thromb. Res.* 133(Suppl. 1), S21–S24. doi: 10.1016/j.thromres.2014.03.012

Garcia, G. R., Gardinassi, L. G., Ribeiro, J. M. C., Anatriello, E., Ferreira, B. R., Moreira, H. N. S., et al. (2014). The sialotranscriptome of *Amblyomma triste*, *Amblyomma parvum* and *Amblyomma cajennense* ticks, uncovered by 454-based RNA-seq. *Parasit. Vectors* 7:430. doi: 10.1186/1756-3305-7-430

Garg, R., Juncadella, I. J., Ramamoorthi, N., Ashish, Ananthanarayanan, S. K., Thomas, V., et al. (2014). Cutting edge: CD4 is the receptor for the tick saliva immunosuppressor, Salp15. *J. Immunol.* 177, 6579–6583. doi: 10.4049/jimmunol.177.10.6579

Gradowski do Nascimento, T., Santos Vieira, P., Campos Cogo, S., Ferreira Dias-Netipanyj, M., de França, F., Dias Câmara, D. A., et al. (2019). Antitumoral effects of *Amblyomma sculptum* berlese saliva in neuroblastoma cell lines involve cytoskeletal deconstruction and cell cycle arrest. *Braz. J. Vet. Parasitol.* 28, 126–133. doi: 10.1590/S1984-296120180098

Hajnická, V., Kocáková, P., Sláviková, M., Slovák, M., Gašperík, J., Fuchsberger, N., et al. (2001). Anti-interleukin-8 activity of tick salivary gland extracts. *Parasite Immunol.* 23, 483–489. doi: 10.1046/j.1365-3024.2001.00403.x

Hajnicka, V., Vancova, I., Kocakova, P., Slovak, M., Gasperik, J., Slavikova, M., et al. (2005). Manipulation of host cytokine network by ticks: a potential gateway for pathogen transmission. *Parasitology* 130, 333–342. doi: 10.1017/s0031182004006535

Hajnicka, V., Vancova-Stibraniova, I., Slovak, M., Kocakova, P., and Nuttall, P. A. (2011). Ixodid tick salivary gland products target host wound healing growth factors. *Int. J. Parasitol.* 41, 213–223. doi: 10.1016/j.ijpara.2010.09.005

Harris, C. L. (2018). Expanding horizons in complement drug discovery: challenges and emerging strategies. *Semin. Immunopathol.* 40, 125–140. doi: 10.1007/s00281-017-0655-658

Hashemzadeh, M., Furukawa, M., Goldsberry, S., and Movahed, M. R. (2008). Chemical structures and mode of action of intravenous glycoprotein IIb/IIIa receptor blockers: a review. *Exp. Clin. Cardiol.* 13, 192–197.

Hayward, J., Sanchez, J., Perry, A., Huang, C., Rodriguez Valle, M., Canals, M., et al. (2017). Ticks from diverse genera encode chemokine-inhibitory evasin proteins. *J. Biol. Chem.* 292, 15670–15680. doi: 10.1074/jbc.M117.807255

Hepburn, N. J., Williams, A. S., Nunn, M. A., Chamberlain-Banoub, J. C., Hamer, J., Morgan, B. P., et al. (2007). *In Vivo* characterization and therapeutic efficacy of a C5-specific inhibitor from the soft tick *Ornithodoros moubata*. J. Biol. Chem. 282, 8292–8299. doi: 10.1074/jbc.m609858200

Hesketh, P. J. (2004). Understanding the pathobiology of chemotherapy induced nausea and vomiting. Providing a basis for therapeutic progress. *Oncology* 18(10 Suppl. 6), 9–14.

Hoffman, R., Benz, E. J., Furie, B., and Shattil, S. J. (2009). *Hematology: Basic Principles and Practice*. California, CA: Churchill Livingstone.

Holíková, V., Štibrániová, I., Bartíková, P., Slovák, M., and Kazimírová, M. (2018). Ixodid tick salivary gland extracts suppress human transforming growth factor-β1 triggered signalling pathways in cervical carcinoma cells. *Biologia* 73, 1109–1122. doi: 10.2478/s11756-018-0129-z

Horka, H., Staudt, V., Klein, M., Taube, C., Reuter, S., Dehzad, N., et al. (2012). The tick salivary protein sialostatin L inhibits the Th9-derived production of the asthma-promoting cytokine IL-9 and is effective in the prevention of experimental asthma. *J. Immunol.* 188, 2669–2676. doi: 10.4049/jimmunol.1100529

Hourcade, D. E., Akk, A. M., Mitchell, L. M., Zhou, H. F., Hauhart, R., and Pham, C. T. (2016). Anti-complement activity of the *Ixodes scapularis* salivary protein Salp20. *Mol. Immunol.* 69, 62–69. doi: 10.1016/j.molimm.2015.11.008

Hovius, J. W. R., Levi, M., and Fikrig, E. (2008). Salivating for knowledge: potential pharmacological agents in tick saliva. *PLoS Med.* 5:e43. doi: 10.1371/journal.pmed.0050043

Iqbal, A., Goldfeder, M. B., Marques-Porto, R., Asif, H., de Souza, J. G., Faria, F., et al. (2017). Revisiting antithrombotic therapeutics; sculptin, a novel specific, competitive, reversible, scissile and tight binding inhibitor of thrombin. *Sci. Rep.* 7:1431. doi: 10.1038/s41598-017-01486-w

Islam, M. K., Tsuji, N., Miyoshi, T., Alim, M. A., Huang, X., Hatta, T., et al. (2009). The Kunitz-like modulatory protein haemangin is vital for hard tick blood-feeding success. *PLoS Pathog.* 5:e1000497. doi: 10.1371/journal.ppat.1000497

Iwanaga, S., Okada, M., Isawa, H., Morita, A., Yuda, M., and Chinzei, Y. (2003). Identification and characterization of novel salivary thrombin inhibitors from the ixodidae tick, *Haemaphysalis longicornis*. *Eur. J. Biochem.* 270, 1926–1934. doi: 10.1046/j.1432-1033.2003.03560.x

Iyer, J. K., Koh, C. Y., Kazimirova, M., Roller, L., Jobichen, C., Swaminathan, K., et al. (2017). Avathrin: a novel thrombin inhibitor derived from a multicopy precursor in the salivary glands of the ixodid tick, *Amblyomma variegatum*. *FASEB J.* 31, 2981–2995. doi: 10.1096/fj.201601216R

Iyer, J. K., Koh, C. Y., Kini, R. M., Kazimirova, M., and Roller, L. (2019). *Novel Thrombin Inhibitors*. U.S. Patent No 15/737,266. Washington, DC: U.S. Patent and Trademark Office.

Jablonka, W., Kotsyfakis, M., Mizurini, D. M., Monteiro, R. Q., Lukszo, J., Drake, S. K., et al. (2015). Identification and mechanistic analysis of a novel tick-derived inhibitor of thrombin. *PLoS One* 10:e0133991. doi: 10.1371/journal.pone.0133991

Juncadella, I. J., Bates, T. C., Suleiman, R., Monteagudo-Mera, A., Olson, C. M., Navasa, N., et al. (2010). The tick saliva immunosuppressor, Salp15, contributes to Th17-induced pathology during experimental autoimmune encephalomyelitis. *Biochem. Biophys. Res. Commun.* 402, 105–109. doi: 10.1016/j.bbrc.2010.09.125

Juncadella, I. C., Garg, R., Ananthnarayanan, S. K., Yengo, C. M., and Anguita, J. (2007). T-cell signaling pathways inhibited by the tick saliva immunosuppressor, Salp15. *FEMS Immunol. Med. Microbiol.* 49, 433–438. doi: 10.1111/j.1574-695X.2007.00223.x

Karczewski, J., Endris, R., and Connolly, T. M. (1994). Disagregin is a fibrinogen receptor antagonist lacking the Arg-Gly-Asp sequence from the tick, *Ornithodoros moubata*. *J. Biol. Chem.* 269, 6702–6708.

Kazimírová, M. (2011). "Pharmacologically active compounds from ticks and other arthropods and their potential use in anticancer therapy" Chapter 3," in *Natural Compounds as Inducers of Cell Death*, Vol. 1, eds M. Diederich and K. Noworyta (Dordrecht: Springer Science+Business Media), 163–182. doi: 10.1007/978-94-007-4575-9_7

Kazimirova, M., Dovinova, I., Rolnikova, T., Tothova, L., and Hunakova, L. (2006). Antiproliferative activity and apoptotic effect of tick salivary gland extracts on human HeLa cells. *Neuro Endocrinol. Lett.* 27(Suppl. 2), 48–52.

Kazimírová, M., Kini, M., and Koh, Y. (2015). *Thrombin Inhibitor*. U.S. Patent No 9,217,027 B2. Washington, DC: U.S. Patent and Trademark Office.

Kazimírová, M., Koh, C. Y., and Kini, R. M. (2010). "Tiny ticks are vast sources of antihaemostatic factors," in *Toxins and Hemostasis*, eds R. Kini, K. Clemetson, F. Markland, M. McLane, and T. Morita (Dordrecht: Springer), 113–130. doi: 10.1007/978-90-481-9295-3_8

Kazimírová, M., and Štibrániová, I. (2013). Tick salivary compounds: their role in modulation of host defences and pathogen transmission. *Front. Cell Infect. Microbiol.* 3:43. doi: 10.3389/fcimb.2013.00043

Keller, P. M., Waxman, L., Arnold, B. A., Schultz, L. D., Condra, C., and Connolly, T. M. (1993). Cloning of the cDNA and expression of moubatin, an inhibitor of platelet-aggregation. *J. Biol. Chem.* 268, 5445–5449.

Klein, M., Brühl, T. J., Staudt, V., Reuter, S., Grebe, N., Gerlitzki, B., et al. (2015). Tick salivary sialostatin L represses the initiation of immune responses by targeting IRF4-dependent transcription in murine mast cells. *J. Immunol.* 195, 621–631. doi: 10.4049/jimmunol.1401823

Koh, C. Y., Kazimirova, M., Nuttall, P. A., and Kini, R. M. (2009). Noncompetitive inhibitor of thrombin. *Chem. Biol. Chem.* 10, 2155–2158. doi: 10.1002/cbic.200900371

Koh, C. Y., Kazimirova, M., Trimnell, A., Takac, P., Labuda, M., Nuttall, P. A., et al. (2007). Variegin, a novel fast and tight binding thrombin inhibitor from the tropical bont tick. *J. Biol. Chem.* 282, 29101–29113. doi: 10.1074/jbc.M705600200

Koh, C. Y., Kumar, S., Kazimirova, M., Nuttall, P. A., Radhakrishnan, U. P., Kim, S., et al. (2011). Crystal structure of thrombin in complex with S-variegin: insights of a novel mechanism of inhibition and design of tunable thrombin inhibitors. *PLoS One* 6:e26367. doi: 10.1371/journal.pone.0026367

Koh, C. Y., Modahl, C. M., Kulkarni, N., and Kini, R. (2018). Toxins are an excellent source of therapeutic agents against cardiovascular diseases. *Semin. Thromb. Hemost.* 44, 691–706. doi: 10.1055/s-0038-1661384

Kotal, J., Langhansova, H., Lieskovska, J., Andersen, J. F., Francischetti, I. M., Chavakis, T., et al. (2015). Modulation of host immunity by tick saliva. *J. Proteomics* 128, 58–68. doi: 10.1016/j.jprot.2015.07.005

Kotál, J., Stergiou, N., Buša, M., Chlastáková, A., Beránková, Z., Řezáčová, P., et al. (2019). The structure and function of Iristatin, a novel immunosuppressive tick salivary cystatin. *Cell Mol. Life Sci.* 76, 2003–2013. doi: 10.1007/s00018-019-03034-3033

Kotsyfakis, M., Horka, H., Salat, J., and Andersen, J. F. (2010). The crystal structures of two salivary cystatins from the tick *Ixodes scapularis* and the effect of these inhibitors on the establishment of *Borrelia burgdorferi* infection in a murine model. *Mol. Microbiol.* 77, 456–470. doi: 10.1111/j.1365-2958.2010.07220.x

Kotsyfakis, M., Karim, S., Andersen, J. F., Mather, T. N., and Ribeiro, J. M. C. (2007). Selective cysteine protease inhibition contributes to blood-feeding success of the tick *Ixodes scapularis*. *J. Biol. Chem.* 282, 29256–29263. doi: 10.1074/jbc.M703143200

Kotsyfakis, M., Sa-Nunes, A., Francischetti, I. M. B., Mather, T. N., Andersen, J. F., and Ribeiro, J. M. C. (2006). Antiinflammatory and immunosuppressive activity of sialostatin L, a salivary cystatin from the tick *Ixodes scapularis*. *J. Biol. Chem.* 281, 26298–26307. doi: 10.1074/jbc.M513010200

Kotsyfakis, M., Schwarz, A., Erhart, J., and Ribeiro, J. M. C. (2015). Tissue- and time-dependent transcription in *Ixodes ricinus* salivary glands and midguts when blood feeding on the vertebrate host. *Sci. Rep.* 5:9103. doi: 10.1038/srep09103

Kuhn, N., Schmidt, C. Q., Schlapschy, M., and Skerra, A. (2016). PASylated Coversin, a C5-specific complement inhibitor with extended pharmacokinetics, shows enhanced anti-hemolytic activity *in vitro*. *Bioconjugate Chem.* 27, 2359–2371. doi: 10.1021/acs.bioconjchem.6b00369

Leboulle, G., Crippa, M., Decrem, Y., Mejri, N., Brossard, M., Bollen, A., et al. (2002). Characterization of a novel salivary immunosuppressive protein from *Ixodes ricinus* ticks. *J. Biol. Chem.* 277, 10083–10089.

Lieskovská, J., Páleníková, J., Langhansová, H., Campos Chagas, A., Calvo, E., Kotsyfakis, M., et al. (2015a). Tick sialostatins L and L2 differentially influence dendritic cell responses to *Borrelia* spirochetes. *Parasit. Vectors* 8:275. doi: 10.1186/s13071-015-0887-1

Lieskovská, J., Paleniková, J., Sirmarová, J., Elsterová, J., Kotsyfakis, M., Campos Chagas, A., et al. (2015b). Tick salivary cystatin sialostatin L2 suppresses IFN responses in mouse dendritic cells. *Parasite Immunol.* 37, 70–78. doi: 10.1111/pim.12162

Lincoff, A. M., Bittl, J. A., Kleiman, N. S., Sarembock, I. J., Jackman, J. D., Mehta, S., et al. (2004). Comparison of bivalirudin versus heparin during percutaneous coronary intervention (the randomized evaluation of PCI linking angiomax to reduced clinical events [REPLACE]-1 trial). *Am. J. Cardiol.* 93, 1092–1096. doi: 10.1016/j.amjcard.2004.01.033

Liu, D., and Chen, Z. (2009). The effects of cantharidin and cantharidin derivates on tumour cells. *Anticancer Agents Med. Chem.* 9, 392–396. doi: 10.2174/1871520610909040392

Liu, X. Y., and Bonnet, S. I. (2014). Hard tick factors implicated in pathogen transmission. *PLoS Negl. Trop. Dis.* 8:e2566. doi: 10.1371/journal.pntd.0002566

Liu, X. Y., de la Fuente, J., Cote, M., Galindo, R. C., Moutailler, S., Vayssier-Taussat, M., et al. (2014). IrSPI, a tick serine protease inhibitor involved in tick feeding and *Bartonella henselae* infection. *PLoS Negl. Trop. Dis.* 8:e2993. doi: 10.1371/journal.pntd.0002993

Lourenço, J. D., Neves, L. P., Olivo, C. R., Duran, A., Almeida, F. M., Arantes, P. M., et al. (2014). A treatment with a protease inhibitor recombinant from the cattle tick *Rhipicephalus (Boophilus) microplus* ameliorates emphysema in mice. *PLoS One* 9:e98216. doi: 10.1371/journal.pone.0098216

Mans, B. J. (2005). Tick histamine-binding proteins and related lipocalins: potential as therapeutic agents. *Curr. Opin. Investig. Drugs* 6, 1131–1135.

Mans, B. J. (2016). "Glandular matrices and secretions: Blood-feeding arthropods," in *Extracellular Composite Matrices in Arthropods*, eds E. Cohen and B. Moussian (Cham: Springer), 625–688. doi: 10.1007/978-3-319-40740-1_17

Mans, B. J., Louw, A. I., and Neitz, A. W. (2003). The major tick salivary gland proteins and toxins from the soft tick, *Ornithodoros savignyi*, are part of the tick lipocalin family: implications for the origins of tick toxicoses. *Mol. Biol. Evol.* 20, 1158–1167. doi: 10.1093/molbev/msg126

Mans, B. J., and Ribeiro, J. M. C. (2008). Function, mechanism and evolution of the moubatin-clade of soft tick lipocalins. *Insect Biochem. Mol. Biol.* 38, 841–852. doi: 10.1016/j.ibmb.2008.06.007

Mans, B. J., Ribeiro, J. M. C., and Andersen, J. F. (2008). Structure, function, and evolution of biogenic amine-binding proteins in soft ticks. *J. Biol. Chem.* 283, 18721–18733. doi: 10.1074/jbc.M800188200

Maria, D. A., de Souza, J. G., Morais, K. L. P., Berra, C. M., de Campos Zampoli, H., Demasi, M., et al. (2013). A novel proteasome inhibitor acting in mitochondrial dysfunction, ER stress and ROS production. *Invest. New Drugs* 31, 493–505. doi: 10.1007/s10637-012-9871-1

Maria, D. A., Will, S. E. A. L., Bosch, R. V., Souza, J. G., Sciani, J. M., Goldfeder, M. B., et al. (2019). Preclinical evaluation of Amblyomin-X, a Kunitz-type protease inhibitor with antitumor activity. *Toxicol. Rep.* 6, 51–63. doi: 10.1016/j.toxrep.2018.11.014

Maritz-Olivier, C., Stutzer, C., Jongejan, F., Neitz, A. W. H., and Gaspar, A. R. M. (2007). Tick anti-hemostatics: targets for future vaccines and therapeutics. *Trends Parasitol.* 23, 397–407. doi: 10.1016/j.pt.2007.07.005

Markwardt, F. (2002). Hirudin as alternative anticoagulant – a historical review. *Semin. Thromb. Hemost.* 28, 405–414. doi: 10.1055/s-2002-35292

Matthijs, M. J., Johnson, S., Sheppard, D., Barber, N. M., Li, Y. I., Nunn, M. A., et al. (2016). Structural basis for therapeutic inhibition of complement C5. *Nat. Struct. Mol. Biol.* 23, 378–386. doi: 10.1038/nsmb.3196

Michalsen, A., Moebus, S., Spahn, G., Esch, T., Langhorst, J., and Dobos, G. J. (2002). Leech therapy for symptomatic treatment of knee osteoarthritis: results and implications of a pilot study. *Altern. Ther. Health Med.* 8, 84–88.

Moed, L., Shwayder, T. A., and Chang, M. W. (2001). Cantharidin revisited: a blistering defense of an ancient medicine. *Arch. Dermatol.* 137, 1357–1360.

Mollnes, T. E., Song, W. C., and Lambris, J. D. (2002). Complement in inflammatory tissue damage and disease. *Trends Immunol.* 23, 61–64. doi: 10.1016/S1471-4906(01)02129-9

Montecucco, F., Mach, F., Lenglet, S., Vonlaufen, A., Gomes Quinderé, A. L., Pelli, G., et al. (2014). Treatment with evasin-3 abrogates neutrophil-mediated inflammation in mouse acute pancreatitis. *Eur. J. Clin. Invest.* 44, 940–950. doi: 10.1111/eci.12327

Monteiro, R. Q., Rezaie, A. R., Ribeiro, J. M. C., and Francischetti, I. M. B. (2005). Ixolaris: a factor Xa heparin-binding exosite inhibitor. *Biochem. J.* 387, 871–877. doi: 10.1042/BJ20041738

Morais, K. L. P., Pasqualoto, K. F. M., Pacheco, M. T. F., Berra, C. M., Alvarez-Flores, M. P., and Chudzinski-Tavassi, A. M. (2014). Rational development of a novel TFPI-like inhibitor from *Amblyomma cajennense* tick. *Toxin Rev.* 33, 48–52. doi: 10.3109/15569543.2013.845217

Murfin, K. E., and Fikrig, E. (2017). Tick bioactive molecules as novel therapeutics: beyond vaccine targets. *Front. Cell Infect. Microbiol.* 7:222. doi: 10.3389/fcimb.2017.00222

Narasimhan, S., Koski, R. A., Beaulieu, B., Anderson, J. F., Ramamoorthi, N., Kantor, F., et al. (2002). A novel family of anticoagulants from the saliva of *Ixodes scapularis*. *Insect Mol. Biol.* 11, 641–650. doi: 10.1046/j.1365-2583.2002.00375.x

Nazareth, R. A., Tomaz, L. S., Ortiz-Costa, S., Atella, G. C., Ribeiro, J. M. C., Francischetti, I. M., et al. (2006). Antithrombotic properties of Ixolaris, a potent

inhibitor of the extrinsic pathway of the coagulation cascade. *Thromb. Haemost.* 96, 7–13. doi: 10.1160/TH06-02-0105

Neeper, M. P., Waxman, L., Smith, D. E., Schulman, C. A., Sardana, M., Ellis, R. W., et al. (1990). Characterization of recombinant tick anticoagulant peptide. A highly selective inhibitor of blood coagulation factor Xa. *J. Biol. Chem.* 265, 17746–17752.

Nunn, M. A., Sharma, A., Paesen, G. C., Adamson, S., Lissina, O., Willis, A. C., et al. (2005). Complement inhibitor of C5 activation from the soft tick *Ornithodoros moubata*. *J. Immunol.* 174, 2084–2091. doi: 10.4049/jimmunol.174.4.2084

Nuttall, P. A. (2018). Wonders of tick saliva. *Ticks Tick Borne Dis.* 10, 470–481. doi: 10.1016/j.ttbdis.2018.11.005

Nuttall, P. A., and Paesen, G. C. (2001a). *Treatment of Allergic Rhinitis. WO-00116164* (2001). South Oak Way Green Park: Evolutec LTD.

Nuttall, P. A., and Paesen, G. C. (2001b). *Treatment of Conjunctivitis. WO-00115719* (2001). South Oak Way Green Park: Evolutec LTD.

Pacheco, M. T., Berra, C. M., Morais, K. L., Sciani, J. M., Branco, V. G., Bosch, R. V., et al. (2014). Dynein function and protein clearance changes in tumor cells induced by a Kunitz-type molecule, Amblyomin-X. *PLoS One* 9:e111907. doi: 10.1371/journal.pone.0111907

Paesen, G. C., Adams, P. L., Harlos, K., Nuttall, P. A., and Stuart, D. I. (1999). Tick histamine-binding proteins: isolation, cloning, and three-dimensional structure. *Mol. Cell* 3, 661–671. doi: 10.1016/S1097-2765(00)80359-80357

Paesen, G. C., Adams, P. L., Nuttall, P. A., and Stuart, D. I. (2000). Tick histamine-binding proteins: lipocalins with a second binding cavity. *Biochim. Biophys. Acta* 1482, 92–101. doi: 10.1016/s0167-4838(00)00168-0

Paesen, G. C., Siebold, C., Harlos, K., Peacey, M. F., Nuttall, P. A., and Stuart, D. I. (2007). A tick protein with a modified Kunitz fold inhibits human tryptase. *J. Mol. Biol.* 368, 1172–1186. doi: 10.1016/j.jmb.2007.03.011

Palenikova, J., Lieskovska, J., Langhansova, H., Kotsyfakis, M., Chmelar, J., and Kopecky, J. (2015). *Ixodes ricinus* salivary serpin IRS-2 affects Th17 differentiation via inhibition of the interleukin-6/STAT-3 signaling pathway. *Infect Immun.* 83, 1949–1956. doi: 10.1128/IAI.03065-14

Parizi, L. F., Ali, A., Tirloni, L., Oldiges, D. P., Sabadin, G. A., Coutinho, M. L., et al. (2018). Peptidase inhibitors in tick physiology. *Med. Vet. Entomol.* 32, 129–144. doi: 10.1111/mve.12276

Paveglio, S. A., Allard, J., Mayette, J., Whittaker, L. A., Juncadella, I., Anguita, J., et al. (2007). The tick salivary protein, Salp15, inhibits the development of experimental asthma. *J. Immunol.* 178, 7064–7071. doi: 10.4049/jimmunol.178.11.7064

Pemberton, R. W. (1999). Insects and other arthropods used as drugs in Korean traditional medicine. *J. Ethnopharmacol.* 65, 207–216. doi: 10.1016/s0378-8741(98)00209-8

Peterková, K., Vančová, I., Hajnická, V., Slovák, M., Šimo, L., and Nuttall, P. A. (2008). Immunomodulatory arsenal of nymphal ticks. *Med. Vet. Entomol.* 22, 167–171. doi: 10.1111/j.1365-2915.2008.00726.x

Poole, N. M., Nyindodo-Ogari, L., Kramer, C., Coons, L. B., and Cole, J. A. (2013). Effects of tick saliva on the migratory and invasive activity of Saos-2 osteosarcoma and MDAMB-231 breast cancer cells. *Ticks Tick Borne Dis.* 4, 120–127. doi: 10.1016/j.ttbdis.2012.09.003

Preston, S. G., Majtán, J., Kouremenou, C., Rysnik, O., Burger, L. F., Cabezas Cruz, A., et al. (2013). Novel immunomodulators from hard ticks selectively reprogramme human dendritic cell Responses. *PLoS Pathog.* 9:e1003450. doi: 10.1371/journal.ppat.1003450

Prevot, P. P., Adam, B., Boudjeltia, K. Z., Brossard, M., Lins, L., Cauchie, P., et al. (2006). Anti-hemostatic effects of a serpin from the saliva of the tick *Ixodes ricinus*. *J. Biol. Chem.* 281, 26361–26369. doi: 10.1074/jbc.M604197200

Prevot, P. P., Beschin, A., Lins, L., Beaufays, J., Grosjean, A., Bruys, L., et al. (2009). Exosites mediate the anti-inflammatory effects of a multifunctional serpin from the saliva of the tick ixodes ricinus. *FEBS J.* 276, 3235–3246. doi: 10.1111/j.1742-4658.2009.07038.x

Radulovič, Ž. M., Kim, T. K., Porter, L. M., Sze, S.-H., Lewis, L., and Mulenga, A. (2014). A 24-48 h fed *Amblyomma americanum* tick saliva immuno-proteome. *BMC Genomics* 15:518. doi: 10.1186/1471-2164-15-518

Ratcliffe, N., Azambuja, P., and Mello, C. B. (2014). Recent advances in developing insect natural products as potential modern day medicines. *Evid. Based Complement. Alternat. Med.* 2014:904958. doi: 10.1155/2014/904958

Ribeiro, J. M. C., Alarcon-Chaidez, F., Francischetti, I. M., Mans, B. J., Mather, T. N., Valenzuela, J. G., et al. (2006). An annotated catalog of salivary gland transcripts from *Ixodes scapularis* ticks. *Insect Biochem. Mol. Biol.* 36, 111–129. doi: 10.1016/j.ibmb.2005.11.005

Roversi, P., Johnson, S., Preston, S. G., Nunn, M. A., Paesen, G. C., Austyn, J. M., et al. (2017). Structural basis of cholesterol binding by a novel clade of dendritic cell modulators from ticks. *Sci. Rep.* 7:16057. doi: 10.1038/s41598-017-16413-2

Roversi, P., Lissina, O., Johnson, S., Ahmat, N., Paesen, G. C., Ploss, K., et al. (2007). The structure of OMCI, a novel lipocalin inhibitor of the complement system. *J. Mol. Biol.* 369, 784–793. doi: 10.1016/j.jmb.2007.03.064

Russo, R. C., Alessandri, A. L., Garcia, C. C., Cordeiro, B. F., Pinho, V., Cassali, G. D., et al. (2011). Therapeutic effects of evasin-1, a chemokine binding protein, in bleomy-cin-induced pulmonary fibrosis. *Am. J. Respir. Cell. Mol. Biol.* 45, 72–80. doi: 10.1165/rcmb.2009-0406OC

Sangamnatdej, S., Paesen, G. C., and Slovak, M. (2002). A high affinity serotonin- and histamine-binding lipocalin from tick saliva. *Insect Mol. Biol.* 11, 79–86. doi: 10.1046/j.0962-1075.2001.00311.x

Sa-Nunes, A., Bafica, A., Antonelli, L. R., Choi, E. Y., Francischetti, I. M. B., Andersen, J. F., et al. (2009). The immunomodulatory action of sialostatin L on dendritic cells reveals its potential to interfere with autoimmunity. *J. Immunol.* 182, 7422–7429. doi: 10.4049/jimmunol.0900075

Schaffer, L. W., Davidson, J. T., Vlasuk, G. P., and Siegl, P. K. S. (1991). Antithrombotic efficacy of recombinant tick anticoagulant peptide. A potent inhibitor of coagulation factor Xa in a primate model of arterial thrombosis. *Circulation* 84, 1741–1748. doi: 10.1161/01.CIR.84.4.1741

Schechter, M. E., Andrade, B. B., He, T., Richter, G. H., Tosh, K. W., Policicchio, B. B., et al. (2017). Inflammatory monocytes expressing tissue factor drive SIV and HIV coagulopathy. *Sci. Transl. Med.* 9, 1–14. doi: 10.1126/scitranslmed.aam5441

Schlehuber, S., and Skerra, A. (2005). Lipocalins in drug discovery: from natural ligand-binding proteins to "anticalins". *Drug Discov. Today* 10, 23–33. doi: 10.1016/S1359-6446(04)03294-3295

Schmidt, M. C. B., Morais, K. L. P., Almeida, M. E. S., Iqbal, A., Goldfeder, M. B., and Chudzinski-Tavassi, A. M. (2018). Amblyomin-X, a recombinant Kunitz-type inhibitor, regulates cell adhesion and migration of human tumor cells. *Cell Adh. Migr.* 25, 1–10. doi: 10.1080/19336918.2018.1516982

Schnirer, I. I., Yao, J. C., and Ajani, J. A. (2003). Carcinoid - a comprehensive review. *Acta Oncol.* 42, 672–692. doi: 10.1080/02841860310010547

Schuijt, T. J., Bakhtiari, K., Daffre, S., Deponte, K., Wielders, S. J. H., Marquart, J. A., et al. (2013). Factor XA activation of factor V is of paramount importance in initiating the coagulation system: lessons from a tick salivary protein. *Circulation* 128, 254–266. doi: 10.1161/CIRCULATIONAHA.113.003191

Schuijt, T. J., Narasimhan, S., Daffre, S., Deponte, K., Hovius, J. W., Veer, C. V., et al. (2011). Identification and characterization of *Ixodes scapularis* antigens that elicit tick immunity using yeast surface display. *PLoS One* 6:e15926. doi: 0.1371/journal.pone.0015926

Schwarz, A., Valdés, J. J., and Kotsyfakis, M. (2012). The role of cystatins in tick physiology and blood feeding. *Ticks Tick Borne Dis.* 3, 117–127. doi: 10.1016/j.ttbdis.2012.03.004

Šimo, L., Kazimirova, M., Richardson, J., and Bonnet, S. I. (2017). The essential role of tick salivary glands and saliva in tick feeding and pathogen transmission. *Front. Cell Infect. Microbiol.* 7:281. doi: 10.3389/fcimb.2017.00281

Simons, S. M., de Júnior, P. L., Faria, F., Batista, I. D., Barros-Battesti, D. M., Labruna, M. B., et al. (2011). The action of *Amblyomma cajennense* tick saliva in compounds of the hemostatic system and cytotoxicity in tumor cell lines. *Biomed. Pharmacother.* 65, 443–450. doi: 10.1016/j.biopha.2011.04.030

Singh, K., Davies, G., Alenazi, Y., Eaton, J. R. O., Kawamura, A., and Bhattacharya, S. (2017). Yeast surface display identifies a family of evasins from ticks with novel polyvalent CC chemokine-binding activities. *Sci. Rep.* 7:4267. doi: 10.1038/s41598-017-04378-4371

Slovák, M., Štibrániová, I., Hajnická, V., and Nuttall, P. A. (2014). Antiplatelet-derived growth factor (PDGF) activity in the saliva of ixodid ticks is linked with their long mouthparts. *Parasite Immunol.* 36, 32–42. doi: 10.1111/pim.12075

Soares, T. S., Oliveira, F., Torquato, R. J. S., Sasaki, S. D., Araujo, M. S., Paschoalin, T., et al. (2016). BmTI-A, a Kunitz type inhibitor from *Rhipicephalus microplus* able to interfere in vessel formation. *Vet. Parasitol.* 219, 44–52. doi: 10.1016/j.vetpar.2016.01.021

Soltys, J., Kusner, L. L., Young, A., Richmonds, C., Hatala, D., Gong, B., et al. (2009). Novel complement inhibitor limits severity of experimentally myasthenia gravis. *Ann. Neurol.* 65, 67–75. doi: 10.1002/ana.21536

Sommerhoff, C. P., and Schaschke, N. (2007). Mast cell tryptase beta as a target in allergic inflammation: an evolving story. *Curr. Pharm. Des.* 13, 313–332. doi: 10.2174/138161207779313579

Sousa, A. C. P., Oliviera, C. J. F., Szabó, M. P. J., and Silva, M. J. B. (2018). Anti-neoplastic activity of *Amblyomma sculptum*, *Amblyomma parvum* and *Rhipicephalus sanguineus* tick saliva on brest tumor cell lines. *Toxicon* 148, 165–171. doi: 10.1016/j.toxicon.2018.04.024

Sousa, A. C. P., Szabó, M. P. J., Oliveira, C. J. F., and Silva, M. J. B. (2015). Exploring the anti-tumoral effects of tick saliva and derived components. *Toxicon.* 102, 69–73. doi: 10.1016/j.toxicon.2015.06.001

Spronk, H. M. H., de Jong, A. M., Crijns, H. J., Schotten, U., Van Gelder, I. C., and Ten Cate, H. (2014). Pleiotropic effects of factor Xa and thrombin: what to expect from novel anticoagulants. *Cardiovasc. Res.* 101, 344–351. doi: 10.1093/cvr/cvt343

Štibrániová, I., Lahová, M., and Bartíková, P. (2013). Immunomodulators in tick saliva and their benefits. *Acta Virol.* 57, 200–216. doi: 10.4149/av_2013_02_200

Stoll, P., Bassler, N., Hagemeyer, C. E., Eisenhardt, S. U., Chen, Y. C., Schmidt, R., et al. (2007). Targeting ligand-induced binding sites on GPIIb/IIIa via single-chain antibody allows effective anticoagulation without bleeding time prolongation. *Arterioscler. Thromb. Vasc. Biol.* 27, 1206–1212. doi: 10.1161/ATVBAHA.106.138875

Stone, G. W., McLaurin, B. T., Cox, D. A., Bertrand, M. E., Lincoff, A. M., Moses, J. W., et al. (2006). Bivalirudin for patients with acute coronary syndromes. *New Engl. J. Med.* 355, 2203–2216. doi: 10.1056/NEJMoa062437

Sun, T., Wang, F., Pan, W., Wu, Q., Wang, J., and Dai, J. (2018). An immunosuppressive tick salivary gland protein DsCystatin interferes with toll-like receptor signaling by downregulating TRAF6. *Front. Immunol.* 9:1245. doi: 10.3389/fimmu.2018.01245

Suppan, J., Engel, B., Marchetti-Deschmann, M., and Nürnberger, S. (2018). Tick attachment cement - reviewing the mysteries of a biological skin plug system. *Biol. Rev.* 93, 1056–1076. doi: 10.1111/brv.12384

Tambourgi, D. V., and van den Berg, C. W. (2014). Animal venoms/toxins and the complement system. *Mol. Immunol.* 61, 153–162. doi: 10.1016/j.molimm.2014.06.020

Tan, A. W. L., Francischetti, I. M. B., Slovak, M., Kini, R. M., and Ribeiro, J. M. C. (2015). Sexual differences in the sialomes of the zebra tick, *Rhipicephalus pulchellus*. *J. Proteomics* 117, 120–144. doi: 10.1016/j.jprot.2014.12.014

Tanaka, A. S., Andreotti, R., Gomes, A., Torquato, R. J., Sampaio, M. U., and Sampaio, C. A. (1999). A double headed serine proteinase inhibitor–human plasma kallikrein and elastase inhibitor–from *Boophilus microplus* larvae. *Immunopharmacology* 45, 171–177. doi: 10.1016/s0162-3109(99)00074-0

Tang, J., Fang, Y. Q., Han, Y. J., Bai, X. W., Yan, X. W., Zhang, Y., et al. (2015). YY-39, a tick anti-thrombosis peptide containing RGD domain. *Peptides* 68, 99–104. doi: 10.1016/j.peptides.2014.08.008

Thiel, S. (2007). Complement activating soluble pattern recognition molecules with collagen-like regions, mannan-binding lectin, ficolins and associated proteins. *Mol. Immunol.* 44, 3875–3888. doi: 10.1016/j.molimm.2007.06.005

Thompson, R. E., Liu, X., Ripoll-Rozada, J., Alonso-García, N., Parker, B. L., Pereira, P. J. B., et al. (2017). Tyrosine sulfation modulates activity of tick-derived thrombin inhibitors. *Nat. Chem.* 9, 909–917. doi: 10.1038/NCHEM.2744

Tian, Y., Yedid, G., Yan, X., Fang, M., Mo, G., Chen, R., et al. (2016). An immunosuppressant peptide from the hard tick *Amblyomma variegatum*. *Toxins* 8:133. doi: 10.3390/toxins8050133

Timp, J. F., Braekkan, S. K., Versteeg, H. H., and Cannegieter, S. C. (2013). Epidemiology of cancer-associated venous thrombosis. *Blood* 122, 1712–1723. doi: 10.1182/blood-2013-04-460121

Tomás-Cortázar, J., Martín-Ruiz, I., Barriales, D., Pascual-Itoiz, M. A., Gutiérrez de Juan, V., Caro-Maldonado, A., et al. (2017). The immunosuppressive effect of the tick protein, Salp15, is long-lasting and persists in a murine model of hematopoietic transplant. *Sci. Rep.* 7:10740. doi: 10.1038/s41598-017-11354-2

Tyson, K., Elkins, C., Patterson, H., Fikrig, E., and de Silva, A. (2007). Biochemical and functional characterization of Salp20, an *Ixodes scapularis* tick salivary protein that inhibits the complement pathway. *Insect Mol. Biol.* 16, 469–479. doi: 10.1111/j.1365-2583.2007.00742.x

Tyson, K. R., Elkins, C., and de Silva, A. M. (2008). A novel mechanism of complement inhi-bition unmasked by a tick salivary protein that binds to properdin. *J. Immunol.* 180, 3964–3968. doi: 10.4049/jimmunol.180.6.3964

Valdés, J. J., Schwarz, A., Cabeza de Vaca, I., Calvo, E., Pedra, J. H. F., Guallar, V., et al. (2013). Tryptogalinin is a tick kunitz serine protease inhibitor with a unique intrinsic disorder. *PLoS One* 8:e62562. doi: 10.1371/journal.pone.0062562

Vančová, I., Hajnická, V., Slovák, M., and Nuttall, P. A. (2010). Anti-chemokine activities of ixodid ticks depend on tick species, developmental stage, and duration of feeding. *Vet. Parasitol.* 167, 274–278. doi: 10.1016/j.vetpar.2009.09.029

Vančová, I., Slovák, M., Hajnická, V., Labuda, M., Simo, L., Peterková, K., et al. (2007). Differential anti-chemokine activity of *Amblyomma variegatum* adult ticks during blood-feeding. *Parasite Immunol.* 29, 169–177. doi: 10.1111/j.1365-3024.2006.00931.x

Valenzuela, J. G. (2002). High-throughput approaches to study salivary proteins and genes from vectors of disease. *Insect Biochem. Mol. Biol.* 32, 1199–1209. doi: 10.1016/S0965-1748(02)00083-88

Valenzuela, J. G., Charlab, R., Mather, T. N., and Ribeiro, J. M. C. (2000). Purification, cloning, and expression of a novel salivary anticomplement protein from the tick, Ixodes scapularis. *J. Biol. Chem.* 275, 18717–18723. doi: 10.1074/jbc.m001486200

van der Locht, A., Stubbs, M. T., Bode, W., Friedrich, T., Bollschweiler, C., Höffken, W., et al. (1996). The ornithodorin thrombin crystal structure, a key to the TAP enigma? *EMBO J.* 15, 6011–6017. doi: 10.1002/j.1460-2075.1996.tb00989.x

Ventura, J. S., Faria, F., Batista, I. F., Simons, S. M., Oliveira, D. G., Morais, K. L., et al. (2013). A Kunitz-type FXa inhibitor affects tumor progression, hypercoagulable state and triggers apoptosis. *Biomed. Pharmacother.* 67, 192–196. doi: 10.1016/j.biopha.2012.11.009

Vieira, A. T., Fagundes, C. T., Alessandri, A. L., Castor, M. G., Guabiraba, R., Borges, V. O., et al. (2009). Treatment with a novel chemokine-binding protein or eosinophil lineage-ablation protects mice from experimental colitis. *Am. J. Pathol.* 175, 2382–2391. doi: 10.2353/ajpath.2009.090093

Wang, X., Coons, L. B., Taylor, D. B., Stevens, S. E., and Gartner, T. K. (1996). Variabilin, a novel RGD-containing antagonist of glycoprotein IIb-IIIa and platelet aggregation inhibitor from the hard tick *Dermacentor variabilis*. *J. Biol. Chem.* 271, 17785–17790. doi: 10.1074/jbc.271.30.17785

Wang, Y., Li, Z., Zhou, Y., Cao, J., Zhang, H., Gong, H., et al. (2016). Specific histamine binding activity of a new lipocalin from *Hyalomma asiaticum* (Ixodidae) and therapeutic effects on allergic asthma in mice. *Parasit. Vectors* 9:506. doi: 10.1186/s13071-016-1790-0

Waxman, L., and Connolly, T. M. (1993). Isolation of an inhibitor selective for collagen-stimulated platelet aggregation from the soft tick *Ornithodoros moubata*. *J. Biol. Chem.* 268, 5445–5449.

Waxman, L., Smith, D. E., Arcuri, K. E., and Vlasuk, G. P. (1990). Tick anticoagulant peptide (TAP) is a novel inhibitor of blood coagulation factor Xa. *Science* 248, 593–596. doi: 10.1126/science.2333510

Wei, A., Alexander, R. S., Duke, J., Ross, H., Rosenfeld, S. A., and Chang, C.-H. (1998). Unexpected binding mode of tick anticoagulant peptide complexed to bovine factor Xa. *J. Mol. Biol.* 283, 147–154. doi: 10.1006/jmbi.1998.2069

Weston-Davies, W. (2004). *Histamine Binding Compounds for Treatment Method for Disease Conditions Mediated by Neutrophils. WO*-2004087188 (2004). South Oak Way Green Park: Evolutec LTD.

Wikel, S. (2013). Ticks and tick-borne pathogens at the cutaneous interface: host defenses, tick countermeasures, and a suitable environment for pathogen establishment. *Front. Microbiol.* 4:337. doi: 10.3389/fmicb.2013.00337

Wikel, S. K. (2018). Tick-host-pathogen systems immunobiology: an interactive trio. *Front. Biosci.* 23, 265–283. doi: 10.2741/4590

Wolf, H., and Hansson, C. (2003). Larval therapy – an effective method of ulcer debridement. *Clin. Exp. Dermatol.* 28, 134–137. doi: 10.1046/j.1365-2230.2003.01226.x

Wu, J., Wang, Y., Liu, H., Yang, H., Ma, D., Li, J., et al. (2010). Two immunoregulatory peptides with antioxidant activity from tick salivary glands. *J. Biol. Chem.* 285, 16606–16613. doi: 10.1074/jbc.M109.094615

Xu, X.-L., Cheng, T.-Y., Yang, H., Yan, F., and Yang, Y. (2015). De novo sequencing, assembly and analysis of salivary gland transcriptome of *Haemaphysalis flava* and identification os sialoprotein genes. *Infect. Genet. Evol.* 32, 135–142. doi: 10.1016/j.meegid.2015.03.010

Yanan, W., Zhuang, L., Yongzhi, Z., Jie, C., Houshuang, Z., Haiyan, G., et al. (2016). Specific histamine binding activity of a new lipocalin from *Hyalomma asiaticum* (Ixodidae) and therapeutic effects on allergic asthma in mice. *Parasit. Vectors* 9:506. doi: 10.1186/s13071-016-1790-0

Yeh, C. H., Fredenburgh, J. C., and Weitz, J. I. (2012). Oral direct factor Xa inhibitors. *Circ. Res.* 111, 1069–1078. doi: 10.1161/CIRCRESAHA.112.276741

Yoshikai, Y. (2001). Roles of prostaglandins and leukotrienes in acute inflammation caused by bacterial infection. *Curr. Opin. Infect. Dis.* 14, 257–263. doi: 10.1097/00001432-200106000-00003

Yu, X., Gong, H., Zhou, Y., Zhang, H., Cao, J., and Zhou, J. (2015). Differential sialotranscriptomes of unfed and fed *Rhipicephalus haemaphysaloides*, with particular regard to differentially expressed genes of cysteine proteases. *Parasit. Vectors.* 8:597. doi: 10.1186/s13071-015-1213-7

Zipfel, P. F., Mihlan, M., and Skerka, C. (2007a). The alternative pathway of complement: a pattern recognition system. *Adv. Exp. Med. Biol.* 598, 80–92. doi: 10.1007/978-0-387-71767-8_7

Zipfel, P. F., Wurzner, R., and Skerka, C. (2007b). Complement evasion of pathogens: common strategies are shared by diverse organisms. *Mol. Immunol.* 44, 3850–3857. doi: 10.1016/j.molimm.2007.06.149

Conflict of Interest Statement: The authors declare that the research was conducted in the absence of any commercial or financial relationships that could be construed as a potential conflict of interest.

frontiers in Physiology

ORIGINAL RESEARCH
published: 16 July 2019
doi: 10.3389/fphys.2019.00793

Seasonal Dynamics, Record of Ticks Infesting Humans, Wild and Domestic Animals and Molecular Phylogeny of *Rhipicephalus microplus* in Khyber Pakhtunkhwa Pakistan

Abid Ali[1], Munsif Ali Khan[1], Hafsa Zahid[1], Pir Muhammad Yaseen[1], Muhammad Qayash Khan[1], Javed Nawab[2], Zia Ur Rehman[3], Muhammad Ateeq[4], Sardar Khan[5] and Mohammad Ibrahim[4]*

[1] Department of Zoology, Abdul Wali Khan University Mardan, Khyber Pakhtunkhwa, Pakistan, [2] Department of Environmental Sciences, Abdul Wali Khan University Mardan, Khyber Pakhtunkhwa, Pakistan, [3] Department of Microbiology, Abdul Wali Khan University Mardan, Khyber Pakhtunkhwa, Pakistan, [4] Department of Chemistry, Abdul Wali Khan University Mardan, Khyber Pakhtunkhwa, Pakistan, [5] Department of Environmental Sciences, University of Peshawar, Khyber Pakhtunkhwa, Pakistan

OPEN ACCESS

Edited by:
Zhijun Yu,
Hebei Normal University, China

Reviewed by:
Nkululeko Nyangiwe,
Dohne Agricultural Development Institute, South Africa
Muhammad Imran Rashid,
University of Veterinary and Animal Sciences, Pakistan

***Correspondence:**
Abid Ali
uop_ali@yahoo.com

Specialty section:
This article was submitted to Invertebrate Physiology, a section of the journal Frontiers in Physiology

Received: *18 March 2019*
Accepted: *06 June 2019*
Published: *16 July 2019*

Citation:
Ali A, Khan MA, Zahid H, Yaseen PM, Qayash Khan M, Nawab J, Ur Rehman Z, Ateeq M, Khan S and Ibrahim M (2019) Seasonal Dynamics, Record of Ticks Infesting Humans, Wild and Domestic Animals and Molecular Phylogeny of Rhipicephalus microplus in Khyber Pakhtunkhwa Pakistan. Front. Physiol. 10:793. doi: 10.3389/fphys.2019.00793

Although ticks prevalent in various agro-systems of Pakistan are associated with economic losses, information is still missing about the tick's diversity, hosts they infest, seasonal dynamics and molecular phylogeny of *Rhipicephalus microplus* in Khyber Pakhtunkhwa (KP) Pakistan. This study for the first time enlisted ticks infesting diverse hosts including humans in various regions of KP. A total of 8,641 ticks were collected across the northern, southern and central regions of KP and were morpho-taxonomically categorized into six genera comprising 17 species, *R. microplus* (*n* = 3,584, 42%), *Hyalomma anatolicum* (*n* = 2,253, 27%), *Argas persicus* (*n* = 1,342, 16%), *Hya. impeltatum* (*n* = 586, 7%), *R. turanicus* (*n* = 161, 2%), *R. haemaphysaloides* (*n* = 142, 2%), *R. annulatus* (*n* = 132, 2%), *Hae. montgomeryi* (*n* = 123, 1.4%), *Hya. marginatum* (*n* = 110, 1.3%), *R. sanguineus* (*n* = 34, 0.4%), and *Hae. longicornis* (*n* = 31, 0.4%). Ticks infesting wild animals included *Amblyomma gervaisi*, *Amb. exornatum, Amb. latum, Dermacentor marginatus,* and *Hae. indica,* while ticks collected from humans included *R. microplus*, *R. annulatus, Hya. anatolicum, Hya. marginatum,* and *Hae. punctata*. The overall prevalence of ticks infesting domestic animals was 69.4% (536/772). Among animal hosts, cattle were found highly infested (87.2%, 157/180) followed by buffalos (79%, 91/114), domestic fowls (74.7%, 112/150), goats (68.3%, 82/120), dogs (66.7%, 32/48), horses (61.3%, 49/80), and sheep (16.3%, 13/80). Analysis revealed that the tick burden significantly differed among domestic animals and was found to be high in cattle, followed by buffalos, goats, sheep, domestic fowl, dogs, and horses. Seasonal patterns of ticks distribution showed highest prevalance in July, August, and September due to the prevailing high temperature and humidity during these months. The phylogenetic analysis of cattle tick *R. microplus* based on partial mitochondrial cytochrome oxidase

subunit I (COX1), 16S ribosomal RNA (16S rRNA) and internal transcribed spacer 2 (ITS2) sequences, revealed that *R. microplus* prevalent in this region belongs to clade C which include ticks originating from Bangladesh, Malaysia, and India. Further large scale studies across the country are necessary to explore the molecular and cross breeding aspects at the geographical overlapping of various tick species and their associated pathogens to facilitate designing control strategies as well as awareness against tick infestation in the region.

Keywords: ticks, hosts, *R. microplus*, Khyber Pakhtunkhwa, Pakistan

INTRODUCTION

Ticks are hematophagous arthropods, notorious vectors of human and animal pathogens and constitute an emerging economic and health problem in tropical and sub-tropical regions (de la Fuente et al., 2017). As a major challenge to public health and veterinary sector, ticks can harbor several pathogens that cause numerous infectious diseases. The emergence and resurgence of several tick-borne diseases pose increasing public health concerns (Gratz, 1999; Paddock and Childs, 2003; Jones et al., 2008). As a vector reservoir for several emerging and re-emerging infectious pathogens of medical and veterinary importance, ticks transmit a wide variety of arboviruses (Crimean-Congo hemorrhagic fever virus, tick-borne encephalitis virus), bacteria (*Rickettsia* spp.), spirochetes (*Anaplasma* spp. *Borrelia* spp. and *Ehrlichia* spp.) and protozoans (*Babesia* spp. and *Theileria* spp.), more than any other blood feeding arthropod (Labruna et al., 2004; Gondard et al., 2017; Schorderet-Weber et al., 2017). These voracious ectoparasites can infest wild, terrestrial, semi-aquatic vertebrates and humans, and are globally distributed from the Arctic to tropical regions (Sherrard-Smith et al., 2012; Yu et al., 2015). Ten percent of the total hard and soft tick species are known to transmit diseases to humans and other animals (Parola and Raoult, 2001; Lew-Tabor and Valle, 2016). Ticks and tick-borne diseases affect approximately 80% of the world's cattle population, particularly in tropical and subtropical countries. Infestation with cattle tick *Rhipicephalus microplus* economically impact the livestock industry in different regions and annual losses due to only this tick have been estimated 22–30 billion US$ (Jabbar et al., 2015; Lew-Tabor and Valle, 2016).

The prevalence of ticks in different regions is mostly associated with various environmental factors that affect tick distribution and adaptation (Estrada-Peña, 2008). Like other hematophagous arthropods, ticks spend their life cycle in such an environment where they depend on host availability, host lifestyle, host interaction with other animals, vegetation coverage, habitat type and geo-climatic conditions (temperature and humidity) for their survival and development (Estrada-Peña, 2008; Gondard et al., 2017). Climatic changes influence tick distribution, shape the biodiversity of ticks and tick-borne pathogens and increase the risks of transmission of pathogens to humans and other hosts (Leger et al., 2013; Dantas-Torres, 2015). The dispersal of ticks in previously tick free areas is consociated with humans and other animals movements due to environmental changes (Estrada-Peña, 2008; Dantas-Torres, 2015) which has resulted in the emergence and re-emergence of tick-borne diseases.

Ticks that belong to the genus *Rhipicephalus* are responsible for severe economic losses in tropical and subtropical agro-systems. Previous studies have enlisted intraspecific variations in genus *Rhipicephalus* based on morpho-taxonomic complications in identification at species level (Lempereur et al., 2010; Barker and Walker, 2014). Morphological variations in *Rhipicephaline* ticks make it difficult to distinguish these tick species morphologically and to date, several valid species of *Rhipicephalus* (*Boophilus*) have been confirmed (Estrada-Peña et al., 2012; Guglielmone et al., 2014; Ali et al., 2016; Coimbra-Dores et al., 2018; Roy et al., 2018). The morpho-taxonomy of *R. microplus* (cattle tick) has been challenged in the last few years due to a hypothesis suggesting that biogeographical and ecological separations have occurred in Boophilid ticks across continents based on morphological and genetic variations (García-García et al., 1999; de la Fuente et al., 2000; Ali et al., 2016; Lew-Tabor et al., 2017). The genetic assemblage study based on mitogenome (12S rRNA and 16S rRNA) and microsatellites markers of *R. microplus* from America, Asia, Australia and Africa have confirmed that *R. microplus* consist of at least two different species (Labruna et al., 2009; Low et al., 2015; Ali et al., 2016; Baron et al., 2018). Mating experiments among these ticks evidenced that reproductive crosses between *R. microplus* ticks from Australia and Argentina or Mozambique are infertile while crosses between Boophilid ticks from Argentina and Mozambique are fertile. These findings based on genetic divergence and reproductive isolation put forward that the Australian *R. microplus* strain is different from the American, Asian and African strain. Phylogenetic analysis of the *R. microplus* mitogenome (COX1 and 16S rRNA) and internal transcribed spacer (ITS) gene revealed that *R. microplus* is a complex of species. The cryptic diversity of *R. microplus* complex includes *R. annulatus*, *R. australis* and two clades of *R. microplus*, clade A and B. Clade A *R. microplus* includes ticks from America and Africa and clade B includes ticks from China (Labruna et al., 2009; Burger et al., 2014; Low et al., 2015; Roy et al., 2018). Recent mitogenome approaches based on COX1 and 16S rRNA haplotypes suggested a distinct genetic assemblage of *R. microplus* from Malaysia resulting in novel clade C which includes ticks from Pakistan, Bangladesh, Myanmar, India and Malaysia (Low et al., 2015; Baron et al., 2018; Roy et al., 2018).

In Pakistan, valid studies have shown the prevalence of five tick genera, including *Hyalomma*, *Haemaphysalis*, *Rhipicephalus, Ornithodoros,* and *Argus* (Karim et al., 2017; Rehman et al., 2017). The notable species compositions of genus *Hyalomma* are *Hya. anatolicum*, *Hya. scupense*, *Hya. kumari*, *Hya. isacci, Hya. turanicum* and *Hya. dromedarii*; genus *Haemaphysalis* are *Hae. bispinosa*, *Hae. montgomeryi*, *Hae. cornupunctata*, *Hae. kashmirensis*, and *Hae. sulcata*; genus *Rhipicephalus* species compositions include *R. microplus, R. annulatus, R. haemaphysaloides, R. turanicus,* and *R. sanguineus;* the genus *Argus* is composed of *Argas persicus* and genus *Ornithodoros* is represented by *Ornithodoros tolozani* (Hoogstraal and Varma, 1962; Kaiser and Hoogstraal, 1964; Robertson et al., 1970; Karim et al., 2017; Rehman et al., 2017).

Pakistan is an agricultural country where livestock plays a crucial role in the national economy. In Pakistan, climatic conditions are extremely favorable for the growth and survival of diverse tick species. These ticks cause severe problems for livestock holders which mainly include low income farmers. The majority of these farmers consider all tick species as one species and are mostly unaware of the capability of pathogens transmission to humans as well as other associated health risks. Tick and tick-borne diseases are prevalent in the province Khyber Pakhtunkhwa (KP) of Pakistan, causing economic loss to livestock holders (Jabbar et al., 2015; Karim et al., 2017; Rehman et al., 2017). However, there is a paucity of documented information about ticks spatial distribution and diversity, their diverse hosts and seasonal dynamics from this region. Therefore, the present endeavor was focused on tick diversity to investigate the present status of tick species infesting various animal hosts, their seasonal dynamics and to obtain the evolutionary information of cattle tick *R. microplus* which is prevalent in the study area.

MATERIALS AND METHODS

Study Area

During the present study five districts namely Charsadda (34°09′49.4″N 71°44′53.4″E), Mardan (34°11′54.6″N 72°01′37.4″E), Peshawar (34°01′36.2″N 71°31′47.4″E), Lower Kohistan (35°19′48.2″N 73°13′50.7″E), and Karak (33°06′37.5″N 71°05′29.0″E), in the northern, southern and central KP (Northwestern geographic state of Pakistan previously known as North-West Frontier Province) were selected to assess the diversity of ticks, their hosts and seasonal dynamics. Nine regions of each aforementioned districts were selected for ticks sampling (**Figure 1**). A Global Positioning System (GPS) was used to obtain geographic coordinates data and loaded onto a Microsoft Excel sheet to develop a distribution map for the study areas using ArcGIS 10.3.1.

Ethics Statement

The protocol for the present study was approved by the ethical committee and board of study members of the Department of Zoology Abdul Wali Khan University Mardan. Written informed consent was obtained from the owners of animals and individuals infested by ticks prior to tick collection.

Ticks Collection

Tick samples were collected during April 2017 to March 2018, from different domestic animals (cattle, buffalo, horse, sheep, goat, dogs, and domestic fowl) at different localities (villages and towns) in various tehsils (an administrative division within the district) of the aforementioned districts (**Figure 1**). For ticks collection, a regular visit was made three times a month and sampling was done randomly with the help of fine tweezers from sampling animals reared at animal farms, houses or grazing in the field. Collected specimens were rinsed with distilled water followed by absolute ethanol to remove any surface confined microbes and host contaminating tissues and stored in properly labeled separate plastic tubes until further analyses. The relevant information including age of host, physical status, previous acaricides or any drugs used against ticks, the body region from where ticks were isolated, date and place of collection were recorded and all the samples were shipped to the Parasitology laboratory of the department of Zoology, Abdul Wali Khan University Mardan. Ticks were immediately identified or preserved (100% ethanol or in a mixture of 95% ethanol, 4% distilled water and 1% glycerol) (Walker et al., 2003) for further study.

During collection, ticks were accidentally found infesting humans and wild goats (locally known as markhor, a national animal of Pakistan mostly found on the Himalaya Mountains). Wild rodents (Indian gray mongoose), wild boars (wild pig), and wild reptiles (monitor lizard and Indian python) were captured by local farmers or found dead on highways. In this collection, ticks were also included from districts other than the above-mentioned districts such as Chitral (35°53′40.9″N 71°41′31.1″E), Haripur (33°59′41.0″N 72°54′35.3″E), Swabi (34°07′29.1″N 72°27′25.7″E), and Nowshera (34°00′27.8″N 71°59′09.8″E) (**Figure 2**).

Morpho-Taxonomic Identification of Ticks

Tick samples were identified morphologically using tick morpho-taxonomic characters under stereozoom microscope (HT Stereozoom) according to the standard relevant identification keys (Walker et al., 2003; Apanaskevich and Horak, 2005, 2008, 2009; Ghosh and Misra, 2012; Nowak-Chmura, 2012; Madder et al., 2014; Caetano et al., 2017).

DNA Extraction and Molecular Identification

A total of 225 (45 per district) morphologically identified *R. microplus* from nine locations in each of the five districts were selected for genomic DNA extraction. Tick samples from each district were separately pooled into five groups, each pool containing ticks of a different location within the district. Ticks were cleaned with distilled water, dried and cut into small pieces using a sterile scalpel and homogenized by a sterile micro pestle in separate 1.5 ml Eppendorf tubes. Genomic DNA

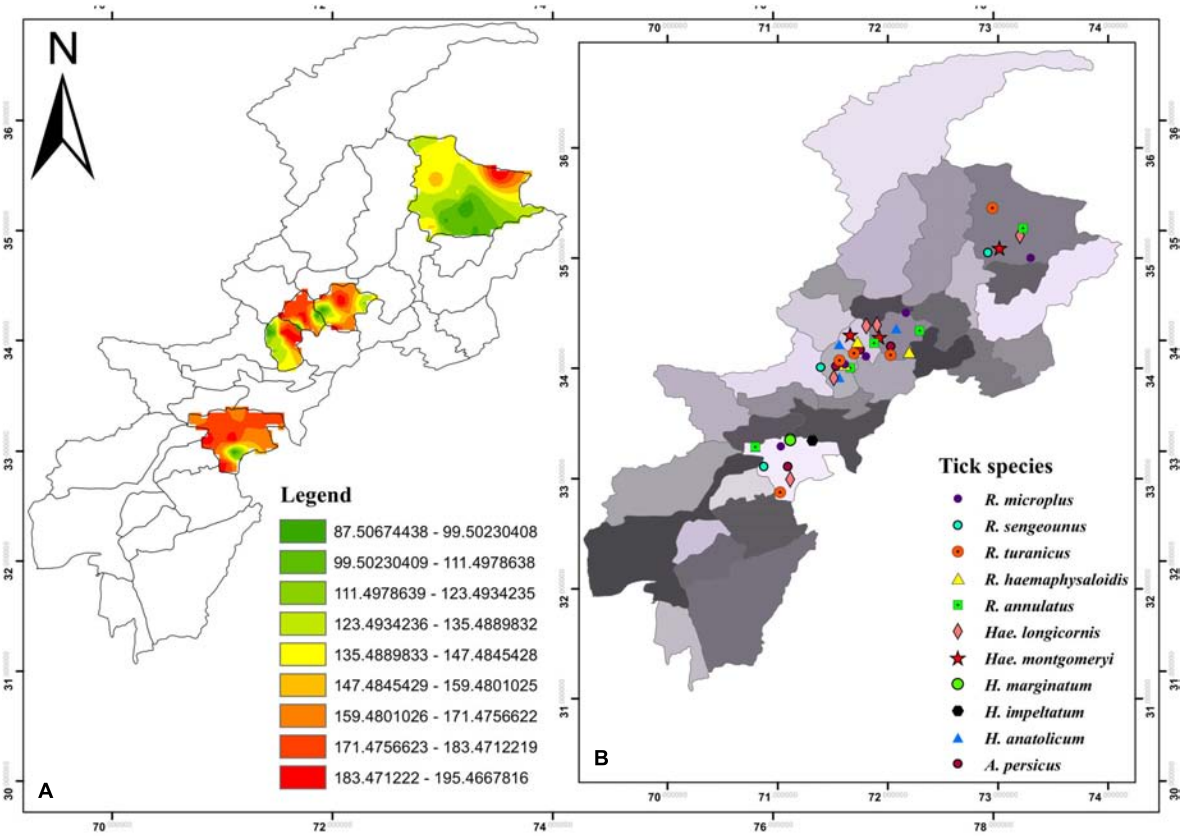

FIGURE 1 | (A) Density map of tick burden in the selected districts **(B)** and spatial distribution of tick species in KP.

was separately extracted from each pool of tick samples using the GeneJET Genomic DNA Purification Kit (Thermo Fisher Scientific) according to the standard DNA extraction protocol of the manufacturer. DNA concentration in the samples was quantified using a Nanodrop ND-100 (Thermo Fisher Scientific) and stored at −20°C until further processing. COX1, 16S rRNA and ITS2 gene fragments of *R. microplus* were amplified by PCR in a thermocycler (HT, ILF, UK) using specific primers (**Table 1**). PCR reactions were performed in a total volume of 25 μL reaction mixture with a composition of 1 μL of each forward and reverse primer, 2 μL of template DNA (50 ng), 7.5 μL of deionized water and 13.5 μL of master mix (Dream*Taq* PCR Master Mix [2X] (Thermo Fisher Scientific). The thermocycling conditions for COX1, 16S rRNA and ITS2 were optimized separately for each reaction. Standardized PCR conditions was, an initial denaturation of 5 min at 95°C followed by 35 cycles of denaturation at 95°C for 30 s, annealing at 53.8°C for COX1, 55.9°C for 16S rRNA and 58°C for ITS2 for 30 s, an extension at 72°C for 30 s and a final extension of 10 min at 72°C. A negative control (distilled water) was included in each run of the amplification reaction for validation. PCR products were confirmed by running the amplified DNA in 2% ethidium bromide stained agarose gel with a 50 bp DNA marker (Thermo Fisher Scientific). The results were visualized using the GeneDoc (UVP BioDoc-It Imaging System).

DNA Purification and Sequencing

The amplified PCR products were purified using the GeneClean II kit (Qbiogene) according to the manufacturer's instructions. For the sequencing of PCR based amplified product, 45 DNA samples of each district were separately grouped containing fifteen samples for each gene fragment. The purified PCR amplicons (45 PCR product samples, 15 samples for each marker) were sequenced unidirectionally by Macrogen Inc. (Seoul, South Korea). The obtained sequences (nucleotide sequences) were analyzed using BioEdit V. 7.0.5 (Hall et al., 2011) and NCBI BLAST[1] (Altschul et al., 1990). All the relevant library sequences of closely related species and of *R. microplus* complex available in GenBank were downloaded and saved for downstream analysis to construct a phylogenetic tree. The obtained sequences were trimmed for the removal of unnecessary nucleotides and those with 100% similarity with each other were discarded. Finally, 12 sequences were uploaded to NCBI GenBank including COX1 (4), 16S rRNA (3) and ITS2 (5).

Phylogenetic Analysis

The obtained trimmed sequences were aligned using ClustalW in BioEdit Sequence Alignment Editor V 7.0.5 (Hall et al., 2011). To test molecular phylogeny of the cattle tick *R. microplus* a

[1]https://blast.ncbi.nlm.nih.gov/Blast.cgi

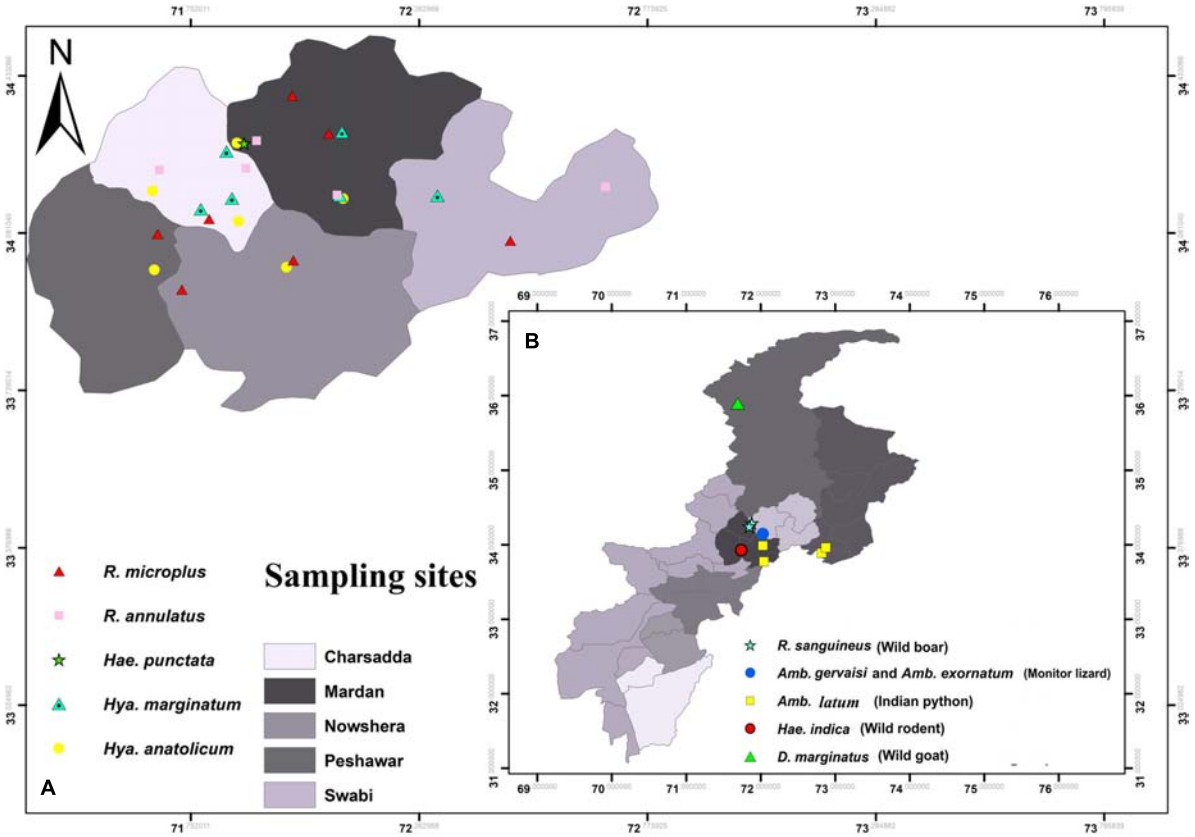

FIGURE 2 | Map showing locations of ticks **(A)** collected from humans **(B)** and wild animals.

multi locus analysis was performed for COX1 (**Figure 3**), 16S rRNA (**Figure 4**), and ITS2 (**Figure 5**) partial sequences using the Maximum likelihood method in MEGA v. X (Kumar et al., 2018) with bootstrapping at 1000 replications (Tamura et al., 2013).

Statistical Analysis

The overall tick prevalence was calculated by the total ticks divided by total hosts, host wise infestation was calculated by the infested hosts divided by total examined. The mean percent of collected ticks and binomial confidence intervals for proportion were calculated (**Table 2**). The median tick burden was analyzed on hosts by applying the Kruskal–Wallis test ($P < 0.001$) among different hosts and the Pearson correlation test was applied for the temporal distribution of ticks. The results were considered statistically significant at $p < 0.05$.

TABLE 1 | Primers used for the amplification of target partial genes of *R. microplus*.

Gene	Primer sequence	Amplicons size (nt)	References
COXI	F: ATTTTACCGCGATGAATATACTCTAC	620 bp	Present study
	R: TCTGTTAATAGTATGGTAATAGCACCTG		
16S rRNA	F: ATTTTGACTATACAAAGGTATTGAAAT	376 bp	Present study
	R: ATTTAAAAGTTGAACAAACTTCTTATTT		
ITS2	F: CACATATCAAGAGAGCCTTCGGC	267 bp	Present study
	R: CATCGTCTTGTGTAGCGTCGC		

RESULTS

Tick's Description and Host Population

Morpho-taxonomic analysis categorized collected ticks into six genera including 17 species (**Figure 1**). The highest number of collected tick species was *R. microplus* (n = 3584, 42%) followed by *Hya. anatolicum* (n = 2,253, 27%), *A. persicus* (n = 1,342, 16%), *Hya. impeltatum* (n = 586, 7%), *R. turanicus* (n = 161, 2%), *R. haemaphysaloides* (n = 142, 2%), *R. annulatus* (n = 132, 2%), *Hae. montgomeryi* (n = 123, 1.4%), *Hya. marginatum* (n = 110, 1.3%), *R. sanguineus* (n = 34, 0.4%), and *Hae. longicornis* (n = 31, 0.4%) (**Table 2** and **Figure 6A**). Cattle were found infested separately by *R. microplus, R. haemaphysaloides, Hya. anatolicum, Hya. impeltatum, Hya. marginatum* and *Hae. montgomeryi* and buffalos were found infested separately by *R. microplus, R. haemaphysaloides*, *Hya. anatolicum,* and *Hae. montgomeryi*. On the other hand, goats were found infested by *Hae. montgomeryi, Hae. longicornis,* and *Hya. impeltatum,* and sheep were infested separately by two species *Hae. longicornis* and *Hya. impeltatum. R. annulatus*

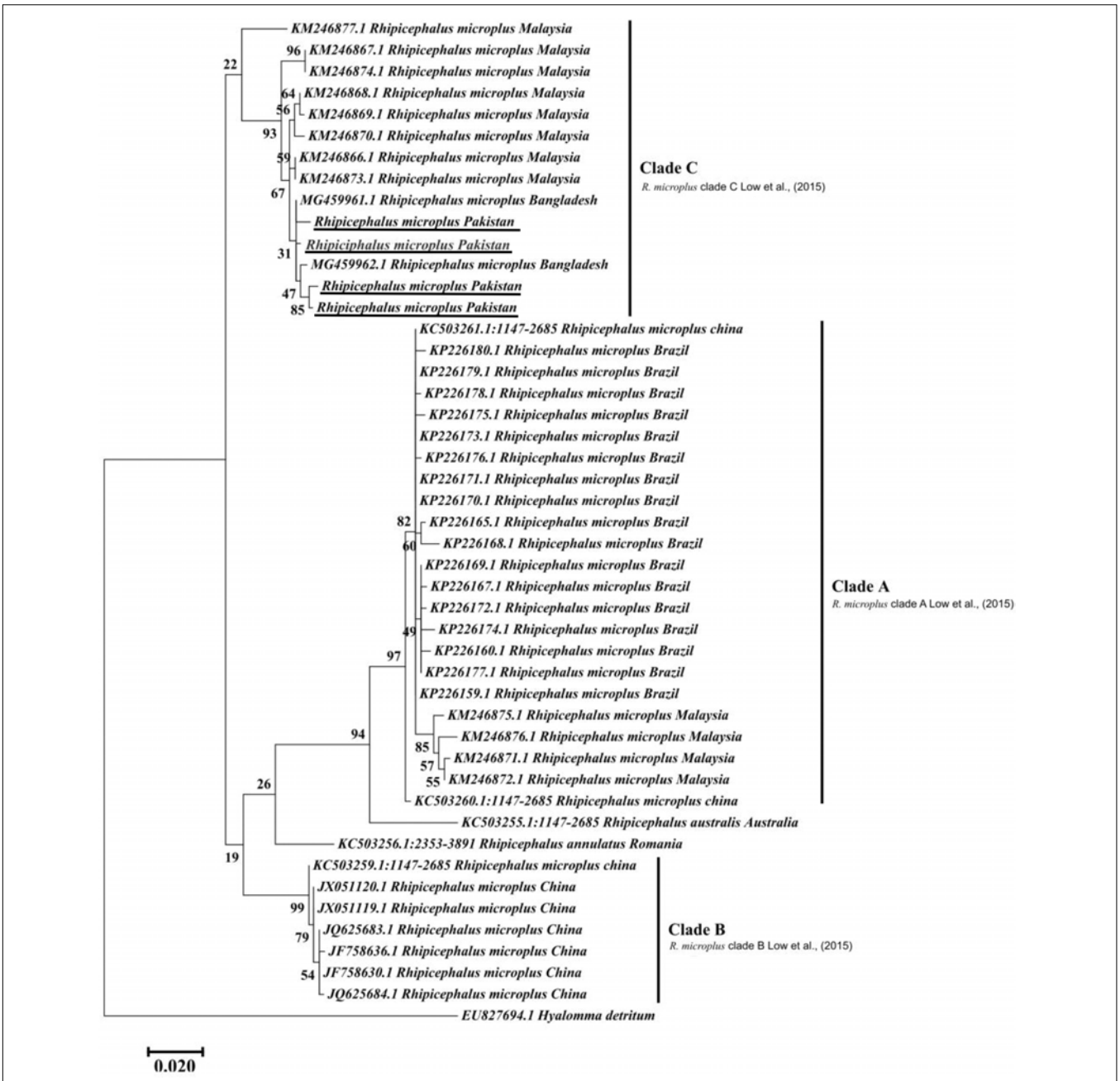

FIGURE 3 | Maximum likelihood tree inferred from COX1 sequences of the genus *Rhipicephalus* and using *Hyalomma* sequence as outgrowth. GenBank accession numbers are followed by species name and location of collection. Clade A includes *R. microplus* ticks from America, Malaysia, and China, clade B includes tick from China and clade C includes ticks from Pakistan, India, Bangladesh, Myanmar, and Malaysia. Support values (Bootstrapping values) were indicated at each node. The bar represents 0.020 substitutions per site. Sequences obtained in the present study were underlined.

and *R. sanguineus* were collected from dogs. Horses and domestic fowls were found to be infested by a single species of *R. turanicus* and *A. persicus,* respectively. Hosts infested by multiple tick species were also recorded. For instance, *R. microplus* and *Hya. anatolicum* were found infesting both cattle and buffaloes (**Table 3**).

A total of 772 animals were observed throughout the study period (April 2017 to March 2018) which included bovine (cattle, 180; buffalos, 114), ovine (sheep, 80), caprine (goats, 120), avian (domestic fowl, 150) equine (horse, 80) and carnivorous (dogs, 48) hosts, from which 8,498 ticks were collected. The overall prevalence of tick infested animals was 69.4% (536/772). Among the tick infested hosts; cattle were found highly infested (87.2%, 157/180) followed by buffalos (79.8%, 91/114), domestic fowl (74.7%, 112/150), goats (68.3%, 82/120), dogs (66.7%, 32/48), horses (61.3%, 49/80), and sheep (16.3%, 13/80).

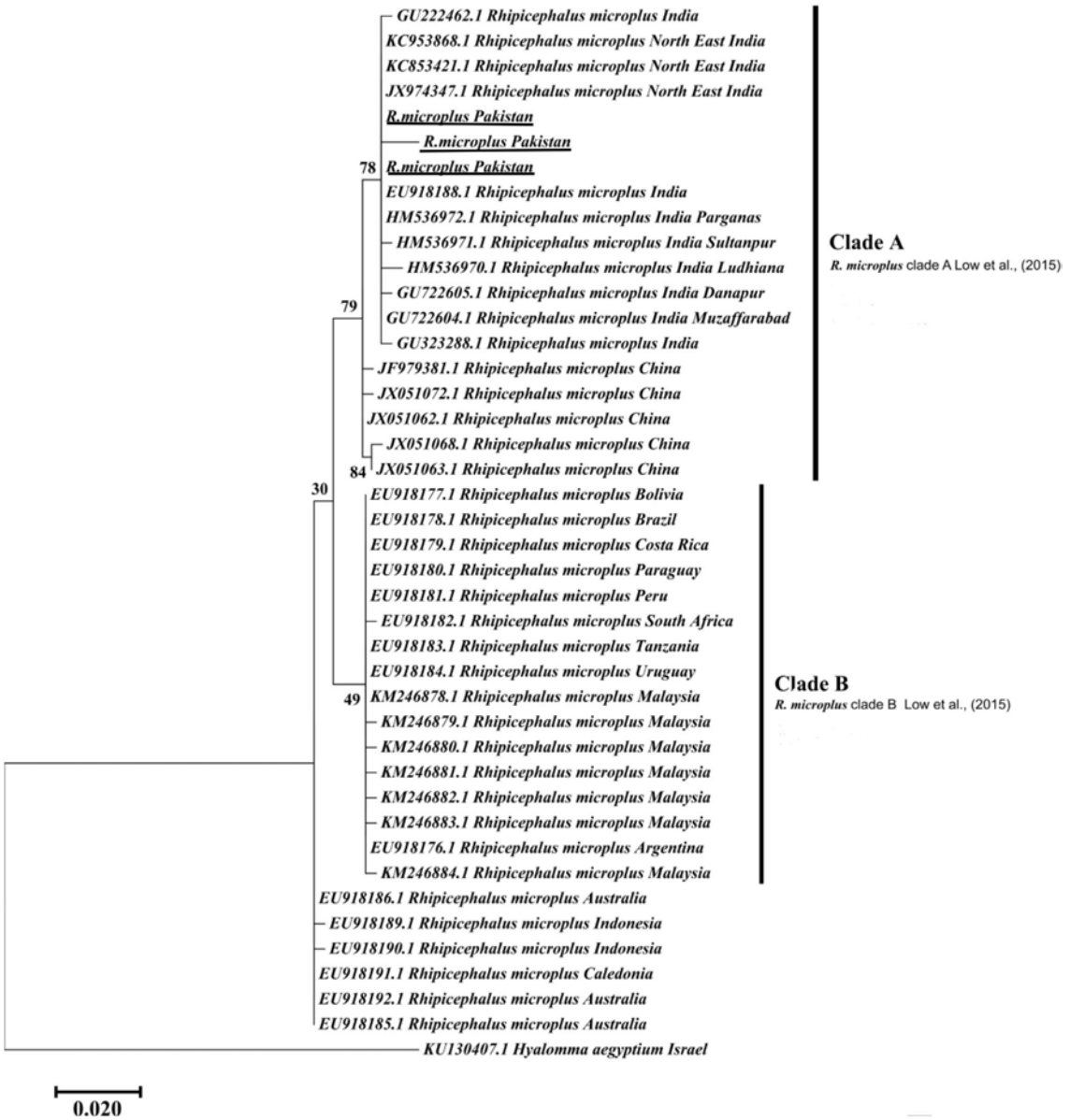

FIGURE 4 | Maximum likelihood tree inferred from 16S rRNA sequences of the genus *Rhipicephalus* and using *Hyalomma* sequence as outgrowth. GenBank accession numbers are followed by species name and location of collection. The clade A includes *R. microplus* from Pakistan, India, and China while Clade B contains *R. microplus* from Africa, Malaysia and South America. Support values (Bootstrapping values) were indicated at each node. The bar represents 0.020 substitutions per site. Sequences obtained in the present study were underlined.

Tick Burden

Median tick burden recorded on host animals was 16 (median 16, Q1-Q3: 9-31) and showed a statistically significant difference among the different host groups ($\chi^2 = 157.83$, $df = 6$, $p < 0.001$). Median tick burden was high in cattle (median 29), followed by buffalos (median 21.5), goats (median 21), sheep (13), domestic fowl (12), dogs (8.5), and horses (6).

Seasonal Dynamics of Ticks

The tick species included in the seasonal dynamics analysis were; *Hya. anatolicum, Hya. marginatum, Hya. impeltatum, R. microplus, R. haemaphysaloides, R. sanguineus, R. turanicus, R. annulatus, Hae. montgomeryi, Hae. longicornis,* and *A. persicus.* Tick species showed spatio-temporal variations in their distribution. Specifically, species of the genus *Hyalomma* were mainly reported in dry regions while species belonging to the genus *Rhipicephalus* were reported in semi-arid regions of the study area (**Figure 6B**). During ticks collection, adult females (partially fed or nymphs) were highly prevalent followed by males and larvae (**Table 2**). Other tick species were not included in the temporal analysis because they were collected by chance from novel hosts (these hosts were not the focus of the present

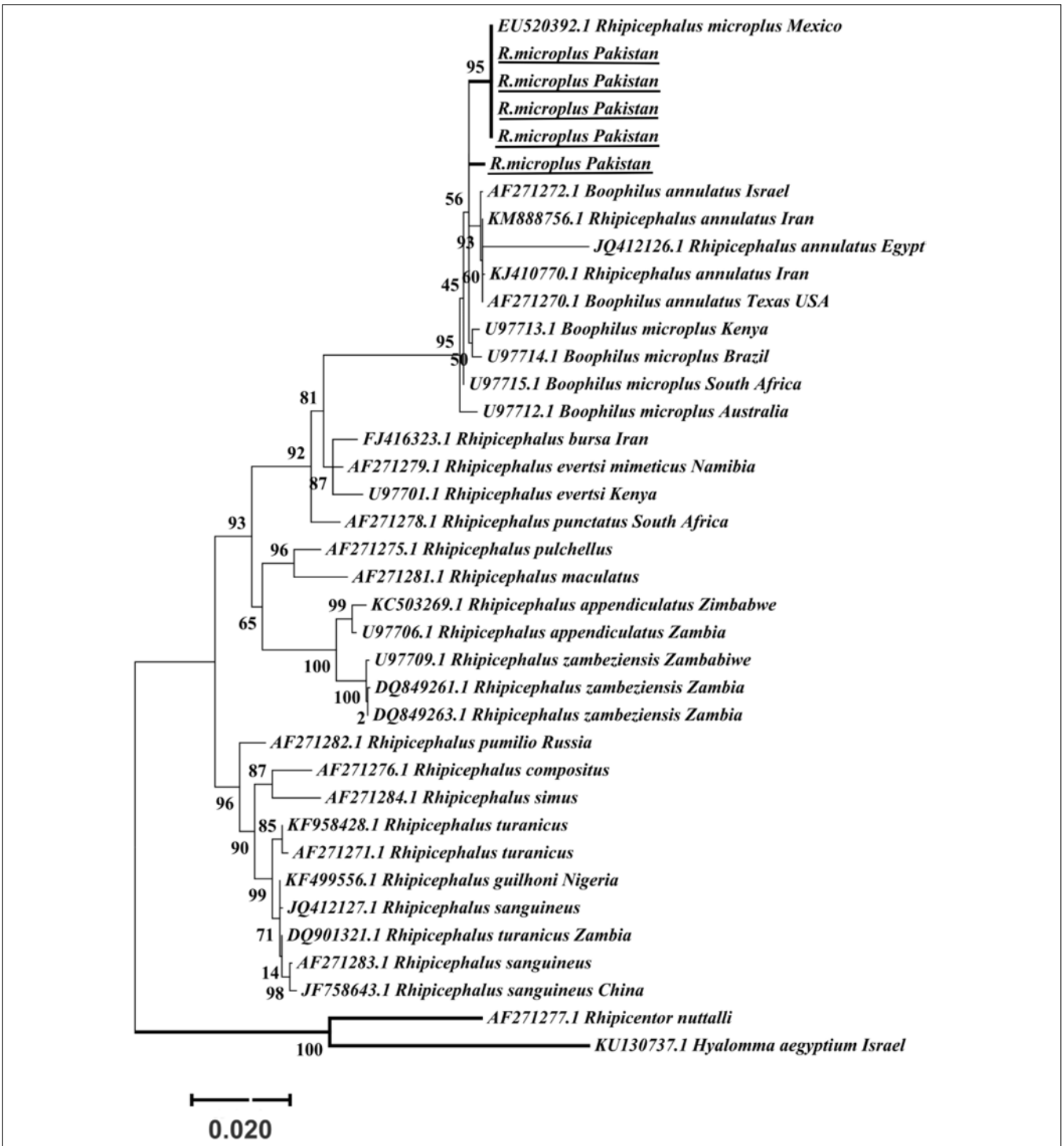

FIGURE 5 | Maximum likelihood tree inferred from ITS2 sequences of the genus *Rhipicephalus* and using *Rhipicentor* and *Hyalomma* sequences as outgrowth. GenBank accession numbers are followed by species name and collection location. Support values (Bootstrapping values) were indicated at each node. The bar represents 0.020 substitutions per site. Sequences obtained in the present study were underlined.

study) either from the study area or from other districts within KP Pakistan, during some parts of the year. This included tick species such as *Amb. gervaisi, Amb. exornatum, Amb. latum, D. marginatus, Hae. indica,* and *R. sanguineus* from monitor lizards, Indian pythons, markhor, mongoose and wild boars, respectively.

The highest number of ticks were collected in July followed by August and September as an increase in the infestation rate

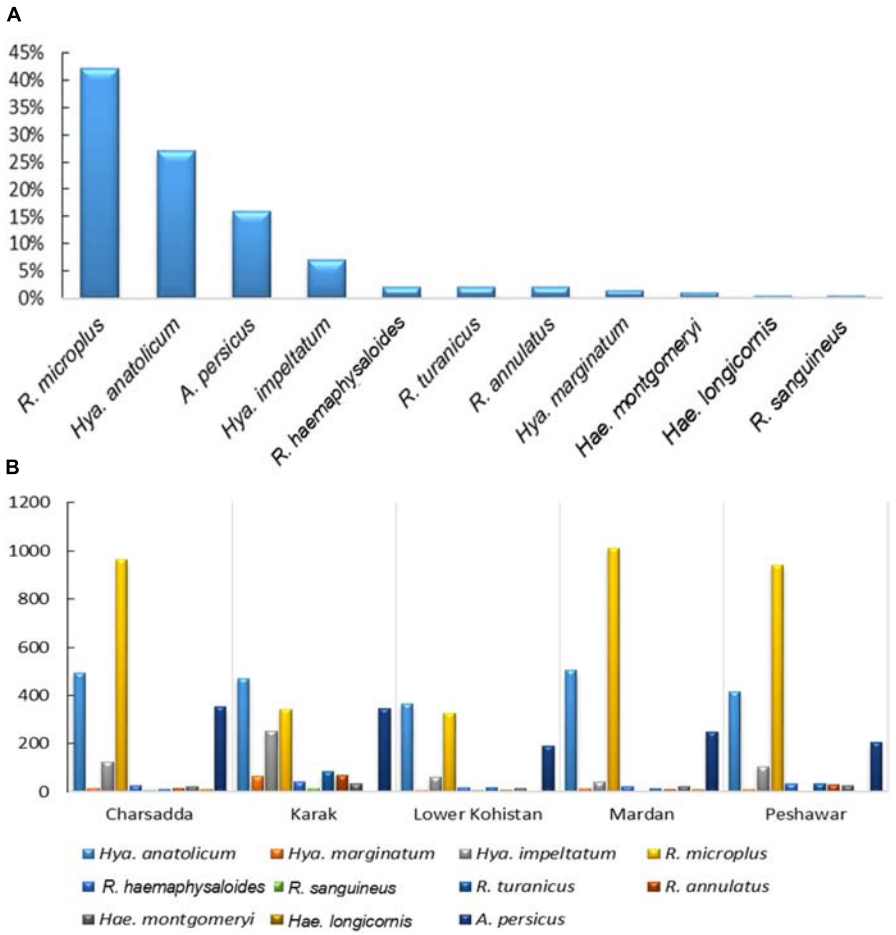

FIGURE 6 | (A) shows percent composition of collected tick species **(B)** and spatial distribution of ticks in various districts of KP, Pakistan.

of ticks were recorded during ticks collection and these finding significantly correlated with an increase in mean temperature [$r(10) = 0.929$, $p < 0.01$] and relative humidity [$r(10) = 0.831$, $p < 0.01$] during these months in the region. As the mean temperature fell and relative humidity decreased, the infestation rate also decreased (**Figure 7**).

Ticks Infesting Humans and Wild Animals

A total of 25 ticks were collected from humans (i.e., three genera and five species including *R. microplus, R. annulatus, Hae. punctata, Hya. marginatum,* and *Hya. anatolicum*). Ticks collected from wild animals included *Hae. indica* (wild rodent, $n = 17$), *Amb. gervaisi* and *Amb. exornatum* (monitor lizard, $n = 21$ and $n = 14$), *Amb. latum* (Indian python, $n = 23$), *D. marginatus* (wild goat, $n = 31$) and *R. sanguineus* (wild boar, $n = 12$) (**Table 4** and **Figure 8**).

Sequence and Phylogenetic Analysis

Genomic DNA extracted from morphologically identified *R. microplus* tick samples were amplified by PCR using COX1, 16S rRNA and ITS2 specific primers (**Table 1**). Results were observed on agarose gel electrophoresis and the resultant amplicons (COX1, 16S rRNA and ITS2) were 620, 376, and 267 bp, respectively. After sequencing, BLAST analysis of the COX1 nucleotide partial sequences showed 95–100% identity with the same sequence reported from Pakistan (accession no. MG459963), Bangladesh (accession no. MG459961, MG459962) Myanmar (accession no. MG459964) and China (accession no. KC503259). In the case of 16S rRNA nucleotide partial sequences, BLAST analysis revealed that it shares a 98–100% identity with previously reported sequences for *R. microplus* from India (accession no. KY458969; MG811555) and China (accession no. KU664521; MH208600). ITS2 partial nucleotide sequences showed that it shares 99% identity with the same sequences reported for the same tick species from India (accession no. JX974346; MG978179), China (accession no. JQ737125; JQ737124; KX450290; MG721034), Laos (accession no. KC503276), Colombia (accession no. MF353138), and Cambodia (accession no. KC503272). Similarly, the sequences of COX1 (accession no. MK812968, MK836289, MK858219, MK858220), 16S rRNA (accession no. MK463980, MK463981, MK463982) and ITS 2 (accession no. MK480725, MK524212,

TABLE 2 | Tick species collected from diverse hosts across KP, Pakistan.

Host animal	*Hyalomma*			*Rhipicephalus*				*Haemaphysalis*		*Argus*
	Hya. anatolicum L/M/F*	*Hya. marginatum* L/M/F	*Hya. impeltatum* L/M/F	*R. microplus* L/M/F	*R. haemaphysaloides* L/M/F	*R. sanguineus* L/M/F	*R. turanicus* L/M/F	*R. annulatus* L/M/F	*Hae. montgomeryi* L/M/F	*Hae. longicornis* L/M/F	*A. persicus* L/M/F
Cow	207/976/561	4/31/23	34/91/161	148/353/1291	8/13/40	1/2/8	10/17/34	19/27/33	0/26/21	0/3/6	–
Buffalo	41/89/39	0/9/12	8/40/87	13/29/182	–	–	3/16/19	–	–	–	–
Goat	11/54/22	2/10/5	0/25/28	7/184/398	4/16/22	–	9/0/2	0/23/14	4/0/8	–	–
Sheep	13/39/53	0/0/3	0/8/13	23/137/296	0/9/18	–	2/13/13	0/11/5	14/17/12	1/2/5	–
Dog	–	–	–	–	–	7/7/9	3/0/14	–	–	7/2/2	–
Horse	19/94/35	0/8/3	12/35/44	61/196/266	0/4/8	–	0/4/2	–	3/4/14	0/0/3	–
Domestic fowl	–	–	–	–	–	–	–	–	–	–	178/317/847
Total	2,253	110	586	3584	142	34	161	132	123	31	1,342
Mean (%)	26.80	1.38	6.88	41.90	1.68	0.44	1.89	1.55	1.48	0.40	15.60
95% CI	(25.8–28.0)	(1.0–2.56)	(5.3–8.0)	(40.2–43.7)	(1.0–2.8)	(0.1–1.12)	(1.1–3.56)	(1.7–2.20)	(1.0–2.31)	(0.1–1.20)	(14.1–17.3)

**Nymphs or partially fed ticks were considered as adults (F). L, larvae; M, male. CI, Confidence Interval.*

TABLE 3 | Collected ticks, their hosts and preferred attachment sites on different hosts observed during present study.

Host	Tick species collected	Tick attachment site on host body
Cattle	*R. microplus, R. haemaphysaloides, Hya. anatolicum, Hya. impeltatum, Hya. marginatum,* and *Hae. montgomeryi*	(belly, dewlap, shoulders and flanks) (axillae, groin, genital areas, perineum and udder)
Buffalos	*R. microplus* *R. haemaphysaloides*, *Hya. anatolicum* and *Hae. montgomeryi*	(neck, shoulders, flanks, axillae, groin, genital areas, perineum, and udder)
Goat	*Hae. longicornis, R. haemaphysaloides* and *Hya. impeltatum*	(neck, shoulder, groin, axillae, genital areas, perineum, and udder)
Dog	*R. annulatus* and *R. sanguineus*	(legs, shoulders, ears, and neck)
Sheep	*Hae. longicornis* and *Hya. impeltatum*	(groin, axilla, lags, genital areas perineum, and udder)
Horses	*R. turanicus*	(shoulder)
Domestic fowl	*A. persicus*	(host plumage and nests)
	Multiple tick species infesting same host	
Cattle		*R. microplus* and *Hya. anatolicum*
Buffalos		*R. microplus* and *Hya. anatolicum*

MK531135, MK578158, MK577644) obtained in the present study were deposited to the NCBI databank.

Maximum likelihood (ML) trees were inferred from COX1, 16S rRNA and ITS2 partial sequences of *R. microplus* to establish its phylogenetic relationship. ML analysis of COX1 nucleotide sequences revealed three clades, clade A includes ticks from America, Malaysia, and China, clade B was comprised of ticks originating from China (Burger et al., 2014; Low et al., 2015) and clade C includes ticks from Pakistan, India, Bangladesh, Myanmar, and Malaysia (**Figure 3**) (Roy et al., 2018). The COX1 phylogenetic analysis provided better support to resolve the evolutionary relationships of *R. microplus*. On the other hand, 16S rRNA partial sequences provided little phylogenetic structure of *R. microplus* complex and divided into two phylogenetic clades, the clade A comprised of the *R. microplus* tick species from China, India and Pakistan. Clade B includes *R. microplus* ticks originating from Malaysia, Africa and America and the *R. australis* (formerly recognized as *R. microplus*) from Australia, Indonesia and New Caledonia formed a separate subclade along with the aforementioned ticks (**Figure 4**). Based on ITS2 analysis, all species of the *R. microplus* complex were clustered together and the ITS2 tree provided support to the monophyly of *R. microplus* complex (**Figure 5**).

DISCUSSION

Climatic change and global warming have a vital impact on the distribution of ticks and tick-borne pathogens, as each tick species selects a set of ecological conditions and biotopes that determine its dispersal and outline risk areas for their

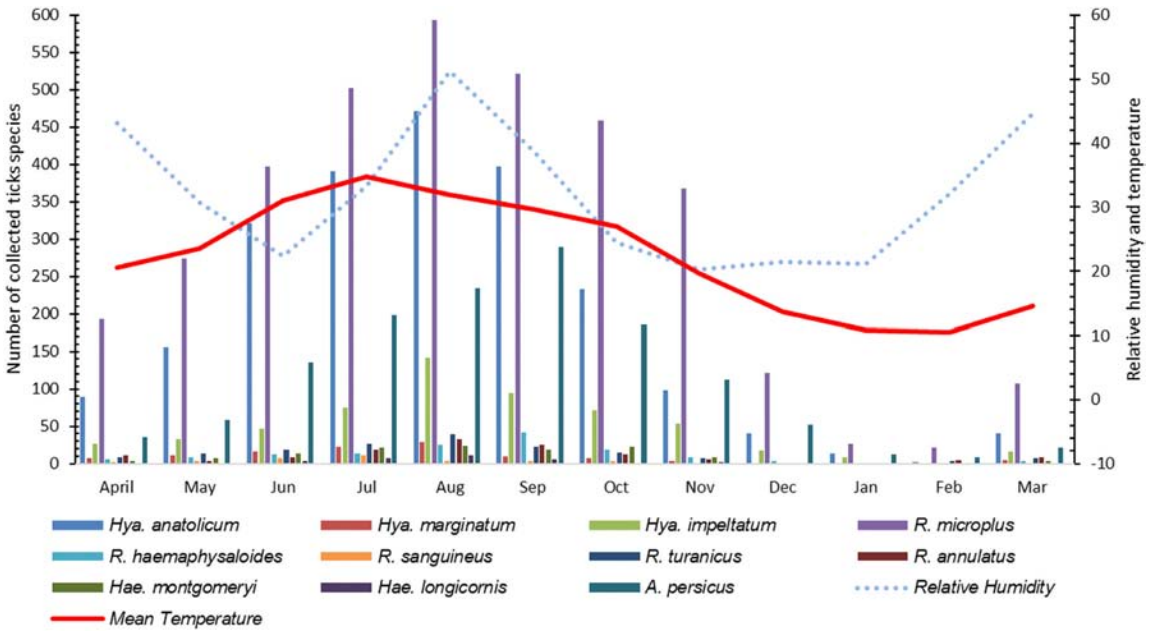

FIGURE 7 | Seasonal dynamics of various tick species recorded during this study.

associated pathogens transmission (Leger et al., 2013). Tick habitat expansion and novel pathogens (protozoans, bacteria, rickettsia, and viruses) are re-emerging in new geographic areas, posing a serious threat to public and veterinary health (Estrada-Peña et al., 2013; Jore et al., 2014). In KP Pakistan, the majority of farmers lack basic knowledge on ticks, their disease causing potential and the wide variety of hosts they infest, mostly resulting in a failure of controlling tick infestations. The present study encompasses the identification of diverse tick species and novel hosts, including humans, along with the seasonal dynamics and molecular phylogeny of *R. microplus* from north-western regions of Pakistan. The collected ticks were categorized into six genera including 17 species of medical and veterinary concern. We reported *Amb. latum*, *Amb. gervaisi*, *Amb. exornatum, A. persicus*, *D. marginatus*, *Hae. indica*, *Hae. longicornis*, *Hae. punctata, Hae. montgomeryi, Hya. impeltatum, H. anatolicum, Hya. marginatum*, *R. annulatus, R. haemaphysaloides*, *R. microplus*, *R. sanguineus,* and *R. turanicus* from the KP province. The majority of these ticks are responsible for the transmission of *Babesia bovis, Theileria annulata*, *Anaplasma marginale,* and *Anaplasma centrale* in the region (Jabbar et al., 2015). Our findings on the tick species prevalent in Pakistan correspond with previously reported studies (Manan et al., 2007; Karim et al., 2017; Rehman et al., 2017). Additionally, these ticks have been shown to be responsible for considerable losses in the livestock industry, causing severe threats to animal hosts and public health (Tadesse et al., 2012; Rehman et al., 2017).

Although ticks infestation on humans has been recorded from other regions of the world (Guglielmone and Robbins, 2018), ticks infesting humans and wild animals have not been previously reported in KP, Pakistan. During this study we found *R. microplus*, *R. annulatus, Hya. anatolicum, Hya. marginatum* and *Hae. punctata* (three genera and five species) infesting humans (**Figure 8**). These ticks, for instance, *R. microplus* (Labruna et al., 2005; Okino et al., 2010; Serra-Freire, 2010), *R. annulatus* (Horak et al., 2005; Bakirci et al., 2014; Kar et al., 2017) *Hya. anatolicum* (Estrada-Peña and Jongejan, 1999; Apanaskevich and Horak, 2005; Papa et al., 2011), *Hya. marginatum* (Santos-Silva et al., 2011), and *Hae. punctata* (Fernández-Soto et al., 2006; Briciu et al., 2011) parasitizing humans have already been reported in other parts of the world. *Hae. indica* from Indian gray mongoose are reported in this study, tick infestation on mongoose have been reported previously (Hoogstraal, 1970; Hoogstraal and Wassef, 1977; Horak et al., 1999; Cheng et al., 2018). In the present study *Amb. gervaisi* and *Amb. exornatum* parasitizing monitor lizards,

TABLE 4 | Tick species collected from wild animals during this study.

Infected host	Collection date	Collected tick species	Number and life stage*
Wild rodent (*Herpestes edwardsi*)	March 17, 2018	*Hae. indica*	17 (4L,10M,3F)
Monitor lizard (*Varanus varanus*)	June 12, 2018	*Amb. gervaisi*	21 (3L,7M,11F)
Monitor lizard (*Varanus varanus*)	July 15, 2018	*Amb. exornatum*	14 (2L,5M,7F)
Wild goat (*Capra falconeri*)	August 21, 2017	*D. marginatus*	31 (5L,9M,17F)
Wild boar (*Sus scrofa*)	May 05, 2017	*R. sanguineus*	12 (2L,6M,4F)
Indian python (*Python molurus*)	July 10, 2018	*Amb. latum*	23 (3L,9M,11F)

**Nymphs or partially fed ticks were considered as adults (F). L, larvae; M, male.*

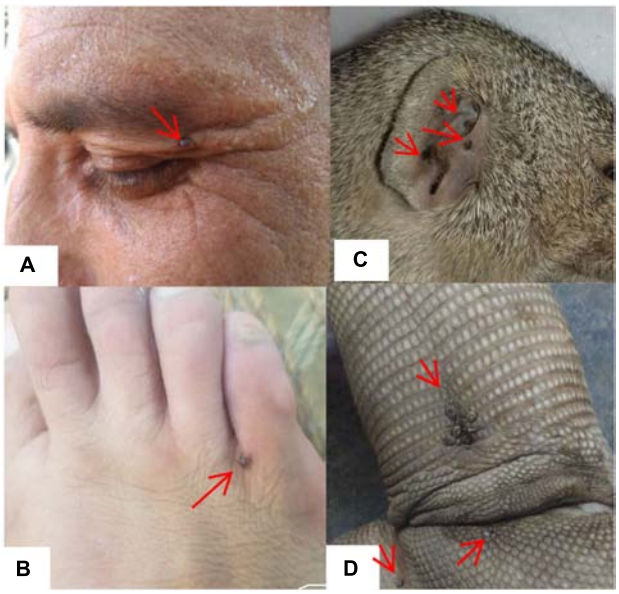

FIGURE 8 | Figure showing ticks infesting humans **(A,B)** (written informed consent was obtained from the individuals for the publication of images), *Hae. indica* collected from mongoose (*Herpestes edwardsi*) **(C)**, and *Amb. gervaisi* collected from monitor lizards (*Varanus varanus*) **(D)**.

and *Amb. latum* infesting Indian pythons were also reported. *Amblyomma* ticks are vectors of several pathogens known to transmit disease causing agents to humans and has never been investigated in Pakistan. *Amblyomma* species infesting reptiles are vectors of *Aeromonas hydrophila* that cause bacterial stomatitis, paralysis and pneumonia in snakes (Tenderio, 1953; Stephen and Achyutha, 1979; Marcus, 1981; Stenos et al., 2005; Hanson et al., 2007). *D. marginatus* were found to infest wild goats (locally known as markhor), which demands further studies to investigate the negative impact of this tick species in markhor which is considered as endangered species. The genus *Dermacentor* is of public and veterinary health concern as a vector reservoir for several pathogens with unknown potential risks in Pakistan. *R. sanguineus,* a vector of microorganisms of medical and veterinary health concern such as *Hepatozoon canis* and *Ehrlichia canis* (Dantas-Torres et al., 2018; Cabezas-Cruz et al., 2019) was collected for the first time from wild boars in the region.

Studies showing the seasonal pattern of tick distributions have never been reported from KP, Pakistan. During this study, information about the tick burden associated with relative humidity and temperature was recorded which is essential for the timing of potential control measures in tick infestation season. The target study region has high temperature and humidity during July, August and September therefore, high tick infestations were recorded during these months. On the other hand, due to the low temperatures during December, January, and February, several tick species were found to exhibit low infestation rates.

Several studies have used COX1, 16S rRNA and ITS2 as genetic markers for the accurate molecular identification and phylogenetic relationship of various organisms, including hard ticks such as *R. microplus* (Burger et al., 2014; Lv et al., 2014; Low et al., 2015; Coimbra-Dores et al., 2018). COX1 sequences have been used to show that cryptic species of *R. microplus* contain and display different population structures in different geographical regions (Burger et al., 2014; Low et al., 2015). Thus, *R. microplus* appears to consist of a complex of distinct genetic assemblages, namely *R. australis*, *R. annulatus*, *R. microplus* clade A (Burger et al., 2014), *R. microplus* clade B (Burger et al., 2014), and *R. microplus* clade C (Low et al., 2015). Burger et al. (2014) showed that *R. microplus* from clade B (Southern China and Northern India) is more closely related to *R. annulatus* than to *R. microplus* from clade A (Asia, South America, and Africa). In accordance with previous studies, phylogenetic trees based on COX1, 16S rRNA and ITS2 of *R. microplus* were obtained to establish the phylogenetic relationship of this tick (Lv et al., 2014; Low et al., 2015; Csordas et al., 2016; Rehman et al., 2017; Roy et al., 2018). COX1 was found to be an established marker for the phylogenetic analyses and informative for *R. microplus* phylogeny as compared to 16S rRNA and ITS2 as the latter provides monophyletic support to Boophild ticks (Burger et al., 2014). The COX1 phylogenetic analysis provided support to resolve the evolutionary relationship of *R. microplus*. Our findings about obtained COX1 sequences and phylogenetic analysis are parallel with previous reports from the region (Roy et al., 2018). ML analysis of COX1 nucleotide sequences revealed that these ticks are closely related to clade C (Low et al., 2015; Roy et al., 2018) (**Figure 3**). On the other hand, 16S rRNA partial sequences provided support to the monophyly of *R. microplus* complex and our tick sequences were clustered with clade A (**Figure 4**) (Brahma et al., 2014; Lv et al., 2014; Low et al., 2015). Based on ITS2 analysis, all species of the *R. microplus* complex were clustered together on the tree and provided support to the monophyly of *R. microplus* complex. The phylogenetic relationship in the *R. microplus* species complex was poor and could not accurately categorized as a sister species since ITS2 is highly conserved and is insufficient in distinguishing these closely related species (**Figure 5**).

CONCLUSION

This study for the first time explored the tick diversity infesting various hosts in KP, Pakistan. The important tick species of domestic animal hosts are *R. microplus, R. annulatus, R. haemaphysaloides, R. sanguineus, R. turanicus, Hae. montgomeryi, Hae. longicornis, Hya. marginatum. Hya. anatolicum, Hya. impeltatum,* and *A. persicus.* The seasonal pattern of several tick species showed high infestation during July, August and September in which high temperature and humidity persists in the region. The collection of tick species parasitizing humans in the study area may facilitate further studies to identify the functional role of these parasites in the transmission of pathogens that cause human diseases.

Altogether, tick species such as *Hae. indica*, *Amb. gervaisi*, *Amb. exornatum, Amb. latum*, *D. marginatus,* and *R. sanguineus* were reported for the first time infesting wild animals in the region. The phylogenetic relationship of cattle tick *R. microplus* explored in this study will further help in defining control strategies. These findings will facilitate awareness among the local population about tick species diversity and their hosts and future control strategies against ticks and tick-borne diseases in Pakistan.

DATA AVAILABILITY

The datasets generated for this study can be found in NCBI, MK463980, MK463981, MK463982, MK480725, MK524212, MK531135, MK578158, MK577644, MK812968, MK836289, MK858219, MK858220.

AUTHOR CONTRIBUTIONS

AA designed the study and acquired the budget. AA, MAK, HZ, SK, PY, JN, ZUR, MA, and MI collected the samples. AA, HZ, SK, MQK, MAK, and JN carried out the statistical analysis. MAK, HZ, PY, ZUR, AA, MA, and MI conducted the experiments. All authors carried out critical revisions and approved the final manuscript.

ACKNOWLEDGMENTS

We acknowledge the financial support provided by the Pakistan Science Foundation and the Higher Education Commission of Pakistan. We would like to thank Dr. Dmitry Apanaskevich, United States National Tick Collection (USNTC) for providing his expertise and facilities in the identification of ticks.

REFERENCES

Ali, A., Parizi, L. F., Ferreira, B. R., Junior, V., and da Silva, I. (2016). A revision of two distinct species of *Rhipicephalus*: *R. microplus* and *R. australis*. *Cienc. Rural* 46, 1240–1248.

Altschul, S. F., Gish, W., Miller, W., Myers, E. W., and Lipman, D. J. (1990). Basic local alignment search tool. *J. Mol. Biol.* 215, 403–410. doi: 10.1006/jmbi.1990.9999

Apanaskevich, D. A., and Horak, I. G. (2005). The genus *Hyalomma*. II The taxonomic status of H. (Euhyalomma) anatolicum Koch 1844 and H. (Euhyalomma) excavatum Koch 1844 with the redescription of all stages. *Acarina* 13, 181–197.

Apanaskevich, D. A., and Horak, I. G. (2008). The genus *Hyalomma* Koch, 1844: V. Re-evaluation of the taxonomic rank of taxa comprising the H. (Euhyalomma) marginatum Koch complex of species (Acari: Ixodidae) with redescription of all parasitic stages and notes on biology. *Int. J. Acarol.* 34, 13–42. doi: 10.1080/01647950808683704

Apanaskevich, D. A., and Horak, I. G. (2009). The genus *Hyalomma* Koch, 1844. IX. Redescription of all parasitic stages of H. (Euhyalomma) impeltatum Schulze & Schlottke, 1930 and H. (E.) somalicum Tonelli Rondelli, 1935 (Acari: Ixodidae). *Syst. Parasitol.* 73, 199–218. doi: 10.1007/s11230-009-9190-x

Bakirci, S., Aysul, N., Eren, H., Unlu, A. H., and Karagenc, T. (2014). Diversity of ticks biting humans in Aydın province of Turkey. *Ank Univ Vet Fak Derg.* 61, 93–98. doi: 10.1501/vetfak_0000002611

Barker, S. C., and Walker, A. R. (2014). Ticks of Australia. The species that infest domestic animals and humans. *Zootaxa.* 3816, 1–144. doi: 10.11646/zootaxa.3816.1.1

Baron, S., van der Merwe, N. A., and Maritz-Olivier, C. (2018). The genetic relationship between *R. microplus* and *R. decoloratus* ticks in South Africa and their population structure. *Mol. Phylogenet. Evol.* 129, 60–69. doi: 10.1016/j.ympev.2018.08.003

Brahma, R. K., Dixit, V., Sangwan, A. K., and Doley, R. (2014). Identification and characterization of *Rhipicephalus* (*Boophilus*) *microplus* and *Haemaphysalis bispinosa* ticks (Acari: Ixodidae) of North East India by ITS2 and 16S rDNA sequences and morphological analysis. *Exp. Appl. Acarol.* 62, 253–265. doi: 10.1007/s10493-013-9732-4

Briciu, V. T., Titilincu, A., Ţăţulescu, D. F., Cârstina, D., Lefkaditis, M., and Mihalca, A. D. (2011). First survey on hard ticks (Ixodidae) collected from humans in Romania: possible risks for tick-borne diseases. *Exp. Appl. Acarol.* 54, 199–204. doi: 10.1007/s10493-010-9418-0

Burger, T. D., Shao, R., and Barker, S. C. (2014). Phylogenetic analysis of mitochondrial genome sequences indicates that the cattle tick *Rhipicephalus* (*Boophilus*) *microplus* contains a cryptic species. *Mol. Phylogenet. Evol.* 76, 241–253. doi: 10.1016/j.ympev.2014.03.017

Cabezas-Cruz, A., Allain, E., Ahmad, A. S., Saeed, M. A., Rashid, I., Ashraf, K., et al. (2019). Low genetic diversity of *Ehrlichia canis* associated with high co-infection rates in *Rhipicephalus sanguineus* (s.l.). *Parasit. Vectors* 12:12. doi: 10.1186/s13071-018-3194-9

Caetano, R. L., Vizzoni, V. F., Bitencourth, K., Carrico, C., Sato, T. P., Pinto, Z. T., et al. (2017). Ultrastructural morphology and molecular analyses of tropical and temperate "species" of *Rhipicephalus sanguineus* sensu lato (Acari: Ixodidae) in Brazil. *J. Med. Entomol.* 54, 1201–1212. doi: 10.1093/jme/tjx066

Cheng, T., Halper, B., Siebert, J., Cruz-Martinez, L., Chapwanya, A., Kelly, P., et al. (2018). Parasites of small Indian mongoose, *Herpestes auropunctatus*, on St. Kitts, West Indies. *Parasitol. Res.* 117, 989–994. doi: 10.1007/s00436-018-5773-2

Coimbra-Dores, M. J., Maia-Silva, M., Marques, W., Oliveira, A. C., Rosa, F., and Dias, D. (2018). Phylogenetic insights on mediterranean and afrotropical *Rhipicephalus* species (Acari: Ixodida) based on mitochondrial DNA. *Exp. Appl. Acarol.* 75, 107–128. doi: 10.1007/s10493-018-0254-y

Csordas, B. G., Garcia, M. V., Cunha, R. C., Giachetto, P. F., Blecha, I. M. Z., and Andreotti, R. (2016). New insights from molecular characterization of the tick *Rhipicephalus* (*Boophilus*) *microplus* in Brazil. *Rev. Bras. Parasitol. Vet.* 25, 317–326. doi: 10.1590/S1984-29612016053

Dantas-Torres, F. (2015). Climate change, biodiversity, ticks and tick-borne diseases: the butterfly effect. *Int. J. Parasitol. Parasites Wildl.* 4, 452–461. doi: 10.1016/j.ijppaw.2015.07.001

Dantas-Torres, F., Latrofa, M. S., Ramos, R. A. N., Lia, R. P., Capelli, G., Parisi, A., et al. (2018). Biological compatibility between two temperate lineages of brown dog ticks. *Rhipicephalus sanguineus* (sensu lato). *Parasit. Vectors* 11:398. doi: 10.1186/s13071-018-2941-2

de la Fuente, J., Antunes, S., Bonnet, S., Cabezas-Cruz, A., Domingos, A. G., Estrada-Peña, A., et al. (2017). Tick-pathogen interactions and vector competence: identification of molecular drivers for tick-borne diseases. *Front. Cell Infect. Microbiol.* 7:114. doi: 10.3389/fcimb.2017.00114

de la Fuente, J., Rodriguez, M., and Garcia-Gari, J. C. (2000). Immunological control of ticks through vaccination with *Boophilus microplus* gut antigens. *Ann. N Y Acad Sci.* 916, 617–621. doi: 10.1111/j.1749-6632.2000.tb05347.x

Estrada-Peña, A. (2008). Climate, niche, ticks, and models: what they are and how we should interpret them. *Parasitol. Res.* 103, 87–95. doi: 10.1007/s00436-008-1056-7

Estrada-Peña, A., Gray, J. S., Kahl, O., Lane, R. S., and Nijhoff, A. M. (2013). Research on the ecology of ticks and tick-borne pathogens—methodological principles and caveats. *Front. Cell Infect. Microbiol.* 3:29. doi: 10.3389/fcimb.2013.00029

Estrada-Peña, A., and Jongejan, F. (1999). Ticks feeding on humans: a review of records on human-biting Ixodoidea with special reference to pathogen transmission. *Exp. Appl. Acarol.* 23, 685–715.

Estrada-Peña, A., Venzal, J. M., Nava, S., Mangold, A., Guglielmone, A. A., Labruna, M. B., et al. (2012). Reinstatement of *Rhipicephalus* (*Boophilus*)

australis (Acari: Ixodidae) with redescription of the adult and larval stages. *J. Med. Entomol.* 49, 794–802. doi: 10.1603/me11223

Fernández-Soto, P., Pérez-Sánchez, R., Álamo-Sanz, R., and Encinas-Grandes, A. (2006). Spotted fever group rickettsiae in ticks feeding on humans in northwestern Spain: is *Rickettsia conorii* vanishing? *Ann. N Y Acad Sci.* 1078, 331–333. doi: 10.1196/annals.1374.063

García-García, J. C., Gonzalez, I. L., González, D. M., Valdés, M., Méndez, L., Lamberti, J., et al. (1999). Sequence variations in the *Boophilus microplus* Bm86 locus and implications for immunoprotection in cattle vaccinated with this antigen. *Exp. Appl. Acarol.* 23, 883–895.

Ghosh, H. S., and Misra, K. K. (2012). Scanning electron microscope study of a snake tick, *Amblyomma gervaisi* (Acari: Ixodidae). *J. Parasit. Dis.* 36, 239–250. doi: 10.1007/s12639-012-0117-0

Gondard, M., Cabezas-Cruz, A., Charles, R. A., Vayssier-Taussat, M., Albina, E., and Moutailler, S. (2017). Ticks and tick-borne pathogens of the Caribbean: current understanding and future directions for more comprehensive surveillance. *Front. Cell Infect. Microbiol.* 7:490. doi: 10.3389/fcimb.2017.00490

Gratz, N. G. (1999). Emerging and resurging vector-borne diseases. *Annu. Rev. Entomol.* 44, 51–75. doi: 10.1146/annurev.ento.44.1.51

Guglielmone, A. A. and Robbins, R. G., (2018). *Hard Ticks (Acari: Ixodida: Ixodidae) Parasitizing Humans*, (New York, NY: Springer), 314.

Guglielmone, A. A., Robbins, R. G., Apanaskevich, D. A., Petney, T. N., Estrada-Peña, A., and Horak, I. G. (2014). *The hard ticks of the world*. Dordrecht: Springer.

Hall, T., Biosciences, I., and Carlsbad, C. (2011). BioEdit: an important software for molecular biology. *GERF Bull. Biosci.* 2, 60–61. doi: 10.1016/j.compbiolchem.2019.02.002

Hanson, B. A., Frank, P. A., Mertins, J. W., and Corn, J. L. (2007). Tick paralysis of a snake caused by *Amblyomma rotundatum* (Acari: Ixodidae). *J. Med. Entomol.* 44, 155–157. doi: 10.1093/jmedent/41.5.155

Hoogstraal, H. (1970). Identity, distribution, and hosts of *Haemaphysalis* (*Rhipistoma*) *indica* Warburton (resurrected) (Ixodoidea: Ixodidae), a carnivore parasite of the Indian subregion. *J. Parasitol.* 56, 1013–1022.

Hoogstraal, H., and Varma, M. G. R. (1962). Haemaphysalis cornupunctata sp. n. and *H. kashmirensis* sp. n. from Kashmir, with Notes on H. sundrai Sharif and H. sewelli Sharif of India and Pakistan (Ixodoidea, Ixodidae). *J. Parasitol.* 48, 185–194.

Hoogstraal, H., and Wassef, H. Y. (1977). Haemaphysalis (Ornithophysalis) kadarsani sp. n. (Ixodoidea: Ixodidae), a rodent parasite of virgin lowland forests in Sulawesi (Celebes). *J. Parasitol.* 63, 1103–1109.

Horak, I. G., Chaparro, F., Beaucournu, J. C., and Louw, J. P. (1999). Parasites of domestic and wild animals in South Africa. XXXVI. Arthropod parasites of yellow mongooses, *Cynictis penicillata* (G. Cuvier, 1829). *Onderstepoort J. Vet. Res.* 66, 33–38.

Horak, I. G., Fourie, L. J., and Braack, L. E. O. (2005). Small mammals as hosts of immature ixodid ticks. *Onderstepoort J. Vet. Res.* 72, 255–261.

Jabbar, A., Abbas, T., Saddiqi, H. A., Qamar, M. F., and Gasser, R. B. (2015). Tick-borne diseases of bovines in Pakistan: major scope for future research and improved control. *Parasit. Vectors* 8:283. doi: 10.1186/s13071-015-0894-2

Jones, K. E., Patel, N. G., Levy, M. A., Storeygard, A., Balk, D., Gittleman, J. L., et al. (2008). Global trends in emerging infectious diseases. *Nature* 451, 990–993. doi: 10.1038/nature06536

Jore, S., Vanwambeke, S. O., Viljugrein, H., Isaksen, K., Kristoffersen, A. B., Woldehiwet, Z., et al. (2014). Climate and environmental change drives *Ixodes ricinus* geographical expansion at the northern range margin. *Parasit. Vectors* 7:11. doi: 10.1186/1756-3305-7-11

Kaiser, M. N., and Hoogstraal, H. (1964). The *Hyalomma* ticks (Ixodoidea, Ixodidae) of Pakistan, India, and Ceylon, with keys to subgenera and species. *Acarologia* 6, 257–286.

Kar, S., Yilmazer, N., Akyildiz, G., and Gargili, A. (2017). The human infesting ticks in the city of Istanbul and its vicinity with reference to a new species for Turkey. *Syst. Appl. Acarol.* 22, 2245–2256.

Karim, S., Budachetri, K., Mukherjee, N., Williams, J., Kausar, A., Hassan, M. J., et al. (2017). A study of ticks and tick-borne livestock pathogens in Pakistan. *PLoS Negl. Trop Dis.* 11:e0005681. doi: 10.1371/journal.pntd.0005681

Kumar, S., Stecher, G., Li, M., Knyaz, C., and Tamura, K. (2018). MEGA X: molecular evolutionary genetics analysis across computing platforms. *Mol. Biol. Evol.* 35, 1547–1549. doi: 10.1093/molbev/msy096

Labruna, M. B., Jorge, R. S., Sana, D. A., Jácomo, A. T., Kashivakura, C. K., Furtado, M. M., et al. (2005). Ticks (Acari: Ixodida) on wild carnivores in Brazil. *Exp. Appl. Acarol.* 36, 149–163.

Labruna, M. B., McBride, J. W., Bouyer, D. H., Camargo, L. M. A., Camargo, E. P., and Walker, D. H. (2004). Molecular evidence for a spotted fever group *Rickettsia* species in the tick *Amblyomma longirostre* in Brazil. *J. Med. Entomol.* 41, 533–537.

Labruna, M. B., Naranjo, V., Mangold, A. J., Thompson, C., Estrada-Peña, A., Guglielmone, A. A., et al. (2009). Allopatric speciation in ticks: genetic and reproductive divergence between geographic strains of *Rhipicephalus* (*Boophilus*) microplus. *BMC Evol. Biol.* 9:46. doi: 10.1186/1471-2148-9-46

Leger, E., Vourc'h, G., Vial, L., Chevillon, C., and McCoy, K. D. (2013). Changing distributions of ticks: causes and consequences. *Exp. Appl. Acarol.* 59, 219–244. doi: 10.1007/s10493-012-9615-0

Lempereur, L., Geysen, D., and Madder, M. (2010). Development and validation of a PCR–RFLP test to identify African *Rhipicephalus* (*Boophilus*) ticks. *Acta Trop.* 114, 55–58. doi: 10.1016/j.actatropica.2010.01.004

Lew-Tabor, A. E., Ali, A., Rehman, G., Rocha-Garcia, G., Zangirolamo, A. F., Malardo, T., et al. (2017). Cattle Tick *Rhipicephalus microplus*-host interface: a review of resistant and susceptible host responses. *Front. Cell Infect Microbiol.* 7:506. doi: 10.3389/fcimb.2017.00506

Lew-Tabor, A. E., and Valle, M. R. (2016). A review of reverse vaccinology approaches for the development of vaccines against ticks and tick borne diseases. *Ticks Tick Borne Dis.* 7, 573–585. doi: doi: 10.1016/j.ttbdis.2015.12.012

Low, V. L., Tay, S. T., Kho, K. L., Koh, F. X., Tan, T. K., Lim, Y. A. L., et al. (2015). Molecular characterisation of the tick *Rhipicephalus microplus* in Malaysia: new insights into the cryptic diversity and distinct genetic assemblages throughout the world. *Parasit. Vectors* 8:341. doi: 10.1186/s13071-015-0956-5

Lv, J., Wu, S., Zhang, Y., Zhang, T., Feng, C., Jia, G., et al. (2014). Development of a DNA barcoding system for the Ixodida (Acari: Ixodida). *Mitochondrial DNA* 25, 142–149. doi: 10.3109/19401736.2013.792052

Madder, M., Horak, I., and Stoltsz, H. (2014). *Tick Identification*. Pretoria: Faculty of veterinary Science University of Pretoria, 58.

Manan, A., Khan, Z., and Ahmad, B. (2007). Prevalence and identification of ixodid tick genera in frontier region Peshawar. *J. Agric. Biol. Sci.* 37, 173–176.

Marcus, L. C. (1981). *Veterinary Biology and Medicine of Captive Amphibians and Reptiles*. Philadelphia, PA: Lea and Febiger.

Nowak-Chmura, M. (2012). Teratological changes in tick morphology in ticks feeding on exotic reptiles. *J. Nat. Hist.* 46, 911–921. doi: 10.1080/00222933.2011.651635

Okino, T., Ushirogawa, H., Matoba, K., and Hatsushika, R. (2010). Bibliographical studies on human cases of hard tick (Acarina: Ixodidae) bites in Japan (5) cases of *Ixodes acutitarsus* and *I. turdus* infestation. *Kawasaki Med. J.* 36, 115–120.

Paddock, C. D., and Childs, J. E. (2003). *Ehrlichia chaffeensis*: a prototypical emerging pathogen. *Clin. Microbiol. Rev.* 16, 37–64. doi: 10.1128/cmr.16.1.37-64.2003

Papa, A., Karabaxoglou, D., and Kansouzidou, A. (2011). Acute West Nile virus neuroinvasive infections: cross-reactivity with dengue virus and tick-borne encephalitis virus. *J. Med. Virol.* 83, 1861–1865. doi: 10.1002/jmv.22180

Parola, P., and Raoult, D. (2001). Ticks and tick-borne bacterial diseases in humans: an emerging infectious threat. *Clin. Infect. Dis.* 32, 897–928. doi: 10.1086/319347

Rehman, A., Nijhof, A. M., Sauter-Louis, C., Schauer, B., Staubach, C., and Conraths, F. J. (2017). Distribution of ticks infesting ruminants and risk factors associated with high tick prevalence in livestock farms in the semi-arid and arid agro-ecological zones of Pakistan. *Parasit. Vectors* 10:190. doi: 10.1186/s13071-017-2138-0

Robertson, R. G., Wisseman, C. L., and Traub, R. (1970). Tick-Borne Rickettsiae of the Spotted Fever Group in West Pakistan: I. isolation of strains from ticks in different habitats. *Am J Epidemiol.* 92, 382–394. doi: 10.1093/oxfordjournals.aje.a121221

Roy, B. C., Krücken, J., Ahmed, J. S., Majumder, S., Baumann, M. P., Clausen, P. H., et al. (2018). Molecular identification of tick-borne pathogens infecting cattle in Mymensingh district of Bangladesh reveals emerging species of Anaplasma and Babesia. *Transbound. Emerg. Dis.* 65, 231–242. doi: 10.1111/tbed.12745

Santos-Silva, M. M., Beati, L., Santos, A. S., De Sousa, R., Núncio, M. S., Melo, P., et al. (2011). The hard-tick fauna of mainland Portugal (Acari:

Ixodidae): an update on geographical distribution and known associations with hosts and pathogens. *Exp. Appl. Acarol.* 55, 85–121. doi: 10.1007/s10493-011-9440-x

Schorderet-Weber, S., Noack, S., Selzer, P. M., and Kaminsky, R. (2017). Blocking transmission of vector-borne diseases. *Int. J. Parasitol. Drugs Drug Resist.* 7, 90–109. doi: 10.1016/j.ijpddr.2017.01.004

Serra-Freire, N. M. (2010). Occurrence of ticks (Acari: Ixodidae) on human hosts, in three municipalities in the State of Pará, Brazil. *Rev. Bras. Parasitol. Vet.* 19, 141–147. doi: 10.1590/s1984-29612010000300003

Sherrard-Smith, E., Chadwick, E., and Cable, J. (2012). Abiotic and biotic factors associated with tick population dynamics on a mammalian host: *Ixodes hexagonus* infesting otters. *Lutra. PloS One* 7:e47131. doi: 10.1371/journal.pone.0047131

Stenos, J., Graves, S. R., and Unsworth, N. B. (2005). A highly sensitive and specific real-time PCR assay for the detection of spotted fever and typhus group *Rickettsiae*. *Am. J. Trop Med. Hyg.* 73, 1083–1085. doi: 10.4269/ajtmh.2005.73.1083

Stephen, S., and Achyutha, R. (1979). Q fever in South Kanara district: natural occurrence of *Coxiella burneti* in the tick (*Aponomma gervaisi*) preliminary report. *Indian J. Med. Res.* 69, 244–246.

Tadesse, F., Abadfaji, G., Girma, S., and Jibat, T. (2012). Identification of tick species and their preferred site on cattles body in and around Mizan Teferi, Southwestern Ethiopia. *Vet. Med. Anim. Health* 4, 1–5.

Tamura, K., Stecher, G., Peterson, D., Filipski, A., and Kumar, S. (2013). MEGA 6 molecular evolutionary genetics analysis version 6.0. *Mol. Biol. Evol.* 30, 2725–2729. doi: 10.1093/molbev/mst197

Tenderio, J. (1953). Alguns dados sobre as stirpes de *Coxiella burneti* isoladas na Guine Portugusea. *Bol. Cult. Guine Port.* 8, 69–87.

Walker, A. R., Bouattour, A., Camicas, J. L., Estrada-Peña, A., Horak, I. G., Latif, A. A., et al. (2003). *Ticks of Domestic Animals in Africa: A Guide to Identification of Species*. Edinburgh: Bioscience Reports.

Yu, Z., Wang, H., Wang, T., Sun, W., Yang, X., and Liu, J. (2015). Tick-borne pathogens and the vector potential of ticks in China. *Parasit. Vectors* 8:24. doi: 10.1186/s13071-014-0628-x

Conflict of Interest Statement: The authors declare that the research was conducted in the absence of any commercial or financial relationships that could be construed as a potential conflict of interest.

frontiers in Physiology

ORIGINAL RESEARCH
published: 26 July 2019
doi: 10.3389/fphys.2019.00977

A Vaccinomics Approach for the Identification of Tick Protective Antigens for the Control of *Ixodes ricinus* and *Dermacentor reticulatus* Infestations in Companion Animals

Marinela Contreras[1†], Margarita Villar[1†] and José de la Fuente[1,2]*

[1] SaBio, Instituto de Investigación en Recursos Cinegéticos (IREC; CSIC-UCLM-JCCM), Ciudad Real, Spain, [2] Department of Veterinary Pathobiology, Center for Veterinary Health Sciences, Oklahoma State University, Stillwater, OK, United States

OPEN ACCESS

Edited by:
Itabajara Silva Vaz Jr., Federal University of Rio Grande do Sul, Brazil

Reviewed by:
Maria Kazimirova, Institute of Zoology, Slovak Academy of Sciences, Slovakia
Luís Fernando Parizi, Federal University of Rio Grande do Sul, Brazil

***Correspondence:**
José de la Fuente
jose_delafuente@yahoo.com

[†] These authors have contributed equally to this work

Specialty section:
This article was submitted to Invertebrate Physiology, a section of the journal Frontiers in Physiology

Received: *13 May 2019*
Accepted: *11 July 2019*
Published: *26 July 2019*

Citation:
Contreras M, Villar M and de la Fuente J (2019) A Vaccinomics Approach for the Identification of Tick Protective Antigens for the Control of Ixodes ricinus and Dermacentor reticulatus Infestations in Companion Animals. Front. Physiol. 10:977. doi: 10.3389/fphys.2019.00977

Ticks and tick-borne pathogens affect health and welfare of companion animals worldwide, and some human tick-borne diseases are associated with exposure to domestic animals. Vaccines are the most environmentally friendly alternative to acaracides for the control of tick infestations, and to reduce the risk for tick-borne diseases affecting human and animal health. However, vaccines have not been developed or successfully implemented for most vector-borne diseases. The main limitation for the development of effective vaccines is the identification of protective antigens. To address this limitation, in this study we used an experimental approach combining vaccinomics based on transcriptomics and proteomics data with vaccination trials for the identification of tick protective antigens. The study was focused on *Ixodes ricinus* and *Dermacentor reticulatus* that infest humans, companion animals and other domestic and wild animals, and transmit disease-causing pathogens. Tick larvae and adult salivary glands were selected for analysis to target tick organs and developmental stages playing a key role during tick life cycle and pathogen infection and transmission. Two *I. ricinus* (heme lipoprotein and uncharacterized secreted protein) and five *D. reticulatus* (glypican-like protein, secreted protein involved in homophilic cell adhesion, sulfate/anion exchanger, signal peptidase complex subunit 3, and uncharacterized secreted protein) proteins were identified as the most effective protective antigens based on the criteria of vaccine $E > 80\%$. The putative function of selected protective antigens, which are involved in different biological processes, resulted in vaccines affecting multiple tick developmental stages. These results suggested that the combination of some of these antigens might be considered to increase vaccine efficacy through antigen synergy for the control of tick infestations and potentially affecting pathogen infection and transmission. These antigens were proposed for commercial vaccine development for the control of tick infestations in companion animals, and potentially in other hosts for these tick species.

Keywords: dog, rabbit, vaccine, tick, *Ixodes*, *Dermacentor*, transcriptomics, proteomics

INTRODUCTION

Tick-borne pathogens cause medically important infections affecting dogs and other pet species worldwide (Liu et al., 2018; Skotarczak, 2018), and some human tick-borne diseases are associated with exposure to domestic animals (Estrada-Peña et al., 2008; Kwit et al., 2018; Escárcega-Ávila et al., 2019). The tick species (Acari: Ixodidae), *Ixodes ricinus* (Linnaeus, 1758) and *Dermacentor reticulatus* (Fabricius, 1794) infest humans, pets and other domestic and wild animals. *I. ricinus* transmits disease-causing pathogens such as *Borrelia* spp. (Lyme disease and various borreliosis), tick-borne encephalitis virus (TBEV; tick-borne encephalitis) and *Anaplasma phagocytophilum* (human and animal anaplasmosis) while *D. reticulatus* is a vector for *Francisella tularensis* (tularemia), *Rickettsia* spp. (human and animal rickettsiosis), Omsk hemorrhagic fever virus (OHFV; Omsk hemorrhagic fever), and *Babesia canis* (canine babesiosis) (Glickman et al., 2006; de la Fuente et al., 2008, 2015; Beugnet and Marié, 2009).

Vaccines have not been developed or successfully implemented for most vector-borne diseases (VBD) affecting humans and animals (de la Fuente et al., 2017b). Therefore, reduction of arthropod vector infestations is important for the control of VBD (de la Fuente and Kocan, 2003; Sperança and Capurro, 2007; Karunamoorthi, 2011; Coller et al., 2012; de la Fuente and Contreras, 2015; de la Fuente et al., 2017b; de la Fuente, 2018). Traditional control methods for arthropod vector infestations are based on the use of chemical acaricides with associated drawbacks such as selection of arthropod-resistant strains and contamination of both the environment and animal products (de la Fuente and Kocan, 2003; de la Fuente et al., 2017b). Vaccination is an environmentally friendly alternative for the control of vector infestations and pathogen infections that allows control of several VBD by targeting their common vector (de la Fuente et al., 2007, 2011, 2017b; de la Fuente and Contreras, 2015; de la Fuente, 2018). Vaccines could be developed to target different tick developmental stages and functions on various hosts with the advantage of avoiding environmental contamination and selection of pesticide resistant arthropod vectors while improving animal welfare and production (de la Fuente et al., 2017b; de la Fuente, 2018). The experience with the only commercial vaccines available for the control of ectoparasite infestations, TickGard and Gavac, demonstrated that these vaccines contribute to the control of cattle tick populations while reducing acaricide applications, but were difficult to introduce into the market because of the absence of immediate effect on tick infestations and the application in combination with other control measures (de la Fuente and Kocan, 2003, 2006; Willadsen, 2004; de la Fuente et al., 2007). The hypothesis behind tick vaccine protective capacity is that ticks feeding on immunized hosts ingest antibodies specific for the target antigen that could reduce its levels and biological activity and/or interact with conserved epitopes in other proteins resulting in reduced tick feeding, development and reproduction (de la Fuente et al., 2011, 2017b; Moreno-Cid et al., 2011; de la Fuente, 2018).

The limiting step in developing tick vaccines is the identification of protective antigens (de la Fuente and Kocan, 2003; de la Fuente et al., 2018). Recent developments in omics analyses of both ticks and tick-borne pathogen and the application of systems biology to the study of tick-host-pathogen molecular interactions have advanced our understanding of the genetic factors and molecular pathways involved at the tick-host, tick-pathogen and host-pathogen interface (de la Fuente, 2012; de la Fuente et al., 2017a). These technologies are generating extensive information, but algorithms are needed to use these data for advancing knowledge on basic biological questions and the discovery of candidate protective antigens for the development of improved vaccines for the control of ticks and VBD (de la Fuente and Merino, 2013; de la Fuente et al., 2016, 2018; Contreras et al., 2018).

Acaricides have been effectively used to reduce tick infestations in companion animals (Otranto, 2018). However, ticks and transmitted pathogens continue to be a major health problem in dogs and other companion animals that require the development of effective vaccines (Otranto, 2018). Previous experiments have shown the possibility of using vaccines with tick gut protein extracts, Subolesin/Akirin and Bm96 for the control of *Rhipicephalus sanguineus* infestations in dogs (de la Fuente et al., 2015), and with pathogen-derived antigens for the control of VBD (e.g., Alhassan et al., 2018; Grosenbaugh et al., 2018). Nevertheless, vaccines for the control of tick infestations and transmitted diseases in companion animals have not been registered and commercialized.

In this study, we used a vaccinomics approach based on transcriptomics and proteomics data (de la Fuente and Merino, 2013; de la Fuente et al., 2016) in combination with vaccination trials for the discovery of tick protective antigens for the control of *I. ricinus* and *D. reticulatus* infestations in companion animals. Dogs and rabbits were used as model animals. Tick larvae and adult salivary glands were selected for analysis. Tick larvae are the first developmental stage to infest hosts and acquire infection or transmit pathogens that are transovarially transmitted. Salivary glands produce a cocktail of anti-clotting, anti-platelet, anti-inflammatory, vasodilatatory and immunomodulatory proteins that interfere with host defenses to aid in tick blood feeding and pathogen infection and transmission (Ayllón et al., 2015; Chmelaø et al., 2016; Nuttall, 2018). The experiments resulted in the identification of new antigens that showed a protective efficacy of vaccination against *I. ricinus* and *D. reticulatus* infestations in rabbits and dogs.

MATERIALS AND METHODS

Ethics Statement

White rabbits (*Oryctolagus cuniculus*) and Beagle dogs (*Canis lupus familiaris*) were used in the experiments. Animal experiments were conducted in strict accordance with the recommendations of the European Guide for the Care and Use of Laboratory Animals. Animals were housed and experiments conducted at LLC ACRO Vet Lab (Pylipovichi village, Kiev region, Ukraine) with the approval and supervision of the Ukrainian Commission for Bioethics and Biosafety for animals under the studies "Tick vaccine experiment on rabbits" number

000369 and "Tick vaccine experiments on dogs" numbers 000576, 000577 and 000761.

Ticks and Sample Preparation

Ixodes ricinus ticks were originally obtained from the reference laboratory colony maintained at the tick rearing facility of the Institute of Parasitology of the Biology Centre of the Academy of Sciences of the Czech Republic (Genomic Resources Development Consortium, Contreras et al., 2014). *D. reticulatus* ticks were obtained from a Dutch colony maintained at the Utrecht Centre for Tick-borne Diseases (UCTD), Department of Infectious Diseases and Immunology, Faculty of Veterinary Medicine, Utrecht University, Utrecht, The Netherlands (Villar et al., 2014). Tick colonies were maintained at the LLC ACRO Vet Lab (Pylipovichi village, Kiev region, Ukraine) and used for analysis and vaccination trials. *I. ricinus* unfed larvae whole internal tissues (IL) and unfed adult salivary glands (ISG), and *D. reticulatus* unfed larvae whole internal tissues (DL) and unfed adult salivary glands (DSG) were processed. RNA and proteins were extracted from approximately 500 larvae using the AllPrep DNA/RNA/Protein Mini Kit (Qiagen, Valencia, CA, United States) and from 50 salivary glands (25 females and 25 males) using Tri Reagent (Sigma-Aldrich, St. Louis, MO, United States) according to manufacturer instructions. RNA was purified with the RNeasy MinElute Cleanup Kit (Qiagen, Valencia, CA, United States) and characterized using the Agilent 2100 Bioanalyzer (Santa Clara, CA, United States) in order to evaluate the quality and integrity of RNA preparations. RNA concentration was determined using the Nanodrop ND-1000 (NanoDrop Technologies Wilmington, DE, United States). Protein concentration was determined using the Pierce BCA Protein Assay Kit (Thermo Scientific, Rockford, IL, United States) with BSA as standard. RNA yield was 10 μg (IL), 4 μg (ISG), 3.5 μg (DL), and 6 μg (DSG). Protein yield was 8 mg (IL and DL), 1.4 mg (ISG), and 3 mg (DSG).

Transcriptomics Data Acquisition for *I. ricinus* and *D. reticulatus* Samples

Purified RNAs were used for library preparation using the TruSeq RNA sample preparation kit v.1 and the standard low throughput procedure (Illumina, San Diego, CA, United States) as previously reported (Genomic Resources Development Consortium, Contreras et al., 2014; Villar et al., 2014). Briefly, 1 μg total RNA was used as starting material for library preparation with the exception of the DL sample for which 0.7 μg were used. Messenger RNA was captured using poly-dT magnetic beads and purified polyA+ RNA was chemically fragmented and reverse-transcribed. Remaining RNA was enzymatically removed, and the second strand generated following an end repair procedure and preparation of double-stranded cDNA for adaptor ligation. Adaptor oligonucleotides containing the signals for subsequent amplification and sequencing were ligated to both ends and cDNA samples were washed using AMPure SPRI-based magnetic beads (Beckman Coulter, IZASA, Barcelona, Spain). Adapters contained identifiers, which allow multiplexing in the sequencing run. An enrichment procedure based on PCR was then performed to ensure that all molecules in the library conserved the adapters at both ends. The number of PCR cycles was adjusted to 10 for all samples except for DL which needed up to 15 cycles. The final amplified library was checked again on a BioAnalyzer 2100 (Agilent, Santa Clara, CA, United States). Libraries were titrated by quantitative PCR using a reference standard to characterize molecule concentration per library (IL, 5.51 nM; ISG, 62.16 nM; DL, 12.44 nM; DSG, 100.95 nM). Libraries were denatured and seeded on the respective lanes of the flowcells at a final concentration after re-naturalization of 10–14 pM. IL and ISG samples were run in single-nucleotide flowcells while DL and DSG samples were run in double-nucleotide flowcells to allow for pair-end sequencing. After binding, clusters were formed in the flowcells by local amplification using a Cluster Station apparatus (Illumina). Following sequencing primer annealing, flowcells were loaded into a GAIIx equipment (Illumina) to perform sequencing using the TruSeq® system (Illumina). IL and ISG samples were run under a 1 × 75 bp single-end read protocol while DL and DSG samples were run under a pair-end 2 × 100 bp protocol for *de novo* RNA sequencing (RNAseq). After sequencing and quality filtering, reads were split according to their different identifiers and fastq files were generated to proceed to quality analysis and gene expression analysis and/or *de novo* transcript assembly. Transcriptomics data was submitted to Dryad Digital Repository[1] or published here (**Supplementary Dataset 1**) and by Villar et al. (2014) for *I. ricinus* and *D. reticulatus* samples, respectively.

Bioinformatics for *I. ricinus* and *D. reticulatus* Transcriptomics Data

I. ricinus

The pipeline used for bioinformatics analysis of *I. ricinus* transcriptomics data was similar to that described by Twine et al. (2011) as previously reported (Genomic Resources Development Consortium, Contreras et al., 2014). The reads from both IL and ISG samples were mapped to the reference *I. scapularis* genome (assembly JCVI_ISG_i3_1.0[2]) using a TopHat-Cufflinks-Cuffdiff pipeline (Langmead et al., 2009; Trapnell et al., 2009). Transcript abundance was estimated using Cufflinks by analyzing the number of reads mapped to each transcript and handling the deviations due to the sample preparation (Langmead et al., 2009). Finally, differential expression between IL and ISG was characterized using Cuffdiff, integrated into the Cufflinks package (Langmead et al., 2009). For analysis of genes coding for secreted proteins, 6 subcellular localization predictors were chosen: WoLF PSORT[3], TargetP[4], Protein Prowler[5], SLP-Local[6], PredSL[7] and CELLO[8]. All these tools have web services that enable batch protein sequence submissions. Results for genes encoding for

[1]https://doi.org/10.5061/dryad.9js92

[2]http://www.ncbi.nlm.nih.gov/nuccore/NZ_ABJB000000000

[3]http://wolfpsort.org

[4]http://www.cbs.dtu.dk/services/TargetP/

[5]http://bioinf.scmb.uq.edu.au:8080/pprowler_webapp_1-2/

[6]https://sunflower.kuicr.kyoto-u.ac.jp/~smatsuda/slplocal.html

[7]http://aias.biol.uoa.gr/PredSL/

[8]http://cello.life.nctu.edu.tw

predicted secreted proteins in IL and ISG were included in **Supplementary Dataset 2**.

D. reticulatus

For *D. reticulatus* transcriptomics data, the 21,838,507 reads (∼2.2 Gb) in DSG were compared against the *I. ricinus* selected reference gene set (**Table 1**) using PROmer (Kurtz et al., 2004). The query sequences were considered in their 3 reading frames and the reference sequences only in the frame 1. PROmer results were filtered by selecting the hits with a minimum length of 60 bp for the extended similarity region and a minimum identity of 80% in this region. Reads with hits fulfilling these requirements were clustered to the selected gene with which they have PROmer hits. We selected the read with hits and always also its paired read. The reads belonging to each cluster were then assembled with Velvet (Zerbino and Birney, 2008; Zerbino et al., 2009) to produce a set of contigs clustered to the reference genes. A BLASTX was then done against all proteins from Ixodidae included in the nr database. For each cluster of contigs, we chose the most similar protein to which the contigs aligned with more similarity, and substituted that protein as the new reference protein for that cluster. As expected, in many cases the most similar protein was identical to the initial *I. ricinus* reference protein. Differential gene expression between DL and DSG samples was determined using χ^2 test statistics with Bonferroni correction ($P = 0.05$) in the IDEG6 software[9].

Proteomics Data Acquisition for *I. ricinus* and *D. reticulatus* Samples

Proteins were resuspended in 5% SDS and frozen at −20°C until use. Two hundred μg of protein extracts from the four samples, IL, ISG, DL and DSG, were mixed with the same quantity of Laemmli sample buffer x2 and applied using a 5-well comb on a conventional SDS-PAGE gel (1.5 mm-thick, 4% stacking, 10% resolving). The electrophoretic run was stopped as soon as the front entered 3 mm into the resolving gel, so that the whole proteome became concentrated in the stacking/resolving gel interface. The unseparated protein bands were visualized by Coomassie Brilliant Blue R-250 staining, excised, cut into cubes (2 × 2 mm) and treated with 0.1% RapiGest SF surfactant (Waters, Milford. MA, United States) according to manufacturer's protocol in order to enhance the subsequent in-gel trypsin digestion. After RapiGest treatment, samples were digested overnight at 37°C with 60 ng/μl trypsin (Promega, Madison, WI, United States) at 5:1 protein:trypsin (w/w) ratio in 50 mM ammonium bicarbonate, pH 8.8 containing 10% (v/v) acetonitrile. The resulting tryptic peptides from each proteome were extracted by 1 h-incubation in 12 mM ammonium bicarbonate, pH 8.8. Trifluoroacetic acid (TFA) was added to a final concentration of 1% and the peptides were finally desalted onto C18 OASIS HLB extraction cartridges (Waters, Milford, MA, United States) and dried-down prior to reverse phase high performance liquid chromatography (RP-HPLC) method coupled with mass spectrometry (RP-HPLC-MS/MS) analysis using a Surveyor LC system coupled to an ion trap mass spectrometer model LCQ Fleet (Thermo-Finnigan, San Jose, CA, United States). Peptides were eluted using a 180-min gradient from 5 to 40% solvent B in solvent A (solvent A: 0.1% formic acid in water; solvent B: 0.1% formic acid in acetonitrile). The LCQ Fleet was programmed to perform a data-dependent MS/MS scan on the 3 most intense precursors detected in a full scan from 400 to 1600 amu (1 μscan, 200 ms injection time). Protein identification was conducted using SEQUEST algorithm (Proteome Discoverer 1.1 package, Thermo Finnigan), allowing optional modifications in Methionine (oxidation) and Cysteine (carboxamidomethylation). Proteomics data was included in **Supplementary Dataset 3** or published by Villar et al. (2014) for *I. ricinus* and *D. reticulatus* samples, respectively.

Bioinformatics for *I. ricinus* and *D. reticulatus* Proteomics Data

The MS/MS raw files were searched against the Ixodidae Uniprot database (28,771 entries in February 2012) with the following constraints: tryptic cleavage after Arginine and Lysine, up to two missed cleavage sites, and tolerances of 0.5 Da for precursor ions and 0.8 Da for MS/MS fragment ions. Protein assignations were first filtered with a SEQUEST XCorr > 2, but only proteins with false discovery rate (FDR) ≤ 0.01 and identified with at least 4 peptides were selected for further analysis from the Ixodidae database. The MS/MS data was also used to search against the database of predicted secreted proteins encoded by the selected top 1,000 expressed genes in both IL and ISG. In this case, proteins with sequence span > 2% were selected for further analysis. Differential protein representation between L and SG samples was determined using χ^2 test statistics with Bonferroni correction ($P = 0.001$) in the IDEG6 software (see footnote 9).

Gene Ontology

Gene ontology (GO) analysis for Molecular Function (MF), Cellular Component (CC) and/or Biological Process (BP) was conducted using the cDNA Annotation System software (dCAS; Bioinformatics and Scientific IT Program (BSIP), Office of Technology Information Systems (OTIS), National Institute of Allergy and Infectious Diseases (NIAID), Bethesda, MD, United States[10]), AmiGO[11] and UniProt[12] using non-redundant sequence database (nr) and databases of tick-specific sequences[13,14]. The GO annotations for selected candidate tick protective antigens were included in **Supplementary Dataset 4**.

Cloning of *I. ricinus* and *D. reticulatus* Genes Encoding for Candidate Protective Antigens

First, selected *I. ricinus* orthologs and *D. reticulatus de novo* generated contigs were amplified by RT-PCR with *I. scapularis*

[9]http://compgen.bio.unipd.it/bioinfo/software/

[10]http://exon.niaid.nih.gov

[11]http://amigo.geneontology.org/amigo

[12]http://www.uniprot.org

[13]http://www.ncbi.nlm.nih.gov

[14]http://www.vectorbase.org/index.php

TABLE 1 | Selected *I. ricinus* genes encoding for candidate tick protective antigens.

***Ixodes* gene ID**	**Genbank accession No. for *I. scapularis***	**Genbank accession No. for *I. ricinus***	**Encoded protein**	**Expression profile**	**Selection criteria**
472	ISCW000027 XM_002433472	GFVZ01075347	Uncharacterized protein	Over in IL	Transcriptomics: Top 1,000 expressed genes in both IL and ISG encoding for putative secreted proteins
529[a]	ISCW002303 XM_002399529	GFVZ01179036	Uncharacterized protein	Over in IL	
752[b]	ISCW002070 XM_002403752	GADI01007371	DNA-bridging protein BAF	Over in IL	
082[c]	ISCW024295 XM_002434082	GFVZ01108982	Secreted protein	Over in IL	
869[a]	ISCW006458 XM_002434869	GFVZ01137642	Uncharacterized protein	Over in IL	
965[a]	ISCW023699 XM_002415965	GFVZ01166334	Conserved hypothetical protein	Over in IL	
922[a,c]	ISCW021228 XM_002403922	GEGO01004220	Vitellogenin 2	Over in IL	Proteomics: Search against Ixodidae database with FDR = 0.01, identification with more than 4 peptides and filtered for BP and redundancy
391[c]	ISCW021710 XM_002411391	GANP01014013	Heme lipoprotein	Over in IL	
749[c]	ISCW016308 XM_002407749	GFVZ01132208	Conserved hypothetical protein	Over in IL	
216[c]	ISCW010436 XM_002406216	GFVZ01099159	Secreted salivary gland peptide	Over in IL	Proteomics: Search against putative secreted proteins encoded by top 1,000 expressed genes in both IL and ISG with XCorr > 2 and sequence span > 2%
892[a]	ISCW002948 XM_002409892	GFVZ01048464	Gap1	Over in IL	
450[a]	ISCW018653 XM_002434450	GFVZ01135723	Vacuolar H+ ATPase	Over in IL	
950[a]	ISCW013911 XM_002415950	GFVZ01068232	Hypothetical protein	Over in IL	
158[c]	ISCW019448 XM_002401158	GEGO01005185	Glypican	Over in IL	
459	ISCW011801 XM_002411459	GFVZ01157992	Hypothetical protein	Over in IL	
251[a]	ISCW023637 XM_002416251	GADI01004860	Secreted metalloprotease	Over in ISG	
178[b]	ISCW017062 XM_002409178	GANP01001334	Zinc finger protein, Palmitoyltransferase	Over in ISG	
623	ISCW015091 XM_002414623	GFVZ01042726	Hypothetical protein	Over in ISG	
738[a]	ISCW012232 XM_002413738	GEFM01006608	Sodium/glucose cotransporter	Over in ISG	
874[a]	ISCW006195 XM_002399874	GFVZ01065454	Fasciclin domain-containing protein	Over in ISG	
908[a]	ISCW014557 XM_002414908	GFVZ01100779	Secreted protein	Over in ISG	

(Continued)

TABLE 1 | Continued

Ixodes gene ID	Genbank accession No. for *I. scapularis*	Genbank accession No. for *I. ricinus*	Encoded protein	Expression profile	Selection criteria
150	ISCW006313 XM_002436150	GANP01003227	Secreted protein	Over in ISG	
556[a]	ISCW006654 XM_002400556	GADI01006770	Gamma-interferon inducible lysosomal thiol reductase	Over in ISG	
016[c]	ISCW019023 XM_002436016	GFVZ01163301	Secreted protein	Over in ISG	
971[a]	ISCW006734 XM_002435971	GADI01005462	Hypothetical protein	Over in ISG	
964[a,c]	ISCW001819 XM_002402964	GFVZ01127380	Conserved hypothetical protein	Over in ISG	Transcriptomics: Biological process (BP) GO for genes predicted as encoding for secreted proteins that were among the top 1,000 expressed genes overexpressed in ISG and filtered for BP and redundancy
427[a]	ISCW015065 XM_002414427	GANP01009473	Solute carrier	Over in ISG	
490[c]	ISCW003957 XM_002399490	GANP01008639	Aquaporin	Over in ISG	
058[c]	ISCW023239 XM_002415058	GANP01004202	Sulfate/anion exchanger	Over in ISG	
912	ISCW002249 XM_002410912	GANP01011997	Sialin	Over in ISG	
078[a]	ISCW005630 XM_002435078	GFVZ01037382	Sialin	Over in ISG	
432	ISCW019986 XM_002404432	GANP01006518	Monocarboxylate transporter	Over in ISG	
098	ISCW013157 XM_002413098	GANP01011927	Sodium-dependent multivitamin transporter	Over in ISG	
624	ISCW015092 XM_002414624	GFVZ01042726	Sodium/solute symporter	Over in SG	
145[a]	ISCW019568 XM_002405145	GFVZ01171589	Signal peptidase 12 kDa subunit	IL = ISG	Transcriptomics: Biological process (BP) GO for genes predicted as encoding for secreted proteins that were among the top 1,000 expressed genes in both IL and ISG and filtered for BP and redundancy
256[a]	ISCW016779 XM_002403256	GFVZ01154332	Signal peptidase complex subunit 3	IL = ISG	

[a]Genes abandoned due to no amplification by RT-PCR or low expression levels in E. coli. [b]Genes removed from further analysis due to the GO CC prediction. [c]Proteins identified in the membrane fraction of IL with FDR < 0.01. IL, I. ricinus larvae and ISG, salivary glands.

or *D. reticulatus* sequence-specific primers and conditions (**Supplementary Table 1**) using IL, ISG, DL and DSG RNA and the iScript One-Step RT-PCR Kit with SYBR Green and the iQ5 thermal cycler (Bio-Rad, Hercules, CA, United States) following manufacturer's recommendations. The genes that did not produce an amplicon after RT-PCR were eliminated from further analyses (**Tables 1**, **2**). Remaining coding regions for *I. scapularis* sequences corresponding to selected *I. ricinus* orthologous sequences and *D. reticulatus de novo* generated contig sequences were synthesized (GenScript, Hong Kong) with optimized codon usage for *Escherichia coli* (**Supplementary Dataset 5**).

Production of Recombinant Proteins and Vaccine Formulations

For gene expression and the production of the recombinant proteins, *E. coli* BL21 Star (DE3) One Shot cells (Invitrogen-Life Technolgies, Inc., Grand Island, NY, United States)

TABLE 2 | Selected *D. reticulatus* genes encoding for candidate tick protective antigens.

Dermacentor gene ID	*Ixodes* gene ID	Genbank accession No. for *D. reticulatus*	Number of reads		Expression profile (overexpressed in)	
			DL	DSG	*I. ricinus*	*D. reticulatus*
S1[a,c]	964	MK895447	250	3206	ISG*	DSG*
S2	256	MK895448	881	1748	ISG*	DSG*
S3[b]	752	NA	68	82	IL	DSG
S4[b]	178	NA	35	181	ISG*	DSG*
S5	892	MK895449	4	216	IL	DSG
S6	912	MK895450	5	49	ISG*	DSG*
S7[c]	490	MK895451	45	2000	ISG*	DSG*
S8[c]	158	MK895452	0	34	IL	DSG
S9	145	MK895453	9	49	ISG*	DSG*
S10[c]	391	MK895454	0	240	IL	DSG
S11	459	MK895455	145	796	IL	DSG
S12	098	MK895456	84	246	NS	DSG
S13	738	MK895457	12	136	ISG*	DSG*
S14[c]	216	MK895458	3585	2088	IL*	DL*
S15	427	MK895459	30	702	ISG*	DSG*
S16	624	MK895460	49	481	NS	DSG
S17[c]	908	MK895461	867	3972	ISG*	DSG*
S18[c]	058	MK895462	23	749	ISG*	DSG*
S19	950	MK895463	2	14	IL	DSG
S20[c]	082	MK895464	67800	1839	IL*	DL*
S21	450	MK895465	64	105	IL	DSG
S22	078	MK895466	5	27	ISG*	DSG*
S23[c]	016	MK895467	9	139	ISG*	DSG*
S24[a]	150	NA	0	1	ISG*	DSG*
S25	874	MK895468	2	39	ISG*	DSG*
S26[a]	529	NA	2	0	IL	NS
S27[a]	749	NA	3	0	IL	NS

**Similar gene expression profile in I. ricinus and D. reticulatus. [a]Genes abandoned due to poor sequence information or low expression in E. coli. [b]Genes removed from further analysis due to the GO CC prediction. [c]Proteins identified in the membrane fraction of DL with FDR < 0.01. NA, no accession number because sequences were not submitted due to poor sequence information or because genes were removed from further analysis due to the GO CC prediction. NS, not significant; IL, I. ricinus larvae and ISG, salivary glands; DL, D. reticulatus larvae and DSG, salivary glands.*

were transformed with the target gene cloned into the pET101/D-TOPO expression vector (Invitrogen-Life Technolgies). Recombinant *E. coli* were inoculated into 10 ml of Luria-Bertani (LB) containing 50 μg/ml ampicillin (Sigma-Aldrich, St Louis, MO, United States) and 0.4% glucose (Laboratorios CONDA S.A., Madrid, Spain) and kept growing overnight at 37°C with shaking. Two ml of the overnight culture was propagated into 250 ml flasks containing 50 ml LB, 50 μg/ml ampicillin and 0.4% glucose for 2 h at 37°C and 200 rpm, and then for 4 h after addition of 0.5 mM final concentration of isopropyl-β-d-thiogalactopyranoside (IPTG, Sigma-Aldrich) for induction of gene expression. The cells were harvested by centrifugation at 3,900 × *g* for 15 min at 4°C and stored at −80°C for protein purification. One g of the cells harvested after induction of gene expression were resuspended in 5 ml of lysis buffer (100 mM Tris-HCl, pH 7.5, 250 mM NaCl, 7 M Urea, 10 mM imidazole) containing protease inhibitor (Ref. 04693132001, Roche, San Cugat del Vallés, Barcelona, Spain) and disrupted using a cell sonicator (Model MS73; Bandelin Sonopuls, Berlin, Germany). After disruption, the insoluble protein fraction containing the recombinant antigens as inclusion bodies were collected by centrifugation at 15,000 × *g* for 15 min at 4°C and stored at −20°C before purification. The purification of the recombinant protein was conducted using the automated Maxwell 16 Polyhistidine Protein Purification Kit (Promega, Madison, WI, United States). The eluted fraction containing the purified denatured proteins was dialyzed against 1000 volumes of PBS (137 mM NaCl, 2.7 mM KCl, 10 mM Na_2HPO_4, 1.8 mM KH_2PO_4), pH 7.4 for 12 h at 4°C. Recombinant proteins were then concentrated using an Amicon Ultra-15 ultrafiltration device (cut off 10 kDa) (Millipore-Merck, Darmstadt, Germany), and adjusted to 0.5 mg/ml. Protein concentration was determined using bicinchoninic acid (Pierce BCA Protein Assay Kit, Thermo Scientific, Rockford, IL, United States). For vaccine formulation, recombinant proteins or saline control were adjuvated in Montanide ISA 50 V2 (Seppic, Paris, France) for rabbit trials or Montanide PET GEL A (Seppic), a ready-to-disperse polymeric adjuvant designed to improve the safety and efficacy of vaccines for

companion animals (Parker et al., 2009) for dog trials to a final protein concentration of 250 μg/ml (Merino et al., 2013; Contreras and de la Fuente, 2016, 2017).

Vaccination Trials in Rabbits

Three two-year-old rabbits per group were assigned to *I. ricinus* or *D. reticulatus* trial injected subcutaneously (dorsum between shoulders) at days 0 (T1) and 14 (T2) with 0.2 ml (50 μg) doses of recombinant protein vaccine formulations or adjuvant/saline using a syringe with removable needle (0.45 × 13 mm). Two weeks after the last immunization (day 28; T3), rabbits in vaccinated and control groups were infested with 200 *I. ricinus* or *D. reticulatus* tick larvae of approximately 21 days after hatching placed on bags located on each rabbit's shaved ear as described previously (Contreras and de la Fuente, 2016, 2017). Immunizations, tick larval infestations, collections and evaluations were done blinded and the key to the experimental groups was not disclosed until the end of the experiment. Engorged tick larvae were collected, counted and weighted as they dropped off between days 31 to 34. Fed larvae were incubated at 21°C, 80–82% humidity with 7 h dark and 17 h light photoperiod until molting. The tick larvae successfully molting to nymphal stage were collected and counted between days 51 to 65. The number of engorged larvae, weight/larvae, and percent of larvae molting to nymphs were evaluated. Data were analyzed statistically to compare results for each tick species between individuals fed on vaccinated and adjuvant/saline injected control rabbits by Student's *t*-test with unequal variance ($P = 0.05$). Vaccine efficacy (E) was calculated as E (%) = 100 [1−(DL × DM_N)], where DL is the reduction in the number of engorged larvae and DM_N is the reduction in the percent of larvae molting to nymphs in ticks fed on vaccinated rabbits when compared to the controls fed on adjuvant/saline injected rabbits (Contreras and de la Fuente, 2016, 2017). Only parameters with statistically significant differences were included in vaccine E calculation. Results were included in **Supplementary Dataset 6**.

Vaccination Trials in Dogs

Three randomly mixed breed male and female dogs (age > 6 months; body weight > 2 Kg) per group were assigned to *I. ricinus* or *D. reticulatus* trial and injected subcutaneously (loose skin on the side of the chest) at days 0 (T1) and 21 (T2) with 0.2 ml (50 μg) doses of recombinant protein vaccine formulations or adjuvant/saline using a syringe with removable needle (0.45 × 13 mm). Two weeks after the last immunization (day 36; T3), dogs in vaccinated and control groups were infested with *I. ricinus* or *D. reticulatus* 25:30 (female:male ratio) adults of at least 10 days after molting and 100 nymphs of approximately 15 days after molting placed on feeding chambers (one chamber per tick stage) glued on each dog's shaved flank. Immunizations, tick infestations, collections and evaluations were done blinded and the key to the experimental groups was not disclosed until the end of the experiment. Engorged tick females were collected, counted and weighted as they dropped off between days 41 and 48. Fed females were incubated at 21°C, 80–82% humidity with 24 h dark photoperiod for approximately 1 month until oviposition. Egg mass per tick was weighted and incubated for fertility determined by counting the number of larvae per tick. Engorged tick nymphs were collected and counted as they dropped off between days 40 to 43. Detached engorged nymphs were incubated at 21°C, 80–82% humidity with 8 h dark and 16 h light photoperiod until molting. The tick nymphs successfully molting to adults were collected and counted approximately 1 month after collection. The number of engorged nymphs and adult females, weight/female, oviposition (egg mass/tick), fertility (No. hatching larvae), and number of nymphs molting to adults were evaluated. Data were analyzed statistically to compare results for each tick species between individuals fed on vaccinated and adjuvant/saline injected control rabbits by Chi^2-test ($P = 0.05$). Vaccine efficacy (E) was calculated as E (%) = 100 [1−(DN × DM_A × DT × DO × DF)], where DN is the reduction in the number of engorged nymphs, DM_A is the reduction in the number of nymphs molting to adults, DT is the reduction in the number of engorged female ticks, DO is the reduction in oviposition, and DF is the reduction in fertility in ticks fed on vaccinated rabbits when compared to the controls fed on adjuvant/saline injected dogs. Only parameters with statistically significant differences were included in vaccine E calculation. Results were included in **Supplementary Dataset 6**.

Analysis of IgG Antibody Response by ELISA and Western Blot

In rabbits, blood samples were collected from each animal before each immunization (T1 and T2) and tick infestation (T3). In dogs, blood samples were collected from each animal before each immunization (T1 and T2), tick infestation (T3) and at day 75 (T4) to better evaluate the duration of the antibody-mediated immune response in the major vaccine target species. Blood samples were collected into sterile tubes and maintained at 4 °C until arrival at the laboratory. Serum was then separated by centrifugation and stored at −20°C. An indirect ELISA test was performed to detect IgG antibodies against recombinant antigens in serum samples from vaccinated and control animals collected at T1–T3 for rabbits or T1–T4 for dogs as described previously (Merino et al., 2013; Contreras and de la Fuente, 2016, 2017). High absorption capacity polystyrene microtiter plates were coated with 50 μl (0.02 μg/ml solution of purified recombinant proteins) per well in carbonate-bicarbonate buffer (Sigma-Aldrich). After an overnight incubation at 4°C, coated plates were blocked with 200 μl/well of blocking solution (5% skim milk in PBS). Serum samples or PBS as negative control were diluted (1:1000, 1:10,000, 1:100,000 v/v; optimal dilution, 1:10,000) in blocking solution and 50 μl/well were added into duplicate wells of the antigen-coated plates. After an overnight incubation at 4°C, the plates were washed three times with a washing solution (PBS containing 0.05% Tween 20). A goat anti-rabbit or anti-dog IgG-peroxidase conjugate (Sigma-Aldrich) was added (diluted 1:3000 v/v in blocking solution) and incubated at RT for 1 h. After three washes with washing solution, 200 μl/well of substrate solution (Fast OPD, Sigma-Aldrich) was added. Finally, the reaction was stopped with 50 μl/well of 3N H_2SO_4 and the optical density (OD) was measured in an ELISA plate reader at 450 nm. Antibody levels in vaccinated and control animals were expressed as the OD_{450nm}

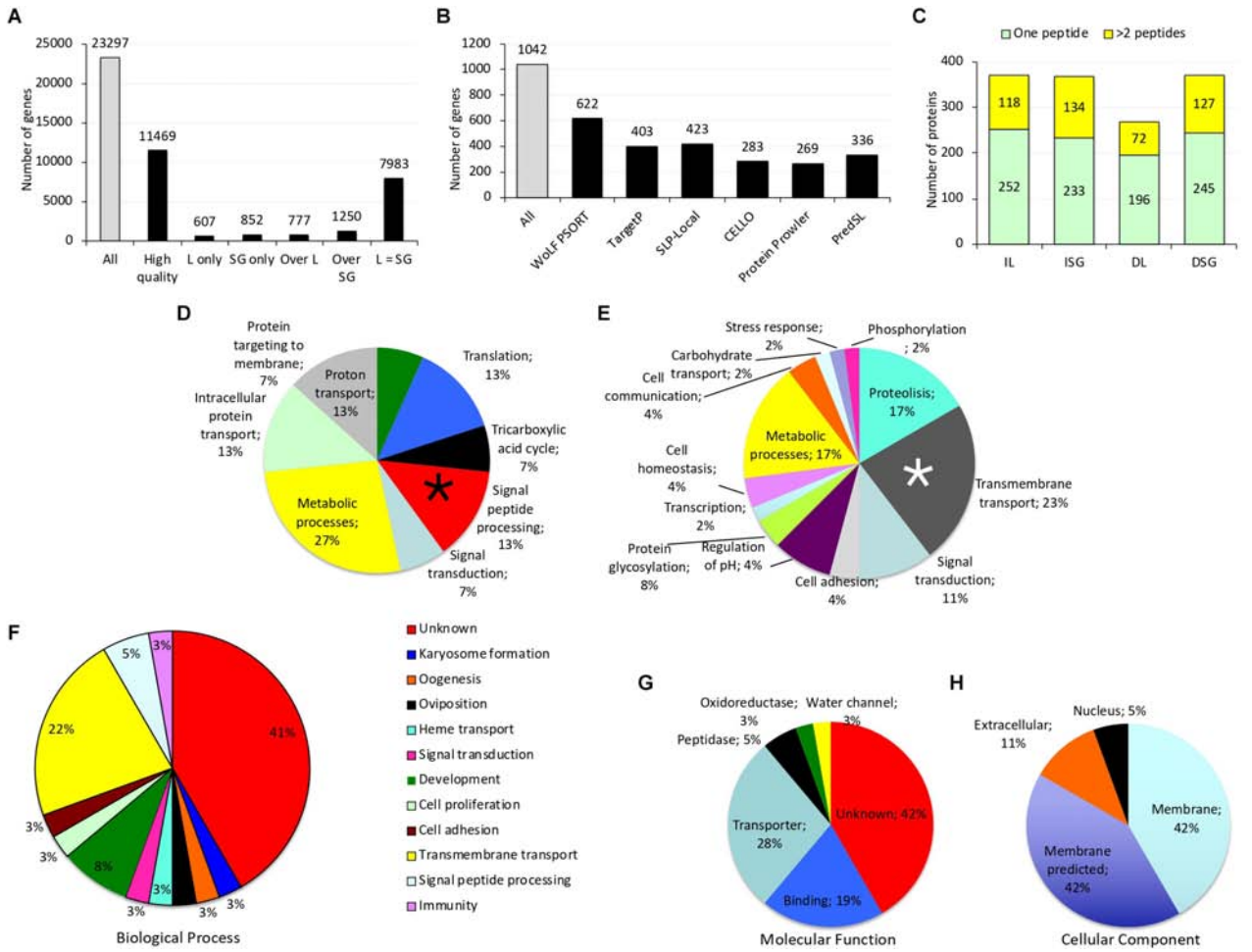

FIGURE 1 | Tick transcriptomics and proteomics data. **(A)** Differential gene expression in *I. ricinus* larvae (L) and salivary gland (SG) samples. **(B)** Genes predicted by different algorithms to encode for secreted proteins in *I. ricinus* larvae (IL) and salivary glands (ISG) samples. **(C)** Proteins identified with XCorr > 2 in the Ixodidae database in IL, ISG, *D. reticulatus* larvae (DL) and salivary gland (DSG) samples. **(D,E)** Biological process (BP) GO for genes predicted as coding for secreted proteins that were either **(D)** among the top 1,000 expressed genes in both IL and ISG or **(E)** overexpressed in ISG. Genes coding for hypothetical proteins or with unknown function were excluded from the graph. The BPs selected for further analysis are marked with asterisks. **(F–H)** GO analysis for **(F)** biological process (BP), **(G)** molecular function (MF) and **(H)** cell component (CC) of genes selected as coding for tick protective antigens. Genes coding for nuclear DNA-binding proteins were removed from further analysis. Complete datasets are on **Supplementary Datasets 1–4**.

($OD_{animal sera} - OD_{PBS control}$) and compared between vaccinated and control groups by ANOVA test ($P = 0.05$).

For Western blot analysis, 10 μg of selected purified recombinant proteins and *Rhipicephalus microplus* Subolesin (Merino et al., 2013) as negative control were separated by electrophoresis in an SDS-12% polyacrylamide gel (Life Science, Hercules, CA, United States) and transferred to a nitrocellulose membrane. The membrane was blocked with 5% BSA (Sigma-Aldrich) for 2 h at room temperature (RT) and washed three times with TBS (50 mM Tris-Cl, pH 7.5, 150 mM NaCl, 0.05% Tween 20). Pooled sera collected at T3 from vaccinated dogs were used as primary antibodies. Primary antibodies were used at a 1:300 dilution in TBS, and the membrane was incubated overnight at 4°C and washed three times with TBS. The membrane was then incubated with an anti-dog IgG-horseradish peroxidase (HRP) conjugate (Sigma-Aldrich) diluted 1:15000 in TBS with 2% BSA. The membrane was washed four times with TBS and finally developed with TMB (3,3′, 5,5′-tetramethylbenzidine) stabilized substrate for HRP (Promega, Madrid, Spain) according to the manufacturer recommendations.

Determination of mRNA Levels by Real-Time RT-PCR

The expression of selected genes was characterized using total RNA extracted from three separate pools of adult tick salivary glands (25 females and 25 males each pool) and larvae (500 larvae each pool) using Tri Reagent (Sigma-Aldrich) according to manufacturer instructions. Real-time RT-PCR was performed on RNA samples using gene-specific oligonucleotide primers (**Supplementary Table 1**) and the iScript One-Step RT-PCR Kit with SYBR Green and the CFX96 Touch Real-Time PCR

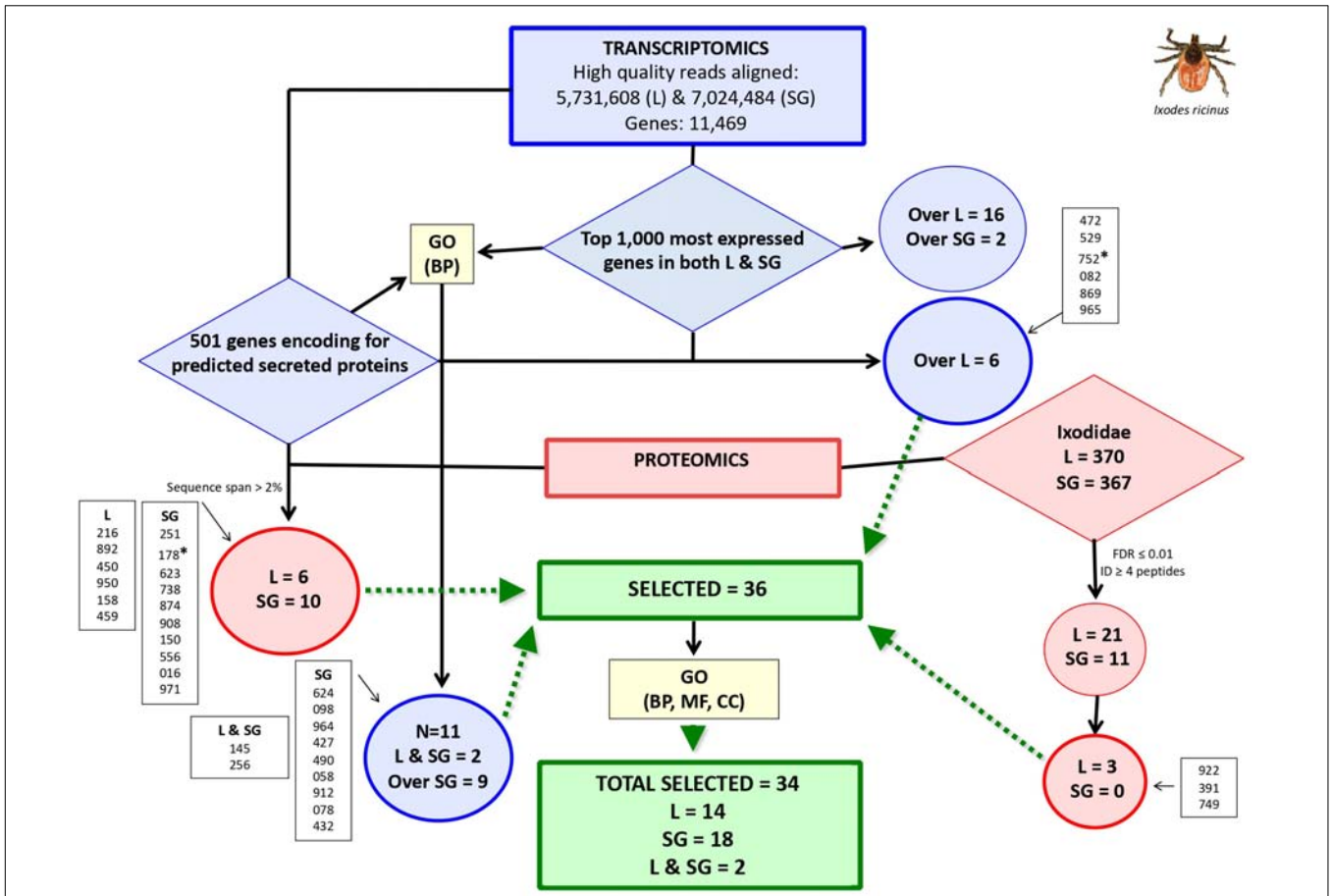

FIGURE 2 | Selection of genes coding for candidate *I. ricinus* tick protective antigens. Trascriptomics data were obtained from *I. ricinus* larvae (L) and salivary gland (SG) samples followed by selection of top 1,000 most expressed genes in both samples and genes coding for secreted proteins. GO analysis for biological process (BP) was then used to select for functionally relevant genes. Proteomics data was used for mining databases of Ixodidae and predicted secreted proteins. Selected genes (*N* = 36; IDs. shown inside boxes) expressed or overexpressed (Over) in *I. ricinus* larvae (IL) and salivary glands (ISG) samples were finally subjected to GO analysis for BP, molecular function (MF) and cell component (CC) to remove two genes coding for nuclear DNA-binding proteins (marked with asterisks), resulting in a final set of 34 selected genes coding for candidate protective antigens. Complete datasets are on **Supplementary Datasets 1–4**.

Detection System (Bio-Rad, Hercules, CA, United States). A dissociation curve was run at the end of the reaction to ensure that only one amplicon was formed and that the amplicons denatured consistently in the same temperature range for every sample. The mRNA levels were normalized against tick *ribosomal protein S4* (*rps4*) as described previously using the genNorm method (ddCT method as implemented by Bio-Rad iQ5 Standard Edition, Version 2.0) (Ayllón et al., 2013). Normalized C_t values were compared between salivary glands and larvae by Student's *t*-test with unequal variance ($P = 0.05$).

Protein Membrane Localization for *I. ricinus* and *D. reticulatus* Candidate Protective Antigens

To characterize the subcellular localization of proteins encoded by selected genes, the proteomes of IL and DL were obtained as described above but purifying membrane proteins prior to analysis. Approximately 200 *D. reticulatus* and *I. ricinus* larvae were pulverized in liquid nitrogen and homogenized with a glass homogenizer (20 strokes) in 4 ml buffer (0.25 M sucrose, 1 mM MgCl2, 10 mM Tris-HCl, pH 7.4) supplemented with complete mini protease inhibitor cocktail (Roche, Basel, Switzerland). Samples were sonicated for 1 min in an ultrasonic cooled bath followed by 10 sec of vortex. After 3 cycles of sonication-vortex, the homogenate was centrifuged at 200 × *g* for 5 min at RT to remove cellular debris. The supernatant was then centrifuged at 12000 × *g* for 30 min at 4°C and the pellet fraction enriched in crude plasma membranes was collected, resuspended in 100 µl Laemmli sample buffer and applied onto 1.2-cm wide wells on a 12% SDS-PAGE gel. The MS/MS raw files were searched against the Ixodida (40,849 entries in June 2013) Uniprot database and the protein database of candidate protective antigens (**Tables 1**, **2**) using the SEQUEST algorithm (Proteome Discoverer 1.3, Thermo Scientific) with the following constraints: tryptic cleavage after Arginine and Lysine, up to two missed cleavage sites, and tolerances of 1 Da for precursor ions and 0.8 Da for MS/MS fragment ions and the

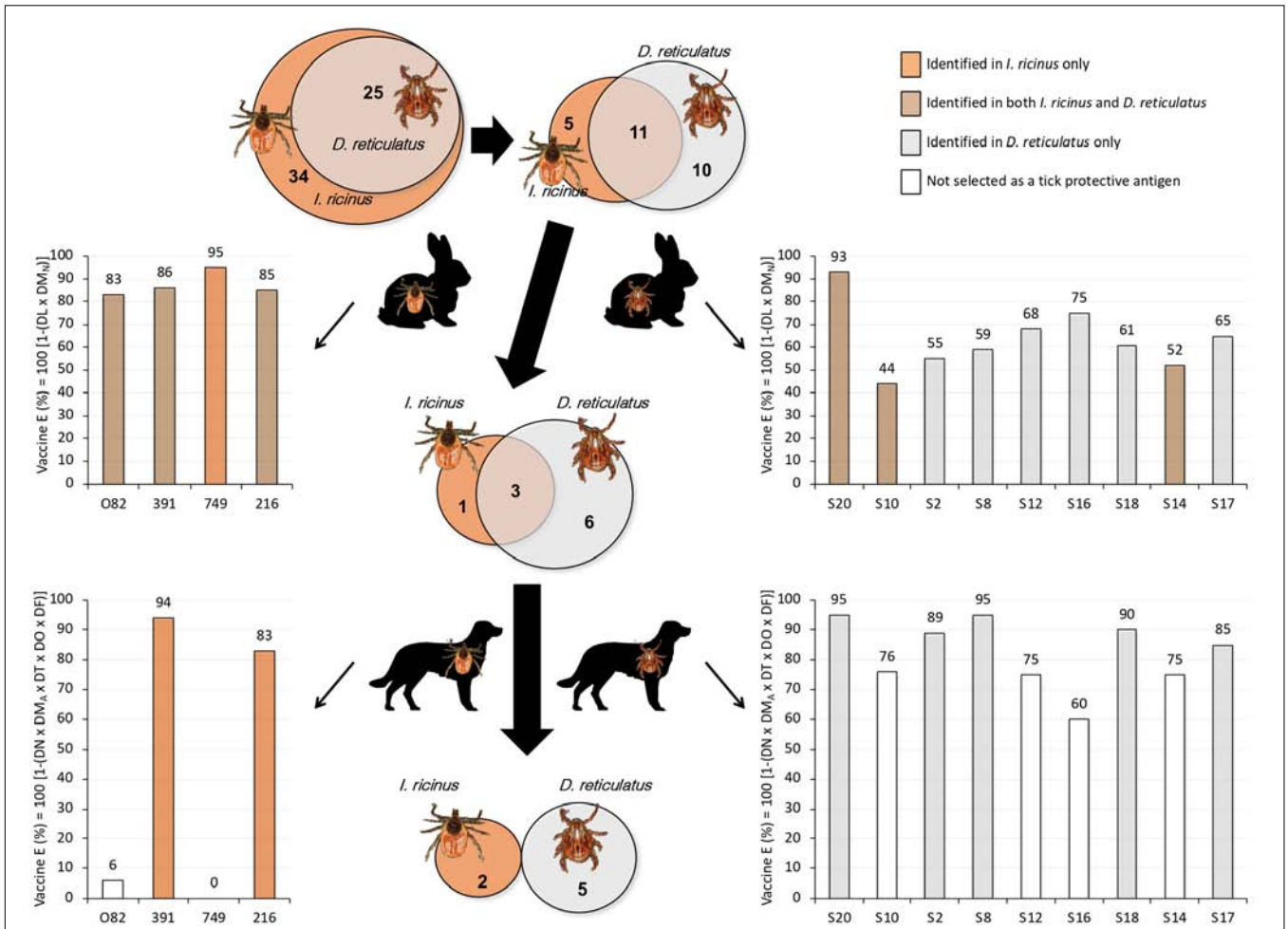

FIGURE 3 | Pipeline for the identification of tick protective antigens. The Venn diagrams depict the set of genes selected for further analysis as coding for candidate tick protective antigens in *I. ricinus* and *D. reticulatus*. The graphs represent the vaccine E after vaccination trials in rabbits and dogs. Of the selected genes coding for *I. ricinus* ($N = 34$) and *D. reticulatus* ($N = 25$) tick protective antigens, only 16 and 21, respectively, were produced as recombinant proteins for initial vaccination screening in rabbits. After vaccination trial in rabbits, the criteria for the final selection of tick protective antigens for vaccination in dogs was based on vaccine $E > 40\%$, resulting in 4 *I. ricinus* and 9 *D. reticulatus* antigens. The vaccination trial in dogs resulted in an overall vaccine $E > 80\%$ for 216 and 391 gene antigens in *I. ricinus*, and S2, S8, S17, S18, and S20 gene antigens in *D. reticulatus*. Full gene description and results are on **Tables 1–3** and **Supplementary Dataset 6**.

searches were performed allowing optional Met oxidation and Cys carbamidomethylation. A FDR < 0.01 was considered as condition for successful peptide assignments. Results are shown in **Tables 1**, **2**.

RESULTS AND DISCUSSION

Algorithm for Selection of Genes Encoding for Candidate Tick Protective Antigens

According to Elvin and Kemp (1994) the conditions necessary and sufficient for an effective tick protective antigen include that (a) host antibodies should be able to gain access to the tick antigen, (b) sufficient antibodies must gain access to the target antigen, and (c) the formation of the antibody-antigen complex should disrupt the normal function of the tick protein. In our study, the hypothesis was that the genes encoding for functionally important secreted proteins that are highly represented in both L and SG would result in good candidate tick protective antigens. These antigens should fulfill the above conditions (a–c) as abundant functionally important secreted proteins would be highly exposed to host antibodies and their interaction should affect protein function, and thus tick feeding and/or development and pathogen infection and transmission.

To fulfill these criteria, an algorithm was developed using a vaccinomics approach to tick protective antigen discovery (de la Fuente and Merino, 2013; de la Fuente et al., 2016). The algorithm included the generation of transcriptomics and proteomics data in tick L and SG, and selection of gene transcripts and proteins highly represented in both samples and encoding for predicted functionally important secreted proteins. The initial dataset was obtained from

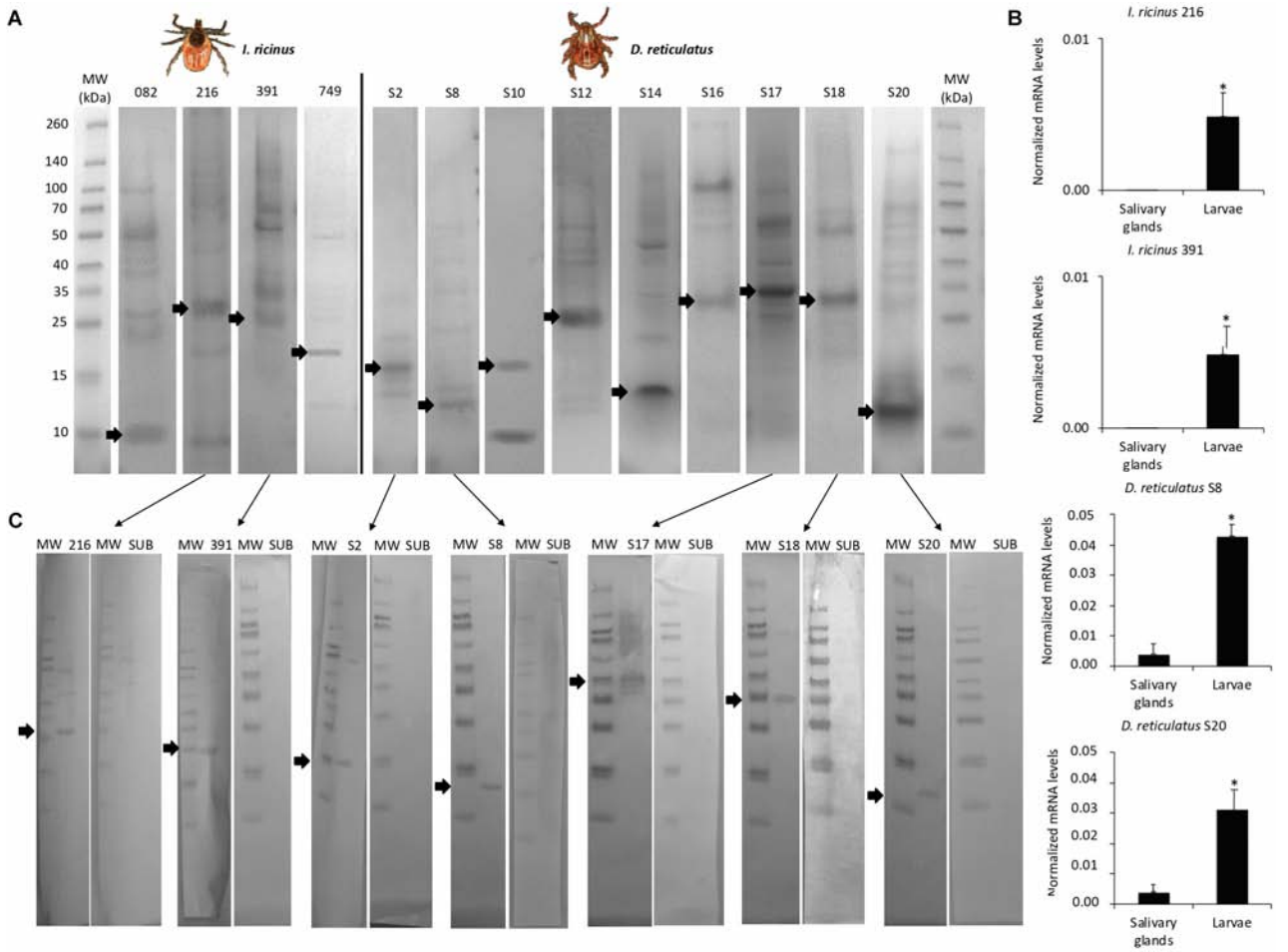

FIGURE 4 | Characterization of candidate tick protective antigens. The 4 *I. ricinus* and 9 *D. reticulatus* candidate protective antigens were selected after vaccination trial in rabbits with vaccine $E > 40\%$. **(A)** The histidine-tagged recombinant proteins were produced using the pET101/D-TOPO expression vector in *E. coli* BL21 Star (DE3) cells. After induction of gene expression with IPTG, collected cells were disrupted and the insoluble protein fraction containing the recombinant antigens as inclusion bodies were collected by centrifugation and purified by affinity to 16 polyhistidine. The eluted fraction containing the purified denatured proteins was dialyzed and concentrated by ultrafiltration to 0.5 mg/ml. Ten μg of purified recombinant antigens were separated by SDS-12% polyacrylamide gel electrophoresis and stained with Coomassie blue. Arrows indicate the position of recombinant antigens based on the predicted molecular weight. **(B)** The mRNA levels of selected genes coding for most effective vaccine antigens in dogs were determined by real-time RT-PCR in tick salivary glands and larvae (IDs refer to annotations in **Tables 1**–**3**). The mRNA levels were normalized against tick *rps4* and normalized C_t values (Ave+SD) were compared between salivary glands and larvae by Student's *t*-test with unequal variance ($^*P < 0.05$; $N = 3$ biological replicates). **(C)** Western blot analysis of selected recombinant proteins and Subolesin as negative control using pooled sera from vaccinated dogs collected at T3. Selected proteins were those corresponding to the most effective protective antigens with vaccine $E > 80\%$. Arrows indicate the position of recombinant antigens. MW, molecular weight marker.

I. ricinus because of the availability of the *I. scapularis* genome sequence for data mining (Gulia-Nuss et al., 2016). Genes selected in *I. ricinus* as encoding for tick candidate protective antigens (**Table 1**) were then used to find orthologous genes in *D. reticulatus* (**Table 2**). Tick IL and ISG were selected to cover both initial (larvae) and final (adult) developmental stages and tissues that are essential for pathogen acquisition and transmission, respectively (Ayllón et al., 2015; Chmelaø et al., 2016; Nuttall, 2018). *I. ricinus* and *D. reticulatus* acquire infection when larvae feed on infected hosts and after transtadial transmission, pathogen is secreted from salivary glands during feeding of nymph and adult ticks. Therefore, affecting these two developmental stages should reduce both tick infestations and pathogen infection/transmission.

Selection of *I. ricinus* Candidate Protective Antigens

After RNAseq, the number of reads/sample corresponded to 27.7 and 27.2 millions for IL and ISG, respectively. Of them, 5,731,608 and 7,024,484 corresponded to pass filter high quality reads aligned to IL and ISG samples, respectively. Of the 23,297 identified gene transcripts, 49% were included in the analysis and not discarded due to not enough alignment, high complexity or shallowly sequenced (**Figure 1A** and

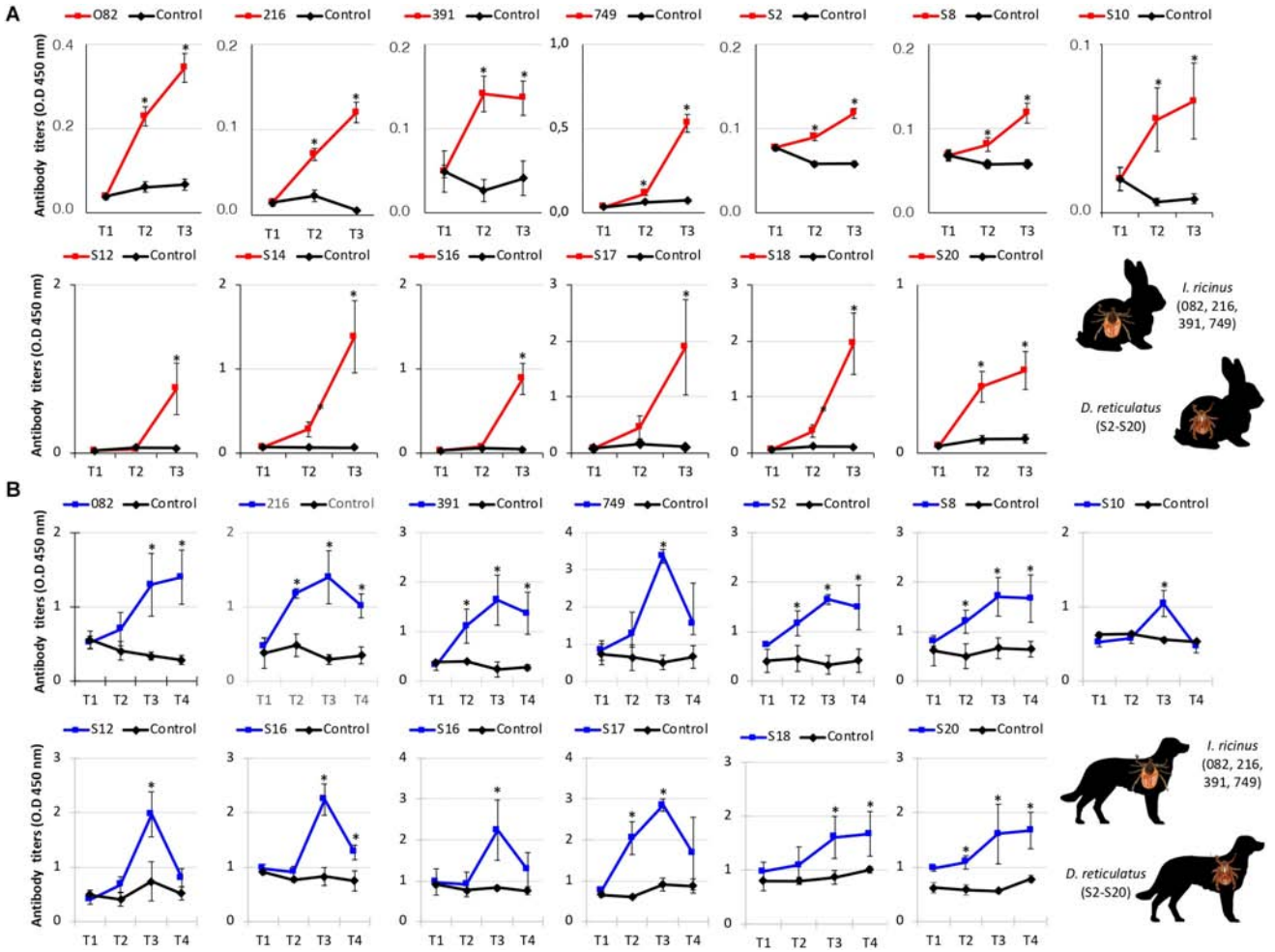

FIGURE 5 | Immune IgG antibody response in vaccinated rabbits and dogs. An indirect ELISA test was performed to detect IgG antibodies against recombinant antigens in serum samples from vaccinated and control **(A)** rabbits and **(B)** dogs. Blood samples were collected from each animal before immunization (T1 and T2) and tick infestation (T3), and at day 75 (T4) in dogs. Serum samples or PBS as negative control were diluted at the optimal dilution of 1:10,000 (v/v). Antibody levels in vaccinated and control animals were expressed as the OD_{450nm} ($OD_{animalsera}$–$OD_{PBScontrol}$) and compared between vaccinated and control groups by ANOVA test (*$P < 0.05$). IDs refer to annotations in **Tables 1**–**3**.

Supplementary Dataset 1). Of them, 13% were expressed in IL or ISG only and 18% were overexpressed on either tissue, but most of the identified genes (70%) did not show differential expression between IL and ISG (**Figure 1A** and **Supplementary Dataset 1**).

Genes encoding for secreted proteins were predicted using different algorithms. Predictor's performance was different with a total of 1,042 genes predicted as encoding for secreted proteins (**Figure 1B**). Protein Prowler performed rather poor (269 predicted proteins) and almost all of them (259 proteins) were identical to those predicted by TargetP. CELLO predicted a low number of secreted proteins. Moreover, it predicted as many as twelve different subcellular localizations, which made the results difficult to analyze. Therefore, the results from Protein Prowler and CELLO were discarded. Five hundred and one genes were selected as encoding for secreted proteins (**Supplementary Dataset 2**). These genes were predicted by at least two predictors. Of them, 208 (41%) were overexpressed in ISG and 97 (19%) were among the top 1,000 expressed genes in both IL and ISG with 6 of them overexpressed in IL (**Supplementary Dataset 2**). These 6 genes were selected as encoding for candidate tick protective antigens (**Figure 2** and **Table 1**).

A total of 3,454 and 2,339 proteins were identified in the Ixodidae database in IL and ISG, respectively. Of them, after applying XCorr > 2, a total of 370 and 367 proteins were identified in IL and ISG, respectively (**Figure 1C** and **Supplementary Dataset 3**). An additional selection criterion using FDR ≤ 0.01 and protein identification with at least 4 peptides resulted in the selection of 21 and 11 proteins in IL and ISG, respectively (**Figure 2**). Finally, after filtering for redundant biological function, 3 genes were selected from IL as encoding for candidate tick protective antigens (**Figure 2** and **Table 1**). The search against the database of predicted

secreted proteins encoded by the selected top 1,000 expressed genes in both IL and ISG (**Supplementary Dataset 4**) using XCorr > 2 and sequence span > 2% resulted in the identification of 6 and 10 proteins in IL and ISG, respectively that were selected as candidate tick protective antigens (**Figure 2** and **Table 1**).

The GO analysis of transcriptomics data resulted in different BP for genes predicted as encoding for secreted proteins that were either overexpressed in ISG or among the top 1,000 expressed genes in both IL and ISG (**Figures 1D,E**). In genes highly expressed in both IL and ISG, metabolic processes was the most represented (27%) BP (**Figure 1D**). In genes overexpressed in ISG, transmembrane transport (23%) and metabolic processes (17%) were the most represented BP (**Figure 1E**). Genes in the signal peptide processing BP (**Figure 1D**) and transmembrane transport (**Figure 1E**) were filtered for highly similar sequences and resulted in 11 genes (9 overexpressed in ISG and 2 highly expressed in both IL and ISG) that were selected as encoding for candidate tick protective antigens (**Figure 2** and **Table 1**).

Finally, GO analysis for BP, MF and CC was conducted for the selected 36 genes encoding for candidate protective antigens (**Figure 2** and **Table 1**). The results showed that approx. 40% of genes had unknown BP and MF (**Figures 1F,G**). As predicted, most of the genes (95%) encoded for membrane and secreted proteins, but two genes (ID Nos. 752 and 178) encoded for predicted nuclear DNA-binding proteins (**Figure 1H**). Although these two genes were initially predicted as encoding for secreted proteins, they were removed from further analysis due to the GO CC prediction (**Figure 2** and **Table 1**). The most represented BP and MF corresponded to transmembrane transport (22%; **Figure 1F**) and transporter activity (28%; **Figure 1G**), respectively. Additionally, BP involved in development (8%), reproduction (oogenesis and oviposition; 6%), protein secretion (signal peptide processing; 3%) and immunity (3%) were also represented (**Figure 1F**).

The final set of genes coding for *I. ricinus* tick candidate protective antigens included 34 candidates (**Figures 2**, **3**, **Table 1**, and **Supplementary Dataset 4**).

TABLE 3 | Results of the vaccination trials in dogs.

Gene ID	DN (%)	DM_A (%)	DT (%)	DW_A (%)	DO (%)	DF (%)	E (%)
I. ricinus							
082	6	0	0	0	0	0	6
216	20	5	33	5	0	67	**83***
391	37	33	9	0	49	68	**94***
749	0	0	0	0	0	0	0
D. reticulatus							
S2	40	41	0	22	69	0	**89***
S8	64	60	0	0	63	0	**95***
S10	10	9	0	1	71	0	76
S12	11	12	0	0	65	9	75
S14	0	0	0	0	75	0	75
S16	0	0	0	0	60	0	60
S17	41	50	11	0	43	0	**85***
S18	55	60	0	0	43	4	**90***
S20	55	63	0	6	67	14	**95***

The number of engorged nymphs and adult females, weight/female, oviposition (egg mass/tick), fertility (No. hatching larvae), and number of nymphs molting to adults were evaluated. Vaccine efficacy (E) was calculated as E (%) = 100 [1−(DN × DM_A × DT × DO × DF)], where DN is the reduction in the number of engorged nymphs, DM_A is the reduction in the number of nymphs molting to adults, DT is the reduction in the number of engorged female ticks, DO is the reduction in oviposition, and DF is the reduction in fertility in ticks fed on vaccinated rabbits when compared to the controls fed on adjuvant/saline injected dogs. Only parameters with statistically significant differences ($P < 0.05$) were included in E calculation. All results are shown in ***Supplementary Dataset 6****. *Antigens with vaccine E > 80% were selected as the most effective tick protective antigens.*

Selection of *D. reticulatus* Candidate Protective Antigens

The number of reads/sample corresponded to 21.7 millions for DL and 21.8 millions for DSG. The 21,838,507 reads (∼2.2 Gb) in DSG were compared against the selected set of *I. ricinus* genes encoding for candidate protective antigens (**Table 1**), clustered and assembled to produce a set of contigs with homology to selected reference genes. These contigs were then analyzed for differential expression between DL and DSG samples and compared to results in *I. ricinus* (**Table 2**). The results showed that 16/27 (59%) of *D. reticulatus* genes had an expression pattern similar to *I. ricinus* (**Table 2**).

A total of 268 and 372 proteins were identified in the Ixodidae database in DL and DSG, respectively, and all remained after data filtering (**Figure 1C** and **Supplementary Dataset 3**). The additional selection criteria using FDR ≤ 0.01 and protein identification with at least 4 peptides did not produce new candidate tick protective antigens.

As previously described for *I. ricinus*, two genes (IDs S3 and S4) were removed from further analysis due to the GO CC prediction (**Figure 2** and **Tables 1**, **2**). Therefore, the final set of genes coding for *D. reticulatus* tick candidate protective antigens included 25 candidates (**Figure 3**, **Table 2**, and **Supplementary Dataset 4**).

Selection of Tick Protective Antigens After Vaccination Trials in Rabbits and Dogs

Of the selected genes encoding for *I. ricinus* ($N = 34$) and *D. reticulatus* ($N = 25$) tick protective antigens, only 16 and 21 respectively were produced as recombinant proteins for initial vaccination screening in rabbits (**Figure 3** and **Tables 1**, **2**). Of them, 11 were identified in both tick species (**Figure 3**). After rabbit vaccination and infestation with *I. ricinus* or *D. reticulatus* tick larvae, the criteria for the final selection of tick protective antigens for vaccination trials in dogs was based on vaccine $E > 40\%$. Selection criteria need to be applied in order to move forward in the vaccinomics pipeline of selecting candidate protective antigens, and $E > 40\%$ was set as the minimum vaccine E for tick larvae. The selection of tick protective antigens resulted in 4 *I. ricinus* and 9

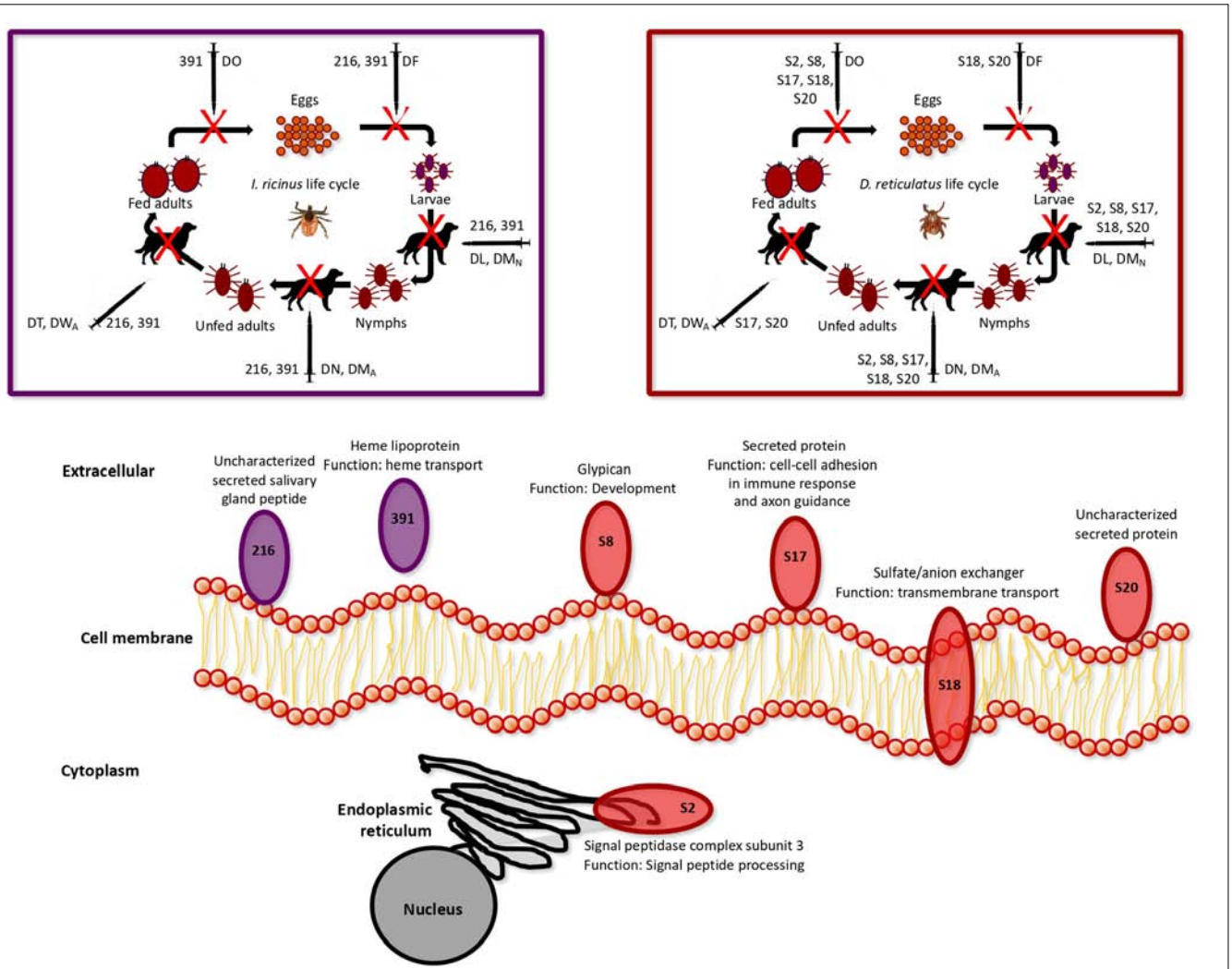

FIGURE 6 | Summary representation of subcellular localization, function and vaccine efficacy of the selected protective antigens after vaccination trial in dogs. Complete GO annotations are in **Supplementary Dataset 4**, and the results of the vaccination trial in rabbits and dogs are in **Table 3** and **Supplementary Dataset 6**. The *I. ricinus* antigens 216 and 391, and the *D. reticulatus* antigens S8, S17, S18 and S20 were identified in the membrane fraction derived from *D. reticulatus* and *I. ricinus* larvae. The effect of vaccination on tick life cycle was based on the parameters used to calculate vaccine E in rabbits and dogs, where DL is the reduction in the number of engorged larvae, DM_N is the reduction in the percent of larvae molting to nymphs, DN is the reduction in the number of engorged nymphs, DM_A is the reduction in the number of nymphs molting to adults, DT is the reduction in the number of engorged female ticks, DO is the reduction in oviposition, and DF is the reduction in fertility in ticks fed on vaccinated animals when compared to the controls fed on adjuvant/saline injected animals. Only parameters with statistically significant differences were included in vaccine E calculation.

D. reticulatus antigens (**Figure 3**, **Table 3**, and **Supplementary Dataset 6**). Of them, 3 were identified in both tick species (**Figure 3**). The results in dogs showed that vaccination with *I. ricinus* antigens affected different tick developmental stages (**Supplementary Dataset 6**) and resulted in an overall vaccine $E > 80\%$ for gene antigens 216 and 391 (**Figure 3** and **Table 3**). Vaccination with *D. reticulatus* antigens mainly affected nymph feeding and molting and oviposition (**Supplementary Dataset 6**) with an overall vaccine E ranging from 75 to 95% (**Figure 3** and **Table 3**). Finally, based on the criteria of vaccine $E > 80\%$, which is considered a good vaccine E for selection of candidate protective antigens, the *I. ricinus* 216 and 391 and the *D. reticulatus* S2, S8, S17, S18, and S20 were identified as the most effective tick protective antigens (**Figure 3** and **Table 3**).

Characterization of Identified Tick Protective Antigens

The candidate protective antigens were produced in *E. coli* and showed a molecular weight similar to that predicted by the amino acid sequence composition (**Figure 4A** and **Supplementary Dataset 5**). The mRNA levels of selected genes coding for the most effective protective antigens were determined by real-time RT-PCR and confirmed the results of the transcriptomics analysis (**Figure 4B** and **Tables 1**, **2**).

The immunogenicity of candidate protective antigens (**Table 3**) was characterized by Western blot (**Figure 4C**) and indirect ELISA (**Figures 5A,B**) tests. The results supported the antigen-specific antibody response in vaccinated animals, and except for S2 and S8 antigens the background IgG levels were low in rabbits (**Figure 5A**). However, in dogs the background IgG levels before vaccination at T1 were higher than in rabbits (**Figure 5B**), suggesting host-specific differences in IgG affinity for tick antigens, and/or possible previous tick infestations at least in some of these dogs. Nevertheless, the IgG antibody response increased in response to vaccination in both rabbits and dogs, and for most antigens remained higher than in control animals until the end of the experiment (**Figures 5A,B**).

Focusing on the selected tick protective antigens after vaccination trials in dogs (**Table 3**), the *I. ricinus* antigens 216 and 391, and the *D. reticulatus* antigens S8, S17, S18 and S20 were identified in the membrane fraction derived from *D. reticulatus* and *I. ricinus* larvae (**Figure 6** and **Tables 1**, **2**), thus confirming the prediction of the algorithms used for selection of membrane/secreted antigens. These antigens showed an effect on different tick developmental stages (**Figure 6**).

Among these proteins, *I. ricinus* 216 and *D. reticulatus* S20 are uncharacterized secreted proteins (**Figure 6**). However, heme lipoproteins such as *I. ricinus* 391 has been proposed as candidate vaccine protective antigens as being among the most abundant proteins involved in heme transport from hemolymph to tissues to complement the loss of the heme synthesis pathway in ticks (Braz et al., 1999; Maya-Monteiro et al., 2000; Lara et al., 2003, 2005; Hajdusek et al., 2009; Kluck et al., 2018). In agreement with this function, vaccination with 391 affected all the developmental stages during *I. ricinus* life cycle (**Figure 6**).

In *D. reticulatus*, a glypican-like protein S8 was identified (**Figure 6**). Glypicans have been used for cancer vaccines against hepatocellular carcinoma (Sun et al., 2016; Li et al., 2018), but not as protective antigens against ectoparasites or vector-borne pathogens. Glypicans are a group of cell-surface glycoproteins involved in the regulation of cellular morphology, growth, motility and differentiation (Li et al., 2018). The results of the vaccination trials suggested that these proteins might play a role in oviposition and development of immature tick stages (**Figure 6**).

The *D. reticulatus* secreted protein S17 was annotated as involved in homophilic cell adhesion via plasma membrane adhesion molecules and axon guidance (**Figure 6**). Proteins with cell-cell adhesion have a role in immune response and neuronal wiring, and are highly conserved across evolution (Samanta and Almo, 2015; Jin and Li, 2019). This protein family has been recently identified in ticks (Jin and Li, 2019), and our results suggested a role for this protein in all tick developmental stages except egg fertility (**Figure 6**).

Sulfate/anion exchanger molecules such as *D. reticulatus* S18 function as transmembrane transporters and are involved in different biological processes including regulation of blood pressure (Wall, 2016). Vaccination with this antigen affected larval and nymphal developmental stages, oviposition and fertility, suggesting a still uncharacterized function of this protein during these developmental processes (**Figure 6**).

The only protein with subcelllular localization in the endoplasmic reticulum (ER) was the *D. reticulatus* S2 antigen (**Figure 6**). This protein was annotated as a signal peptidase complex subunit 3, which is involved in protein targeting to ER through signal peptide processing. The disruption of the catalytic subunit of these conserved proteins leads to cell death in yeast (Bohni et al., 1988; Fang et al., 1997), *Plasmodium falciparum* (Tuteja et al., 2008), and *Leishmania manilensis major* (Taheri et al., 2010). Furthermore, knockdown by RNA interference of the gene coding for this enzyme in *Locusta migratoria* (*LmSPC1*) affected insect molting, feeding, reproduction and embryonic development (Zhang and Xia, 2014). Vaccination with this antigen reduced development of tick immature stages and oviposition, supporting the role of this protein in tick survival (**Figure 6**).

CONCLUSION

The experimental approach used in this study resulted in the identification of tick protective antigens by using a vaccinomics approach in combination with vaccination trials. Based on the criteria of vaccine $E > 80\%$, two *I. ricinus* and five *D. reticulatus* proteins were identified as the most effective protective antigens (**Figure 6**). Consequently, these antigens were proposed for commercial vaccine development for the control of tick infestations in companion animals, and other hosts for these tick species.

The putative function of selected protective antigens, which are involved in different biological processes, resulted in vaccines affecting multiple tick developmental stages (**Figure 6**). These results suggested that the combination of some of these antigens might be considered to increase vaccine efficacy through antigen synergy for the control of tick infestations and potentially affecting pathogen infection and transmission.

Finally, additional facts should be considered for vaccine development including that (a) a protective antigen is necessary but not sufficient for an effective vaccine as vaccine formulation, adjuvant and antigen composition including tick-derived and pathogen-derived antigens highly influence the final vaccine efficacy, (b) tick vaccines cannot be designed to prevent tick attachment and feeding because the immune response to vaccination (e.g., antibodies) needs to interact with target antigens in order to have an effect on different biological processes affecting life cycle of ticks and transmitted pathogens, (c) tick vaccines for wild animals are difficult to deliver, but appropriate vaccine formulations (i.e., virus-based) may address this problem, and (d) vaccines for companion animals may be acceptable if they increase animal welfare and health by reducing the duration of tick feeding and pathogen transmission.

DATA AVAILABILITY

All datasets generated for this study are included in the manuscript and/or the **Supplementary Files**.

ETHICS STATEMENT

White rabbits (*Oryctolagus cuniculus*) and Beagle dogs (*Canis lupus familiaris*) were used in the experiments. Animal experiments were conducted in strict accordance with the recommendations of the European Guide for the Care and Use of Laboratory Animals. Animals were housed and the experiments were conducted at LLC ACRO Vet Lab (Pylipovichi Village, Kyiv Region, Ukraine) with the approval and supervision of the Ukrainian Commission for Bioethics and Biosafety for animals under the studies "Tick vaccine experiment on rabbits" number 000369 and "Tick vaccine experiments on dogs" numbers 000576, 000577, and 000761.

AUTHOR CONTRIBUTIONS

MV and JdlF conceived the study and designed the experiments. MC and MV performed the experiments. All authors performed the data analysis, wrote the manuscript, and contributed to the final version of the manuscript and approved it for publication.

FUNDING

This research was financially supported by Beaphar B.V. (Raalte, Netherlands). MC was funded by the Consejo Superior de Investigaciones Científicas (CSIC), Spain. MV was funded by the Universidad de Castilla–La Mancha (UCLM), Spain.

ACKNOWLEDGMENTS

We thank Francisco Ruiz-Fons (SaBio, IREC, Spain) for the tick pictures included in the figures.

SUPPLEMENTARY MATERIAL

The Supplementary Material for this article can be found online at: https://www.frontiersin.org/articles/10.3389/fphys.2019.00977/full#supplementary-material

REFERENCES

Alhassan, A., Liu, H., McGill, J., Cerezo, A., Jakkula, L. U. M. R., Nair, A. D. S., et al. (2018). *Rickettsia rickettsii* whole cell antigens offer protection against rocky mountain spotted fever in the canine host. *Infect. Immun.* 87:e00628-18. doi: 10.1128/IAI.00628-18

Ayllón, N., Villar, M., Busby, A. T., Kocan, K. M., Blouin, E. F., Bonzón-Kulichenko, E., et al. (2013). *Anaplasma phagocytophilum* inhibits apoptosis and promotes cytoskeleton rearrangement for infection of tick cells. *Infect. Immun.* 81, 2415–2425. doi: 10.1128/IAI.00194-13

Ayllón, N., Villar, V., Galindo, R. C., Kocan, K. M., Šíma, R., López, J. A., et al. (2015). Systems biology of tissue-specific response to Anaplasma phagocytophilum reveals differentiated apoptosis in the tick vector Ixodes scapularis. *PLoS Genet.* 11:e1005120. doi: 10.1371/journal.pgen.1005120

Beugnet, F., and Marié, J. L. (2009). Emerging arthropod-borne diseases of companion animals in europe. *Vet. Parasitol.* 163, 298–305. doi: 10.1016/j.vetpar.2009.03.028

Bohni, P. C., Deshaies, R. J., and Schekman, R. W. (1988). SEC11 is required for signal peptide processing and yeast cell growth. *J. Cell. Biol.* 106, 1035–1042. doi: 10.1083/jcb.106.4.1035

Braz, G. R., Coelho, H. S., Masuda, H., and Oliveira, P. L. (1999). A missing metabolic pathway in the cattle tick *Boophilus microplus*. *Curr. Biol.* 9, 703–706. doi: 10.1016/s0960-9822(99)80312-1

Chmelař, J., Kotál, J., Karim, S., Kopacek, P., Francischetti, I. M. B., Pedra, J. H. F., et al. (2016). Sialomes and mialomes: a systems-biology view of tick tissues and tick-host interaction. *Trends Parasitol.* 32, 242–254. doi: 10.1016/j.pt.2015.10.002

Coller, B. A., Clements, D. E., Martyak, T., Yelmene, M., Thorne, M., and Parks, D. E. (2012). Advances in flavivirus vaccine development. *IDrugs* 13, 880–884.

Contreras, M., and de la Fuente, J. (2016). Control of ixodes ricinus and dermacentor reticulatus tick infestations in rabbits vaccinated with the Q38 subolesin/akirin chimera. *Vaccine* 34, 3010–3013. doi: 10.1016/j.vaccine.2016.04.092

Contreras, M., and de la Fuente, J. (2017). Control of infestations by ixodes ricinus tick larvae in rabbits vaccinated with aquaporin recombinant antigens. *Vaccine* 35, 1323–1328. doi: 10.1016/j.vaccine.2017.01.052

Contreras, M., Villar, M., Artigas-Jerónimo, S., Kornieieva, L., Mótrofanov, S., and de la Fuente, J. (2018). A reverse vaccinology approach to the identification and characterization of Ctenocephalides felis candidate protective antigens for the control of cat flea infestations. *Parasite. Vectors* 11:43. doi: 10.1186/s13071-018-2618-x

de la Fuente, J. (2012). Vaccines for vector control: exciting possibilities for the future. *Vet. J.* 194, 139–140. doi: 10.1016/j.tvjl.2012.07.029

de la Fuente, J. (2018). Controlling ticks and tick-borne diseases looking forward. *Ticks Tick Borne Dis.* 9, 1354–1357. doi: 10.1016/j.ttbdis.2018.04.001

de la Fuente, J., Almazán, C., Canales, M., Pérez de la Lastra, J. M., Kocan, K. M., and Willadsen, P. (2007). A ten-year review of commercial vaccine performance for control of tick infestations on cattle. *Anim. Health Res. Rev.* 8, 23–28. doi: 10.1017/s1466252307001193

de la Fuente, J., Antunes, S., Bonnet, S., Cabezas-Cruz, A., Domingos, A., Estrada-Peña, A., et al. (2017a). Tick-pathogen interactions and vector competence: identification of molecular drivers for tick-borne diseases. *Front. Cell. Infect. Microbiol.* 7:114. doi: 10.3389/fcimb.2017.00114

de la Fuente, J., and Contreras, M. (2015). Tick vaccines: current status and future directions. *Expert Rev. Vaccines* 14, 1367–1376. doi: 10.1586/14760584.2015.1076339

de la Fuente, J., Contreras, M., Estrada-Peña, A., and Cabezas-Cruz, A. (2017b). Targeting a global health problem: vaccine design and challenges for the control of tick-borne diseases. *Vaccine* 35, 5089–5094. doi: 10.1016/j.vaccine.2017.07.097

de la Fuente, J., Estrada-Peña, A., Venzal, J. M., Kocan, K. M., and Sonenshine, D. E. (2008). Overview: Ticks as vectors of pathogens that cause disease in humans and animals. *Front. Biosci.* 13, 6938–6946. doi: 10.2741/3200

de la Fuente, J., and Kocan, K. M. (2003). Advances in the identification and characterization of protective antigens for development of recombinant vaccines against tick infestations. *Expert Rev. Vaccines* 2, 583–593. doi: 10.1586/14760584.2.4.583

de la Fuente, J., and Kocan, K. M. (2006). Strategies for development of vaccines for control of ixodid tick species. *Parasite Immunol.* 28, 275–283. doi: 10.1111/j.1365-3024.2006.00828.x

de la Fuente, J., Kopáèek, P., Lew-Tabor, A., and Maritz-Olivier, C. (2016). Strategies for new and improved vaccines against ticks and tick-borne diseases. *Parasite Immunol* 38, 754–769. doi: 10.1111/pim.12339

de la Fuente, J., and Merino, O. (2013). Vaccinomics, the new road to tick vaccines. *Vaccine* 31, 5923–5929. doi: 10.1016/j.vaccine.2013.10.049

de la Fuente, J., Moreno-Cid, J. A., Canales, M., Villar, M., Pérez de la Lastra, J. M., Kocan, K. M., et al. (2011). Targeting arthropod subolesin/akirin for

the development of a universal vaccine for control of vector infestations and pathogen transmission. *Vet. Parasitol.* 181, 17–22. doi: 10.1016/j.vetpar.2011.04.018

de la Fuente, J., Villar, M., Contreras, M., Moreno-Cid, J. A., Merino, O., Pérez de la Lastra, J. M., et al. (2015). Prospects for vaccination against the ticks of pets and the potential impact on pathogen transmission. *Vet. Parasitol.* 208, 26–29. doi: 10.1016/j.vetpar.2014.12.015

de la Fuente, J., Villar, M., Estrada-Peña, A., and Olivas, J. A. (2018). High throughput discovery and characterization of tick and pathogen vaccine protective antigens using vaccinomics with intelligent big data analytic techniques. *Expert Rev. Vaccines* 17, 569–576. doi: 10.1080/14760584.2018.1493928

Elvin, C. M., and Kemp, D. H. (1994). Generic approaches to obtaining efficacious antigens from vector arthropods. *Int. J. Parasitol.* 24, 67–79. doi: 10.1016/0020-7519(94)90060-4

Escárcega-Ávila, A. M., de la Mora-Covarrubias, A., Quezada-Casasola, A., and Jiménez-Vega, F. (2019). Occupational risk for personnel working in veterinary clinics through exposure to vectors of rickettsial pathogens. *Ticks Tick Borne Dis.* 10, 299–304. doi: 10.1016/j.ttbdis.2018.10.012

Estrada-Peña, A., Venzal, J. M., Kocan, K. M., and Sonenshine, D. E. (2008). Overview: ticks as vectors of pathogens that cause disease in humans and animals. *Front. Biosci.* 13:6938–6946.

Fang, H., Mullins, C., and Green, N. (1997). In addition to SEC11, a newly identified gene, SPC3, is essential for signal peptidase activity in the yeast endoplasmic reticulum. *J. Biol. Chem.* 272, 13152–13158. doi: 10.1074/jbc.272.20.13152

Genomic Resources Development Consortium, Contreras, M., de la Fuente, J., Estrada-Peña, A., Grubhoffer, L., and Tobes, R. (2014). Genomic Resources Notes accepted 1 April 2014 – 31 May 2014. *Mol. Ecol. Resour.* 14:1095. doi: 10.1111/1755-0998.12298

Glickman, L. T., Moore, G. E., Glickman, N. W., Caldanaro, R. J., Aucoin, D., and Lewis, H. B. (2006). Purdue University-Banfield National Companion Animal Surveillance Program for emerging and zoonotic diseases. *Vector Borne Zoonotic Dis.* 6, 14–23. doi: 10.1089/vbz.2006.6.14

Grosenbaugh, D. A., De Luca, K., Durand, P. Y., Feilmeier, B., DeWitt, K., Sigoillot-Claude, C., et al. (2018). Characterization of recombinant OspA in two different borrelia vaccines with respect to immunological response and its relationship to functional parameters. *BMC Vet. Res.* 14:312. doi: 10.1186/s12917-018-1625-7

Gulia-Nuss, M., Nuss, A. B., Meyer, J. M., Sonenshine, D. E., Roe, R. M., Waterhouse, R. M., et al. (2016). Genomic insights into the ixodes scapularis tick vector of lyme disease. *Nat. Commun.* 7:10507. doi: 10.1038/ncomms10507

Hajdusek, O., Sojka, D., Kopacek, P., Buresova, V., Franta, Z., Sauman, I., et al. (2009). Knockdown of proteins involved in iron metabolism limits tick reproduction and development. *Proc. Natl. Acad. Sci. U.S.A.* 106, 1033–1038. doi: 10.1073/pnas.0807961106

Jin, Y., and Li, H. (2019). Revisiting DSCAM diversity: lessons from clustered protocadherins. *Cell. Mol. Life Sci.* 76, 667–680. doi: 10.1007/s00018-018-2951-4

Karunamoorthi, K. (2011). Vector control: a cornerstone in the malaria elimination campaign. *Clin. Microbiol. Infect.* 17, 1608–1616. doi: 10.1111/j.1469-0691.2011.03664.x

Kluck, G. E. G., Silva Cardoso, L., De Cicco, N. N. T., Lima, M. S., Folly, E., and Atella, G. C. (2018). A new lipid carrier protein in the cattle tick *Rhipicephalus microplus*. *Ticks Tick Borne Dis.* 9, 850–859. doi: 10.1016/j.ttbdis.2018.03.010

Kurtz, S., Phillippy, A., Delcher, A. L., Smoot, M., Shumway, M., Antonescu, C., et al. (2004). Versatile and open software for comparing large genomes. *Genome Biol.* 5:R12.

Kwit, N. A., Schwartz, A., Kugeler, K. J., Mead, P. S., and Nelson, C. A. (2018). Human tularaemia associated with exposure to domestic dogs-United States, 2006-2016. *Zoonoses Public Health* 2018, 1–5. doi: 10.1111/zph.12552

Langmead, B., Trapnell, C., Pop, M., and Salzberg, S. L. (2009). Ultrafast and memory-efficient alignment of short DNA sequences to the human genome. *Genome Biol.* 10:R25. doi: 10.1186/gb-2009-10-3-r25

Lara, F. A., Lins, U., Bechara, G. H., and Oliveira, P. L. (2005). Tracing heme in a living cell: hemoglobin degradation and heme traffic in digest cells of the cattle tick *Boophilus microplus*. *J. Exp. Biol.* 208, 3093–3101. doi: 10.1242/jeb.01749

Lara, F. A., Lins, U., Paiva-Silva, G., Almeida, I. C., Braga, C. M., Miguens, F. C., et al. (2003). A new intracellular pathway of haem detoxification in the midgut of the cattle tick *Boophilus microplus*: aggregation inside a specialized organelle, the hemosome. *J. Exp. Biol.* 206, 1707–1715. doi: 10.1242/jeb.00334

Li, N., Gao, W., Zhang, Y. F., and Ho, M. (2018). Glypicans as cancer therapeutic targets. *Trends Cancer.* 4, 741–754. doi: 10.1016/j.trecan.2018.09.004

Liu, J., Drexel, J., Andrews, B., Eberts, M., Breitschwerdt, E., and Chandrashekar, R. (2018). Comparative evaluation of 2 in-clinic assays for vector-borne disease testing in dogs. *Top. Companion Anim. Med.* 33, 114–118. doi: 10.1053/j.tcam.2018.09.003

Maya-Monteiro, C. M., Daffre, S., Logullo, C., Lara, F. A., Alves, E. W., Capurro, M. L., et al. (2000). HeLp, a heme lipoprotein from the hemolymph of the cattle tick. *Boophilus microplus*. *J. Biol. Chem.* 275, 36584–36589. doi: 10.1074/jbc.m007344200

Merino, M., Antunes, S., Mosqueda, J., Moreno-Cid, J. A., Pérez de la Lastra, J. M., Rosario-Cruz, R., et al. (2013). Vaccination with proteins involved in tick-pathogen interactions reduces vector infestations and pathogen infection. *Vaccine* 31, 5889–5896. doi: 10.1016/j.vaccine.2013.09.037

Moreno-Cid, J. A., Jiménez, M., Cornelie, S., Molina, R., Alarcón, P., Lacroix, M. N., et al. (2011). Characterization of *Aedes albopictus* akirin for the control of mosquito and sand fly infestations. *Vaccine* 29, 77–82. doi: 10.1016/j.vaccine.2010.10.011

Nuttall, P. A. (2018). Wonders of tick saliva. *Ticks Tick Borne Dis.* 10, 470–481. doi: 10.1016/j.ttbdis.2018.11.005

Otranto, D. (2018). Arthropod-borne pathogens of dogs and cats: from pathways and times of transmission to disease control. *Vet. Parasitol.* 251, 68–77. doi: 10.1016/j.vetpar.2017.12.021

Parker, R., Deville, S., Dupuis, L., Bertrand, F., and Aucouturier, J. (2009). Adjuvant formulation for veterinary vaccines: montanidetm gel safety profile. *Procedia Vaccinol.* 1, 140–147. doi: 10.1016/j.provac.2009.07.026

Samanta, D., and Almo, S. C. (2015). Nectin family of cell-adhesion molecules: structural and molecular aspects of function and specificity. *Cell. Mol. Life Sci.* 72, 645–658. doi: 10.1007/s00018-014-1763-4

Skotarczak, B. (2018). The role of companion animals in the environmental circulation of tick-borne bacterial pathogens. *Ann. Agric. Environ. Med.* 25, 473–480. doi: 10.26444/aaem/93381

Sperança, M. A., and Capurro, M. L. (2007). Perspectives in the control of infectious diseases by transgenic mosquitoes in the post-genomic era-a review. *Mem. Inst. Oswaldo Cruz* 102, 425–433. doi: 10.1590/s0074-02762007005000054

Sun, Z., Zhu, Y., Xia, J., Sawakami, T., Kokudo, N., and Zhang, N. (2016). Status of and prospects for cancer vaccines against hepatocellular carcinoma in clinical trials. *Biosci. Trends* 10, 85–91. doi: 10.5582/bst.2015.01128

Taheri, T., Salmanian, A.-H., Gholami, E., Doustdari, F., Zahedifard, F., and Rafati, S. (2010). Leishmania major: disruption of signal peptidase type I and its consequences on survival, growth and infectivity. *Exp. Parasitol.* 126, 135–145. doi: 10.1016/j.exppara.2010.04.009

Trapnell, C., Pachter, L., and Salzberg, S. L. (2009). TopHat: discovering splice junctions with RNA-Seq. *Bioinformatics* 25, 1105–1111. doi: 10.1093/bioinformatics/btp120

Tuteja, R., Pradhan, A., and Sharma, S. (2008). Plasmodium falciparum signal peptidase is regulated by phosphorylation and required for intra-erythrocytic growth. *Mol. Biochem. Parasitol.* 157, 137–147. doi: 10.1016/j.molbiopara.2007.10.007

Twine, N. A., Janitz, K., Wilkins, M. R., and Janitz, M. (2011). Whole transcriptome sequencing reveals gene expression and splicing differences in brain regions affected by alzheimer's disease. *PLoS One* 6:e16266. doi: 10.1371/journal.pone.0016266

Villar, M., Popara, M., Ayllón, N., Fernández de Mera, I. G., Mateos-Hernández, L., Galindo, R. C., et al. (2014). A systems biology approach to the characterization of stress response in *Dermacentor reticulatus* tick unfed larvae. *PLoS One* 9:e89564. doi: 10.1371/journal.pone.0089564

Wall, S. M. (2016). The role of pendrin in blood pressure regulation. *Am. J. Physiol. Renal Physiol.* 310, F193–F203. doi: 10.1152/ajprenal.00400.2015

Willadsen, P. (2004). Anti-tick vaccines. *Parasitol.* 129, S367–S874.

Zerbino, D. R., and Birney, E. (2008). Velvet: algorithms for de novo short read assembly using de bruijn graphs. *Genome Res.* 18, 821–829. doi: 10.1101/gr.074492.107

Zerbino, D. R., McEwen, G. K., Margulies, E. H., and Birney, E. (2009). Pebble and rock band: heuristic resolution of repeats and scaffolding in the velvet short-read de novo assembler. *PLoS One* 4:e8407. doi: 10.1371/journal.pone.0008407

Zhang, W., and Xia, Y. (2014). ER type I signal peptidase subunit (LmSPC1) is essential for the survival of *Locusta migratoria manilensis* and affects moulting, feeding, reproduction and embryonic development. *Insect Mol. Biol.* 23, 269–285. doi: 10.1111/imb.12080

Conflict of Interest Statement: The authors declare that the research was conducted in the absence of any commercial or financial relationships that could be construed as a potential conflict of interest.

frontiers in Physiology

ORIGINAL RESEARCH
published: 30 July 2019
doi: 10.3389/fphys.2019.00982

The Complete Mitochondrial Genome and Expression Profile of Mitochondrial Protein-Coding Genes in the Bisexual and Parthenogenetic *Haemaphysalis longicornis*

Tianhong Wang, Shiqi Zhang, Tingwei Pei, Zhijun Yu and Jingze Liu**

Hebei Key Laboratory of Animal Physiology, Biochemistry and Molecular Biology, College of Life Sciences, Hebei Normal University, Shijiazhuang, China

OPEN ACCESS

Edited by:
Abid Ali,
Abdul Wali Khan University Mardan, Pakistan

Reviewed by:
Shahid Karim,
The University of Southern Mississippi, United States
Yuxin Yin,
University of California, Los Angeles, United States
Maria Dolores Esteve-Gasent,
Texas A&M University, United States

***Correspondence:**
Zhijun Yu
yuzhijun@hebtu.edu.cn
Jingze Liu
liujingze@hebtu.edu.cn

Specialty section:
This article was submitted to Invertebrate Physiology, a section of the journal Frontiers in Physiology

Received: *03 April 2019*
Accepted: *15 July 2019*
Published: *30 July 2019*

Citation:
Wang T, Zhang S, Pei T, Yu Z and Liu J (2019) The Complete Mitochondrial Genome and Expression Profile of Mitochondrial Protein-Coding Genes in the Bisexual and Parthenogenetic Haemaphysalis longicornis. Front. Physiol. 10:982. doi: 10.3389/fphys.2019.00982

The tick *Haemaphysalis longicornis* is widely distributed in eastern Asia, New Zealand and Australia, and is well-known as a vector of multiple zoonotic pathogens. This species exhibits two reproductive strategies, bisexual and obligate parthenogenetic reproduction. Hence, in the current study, the complete mitochondrial genomes of the bisexual and parthenogenetic populations were assembled and analyzed, and the expression of the mitochondrial protein-coding genes was evaluated and compared between the two reproductive populations. The results indicated that the length of the mitochondrial genomes of the two reproductive populations is 14,694 and 14,693 bp in the bisexual and parthenogenetic populations, respectively. The AT content in the mitochondrial genome of the bisexual and obligate parthenogenetic population reached 77.22 and 77.34%, respectively. The phylogenetic tree was constructed combining 13 protein-coding genes, which showed that the genetic distance between the bisexual and parthenogenetic populations was less than that between the subspecies. The expression of the mitochondrial protein-coding genes was quantitatively analyzed at different feeding status for the bisexual and parthenogenetic populations, and the results showed significant differences in the expression patterns of these genes, suggesting that they might trigger specific energy utilization mechanisms due to their different reproductive strategies and environmental pressures.

Keywords: *Haemaphysalis longicornis*, mitochondrial genome, bisexual and parthenogenetic, mitochondrial protein-coding genes, expression profile

INTRODUCTION

Ticks are obligate blood-sucking ectoparasites with global distribution, and they can feed on a broad range of animals (Kaufman, 2010). They are notorious vectors of zoonotic pathogens. Furthermore, tick-borne diseases (TBDs) are increasingly threatening animal and human health and thus causing great economic damages (Jongejan and Uilenberg, 2004; Kovalev and Mukhacheva, 2013). The global annual financial losses due to ticks and TBDs are estimated in billions of dollars (Burger et al., 2014b). In China, 117 species of ticks in 7 genera have been recorded, and more than 60 tick

species have shown vector potential (Yu et al., 2015). The tick *Haemaphysalis longicornis* is widely distributed in eastern Asia, New Zealand and Australia and is well-known as a vector of multiple zoonotic pathogens (Hoogstraal et al., 1968; Herrin and Oliver, 1974). These pathogens include *Anaplasma bovis*, *Babesia ovate*, *Borrelia burgdorfer*, *Rickettsia japonica*, *Theileria orientalis*, and severe fever with thrombocytopenia syndrome virus (SFTSV) (Fujisaki et al., 1994; Jongejan and Uilenberg, 2004; Matsuo et al., 2013; Takahashi et al., 2014; Qin et al., 2018; Zhang et al., 2019). Human infection of tick *H. longicornis* was reported in at least 23 provinces in China (Chen et al., 2010, 2015; Zhan et al., 2017) with a case fatality rate of 10−30% (Liu et al., 2014). In America, this species has been expanded to 19 counties in 8 states since the first detection in 2013 (Magori, 2018).

In *H. longicornis*, the life history of a bisexual and parthenogenetic population is different (Hoogstraal et al., 1968). The parthenogenetic population can feed engorged and oviposit without males and thus might have stronger reproductive capacity and spreading ability. However, the distribution of the parthenogenetic population was only reported in Shanghai, Gansu and Sichuan provinces in China (Zhou Z. et al., 2004; Yang et al., 2007; Chen et al., 2010). The parthenogenetic species were historically a critical problem for early taxonomic studies (Monis et al., 2002). The number of eggs laid by the parthenogenetic population was significantly lower than that of the bisexual population (Oliver, 1977), whereas the engorgement body weight of females and egg size of the parthenogenetic population were considerably higher than that of the bisexual population, but the hatching rate of eggs was still lower in the parthenogenetic population (Chen et al., 2014). In recent years, scanning electron microscopy (SEM) has been used to describe the morphological characteristics of the two reproductive populations (Yang et al., 2007; Wang et al., 2013).

Mitochondrial genomes are characterized by simple structure, small molecular weight, rapid evolutionary rate, and matrilineal inheritance, which is particularly crucial in phylogenetic studies (Lin and Danforth, 2004; Gissi et al., 2008; Li and Liang, 2018). To date, more than 20 complete mitochondrial genomes in ixodid ticks have been available for phylogenetic analysis (Burger et al., 2014b). Additionally, structural genomic features, such as secondary structures of tRNA and rRNA, are also applied in comparative and evolutionary genomics (Qin et al., 2015; Kim et al., 2017). Compared with a phylogenetic analysis of a single gene sequence, a combined study of multiple mitochondrial genes can more accurately evaluate the genetic distance among or within species (Papanicolaou et al., 2008; Timmermans et al., 2014). Hence, investigations on the genetic relatedness of mitochondrial genomes will be helpful in making taxonomic determinations. Additionally, the protein-coding genes (PCGs) play a vital role in activity changes of the arthropod mitochondrial complex (Uno et al., 2004; Fontanillas et al., 2010). Evaluation of the differential expression profiling of PCGs will help to elucidate the energy utilization of different reproductive strategies.

In the current study, the complete mitochondrial genomes of the bisexual and parthenogenetic populations of *H. longicornis* were assembled and analyzed, and the expression of the mitochondrial PCGs was evaluated and compared between the two reproductive populations. The differences in survival climate may have influenced the survival strategies of *H. longicornis* and may have resulted from mutations in the parthenogenetic population. These results may help to elucidate the possible interconnections among environmental stress, genetic evolution, and parthenogenetic patterns.

MATERIALS AND METHODS

Sample Collection and DNA Extraction

The bisexual population of *H. longicornis* was collected from Xiaowutai National Nature Reserve Area of Zhuolu County (40° 03′ 03″ N, 115° 23′ 15″ E), Zhangjiakou City, Hebei Province, China. The parthenogenetic population was collected in Cangxi County (31° 44′ 35″ N, 105° 49′ 04″ E), Guangyuan City, Sichuan Province, China. The free-living nymphal collection was conducted in the above two locations using a white cloth flag in April of each year. The collected ticks were placed into perforated, clean centrifugal tubes with ventilated lids on one side through a 4-mm-diameter hole sealed with plastic screen. After the nymphs molted, delimitation between the two populations was performed based on our previous publications (Yang et al., 2007; Chen X. et al., 2012; Chen Z. et al., 2012; Wang et al., 2013). The distinguishing feature between the two populations is whether males appear in the adult population after molting nymphs.

The ticks were fed on the New Zealand white rabbit ear until engorged and were maintained under standard environmental chamber conditions (26 ± 1°C, 75% ± 5 RH, and 12 h: 12 h L:D). All experimental procedures in this study were approved by the Animal Ethics Committee of the Hebei Normal University (Protocol Number: IACUC-157026).

Three mitochondrial genome samples were sequenced as follows: 10 unfed adults of parthenogenetic female, bisexual female and bisexual male were separately placed in a 1.5-ml centrifuge tube, washed with 75% ethanol for 30 s, and then homogenized under liquid nitrogen. DNA was extracted using the EasyPure®genomic DNA kit (TransGen Biotech Co., Ltd., Beijing, China). DNA concentration was estimated using a TU-1950 spectrophotometer (Xi'an Yima Opto-electrical Technology Co., Ltd., Xi'an, China). The extracted DNA was visualized on 1% agarose gel to ensure strong bands and purified using the EasyPure®quick gel extraction kit (TransGen Biotech Co., Ltd., Beijing, China). All purified DNA was stored at −80°C until use.

Next Generation Sequencing Library Construction and Sequence Analysis

For the sequencing library construction, the fragmented tick genomic DNA (400−500 bp) was obtained by sharing 2-μg of tick DNA using Covaris M220 Focused-ultrasonicator (Convaris, Inc., Woburn, MA, United States). Subsequent reaction steps using TruSeq™ DNA Sample HT Prep Kit (Illumina Inc., San Diego, CA, United States), which include repaired ends, adenylated 3′ ends, added A-Tailing and ligated adapter, and then the ligation products were purified with agarose electrophoresis and enriched the DNA fragments with a PCR primer cocktail

that annealed to the ends of the adapters. Finally, the library was quantified and sequenced on illumina Hiseq X Ten sequencing platform according to the standard operation.

In this study, we annotated our next-generation sequencing (NGS) data with the mitochondrial genome of three different species of *Haemaphysalis* from the National Center of Biotechnology Information (NCBI) nucleotide database, as the Genebank number: AB075954 (*H. flava*), JX573135 (*H. formosensis*) and JX573136 (*H. parva*). SOAPdenovo v2.04[1] was used for sequence filtering and assembly (Xie et al., 2014). GapCloser v1.12 software (a SOAP suite tool) was used to perform vulnerability completion and base correction. The splicing of the original mitochondrial genome sequencing data was reflected in the (**Supplementary Table S1**). The mitochondrial circular map was assembled by Organellar Genome DRAW[2] (Lohse et al., 2013). The three complete mitochondrial genome circular maps of *H. longicornis* were uploaded to the (**Supplementary Figures S1−S3**). The complete mitochondrial genome sequence was deposited in the NCBI nucleotide database accession numbers: MK450606 (The bisexual population of *H. longicornis*) and MK439888 (The parthenogenetic population of *H. longicornis*).

The PCGs, tRNA, rRNA and non-coding regions (NCRs) of the genome were predicted using MITOS[3] online analysis software (Bernt et al., 2013). The PCGs were blasted using the GO[4] database. MEGA v7.0 for Windows (Kumar et al., 2016) was used to analyze the base content and the similarity. The calculation formula of the base skew is AT skew = (A−T)/(A+T); GC skew = (G−C)/(G+C) (Alexandre et al., 2005). The relative synonymous Codon usage (RSCU) analysis was carried out using Codon W software version 2.7.2.1 for Windows (Cancilla et al., 1995). The tRNAscan-SE[5] was used to identify the tRNA structure (Burger et al., 2014a). The genome tandem repeats of NCRs were predicted using Tandem Repeats Finder[6] (Benson, 1999).

Polymorphism Detection and Circular Map Comparison

Based on our previous studies (Chen X. et al., 2012; Chen et al., 2015), we speculated that the differentiation of the bisexual population might generate the parthenogenetic population. In this experiment, we analyzed the mitochondrial genome data of the bisexual population as the treatment group to assess the polymorphism and small insertion-deletion of the parthenogenetic population. Burrows-Wheeler Aligner[7] and Genome Analysis Toolkit[8] were used to match the genome sequence, and nucleotide polymorphism analysis (Lines et al., 2014; Mccormick et al., 2015). OrthoMCL DB[9] was used to draw the three circular maps of the mitochondrial genomes (conditions: *E*-value: 1−5, E percent identity cutoff: 0, Markov plus index: 1.5) (Fischer et al., 2011).

Phylogenetic Development and Homologous Gene

The mitochondrial genomes of 24 ixodid ticks and *Nuttalliella namaqua* were obtained from the NCBI[10] nucleotide databases. RAxML v8.0[11] was used to construct a phylogenetic tree with bootstrap replicated evaluation nodes 1000 times (Stamatakis, 2015). Sequence alignments and filtering of the PCGs were carried out using MAFFT v7.0[12] and Gblocks[13]. A Venn diagram of homologous genes was drawn using CGV software (Tominski et al., 2009).

Mitochondrial Genome Protein-Coding Genes at Different Feeding Status

The expression profiling of the mitochondrial genome protein-coding genes of *H. longicornis* at different feeding status was quantitatively analyzed using real-time quantitative PCR (qPCR). The weights of the bisexual and parthenogenetic population samples were similar in this experiment. RNA was extracted using the EasyPure®RNA Kit (TransGen Biotech Co., Ltd., Beijing, China) from *H. longicornis* at different feeding status, including unfed female (without feeding), partially fed (feed without mating) and engorged (fully engorged and detached).

Then, cDNA was synthesized using 500-ng RNA and 10-μl purity water combined with TranScript®First-Strand cDNA Synthesis SuperMix (TransGen Biotech Co., Ltd., Beijing, China). Samples were incubated at 65°C for 5 min, chilled on ice for 2 min, and then incubated at 42°C for 15 min. The cDNA products were stored at −20°C. The length of the quantitative product was designed between 100 and 200 bp (**Supplementary Table S2**), and a 20-μl master mix was prepared using SYBRGreen PCR buffer, HotStarTaq DNA polymerase, SYBRGreen I dye, dNTPs (TransGen Biotech Co., Ltd., Beijing, China), PCR stabilizer. PCR was performed using SimpliAmp Thermal Cycler A24811 (Applied Biosystems Shanghai Co., Ltd., Shanghai, China). The qPCR conditions were set as follows: 95°C for 30 s; 40 cycles of 95°C for 5 s, 55°C for 15 s, 72°C for 10 s. Relative expression of these genes was calculated using the $2^{-\Delta\Delta Ct}$ method. If the relative expression ratio was <1, there was down regulation of the comparison gene in the sample (dotted line group). Conversely, if the expression ratio was >1, there was up regulation in the expression of the sample (dotted line group). All samples were prepared from at least two female individuals, and three parallel experiments were performed to improve the accuracy. The statistical analysis was determined using Duncan's multiple range test with analysis of variance (ANOVA), and calculations were performed using SPSS v17.0 for Windows (SPSS Inc., Chicago, IL, United States).

[1] https://sourceforge.net/projects/soapdenovo2/
[2] http://ogdraw.mpimp-golm.mpg.de/
[3] http://mitos.bioinf.uni-leipzig.de/index.py
[4] http://www.geneontology.org
[5] http://lowelab.ucsc.edu/tRNAscan-SE
[6] http://tandem.bu.edu/trf/trf.html
[7] http://bio-bwa.sourceforge.net
[8] https://software.broadinstitute.org/gatk
[9] http://orthomcl.org/orthomcl
[10] https://www.ncbi.nlm.nih.gov/
[11] https://cme.h-its.org/exelixis/web/software/raxml/index.html
[12] https://mafft.cbrc.jp/alignment/software/
[13] http://molevol.cmima.csic.es/castresana/Gblocks.html

RESULTS

Base Features and Gene Composition

The length of the complete genome of the bisexual and parthenogenetic populations *H. longicornis* is 14,694 and 14,693 bp, respectively. The circular structure of the mitochondrial genomes of the two populations was successfully predicted, and the gene arrangement of the mitochondrial genomes included 13 PCGs, 22 tRNA and 2 rRNA. The contents of the four bases in the base composition of the mitochondrial genome are approximately 38% (A), 39% (T), 13% (C), and 9% (G), respectively. The A+T contents of the mitochondrial genome account for 77.22% in the bisexual population and 77.34% in the parthenogenetic population. The frequency of base used in both reproductive populations was highly similar. The GC-skew and AT-skew of the two reproductive populations were negative; GC-skew in the bisexual population was −0.1446, and AT-skew in the bisexual population was −0.0104. In the parthenogenetic population, GC-skew was −0.1502, and AT-skew was −0.0092 (**Table 1**).

Polymorphism and Circular Map of the Mitochondrial Genome

Bisexual female and male ticks share the same mitochondrial genome. Polymorphism analysis of the parthenogenetic population revealed 199 bases differences, but no small indel differences were found (**Supplementary Figure S4**). Only one site on the *nad3* gene displayed a non-synonymous mutation. The circular maps of the mitochondrial genomes were assembled and compared. No significant differences in gene direction and arrangement were observed between the bisexual and parthenogenetic populations (**Figure 1**).

Mitochondrial Protein-Coding Gene and Codon Analysis

The length of the PCGs in the bisexual population was 10,434 bp, accounting for 71.01% of the total mitochondrial genome, and was 10,464 bp in the parthenogenetic population, accounting for 71.22%. The heavy strand contains 9 genes (*cox1*, *cox2*, *cox3*, *cytb*, *nad2*, *nad3*, *nad6*, *atp6*, and *atp8*), and the light strand contains 4 genes (*nad1*, *nad4*, *nad4l*, and *atp8*). Mitochondrial genes of *H. longicornis* displayed distinct rearrangement characteristics from *Haemaphysalis* genus (Liu et al., 2018), and the arrangement and distribution of 13 PCGs were completely consistent in the two reproductive populations. Four start codons (ATA, ATT, ATG, and ATC) were detected in *H. longicornis*. Among these start codons, ATT was adopted by 7 genes (*cox1*, *cox2*, *nad1*, *nad2*, *nad3*, *nad4l*, and *nad5*), ATA was used by 3 genes (*cox3*, *cytb*, and *atp8*), ATG and ATC were used by 3 genes (*nad4*, *atp6,* and *nad6*). The termination codon TAA was used by 9 PCGs (*cox1*, *cox3, atp6*, *atp8*, *nad1, nad2*, *nad3*, *nad5*, and *nad6*). The incomplete codon T was used in genes including *cox2*, *nad3*, and *nad4*. Only *nad4L* used TAG as the termination codon (**Supplementary Table S3**). The two populations are identical in the usage of the initiation codon and termination codon.

Codons including TTT (Phe), ATT (Ile) and AAA (Lys) showed the highest utilization rate. Codons of GCG (Ala), CCG (Pro), CGG (Arg), CGC (Arg) and ACG (Thr) containing "CG" showed relatively lower utilization rates, that is, less than 10 times (**Supplementary Table S4**). In tRNA, Phe and Leu2 were used more than 400 times in the bisexual population, and Phe, Ile and Lys were the most frequently used in the parthenogenetic population, being used more than 400 times. The lowest tRNA usage was Arg in the two reproductive populations (**Figure 2**).

Transfer RNA and Ribosomal RNA

The mitochondrial genome in *H. longicornis* contains 22 tRNA and 2 rRNA. The secondary structure of all tRNA was successfully predicted, and the length ranged from 53 to 68 bp, with the longest *trnQ*, and the shortest *trnC* (**Supplementary Figures S5**, **S6**). The rRNA of *H. longicornis* displayed a significant AT bias. The total length of the tRNA in the two populations was identical, reaching 1,352 bp. The length of *rrnL* was 995 bp (AT = 82.21%), and the *rrnS* length was 778 bp (AT = 79.56%) in the bisexual population. In the parthenogenetic population, the *rrnL* length was 997 bp (AT = 82.25%), and the *rrnL* length was 777 bp (AT = 79.51%).

Gene Rearrangement and Position Variance

The mitochondrial genome of *H. longicornis* was characterized by obvious rearrangement in major genes. Five PCGs, including *nad5-nad4-nad4l-nad6-cytb,* were rearranged in new regions, which resulted in the displacement of the NCRs. The tRNA genes *trnF*, *trnH*, *trnT*, *trnP, trnS2*, *trnL1*, *trnC,* and *trnL2* changed the *Drosophila* genus arrangement. The displacement of tRNA was also observed in the two reproductive populations (**Figure 3**).

Non-coding Regions and Gene Overlapping

Most mitochondrial genes of *H. longicornis* displayed overlapping regions or spacer regions. A total of 22 spacer regions and seven overlapping regions of genes were found in the mitochondrial genome of *H. longicornis*, with overlapping regions ranging

TABLE 1 | Base composition and skewness in the mitochondrial genome of *Haemaphysalis longicornis*.

Populations	A	Ratio%	T	Ratio%	C	Ratio%	G	Ratio%	AT-skew	GC-skew	CG%	All length
Female (Bisexual)	5614	38.21%	5732	39.01%	1916	13.04%	1432	9.75%	−0.0104	−0.1446	22.78%	14694
Male (Bisexual)	5614	38.21%	5732	39.01%	1916	13.04%	1432	9.75%	−0.0104	−0.1446	22.78%	14694
Parthenogenetic	5629	38.31%	5734	39.03%	1915	13.03%	1415	9.63%	−0.0092	−0.1502	22.66%	14693

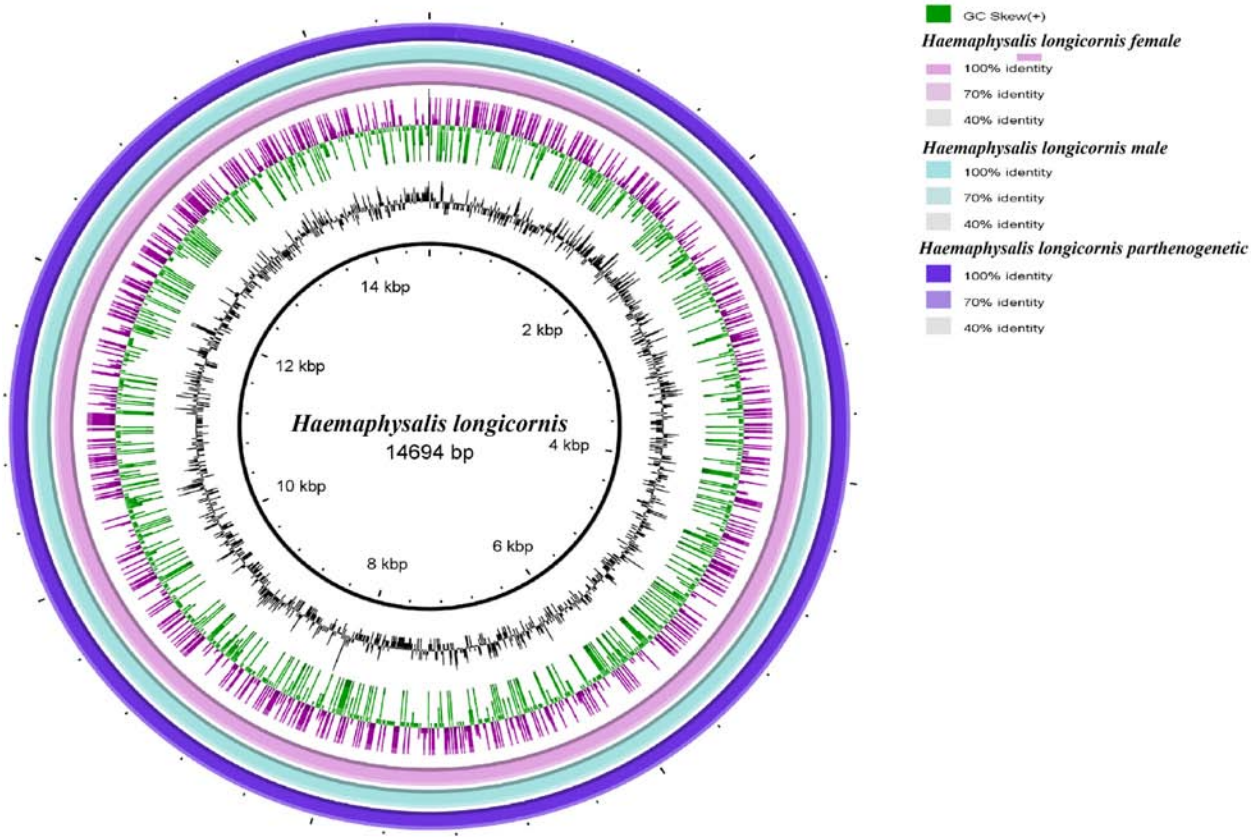

FIGURE 1 | Circular maps of the mitochondrial genome of the bisexual and parthenogenetic *Haemaphysalis longicornis*. The color change of the ring indicates the level of difference between the bisexual female, bisexual male, and the parthenogenetic population.

from 1 to 9 bp. The special region was *atp6*: in the bisexual population, *atp6* overlapped by four bases, whereas in the parthenogenetic population, there was an interval region of eight bases. Four regions showed length differences between bisexual and parthenogenetic populations. The mitochondrial genome of *H. longicornis* contains three NCRs with a total length of more than 100 bp. NCR1 was located between *rrnL* and *trnV*, with a length of 159 bp; NCR2 was located between *rrnS* and *trnI*, with a length of 240 bp; and NCR3 was located between *trnL1* and *trnC*, with a length of 309 bp (**Supplementary Table S3**). The content of A+T in the NCRs of *H. longicornis* was only 60−70%.

Phylogenetic and Homologous Gene Analysis

The phylogeny of the bisexual and the parthenogenetic population of *H. longicornis* was constructed with 24 tick species with complete mitochondrial genome available from the NCBI database. The results demonstrated that ticks in genera *Ixodes*, *Bothriocroton*, *Amblyomma* and *Haemaphysalis* were clustered into an independent branch, and ticks in *Dermacentor* and *Rhipicephalus* were grouped in Rhipicephalinae. *N. namaqua* and Ixodidae ticks were in different evolutionary branches. The two reproductive populations of *H. longicornis* were assigned to the cluster of the *Haemaphysalis* genus (**Figure 4**). In addition, homologous gene analysis showed that among 11 orthologous genes in these ticks, only one unique homologous gene was found in 10 ixodid ticks, and two novel homologous genes were found in *N. namaqua*. There were no unique homologous genes observed in the bisexual and parthenogenetic populations of *H. longicornis* (**Figure 5**).

Quantitative Analysis of the Mitochondrial Protein-Coding Genes

The expression profiling of the 13 PCGs was detected in the females of the two populations during unfed, partially fed and engorgement, respectively. In the partially fed stage, the expression levels of most mitochondrial genes were similar to the unfed stage. The expression levels of *cox2*, *nad6*, *atp6*, and *atp8* genes were increased in the bisexual population, and *cytb* and *nad4* genes were significantly down regulated ($P < 0.01$).

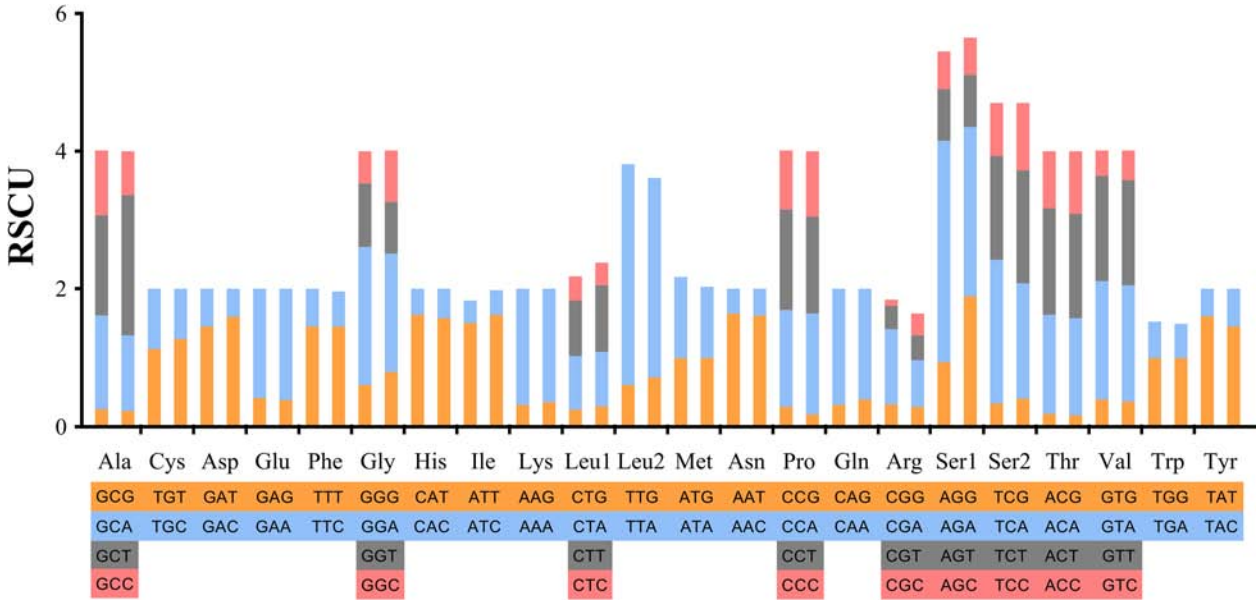

FIGURE 2 | Relative synonymous codon usage in protein-coding genes of *Haemaphysalis longicornis* bisexual population and parthenogenetic population. The different amino acids are shown in four colors at most.

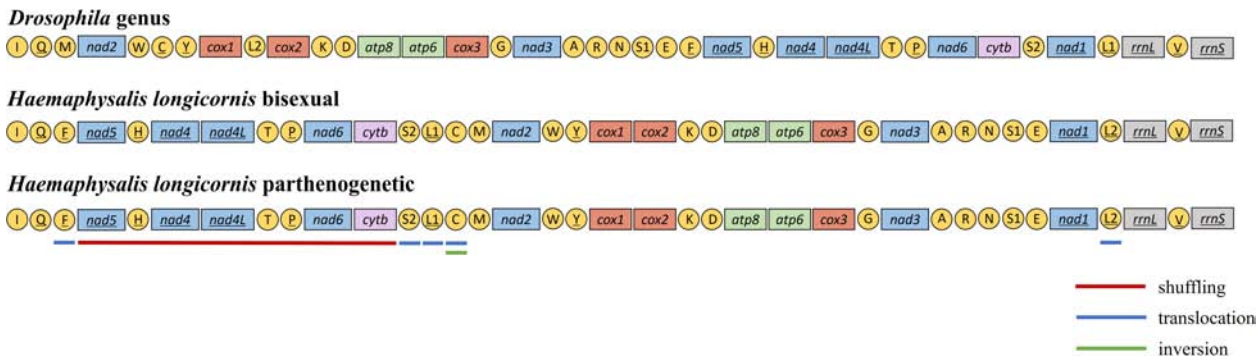

FIGURE 3 | Mitochondrial gene arrangement characteristics of *Haemaphysalis longicornis*. The different color underlines highlighted the genes and rearrangements.

The expression of the *cox1* and *atp8* genes of the parthenogenetic population was significantly up regulated ($P < 0.01$). In contrast, the expression of the *nad3* genes was significantly decreased ($P < 0.01$). The *atp8* gene expression was considerably increased in the two populations at the partially fed and engorgement stages (**Supplementary Figures S7**, **S8**).

When the gene expression of the parthenogenetic population was used as a reference, all genes in the bisexual population were differentially expressed, among which *cox2*, *cox3,* and *nad3* were most significantly expressed. The *cox3* gene expression of the bisexual population in the unfed stage was 60-fold upregulated, whereas it was 16-fold upregulated to the partially fed and engorgement stages. No changes were observed in the expression level of *nad3* in the unfed and engorgement stages in the parthenogenetic population, but it was significantly down regulated in the bisexual population ($P < 0.01$), which resulted in 20-fold variation between the two populations (**Figure 6**).

DISCUSSION

In the current study, the complete mitochondrial genomes of the bisexual and parthenogenetic populations of *H. longicornis* were assembled. The A+T content in *H. longicornis* was approximately 77%, and an obvious AT bias was also observed in most tick mitochondrial genomes (Black and Roehrdanz, 1998; Xiong et al., 2013; Williamsnewkirk et al., 2015). The A+T content affected both the codon usage pattern and amino acid composition of proteins (Breinholt and Kawahara, 2013). The GC and AT skew values of the two populations were negative, indicating that the mitochondrial genome has a slight preference in the usage of "T" and "C." Previous studies have shown that the reversal of GC-skew might be related to the direction of replication but does not affect the direction of genes, whereas AT-skew can vary with changes in the direction of genes, replication and codon location

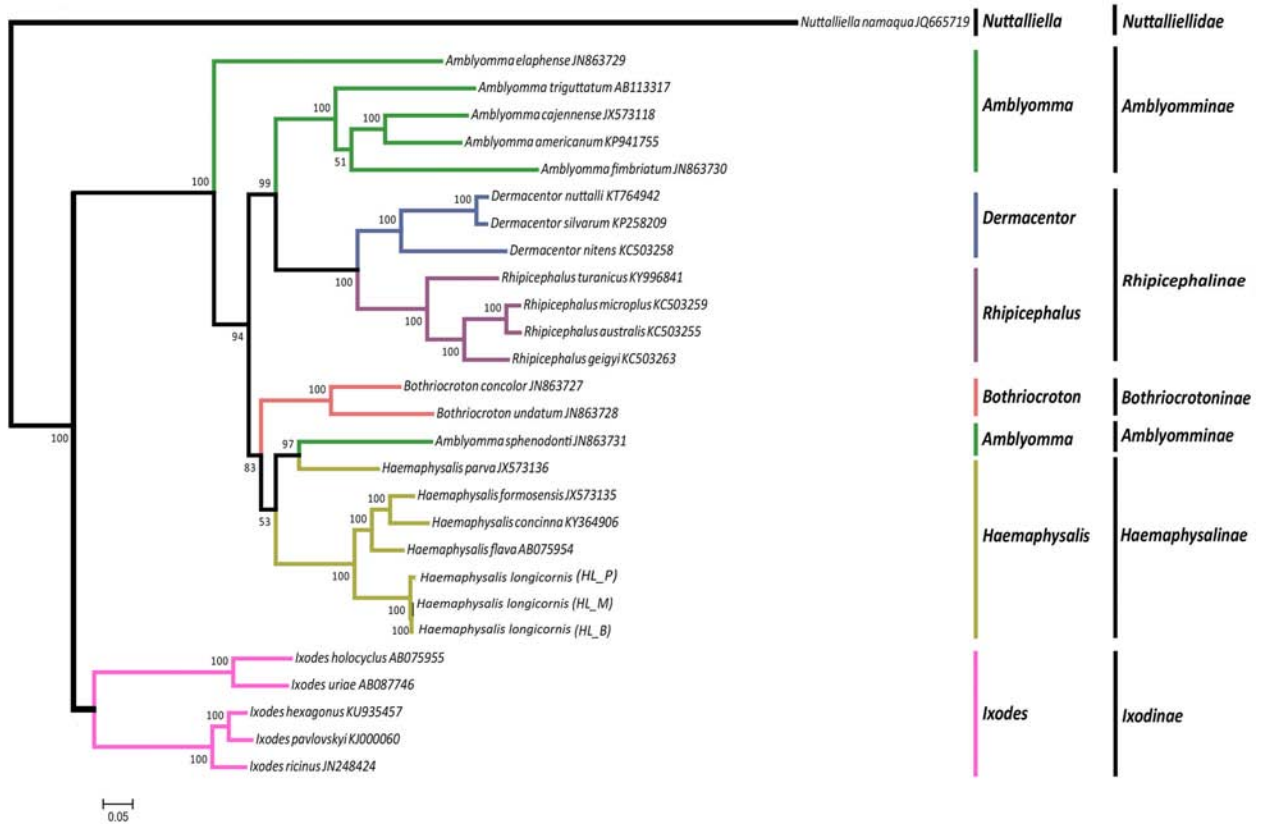

FIGURE 4 | Phylogenetic tree combining 13 protein-coding genes of *Haemaphysalis longicornis*. Using ML analysis based on 24 Ixodidae mitochondrial genome data, different species were marked. The *Nuttalliella namaqua* (JQ665719) is the outgroup. In the phylogenetic tree, the scale bar represents the number of expected changes per site. The percentage of the ML bootstrap support was given at each node. The *Haemaphysalis longicornis* mitochondrial genome of the bisexual and parthenogenetic populations were in the same branch with strong support.

(Wei et al., 2010). In the polymorphism analysis, we found that the mitochondrial sequences were entirely consistent between male and female ticks in the bisexual population, and no special structure was discovered, which maybe attributable to the maternal inheritance of the mitochondrial genome (Burger et al., 2013).

The arrangement of PCGs was similar to other tick species (Burger et al., 2013; Williamsnewkirk et al., 2015; Guo et al., 2016). The starting codon used by *H. longicornis* contained four common "ATN" types, and no special form of the first codon subtype was found. In *H. longicornis*, ATT was used as the initial codon for *cox1*, which is different from "CGA" used in some insect species (Zhu et al., 2013). Three termination codons, including TAA, TAG and "T," were found in *H. longicornis*, and the incomplete termination codons "T" were common in mitochondrial genes (Pan et al., 2008; Dai et al., 2016), which might be converted to complete TAA codons by polyadenylation (Ojala et al., 1981).

In the tick *H. longicornis*, the most frequently used *trnS1* and *trnS2* displayed A and T bases preference in codon usage. Correspondingly, the TTA codon improved the higher usage of *trnL2*. A low utilization rate was observed in "CGC" and "CGG," which resulted in the lower usage of *trnR*. In addition, *trnW* showed the lowest utilization rate. Changes in codon usage are generally regarded as important factors affecting protein expression levels (Zhou J. L. et al., 2004; Fang et al., 2015). Although some differences in codon usage were observed between the two reproductive populations, there was no significant difference in genetic structure or polymorphism between the bisexual and parthenogenetic populations.

The secondary structure of tRNA differs only at a few bases between the two reproductive populations. The DHU arms of *trnC* and *trnS1* were absent in the two populations, which were common features in ticks and insects (Jühling et al., 2009; Cameron, 2014; Williamsnewkirk et al., 2015; Yuan et al., 2015; Liu et al., 2018). The base mismatch of mitochondrial tRNA genes is a common phenomenon (Jühling et al., 2012), which mainly appears in four tRNA structures: the amino acid acceptor arm (AA), the TΨC arm (T), the anticodon arm (AC) and the dihydrouridine arm (DHU) (Zhang et al., 2012). A total of 11 base mismatches were observed in the tRNA genes of *H. longicornis*, among which G-U mismatches occurred 9 times, and the remaining two pairs were U-U mismatches. The mismatch was similar between the bisexual and parthenogenetic populations. The RNA editing

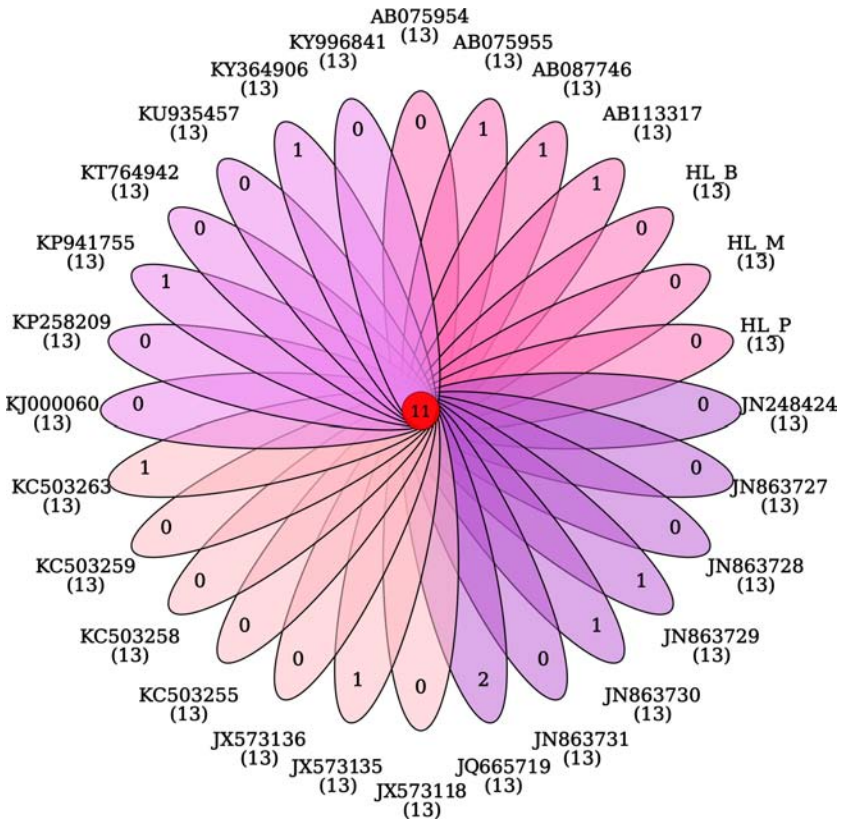

FIGURE 5 | Venn map analysis of the homologous genes in *Haemaphysalis longicornis*. There are no unique homologous genes in the bisexual and parthenogenetic populations of the *Haemaphysalis longicornis* mitochondrial genome.

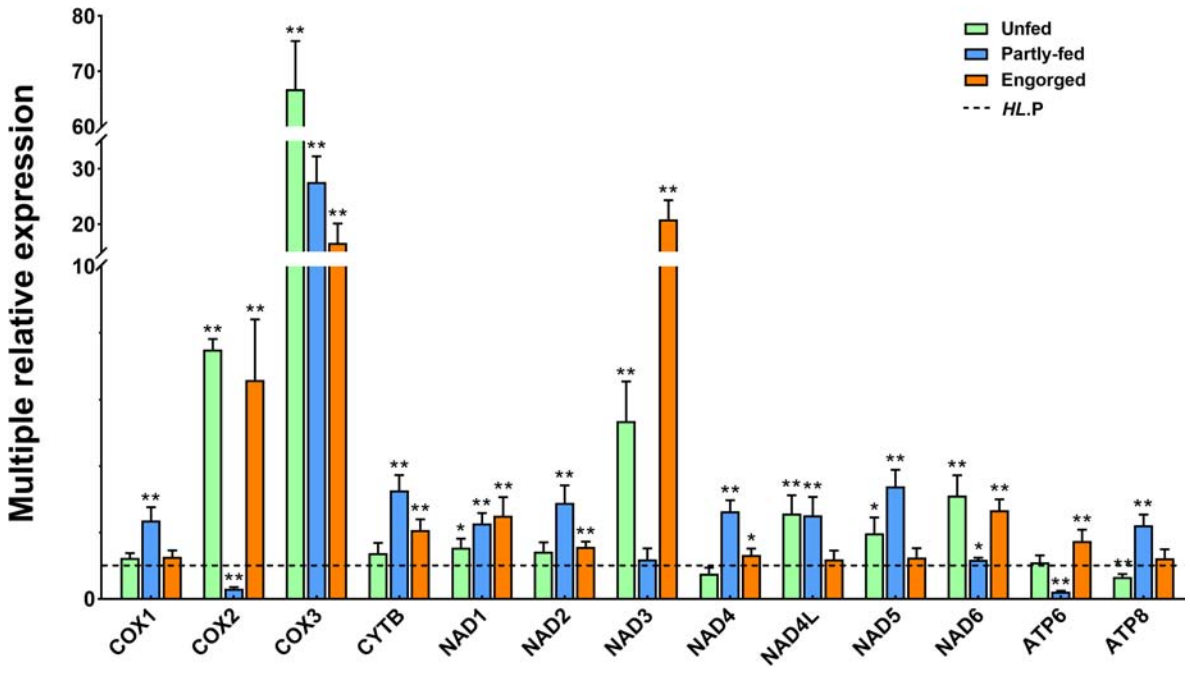

FIGURE 6 | Comparative expression of the different feeding status of *Haemaphysalis longicornis*. The dotted line represents the expression of the parthenogenetic population. The asterisk indicates a level of significant difference (*$P < 0.05$, **$P < 0.01$) in gene expression between the different groups.

process can correct the base mismatch without affecting the tRNA transport function (Bae et al., 2004). However, the base mismatch may jeopardize the survival ability of living organisms (Hendrickson, 2001) and hence result in the evolution of species (Watanabe et al., 1994). The gene length, base skew, and arrangement position of the rRNA in the bisexual and parthenogenetic *H. longicornis* were similar to those of other insects (Breinholt and Kawahara, 2013).

In most cases, the mitochondrial genomes displayed conservative gene arrangement and stable gene structure. Despite rapid evolution over time, the genomic arrangement of most arthropod mitochondria usually remains unchanged (Boore, 1999), and there is no similarity in mitochondrial gene rearrangement (Cameron et al., 2006). The genetic arrangement in the *Drosophila* genus was generally considered to be the original form of insects (Boore, 1999). Mitochondrial gene rearrangement includes major gene rearrangement and minor gene rearrangement (Boore and Brown, 2000). Like insects, two patterns of mitochondrial gene rearrangement were found in different genera of ticks. The minor rearrangement type was relatively common and occurred only in exchanges of the tRNA position (Cameron et al., 2007). This kind of rearrangement was common in *Ixodes* genus, but the rearrangement degree was significantly lower than that observed in other genera of ticks (Liu et al., 2018). The major gene rearrangement referred to the rearrangement or inversion of PCG or rRNA genes and infrequently occurred in insects. Liu et al. reported the major gene rearrangement from some tick genera, such as *Haemaphysalis*, *Amblyomma*, and *Rhipicephalus* (Liu et al., 2018). There were three types of tRNA gene position changes: shuffling (local rearrangements), translocation (cross-gene displacement) and inversion (change the encoding or transcriptional direction) (Dowton and Austin, 1999). Three different displacements were observed in *H. longicornis* tRNA: shuffling was found in *trnH*, *trnT* and *trnP*, translocation was observed in 5 genes (*trnF*, *trnS2*, *trnL1*, *trnC,* and *trnL2*), and *trnC* experienced gene inversion. The tRNA gene rearrangement was interpreted as a result of tandem duplication and random loss (Jühling et al., 2012; Xia et al., 2016), which could provide important genetic and phylogenetic information (Boore et al., 1998; Cameron et al., 2006).

Mitochondrial genomes generally have no introns. Although there are some intergenic regions, most of the arthropod mitochondrial genes are closely linked (Boore, 1999). The mitochondrial genomes of ticks contain different sizes of overlapping regions, including intergenic regions and NCRs. These regions are generally regarded as being involved in gene expression and regulation. The current study found three NCRs in the mitochondrial genome of *H. longicornis*. NCR1 was speculated to be a randomly insert fragment, which was also reported previously in *Dermacentor* and *Rhipicephalus* and possibly related to the tRNA structure (Cameron and Whiting, 2008; Burger et al., 2014b; Mccooke et al., 2015; Guo et al., 2016). The NCR2 and NCR3 were situated in similar positions with other tick species (Burger et al., 2012; Montagna et al., 2012; Williamsnewkirk et al., 2015). No difference was observed in the length or location of NCRs between the bisexual and parthenogenetic populations of *H. longicornis*. The NCRs were considered as a gene control region in arthropod, and the number of repeat sequences and conserved structures could directly affect the length and base skew of the NCRs (Simon, 1991; Montagna et al., 2012; Cameron, 2014; Li and Liang, 2018), which may be the reason for the lower A+T content of NCRs (60−70%) in *H. longicornis*. Recently, a "Tick-Box" structure was found in ticks, and metazoan, which is a 17-bp-long conserved sequence (*TTGyrTChwwwTwwGdA*) in the mitochondrial genome, was connected to transcription termination and gene alignment (Montagna et al., 2012). This conserved sequence was also found in two reproductive populations of *H. longicornis*, which were the same as other species of *Haemaphysalis* (*TTGCATCAATTTTTGGA*). Also, the conserved "ATGATAA" repeat sequence was found between *atp8* and *atp6* in *H. longicornis*, which has been reported in other ticks and insects (Stewart and Beckenbach, 2006; Williamsnewkirk et al., 2015).

Phylogenetic tree analysis showed that the independent branches of *Ixodes*, *Rhipicephalus*, *Amblyomma* and *Dermacentor* species were similar to the findings of Burger et al. (2014a). The conjoint analysis using all PCG genes could improve the stability and reliability of phylogenetic reconstruction (Sheffield et al., 2009). The two reproductive populations of *H. longicornis* were the most closely related and were less than the criteria for subspecies identification, which was consistent with previous results (Chen et al., 2010; Chen X. et al., 2012). Only one non-synonymous site of PCGs was observed in the two populations, whereas nearly 200 polymorphic sites were detected, but no apparent changes were observed in gene structure and arrangement under the evolutionary pressure of different environments.

The mitochondrion is essential for energy metabolism and is also involved in many critical processes, including cell transport, signal transduction, temperature regulation and immune activity (Brand, 2000; Detmer and Chan, 2007). Mitochondrial genes may lead to significant changes in metabolism and adaptability in the process of evolution (Ballard and Pichaud, 2014), and their genetic diversity was mainly formed by random genetic drift and natural selection (Sun et al., 2018). Multiple genes of *H. longicornis* were significantly upregulated in the partially fed and engorgement stages; among these genes, the most significant changes were detected in *atp6* and *atp8*, which are the core subunits of ATP synthase (Fontanillas et al., 2010). The expression of these genes might provide guarantees for oxidative phosphorylation (OXPHOS) of cells and changes in the metabolism of body temperature. In previous studies, *cox1* was considered to be the essential gene for COX activity changes (Uno et al., 2004; Singtripop et al., 2007). In the bisexual *H. longicornis*, the upregulation of *cox1* was not evident compared with the other two subunits (*cox2* and *cox3*). In parthenogenetic *H. longicornis*, changes in the *cox1* gene were noticeable, but down-regulation in *cox2* and *cox3* was observed. These results suggested that the dynamic changes of the *cox* subunit

were not solely related to the *cox1* gene. The *cox3* gene in the bisexual population was considerably higher than that in the parthenogenetic population at each feeding status. This differential expression may be attributed to the living environment of the bisexual population, where it is characterized by higher altitude and latitude, and the climatic conditions of temperature and humidity are more severe.

The most specific gene in the NADH complex is *nad3* (Sanz et al., 2010). Only one non-synonymous site was observed in this gene, and this mutation was likely to change the gene expression patterns and functions in the two populations. The expression of *nad3* was significantly downregulated in the bisexual and parthenogenetic *H. longicornis* at different status, whereas it was also multiple times higher in the engorgement stage in parthenogenetic *H. longicornis* compared with that in the bisexual population. The structural changes of PCGs were required events for environmental adaptation, and most genes were maintained or upregulated during blood feeding or at the engorgement stage, which suggested that the metabolic level in the body was increased or the number of mitochondria was increased. These changes will guarantee rapid development and reproduction in *H. longicornis*.

CONCLUSION

In the current study, the mitochondrial genomes of the bisexual and parthenogenetic *H. longicornis* were analyzed, and the gene structure and position arrangement were similar between the two reproductive populations. However, single nucleotide polymorphism analysis showed that approximately 200 bases were different. Phylogenetic analysis suggested that the bisexual and parthenogenetic populations were more closely related than the subspecies. Quantitative results of PCGs showed that the expression patterns of genes in the two reproductive populations were significantly distinctive at different feeding status, which may be similarly associated with environmental differences and reproductive patterns.

DATA AVAILABILITY

The datasets generated for this study can be found in NCBI with the accession numbers: MK450606 (bisexual populations of *H. longicornis*) and MK439888 (parthenogenetic populations of *H. longicornis*).

ETHICS STATEMENT

All experimental procedures were approved by the Animal Ethics Committee of Hebei Normal University (protocol number: IACUC-157026).

AUTHOR CONTRIBUTIONS

ZY conceived the experiments. TW performed the experiments. SZ and TP analyzed the data. ZY and TW drafted and edited the manuscript. JL reviewed and corrected the manuscript.

FUNDING

This work was supported by the National Natural Science Foundation of China (31672365), the Youth Top Talent Support Program of Hebei Province to ZY, the Natural Science Foundation of Hebei Province (C2019205064), the Financial Assistance for the Introduction of Overseas Researchers (C20190350), the Natural Science Research Programs of the Educational Department of Hebei Province (BJ2016032), the Science Foundation of Hebei Normal University (L2018J04), and the Postgraduate Innovation Foundation of Hebei (CXZZBS2018094).

ACKNOWLEDGMENTS

We are very grateful to Dr. Abolfazl Masoudi from our laboratory for reviewing the manuscript and providing valuable comments.

SUPPLEMENTARY MATERIAL

The Supplementary Material for this article can be found online at: https://www.frontiersin.org/articles/10.3389/fphys.2019.00982/full#supplementary-material

FIGURE S1 | Mitochondrial genome circular map of *Haemaphysalis longicornis* bisexual female.

FIGURE S2 | Mitochondrial genome circular map of *Haemaphysalis longicornis* bisexual male.

FIGURE S3 | Mitochondrial genome circular map of the *Haemaphysalis longicornis* parthenogenetic population.

FIGURE S4 | Nucleotide polymorphisms in the parthenogenetic population with the bisexual population considered as the reference.

FIGURE S5 | Secondary structures of tRNA in the bisexual population of *Haemaphysalis longicornis*.

FIGURE S6 | Secondary structures of tRNAs in the parthenogenetic population of *Haemaphysalis longicornis*.

FIGURE S7 | Quantitative expression of the different feeding status of the bisexual population. The asterisk indicates a level of significant difference ($*P < 0.05$, $**P < 0.01$) in gene expression between the different groups.

FIGURE S8 | Quantitative expression of the different feeding status of the parthenogenetic population. The asterisk indicates a level of significant difference ($*P < 0.05$, $**P < 0.01$) in gene expression between the different groups.

TABLE S1 | Original mitochondrial genome sequencing data of *Haemaphysalis longicornis*.

TABLE S2 | Quantitative primers in the mitochondrial genome of *Haemaphysalis longicornis*.

TABLE S3 | Comparison of the mitochondrial gene position and arrangement in the bisexual and parthenogenetic population of *Haemaphysalis longicornis*.

TABLE S4 | Codon usage of *Haemaphysalis longicornis* in the mitochondrial protein-coding genes.

REFERENCES

Alexandre, H., Nelly, L., and Jean, D. J. (2005). Evidence for multiple reversals of asymmetric mutational constraints during the evolution of the mitochondrial genome of metazoa, and consequences for phylogenetic inferences. *Syst. Biol.* 54, 277–298. doi: 10.1080/10635150590947843

Bae, J. S., Kim, I., Sohn, H. D., and Jin, B. R. (2004). The mitochondrial genome of the firefly, *Pyrocoelia rufa*: complete DNA sequence, genome organization, and phylogenetic analysis with other insects. *Mol. Phylogenet. Evol.* 32, 978–985. doi: 10.1016/j.ympev.2004.03.009

Ballard, J. W., and Pichaud, N. J. (2014). Mitochondrial DNA: more than an evolutionary bystander. *Funct. Ecol.* 28, 218–231. doi: 10.1111/1365-2435.12177

Benson, G. (1999). Tandem repeats finder: a program to analyze DNA sequences. *Nucleic Acids Res.* 27, 573–580. doi: 10.1093/nar/27.2.573

Bernt, M., Donath, A., Jühling, F., Externbrink, F., Florentz, C., Fritzsch, G., et al. (2013). MITOS: improved de novo metazoan mitochondrial genome annotation. *Mol. Phylogenet. Evol.* 69, 313–319. doi: 10.1016/j.ympev.2012.08.023

Black, W. C., and Roehrdanz, R. L. (1998). Mitochondrial gene order is not conserved in arthropods: prostriate and metastriate tick mitochondrial genomes. *Mol. Biol. Evol.* 15, 1772–1785. doi: 10.1093/oxfordjournals.molbev.a025903

Boore, J. L. (1999). Survey and summary animal mitochondrial genomes. *Nucleic Acids Res.* 27, 1767–1780. doi: 10.1093/nar/27.8.1767

Boore, J. L., and Brown, W. M. (2000). Mitochondrial genomes of *Galathealinum*, *Helobdella*, and *Platynereis*: sequence and gene arrangement comparisons indicate that Pogonophora is not a phylum and Annelida and Arthropoda are not sister taxa. *Mol. Biol. Evol.* 17, 87–106. doi: 10.1093/oxfordjournals.molbev.a026241

Boore, J. L., Lavrov, D. V., and Brown, W. M. (1998). Gene translocation links insects and crustaceans. *Nature* 392, 667–668. doi: 10.1038/33577

Brand, M. D. (2000). Uncoupling to survive? The role of mitochondrial inefficiency in ageing. *Exp. Gerontol.* 35, 811–820. doi: 10.1016/S0531-5565(00)00135-2

Breinholt, J. W., and Kawahara, A. Y. (2013). Phylotranscriptomics: saturated third codon positions radically influence the estimation of trees based on next-gen data. *Genome Biol. Evol.* 5, 2082–2092. doi: 10.1093/gbe/evt157

Burger, T. D., Shao, R., and Barker, S. C. (2013). Phylogenetic analysis of the mitochondrial genomes and nuclear rRNA genes of ticks reveals a deep phylogenetic structure within the genus *Haemaphysalis* and further elucidates the polyphyly of the genus *Amblyomma* with respect to *Amblyomma sphenodonti* and *Amblyomma elaphense*. *Ticks Tick Borne Dis.* 4, 265–274. doi: 10.1016/j.ttbdis.2013.02.002

Burger, T. D., Shao, R., Beati, L., Miller, H., and Barker, S. C. (2012). Phylogenetic analysis of ticks (Acari: Ixodida) using mitochondrial genomes and nuclear rRNA genes indicates that the genus *Amblyomma* is polyphyletic. *Mol. Phylogenet. Evol.* 64, 45–55. doi: 10.1016/j.ympev.2012.03.004

Burger, T. D., Shao, R., and Barker, S. C. (2014a). Phylogenetic analysis of mitochondrial genome sequences indicates that the cattle tick, *Rhipicephalus* (*Boophilus*) *microplus*, contains a cryptic species. *Mol. Phylogenet. Evol.* 76, 241–253. doi: 10.1016/j.ympev.2014.03.017

Burger, T. D., Shao, R., Labruna, M. B., and Barker, S. C. (2014b). Molecular phylogeny of soft ticks (Ixodida: Argasidae) inferred from mitochondrial genome and nuclear rRNA sequences. *Ticks Tick Borne Dis.* 5, 195–207. doi: 10.1016/j.ttbdis.2013.10.009

Cameron, S. L. (2014). Insect mitochondrial genomics: implications for evolution and phylogeny. *Annu. Rev. Entomol.* 59, 95–117. doi: 10.1146/annurev-ento-011613-162007

Cameron, S. L., Beckenbach, A. T., Dowton, A., and Whiting, M. F. (2006). Evidence from mitochondrial genomics on interordinal relationships. *Arthropod Syst. Phylogeny* 64, 27–34.

Cameron, S. L., Johnson, K. P., and Whiting, M. F. (2007). The mitochondrial genome of the screamer *Louse Bothriometopus* (Phthiraptera: Ischnocera): effects of extensive gene rearrangements on the evolution of the genome. *J. Mol. Evol.* 65, 589–604. doi: 10.1007/s00239-007-9042-8

Cameron, S. L., and Whiting, M. F. (2008). The complete mitochondrial genome of the tobacco hornworm, *Manduca sexta*, (Insecta: Lepidoptera: Sphingidae), and an examination of mitochondrial gene variability within butterflies and moths. *Gene* 408, 112–123. doi: 10.1016/j.gene.2007.10.023

Cancilla, M. R., Hillier, A. J., and Davidson, B. E. (1995). *Lactococcus lactis* glyceraldehyde 3 phosphate dehydrogenase gene, gap-further evidence for strongly biased codon usage in glycolytic pathway genes. *Microbiology* 141, 1027–1036. doi: 10.1099/13500872-141-4-1027

Chen, X., Xu, S., Yu, Z., Guo, L., Yang, S., Liu, L., et al. (2014). Multiple lines of evidence on the genetic relatedness of the parthenogenetic and bisexual *Haemaphysalis longicornis* (Acari: Ixodidae). *Infect. Genet. Evol.* 21, 308–314. doi: 10.1016/j.meegid.2013.12.002

Chen, X., Yu, Z. Y., Guo, L. D., Li, L. X., Meng, H., Wang, D., et al. (2012). Life cycle of *Haemaphysalis doenitzi* (Acari: Ixodidae) under laboratory conditions and its phylogeny based on mitochondrial 16S rDNA. *Exp. Appl. Acarol.* 56, 143–150. doi: 10.1007/s10493-011-9507-8

Chen, Z., Li, Y. Q., Ren, Q. Y., Liu, Z. J., Luo, J., Li, K., et al. (2015). Does *Haemaphysalis bispinosa* (Acari: Ixodidae) really occur in China? *Exp. Appl. Acarol.* 65, 249–257. doi: 10.1007/s10493-014-9854-3

Chen, Z., Yang, X. J., Bu, F. J., Yang, X. H., Yang, X. L., and Liu, J. Z. (2010). Ticks (Acari: Ixodoidea: Argasidae, Ixodidae) of China. *Exp. Appl. Acarol.* 51, 393–404. doi: 10.1007/s10493-010-9335-2

Chen, Z., Yang, X. J., Bu, F. J., Yang, X. L., and Liu, J. Z. (2012). Morphological, biological and molecular characteristics of bisexual and parthenogenetic *Haemaphysalis longicornis*. *Vet. Parasitol.* 189, 344–352. doi: 10.1016/j.vetpar.2012.04.021

Dai, L. S., Zhu, B. J., Zhao, Y., Zhang, C. F., and Liu, C. L. (2016). Comparative mitochondrial genome analysis of *Eligma narcissus* and other Lepidopteran insects reveals conserved mitochondrial genome organization and phylogenetic relationships. *Sci. Rep.* 6:26387. doi: 10.1038/srep26387

Detmer, S. A., and Chan, D. C. (2007). Functions and dysfunctions of mitochondrial dynamics. *Nat. Rev. Mol. Cell Biol.* 8, 870–879. doi: 10.1038/nrm2275

Dowton, M., and Austin, A. D. (1999). Evolutionary dynamics of a mitochondrial rearrangement "hot spot" in the Hymenoptera. *Mol. Biol. Evol.* 16, 298–309. doi: 10.1093/oxfordjournals.molbev.a026111

Fang, B., Jiang, W., Zhou, Q., and Wang, S. J. (2015). Codon-optimized NADH oxidase gene expression and gene fusion with glycerol dehydrogenase for bienzyme system with cofactor regeneration. *PLoS One* 10:e0128412. doi: 10.1371/journal.pone.0128412

Fischer, S., Brunk, B. P., Chen, F., Gao, X., Harb, O. S., and Iodice, J. B. (2011). Using OrthoMCL to assign proteins to OrthoMCL-DB groups or to cluster proteomes into new ortholog groups. *Curr. Protoc. Bioinformatics* 6, 6.12.1–6.12.19. doi: 10.1002/0471250953.bi0612s35

Fontanillas, P., Dépraz, A., Giorgi, M. S., and Perrin, N. (2010). Nonshivering thermogenesis capacity associated to mitochondrial DNA haplotypes and gender in the greater white-toothed shrew *Crocidura russula*. *Mol. Ecol.* 14, 661–670. doi: 10.1111/j.1365-294X.2004.02414.x

Fujisaki, K., Kawazu, S., and Kamio, T. (1994). The taxonomy of the bovine *Theileria* spp. *Parasitol. Today* 10, 31–33. doi: 10.1016/0169-4758(94)90355-7

Gissi, C., Iannelli, F., and Pesole, G. J. (2008). Evolution of the mitochondrial genome of metazoa as exemplified by comparison of congeneric species. *Heredity* 101, 301–320. doi: 10.1038/hdy.2008.62

Guo, D. H., Zhang, Y., Fu, X., Gao, Y., Liu, Y. T., Qiu, J. H., et al. (2016). Complete mitochondrial genomes of *Dermacentor silvarum* and comparative analyses with another hard tick *Dermacentor nitens*. *Exp. Parasitol.* 169, 22–27. doi: 10.1016/j.exppara.2016.07.004

Hendrickson, T. L. (2001). Recognizing the D-loop of transfer RNAs. *Proc. Natl. Acad. Sci. U.S.A.* 98, 13473–13475. doi: 10.1073/pnas.251549298

Herrin, C. S., and Oliver, J. H. (1974). Numerical taxonomic studies of parthenogenetic and bisexual populations of *Haemaphysalis longicornis* and related species (Acari: Ixodidae). *J. Parasitol.* 60, 1025–1036. doi: 10.2307/3278542

Hoogstraal, H., Roberts, F. H. S., Kohls, G. M., and Tipton, V. J. (1968). Review of *Haemaphysalis* (*Kaiseriana*) *longicornis* Neumann (resurrected) of Australia, New Zealand, New Caledonia, Fiji, Japan, Korea, and Northeastern China and USSR, and its parthenogenetic and bisexual populations (Ixodoidea, Ixodidae). *J. Parasitol.* 54, 1197–1213. doi: 10.2307/3276992

Jongejan, F., and Uilenberg, G. (2004). The global importance of ticks. *Parasitology* 129, S3–S14. doi: 10.1017/S0031182004005967

Jühling, F., Mörl, M., Hartmann, R. K., Sprinzl, M., Stadler, P. F., and Pütz, J. J. (2009). tRNAdb 2009: compilation of tRNA sequences and tRNA genes. *Nucleic Acids Res.* 37, 159–162. doi: 10.1093/nar/gkn772

Jühling, F., Pütz, J., Bernt, M., Donath, A., Middendorf, M., Florentz, C., et al. (2012). Improved systematic tRNA gene annotation allows new insights into the evolution of mitochondrial tRNA structures and into the mechanisms of mitochondrial genome rearrangements. *Nucleic Acids Res.* 40, 2833–2845. doi: 10.1093/nar/gkr1131

Kaufman, W. R. (2010). Ticks: physiological aspects with implications for pathogen transmission. *Ticks Tick Borne Dis.* 1, 11–22. doi: 10.1016/j.ttbdis.2009.12.001

Kim, J., Kern, E., Kim, T., Sim, M., Kim, J., Kim, Y., et al. (2017). Phylogenetic analysis of two *Plectus* mitochondrial genomes (Nematoda: Plectida) supports a sister group relationship between Plectida and Rhabditida within Chromadorea. *Mol. Phylogenet. Evol.* 107, 90–102. doi: 10.1016/j.ympev.2016.10.010

Kovalev, S. Y., and Mukhacheva, T. A. (2013). Cluster on structure of tick-borne encephalitis virus populations. *Infect. Genet. Evol.* 14, 22–28. doi: 10.1016/j.meegid.2012.10.011

Kumar, S., Stecher, G., and Tamura, K. J. (2016). MEGA7: molecular evolutionary genetics analysis version 7.0 for bigger datasets. *Mol. Biol. Evol.* 33, 1870–1874. doi: 10.1093/molbev/msw054

Li, K., and Liang, A. P. (2018). Hemiptera mitochondrial control region: new sights into the structural organization, phylogenetic utility, and roles of tandem repetitions of the noncoding segment. *Int. J. Mol. Sci.* 19:E1292. doi: 10.3390/ijms19051292

Lin, C. P., and Danforth, B. N. (2004). Evolution, how do insect nuclear and mitochondrial gene substitution patterns differ? Insights from bayesian analyses of combined datasets. *Mol. Phylogenet. Evol.* 30, 686–702. doi: 10.3390/ijms19051292

Lines, M. A., Jobling, R., Brady, L., Marshall, C. R., Scherer, S. W., and Rodriguez, A. R. (2014). Peroxisomal D-bifunctional protein deficiency: three adults diagnosed by whole-exome sequencing. *Neurology* 82, 963–968. doi: 10.1212/WNL.0000000000000219

Liu, Q., He, B., Huang, S. Y., Wei, F., and Zhu, X. Q. (2014). Severe fever with thrombocytopenia syndrome, an emerging tick-borne zoonosis. *Lancet Infect. Dis.* 14, 763–772. doi: 10.1016/S1473-3099(14)70718-2

Liu, Z. Q., Liu, Y. F., Kuermanali, N., Wang, D. F., Chen, S. J., Guo, H. L., et al. (2018). Sequencing of complete mitochondrial genomes confirms synonymization of *Hyalomma asiaticum asiaticum* and *kozlovi*, and advances phylogenetic hypotheses for the Ixodidae. *PLoS One* 13:e0197524. doi: 10.1371/journal.pone.0197524

Lohse, M., Drechsel, O., Kahlau, S., and Bock, R. J. (2013). OrganellarGenomeDRAW—a suite of tools for generating physical maps of plastid and mitochondrial genomes and visualizing expression data sets. *Nucleic Acids Res.* 41, 575–581. doi: 10.1093/nar/gkt289

Magori, K. (2018). Preliminary prediction of the potential distribution and consequences of *Haemaphysalis longicornis* (Ixodida: Ixodidae) in the United States and North America, using a simple rule-based climate envelope model. *bioRxiv* [Preprint]. doi: 10.1101/389940

Matsuo, T., Okura, N., Kakuda, H., and Yano, Y. (2013). Reproduction in a Metastriata tick, *Haemaphysalis longicornis* (Acari: Ixodidae). *J. Acarol. Soc. Jpn.* 22, 1–23. doi: 10.1046/j.1463-6395.2000.00035.x

Mccooke, J. K., Guerrero, F. D., Barrero, R. A., Black, M., Hunter, A., Bell, C., et al. (2015). The mitochondrial genome of a Texas outbreak strain of the cattle tick, *Rhipicephalus* (*Boophilus*) *microplus*, derived from whole genome sequencing Pacific Biosciences and Illumina reads. *Gene* 571, 135–141. doi: 10.1016/j.gene.2015.06.060

Mccormick, R. F., Truong, S. K., and Mullet, J. E. (2015). RIG: recalibration and interrelation of genomic sequence data with the GATK. *G3* 5, 655–665. doi: 10.1534/g3.115.017012

Monis, P. T., Andrews, R. H., and Saint, C. P. (2002). Molecular biology techniques in parasite ecology. *Int. J. Parasitol.* 32, 551–562. doi: 10.1016/s0020-7519(01)00352-6

Montagna, M., Sassera, D., Griggio, F., Epis, S., Bandi, C., and Gissi, C. J. (2012). Tick-Box for 3′-End formation of mitochondrial transcripts in Ixodida, basal Chelicerates and *Drosophila*. *PLoS One* 7:e47538. doi: 10.1371/journal.pone.0047538

Ojala, D., Montoya, J., and Attardi, G. J. (1981). tRNA punctuation model of RNA processing in human mitochondria. *Nature* 290, 470–474. doi: 10.1038/290470a0

Oliver, H. J. (1977). Cytogenetics of mites and ticks. *Annu. Rev. Entomol.* 22, 407–429. doi: 10.1146/annurev.en.22.010177.002203

Pan, M. H., Yu, Q. Y., Xia, Y. L., Dai, F. Y., Liu, Y. Q., and Lu, C. (2008). Characterization of mitochondrial genome of Chinese wild mulberry silkworm, *Bombyx mandarina* (Lepidoptera: Bombycidae). *Sci. China Life Sci.* 51, 693–701. doi: 10.1007/s11427-008-0097-6

Papanicolaou, A., Gebauerjung, S., Blaxter, M. L., Mcmillan, W. O., and Jiggins, C. D. (2008). ButterflyBase: a platform for lepidopteran genomics. *Nucleic Acids Res.* 36, D582–D587. doi: 10.1093/nar/gkm853

Qin, J., Zhang, Y., Zhou, X., Kong, X., Wei, S., Ward, R. D., et al. (2015). Mitochondrial phylogenomics and genetic relationships of closely related pine moth (Lasiocampidae: *Dendrolimus*) species in China, using whole mitochondrial genomes. *BMC Genomics* 16:428. doi: 10.1186/s12864-015-1566-5

Qin, X. R., Han, F. J., Luo, L. M., Zhao, F. M., Han, H. J., Zhang, Z. T., et al. (2018). *Anaplasma* species detected in *Haemaphysalis longicornis* tick from china. *Ticks Tick Borne Dis.* 9, 840–843. doi: 10.1016/j.ttbdis.2018.03.014

Sanz, A., Soikkeli, M., Portero-Otín, M., Wilson, A., Kemppainen, E., and Mcilroy, G. (2010). Expression of the yeast NADH dehydrogenase Ndi1 in *Drosophila* confers increased lifespan independently of dietary restriction. *Proc. Natl. Acad. Sci. U.S.A.* 107, 9105–9110. doi: 10.1073/pnas.0911539107

Sheffield, N. C., Song, H., Cameron, S. L., and Whiting, M. F. (2009). Nonstationary evolution and compositional heterogeneity in beetle mitochondrial phylogenomics. *Syst. Biol.* 58, 381–394. doi: 10.1093/sysbio/syp037

Simon, C. (1991). "Molecular systematics at the species boundary: exploiting conserved and variable regions of the mitochondrial genome of animals via direct sequencing from amplified DNA," in *Molecular Techniques in Taxonomy*, eds G. M. Hewitt, A. W. B. Johnston, and J. P. W. Young (Berlin: Springer-Verlag), 33–71. doi: 10.1007/978-3-642-83962-7_4

Singtripop, T., Saeangsakda, M., Tatun, N., Kaneko, Y., and Sakurai, S. (2007). Correlation of oxygen consumption, cytochrome c oxidase, and cytochrome c oxidase subunit I gene expression in the termination of larval diapause in the bamboo borer, *Omphisa fuscidentalis*. *J. Insect Physiol.* 53, 933–939. doi: 10.1016/j.jinsphys.2007.03.005

Stamatakis, A. (2015). Using RAxML to infer phylogenies. *Curr. Protoc. Bioinformatics* 51, 6.14.1–6.14.14. doi: 10.1002/0471250953.bi0614s51

Stewart, J. B., and Beckenbach, A. T. (2006). Insect mitochondrial genomics 2: the complete mitochondrial genome sequence of a giant stonefly, *Pteronarcys princeps*, asymmetric directional mutation bias, and conserved plecopteran A+T-region elements. *Genome* 52, 815–824. doi: 10.1139/G08-098

Sun, J. T., Jin, P. Y., Hoffmann, A. A., Duan, X. Z., Dai, J., Hu, G., et al. (2018). Evolutionary divergence of mitochondrial genomes in two *Tetranychus* species distributed across different climates. *Insect Mol. Biol.* 27, 698–709. doi: 10.1111/imb.12501

Takahashi, T., Maeda, K., Suzuki, T., and Ishido, A. (2014). The first identification and retrospective study of severe fever with thrombocytopenia syndrome in Japan. *J. Infect. Dis.* 209, 816–827. doi: 10.1093/infdis/jit603

Timmermans, M. J., Lees, D. C., and Simonsen, T. J. (2014). Towards a mitogenomic phylogeny of Lepidoptera. *Mol. Phylogenet. Evol.* 79, 169–178. doi: 10.1016/j.ympev.2014.05.031

Tominski, C., Abello, J., and Schumann, H. J. (2009). Technical section: CGV-An interactive graph visualization system. *Comput. Graph.* 33, 660–678. doi: 10.1016/j.cag.2009.06.002

Uno, T., Nakasuji, A., Shimoda, M., and Aizono, Y. J. (2004). Expression of cytochrome c oxidase subunit 1 gene in the brain at an early stage in the termination of pupal diapause in the sweet potato hornworm, *Agrius convolvuli*. *J. Insect Physiol.* 50, 35–42. doi: 10.1016/j.jinsphys.2003.09.011

Wang, D., Hu, Y. H., and Liu, J. Z. (2013). Ultrastructure and development of the Haller's organ of parthenogenetic *Haemaphysalis longicornis* (Acari: Ixodidae). *Acta Entomol. Sin.* 56, 306–311.

Watanabe, Y., Kawai, G., Yokogawa, T., Hayashi, N., Kumazawa, Y., Ueda, T., et al. (1994). Higher-order structure of bovine mitochondrial tRNASerUGA: chemical modification and computer modeling. *Nucleic Acids Res.* 22, 5378–5384. doi: 10.1093/nar/22.24.5378

Wei, S. J., Shi, M., Chen, X. X., Sharkey, M. J., Achterberg, C. V., Ye, G. Y., et al. (2010). New views on strand asymmetry in insect mitochondrial genomes. *PLoS One* 5:e12708. doi: 10.1371/journal.pone.0012708

Williamsnewkirk, A. J., Burroughs, M., Changayil, S. S., and Dasch, G. A. (2015). The mitochondrial genome of the lone star tick (*Amblyomma americanum*). *Ticks Tick Borne Dis.* 6, 793–801. doi: 10.1016/j.ttbdis.2015.07.006

Xia, Y., Zheng, Y., Murphy, R. W., and Zeng, X. (2016). Intraspecific rearrangement of mitochondrial genome suggests the prevalence of the tandem duplication-random loss (TDLR) mechanism in *Quasipaa boulengeri*. *BMC Genomics* 17:965. doi: 10.1186/s12864-016-3309-7

Xie, Y., Wu, G., Tang, J., Luo, R., Patterson, J., Liu, S., et al. (2014). SOAPdenovo-Trans: de novo transcriptome assembly with short RNA-Seq reads. *Bioinformatics* 30, 1660–1666. doi: 10.1093/bioinformatics/btu077

Xiong, H., Barker, S. C., Burger, T. D., Raoult, D., and Shao, R. F. (2013). Heteroplasmy in the mitochondrial genomes of human lice and ticks revealed by high throughput sequencing. *PLoS One* 8:e73329. doi: 10.1371/journal.pone.0073329

Yang, C. M., Yang, G. Y., Xie, Y. X., Wu, K. B., and Yong, J. X. (2007). Morphological observation of parthenogenetic *Haemaphysalis longicornis* with scanning electron microscope. *Acta Parasitol. Med. Entomol. Sin.* 14, 104–109.

Yu, Z. J., Wang, H., Wang, T. H., Sun, W. Y., Yang, X. L., and Liu, J. Z. (2015). Tick-borne pathogens and the vector potential of ticks in China. *Parasit. Vectors* 8:24. doi: 10.1186/s13071-014-0628-x

Yuan, M. L., Zhang, Q. L., Guo, Z. L., Wang, J., and Shen, Y. Y. (2015). Comparative mitogenomic analysis of the superfamily Pentatomoidea (Insecta: Hemiptera: Heteroptera) and phylogenetic implications. *BMC Genomics* 16:460. doi: 10.1186/s12864-015-1679-x

Zhan, J., Wang, Q., Cheng, J., Hu, B., Li, J., Zhan, F., et al. (2017). Current status of severe fever with thrombocytopenia syndrome in china. *Virol. Sin.* 32, 51–62. doi: 10.1007/s12250-016-3931-1

Zhou, J. L., Zhou, Y. Z., Gong, H. Y., Chen, L. Z., and Cao, J. (2004). Discovery of parthenogenesis population of *Haemaphysalis longicornis* in China and its biological characteristic. *Chin J. Vector Biol. Control* 15, 173–174.

Zhang, M., Nie, X., Cao, T., Wang, J., Li, T., Zhang, X., et al. (2012). The complete mitochondrial genome of the butterfly *Apatura metis* (Lepidoptera: Nymphalidae). *Mol. Biol. Rep.* 39, 6529–6536. doi: 10.1007/s11033-012-1481-7

Zhang, R. L., Huang, Z. D., Yu, G. F., and Zhang, Z. (2019). Characterization of microbiota diversity of field-collected *Haemaphysalis longicornis* (Acari: Ixodidae) with regard to sex and blood meals. *J. Basic Microbiol.* 59, 215–223. doi: 10.1002/jobm.201800372

Zhou, Z., Schnake, P., Xiao, L., and Lal, A. A. (2004). Enhanced expression of a recombinant malaria candidate vaccine in *Escherichia coli* by codon optimization. *Protein Expr. Purif.* 34, 87–94. doi: 10.1016/j.pep.2003.11.006

Zhu, B. J., Liu, Q. N., Dai, L. S., Wang, L., Sun, Y., Lin, K. Z., et al. (2013). Characterization of the complete mitochondrial genome of *Diaphania pyloalis* (Lepidoptera: Pyralididae). *Gene* 527, 283–291. doi: 10.1016/j.gene.2013.06.035

Conflict of Interest Statement: The authors declare that the research was conducted in the absence of any commercial or financial relationships that could be construed as a potential conflict of interest.

frontiers in Physiology

ORIGINAL RESEARCH
published: 31 July 2019
doi: 10.3389/fphys.2019.00965

TOR as a Regulatory Target in *Rhipicephalus microplus* Embryogenesis

*Camila Waltero[1], Leonardo Araujo de Abreu[1,2], Thayná Alonso[1], Rodrigo Nunes-da-Fonseca[1,2], Itabajara da Silva Vaz Jr.[2,3] and Carlos Logullo[1,2]**

[1] Laboratório Integrado de Bioquímica Hatisaburo Masuda and Laboratório Integrado de Ciências Morfofuncionais, Instituto de Biodiversidade e Sustentabilidade NUPEM, Universidade Federal do Rio de Janeiro, Macaé, Brazil, [2] Instituto Nacional de Ciência e Tecnologia em Entomologia Molecular (INCT-EM), Rio de Janeiro, Brazil, [3] Centro de Biotecnologia, Faculdade de Veterinária, Universidade Federal do Rio Grande do Sul, Porto Alegre, Brazil

Embryogenesis is a metabolically intensive process carried out under tightly controlled conditions. The insulin signaling pathway regulates glucose homeostasis and is essential for reproduction in metazoan model species. Three key targets are part of this signaling pathway: protein kinase B (PKB, or AKT), glycogen synthase kinase 3 (GSK-3), and target of rapamycin (TOR). While the role of AKT and GSK-3 has been investigated during tick embryonic development, the role of TOR remains unknown. In this study, TOR and two other downstream effectors, namely S6 kinase (S6K) and eukaryotic translation initiation factor 4E-binding protein 1 (4E-BP1), were investigated in *in vitro* studies using the tick embryonic cell line BME26. First, we show that exogenous insulin can stimulate TOR transcription. Second, TOR chemical inhibition led to a decrease in BME26 cell viability, loss of membrane integrity, and downregulation of S6K and 4E-BP1 transcription. Conversely, treating BME26 cells with chemical inhibitors of AKT or GSK-3 did not affect S6K and 4E-BP1 transcription, showing that TOR is specifically required to activate its downstream targets. To address the role of TOR in tick reproduction, *in vivo* studies were performed. Analysis of relative transcription during different stages of tick embryonic development showed different levels of transcription for TOR, and a maternal deposition of S6K and 4E-BP1 transcripts. Injection of TOR double-stranded RNA (dsRNA) into partially fed females led to a slight delay in oviposition, an atypical egg external morphology, decreased vitellin content in eggs, and decreased larval hatching. Taken together, our data show that the TOR signaling pathway is important for tick reproduction, that TOR acts as a regulatory target in *Rhipicephalus microplus* embryogenesis and represents a promising target for the development of compounds for tick control.

Keywords: target of rapamycin, embryogenesis, tick embryonic cells, BME26, *Rhipicephalus microplus*

OPEN ACCESS

Edited by:
Bin Tang,
Hangzhou Normal University, China

Reviewed by:
Zhongxiang Sun,
Fujian Agriculture and Forestry University, China
Agus Suryawan,
Baylor College of Medicine, United States

***Correspondence:**
Carlos Logullo
carlos.logullo@bioqmed.ufrj.br;
carloslogullo@yahoo.com.br

Specialty section:
This article was submitted to Invertebrate Physiology, a section of the journal Frontiers in Physiology

Received: *19 March 2019*
Accepted: *11 July 2019*
Published: *31 July 2019*

Citation:
Waltero C, Abreu LA, Alonso T, Nunes-da-Fonseca R, da Silva Vaz I Jr and Logullo C (2019) TOR as a Regulatory Target in Rhipicephalus microplus Embryogenesis. Front. Physiol. 10:965. doi: 10.3389/fphys.2019.00965

INTRODUCTION

The cattle tick, *Rhipicephalus microplus,* is an obligate hematophagous ectoparasite of veterinary and economical relevance in tropical and subtropical regions, due to its role as animal disease vector for *Babesia* spp. and *Anaplasma* spp., and its impact on livestock production (Grisi et al., 2002; Guerrero et al., 2012; Parizi et al., 2012). Current methods for tick and tick-borne disease control

depend heavily on the application of acaricides; however, excessive reliance on these pesticides is unsustainable due to the widespread resistance in tick populations, as well as an increasing public concern about residues found in animal products, environmental pollution, and the high costs of developing and registering these products (Graf et al., 2004; Ghosh et al., 2007; de la Fuente et al., 2008; Rodriguez-Vivas et al., 2011; Parizi et al., 2012; Merino et al., 2013). Thus, a better understanding of tick biology may greatly improve both current and novel control strategies.

Embryogenesis is one of the most important aspects of *R. microplus* tick life-cycle (Campos et al., 2006; Moraes et al., 2007; Santos et al., 2013). The study of molecules involved in metabolic pathways during embryogenesis could reveal regulatory networks that govern metabolism during this critical stage (Martins et al., 2015). Insulin signaling pathway (ISP) and its components, phosphatidylinositol 3-OH kinase (PI3K), protein kinase B (PKB or AKT) and glycogen synthase kinase 3 (GSK-3), play important roles in metabolic control (**Supplementary Figure S1**) (de Abreu et al., 2009, 2013; Fabres et al., 2010). In previous studies, we demonstrated that *R. microplus* embryonic cell line, BME26, harbors an insulin-responsive machinery, and that AKT/GSK3 axis integrates glycogen metabolism and cell survival (de Abreu et al., 2009, 2013). We also observed that GSK-3, a key enzyme in glycogen metabolism, is required for cell viability, oviposition, and larval hatching in the cattle tick (Fabres et al., 2010; de Abreu et al., 2013) (**Supplementary Figure S1**). In order to improve the current knowledge of tick physiology, new targets must be identified and studied.

Target of rapamycin (TOR) signaling pathway (TSP) is regulated by ISP in several animal species (Hay and Sonenberg, 2004; Jia et al., 2004; Wullschleger et al., 2006; Hassan et al., 2013; Hatem et al., 2015; Yoon, 2017). This pathway acts controlling energy metabolism, and monitoring the nutritional status of eukaryotic cells. TSP plays a role in protein synthesis, transcription, cell growth, proliferation, metabolism, aging, and autophagy, from yeasts to mammals (Wullschleger et al., 2006; Guertin and Sabatini, 2007; Jung et al., 2010; Katewa and Kapahi, 2011; Kim and Guan, 2011; Beauchamp and Platanias, 2013). However, the role of TOR target in tick embryogenesis is still unknown.

In the present study, we characterized TSP during *R. microplus* embryogenesis, studying the effects of chemical inhibition on regulation and cell viability *in vitro*. Additionally, to evaluate the dynamics of this pathway *in vivo*, we analyzed the relative transcription of other members of the TOR pathway, S6 kinase (S6K) and eukaryotic translation initiation factor 4E-binding protein 1 (4E-BP1) during embryogenesis. We also describe the effects of TOR gene silencing in partially fed females, particularly in ovarian growth, egg development, and larval hatching. Altogether, our study shows that TSP is important for tick reproductive physiology, that TOR acts as a regulatory target during *Rhipicephalus microplus* embryogenesis and can be considered an important target for tick control.

MATERIALS AND METHODS

Ethics Statement

Animals used in the experiments were housed at Faculdade de Veterinária, Universidade Federal do Rio Grande do Sul (UFRGS) facilities. This research was conducted according to the ethics and methodological guidance, in agreement with the International and National Directives and Norms for Animal Experimentation Ethics Committee of Universidade Federal do Rio Grande do Sul (process number 14403).

Chemicals

Insulin, TOR inhibitor rapamycin, GSK3 inhibitor alsterpaullone {9-Nitro-7, 12-dihydroindolo [3,2-d][1]benzazepin-6(5H)-one}, MTT [3-(4,5-Dimethyl-2-thiazolyl)-2,5-diphenyl-2H-tetrazolium bromide], and Leibovitz's 15 culture medium were purchased from Sigma-Aldrich (St. Louis, MO, United States). AKT inhibitor 10-DEBC {10-[4′-(N,N-Diethylamino)butyl]-2-chlorophenoxazinehydrochloride} was purchased from Tocris Bioscience (Ellisville, MO, United States). Fetal bovine serum (FBS) was obtained from Nutricell Nutrientes Celulares (Campinas, SP, Brazil). Other reagents and chemicals used were of analytical grade and locally purchased.

BME26 Cell Line and *Rhipicephalus microplus* Females and Eggs

BME26 cell line is derived from *R. microplus* embryos at different stages of embryogenesis, first isolated in the 1980s and described by Esteves et al. (2008). Cell cultures were maintained as previously described (Esteves et al., 2008; de Abreu et al., 2013). Leibovitz L15 culture medium (Sigma-Aldrich, United States) was diluted in sterile ultra-pure water (3:1) and supplemented with inactivated fetal bovine serum (20%, Nutricell, Brazil), tryptose phosphate broth (10% Sigma- Aldrich, United States), 100 mL^{-1} penicillin units (Gibco, United States) and 100 μg mL^{-1} streptomycin (Gibco, United States). This fresh complete medium was used for cell culture.

Cells adhered to 25 cm^2 flasks were resuspended in 5 mL of the medium described above using a 22 gauge needle (0.7 × 25 mm) with the folded tip mounted in a 5 mL plastic syringe. Culture cell density was determined using Neubauer's chamber (hemocytometer) and cell viability was determined using the trypan blue labeled cell exclusion method (0.4%, Sigma-Aldrich, United States). Aliquots of 1×10^7 cells were transferred to new flasks filled with 5 mL fresh complete medium. The flasks were incubated at 34°C for 2 weeks and the medium replaced weekly to promote cell proliferation. Cells maintained in these flasks, with approximately 4×10^6 cells/mL, were used in later experiments in order to maintain homogenous characteristics between the cells used. Each of these flasks are considered independent biological samples.

Rhipicephalus microplus ticks (Porto Alegre strain) were collected from bovines housed in individual tick-proof pens on slatted floors. These ticks are free of pathogens such as *Babesia* spp. and *Anaplasma* spp. (Reck et al., 2009). Partially engorged tick females (20–60 mg each) were manually removed from

cattle and used for RNA interference (RNAi) experiments as described below. Two independent experiments were performed, with approximately 20 individuals per treatment for each independent experiment. Fully engorged adult female ticks were collected in Petri dishes and incubated at 28°C and 80% relative humidity until completing oviposition. After oviposition, eggs were separated according to age and maintained under the same conditions. Eggs were collected on different days during the embryogenesis for RNA extraction, determination of vitellin content, or were observed until hatching.

RNA Extraction and cDNA Synthesis

Total RNA was extracted from BME26 cells (5×10^5 cells in each experimental condition in three biological replicates), from ovaries of partially engorged females in RNAi experiment (three ovaries in each experimental condition in two biological replicates), and from eggs on different days of embryogenesis (50 mg for each day in three biological replicates), using TRIzol®reagent (Invitrogen, Waltham, CA, United States) following the manufacturer's recommendations. RNA concentration was determined by spectrophotometry at 260 and 280 nm (Picodrop Ltd, United States). Extracted RNA (2 μg) was resuspended in diethylpyrocarbonate (DEPC)-treated water and treated with DNase I (Invitrogen, Waltham, CA, United States). Reverse transcription reaction was performed using High-Capacity cDNA Reverse Transcription Kit (Applied Biosystems, Waltham, CA, United States) following the manufacturer's protocol, and the resulting cDNA samples were stored at −20°C for analyses of relative transcription.

Cloning of RmTOR, RmS6K and Rm4E-BP1 ORFs, and Phylogenetic Analysis

RT-PCR was performed using specific primers to clone three open reading frames (ORF): RmTOR, RmS6K, and Rm4E-BP1. The primers (**Supplementary Table S1**) were designed based on *R. microplus* transcriptome database (RmINCT-EM) created by our research group using Illumina sequencing (unpublished). BME26 cDNA was used as a template. The PCR products were separated by electrophoresis on 1.5% agarose gel and each fragment was excised and purified using GFX™ PCR and Gel Band Purification Kit (GE Healthcare, Chicago, IL, United States). The amplified fragments were ligated into pGEM-T easy vector (Promega) according to the manufacturer's instructions. Plasmids were transformed into *Escherichia coli* TOP10 cells by electroporation. Recombinant plasmid DNA was extracted using PlasmidPrep Mini Spin Kit (GE Healthcare) and DNA sequencing was performed using T7 and SP6 vector-specific primers (**Supplementary Table S1**) in 3500 Genetic Analyzer (Applied Biosystems, Hitachi, United States). A total of 4 sequencing efforts were performed for each target. DNA sequence alignment, amino acid translations, and amino acid sequence alignments were done using BioEdit version 7.2.6 software (Hall, 1999). The sequences are listed under GenBank accession numbers: MK598842 (RmTOR), MK598841 (RmS6K), and MK598840 (Rm4E-BP1). Phylogenetic analyses were performed in MEGA software, version 5.05, using coding mRNA sequences (Tamura et al., 2011) and the neighbor-joining method. Bootstrap support was assessed using 1,000 replicates. The sequences included in the phylogenetic analyses are listed under GenBank accession numbers: BAM28764.1 (*Haemaphysalis longicornis);* EFX81736.1 (*Daphnia pulex*); KRT79235.1 (*Oryctes borbonicus*); KZS19304.1 (*Daphnia magna);* XP_002404524.1 (*Ixodes scapularis);* XP_003740398.1 (*Galendromus occidentalis);* XP_008468645.1 (*Diaphorina citri*); XP_013779553.1 (*Limulus Polyphemus);* XP_015792963.1 (*Tetranychus urticae);* XP_015908828.1 (*Parasteatoda tepidariorum);* XP_018027170.1 (*Hyalella Azteca);* NP_477295.1 (*Drosophila melanogaster*); XP_001846418.1 (*Culex quinquefasciatus);* XP_006569762.1 (*Apis mellifera);* and XP_317732.2 (*Anopheles gambiae).*

BME26 Cell Treatment With Exogenous Insulin

Cells were treated with exogenous insulin as previously described (de Abreu et al., 2009). BME26 cells were resuspended from flasks in which cell proliferation was promoted. Thereafter, cell density of the culture was determined using Neubauer's chamber (hemocytometer) and cell viability was determined using the trypan blue-labeled cell exclusion method (0.4%, Sigma-Aldrich, United States). A total of 5×10^5 cells were plated into wells (16.25 mm diameter and 1.93 cm^2 growth area) of 24 well plates and the final volume of 500 μL was completed with fresh complete medium. Cell plates were incubated at 34°C for a period of 24 h to allow cell adhesion. After this time, complete medium was replaced with medium without fetal bovine serum or with fresh complete medium for 24 h. Subsequently, some cells were exposed to insulin (final concentration 1 μM, Sigma-Aldrich, United States). The plate was incubated at 34°C for 30 min. Finally, all cells were lysed for RNA extraction (described above). All treatments were performed in three independent biological samples and three technical replicates.

Chemical Inhibition of TOR, AKT and GSK3

BME26 cells were seeded in 24-well plates (5×10^5 cells/well) in 500 μL of complete medium and allowed to settle. After 24 h at 34°C, medium culture was replaced and chemical inhibitors or vehicle control (0.073% DMSO) were added as indicated. BME26 cells were treated with one of the following inhibitors: 0.03 to 2 μM of rapamycin (TOR inhibitor); 12 μM of 10-DEBC (AKT inhibitor, non-lethal concentration); or 40, 400, and 4000 nM of alsterpaullone (GSK inhibitor, non-lethal concentration). After 24 h of incubation at 34°C, cells were processed for total RNA extraction and analysis of S6K and 4E-BP1 relative transcription. Alternatively, cells treated with rapamycin were incubated for 48 h and analyzed for cell viability and membrane integrity as described below. All treatments were performed in three independent biological samples and three technical replicates.

Cell Viability and Membrane Integrity Assays

After 48 h of TOR chemical inhibition, BME26 cells were subjected to MTT assay (viability assay), following de Abreu et al. (2013). In each well, 50 μL of MTT (12 mM prepared in L15 medium without fetal bovine serum) was added. The plate was incubated at 34°C for 2 h and protected from light. Subsequently, the solution was completely discarded and 1 mL of isopropyl alcohol (0.15% HCl in isopropyl alcohol) was added to each well to dissolve the formazan crystals. The mixture was transferred to 1.5 mL tubes, centrifuged at 6000 × *g* for 15 min and the supernatant was collected in new tubes to measure the absorbance at 570 nm using quartz cuvettes on a UVmini-1240 UV-VIS spectrophotometer (Shimadzu, Japan). The absorbance values of the control treatment (cells treated with 0.073% DMSO) were used for normalization (100% viability). All samples were analyzed in three independent experiments performed in technical triplicates. Additionally, cell viability was determined by trypan blue (0.4%, Sigma-Aldrich, United States) exclusion technique using a Neubauer hemocytometer. The experimental procedure and calculations were performed according to standard methodology (Louis and Siegel, 2011). All samples were analyzed in three independent experiments performed in three technical triplicates.

Membrane integrity in rapamycin-treated BME26 cells was analyzed following de Abreu et al. (2013). Cells were distributed over glass coverslips placed at the bottom of 24-well plate (2×10^5 cells/well). Cells were treated with rapamycin as described above and incubated for 48 h, after which culture medium was gently removed and replaced with PBS. Hoechst 33342 (0.08 mM) was added and incubated for 5 min, followed by addition of propidium iodide (14.8 μM) and further 5-min incubation, always at room temperature and protected from light. The solution was discarded, and coverslips were washed with PBS and mounted over glass slides containing 5 μL of glycerol. BME26 cells were observed under a confocal fluorescence microscope (LSM 780-NLO Zeiss Axio Observer Z.1, Carl Zeiss AG, Germany) using 405 and 488 nm lasers. Images were obtained at 400x magnification.

Double-Stranded RNA (dsRNA) Synthesis, and Delivery Into BME26 Cells or Female Ticks

A dsRNA based on *R. microplus* TOR coding sequence was designed (dsTOR). Suitable regions of the gene and RNA sequence were screened using BLAST to determine specificity. dsRNA specificity and potential off-targets were estimated from similar genes in other species with the dsCheck program (Naito et al., 2005). *In vitro* dsRNA synthesis was performed using BME26 cDNA as a template and oligonucleotide primers containing T7 promoter sequences (**Supplementary Table S2**). The amplicon was analyzed by electrophoresis on 1.5% agarose gel, purified using GFX™ PCR and Gel Band Purification Kit (GE Healthcare), and quantified by spectrophotometry at 260 nm (Picodrop Ltd, United States). dsRNA was transcribed *in vitro* from 1 μg of purified cDNA, using the T7 RiboMAX™ Express RNAi System (Promega), and purified according to manufacturer's instructions. Final yield was estimated by absorbance measurement at 260 nm and quality confirmed by 1.5% agarose gel electrophoresis. The final size of dsRNA was 519 bp. dsRNA synthesis for RmAKT and RmGSK-3β was performed as described previously in Fabres et al. (2010) and de Abreu et al. (2013), respectively. An unrelated 600 bp-long dsRNA of green fluorescent protein (dsGFP) (**Supplementary Table S2**) was kindly provided by Dr. Albert Mulenga (Texas A&M University, United States).

dsRNA delivery into BME26 cells was performed following de Abreu et al. (2013). A total of 5×10^5 cells were plated into wells (16.25 mm diameter and 1.93 cm^2 growth area) of 24-well plates, and the final volume of 500 μL was completed with fresh complete medium. Cell plates were incubated at 34°C for a period of 24 h to allow cell adhesion. Subsequently, the culture medium was replaced with 200 μL of fresh medium containing 4 μg of dsRNA and the plate was gently mixed. After 24 h of incubation at 34°C, cells were collected and processed for RNA extraction. RNA from cells treated with dsGFP was used as a control group. All treatments were performed in three independent biological samples and three technical replicates.

dsRNA injection into female ticks was performed according to Fabres et al. (2010). Females with a weight between 20 and 60 mg were manually removed from the cattle and injected with 4 μg of dsRNA in a maximum volume of 2 μL in the lower quadrant of the ventral surface using a Hamilton syringe. Two control groups were injected: one with unrelated dsRNA (4 μg of dsGFP in a maximum volume of 2 μL) and the other with buffer (2 μL of 10 mM PBS, pH 7.4). A third group was injected with TOR dsRNA (4 μg of dsTOR in a maximum volume of 2 μL). The females were fixed on expanded polystyrene plates with double-sided adhesive tape for artificial feeding by capillaries (Gonsioroski et al., 2012). Capillaries were filled with non-infested bovine blood that was collected in heparinized tubes and were replaced every 3 h. The females were maintained with this feeding for 28 h. For confirmation of silencing, ovaries from three females for each independent experiment were collected and processed for RNA extraction after 48 h of dsRNA or PBS injection. Two independent experiments were performed, with approximately 20 individuals per treatment for each independent experiment.

Analysis of Relative Transcription by qPCR

qPCR reactions were carried out on Applied Biosystems StepOne™ platform, in a total volume of 15 μL, with 100 ng of cDNA, 250 nM of primers (final concentration) and Power Sybr Green Mix (Thermo Fisher, United States), following the manufacturer's recommendations. Specific primers are described in **Supplementary Table S3**. The cycling parameters for analyzing RmTOR, RmS6K and Rm4E-BP1 relative transcription were: 10 min at 95°C, followed by 40 cycles of denaturation at 95°C for 15 s and annealing at 60°C for 1 min. For the melt curve stage, the cycling parameters were: 95°C for 15 s, 1 min at 60°C, followed by 35 cycles, with a temperature

increase of 0.3°C in each cycle until reaching a final temperature of 95°C. Other cycling parameters for analyzing RmAKT and RmGSK-3β relative transcription were selected according to de Abreu et al. (2013) and Martins et al. (2015). Relative transcription was determined using the Ct values from each run on Relative transcription Software Tool—REST (Pfaffl, 2001). Elongation factor-1A (ELF-1A) was used as a reference gene (Nijhof et al., 2009). These and other features are detailed in **Supplementary File S1**.

Analysis of relative transcription by qPCR was used in five different experiments: (i) to evaluate relative transcription of RmTOR and RmAKT in BME26 cells treated with exogenous insulin; (ii) to evaluate relative transcription of RmS6K and Rm4E-BP1 after treatment with chemical inhibitors; (iii) to evaluate relative transcription of RmS6K and Rm4E-BP1 after gene silencing following dsRNA treatment; (iv) to evaluate the relative transcription of RmTOR, RmS6K, and Rm4E-BP1 in eggs at different stages of embryogenesis, using cDNA from 1st, 3rd, 5th, 7th, 9th, 12th, 15th, and 18th day of embryogenesis; and (v) to verify gene silencing following dsRNA treatment. All samples were analyzed in triplicates, in three independent experiments, except for dsRNA injection into tick females, which was performed in two independent experiments.

Determination of Ovarian Growth and Biological Parameters in dsRNA-Treated Females

After 48 h of dsRNA injection, ticks were dissected and 2 ovaries were collected for determination of ovarian growth, using the ovarian growth phase (OGP) system (Seixas et al., 2008). The ovaries were examined in a stereoscope and pictures were analyzed using the software ImageJ (Abràmoff et al., 2004). The proportion of mature oocytes was analyzed by measuring the area occupied by mature and immature oocytes in each image. Additionally, females treated with dsRNA or PBS injection, as well as eggs were collected for examination in a stereoscope and pictures were analyzed.

The biological parameters analyzed were: nutritional efficacy index (final weight of engorged tick/initial weight of engorged tick), eggs production index (EPI) [(weight of eggs/final weight of engorged tick) × 100)], weight of eggs 10 days after oviposition, weight of larvae 40 days after oviposition, and hatching rate (%) (Bennett, 1974; Fabres et al., 2010; Gonsioroski et al., 2012). Two independent experiments were performed, with approximately 20 individuals per treatment for each independent experiment.

Determination of Vitellin (Vt) Content in Eggs by SDS-PAGE and Dot Blot

Eggs from female ticks treated with dsRNA or PBS injection were collected 9 days after oviposition (10 eggs from each group) and homogenized in 10 mM Tris-HCl buffer, pH 7.4, containing a protease inhibitor cocktail (4EBSF, aprotinin, bestatin hydrochloride, E-64, EDTA, leupeptin hemisulfate salt), pepstatin A (1 mM), and Triton X-100 10%. The samples were kept on ice and immediately used for determination of vitellin content by sodium dodecyl sulfate polyacrylamide gel electrophoresis (SDS-PAGE) and dot blot.

SDS-PAGE was performed under denaturing conditions following the method of Laemmli (1970), followed of silver staining. For dot blot, each sample was spotted onto nitrocellulose membrane (5 μL per spot) and allowed to dry. The membranes were processed as follows: 1 h at room temperature with blocking solution (5% non-fat dry milk/PBS); overnight at 4°C with anti-Vt rabbit serum (1:1000 in blocking solution) (Canal et al., 1995), or blocking solution only, as control; three times 5-min washes with PBS; 1 h at room temperature with secondary antibody (anti-IgG alkaline phosphatase conjugate 1:5000 in blocking solution). Alkaline phosphatase detection was performed with nitro blue tetrazolium (NBT) and 5-bromo4-chloro-3- indolyl phosphate (BCIP) (Promega, United States) in 100 mM Tris pH 9.5 containing 5 mM $MgCl_2$ and 100 mM NaCl.

Statistical Analyses

Unpaired *t*-tests were used for relative transcription analyses, in the insulin-stimulation experiment, chemical inhibition, and gene silencing experiments. ANOVA followed by Dunnett's test was used in cell viability and cell counting experiments, for analysis of relative transcription during embryogenesis, and for assessment of biological parameters. All statistical analyses were performed using Graph Pad Prism version 6.01 Software (Graph Pad Software, Inc.).

RESULTS

TSP Components Are Conserved in *R. microplus*

In this study, we attempted to clone the ORFs of three members of the TSP: RmTOR, RmS6K, and Rm4E-BP1. We were able to sequence a partial RmTOR ORF of 1378 bp (GenBank accession MK598842), which encodes a 458-amino acid polypeptide. Multiple alignment of the deduced amino acid sequence for RmTOR showed 95% identity with the orthologous sequence from the tick *Haemaphysalis longicornis*. We also sequenced a partial RmS6K ORF of 425 bp (GenBank accession MK598841). Multiple alignment of the transcript encoding a S6K protein showed a highly conserved catalytic domain. The identity was 78% with the putative sequence from the tick *Ixodes scapularis*.

The complete sequence of a transcript encoding 4E-BP1 protein was obtained, corresponding to an ORF of 381 nucleotides (GenBank accession MK598840). The encoded protein has 126 amino acids and a predicted molecular weight of 13.3 kDa. Multiple alignment of the deduced amino acid sequence to Rm4E-BP1 identified highly conserved motifs and a high identity level with the orthologous sequences from *H. longicornis* and *I. scapularis* ticks (84 and 74%, respectively).

Phylogenetic analysis was performed using the complete amino acid sequence obtained for Rm4E-BP1 (**Supplementary Figure S2**). Sequences from 16 species of arthropods were used in the construction of a neighbor-joining tree. The analysis indicates divergences between tick species and other groups of arthropods; for example, sequences from *R. microplus* and

H. longicornis formed a single clade, while *I. scapularis* sequences were assigned to a distinct clade. Distant clades correspond to insects, such as bees, flies and mosquitoes. Taken together, these results demonstrate that RmTOR, RmS6K, and Rm4E-BP1 are conserved in *R. microplus* tick.

Exogenous Insulin Can Stimulate RmTOR Relative Transcription

ISP regulates TSP in several animal species (Hay and Sonenberg, 2004; Wullschleger et al., 2006; Hassan et al., 2013; Hatem et al., 2015; Yoon, 2017). To assess whether TSP can be regulated/stimulated by insulin in the cattle tick, BME26 embryonic cells were cultured in the absence or presence of fetal bovine serum (FBS), then incubated with or without exogenous insulin (de Abreu et al., 2009). After exposure to insulin, we evaluated the relative transcription of two targets of ISP and TSP: RmAKT and RmTOR (**Figure 1**).

We observed a higher relative transcription of both RmAKT and RmTOR when cells were incubated with insulin in the absence of FBS compared to cells incubated without insulin and with FBS (normal condition of the cells) (**Figure 1**). In addition, a statistical difference in RmAKT relative transcription was observed when cells were incubated with insulin in the absence of FBS compared to cells treated without insulin and without FBS (**Figure 1A**). However, we did not observe a statistical difference in RmTOR relative transcription when cells were incubated with insulin in the absence of FBS compared to cells incubated without insulin and without FBS (**Figure 1B**).

These results suggest that there is an insulin signaling that stimulates the relative transcription of targets of ISP and TSP in the cattle tick.

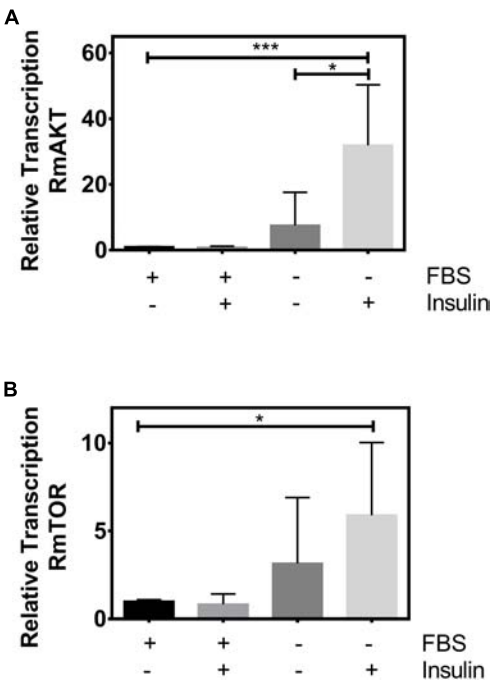

FIGURE 1 | Exogenous insulin stimulates RmAKT and RmTOR relative transcription. BME26 cells were cultured in the absence or presence of fetal bovine serum (FBS), then incubated with or without exogenous insulin (1 μM). Relative transcription of **(A)** RmAKT and **(B)** RmTOR were evaluated using the Pfaffl (2001) method with ELF-1A as reference gene (Nijhof et al., 2009). The plots represent mean ± SD of three independent experiments (*$p < 0.05$; ***$p < 0.0001$).

TOR Inhibition Affects Cell Viability and Membrane Integrity in BME26 Cells

Given the fundamental role played by TOR in cell viability in other species, we studied the effects of TOR chemical inhibition in the cattle tick, using tick embryonic BME26 cells. After treatment with different concentrations of rapamycin for 48 h, cell viability was evaluated by MTT assay (**Figure 2A**) and cell counting (**Figure 2A**, insert). Rapamycin concentrations above 0.12 μM caused significant reduction in cell viability, reaching 34% decrease at 2 μM, compared to control cells (cells treated with 0.073% DMSO) (**Figure 2A**); accordingly, we observed a significant reduction in cell density at rapamycin concentrations between 0.25 and 2 μM compared to control cells (**Figure 2A** insert).

Additionally, membrane integrity was analyzed in BME26 cells upon rapamycin treatment (**Figure 2B**). Rapamycin concentrations above 0.2 μM caused the cells to stain more intensely with propidium iodide, compared to control cells (red staining highlighted with yellow arrows in **Figure 2B**). Cells with intact membrane are generally not permeable to propidium iodide, therefore the intense staining indicated membrane damage. BME26 cells treated with rapamycin also exhibited chromatin condensation (pyknosis, indicated by green arrowheads in **Figure 2B**), a possible indication of cell death by apoptosis. Taken together, these results suggest that TOR is important for cell viability in BME26 cells.

TOR Regulates S6K and 4E-BP1 in BME26 Cells

To further investigate the possible interaction between ISP and TSP components in *R. microplus,* we performed gene silencing of three signaling components (RmAKT, RmGSK-3β and RmTOR) in BME26 cells. First, we confirmed gene silencing by qPCR (**Supplementary Figure S3**) and evaluated the relative transcription of downstream targets (**Supplementary Figure S4**). Gene silencing efficiency was 75% for RmAKT, 45% for RmGSK-3β, and 80% for RmTOR (**Supplementary Figure S3**). No difference was observed in the transcription of any of these targets upon dsRNA treatment (**Supplementary Figure S4**). However, a contrasting result was observed when using chemical inhibitors of each of the signaling components, namely 10-DEBC (AKT inhibitor), alsterpaullone (GSK inhibitor), and rapamycin (TOR inhibitor). Rapamycin treatment caused reduced transcription levels of RmS6K and Rm4E-BP1 when compared to control treatment (**Figure 3C**). In contrast, AKT and GSK-3β chemical inhibition (**Figures 3A,B**) did not cause any detectable difference in the relative transcription of the downstream targets. Taken together, these results lead us to believe that TOR regulates S6K and 4E-BP1 in BME26 cells.

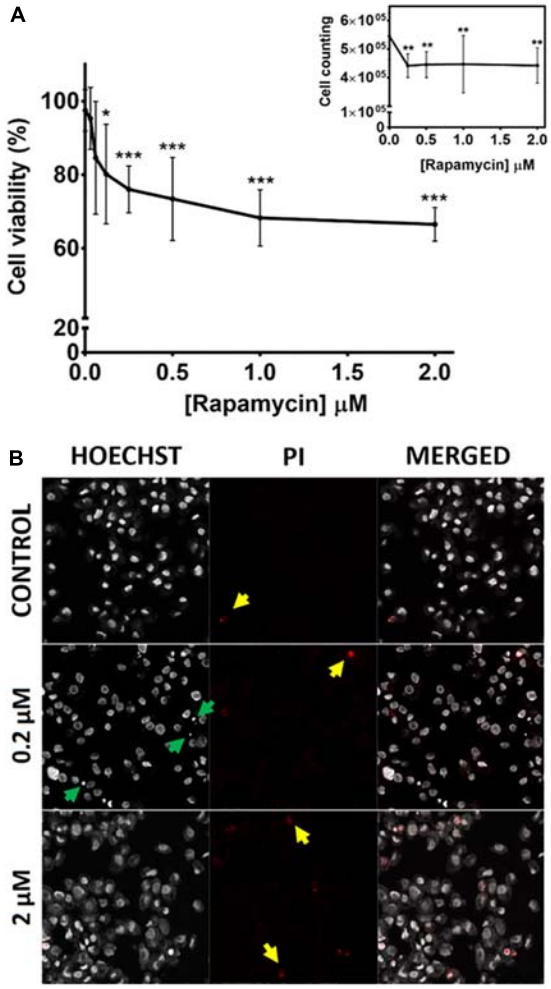

FIGURE 2 | TOR inhibition affects viability and membrane integrity in BME26 cells. BME26 cells were treated with rapamycin (0.03 to 2 μM) for 48 h. Cells treated with 0.073% DMSO were used as the control group. **(A)** Cell viability was analyzed by MTT assay and cell counting (insert). Results were normalized to control exposed to vehicle alone (DMSO). Plots present mean ± SD of three independent experiments (*$p < 0.05$; **$p < 0.005$; ***$p < 0.0001$). **(B)** Membrane integrity of the treated cells was evaluated following de Abreu et al. (2013). Cells were stained with Hoechst 33342 (left column) and propidium iodide (center column and yellow arrows). Events of pyknosis are indicated by green arrows. Images were obtained in a confocal fluorescence microscope at 400x magnification.

RmTOR Is Transcribed During Tick Embryogenesis

With the main goal of investigating the role of TSP in *R. microplus* embryogenesis, we evaluated the transcriptional profile of RmTOR, RmS6K, and Rm4E-BP1 during embryo development (**Figure 4**). Developmental stages are depicted in **Figure 4A**: the initial stage represents the 1st to 3rd day after oviposition (DAO), characterized by cleavages starting inside the yolk and further cell divisions; the middle stage corresponds to the end of 6th to 7th DAO, characterized by the beginning of germ band extension and generation of abdominal segments; the final stage comprises the 15th to 18th DAO, characterized by a nearly complete dorsal closure. The highest level of RmTOR relative transcription was observed in the first day, decreasing to about half the initial levels in the subsequent days, then surging again in the final developmental stage, between days 15 and 18 (**Figure 4B**). On the other hand, RmS6K and Rm4E-BP1 transcriptional levels, which were also highest on the first day after oviposition, markedly decreased during all the remaining of the embryogenesis period (**Figures 4C,D**). The data might indicate a role for TOR during tick development.

RmTOR Gene Silencing in Female Ticks Affects Ovarian Development, Vitellin Content in Eggs, and Egg Hatching

RmTOR was silenced by RNAi in partially engorged female ticks in order to study its role during *R. microplus* embryogenesis. We observed lower levels of TOR transcripts in ovaries from ticks treated with RmTOR-dsRNA compared to dsGFP-injected control (gene silencing efficiency was 77%) (**Supplementary Figure S5**). After 48 h of injection, ovaries dissected from females treated with dsTOR showed a slightly delayed development compared with controls (**Figure 5A**). According to the ovarian growth phase (OGP) system proposed by Seixas et al. (2008), dsTOR-injected females had ovaries classified as stage 3, while ovaries from the PBS control group were classified as stage 4. Also, ovaries from dsTOR group showed a reduced proportion of mature follicles (**Figure 5A**, black area in pie charts).

Eggs laid by females treated with dsTOR showed an atypical external appearance when observed on day 10 after the start of oviposition, in contrast to the typical morphology observed in eggs from the control groups (PBS and dsGFP) (**Figure 5B**). Recognizing that vitellogenesis is a fundamental process in tick development which can be regulated by TSP via S6K (Umemiya-Shirafuji et al., 2012), we investigated vitellin content in eggs from females subjected to gene silencing (**Figure 6**). Eggs from female ticks treated with dsRNA or PBS injection were collected 9 days after oviposition, when important morphological and biochemical events occur, including: the final development of the germ band, formation of the abdominal segments, early formation of the four pairs of legs. Also at this stage, a great reduction in carbohydrate content takes place, suggesting that gluconeogenic processes are necessary to sustain egg development (Moraes et al., 2007; Logullo et al., 2009; Santos et al., 2013; Martins et al., 2018). SDS-PAGE, followed by densitometric analyses of the three major VT subunits (120, 105, and 70 kDa), and dot blot demonstrated a lower vitellin content in eggs laid by dsTOR-treated females when compared with controls. Accordingly, we also observed a lower total protein content in these eggs.

The nutritional efficacy index was not affected by RmTOR gene knockdown (**Figure 7A**), indicating that dsRNA injection did not affect feeding behavior. Also, egg weight and the egg production index remained unaffected in dsTOR-injected group (**Figures 7B,C**). In contrast, a significant reduction in the weight of larvae and in hatching rate was observed after TOR gene silencing in comparison with control groups after 40 days

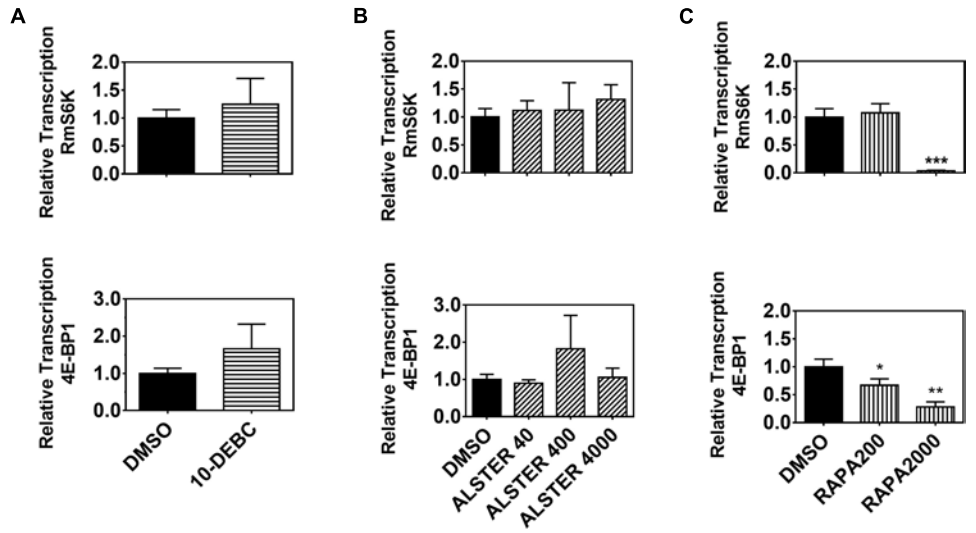

FIGURE 3 | Transcription of downstream ISP/TSP targets requires TOR enzymatic activity. Relative transcription of two downstream targets (S6K and 4E-BP1) was evaluated 24 h after BME26 cells were treated with chemical inhibitors of: **(A)** AKT (10-DEBC 12 μM), **(B)** GSK (alsterpaullone 40, 400 and 4000 nM), or **(C)** TOR (rapamycin 200 and 2000 nM) or vehicle (0.073% DMSO) as control. Relative transcription was calculated according to the Pfaffl (2001) method using ELF-1A as reference gene (Nijhof et al., 2009), and data were analyzed in unpaired t-test. The plots present mean ± SD from three independent experiments (*$p < 0.05$; **$p < 0.005$; ***$p < 0.0001$).

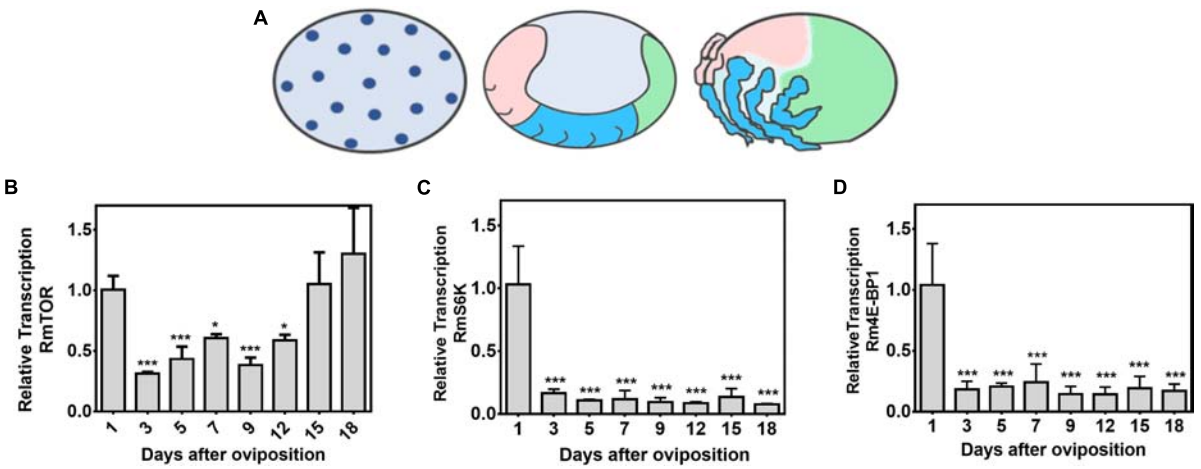

FIGURE 4 | RmTOR, but not RmS6K and Rm4E-BP1, is transcribed at different stages during tick embryogenesis. The different stages of *R. microplus* embryo development (according to Santos et al., 2013) are depicted in **(A)** (initial stage; middle stage; and final stage). Relative transcription of RmTOR **(B)**, RmS6K **(C)**, and Rm4E-BP1 **(D)** was determined by qPCR using cDNA from eggs collected on different days of embryogenesis. Relative transcription was calculated according to the Pfaffl (2001) method using ELF-1A as reference gene (Nijhof et al., 2009), and data were analyzed by one-way ANOVA, followed by Dunnett's test, where all samples were compared with 1-day-old eggs. Plots present mean ± SD from three independent experiments (*$p < 0.05$; ***$p < 0.0001$ compared with first day after oviposition).

(**Figures 7D,E**). Taken together, these results led us to believe that TOR is important for tick reproduction.

DISCUSSION

TSP is a central regulatory pathway in energy metabolism, and nutritional status monitoring in eukaryotic cells. TSP is fundamental for protein synthesis, transcription, cell growth, cell survival, proliferation, aging, and autophagy, from yeast to vertebrates (Hawkins et al., 2006; Wullschleger et al., 2006; Guertin and Sabatini, 2007; Jung et al., 2010; Katewa and Kapahi, 2011; Kim and Guan, 2011; Laplante and Sabatini, 2012; Beauchamp and Platanias, 2013; Na et al., 2015; Kennedy et al., 2016). This paper demonstrates that the role of TOR is conserved in ticks and fundamental in the embryogenesis of the cattle tick *R. microplus*.

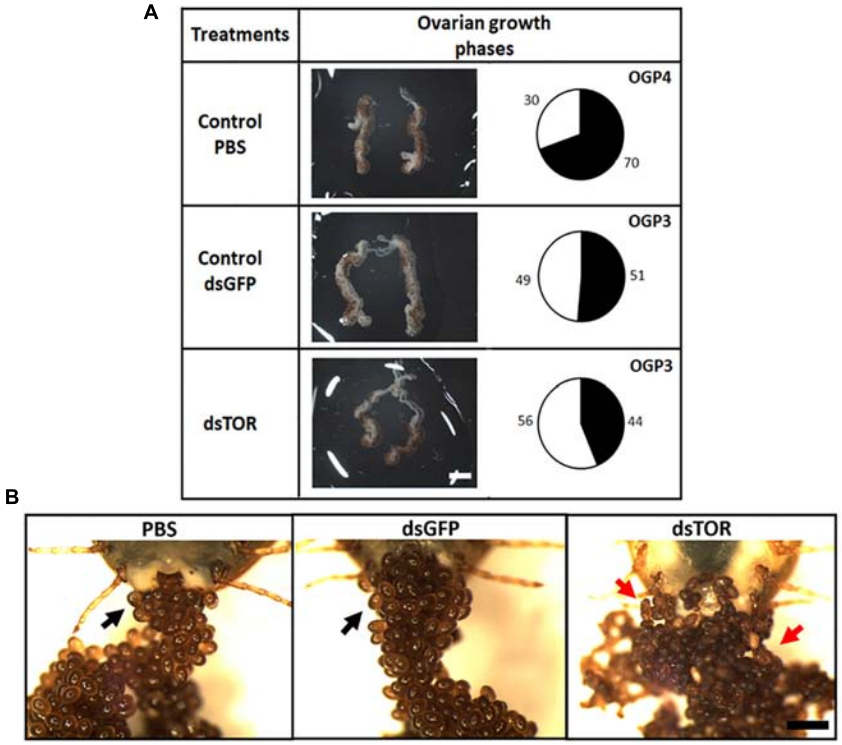

FIGURE 5 | TOR gene silencing delays ovarian development and affects oviposition in *R. microplus*. **(A)** Females were dissected 48 h after dsRNA treatment for optical assessment of ovarian development. Ovaries were examined in a stereoscope. The relative proportion of mature to immature oocytes was analyzed by area measurements, as described in Section "Materials and Methods." Proportion of area occupied by developed oocytes is indicated in pie charts (black). Scale bar: 2 mm. **(B)** Representative images show the effect on oviposition of dsRNA injection (dsTOR, dsGFP or PBS control) in partially engorged female ticks. Eggs were examined under stereoscope 10 days after the start of oviposition. Normal eggs are indicated by black arrows and atypical eggs are indicated by red arrows. Scale bar: 1 mm.

In order to investigate components of TSP in the cattle tick *R. microplus*, we sequenced and analyzed either partial or complete nucleotide sequences coding for RmTOR, RmS6K and Rm4E-BP1.

TOR is an atypical serine/threonine kinase of the phosphatidylinositol kinase-related kinase (PIKK) family, that comprises two conserved complexes, named TOR complex 1 (TORC1) and TOR complex 2 (TORC2) (Hay and Sonenberg, 2004; Wullschleger et al., 2006; Soulard et al., 2009; Loewith, 2011; Laplante and Sabatini, 2012; Sabatini, 2017). TORC1 acts as an integrator of extracellular and intracellular signals, such as the nutrient availability, growth factors, and stress energy levels (Hay and Sonenberg, 2004; Reiling and Sabatini, 2006; Wullschleger et al., 2006; Zoncu et al., 2011). These signals can be cooperative or antagonists, enabling the cell to adjust and perform appropriate responses for each condition (Howell and Manning, 2011). This TOR complex stimulates S6 kinase (S6K) activity, as well as phosphorylating factor 4E-Binding Protein 1 (4E-BP1) that leads to the release of eukaryotic initiation factor 4E (eIF4E), thus initiating translation of specific mRNAs (Engelman et al., 2006; Shaw and Cantley, 2006; Ma and Blenis, 2009). A domain associated with the complex regulator known as Raptor (regulatory-associated protein of mTOR) defines mTORC1, and is inhibited by rapamycin, a property that originated the protein name, 'Target Of Rapamycin' (Loewith, 2011).

On the other hand, the less studied TORC2 has been considered to be insensitive to nutrient levels, but responsive to growth factor signaling, possibly by associating with translating ribosomes in response to growth factor receptor-PI3K activation (Oh et al., 2010; Zinzalla et al., 2011), and to function mainly by activating protein kinase B (AKT) via Ser473 phosphorylation (Sarbassov et al., 2005; Masui et al., 2014). It can also phosphorylate other protein kinase A, G, and C families (AGC kinases). TORC2 may also be regulated by amino acids, depending on specific substrates and cellular context. Ribosomes have been reported to be direct activators of mTORC2 in response to insulin (Zinzalla et al., 2011; Takahara and Maeda, 2013).

Target of rapamycin protein is structurally defined by the presence of several conserved domains such as the HEAT repeat, focal adhesion target (FAT), FKBP12/rapamycin binding (FRB), kinase, and FAT C-terminal (FATC) domains, starting from the N-terminus (Yang et al., 2013; Maegawa et al., 2015). In the cattle tick *R. microplus,* the amino acid sequence of RmTOR is composed of three classical domains: FRB domain, a catalytic domain, and FATC domain. In the amino acid sequence of RmS6K, we found a conserved catalytic domain (Hanks and Quinn, 1991; Hunter, 1991). Investigating

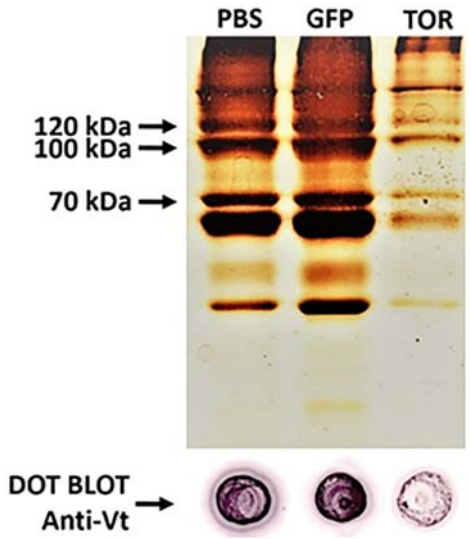

FIGURE 6 | TOR gene silencing decreased vitellin (Vt) content in eggs. Eggs from female ticks treated with dsRNA injection (PBS, dsGFP and dsTOR) were collected 9 days after oviposition (middle stage). The samples were used for determination of vitellin content by SDS-PAGE **(top)** and dot blot **(bottom)**. Arrows on the **(top)** panel indicate the approximate molecular weight of the three major VT subunits (120, 105, and 70 kDa).

the identity of RmTOR and RmS6K with orthologous sequences, a high identity with other ticks was observed, proving the conservation of these proteins.

From full-length 4E-BP1 cDNA, the deduced amino acid sequence presented three motifs: RAIP, TOS, and YXXXXLφ, important regulatory sites highly conserved among invertebrate and vertebrate organisms (Mader et al., 1995; Lawrence and Abraham, 1997; Gingras et al., 1999; Schalm and Blenis, 2002; Tee and Proud, 2002). It is worth noting that three isoforms were identified from vertebrates (Pause et al., 1994; Rousseau et al., 1996; Poulin et al., 1998), while only one isoform was identified in arthropods (Gutzeit et al., 1994; Bernal and Kimbrell, 2000; Lasko, 2000; Cormier et al., 2001; Miron et al., 2001; Gu et al., 2011; Kume et al., 2012). In the present study, only one 4E-BP1 isoform was identified from *R. microplus,* and showed high identity with the orthologous sequences from *H. longicornis* and *I. scapularis* ticks.

Recognizing that the TSP is conserved in *R. microplus,* our main goal was to investigate the role of this pathway in *R. microplus* embryogenesis. Therefore, we evaluated the transcriptional profile of RmTOR, RmS6K, and Rm4E-BP1 during embryo development (**Figures 4B–D**). Transcriptional levels of RmS6K and Rm4E-BP1 were highest on the first day after oviposition, which suggests that these transcripts are of maternal origin. In the tick *H. longicornis*, TOR controls vitellogenesis via activation of S6 kinase (S6K) in pre-ovipositional stage (Umemiya-Shirafuji et al., 2012), and 4E-BP1 is highly relevant for lipid storage during the non-feeding starvation period (Kume et al., 2012). S6K and 4E-BP1 have also been implicated in embryo development in other models. For example, in *Xenopus laevis*, S6K activity is high immediately after fertilization, presumably for altering the translational capacity available for mRNAs lacking a 5′-TOP region (Schwab et al., 1999). Also, in sea urchin embryos, dissociation of 4E-BP1 of its target, the eukaryotic initiation factor 4E (eIF4E), is functionally important for the first mitotic division (Salaün et al., 2004; Salaun et al., 2005). In the mosquito *Aedes aegypti,* RNA-interference-mediated depletion of S6K demonstrated that the TOR pathway is required for mosquito egg development (Hansen et al., 2005), while depletion of 4E-BP1 affects mosquito longevity and is critical in modulating translational events that are dependent on nutritional, developmental and stress conditions (Roy and Raikhel, 2012).

RmTOR transcriptional profile demonstrated a large mRNA deposition by the mother in 1-day-old eggs, followed by lower levels during the middle stage of embryogenesis. Toward the final stage, when dorsal closure is undergoing, TOR transcript levels rise again to levels equivalent to the initial stage (**Figure 4B**). In mosquitoes, TOR serves as a key regulator to complete vitellogenesis (Hansen et al., 2004, 2005). Previous studies showed that chemical inhibition of TOR with rapamycin or RNAi-mediated gene depletion resulted in significant down-regulation of vitellogenin transcription after amino acid stimulation in fat body culture system *in vitro*, as well as in inhibition of egg development *in vivo* (Hansen et al., 2004, 2005). In *Drosophila*, TSP activation promotes yolk catabolism in embryos (Kuhn et al., 2015). It remains to be determined if these *R. microplus* TSP components function in similar ways.

To further elucidate the role of TOR in *R. microplus* embryogenesis, two strategies were employed in this study: chemical inhibition in tick embryonic cell line (BME26), and RNAi in partially engorged female ticks. It is known that the study of TSP functions in invertebrate and vertebrate organisms has been greatly advanced by exploring the mechanism of action of rapamycin, a specific inhibitor of TOR, which has several clinical applications as immunosuppressive, antifungal, and anticancer (Shor et al., 2009; Thoreen et al., 2009; Wu and Hu, 2010; Zaytseva et al., 2012). BME26 cells treated with concentrations of rapamycin greater than 0.12 μM showed a significant decrease in cell viability and cell counting (**Figure 2A**). Furthermore, we observed that BME26 cells treated with concentrations greater than 0.2 μM showed a higher intensity of staining with propidium iodide compared with control cells, and exhibited chromatin condensation (**Figure 2B**). Similar results have been described for T lymphocytes and endothelial cells (Barilli et al., 2008; Wang et al., 2012). It has been shown that rapamycin causes G1 arrest and blocks G1 to S phase transition in fibroblasts and B-CLL cells (Hashemolhosseini et al., 1998; Decker et al., 2003). It can also cause dysregulation of the two effector proteins of the TSP pathway, S6K and 4E-BP1, causing negative impact in cap-dependent initiation of translation (Beretta et al., 1996), in cellular migration (Poon et al., 1996), and activating cell death by apoptosis or necrosis (Shi et al., 1995; Barilli et al., 2008). Our results demonstrate that TOR directly affects cell viability in tick embryonic cells.

To assess whether TSP can be regulated/stimulated by insulin in the cattle tick, BME26 embryonic cells were exposed to insulin,

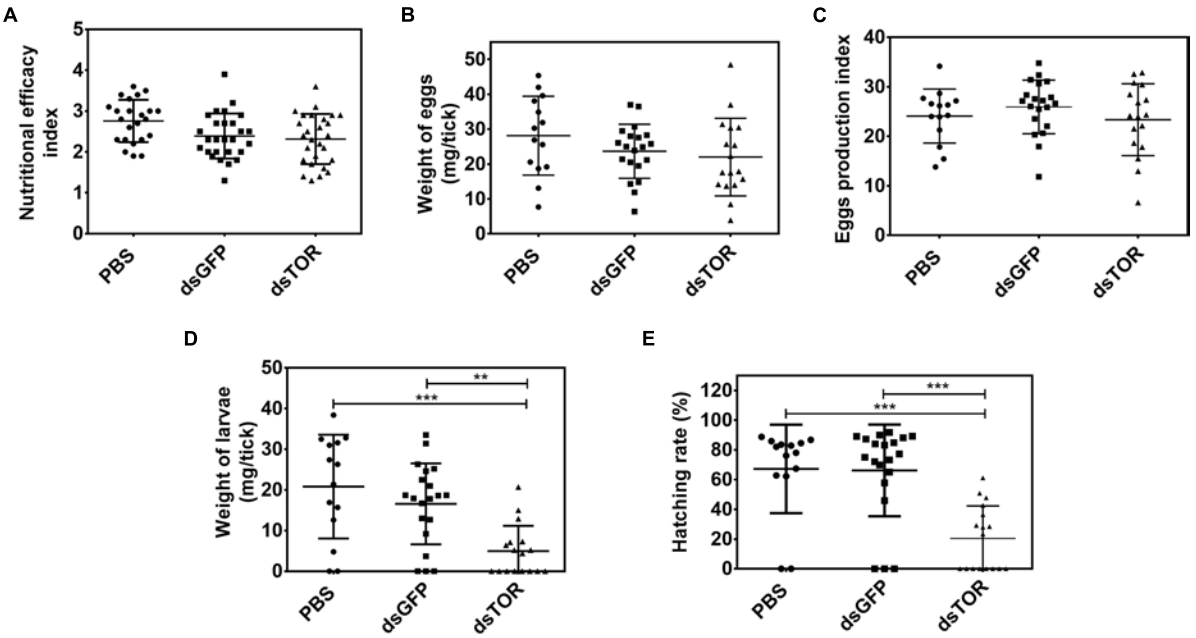

FIGURE 7 | TOR gene silencing affects egg hatching in *R. microplus*. Biological parameters were analyzed after dsRNA treatment (dsTOR, dsGFP, or PBS control) in partially engorged female ticks. **(A)** Nutritional efficacy index; **(B)** weight of eggs (mg/tick); **(C)** egg production index (EPI); **(D)** weight of larvae (mg/tick); and **(E)** hatching rate (%). Plots present mean ± SD from two independent experiments (**$p < 0.005$; ***$p < 0.0001$).

and the relative transcription of two components of ISP and TSP pathways (AKT and TOR) was evaluated (**Figure 1**). We observed a higher relative transcription of TOR when cells were incubated with insulin in the absence of FBS (**Figure 1B**), indicating that TOR can be stimulated by exogenous insulin. This interaction between the two pathways has also been demonstrated in other species (Hay and Sonenberg, 2004; Wullschleger et al., 2006; Hassan et al., 2013; Hatem et al., 2015; Yoon, 2017). Also, AKT relative transcription was higher when cells were incubated with insulin in the absence of FBS when compared to control cells (**Figure 1A**), an even more marked increase than observed for TOR. This can be attributed to the direct regulation of AKT by insulin (de Abreu et al., 2009, 2013). In previous studies, we demonstrated that *R. microplus* embryonic cell line (BME26) displays an insulin-responsive machinery, and that AKT/GSK3 axis integrates glycogen metabolism and cell survival (de Abreu et al., 2009, 2013). Likewise, our results suggest that ISP can stimulate/regulate TSP in the tick *R. microplus*.

Target of rapamycin gene silencing in partially engorged females caused a slight delay in ovary development (**Figure 5A**), an atypical external appearance in 10-day-old eggs (**Figure 5B**), lower vitellin and protein content (**Figure 6**), and decreased hatching rate in comparison with control groups (**Figure 7**), results that altogether suggest TOR is important for tick embryo development and tick reproduction. Collectively, our data agree with studies developed in other arthropods. For example, in *Drosophila,* using maternal short hairpin RNAs technology (shRNA), it was observed that shRNA-TOR embryos were smaller than control embryos, and showed significant DNA fragmentation post-cellularization (Kuhn et al., 2015). According to a recent report in *Lepeophtheirus salmonis*, RNAi mediated knockdown of TOR pathway genes resulted in inhibition of egg development and maturation (Sandlund et al., 2018). In other models, TSP has been studied for its role in oogenesis or/and vitellogenesis, for example in the red flour beetle *Tribolium castaneum* (Parthasarathy and Palli, 2011), the brown planthopper *Nilaparvata lugens* (Zhai et al., 2015; Lu et al., 2016), in the mosquito *Aedes aegypti* (Hansen et al., 2004, 2005), and in *H. longicornis* tick (Umemiya-Shirafuji et al., 2012). However, this is the first study reporting the importance of TSP during embryogenesis in ticks. It has been demonstrated that, in several insect species, ISP and TSP serve as important sensors of nutritional status and are required for initiation of reproductive events, such as oocyte maturation and vitellogenin synthesis. Previous work by our group demonstrated that vitellin, the main tick yolk protein, is internalized by the oocyte (Seixas et al., 2018) and it is a reservoir of heme for embryo development (Logullo et al., 2002). We show in the present study that TOR silencing decreases vitellin content in eggs 9 days after oviposition (**Figure 6**), which means that development will likely be affected. Accordingly, we also observed a lower total protein content in eggs laid by dsTOR-treated females when compared with controls; this may be related to the fact that TOR is involved in the processes of ribosomal biogenesis and protein biosynthesis (Oh et al., 2010; Zinzalla et al., 2011).

Finally, with the aim of studying the interconnection between ISP/TSP signaling pathways in *R. microplus,* we investigated the transcription of downstream targets (S6K and 4E-BP1) in BME26 embryonic cell line treated with chemical inhibition or RNAi of upstream regulators (**Figure 4** and **Supplementary Figure S3**).

The results show a lower relative transcription for S6K and 4E-BP1 when treated with rapamycin, in comparison with untreated cells, demonstrating a consistent inhibitory effect and suggesting a potentially conserved function of TSP pathway in ticks (**Figure 3**). Rapamycin treatment has allowed the investigation of TSP roles in diverse processes, for example: regulation of juvenile hormone and expression of vitellogenin in the cockroach *Blattella germanica* (Maestro et al., 2009); deposition of proteins important for embryogenesis in blood-fed *A. aegypti* females (Gulia-Nuss et al., 2011; Pérez-Hedo et al., 2013); and regulation of S6K and 4E-BP proteins in different organisms (Stewart et al., 1996; Montagne et al., 1999; Oldham et al., 2000; Umemiya-Shirafuji et al., 2012). In contrast, we did not observe any difference in the relative transcription of downstream targets in BME26 cells treated with chemical inhibitor of AKT or GSK3, suggesting that, unlike TOR, these proteins are not involved in S6K and 4E-BP1 regulation. When BME26 cells were treated with RNAi for AKT, GSK3, or TOR, the transcription of downstream targets seemed to be unaffected (**Supplementary Figure S4**), suggesting that the effect of gene silencing was not sufficient to affect protein function, and that regulation occurs mainly at the post-transcriptional level, as classically described in kinase pathways (Woodgett, 2001; Riehle and Brown, 2003; Hay and Sonenberg, 2004; Sarbassov et al., 2005; Albert and Hall, 2015).

The cattle tick *R. microplus* is an obligate hematophagous arthropod that poses a serious threat to dairy and cattle production. Amongst the indirect effects of its diet is the transmission of various pathogens, and the resulting diseases can cause large losses in livestock production, reduce farm incomes, increase costs for consumers, and threaten trade between regions and/or world markets (Tabor et al., 2017). Strategies for the control of diseases transmitted by this arthropod vector have been managed mainly with two general approaches: (i) focusing on interventions, such as vaccines or drug treatments, and (ii) focusing on the development of strategies based on vector knowledge, aimed at reducing transmission by reducing vector density or interfering with the vector's ability to transmit the disease-causing pathogen (Murray et al., 2012). Our research group focuses on this second strategy, aiming to contribute knowledge to the understanding of *R. microplus* tick biology, studying mainly the aspects related to energy metabolism during embryogenesis. ISP/TSP signaling pathways are the main bridge between nutrient detection system and development of different cellular processes, such as cell viability, growth, and proliferation in arthropods (Grewal, 2009; Benmimoun et al., 2012; Pérez-Hedo et al., 2013).

Here, we demonstrate that the role of TOR is conserved in ticks and fundamental for tick reproductive physiology. Combined with previous work by our group (de Abreu et al., 2013), we show that TOR is a regulatory target in *R. microplus* embryogenesis and can be considered an important target for tick control. Future studies should be able to understand the side effects of chemical inhibition in other cellular processes in the cattle tick.

DATA AVAILABILITY

The datasets generated for this study can be found in GenBank with the accession numbers MK598842, MK598841, and MK598840.

ETHICS STATEMENT

Animals used in the experiments were housed at Faculdade de Veterinária, Universidade Federal do Rio Grande do Sul (UFRGS) facilities. This research was conducted according to the ethics and methodological guidance, in agreement with the International and National Directives and Norms for Animal Experimentation Ethics Committee of Universidade Federal do Rio Grande do Sul (Process No. 14403).

AUTHOR CONTRIBUTIONS

CW, LA, and CL conceived and designed the experiments. CW and TA performed the experiments. CW, RN-d-F, ISV, and CL contributed reagents, materials, and analysis tools. CW, LA, RN-d-F, ISV, and CL drafted the manuscript. CW, LA, RN-d-F, ISV, and CL critically revised the manuscript.

FUNDING

This study was financed in part by the Coordenação de Aperfeiçoamento de Pessoal de Nível Superior - Brazil (CAPES) - Finance Code 001. We acknowledge the support by grants from the CNPq-Instituto Nacional de Ciência e Tecnologia de Entomologia Molecular, FAPERJ, and FAPERGS (Brazil).

SUPPLEMENTARY MATERIAL

The Supplementary Material for this article can be found online at: https://www.frontiersin.org/articles/10.3389/fphys.2019.00965/full#supplementary-material

REFERENCES

Abràmoff, M., Magalhães, P., and Ram, S. (2004). Image processing with imageJ. *Biophotonics Int.* 11, 36–42. doi: 10.1117/1.3589100

Albert, V., and Hall, M. N. (2015). mTOR signaling in cellular and organismal energetics. *Curr. Opin. Cell Biol.* 33, 55–66. doi: 10.1016/j.ceb.2014.12.001

Barilli, A., Visigalli, R., Sala, R., Gazzola, G. C., Parolari, A., Tremoli, E., et al. (2008). In human endothelial cells rapamycin causes mTORC2 inhibition and impairs cell viability and function. *Cardiovasc. Res.* 78, 563–571. doi: 10.1093/cvr/cvn024

Beauchamp, E. M., and Platanias, L. C. (2013). The evolution of the TOR pathway and its role in cancer. *Oncogene* 32, 3923–3932. doi: 10.1038/onc.2012.567

Benmimoun, B., Polesello, C., Waltzer, L., and Haenlin, M. (2012). Dual role for Insulin/TOR signaling in the control of hematopoietic progenitor maintenance in *Drosophila*. *Development* 139, 1713–1717. doi: 10.1242/dev.080259

Bennett, G. F. (1974). Oviposition of *Boophilus microplus* (Canestrini) (*Acarida*: *Ixodidae*). II. Influence of temperature, humidity and light. *Acarologia* 16, 251–257.

Beretta, L., Gingras, A. C., Svitkin, Y. V., Hall, M. N., and Sonenberg, N. (1996). Rapamycin blocks the phosphorylation of 4E-BP1 and inhibits cap-dependent initiation of translation. *EMBO J.* 15, 658–664. doi: 10.1002/j.1460-2075.1996.tb00398.x

Bernal, A., and Kimbrell, D. A. (2000). *Drosophila* thor participates in host immune defense and connects a translational regulator with innate immunity. *Proc. Natl. Acad. Sci. U.S A.* 97, 6019–6024. doi: 10.1073/pnas.100391597

Campos, E., Moraes, J., Façanha, A. R., Moreira, E., Valle, D., Abreu, L., et al. (2006). Kinetics of energy source utilization in *Boophilus microplus* (Canestrini, 1887) (*Acari*: *Ixodidae*) embryonic development. *Vet. Parasitol.* 138, 349–357. doi: 10.1016/j.vetpar.2006.02.004

Canal, C. W., Maia, H. M., Vaz Júnior, I. S., Chies, J. M., Farias, N. A., Masuda, A., et al. (1995). Changing patterns of vitellin-related peptides during development of the cattle tick *Boophilus microplus*. *Exp. Appl. Acarol.* 19, 325–336. doi: 10.1007/bf00052390

Cormier, P., Pyronnet, S., Morales, J., Mulner-Lorillon, O., Sonenberg, N., and Bellé, R. (2001). eIF4E association with 4E-BP decreases rapidly following fertilization in sea urchin. *Dev. Biol.* 232, 275–283. doi: 10.1006/dbio.2001.0206

de Abreu, L. A., Calixto, C., Waltero, C. F., Della Noce, B. P., Githaka, N. W., Seixas, A., et al. (2013). The conserved role of the AKT/GSK3 axis in cell survival and glycogen metabolism in *Rhipicephalus* (*Boophilus*) microplus embryo tick cell line BME26. *Biochim. Biophys. Acta* 1830, 2574–2582. doi: 10.1016/j.bbagen.2012.12.016

de Abreu, L. A., Fabres, A., Esteves, E., Masuda, A., da Silva Vaz, I., Daffre, S., et al. (2009). Exogenous insulin stimulates glycogen accumulation in *Rhipicephalus* (*Boophilus*) microplus embryo cell line BME26 via PI3K/AKT pathway. *Comp. Biochem. Physiol. B Biochem. Mol. Biol.* 153, 185–190. doi: 10.1016/j.cbpb.2009.02.016

de la Fuente, J., Estrada-Pena, A., Venzal, J. M., Kocan, K. M., and Sonenshine, D. E. (2008). Overview: ticks as vectors of pathogens that cause disease in humans and animals. *Front. Biosci.* 13, 6938–6946. doi: 10.2741/3200

Decker, T., Hipp, S., Ringshausen, I., Bogner, C., Oelsner, M., Schneller, F., et al. (2003). Rapamycin-induced G1 arrest in cycling B-CLL cells is associated with reduced expression of cyclin D3, cyclin E, cyclin A, and survivin. *Blood* 101, 278–285. doi: 10.1182/blood-2002-01-0189

Engelman, J. A., Luo, J., and Cantley, L. C. (2006). The evolution of phosphatidylinositol 3-kinases as regulators of growth and metabolism. *Nat. Rev. Genet.* 7, 606–619. doi: 10.1038/nrg1879

Esteves, E., Lara, F. A., Lorenzini, D. M., Costa, G. H. N., Fukuzawa, A. H., Pressinotti, L. N., et al. (2008). Cellular and molecular characterization of an embryonic cell line (BME26) from the tick *Rhipicephalus* (*Boophilus*) microplus. *Insect Biochem. Mol. Biol.* 38, 568–580. doi: 10.1016/j.ibmb.2008.01.006

Fabres, A., De Andrade, C., Guizzo, M., Sorgine, M., De, O., Paiva-Silva, G., et al. (2010). Effect of GSK-3 activity, enzymatic inhibition and gene silencing by RNAi on tick oviposition and egg hatching. *Parasitology* 137, 1537–1546. doi: 10.1017/S0031182010000284

Ghosh, S., Azhahianambi, P., and Yadav, M. P. (2007). Upcoming and future strategies of tick control: a review. *J. Vector Borne Dis.* 44, 79–89.

Gingras, A. C., Gygi, S. P., Raught, B., Polakiewicz, R. D., Abraham, R. T., Hoekstra, M. F., et al. (1999). Regulation of 4E-BP1 phosphorylation: a novel two-step mechanism. *Genes Dev.* 13, 1422–1437. doi: 10.1101/gad.13.11.1422

Gonsioroski, A. V., Bezerra, I. A., Utiumi, K. U., Driemeier, D., Farias, S. E., da Silva Vaz, I., et al. (2012). Anti-tick monoclonal antibody applied by artificial capillary feeding in *Rhipicephalus* (*Boophilus*) microplus females. *Exp. Parasitol.* 130, 359–363. doi: 10.1016/J.EXPPARA.2012.02.006

Graf, J. F., Gogolewski, R., Leach-Bing, N., Sabatini, G. A., Molento, M. B., Bordin, E. L., et al. (2004). Tick control: an industry point of view. *Parasitology* 129(Suppl), S427–S442.

Grewal, S. S. (2009). Insulin/TOR signaling in growth and homeostasis: a view from the fly world. *Int. J. Biochem. Cell Biol.* 41, 1006–1010. doi: 10.1016/j.biocel.2008.10.010

Grisi, L., Massard, C. L., Moya Borja, G. E., and Pereira, J. B. (2002). Impacto econômico das principais ectoparasitoses em bovinos no Brasil. *Hora Vet.* 125, 8–10.

Gu, S.-H., Young, S.-C., Tsai, W.-H., Lin, J.-L., and Lin, P.-L. (2011). Involvement of 4E-BP phosphorylation in embryonic development of the silkworm. *Bombyx mori. J. Insect Physiol.* 57, 978–985. doi: 10.1016/j.jinsphys.2011.04.014

Guerrero, F. D., Miller, R. J., and Pérez de León, A. A. (2012). Cattle tick vaccines: many candidate antigens, but will a commercially viable product emerge? *Int. J. Parasitol.* 42, 421–427. doi: 10.1016/j.ijpara.2012.04.003

Guertin, D. A., and Sabatini, D. M. (2007). Defining the role of mTOR in cancer. *Cancer Cell* 12, 9–22. doi: 10.1016/j.ccr.2007.05.008

Gulia-Nuss, M., Robertson, A. E., Brown, M. R., and Strand, M. R. (2011). Insulin-like peptides and the target of rapamycin pathway coordinately regulate blood digestion and egg maturation in the mosquito *Aedes aegypti*. *PLoS One* 6:e20401. doi: 10.1371/journal.pone.0020401

Gutzeit, H. O., Zissler, D., Grau, V., Liphardt, M., and Heinrich, U. R. (1994). Glycogen stores in mature ovarian follicles and young embryos of *Drosophila*: ultrastructural changes and some biochemical correlates. *Eur. J. Cell Biol.* 63, 52–60.

Hall, T. (1999). BioEdit: a user-friendly biological sequence aligment editor and analysis program for Windows 95/98/NT. *Nucleic Acids Symp. Ser.* 41, 95–98.

Hanks, S. K., and Quinn, A. M. (1991). Protein kinase catalytic domain sequence database: identification of conserved features of primary structure and classification of family members. *Methods Enzymol.* 200, 38–62. doi: 10.1016/0076-6879(91)00126-h

Hansen, I. A., Attardo, G. M., Park, J.-H., Peng, Q., and Raikhel, A. S. (2004). Target of rapamycin-mediated amino acid signaling in mosquito anautogeny. *Proc. Natl. Acad. Sci. U.S.A.* 101, 10626–10631. doi: 10.1073/pnas.0403460101

Hansen, I. A., Attardo, G. M., Roy, S. G., and Raikhel, A. S. (2005). Target of rapamycin-dependent activation of S6 kinase is a central step in the transduction of nutritional signals during egg development in a mosquito. *J. Biol. Chem.* 280, 20565–20572. doi: 10.1074/jbc.M500712200

Hashemolhosseini, S., Nagamine, Y., Morley, S. J., Desrivières, S., Mercep, L., and Ferrari, S. (1998). Rapamycin inhibition of the G1 to S transition is mediated by effects on cyclin D1 mRNA and protein stability. *J. Biol. Chem* 273, 14424–14429. doi: 10.1074/jbc.273.23.14424

Hassan, B., Akcakanat, A., Holder, A. M., and Meric-Bernstam, F. (2013). Targeting the PI3-kinase/Akt/mTOR signaling pathway. *Surg. Oncol. Clin. N. Am.* 22, 641–664. doi: 10.1016/j.soc.2013.06.008

Hatem, N. E., Wang, Z., Nave, K. B., Koyama, T., and Suzuki, Y. (2015). The role of juvenile hormone and insulin/TOR signaling in the growth of *Manduca sexta*. *BMC Biol.* 13:44. doi: 10.1186/s12915-015-0155-z

Hawkins, P. T., Anderson, K. E., Davidson, K., and Stephens, L. R. (2006). Signalling through Class I PI3Ks in mammalian cells. *Biochem. Soc. Trans.* 34, 647–662. doi: 10.1042/BST0340647

Hay, N., and Sonenberg, N. (2004). Upstream and downstream of mTOR. *Genes Dev.* 18, 1926–1945. doi: 10.1101/gad.1212704

Howell, J. J., and Manning, B. D. (2011). mTOR couples cellular nutrient sensing to organismal metabolic homeostasis. *Trends Endocrinol. Metab.* 22, 94–102. doi: 10.1016/j.tem.2010.12.003

Hunter, T. (1991). Protein kinase classification. *Methods Enzymol.* 200, 3–37. doi: 10.1016/0076-6879(91)00125-G

Jia, K., Chen, D., and Riddle, D. L. (2004). The TOR pathway interacts with the insulin signaling pathway to regulate C. elegans larval development, metabolism and life span. *Development* 131, 3897–3906. doi: 10.1242/dev.01255

Jung, C. H., Ro, S.-H., Cao, J., Otto, N. M., and Kim, D.-H. (2010). mTOR regulation of autophagy. *FEBS Lett.* 584, 1287–1295. doi: 10.1016/j.febslet.2010.01.017

Katewa, S. D., and Kapahi, P. (2011). Role of TOR signaling in aging and related biological processes in *Drosophila melanogaster*. *Exp. Gerontol.* 46, 382–390. doi: 10.1016/j.exger.2010.11.036

Kennedy, B. K., Lamming, D. W., Albert, V., Svensson, K., Shimobayashi, M., Colombi, M., et al. (2016). The mechanistic target of rapamycin: the grand conducTOR of metabolism and aging. *Cell Metab.* 23, 990–1003. doi: 10.1016/j.cmet.2016.05.009

Kim, J., and Guan, K.-L. (2011). Amino acid signaling in TOR activation. *Annu. Rev. Biochem.* 80, 1001–1032. doi: 10.1146/annurev-biochem-062209-4

Kuhn, H., Sopko, R., Coughlin, M., Perrimon, N., and Mitchison, T. (2015). The atg1-tor pathway regulates yolk catabolism in *Drosophila embryos*. *Development* 142, 3869–3878. doi: 10.1242/dev.125419

Kume, A., Boldbaatar, D., Takazawa, Y., Umemiya-Shirafuji, R., Tanaka, T., and Fujisaki, K. (2012). RNAi of the translation inhibition gene 4E-BP identified from the hard tick, *Haemaphysalis longicornis*, affects lipid storage during the off-host starvation period of ticks. *Parasitol. Res.* 111, 889–896. doi: 10.1007/s00436-012-2915-9

Laemmli, U. K. (1970). Cleavage of structural proteins during the assembly of the head of bacteriophage T4. *Nature* 227, 680–685. doi: 10.1038/227680a0

Laplante, M., and Sabatini, D. M. (2012). mTOR Signaling. *Cold Spring Harb. Perspect. Biol.* 4, doi: 10.1101/cshperspect.a011593

Lasko, P. (2000). The *Drosophila melanogaster* genome: translation factors and RNA binding proteins. *J. Cell Biol.* 150, F51–F56. doi: 10.1080/19336934.2016.1220464

Lawrence, J. C., and Abraham, R. T. (1997). PHAS/4E-BPs as regulators of mRNA translation and cell proliferation. *Trends Biochem. Sci.* 22, 345–349. doi: 10.1016/s0968-0004(97)01101-8

Loewith, R. (2011). A brief history of TOR. *Biochem. Soc. Trans.* 39, 437–442. doi: 10.1042/BST0390437

Logullo, C., Moraes, J., Dansa-Petretski, M., Vaz, I. S. Jr., Masuda, A., Sorgine, M. H. F., et al. (2002). Binding and storage of heme by vitellin from the cattle tick, *Boophilus microplus*. *Insect Biochem. Mol. Biol.* 32, 1805–1811. doi: 10.1016/S0965-1748(02)00162-5

Logullo, C., Witola, W. H., Andrade, C., Abreu, L., Gomes, J., da Silva Vaz, I., et al. (2009). Expression and activity of glycogen synthase kinase during vitellogenesis and embryogenesis of *Rhipicephalus* (*Boophilus*) microplus. *Vet. Parasitol.* 161, 261–269. doi: 10.1016/j.vetpar.2009.01.029

Louis, K., and Siegel, A. (2011). "Cell viability analysis using trypan blue: manual and automated methods," in *Mammalian Cell Viability*, eds J. Martin and Stoddart (New York, NY: Humana Press).

Lu, K., Chen, X., Liu, W.-T., and Zhou, Q. (2016). TOR pathway-mediated juvenile hormone synthesis regulates nutrient-dependent female reproduction in nilaparvata lugens (Stål). *Int. J. Mol. Sci.* 17:438. doi: 10.3390/ijms17040438

Ma, X. M., and Blenis, J. (2009). Molecular mechanisms of mTOR-mediated translational control. *Nat. Rev. Mol. Cell Biol.* 10, 307–318. doi: 10.1038/nrm2672

Mader, S., Lee, H., Pause, A., and Sonenberg, N. (1995). The translation initiation factor eIF-4E binds to a common motif shared by the translation factor eIF-4 gamma and the translational repressors 4E-binding proteins. *Mol. Cell. Biol.* 15, 4990–4997. doi: 10.1128/MCB.15.9.4990

Maegawa, K., Takii, R., Ushimaru, T., and Kozaki, A. (2015). Evolutionary conservation of TORC1 components, TOR, Raptor, and LST8, between rice and yeast. *Mol. Genet. Genomics* 290, 2019–2030. doi: 10.1007/s00438-015-1056-0

Maestro, J. L., Cobo, J., and Bellés, X. (2009). Target of rapamycin (TOR) mediates the transduction of nutritional signals into juvenile hormone production. *J. Biol. Chem.* 284, 5506–5513. doi: 10.1074/jbc.M807042200

Martins, R., Noce, B. Della, Waltero, C. F., Pessoa Costa, E., Araujo De Abreu, L., Githaka, N. W., et al. (2015). Non-Classical gluconeogenesis-dependent glucose metabolism in *Rhipicephalus* microplus embryonic cell line BME26. *Int. J. Mol. Sci.* 16, 1821–1839. doi: 10.3390/ijms16011821

Martins, R., Ruiz, N., Fonseca, R. N., da Vaz Junior, I., da, S., and Logullo, C. (2018). The dynamics of energy metabolism in the tick embryo. *Rev. Bras. Parasitol. Vet.* 27, 259–266. doi: 10.1590/S1984-296120180051

Masui, K., Cavenee, W. K., and Mischel, P. S. (2014). mTORC2 in the center of cancer metabolic reprogramming. *Trends Endocrinol. Metab.* 25, 364–373. doi: 10.1016/j.tem.2014.04.002

Merino, O., Alberdi, P., Pérez de la Lastra, J. M., and de la Fuente, J. (2013). Tick vaccines and the control of tick-borne pathogens. *Front. Cell. Infect. Microbiol.* 3:30. doi: 10.3389/fcimb.2013.00030

Miron, M., Verdú, J., Lachance, P. E., Birnbaum, M. J., Lasko, P. F., and Sonenberg, N. (2001). The translational inhibitor 4E-BP is an effector of PI(3)K/Akt signalling and cell growth in *Drosophila*. *Nat. Cell Biol.* 3, 596–601. doi: 10.1038/35078571

Montagne, J., Stewart, M. J., Stocker, H., Hafen, E., Kozma, S. C., and Thomas, G. (1999). *Drosophila* S6 kinase: a regulator of cell size. *Science* 285, 2126–2129. doi: 10.1126/science.285.5436.2126

Moraes, J., Galina, A., Alvarenga, P. H., Rezende, G. L., Masuda, A., da Silva Vaz, I., et al. (2007). Glucose metabolism during embryogenesis of the hard tick *Boophilus microplus*. *Comp. Biochem. Physiol. A Mol Integr. Physiol.* 146, 528–533. doi: 10.1016/j.cbpa.2006.05.009

Murray, C. J. L., Vos, T., Lozano, R., Naghavi, M., Flaxman, A. D., Michaud, C., et al. (2012). Disability-adjusted life years (DALYs) for 291 diseases and injuries in 21 regions, 1990-2010: a systematic analysis for the global burden of disease study 2010. *Lancet* 380, 2197–2223. doi: 10.1016/S0140-6736(12)61689-4

Na, H.-J., Park, J.-S., Pyo, J.-H., Jeon, H.-J., Kim, Y.-S., Arking, R., et al. (2015). Metformin inhibits age-related centrosome amplification in *Drosophila* midgut stem cells through AKT/TOR pathway. *Mech. Ageing Dev.* 149, 8–18. doi: 10.1016/j.mad.2015.05.004

Naito, Y., Yamada, T., Matsumiya, T., Ui-Tei, K., Saigo, K., and Morishita, S. (2005). dsCheck: highly sensitive off-target search software for double-stranded RNA-mediated RNA interference. *Nucleic Acids Res.* 33, W589–W591. doi: 10.1093/nar/gki419

Nijhof, A. M., Balk, J. A., Postigo, M., and Jongejan, F. (2009). Selection of reference genes for quantitative RT-PCR studies in *Rhipicephalus* (*Boophilus*) microplus and *Rhipicephalus* appendiculatus ticks and determination of the expression profile of Bm86. *BMC Mol. Biol.* 10:112. doi: 10.1186/1471-2199-10-112

Oh, W. J., Wu, C., Kim, S. J., Facchinetti, V., Julien, L.-A., Finlan, M., et al. (2010). mTORC2 can associate with ribosomes to promote cotranslational phosphorylation and stability of nascent Akt polypeptide. *EMBO J.* 29, 3939–3951. doi: 10.1038/emboj.2010.271

Oldham, S., Montagne, J., Radimerski, T., Thomas, G., and Hafen, E. (2000). Genetic and biochemical characterization of dTOR, the *Drosophila* homolog of the target of rapamycin. *Genes Dev.* 14, 2689–2694. doi: 10.1101/gad.845700

Parizi, L. F., Githaka, N. W., Logullo, C., Konnai, S., Masuda, A., Ohashi, K., et al. (2012). The quest for a universal vaccine against ticks: cross-immunity insights. *Vet. J.* 194, 158–165. doi: 10.1016/j.tvjl.2012.05.023

Parthasarathy, R., and Palli, S. R. (2011). Molecular analysis of nutritional and hormonal regulation of female reproduction in the red flour beetle, Tribolium castaneum. Insect Biochem. *Mol. Biol.* 41, 294–305. doi: 10.1016/j.ibmb.2011.01.006

Pause, A., Belsham, G. J., Gingras, A.-C., Donzé, O., Lin, T.-A., Lawrence, J. C., et al. (1994). Insulin-dependent stimulation of protein synthesis by phosphorylation of a regulator of 5'-cap function. *Nature* 371, 762–767. doi: 10.1038/371762a0

Pérez-Hedo, M., Rivera-Perez, C., and Noriega, F. G. (2013). The insulin/TOR signal transduction pathway is involved in the nutritional regulation of juvenile hormone synthesis in *Aedes aegypti*. *Insect Biochem. Mol. Biol.* 43, 495–500. doi: 10.1016/j.ibmb.2013.03.008

Pfaffl, M. W. (2001). A new mathematical model for relative quantification in real-time RT-PCR. *Nucleic Acids Res.* 29, e45.

Poon, M., Marx, S. O., Gallo, R., Badimon, J. J., Taubman, M. B., and Marks, A. R. (1996). Rapamycin inhibits vascular smooth muscle cell migration. *J. Clin. Invest.* 98, 2277–2283. doi: 10.1172/JCI119038

Poulin, F., Gingras, A. C., Olsen, H., Chevalier, S., and Sonenberg, N. (1998). 4E-BP3, a new member of the eukaryotic initiation factor 4E-binding protein family. *J. Biol. Chem.* 273, 14002–14007. doi: 10.1074/jbc.273.22.14002

Reck, J., Berger, M., Terra, R. M. S., Marks, F. S., da Silva Vaz, I., Guimarães, J. A., et al. (2009). Systemic alterations of bovine hemostasis due to *Rhipicephalus* (*Boophilus*) microplus infestation. *Res. Vet. Sci.* 86, 56–62. doi: 10.1016/j.rvsc.2008.05.007

Reiling, J. H., and Sabatini, D. M. (2006). Stress and mTORture signaling. *Oncogene* 25, 6373–6383. doi: 10.1038/sj.onc.1209889

Riehle, M. A., and Brown, M. R. (2003). Molecular analysis of the serine/threonine kinase akt and its expression in the mosquito *Aedes aegypti*. *Insect Mol. Biol.* 12, 225–232. doi: 10.1046/j.1365-2583.2003.00405.x

Rodriguez-Vivas, R. I. I., Trees, A. J. J., Rosado-Aguilar, J. A. A., Villegas-Perez, S. L. L., and Hodgkinson, J. E. E. (2011). Evolution of acaricide resistance: phenotypic and genotypic changes in field populations of Rhipicephalus (*Boophilus*) microplus in response to pyrethroid selection pressure. *Int. J. Parasitol.* 41, 895–903. doi: 10.1016/j.ijpara.2011.03.012

Rousseau, D., Gingras, A. C., Pause, A., and Sonenberg, N. (1996). The eIF4E-binding proteins 1 and 2 are negative regulators of cell growth. *Oncogene* 13, 2415–2420.

Roy, S. G., and Raikhel, A. S. (2012). Nutritional and hormonal regulation of the TOR effector 4E-binding protein (4E-BP) in the mosquito *Aedes aegypti*. *FASEB J.* 26, 1334–1342. doi: 10.1096/fj.11-189969

Sabatini, D. M. (2017). Twenty-five years of mTOR: uncovering the link from nutrients to growth. *Proc. Natl. Acad. Sci. U.S.A.* 114, 11818–11825. doi: 10.1073/pnas.1716173114

Salaun, P., Boulben, S., Mulner-Lorillon, O., Bellé, R., Sonenberg, N., Morales, J., et al. (2005). Embryonic-stage-dependent changes in the level of eIF4E-binding proteins during early development of sea urchin embryos. *J. Cell Sci.* 118, 1385–1394. doi: 10.1242/jcs.01716

Salaün, P., Le Breton, M., Morales, J., Bellé, R., Boulben, S., Mulner-Lorillon, O., et al. (2004). Signal transduction pathways that contribute to CDK1/cyclin B activation during the first mitotic division in sea urchin embryos. *Exp. Cell Res.* 296, 347–357. doi: 10.1016/j.yexcr.2004.02.013

Sandlund, L., Kongshaug, H., Nilsen, F., and Dalvin, S. (2018). Molecular charaLepeophthei cterization and functional analysis of components of the TOR pathway of the salmon louse, rus salmonis (Krøyer, 1838). *Exp. Parasitol.* 88, 83–92. doi: 10.1016/j.exppara.2018.04.004

Santos, V. T., Ribeiro, L., Fraga, A., de Barros, C. M., Campos, E., Moraes, J., et al. (2013). The embryogenesis of the tick *Rhipicephalus* (*Boophilus*) microplus: the establishment of a new chelicerate model system. *Genesis* 51, 803–818. doi: 10.1002/dvg.22717

Sarbassov, D. D., Guertin, D. A., Ali, S. M., and Sabatini, D. M. (2005). Phosphorylation and regulation of Akt/PKB by the rictor-mTOR complex. *Science* 307, 1098–1101. doi: 10.1126/science.1106148

Schalm, S. S., and Blenis, J. (2002). Identification of a conserved motif required for mTOR signaling. *Curr. Biol.* 12, 632–639. doi: 10.1016/S0960-9822(02)00762-5

Schwab, M. S., Kim, S. H., Terada, N., Edfjäll, C., Kozma, S. C., Thomas, G., et al. (1999). p70(S6K) controls selective mRNA translation during oocyte maturation and early embryogenesis in *Xenopus laevis*. *Mol. Cell. Biol.* 19, 2485–2494. doi: 10.1128/mcb.19.4.2485

Seixas, A., Alzugaray, M. F., Tirloni, L., Parizi, L. F., Pinto, A. F. M., Githaka, N. W., et al. (2018). Expression profile of *Rhipicephalus* microplus vitellogenin receptor during oogenesis. *Ticks Tick Borne Dis.* 9, 72–81. doi: 10.1016/j.ttbdis.2017.10.006

Seixas, A., Friesen, K. J., and Kaufman, W. R. (2008). Effect of 20-hydroxyecdysone and haemolymph on oogenesis in the ixodid tick Amblyomma hebraeum. *J. Insect Physiol.* 54, 1175–1183. doi: 10.1016/j.jinsphys.2008.05.004

Shaw, R. J., and Cantley, L. C. (2006). Ras, PI(3)K and mTOR signalling controls tumour cell growth. *Nature* 441, 424–430. doi: 10.1038/nature04869

Shi, Y., Frankel, A., Radvanyi, L. G., Penn, L. Z., Miller, R. G., and Mills, G. B. (1995). Rapamycin enhances apoptosis and increases sensitivity to cisplatin in vitro. *Cancer Res.* 55, 1982–1988.

Shor, B., Gibbons, J. J., Abraham, R. T., and Yu, K. (2009). Targeting mTOR globally in cancer. thinking beyond rapamycin. *Cell Cycle* 8, 3831–3837. doi: 10.4161/cc.8.23.10070

Soulard, A., Cohen, A., and Hall, M. N. (2009). TOR signaling in invertebrates. *Curr. Opin. Cell Biol.* 21, 825–836. doi: 10.1016/j.ceb.2009.08.007

Stewart, M. J., Berry, C. O., Zilberman, F., Thomas, G., and Kozma, S. C. (1996). The *Drosophila* p70s6k homolog exhibits conserved regulatory elements and rapamycin sensitivity. *Proc. Natl. Acad. Sci. U S.A.* 93, 10791–10796. doi: 10.1073/pnas.93.20.10791

Tabor, A. E., Ali, A., Rehman, G., Rocha Garcia, G., Zangirolamo, A. F., Malardo, T., et al. (2017). Cattle tick *Rhipicephalus* microplus-host interface: a review of resistant and susceptible host responses. *Front. Cell. Infect. Microbiol.* 7:506. doi: 10.3389/fcimb.2017.00506

Takahara, T., and Maeda, T. (2013). Evolutionarily conserved regulation of TOR signalling. *J. Biochem.* 154, 1–10. doi: 10.1093/jb/mvt047

Tamura, K., Peterson, D., Peterson, N., Stecher, G., Nei, M., and Kumar, S. (2011). MEGA5: Molecular evolutionary genetics analysis using maximum likelihood, evolutionary distance, and maximum parsimony methods. *Mol. Biol. Evol.* 28, 2731–2739. doi: 10.1093/molbev/msr121

Tee, A. R., and Proud, C. G. (2002). Caspase cleavage of initiation factor 4E-binding protein 1 yields a dominant inhibitor of cap-dependent translation and reveals a novel regulatory motif. *Mol. Cell. Biol.* 22, 1674–1683. doi: 10.1128/MCB.22.6.1674-1683.2002

Thoreen, C. C., Kang, S. A., Chang, J. W., Liu, Q., Zhang, J., Gao, Y., et al. (2009). An ATP-competitive mammalian target of rapamycin inhibitor reveals rapamycin-resistant functions of mTORC1. *J. Biol. Chem.* 284, 8023–8032. doi: 10.1074/jbc.M900301200

Umemiya-Shirafuji, R., Boldbaatar, D., Liao, M., Battur, B., Rahman, M. M., Kuboki, T., et al. (2012). Target of rapamycin (TOR) controls vitellogenesis via activation of the S6 kinase in the fat body of the tick, *Haemaphysalis longicornis*. *Int. J. Parasitol.* 42, 991–998. doi: 10.1016/j.ijpara.2012.08.002

Wang, B., He, Q., Mao, Y., Chen, Z., Jiang, H., and Chen, J. (2012). Rapamycin inhibiting Jurkat T cells viability through changing mRNA expression of serine/threonine protein phosphatase 2A. *Transpl. Immunol.* 26, 50–54. doi: 10.1016/j.trim.2011.10.004

Woodgett, J. R. (2001). Judging a protein by more than its name: GSK-3. *Sci. STKE* 2001:re12. doi: 10.1126/stke.2001.100.re12

Wu, P., and Hu, Y.-Z. (2010). PI3K/Akt/mTOR pathway inhibitors in cancer: a perspective on clinical progress. *Curr. Med. Chem.* 17, 4326–4341. doi: 10.2174/092986710793361234

Wullschleger, S., Loewith, R., and Hall, M. N. (2006). TOR signaling in growth and metabolism. *Cell* 124, 471–484. doi: 10.1016/j.cell.2006.01.016

Yang, H., Rudge, D. G., Koos, J. D., Vaidialingam, B., Yang, H. J., and Pavletich, N. P. (2013). mTOR kinase structure, mechanism and regulation. *Nature* 497, 217–223. doi: 10.1038/nature12122

Yoon, M.-S. (2017). The Role of mammalian target of rapamycin (mTOR) in insulin signaling. *Nutrients* 9:E1176. doi: 10.3390/nu9111176

Zaytseva, Y. Y., Valentino, J. D., Gulhati, P., Evers, B. M., and Mark Evers, B. (2012). mTOR inhibitors in cancer therapy. *Cancer Lett.* 319, 1–7. doi: 10.1016/j.canlet.2012.01.005

Zhai, Y., Sun, Z., Zhang, J., Kang, K., Chen, J., and Zhang, W. (2015). Activation of the TOR signalling pathway by glutamine regulates insect fecundity. *Sci. Rep.* 5:10694. doi: 10.1038/srep10694

Zinzalla, V., Stracka, D., Oppliger, W., and Hall, M. N. (2011). Activation of mTORC2 by association with the ribosome. *Cell* 144, 757–768. doi: 10.1016/j.cell.2011.02.014

Zoncu, R., Efeyan, A., and Sabatini, D. M. (2011). mTOR: from growth signal integration to cancer, diabetes and ageing. *Nat. Rev. Mol. Cell Biol.* 12, 21–35. doi: 10.1038/nrm3025

Conflict of Interest Statement: The authors declare that the research was conducted in the absence of any commercial or financial relationships that could be construed as a potential conflict of interest.

frontiers in Physiology

ORIGINAL RESEARCH
published: 07 August 2019
doi: 10.3389/fphys.2019.01008

The Cattle Fever Tick, *Rhipicephalus microplus,* as a Model for Forward Pharmacology to Elucidate Kinin GPCR Function in the Acari

*Caixing Xiong[1], Dwight Baker[2] and Patricia V. Pietrantonio[1]**

[1] Department of Entomology, Texas A&M University, College Station, TX, United States, [2] Department of Biochemistry and Biophysics, Texas A&M University, College Station, TX, United States

The success of the acaricide amitraz, a ligand of the tick tyramine/octopamine receptor (a G protein-coupled receptor; GPCR), stimulated interest on arthropod-specific GPCRs as targets to control tick populations. This search advances tick physiology because little is known about the pharmacology of tick GPCRs, their endogenous ligands or their physiological functions. Here we explored the tick kinin receptor, a neuropeptide GPCR, and its ligands. Kinins are pleiotropic insect neuropeptides but their function in ticks is unknown. The endogenous tick kinins are unknown and their cDNAs have not been cloned in any species. In contrast, more than 271 insect kinin sequences are available in the DINeR database. To fill this gap, we cloned the kinin cDNA from the cattle fever tick, *Rhipicephalus microplus,* which encodes 17 predicted kinins, and verified the kinin gene structure. We predicted the kinin precursor sequences from additional seven tick species, including *Ixodes scapularis*. All species showed an expansion of kinin paracopies. The "kinin core" (minimal active sequence) of tick kinins FX_1X_2WGamide is similar to those in insects. Pro was predominant at the X_2 position in tick kinins. Toward accelerating the discovery of kinin function in ticks we searched for novel synthetic receptor ligands. We developed a dual-addition assay for functional screens of small molecules and/or peptidomimetics that uses a fluorescent calcium reporter. A commercial library of fourteen small molecules antagonists of mammalian neurokinin (NK) receptors was screened using this endpoint assay. One acted as full antagonist (TKSM02) with inhibitory concentration fifty (IC_{50}) of ∼45 μM, and three were partial antagonists. A subsequent calcium bioluminescence assay tested these four antagonists through kinetic curves and confirmed TKSM02 as full antagonist and one as partial antagonist (TKSM14). Antagonists of NK receptors displayed selectivity (>10,000-fold) on the tick kinin receptor. Three peptidomimetic ligands of the mammalian NK receptors (hemokinin 1, antagonist G, and spantide I) were tested in the bioluminescence assay but none were active. Forward approaches may accelerate discovery of kinin ligands, either as reagents for tick physiological research or as lead molecules for acaricide development, and they demonstrate that selectivity is achievable between mammalian and tick neuropeptide systems.

Keywords: leucokinin receptor, endogenous tick kinins, neuropeptide GPCR, dual-addition assay, small molecule screen, neurokinin antagonists, southern cattle tick

OPEN ACCESS

Edited by:
Itabajara Silva Vaz Jr., Federal University of Rio Grande do Sul, Brazil

Reviewed by:
Greg Pask, Bucknell University, United States
Yoonseong Park, Kansas State University, United States

****Correspondence:***
Patricia V. Pietrantonio
p-pietrantonio@tamu.edu

Specialty section:
This article was submitted to Invertebrate Physiology, a section of the journal Frontiers in Physiology

Received: *03 May 2019*
Accepted: *22 July 2019*
Published: *07 August 2019*

Citation:
Xiong C, Baker D and Pietrantonio PV (2019) The Cattle Fever Tick, Rhipicephalus microplus, as a Model for Forward Pharmacology to Elucidate Kinin GPCR Function in the Acari. Front. Physiol. 10:1008. doi: 10.3389/fphys.2019.01008

INTRODUCTION

The cattle fever tick or southern cattle tick, *Rhipicephalus microplus* (Canestrini), and the diseases it transmits cause significant losses to the livestock industry in tropical and subtropical regions of the world (Pérez de León et al., 2012). Considering the lack of effective vaccines against many of these vector-borne pathogens, vector control is still the most efficient approach to block disease transmission. However, worldwide distribution of tick resistance to the most commonly used acaricides, such as amitraz (formamidines), pyrethroids, organophosphates, and ivermectin was detected in tick populations (Guerrero et al., 2012; Pohl et al., 2012). In the near future, the current available pesticides will fail to control populations of these ticks as many exhibit multiple mechanisms of resistance with apparently no fitness cost. Pesticides safe to non-target species with novel modes of actions in vectors are needed. Here we describe a model study using a forward pharmacological approach to investigate a tick neuropeptide G protein-coupled receptor (GPCR) as potential target for tick control (**Figure 1**). This receptor, known as leucokinin-like peptide receptor (LKR) (accession AF228521), or myokinin receptor (Holmes et al., 2000, 2003) has been suggested as a promising novel target for pest control (Lees et al., 2010; Audsley and Down, 2015; Guerrero et al., 2016; Pietrantonio et al., 2018). A kinin peptidomimetic is antifeedant and lethal to the pea aphid (Smagghe et al., 2010), prevents the blood feeding to repletion in the kissing bug, *Rhodnius prolixus,* decreasing the chance of a successful molt (Lange et al., 2016) and triggers avoidance behavior in the mosquito *Aedes aegypti* when given in a sucrose solution (Kwon et al., 2016).

Kinin receptors are invertebrate-specific neuropeptide GPCRs (Pietrantonio et al., 2018). The kinin system is widely distributed in the Acari and in nearly every order of insects, except Coleoptera (beetles) (Halberg et al., 2015; Derst et al., 2016). Insect kinins are involved in many important physiological processes: they regulate diuresis (Hayes et al., 1989; Kersch and Pietrantonio, 2011), feeding (Al-Anzi et al., 2010; Kwon et al., 2016; Zandawala et al., 2018), pre-ecdysis (Kim et al., 2006) as well as tracheal air clearance post-ecdysis (Adams et al., 2000). In the fruit fly *D. melanogaster*, both leucokinin- and leucokinin receptor (LKR; also known as drosokinin receptor) loss-of-function mutant strains showed significant increases in resistance to desiccation, ionic stress (only tested in LK-mutant fly), and starvation (Cannell et al., 2016; Zandawala et al., 2018). Prior work has deorphanized kinin receptors of two vector species, the yellow fever mosquito *Ae. aegypti* (Pietrantonio et al., 2005) and the cattle fever tick *R. microplus* (Holmes et al., 2003), and found the kinin system is important in regulating diuresis and sugar feeding in *Ae. aegypti* (Kersch and Pietrantonio, 2011; Kwon et al., 2016). The most recent RNAi-mediated silencing of the kinin receptor in the cattle fever tick caused a reproductive fitness cost (Brock et al., 2019). While our cloning of this receptor represented the first known neuropeptide GPCR in the Acari, there has been no urgent need in establishing the endogenous ligand of the *R. microplus* tick. This was because receptor functional studies were performed using insect kinin core peptide analogs that activated the tick receptor. The endogenous ligands of the kinin receptor(s) feature a short C-terminal pentapeptide (Phe-X_1-X_2-Trp-Gly-NH_2) as the minimal peptide core required for activity (Nachman et al., 2002). Insect kinins are among the most well characterized neuropeptides with currently 271 endogenous kinins identified in insects (Yeoh et al., 2017). In the synganglion of the tick *Ixodes ricinus*, we previously identified kinin peptide (leucokinin-like) immunoreactivity, and mass spectral analyses of synganglia of adult *R. microplus* and *Ix. ricinus* detected a strong signal at ∼1,008 Da, consistent with the mass of kinin peptides (Neupert et al., 2005). However, the endogenous cDNAs for kinin peptides have not yet been cloned in any tick species and tick sequences are unknown. Herein, we predicted and cloned the putative kinin cDNA which shows an amplification in the number of kinin ligands in *R. microplus,* similar to what was predicted for *Ix. scapularis* (Gulia-Nuss et al., 2016).

Previous functional studies with mosquito- and tick-kinin recombinant receptors tested insect kinin peptides, or kinin peptidomimetics designed for increased stability and/or penetration through the arthropod cuticle (Taneja-Bageshwar et al., 2006; Xiong et al., 2019). Results showed that the tick kinin receptor was a more permissive receptor; i.e., it was activated by more ligands and with lower EC_{50} than the mosquito receptor. There are no true orthologous mammalian receptors of the tick kinin receptor, which makes it an attractive potential selective target. However, the most similar mammalian receptors are the neurokinin receptors that mediate the biological actions of tachykinins (Pennefather et al., 2004). As also the tick kinin receptor is activated by the tachykinin of the stable fly (Holmes et al., 2003), we hypothesized that ligands of the mammalian neurokinin receptors could be active on the permissive tick kinin receptor.

To test this, a dual-addition assay was developed to determine the activity of peptidomimetics and small molecule ligands of neurokinin receptors on the tick kinin receptor. This assay allows discriminating agonist and antagonist activity in a single assay. Here we report the first small molecule ligands showing antagonistic activities on the tick kinin receptor. Although these small molecules did not exhibit high potency, this exploratory screen provides the methodological foundation for future screens of small molecule libraries in high-throughput mode. The results suggested mammalian NK receptor ligands displayed high selectivity over the arthropod kinin receptor. Additionally, the quantified activities of antagonists provide structure-activity data that helps define ligand-receptor interactions in computational models.

MATERIALS AND METHODS

In silico Prediction of the Kinin Precursor cDNA Sequence in *R. microplus*

In search of the gene encoding the kinin precursor of the cattle fever tick, *R. microplus*, we first manually curated the protein sequence of the identified orthologous gene from the black legged tick, *Ixodes scapularis*, present in the genomic

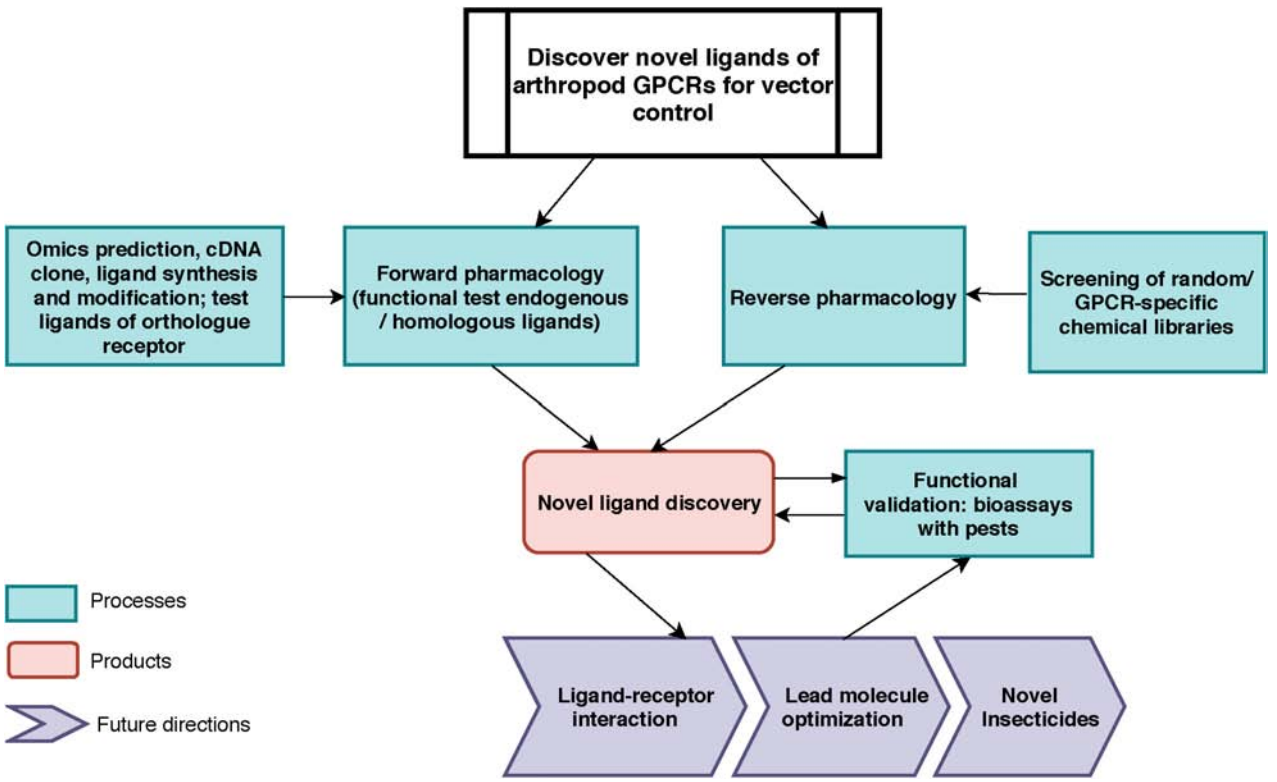

FIGURE 1 | Toward vector control: General work-flow for the discovery of novel ligands for arthropod vector GPCRs. For forward pharmacological characterization of GPCR, endogenous ligands can be identified by *in silico* predictions, cloning, tissue extraction and purification, and subsequently be synthesized (e.g., neuropeptides). Ligands from known orthologs or pseudo-orthologous GPCRs from other animals could be tested (this work). For reverse pharmacology, GPCR-specific or random molecule libraries can be screened on the target GPCR. In both approaches, the active endogenous ligands and screened molecules will be validated through bioassays for their physiological functions *in vivo*. The outputs of this pipeline are: (1) endogenous ligand(s) identification; (2) novel small molecule discovery (3) knowledge of novel biological function of neuropeptide receptor; (4) data for receptor-ligand interactions modeling and for novel chemistry design.

scaffold (DS680282| 583-1410) (Gulia-Nuss et al., 2016). This predicted nucleotide sequence of the kinin gene was translated in the six potential frames. Once the correct open reading frame encoding 19 putative kinin peptides was identified, the putative start codon was located but the stop codon could not be predicted within that scaffold. The curated protein sequence was used as the query for local TBLASTN analyses at the National Center for Biotechnology Information (NCBI)[1] against the *R. microplus* (taxid: 6941) whole genome shotgun contig (WGS) (Rmi2.0; 2017), and its transcriptome shotgun assembly (TSA). The respective identified genomic fragments and transcripts were aligned with MegAlign (Lasergene, Madison, WI, United States) to assist with primer design for cDNA cloning. All sequence analyses in this study were performed with DNASTAR (Lasergene).

Cloning the Kinin Precursor cDNA

The synganglia of females fed for 5 days (non-repleted) of the pesticide-susceptible Gonzalez strain of *R.* (*Boophilus*) *microplus* were used for cDNA synthesis. Details on tick dissection, mRNA extraction and 3′- and 5′-RACE ready cDNA syntheses were as described previously (Yang et al., 2013). To obtain the cDNA that encodes the putative kinin precursor from *R. microplus*, specific primers (**Supplementary Table S1**) were designed based on the predicted transcript available in NCBI (GEEZ01003316). For 5′- or 3′-RACE (**Supplementary Figure S1**), reactions were carried out in 50 μl volume, as follows: 2 μl of 5′- or 3′-RACE-ready cDNA of synganglia was added into the mix of 1 × Phusion HF buffer, 0.2 mM each dNTPs, 0.5 μM of UPM (5′, 3′ Race kit, Clontech®, Mountain View, CA), and 0.4 μM of RmkininP1R (for 5′ RACE) or RmkininP1F (for 3′ RACE), and 0.5 μl Phusion® High-fidelity DNA polymerase (New England Biolabs® Inc., Ipswich, MA). For 5′-RACE, touchdown PCR was as follows: 98°C for 30 s; followed by 5 cycles of 98°C for 10 s, 72°C for 1 min, followed by 5 cycles of 98°C for 10 s, 70°C for 30, 72°C for 1 min, followed by 25 cycles of 98°C for 10 s, 68°C for 30 s, 72°C for 1 min, with a final extension step of 72°C for 10 min. For 3′ RACE, touchdown PCR was as follows: 5 cycles of 98°C for 30 s, 72°C for 3 min, followed by 5 cycles of 98°C for 30 s, 70°C for 30 s, 72°C for 3 min, followed by 40 cycles of 98°C for 30 s, 68°C for 30 s, 72°C for 3 min, with a final extension step of 72°C for 5 min. The products from 5′- and 3′-RACE were purified with Zymoclean gel DNA recovery kit (Zymo^{TM} Research) and cloned into pCR^{TM}2.1 Vector

[1]https://www.ncbi.nlm.nih.gov/

(Invitrogen). Chemical transformation was used to incorporate the plasmids containing PCR products into premade competent *E. coli* cells DH5α (Zymo^{TM} 5α) (Zymo^{TM} Research, Irvine, CA, United States). Transformants were screened by blue/white colony selection and 100 μg/ml ampicillin (Cayman Chemical, Ann Arbor, MI, United States). Plasmids were isolated using the Zyppy^{TM} plasmid miniprep (Zymo^{TM} Research) and sent to (Eton Bioscience Inc., San Diego, CA, United States) for Sanger sequencing. The full length of cDNA sequence was deduced by aligning the overlapping 5′- and 3′-end DNA fragments (**Supplementary Figure S1A**). To obtain the coding sequence of the cDNA (ORF) in a single product, gene-specific primers were designed (Rmk-ORF-F/R) outside of the ORF region to amplify the cDNA, using similar reagents as above (**Supplementary Table S1**). Specifically, in a 50 μl volume, 2 μl of 3′-ready cDNA was added into the mixture of 1 × Phusion HF buffer, 0.2 mM each dNTPs, 0.4 μM of both Rmk-ORF forward and reverse primers, and 0.5 μl Phusion® High-fidelity DNA polymerase. The reaction was run at the following conditions: 98°C for 30 s, followed by 30 cycles of 98°C for 10 s, 72°C for 90 s, with a final extension step of 72°C for 10 min. The PCR product was purified, cloned into pCR^{TM}2.1 Vector, and verified by sequencing as described above.

R. microplus Kinin Gene Structural Characterization

The blastn "hits" obtained on the *R. microplus* genome with the cloned kinin cDNA sequence only overlapped the genome sequence toward the 3′ end of the cDNA. Thus, to define the structure of the putative kinin gene, i.e., to determine the precise number and length (bp) of introns and exons, several PCR reactions were performed (**Supplementary Figure S1B**). The genomic DNA template was extracted from the acaricide-susceptible Deutch strain of *R. microplus* because the Gonzalez strain used for cDNA synthesis is no longer available. Genomic DNA was extracted from one female tick using Zymo^{TM} *Quick*-DNA miniprep kit (Zymo^{TM} Research). To obtain the sequence of the predicted ORF, first, gene-specific primers located toward the 5′- and 3′- ends of the cDNA sequence (Rmk-ORF-F/R) (**Supplementary Figure S1B**) were used to amplify the genomic DNA. In a 50 μl volume, 100 ng of genomic DNA was added into the mixture of 1 × Phusion HF buffer, 0.2 mM of each dNTPs, 0.4 μM of both Rmk-ORF forward and reverse primers, and 0.5 μl Phusion High-fidelity DNA polymerase. The reaction was run at 98°C for 30 s, followed by 30 cycles of 98°C for 10 s, 72°C for 120 s, with a final extension step of 72°C for 10 min. A 4 kb PCR product was amplified, and it was purified with Select-a-Size DNA clean and concentrator^{TM} kit (Zymo^{TM} research, Irvine, CA, United States). Three forward primers and two reverse primers were designed to "walk" the ∼4 kb PCR product obtained for Sanger sequencing (**Supplementary Figure S1B**). Secondly, a gene-specific forward primer (Bmkinin-g-long-F) and a reverse primer outside the 4 kb product region (Bmkinin-g-long-R) were designed to amplify a 1,375 bp product that includes 40 bp toward the 3′ end of the kinin gene. For the reverse primer design, the sequence of the genomic contig (LYUQ01126194.1) was used (**Supplementary Figure S1B**). Thirdly, gene specific primers were designed based on the cDNA sequence (**Supplementary Figure S1B**) to amplify a ∼3.5 kb product containing additional 20 bp toward the 5′ end of the gene.

R. microplus Kinin Peptide Precursor Characterization

The signal peptide of the translated *R. microplus* kinin peptide precursor sequence was predicted with SignaIP v. 5.0[2] (Armenteros et al., 2019). The cleavage sites on the precursor were predicted following the principles summarized by Veenstra (2000). The conserved motif logos of the C-terminal pentapeptide of kinins in *R. microplus* and *Ix. scapularis* were created separately by WebLogo[3] (Crooks et al., 2004).

Prediction of Tick Kinin Peptide Precursors and Phylogenetic Analysis

The nucleotide sequences encoding the orthologous kinin precursors from other Acari species were predicted through tblastn on NCBI using the cloned kinin precursor of the *R. microplus* tick as query against the transcriptome data of Acari (taxi: 6933). The protein sequence was manually curated by translating the DNA sequence on ExPASy[4]. For species with more than one hit in the BLAST results, nucleotide sequences were downloaded and aligned by SeqMan Pro (DNASTAR Lasergene, Madison, WI, United States), before being used for protein curation. For specific genes for which the nucleotide sequences of two hits did not overlap, the encoding polypeptides were curated separately, and later combined from N-terminus to C-terminus retaining a gap between two polypeptides. This procedure applies for the predicted kinin precursor of *Amblyomma sculptum* and *Dermacentor variabilis*. To predict the *Ix. scapularis* kinin precursor, the transcript sequences identified by tblastn were used in combination with the sequence of the genome scaffold (DS680282) which had been previously reported to encode the kinin gene with 19 kinin peptides, with no other details provided (Gulia-Nuss et al., 2016). All the curated kinin precursor protein sequences start with methionine, and their predicted coding sequences end with a stop codon, except for that of *A. sculptum,* in which a stop codon was not present. To help verify the predicted methionine, all deduced tick kinin precursors were aligned using the Clustal W method with MegAlign (Lasergene). The kinin precursor sequence of the common bed bug, *C. lectularius*, was obtained from Predel et al. (2017). Additional insect kinin sequences were obtained from the DINeR database and references therein[5] (Yeoh et al., 2017). Those sequences are from one hemipteran, *R. prolixus* [DAA34788.1] (Bhatt et al., 2014), and four dipterans, *Aedes aegypti* [AAC47656.1] (Veenstra et al., 1997), *Culex quinquefasciatus* [EDS35029.1] (Schooley et al., 2012), *Stomoxys calcitrans* [XP_013117801.1], and *Drosophila melanogaster* [NP_524893.2]. Fourteen protein sequences of putative arthropod kinin precursors were included

[2]http://www.cbs.dtu.dk/services/SignalP/

[3]https://weblogo.berkeley.edu/logo.cgi

[4]https://web.expasy.org/translate

[5]http://www.neurostresspep.eu/home

in the phylogenic analysis. The protein sequences were first aligned by MAFFT with the iterative refinement algorithm E-INS-i, because of the occurrence of known insertions and deletions during the evolution of neuropeptide genes[6], (Katoh and Standley, 2013), with the default online settings. The aligned sequences were processed through Mesquite version 3.6 (build 917) (Maddison, 2005) to convert the terminal gaps into missing data. Phylogeny was constructed using MrBayes version 3.2.6 (Ronquist et al., 2012) executable for Windows 64-bit with four chains and four runs in the mixed amino acid model for 1,000,000 generations. The traces of parameters were visualized in Tracer version 1.7.1 (Rambaut et al., 2018) to confirm that the four runs reached convergence. The consensus tree was generated with 10% burnins and output through FigTree version 1.4.4 (Rambaut, 2012).

Cell Lines

BMLK3 is a CHO-K1 cell line stably expressing the southern cattle tick (*R. microplus*) kinin receptor, and served to characterize the functional activity of compounds on the receptor. Receptor cloning, transfection and selection of single clonal cell lines expressing this kinin receptor was reported previously (Holmes et al., 2000, 2003). A cell line similarly transfected with empty vector plasmid pcDNA3.1 (Invitrogen, Carlsbad, CA, United States) was designated as a "vector only" cell line and used as the negative control in all experiments. Cells were maintained in T-25 or T-75 flasks (CELLSTAR®, Greiner® Bio-one) with maintenance medium consisting of F-12K medium (Corning™ Cellgro™, Mediatech, Inc., Manassas, VA, United States), fetal bovine serum (FBS) (10%) (Equitech-Bio, Kerrville, TX, United States) and 400 μg/ml G418 Sulfate (Gibco® Invitrogen, New York, United States). Cells were maintained in a humidified incubator at 37°C, 5% CO_2. Cells were incubated under the above conditions unless specified otherwise.

Two different calcium reporters (Fluo-8 AM or aequorin/coelenterazine) were utilized in dual-addition assays, which are described in detail in the sections below. Both assays allow the discrimination of agonistic or antagonistic activity of compounds. Briefly, a primary screen of compounds measured the endpoint fluorescence from cells cultured in a 384-well plate format. Compounds that showed potential activity in this screen were further tested at various concentrations with a kinetic assay that measured calcium bioluminescence in a 96-well plate format.

Preparation of Small Molecule Library Plates

A commercial library of fourteen small molecule antagonists of mammalian neurokinin receptors (NK1-3) was purchased from Tocris® Bioscience (R&D System, Bristol, United Kingdom) (for information on chemicals see **Supplementary Table S2**) to be screened on the BMLK3 cells in 384-well format. Additionally, thapsigargin, which discharges intracellular Ca^{2+} stores by inhibition of the Ca^{2+} ATPase in endoplasmic reticulum (Thastrup et al., 1990), and 2-APB (2-aminoethoxydiphenyl borate), which blocks of store-operated Ca^{2+} entry and may block InsP3-induced Ca^{2+} release (Bootman et al., 2002), were purchased from Tocris® Bioscience and used as positive and negative controls, respectively, for the Ca^{2+} signal assay readout.

All small molecule stock solutions (for library and controls) were prepared in 100% DMSO (Sigma-Aldrich, St. Louis, MO, United States) and aliquoted and stored at −20°C before use. For the initial screening in the fluorescence assay, compounds were initially prepared in a V-bottom, 384-well plate (Corning®, NY, United States) in Hanks' Saline Buffer containing 20 mM Hepes (HHBS), 2% DMSO, at a 10× concentration of the final concentration in the assay. The sixteen small molecules were serially diluted in this plate into 22 dosages using a dilution ratio of 1:1.4, starting at 1 mM (except thapsigargin started at 100 μM, **Supplementary Table S3**) using an automatic-8 channel EPMotion™ liquid handler (Eppendorf Biotech company, Hamburg, Germany).

Ten selected molecules, which were either active in the first screening or could not be dissolved in 2% DMSO, were further prepared in a V-bottom 384-well plate in HHBS, 10% DMSO at a 10× concentration of the final concentration in the assay; thapsigargin and 2-APB were also prepared in the same solvent. The twelve small molecules (including thapsigargin and 2-APB) were serially diluted in the plate (dilution ratio 1:1.4) into 10 dosages starting from various concentrations (10 μM to 1 mM) depending on the solubility of each molecule (**Supplementary Table S4**, Panel A). In this "library subset" plate, each concentration of the small molecules was dispensed into a duplicate well for testing both the kinin-receptor expressing cell line (BMLK3 cells) and the cells transfected with the vector plasmid only, respectively. In both 384-well library plates, 64 wells in four edge columns were filled with blank solvent (first addition) (**Supplementary Tables S3**, **S4**).

Preliminary Screen of a Small Molecule Library in an End-Point Fluorescence Assay

The screening of the potential antagonists on BMLK3 cells was performed with an endpoint fluorescence assay in a black/clear 384-well plate (CELLSTAR®, Greiner Bio-one, 781077) coated with Poly-D-Lysine (Sigma-Aldrich). This assay uses Fluo-8 AM (Fluo-8 Calcium Flux Assay Kit - No Wash, Abcam®, Cambridge, United Kingdom) as the calcium indicator. Unless specified, the pipetting steps in the 384-well plate fluorescence assay were performed by an automated CyBio® Well Vario System using a 384 pipette-head that allows to simultaneously deliver a volume of up to 60 μl per well. The screening of the first library prepared in 2% DMSO was performed on BMLK3 cells only (**Supplementary Table S3**). The screening of the second library plate prepared in 10% DMSO ("library subset") was tested with half of plate with BMLK3 and another half with vector only cells (**Supplementary Table S4**).

BMLK3 or vector only cells were cultured in T-75 flasks. When they reached about 90% confluency, they were trypsinized and suspended in F-12K medium containing 1% FBS and 400 μg/ml

[6]https://mafft.cbrc.jp/alignment/server/

of G418 Sulfate at 4 × 10^5 cells/ml to be seeded in 384-well plates. For this, the cell suspension (25 μl; ∼10,000 cells/well) was dispensed into all 384 wells of the plate. To distribute cells evenly, mixing was by aspirating and immediately re-dispensing 10 μl of the applied cell suspension three times. Plates were incubated overnight at 37°C under 5% CO_2. On the next day, cells were prepared for the assay following the kit's instructions: the old media in the assay plate was fully removed by inverting the plate and gently blotting it on paper towels, and media was replaced with 45 μl of Fluo-8 AM loading dye (1×). The plate was incubated at 37°C under 5% CO_2 for 30 min, then equilibrated at room temperature in the dark for 30 min. The screening of the small molecule library was achieved by a dual-addition assay. The "first addition" consisted of 5 μl of either the blank solvent or a 10 × solution of the potential antagonist transferred from the 384-well library plate, to reach 1 × concentration in the wells. After 5 min incubation with cells, a second addition of 5.6 μl of 10 μM kinin receptor-specific agonist peptide (FFFSWGamide) resulted in a final concentration of 1 μM. The calcium fluorescence signal was read by a Varioskan LUX™ (Thermos Scientific, Waltham, MA, United States) plate reader set for fluorescence plate-mode with Ex/Em = 490/525 nm and kept at 29°C. Endpoint responses were read immediately after the first addition and 5 min after the second addition of agonist. The plate was read from both forward and reverse orientations by rotating the plate (180°) on the instrument to compensate the variation in signal kinetics during the lapse in plate reading, because there was a 2 min lag time between the readings of the first and the last well. The response to each addition was represented as the average value of both forward and reverse plate readings (**Supplementary Tables S3**, **S4**, Panels B,C). The antagonist activity was calculated as the percentage of the response to 1 μM FFFSWGa of cells that had been incubated with the putative antagonist compound in comparison to the response of cells that had been incubated with blank solvent only. A compound was considered to have antagonistic activity, if it minimally inhibited 50% of the response to the agonist FFFSWGa (1 μM) applied in the second addition. These candidates were selected for further validation in a dose-response kinetic calcium mobilization bioluminescence assay.

Kinetic, Dose-Response Calcium Mobilization Bioluminescence Assay

The calcium bioluminescence assay was used for the kinetic analysis of dose-responses to the compounds identified in the primary screen. Aequorin is the calcium reporter, transiently expressed in the BMLK3 cells (Lu et al., 2011b). This "dual-addition" kinetic assay was conceived to characterize the diverse activity patterns the putative ligands may display. The "first addition" consists of the compound being tested, either a small molecule or a peptidomimetic; the bioluminescence response elicited is measured for 30 s (if the compound is an agonist there will be bioluminescence response during this first 30 s period). Immediately after, at 32 s, a "second addition" with a single concentration of agonist follows (FFFSWGa, 1 μM), and the response continues to be measured for another 30 s. It is important to emphasize that the response measured after this addition of agonist is influenced by the presence of the unknown compound applied in the first addition. If the compound is an antagonist, the response to the agonist applied in the second addition will be reduced with respect to that of the positive control (buffer + agonist). The pharmacological activity of the unknown molecule can be determined based on the integrated area under the bioluminescence response curve registered during both these 30 s periods (total bioluminescence expressed as average bioluminescence units per second). That is, it can be inferred if the unknown molecule is a full agonist, full antagonist, partial agonist, partial antagonist, or an allosteric modulator. This approach is widely applied in GPCR drug discovery (Ma et al., 2017).

Selected small molecules were solubilized in 1 × DMEM medium (Gibco®, Invitrogen) with 10% DMSO and prepared from 500 nM to 500 μM as 5× of the final concentration. In addition, three peptidomimetic ligands of neurokinin receptors were purchased from Tocris® Bioscience: one agonist, hemokinin 1 (human), and two antagonists, antagonist G and spantide I. These peptidomimetics were solubilized in 80% acetonitrile: 0.01% trifluoroacetic acid and then aliquoted (100 nm per tube) and freeze-dried; the dry peptidomimetics were stored at −20°C before use. For the assay, the peptidomimetics were solubilized and diluted in assay buffer (1 × DMEM) containing 1% DMSO from 10 nM to 100 μM as 10× of the final concentrations in the assay. All compounds, either small molecules or peptidomimetics were tested in three independent replicates, each with 2-3 wells as pseudo-replicates. Responses from each assay were calculated as the average of individual responses from the pseudo-replicate wells.

The cells preparation was described in detail elsewhere (Lu et al., 2011b). In brief, the BMLK3 and vector-only cells were cultured to ∼ 90% confluency in T-25 flasks. The cells were trypsinized and suspended in maintenance medium, counted, and diluted to 1 × 10^5 cells/ml; 2 ml of this cell suspension was placed into each well of 6-well-plates (CELLSTAR®, Greiner Bio-one). After overnight incubation, when the cells reached a confluency of 40–60%, old medium was replaced with 1 ml of serum-reduced Opti-MEM™ medium (Gibco®, Invitrogen) in each well. Following the instructions of the transfection reagent manufacturer, cells in each well of the 6-well plate were transiently transfected with 1 μg mtAequorin/pcDNA1 plasmid mixed in 4 μl of FuGENE6 (Promega, Madison, WI, United States) and 96 μl of Opti-MEM™ medium. After 6 h of incubation, the old medium was replaced with 2 ml of F-12K medium with FBS (10%) (antibiotic-free medium). Following 24 h incubation, cells were trypsinized, seeded into white/clear 96-well-plates (CELLSTAR®, Greiner Bio-one) (20,000 cells/well in 100 μl of antibiotic-free medium), and incubated overnight until they reached optimal confluence of 80%. BMLK3 cells and vector only cells were prepared in the same plate to test different concentrations of each compound. To reconstitute the aequorin-complex, cells were incubated with 90 μl per well of calcium-free DMEM (1×) containing coelenterazine (5 μM) (Regis™ Technology, Inc., Morton Grove, IL, United States). After 3 h of incubation in the dark, cells were ready for the assay.

The "dual-addition" assays were performed with a Clariostar™ (BMG LABTECH, Chicago, IL, United States) plate reader set at 29°C and for bioluminescence and "well" mode at 469 nm emission wavelength. The two additions were performed by the built-in injectors of the Clariostar™ plate reader. The first addition was performed after 2 s of initiating the recording of the bioluminescence response, which continued for 30 s. This addition applied either 22.5 μl (5×) of certain small molecule antagonist at a specific concentration or blank solvent, or 10 μl of peptidomimetic (10×). At 32 s, a second addition of 12.5 μl of agonist peptide FFFSWGa was executed with the second injector into the same well containing the test compound or blank solvent, to reach a final concentration of 1 μM. For peptidomimetics, 11 μl were applied. Recording continued for another 30 s; in sum, the kinetic response of each well was recorded for a total of 65 s at 1 s intervals. The same procedure was performed for each concentration of the ligand tested. The kinetic response to both additions were recorded immediately after addition for 30 s, with 1 s interval, and is expressed as bioluminescence units (BU) per second. The total response of the cells to each addition was represented as the percentage of the averaged BU per second obtained in each of the two 30 s-ranges, relative to the average BU to the PC (blank solvent + 1 μM FFFSWGa) in the 2nd range (average BU of the PC curve from 35 to 65 s).

Effect of a Prolonged Pre-incubation With Various Concentrations of TKSM14 on the Agonist-Induced Response

Because TKSM14 displayed antagonistic activity in the fluorescence assay but not in the calcium bioluminescence assay, a modified calcium bioluminescence assay was performed in which the incubation time (previously 30 s) was increased to 5 min, as in the fluorescence assay. The first addition was performed manually to add 22.5 μl of the blank buffer or different dosages of the TKSM14 (5 × solutions), to achieve final concentrations of 1, 10, 30, 50, and 100 μM. The second addition was performed with the built-in injector of the Clariostar™ plate reader (12.5 μl of the 10× agonist FFFSWGa solution for a final concentration of 1 μM), as described in the previous section. The response to the agonist in the second addition was recoded for 30 s, at 1 s intervals. Similarly, as before, three independent assays were performed, with each assay containing 3–4 pseudo-replicates. Responses from each assay were calculated as the average of individual responses from the pseudo-replicate wells. The antagonistic activity was represented as a percentage of the average bioluminescence units obtained during the 30 s after the second addition (wells containing both the small molecule being analyzed and FFFSWGa), divided by the average bioluminescence units obtained from wells containing FFFSWGa only.

Statistical Analyses

All statistical analyses were performed with Prism 6.0 (GraphPad Software, La Jolla, CA, United States). In the end-point fluorescence assay, dose-response curves and IC_{50} values were calculated with "log [inhibitor] vs. response – Variable slope (four parameters)" function in Prism 6.0. IC_{50}s of the antagonists were defined as the concentration of antagonist that inhibits agonist response in the mid-range of the respective fitted dose-response curve (this is not the concentration that inhibits 50% of the agonist response). In the kinetic calcium bioluminescence assay, to determine the statistical significance of the inhibitory effect from various concentrations of the same compound, the response after the second addition for each concentration within each molecule was compared to the corresponding blank control by one-way ANOVA (n = 3) followed by Tukey's multiple comparisons test.

RESULTS

Our long-term approach for discovering novel ligands for arthropod GPCRs is summarized in **Figure 1**. In this study, we focused on processes on the left of the figure, by using transcriptomics and genomic data to clone the kinin cDNA, followed by forward pharmacological approaches toward the identification of novel ligands for the kinin receptor of the southern cattle tick, *R. microplus*.

R. microplus cDNA Sequence and Gene Structure

We first identified the predicted 332 amino acid residue protein sequence of the putative kinin precursor of *Ix. scapularis* from a genome fragment (DS680282: 583-1410) (Gulia-Nuss et al., 2016). Although it was reported that the gene encoded 19 kinins (Gulia-Nuss et al., 2016), the exact sequences of kinins were not provided. Herein, we listed the sequence of the 19 paracopies of putative bioactive kinins from *Ix. scapularis* (**Table 1**). Using this curated precursor protein as query, the tBLASTn results against WGS assembly and TSA of *R. microplus* (taxid: 6941) identified a genomic DNA fragment of accession number LYUQ01126194.1 and four transcripts with high similarities. Our cloning of the putative kinin precursor cDNA from *R. microplus* verified the full-length cDNA sequence is 1,398 bp long encoding a 1,227 bp open reading frame (ORF). The predicted precursor protein of 409 amino acid residues has a predicted molecular mass of 44.72 kDa (GenBank QDO79406) (**Supplementary Figure S2**). The 5′- and 3′-untranslated regions (UTRs) are 85 bp and 86 bp, respectively.

Alignment of the cloned cDNA to the genome sequence revealed that the 5′-end was missing in the genome, as determined by BLAST (**Figure 2A**). We were able to obtain this missing sequence by genomic PCR amplification using a primer designed based on the sequence of the cDNA 5′-end (**Supplementary Figure S1** and **Supplementary Table S1**). By further amplification of the genomic DNA with gene-specific primers we sequenced the putative kinin gene of *R. microplus,* that is encoded in approximately 4.1 kb (GenBank MK875970) (**Figure 2B**), composed of two exons and one intron. The first exon is 140 bp long and the second exon is 1,253 bp long; in between there is an intron of ∼ 2,700 bp. Although the genomic DNA and cDNA sequences obtained were from different strains of *R. microplus*, the alignment of their ORF region showed 99% identity.

Analysis of the *R. microplus* Kinin Precursor

The first 38 amino acid residues of the *R. microplus* kinin precursor were predicted with SignalP v 5.0 as belonging to a signal peptide with only 50% probability, denying such conclusive identification. Seventeen paracopies of putative bioactive kinins were encoded by this single cDNA (**Table 1**). Three of them (Rmkinin 10, 13, and 15) have a predicted molecular weight of about 1,009 Da, which was the mass of putative *R. microplus* kinin detected through mass spectrometry in a previous study (Neupert et al., 2005). The *R. microplus* kinins showed the canonical critical residues and necessary characteristics for activity of the insect kinins (FX_1X_2WGa): Phe and Trp at the first and fourth position of the pentapeptide minimally active core, respectively, as well as the amidated Gly at the fifth position. Noticeably, the second variable position (X_2) was dominated by Pro; only two out of 17 kinin paracopies from *R. microplus* have a different amino acid other than Pro on the X_2 position (**Table 1**). This consensus pattern of the kinin C-terminal pentapeptide (FX_1PWGa) was prevalent in other tick species as well (**Table 1** and **Figure 3A**).

TABLE 1 | Predicted bioactive kinins from *Rhipicephalus microplus* and *Ixodes scapularis.*

Name	*Rhipicephalus microplus*	Predicted molecular weight (Daltons)
Rmkinin1	QFSPWGa	720
Rmkinin2	LHPVDIAVRAADLFSPWGa	1963
Rmkinin3	DKDQTFNPWGa	1206
Rmkinin4	AGDHF**G**SWGa	932
Rmkinin5	DTFSAWGa	782
Rmkinin6	QQDSKNAFSPWGa	1363
Rmkinin7	AVRSPTARNDAARAKQED GEEDEERSF**A**PWGa	3446
Rmkinin8	GTGEDQAFSPWGa	1250
Rmkinin9	GDDGDTSF**T**PWGa	1253
Rmkinin10	DDRFNPWGa	**1005**
Rmkinin11	EGPFSPWGa	875
Rmkinin12	DGSNKEGFFNPWGa	1454
Rmkinin13	GADDPFNPWGa	**1074**
Rmkinin14	QDSFNPWGa	949
Rmkinin15	EDGVF**R**PWGa	**1061**
Rmkinin16	EDNVF**R**PWGa	1118
Rmkinin17	EGNVF**G**PWGa	961
	Ixodes scapularis	
Ixkinin1	QFSPWGa	720
Ixkinin2	GDKQPEDEAFNPWGa	1589
Ixkinin3	ENDKDKELSFNPWGa	1678
Ixkinin4	GSFSSWGa	726
Ixkinin5	DTF**G**SWGa	768
Ixkinin6	DTF**G**PWGa	768
Ixkinin7	DTF**G**PWGa	768
Ixkinin8	DTF**G**PWGa	768
Ixkinin9	DTF**G**PWGa	768
Ixkinin10	DTF**G**PWGa	768
Ixkinin11	QDKESGFNPWGa	1263
Ixkinin12	DPFNPWGa	831
Ixkinin13	EDKNAFSPWGa	1149
Ixkinin14	DQNFNPWGa	976
Ixkinin15	TTKDSTFSPWGa	1225
Ixkinin16	EGPFNPWGa	902
Ixkinin17	GDSDTAF**A**PWGa	1122
Ixkinin18	DNNFNPWGa	962
Ixkinin19	DNGNKDSSFSPWGa	1409

Under name, ordinal numbers reflect the order in which each sequence appears from the 5′ to 3′ direction either in the cDNA (R.m.) or in the predicted gene (Ix.). The bolded predicted molecular weights were similar to previously predicted kinin masses (approximately 1,009 Da) (Neupert et al., 2005).

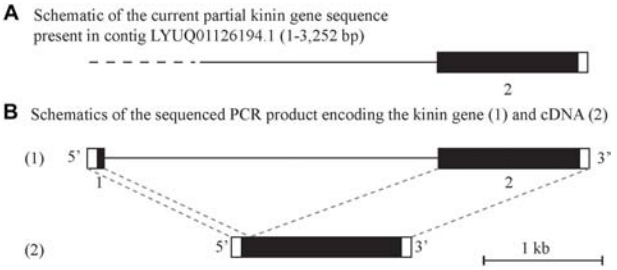

FIGURE 2 | Schematic of the kinin gene and cDNA from *Rhipicephalus microplus*. The black boxes represent the protein-encoding regions and the white boxes are the untranslated regions on the 5′ and 3′-end of the kinin gene or cDNA. **(A)** Depicts a genome contig fragment (the full length of 7,784 bp is not represented here) encoding the 3′-end fragment of the predicted *R. microplus* kinin gene (position 1 to 3,252). The dashed line represents the sequence gap at the 5′-end of the kinin gene in the genome assembly (Rm2.0; NCBI). **(B)** (1) Depicts the amplified 4.1 kb PCR product sequenced that encodes the kinin gene. The gene is composed of two exons (140 and 1,254 bp, respectively, represented by boxes) and one intron (2.7 kb black line). This structure was verified by aligning the gene sequence with the 1398 bp cDNA (2) obtained in this study.

Kinin Precursors From Other Tick Species

Using the *R. microplus* kinin precursor as query for TBLASTN against the transcriptomes of all Acari (taxid: 6933) on NCBI, we predicted amino acid sequences of the putative kinin precursors from another seven tick species. Four full amino acid sequences were obtained, those from the relapsing fever tick, *Ornithodoros turicata,* the castor bean tick, *Ix. ricinus,* the brown dog tick, *R. sanguineus*, and the curated kinin precursor of *Ix. scapularis.*

The precursor from *Ix. scapularis* was predicted by aligning the kinin precursors deduced from three transcripts and the genomic scaffold. Missing sequences were identified from each of these: the transcripts provided a sequence of 23 amino acid residues at the N-terminus containing part of the signal peptide, and an additional C-terminal sequence of 23 amino acid residues followed by the stop codon. These sequences are absent in the genomic scaffold. However, the protein deduced from the transcriptome lack 40 amino acid residues, which are present in the genomic scaffold, distributed in two gaps within positions 250–293 in the alignment (see **Supplementary Figure S3**). These

A

GDIE01101972.1 ***Ornithodoros turicata*** 283 aa (10)
MAPAARSSQTFCTLRYLILSISLLASYASVEESDGDSRDDDSFEDMVIRWNISPDTLQRLRARREAIARPFVPRWG
NQIQGDAAVGKPYGNYRDVWIYG**KK**DAHFNPWGG**KR**DGTHTRSGLDDSSGSWSE**KK**DNFNPWGG**KK**EASFN
PWGG**KR**DNFNPWGG**KK**DNFNPWGG**KK**DSSIFNPWGG**KR**SDGSKDKELSFNPWGG**KR**QDGVGTIFGPWGG**K**
RENLFNPWGG**KR**EKSEMTFNPWGG**KK**SELAFSPWMSASSRIKRDSTINTDMFIQHPKVQKASPRPL*

GFVZ01012512.1_GFVZ01032577.1_***Ixodes ricinus*** 348 aa (16)
MELRGHDAQELRFLWTLLATTFLMSMGGLCQDVDSGSGDLGRSSRVGESFIRWNISPATLQHMRSESF**KR**QFSP
WGG**KR**GVLDQALPTAHRLSGPLYLYKALHSPGAMGE**RR**GDKQPDDETFNPWGG**KR**ENDKDKELSFNPWGG**K**
RGTFSSWGG**KR**DTFGPWGG**KR**DTFGAWGG**KR**DTFGPWGG**KR**QDKESGFNPWGG**KR**EDPFNPWGG**KK**EDK
NAFSPWGG**KR**EQNFNPWGG**KK**TSKDSTFSPWGG**KR**EGPFNPWGG**KK**GDSDTAFAPWGG**KR**DNNFNPWGG
KRDNGNKDSSFSPWGG**KR**ESFGVQASDPDSLEDHSPSRNKRDSSSRVPKTKNSARSAISSVAKTF*

DS680282 (genome scaffold) GBBN01023680.1_GGIX01408871.1_ GBBN01027580.1_ ***Ixodes scapularis*** 378 aa (19)
MELRGHDAQELRFLWTLLATTFLMSMGGLCQDVDSGSGDLGRSSRVGESFIRWNISPATLQHMRSESF**KR**QFSP
WGG**KR**GVLDQALPTAHRLSGPLYLYKALHSPRAMGE**RR**GDKQPEDEAFNPWGG**KR**ENDKDKELSFNPWGG**K**
RGSFSSWGG**KR**DTFGSWGG**KR**DTFGPWGG**KR**DTFGPWGG**KR**DTFGPWGG**KR**DTFGPWGG**KR**DTFGPWG
G**KR**QDKESGFNPWGG**KR**EDPFNPWGG**KK**EDKNAFSPWGG**KR**DQNFNPWGG**KK**TTKDSTFSPWGG**KR**EGP
FNPWGG**KK**GDSDTAFAPWGG**KR**DNNFNPWGG**KR**DNGNKDSSFSPWGG**KR**ESFGVQALDPDSLEDHSPSRN
KRDSSSRVPKTKNSAQSTIRSVAKTF*

GFGI01134859.1_GFGI01059497.1_***Hyalomma dromedarii*** C-terminal protein, 282 aa (16)
MRSESF**KR**QFSPWGG**KR**NAALLESLLDSPGNQESRRHHLAADASYKV**RR**LHPAGVRDADSFNPWGG**KR**TDD**K**
KDKDQTFNPWGG**KR**DSVRVKQEDGEEDEERSFAPWGG**KR**GAGEDQAFSPWGG**KK**RDDGDTSFAPWGG**KR**E
DRFNPWGG**KR**EGPFNPWGG**KR**DGSNKEGFFNPWGG**KR**GADDSFNPWGG**KR**GADDSFNPWGG**KR**QDSFNP
WGG**KR**EDGVFRPWGG**KK**DDNVFRPWGG**KK**EDNVFGPWGG**KR**EDAGSLRKKRDSSTSEHKVTTSHGGKSAS
A*

GGTZ01063774.1_GGQS01017149.1_GGQS01017150.1_***Dermacentor variabilis*** C-terminal protein, internal gap, 257 aa (11)
MRSESF**KR**QFSPWGG**KR**NTAAFESLLDSPGDQQSHRHQLAADASYKVRRLHHTGSPRNADSFSP…ERSFAPW
GG**KR**GAAEDQAFSPWGG**KR**DSEEDTSFAPLGG**KR**EDRFNPWGG**KR**EGPFNPWGG**KR**EGSNKEGFFNPWGG
KRGADDSFNPWGG**KR**QDSFNPWGG**KR**ESGVFRPWGG**KK**EDKVFGPWGG**KR**DDDVFGPWGG**KR**EQVSSSS
SHSAGRGFPFGGATEHGVDAESLRKKRDSSMSEHQVTTSYSGKSGGT*

GEEX01014746.1_ GEEX01012161.1_***Amblyomma sculptum***, N-terminal protein, internal gap, 296 aa (15)
MGLRRRAAAGETLLLRVFLVASVLSLDVSAQHMVGSDEARSLLSRGGDTLIRWNISPATLQHMRSESF**KR**QFSP
WGG**KR**NAAFDYLLDAPGGDHQVADAASSYKVRRVHHTPSLRN…VFAPWGG**KR**AAEDRAFSPWGG**KR**GGDG
DGGETFAPWGG**KR**EDRFNPWGG**KR**EGPFNPWGG**KR**EGSNKEGFFNPWGG**KR**GADDSFNPWGG**KR**GADDA
FNPWGG**KG**GADAAFNPWGG**KR**QDSFNPWGG**KR**EDVVFRPWGG**KK**EDNVFRPWGG**KK**EDNVFRPWGG**KR**
QGDGFKPWGG**KR**EEDT

HACP01031283.1_***Rhipicephalus sanguineus*** 411 aa (17)
MGTVLRRRGAAGANFAVGETLMLQLLLVVIAFSSDAWAQHVVGSDEARSLLSRGGDTLIRWNISPAALQHMRSE
NF**KR**QFSPWGG**KR**NTAAFESLLDSAGNQESRRHHLAADASYKV**RR**LHPASIGVRDADSFSPWGG**KR**TDD**KK**DK
DQTFNPWGG**KR**AAAGDRFGSWGG**KR**ETFNAWGG**KR**QQDKNSFSPWGG**KR**AVRSPTARNEDAARARQDDGE
EDEERSFAPWGG**KR**GTGEDQAFSPWGG**KR**GDDGDTSFTPWGG**KR**EDRFNPWGG**KR**EGPFNPWGG**KR**DGS
NKEGFFNPWGG**KR**GADDSFNPWGG**KR**QDSFNPWGG**KR**EDGVFRPWGG**KK**EDNVFRPWGG**KK**EDNVFAPW
GG**KR**EDALPSLYVGRGFNYGGTASHGVDAGSLRKKRDSSTSEHKGTTSYGGKSGST*

cloned ***Rhipicephalus microplus*** 409 aa (17)
MGTVLHRRGAAGANFTVGESLVLLLVLGVIAFPLDAWAQHVVGSDEARSLLSRGGDTLIRWNISPAALQHMRSES
F**KR**QFSPWGG**KR**NAAAFESLLDAAGNQESHRHRLAADASYKV**RR**LHPVDIAVRAADLFSPWGG**KR**TDDKKDKD
QTFNPWGG**KR**AGDHFGSWGG**KR**DTFSAWGG**KR**QQDSKNAFSPWGG**KR**AVRSPTARNDAARAKQEDGEEDE
ERSFAPWGG**KR**GTGEDQAFSPWGG**KR**GDDGDTSFTPWGG**KR**DDRFNPWGG**KR**EGPFSPWGG**KR**DGSNKE
GFFNPWGG**KR**GADDPFNPWGG**KR**QDSFNPWGG**KK**EDGVFRPWGG**KK**EDNVFRPWGG**KK**EGNVFGPWGG
KREDATPSLSVSRALNYGGPASHDVDAGSLRKKRDSSASEQKGTTSNGEKSGRT*

B

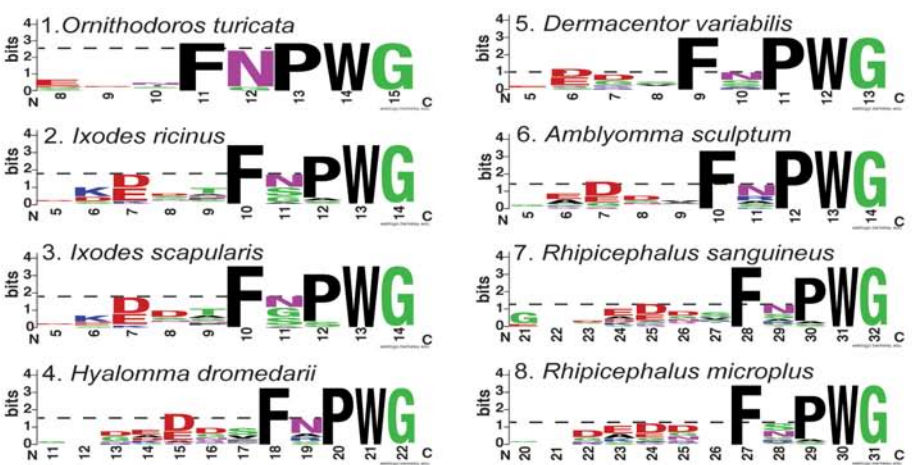

FIGURE 3 | Continued

FIGURE 3 | Amino acid sequences of kinin precursors from eight tick species. **(A)** Amino acid sequences were manually curated after mining the available transcriptomes on NCBI. The number of kinin paracopies in each precursor are denoted in the parentheses. The gaps within the protein are denoted with "**. . .**." The signal peptides predicted by SignalP 5.0 were underlined. The predicted cleavage sites are in bold, and potential bioactive kinins containing the kinin C-terminal motif, FX_1X_2WG-amide, are highlighted with gray color. The sequence of kinin precursor from *Ixodes scapularis* was curated based on the putative kinin gene in the genome scaffold (DS680282), while the additional N- and C- terminal sequences were deduced from sequences of three transcripts (**Supplementary Figure S3**). The number 1 to the left of the *Amblyomma sculptum* sequence points to an unusual cleavage site (K) or a potential sequencing error at this site (K followed by G) (in black square frame). The version numbers are listed on the top of each sequence (accession numbers are identical except do not contain the 0.1 at the end). **(B)** Sequence logos of the kinins from eight tick species. The logos were created by WebLogo (Crooks et al., 2004) using the amino acid sequences from each tick kinin precursor between predicted cleavage sites (highlighted in panel **A**). The overall height of each letter stack indicates the sequence conservation at that position (measured in bits), whereas the height of amino acid symbols within the stack reflects the relative frequency of the corresponding residue at that position. On the *X* axis, the numbers refer to the amino acid position within the alignment, which was anchored to the conserved C-terminal amidated-glycine residue, similarly as shown in the DINeR database (Yeoh et al., 2017). Toward the N-terminus, logos begin at the position within the alignment where bits are above 0 value. Polar amino acids containing an amide group (Q, N) are in purple, other polar amino acids (G, S, T, Y, C) are in green, basic (K, R, H) are in blue, acidic (D, E) in red and hydrophobic (A, V, L, I, P, W, F, M) amino acids are in black. The dashed-line indicates the bit value of the amino acid residue at the first variable position (X_1) of the kinin C-terminal pentapeptide motif (FX_1X_2WGamide).

gaps may have arisen from errors in the transcriptome assembly because this genomic region encodes four repeats of the sequence "DTFGPWGGKR." Therefore, the hypothetical kinin precursor from *Ix. scapularis,* is predicted as a protein of 378 amino acid residues (**Figure 3A**).

Three partial kinin precursors were predicted from the American dog tick, *Dermacentor variabilis,* and from *Amblyomma sculptum* and *Hyalomma dromedarii*. The former two were predicted with a gap retained in both amino acid sequences (**Figure 3A**). Whereas the *H. dromedarii* precursor, while missing approximately 70 amino acid residues at the N-terminus, should contain all the kinin paracopies as inferred from the alignment of tick kinin precursors (**Supplementary Figure S3**). Similarly, the deduced amino acid sequence of *D. variabilis* kinin precursor appeared to miss the same 70 residues sequence at the N-terminus (**Supplementary Figure S3**). Among the seven deduced protein sequences, only the *A. sculptum* kinin precursor lacked the stop codon. Among the eight tick kinin precursors analyzed, SignalP 5.0 predicted the signal peptide from those of *O. turicata*, *Ix. scapularis*, *Ix. ricinus*, and *A. sculptum* (**Figure 3A**). For *O. turicata*, the signal peptide includes the first 28 amino acid residues, with a cleavage site between residues A and S (**Figure 3A**). For the latter three species, the signal peptide includes the first 30 amino acid residues, with the cleavage site between C and Q for *Ixodes* spp., and between A and Q for *A. sculptum*.

Putative enzyme cutting sites, characterized by contiguous basic residues (Veenstra, 2000), and those for kinin sequences were predicted in the translated precursor sequences (**Figure 3A**). The number of kinin paracopies was high, especially in hard ticks. In the curated full-length kinin precursor of four hard tick species, 17 paracopies of kinins were predicted, in average. The transcript of the only soft tick kinin gene analyzed (*O. turicata)* is predicted to encode 10 kinin paracopies.

Within the functional C-terminal pentapeptide ($\underline{F}X_1X_2\underline{WG}$amide) core of insect kinins, the first (F), fourth (W), and fifth (G) amino acid residues are highly conserved, and similar conservation was observed in tick kinins. However, the second variable position predominantly featured proline in all eight tick species (**Figure 3B**), and the first variable position showed lower conservation in all analyzed tick species. Asparagine (N) predominately occupied the X_1 position in the soft tick *O. turicata* kinins, while in the *Ixodes* ticks (Prostriata), the X_1 position was equally occupied by either N, G, or S. The amino acid residue in the X_1 position was even less conserved (lower bits value) in ticks of the Metastriata group (**Figures 3B**, **4**–**8**).

Phylogenetic Analysis of Kinin Precursors

To establish how conserved the kinin precursors are between ticks and other insect blood feeders, a phylogenetic Bayesian analysis was performed with the putative kinin precursors from eight tick species and those known from five blood-feeding insect species (**Figure 4**). Bhatt et al. (2014) validated the *in vivo* activity of the *R. prolixus* kinin sequences used to construct this tree, and the three aedeskinins are active on the cognate receptor (Pietrantonio et al., 2005). The kinins from *C. lectularius* were detected in the CNS by mass spectrometry by Predel et al. (2017).

The number of kinin paracopies in different arthropod species varied dramatically. However, the selection pressure behind these putative insertions or deletions is unclear. The number of kinin copies was high in ticks and some hematophagous insects, but not in all (**Figure 4**). With the support of the phylogenetic unrooted tree, we found that the kinin precursors from ticks and insects were separated into two different groups. Similarly, within each branch, arthropods that are phylogenetically closer to each other clustered in the same group, indicating substantial conservation of kinin precursors across broad taxonomic groups. The only exception was that a soft tick, *O. turicata*, clustered with *Ixodes* ticks (hard ticks) but with a posterior node probability of 0.76. Insect kinin precursors, even those from species with several paracopies as in the case of ticks (i.e., up to 15 in *R. prolixus*), were more similar among themselves than to tick kinin precursors (**Supplementary Figure S4**). Thus, the number of kinin paracopies, does not appear to differentiate sequences of ticks from those of insects.

Small Molecule Screening on Recombinant Tick Kinin Receptor

Toward the discovery of novel "small-molecule" ligands (Lipinski, 2016) for the target GPCR, we initiated a small-scale screening with the dual-addition assay we developed. Because

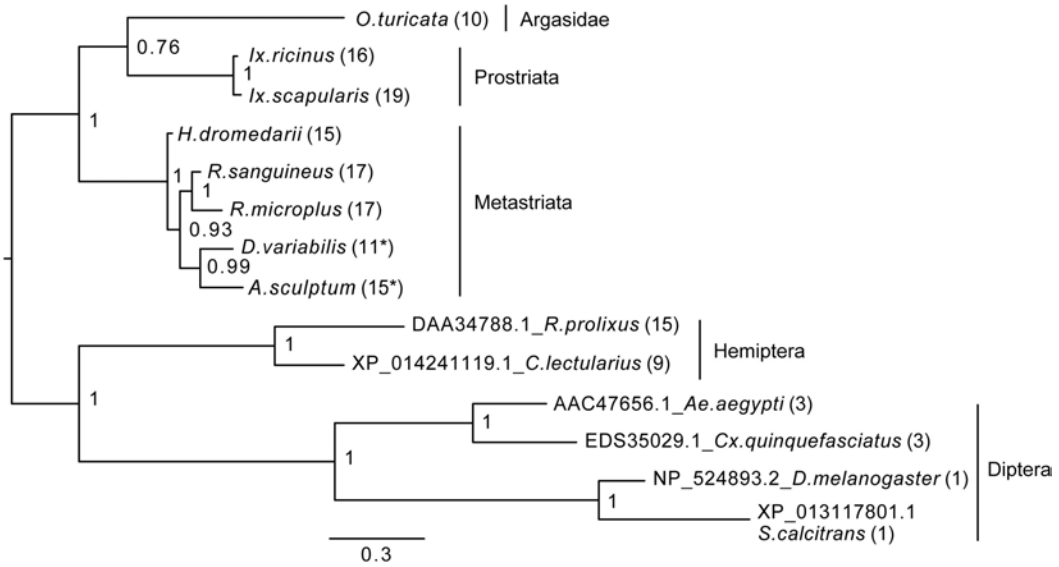

FIGURE 4 | Bayesian phylogenetic analysis of kinin precursor. The phylogenetic tree was constructed in MrBayes with four chains and four runs of the mixed amino acid model for 1,000,000 generations with a 10% burnins. Node values are Bayesian posterior probability rounded to two significant figures. Scale refers to branch length and represents the probability of an amino acid substitution along that interval. The number of kinin paracopies encoded by each precursor is denoted in the parentheses. "*" Indicates there could be more kinin paracopies present in this species as the predicted amino acid sequence likely only encodes a fragment of the kinin precursor due to gaps present in the predicted transcripts in NCBI. The curated protein sequences and version numbers of corresponding transcript sequences are in **Figure 3A**.

kinin receptors are invertebrate-specific GPCRs, there is no available commercial library of ligands from any ortholog mammalian GPCR (**Figure 1**). To explore the opportunity for discovery of antagonists, we selected a small-molecule library of known antagonists of those mammalian GPCRs that have the highest amino acid sequence identity to the tick kinin receptor. These are the neurokinin receptors (NK1-3 receptors), with approximately 36% amino acid sequence identity to the tick kinin receptor, as per Blast analyses in NCBI. The preliminary screening of fourteen small molecules was performed with an end-point calcium fluorescence assay. The screening of these small molecules was with 22 concentrations of antagonists prepared in 2% DMSO, performed on the BMLK3 cell line only. Four compounds, TKSM02, TKSM10, TKSM13 and TKSM14 showed some antagonistic activities, as they showed increasing values of fluorescence with decreasing concentrations (**Supplementary Table S3**, panel D, rows C, K, N, and O). It was noticed during the plate preparation that compounds TKSM04, TKSM05, TKSM08, TKSM09 and TKSM14 may have precipitated out when prepared in 2% DMSO at 1 mM. Indeed, fluorescence endpoint readings of some of them confirmed this suspicion due to randomness of their values. Therefore, a second small-molecule plate was made in 10% DMSO with ten selected compounds prepared in 10 serial concentrations (**Supplementary Table S4**, panel A). These small molecules included the four active small molecules from the first screen; those four more hydrophobic molecules that had precipitated; and the small molecules TKSM06 and TKSM07 that had showed erratic activity in the first screen (**Supplementary Table S3**, panel D, rows G and H). When TKSM02 and TKSM14 were tested after being prepared in 10% DMSO, they showed dose-dependent antagonistic activities that allowed the estimation of IC_{50}s and confidence intervals (**Figures 5A,D**). TKSM02 acted as a full antagonist with IC_{50} = 45 μM (95% confidence interval of 31–61 μM) (**Figure 5A**). Three small molecules showed partial antagonism: TKSM14, with IC_{50} = 23 μM (95% confidence interval of 17–30 μM), only inhibited 60% of the agonist response at the highest concentrations tested of 35 and 50 μM (**Figure 5D**), and TKSM10 and TKSM13 did not have meaningful IC_{50} values because their 95% confidence intervals were too wide (**Figures 5B,C**). Nevertheless, TKSM10 exhibited antagonist activity at concentrations above 70 μM and inhibited 80% of agonist response when applied at 100 μM (**Figure 5B**). Although TKSM13 showed an overall weak antagonistic activity across concentrations, it acted as a potential antagonist (**Figure 5C**) as it inhibited approximately 50% of the agonist response at concentrations above 25 μM. The rest of the compounds re-tested (TKSM04-TKSM09) did not show any activity (**Supplementary Table S4**, panel D).

The small molecule library prepared for the second screening of potentially insoluble molecules (10% DMSO), was screened on both BMLK3 cells and "vector only" cells to test for the tick receptor specificity of the agonist responses observed after the first addition of small molecules, because the endogenous expression of NK receptors in CHO-K1 cells is assumed. Counter screening on vector only cells (**Supplementary Table S4**). confirmed that none of the agonistic responses observed after the first addition were specific for the tick kinin receptor because the vector only cells showed equivalent agonistic responses to these molecules as BMLK3 cells did (**Supplementary Table S4**,

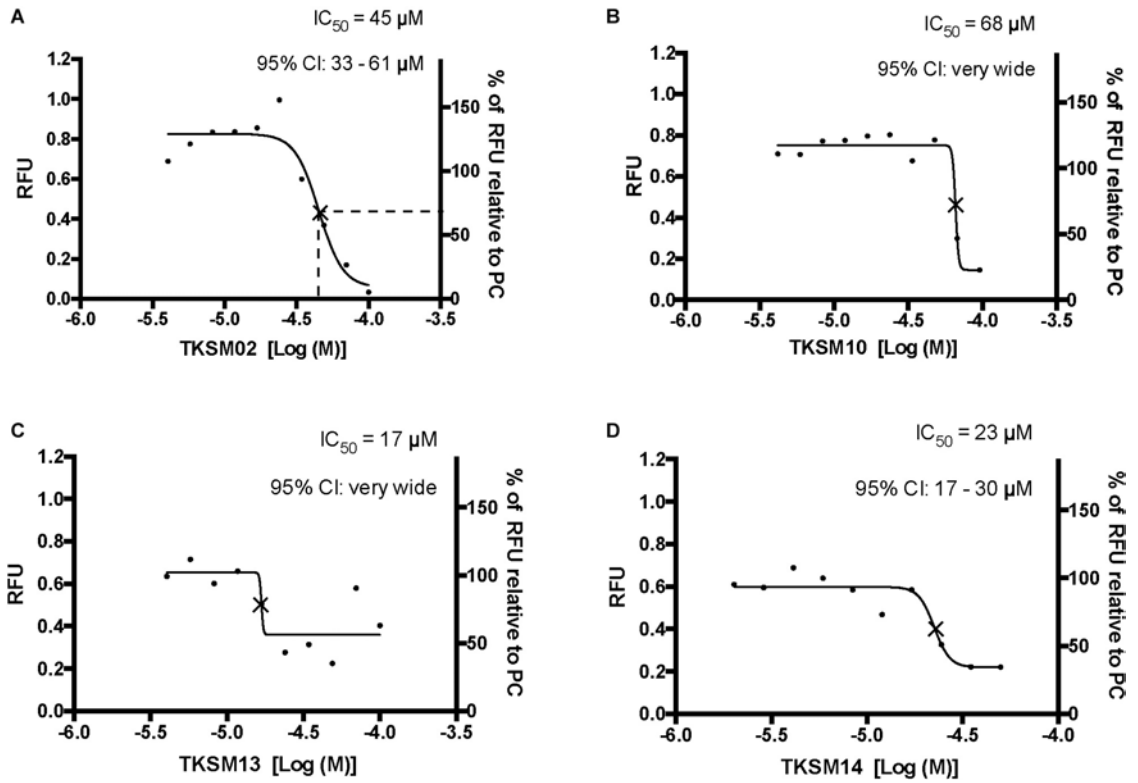

FIGURE 5 | Four small molecules antagonized the tick kinin receptor activity. Only four molecules out of the 10 tested exhibited antagonistic activities. **(A–D)** Dose-responses of the tick kinin receptor (in the BMLK3 cell line) to small-molecule ligands of mammalian neurokinin receptors were measured in a calcium fluorescence assay. Ten dosages were applied for each compound, starting from 100 μM (except TKSM14, starting from 50 μM) and following a 1:1.4 dilution series. The antagonist activity of 10 selected small molecules was tested by first dispensing the blank buffer or small molecules at various concentration [Log (Molar) on the *X*-axis] from the library plate into the assay plate. This was followed by incubation with the cells for 5 min, after which the kinin agonist (1 μM FFFSWGa) of the tick kinin receptor was dispensed into all wells and incubated for another 5 min. The end-point relative fluorescence units (RFU) from each well was represented as the average RFU (left *Y*-axis) of two end-point reads obtained by inverting the orientation of the plate in a Varioskan LUX™ (Thermos Scientific, Waltham, MA, United States) plate reader. Additionally, the right *Y*-axis represents the percentage of RFU relative to the averaged responses from cells to the PC (blank buffer + agonist). Non-linear dose-response curves IC_{50}s were defined as the concentration of antagonist that inhibits agonist response in the mid-range of its respective fitted dose-response curve and they are marked with a cross (×) on the curve. The IC_{50}s and corresponding 95% confidence intervals of IC_{50S} were calculated with "log(inhibitor) vs. response- Variable slope (four parameters)" in GraphPad 6.0. The IC_{50s} shown here are not the concentrations that inhibit 50% of the agonist response.

panel B, compare row F, wells 2-12 to row F, wells 22 to 13). Therefore, only antagonistic activities remain to be demonstrated in tick bioassays.

Kinetic Responses to Selected Small Molecules and Peptidomimetics in a Dual-Addition Calcium Bioluminescence Assay

The primary screen using fluorescence provided only one end-point reading after 5 min of incubation with cells. A kinetic calcium bioluminescence assay was subsequently performed with molecules identified in the first screen. This was to determine the kinetic responses during the first 30 s after the addition of compound of unknown activity (small molecule or peptidomimetic) and the response after the subsequent addition of known agonist (1 μM FFFSWGa) (**Figure 6**). In contrast to the results of the fluorescence assay, nearly no agonist responses were detected in the kinetic assay in the first 30 s after the addition of small molecules (**Figures 6A–E**, right panel, black bars). The statistical analyses of antagonist activities based on the responses after the agonist addition were calculated by one-way ANOVA followed by Tukey's multiple comparison test among all dosages. Consistent with the preliminary screen, TKSM02 was the most potent antagonist on the tick kinin receptor and inhibited 82.7 ± 1.8% of the FFFSWGa agonist response at 100 μM (**Figure 6A**; black curve in the left panel and in the histogram, last gray bar). The bioluminescence response of TKSM02 at 100 μM was significantly lower than the responses to the four lower concentrations tested from 100 nM–30 μM (histogram, four bars to the left), and significantly lower than the response to agonist only (Blank bar), as expected ($p < 0.0001$) (**Figure 6A**). A dose-dependent trend of antagonistic responses was observed for TKSM10 from 1 to 100 μM (**Figure 6B**, decreasing bar heights in histogram), with the lowest cell response being 84 ± 6% of the response to agonist only (16% inhibition). However, the

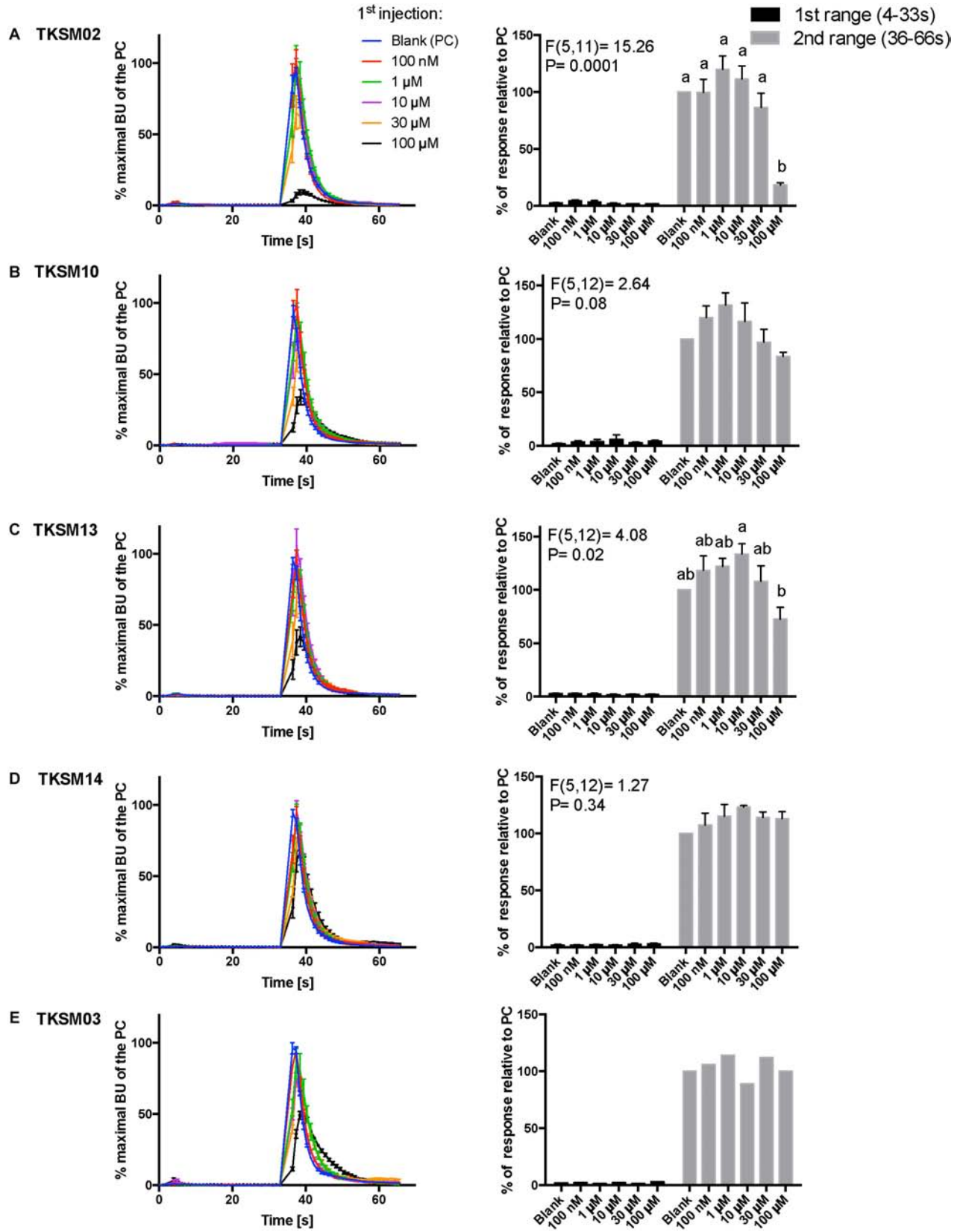

FIGURE 6 | Continued

FIGURE 6 | Kinetic dose-responses of the BMLK3 cell line to five selective small molecules. Kinetic bioluminescence responses of tick kinin receptor recombinant cells to **(A–D)** four antagonist candidates (n = 3), and **(E)** TKSM03 [negative control (n = 1)] in the "dual-addition" calcium bioluminescence assay. All small molecules were tested at five different concentrations from 100 nM to 100 μM. Two additions were performed by the two injectors built-in the Clariostar^{TM} plate reader (BMG LABTECH) as follows: the first addition of various concentrations of small molecules (5×) or corresponding blank buffer, was performed at 2 s after initiation of the recording. The response to the first addition was recorded for 30 s with 1 s intervals (first range). At 32 s, the second addition of the agonist of tick kinin receptor used in this study (1 μM FFFSWGa) was performed in the same well, and the cell response was recorded for another 30 s with 1 s intervals (second range). Curves on the left of each panel depict in different colors the kinetic response in bioluminescence units (BU) per second to each concentration (4–9 wells) from three independent assays (except TKSM03 n = 2 wells from one assay). The Y-axis represents the percentage BU of each concentration normalized to the maximal BU of the positive control (blank buffer + agonist, blue curve) (mean ± SEM). The histogram on the right of each panel shows sequentially the total BU responses of cells to the two additions, the first (black) and second (gray) range recordings, respectively. The total response in each range was expressed as the percentages of the average BU (per second) obtained in each of the two 30 s-ranges, relative to the average units to the PC in the second range (average BU of the blue curve at 35–65 s). In each independent assay, the total response to each concentration of each small molecule in the first addition or to the agonist in the second addition was calculated as the average of 2–3 pseudo-replicate wells (Y axis: mean ± SEM; n = 3 independent assays). None of the tested compounds showed agonist activity. Statistical differences in inhibitory activities between different concentrations of each compound were analyzed by one-way ANOVA (n = 3) followed by Tukey's multiple comparison test ($p \leq 0.05$) with GraphPad 6.0 (GraphPad Software, La Jolla, CA, United States). Bars with different letter superscripts indicate significant differences.

increasing trend of inhibition with higher concentrations was not detected as statistically significant by ANOVA (p = 0.08). The ANOVA for TKSM13 detected significant variation in the response among concentrations (p = 0.02) and Tukey's test detected a significant decrease in the response to the agonist of 72 ± 19% at 100 μM with respect to the 133 ± 17% response to 10 μM concentration ($p < 0.05$) (**Figure 6C**). Unexpectedly, TKSM14 did not show any antagonistic activity in the calcium bioluminescence assay, which was inconsistent with the result of the primary screen in the fluorescence assay. We then asked whether increasing the preincubation time to 5 min in the bioluminescence assay (previously, 30 s), similar to the fluorescence assay, could reveal TKSM14 antagonistic activity. Indeed, when the preincubation with TKSM14 was 5 min, a dose-dependent antagonistic response was detected after agonist addition (**Figures 7A,B**). Tukey's test showed significant antagonistic activities of TKSM14 at both 50 μM (63 ± 8%) and 100 μM (55 ± 4%) which inhibited ∼ 40 and 45% of the agonist response (**Figure 7A**, orange and black curves on the left panel and last two bars on the histogram to the right). This activity matched the result observed in the first screen. This suggested that TKSM14 might have a lower binding affinity, reflected in the longer incubation time with the cells required to block the receptor.

Compound TKSM03 was chosen as a negative control for the bioluminescence assay with small molecules due to its lack of activity in the fluorescence screen. Its lack of activity was confirmed in the bioluminescence assay, as this compound did not decrease the agonist response even at the highest concentration tested of 100 μM (**Figure 6E**, histogram on right). The corresponding black curve on the left panel (**Figure 6E**) could be misleading at first sight, giving the impression that TKSM03 could be an antagonist, as the black curve appeared to be lower than other curves. However, it must be emphasized that although the maximal bioluminescence units per second at about 40 s is diminished with respect to the other concentrations, the area under the curve did not change with respect to that of the blank control (**Figure 6E**, right panel). This is why it is important to consider the total, integrated bioluminescence response and not only the peak response.

In addition, three peptidomimetic ligands of mammalian neurokinin receptors were tested using this approach. These ligands of NK receptors showed neither agonistic nor antagonistic activities on the tick kinin receptor within the tested concentration range (1 nM–10 μM) (**Figures 8A–C**) (ANOVA $p > 0.1$ for all three peptidomimetics). In **Figure 8B**, a slight agonistic activity of antagonist G at 1-, 3- and 10-μM can be detected, peaking at about 14 s; the same activity is reflected in the histogram to the right. However, this activity was only observed in the first independent replication and could not be seen in the two other independent replications. This agonist response was also not detected in the vector only cells (not shown). We do not know what could have caused this effect.

DISCUSSION

The insect kinins were named leucokinins after first being isolated from the roach *Leucophaea maderae* for their myotropic activity (Holman et al., 1986). The kinin neuropeptide signaling system is pleiotropic in insects, regulating physiological functions both at the central and peripheral levels. They regulate myotropic and diuretic activities, orchestrate innate behaviors during pre-ecdysis and influence feeding behavior (Veenstra et al., 1997; Kim et al., 2006; Kersch and Pietrantonio, 2011; Schooley et al., 2012; Kwon et al., 2016; Pietrantonio et al., 2018). However, the kinin functions in ticks have remained elusive. In the tick *R. microplus* LKR was immunolocalized on the midgut outer surface, and LKR-silenced females displayed variations in gut discoloration, had a reduction in body weight of ∼30%, reduced weight of their egg masses, and experienced decreased egg hatching. Thus, LKR silencing in female ticks caused a reproductive fitness cost, perhaps related to defects in heme metabolism because some guts from silenced females were completely white (Brock et al., 2019). In agreement, the LKR transcript of the tick *R. sanguineous* was apparently expressed at higher levels in the gut and salivary glands than in other tissues, as inferred from RT-PCR analyses (Lees et al., 2010).

Most information on tick GPCRs was obtained from recombinant receptor systems (Yang et al., 2013, 2015; Gross et al., 2015; Gondalia et al., 2016; Kim et al., 2018). Transcripts for

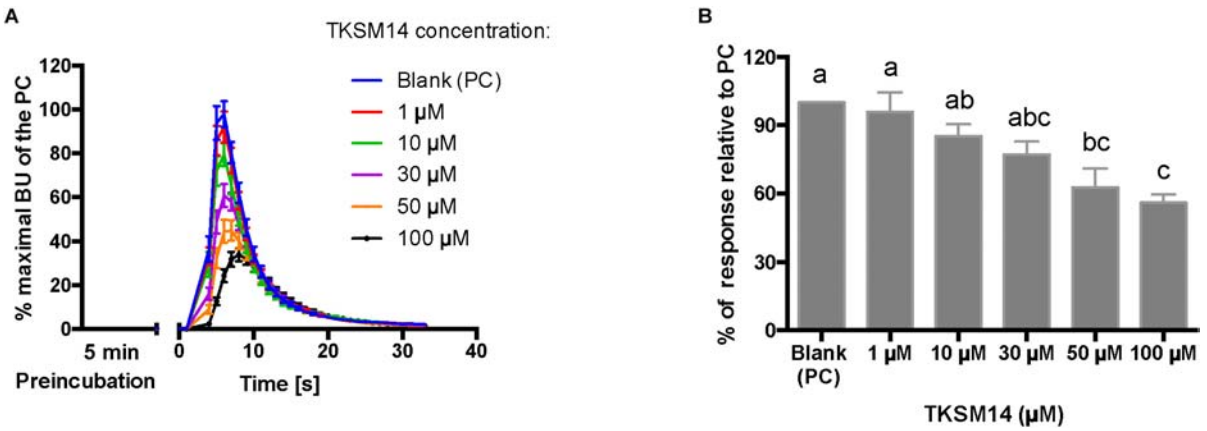

FIGURE 7 | BMLK3 preincubation (5 min) with dosages of TKSM14 before agonist addition, enhances its antagonistic activity in the calcium bioluminescence assay. **(A)** The kinetic responses of BMLK3 cells to the agonist (1 µM FFFSWGa) after being incubated with various concentrations of TKSM14 (1–100 µM) or blank solvent for 5 min. The response was recorded for 30 s at 1 s intervals by the Clariostar^{TM} plate reader (BMG LABTECH). The kinetic response is represented as the percentage of the maximal bioluminescence units (BU) of the positive control (PC = blank buffer + agonist, blue curve) in each assay (Mean ± SEM, n = 9–10 wells from three independent assays). **(B)** The total cellular response in each well is expressed as the percentage of the average BU (per second) obtained in the 30 s relative to the average response units to the PC in 30 s. Three independent assays were performed. Responses from each assay were calculated as the average of individual responses from 3-4 pseudo-replicate wells (Y axis: mean ± SEM). Statistical differences in inhibitory activities between different treatment were analyzed by one-way ANOVA (n = 3) followed by Tukey's multiple comparison test ($p \leq 0.05$) with GraphPad 6.0 (GraphPad Software, La Jolla, CA, United States). Bars with different letter superscripts indicate significant differences.

tick GPCRs are often expressed *in vivo* at very low levels, which complicates their physiological characterization. For example, results of qRT-PCR after gene silencing is often highly variable in diverse tick tissues due to their normal low expression levels (Brock et al., 2019). To address this challenge, additional future approaches to elucidate the physiological function of the tick kinin system through loss-of-function experiments include the knockdown of the endogenous kinin neuropeptide transcript and a pharmacological approach to block receptor function. With these approaches in mind, we cloned the kinin cDNA from *R. microplus*, and developed a dual addition assay to discover antagonists of the receptor to block the response to endogenous ligands and impair the normal physiology of ticks (**Figure 1**). To expand our current knowledge on the kinin system of the cattle fever tick, *R. microplus,* we used a forward pharmacological approach (**Figure 1**). Herein, we integrated the cloning of the cDNA encoding the tick endogenous kinins from the synganglion of female *R. microplus* and predicted kinin sequences from other Acari.

Kinins arose before the shared common ancestor of Mollusca, Insecta and Acari, and the lymnokinin receptor (leucokinin-like) was functionally characterized in the pond snail, *Lymnaea stagnalis* (Cox et al., 1997; Grimmelikhuijzen and Hauser, 2012).

In the cattle fever tick, we identified a single cDNA that encodes 17 potential bioactive kinins, all different (**Table 1**). This is the first report for the cloning of a kinin-encoding cDNA from any tick species. Similar to *R. microplus*, the additional tick species analyzed also showed an expansion in the number of predicted kinins (**Figure 3**), underscoring the potential importance of the kinin system in ticks. Most of the *R. microplus* kinins featured the conserved C-terminal pentapeptide motif found in insects (FX_1X_2WGa). We predict the kinins reported in this study are active because they satisfy the minimal requirement for activity and we have experimental evidence of activity of similar kinin analogs and insect kinins on the *R. microplus* receptor expressed in CHO-K1 cells (Holmes et al., 2003; Taneja-Bageshwar et al., 2006, 2009; Xiong et al., 2019). However, the variable position X_1 that in insect kinins is occupied by His, Asn, Ser or Tyr (Torfs et al., 1999), is different in some of the *R. microplus* kinins, featuring instead Gly, Ala, Thr, or Arg (Bold amino acids in **Table 1**). *R. microplus* retained the same variable residues as in the insect kinins in position X_2 (Ser/Pro/Ala) (Torfs et al., 1999), with Pro being more frequent in tick kinins (**Table 1**). These seventeen predicted kinins await to be synthesized and tested in the receptor functional assay to verify their biological activities.

The genome analysis of *Ix. scapularis* identified a putative kinin-encoding gene and four genes encoding kinin receptors (Gulia-Nuss et al., 2016). In contrast, BLAST of *R. microplus* LKR against the updated genome assembly (Rm2.0; NCBI) of this species identified only one receptor and did not reveal kinin receptor paralogs. The same sequence of 1,481 bp was identified in two contigs (sequences ID LYUQ01138740.1 and LYUQ01085891.1), and it matched the 3′-half of the *R. microplus* LKR cDNA with 99.9% identity. Therefore, it appears that in *R. microplus* there is only one kinin receptor gene, or perhaps an identical duplicate. In the genomes of six non-tick chelicerate species (spiders, the house dust mite and a scorpion), five species have one gene for both the kinin peptide and receptor, except that the African social velvet spider (*Stegodyphus mimosarum*) has 3 LKR paralogs (Veenstra, 2016). The transcript expression level of kinin and its receptor(s) seems to be generally low in ticks because transcripts were not reported in transcriptomes from synganglia of females of *R. microplus* from Texas, *Ix. scapularis*

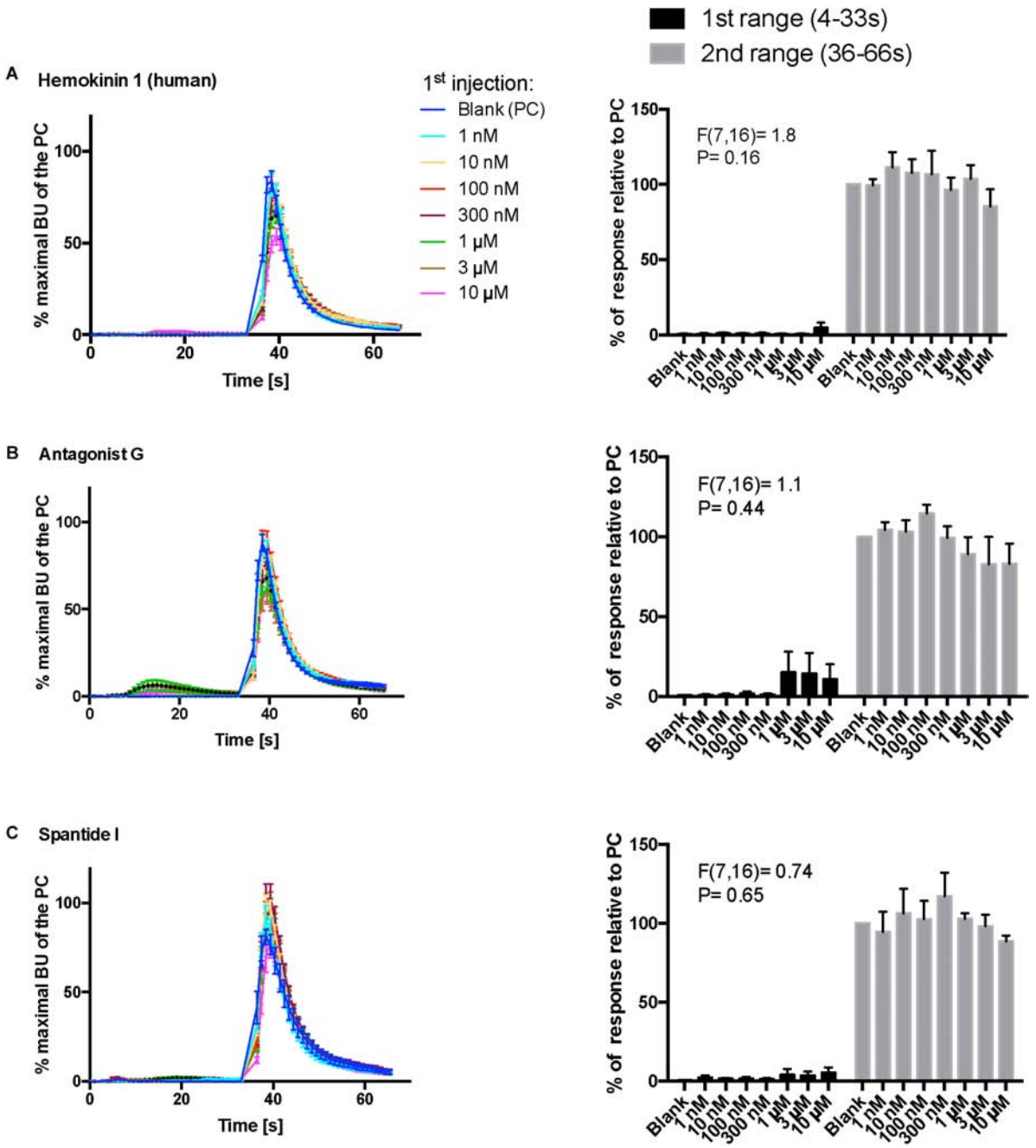

FIGURE 8 | Kinetic dose-responses of the BMLK3 cell to three peptidomimetic ligands of mammalian neurokinin receptors in the "dual-addition" calcium bioluminescence assay. Kinetic bioluminescence responses of tick kinin receptor recombinant cells to **(A–C)** three peptidomimetics (1 nM–10 µM, *n* = 3). Two additions were performed by the two injectors built-in the Clariostar™ plate reader (BMG LABTECH) as follows: the first addition of various concentrations of peptidomimetics (10×), or corresponding blank buffer, was performed at 2 s after initiation of the recording. The response to the first addition was recorded for 30 s with 1 s intervals (first range). At 32 s, the second addition of the agonist of tick kinin receptor (1 µM FFFSWGa) was performed in the same well, and the cellular response was recorded for another 30 s with 1 s intervals (second range). Curves on the left of each panel depict in different colors the kinetic response in bioluminescence units (BU) per second to each concentration (8–9 wells from three independent assays). The *Y*-axis represents the percentage BU of each concentration normalized to the maximal BU of the positive control (blank buffer + agonist, blue curve) (mean ± SEM). The histogram on the right of each panel shows sequentially the total BU responses of cells to the two additions, the first and second range recordings, respectively. The total responses in each range was expressed as the percentages of the average BU (per second) obtained in each of the two 30 s-ranges, relative to the average units to the PC in the second range (average BU of the blue curve at 35–65 s). In each independent assay, the total response to each concentration of each peptidomimetic in the first addition or to the agonist in the second addition was calculated as the average of 2–3 pseudo-replicate wells (*Y* axis: mean ± SEM, *n* = 3 independent assays). None of the tested compounds showed agonist activity (for **B** panel, first range, see explanation in text). Statistical differences in inhibitory activities between different concentrations of each compound were analyzed by one-way ANOVA (*n* = 3) but no statistical differences were detected.

and *O. turicata* (Egekwu et al., 2014, 2016; Guerrero et al., 2016). As the kinin receptor transcript level is low in ticks (as well as the level of receptor protein (Brock et al., 2019), it is tempting to speculate that kinin signaling may be regulated by changes in the expression and release of their expanded kinin peptide repertoire. A detailed temporal quantitative analysis of receptor and kinin precursor mRNA transcripts is still lacking. It is also yet unknown whether the high copy number of the tick kinins will result in increased peptide expression (i.e., concentration) or in sustained, constitutive expression. It is worth noting, however, that kinins are active at nanomolar levels (low concentrations) (Holmes et al., 2003; Xiong et al., 2019).

Kinins arose before the shared common ancestor of Mollusca, Insecta and Acari, and the lymnokinin receptor (leucokinin-like) was functionally characterized in the pond snail, *Lymnaea stagnalis* (Cox et al., 1997; Grimmelikhuijzen and Hauser, 2012). Among ticks, the Argasidae are considered a basal group to the Ixodidae (Geraci et al., 2007). Arthropod molecular phylogenetic studies have suggested Prostriata are more ancient than Metastriata (Jeyaprakash and Hoy, 2009). Although the pentapeptide core of tick kinins is largely conserved, it is noteworthy that more ancient species show higher conservation on the X_1 position of this core, with asparagine (N), glycine (G) or serine (S) being more frequent. Further, although the Prostriata and Metastriata have a similar number of kinin paracopies (∼17), the tick kinins of the Metastriata showed more frequent amino acid substitutions than those of the Prostriata. Specifically, *Ix. scapularis* and *Ix. ricinus* (Prostriata) have multiple iterations of the same kinin sequence (DTFGPWGa) in the kinin precursor, whereas ticks from the Metastriata showed no repetition in the sequence of kinin paracopies (**Table 1** and **Figure 3A**).

The unrooted phylogenetic tree revealed kinin sequence differences between ticks and insect blood feeders (**Figure 4**). Although the number of paracopies does not appear to differentiate kinin sequences of ticks from those of insects, we have experimental evidence that kinin receptors from insects and ticks have different ligand structure-activity relationships, as manifested in the differential potency of the same set of kinin analogs (Taneja-Bageshwar et al., 2006; Xiong et al., 2019). Therefore, differences in the sequences of the mature kinin peptides between ticks and insects further support this differential activation. Additionally, we reiterate that kinins have pleiotropic functions in insects and therefore, it is possible that they are similarly pleiotropic in ticks. We speculate this pleiotropism could be achieved in ticks either by diversification of receptors or ligands. In *Ixodes* (Prostriata), despite low variation in the kinin sequences, up to four kinin receptors may be present (Gulia-Nuss et al., 2016). In contrast, *Rhipicephalus microplus* appears to have only one receptor but exhibits high variation in the sequences of the kinin ligands (**Table 1**). As a mechanism for pleiotropism, there is evidence that in the mosquito renal organ different kinin analogs promote differential downstream tissue responses, either fluid secretion or changes membrane voltage (Schepel et al., 2010), apparently through the same receptor because only one kinin receptor has been identified in this tissue (Lu et al., 2011a).

To advance the discovery of novel ligands toward application, we tested potential synthetic ligands (small molecules and peptidomimetics) of mammalian neurokinin receptors on the recombinant tick receptor (**Figure 1**). Our previous success with a kinin mimetic, named 1728, that elicits aversive behavior in the mosquito and inhibits the sugar neuron provided the proof of principle to pursue this approach (Kwon et al., 2016). The NK receptors are considered "pseudo-orthologs" of the arthropod kinin receptor because while tachykinins exist in both mammals and arthropods, the kinin system is arthropod-specific (Nachman et al., 1999). To accelerate discovery and reduce the cost of screening a commercial GPCR-specific small molecule library and selected peptidomimetics, we developed a dual-addition functional assay using two reporters for calcium, in fluorescence and bioluminescence modes, respectively. A comparable pipeline was developed by Ejendal et al. (2012) for validating the dopamine receptor of *Ix. scapularis* as acaricide target, except their functional assay detects cAMP as the secondary messenger. Using a reverse pharmacological approach, Duvall et al. (2019) recently discovered a novel small molecule ligand of the mosquito neuropeptide receptor, NPY receptor, which discourages the biting behavior of mosquito (Duvall et al., 2019).

In this study, through the primary screening of a small molecule library of NK receptor antagonists, and their secondary validation by a bioluminescence assay, a small molecule, named TKSM02, was identified as a "full antagonist" of the tick kinin receptor with an IC_{50} of 45 μM (**Figure 5A**), as it fully blocked receptor activity at 100 μM. Although of weak potency, we believe this is the first antagonist reported for a kinin receptor of any arthropod species. However, it should be noted that we used a generic kinin receptor agonist, FFFSWGa, in the antagonist screen. Therefore, the antagonists identified with this screen may not similarly antagonize endogenous tick kinins on the cognate receptor. Overall, ligands of NK receptors displayed more than a 10,000-fold reduced potency on the tick kinin receptor. The quantitative functional data reported here will provide valuable information to constrain the ligand-receptor interaction surface in computational modeling.

Agonists and antagonist peptidomimetics of NK receptors were tested: hemokinin 1 (human) is an agonist of the NK1 receptor with active concentration at the nanomolar level, antagonist G is a broad antagonist on NK receptors, and spantide I is a selective potent antagonist of the NK1 receptor (**Supplementary Table S2**). Our results provided additional functional evidence that the tick kinin receptor is pharmacologically different from the insect tachykinin receptor as none of the peptidomimetic ligands of NK receptors showed any activity on the tick kinin receptor. However, spantide I antagonizes insect tachykinins in recombinant tachykinin receptors of the stable fly and fruit fly at 1 and 50 μM, respectively (Torfs et al., 2002; Poels et al., 2009).

In summary, we report for the first time putative tick kinin sequences. Further, our small molecule screening results confirmed in one direction the target selectivity of the kinin receptor for arthropod vector control, as only one of the small

molecule NK antagonists was active. The dual addition assay we developed is amenable and ready for the high throughput screening of random small molecule libraries on the tick kinin receptor or other tick neuropeptide receptors signaling through the calcium cascade. While receptor "hits" of random molecules are expected, the next frontier is to develop suitable tick bioassays to elucidate the physiological functions of kinins that could be impaired by these synthetic ligands.

DATA AVAILABILITY

The DNA sequence of the PCR product verifying the *R. microplus* kinin gene sequence with mRNA sequence of the kinin precursor were uploaded in NCBI with GenBank accession number (MK875970). The raw data of the fluorescence dual-addition assay are under **Supplementary Tables S3**, **S4**. The raw data of the calcium bioluminescence assay can be made available upon request.

AUTHOR CONTRIBUTIONS

PP and CX designed the study, developed the fluorescence assay, performed the data analyses and wrote the manuscript. CX was responsible for performing the molecular cloning, cell culture and calcium bioluminescence assay. DB advised on composition of small molecule library. CX and DB performed the 384-well-plate calcium fluorescence assay. All authors edited and approved the final manuscript.

FUNDING

This work was supported by NIFA-AFRI Animal Health and Well-Being Award 2016-67015-24918 to Patricia V. Pietrantonio and Kevin Temeyer and from competitive funds from the Texas A&M AgriLife Research Insect Vector Diseases Grant Program (FY19-21) to PP. NIFA also supports PP program through Hatch project TX (TEX0-2-9206), accession 1002279 (Y 2018-2023).

ACKNOWLEDGMENTS

We thank Distinguished Professor James C. Sacchettini (Deptartment of Biochemistry and Biophysics, Texas A&M University) for the support of his staff and for the use of facilities for high throughput screening. Dr. Wen Dong is acknowledged for training CX in the use of the Cybio® system. We thank the A.W.E.S.O.M.E. faculty group in the College of Agriculture and Life Sciences at Texas A&M University for assistance with editing the manuscript. We acknowledge Professor James Woolley for his advice on the construction of the unrooted phylogenetic tree. We also thank both reviewers for their input to improving this manuscript.

SUPPLEMENTARY MATERIAL

The Supplementary Material for this article can be found online at: https://www.frontiersin.org/articles/10.3389/fphys.2019.01008/full#supplementary-material

REFERENCES

Adams, M. D., Celniker, S. E., Holt, R. A., Evans, C. A., Gocayne, J. D., Amanatides, P. G., et al. (2000). The genome sequence of *Drosophila melanogaster*. *Science* 287, 2185–2195. doi: 10.1126/science.287.5461.2185

Al-Anzi, B., Armand, E., Nagamei, P., Olszewski, M., Sapin, V., Waters, C., et al. (2010). The leucokinin pathway and its neurons regulate meal size in *Drosophila*. *Curr. Biol.* 20, 969–978. doi: 10.1016/j.cub.2010.04.039

Armenteros, J. J. A., Tsirigos, K. D., Sønderby, C. K., Petersen, T. N., Winther, O., Brunak, S., et al. (2019). SignalP 5.0 improves signal peptide predictions using deep neural networks. *Nat. Biotechnol.* 37, 420–423. doi: 10.1038/s41587-019-0036-z

Audsley, N., and Down, R. E. (2015). G protein coupled receptors as targets for next generation pesticides. *Insect Biochem. Molec.* 67(Suppl. C), 27–37. doi: 10.1016/j.ibmb.2015.07.014

Bhatt, G., da Silva, R., Nachman, R. J., and Orchard, I. (2014). The molecular characterization of the kinin transcript and the physiological effects of kinins in the blood-gorging insect. *Rhodnius prolixus. Peptides.* 53, 148–158. doi: 10.1016/j.peptides.2013.04.009

Bootman, M. D., Collins, T. J., MacKenzie, L., Roderick, H. L., Berridge, M. J., and Peppiatt, C. M. (2002). 2-aminoethoxydiphenyl borate (2-APB) is a reliable blocker of store-operated Ca2+ entry but an inconsistent inhibitor of InsP3-induced Ca2+ release. *FASEB J.* 16, 1145–1150. doi: 10.1096/fj.02-0037rev

Brock, C. M., Temeyer, K. B., Tidwell, J., Yang, Y., Blandon, M. A., Carreón-Camacho, D., et al. (2019). The leucokinin-like peptide receptor from the cattle fever tick, *Rhipicephalus microplus*, is localized in the midgut periphery and receptor silencing with validated double-stranded RNAs causes a reproductive fitness cost. *Int. J. Parasitol.* 49, 287–299. doi: 10.1016/j.ijpara.2018.11.006

Cannell, E., Dornan, A. J., Halberg, K. A., Terhzaz, S., Dow, J. A., and Davies, S.-A. (2016). The corticotropin-releasing factor-like diuretic hormone 44 (DH44) and kinin neuropeptides modulate desiccation and starvation tolerance in *Drosophila melanogaster*. *Peptides* 80, 96–107. doi: 10.1016/j.peptides.2016.02.004

Cox, K. J., Tensen, C. P., Van der Schors, R. C., Li, K. W., van Heerikhuizen, H., Vreugdenhil, E., et al. (1997). Cloning, characterization, and expression of a G-protein-coupled receptor from *Lymnaea stagnalis* and identification of a leucokinin-like peptide, PSFHSWSamide, as its endogenous ligand. *J. Neurosci* 17, 1197–1205. doi: 10.1523/jneurosci.17-04-01197.1997

Crooks, G. E., Hon, G., Chandonia, J.-M., and Brenner, S. E. (2004). WebLogo: a sequence logo generator. *Genome Res.* 14, 1188–1190. doi: 10.1101/gr.849004

Derst, C., Dircksen, H., Meusemann, K., Zhou, X., Liu, S., and Predel, R. (2016). Evolution of neuropeptides in non-pterygote hexapods. *BMC Evol. Biol.* 16:51. doi: 10.1186/s12862-016-0621-4

Duvall, L. B., Ramos-Espiritu, L., Barsoum, K. E., Glickman, J. F., and Vosshall, L. B. (2019). Small-molecule agonists of Ae. aegypti neuropeptide Y receptor block mosquito biting. *Cell* 176, 687–701.e5. doi: 10.1016/j.cell.2018.12.004

Egekwu, N., Sonenshine, D., Garman, H., Barshis, D., Cox, N., Bissinger, B., et al. (2016). Comparison of synganglion neuropeptides, neuropeptide receptors and neurotransmitter receptors and their gene expression in response to feeding in *Ixodes scapularis* (Ixodidae) vs. *O rnithodoros turicata (Argasidae). Insect Mol. Biol.* 25, 72–92. doi: 10.1111/imb.12202

Egekwu, N., Sonenshine, D. E., Bissinger, B. W., and Roe, R. M. (2014). Transcriptome of the female synganglion of the black-legged tick *Ixodes scapularis* (*Acari*: *Ixodidae*) with comparison between Illumina and 454 systems. *PLoS One.* 9:e102667. doi: 10.1371/journal.pone.0102667

Ejendal, K. F. K., Meyer, J. M., Brust, T. F., Avramova, L. V., Hill, C. A., and Watts, V. J. (2012). Discovery of antagonists of tick dopamine receptors via chemical

library screening and comparative pharmacological analyses. *Insect Biochem. Molec.* 42, 846–853. doi: 10.1016/j.ibmb.2012.07.011

Geraci, N. S., Johnston, J. S., Robinson, J. P., Wikel, S. K., and Hill, C. A. (2007). Variation in genome size of argasid and ixodid ticks. *Insect Biochem. Molec.* 37, 399–408. doi: 10.1016/j.ibmb.2006.12.007

Gondalia, K., Qudrat, A., Bruno, B., Medina, J. F., and Paluzzi, J.-P. V. (2016). Identification and functional characterization of a pyrokinin neuropeptide receptor in the Lyme disease vector, *Ixodes scapularis*. *Peptides* 86, 42–54. doi: 10.1016/j.peptides.2016.09.011

Grimmelikhuijzen, C. J., and Hauser, F. (2012). Mini-review: the evolution of neuropeptide signaling. *Regul. pept.* 177, S6–S9. doi: 10.1016/j.regpep.2012.05.001

Gross, A. D., Temeyer, K. B., Day, T. A., Pérez de León, A. A., Kimber, M. J., and Coats, J. R. (2015). Pharmacological characterization of a tyramine receptor from the southern cattle tick, *Rhipicephalus (Boophilus) microplus*. *Insect Biochem. Molec.* 63, 47–53. doi: 10.1016/j.ibmb.2015.04.008

Guerrero, F. D., Kellogg, A., Ogrey, A. N., Heekin, A. M., Barrero, R., Bellgard, M. I., et al. (2016). Prediction of G protein-coupled receptor encoding sequences from the synganglion transcriptome of the cattle tick, *Rhipicephalus microplus*. *Ticks. Tick-Borne. Dis.* 7, 670–677. doi: 10.1016/j.ttbdis.2016.02.014

Guerrero, F. D., Lovis, L., and Martins, J. R. (2012). Acaricide resistance mechanisms in *Rhipicephalus (Boophilus) microplus*. *Rev. Bras. Parasitol. V.* 21, 1–6. doi: 10.1590/s1984-29612012000100002

Gulia-Nuss, M., Nuss, A. B., Meyer, J. M., Sonenshine, D. E., Roe, R. M., Waterhouse, R. M., et al. (2016). Genomic insights into the *Ixodes scapularis* tick vector of Lyme disease. *Nat. Commun.* 7:10507. doi: 10.1038/ncomms10507

Halberg, K. A., Terhzaz, S., Cabrero, P., Davies, S. A., and Dow, J. A. (2015). Tracing the evolutionary origins of insect renal function. *Nat. Commun.* 6:6800. doi: 10.1038/ncomms7800

Hayes, T., Pannabecker, T. L., Hinckley, D., Holman, G., Nachman, R., Petzel, D., et al. (1989). Leucokinins, a new family of ion transport stimulators and inhibitors in insect malpighian tubules. *Life Sci.* 44, 1259–1266. doi: 10.1016/0024-3205(89)90362-7

Holman, G., Cook, B., and Nachman, R. (1986). Isolation, primary structure and synthesis of two neuropeptides from *Leucophaea maderae*: members of a new family of cephalomyotropins. *Comp. Biochem. Phys. C* 84, 205–211. doi: 10.1016/0742-8413(86)90084-8

Holmes, S., Barhoumi, R., Nachman, R., and Pietrantonio, P. (2003). Functional analysis of a G protein-coupled receptor from the Southern cattle tick *Boophilus microplus* (*Acari*: *Ixodidae*) identifies it as the first arthropod myokinin receptor. *Insect Mol. Biol.* 12, 27–38. doi: 10.1046/j.1365-2583.2003.00384.x

Holmes, S., He, H., Chen, A., Lvie, G., and Pietrantonio, P. (2000). Cloning and transcriptional expression of a leucokinin-like peptide receptor from the Southern cattle tick, *Boophilus microplus* (*Acari*: *Ixodidae*). *Insect Mol. Biol.* 9, 457–465. doi: 10.1046/j.1365-2583.2000.00208.x

Jeyaprakash, A., and Hoy, M. A. (2009). First divergence time estimate of spiders, scorpions, mites and ticks (subphylum: *Chelicerata*) inferred from mitochondrial phylogeny. *Exp. Appl. Acarol.* 47, 1–18. doi: 10.1007/s10493-008-9203-5

Katoh, K., and Standley, D. M. (2013). MAFFT multiple sequence alignment software version 7: improvements in performance and usability. *Mol. Biol. Evol.* 30, 772–780. doi: 10.1093/molbev/mst010

Kersch, C. N., and Pietrantonio, P. V. (2011). Mosquito *Aedes aegypti* (L.) *leucokinin receptor* is critical for in vivo fluid excretion post blood feeding. *FEBS Lett.* 585, 3507–3512. doi: 10.1016/j.febslet.2011.10.001

Kim, D., Šimo, L., and Park, Y. (2018). Molecular characterization of neuropeptide elevenin and two elevenin receptors, IsElevR1 and IsElevR2, from the blacklegged tick, *Ixodes scapularis*. *Insect Biochem. Molec.* 101, 66–75. doi: 10.1016/j.ibmb.2018.07.005

Kim, Y.-J., Žitňan, D., Cho, K.-H., Schooley, D. A., Mizoguchi, A., and Adams, M. E. (2006). Central peptidergic ensembles associated with organization of an innate behavior. *Proc. Natl. Acad. Sci. U.S.A.* 103, 14211–14216. doi: 10.1073/pnas.0603459103

Kwon, H., Agha, M. A., Smith, R. C., Nachman, R. J., Marion-Poll, F., and Pietrantonio, P. V. (2016). Leucokinin mimetic elicits aversive behavior in mosquito *Aedes aegypti* (L.) and inhibits the sugar taste neuron. *Proc. Natl. Acad. Sci. U.S.A.* 113, 6880–6885. doi: 10.1073/pnas.1520404113

Lange, A. B., Nachman, R. J., Kaczmarek, K., and Zabrocki, J. (2016). Biostable insect kinin analogs reduce blood meal and disrupt ecdysis in the blood-gorging Chagas' disease vector. *Rhodnius prolixus. Peptides.* 80, 108–113. doi: 10.1016/j.peptides.2016.01.012

Lees, K., Woods, D., and Bowman, A. S. (2010). Transcriptome analysis of the synganglion from the brown dog tick, *Rhipicephalus sanguineus*. *Insect Mol. Biol.* 19, 273–282. doi: 10.1111/j.1365-2583.2009.00968.x

Lipinski, C. A. (2016). Rule of five in 2015 and beyond: target and ligand structural limitations, ligand chemistry structure and drug discovery project decisions. *ADV Drug Deliver. Rev.* 101, 34–41. doi: 10.1016/j.addr.2016.04.029

Lu, H. L., Kersch, C., and Pietrantonio, P. V. (2011a). The kinin receptor is expressed in the Malpighian tubule stellate cells in the mosquito *Aedes aegypti* (L.): a new model needed to explain ion transport?. *Insect Biochem. Molec.* 41, 135–140. doi: 10.1016/j.ibmb.2010.10.033

Lu, H. L., Kersch, C. N., Taneja-Bageshwar, S., and Pietrantonio, P. V. (2011b). A calcium bioluminescence assay for functional analysis of mosquito (*Aedes aegypti*) and Tick (*Rhipicephalus microplus*) G protein-coupled receptors. *Jove-J. Vis. Exp.* 20, 2732. doi: 10.3791/2732

Ma, Q., Ye, L., Liu, H., Shi, Y., and Zhou, N. (2017). An overview of Ca2+ mobilization assays in GPCR drug discovery. *Expert Opin. Drug Dis.* 12, 511–523. doi: 10.1080/17460441.2017.1303473

Maddison, W. P. (2005). *Mesquite: a Modular System for Evolutionary Analysis. Version 1.06*. Available at: http://mesquiteproject.org

Nachman, R. J., Moyna, G., Williams, H. J., Zabrocki, J., Zadina, J. E., Coast, G. M., et al. (1999). Comparison of active conformations of the insectatachykinin/tachykinin and insect kinin/Tyr-W-MIF-1 neuropeptide family pairs. *Ann. NY. Acad. Sci.* 897, 388–400. doi: 10.1111/j.1749-6632.1999.tb07908.x

Nachman, R. J., Zabrocki, J., Olczak, J., Williams, H. J., Moyna, G., Scott, A. I., et al. (2002). cis-Peptide bond mimetic tetrazole analogs of the insect kinins identify the active conformation. *Peptides* 23, 709–716. doi: 10.1016/s0196-9781(01)00651-9

Neupert, S., Predel, R., Russell, W. K., Davies, R., Pietrantonio, P. V., and Nachman, R. J. (2005). Identification of tick periviscerokinin, the first neurohormone of *Ixodidae*: single cell analysis by means of MALDI-TOF/TOF mass spectrometry. *Biochem. Bioph. Res. Co.* 338, 1860–1864. doi: 10.1016/j.bbrc.2005.10.165

Pennefather, J. N., Lecci, A., Candenas, M. L., Patak, E., Pinto, F. M., and Maggi, C. A. (2004). Tachykinins and tachykinin receptors: a growing family. *Life Sci.* 74, 1445–1463. doi: 10.1016/j.lfs.2003.09.039

Pérez de León, A. A., Teel, P. D., Auclair, A. N., Messenger, M. T., Guerrero, F. D., Schuster, G., et al. (2012). Integrated strategy for sustainable cattle fever tick eradication in USA is required to mitigate the impact of global change. *Front. Physiol.* 3:195. doi: 10.3389/fphys.2012.00195

Pietrantonio, P., Jagge, C., Taneja-Bageshwar, S., Nachman, R., and Barhoumi, R. (2005). The mosquito *Aedes aegypti* (L.) *leucokinin* receptor is a multiligand receptor for the three *Aedes kinins*. *Insect Mol. Biol.* 14, 55–67. doi: 10.1111/j.1365-2583.2004.00531.x

Pietrantonio, P., Xiong, C., Nachman, R., and Shen, Y. (2018). G protein-coupled receptors in arthropod vectors: omics and pharmacological approaches to elucidate ligand-receptor interactions and novel organismal functions. *Curr. Opin. Insect Sci.* 29, 12–20. doi: 10.1016/j.cois.2018.05.016

Poels, J., Birse, R. T., Nachman, R. J., Fichna, J., Janecka, A., Broeck, J. V., et al. (2009). Characterization and distribution of NKD, a receptor for *Drosophila* tachykinin-related peptide 6. *Peptides* 30, 545–556. doi: 10.1016/j.peptides.2008.10.012

Pohl, P. C., Klafke, G. M., Júnior, J. R., Martins, J. R., da Silva Vaz, I., and Masuda, A. (2012). ABC transporters as a multidrug detoxification mechanism in *Rhipicephalus (Boophilus)* microplus. *Parasitol. Res.* 111, 2345–2351. doi: 10.1007/s00436-012-3089-1

Predel, R., Neupert, S., Derst, C., Reinhardt, K., and Wegener, C. (2017). Neuropeptidomics of the bed bug *Cimex lectularius*. *J. Proteome. Res.* 17, 440–454. doi: 10.1021/acs.jproteome.7b00630

Rambaut, A. (2012). *FigTree Version 1.4.4*.

Rambaut, A., Drummond, A., Xie, D., Baele, G., and Suchard, M. (2018). *Tracer Version 1.7.1*.

Ronquist, F., Teslenko, M., Van Der Mark, P., Ayres, D. L., Darling, A., Höhna, S., et al. (2012). MrBayes 3.2: efficient bayesian phylogenetic inference and model

choice across a large model space. *Syst. Biol.* 61, 539–542. doi: 10.1093/sysbio/sys029

Schepel, S. A., Fox, A. J., Miyauchi, J. T., Sou, T., Yang, J. D., Lau, K., et al. (2010). The single kinin receptor signals to separate and independent physiological pathways in malpighian tubules of the yellow fever mosquito. *Am. J. Physiol.Regul. Integr. Comp. Physiol.* 299, R612–R622. doi: 10.1152/ajpregu.00068.2010

Schooley, D., Horodyski, F., and Coast, G. M. (2012). "Hormones controlling homeostasis in insects," in *Insect Endocrinology*, ed. L. I. Gilbert, (Cambridge, MA: Academic Press), 366–429. doi: 10.1016/b978-0-12-384749-2.10009-3

Smagghe, G., Mahdian, K., Zubrzak, P., and Nachman, R. J. (2010). Antifeedant activity and high mortality in the pea aphid *Acyrthosiphon pisum* (*Hemiptera*: *Aphidae*) induced by biostable insect kinin analogs. *Peptides* 31, 498–505. doi: 10.1016/j.peptides.2009.07.001

Taneja-Bageshwar, S., Strey, A., Isaac, R. E., Coast, G. M., Zubrzak, P., Pietrantonio, P. V., et al. (2009). Biostable agonists that match or exceed activity of native insect kinins on recombinant arthropod GPCRs. *Gen. Comp. Endocrinol.* 162, 122–128. doi: 10.1016/j.ygcen.2008.10.013

Taneja-Bageshwar, S., Strey, A., Zubrzak, P., Pietrantonio, P. V., and Nachman, R. J. (2006). Comparative structure-activity analysis of insect kinin core analogs on recombinant kinin receptors from Southern cattle tick *Boophilus microplus* (*Acari*: *Ixodidae*) and mosquito *Aedes aegypti* (*Diptera*: *Culicidae*). *Arch. Insect Biochem.* 62, 128–140. doi: 10.1002/arch.20129

Thastrup, O., Cullen, P. J., Drøbak, B., Hanley, M. R., and Dawson, A. P. (1990). Thapsigargin, a tumor promoter, discharges intracellular Ca2+ stores by specific inhibition of the endoplasmic reticulum Ca2 (+)-ATPase. *Proc. Natl. Acad. Sci. U.S.A.* 87, 2466–2470. doi: 10.1073/pnas.87.7.2466

Torfs, H., Poels, J., Detheux, M., Dupriez, V., Van Loy, T., Vercammen, L., et al. (2002). Recombinant aequorin as a reporter for receptor-mediated changes of intracellular Ca 2+-levels in *Drosophila* S2 cells. *Invertebr. Neurosci.* 4, 119–124. doi: 10.1007/s10158-001-0013-2

Torfs, P., Nieto, J., Veelaert, D., Boon, D., Van De Water, G., Waelkens, E., et al. (1999). The kinin peptide family in invertebrates. *Ann. NY. Acad. Sci.* 897, 361–373. doi: 10.1111/j.1749-6632.1999.tb07906.x

Veenstra, J. A. (2000). Mono-and dibasic proteolytic cleavage sites in insect neuroendocrine peptide precursors. *Arch. Insect Biochem.* 43, 49–63. doi: 10.1002/(sici)1520-6327(200002)43:2<49::aid-arch1>3.0.co;2-m

Veenstra, J. A. (2016). Neuropeptide evolution: *Chelicerate* neurohormone and neuropeptide genes may reflect one or more whole genome duplications. *Gen. Comp. Endocrinol.* 229, 41–55. doi: 10.1016/j.ygcen.2015.11.019

Veenstra, J. A., Pattillo, J. M., and Petzel, D. H. (1997). A single cDNA encodes all three aedesleucokinins, which stimulate both fluid secretion by the malpighian tubules and hindgut contractions. *J. Biol. Chem.* 272, 10402–10407. doi: 10.1074/jbc.272.16.10402

Xiong, C., Kaczmarek, K., Zabrocki, J., Pietrantonio, P. V., and Nachman, R. J. (2019). Evaluation of Aib and PEG-polymer insect kinin analogs on mosquito and tick GPCRs identifies potent new pest management tools with potentially enhanced biostability and bioavailability. *Gen. Comp. Endocrinol.* 278, 58–67. doi: 10.1016/j.ygcen.2018.08.002

Yang, Y., Bajracharya, P., Castillo, P., Nachman, R. J., and Pietrantonio, P. V. (2013). Molecular and functional characterization of the first tick CAP2b (periviscerokinin) receptor from *Rhipicephalus (Boophilus) microplus* (*Acari*: *Ixodidae*). *Gen. Comp. Endocrinol.* 194, 142–151. doi: 10.1016/j.ygcen.2013.09.001

Yang, Y., Nachman, R. J., and Pietrantonio, P. V. (2015). Molecular and pharmacological characterization of the chelicerata pyrokinin receptor from the southern cattle tick, *Rhipicephalus (Boophilus)* microplus. *Insect Biochem. Molec.* 60, 13–23. doi: 10.1016/j.ibmb.2015.02.010

Yeoh, J. G. C., Pandit, A. A., Zandawala, M., Nässel, D. R., Davies, S.-A., and Dow, J. A. T. (2017). DINeR: database for insect neuropeptide research. *Insect Biochem. Molec.* 86, 9–19. doi: 10.1016/j.ibmb.2017.05.001

Zandawala, M., Yurgel, M. E., Texada, M. J., Liao, S., Rewitz, K. F., Keene, A. C., et al. (2018). Modulation of Drosophila post-feeding physiology and behavior by the neuropeptide leucokinin. *PloS Genet.* 14:e1007767. doi: 10.1371/journal.pgen.1007767

Conflict of Interest Statement: The authors declare that the research was conducted in the absence of any commercial or financial relationships that could be construed as a potential conflict of interest.

frontiers in Veterinary Science

ORIGINAL RESEARCH
published: 06 February 2020
doi: 10.3389/fvets.2020.00040

Experimental *Ixodes ricinus*-Sheep Cycle of *Anaplasma phagocytophilum* NV2Os Propagated in Tick Cell Cultures

Consuelo Almazán[1], Lisa Fourniol[1], Clotilde Rouxel[1], Pilar Alberdi[2], Christelle Gandoin[1], Anne-Claire Lagrée[1], Henri-Jean Boulouis[1], José de la Fuente[2,3] and Sarah I. Bonnet[1]**

[1] UMR BIPAR, INRAE, Ecole Nationale Vétérinaire d'Alfort, ANSES, Université Paris-Est, Maisons-Alfort, France, [2] SaBio, Instituto de Investigación en Recursos Cinegéticos IREC (CSIC-UCLM-JCCM), Ciudad Real, Spain, [3] Department of Veterinary Pathobiology, Center for Veterinary Health Sciences, Oklahoma State University, Stillwater, OK, United States

OPEN ACCESS

Edited by:
Armanda Bastos, University of Pretoria, South Africa

Reviewed by:
Eliane Esteves, University of São Paulo, Brazil
Itabajara Silva Vaz Jr., Federal University of Rio Grande do Sul, Brazil

***Correspondence:**
Consuelo Almazán
consuelo.almazan@anses.fr
Sarah I. Bonnet
sarah.bonnet@vet-alfort.fr

Specialty section:
This article was submitted to Veterinary Infectious Diseases, a section of the journal Frontiers in Veterinary Science

Received: *05 September 2019*
Accepted: *15 January 2020*
Published: *06 February 2020*

Citation:
Almazán C, Fourniol L, Rouxel C, Alberdi P, Gandoin C, Lagrée A-C, Boulouis H-J, de la Fuente J and Bonnet SI (2020) Experimental Ixodes ricinus-Sheep Cycle of Anaplasma phagocytophilum NV2Os Propagated in Tick Cell Cultures. Front. Vet. Sci. 7:40. doi: 10.3389/fvets.2020.00040

The causative agent of tick-borne fever and human granulocytic anaplasmosis, *Anaplasma phagocytophilum,* is transmitted by *Ixodes ricinus*, and is currently considered an emerging disease throughout Europe. In this study, we established a model of *A. phagocytophilum* sheep infection and *I. ricinus* transmission using the European Norway variant 2 ovine strain (NV2Os) propagated in both IDE8 and ISE6 tick cells. Two sheep were inoculated with IDE8 tick cells infected with NV2Os. Both sheep developed *A. phagocytophilum* infection as determined by qPCR and PCR, the presence of fever 4 days post inoculation (dpi), the observation of morulae in granulocytes at 6 dpi, and the detection of *A. phagocytophilum* antibodies at 14 dpi. *A. phagocytophilum* was detected by PCR in skin, lung, small intestine, liver, spleen, uterus, bone marrow, and mesenteric lymph node from necropsies performed at 14 and 15 dpi. One sheep was infested during the acute phase of infection with *I. ricinus* nymphs from a pathogen-free colony. After molting, *A. phagocytophilum* transstadial transmission in ticks was validated with qPCR positive bacterial detection in 80% of salivary glands and 90% of midguts from female adults. Infected sheep blood collected at 14 dpi was demonstrated to be able to infect ISE6 tick cells, thus enabling the infection of two additional naive sheep, which then went on to develop similar clinical signs to the sheep infected previously. One of the sheep remained persistently infected until 115 dpi when it was euthanized, and transmitted bacteria to 70 and 2.7% of nymphs engorged as larvae during the acute and persistent infection stages, respectively. We then demonstrated that these infected nymphs were able to transmit the bacteria to one of two other naive infested sheep. As expected, when *I. ricinus* females were engorged during the acute phase of infection, no *A. phagocytophilum* transovarial transmission was detected. The development of this new experimental model will facilitate future research on this tick-borne bacterium of increasing importance, and enable the evaluation of any new tick/transmission control strategies.

Keywords: *Anaplasma phagocytophilum*, *Ixodes ricinus*, sheep, NV2Os, tick cell cultures

INTRODUCTION

Anaplasma phagocytophilum (Rickettsiales: Anaplasmataceae), is an obligate intracellular Gram negative bacterium mainly transmitted by *I. scapularis* and *I. pacificus* in the United States, *I. persulcatus* in Asia, and *I. ricinus* in Europe (1). *A. phagocytophilum* is the causative agent of human granulocytic anaplasmosis (HGA) and tick-borne fever (TBF), affecting both humans and a variety of domestic and wild animal species (2–4). Tick-borne fever was first identified in sheep from Scotland in 1932 (5), and the discovery of the etiological disease agent followed in 1940 (6). Throughout Europe, sheep are exposed to *A. phagocytophilum* (7)—with seroprevalence as high as 80% in sheep grazing in tick-infested Norwegian pastures—resulting in considerable economic and animal welfare consequences (8, 9).

The wide range of potential hosts, as well as incidence and severity of the disease in a particular host appear to vary according to geographical region (1). *A. phagocytophilum* infects granulocytes, mostly neutrophils, and exists as macrocolonies or morulae within intracytoplasmic vacuole (10, 11). Approximatively within a week of exposure to an infectious tick bite, TBF disease becomes clinically evident and is characterized by fever, leukopenia, marked neutropenia, and thrombocytopenia (12). In sheep, *A. phagocytophilum* infection causes a fever lasting from 1 to 2 weeks, and which may vary according to animal age, the *A. phagocytophilum* variant, the host breed and its immunological status (13). Anorexia, depression (14), reduced weight gain (15), as well as abortions (16) have also been reported. In addition, because of the severe hematological and immune disorders associated with *A. phagocytophilum* infection, animals are more susceptible to secondary infections, including tick pyemia, caused by *Staphylococcus* spp. (14).

A. phagocytophilum has a large number of genetic variants which vary in virulence and clinical manifestation, and which can be differentiated by sequencing 16S rRNA (9) or *mps4* genes (17, 18). Four variants that differ in pathogenicity and immunogenicity were identified as circulating in sheep flocks from Norway (9). Among them, *A. phagocytophilum* variant 1 (var1) is believed to be associated with the majority of fatal TBF cases in sheep (19). In contrast, *A. phagocytophilum* variant 2 (var2), which is also frequently found circulating in naturally-infected sheep, produces a less severe clinical manifestation with shorter periods of fever and bacteremia, and a less severe neutropenia (20–22). Indeed, as it produces mild TBF in sheep, *A. phagocytophilum* var2 could be a useful model for studying bacterial infection processes in sheep, tick transmission modalities, and could also be used in vaccine trials.

Tick cell lines are well-established systems in which tick-borne pathogens—including *Anaplasma* species—can be propagated (23). Both HGA and equine granulocytic anaplasmosis variants were initially cultivated in the human promyelocytic cell line HL-60 (24), and then in IDE8 and ISE6 tick cell lines derived from *I. scapularis* embryos (25, 26). TBF variants were successfully cultivated in these tick cell lines, including variants isolated from sheep, such as the Old Sourhope strain, which, after three culture passages, was shown to be infectious in susceptible sheep (27). The *A. phagocytophilum* Norway var2 ovine strain (NV2Os), isolated from Norwegian sheep (9), was also successfully propagated in IDE8 embryonic tick cells (28), but, to the best of our knowledge, sheep infection from this cell culture has never been experimentally achieved to date.

The present study aims to investigate whether the *A. phagocytophilum* NV2Os propagated in both IDE8 and ISE6 tick cells can be used in the laboratory to experimentally recreate the entire bacterial transmission cycle from sheep to ticks and from ticks to sheep, thus creating an experimental model in which both tick-host-pathogen interactions, as well as novel tick/transmission control strategies, such as anti-tick or anti-transmission vaccines, can be studied. We report that the development of this model enabled successful sheep infection, the production of infected *I. ricinus* from both acute and persistently *A. phagocytophilum*-infected sheep, as well as the re-transmission of the bacteria to naïve sheep by these ticks.

MATERIALS AND METHODS

Experimental Design

The experimental design of the study is presented in **Figure 1**. Two 9-month-old Romane breed female sheep (identification numbers 128 and 320) were inoculated with IDE8 tick cells infected with *A. phagocytophilum* NV2Os into the jugular vein, and euthanized at 14 and 15 days post inoculation (dpi), due to clinical signs of distress. During the acute phase of *A. phagocytophilum* infection at 6 dpi, sheep 320 was infested with *I. ricinus* nymphs. In addition, infected blood obtained from sheep 320 was used to assess whether NV2Os could be propagated in ISE6 tick cells. These *A. phagocytophilum*-infected ISE6 tick cells were then intrajugularly inoculated into two 11-month-old Romane breed female sheep (identification numbers 381 and 648). Unexpectedly, sheep 648 died at 12 dpi, and no necropsy could be performed. Sheep 381 however, recovered after the acute phase and remained without signs of infection until 115 dpi, when it was euthanized. *A. phagocytophilum* tick transmission was evaluated by infesting both sheep 381 and 648 during the acute phase of infection at 7 and 6 dpi, respectively, as well as sheep 381 during the persistent phase of infection at 108 dpi with *I. ricinus* larvae, and the infection assessed after molting into nymphal stages. The infectious status of nymphs molted from larvae fed on infected sheep 381 and 648 was assessed by feeding them on two naive PreAlps breed sheep (identification numbers 572 and 615). For sheep 128 and 320, blood samples were obtained every day from day 0 to 14 and 15 dpi, respectively. Sheep 648 was bled every day from day 0 until 12 dpi, when it died. Sheep 381 was bled every day from day 0 to 15 dpi, and then every 15 days until 115 dpi. Sheep infected with *I. ricinus* nymphs (572 and 615) were bled every 5 days from day 0 to day 25 post tick infestation.

Culture of *A. phagocytophilum* NV2Os in IDE8 and ISE6 Tick Cells

IDE8 and ISE6 embryonic tick cell cultures were maintained according to Munderloh and Kurtti (29) and Munderloh et

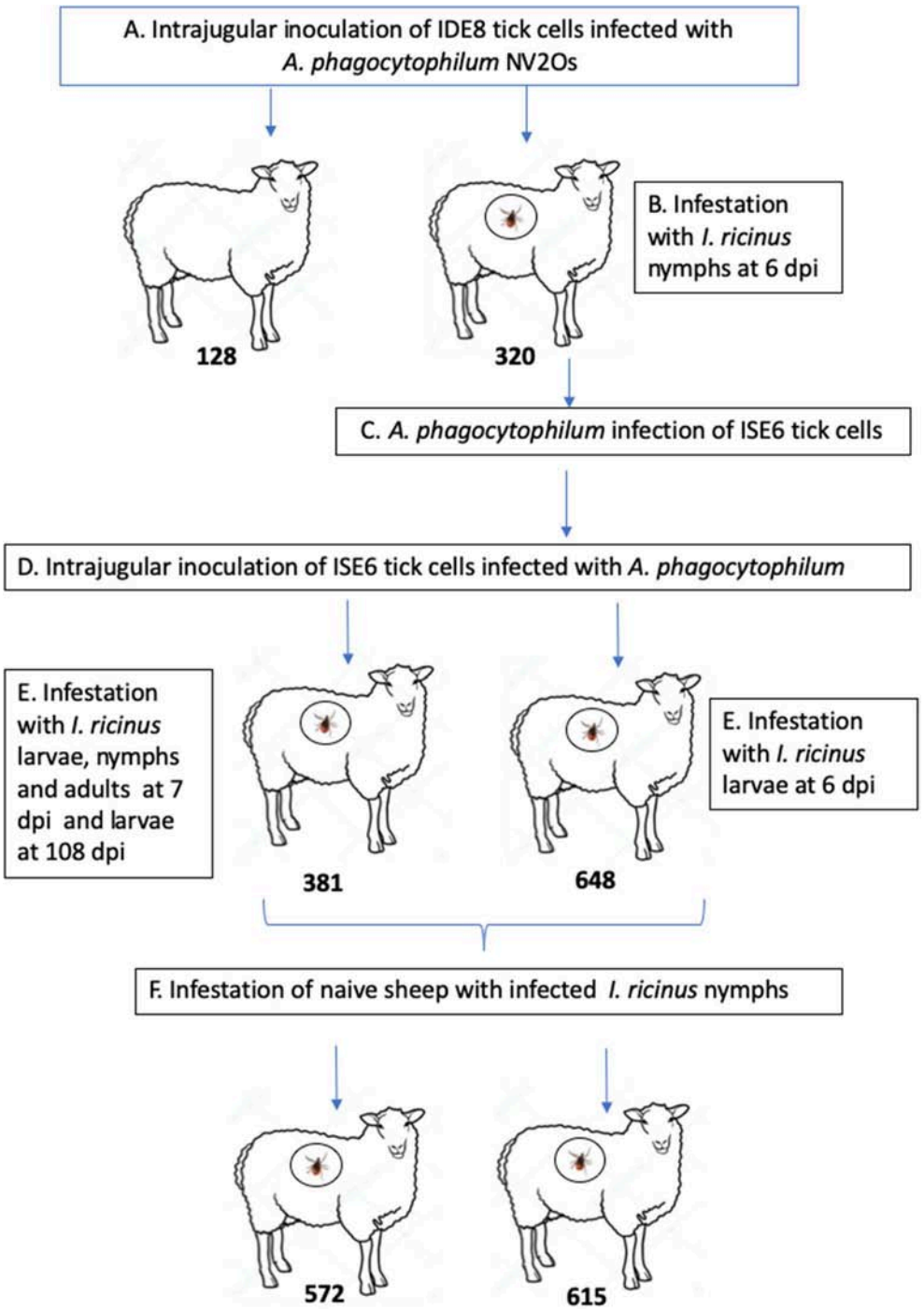

FIGURE 1 | Schematic representation of the experimental design. **(A)** Infection of Romane sheep (identification numbers 128 and 320) with *Anaplasma phagocytophilum* NV2Os propagated in IDE8 tick cells; **(B)** *Ixodes ricinus* infestation; **(C)** Infection of ISE6 tick cells with the *A. phagocytophilum* NV2Os from sheep 320; **(D)** Inoculation of Romane sheep (identification numbers 381 and 648) with the *A. phagocytophilum* NV2Os propagated in ISE6 tick cells; **(E)** Transmission of *A. phagocytophilum* from sheep to *I. ricinus* ticks during both acute (sheep 381 and 648) and persistent infection (sheep 381); **(F)** Tick transmission of *A. phagocytophilum* to naive PreAlps sheep (identification numbers 572 and 615).

al. (30), respectively. Healthy tick cells from both cell lines were propagated in L-15B medium, whereas infected cells were cultured in L-15B supplemented with 0.1% $NaHCO_3$ and 10 mM HEPES and the pH was adjusted to 7.5. Both uninfected and infected IDE8 and ISE6 cells were maintained at 31 and 34°C, respectively. The *A. phagocytophilum* NV2Os was propagated in

IDE8 tick cells (approximate passage of 110) as described by Alberdi et al. (28). *A. phagocytophilum* infection was propagated by transferring 1/10th of an infected IDE8 cell culture to a new flask of healthy cells, every 4 days. To determine the level of infection, 60 μl of RPMI medium with suspended cells were centrifuged on slides with a cytocentrifuge Shandon Cytospin (Thermo Fisher Scientific, Sweden) for 5 min at 1,000 rpm, stained using the Hemacolor® staining kit (Merck, Darmstadt, Germany) and observed under a light microscope.

Blood from *A. phagocytophilum*-infected sheep 320 collected at 14 dpi was used to infect ISE6 tick cells. A 500 μl drop of blood was added to two 25 cm^2 culture flasks of ISE6 cells (approximate passage of 90). Cytocentrifuged slides were stained twice a week using Hemacolor® kit (Merck Millipore, Darmstadt, Germany) in order to determine the level of infection. Once infection reached 70%, cells ($\sim 1 \times 10^7$ infected cells) were collected and centrifuged for 5 min at 200 × g, then resuspended in 2 ml of sterile RPMI to prepare the inoculum (31).

Sheep Inoculation

Four 9-month-old Romane breed female sheep, originally from the INRA Experimental Animal Center at Bressonvilliers, France, and reared in a secure sheepfold at the Biomedical Research Center (CRBM) facilities, National School of Veterinary Medicine of Alfort (ENVA), were used. First, two sheep identified with numbers 128 and 320 (**Figure 1**) were inoculated with 1 ml of medium containing 1×10^7 *A. phagocytophilum*-infected IDE8 cells with a 70% infection level into the jugular vein with a 6 cc syringe and a 20-gauge 1" needle (Terumo) after skin disinfection. Two months later, the two other sheep, with identification numbers 381 and 648 (**Figure 1**) were inoculated with 1 ml of medium containing 5×10^6 ISE6 cells infected with *A. phagocytophilum* obtained from sheep 320 and with a 70% infection level.

Detection of *A. phagocytophilum* in Sheep's Blood by PCR and Determination of Infection Levels by Quantitative PCR (qPCR)

PCR detection of *A. phagocytophilum msp4* was performed using DNA obtained from blood collected daily, from day 0 to 14 or 15 dpi in sheep inoculated with IDE8 infected cells (sheep 320 and 128, respectively), and from day 0 to 12 or 15 dpi in sheep inoculated with ISE6 infected cells (sheep 648 and 381, respectively). For sheep infected by *I. ricinus* nymphs (572, 615), PCR detection was performed every 5 days from 0 to 25 days post tick infestation and until euthanasia. Blood was collected from the jugular vein, and drawn into 10 ml EDTA vacutainer tubes. The PCR protocol described by Kocan et al. was followed (32). Briefly, DNA was extracted using a NucleoSpin Blood kit (Macherey-Nagel, Germany) from 200 μl of blood. PCR reactions were then performed using the oligonucleotide primers msp4-F (5′-CCTTGGCTGCAGCACCACCTG-3′), and msp4-R (5′-TGCTGTGGGTCGTGACGCG-3′), in 20 μl of final volume using the Takara Ex Taq system (Bio Europe, France). For positive and negative controls, DNA from *A. phagocytophilum*-infected ISE6 tick cells and nuclease free water were used, respectively. PCR products were visualized by 2% agarose gel electrophoresis. PCR products were purified using the PCR Clean-Up kit (Macherey Nagel, Germany), and were sequenced by the Eurofins sequencing service (France). The obtained sequences were submitted to the BLAST (basic local alignment search tool) platform to search for sequences with homology to *A. phagocytophilum* NV2Os.

A. phagocytophilum infection levels in sheep were determined by qPCR targeting the *msp4* gene using DNA obtained from blood collected every 3 days from sheep 320 and 128, starting at day 0 until euthanasia (14 and 15 dpi, respectively), and from sheep 648 and 381 until 12 and 15 dpi respectively. For sheep 381, qPCR was performed every 15 days until 115 dpi. Samples were processed according to the protocol described by Reppert et al. (31). DNA concentration was evaluated with a NanoDrop™ 2000 (Thermo Scientific, USA) and 20 ng of DNA was then mixed in a 20 μl reaction containing the primers qmsp4F (5-ATGAATTACAGAGAATTGCTTGTAGG-3), and qmsp4R (5-TTAATTGAAAGCAAATCTTGCTCCTATG-3) using the SsoAdvanced™ SYBR® Green Supermix (Bio-Rad, Hercules, CA, USA). Reactions were performed in a LightCycler® 480 (Roche Life Science, Indianapolis, IN, USA). The *Ovis aries* aldolase B gene (*ALDOB*) was used for normalization, with the primers Oa-AldBF (5′-CCCATCTTGCTATCCAGGAA-3′) and Oa-AldBR (5′-TACAGCAGCCAGGACCTTCT-3′). The same mix without DNA, or DNA from infected ISE6 cell culture were used as negative and positive controls, respectively. Triplicate values from each sample were normalized by calculating the ratio of *A. phagocytophilum msp4* DNA to the averaged *ALDOB* gene. The standard errors of the averaged normalized values of the mean were determined and values analyzed by the Student's *t*-test ($p = 0.05$).

Detection of *A. phagocytophilum* Intracellular Inclusions in Blood Smears

Blood smears were performed on blood samples collected daily in EDTA tubes, starting at day 0 until 14 dpi for sheep 320, 15 dpi for sheep 128 and 381, and 12 dpi for sheep 648. Blood smears were stained using the Hemacolor® staining kit (Merck, Darmstadt, Germany). Slides were observed under a light microscope and 100 white cells per slide were examined to determine the percentage of infected neutrophils. When basophilic inclusions consistent with *A. phagocytophilum* organisms were found, slides were then examined under an Imager 21 Zeiss microscope adapted to an AxioCam HRC Zeiss camera to record images.

Gross Lesions and Detection of *A. phagocytophilum* in Sheep Tissues

In order to detect gross lesions, necropsies were performed immediately after euthanasia, which was carried out via intravenous injection of 18% sodium pentobarbital. Euthanasia occurred at 14 and 15 dpi for sheep 320 and 128 during the acute phase of the infection, and at day 115 for sheep 381 during

the persistent phase of the infection. For PCR detection of the *A. phagocytophilum msp4* gene, ∼1 cm^2 of skin from the tick infestation area, and samples from sheep lung, myocardium, liver, spleen, stomach, small intestine, lymph nodes, brain, uterus, ovary, cerebellum, bone marrow, kidney, and gallbladder were obtained, deposited into sterile tubes and stored at −80°C until later use. DNA was extracted using a NucleoSpin® tissue kit (Macherey-Nagel, Germany) from 25 mg of each tissue. DNA concentration was evaluated with a NanoDrop™ 2000 (Thermo Scientific, USA) and PCR reactions were performed using 20 ng of DNA in a final volume of 20 µl as described for blood in section Detection of *A. phagocytophilum* in Sheep's Blood by PCR and Determination of Infection Levels by Quantitative PCR (qPCR).

Indirect Immunofluorescence Antibody Assay (IFA)

The detection of anti-*A. phagocytophilum* antibodies was performed using the indirect immunofluorescence antibody assay (IFA) on serum samples obtained at day 0 (for negative controls), and at 14 dpi and 15 dpi from sheep 320 and 128, respectively; and every 15 days until 115 dpi for sheep 381. Blood samples were collected from the jugular vein, and serum obtained by centrifugation. Serial dilutions of serum starting from 1:50 were analyzed using the Mega-Screen Fluo *A. phagocytophilum*-coated slides (MegaCor, Hoerbranz, Austria), following manufacturer's instructions. Briefly, the *A. phagocytophilum*-coated slides were incubated with serial dilutions of serum for 30 min at 37°C. Slides were rinsed with PBS and incubated with 25 µl of 1:50 fluorescein isothiocyanate-conjugated rabbit anti-sheep IgG (H + L) (Jackson Immuno Research, Cambridge, UK) in Evans blue solution (Biomerieux, Hampshire, UK) for counterstaining. After incubation for 30 min at 37°C, slides were rinsed and mounting medium (Bio-Rad, Hercules, CA, USA) was added. Finally, slides were analyzed with a fluorescent microscope. A titer of 1.69 (Log_{10} reciprocal of 1:50) or higher was considered positive (8).

Tick Infestation

I. ricinus ticks originally collected from the Sénart Forest, France (coordinates 48°40′00″N 2°29′00″E), and maintained as a pathogen-free colony reared at 22°C with 95% relative humidity and a 12-h light/dark cycle as previously described (33), were used for sheep infestation. For feeding, ticks were enclosed into stockinet cells attached to the back of each sheep, following a protocol adapted from cattle and rabbits (34, 35). Nine hundred nymphs of *I. ricinus* were engorged on sheep 320 when *A. phagocytophilum* was detected by PCR, during the highest fever spike (6 dpi) (**Figure 1**). Engorged nymphs were collected after 6 days of feeding. Collected engorged ticks were cleaned and reared until they molted into adults. The transmission of *A. phagocytophilum* to *I. ricinus* ticks during acute infection of sheep was tested by infesting 950 naive nymphs on sheep 381 and 2,000 naive larvae on sheep 381 and 648 at 7 and 6 dpi, respectively (**Figure 1**). Engorged larvae were collected after 3–5 days of feeding and then incubated in order to test for *A. phagocytophilum* presence in both engorged ticks and recently molted nymphs. Transovarial transmission of *A. phagocytophilum* was tested by infesting 15 adult couples on sheep 381 at 7 dpi. Engorged females were collected after 9 days of feeding and reared until oviposition. The transmission of *A. phagocytophilum* to *I. ricinus* ticks during persistent infection of sheep was tested by infesting 4,000 naive larvae on sheep 381 at 108 dpi (**Figure 1**). Finally, in order to test if nymphs molted from larvae fed on *A. phagocytophilum*-infected sheep 381 and 648 were able to transmit the bacteria to naive sheep, two 8-month-old male PreAlps breed sheep, identified as 572 and 615, were infested with 45 nymphs each (**Figure 1**).

Detection of *A. phagocytophilum* in Ticks

A. phagocytophilum detection by qPCR was performed using DNA obtained from salivary glands and midguts from adult ticks engorged as nymphs on infected sheep 320, whole nymphs engorged as larvae on sheep 381 and 648, as well as egg masses obtained from females engorged on sheep 381 (**Figure 1**). DNA was extracted from each individual tick with the NucleoSpin tissue kit (Macherey Nagel, Germany), and 20 ng of DNA was mixed in a 20 µl reaction containing the primers msp2-F (5-ATGGAAGGTAGTGTTGGTTATGGTATT-3), and msp2-R (5-TTGGTCTTGAAGCGCTCGTA), adapted from the protocol described by Courtney et al. (36), using the SsoAdvanced™ SYBR® Green Supermix (Bio-Rad, Hercules, CA, USA). Reactions were performed in triplicate in a LightCycler® 480 (Roche Life Science, Indianapolis, IN, USA). Normalization was performed using the tick ribosomal protein S4 gene (*rps4*) with primers rps4F 5- GGTGAAGAAGATTGTCAAGCAGAG-3 and rps4R 5- TGAAGCCAGCAGGGTAGTTTG-3 (37).

RESULTS

A. phagocytophilum NV2Os Propagated in Both IDE8 and ISE6 Tick Cells Can Infect Sheep

The two sheep (128, 320) inoculated with the *A. phagocytophilum* NV2Os propagated in IDE8 tick cells developed an infection as demonstrated by clinical signs, observation of morulae inclusions in neutrophils, positive PCR and qPCR results, anti-*A. phagocytophilum* antibody detection, as well as the presence of lesions detected during necropsies after euthanasia. The first sign of infection was increased temperature by the 3rd dpi with peaks of 41.5°C at 5 and 6 dpi in sheep 128 and 320, respectively (**Figure 2A**). After 7 dpi, a decrease in appetite, and the presence of nasal discharge and conjunctivitis were observed in both animals. Sheep 320 maintained a temperature over 40°C until 13 dpi, at which point nasal discharge and lacrimal secretions increased, it then became lethargic with tachypnea, prostration, and stopped drinking water. Due to animal welfare regulations and ethics, euthanasia was performed at 14 and 15 dpi for sheep 320 and 128, respectively. *A. phagocytophilum msp4* PCR was positive from 5 dpi until 12 dpi in both sheep (**Figure 2B**). For both sheep, qPCR-determined *A. phagocytophilum* infection levels increased after 3 dpi, showed the highest fold change at 6 dpi, and then decreased drastically at 9 dpi. However, *A. phagocytophilum* DNA remained at detectable levels until 14 dpi in sheep 128 (**Figure 3A**). The statistical analysis of the averaged normalized values of the mean indicated that the fold change was

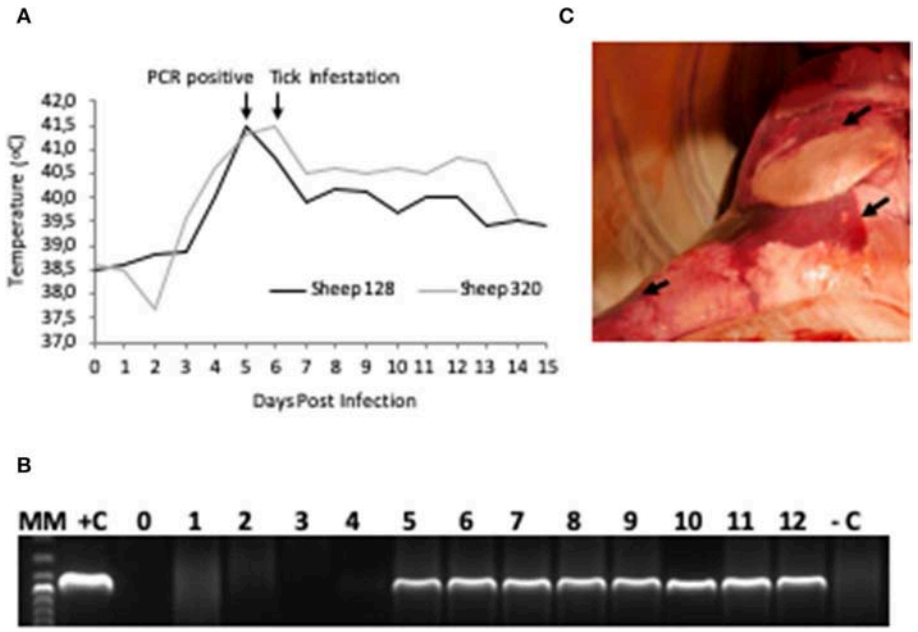

FIGURE 2 | *A. phagocytophilum* infection in sheep experimentally infected with NV2O-infected IDE8 tick cells. **(A)** Temperature (°C) recorded daily from day 0 post-infection to the day of euthanasia for sheep 128 and 320; **(B)** PCR detection of *A. phagocytophilum msp4* gene in sheep 320 blood samples from day 0 to day 12 post-infection, MM, molecular marker; +C, positive control; –C, negative control; **(C)** Lung necropsy of sheep 320 14 days post infection. Arrows indicate patches of red coloration contrasting with the pink normal color.

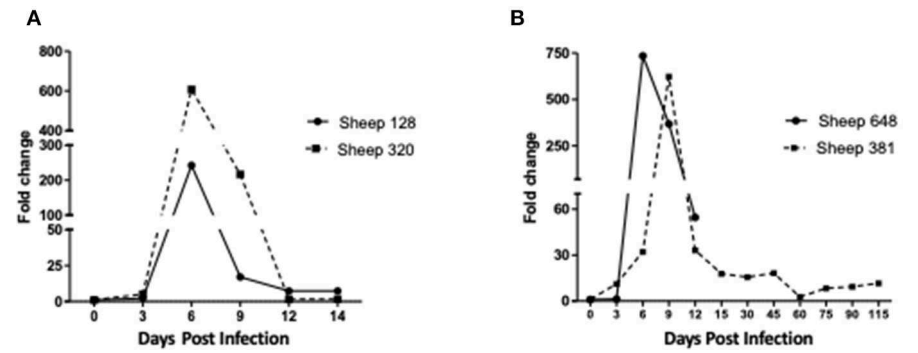

FIGURE 3 | Infection levels in sheep inoculated with *A. phagocytophilum* NV2Os propagated in tick cells. Infection levels were determined from day 0 post-infection to the day of euthanasia and according to *A. phagocytophilum msp4* gene expression as assessed by quantitative PCR (qPCR) relative to the *aldolase B* (*ALDOB*) gene of *Ovis aries.* Triplicate values from each sample were normalized by calculating the ratio of *A. phagocytophilum msp4* DNA to the averaged *ALDOB* gene. **(A)** Sheep 128 and 320 inoculated with NV2Os cultivated in IDE8 tick cells; **(B)** Sheep 381 and 648 inoculated with NV2Os cultivated in ISE6 tick cells.

significant ($p = 0.05$) from 3 dpi until 14 dpi. *A. phagocytophilum* morulae were found in neutrophils from both infected sheep at 6 and 7 dpi, whereas no other blood infection was detected (**Figure 4**). The highest cellular infection level was observed at 8 dpi with 47 and 60% of neutrophils infected in sheep 128 and 320, respectively (**Figure 4**). Few morulae were seen at 10 dpi and no further intracellular inclusions were found after 12 dpi.

The main gross lesions observed during necropsies of the two sheep 128 and 320 at 14 and 15 dpi corresponded to a moderate hepatomegaly and splenomegaly. The spleens from both sheep showed rounded borders and mild enlargement. While the use of barbiturates for euthanasia may have contributed to the observed mild splenomegaly, the absence of bleeding during necropsy suggests that it was mainly due to infection with *A. phagocytophilum*. In addition, in contrast to a normal pink lung color, patches of red coloration in sheep 320 lungs were observed (**Figure 2C**), as well as abundant bronchial and tracheal liquid. Mesenteric, axillar, and mandibular lymph nodes from both sheep were also mildly increased in size. Lesions were not detected in the remainder of examined tissues. *A. phagocytophilum msp4* PCR on necropsies yielded positive results in lung, liver, spleen, uterus, and the small intestine from sheep

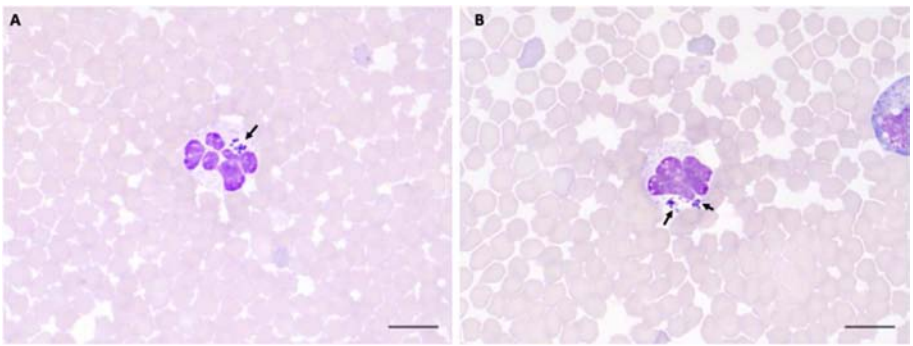

FIGURE 4 | *A. phagocytophilum* morula (arrowheads) in peripheral blood neutrophils from sheep infected with NV2Os propagated in IDE8 tick cells. Blood smears were performed at day 8 post-infection and stained with the Hemacolor® staining kit (Merck). **(A)** Sheep 320; **(B)** Sheep 128. Scale bars = 10 μm.

128, while in sheep 320, skin, spleen, lung, small intestine, bone marrow, and mesenteric lymph nodes were positive (**Table 1**).

The two sheep (381, 648) inoculated with *A. phagocytophilum* propagated in ISE6 tick cells showed clinical signs similar to sheep 128 and 320. Increased temperature was observed at 5 dpi with a 42°C peak at 6 dpi. Sheep 648 presented with other clinical signs, such as trembling, total loss of appetite, and excessive salivation, and died at 12 dpi. Sheep 381, on the other hand, recovered after the febrile process, without any clinical signs until 115 dpi, when it was euthanized. *A. phagocytophilum msp4* PCR was positive for both sheep at 5 dpi, and sheep 381 became negative at 15 dpi (data not shown). qPCR-Determined infection levels showed the highest fold change at 6 dpi in sheep 648, and at 9 dpi in sheep 381 followed by a drastic decrease at 12 dpi for both sheep (**Figure 3B**). For sheep 381, significant values ($p = 0.05$) were obtained until the end of the experiment, except at 60 dpi. Granular inclusions consistent with *A. phagocytophilum* morulae were detected in both sheep, with the highest percentages of infected neutrophils at 8 dpi with 47 and 60% in sheep 381 and 648, respectively. No other blood pathogens were identified via the blood smears from the two sheep, including sheep 648 that died at 12 dpi. For sheep 381, except for a mild splenomegaly, no gross lesion was observed at 115 dpi and all tested tissues were negative for *A. phagocytophilum* by PCR (**Table 1**).

Antibody detection by IFA indicated that the four sheep, 128, 320, 381, and 648 were negative prior to experimental inoculations (titer ≤ 1.6), and sheep 128, 320, and 381 became positive at 14 dpi (titer = 2.0). Sheep 648 died at 12 dpi before seroconversion, and sheep 381 remained positive with antibody titers between 2.0 and 2.77 from 14 to 115 dpi, until the animal was euthanized.

Transmission of *A. phagocytophilum* NV2Os by *I. ricinus*

The percentages of engorged ticks collected after feeding on infected sheep, as well as the rate of *A. phagocytophilum* detection in molted ticks are shown in **Table 2**. On all sheep, 67.5 and 11.3% of larvae and nymphs underwent successful engorgement, respectively. On sheep 320 inoculated with *A. phagocytophilum*-infected IDE8 tick cells, 17.7% of tick nymphs became engorged, and 50% underwent molting. *A. phagocytophilum* transstadial transmission was demonstrated by qPCR in 8 salivary glands (80%) and 9 midgut samples (90%) obtained from 10 dissected females infected at the nymphal stage. For sheep 648 inoculated with *A. phagocytophilum*-infected ISE6 tick cells, 46.2% of tick larvae became engorged, and where no transstadial transmission was detected in 10 recently-molted nymphs engorged at the larval stage. However, when testing sheep 381—also infected with ISE6 cells—during both the acute (7 dpi) and persistent phases of infection (108 dpi), *A. phagocytophilum* acquisition and transstadial transmission from larvae to nymphs was demonstrated. In fact, at 7 dpi, 7 of the 10 recently-molted nymphs infected at the larval stage were positive for *A. phagocytophilum* infection, whereas at 108 dpi, only 2.7% (2/72) were positive despite an 85.3% larval engorgement success rate. At 7 dpi, only 4.5% of nymphs became engorged, with 34.9% of engorged nymphs then molting into adults. Following the engorgement of 15 pairs of adult ticks on infected sheep 381 at 7 dpi, *A. phagocytophilum* transovarial transmission was tested using DNA extracted from five egg masses obtained from engorged females, and all samples were negative (data not shown).

Finally, the transmission of *A. phagocytophilum* by *I. ricinus* nymphs fed as larvae on infected sheep 381 and 648, was tested by infesting two PreAlps sheep (572 and 615) with 45 nymphs each. To achieve this, a mixed pool of nymphs from both sheep was used, leading to an estimated 42% infection level in each tick batch. Nymph engorgement was as low as 3/45 (7%) in sheep 572, and 10/45 (22%) in sheep 615. Although sheep 572 remained healthy and *A. phagocytophilum* was not detected, sheep 615 developed hyperthermia above 40°C with inappetence, lethargy, and reluctance to drink water, which led us to perform euthanasia at 15 days post nymph infestation. These clinical signs were then similar to what was previously observed during an NV2Os infection, and this infection was confirmed by positive qPCR bacterial detection in blood samples as early as the 5th day post tick infestation. Sequencing the PCR-amplified *msp4* gene demonstrated that the isolate corresponded to *A. phagocytophilum* NV2Os, Gene Bank accession number CP015376.1.

TABLE 1 | PCR detection of *Anaplasma phagocytophilum* in necropsies obtained after euthanasia of sheep 320 and 128 infected with infected IDE8 cells, at 14 and 15 dpi, respectively, and of sheep 381 infected with ISE6 cells at 115 dpi.

Sheep n°	Skin	Lungs	Myocardium	Liver	Spleen	Stomach	Kidney	Gallbladder	Small intestine (Duodenum)	Mesenteric lymph nodes	Axillary lymph nodes	Prescapular lymph nodes	Uterus	Ovary	Brain	Cerebellum	Bone marrow
320	+	+	−	−	+	−	−	−	+	+	−	−	−	−	−	−	+
128	−	+	−	+	+	−	−	−	+	−	−	−	+	−	−	−	Not analyzed
381	−	−	−	−	−	−	−	−	−	−	−	−	−	−	−	−	−

DISCUSSION

As the etiological agent causing both HGA in humans and TBF in domestic animals, *A. phagocytophilum* receives growing scientific interest due to its importance in public health, to livestock welfare, and national economies. In the United Kingdom, there are an estimated 300,000 cases of tick pyaemia each year caused by immunosuppression in *A. phagocytophilum*-infected animals (14). A similarly high number of *A. phagocytophilum*-infected lambs has been reported in Norway (8). For livestock exposed to tick-infested pastures, current control methods are based on the use of long-acting antibiotics—given before animals are moved from tick-free environments into tick-infested pasture—and by reducing tick infestation with acaricides. Due to the multiple disadvantages of such chemical control measures (development of resistance, environmental hazard, contamination of milk, and meat products with drug residues, high cost), new approaches are urgently needed. The development of such approaches requires the establishment of relevant laboratory models. Therefore, the purpose of the present study was to develop an *I. ricinus*-sheep model that enabled us to mimic the natural *A. phagocytophilum* infection cycles of both sheep and ticks. This would facilitate future studies on tick-host-pathogen interactions, as well as enabling the evaluation of new control methods, such as anti-tick vaccines or transmission-blocking vaccines. It is well-known that for both vertebrates and ticks, tick-borne pathogen acquisition differs between natural infection via tick bites and experimental infection through injection due to, among other reasons, saliva-assisted transmission mechanisms (38).

In this study, only a limited number of sheep were included for this first experiment which aimed to validate our experimental model. Therefore, infection follow-up results and clinical observations should be taken with caution, and should ideally be reproduced to take into account any individual sheep variation and be generalized to the NV2Os/Romane breed sheep pair.

It has been reported that the delay in detecting *A. phagocytophilum* in sheep may vary according to the infectious dose, bacterial genotypes, infection source (infected blood or cell culture), as well as to the immune status and susceptibility of animal breeds [see review in (1)]. Here we report for the first time that the Norway variant 2 ovine strain (NV2Os) propagated in both IDE8 and ISE6 tick cell cultures was able to successfully infect Romane breed female sheep. Following infection with NV2Os-infected IDE8 cells, the bacteria were detected in sheep blood at 4 dpi by qPCR, 5 dpi by conventional PCR and 6 dpi by microscopic examination of blood smears, which is consistent with the assumed sensitivity of these detection techniques. Such a prepatent period in sheep is shorter than what was reported with the human strain NY-18 (10–21 dpi) (31, 32), longer than with the var1 (13, 22), but in accordance with what was observed with var2 in Norwegian Dala breed lambs (22). According to qPCR results, bacteremia peaked at 6 dpi, except for sheep 381 that recovered after the acute phase with a peak at 9 dpi following infection with *A. phagocytophilum* NV2Os propagated in ISE6 cells. Nevertheless, blood smears demonstrated a detection lag, with the maximum number of infected neutrophils (47 and 60%) at 8 dpi for sheep infected with IDE8 cells, suggesting also that

TABLE 2 | *Ixodes ricinus* ticks collected after feeding on *A. phagocytophilum*-infected sheep during both the acute or the persistent phases of infection, and detection of infection in engorged and molted ticks.

Sheep n°	Day post-infection	Number of infesting ticks		Number of engorged ticks (%)		Number of ticks recovered after molting (%)		*A. phagocytophilum*-positive molted ticks/tested ticks (%)	
		Larvae	Nymphs	Larvae	Nymphs	Nymphs	Adults	Nymphs	Adults
320	6	–	900	–	160 (17.7%)	–	80 (50%) (37 females, 43 males)	–	8/10 Salivary glands (80%) 9/10 midgut (90%)
648	6	2000	–	925 (46.2%)	–	252 (27.2%)		0/10	–
381	7	2000	950	1060 (53%)	43 (4.5%)	411 (38.8%)	15 (34.9%) (9 females, 6 males)	7/10 (70%)	–
	108	4000	–	3414 (85.3%)	–	2236 (65.5%)	–	2/72 (2.8%)	–

qPCR detection is more reliable. The observed initial bacteremia period with a mean duration of 10.75 (±1.7) days, as determined by qPCR, was also similar to that reported by Granquist et al. for the Var2 where the mean was 11.4 (±1.8) (22). Lastly, infection monitoring in sheep 381 and positive qPCR bacterial detection until 115 dpi confirmed that *A. phagocytophilum* can establish long-term infections in immune competent sheep, and has previously been reported for as long as 6–25 months (22, 39–41). Such persistent cyclic activity was suggested to be linked to variant-specific antigen immune responses to the bacteria (42, 43), and is epidemiologically very important in the maintenance of *A. phagocytophilum* infection in the field, especially during periods of no tick activity.

The indirect immunofluorescence assay, adapted to detect antibodies against *A. phagocytophilum,* and which has been extensively used in experimental and natural infections (8, 9, 21, 22) was used to test seroconversion in infected sheep. Our findings showed that antibodies were detected in all infected sheep at 14 dpi. Although the titers varied during the persistent infection of sheep 381, the results remained positive until 115 dpi, when the animal was euthanized. These results are consistent with studies in naturally- and experimentally-infected sheep (9, 13, 22).

In accordance with previous studies using the same strain but in Norwegian Dala sheep by Stuen et al. and Granquist et al. (21, 22), the first clinical sign was an increase in temperature up to 41.5°C between 3 and 6 dpi dependent on the sheep. However, a discrepancy was observed that may be explained by the genetic susceptibility of the French breeds used in this study, where the febrile process lasted between 8 and 9 days here and 2.2–3 days in their studies. All infected sheep also showed signs of loss of appetite and lethargy until euthanasia, except for sheep 381 that recovered after the acute phase of infection, and showed no clinical signs until euthanasia at 115 dpi.

Few studies have been performed in order to evaluate the existence of tissue that may act as *A. phagocytophilum* reservoirs in persistently-infected sheep and which could explain the maintenance of the bacteria in the field, especially during periods of vector tick non-activity. When the Suffolk breed was infected with the NY-18 human strain, no bacteria could be detected in any internal organ 1 month after infection, even with quantitative PCR (31). However, when the Norwegian Dala breed was infected with a Norway ovine field isolate, several organs (bone marrow, intestinal and bladder walls, kidney, lymph node, and thymus) were PCR positive 3 months after infection (44). Here we observed positive PCR results in several organs from sheep euthanized 2 weeks after the infection, but no infection was detected by PCR during necropsies performed at 115 days post infection. These varying results may reflect differences due to the bacterial strain or sheep breed, but the main conclusion is that more experiments with more animals are needed to answer this question. However, preferential involvement of lymphoid tissue may suggest that these tissues could represent a source of infected cells that, when released into the blood, would enable tick infection (44). As for the lesions, *A. phagocytophilum* infection has been reported to be associated with moderate tissue damage, which targets lymphoid tissues and the spleen in particular (31, 32, 45), as confirmed by our study.

Experimentally-infected sheep here proved to be excellent hosts for the production of *I. ricinus* ticks infected with ovine NV2Os, with feeding success rates of 67, 11, and 60% for larvae, nymphs, and female adults, respectively. Unlike laboratory animals, such as mice or rabbits, the large size of sheep makes it possible to feed many ticks at once without animal suffering in the absence of infection. This result is very encouraging considering the fact that in an experimental study with *I. scapularis*, Kocan et al. reported larvae feeding failure but, like us, poor performance of nymphs feeding on sheep (32). After engorgement during the acute phase, ticks acquired *A. phagocytophilum*, with an estimation of 80% acquisition in both engorged larvae and nymphs (data not shown). Similar *A. phagocytophilum* acquisition percentages in field populations of *I. ricinus* have been reported in a study performed in the United Kingdom. There, sheep naturally exposed to tick-infested pasture for a minimum of 4 weeks, resulted in 59 and 72% of PCR-positive engorged larvae and nymphs, respectively, after feeding on sheep. It must be taken into consideration however, that nymphs may have been previously infected (46).

In this last study, the authors reported that after molting, engorged larvae led to 18.5% of infected nymphs, where engorged nymphs led to 48% of infected adults (46). Here, higher transstadial infection rates were recovered after feeding larvae and nymphs on *A. phagocytophilum*-experimentally-infected sheep during the acute phase, with 70% of nymphs infected, and

80 and 90% of female tick salivary glands and midguts infected, respectively. The differences could be due to bacterial strain and sheep breed, and/or to the fact that in our study, ticks were fed during the acute phase of the infection, at the point where bacteria reached their highest peak in blood, as demonstrated by qPCR. Indeed, in the study performed by Ogden and coworkers, ticks were collected from sheep undergoing both acute and post-acute phases of infection at different time points over 9 weeks (46). In addition, it has been reported that tick acquisition efficiency gradually declines from high levels in the acute and immediate post-acute infection phases, to low levels in sheep that have been infected for much longer periods (47).

This last observation was confirmed by our results on transstadial transmission efficiency of *A. phagocytophilum* in *I. ricinus* ticks fed during acute or persistent infection of the sheep 381 with 70% and only 2.7% infection levels in molted nymphs, respectively. These last low infection rates can be explained by the low bacteremia in persistently-infected sheep, and the fact that larvae ingest small amounts of blood—and hence bacteria—within blood meals. Indeed, in nymphs or adults, which ingest larger volumes of blood and consequently have access to higher infectious bacterial doses, we can expect higher infection percentages. In addition, it has been suggested that a greater number of feeding adult ticks stimulates bacterial multiplication at the tick bite site and thus increases the *A. phagocytophilum* infectious dose for ticks (48, 49). Here, only larvae were used to infest sheep during the persistent infection, when both larvae and nymphs were used during the acute infection, which may also explain the observed difference in tick infection levels. However, bacterial transmission to ticks from persistently-infected sheep with no clinical signs, no positive PCR bacterial detection in blood, and for which all necropsies were PCR negative, has a real epidemiological importance for bacteria and disease maintenance and propagation in the field.

Our results also showed that larvae which had acquired *A. phagocytophilum* NV2Os from an infected sheep were able to retransmit it, as nymphs, to a naive sheep, thus validating that the transstadial transmitted bacteria remained infectious. This is the first demonstration of a complete NV2Os transmission cycle, from an *in vitro* bacterial culture to *I. ricinus* ticks. Finally, the failure to detect bacteria in eggs laid by adult ticks engorged on infected sheep during the acute phase, confirms that transovarial transmission of *A. phagocytophilum* is not likely to occur, in correlation with previous studies (32, 46).

CONCLUSION

Here we established a sheep model of IDE8 and ISE6 tick cell culture-propagated *A. phagocytophilum* NV2Os infection and tick transmission successfully mimicking the entire transmission cycle in the laboratory. Previously, sheep were experimentally infected with *A. phagocytophilum* NV2Os by inoculating blood obtained from infected sheep, but to our knowledge, this is the first time that this strain propagated in IDE8 or ISE6 tick cells has been used to infect sheep, and which produced clinical signs due to *A. phagocytophilum* infection. Our results also showed that not only were infected sheep able to transmit the bacteria to ticks during the acute phase of the infection, but also during the chronic persistent infection phase, a finding which has important epidemiological significance. Moreover, we demonstrated that nymphs infected on sheep during the preceding infection stage were also able to transmit the bacteria to naive sheep. The establishment of such a model opens an entire spectrum of possibilities in which to study the molecular events of *A. phagocytophilum* infection in both vertebrate and invertebrate hosts, tick-host-pathogen interactions, as well as testing the efficacy of vaccine candidates against *I. ricinus* and *A. phagocytophilum.*

DATA AVAILABILITY STATEMENT

The datasets generated for this study are available on request to the corresponding author.

ETHICS STATEMENT

The animal study was reviewed and approved by ComEth Anses/ENVA/UPEC; Permit Number 2016092716395004, ComEth Anses/ENVA/UPEC; Permit Number 2015081414257726.

AUTHOR CONTRIBUTIONS

CA and SB conceived and designed the study, analyzed the results, and wrote the paper. JF advised on experimental design. CA and LF performed animal experiments and performed laboratory analyses. H-JB, CA, and LF performed necropsies. PA and CR performed the cell cultures. CG performed IFA. PA, CR, and A-CL edited the manuscript. All authors read and approved the final paper.

FUNDING

This study received funding from the French Government's *Investissement d'Avenir* program, *Laboratoire d'Excellence* Integrative Biology of Emerging Infectious Diseases (grant n°ANR-10-LABX-62-IBEID) and from the SATTIdF Innov.

ACKNOWLEDGMENTS

We thank Snorre Stuen (Norwegian University of Life Sciences) for providing the *A. phagocytophilum* NV2Os strain. Benoit Lecuelle, Francis Moreau, and Michael Jacob (Biomedical Research Center, Ecole Nationale Vétérinaire d'Alfort) are acknowledged for their technical assistance during the sheep infections. We are in debt to Jean-Luc Servely (Bio-Pole, Ecole Nationale Vétérinaire d'Alfort) for his valuable imaging assistance. Gilberto Reyes de Luna, MSc student from the University of Queretaro, Mexico, is also acknowledged for his assistance on sheep infection and tick infestation, as well as DNA isolation from sheep tissues.

REFERENCES

1. Woldehiwet Z. The natural history of *Anaplasma phagocytophilum*. *Vet Parasitol*. (2010) 167:108–22. doi: 10.1016/j.vetpar.2009.09.013
2. Stuen S, Granquist EG, Silaghi C. *Anaplasma phagocytophilum*–a widespread multi-host pathogen with highly adaptive strategies. *Front Cell Infect Microbiol*. (2013) 3:31. doi: 10.3389/fcimb.2013.00031
3. Dahlgren FS, Heitman KN, Drexler NA, Massung RF, Behravesh CB. Human granulocytic anaplasmosis in the United States from 2008 to 2012: a summary of national surveillance data. *Am J Trop Med Hyg*. (2015) 93:66–72. doi: 10.4269/ajtmh.15-0122
4. Dziegiel B, Adaszek L, Winiarczyk S. Wild animals as reservoirs of *Anaplasma phagocytophilum* for humans. *Przegl Epidemiol*. (2016) 70:428–35.
5. Macleod J. Preliminary studies in tick transmission of louping ill. II A study of the reaction of sheep to tick infestation. *Vet J*. (1932) 88:276–84. doi: 10.1016/S0372-5545(17)39756-0
6. Gordon W, Briownlee A, Wilson D. Studies on louping ill, tick-borne fever and scrapie. In: *3rd International* Conference on *Microbiology*. New York, NY (1940). p. 362.
7. Granquist EG. *Anaplasma phagocytophilum* in sheep. In: Thomas S, editor. *Rickettsiales*. Cham: Springer (2016). p. 137–54.
8. Stuen S, Bergstrom K. Serological investigation of granulocytic Ehrlichia infection in sheep in Norway. *Acta Vet Scand*. (2001) 42:331–8. doi: 10.1186/1751-0147-42-331
9. Stuen S, Van De Pol I, Bergstrom K, Schouls LM. Identification of *Anaplasma phagocytophila* (formerly *Ehrlichia phagocytophila*) variants in blood from sheep in Norway. *J Clin Microbiol*. (2002) 40:3192–7. doi: 10.1128/jcm.40.9.3192-3197.2002
10. Woldehiwet Z. The effects of tick-borne fever on some functions of polymorphonuclear cells of sheep. *J Comp Pathol*. (1987) 97:481–5. doi: 10.1016/0021-9975(87)90026-0
11. Walker DH, Dumler JS. Human monocytic and granulocytic ehrlichioses. Discovery and diagnosis of emerging tick-borne infections and the critical role of the pathologist. *Arch Pathol Lab Med*. (1997) 121:785–91.
12. Gokce HI, Woldehiwet Z. Differential haematological effects of tick-borne fever in sheep and goats. *Zentralbl Veterinarmed B*. (1999) 46:105–15. doi: 10.1111/j.0931-1793.1999.00211.x
13. Stuen S, Grova L, Granquist EG, Sandstedt K, Olesen I, Steinshamn H. A comparative study of clinical manifestations, haematological and serological responses after experimental infection with *Anaplasma phagocytophilum* in two Norwegian sheep breeds. *Acta Vet Scand*. (2011) 53:8. doi: 10.1186/1751-0147-53-8
14. Brodie TA, Holmes PH, Urquhart GM. Some aspects of tick-borne diseases of British sheep. *Vet Rec*. (1986) 118:415–8. doi: 10.1136/vr.118.15.415
15. Stuen S, Bergstrom K, Palmer E. Reduced weight gain due to subclinical *Anaplasma phagocytophilum* (formerly *Ehrlichia phagocytophila*) infection. *Exp Appl Acarol*. (2002) 28:209–15. doi: 10.1023/a:1025350517733
16. Garcia-Perez AL, Barandika J, Oporto B, Povedano I, Juste RA. *Anaplasma phagocytophila* as an abortifacient agent in sheep farms from northern Spain. *Ann N Y Acad Sci*. (2003) 990:429–32. doi: 10.1111/j.1749-6632.2003.tb07406.x
17. de la Fuente J, Massung RF, Wong SJ, Chu FK, Lutz H, Meli M, et al. Sequence analysis of the msp4 gene of *Anaplasma phagocytophilum* strains. *J Clin Microbiol*. (2005) 43:1309–17. doi: 10.1128/JCM.43.3.1309-1317.2005
18. Ladbury GA, Stuen S, Thomas R, Bown KJ, Woldehiwet Z, Granquist EG, et al. Dynamic transmission of numerous *Anaplasma phagocytophilum* genotypes among lambs in an infected sheep flock in an area of anaplasmosis endemicity. *J Clin Microbiol*. (2008) 46:1686–91. doi: 10.1128/JCM.02068-07
19. Stuen S, Nevland S, Moum T. Fatal cases of Tick-borne fever (TBF) in sheep caused by several 16S rRNA gene variants of *Anaplasma phagocytophilum*. *Ann N Y Acad Sci*. (2003) 990:433–4. doi: 10.1111/j.1749-6632.2003.tb07407.x
20. Stuen S, Bergstrom K, Petrovec M, Van De Pol I, Schouls LM. Differences in clinical manifestations and hematological and serological responses after experimental infection with genetic variants of *Anaplasma phagocytophilum* in sheep. *Clin Diagn Lab Immunol*. (2003) 10:692–5. doi: 10.1128/cdli.10.4.692-695.2003
21. Stuen S, Torsteinbo WO, Bergstrom K, Bardsen K. Superinfection occurs in *Anaplasma phagocytophilum* infected sheep irrespective of infection phase and protection status. *Acta Vet Scand*. (2009) 51:41. doi: 10.1186/1751-0147-51-41
22. Granquist EG, Bardsen K, Bergstrom K, Stuen S. Variant -and individual dependent nature of persistent *Anaplasma phagocytophilum* infection. *Acta Vet Scand*. (2010) 52:25. doi: 10.1186/1751-0147-52-25
23. Bell-Sakyi L, Zweygarth E, Blouin EF, Gould EA, Jongejan F. Tick cell lines: tools for tick and tick-borne disease research. *Trends Parasitol*. (2007) 23:450–7. doi: 10.1016/j.pt.2007.07.009
24. Goodman JL, Nelson C, Vitale B, Madigan JE, Dumler JS, Kurtti TJ, et al. Direct cultivation of the causative agent of human granulocytic ehrlichiosis. *N Engl J Med*. (1996) 334:209–15. doi: 10.1056/NEJM199601253340401
25. Munderloh UG, Madigan JE, Dumler JS, Goodman JL, Hayes SF, Barlough JE, et al. Isolation of the equine granulocytic ehrlichiosis agent, Ehrlichia equi, in tick cell culture. *J Clin Microbiol*. (1996) 34:664–70. doi: 10.1128/JCM.34.3.664-670.1996
26. Munderloh UG, Jauron SD, Fingerle V, Leitritz L, Hayes SF, Hautman JM, et al. Invasion and intracellular development of the human granulocytic ehrlichiosis agent in tick cell culture. *J Clin Microbiol*. (1999) 37:2518–24. doi: 10.1128/JCM.37.8.2518-2524.1999
27. Woldehiwet Z, Horrocks BK, Scaife H, Ross G, Munderloh UG, Bown K, et al. Cultivation of an ovine strain of *Ehrlichia phagocytophila* in tick cell cultures. *J Comp Pathol*. (2002) 127:142–9. doi: 10.1053/jcpa.2002.0574
28. Alberdi P, Ayllon N, Cabezas-Cruz A, Bell-Sakyi L, Zweygarth E, Stuen S, et al. Infection of Ixodes spp. tick cells with different *Anaplasma phagocytophilum* isolates induces the inhibition of apoptotic cell death. *Ticks Tick Borne Dis*. (2015) 6:758–67. doi: 10.1016/j.ttbdis.2015.07.001
29. Munderloh UG, Kurtti TJ. Formulation of medium for tick cell culture. *Exp Appl Acarol*. (1989) 7:219–29.
30. Munderloh UG, Liu Y, Wang M, Chen C, Kurtti TJ. Establishment, maintenance and description of cell lines from the tick *Ixodes scapularis*. *J Parasitol*. (1994) 80:533–43. doi: 10.2307/3283188
31. Reppert E, Galindo RC, Ayllon N, Breshears MA, Kocan KM, Blouin EF, et al. Studies of *Anaplasma phagocytophilum* in sheep experimentally infected with the human NY-18 isolate: characterization of tick feeding sites. *Ticks Tick Borne Dis*. (2014) 5:744–52. doi: 10.1016/j.ttbdis.2014.05.014
32. Kocan KM, Busby AT, Allison RW, Breshears MA, Coburn L, Galindo RC, et al. Sheep experimentally infected with a human isolate of *Anaplasma phagocytophilum* serve as a host for infection of *Ixodes scapularis* ticks. *Ticks Tick Borne Dis*. (2012) 3:147–53. doi: 10.1016/j.ttbdis.2012.01.004
33. Bonnet S, Jouglin M, Malandrin L, Becker C, Agoulon A, L'hostis M, et al. Transstadial and transovarial persistence of Babesia divergens DNA in *Ixodes ricinus* ticks fed on infected blood in a new skin-feeding technique. *Parasitology*. (2007) 134:197–207. doi: 10.1017/S0031182006001545
34. Almazán C, Lagunes R, Villar M, Canales M, Rosario-Cruz R, Jongejan F, et al. Identification and characterization of Rhipicephalus (Boophilus) microplus candidate protective antigens for the control of cattle tick infestations. *Parasitol Res*. (2010) 106:471–9. doi: 10.1007/s00436-009-1689-1
35. Almazán C, Bonnet S, Cote M, Slovak M, Park Y, Simo L. A versatile model of hard tick infestation on laboratory rabbits. *J Vis Exp*. (2018) 140:e57994. doi: 10.3791/57994
36. Courtney JW, Kostelnik LM, Zeidner NS, Massung RF. Multiplex real-time PCR for detection of *Anaplasma phagocytophilum* and *Borrelia burgdorferi*. *J Clin Microbiol*. (2004) 42:3164–8. doi: 10.1128/JCM.42.7.3164-3168.2004
37. Koci J, Simo L, Park Y. Validation of internal reference genes for real-time quantitative polymerase chain reaction studies in the tick, *Ixodes scapularis* (Acari: Ixodidae). *J Med Entomol*. (2013) 50:79–84. doi: 10.1603/me12034

38. Simo L, Kazimirova M, Richardson J, Bonnet SI. The essential role of tick salivary glands and saliva in tick feeding and pathogen transmission. *Front Cell Infect Microbiol*. (2017) 7:281. doi: 10.3389/fcimb.2017.00281
39. Foggie A. Studies on the infectious agent of tick-borne fever in sheep. *J Pathol Bacteriol*. (1951) 63:1–15. doi: 10.1002/path.1700630103
40. Stuen S, Engvall EO, Artursson K. Persistence of *Ehrlichia phagocytophila* infection in lambs in relation to clinical parameters and antibody responses. *Vet Rec*. (1998) 143:553–5. doi: 10.1136/vr.143.20.553
41. Stuen S, Bergstrom K. Persistence of *Ehrlichia phagocytophila* infection in two age groups of lambs. *Acta Vet Scand*. (2001) 42:453–8. doi: 10.1186/1751-0147-42-453
42. Wang X, Rikihisa Y, Lai TH, Kumagai Y, Zhi N, Reed SM. Rapid sequential changeover of expressed p44 genes during the acute phase of *Anaplasma phagocytophilum* infection in horses. *Infect Immun*. (2004) 72:6852–9. doi: 10.1128/IAI.72.12.6852-6859.2004
43. Granquist EG, Stuen S, Crosby L, Lundgren AM, Alleman AR, Barbet AF. Variant-specific and diminishing immune responses towards the highly variable MSP2(P44) outer membrane protein of *Anaplasma phagocytophilum* during persistent infection in lambs. *Vet Immunol Immunopathol*. (2010) 133:117–24. doi: 10.1016/j.vetimm.2009.07.009
44. Stuen S, Casey AN, Woldehiwet Z, French NP, Ogden NH. Detection by the polymerase chain reaction of *Anaplasma phagocytophilum* in tissues of persistently infected sheep. *J Comp Pathol*. (2006) 134:101–4. doi: 10.1016/j.jcpa.2005.06.006
45. Lepidi H, Bunnell JE, Martin ME, Madigan JE, Stuen S, Dumler JS. Comparative pathology, and immunohistology associated with clinical illness after *Ehrlichia phagocytophila*-group infections. *Am J Trop Med Hyg*. (2000) 62:29–37. doi: 10.4269/ajtmh.2000.62.29
46. Ogden NH, Casey AN, Woldehiwet Z, French NP. Transmission of *Anaplasma phagocytophilum* to *Ixodes ricinus* ticks from sheep in the acute and post-acute phases of infection. *Infect Immun*. (2003) 71:2071–8. doi: 10.1128/IAI.71.4.2071-2078.2003
47. Ogden NH, Casey AN, French NP, Bown KJ, Adams JD, Woldehiwet Z. Natural *Ehrlichia phagocytophila* transmission coefficients from sheep 'carriers' to *Ixodes ricinus* ticks vary with the numbers of feeding ticks. *Parasitology*. (2002) 124:127–36. doi: 10.1017/s003118200100107x
48. Ogden NH, Casey AN, French NP, Adams JD, Woldehiwet Z. Field evidence for density-dependent facilitation amongst *Ixodes ricinus* ticks feeding on sheep. *Parasitology*. (2002) 124:117–25. doi: 10.1017/s0031182001001081
49. Ogden NH, Casey AN, French NP, Woldehiwet Z. A review of studies on the transmission of *Anaplasma phagocytophilum* from sheep: implications for the force of infection in endemic cycles. *Exp Appl Acarol*. (2002) 28:195–202. doi: 10.1023/a:1025394315915

Conflict of Interest: The authors declare that the research was conducted in the absence of any commercial or financial relationships that could be construed as a potential conflict of interest.

frontiers in Physiology

MINI REVIEW
published: 25 February 2020
doi: 10.3389/fphys.2020.00152

Tick Cell Lines in Research on Tick Control

*Ahmed Al-Rofaai and Lesley Bell-Sakyi**

Department of Infection Biology, Institute of Infection and Global Health, University of Liverpool, Liverpool, United Kingdom

Ticks and the diseases they transmit are of huge veterinary, medical and economic importance worldwide. Control of ticks attacking livestock and companion animals is achieved primarily by application of chemical or plant-based acaricides. However, ticks can rapidly develop resistance to any new product brought onto the market, necessitating an ongoing search for novel active compounds and alternative approaches to tick control. Many aspects of tick and tick-borne pathogen research have been facilitated by the application of continuous cell lines derived from some of the most economically important tick species. These include cell lines derived from acaricide-susceptible and resistant ticks, cell sub-lines with *in vitro*-generated acaricide resistance, and genetically modified tick cells. Although not a replacement for the whole organism, tick cell lines enable studies at the cellular and molecular level and provide a more accessible, more ethical and less expensive *in vitro* alternative to *in vivo* tick feeding experiments. Here we review the role played by tick cell lines in studies on acaricide resistance, mode-of-action of acaricides, identification of potential novel control targets through better understanding of tick metabolism, and anti-tick vaccine development, that may lead to new approaches to control ticks and tick-borne diseases.

Keywords: *Rhipicephalus microplus*, *Ixodes* spp., control, tick cell line, acaricide, resistance, metabolism, anti-tick vaccine

OPEN ACCESS

Edited by:
Itabajara Silva Vaz Jr., Federal University of Rio Grande do Sul, Brazil

Reviewed by:
Eliane Esteves, University of São Paulo, Brazil
Ulrike G. Munderloh, University of Minnesota Twin Cities, United States

****Correspondence:***
Lesley Bell-Sakyi
L.Bell-Sakyi@liverpool.ac.uk

Specialty section:
This article was submitted to Invertebrate Physiology, a section of the journal Frontiers in Physiology

Received: *16 December 2019*
Accepted: *12 February 2020*
Published: *25 February 2020*

Citation:
Al-Rofaai A and Bell-Sakyi L (2020) Tick Cell Lines in Research on Tick Control. Front. Physiol. 11:152. doi: 10.3389/fphys.2020.00152

INTRODUCTION

Ticks are obligate, haematophagous ectoparasites. Like mosquitoes, they cause problems to their hosts both from skin irritation and damage during blood feeding and by transmitting numerous pathogens including viruses, bacteria and protozoa. Consequently, ticks and tick-borne pathogens (TBPs) are of huge veterinary, medical and economic importance due to their negative impact on the health of humans and domestic animals (de la Fuente et al., 2008). Therefore, many control strategies have been devised to eliminate or avoid ticks and reduce the spread of TBPs, such as personal protection, landscape management, chemicals, vaccination, and biological control (Stafford et al., 2017). Amongst these, chemical control using a variety of acaricidal compounds is still the main strategy for controlling ticks affecting livestock and companion animals. However, many tick species develop resistance to these chemicals, which has led to attempts to find natural alternatives by studying the effects of some natural products on ticks and TBPs (Rodriguez-Vivas et al., 2018). Globally, the most economically important species, the invasive Asian cattle tick

Rhipicephalus (*Boophilus*) *microplus*, is also the most notorious for rapid development of resistance to every new acaricidal product brought onto the market (Jonsson and Hope, 2007; Abbas et al., 2014). Acaricide-resistant *R. microplus* are widespread throughout tropical and sub-tropical Asia, Latin America and Australia (Abbas et al., 2014), and are rapidly spreading in Southern, Central and West Africa (Nyangiwe et al., 2018; Silatsa et al., 2019).

Tick cell lines have an invaluable role to play in many aspects of tick and TBP research including tick biology, host-vector-pathogen relationships, genetic manipulation, genomics and proteomics (Bell-Sakyi et al., 2007). In addition, tick cell lines play a major role as essential tools in *in vitro* studies to examine and assess the impact of chemical molecules and vaccines against ticks and TBPs, as well as to investigate the mechanisms of resistance and tick metabolism which can lead to the development of novel approaches to control ticks and TBPs (Bell-Sakyi et al., 2018). While >60 continuous cell lines have now been established from 16 ixodid and three argasid tick species (Bell-Sakyi et al., 2018), studies on tick and pathogen control have predominantly centered around cell lines derived from, not surprisingly, *R. microplus*. A smaller number of studies have used cell lines derived from other tropical *Rhipicephalus* species of veterinary importance, from *Ixodes ricinus*, a European tick that feeds on a wide range of domestic and wild animal hosts as well as attacking humans, and from the medically important North American species *Ixodes scapularis* (**Table 1**).

This Mini Review focuses on the role of tick cell lines in studies on control of ticks and the few studies dealing with approaches to combined control of ticks and TBPs. While tick cell lines have been used in many studies contributing to aspects of pathogen control *per se*, these are beyond the scope of our review. Here we review selected studies to highlight how tick cell lines can contribute to tick control research, bearing in mind that results gained *in vitro* should be validated *in vivo*.

TICK CELL LINES IN STUDIES ON ACARICIDE RESISTANCE

Tick cell lines have been investigated for their potential as cheap and ethical tools to study acaricide resistance. Some studies focused on establishing drug-resistant cell lines which provide a useful tool to study and understand the mechanisms of resistance, an important step toward improving detection and prevention of tick resistance against acaricides. Tick cell lines are also a useful resource for identifying genes responsible for acaricide resistance and some published studies have focused on this aspect.

Generation and Application of Acaricide-Resistant Tick Cell Lines

Cossio-Bayugar et al. (2002b) generated three organophosphate-resistant *R. microplus* cell sub-lines by exposing the *R. microplus* BmVIII-SCC cell line (Holman, 1981), originally derived from embryos of acaricide-susceptible ticks, to gradually increasing concentrations of the organophosphate compound coumaphos (**Table 2**). They then assessed the levels of esterase, an enzyme that, when present at high levels, is responsible for causing resistance by modifying the organophosphate target site to be less sensitive. After exposure to coumaphos, there were higher levels of esterase in the resistant sub-lines compared to the original susceptible cell line. These findings, which were in line with previous *in vivo* studies (Miranda et al., 1995; Rosario-Cruz et al., 1997), validated the use of tick cell lines to study development of resistance in ticks, which could thereafter help to determine a suitable approach to formulating acaricides that would be less likely to induce resistance.

This group then used the coumaphos-resistant *R. microplus* cell sub-lines to evaluate the mechanisms that may contribute to acaricide resistance by further characterizing them compared to susceptible control cells (Cossio-Bayugar et al., 2002a). In addition to higher esterase levels, they found that the resistant cells exhibited higher levels of intracellular calcium and glutathione, decreased glutathione S-transferase activity, and reduced plasma and mitochondrial membrane potentials. Their results were consistent with the *in vivo* observations of increased esterase activity in organophosphate-resistant ticks, as well as resistance mechanisms found in other cell systems. One of the coumaphos-resistant *R. microplus* cell sub-lines played an important role in a further study (Cossio-Bayugar et al., 2005) that identified amino acid substitutions in the protein encoded by the phospholipid hydroperoxide glutathione peroxidase (PHGPx) gene in susceptible and resistant *R. microplus*, highlighting the possibility of its relationship with acaricide resistance in these tick populations.

A study conducted by Pohl et al. (2014) also focused on understanding the mechanisms of acaricide resistance in *R. microplus*. In this study, the authors established an ivermectin-resistant sub-line (BME26-IVM) of the *R. microplus* embryo-derived cell line BME26 (Kurtti et al., 1988; Esteves et al., 2008) by exposing susceptible cells to increasing concentrations of ivermectin (**Table 2**) over 46 weeks. Using the BME26-IVM sub-line, the contribution of the ATP-binding cassette (ABC) transporter mechanism was investigated by evaluating mRNA expression using quantitative RT-PCR. This study demonstrated increased levels of ABC transporter gene transcripts in the ivermectin-resistant cells compared to the original susceptible BME26 cells.

Effect of Acaricide Treatment of "Susceptible" Tick Cell Lines on Expression of Genes Associated With Resistance

Taking a different approach and using a cell line expected to be susceptible to ivermectin, Mangia et al. (2016) evaluated the expression of selected members of the ABC transporter subfamily B genes encoding P-glycoproteins (PgPs) in the *I. ricinus* embryo-derived cell line IRE/CTVM19 following treatment with ivermectin. The authors showed that ABC pump expression was not significantly modulated by ivermectin treatment, and expression of one of the subfamily genes was not detected. Interestingly, this study revealed that the IRE/CTVM19 cell line was able to tolerate a much higher concentration of ivermectin

TABLE 1 | Tick cell lines used in studies on tick control reviewed in this article.

Tick species	Distribution	Economic importance	Cell line	Geographic origin of parent ticks	Original references
Rhipicephalus microplus	Worldwide tropical and sub-tropical	Serious ectoparasitic pest of cattle; transmits anaplasmosis and babesiosis; high propensity to develop acaricide resistance	BmVIII-SCC	Mexico	Holman, 1981
			BME26	Mexico	Kurtti et al., 1988
			BME/CTVM2	Costa Rica	Bell-Sakyi, 2004
			BME/CTVM5	Colombia	Bell-Sakyi et al., 2007
			BME/CTVM6	Colombia	Bell-Sakyi, 2004
			BME/CTVM23	Mozambique	Alberdi et al., 2012
			BME/CTVM30	Mozambique	Alberdi et al., 2012
Rhipicephalus appendiculatus	East, Central and Southern Africa	Transmits East Coast fever of cattle and Nairobi sheep disease	RAN/CTVM3	Kenya	Bekker et al., 2002
			RA243	East Africa	Varma et al., 1975
Rhipicephalus evertsi	Sub-Saharan Africa	Transmits equine babesiosis, bovine anaplasmosis and causes tick toxicosis in ruminants	REN/CTVM32	South Africa	Bell-Sakyi et al., 2015
Rhipicephalus sanguineus	Worldwide tropical, sub-tropical and temperate	Transmits canine babesiosis, ehrlichioses and human rickettsioses	RSE/PILS35	France	Koh-Tan et al., 2016
			RML-RSE	United States	Yunker et al., 1981; Bell-Sakyi et al., 2015
Ixodes ricinus	Europe	Transmits borreliosis, neoehrlichiosis, anaplasmosis, babesiosis, tick-borne encephalitis, louping ill	IRE/CTVM19	United Kingdom	Bell-Sakyi et al., 2007
			IRE/CTVM20	United Kingdom	Bell-Sakyi et al., 2007
Ixodes scapularis	North America	Transmits Lyme borreliosis, human anaplasmosis and babesiosis, Powassan encephalitis	IDE8	United States	Munderloh et al., 1994
			ISE6	United States	Kurtti et al., 1996

TABLE 2 | Acaricides and pesticides used with tick cell lines in studies on tick control reviewed in this article.

Name	Chemical class	Route of application to animals	Mode of action
Amitraz	Amidines	Spot-on, spraying and dipping	Has an antagonistic effect on octopaminergic G protein-coupled receptors of the nerve cells causing paralysis and hyperexcitation in ticks
Coumaphos	Organophosphate compounds	Spraying and dipping	Acts on the nervous system as an inhibitor of transmission of nervous signals causing paralysis in the parasite
Fipronil	Phenylpyrazole compounds	Pour-on, spot-on and spraying	Inhibitor of GABA (gamma-aminobutyric acid), a key neurotransmitter in the central nervous system.
Ivermectin	Avermectins (macrocyclic lactones)	Pour-on, orally and by injection	Acts as inhibitor of GABA causing neuromuscular blockage, also opens chloride ion channels in membranes of the nervous system and further depresses neuronal function.
Paraquat	Dipyridylium (viologen)	Not applied to animals	A highly toxic herbicide known to induce oxidative stress in cells because of its ability to induce generation of superoxide ions
Permethrin	Synthetic pyrethroids	Pour-on, spot-on, spraying and dipping	Acts on the membrane of nerve cells blocking the closure of the ion gates of the sodium channel during re-polarization, and thereby disrupts transmission of nervous impulses.

(30 μg/ml) than the *R. microplus*-derived line BME26 that did not survive after exposure to 12.5 μg/ml ivermectin (Pohl et al., 2014). This could have been due to biological differences between the two tick species from which the cell lines were derived, differences in the phenotypic composition of the cell lines and/or in the culture conditions used. This should be considered when conducting such *in vitro* experiments using tick cell lines.

In a further study, Mangia et al. (2018) treated IRE/CTVM19 cultures with different concentrations of the acaricides permethrin, amitraz and fipronil (**Table 2**). They assessed cell viability, morphology, metabolic activity and expression of ABC genes at day 10 post-treatment. In general, the results showed that fipronil had the greatest significant negative effects on cell viability and metabolic activity, followed by permethrin, while amitraz only caused a significant decrease in these parameters at the highest concentration tested. The negative effects of fipronil and permethrin were confirmed by their effects on ABC gene expression with upregulation of ABCB6, ABCB8, and ABCB10, while amitraz had little or no effect on expression of any of the ABC genes tested.

Exploiting Tick Cell Lines Derived From Susceptible and Resistant Ticks to Identify Genes Involved in Acaricide Resistance

For some of the currently available *R. microplus* cell lines, the acaricide resistance status of the parent ticks from which the

cultures were derived is known. As already mentioned, the parent BmVIII-SCC and BME26 cells used by, respectively, Cossio-Bayugar et al. (2002b) and Pohl et al. (2014) to derive acaricide-resistant sub-lines *in vitro* were originally susceptible to the compounds used, implying that the parent ticks of both lines, originally from Mexico, were also acaricide-susceptible. Two additional *R. microplus* cell lines, BME/CTVM2 (Bell-Sakyi, 2004) and BME/CTVM4 (Bell-Sakyi et al., 2007), were derived from known acaricide-susceptible ticks from Costa Rica, while two other cell lines, BME/CTVM5 (Bell-Sakyi et al., 2007) and BME/CTVM6 (Bell-Sakyi, 2004) were derived from Colombian ticks known to be resistant to organophosphates, organochlorines and amitraz (Koh-Tan et al., 2016). While these cells whose natural resistance status derives from their parent ticks offer a potentially very interesting complement to the *in vitro*-derived resistant *R. microplus* cell lines of Cossio-Bayugar et al. (2002b) and Pohl et al. (2014), to date they have only been exploited in a single study. Koh-Tan et al. (2016) investigated the expression of the β-adrenergic octopamine receptor (βAOR) gene, associated with amitraz resistance, and the ATP-binding cassette B10 (ABCB10) gene, associated with macrocyclic lactone resistance, in tick cell lines derived from *R. microplus*, including BmVIII-SCC, BME/CTVM2, BME/CTVM5 and BME/CTVM6, *Rhipicephalus appendiculatus*, *Rhipicephalus sanguineus*, and *Rhipicephalus evertsi* (**Table 1**). Expression of the βAOR gene was detected in all the *Rhipicephalus* spp. cell lines, but in BME/CTVM6, derived from amitraz-resistant ticks, a novel larger amplicon was detected. This was found to encode a 12-amino acid insertion identified as a duplication of the immediately upstream sequence; the insertion was also present in genomic DNA from BME/CTVM5 cells, similarly derived from amitraz-resistant ticks, but transcription of the novel amplicon was not detectable. Expression of the ABC10 gene was approximately seven-fold higher in BME/CTVM6 cells compared to all other cell lines examined including BME/CTVM5. These findings suggest that BME/CTVM6 cells in particular could be a useful model system for studying resistance to multiple acaricide groups in *R. microplus*; further experiments are needed to determine whether additional genes are mutated in this cell line.

TICK CELL LINES ELUCIDATE NOVEL ASPECTS OF TICK CELL METABOLISM TO IDENTIFY POTENTIAL CONTROL TARGETS

Tick cell lines have also played a valuable role in the study of tick cell metabolism which can help in developing novel control methods. De Abreu et al. (2013) investigated the role of protein kinase B (AKT) and glycogen synthase kinase 3 (GSK3) in glycogen metabolism and cell viability using the *R. microplus* cell line BME26, and the results revealed an antagonistic role for AKT and GSK3. A reduction in AKT caused a decrease in glycogen content, cell viability and altered cell membrane permeability, whereas the inhibition of GSK3 promoted an increase in glycogen content.

To better understand energy metabolism during embryonic development in ticks, Da Silva et al. (2015) used the BME26 cell line to evaluate several genes involved in gluconeogenesis, glycolysis and glycogen metabolism, the major pathways for carbohydrate catabolism and anabolism. Their results showed that several genes displayed mutual regulation in response to glucose treatment, and the transcription of gluconeogenic genes in tick cells is controlled by GSK3.

The BME26 cell line also played an essential and effective role in the first report on characterization of a cell cycle protein in arachnids, and the reversal of its functions with an inhibitor (Gomes et al., 2013). The BME26 cell line was used in an *in vitro* inhibition assay to determine the inhibitory effects of roscovitine, a purine derivative, on tick cyclin-dependent kinases (CDKs), which are essential for cell cycle progression, and the results suggested that CDKs may present an alternative strategy for designing a novel acaricide that targets both oogenesis and embryogenesis processes.

The *I. scapularis* embryo-derived tick cell line ISE6 (Kurtti et al., 1996) is the one of the most widely used tick cell lines due to its susceptibility to a wide range of TBPs (Oliver et al., 2015). ISE6 cells were used by Cabezas-Cruz et al. (2017) to study possible control of infection with the obligate intracellular bacterium *Anaplasma phagocytophilum*, causative agent of disease in humans, ruminants, horses and dogs, by increasing the synthesis of phosphoenolpyruvate from tyrosine. Ferritins (FER) are iron-storage proteins that act to store excess iron available in the cellular iron pool by the binding and oxidation of the ferrous ion (Fe2+) and the formation of ferric ion (Fe3+) in the FER core cavity (Galay et al., 2015). Hernandez et al. (2018) were able to induce intracellular ferritin (FER1) protein expression by exposing ISE6 cells to various concentrations of ferrous sulfate. They showed that silencing of FER1 expression by RNA interference led to a decrease in ISE6 cell proliferation and an increase in mortality, concluding that ISE6 cells could be a good tool to further understanding of the mechanism of FER1 action. Thereafter, Hernandez et al. (2019) characterized the activity of an iron-inducible tick promoter derived from the tick *Haemaphysalis longicornis*, previously identified by Kusakisako et al. (2018b), in ISE6 cells, which could be a valuable tool in the development of a gene-manipulation system to control ticks and TBPs. Kusakisako et al. (2018a) established methods to visualize H_2O_2 in ISE6 cells using an intracellular H_2O_2 probe and observed that paraquat, known to induce oxidative stress in mammalian cells (**Table 2**), was also effective in this respect in ISE6 tick cells. Iron derived from host blood may react with oxygen in the tick's body and lead to high levels of H_2O_2, causing oxidative stress such as DNA strand breaks, lipid peroxidation and degradation of other molecules (Kusakisako et al., 2018a; Hernandez et al., 2019).

GENETIC MANIPULATION OF TICK CELL LINES

The development of new strategies for control of ticks could be greatly enhanced by exploring genetic manipulation of ticks

and tick cell lines. Demonstrating proof of concept, Kurtti et al. (2006) first reported stable transfection of the *I. scapularis* cell line ISE6 with a gene encoding a fluorescent protein using the Sleeping Beauty transposon system. In a different approach, Cossio-Bayugar and Miranda-Miranda (2007) reported retroviral transfection of primary *R. microplus* cell cultures with green fluorescent protein; fluorescence was detectable for up to 2 weeks following retroviral transfection. Using yet another approach, Machado-Ferreira et al. (2015) achieved the expression of transgenes in *R. microplus* ticks and the cell line BME/CTVM2 using *Agrobacterium tumefaciens* T-DNA constructs; evidence of transcription and protein synthesis were detectable for 2–3 weeks by fluorescence microscopy, western blot analyses and RT-PCR. These studies demonstrate that genetic manipulation approaches used with other animal cell systems can equally be applied to tick cell lines, and raise the possibility of modifying ticks to render them incapable of developing acaricide resistance.

TICK CELL LINES CONTRIBUTE TO ANTI-TICK VACCINE DEVELOPMENT

Vaccination with recombinant tick antigens represents a promising tick control strategy. Vaccines containing recombinant tick antigens demonstrated advantages including reduction in acaricide application, cost-effectiveness and reducing the prevalence of tick-borne diseases through reducing exposure of cattle to infected ticks. However, the efficacies of these vaccines vary considerably between tick species and geographic location (de la Fuente et al., 2007). Tick cell lines have played a central role in identifying tick protective antigens to produce a variety of vaccines that contribute to the prevention and control of tick infestations and TBP infections. For example, three embryo-derived tick cell lines, *R. microplus* BME/CTVM2 and *I. scapularis* IDE8 (Munderloh et al., 1994) and ISE6, were used in a study conducted by Antunes et al. (2014) to identify tick proteins involved in tick-pathogen interactions. The aim was to identify candidate protective antigens that could be used as vaccines for the control of cattle infestations with *R. microplus* ticks and infection with the TBPs *Anaplasma marginale* and *Babesia bigemina* transmitted by *R. microplus*. As an important part of the experiment, antibodies produced against the *R. microplus* protein subolesin were tested using immunofluorescence and showed positive reactions in the three cell lines, but no effect was observed on pathogen DNA levels. In contrast, using the *I. scapularis* cell line ISE6 and the *I. ricinus* cell line IRE/CTVM20 (Bell-Sakyi et al., 2007), Contreras et al. (2017) determined that two candidate tick-protective antigens – *I. scapularis* lipocalin (ISCW005600) and lectin pathway inhibitor (AAY66632), and their *I. ricinus* homologs – constitute candidate protective antigens for the control of tick infestations as well as *A. phagocytophilum* infection. They showed that anti ISCW005600 and AAY66632 IgG significantly increased the percentage of apoptotic tick cells and decreased pathogen infection, which could help in the development of effective anti-tick and anti-pathogen vaccines.

CONCLUSION

Ticks and TBPs have huge negative impacts on global livestock and public health and national economies. Scientific research has focused on creating and developing a variety of strategies to prevent and control ticks and TBPs. Tick cell lines represent essential tools in this area of research: *in vitro*-generated acaricide-resistant cell lines, cell lines derived from acaricide-resistant and susceptible ticks, genetically modified cell lines and cell lines supporting growth of intracellular TBPs all have a role to play. Experimental parameters can be easily controlled, effects at the cellular and molecular level can be determined, and cell lines reduce, while not ultimately replacing, the need for expensive *in vivo* studies involving maintenance of tick colonies and feeding on laboratory animals. As the numbers of cell lines derived from economically important tick species increase, so do the opportunities for exploiting them in a wide range of studies. For example, the potential for developing high-throughput preliminary screens of novel, potentially acaricidal compounds using cell lines from multiple tick species remains unexplored; such screens could greatly increase the number of active compounds identified for further testing at relatively low cost, and could be applied both to compound libraries held by pharmaceutical companies and to natural plant products. It is anticipated that gene editing of tick cell lines by technologies such as CRISPR will add another facet to the control portfolio. The Tick Cell Biobank (Bell-Sakyi et al., 2018), which houses all the cell lines mentioned in this review as well as cell lines derived from many other species of veterinary and medical concern, will continue to underpin research on tick and TBP control.

AUTHOR CONTRIBUTIONS

AA-R drafted the manuscript, LB-S edited the draft and both authors produced and agreed the final version.

FUNDING

AA-R is supported by the Council for At-Risk Academics (CARA) and the University of Liverpool. LB-S is supported by the United Kingdom Biotechnology and Biological Sciences Research Council grant number BB/P024270/1.

ACKNOWLEDGMENTS

We would like to thank staff of the Council for At-Risk Academics (CARA) and Dr. Benjamin Makepeace for their instrumental roles in bringing AA-R to the University of Liverpool.

REFERENCES

Abbas, R. Z., Zaman, M. A., Colwell, D. D., Gilleard, J., and Iqbal, Z. (2014). Acaricide resistance in cattle ticks and approaches to its management: the state of play. *Vet. Parasitol.* 203, 6–20. doi: 10.1016/j.vetpar.2014.03.006

Alberdi, M. P., Dalby, M. J., Rodriguez-Andres, J., Fazakerley, J. K., Kohl, A., and Bell-Sakyi, L. (2012). Detection and identification of putative bacterial endosymbionts and endogenous viruses in tick cell lines. *Ticks Tick Borne Dis.* 3, 137–146. doi: 10.1016/j.ttbdis.2012.05.002

Antunes, S., Merino, O., Mosqueda, J., Moreno-Cid, J. A., Bell-Sakyi, L., Fragkoudis, R., et al. (2014). Tick capillary feeding for the study of proteins involved in tick-pathogen interactions as potential antigens for the control of tick infestation and pathogen infection. *Parasit. Vectors* 7:42. doi: 10.1186/1756-3305-7-42

Bekker, C. P. J., Bell-Sakyi, L., Paxton, E. A., Martinez, D., Bensaid, A., and Jongejan, F. (2002). Transcriptional analysis of the major antigenic protein 1 multigene family of *Cowdria ruminantium*. *Gene* 285, 193–201. doi: 10.1016/s0378-1119(02)00408-0

Bell-Sakyi, L. (2004). *Ehrlichia ruminantium* grows in cell lines from four ixodid tick genera. *J. Comp. Pathol.* 130, 285–293. doi: 10.1016/j.jcpa.2003.12.002

Bell-Sakyi, L., Darby, A., Baylis, M., and Makepeace, B. L. (2018). The tick cell biobank: a global resource for *in vitro* research on ticks, other arthropods and the pathogens they transmit. *Ticks Tick Borne Dis.* 9, 1364–1371. doi: 10.1016/j.ttbdis.2018.05.015

Bell-Sakyi, L., Palomar, A., Bradford, E. L., and Shkap, V. (2015). Propagation of the Israeli vaccine strain of *Anaplasma centrale* in tick cell lines. *Vet. Microbiol.* 179, 270–276. doi: 10.1016/j.vetmic.2015.07.008

Bell-Sakyi, L., Zweygarth, E., Blouin, E. F., Gould, E. A., and Jongejan, F. (2007). Tick cell lines: tools for tick and tick-borne disease research. *Trends Parasitol.* 23, 450–457. doi: 10.1016/j.pt.2007.07.009

Cabezas-Cruz, A., Espinosa, P. J., Obregon, D. A., Alberdi, P., and de la Fuente, J. (2017). *Ixodes scapularis* tick cells control *Anaplasma phagocytophilum* infection by increasing the synthesis of phosphoenolpyruvate from tyrosine. *Front. Cell. Infect. Microbiol.* 7:375. doi: 10.3389/fcimb.2017.00375

Contreras, M., Alberdi, P., Fernandez de Mera, I. G., Krull, C., Nijhof, A., Villar, M., et al. (2017). Vaccinomics approach to the identification of candidate protective antigens for the control of tick vector infestations and *Anaplasma phagocytophilum* infection. *Front. Cell. Infect. Microbiol.* 7:360. doi: 10.3389/fcimb.2017.00360

Cossio-Bayugar, R., Barhoumi, R., Burghardt, R. C., Wagner, G. G., and Holman, P. J. (2002a). Basal cellular alterations of esterase, glutathione, glutathione S-transferase, intracellular calcium, and membrane potentials in coumaphos-resistant *Boophilus microplus* (Acari: Ixodidae) cell lines. *Pesticide Biochem. Physiol.* 72, 1–9. doi: 10.1006/pest.2001.2578

Cossio-Bayugar, R., Miranda, E., and Holman, P. J. (2005). Molecular cloning of a phospholipid-hydroperoxide glutathione peroxidase gene from the tick *Boophilus microplus* (Acari: Ixodidae). *Insect Biochem. Molec. Biol.* 35, 1378–1387. doi: 10.1016/j.ibmb.2005.08.008

Cossio-Bayugar, R., and Miranda-Miranda, E. (2007). Heterologus gene expression in a cattle tick *Rhipicephalus microplus* embryonic cell culture. *J. Anim. Vet. Adv.* 6, 1214–1218.

Cossio-Bayugar, R., Wagner, G. G., and Holman, P. J. (2002b). *In vitro* generation of organophosphate resistant *Boophilus microplus* (Acari: Ixodidae) cell lines. *J. Med. Entomol.* 39, 278–284. doi: 10.1603/0022-2585-39.2.278

Da Silva, R. M., Noce, B. D., Waltero, C. F., Costa, E. P., de Abreu, L. A., Githaka, N. W., et al. (2015). Non-classical gluconeogenesis-dependent glucose metabolism in *Rhipicephalus microplus* embryonic cell line BME26. *Int. J. Mol. Sci.* 16, 1821–1839. doi: 10.3390/ijms16011821

De Abreu, L. A., Calixto, C., Waltero, C. F., Della Noce, B. P., Githaka, N. W., Seixas, A., et al. (2013). The conserved role of the AKT/GSK3 axis in cell survival and glycogen metabolism in *Rhipicephalus Boophilus microplus* embryo tick cell line BME26. *Biochim. Biophys. Acta* 1830, 2574–2582. doi: 10.1016/j.bbagen.2012.12.016

de la Fuente, J., Almazán, C., Canales, M., Pérez de la Lastra, J. M., Kocan, K. M., and Willadsen, P. (2007). A ten-year review of commercial vaccine performance for control of tick infestations on cattle. *Anim. Health Res. Rev.* 8, 23–28. doi: 10.1017/s1466252307001193

de la Fuente, J., Estrada-Pena, A., Venzal, J. M., Kocan, K. M., and Sonenshine, D. E. (2008). Overview: ticks as vectors of pathogens that cause disease in humans and animals. *Front. Biosci.* 13:6938–6946. doi: 10.2741/3200

Esteves, E., Lara, F. A., Lorenzini, D. M., Costa, G. H. N., Fukuzawa, A. H., Pressinotti, L. N., et al. (2008). Cellular and molecular characterization of an embryonic cell line (BME26) from the tick *Rhipicephalus* (*Boophilus*) *microplus*. *Insect Biochem. Mol. Biol.* 38, 568–580. doi: 10.1016/j.ibmb.2008.01.006

Galay, R. L., Umemiya-Shirafuji, R., Mochizuki, M., Fujisaki, K., and Tanaka, T. (2015). Iron metabolism in hard ticks (Acari: Ixodidae): the antidote to their toxic diet. *Parasitol. Int.* 64, 182–189. doi: 10.1016/j.parint.2014.12.005

Gomes, H., Romeiro, N. C., Braz, G. R. C., de Oliveira, E. A. G., Rodrigues, C., da Fonseca, R. N., et al. (2013). Identification and structural-functional analysis of cyclin-dependent kinases of the cattle tick *Rhipicephalus (Boophilus) microplus*. *PLoS One* 8:e76128. doi: 10.1371/journal.pone.0076128

Hernandez, E. P., Kusakisako, K., Hatta, T., and Tanaka, T. (2019). Characterization of an iron-inducible *Haemaphysalis longicornis* tick-derived promoter in an *Ixodes scapularis*-derived tick cell line (ISE6). *Parasit. Vectors* 12:321. doi: 10.1186/s13071-019-3574-9

Hernandez, E. P., Kusakisako, K., Talactac, M. R., Galay, R. L., Yoshii, K., and Tanaka, T. (2018). Induction of intracellular ferritin expression in embryo-derived *Ixodes scapularis* cell line (ISE6). *Sci. Rep.* 8:16566. doi: 10.1038/s41598-018-34860-3

Holman, P. J. (1981). Partial characterization of a unique female diploid cell strain from the tick *Boophilus microplus* (Acari: Ixodidae). *J. Med. Entomol.* 18, 84–88. doi: 10.1093/jmedent/18.1.84

Jonsson, N. N., and Hope, M. (2007). Progress in the epidemiology and diagnosis of amitraz resistance in the cattle tick *Boophilus microplus*. *Vet. Parasitol.* 146, 193–198. doi: 10.1016/j.vetpar.2007.03.006

Koh-Tan, H. H. C., Strachan, E., Cooper, K., Bell-Sakyi, L., and Jonsson, N. N. (2016). Identification of a novel β-adrenergic octopamine receptor-like gene (βAOR-like) and increased ATP-binding cassette B10 (ABCB10) expression in a *Rhipicephalus microplus* cell line derived from acaricide-resistant ticks. *Parasit. Vectors* 9:425.

Kurtti, T. J., Felsheim, R. F., Mattila, J. T., Baldridge, G. D., Burkhardt, N. Y., and Munderloh, U. G. (2006). Stable transformation of a tick (*Ixodes scapularis*) cell line with the *Sleeping Beauty* transposon system. *Soc. Vitro Biol. J.* 42:32.

Kurtti, T. J., Munderloh, U. G., and Ahlstrand, G. G. (1988). Tick tissue and cell culture in vector research. *Adv. Dis. Vector Res.* 5, 87–109.

Kurtti, T. J., Munderloh, U. G., Andreadis, T. G., Magnarelli, L. A., and Mather, T. N. (1996). Tick cell culture isolation of an intracellular prokaryote from the tick *Ixodes scapularis*. *J. Invert. Pathol.* 67, 318–321. doi: 10.1006/jipa.1996.0050

Kusakisako, K., Hernandez, E. P., Talactac, M. R., Yoshii, K., Umemiya-Shirafuji, R., Fujisaki, K., et al. (2018a). Peroxiredoxins are important for the regulation of hydrogen peroxide concentrations in ticks and tick cell line. *Ticks Tick Borne Dis.* 9, 872–881. doi: 10.1016/j.ttbdis.2018.03.016

Kusakisako, K., Ido, A., Masatan, T., Morokuma, H., Hernandez, E. P., Talactac, M. R., et al. (2018b). Transcriptional activities of two newly identified *Haemaphysalis longicornis* tick-derived promoter regions in the *Ixodes scapularis* tick cell line (ISE6). *Insect Mol. Biol.* 27, 590–602. doi: 10.1111/imb.12497

Machado-Ferreira, E., Balsemão-Pires, E., Dietrich, G., Hojgaard, A., Vizzoni, V. F., Scoles, G., et al. (2015). Transgene expression in tick cells using *Agrobacterium tumefaciens*. *Exp. Appl. Acarol.* 67, 269–287. doi: 10.1007/s10493-015-9949-5

Mangia, C., Vismarra, A., Genchi, M., Epis, S., Bandi, C., Grandi, G., et al. (2018). Exposure to amitraz, fipronil and permethrin affects cell viability and ABC transporter gene expression in an *Ixodes ricinus* cell line. *Parasit. Vectors* 11:437. doi: 10.1186/s13071-018-3020-4

Mangia, C., Vismarra, A., Kramer, L., Bell-Sakyi, L., Porretta, D., Otranto, M., et al. (2016). Evaluation of the *in vitro* expression of ATP binding-cassette (ABC) proteins in an *Ixodes ricinus* cell line exposed to ivermectin. *Parasit. Vectors* 9:215. doi: 10.1186/s13071-016-1497-2

Miranda, E., Cossio-Bayugar, R., Tellez-Alanis, M. R., Garcia-Vazquez, Z., Rosario-Cruz, R., and Ortiz-Estrada, M. (1995). An enzymatic marker for ixodicide resistance detection in the cattle tick *Boophilus microplus*. *Adv. Agric. Res.* 4, 1–8.

Munderloh, U. G., Liu, Y., Wang, M., Chen, C., and Kurtti, T. J. (1994). Establishment, maintenance and description of cell lines from the tick *Ixodes scapularis*. *J. Parasitol.* 80, 533–543.

Nyangiwe, N., Yawa, M., and Muchenje, V. (2018). Driving forces for changes in geographic range of cattle ticks (Acari: Ixodidae) in Africa: a review. *South Afr. J. Anim. Sci.* 48, 829–841.

Oliver, J. D., Chavez, A. S., Felsheim, R. F., Kurtti, T. J., and Munderloh, U. G. (2015). An *Ixodes scapularis* cell line with a predominantly neuron-like phenotype. *Exp. Appl. Acarol.* 66, 427–442. doi: 10.1007/s10493-015-9908-1

Pohl, P. C., Carvalho, D. D., Daffre, S., da Silva Vaz, I., and Masuda, A. (2014). *In vitro* establishment of ivermectin-resistant *Rhipicephalus microplus* cell line and the contribution of ABC transporters on the resistance mechanism. *Vet. Parasitol.* 204, 316–322. doi: 10.1016/j.vetpar.2014.05.042

Rodriguez-Vivas, R. I., Jonsson, N. N., and Bhushan, C. (2018). Strategies for the control of *Rhipicephalus microplus* ticks in a world of conventional acaricide and macrocyclic lactone resistance. *Parasitol. Res.* 117, 3–29. doi: 10.1007/s00436-017-5677-5676

Rosario-Cruz, R., Miranda-Miranda, E., Garcia-Vazquez, Z., and Ortiz-Estrada, M. (1997). Detection of esterase activity in susceptible and organophosphate resistant strains of the cattle tick *Boophilus microplus*. *Bull. Entomol. Res.* 87, 197–202. doi: 10.1017/s0007485300027358

Silatsa, B. A., Simo, G., Githaka, N., Mwaura, S., Kamga, R. M., Oumarou, F., et al. (2019). A comprehensive survey of the prevalence and spatial distribution of ticks infesting cattle in different agro-ecological zones of Cameroon. *Parasit. Vectors* 12:489. doi: 10.1186/s13071-019-3738-7

Stafford, K. C., Williams, S. C., and Molaei, G. (2017). Integrated pest management in controlling ticks and tick-associated diseases. *J. Integr. Pest Manag.* 8:28. doi: 10.1093/jipm/pmx018

Varma, M. G. R., Pudney, M., and Leake, C. J. (1975). The establishment of three cell lines from the tick *Rhipicephalus appendiculatus* (Acari: Ixodidae) and their infection with some arboviruses. *J. Med. Entomol.* 11, 698–706. doi: 10.1093/jmedent/11.6.698

Yunker, C. E., Cory, J., and Meibos, H. (1981). Continuous cell lines from embryonic tissues of ticks (Acari: Ixodidae). *In Vitro* 17, 139–142. doi: 10.1007/bf02618071

Conflict of Interest: The authors declare that the research was conducted in the absence of any commercial or financial relationships that could be construed as a potential conflict of interest.

The reviewer UM declared a past co-authorship with one of the authors LB-S to the handling Editor.

frontiers in Veterinary Science

ORIGINAL RESEARCH
published: 06 March 2020
doi: 10.3389/fvets.2020.00111

Global Transcription Profiles of *Anaplasma phagocytophilum* at Key Stages of Infection in Tick and Human Cell Lines and Granulocytes

*Curtis M. Nelson[1], Michael J. Herron[1], Xin-Ru Wang[1], Gerald D. Baldridge[1], Jonathan D. Oliver[2] and Ulrike G. Munderloh[1]**

[1] Department of Entomology, College of Food, Agriculture, and Natural Resource Sciences, University of Minnesota, Minneapolis, MN, United States, [2] Division of Environmental Health Sciences, School of Public Health, University of Minnesota, Minneapolis, MN, United States

The incidence of human diseases caused by tick-borne pathogens is increasing but little is known about the molecular interactions between the agents and their vectors and hosts. *Anaplasma phagocytophilum* (Ap) is an obligate intracellular, tick-borne bacterium that causes granulocytic anaplasmosis in humans, dogs, sheep, and horses. In mammals, neutrophil granulocytes are a primary target of infection, and in ticks, Ap has been found in gut and salivary gland cells. To identify bacterial genes that enable Ap to invade and proliferate in human and tick cells, labeled mRNA from Ap bound to or replicating within human and tick cells (lines HL-60 and ISE6), and replicating in primary human granulocytes *ex vivo*, was hybridized to a custom tiling microarray containing probes representing the entire Ap genome. Probe signal values plotted over a map of the Ap genome revealed antisense transcripts and unannotated genes. Comparisons of transcript levels from each annotated gene between test conditions (e.g., Ap replicating in HL-60 vs. ISE6) identified those that were differentially transcribed, thereby highlighting genes associated with each condition. Bacteria replicating in HL-60 cells upregulated 122 genes compared to those in ISE6, including numerous *p44* paralogs, five *HGE-14* paralogs, and 32 hypothetical protein genes, of which 47% were predicted to be secreted or localized to the membrane. By comparison, 60% of genes upregulated in ISE6 encoded hypothetical proteins, 60% of which were predicted to be secreted or membrane associated. In granulocytes, Ap upregulated 120 genes compared to HL-60, 33% of them hypothetical and 43% of those predicted to encode secreted or membrane associated proteins. HL-60-grown bacteria binding to HL-60 cells barely responded transcriptionally, while ISE6-grown bacteria binding to ISE6 cells upregulated 48 genes. HL-60-grown bacteria, when incubated with ISE6 cells, upregulated the same genes that were upregulated by ISE6-grown bacteria exposed to uninfected ISE6. Hypothetical genes (constituting about 29% of Ap genes) played a disproportionate role in most infection scenarios, and particular sets of them were consistently upregulated in bacteria binding/entering both ISE6 and HL-60 cells. This suggested that the encoded proteins played central roles in establishing infection in ticks and humans.

Keywords: human anaplasmosis, tick-borne pathogen, tiling microarray, obligate intracellular bacterium, *Ixodes scapularis*, differential gene expression, host-cell invasion, intracellular replication

OPEN ACCESS

Edited by:
Itabajara Silva Vaz Jr, Federal University of Rio Grande Do Sul, Brazil

Reviewed by:
Pilar Alberdi, Institute of Game and Wildlife Research (CSIC), Spain
Andréa Cristina Fogaça, University of São Paulo, Brazil

***Correspondence:**
Ulrike G. Munderloh
munde001@umn.edu

Specialty section:
This article was submitted to Veterinary Infectious Diseases, a section of the journal Frontiers in Veterinary Science

Received: *29 October 2019*
Accepted: *13 February 2020*
Published: *06 March 2020*

Citation:
Nelson CM, Herron MJ, Wang X-R, Baldridge GD, Oliver JD and Munderloh UG (2020) Global Transcription Profiles of Anaplasma phagocytophilum at Key Stages of Infection in Tick and Human Cell Lines and Granulocytes. Front. Vet. Sci. 7:111. doi: 10.3389/fvets.2020.00111

INTRODUCTION

Anaplasma phagocytophilum (Ap) is an obligate intracellular bacterium that is spread by blacklegged ticks (*Ixodes scapularis* and *Ixodes pacificus*). It causes human anaplasmosis, a serious disease that has steadily increased in prevalence in the United States from 350 cases in 2000 to 5,762 in 2017 (https://www.cdc.gov/anaplasmosis/stats/index.html). Ap alternately infects ticks and mammals to perpetuate itself. In humans and other mammals, infected cells include microvascular endothelium which participates in antigen presentation, and granulocytes that are an important component of the innate immune system. This steers the host toward an ineffective, pro-inflammatory T2-dominated response that induces high fever and liver damage characteristic of human anaplasmosis. A T2 immune response is dominated by production of antibodies as opposed to induction of cytotoxic lymphocytes (a T1 response). The former is ineffective in protecting the host against primary infection with intracellular pathogens (1, 2).

Cell lines from specific host species and tissues are invaluable research tools for analysis of intracellular pathogen–host interactions at the cellular and molecular levels to identify specific host proteins and pathogen factors at play. As models of human infection, relevant cell lines include HMEC-1, a microvascular endothelial cell line, and HL-60, representing human granulocyte precursors, while the tick cell line ISE6 from *Ixodes scapularis* embryos commonly serves to investigate tick infection (3–5). *In vitro* studies further benefit from the availability of complete genome sequences for both hosts and Ap. Despite the many advantages offered by established cell lines for analysis of intracellular bacteria, including ready availability of a well-defined and standardized system, *ex vivo* use of a definitive target cell can reveal molecular mechanisms of pathogenesis that may not otherwise be evident. With the notable exception of granulocytes, cells derived from peripheral blood are conveniently accessible and tractable. Neutrophil granulocytes, however, are first line responders of the innate immune system, and though relatively abundant, when placed *ex vivo*, they rapidly induce defense responses to stimuli designed to efficiently kill invading pathogens. This and their short life span pose special challenges that must be overcome when working with them in a culture system *in vitro* to prevent inadvertent activation and avoid use of senescent cells (6).

Ticks and humans are separated by a large evolutionary distance and are biologically widely divergent, which presents unique challenges to intracellular pathogens that infect these disparate hosts using the limited resources of their small genomes. We have previously shown that Ap activates transcription from specific sets of genes depending on the host cell within which they reside, which is even true for different cell types from the same species (7). These earlier experiments used bacteria harvested from asynchronous, heavily infected cultures, and were not designed to determine a detailed time-course of gene activation during cell invasion and the subsequent intracellular life cycle of Ap, nor did they track changes induced when Ap encounters the alternate host. In the current manuscript, we present a picture of sequential gene activation in bacteria harvested from HL-60 or ISE6 cells and then incubated with fresh uninfected cells. As a control, Ap were held in sterile culture medium in the absence of any host cell stimuli. Samples were collected during phases corresponding to host cell adhesion and invasion, and subsequent intracellular replication. All transcripts, whether from annotated or unannotated genome regions, coding or non-coding DNA strands, were mapped to the genome of the specific Ap isolate used, and quantified. The knowledge gained will facilitate identification of function of the many hypothetical protein genes (those without any known homologs in the data bases) in the Ap genome, as well as provide a basis for rational selection of molecular targets for the prevention or cure of human anaplasmosis.

MATERIALS AND METHODS

Cells, Ap Isolate, and Culture Conditions

HL-60 (human promyeloblast, ATCC #CCL240) cells were maintained between 1×10^5 and 1.5×10^6 cells/mL in RPMI-1640 supplemented with 2 mM glutaMAX, 2 mM L-glutamine, 25 mM HEPES, and 10% FBS (HL-60 medium) in a water saturated, 5% CO_2 atmosphere at 37°C. ISE6 (*I. scapularis*) cells were maintained as previously described (3) except they were kept at 34°C and the culture medium for Ap-infected cells contained 10% FBS. Human peripheral blood granulocytes were isolated from 5 mL of blood anticoagulated with 50 μL of 0.5 M EDTA from a healthy adult using Ficoll-Paque PREMIUM (GE Healthcare). Blood was mixed with 5 mL of room temperature (RT) RPMI-1640 containing 25 mM HEPES and 2 mM GlutaMAX. Tubes containing 3 mL of Ficoll-Paque were overlaid with 4 mL of diluted blood and centrifuged at 400 × g for 35 min at 20°C in a swinging bucket rotor with the brake off. Layers above the granulocyte/erythrocyte layer were discarded and granulocytes were aspirated (∼1.0 mL) from the erythrocyte layer and mixed with 10 mL of RBC Lysis Solution (Qiagen, United States). After 10 min at RT, the erythrocyte-free granulocytes were centrifuged at 400 × g for 10 min at 20°C, washed once with 5 mL of HL-60 medium, and resuspended in 1 mL of medium. HGE1 (passage 10–20), a sequenced [(8), APHH00000000.1] human Ap isolate from Minnesota (9) was used throughout the study. To maintain HGE1 in HL-60, a 4 mL-culture of 10^5 HL-60 cells/mL was inoculated with 50 μL of HGE1-infected HL-60 (50–90% of infected cells) every 3–4 days. To maintain HGE1 in ISE6, a light monolayer of ISE6 (∼3×10^6 cells) in a 25-cm^2 flask containing 5 mL of medium for Ap-infected cells was inoculated with 100 μL of ∼90% infected ISE6 cells. The sealed flask was incubated at 34°C and fed three times per week until the cells began to lift off at about 2 weeks, when the culture was again ∼90% infected.

Cell-Free Bacteria Preparation

Routine maintenance procedures as described above result in asynchronous infections, in which only a proportion of bacteria represent the infectious, dense-core form (10). To achieve standardized infections in HL-60 and ISE6 cultures that produced maximum numbers of infectious bacteria needed for experiments, we used saturating levels of cell-free bacteria at a

multiplicity of infection (MOI) of 10–50 bacteria/cell (11) for two successive passages. This resulted in synchronously infected samples for tiling array analysis. To harvest cell-free bacteria from such standardized HL-60 cultures, 3–5 × 10^6 cells that were ≥95% infected (∼72 h post-inoculation, pi, determined by microscopic examination of Giemsa-stained cells deposited onto slides using a Cytospin centrifuge; Thermo Scientific) were resuspended in 3 mL of culture medium. The cell suspension was passed six times through a syringe fitted with a 27-gauge needle to release bacteria, intact cells were removed by centrifugation (710 × g, 6 min), and the supernatant was passed through a 2 μm syringe filter to remove cell nuclei and debris. Bacteria were collected from the filtrate (5,000 × g for 5 min), and resuspended in 100 μL of culture medium. These HL-60-derived bacteria were used either for propagation (another round of HL-60 infection) or to produce samples of infected HL-60 cells or human granulocytes for array analysis. To prepare cell-free bacteria from tick cells, a culture of 3–5 × 10^6 infected ISE6 cells (about 14 days pi) was resuspended in 3 mL of culture medium, and bacteria were isolated as described above.

Sample Preparation

The experimental conditions that Ap bacteria were subject to and host cells of origin are listed in **Table 1**, and are subsequently referred to by their assigned numbers (samples 1–8).

Transcript signals from the entire chromosome of Ap isolate HGE1 (representing the positive and the negative strand, including all coding, non-coding, annotated, and unannotated regions) were measured at two time-points when bacteria were binding to and entering HL-60 or ISE6 cells (2 and 4 h, respectively; **Tables S3, S4**), and at one time-point when bacteria were replicating in each cell type: 24 h for HL-60 and human granulocytes, and 48 h for ISE6 (**Tables S1, S2, S8**). All replicates were biological replicates.

To test gene expression in bacteria derived from HL-60 cells and exposed to or cultured in fresh HL-60 cells or human granulocyte samples (samples 1, 2, 6, and 8), 2 × 10^6 cells in 0.5 mL of HL-60 medium were mixed with 30 μL of cell-free bacteria (MOI: 10–50) in 1.5 mL microfuge tubes and incubated at 37°C for 2 h (sample 1) or 4 h (sample 2). Tubes were manually inverted to gently mix contents every 15 min to maximize contact between bacteria and cells. Cells were allowed to settle for a final 15 min period, and the medium containing unbound bacteria was aspirated. Cells with bound bacteria were washed once by centrifugation at 350 × g for 6 min in 5 mL of medium pre-warmed to 37°C, and dissolved in 1 mL of Tri Reagent (Sigma-Aldrich) to extract RNA for measurement of transcription associated with cell binding/entry. To measure transcription when bacteria were replicating, cells infected as described were resuspended in 20 mL of medium and further incubated at 37°C for 24 h (samples 6 and 8). They were then pelleted (350 × g, 6 min) and dissolved in 1 mL of Tri Reagent. Control samples consisted of 30 μL of cell-free bacteria prepared identically in parallel in 0.5 mL of medium alone, to measure bacterial transcription after incubation in the absence of host cells, or 2 × 10^6 HL-60 cells or 3 × 10^6 ISE6 cells without Ap (samples 6 and 10, respectively). Following collection by centrifugation at 4,000 × g for 6 min, bacteria were dissolved in 1 mL of Tri Reagent. Granulocytes are less transcriptionally active than other leukocytes or HL-60 cells (12), and thus contribute much less cellular mRNA. To equalize the RNA concentration in sample 8 to the other samples, 1 × 10^6 sterile HL-60 cells were added to sample 8 after addition of Tri Reagent. The same was done with control samples of bacteria in fresh medium alone, as described below under RNA isolation. For ISE6 samples, 3 × 10^6 ISE6 cells established as a light monolayer (∼80% confluent) in a 25-cm^2 flask were inoculated with 30 μL of ISE6-derived bacteria in 1 mL of ISE6 growth medium (MOI: 10–50) and incubated for 2 h (sample 3) or 4 h (sample 4) at 34°C with gentle hand rocking at 15-min intervals to redistribute the bacteria across the monolayer. To remove unbound bacteria, the medium was discarded, and the monolayer rinsed with 5 mL of medium warmed to 34°C, then flooded with 3 mL of Tri Reagent to collect RNA from bacteria binding/entering ISE6. To measure gene transcription when bacteria were replicating in ISE6 cells, cultures were incubated for another 48 h at 34°C in 5 mL of medium (sample 7), and RNA was then isolated from the monolayer as above.

To visualize Ap binding/entering HL-60 cells at 2 and 4 h, 1 × 10^4 cells from preparations used for RNA isolation (samples 1 and 2; **Figures 1A,B**), were deposited onto microscope slides using a Cytospin centrifuge, air dried five min, and fixed in methanol five min. Bacteria were labeled with antibody by incubating first with dog anti-Ap serum (1/2,000 dilution) followed with goat anti-dog IgG-FITC (13). Preparations were overlaid with PBS containing 0.15 μg DAPI/mL to stain HL-60 cell nuclei (blue). For Ap exposed to ISE6 for 2 and 4 h (corresponding to samples 3, 4, and 5; **Figures 1C–E**), cells were first established in glass bottom dishes (MatTek Corporation) then incubated with bacteria at the same concentration and MOI as for microarray samples. After washing, cells and bacteria were fixed by flooding dishes with methanol, air dried, stained as above, and imaged within the dishes. Cells with bound Ap were

TABLE 1 | Samples for RNA extraction.

Sample Nr./ Replicates[a]	Origin host cell[b]	Target host cell[c]	Control[d]	Sampling time[e]
1/1	Ap from HL-60	HL-60	Ap w/o host cells	2 h
2/3	Ap from HL-60	HL-60	Ap w/o host cells	4 h
3/1	Ap from ISE6	ISE6	Ap w/o host cells	2 h
4/3	Ap from ISE6	ISE6	Ap w/o host cells	4 h
5/1	Ap from HL-60	ISE6	Ap w/o host cells	2 h
6/4	Ap from HL-60	HL-60	Uninfected HL-60	24 h
7/3	Ap from ISE6	ISE6	Uninfected ISE6	48 h
8/3	Ap from HL-60	PMN[f]	–	24 h

[a] *Sample number and number of biological replicates used.*
[b] *Host cells from which A. phagocytophilum were purified.*
[c] *Host cells to which purified A. phagocytophilum were exposed.*
[d] *Purified A. phagocytophilum incubated in freshly-made cell culture medium alone.*
[e] *Time post of addition of A. phagocytophilum to target host cells when samples were taken.*
[f] *Human granulocytes.*

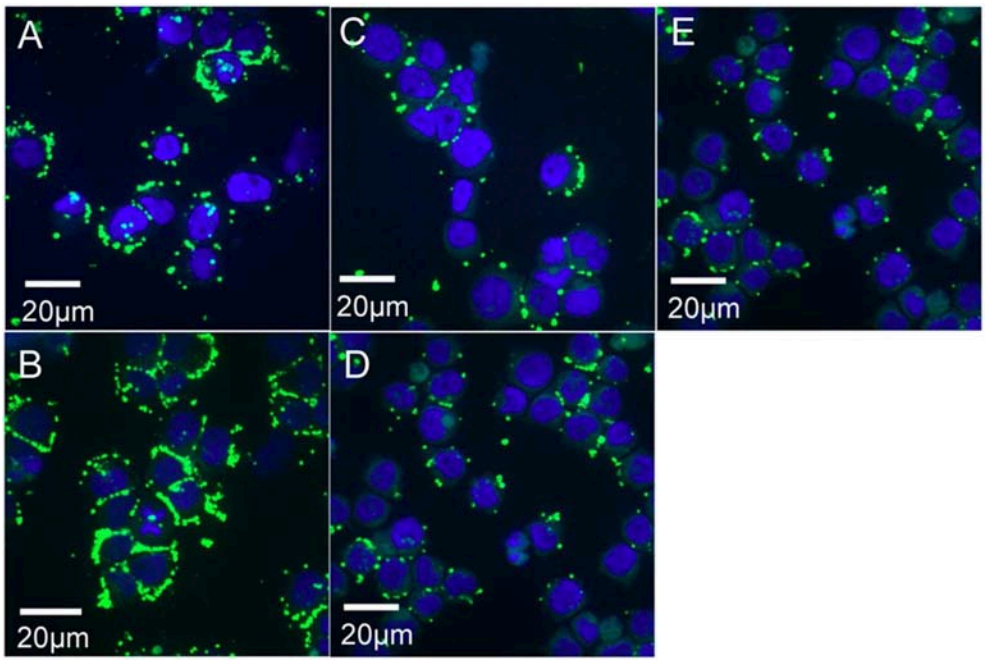

FIGURE 1 | Confocal microscopy images of *A. phagocytophilum* (Ap) binding/entering HL-60 and ISE6 cells. Cell nuclei are stained blue with DAPI, bacteria green by immunofluorescence (primary antibody: dog anti-Ap serum; secondary antibody: goat anti-dog IgG-FITC). **(A)** Sample 1 (Ap incubated with HL-60 for 2 h; **(B)** Sample 2 (Ap incubated with HL-60 for 4 h); **(C)** Sample 3 (Ap incubated with ISE6 for 2 h; **(D)** Sample 4 (Ap incubated with ISE6 for 4 h); and **(E)** Sample 5 (HL-60-grown bacteria incubated with ISE6 cells for 2 h).

viewed on an Olympus BX61 confocal microscope (Olympus America, Pennsylvania) equipped with a DSU-D2 confocal disk-scanning unit, and images were acquired with a Photometrics QuantEM:512SC EMCCD camera (Photometrics, Arizona) or a QFire color camera (Qimaging, California).

RNA Isolation

Total RNA for each sample was extracted from 2×10^6 infected HL-60 cells or 3×10^6 infected ISE6 cells, and purified according to the product protocol. Finally, the RNA pellets were washed in 75% ethanol and stored in fresh 75% ethanol at −20°C for 1–2 weeks. For array analysis, ethanol was removed, the RNA pellet was dried briefly, dissolved in 30 μL RNase-free water, and sent on dry ice to MOgene, LC (St. Louis, MO) where 2 μg of each sample was used for labeling, array hybridization, and scanning (14). The RNA content of control samples of bacteria incubated in fresh medium alone was adjusted to that in samples of infected cells by adding an equal number of the appropriate sterile host cells (2×10^6 HL-60 or 3×10^6 ISE6) to the control samples immediately after the bacteria had been dissolved in Tri Reagent.

Tiling Microarray Design

The Agilent microarray design tool, eArray, was used to design a custom, whole genome tiling array for HGE1 based on its genomic sequence (contig 1 GI: 546157146, contig 2 GI: 482614209; accessible at NCBI, numbers APHH01000001.1 and APHH01000002.1, respectively) and was manufactured by Agilent in an 8-plex format (eight arrays per slide). Each array contained 60,000 60-mer oligonucleotides, each overlapping its genomic neighbor by 10 bases to represent all genomic sequences on both DNA strands, allowing detection and relative quantification of any transcribed RNA, whether from annotated genes, intergenic regions, or sequences on the opposite (non-coding) DNA strand (antisense transcripts).

Microarray Analysis

In our first approach to preparing labeled samples (i.e., targets) from Ap culture RNA, Agilent's FairPlay III kit was used according to manufacturer's instructions. This kit employs a mutant of the MMLV reverse transcriptase and random primers to generate cDNA labeled with Cy3. To prevent second strand cDNA synthesis, actinomycin D (6 μg/mL) was incorporated into the reverse transcription step (15). In our second approach, which was used to generate all data presented here, total RNA isolated from Ap-infected host cells was directly labeled chemically using the Kreatech (Leica Biosystems) ULS Labeling Kit and protocol. A platinum complex linked to Cy3 forms a coordinate bond with guanine at the N7 position of RNA, and no enzyme is involved. With this method, 2 μg of labeled RNA is sufficient for array hybridization, which serves to reduce background noise (14). Labeled RNA was fragmented with 1X Agilent fragmentation buffer at 60°C for 30 min, and the reaction was quenched by the addition of hybridization buffer. Samples were hybridized with the tiling arrays at 65°C for 17 h with continuous mixing at 10 rpm and scanned on an Agilent C high-resolution scanner with 20-bit imaging.

Array Data Analysis

We extracted probe intensity data from tabular text files provided by MOgene, reformatted them, and intermittent spikes with intensities >5 times the sum of immediately adjacent probes were filtered by replacing them with the average of those values, as done previously (7). Data from independent samples were quantile normalized (16) except where otherwise noted. Transcription values for entire genes (1,189 locus tags) were calculated as the sum of hybridization values of all probes corresponding to each gene. The 1,189 locus tags measured included 13 truncated *p44* pseudogenes consisting of only conserved sequence, referred to as *p44* fragments, and 93 others that contained conserved and hypervariable sequence (HVR). Since actually transcribed pseudogenes should show elevated HVR signals, all 93 pseudogenes were visually assessed in Artemis plots under each of the 12 conditions tested, with signal levels from only the HVRs rated on a scale from 0 (not transcribed) to 4 (strongly transcribed), as listed in **Table S9** and illustrated in **Figure 2**. Gene transcription values from samples with three or more replicates were compared using the paired two-tailed Student's t-test to those in relevant samples (e.g., Ap replicating in HL60 vs. in ISE6). Values that were statistically

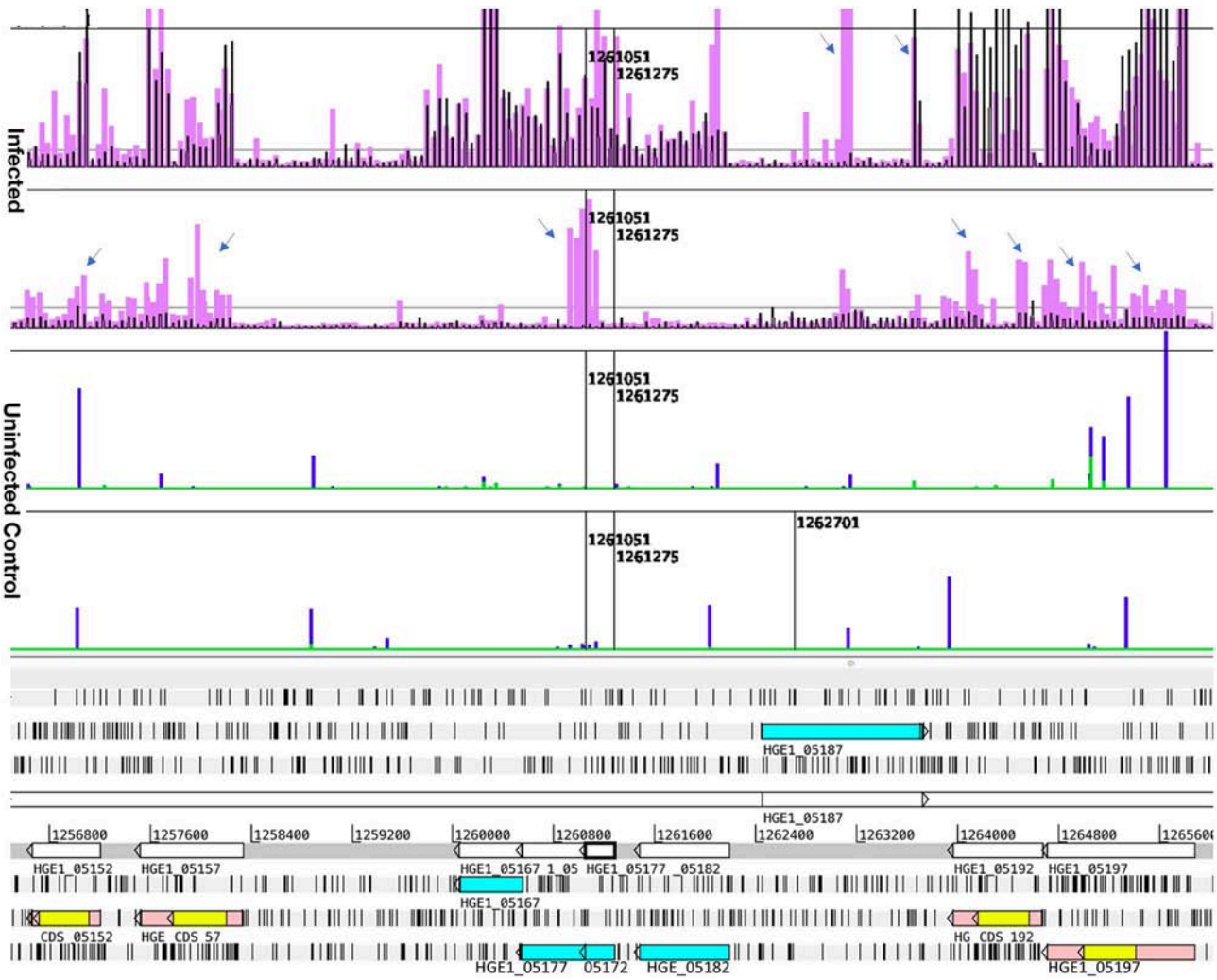

FIGURE 2 | Transcript levels in Sample 1 and sample 3, illustrating differential *p44* transcription in HL-60 and ISE6, and antisense transcripts. Transcription data (top four graphs) plotted over the annotated genome sequence (sections at the bottom; turquoise boxes denote coding regions of annotated genes, pink boxes denote *p44* conserved sequences with yellow boxes denoting their center hypervariable region) of *A. phagocytophilum* (Ap) strain HGE1 using the Artemis genome browser. Black bars represent *A. phagocytophilum* (Ap) transcription in sample 1 (2 h with HL-60 cells), and lavender bars transcription signal in sample 3 (2 h with ISE6 cells) (Infected). Each bar corresponds to one 60-mer probe on the tiling array. The bottom (Uninfected) graphs depict lack of signal from uninfected controls (HL-60 green, ISE6 blue). Prominent antisense signals in sample 3 are indicated (arrows), especially at the junction of HGE1_05172 (putative ATP synthase FO, B subunit) and HGE1_05177 (ATP synthase subunit C), but also from the *p44* paralogs (pink bars with yellow centers) and HGE1_05187. HGE1_05192 (*p44*-18) has strong signal corresponding to its hypervariable region (yellow) indicating that it is specifically transcribed in sample 1. Nucleotide positions in the genome are indicated by numbers above the gray line.

significant ($p \leq 0.05$) and ≥1.5- or 2-fold elevated or reduced relative to comparison samples were identified as differentially transcribed and ranked in order of transcript abundance. Differential transcription values from single sample comparisons (2-h incubations) were not assessed for statistical significance and genes were ranked only if differing by ≥2-fold. For easy visualization of transcripts from genes and intergenic and antisense sequences, transcription profiles of selected genome regions were displayed graphically by plotting hybridization values from 60-mer probes above the annotated genome of HGE1 in the genome browser Artemis (17) (**Figures S1**–**S9**).

Raw microarray data have been deposited in the Dryad database, available at https://doi.org/10.5061/dryad.18931zcs5.

RESULTS

Sample Labeling

Addition of actinomycin D during reverse transcription did not prevent synthesis of spurious second strand cDNA when using the FairPlay III kit to generate labeled samples. This was evident when comparing transcription signals from the same sample prepared with either indirectly labeled cDNA or directly labeled RNA (**Figure S1**). Direct labeling produced stronger sense signals without the prominent false antisense signals seen with the reverse transcriptase-based method. Genuine antisense signals can be seen in Artemis plots of the subsequent transcription data from Kreatech-labeled samples.

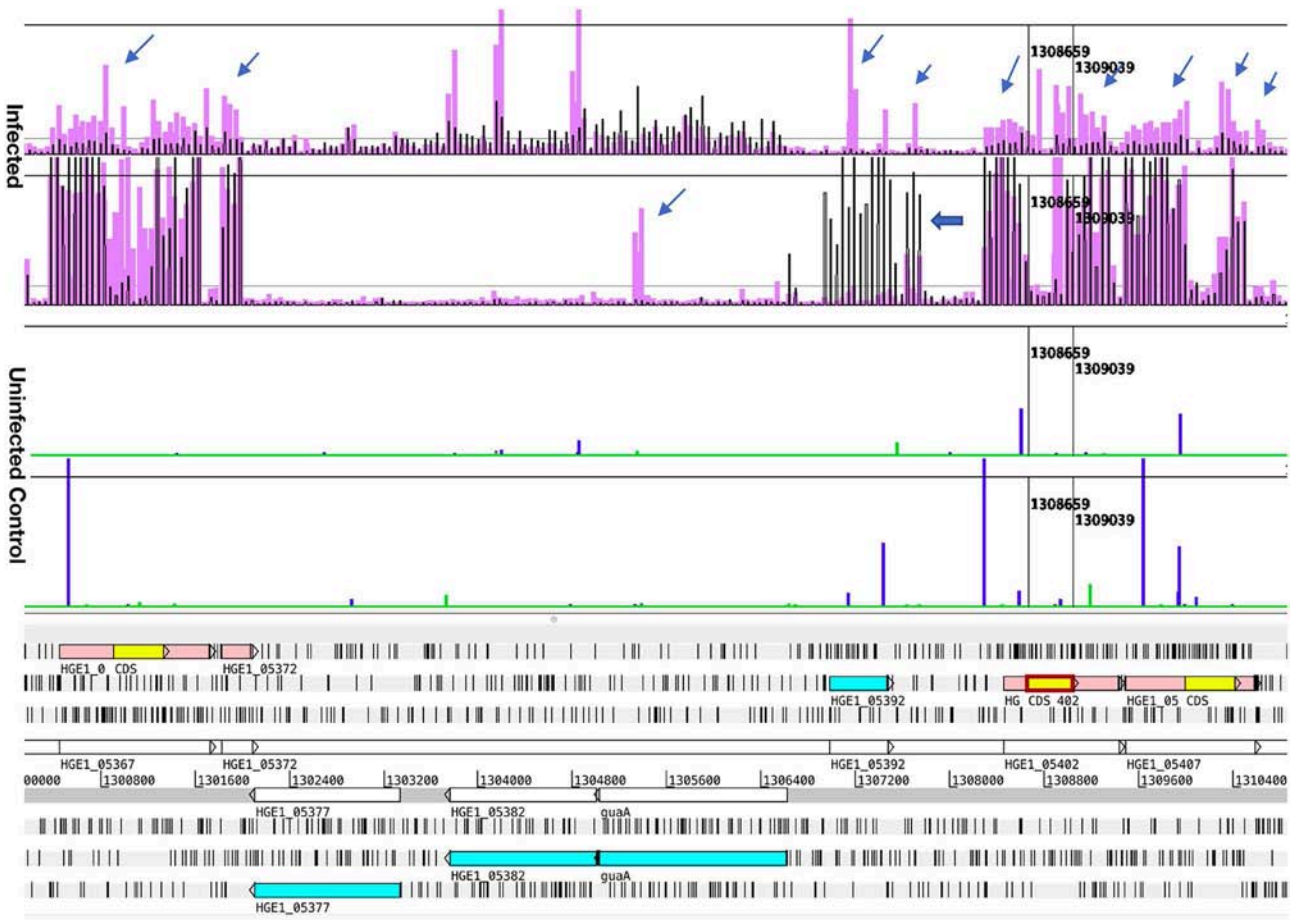

FIGURE 3 | Comparison of transcript signal from Samples 1 and 3, illustrating antisense transcripts and transcription from an unannotated gene. Transcription data (top four graphs) plotted over the annotated genome sequence (sections at the bottom; turquoise boxes denote coding regions of annotated genes, pink boxes denote *p44* conserved sequences with yellow boxes denoting their center hypervariable region) of *A. phagocytophilum* (Ap) strain HGE1 using the Artemis genome browser. The top two graphs (Infected) represent Ap transcription in Sample 1 (black bars, 2 h with HL-60 cells) vs. in Sample 3 (lavender bars, 2 h with ISE6 cells). Each vertical bar corresponds to one 60-mer probe on the tiling array. The two graphs below (Uninfected control) are plots of data from uninfected cells (HL-60, green; ISE6, blue), to demonstrate that host cell transcripts are not responsible for antisense signals. Occasional probes produce signals but overall the sterile cell graphs are flat. Prominent antisense signals generated by Ap from ISE6 are indicated by slender arrows, including those associated with the *p44* conserved regions (pink boxes). Also shown is a *p44* paralog (HGE_05367; at base position 1,300,800 in the genome) specifically transcribed in Sample 3, as indicated by signal corresponding to the center hypervariable region (yellow box). Note a hypothetical gene, HGE1_05392, with elevated transcript levels in Sample 1 (and with antisense signals in Sample 3). Immediately downstream, a transcription peak indicates the presence of a small, unannotated gene (bold arrow). Transcription levels from the HVRs of *p44*s HGE_05367, HGE1_05402, and 05407 were rated 1, 0, and 2 in HL-60, and 4, 0, and 1 in ISE6, respectively. Nucleotide positions in the genome are indicated by numbers above the gray line.

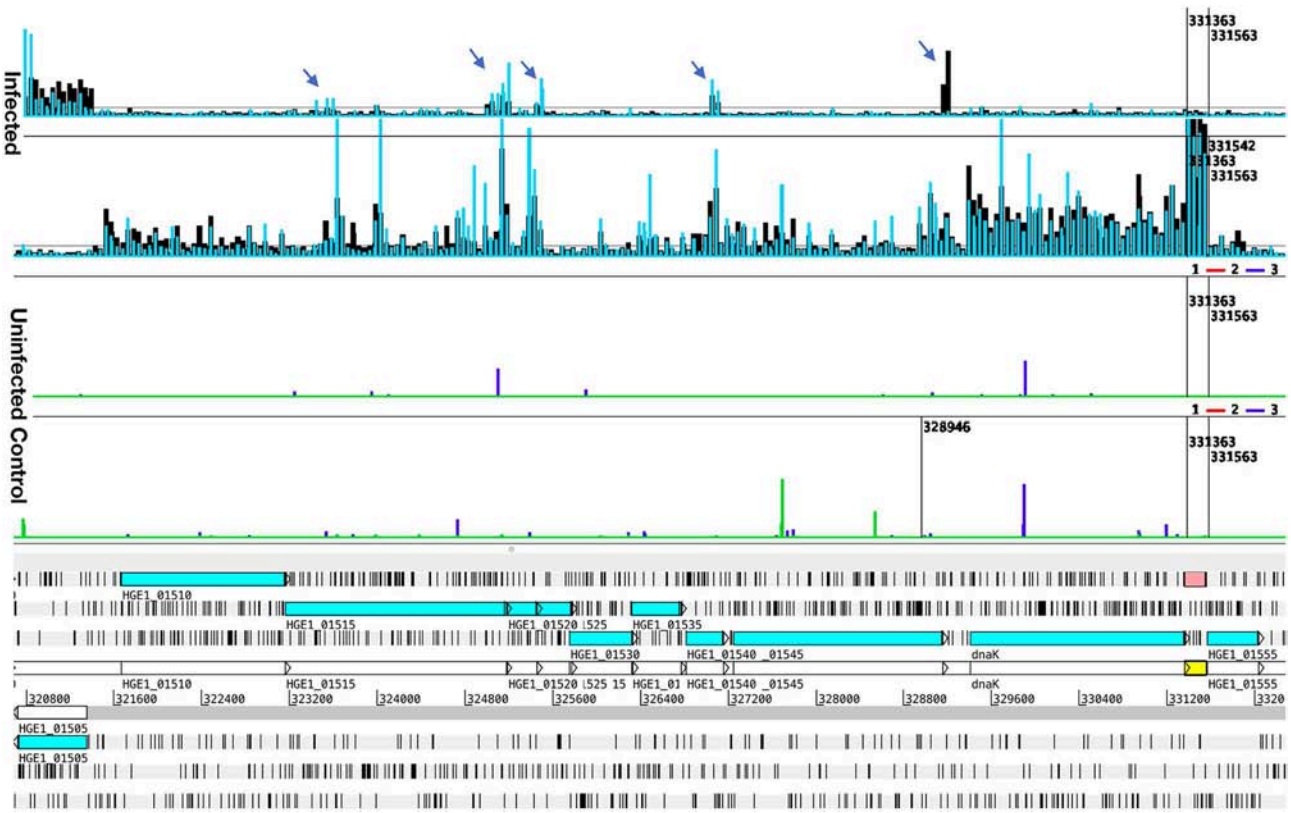

FIGURE 4 | Transcript levels in Samples 6 and 8, illustrating antisense signals and transcription from an unannotated gene. Transcription data (top four graphs) plotted over the annotated genome sequence (sections at the bottom; turquoise boxes denote coding regions of annotated genes) of *A. phagocytophilum* (Ap) strain HGE1 using the Artemis genome browser. Blue and black bars (top two graphs) represent Ap transcription in sample 6 (Ap replicating in HL-60 cells for 24 h, blue bars), and in and sample 8 (Ap replicating in human granulocytes, PMN, for 24 h, black bars). Each bar corresponds to one 60-mer probe on the tiling array. The bottom (Uninfected) graphs depict lack of signal from uninfected controls (HL-60 green, PMN blue). Antisense signals from infected HL-60 cells and granulocytes are indicated (arrows). A strong transcription signal (pink box) is visible from an unannotated gene immediately downstream of dnaK. Nucleotide positions in the genome are indicated by numbers above the gray line.

They were especially common in bacteria infecting ISE6 cells (**Figure 3**), but can also be seen in infected HL-60 cells and human granulocytes (**Figure 4**), and were often associated with reduced sense transcription. The conserved sequences of *p44* pseudogenes consistently showed antisense signals. Anti-sense transcripts were not derived from host cell mRNA (**Figures 1–3**, Uninfected Control).

Transcription Associated With Host Cell Binding/Entry

Table 2 lists the most differentially regulated genes in the various culture conditions examined.

Transcript profiles from sample 1 (Ap from HL-60 cells exposed to uninfected HL-60 cells for 2 h) showed that three genes were ≥2-fold elevated with HL-60 cells compared to six in the fresh medium control (**Table S3A**). Comparison of gene transcription values from sample 2 (4 h with HL-60) to those of the control samples showed that none were differentially transcribed (≥2-fold elevated, $p \leq 0.05$). Thus, HL-60-produced bacteria that bound to/entered fresh HL-60 cells showed little transcription induced by cell contact, suggesting that before 2 h, and probably upon release from parent cells, the genes necessary for HL-60 cell binding and entry were already expressed. To determine if there was a change in transcription over time, samples 1 and 2 were compared to each other, identifying seven genes with elevated transcript levels at 2 h (three that encode tRNAs) vs. 45 at 4 h (**Table S3B**). Because the comparison of sample 2 (4 h with HL-60 cells) to controls showed no differences, upregulation of genes at 4 h compared to 2 h occurred through passage of time rather than as a result of bacterial interactions with HL-60 cells.

Bacteria bound to and entering ISE6 host cells after 2 h incubation (sample 3) showed increased mRNA levels for 48 genes relative to the medium only control in which 24 genes were upregulated (**Table S4A**). After 4 h with ISE6 (sample 4), eight genes had elevated levels (2.0- to 8.7-fold) vs. 37 in controls (**Table S4B**). The 48 genes with elevated transcription in sample 3 (2 h incubation with ISE6) included 18 hypothetical

TABLE 2 | Most differentially regulated genes in the cell culture systems used in this study.

Sample	Locus tag	Function	Ratio (*P*-value)
Sample 6 (24 h in HL-60) vs. Sample 7 (48 h in ISE6)	HGE1_00140	Hypothetical, localizes to morulae membrane (18)	5.89 (0.045)
	HGE1_05192	*p44-18*	3.83 (0.008)
	HGE1_04712	Phage repressor protein C	3.92 (0.026)
Sample 5 (HL-60 grown Ap exposed to ISE6) vs. Sample 1 (2 h with HL-60)	HGE1_05312	Transcriptional regulator tr1 (at p44 expression locus) (19, 23, 24)	9.94 (not done)
	HGE1_02797	Hypothetical	6.06 (not done)
	HGE1_02157	Single-stranded DNA-binding protein	5.97 (not done)
Sample 6 (24 h in HL-60 vs. 24 h in PMN (sample 8)	HGE1_01702	tRNA-Arg	7.561 (0.018)
	HGE1_06226	tRNA-Lys	7.45 (0.050)
	HGE1_06206	tRNA-Met	5.36 (0.000)

HL-60, human promyelocyte cells; ISE6, Ixodes scapularis tick cells; PMN, human granulocytes.

genes of which ten were predicted by CELLO or secP to be localized to the bacterial membranes or to be secreted. Additional genes with elevated transcript levels were: the *tr1* transcription regulator (HGE1_05312, 3.4-fold) that was also upregulated in sample 7 (Ap replicating in ISE6) and sample 8 (Ap replicating in granulocytes) relative to sample 6 (Ap replicating in HL-60); HGE1_03902 [2.8-fold; encoding the invasin AipA; (25)]; three *vir* genes (two *virB2* and *virB6*); and an *HGE-14* paralog (HGE1_01777) that was not among those paralogs upregulated during replication in any of the cell types. The 24 genes with elevated mRNA signals in the 2 h control for sample 3 included 10 hypothetical genes. Eight genes upregulated in sample 4 (4 h in the presence of ISE6 cells) included two that encode guanylate kinases (8.7- and 4.5-fold elevated), which have roles in nucleotide transport and metabolism, three hypothetical genes (one predicted by secP to encode a secreted protein), and two with roles in translation, ribosomal structure and biogenesis (**Table S4B**). The 37 upregulated genes in the controls for sample 4 included 12 *p44* pseudogenes and omp-1A, six hypothetical genes, six that encode tRNAs, and two *virB2* genes. Thus, bacteria incubated for 2 h with ISE6 cells (sample 3) responded to them specifically, as 67% of differentially transcribed genes were upregulated in comparison to the control. At 4 h (sample 4), 82% of genes were upregulated in the control, indicating that most of the host cell-specific response occurred by 2 h.

Comparison of the two ISE6 samples 3 and 4 (2 vs. 4 h; **Table S4C**) identified 232 differentially transcribed genes; 167 were upregulated in sample 3 (2 h), including 50 *p44* pseudogenes (vs. none in sample 4); 22 tRNA genes (vs. five in sample 4); 14 genes with roles in translation, ribosomal structure and biogenesis (vs. three in sample 4); ten genes involved in post-translational modification, protein turnover, chaperones (vs. three in sample 4); seven genes involved in intracellular trafficking, secretion, and vesicular transport (vs. one in sample 4), and six genes with roles in replication, recombination and repair (vs. one in sample 4) (**Table S4C**). In sample 3, *p44* pseudogenes along with recombination- and secretion-related genes were upregulated compared to sample 4, in which the gene encoding major surface protein 4 (*msp4*) was upregulated and hypothetical genes predominated. Of these, 57% were predicted by secP, sigP, or CELLO to be secreted or localized to the bacterial membranes or periplasm, including HGE1_05392 (12.5-fold upregulated; **Figure 1**), the product of which is associated with dense core organisms (10), and HGE1_03697 that encodes Ats-1, which is translocated to mitochondria for inhibition of apoptosis, and induction of autophagosome formation (26). Transcription of *p44* was upregulated in sample 3 (**Figure 2**) and declined in sample 4, but levels remained elevated in the 4 h controls (no host cells), indicating that in addition to causing the upregulation of the genes noted above, bacterial contact with uninfected ISE6 cells was responsible for the drop in *p44* mRNA levels.

Sample 5 (bacteria from HL-60 cells incubated with ISE6 cells for 2 h) was included to determine how bacteria produced in human cells would adjust their transcription pattern to express genes required for tick cell binding and entry. Compared to sample 1 (Ap from HL-60 incubated with fresh HL-60 cells for 2 h), 127 genes were differentially transcribed: 54 in sample 5 (20 hypothetical genes) and 72 in sample 1 (13 hypothetical) (**Table S5A**). Seventeen of the 21 hypothetical genes with elevated transcripts in sample 5 were also upregulated in sample 3 when compared to sample 1 (below), and eight of these were predicted to encode proteins localized to the bacterial membranes, periplasm, or to be secreted. In addition, the transcription regulator *tr1* (HGE1_05312), shown to be upregulated 9.1-fold in sample 3 (2 h with ISE6) relative to sample 1 (2 h with HL-60; **Table S6A**), was the most upregulated gene in sample 5 (9.9-fold). Also upregulated in sample 5, and in sample 3 relative to sample 1, was HGE1_00935, which encodes an effector protein that interacts with the trans-Golgi network (27). Through contact with ISE6 cells, the HL-60-grown bacteria (sample 5) shifted their transcription, and early ISE6-specific effectors and membrane proteins were upregulated. When confronted with the homologous host (sample 1), 31 of the 72 genes with elevated transcript levels had roles in translation, ribosomal structure and biogenesis, indicating that transcription had already shifted to pathways that support bacterial growth and replication (**Table S5B**).

These comparisons showed that the 2 h samples identified host cell-specific transcription, whereas the 4 h samples included time-dependent changes in transcription in addition to those seen at 2 h. Therefore, in subsequent comparisons to identify genes specific to human- and tick-cell binding and entry, and to distinguish replication-specific genes, the 2 h data were used.

Transcriptional Differences Between Bacteria Binding/Entering HL-60 and ISE6 Cells

To distinguish the earliest human- and tick-cell-specific gene activity, sample 1 (2 h with HL-60) and sample 3 (2 h with ISE6) samples were compared, revealing 205 differentially transcribed (≥2-fold elevated transcripts) genes (**Table S6A**): 126 in Ap incubated with HL-60, of which 36 were hypothetical genes, and 79 in Ap incubated with ISE6, including 39 hypothetical genes (**Figure S4**). Of the 36 hypothetical genes with elevated transcript levels in sample 1, 25 encode proteins predicted by secP or CELLO to be secreted or localized to the bacterial membranes or periplasm. Among hypothetical genes, HGE1_03552 was strongly upregulated in sample 3, but not in sample 1, and HGE1_03512, was upregulated at 2 h in sample 1, but not in sample 3. Antisense signals were evident especially in sample 3 from several of the genes, as well as an unannotated peak just upstream of HGE1_03517 (**Figure S4**). Also upregulated in sample 1 were 25 genes with roles in translation, ribosomal structure, and biogenesis (vs. only three in sample 3); six *HGE-14* paralogs (HGE1_01782, 01772, 01752, 02095, 02107, and 02100, vs. one, HGE1_02092, in sample 3), including three known type IV secretion system (T4SS) substrates translocated to host cell nuclei (21); and five genes each involved in signal transduction mechanisms and energy production and conversion (vs. none in either category in sample 3; **Table S6A**). Additional notable HGE1 genes with elevated transcripts in sample 1 included: HGE1_05392 (**Figure 1**) known to be expressed by dense-cored, infectious bacteria [(10), which was 17-fold upregulated; this gene was also upregulated in sample 4]. By contrast, Ap entering ISE6 tick cells did not express HGE1_05392, and in fact, produced strong anti-sense signal possibly indicative of a regulatory mechanism. This result indicates that this gene product does not participate in invasion of ISE6 cells. Similarly, prominent antisense signals in sample 3 are evident at the junction of HGE1_05172 (putative ATP synthase FO, B subunit) and 05177 (ATP synthase subunit C; **Figure 2**), suggesting this ATP synthase is not required for invasion of ISE6 cells. HGE1_00140, which was 7-fold elevated, had previously been shown to localize to the cytosolic side of the morula membrane (18); *dnaK*, 5-fold elevated, involved in cell infection (28); HGE1_02357 encoding ApxR, 4.8-fold elevated, associated with upregulation of *p44* expression in HL-60 cells (23, 24) but which was not elevated in sample 6 (24 h in HL-60; **Table S1A**); HGE1_03232, 3.9-fold elevated, encoding the effector AnkA (29), and *omp1A* (HGE1_01505), 3.5-fold elevated, an outer-membrane-expressed protein that interacts with mammalian host cells (30). Genes that were upregulated 2- to 3-fold in sample 1 included: HGE1_03697, encoding Ats-1, which is imported to mitochondria, inhibits apoptosis and induces autophagosome formation (26); HGE1_01090, encoding Asp14, which is surface-expressed and critical for infection (31); and HGE1_03902, encoding AipA, an invasin necessary for infection of mammalian cells (25). HGE1 genes upregulated in sample 3 (2 h with ISE6 cells) included the *p44*ES transcription regulator, *tr1* [HGE1_05312; (19)], which was the second-most elevated (9.1-fold, **Figure S5**), and likely drives expression of *p44* paralogs specifically expressed in ISE6 cells, i.e., HGE1_05312 (**Figure S5**), and several others at later times; HGE1_00935 (upregulated 9.9-fold in sample 5) encoding an effector that interacts with the trans-Golgi network (27); and 39 hypothetical genes, 19 of which were predicted to be secreted or localized to the bacterial membranes or periplasm.

Transcriptional Differences Between Bacteria Binding/Entering and Replicating in HL-60 and ISE6 Cells

For each cell line, the Ap replication/growth samples were compared to the earliest binding/entry sample to further differentiate genes involved in those two infection stages in human and tick host cells. Comparison of sample 6 (24 h in HL-60) to sample 1 (2 h with HL-60) revealed 80 differentially transcribed (≥2-fold elevated) genes, 34 at 24 h and 46 at 2 h. Genes in the 24 h list included 15 that encode hypothetical proteins, six that encode proteins predicted by secP or CELLO to be secreted or localized to the bacterial membranes or periplasm, eight *p44* pseudogenes, and the transcription regulator *tr1* (2.3-fold) (**Table S7**).

In sample 1 (2 h with HL-60), half of the upregulated genes (23) encoded hypothetical proteins (**Table S3A**), 18 of which were also upregulated in sample 1 compared to sample 3 (**Table S6A**); 15 of these encode proteins predicted to be secreted or localized to the bacterial membrane or periplasm. Also upregulated in sample 1 were five *HGE-14* paralogs (**Table S3A**) that were still upregulated in sample 6 compared to sample 7 (48 h in ISE6; **Table S1A**), and in sample 1 when compared to sample 3 (**Table S6A**). In addition, several genes whose products are membrane-expressed or secreted early by infectious bacteria, especially those incubated with HL-60 cells, were upregulated in sample 1 (**Table S7**).

Comparison of sample 7 (48 h in ISE6) to sample 3 (2 h in ISE6) identified 65 differentially transcribed (≥2-fold elevated) genes, 43 with elevated transcript levels at 48 h and 22 at 2 h (**Table S8A**). Of those upregulated at 48 h, 20 encode hypothetical proteins, 12 of which were predicted to localize to the bacterial membranes or periplasm or to be secreted. Also upregulated in sample 7 was HGE1_05392, which was previously found to be expressed by infectious bacteria (10). In the present study, it was upregulated 4.4-fold in sample 7 relative to sample 3, but even more so (upregulated 12.5-fold) in sample 4 compared to sample 3 (**Table S4C**). HGE1_01872, predicted by both secP and sigP to encode a secreted protein, was upregulated in sample 4 (4 h) compared to sample 3 (2 h; **Figure S9**). Interestingly, *msp4* was 3.6-fold elevated in sample 7, and similarly elevated in sample 4 compared to sample 3 (**Table S4C**) suggesting a role following invasion. In addition, eight genes involved in translation, ribosomal structure and biogenesis were elevated at 48 h in sample 7 (vs. one in sample 3), which is consistent with the activities of growing/replicating organisms.

In sample 3 (2 h), 11 of 22 upregulated genes encoded hypothetical proteins, five of which were also upregulated when compared to sample 1 (2 h with HL-60; **Table S6A**). These included HGE1_05647 and HGE1_02122 that were among the 17 upregulated in HL-60-grown bacteria after 2 h incubation with ISE6 cells (sample 5; **Table S5A**). Another of these early ISE6 hypothetical genes, HGE1_03797, whose product was predicted by secP to be secreted, was the most upregulated gene (27-fold) at 48 h, and was also upregulated at 4 h compared to 2 h (**Table S4C**), indicating that its role extends beyond the early stages of ISE6 cell infection. Two others on the early ISE6 genes list, HGE1_03547 and HGE1_03167, and one not on the list but upregulated at 2 h with ISE6 vs. 2 h with HL-60, HGE1_03492, were also upregulated at 48 h, indicating that they, too, encode proteins with functions early and at 48 h in ISE6. HGE1_04797, the most upregulated gene at 2 h (relative to 48 h), was upregulated 3.2-fold after 2 h incubation with ISE6 compared to control bacteria (**Table S4A**), suggesting that its role in ISE6 infection is specifically early. Also elevated at 2 h were three full-length *p44* pseudogenes (**Figure S9**). In Ap incubated with ISE6 cells, *p44* transcripts were elevated at 2 h, diminished by 4 h, and remained low at 48 h.

Transcriptional Differences Between Bacteria Replicating in HL-60, Granulocytes, and ISE6

Figure 5 demonstrates the appearance of infected cells in Giemsa-stained samples to show that morulae containing large numbers of Ap were produced in HL-60 cells (panel A), ISE6 cells (panel B), and human granulocytes (panel C). Transcript levels of all genes from bacteria replicating in the human cell line (sample 6) and human granulocytes (sample 8) vs. those from bacteria replicating in the tick cell line (sample 7) showed host-cell specific profiles when using Ap incubated in culture medium in the absence of the respective host cells as controls. Of 164 differentially transcribed genes ($\geq$1.5-fold elevated, $p \leq 0.05$), 122 had elevated mRNA levels in HL-60 cells and 42 in ISE6 cells (**Table S1A**). The HL-60 list was dominated by genes found only in the family Anaplasmataceae (43, 35% of total), hereafter referred to as unique Anaplasmataceae genes. These included 37 *p44* pseudogenes, five *HGE-14* paralogs (HGE1_01782, 01752, 01772, 02100, and 02107 in descending order of transcript signal abundance), and HGE1_05792, an msp2 family gene (**Figures S2**, **S7**). These genes encode bacterial cell surface proteins (P44 and Msp2 family) and putative type 4 secretion system (T4SS) effectors that are translocated into the HL-60 cell nucleus [*HGE-14*; (21)]. Hypothetical protein genes were the next most numerous (32) category in HL-60 cells (**Table S1A**). Hypothetical proteins were assessed using three computational models: the SecretomeP 2.0 Server (secP) (32), which predicts non-signal-peptide-triggered protein secretion; the SignalP-5.0 Server (sigP) (33), which predicts the presence of signal peptides; and CELLO, a subcellular localization predictor (34). Fifteen of the 32 were predicted by secP as secreted or by CELLO as localized to the bacterial cell membranes, periplasm, or as extracellular (none were by sigP) (**Table S1A**). HGE1_00140, the most upregulated gene (hypothetical) in HL-60 (5.9-fold), is localized to the morulae membrane late in HL-60 cell infection (18). Surface protein gene, HGE1_05792, which encodes an MSP2 family outer membrane protein, was upregulated during replication in HL-60 cells (sample 6), but not in ISE6 cells (sample 7; **Figure S2**). Next in abundance were 11 genes annotated by Clusters of Orthologous Groups (COGs) as translation, ribosome structure and biogenesis (vs. two in ISE6), followed by four genes each in COGs categories transcription and energy production and conservation (vs. none in either in ISE6). Another 20 genes with elevated transcript levels in HL-60 have diverse or unknown functions (**Table S1B**). Twenty-five of 42 genes displaying increased transcript levels in ISE6 cells were hypothetical genes, 15 of which were predicted to be secreted or membrane associated. Also upregulated in ISE6 cells were four genes with roles in replication, recombination and repair (vs. one in HL-60), and the transcription regulator *tr1* (HGE1_05312), which is the first of four genes that constitute the *p44* expression site (*p44*ES) (20). *tr1* and a *p44* paralog, HGE_05367, located just downstream were specifically and significantly upregulated in Sample 3 (**Figure 3**), as indicated by signal corresponding to the center

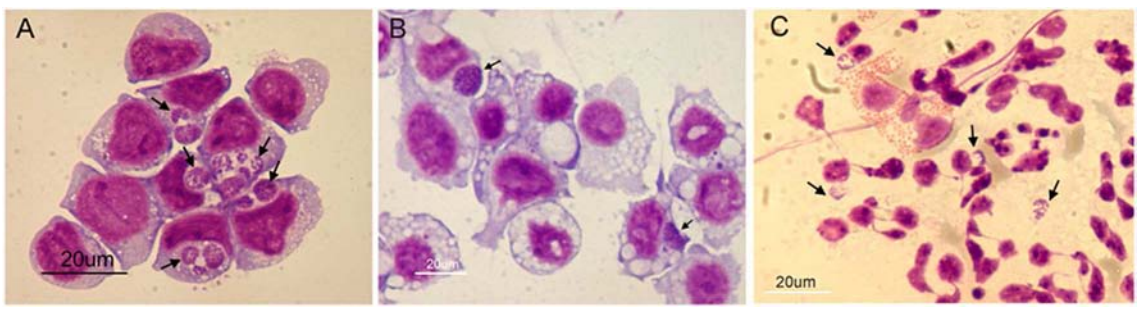

FIGURE 5 | Light microscopy images of Giemsa-stained cells used for transcriptome analysis of *A. phagocytophilum* (Ap) replicating in three cell types. Panel **(A)** HL-60 cells infected 24 h, **(B)** ISE6 cells infected 48 h, and **(C)** human granulocytes infected 24 h. Arrows indicate morulae (Ap colonies within vacuoles). Cytospin slides of each sample were air dried, fixed in methanol and Giemsa-stained. Scale bars = 20 μm.

hypervariable region, but none of the other *p44* pseudogenes were (**Table S1B**).

Comparison of samples taken during replication of Ap in human granulocytes (24 h) (**Figure 5C**, Giemsa-stained) to those of Ap replicating in HL-60 cells (**Figure 5A**) showed similar profiles over large sections of the genome (**Figure 3**), but also identified 225 differentially transcribed genes (≥1.5-fold elevated, $p \leq 0.05$), 105 with elevated mRNA levels in HL-60 cells and 120 in granulocytes (**Table S2A**). Genes elevated in HL-60 cells relative to granulocytes included 28 with roles in translation, ribosomal structure and biogenesis (vs. nine in granulocytes); 10 that encode tRNA (vs. one in granulocytes); six unique Anaplasmataceae genes (five *p44* pseudogenes and HGE1_06087 (**Figure S3**); six with roles in nucleotide transport and metabolism (vs. three in granulocytes); five with roles in lipid transport and metabolism (vs. two in granulocytes); four involved in cell wall/membrane/envelope biogenesis (vs. one in granulocytes); and four genes that participate in transcription (vs. one in granulocytes; **Table S2B**). The disproportionate upregulation of genes in these categories suggests an emphasis on bacterial growth in HL-60. An exception is HGE1_06087, a unique Anaplasmataceae gene encoding a 100-kDa immune-dominant antigen, HGE-2, that has been shown to be surface-expressed on bacteria within morulae and on the morulae membrane (18), is also upregulated in HL-60 cells (**Figure S3**). Over-represented genes in granulocytes included 40 hypothetical genes (vs. 15 in HL-60), 10 unique Anaplasmataceae genes (seven *p44* pseudogenes and three msp2 paralogs), and nine genes each in the following COGs categories: coenzyme transport and metabolism (vs. three in HL-60), post-translational modification, protein turnover, chaperones (vs. three in HL-60), energy production and conversion (vs. three in HL-60), and intracellular trafficking, secretion, and vesicular transport (vs. two in HL-60; **Table S2B**). The transcription regulator *tr1* was upregulated 3.2-fold in granulocytes and several full-length *p44* pseudogenes were upregulated in both cell types. CELLO, secP, and sigP analyses of hypothetical proteins predicted that 17 of those elevated in granulocytes and seven of those elevated with HL-60 cells are either secreted (by secP) or localized to the bacterial cell membranes or periplasm (**Table S2A**).

P44 Hypervariable Region Signals

Antigenic variation in Ap is mediated by recombination within the HVR of P44 transcribed from the specific *p44* copy located in the expression site (35). The 93 *p44* pseudogenes that occur in the genome of Ap isolate HGE1 differ primarily in their hypervariable region (HVR) sequences (bound by LAKT residues, depicted yellow in Artemis plots), which often showed little corresponding signal even when signal from the whole pseudogene (including from conserved sequences flanking the HVR) met the threshold for being designated as differentially transcribed. Actually transcribed *p44* HVRs with their associated anti-sense signals are illustrated in **Figure 2** and listed in **Table S9**.

As with the whole gene measurement method, the HVR only ratings indicated that *p44* transcription levels were highest after 2 h with ISE6 and at 24 h in HL-60 (average HVR signal levels were 1.7 for each). This evaluation of HL-60 and ISE6 specific HVRs revealed a spatial pattern of *p44* pseudogene usage. In HL-60, the HVRs of *p44-37* and *p44-37b*, which are essentially duplicates, displayed strong signals from 2 h after exposure to fresh host cells through 24 h. A *p44* that has been identified as expressed during infection of HL-60 (36, 37), *p44-18*, showed prominent HVR signals at 2 h in the presence or absence HL-60 cells, and at 24 h during replication in HL-60. In ISE6, the HVR of *p44-65* showed a strong signal at 2 h (vs. none at 2 h with HL-60), and the HVRs of HGE1_04365, *p44-62*, *p44-26*, *p44-51*, and *p44-11*, all had strong signals, especially at 4 h and 48 h.

P44 genes nearer the genomic origin of replication (toward the top and bottom of the sequential *p44* list in **Table S9**) tended to display higher HVR signals, and a run of seven (HGE1_04617-04807) further from the origin showed very little transcription signals in all three host cell types. This pattern of *p44* pseudogene usage by Ap is in agreement with findings by Foley et al. (38), although pseudogenes closer to the *p44*ES were no more likely to occupy it than more distant ones (**Table S9**). Ap infecting human granulocytes at 24 h showed an HVR transcription profile most similar to that of infected HL-60 cells at 24 h, whereas HL-60-grown bacteria incubated with ISE6 cells 2 h (Sample 5) had shifted to a *p44* profile resembling that in Sample 3 (ISE6-grown bacteria exposed to ISE6 cells 2 h).

DISCUSSION

The near lack of differential transcription between sample 1 and bacteria incubated for the same period by themselves suggested that cell-free bacteria either did not alter their gene transcription in response to contact with uninfected HL-60 cells, or that 2 h of co-incubation with uninfected host cells was insufficient time to detect a shift in transcription. HL-60-grown Ap bacteria exposed to fresh HL-60 cells for 2 h (sample 1) upregulated only three genes relative to control bacteria in medium alone (**Table S3A**), and after 4 h (sample 2), there were no differences with control bacteria. This failure of host cell contact to induce substantial new bacterial transcription suggested that, upon release from parent host cells, those genes required for invasion of new HL-60 cells were already expressed. The shift to ISE6-specific genes by HL-60-grown bacteria exposed to ISE6 cells in Sample 5 (**Table S5A**) indirectly supported this conclusion. Moreover, it demonstrated an induced bacterial response and suggested that tick cell membranes are sufficiently different to require retooling of the bacterial membrane to facilitate cell attachment and invasion. In HL-60 cells and human granulocytes, P-selectin glycoprotein ligand 1 (PSGL-1) is the receptor mediating infection by Ap (4), which is absent in arthropods where sialylated glycoproteins are rare. Overall, the arthropod glycome is quite different from that of mammals (39),

and arthropod-borne pathogens thus utilize different cell surface moieties to colonize the vector vs. the mammalian host, although basic strategies are conserved (40).

In contrast, Ap bacteria from ISE6 tick cells had a strong transcriptional response to contact with uninfected tick cells (Sample 3, **Table S4A**), displaying 48 genes that were upregulated in comparison to the control (2 h in medium). These included several genes that encoded structural components of the type 4 secretion system (T4SS) of Ap (two *virB2*, one *virB6*), or were predicted to be effectors, i.e., HGE1_01777, an *HGE-14* paralog, and six hypothetical genes (21, 22). The specific ISE6 host components that these putative effectors interact with are unknown, but it is predictable based on the divergent biology and structure of tick vs. human cells that Ap should be using specific effectors for vector and human host cells. Among 17 upregulated genes associated with early infection of ISE6, there were four hypothetical genes (HGE1_02797, 03277, 05647, and 02747) (**Table S5A**). The 17 genes were found to be upregulated both in ISE6-grown bacteria incubated with ISE6 cells (sample 3) and in HL-60-grown bacteria incubated with ISE6 cells (Sample 5), when each was compared to Samples 1 and 2 (HL-60-grown bacteria incubated with HL-60 cells). Two of them (HGE1_05647 and HGE1_02122) had elevated mRNA levels in sample 3 compared to sample 7, suggesting that their role was restricted to invasion, while three others had elevated transcript levels in Sample 7 (**Table S8**) including HGE1_03797 (27-fold elevated). This indicated that their gene products had roles primarily in subsequent intracellular replication. The strongly upregulated HGE1_03797 encodes a hypothetical protein predicted by CELLO to localize to the bacterial cytoplasm and by secP to be secreted, which reflects our lack of understanding how Ap proteins function.

The conserved flanking regions of 50 *p44* pseudogenes displayed elevated transcript levels in sample 3 (2 h with ISE6) compared to sample 4 (4 h; **Table S4C**), but only three did in comparison to the 2 h control (**Table S4A**). This phenomenon reflected upregulation of a subset of *p44* genes in which HVRs showed transcript signals at the same time, and not of all of them. Apparently, *p44* transcript levels were already high in the control, likely upon release from parent ISE6 cells. By 4 h of co-incubation with ISE6 host cells (sample 4), the number of upregulated Ap genes had declined to eight, while in controls (bacteria incubated alone in medium), elevated transcript levels were still seen in 37, including conserved regions of many *p44*s (**Table S4B**), indicating a transition away from cell-specific transcription. The decreased *p44* transcript levels after 4 h incubation with ISE6 vs. their elevation in the 4 h control suggested that cell contact led to the decrease. Research with the related *A. marginale* bovine anaplasmosis agent similarly demonstrated that the diversity of *msp2* sequences in the expression site of bacteria harvested from tick cells was reduced in comparison to bacteria harvested from blood or from mammalian cell lines (41). This was taken to indicate that the type of MSP2 produced changed in response to immune pressure (which is more complex in cattle than in ticks) as well as during invasion of different host cells that present diversities in membrane structure (42, 43).

The apparent transcription of 50 *p44* pseudogenes in ISE6 tick cell-grown Ap after 2 h incubation with fresh ISE6 (**Table S4C**) and of 37 in Ap replicating in the human cell line (**Table S1**) is striking. However, transcription data showed that many of them had elevated signals corresponding to the conserved ends of the pseudogenes only, but not to intervening hypervariable regions (HVRs). This suggested that they were not transcribed from the expression site (*p44*ES), consistent with our previous study (7). Conserved sequence transcripts of all bacteria in the population generated from pseudogenes occupying the *p44*ES likely hybridized not only to probes corresponding to the specifically transcribed pseudogenes but to all probes that were homologous (those representing conserved sequences of other *p44*s), giving an inflated impression of *p44* transcription diversity. The appearance of *p44* fragments in differential gene transcription lists is further evidence of this. In HGE1, 13 of these truncated *p44*s consist of only conserved sequences, and their elevated signals must result from hybridization to homologous transcripts from specifically transcribed pseudogenes. Thus, the apparent transcription of numerous *p44* pseudogenes may be better understood as increased transcription of fewer pseudogenes, which were identified through HVR signal assessment (**Table S9**). However, the existence of duplicate pseudogenes, such as *p44-37* and *-37b*, which both showed strong HVR signals in HL-60, as well as other HVRs with significant sequence identity, means care must be taken in interpreting even HVR signals. Possibly only either *p44-37* or *-37b* was specifically transcribed, with signal from the other the result of cross hybridization, as in the conserved sequences above. Our data presented here are consistent with results demonstrating differential transcription of *p44*s in the tick vector and in different hosts with specific immune defects, as well as *in vitro* (44). Such studies reinforce the idea of molecular adaptation of Ap conferred by P44 to colonize its tick vector and its mammalian hosts, and of P44-mediated immune evasion.

P44 acts as a porin thought to allow diffusion of metabolic intermediates from the host cell into the bacterium (45), with the HVR providing antigenic variation for immunoevasion. A further role in cell binding is suggested by the host cell specific expression of particular pseudogenes that have been identified in infected cell lines previously (36, 37) and here in HL-60 and ISE6. The upregulation of *p44*s during Ap replication in HL-60 cells (sample 6; **Figure S3**) suggested that the porin function was called for, and by ISE6-grown bacteria after 2 h incubation with fresh ISE6 cells (sample 3), that a function in cell binding was important for the largely extracellular bacteria (**Figure 3**, **Figure S5**). Spatial clustering within the genome of specifically transcribed *p44*s (with elevated HVR signals) around the origin of replication is consistent with the findings of Foley et al. (38), and the run of seven barely transcribed *p44*s is an interesting example of genomic location correlating with a lack of use. The overrepresentation of conserved sequence transcripts

is reminiscent of the antisense signals seen corresponding to conserved *p44* sequences in Artemis plots of the data (**Figures 2**, **3**), which, given their particular prominence in ISE6-grown Ap, may serve to keep *p44* expression low.

In general, there was a negative relationship between *tr1* (HGE1_05312) activity and *p44* transcription in Ap derived from ISE6 tick cells when interacting with uninfected tick cells, suggesting that this transcriptional regulator dampened *p44* transcription under these circumstances. In HL-60-grown Ap incubated 2 h with fresh HL-60, *apxR*, a regulator of *tr1* linked to increased *p44* transcription in mammalian cells (23, 24), was upregulated 4.8-fold relative to the 2 h ISE6 sample (**Table S6A**). However, *p44* transcription appears to be greater at 2 h with ISE6 (**Tables S6A, S9**) instead of at 2 h with HL-60, and *tr1* is upregulated 9.1-fold in the ISE6 sample. This counter-intuitive situation—*apxR* elevated but *p44* low (2 h in HL-60) and both *tr1* and *p44* elevated (2 h in ISE6)—hints at a more complex regulatory process behind *p44* transcription.

The overall greater differential transcription seen in Ap incubated with ISE6 when comparing the 2 h time-point to the 4 h time-point (167 genes at 2 h, 65 at 4 h) than was evident in comparisons to controls (48 genes at 2 h, 8 genes at 4 h) (**Tables S4A–S4C**), suggests that much of the change occurred as a function of time rather than in response to cell contact. This was essentially entirely the case with HL-60 in which 45 bacterial genes were upregulated at 4 h in comparison to 2 h (**Table S3B**), but none were in comparison to the 4 h control. Nonetheless, when compared to bacteria replicating in HL-60 (**Table S7**) or binding/entering ISE6 (**Table S6**), numerous genes with elevated transcript levels were identified in the 2 h HL-60 sample, including five *HGE-14* paralogs (HGE1_01782, 01772, 01752, 02107, and 02100) in both comparisons and with transcript levels in the same order by abundance. These paralogs were also upregulated, and in a similar order of transcript abundance (HGE1_01782, 01752, 01772, 02100, and 02107), in HL-60 replication samples relative to ISE6 replication samples, suggesting a role specifically in manipulating the mammalian host. Bacteria binding/entering ISE6 cells for 2 h upregulated their own *HGE-14* paralogs: HGE1_02092 in comparison to bacteria incubated 2 h with HL-60 (**Table S6**); and HGE1_01777 in comparison to the control (**Table S4A**), and in Sample 5 in comparison to 2 h HL-60 (**Table S5**). Thus, five particular *HGE-14* paralogs (of ten that are annotated and an eleventh that is indicated by transcription plots, **Figure S7**) were upregulated at consistent individual levels in bacteria binding/entering and replicating in HL-60, as were two others in bacteria binding/entering ISE6 cells. The suggestion is that these nucleus-targeting effectors are specific to mammalian or tick host cells and in human cells operate collectively but with discrete functions. Since no *HGE-14* paralogs were differentially transcribed in the 24 h HL-60/24 h granulocyte comparison, it can be inferred that the five were transcribed at similar levels in granulocytes. The expression of fewer *HGE-14* paralogs in ISE6 than human cells may reflect the lower complexity of the tick host system that requires less manipulation of a more primitive immune system for Ap to infect and thrive.

Other notable genes with elevated transcript levels in bacteria binding/entering HL-60, both in comparison to those replicating in HL-60 (**Table S7**) and those binding/entering ISE6 cells (**Table S6**), included: HGE1_05392 (product predicted to be secreted), shown to be expressed by infectious organisms (10); HGE1_00140 (product predicted to be secreted), identified on the morulae membrane (18); HGE1_01550, encoding DnaK, which localizes to the bacterial membrane (28); HGE1_03902, encoding AipA, an invasin of mammalian cells (25); and HGE1_01090, encoding a protein expressed on the bacterial surface and required for infection (31). Upregulation of these genes encoding surface-expressed or secreted proteins with roles in cell infection was specifically associated with HL-60 cell binding and entry in this study, consistent with the studies mentioned.

As in the tick cells, a set of bacterial genes that encode hypothetical proteins was specifically upregulated in bacteria binding/entering the human cell line. In comparison to bacteria either replicating in HL-60 or binding/entering ISE6, 18 hypothetical genes were upregulated in bacteria binding/entering HL-60 cells, 15 of which were predicted to be secreted or localized to the bacterial membrane or periplasm (**Table S7**). These bacterial-membrane-associated proteins as well as those encoded by genes upregulated early during ISE6 cell infection, likely facilitate host cell binding, invasion, and immune avoidance in ways unique to Ap, and are thus of particular interest for functional studies.

Bacteria replicating in HL-60 vs. ISE6 displayed more genes involved in translation, ribosome structure and biogenesis (11 vs. 2 in ISE6), transcription (4 vs. 1 in ISE6), energy production and conversion (4 vs. 0 in ISE6), and lipid transport and metabolism (3 vs. 0 in ISE6; **Table S1B**), suggesting that comparatively robust synthetic processes were underway in the human cells. This may be a reflection of the slower growth of Ap in the tick cells, which require about 2 weeks to become maximally infected compared to 4 days in HL-60.

In human granulocytes vs. HL-60 cells, bacterial transcription showed major differences in three gene categories: translation, ribosomal structure, and biogenesis (28 genes upregulated in HL-60 vs. 9 in granulocytes); hypothetical genes (15 in HL-60 vs. 40 in granulocytes); and transfer RNA genes (10 in HL-60 vs. 1 in granulocytes; **Table S2B**). The comparatively high tRNA transcript levels in bacteria infecting HL-60 cells included the six most differentially transcribed genes (4.4- to 7.6-fold elevated, **Table S2A**), and in conjunction with no differences in tRNA levels between HL-60 and ISE6 replication samples (**Table S1A**), indicated that bacterial tRNA levels in granulocytes were especially low. Transfer RNA genes were also relatively upregulated at 2 h with ISE6 compared to 4 h (**Table S4C**), and at 4 h with HL-60 compared to 2 h (**Table S3B**). Aside from their obvious role in protein biosynthesis, prokaryotic tRNAs have diverse functions encompassing regulation of gene expression including suppression, and as substrates for cell wall formation, protein degradation, aminoacylation of phospholipids in cell membranes, and antibiotic biosynthesis [reviewed by Raina and Ibba (46) and Shepherd and Ibba (47)].

In this study, tRNA transcription was low in the primary host cells (human granulocytes), but high in the cell lines, consistent

with the observation that in humans, relatively few granulocytes are infected that support limited Ap growth and replication. Differentiated neutrophil granulocytes secrete branched-chain, aromatic and positively charged free amino acids upon adhesion to extracellular matrix (48), and inhibition of this response may increase availability to intracellular Ap (49). Evidence derived from *in vitro* studies of Ap and also *in vivo* with the related *Anaplasma marginale* indicates that microvascular endothelial cells are a nidus of infection (50–52), and these long-lived cells likely offer an environment supportive of growth and replication that requires import of amino acids. This and the substantial increase in hypothetical genes upregulated in granulocytes illustrates how little we understand of the interaction between Ap and granulocytes and highlights the need for follow-up testing *in vivo* or with primary cells. Other differences in Ap transcription between granulocytes and HL-60 cells included three times as many upregulated genes in granulocytes with roles in coenzyme transport and metabolism, post-translational modification, protein turnover, chaperones, energy production and conversion, and intracellular trafficking, secretion, and vesicular transport. This shows that Ap is very active during its residence in these cells, re-programming cellular defense responses to turn these professional phagocytes that predominantly utilize glycolysis for generation of energy (53) into a supportive host cell (54, 55).

We noted that direct labeling of total RNA from Ap-infected cells produced strong, specific signals that corresponded to the genomic source and relative abundance of all Ap mRNA transcripts on a whole genome tiling array. In addition to providing transcript levels for all predicted bacterial genes during the earliest stage of human and tick cell infection and proliferation in both cell lines and human granulocytes, specific transcription peaks indicated the presence of unannotated genes and antisense transcripts that may play roles in host cell infection. Genes that encode hypothetical proteins that are unique to Ap and particularly enable the pathogen to manipulate tick and mammalian host cells are key to understanding how those processes work and can themselves be manipulated to prevent infection. Current work in our laboratory and others with mutant libraries containing single-insertion mutants, many into genes encoding hypothetical proteins, will be guided by these data, which identify the genes (the mutants) to prioritize in phenotypic screens designed to reveal gene function.

CONCLUSIONS

The gene expression profiles of Ap isolate HGE1 during invasion and replication in cell cultures from its vector and human host reflected its need to adapt to these biologically divergent hosts. Analysis of gene activation in Ap from human promyelocytes (HL-60) exposed to uninfected HL-60 cells showed little change, and the bacteria appeared pre-programmed for invasion of the same mammalian host cell. By contrast, the expression profiles of HL-60 grown or tick cell (ISE6) culture-derived Ap when incubated with uninfected ISE6 cells, demonstrated significant new gene upregulation, suggesting Ap were primed for multiple rounds of infection and invasion of mammalian cells, but not tick cells. These results indicated that Ap recognized the host species cell they are exposed to, and adapted quickly, a conclusion further supported by upregulation of host-cell specific genes encoding effectors and T4SS components that would facilitate control of host cell transcription. Remarkably, Ap gene expression in human granulocytes *ex-vivo* included a large set of hypothetical genes and genes in categories related to production of proteins and metabolites, but was otherwise similar to that seen in HL-60 cells. This is consistent with the fact that HL-60 cells replicate in culture, while granulocytes do not. With our research, many hypothetical genes are now linked to specific events during the life cycle of Ap, which provides important clues to their function. Given the significant involvement of hypothetical gene products in important Ap functions, such as replication in human neutrophils, which is linked to pathogenicity of anaplasmosis, it would be very rewarding to determine their function.

DATA AVAILABILITY STATEMENT

Raw microarray data have been deposited in the Dryad database, available at https://doi.org/10.5061/dryad.18931zcs5.

ETHICS STATEMENT

The studies involving human participants were reviewed and approved by the Internal Review Board of the University of Minnesota. The patients/participants provided their written informed consent to participate in this study.

AUTHOR CONTRIBUTIONS

CN designed the custom tiling array, designed and carried out the study, and wrote the manuscript. MH normalized the microarray data, performed the statistical analyses, and prepared the data for viewing in Artemis. X-RW did the confocal microscopy and assisted with preparing figures. GB provided the editorial assistance with the manuscript. JO helped to interpret the results and submitted the data sets to the Dryad repository for sharing with other researchers. UM was the principal investigator, oversaw the study and assisted with writing the manuscript.

FUNDING

Generous funding for the research was provided by a grant from the National Institutes of Health, NIAID, Nr. R01AI042792. The funder had no role in the design or execution of the research.

ACKNOWLEDGMENTS

We gratefully acknowledge generous support from NIH/NIAID for this research under grant R01AI042792 to UM.

SUPPLEMENTARY MATERIAL

The Supplementary Material for this article can be found online at: https://www.frontiersin.org/articles/10.3389/fvets.2020.00111/full#supplementary-material

Figure S1 | Blue bars (arrows) represent *A. phagocytophilum* transcription signals detected with Cy3-labeled cDNA in sample 6 (24 h in HL-60 cells), using the FairPlay III kit from Agilent. Actinomycin D was added in an attempt to prevent spurious second strand cDNA synthesis. Black bars represent *A. phagocytophilum* transcription signals detected using the same sample 6 material in which RNA was directly Cy3-labeled via the Kreatech kit (Leica Biosystems). Turquoise boxes below the transcript plots denote coding regions of annotated genes. Each bar corresponds to one 60-mer probe on the tiling array representing positive (upper panel) and negative (lower panel) strands of the genome between genes HGE1_04417 and *tolB*. Direct labeling avoids reverse transcriptase-mediated production of cDNA, which may continue to produce second strand cDNA that hybridizes to anti-sense DNA (blue bars, lower plot). The direct labeling method (black bars) produced stronger transcription signals without the false antisense signals seen with the indirect method. Labeled cDNA or RNA from sample 6 was hybridized to arrays contained on the same 8-plex slide and the data were not normalized. Subsequently, only directly labeled RNA from all samples was used. Nucleotide positions in the genome are indicated by numbers above the gray line.

Figure S2 | Transcription data (top two graphs) plotted over the annotated genome sequence (sections at the bottom) using the Artemis genome browser. Turquoise boxes denote coding regions of annotated genes, and pink boxes denote *p44* conserved sequences with yellow boxes denoting their center hypervariable region. Each bar corresponds to one 60-mer probe on the tiling array. Black bars represent Ap transcription in HL-60 cells at 24 h (sample 6), red bars represent Ap transcription in ISE6 cells at 48 h (sample 7). HGE1_05792, which encodes an MSP2 family outer membrane protein, is upregulated during replication in HL-60 cells (sample 6), but not in ISE6 cells (sample 7). Three *p44* paralogs (HGE1_05805, HGE1_05812, HGE1_05817) show characteristic signals associated with their conserved ends (pink) but little specific signal corresponding to their hypervariable regions (yellow). Nucleotide positions in the genome are indicated by numbers above the gray line.

Figure S3 | Transcription data (top two graphs) plotted over the annotated genome sequence (sections at the bottom) using the Artemis genome browser. Turquoise boxes denote coding regions of annotated genes, and pink boxes denote *p44* conserved sequences with yellow boxes denoting their center hypervariable region. Each bar corresponds to one 60-mer probe on the tiling array. Black bars represent Ap transcription in HL-60 cells at 24 h (sample 6), and blue bars represent Ap transcription in human granulocytes at 24 h (sample 8). HGE1_06087, a unique Anaplasmataceae gene encoding HGE-2 that is surface-expressed on bacteria within morulae and on the morulae membrane (18), is upregulated in HL-60 cells. Two *p44* paralogs, HGE1_06097 and 06102, have strong transcription signals associated with their conserved ends (pink boxes) but not their hypervariable regions (yellow boxes), while two others (HGE1_06127 = p44-37, HGE1_06132 = p44-37b) show strong signals that include their hypervariable regions, indicating transcription from the *p44* expression site by a substantial percentage of the bacteria. All *p44* paralogs show greater transcription in HL-60 cells than in human granulocytes. Nucleotide positions in the genome are indicated by numbers above the gray line.

Figure S4 | Transcription data (top two graphs) plotted over the annotated genome sequence (sections at the bottom) using the Artemis genome browser. Turquoise boxes denote coding regions of annotated genes. Each bar corresponds to one 60-mer probe on the tiling array. Black bars represent Ap transcription at 2 h with HL-60 cells (sample 1), red bars represent Ap transcription at 2 h with ISE6 cells (sample 3). Each bar corresponds to one 60-mer probe on the tiling array. HGE1_03552, a hypothetical gene, is strongly upregulated in sample 3, but not in sample 1. Another hypothetical gene, HGE1_03512, is upregulated at 2 h in sample 1, but not in sample 3. Antisense signals, especially from sample 3 (red bars), can be seen opposite sense transcription signals from several of the genes. Also of note is an unannotated peak just upstream of HGE1_03517. Nucleotide positions in the genome are indicated by numbers above the gray line.

Figure S5 | Transcript signals from Samples 1 and 3 in *A. phagocytophilum* (Ap) strain HGE1. Transcription data (top two graphs) plotted over the annotated genome sequence (sections at the bottom) using the Artemis genome browser. Turquoise boxes denote coding regions of annotated genes, and pink boxes denote *p44* conserved sequences with yellow boxes denoting their center hypervariable region. Each bar corresponds to one 60-mer probe on the tiling array. Black bars represent Ap transcription at 2 h with HL-60 cells (sample 1), red bars represent Ap transcription at 2 h with ISE6 cells (sample 3). Transcription regulator 1 (*tr1*) (HGE1_05312) is upregulated only in sample 3, and is positioned at the beginning of the *p44* expression site (p44ES) (19), which includes *omp-1x* (HGE1_05317), *omp-1N* (HGE1_05322), and the particular *p44* paralog being expressed (HGE1_05327) all polycistronically transcribed (20). Notably, recombinase A (HGE1_05332) is co-transcribed in both tick and human cells, suggesting a possible role in *p44* recombination. Nucleotide positions in the genome are indicated by numbers above the gray line.

Figure S6 | Transcription data (top two graphs) plotted over the annotated genome sequence (sections at the bottom) using the Artemis genome browser. Turquoise boxes denote coding regions of annotated genes. Each bar corresponds to one 60-mer probe on the tiling array. Green bars represent Ap transcription in sample 1 (2 h with HL-60), black bars represent Ap transcription in sample 6 (24 h in HL-60). HGE1_01020, a hypothetical gene whose product is predicted by CELLO to localize to the bacterial inner membrane, and groEL, which is translocated into host cell nuclei (21), are upregulated in sample 1, suggesting that Ap may alter host cell responses even before or immediately after host cell invasion. Nucleotide positions in the genome are indicated by numbers above the gray line.

Figure S7 | Transcription data (top two graphs) plotted over the annotated genome sequence (sections at the bottom) using the Artemis genome browser. Turquoise boxes denote coding regions of annotated genes. Each bar corresponds to one 60-mer probe on the tiling array. Green bars represent Ap transcription in sample 1 (2 h with HL-60), black bars represent Ap transcription in sample 6 (24 h in HL-60). Three annotated HGE-14 genes (HGE1_01752, HGE1_01772, and HGE1_01782) and one on the same DNA strand between HGE1_01752 and HGE1_01772 that is not annotated are upregulated at 2 h with HL-60. HGE-14 proteins are putative effectors predicted to enter the host nucleus and alter transcription (21, 22). Nucleotide positions in the genome are indicated by numbers above the gray line.

Figure S8 | Transcription data (top two graphs) plotted over the annotated genome sequence (sections at the bottom) using the Artemis genome browser. Turquoise boxes denote coding regions of annotated genes. Each bar corresponds to one 60-mer probe on the tiling array. Green bars represent Ap transcription in sample 3 (2 h with ISE6), red bars represent Ap transcription in sample 7 (48 h in ISE6 cells). HGE1_01872, a hypothetical gene, is upregulated in replicating bacteria. Nucleotide positions in the genome are indicated by numbers above the gray line.

Figure S9 | Transcription data (top two graphs) plotted over the annotated genome sequence (sections at the bottom) using the Artemis genome browser. Turquoise boxes denote coding regions of annotated genes, and pink boxes denote *p44* conserved sequences with yellow boxes denoting their center hypervariable region. Each bar corresponds to one 60-mer probe on the tiling array. Green bars represent Ap transcription in sample 3 (2 h with ISE6), red bars represent Ap transcription in sample 7 (48 h in ISE6 cells). HGE1_05412 encoding MSP4 is upregulated during bacterial replication, whereas three *p44* paralogs (HGE1_05402, HGE1_05407, and HGE1_05427) are upregulated at 2 h with ISE6 cells.

REFERENCES

1. Lofthouse SA, Apostolopoulos V, Pietersz GA, Li W, McKenzie IF. Induction of T1 (cytotoxic lymphocyte) and/or T2 (antibody) responses to a mucin-1 tumour antigen. *Vaccine*. (1997) 14:1586–93. doi: 10.1016/S0264-410X(97)00077-7
2. Brown WC. Adaptive immunity to *Anaplasma* pathogens and immune dysregulation: implications for bacterial persistence. *Comp Immunol Microbiol Infect Dis*. (2012) 35:241–52. doi: 10.1016/j.cimid.2011.12.002
3. Munderloh UG, Jauron SD, Fingerle V, Leitritz L, Hayes SF, Hautman JM, et al. Invasion and intracellular development of the human granulocytic ehrlichiosis agent in tick cell culture. *J Clin Microbiol*. (1999) 8:2518–24. doi: 10.1128/JCM.37.8.2518-2524.1999
4. Herron MJ, Nelson CM, Larson J, Snapp KR, Kansas GS, Goodman JL. Intracellular parasitism by the human granulocytic ehrlichiosis bacterium through the P-selectin ligand, PSGL-1. *Science*. (2000) 288:1653–6. doi: 10.1126/science.288.5471.1653
5. Truchan HK, Seidman D, Carlyon JA. Breaking in and grabbing a meal: *Anaplasma phagocytophilum* cellular invasion, nutrient acquisition, and promising tools for their study. *Microbes Infect*. (2013) 15:1017–25. doi: 10.1016/j.micinf.2013.10.010
6. Kuhns DB, Priel DAL, Chu J, Zarember KA. Isolation and functional analysis of human neutrophils. *Curr Protoc Immunol*. (2015) 111:7.23.1–16. doi: 10.1002/0471142735.im0723s111
7. Nelson CM, Herron MJ, Felsheim RF, Schloeder BR, Grindle SM, Chavez AO, et al. Whole genome transcription profiling of *Anaplasma phagocytophilum* in human and tick host cells by tiling array analysis. *BMC Genomics*. (2008) 9:364. doi: 10.1186/1471-2164-9-364
8. Barbet AF, Al-Khedery B, Stuen S, Granquist EG, Felsheim RF, Munderloh UG. An emerging tick-borne disease of humans is caused by a subset of strains with conserved genome structure. *Pathogens*. (2013) 2:544–55. doi: 10.3390/pathogens2030544
9. Goodman JL, Nelson CM, Vitale B, Madigan JE, Dumler JS, Kurtti TJ, et al. Direct cultivation of the causative agent from patients with human granulocytic ehrlichiosis. *N Engl J Med*. (1996) 334:209–15. doi: 10.1056/NEJM199601253340401
10. Troese MJ, Kahlon A, Ragland SA, Ottens AK, Ojogun N, Nelson KT, et al. Proteomic analysis of *Anaplasma phagocytophilum* during infection of human myeloid cells identifies a protein that is pronouncedly upregulated on the infectious dense-cored cell. *Infect Immun*. (2011) 79:4696–707. doi: 10.1128/IAI.05658-11
11. Goodman JL, Nelson CM, Klein MB, Hayes SF, Weston BW. Leukocyte infection by the granulocytic ehrlichiosis agent is linked to expression of a selectin ligand. *J Clin Invest*. (1999) 103:407–12. doi: 10.1172/JCI4230
12. Jiang K, Sun X, Chen Y, Shen Y, Jarvis JN. RNA sequencing from human neutrophils reveals distinct transcriptional differences associated with chronic inflammatory states. *BMC Med Genomics*. (2015) 8:55. doi: 10.1186/s12920-015-0128-7
13. Chávez AS, Fairman JW, Felsheim RF, Nelson CM, Herron JM, Higgins L, et al. An O-methyltransferase is required for infection of tick cells by *Anaplasma phagocytophilum*. *PLoS Pathog*. (2015) 11:e1005248. doi: 10.1371/journal.ppat.1005248
14. Gupta V, Cherkassky A, Chatis P, Joseph R, Johnson AL, Broadbent J, et al. Directly labeled mRNA produces highly precise and unbiased differential gene expression data. *Nucleic Acids Res*. (2003) 31:e13. doi: 10.1093/nar/gng013
15. Perocchi F, Xu Z, Clauder-Münster S, Steinmetz LM. Antisense artifacts in transcriptome microarray experiments are resolved by actinomycin D. *Nucleic Acids Res*. (2007) 35:e128. doi: 10.1093/nar/gkm683
16. Royce TE, Rozowsky JS, Luscombe NM, Emanuelsson O, Yu H, Zhu X, et al. Extrapolating traditional DNA microarray statistics to tiling and protein microarray technologies. *Methods Enzymol*. (2006) 411:282–311. doi: 10.1016/S0076-6879(06)11015-0
17. Carver T, Harris SR, Berriman M, Parkhill J, McQuillan JA. Artemis: an integrated platform for visualization and analysis of high-throughput sequence-based experimental data. *Bioinformatics*. (2012) 4:464–9. doi: 10.1093/bioinformatics/btr703
18. Huang B, Troese MJ, Ye S, Sims JT, Galloway NL, Borjesson DL, et al. *Anaplasma phagocytophilum* APH_1387 is expressed throughout bacterial intracellular development and localizes to the pathogen-occupied vacuolar membrane. *Infect Immun*. (2010) 78:1864–73. doi: 10.1128/IAI.01418-09
19. Barbet AF, Agnes JT, Moreland AL, Lundgren AM, Alleman AR, Noh SM, et al. Identification of functional promoters in the msp2 expression loci of *Anaplasma marginale* and *Anaplasma phagocytophilum*. *Gene*. (2005) 353:89–97. doi: 10.1016/j.gene.2005.03.036
20. Barbet AF, Meeus PFM, Bélanger M, Bowie MV, Yi J, Lundgren AM, et al. Expression of multiple outer membrane protein sequence variants from a single genomic locus of *Anaplasma phagocytophilum*. *Infect Immun*. (2003) 71:1706–18. doi: 10.1128/IAI.71.4.1706-1718.2003
21. Sinclair SH, Garcia-Garcia JC, DumLer JS. Bioinformatic and mass spectrometry identification of *Anaplasma phagocytophilum* proteins translocated into host cell nuclei. *Front Microbiol*. (2015) 5:274. doi: 10.3389/fmicb.2015.00055
22. Esna Ashari Z, Brayton KA, Broschat SL. Prediction of T4SS effector proteins for *Anaplasma phagocytophilum* using OPT4e, A new software tool. *Front Microbiol*. (2019) 10:1391. doi: 10.3389/fmicb.2019.01391
23. Wang X, Kikuchi T, Rikihisa Y. Proteomic identification of a novel *Anaplasma phagocytophilum* DNA binding protein that regulates a putative transcription factor. *J Bacteriol*. (2007) 189:4880–6. doi: 10.1128/JB.00318-07
24. Wang X, Cheng Z, Zhang C, Kikuchi T, Rikihisa Y. *Anaplasma phagocytophilum* p44 mRNA expression is differentially regulated in mammalian and tick host cells: involvement of the DNA binding protein ApxR. *J Bacteriol*. (2007) 189:8651–9. doi: 10.1128/JB.00881-07
25. Seidman D, Ojogun N, Walker NJ, Mastronunzio J, Kahlon A, Hebert KS, et al. *Anaplasma phagocytophilum* surface protein AipA mediates invasion of mammalian host cells. *Cell Microbiol*. (2014) 16:1133–45. doi: 10.1111/cmi.12286
26. Niu H, Rikihisa Y. Ats-1: a novel bacterial molecule that links autophagy to bacterial nutrition. *Autophagy*. (2013) 9:787–8. doi: 10.4161/auto.23693
27. Zhu J, He M, Xu W, Li Y, Huang R, Wu S, et al. Development of TEM-1 β-lactamase based protein translocation assay for identification of *Anaplasma phagocytophilum* type IV secretion system effector proteins. *Sci Rep*. (2019) 9:4235. doi: 10.1038/s41598-019-40682-8
28. Contreras M, Alberdi P, Mateos-Hernández L, Fernández de Mera IG, García-Pérez AL, Vancová M, et al. *Anaplasma phagocytophilum* MSP4 and HSP70 proteins are involved in interactions with host cells during pathogen infection. *Front Cell Infect Microbiol*. (2017) 7:307. doi: 10.3389/fcimb.2017.00307
29. Caturegli P, Asanovich KM, Walls JJ, Bakken JS, Madigan JE, Popov VL, et al. ankA: an *Ehrlichia phagocytophila* group gene encoding a cytoplasmic protein antigen with ankyrin repeats. *Infect Immun*. (2000) 68:5277–83. doi: 10.1128/IAI.68.9.5277-5283.2000
30. Ojogun N, Kahlon A, Ragland SA, Troese MJ, Mastronunzio JE, Walker NJ, et al. *Anaplasma phagocytophilum* outer membrane protein A interacts with sialylated glycoproteins to promote infection of mammalian host cells. *Infect Immun*. (2012) 80:3748–60. doi: 10.1128/IAI.00654-12
31. Kahlon A, Ojogun N, Ragland SA, Seidman D, Troese MJ, Ottens AK, et al. *Anaplasma phagocytophilum* Asp14 is an invasin that interacts with mammalian host cells via its C terminus to facilitate infection. *Infect Immun*. (2013) 81:65–79. doi: 10.1128/IAI.00932-12
32. Bendtsen JD, Kiemer L, Fausbøll A, Brunak S. Non-classical protein secretion in bacteria. *BMC Microbiol*. (2005) 5:58. doi: 10.1186/1471-2180-5-58
33. Almagro Armenteros JJ, Tsirigos KD, Sønderby CK, Petersen TN, Winther O, et al. SignalP 5.0 improves signal peptide predictions using deep neural networks. *Nat Biotechnol*. (2019) 37:420–3. doi: 10.1038/s41587-019-0036-z
34. Yu CS, Lin CJ, Hwang JK. Predicting subcellular localization of proteins for Gram-negative bacteria by support vector machines based on n-peptide compositions. *Protein Sci*. (2004) 13:1402–6. doi: 10.1110/ps.03479604
35. Rejmanek D, Foley P, Barbet A, Foley J. Evolution of antigen variation in the tick-borne pathogen *Anaplasma phagocytophilum*. *Mol Biol Evol*. (2012) 29:391–400. doi: 10.1093/molbev/msr229
36. Sarkar M, Troese MJ, Kearns SA, Yang T, Reneer DV, Carlyon JA. *Anaplasma phagocytophilum* MSP2(*P44*)-18 predominates and is modified into multiple isoforms in human myeloid cells. *Infect Immun*. (2008) 76:2090–8. doi: 10.1128/IAI.01594-07
37. Shimada M, Takamoto N, Su H, Sasahara H, Shimamura Y, Ando S, et al. Predominant shift of different *P44*-expressing *Anaplasma phagocytophilum* in

infected HL-60, THP-1, NB4, and RF/6A cell lines. *Jpn J Infect Dis*. (2019) 72:73–80. doi: 10.7883/yoken.JJID.2018.230
38. Foley JE, Nieto NC, Barbet A, Foley P. Antigen diversity in the parasitic bacterium *Anaplasma phagocytophilum* arises from selectively-represented, spatially clustered functional pseudogenes. *PLoS ONE*. (2009) 4:e8265. doi: 10.1371/journal.pone.0008265
39. Zhu F, Dong L, Keping C. Structures and functions of invertebrate glycosylation. *Open Biol*. (2019) 9:180232. doi: 10.1098/rsob.180232
40. Dinglasan RR, Jacobs-Lorena M. Insight into a conserved lifestyle: protein-carbohydrate adhesion strategies of vector-borne pathogens. *Infect Immun*. (2005) 73:7797–807. doi: 10.1128/IAI.73.12.7797-7807.2005
41. Oliva Chávez AS, Felsheim RF, Kurtti TJ, Ku PS, Brayton KA, Munderloh UG. Expression patterns of *Anaplasma marginale* Msp2 variants change in response to growth in cattle, and tick cells versus mammalian cells. *PLoS ONE*. (2012) 7:e36012. doi: 10.1371/journal.pone.0036012
42. Brayton KA, Knowles DP, McGuire TC, Palmer GH. Efficient use of a small genome to generate antigenic diversity in tick-borne ehrlichial pathogens. *Proc Natl Acad Sci USA*. (2001) 98:4130–5. doi: 10.1073/pnas.071056298
43. de la Fuente J, Kocan KM. Expression of *Anaplasma marginale* major surface protein 2 variants in persistently infected ticks. *Infect Immun*. (2001) 69:5151–6. doi: 10.1128/IAI.69.8.5151-5156.2001
44. Ijdo JW, Wu C, Telford SR III, Fikrig E. Differential expression of the p44 gene family in the agent of human granulocytic ehrlichiosis. *Infect Immun*. (2002) 70:5295–8. doi: 10.1128/IAI.70.9.5295-5298.2002
45. Huang H, Wang X, Kikuchi T, Kumagai Y, Rikihisa Y. Porin activity of *Anaplasma phagocytophilum* outer membrane fraction and purified *P44*. *J Bacteriol*. (2007) 189:1998–2006. doi: 10.1128/JB.01548-06
46. Raina M, Ibba M. tRNAs as regulators of biological processes. *Front Genet*. (2014) 5:171. doi: 10.3389/fgene.2014.00171
47. Shepherd J, Ibba M. Bacterial transfer RNAs. *FEMS Microbiol Rev*. (2015) 39:280–300. doi: 10.1093/femsre/fuv004
48. Galkina SI, Fedorova NV, Ksenofontov AL, Stadnichuk VI, Baratova LA, Sud'Ina GF. Neutrophils as a source of branched-chain, aromatic and positively charged free amino acids. *Cell Adh Migr*. (2019) 13:98–105. doi: 10.1080/19336918.2018.1540903
49. Choi KS, Garyu J, Park J, DumLer JS. Diminished adhesion of *Anaplasma phagocytophilum*-infected neutrophils to endothelial cells is associated with reduced expression of leukocyte surface selectin. *Infect Immun*. (2003) 71:4586–94. doi: 10.1128/IAI.71.8.4586-4594.2003
50. Munderloh UG, Lynch MJ, Herron MJ, Palmer AT, Kurtti TJ, Nelson RD, et al. Infection of endothelial cells with *Anaplasma marginale* and *A. phagocytophilum*. *Vet Microbiol*. (2004) 101:53–64. doi: 10.1016/j.vetmic.2004.02.011
51. Wamsley HL, Alleman AR, Johnson CM, Barbet AF, Abbott JR. Investigation of endothelial cells as an *in vivo* nidus of *Anaplasma marginale* infection in cattle. *Vet Microbiol*. (2011) 153:264–73. doi: 10.1016/j.vetmic.2011.05.035
52. Noh SM, Ueti MW, Palmer GH, Munderloh UG, Felsheim RF, Brayton KA. Stability and tick transmission phenotype of gfp-transformed *Anaplasma marginale* through a complete *in vivo* infection cycle. *Appl Environ Microbiol*. (2011) 77:330–4. doi: 10.1128/AEM.02096-10
53. Borregaard N, Herlin T. Energy metabolism of human neutrophils during phagocytosis. *J Clin Invest*. (1982) 70:550–7. doi: 10.1172/JCI110647
54. Carlyon JA, Abdel-Latif D, Pypaert M, Lacy P, Fikrig E. *Anaplasma phagocytophilum* utilizes multiple host evasion mechanisms to thwart NADPH oxidase-mediated killing during neutrophil infection. *Infect Immun*. (2004) 72:4772–83. doi: 10.1128/IAI.72.8.4772-4783.2004
55. Lee HC, Kioi M, Han J, Puri RK, Goodman JL. *Anaplasma phagocytophilum*-induced gene expression in both human neutrophils and HL-60 cells. *Genomics*. (2008) 92:144–51. doi: 10.1016/j.ygeno.2008.05.005

Conflict of Interest: The authors declare that the research was conducted in the absence of any commercial or financial relationships that could be construed as a potential conflict of interest.

frontiers in Physiology

ORIGINAL RESEARCH
published: 19 May 2020
doi: 10.3389/fphys.2020.00502

Porin Expression Profiles in *Haemaphysalis longicornis* Infected With *Babesia microti*

Weiqing Zheng[1,2], Rika Umemiya-Shirafuji[1], Qian Zhang[3], Kiyoshi Okado[1], Paul Franck Adjou Moumouni[1], Hiroshi Suzuki[1], Haiying Chen[2], Mingming Liu[1] and Xuenan Xuan[1]**

[1] National Research Center for Protozoan Diseases, Obihiro University of Agriculture and Veterinary Medicine, Obihiro, Japan, [2] The Collaboration Unit for Field Epidemiology of State Key Laboratory for Infectious Disease Prevention and Control, Jiangxi Provincial Key Laboratory of Animal-origin and Vector-Borne Diseases, Nanchang Center for Disease Control and Prevention, Nanchang, China, [3] The Ophthalmology Department, The Second Affiliated Hospital of Nanchang University, Nanchang, China

OPEN ACCESS

Edited by:
Itabajara Silva Vaz Jr., Federal University of Rio Grande do Sul, Brazil

Reviewed by:
Stephen Lu, National Institute of Allergy and Infectious Diseases (NIH), United States
Jose Octavio Merino, Instituto de Investigacion en Recursos Cinegèticos, Spain

***Correspondence:**
Rika Umemiya-Shirafuji
umemiya@obihiro.ac.jp
Xuenan Xuan
gen@obihiro.ac.jp

Specialty section:
This article was submitted to Invertebrate Physiology, a section of the journal Frontiers in Physiology

Received: *14 February 2020*
Accepted: *23 April 2020*
Published: *19 May 2020*

Citation:
Zheng W, Umemiya-Shirafuji R, Zhang Q, Okado K, Adjou Moumouni PF, Suzuki H, Chen H, Liu M and Xuan X (2020) Porin Expression Profiles in Haemaphysalis longicornis Infected With Babesia microti. Front. Physiol. 11:502. doi: 10.3389/fphys.2020.00502

The *porin* gene is widely disseminated in various organisms and has a pivotal role in the regulation of pathogen infection in blood-sucking arthropods. However, to date, information on the *porin* gene from the *Haemaphysalis longicornis* tick, an important vector of human and animal diseases, remains unknown. In this study, we identified the *porin* gene from *H. longicornis* and evaluated its expression levels in *Babesia microti*-infected and -uninfected *H. longicornis* ticks at developmental stages. We also analyzed *porin* functions in relation to both tick blood feeding and *Babesia* infection and the relationship between *porin* and *porin*-related apoptosis genes such as *B-cell lymphoma* (*Bcl*), *cytochrome complex* (*Cytc*), *caspase 2* (*Cas2*), and *caspase 8* (*Cas8*). The coding nucleotide sequence of *H. longicornis porin* cDNA was found to be 849 bp in length and encoded 282 amino acids. Domain analysis showed the protein to contain six determinants of voltage gating and two polypeptide binding sites. *Porin* mRNA levels were not significantly different between 1-day-laid and 7-day-laid eggs. In the nymphal stage, higher *porin* expression levels were found in unfed, 12-h-partially-fed (12 hPF), 1-day-partially-fed (1 dPF), 2 dPF nymphs and nymphs at 0 day post-engorgement (0 dAE) vs. nymphs at 2 dAE. *Cytc* and *Cas2* mRNA levels were higher in 2 dPF nymphs in contrast to nymphs at 2 dAE. *Porin* expression levels appeared to be higher in the infected vs. uninfected nymphs during blood feeding except at 1 dPF and 0–1 dAE. Especially, the highest *B. microti* burden negatively affected *porin* mRNA levels in both nymphs and female adults. *Porin* knockdown affected body weight and *Babesia* infection levels and significantly downregulated the expression levels of *Cytc* and *Bcl* in *H. longicornis* female ticks. In addition, this study showed that infection levels of the *B. microti* Gray strain in nymphal and female *H. longicornis* peaked at or around engorgement from blood feeding to post engorgement. Taken together, the research conducted in this study suggests that *H. longicornis porin* might interfere with blood feeding and *B. microti* infection.

Keywords: *Haemaphysalis longicornis*, tick, *Babesia microti*, protozoan parasite, *porin*, expression profiles

INTRODUCTION

The Asian longhorned tick, *Haemaphysalis longicornis*, is widely distributed in eastern Asia, Australia, and New Zealand and was recently found in the US (Heath, 2016; Rainey et al., 2018; Raghavan et al., 2019; Wormser et al., 2019; Zheng et al., 2019). *H. longicornis*, known as a harmful ectoparasite for domestic animals, spreads diseases including babesioses to livestock (McFadden et al., 2011). The tick has also been associated with several other tick-borne diseases in humans, including bacterioses and viroses (Chae and Lee, 2010; Fang et al., 2015; Zheng et al., 2018; Zhuang et al., 2018).

Over millions of years, ticks have co-evolved with a variety of microorganisms including *Babesia*. When *Babesia* parasites enter the tick body, ticks activate their immune system to inhibit *Babesia* invasion, and in turn, *Babesia* parasites hijack various tick molecules to facilitate their own transmission (de la Fuente et al., 2017). Several molecules are essential for tick-*Babesia* interaction, such as defensins, microplusin/hebraein, Kunitz domain-containing proteins, lipocalins, and proteases (Antunes et al., 2017). It is speculated that *porin*, also termed a voltage-dependent anion-selective channel (VDAC), plays paramount roles in modulating pathogen infection in vectors, including bacteria and protozoa in ticks, and viruses in mosquitoes (Fongsaran et al., 2014; Alberdi et al., 2015; Rodríguez-Hernández et al., 2015; Jitobaom et al., 2016). To date, *porin* has been described in at least three tick species, including *Ixodes scapularis*, *Rhipicephalus microplus*, and *Amblyomma variegatum* (Ribeiro et al., 2011; Rodríguez-Hernández et al., 2011; Alberdi et al., 2015). *Porin* in *R. microplus* was identified when it was exposed to *Babesia bigemina* infection (Rodríguez-Hernández et al., 2011).

Various *Babesia* parasites including *Babesia microti* have been experimentally transmitted by or detected in the Asian longhorned tick (Ikadai et al., 2007; Sivakumar et al., 2014; Fang et al., 2015; Zhang et al., 2017). *B. microti* is the most malignant human *Babesia* parasite with high morbidity and wide distribution around the globe (Vannier and Krause, 2012; Chen et al., 2019; Krause, 2019), and *Ixodes* ticks have historically been considered as common vectors of *B. microti* (Mather et al., 1990; Krause, 2019). However, *B. microti* DNA can be detected in *H. longicornis* collected from the field (Zhang et al., 2017) and can be acquired by the tick when feeding on mice infected with the *B. microti* Munich strain (Kusakisako et al., 2015). The transmission of *B. microti* from *H. longicornis* to mice has also been achieved (Wu et al., 2017), suggesting that the tick is a potential vector of the protozoan parasite. However, the molecular mechanisms underlying *H. longicornis-B. microti* interactions remain unclear.

On the basis of the above information, we hypothesized that *H. longicornis porin* might have roles in modulating *B. microti* infection in the ticks, and thus we designed experiments to confirm the hypothesis in this study. First, a homolog of *porin* was identified and characterized in *H. longicornis* using an Expressed Sequence Tags (ESTs) database, and then the expression levels of *porin* mRNA in *H. longicornis* eggs and nymphs were analyzed by real-time PCR. Moreover, we established a *H. longicornis-B. microti* Gray strain (a human-pathogenic strain) infection model and determined the dynamics of *B. microti* loads in nymphal and female ticks during the blood feeding stage. *Porin* mRNA transcripts were then compared between *B. microti*-infected and -uninfected ticks. Finally, *porin* functional analyses were carried out by RNA interference (RNAi) to determine its potential roles in blood feeding and *B. microti* infection.

MATERIALS AND METHODS

Ticks, Parasites, and Animals

Parthenogenetic *H. longicornis* ticks (Okayama strain) were kept at the National Research Center for Protozoan Diseases (NRCPD), Obihiro University of Agriculture and Veterinary Medicine, Obihiro, Japan, and maintained by feeding on the ears of Japanese white rabbits (Japan SLC, Shizuoka, Japan) (Umemiya-Shirafuji et al., 2019a). In the present study, two rabbits were used to maintain the nymphal and female ticks. The *B. microti* Gray strain was used to produce *B. microti*-infected ticks. Cryopreserved protozoan parasites were kept in liquid nitrogen in NRCPD and thawed using the methods mentioned in The Global Bioresource Center (ATCC® 30221™). Seven 8-week-old female hamsters (Japan SLC, Shizuoka, Japan) were inoculated with thawed *B. microti* and then used for blood feeding to produce *B. microti*-infected ticks. In parallel, seven uninfected hamsters were used for blood meal and production of uninfected ticks. All animals used in this study were reared in a temperature- and humidity-regulated room under controlled lighting, given water and commercial regular chow, and were cared for in accordance with the guidelines approved by the Animal Care and Use Committee (Animal exp.: 19–74 for rabbits and 19–77 for hamsters) of Obihiro University of Agriculture and Veterinary Medicine.

Identification and Characterization of the cDNA Encoding *Porin*

ESTs were previously constructed by random partial sequencing of the 5′- terminal of the cDNA clones from cDNA libraries established with salivary glands of 4-day-fed *H. longicornis* females, and the similarities in the protein databases were examined using the BLASTp program (Liao et al., 2009). The plasmids containing the *porin* gene-encoding insert were extracted using a Qiagen DNA purification kit (Qiagen, Hilden, Germany) and subsequently subjected to analysis on an ABI PRISM 3100 DNA sequencer (Applied Biosystems, Waltham, MA, United States) using plasmid (pGCAP1 vector)-specific primers and walking primers thereafter.

The full length of the *porin* coding region was searched with the BLASTx program in the National Center for Biotechnology Information (NCBI)[1]. The domain structure was determined using the Conserved Protein Domain Family search program in the NCBI[2]. The deduced amino acid translation of the

[1]https://blast.ncbi.nlm.nih.gov

[2]https://www.ncbi.nlm.nih.gov/Structure/cdd/cddsrv.cgi

porin sequence was performed using an online tool Nucleotide Amino acid Derived Visualization[3]. Alignment of the *porin* amino acid sequences from different tick species was viewed with the Multiple Align Show[4]. The identity and similarity between *H. longicornis* and other tick species were calculated with the Ident and Sim program of the Sequence Manipulation Suite. The similar amino acids were classified into the same group for the similarity calculation: GAVLI, FYW, CM, ST, KRH, DENQ, and P[5]. The theoretical pI (isoelectric point) and Mw (molecular weight) were determined by the Compute pI/Mw[6].

Real-Time PCR Analysis

The expression levels of the *porin* gene were analyzed in ticks at egg, nymph, or adult stage, in ticks incubated at 15°C or 25°C, and in *B. microti*-infected or -uninfected ticks. Three duplicates were made for each group of tick samples. After two washes with double distilled water and one wash with 70% ethanol, 10 mg of eggs, whole body of four nymphs, and three unfed and two partially fed or engorged female ticks with host blood removed were homogenized in TRI reagent (Sigma-Aldrich, St. Louis, MO, United States) using pestles. RNA extraction, cDNA synthesis, and real-time PCR were performed as described elsewhere (Umemiya-Shirafuji et al., 2019b). The same amount of cDNA was used in a real-time PCR reaction system to assess the stability of internal control genes in ticks at different developmental stages under unfed, uninfected, or infected conditions. The candidate internal control genes evaluated in this study included glyceraldehyde-3-phosphate dehydrogenase (*GAPDH*), *L23*, *HlP0*, and *Hlactin*. The most stable one was used for analysis of the relative mRNA level of the *porin* gene. *Porin*-related apoptosis genes such as *B-cell lymphoma* (*Bcl*), *cytochrome complex* (*Cytc*), *caspase 2* (*Cas2*), and *caspase 8* (*Cas8*) were also assessed by real-time PCR. The *H. longicornis Bcl* sequence was identified using the EST database as described above, and for the other genes, previously published sequences were used (GenBank database under accession number DQ666174 for *Cas2*, DQ660369 for *Cas8*, and NC_037493 for *Cytc*). The primers used in our study are listed in **Supplementary Table S1**. The mRNA levels were normalized separately against mRNA levels of the internal control gene using the ΔCT $\{2^{\wedge[-(CT_{\text{target gene}} - CT_{\text{internal control gene}})]}\}$ method.

Analyses of *B. microti* Burdens in Ticks

B. microti burdens were calculated in nymphal and female ticks by standardizing the relative amount of *Babesia* 18S rRNA against tick ITS-2 in infected ticks with the values obtained in uninfected ones. The amounts of *Babesia* 18S rRNA and tick ITS-2 in the samples were evaluated using genomic DNA samples for real-time PCR, and the practice was repeated thrice for each group. Tick samples consisted of nymphs, which were allowed to feed on *B. microti*-infected hamsters with ∼10% parasitemia, and female ticks, which fed on hamsters with ∼5% parasitemia. Genomic DNA was isolated from *B. microti*-infected ticks using a NucleoSpin® Tissue kit (Macherey-Nagel, Duren, Germany) according to the manufacturer's manual. In addition, conventional PCR using KOD-Plus-Neo DNA polymerase (Toyobo, Osaka, Japan) and *B. microti* β-*tubulin*-specific primers and *H. longicornis actin*-specific primers (control gene) was performed on nymphal samples to detect *B. microti* DNA. The PCR products were electrophoresed on a 1.5% agarose gel and stained with ethidium bromide (EB). Conventional PCR was performed in triplicate for each group. The primers used in this study are listed in **Supplementary Table S1**. The genetic amount of *B. microti* 18S rRNA (Bm18S rRNA) was normalized against that of *H. longicornis* ITS-2 (HlITS-2) using the ΔCT $\{2^{\wedge[-(CT_{\text{Bm18S rRNA}} - CT_{\text{HlITS-2}})]}\}$ method.

Suppression Subtractive Hybridization (SSH) cDNA Construction and Analysis

The technique of SSH was used to compare the expression levels of the *porin* gene in *B. microti*-infected and -uninfected engorged female ticks. *Babesia* DNA in ticks was detected by conventional PCR with β-*tubulin* gene primers as described above. Forward and reverse suppression subtraction cDNA libraries were constructed using the Super SMART™ PCR cDNA synthesis kit according to the manufacturer's instructions (Clontech, Mountain View, CA, United States). Briefly, in the forward suppression subtraction cDNA library, cDNA prepared from 15 *Babesia*-infected ticks served as the "Tester," and cDNA prepared from 15 uninfected ticks served as the "Driver" in the subtraction procedure to enrich for cDNAs preferentially expressed and upregulated in the *Babesia*-infected ticks. In the reverse suppression subtraction cDNA library, cDNA from 15 infected ticks (driver) was used in excess to hybridize cDNA from 15 uninfected ticks (tester) to enrich for cDNAs preferentially expressed and upregulated in the uninfected ticks. Two PCR amplifications were performed to enrich differentially expressed transcripts in infected ticks from the forward suppression subtraction cDNA library and in uninfected ticks from the reverse suppression subtraction cDNA library. The amounts of *porin* transcripts in the forward and reverse suppression subtraction cDNA libraries and in unsubtracted cDNA libraries were determined by relative band brightness of its PCR products on an electrophoresed gel stained with EB.

RNAi and the Effect of *Porin* Knockdown on Tick Blood Feeding and *Babesia* Infection

RNAi was used to analyze the effect of *porin* knockdown on blood feeding, *Babesia* infection, and the *porin*-related apoptosis signaling pathway. The *porin* double-strand RNA (dsRNA) was constructed with the primer set including the T7 promoter sequence (underlined with double solid lines) at the 5′-end of both primers (*porin* RNAiF: 5′-GATA TCTAATACGACTCACTATAGGTGCACACCAACGTGAACG

[3]http://nadv.herokuapp.com/

[4]http://www.bioinformatics.org/SMS/multi_align.html

[5]https://www.bioinformatics.org/sms2/ident_sim.html

[6]https://web.expasy.org/compute_pi/

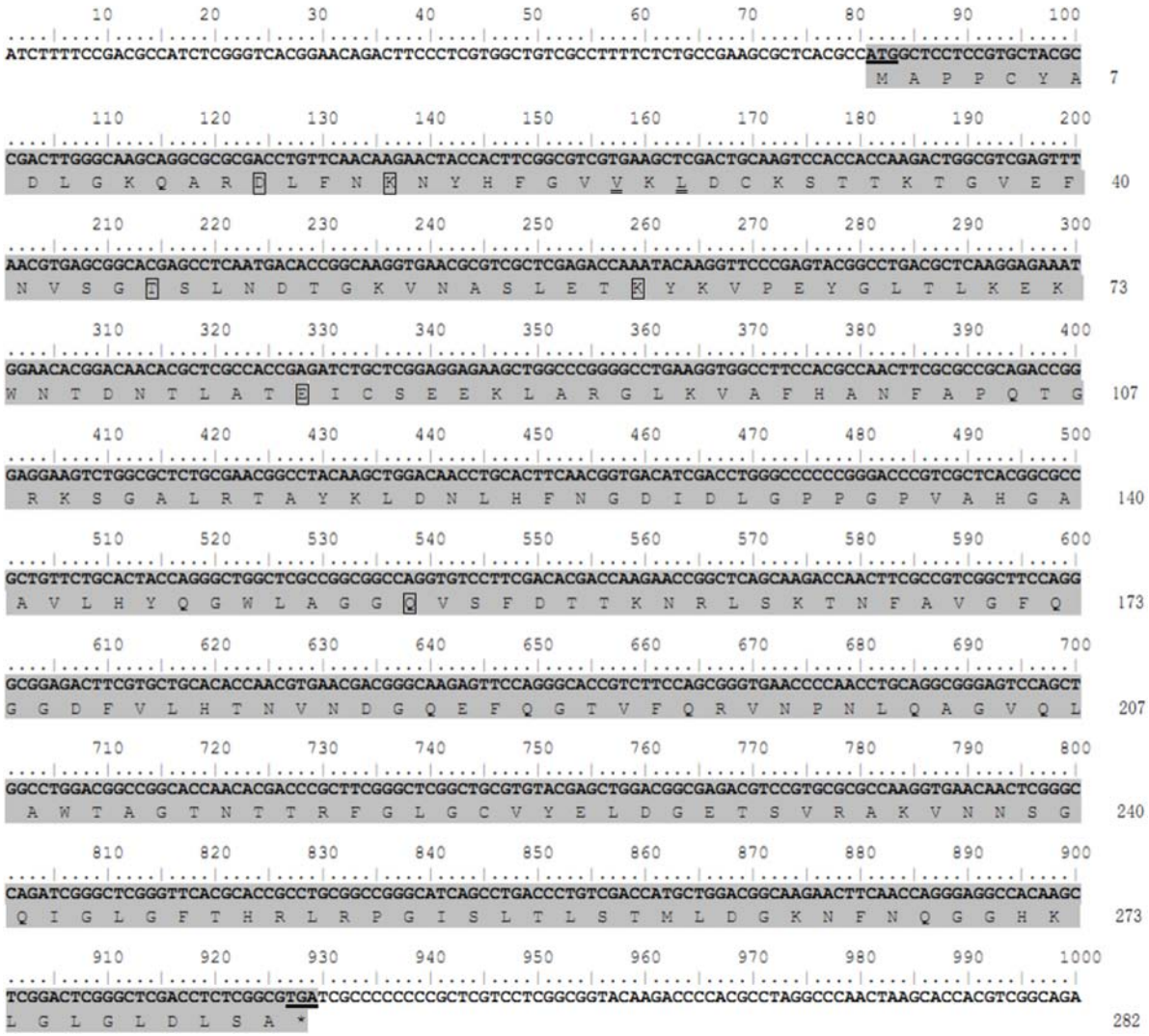

FIGURE 1 | Nucleotide and deduced amino acid sequences of the *porin* gene from the *H. longicornis* tick. The protein coding region for the *porin* gene is indicated by gray shading. The residuals in the boxes show putative determinants of voltage gating, and the residuals with double underlines are putative polypeptide binding sites. The start codon ATG and stop codon TGA are underlined. Nucleotides are numbered above each line, and amino acid numbering is on the right.

AC-3′; *porin* RNAiR: 5′-GATATCTAATACGACTCACTATAGG AAAAGATAGGAAGGGTCTGCCG-3′). Female ticks were used for RNAi experiments as described previously (Liao et al., 2009). The dsRNA-injected ticks were allowed to rest 1 day and then put in chambers attached to the hair-shaved back of hamsters. Each hamster was challenged with 15 dsRNA-injected ticks in the control group or experimental group. The practice was repeated three times. To examine *porin* knockdown efficiency during blood feeding after dsRNA injection, two 0-to-7-day-fed ticks from the infested hamsters were collected from the *porin* dsRNA-injected group and a firefly *luciferase* dsRNA-injected group as a control. Determination of the expression of *porin* was done as described in Section Real-Time PCR Analysis. In contrast, *B. microti* burdens and the expression levels of *porin*-related apoptosis genes were assessed by real-time PCR using genomic DNA and cDNA, respectively. The feeding success of the remaining ticks was investigated by measuring the feeding period and body weight at engorgement.

Statistical Analysis

The mean ranks of *Babesia* burdens in the *porin* RNAi or control group and mRNA levels of *porin* or its related apoptosis genes in the uninfected or infected ticks, *porin* RNAi or control group, 1-day-laid or 7-day-laid eggs, and 2-day-partially-fed (2 dPF) or 2 days after engorgement (2 dAE) nymphs were compared using the Mann-Whitney *U* test. The difference in the mean ranks of *B. microti* burdens, and mRNA levels of *porin* in nymphal and female adult ticks during the blood-feeding process, was analyzed with the Kruskal-Wallis *H* test followed by the Dunn's multiple comparisons test. A p-value of <0.05 was considered statistically significant.

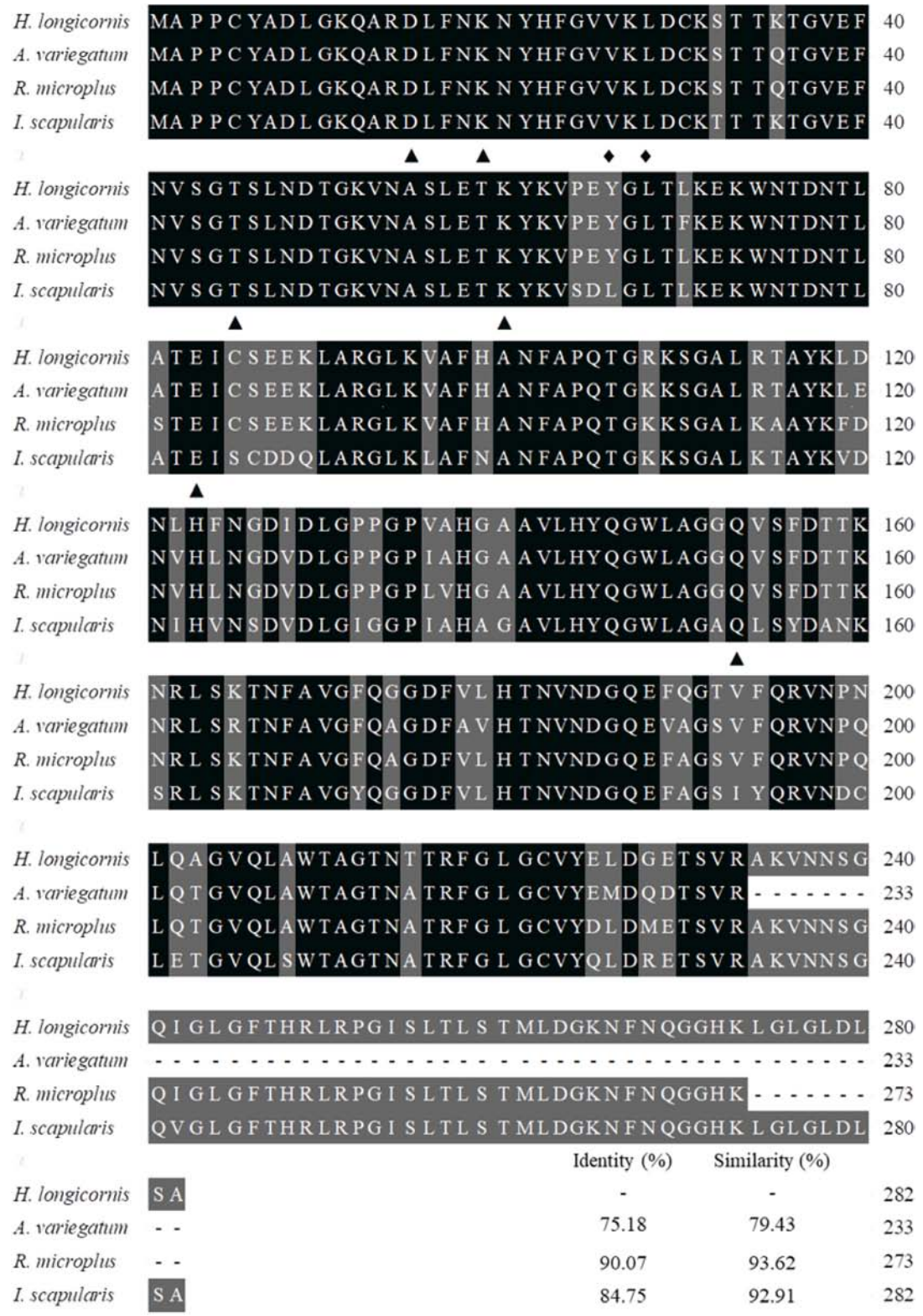

FIGURE 2 | Alignment of the amino acid sequence of the *porin* gene of *H. longicornis* was compared with those of the ixodid ticks *Ixodes scapularis* (XP_002408065), *Rhipicephalus microplus* (ADT82652), and *Amblyomma variegatum* (DAA34069). Identical residues are darkly shaded and similarity residues are gray shaded. Amino acid numbering is on the right. The putative determinants of voltage gating and polypeptide binding sites are shown at the bottom of the sub-columns with triangles and diamonds, respectively.

Nucleotide Sequence Accession Number

The sequences of the *porin* gene of *H. longicornis* and its related apoptosis gene *Bcl* were submitted to the GenBank database under accession numbers MN584740 and MN584741, respectively.

RESULTS

Porin Characterization

The coding nucleotide sequence of the *porin* cDNA was found to be 849 bp in length and encoded 282 amino acids with an expected isoelectric point of 8.95 and molecular weight of 30.4 kDa. The protein is glycine-and-leucine rich with 35 glycines and 31 leucines. Domain analysis showed *porin* to contain six determinants of voltage gating and two polypeptide binding sites (**Figure 1**). Multiple alignment of the amino acid sequence with the homolog sequences from other tick species, including *I. scapularis*, *R. microplus*, and *A. variegatum*, revealed that the determinants of voltage gating and the polypeptide binding sites are conserved among these four tick species. The *H. longicornis porin* amino acids showed the highest homology with that of *R. microplus*, with 90.07% identity and 93.62% similarity, in contrast to 84.75% identity and 92.91% similarity with that of *I. scapularis*, and 75.18% identity and 79.43% similarity with that of *A. variegatum* (**Figure 2**).

Expression Profiles of *Porin* Gene and *Porin*-Related Apoptosis Genes in *H. longicornis* Ticks

GAPDH was the most stably expressed internal control gene in ticks at developmental stages compared with *L23*, *HlP0*, and *Hlactin* and was used as the internal control gene in this study (**Supplementary Figure S1**). Real-time PCR revealed that *porin* mRNA was expressed in the eggs and unfed and fed nymphs (**Figures 3A,B**). There were no differences in *porin* mRNA levels between 1-day-laid eggs and 7-day-laid eggs (**Figure 3A**). *Porin* showed no significant change in expression levels between unfed nymphs incubated at 15 and 25°C (**Supplementary Figure S2**). *Porin* expression levels were higher in the unfed nymphs, 12-h-partially-fed (12 hPF) to 2-d-partially-fed (2 dPF) nymphs, and the nymphs at 0 dAE than the nymphs at 2 dAE ($p < 0.05$) (**Figure 3B**). Subsequently, nymphal samples at 2 dPF and 2 dAE were used to examine expression levels of *porin*-related apoptosis genes. *Cytc* and *Cas2* were significantly less expressed in 2 dAE nymphs than in 2 dPF nymphs ($p < 0.05$) (**Figure 3C**). However, mRNA levels of *Bcl* and *Cas8* in nymphs were not significantly different at 2 dAE vs. 2 dPF (**Figure 3C**).

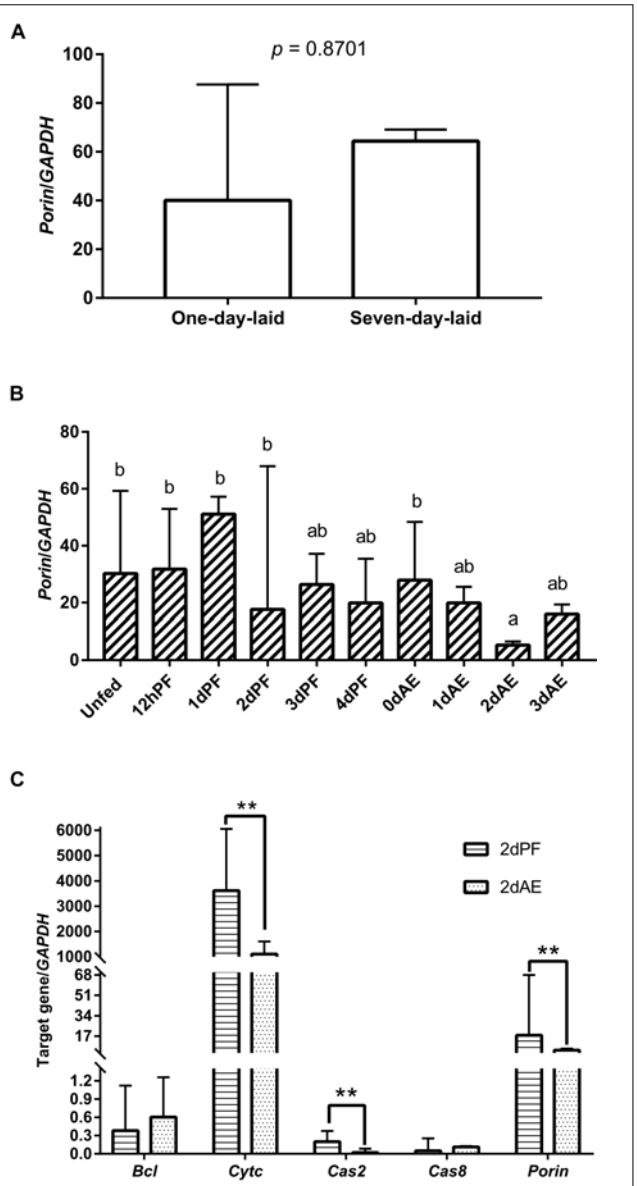

FIGURE 3 | *Porin* expression levels at developmental stages of *H. longicornis* ticks. **(A)** *Porin* gene expression levels at egg stage (1-day-laid eggs and 7-day-laid eggs). **(B)** *Porin* gene expression levels in unfed nymphs, partially fed nymphs (12 hPF to 4 dPF), and nymphs at 0–3 days after engorgement (0 dAE to 3 dAE). **(C)** Comparison of mRNA expression levels of *porin* and its caspase-related apoptosis signal pathway genes between 2 dAE nymphs and 2 dPF nymphs. The bar indicates the median with 95% confidence interval (CI) of three biological repeats. Different letters above the bars represent significant differences ($p < 0.05$). $^{**}p < 0.01$.

B. microti Gray Strain Burdens in *H. longicornis* Ticks

Nymphs fed on *B. microti*-infected hamsters for 12 h and 1–3 days (12 hPF nymphs to 3 dPF nymphs) had lower levels of *Babesia* burdens compared with those fed for 4 days (4 dPF nymphs) and ticks at the onset of engorgement (0 dAE) (**Figure 4**). Real-time PCR analysis showed that the largest amount of *Babesia* DNA was detected at 0 dAE and then decreased at 1–3 dAE, which was further confirmed by conventional PCR analysis (gel electrophoresis image in **Figure 4**). A similar phenomenon was found in female ticks injected with dsRNA of firefly *luciferase* (control group) during blood feeding as evidenced

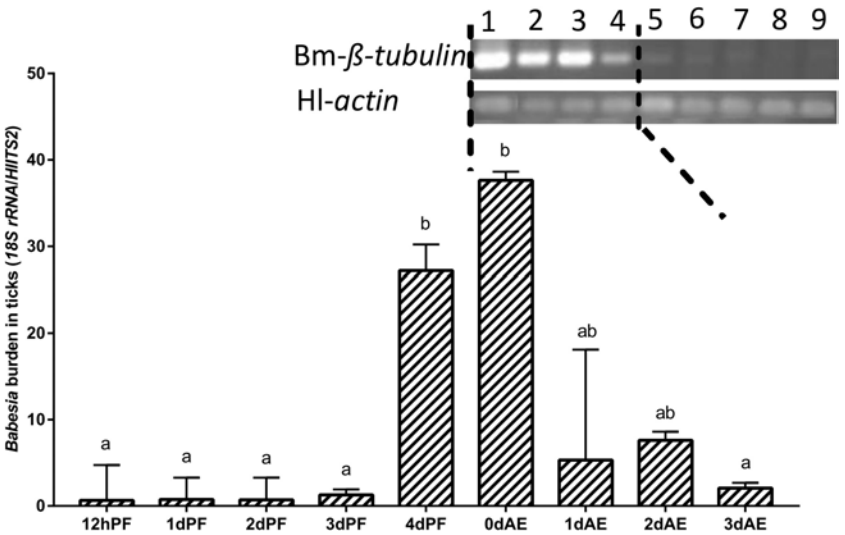

FIGURE 4 | *Babesia* burdens in nymphal *H. longicornis* ticks. Gel electrophoresis image shows the result of a conventional PCR analysis of *Babesia* infection in nymphal ticks at 0–7 days after engorgement (lanes 1–8). Lane 9, negative control. β-*tubulin* (1,341 bp; Bm-β-*tubulin*) was amplified to detect *Babesia microti*, and a 143-bp fragment of the *H. longicornis actin* was amplified as a control. Data sets plotted in histogram are for 12-h partially fed nymphs to 4-day partially-fed nymphs (12 hPF to 4 dPF) and engorged nymphs at 0–3 days after engorgement (0 dAE to 3 dAE). The bar indicates the median with 95% CI of three biological repeats, and different letters above the bars represent significant differences ($p < 0.05$).

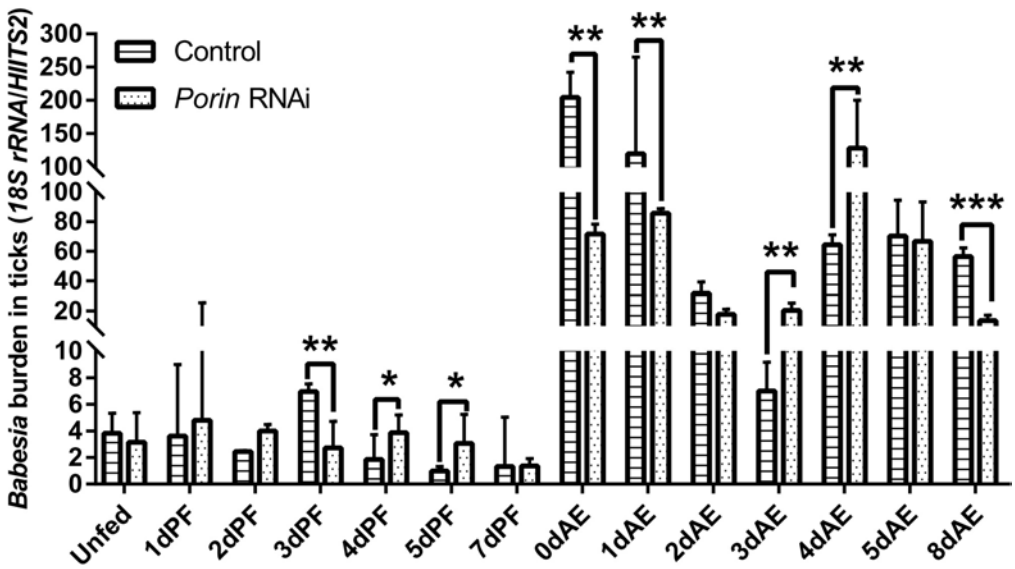

FIGURE 5 | *Babesia* burdens in *porin* RNAi and control ticks during blood feeding. The bar indicates the median with 95% CI of three biological repeats. The asterisks above the bars indicate significant differences in *Babesia* burdens between *porin* RNAi and control groups. *$p < 0.05$; **$p < 0.01$; ***$p < 0.001$.

by the peak of *Babesia* burden at 0 dAE and its subsequent reduction (**Figure 5**).

Comparison of Expression Levels of *Porin* Gene Between Uninfected and Infected Nymphal and Female Ticks

Expression of the *porin* gene was found in *B. microti*-infected or -uninfected nymphs (**Figure 6A**). *Porin* expression levels were higher in the infected vs. uninfected nymphs at 2 and 3 dAE (**Figure 6A**). The expression levels appeared to be higher in infected nymphs during blood feeding (2, 3, and 4 dPF) compared with uninfected nymphs. When the highest *Babesia* load was reached at 0 dAE (**Figure 4**), it appeared that the *porin* expression level in the infected nymphs was decreased ($p = 0.43$) (**Figure 6A**). We then performed an experiment to validate whether the identical phenomenon occurred in female ticks (**Figures 6B–D**). The

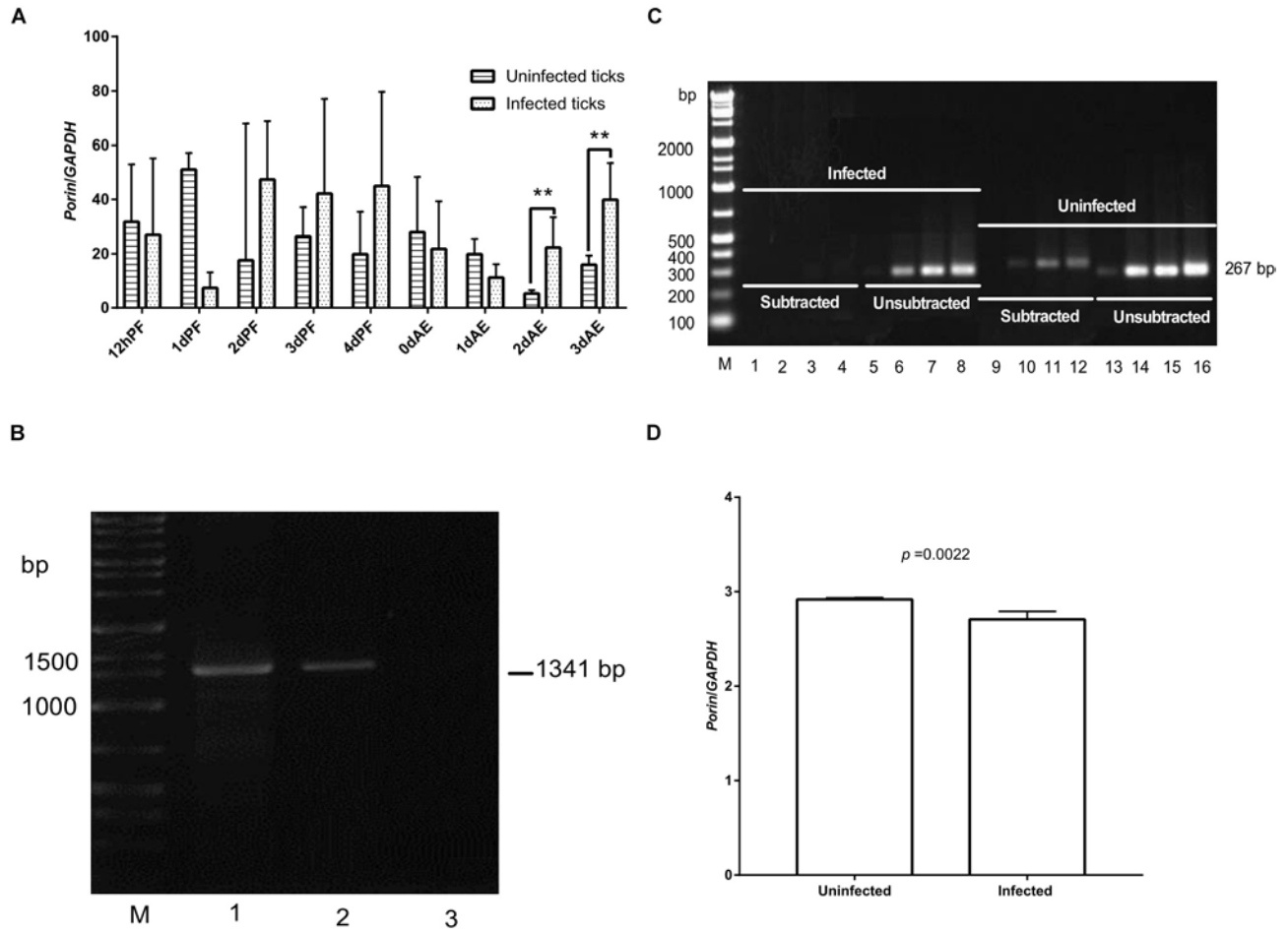

FIGURE 6 | Expression levels of the *porin* gene between uninfected and infected nymphal and female ticks. **(A)** *Porin* gene expression level in *B. microti*-infected or -uninfected nymphal *H. longicornis*. **(B)** Gel electrophoresis analysis of conventional PCR products of *Babesia* β-*tubulin* (1,341 bp) in *B. microti*-infected and -uninfected female ticks at engorgement. Lane 1, infected tick sample; lane 2, positive control; lane 3, uninfected tick sample. **(C)** SSH analysis of *porin* expression levels in infected ticks. No or weak bands were visualized on a gel for PCR products of *porin* amplified from cDNA of infected ticks subtracted with that of uninfected ticks. Bright bands were visualized on a gel for PCR products of *porin* amplified from cDNA of uninfected ticks subtracted with that of infected ticks. Lanes 1, 5, 9, and 13: PCR products amplified by 18 cycles from *porin* gene; lanes 2, 6, 10, and 14: PCR products amplified by 23 cycles; lanes 3, 7, 11, and 15: PCR products amplified by 28 cycles; lanes 4, 8, 12, and 16: PCR products amplified by 33 cycles. **(D)** Real-time PCR analysis of *porin* mRNA expression in whole body of *B. microti*-infected and -uninfected engorged female ticks. The bar indicates the median with 95% CI of three biological repeats. The asterisks above the bar indicate a significant difference in *porin/GAPDH* between uninfected and *B. microti*-infected ticks (**$p < 0.01$).

band on a gel in *porin* PCR products amplified from the reverse SSH cDNA library was brighter than those from the forward SSH cDNA library (**Figure 6C**). The significantly higher mRNA levels of *porin* in uninfected engorged female ticks were further confirmed by real-time PCR ($p = 0.0022$) (**Figure 6D**).

Effect of *Porin* Knockdown on Blood Feeding, *Babesia* Infection, and Expression Profiles of *Porin*-Related Apoptosis Genes in Female Ticks

When each tick was injected with 1 μg of *porin* dsRNA, a gradual reduction in gene silencing efficiency was seen in the hamster-infested ticks after 2 days from tick attachment (**Figure 7A**). The gene was knocked down by 90.24% in female ticks fed on hamsters for 2 days (**Figure 7A**). The body weight of the engorged female ticks in the control group was significantly higher ($p < 0.001$) than that of the RNAi group (**Figure 7B**). No differences in feeding period were seen in the control and *porin*-knockdown groups (data not shown). The effect of *porin* silencing on *Babesia* burdens in the female ticks was time-course dependent. At 3dPF, 0 dAE, 1 dAE, and 8 dAE, the RNAi ticks had 2.34, 2.91, 2.16, and 4.26-fold lower *Babesia* burdens in comparison with the control ticks, respectively (**Figure 5**). However, at 4 dPF, 5 dPF, 3 dAE and 4 dAE, 2.04, 3.14, 2.82, and 2.41-fold higher amounts of *Babesia* DNA were detected in the *porin*-knockdown ticks, respectively (**Figure 5**). Furthermore, at 0 dAE the expression levels of *Cytc* and *Bcl* in the *porin*-knockdown female ticks significantly decreased in contrast to

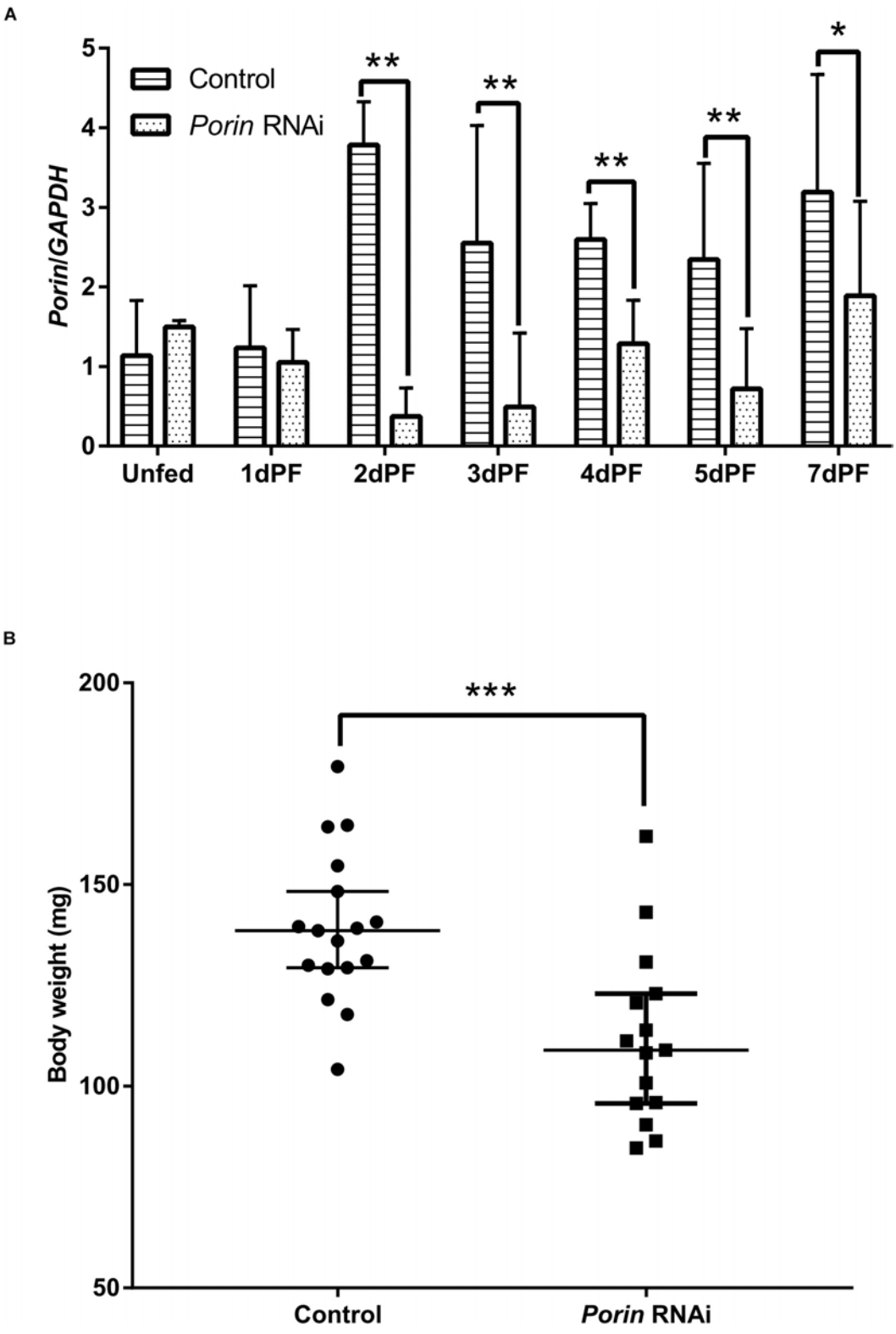

FIGURE 7 | The effect of *porin* silencing on body weight of female ticks at engorgement. **(A)** Expression analysis of *porin* mRNA in whole body of dsRNA-injected female ticks; **(B)** Body weights of female ticks at engorgement in *porin* RNAi and control ticks. The bar indicates the median with 95% CI of three biological repeats. The asterisks above the bars indicate significant differences in *porin*/*GAPDH* and body weight between *porin* RNAi and control groups. $^{*}p < 0.05$; $^{**}p < 0.01$; $^{***}p < 0.001$.

that in the control ticks ($p < 0.01$ and $p < 0.05$), whereas the mRNA levels of *Cas2* and *Cas8* did not show obvious changes in the *porin*-RNAi ticks compared with the control ticks (**Figure 8**).

DISCUSSION

Porin in *H. longicornis* is a 30.4 kDa protein with 282 amino acids, as is reported in other organisms (Sardiello et al., 2003; Wang et al., 2010; Rodríguez-Hernández et al., 2011). Additionally, our study showed that determinants of voltage gating and polypeptide binding sites in *porin* protein are conserved among tick species (**Figure 2**), suggesting that they play a primary role in the regulation of ion and molecular flow and in metabolism inside and outside the mitochondrial membrane among ticks. It was reported that *porin* might be involved in tick feeding and/or digestion of blood meals and its development (Ayllón et al., 2013; Rodríguez-Hernández et al., 2015). *Porin* mRNA levels of *I. scapularis* increased from egg to adult stages and from the non-feeding to feeding periods of female ticks. Knockdown of the gene resulted in about a 40% reduction in female tick weight after feeding compared to the weight of controls (Ayllón et al., 2013). *Porin* expression levels in the midgut of adult *R. microplus* ticks first increased to a maximum and then decreased at 0 to 72 h post repletion (Rodríguez-Hernández et al., 2015). In the present study, a similar expression level of *porin* mRNA was found in 1-day-laid and 7-day-laid eggs (**Figure 3A**), and the mRNA levels were appeared to be higher in the unfed nymphs, 12 hPF to 2 dPF nymphs, and the nymphs at 0 dAE than the nymphs at 2 dAE (**Figure 3B**). However, their expression levels increased in female ticks when taking blood from the hosts (**Figure 7A**). *Porin* silencing mediated by RNAi significantly decreased the body weight of engorged adults but did not alter the blood feeding period (**Figure 7B**).

When confronting stressful situations and adverse conditions, remodeling of the cell skeleton, inhibition of cell apoptosis, and manipulation of the innate or specific immune system can help hosts remove the damaged cells to maintain tissue homeostasis and therefore benefit the remaining cells (de la Fuente et al., 2016). In the regulated process of cell apoptosis, *porin* plays a pivotal role in releasing an apoptogenic factor, namely *Cytc*. Pathogen infection activates the Janus kinase/signal transducers and activators of transcription (JAK/STAT) to down-regulate *porin* expression and therefore inhibit cell apoptosis as an aid to pathogen infection, survival, development, and multiplication inside infected cells (Alberdi et al., 2015; de la Fuente et al., 2016). In the present study, *porin* mRNA expression levels appeared to be lower in *B. microti*-infected ticks than in uninfected ticks at engorgement when the highest *Babesia* burden occurred (**Figures 5A,C,D**), suggesting that the invasion of a large number of *Babesia* might inhibit cell apoptosis in ticks via suppression of *porin* expression. However, some other studies have reported opposite findings, showing the same or higher levels of *porin* expression in vectors when they have the highest pathogen load (Fongsaran et al., 2014; Rodríguez-Hernández et al., 2015; Jitobaom et al., 2016). These studies showed that *porin* may function as an activator of pathogen receptors (such as plasminogen) or a part of a pathogen receptor (such as *porin* plus *GRP78* complex). The formation of pathogen receptor facilitates pathogen entry into cells, for example, the dissemination of *Borrelia burgdorferi* in *Ixodes* ticks, *B. bigemina* in *Rhipicephalus* ticks, and the invasion of Japanese encephalitis virus, dengue virus, and *Plasmodium* spp. into the midgut cells of mosquitoes. Our data showed that nymphal and adult ticks acquired *B. microti* via blood sucking. During the blood feeding process, we found that the amount of babesial DNA in ticks increased at 4 dPF and 0 dAE, and then decreased thereafter, suggesting that *B. microti* infected and proliferated in the tick body at these timings. Moreover, *porin* mRNA expression levels appeared to be lower at 1 dPF, higher at 2–4 dPF, lower at 0–1 dAE, and higher at 2–3 dAE in the infected nymphs vs. the uninfected nymphs. The *porin* expression dynamics might be related to *Babesia* infection in a time-dependent manner. RNAi of *porin* changed the *Babesia* infection level in dsRNA-injected ticks in contrast to the control ticks. The peak of *Babesia* burden in control ticks was observed at 0 dAE, however, the peak in *porin* dsRNA-injected ticks was found at 4 dAE. Taken together, our results indicate that during the blood feeding *Babesia* infection might cause the inhibition of cell apoptosis at one time point and/or activation of *porin* expression for pathogen invasion at another time point (Alberdi et al., 2015; Rodríguez-Hernández et al., 2015; de la Fuente et al., 2016). For better understanding the interactions between *B. microti* and porin and the related molecules, further analyses will be needed focusing on an important organ for *Babesia* infection, such as the midgut.

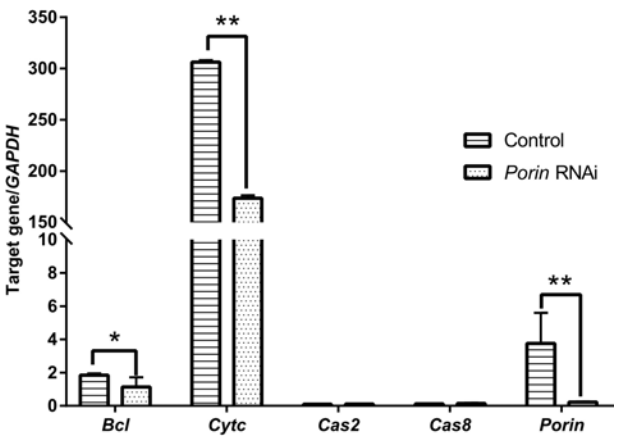

FIGURE 8 | Impact of *porin* RNAi on *porin*-related apoptosis gene expression in engorged female ticks. The bar indicates the median with 95% CI of three biological repeats. The asterisks above the bars indicate significant differences in target gene/*GAPDH* between *porin* RNAi and control groups. $*p < 0.05$; $**p < 0.01$.

Most *caspases* play a role in programmed cell death, including apoptosis and pyroptosis, and as initiators, executioners, or inflammatory types (Galluzzi et al., 2016). *Hlcaspase-2* (termed *Cas2* in our study) and *Hlcaspase-8* (termed *Cas8*) previously identified from *H. longicornis* (Tanaka et al., 2007) are two members of initiator *caspases* that might play important roles in inducing cell death by apoptosis. In addition to apoptosis, *Cas8* is required for the inhibition of necroptosis (Denecker et al., 2008). During times of cellular stress, mitochondrial *Cytc* binding to an adaptor protein (APAF-1) recruits initiator *caspases*, which helps to form a *caspase*-activating multiprotein complex called the apoptosome. Once activated, initiator *caspases* will modulate other executioner *caspases*. This leads to degradation of cellular components for apoptosis (Creagh, 2014). In our study, highly down-regulated *Cytc* induced by *porin* silencing did not suppress the expression levels of the initiator *caspase, Cas8* (**Figure 8**). The same phenomenon was observed in nymphs at 2 dAE and 2 dPF (**Figure 3C**), which might be explained by an extrinsic, and not intrinsic, apoptotic pathway available to *Cas8* (Creagh, 2014). Further experiments at protein level will be required to evaluate the role of *porin* in the activating *caspases*-interfered apoptotic pathway.

CONCLUSION

In conclusion, the present experiments identified the *porin* gene from *H. longicornis* and evaluated its expression levels in *B. microti*-infected and -uninfected *H. longicornis* ticks at developmental stages. Our data suggest that *porin* might positively regulate expression of the *Cytc* gene, which is known to be vital for *caspases*-interfered cell apoptosis. *Porin* knockdown reduced body weight and changed *Babesia* infection levels in *H. longicornis* ticks. In addition, we detected DNA of the *B. microti* Gray strain in both nymphal and adult stages that fed on infected hamsters by using conventional and real-time PCR analyses. *Babesia* loads in nymphs and adults remained at low levels before engorgement, peaked at/around onset of engorgement, and then gradually decreased to low levels such as those in initial blood feeding stages, which is consistent with a previous observation of *B. microti* Munich strain infection in mice (Kusakisako et al., 2015). This *H. longicornis-B. microti* experimental infection model using hamsters will be used for further investigation of the interaction between ticks and human *Babesia*. Taken together, our findings will be useful for better understanding the roles of *H. longicornis porin* in tick development, blood feeding, and *B. microti* infection.

DATA AVAILABILITY STATEMENT

The datasets generated for this study can be found in the GenBank database under accession numbers MN584740 for porin and MN584741 for Bcl.

ETHICS STATEMENT

The animal study was reviewed and approved by Animal Care and Use Committee of Obihiro University of Agriculture and Veterinary Medicine.

AUTHOR CONTRIBUTIONS

XX, RU-S, HS, QZ, and HC conceived and designed the study. WZ performed most of the experimental work. WZ and RU-S wrote the manuscript. WZ, KO, PAM, and ML collected and analyzed the data.

FUNDING

This study was financially supported by grants from the Jiangxi Provincial Department of Science and Technology (Grant Nos. 20192BBHL80013, 2016BBG70005), the Health Commission of Jiangxi Province (Grant No. 20162007), and the Ministry of Education, Culture, Sports, Science and Technology (MEXT) of Japan as a project for Joint Usage/Research Center. WZ was supported by a Sasakawa Medical Fellowship through the Japan-China Medical Association.

ACKNOWLEDGMENTS

We appreciate Mr. Hiroyuki Sugawara (Obihiro University of Agriculture and Veterinary Medicine) for his great work in rabbit and hamster rearing and in aiding in attaching chambers to the backs of the hamsters. We thank Ms. Maki Kuniyori (Obihiro University of Agriculture and Veterinary Medicine) for assistance with the methodology.

SUPPLEMENTARY MATERIAL

The Supplementary Material for this article can be found online at: https://www.frontiersin.org/articles/10.3389/fphys.2020.00502/full#supplementary-material

REFERENCES

Alberdi, P., Ayllón, N., Cabezas-Cruz, A., Bell-Sakyi, L., Zweygarth, E., Stuen, S., et al. (2015). Infection of Ixodes spp. tick cells with different *Anaplasma phagocytophilum* isolates induces the inhibition of apoptotic cell death. *Ticks Tick Borne Dis.* 6, 758–767. doi: 10.1016/j.ttbdis.2015.07.001

Antunes, S., Rosa, C., Couto, J., Joana, F., and Domingos, A. (2017). Deciphering babesia-vector interactions. *Front. Cell. Infect. Microbiol.* 7:429. doi: 10.3389/fcimb.2017.00429

Ayllón, N., Villar, M., Busby, A. T., Kocan, K. M., Blouin, E. F., Bonzón-Kulichenko, E., et al. (2013). *Anaplasma phagocytophilum* inhibits apoptosis and promotes cytoskeleton rearrangement for infection of tick cells. *Infect. Immun.* 81, 2415–2425. doi: 10.1128/IAI.00194-13

Chae, J. S., and Lee, M. J. (2010). Molecular detection of *Ehrlichia chaffeensis* and *Anaplasma bovis* in the salivary glands from *Haemaphysalis longicornis* ticks. *Vect. Borne Zoon. Dis.* 10, 411–443. doi: 10.1089/vbz.2008.0215

Chen, Z., Li, H., Gao, X., Bian, A., Yan, H., Kong, D., et al. (2019). Human babesiosis in China: a systematic review. *Parasitol. Res.* 118, 1103–1112. doi: 10.1007/s00436-019-06250-9

Creagh, E. M. (2014). Caspase crosstalk: integration of apoptotic and innate immune signalling pathways. *Trends Immunol.* 35, 631–640. doi: 10.1016/j.it.2014.10.004

de la Fuente, J., Antunes, S., Bonnet, S., Cabezas-Cruz, A., Domingos, A. G., Estrada-Peña, A., et al. (2017). Tick-pathogen interactions and vector competence: identification of molecular drivers for tick-borne diseases. *Front. Cell. Infect. Microbiol.* 7:114. doi: 10.3389/fcimb.2017.00114

de la Fuente, J., Estrada-Peña, A., Cabezas-Cruz, A., and Kocan, K. M. (2016). *Anaplasma phagocytophilum* uses common strategies for infection of ticks and vertebrate hosts. *Trends Microbiol.* 24, 173–180. doi: 10.1016/j.tim.2015.12.001

Denecker, G., Ovaere, P., Vandenabeele, P., and Declercq, W. (2008). Caspase-14 reveals its secrets. *J. Cell. Biol.* 180, 451–458. doi: 10.1083/jcb.200709098

Fang, L. Q., Liu, K., Li, X. L., Liang, S., Yang, Y., Yao, H. W., et al. (2015). Emerging tick-borne infections in mainland China: an increasing public health threat. *Lancet Infect. Dis.* 15, 1467–1479. doi: 10.1016/S1473-3099(15)00177-2

Fongsaran, C., Phaonakrop, N., Roytrakul, S., Thepparit, C., Kuadkitkan, A., and Smith, D. R. (2014). Voltage dependent anion channel is redistributed during Japanese encephalitis virus infection of insect cells. *Sci. World J.* 2014:976015. doi: 10.1155/2014/976015

Galluzzi, L., López-Soto, A., Kumar, S., and Kroemer, G. (2016). Caspases connect cell-death signaling to organismal homeostasis. *Immunity* 44, 221–231. doi: 10.1016/j.immuni.2016.01.020

Heath, A. (2016). Biology, ecology and distribution of the tick, *Haemaphysalis longicornis* neumann (Acari: Ixodidae) in New Zealand. *N. Z. Vet. J.* 64, 10–20. doi: 10.1080/00480169.2015.1035769

Ikadai, H., Sasaki, M., Ishida, H., Matsuu, A., Igarashi, I., Fujisaki, K., et al. (2007). Molecular evidence of Babesia equi transmission in *Haemaphysalis longicornis*. *Am. J. Trop. Med. Hyg.* 76, 694–697.

Jitobaom, K., Tongluan, N., and Smith, D. R. (2016). Involvement of voltage-dependent anion channel (VDAC) in dengue infection. *Sci. Rep.* 6:35753. doi: 10.1038/srep35753

Krause, P. J. (2019). Human babesiosis. *Int. J. Parasitol.* 49, 165–174. doi: 10.1016/j.ijpara.2018.11.007

Kusakisako, K., Maeda, H., Galay, R. L., Matsuo, T., Tsujio, M., Umemiya-Shirafuji, R., et al. (2015). The vector potential of *Haemaphysalis longicornis* ticks for *Babesia microti* parasites under experimental condition. *J. Protozool. Res.* 25, 8–17.

Liao, M., Zhou, J., Gong, H., Boldbaatar, D., Shirafuji, R., Battur, B., et al. (2009). Hemalin, a thrombin inhibitor isolated from a midgut cDNA library from the hard tick *Haemaphysalis longicornis*. *J. Insect Physiol.* 55, 164–173. doi: 10.1016/j.jinsphys.2008.11.004

Mather, T. N., Telford, S. R., Moore, S. I., and Spielman, A. (1990). *Borrelia burgdorferi* and *Babesia microti*: efficiency of transmission from reservoirs to vector ticks (*Ixodes dammini*). *Exp. Parasitol.* 70, 55–61. doi: 10.1016/0014-4894(90)90085-q

McFadden, A. M., Rawdon, T. G., Meyer, J., Makin, J., Morley, C. M., Clough, R. R., et al. (2011). An outbreak of *Haemolytic anaemia* associated with infection of *Theileria orientalis* in naive cattle. *N. Z. Vet. J.* 59, 79–85. doi: 10.1080/00480169.2011.552857

Raghavan, R. K., Barker, S. C., Cobos, M. E., Barker, D., Teo, E., Foley, D. H., et al. (2019). Potential spatial distribution of the newly introduced long-horned tick, *Haemaphysalis longicornis* in North America. *Sci. Rep.* 9:498. doi: 10.1038/s41598-018-37205-2

Rainey, T., Occi, J. L., Robbins, R. G., and Egizi, A. (2018). Discovery of *Haemaphysalis longicornis* (Ixodida: Ixodidae) parasitizing a sheep in New Jersey, United States. *J. Med. Entomol.* 55, 757–759. doi: 10.1093/jme/tjy006

Ribeiro, J. M., Anderson, J. M., Manoukis, N. C., Meng, Z., and Francischetti, I. M. (2011). A further insight into the sialome of the tropical bont tick, *Amblyomma variegatum*. *BMC Genomics* 12:136. doi: 10.1186/1471-2164-12-136

Rodríguez-Hernández, E., Mosqueda, J., Alvarez-Sánchez, M. E., Neri, A. F., Mendoza-Hernández, G., and Camacho-Nuez, M. (2011). The identification of a VDAC-like protein involved in the interaction of *Babesia bigemina* sexual stages with *Rhipicephalus microplus* midgut cells. *Vet. Parasitol.* 187, 538–541. doi: 10.1016/j.vetpar.2012.01.028

Rodríguez-Hernández, E., Mosqueda, J., León-Ávila, G., Castañeda-Ortiz, E. J., Álvarez-Sánchez, M. E., Camacho, A. D., et al. (2015). BmVDAC upregulation in the midgut of *Rhipicephalus microplus*, during infection with *Babesia bigemina*. *Vet. Parasitol.* 212, 368–374. doi: 10.1016/j.vetpar.2015.06.016

Sardiello, M., Tripoli, G., Oliva, M., Santolamazza, F., Moschetti, R., Barsanti, P., et al. (2003). Comparative study of the porin genes encoding VDAC, a voltage-dependent anion channel protein, in *Anopheles gambiae* and *Drosophila melanogaster*. *Gene* 317, 111–112. doi: 10.1016/s0378-1119(03)00658-9

Sivakumar, T., Tattiyapong, M., Okubo, K., Suganuma, K., Hayashida, K., Igarashi, I., et al. (2014). PCR detection of *Babesia ovata* from questing ticks in Japan. *Ticks Tick Borne Dis.* 5, 305–310. doi: 10.1016/j.ttbdis.2013.12.006

Tanaka, M., Liao, M., Zhou, J., Nishikawa, Y., Xuan, X., and Fujisaki, K. (2007). Molecular cloning of two caspase-like genes from the hard tick *Haemaphysalis longicornis*. *J. Vet. Med. Sci.* 69, 85–90. doi: 10.1292/jvms.69.85

Umemiya-Shirafuji, R., Fujisaki, K., Okado, K., Adjou Moumouni, P. F., Yokoyama, N., Hiroshi, S., et al. (2019a). Hard ticks as research resources for vector biology: from genome to whole-body level. *Med. Entomol. Zool.* 70, 181–188. doi: 10.7601/mez.70.181

Umemiya-Shirafuji, R., Mihara, R., Fujisaki, K., and Suzuki, H. (2019b). Intracellular localization of vitellogenin receptor mRNA and protein during oogenesis of a parthenogenetic tick, *Haemaphysalis longicornis*. *Parasit. Vect.* 12:205. doi: 10.1186/s13071-019-3469-9

Vannier, E., and Krause, P. J. (2012). Human babesiosis. *N. Engl. J. Med.* 366, 2397–2407. doi: 10.1056/NEJMra1202018

Wang, K. C., Kondo, H., Hirono, I., and Aoki, T. (2010). The *Marsupenaeus japonicus* voltage-dependent anion channel (MjVDAC) protein is involved in white spot syndrome virus (WSSV) pathogenesis. *Fish Shellfish Immunol.* 29, 94–103. doi: 10.1016/j.fsi.2010.02.020

Wormser, G. P., McKenna, D., Piedmonte, N., Vinci, V., Egizi, A. M., Backenson, B., et al. (2019). First recognized human bite in the United States by the Asian longhorned tick, *Haemaphysalis longicornis*. *Clin. Infect. Dis.* 70, 314–316. doi: 10.1093/cid/ciz449

Wu, J., Cao, J., Zhou, Y., Zhang, H., Gong, H., and Zhou, J. (2017). Evaluation on infectivity of *Babesia microti* to domestic animals and ticks outside the *Ixodes genus*. *Front. Microbiol.* 8:1915. doi: 10.3389/fmicb.2017.01915

Zhang, H., Sun, Y., Jiang, H., and Huo, X. (2017). Prevalence of severe febrile and thrombocytopenic syndrome virus, *Anaplasma* spp. and *Babesia microti* in hard ticks (Acari: Ixodidae) from Jiaodong peninsula, Shandong Province. *Vector Borne Zoonotic Dis.* 17, 134–140. doi: 10.1089/vbz.2016.1978

Zheng, W., Xuan, X., Fu, R., Tao, H., Xu, R., Liu, Y., et al. (2019). Preliminary investigation of ixodid ticks in jiangxi province of Eastern China. *Exp. Appl. Acarol.* 77, 93–104. doi: 10.1007/s10493-018-0324-1

Zheng, W. Q., Xuan, X. N., Fu, R. L., Tao, H. Y., Liu, Y. Q., Liu, X. Q., et al. (2018). Tick-borne pathogens in ixodid ticks from Poyang Lake Region, southeastern China. *Korean J. Parasitol.* 56, 589–596. doi: 10.3347/kjp.2018.56.6.589

Zhuang, L., Sun, Y., Cui, X. M., Tang, F., Hu, J. G., Wang, L. Y., et al. (2018). Transmission of severe fever with thrombocytopenia syndrome virus by *Haemaphysalis longicornis* ticks, China. *Emerg. Infect. Dis.* 24, 868–871. doi: 10.3201/eid2405.151435

Conflict of Interest: The authors declare that the research was conducted in the absence of any commercial or financial relationships that could be construed as a potential conflict of interest.

Advantages of publishing in Frontiers

OPEN ACCESS
Articles are free to read for greatest visibility and readership

FAST PUBLICATION
Around 90 days from submission to decision

HIGH QUALITY PEER-REVIEW
Rigorous, collaborative, and constructive peer-review

TRANSPARENT PEER-REVIEW
Editors and reviewers acknowledged by name on published articles

Frontiers
Avenue du Tribunal-Fédéral 34
1005 Lausanne | Switzerland

Visit us: www.frontiersin.org
Contact us: info@frontiersin.org | +41 21 510 17 00

REPRODUCIBILITY OF RESEARCH
Support open data and methods to enhance research reproducibility

DIGITAL PUBLISHING
Articles designed for optimal readership across devices

FOLLOW US
@frontiersin

IMPACT METRICS
Advanced article metrics track visibility across digital media

EXTENSIVE PROMOTION
Marketing and promotion of impactful research

LOOP RESEARCH NETWORK
Our network increases your article's readership